

Complexity

Complexity in Economics and Business

Lead Guest Editor: Baogui Xin

Guest Editors: Abdelalim Elsadany and Lei Xie





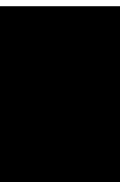
Complexity in Economics and Business

Complexity

Complexity in Economics and Business

Lead Guest Editor: Baogui Xin


Guest Editors: Abdelalim Elsadany and Lei Xie



Copyright © 2020 Hindawi Limited. All rights reserved.

This is a special issue published in "Complexity." All articles are open access articles distributed under the Creative Commons Attribution License, which permits unrestricted use, distribution, and reproduction in any medium, provided the original work is properly cited.

Chief Editor

Hiroki Sayama , USA

Associate Editors

Albert Diaz-Guilera , Spain
Carlos Gershenson , Mexico
Sergio Gómez , Spain
Sing Kiong Nguang , New Zealand
Yongping Pan , Singapore
Dimitrios Stamovlasis , Greece
Christos Volos , Greece
Yong Xu , China
Xinggang Yan , United Kingdom

Academic Editors

Andrew Adamatzky, United Kingdom
Marcus Aguiar , Brazil
Tarek Ahmed-Ali, France
Maia Angelova , Australia
David Arroyo, Spain
Tomaso Aste , United Kingdom
Shonak Bansal , India
George Bassel, United Kingdom
Mohamed Boutayeb, France
Dirk Brockmann, Germany
Seth Bullock, United Kingdom
Diyi Chen , China
Alan Dorin , Australia
Guilherme Ferraz de Arruda , Italy
Harish Garg , India
Sarangapani Jagannathan , USA
Mahdi Jalili, Australia
Jeffrey H. Johnson, United Kingdom
Jurgen Kurths, Germany
C. H. Lai , Singapore
Fredrik Liljeros, Sweden
Naoki Masuda, USA
Jose F. Mendes , Portugal
Christopher P. Monterola, Philippines
Marcin Mrugalski , Poland
Vincenzo Nicosia, United Kingdom
Nicola Perra , United Kingdom
Andrea Rapisarda, Italy
Céline Rozenblat, Switzerland
M. San Miguel, Spain
Enzo Pasquale Scilingo , Italy
Ana Teixeira de Melo, Portugal




Shahadat Uddin , Australia
Jose C. Valverde , Spain
Massimiliano Zanin , Spain

Contents


An Evaluation on Investment of Research Funds with a Neural Network Algorithm in “Double First-Class” Universities

Jihong Sun , Yahui Li , Xiaoyun Zhao , and Nanxing Zhang 
Research Article (8 pages), Article ID 7496126, Volume 2020 (2020)


A Hybrid Approach Integrating Multiple ICEEMDANs, WOA, and RVFL Networks for Economic and Financial Time Series Forecasting

Jiang Wu , Tengfei Zhou , and Taiyong Li 
Research Article (17 pages), Article ID 9318308, Volume 2020 (2020)


An Analytical Optimisation Framework for Airport Terminal Capacity Expansion

Sultan Alodhaibi , Robert L. Burdett, and Prasad K. D. V. Yarlagadda
Research Article (10 pages), Article ID 2976281, Volume 2020 (2020)

Scheduling on a Single Machine and Parallel Machines with Batch Deliveries and Potential Disruption

Hua Gong , Yuyan Zhang, and Puyu Yuan 
Research Article (10 pages), Article ID 6840471, Volume 2020 (2020)


Complex Dynamic Analysis for Game Model under Different Regulatory Levels in China’s Housing Rental Market

Lingling Mu, Xiangyu Qin, Yuan Li, and Ping Liu 
Research Article (10 pages), Article ID 7370868, Volume 2020 (2020)

A New Method for Interindustry Linkage Analysis Based on Demand-Driven and Multisector Input-Output Model and Its Application in China’s Manufacturing and Producer Services

Xiao Liu  and Jinchuan Shi 
Research Article (16 pages), Article ID 3857981, Volume 2020 (2020)

A Dynamic Duopoly Cournot Model with R&D Efforts and Its Dynamic Behavior Analysis

Wei Zhou , Jie Zhou, Tong Chu, and Hui Li
Research Article (19 pages), Article ID 9634878, Volume 2020 (2020)

Numerical Solutions to Optimal Portfolio Selection and Consumption Strategies under Stochastic Volatility

Lei Ge  and Qiang Zhang
Research Article (16 pages), Article ID 9548060, Volume 2020 (2020)




Adaptive Finite-Time Congestion Control for Uncertain TCP/AQM Network with Unknown Hysteresis

Weimin Zheng, Yanxin Li , Xiaowen Jing, and Shangkun Liu
Research Article (9 pages), Article ID 4138390, Volume 2020 (2020)

Decisions and Coordination in a Capacity Sharing Supply Chain considering Production Cost Misreporting

Daozhi Zhao  and Hongshuai Han 
Research Article (12 pages), Article ID 1926035, Volume 2020 (2020)

Supply Chain Decision-Making and Coordination considering Anticipated Regret under Price Discount

Jie Jian , Huipeng Li, Nian Zhang , and Jiafu Su 



Research Article (14 pages), Article ID 6091702, Volume 2020 (2020)

Digital Twin Driven Green Performance Evaluation Methodology of Intelligent Manufacturing: Hybrid Model Based on Fuzzy Rough-Sets AHP, Multistage Weight Synthesis, and PROMETHEE II

Lianhui Li , Chunlei Mao, Hongxia Sun, Yiping Yuan , and Bingbing Lei 


Research Article (24 pages), Article ID 3853925, Volume 2020 (2020)

Stock Market Temporal Complex Networks Construction, Robustness Analysis, and Systematic Risk Identification: A Case of CSI 300 Index

Xiaole Wan , Zhen Zhang, Chi Zhang, and Qingchun Meng 

Research Article (19 pages), Article ID 7195494, Volume 2020 (2020)

Research on Dynamic and Complexity of Energy-Saving Investment about Multichannel and Multienergy Supply Chain

Fang Wu 



Research Article (10 pages), Article ID 2409636, Volume 2020 (2020)

Complexity Analysis of Pricing in a Multichannel Supply Chain with Spillovers from Online to Offline Sales

Fengxia Mai, Jianxiong Zhang , Rui Yang, and Xiaojie Sun 


Research Article (17 pages), Article ID 3145478, Volume 2020 (2020)

Dynamic Investigation in Green Supply Chain considering Channel Service

Qiuxiang Li , Mengmeng Li, and Yimin Huang 




Research Article (18 pages), Article ID 1640724, Volume 2020 (2020)

Forecasting CDS Term Structure Based on Nelson–Siegel Model and Machine Learning

Won Joong Kim, Gunho Jung, and Sun-Yong Choi 


Research Article (23 pages), Article ID 2518283, Volume 2020 (2020)

Evolutionary Game Model of Integrating Health and Care Services for Elder People

Tingqiang Chen , Jinnan Pan, Yuanping He , and Jining Wang 




Research Article (13 pages), Article ID 5846794, Volume 2020 (2020)

Dynamic Green Innovation Decision of the Supply Chain with Innovating and Free-Riding Manufacturers: Cooperation and Spillover

Feifei Zhang, Zaixu Zhang, Yawei Xue, Jian Zhang , and Yang Che

Research Article (17 pages), Article ID 8937847, Volume 2020 (2020)



Habit or Utility: A Key Choice Point in Promoting the Adoption of Telehealth in China

Yun Fan , Sifeng Liu, Jun Liu, Saad Ahmed Javed , and Zhigeng Fang 

Research Article (11 pages), Article ID 5063756, Volume 2020 (2020)

Contents

“Buy Online, Pick Up in Store” under Fit Uncertainty: To Offer or Not to Offer

Huijing Li, Shilei Yang, Haiyan Kang , and Victor Shi 


Research Article (12 pages), Article ID 3095672, Volume 2020 (2020)

Risk Evaluation of Sewage Treatment PPPABS Projects Using Combination Weight Method and D-S Evidence Theory

Hui Zhao , Zehui Bu, and Shengbin Ma



Research Article (12 pages), Article ID 4167130, Volume 2020 (2020)

Analysis of Complex Dynamics in Different Bargaining Systems

Xiaogang Ma, Chunyu Bao , and Lin Su

Research Article (16 pages), Article ID 8406749, Volume 2020 (2020)

Economic Development Forecast of China’s General Aviation Industry

Hongqing Liao, Zhigeng Fang , Chuanhui Wang, and Xiaqing Liu 


Research Article (8 pages), Article ID 3747031, Volume 2020 (2020)

Evaluation and Selection of Manufacturing Suppliers in B2B E-Commerce Environment

Quan Zhang , Zhen Guo , Feiyu Man , and Jiyun Ma 



Research Article (8 pages), Article ID 8690402, Volume 2020 (2020)

A Dynamic Thermal-Allocation Solution to the Complex Economic Benefit for a Data Center

Hui Liu , Wenyu Song, Tianqi Jin, Zhiyong Wu, Fusheng Yan, and Jie Song

Research Article (12 pages), Article ID 5934747, Volume 2020 (2020)

The Applications and Complexity Analysis Based on Network Embedding Behaviors under Evolutionary Game Framework

Xin Su , Hui Zhang, and Shubing Guo 


Research Article (23 pages), Article ID 3714564, Volume 2020 (2020)

The Pricing Strategy of Dual Recycling Channels for Power Batteries of New Energy Vehicles under Government Subsidies

Xiaodong Zhu  and Wei Li


Research Article (16 pages), Article ID 3691493, Volume 2020 (2020)

DLI: A Deep Learning-Based Granger Causality Inference

Wei Peng 



Research Article (6 pages), Article ID 5960171, Volume 2020 (2020)

Research on the Complexity of Game Model about Recovery Pricing in Reverse Supply Chain considering Fairness Concerns

Ting Li , Dongyun Yan, and Shuxia Sui

Research Article (13 pages), Article ID 9621782, Volume 2020 (2020)

Feedback Control of a Chaotic Finance System with Two Delays

Zhichao Jiang  and Tongqian Zhang 


Research Article (17 pages), Article ID 4937569, Volume 2020 (2020)

Production Decision and Coordination Mechanism of Socially Responsible Closed-Loop Supply Chain

Xiaofeng Long , Jiali Ge , Tong Shu , and Chunxia Liu 


Research Article (10 pages), Article ID 9095215, Volume 2020 (2020)

Dynamics of a Cournot Duopoly Game with a Generalized Bounded Rationality

A. Al-khedhairi 



Research Article (10 pages), Article ID 8903183, Volume 2020 (2020)

Decision-Making of Electronic Commerce Supply Chain considering EW Service

Yuyan Wang , Zhaoqing Yu, Liang Shen, and Runjie Fan


Research Article (13 pages), Article ID 8035045, Volume 2020 (2020)

Supply Chain Flexibility Evaluation Based on Matter-Element Extension

Xiaochun Luo , Zilong Wang, Lin Lu , and Yan Guan

Research Article (12 pages), Article ID 8057924, Volume 2020 (2020)

The Effect of Shadow Banking on the Systemic Risk in a Dynamic Complex Interbank Network System

Hong Fan  and Hongjie Pan



Research Article (10 pages), Article ID 3951892, Volume 2020 (2020)

Analyzing Interactions between Japanese Ports and the Maritime Silk Road Based on Complex Networks

Zhi-Hua Hu , Chan-Juan Liu, and Paul Tae-Woo Lee

Research Article (18 pages), Article ID 3769307, Volume 2020 (2020)

Reliability Modeling for Multistate System with Preventive Maintenance under Customer Demand

Jinlei Qin  and Zheng Li 

Research Article (9 pages), Article ID 3165230, Volume 2020 (2020)

The Formation Mechanism of Green Dairy Industry Chain from the Perspective of Green Sustainable Development

Hongli Chen  and Xiuli Liu 

Research Article (12 pages), Article ID 2927153, Volume 2020 (2020)

An Eco-Inefficiency Dominance Probability Approach for Chinese Banking Operations Based on Data Envelopment Analysis

Feng Li , Lunwen Wu, Qingyuan Zhu , Yanling Yu, Gang Kou , and Yi Liao 

Research Article (14 pages), Article ID 3780232, Volume 2020 (2020)



Contents

The Dominance Degree-Based Heterogeneous Linguistic Decision-Making Technique for Sustainable 3PRLP Selection

Xiaolu Zhang  and Ting Su



Research Article (18 pages), Article ID 6102036, Volume 2020 (2020)

Research on Coordination Complexity of E-Commerce Logistics Service Supply Chain

Yaoguang Zhong, Fangfang Guo, Huajun Tang , and Xumei Chen 

Research Article (21 pages), Article ID 7031543, Volume 2020 (2020)

Supply Chain Decisions and Coordination under the Combined Effect of Overconfidence and Fairness Concern

Zhang Zhijian, Peng Wang , Miyu Wan, Junhua Guo, and Jian Liu 

Research Article (16 pages), Article ID 3056305, Volume 2020 (2020)

Cooperative Innovation in the Medical Supply Chain Based on User Feedback

Ran Chen, Gui-sheng Hou, and Yu Wang 

Research Article (9 pages), Article ID 7106917, Volume 2020 (2020)

Research Article

An Evaluation on Investment of Research Funds with a Neural Network Algorithm in “Double First-Class” Universities

Jihong Sun ¹, Yahui Li ², Xiaoyun Zhao ² and Nanxing Zhang ¹

¹China National Institute of Education Science, Beijing 100088, China

²School of Economics, Qufu Normal University, Qufu 276800, China

Correspondence should be addressed to Nanxing Zhang; zhangnx2014@126.com

Received 8 May 2020; Accepted 4 August 2020; Published 4 November 2020

Academic Editor: Abdelalim A. Elsadany

Copyright © 2020 Jihong Sun et al. This is an open access article distributed under the Creative Commons Attribution License, which permits unrestricted use, distribution, and reproduction in any medium, provided the original work is properly cited.

In the current context of the establishment of world-class universities and disciplines in China, this study examined the investment of research funds at universities. First, six variables were selected as evaluation indicators from the perspective of fixed assets, teaching configuration, research instruments, and the number of books in libraries. Seventy-two universities were investigated from 2013 to 2017. Second, an evaluation system was constructed using the BP (backpropagation) neural network method and its applicability was verified. Finally, by adjusting the six indicators, the investment of university research funds could be adjusted and predicted to provide a reference for the construction of “first-class” universities and disciplines.

1. Introduction

Since reform and opening up, China has been attached greater importance to education, particularly at a time when the world is undergoing great development, change, and adjustment, with rapid scientific and technological progress, deepening economic globalization, and fierce competition for high-skilled workers. At the same time, the development of higher education in China has attracted worldwide attention. The initial formation of a socialist system of higher education has been constructed, which is multiform, multilevel, and full of disciplines to meet the needs of economic construction and social development, where a large number of outstanding and top-notch high-skilled workers have been trained for socialist modernisation and play a great role in the country's economic construction, scientific and technological progress, and social development. Today, in the era of the knowledge economy, the previously implemented “211” project and “985” project of higher education policy have exposed some problems, such as low resource utilisation, identity consolidation, and lack of fair and effective competition among other factors. The country's development requires improving the quality of our people and training innovative high-skilled workers. Considering

the current state of China and its critical period of reform as well as the international experience of advanced higher education, the Government has introduced a policy of “double first-class” university system.

The study of investment in scientific research funds from each university in terms of infrastructure and equipment is more favourable to the understanding and grasp of the current “first-class” universities in all aspects. The increase in fixed assets of universities, the purchase of scientific research instruments and equipment, and the expansion of library books are more conducive to determining the scope of funding, facilitating the use of funds in practise, and efficiently promoting the construction and development of first-class universities and first-class disciplines in China with high efficiency.

2. Literature Review

2.1. Research on Evaluation of School Facilities. By analysing the current status of the development of teaching laboratories in universities, Gao [1] propose optimising teaching laboratories in terms of both informational construction and social services, so that teaching laboratories can better contribute to the development of “double first-class”

schools. Zhang [2] discusses the important role of first-class laboratory construction in “double first-class” universities and provides reference opinions for promoting the development of “double first-class” construction projects in three aspects: laboratory management mechanisms, laboratory conditions construction, and laboratory teacher team configuration.

Liu and Ding [3] use the Shanghai University Library as an example to study the availability of subject literature resources in the construction of “double first-class” universities. It is proposed that the establishment of a document resource guarantee system should be suitable for the construction of first-class disciplines in colleges and universities, with a focus on the construction of document resources in discipline groups and on regular evaluation and assessment. Zhang and Zheng [4] summarised the current status of the opening and sharing of large-scale instruments and equipment in colleges and universities. They proposed a new method of open sharing of these resources under the realistic background of the construction of “double first-class” universities. Jiang et al. [5] analysed the importance of the current “double first-class” construction on the new experimental teaching platform. Deep three-dimensional teaching designs, such as online resources and testing, are discussed. The emphasis is on cultivating students’ basic experimental skills and innovation awareness as well as enhancing the ability of experimental teachers. Wu and Ma [6] took 42 “double first-class” university libraries as research objects and highlighted major issues in the opening of scientific research achievements. It is believed that the formulation and improvement of policies should be strengthened to realise early open access to scientific research results. Fan et al. [7] studied and evaluated the requirements of the construction of “double first-class” universities on the construction of library resources. They proposed corresponding measures for the operation of the library’s ladder-type resource construction model and related policy mechanisms.

2.2. Research on the Evaluation of Infrastructure with Neural Network Universities. Wang [8] used a BP neural network to establish an evaluation index system for the quality of electronic resources of libraries. Through empirical research on the library’s electronic resources, the effectiveness of management evaluation is clarified. Liu and Li [9] used the SOM (self-organizing map) neural network clustering algorithm to study the outstanding problems in the digital construction of university libraries. They screen and process related data resources of users to form related data sets and combine related technologies to establish a personalised recommendation service system for users in university libraries. Zhang et al. [10] conducted a comprehensive and scientific evaluation of the information dissemination capability of the think tank on the We Chat public platform. They conducted simulation verification using the BP neural network model. The evaluation model has strong operability and practicability and can provide new methods and ideas for information dissemination.

Zhang et al. [11] used a BP neural network to establish an evaluation system. They use the capability maturity model to study the think tank service capabilities of university libraries. It is conducive to college libraries to determine their own think tank service capability level and optimise and improve it in a targeted manner.

2.3. Research on the Evaluation of the Teaching Quality Neural Network Universities. Zheng and Yan [12] used a teaching evaluation mechanism to measure teaching quality. Through the three aspects of the difference in teaching quality, the unity of teaching evaluation subjects, and the difficult operation of teaching evaluation methods, a comprehensive teaching quality evaluation system was established. Fan and Ma [13] evaluated the teaching quality of college teachers by establishing a complex nonlinear relationship between the evaluation results of teaching quality and various indicators. Zhu and Wang [14] used a particle swarm optimisation method to establish a BP neural network evaluation model. It solved the problem of scientific research performance evaluation faced by the Scientific Research Management Department of Colleges and Universities. It used particle swarm optimisation to optimise the initial weights and thresholds of the BP neural network model and then made predictions.

In summary, most of the research on the construction of “double first-class” universities has been carried out in combination with the basic supporting facilities of universities, the quality of education and teaching, and other aspects. There are few studies on research funding at universities, and there is a lack of research that uses neural networks for in-depth analysis. This study uses a neural network model to discuss the investment in scientific research funds of various universities from the aspects of infrastructure and hardware equipment of “double first-class” universities and discusses the related implications.

3. BP Neural Network Model

An artificial neurone emulates the abstraction, simplification, and simulation of biological neurones. It is the basic processing unit of an artificial neural network. Neural network learning is one of the basic algorithms in the field of artificial intelligence. It was a mathematical model proposed by the psychologist McCulloch and mathematician Pitts in 1943. Its main application areas involve pattern recognition, intelligent robots, nonlinear system recognition, knowledge processing, and other factors.

3.1. Mathematical Model of Neural Network Perceptron. The most common neural network model with only a single hidden layer is a three-layer perceptron. These three layers are the input layer, hidden layer, and output layer. There is a mathematical relationship between the signals of each layer as follows:

For the hidden layer,

$$\begin{cases} y_i = f(\text{net}_j), & j = 1, 2, \dots, m, \\ \text{net}_j = \sum_{i=0}^n v_{ij}x_i, & j = 1, 2, \dots, m. \end{cases} \quad (1)$$

For the output layer,

$$\begin{cases} o_k = f(\text{net}_k), & k = 1, 2, \dots, l, \\ \text{net}_k = \sum_{j=0}^m w_{jk}y_j, & k = 1, 2, \dots, l. \end{cases} \quad (2)$$

In formulas (1) and (2), the transformation function $f(x)$ is usually a unipolar sigmoid function, which we call

$$f(x) = \frac{1}{1 + e^{-x}}. \quad (3)$$

The sigmoid function is derivative and continuous. For equation (3), we call

$$f'(x) = f(x)[1 - f(x)]. \quad (4)$$

If necessary, you can also use the bipolar sigmoid function:

$$f(x) = \frac{1 - e^{-x}}{1 + e^{-x}}. \quad (5)$$

To reduce the computational complexity, the output layer can also use linear functions as needed:

$$f(x) = kx. \quad (6)$$

3.2. Derivation of the BP Algorithm. The following uses the three-layer BP neural network model as an example to derive the BP learning algorithm.

(1) Network error

If the network output is not equal to the expected output, then there is an output error E as follows:

$$E = \frac{1}{2}(d - O)^2 = \frac{1}{2} \sum_{k=1}^l (d_k - O_k)^2. \quad (7)$$

Expanding the above error to the hidden layer,

$$E = \frac{1}{2} \sum_{k=1}^l [d_k - f(\text{net}_k)]^2 = \frac{1}{2} \sum_{k=1}^l \left[d_k - f\left(\sum_{j=0}^m w_{jk}y_j\right) \right]^2. \quad (8)$$

Further, expand to the input layer:

$$E = \frac{1}{2} \sum_{k=1}^l \left\{ d_k - f\left[\sum_{j=0}^m w_{jk}f(\text{net}_j)\right] \right\}^2 = \frac{1}{2} \sum_{k=1}^l \left\{ d_k - f\left[\sum_{j=0}^m w_{jk}f\left(\sum_{i=0}^n v_{ij}x_i\right)\right] \right\}^2. \quad (9)$$

(2) Network weight adjustment based on gradient descent

From equation (9), the input error of the neural network is a function of weights w_{jk} and v_{ij} of each layer. By adjusting the weight value, the error E can be changed, so that the adjustment amount of the weight value is proportional to the gradient decrease of the error, namely,

$$\Delta w_{jk} = -\eta \frac{\partial E}{\partial w_{jk}}, \quad k = 1, 2, \dots, l, \quad j = 1, 2, \dots, m, \quad (10)$$

$$\Delta v_{ij} = -\eta \frac{\partial E}{\partial v_{ij}}, \quad i = 1, 2, \dots, n, \quad j = 1, 2, \dots, m. \quad (11)$$

In the above formula, the minus sign indicates gradient descent. The constant $\eta \in (0, 1)$ is a scale factor, which reflects the learning rate. Surely, the BP algorithm belongs to the σ learning rule.

Equations (10) and (11) only express the idea of adjusting the weights mathematically. The calculation formula derivation of the weight adjustment of the three-layer BP algorithm is as follows. It is assumed that

in all the derivation processes, there is $j = 0, 1, 2, \dots, m$, $k = 1, 2, \dots, l$ for each output layer and $i = 0, 1, 2, \dots, n$, $j = 1, 2, \dots, m$ for each hidden layer.

For the output layer, equation (10) can be written as

$$\Delta w_{jk} = -\eta \frac{\partial E}{\partial w_{jk}} = -\eta \frac{\partial E}{\partial \text{net}_k} \frac{\partial \text{net}_k}{\partial w_{jk}}. \quad (12)$$

Equation (11) can be written as

$$\Delta v_{ij} = -\eta \frac{\partial E}{\partial v_{ij}} = -\eta \frac{\partial E}{\partial \text{net}_j} \frac{\partial \text{net}_j}{\partial v_{ij}}. \quad (13)$$

We define an error signal for the output layer and the hidden layer.

$$\delta_k^o = -\frac{\partial E}{\partial \text{net}_k}, \quad (14)$$

$$\delta_j^y = -\frac{\partial E}{\partial \text{net}_j}. \quad (15)$$

Comprehensive application of formulas (2) and (14): the weight adjustment formula of (12) can be rewritten as

$$\Delta w_{jk} = \eta \delta_k^o y_j. \quad (16)$$

Comprehensive application of formulas (4) and (15): the weight adjustment formula of (13) can be rewritten as

$$\Delta v_{ij} = \eta \delta_j^y x_i. \quad (17)$$

Calculate the error signals δ_k^o and δ_j^y in formulas (14) and (15); then, the calculation and derivation of the weight adjustment amount are also completed.

The output layer δ_k^o can be expanded to

$$\delta_k^o = -\frac{\partial E}{\partial \text{net}_k} = -\frac{\partial E}{\partial o_k} \frac{\partial o_k}{\partial \text{net}_k} = -\frac{\partial E}{\partial o_k} f'(\text{net}_k). \quad (18)$$

The hidden layer δ_j^y can be expanded to

$$\delta_j^y = -\frac{\partial E}{\partial \text{net}_j} = -\frac{\partial E}{\partial y_j} \frac{\partial y_j}{\partial \text{net}_j} = -\frac{\partial E}{\partial y_j} f'(\text{net}_j). \quad (19)$$

Next, according to formulas (18) and (19), we find the partial derivative of the network error to the output of each layer.

Output layer: using equation (7), the partial derivative can be obtained:

$$\frac{\partial E}{\partial o_k} = -(d_k - o_k). \quad (20)$$

Hidden layer: using equation (8), the partial derivative can be obtained:

$$\frac{\partial E}{\partial y_j} = -\sum_{k=1}^l (d_k - o_k) f'(\text{net}_k) w_{jk}. \quad (21)$$

Substituting the above results into formulas (18) and (19), and applying equation (4), $f'(x) = f(x)[1 - f(x)]$, we obtain

$$\delta_k^o = (d_k - o_k) o_k (1 - o_k), \quad (22)$$

$$\begin{aligned} \delta_j^y &= \left[\sum_{k=1}^l (d_k - o_k) f'(\text{net}_k) w_{jk} \right] f'(\text{net}_j) \\ &= \left(\sum_{k=1}^l \delta_k^o w_{jk} \right) y_j (1 - y_j). \end{aligned} \quad (23)$$

Substituting equations (22) and (23) into equations (16) and (17), the calculation formula for the weight adjustment of the BP learning algorithm of the three-layer perceptron can be obtained:

$$\begin{aligned} \Delta w_{jk} &= \eta \delta_k^o y_j = \eta (d_k - o_k) o_k (1 - o_k) y_j, \\ \Delta v_{ij} &= \eta \delta_j^y x_i = \eta \left(\sum_{k=1}^l \delta_k^o w_{jk} \right) y_j (1 - y_j) x_i. \end{aligned} \quad (24)$$

(3) Vector form of BP learning algorithm

Output layer: assuming $Y = (y_1, y_2, \dots, y_j, \dots, y_m)^T$, $\delta^o = (\delta_1^o, \delta_2^o, \dots, \delta_k^o, \dots, \delta_l^o)^T$, the weight matrix adjustment from the hidden layer to the output layer is

$$\Delta W = \eta (\delta^o Y^T)^T. \quad (25)$$

Hidden layer: assuming $X = (x_1, x_2, \dots, x_i, \dots, x_m)^T$, $\delta^y = (\delta_1^y, \delta_2^y, \dots, \delta_k^y, \dots, \delta_l^y)^T$, the weight matrix adjustment from the input layer to the hidden layer is

$$\Delta V = \eta (\delta^y X^T)^T. \quad (26)$$

According to formulas (25) and (26), in the BP learning algorithm, the adjustment formula of the weights of each layer is identical in the same form. They all require three factors, the learning rate η , the error signal δ output by this layer, and the input signal Y (or X) of this layer. The error signal of each hidden layer is related to the error signal of each previous layer, and it is transmitted from the output layer and back to the input layer.

3.3. Determination of Input Variables and Output Variables

3.3.1. Input Dimensionality Reduction. For image data, adjacent pixels are highly correlated, so the input data is somewhat redundant. Suppose a 16×16 grey value image is processed. The input is a 256-dimensional vector $x \in R^{256}$, where the feature value x_j corresponds to the brightness value of each pixel. Because of the correlation between adjacent pixels, the input vector needs to be converted into an approximate vector with a lower dimension. At this time, the error is very small, which does not affect the processing result, but the amount of calculation is greatly reduced.

Principal Component Analysis (PCA) is a statistical analysis method to identify the main contradictions of things. The purpose of calculating the principal component is to find r ($r < n$) new variables. Each new variable is a linear combination of the original n variables. They reflect the influence of the original n variables, and these new variables are uncorrelated.

3.3.2. Preprocessing of Input and Output Data. Scale normalization is a linear transformation. It readjusts the value of each input component of the data. These dimensions may be independent of each other. Ensure that the final data vector falls within the interval $[0, 1]$ or $[-1, 1]$. The pixel values obtained when processing natural images are in the range $[0, 255]$. A common process is to divide these pixel values by 255 to scale them to $[0, 1]$. Transform the input and output data to the value of the interval $[0, 1]$:

$$x'_i = \frac{x_i - x_{\min}}{x_{\max} - x_{\min}}, \quad (27)$$

where x_i represents the input or output data, x_{\min} represents the minimum value of the data change, and x_{\max} represents the maximum value of the data change range.

If the input or output data is converted to a value in the range $[-1, 1]$, the following conversion formulas are commonly used:

$$\begin{aligned} x_{\text{mid}} &= \frac{x_{\max} + x_{\min}}{2}, \\ x'_i &= \frac{x_i - x_{\text{mid}}}{1/2(x_{\max} - x_{\min})}. \end{aligned} \quad (28)$$

x_{mid} represents the middle value of the data change range. After changing according to the above transformation, the intermediate value of the original data is converted to zero. The maximum value is converted to 1, and the minimum value is converted to -1 .

3.3.3. Training Sample Set. The laws in neural network training can be extracted from the samples. Therefore, a high-quality data sample set is an important and critical step. The selection of samples should not only be representative, but also eliminate invalid data and erroneous data. At the same time, we must unify the sample category and sample size. Normally, if the number of training samples is large, the training results will more accurately reflect their internal laws. However, when the number of samples reaches a certain upper limit, it is more difficult to improve the accuracy of the network. Generally, the number of training samples is 5–10 times the total number of network connection weights.

3.4. BP Network Structure Design. Through training samples, the number of nodes in the input and output layers of the network can be determined. The structural design of the BP network is mainly used to determine the number of hidden layers, the number of nodes in each hidden layer, and the neurone activation function of each node.

Determination of the number of hidden layers: according to theory, if a feedforward network has a single hidden layer when designing a multilayer BP network, it will first consider designing only one hidden layer. When there are too many hidden nodes in a hidden layer and the network performance cannot be improved, the second hidden layer will be considered.

Determining the number of hidden layer nodes: the role of hidden layer nodes is to extract internal laws from samples and store them. The commonly used empirical formulas for determining the number of hidden nodes are as follows:

$$\begin{aligned} m &= \sqrt{n+l} + \alpha, \\ m &= \text{lbn}, \\ m &= \sqrt{n \cdot l}. \end{aligned} \quad (29)$$

In the above formula, m is the number of hidden layer nodes and n is the number of input layer nodes. l is the number of nodes in the output layer, and α is a constant between 1 and 10.

Approximation and generalisation considerations: the total number of weights and thresholds reflects the information capacity of the network. The “overdesign” of the number of hidden nodes may lead to “overfitting.” The noise in the sample is retained, but it reduces the generalisation ability. The above design uses a combination of experience and trial. The theoretical guidance of neural network design still needs to be improved. The research shows that the number of training samples P , the given training error ε , and the network information capacity n_w should meet the following matching relationship:

$$P = \frac{n_w}{\varepsilon} \quad (30)$$

4. An Empirical Analysis of the Scientific Research Fund with BP Neural Network in Higher Education

In this study, six evaluation indicators—fixed assets, number of teaching and research instruments and equipment, amount of teaching and research instruments and equipment, number of large teaching and research equipment over 400,000, amount of large teaching and research equipment over 400,000, and number of books in libraries—are selected as input variables. Fixed assets, teaching and research equipment, and library collection are the tools used by students and teachers to acquire new knowledge and solve research problems, which are important in improving the quality of education and research. In addition, with the continuous improvement of the level of science and technology and the continuous acceleration of the process of informationisation in this era, teaching and research instruments and equipment are becoming much more advanced, playing an increasingly important role in conducting relevant teaching experiments. In 2018, China’s dual-class universities invested about 388.2 billion yuan in fixed assets, a total of 6.31 million pieces of teaching and research instruments, with an investment of about 126.6 billion yuan, of which more than 400,000 large teaching and research equipment of about 32.6 billion yuan, or 25.8% of the total investment in teaching and research equipment. The library collection was about 250 million books. Generally speaking, fixed assets, research instruments, and library collections comprise the infrastructure for teaching and research in universities, and they are also the basic requirements for the construction of China’s “double first-class” universities.

As study subjects, 72 colleges and universities among the “double first-class” colleges and universities in 2017 were selected, and the aforementioned indicators were used as network input, the number of scientific research activities was used as the network output, and the number of implicit layer nodes was determined according to the empirical formula of the number of implicit nodes, thus forming a 6-3-1 neural network structure. The BP neural network is created using the software *R*, and weights and thresholds are determined using correlation functions. The minimum-maximum normalisation method is used to normalise the

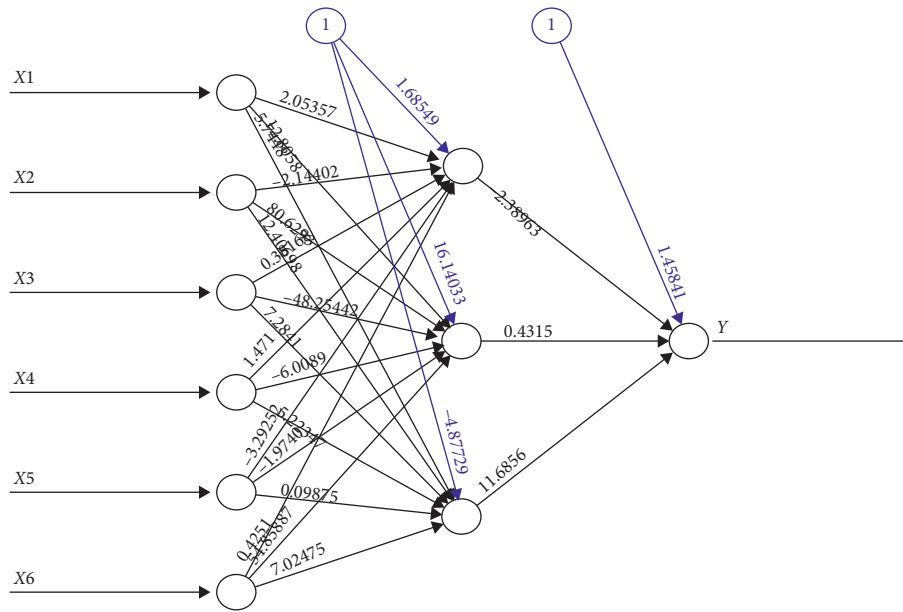


FIGURE 1: The neural network model of university samples in 2017.

sample indicator data with the total score, and the neural net function is used to create the forward network to achieve an arbitrary mapping of the neural network from input to output. The algorithm for computing the neural network is rprop+, the incentive function from the input layer to the implicit layer is Tansig, the incentive function from the implicit layer to the output layer is Purelin, the learning rate is set to 0.01, and the number of neurones in the implicit layer is 3. The stop queue for the error function is 0.001, the maximum number of iterative training allowed is 100000, and the number of training sessions is 1000. Set the error performance index of network convergence as MSE (mean square error); the set output mode is linear output, and the default value is selected for all other parameters. By default, the algorithm used in the neural net function is based on elastic backpropagation with upweighted regression and an additional modification of either the learning rate associated with the minimum absolute gradient or the minimum learning rate itself.

The colleges in the sample in 2017 are divided into training and test sets, and the constructed neural network is shown in Figure 1. X1 is a fixed asset. X2 is the number of teaching and research instruments and equipment. X3 is the amount of teaching and research equipment. X4 is the number of large-scale teaching and research equipment. X5 is the amount of large-scale teaching and research equipment. X6 is the number of books in libraries. Y is the funding for scientific research activities.

The maximum step of training the neural network was 88143. When this value is reached, the training process of the neural network stops. Specify the threshold value of the partial derivative of the error function, which is the stop threshold of the error function, to reach 0.00098. The error rate of this neural network model was 0.07809. The black line (the line starting from the input node) shows the connection between each layer and the weight on each connection, while

the blue line (the lines start from the deviation nodes distinguished by 1) shows the deviation added at each step. It can be considered that the deviation is the intercept of the linear model. The deviation of the first node of the hidden layer was 1.68549. The deviation of the second node of the hidden layer was 16.14033. The deviation of the third node of the hidden layer was -4.87729 . The deviation of the output layer node was 1.45841. The specific values of the weights between the nodes of each layer are shown in Table 1.

From Table 1, the weights of the first node of the hidden layer have a greater impact on the indicator of the number of teaching and research equipment and the indicator of the number of large teaching and research equipment, both of which play an inhibitory role. The weights for the second node of the hidden layer have a greater impact on the number of teaching and research equipment, which is a facilitator, and the number of books in libraries, which is disincentive. The weights of the third node of the hidden layer have a greater impact on the number of teaching and research equipment indicators and the number of teaching and research equipment indicators, with the former acting as an inhibitor and the latter as a facilitator. The relationship between the hidden layer and the output layer has a greater impact on the third and first nodes.

The MSE of the neural network with a value of 651133098 is significantly smaller than that of the linear regression model with a value of 1723270943, which indicates that the neural network model is better. Furthermore, it is possible to predict the funding for higher education research activities of “double-first-class” universities through a neural network evaluation model. As long as the data of those indicators are collected for a certain university in a certain year, it is possible to predict the approximate range of funding for scientific research activities of that university, which provides an effective reference for the funding of college education in China.

TABLE 1: Weight table of neural network of university samples in 2017.

	Hidden layer first node	Hidden layer second node	Hidden layer third node	Output layer
Fixed assets	2.053567	-12.80568	5.744475	—
Number of teaching and research equipment	-2.144015	80.63330	-12.48698	—
Amount of teaching and research equipment	0.3614817	-48.25442	7.784177	—
Number of large-scale teaching and research equipment	1.471630	-6.008896	-5.223469	—
Amount of large-scale teaching and research equipment	-3.292561	-1.974632	0.098747	—
Number of books in libraries	0.425100	-54.85887	7.024750	—
Hidden layer first node	—	—	—	-2.389628
Hidden layer second node	—	—	—	0.4314989
Hidden layer third node	—	—	—	11.68560

5. Summary

In the current context of the creation of world-class universities and disciplines in China, this paper examines the investment of research funds at universities. Six variables were selected as evaluation indicators from the perspective of fixed assets, teaching configuration and research equipment, and the number of books in libraries, and the data of 72 universities from 2013 to 2017 were analysed. The MSE is 651133098 for the neural network and 1723270943 for the regression model, which proved that the neural network model is more effective than the regression model. The theoretical model can be applied to practice, and the findings show that it is possible to modify and predict the investment strategy of the scientific research expenses of universities through adjusting the six indicators, which provides an effective reference for the construction of “world-class” universities and disciplines.

Appendix

A. Neural Network Algorithm

```
library("neuralnet")
#Load package
set.seed(1)
max_data <- apply(data, 2, max)
min_data <- apply(data, 2, min)
data_scaled <- scale(data, center = min_data, scale = max_data - min_data)
#The function scale is a general function for data standardization, The default method is to center or scale the columns of a numeric matrix.
index = sample(1:nrow(data), round(0.70*nrow(data)))
#70% of the data is used to train the neural network, and the remaining 30% is used to test the neural network.
train_data <- as.data.frame(data_scaled[index,])
test_data <- as.data.frame(data_scaled[-index,])
```

```
#The data is divided into two new data frames, called train_data and test_data
```

```
n = names(data)
```

```
f = as.formula(paste("Y~", paste(n[!n%in%
"Y"], collapse = "+")))
```

```
#Build the formula that will be used to build the neural network
```

```
net_data = neuralnet(f, data = train_data,
hidden = 3, threshold = 0.001, learningrate =
0.01, linear.output = T)
```

```
#Use neuralnet functions to build and train neural networks. There are 3 hidden layers, the stop threshold of the error function is 0.001, and the learning rate is 0.01.
```

```
net_data$result.matrix
```

```
#Output weight value and threshold value
```

```
plot(net_data)
```

```
#Drawing a neural network
```

```
predict_net_test <- compute(net_data, test_data[, 1:6])
```

```
predict_net_test_start <- predict_net_test$net.result * (max(data$Y) ± min(data$Y)) + min(data$Y)
#Using neural networks to make predictions.
```

```
test_start <- as.data.frame(((test_data$Y) * (max(data$Y) ± min(data$Y)) + min(data$Y))
MSE.net_data <- sum(((test_start - predict_net_test_start)^2) / nrow(test_start)) #Define the mean square error formula.
```

```
Regression_Model <- lm(Y~., data = data)
```

```
#Establish a linear regression model to understand the accuracy of neural network predictions.
```

```
summary(Regression_Model)
```

```
test <- data[-index,]
```

```
predict_lm <- predict(Regression_Model, test)
```

```
MSE.lm <- sum((predict_lm - test$Y)^2) / nrow(test)
```

```
MSE.net_data
```

```
#Calculate the MSE value of the neural network
```

```
MSE.lm
```

```
#Calculate the MSE value of the regression model
```

Data Availability

The data used to support the findings of this study are included within the article.

Conflicts of Interest

The authors declare that they have no conflicts of interest.

Acknowledgments

This article is a phased result of the research program “Decade Research on the Performance Evaluation of Colleges and Universities,” National Institute of Education Sciences (Grant no. GYH2019010).

References

- [1] L. Gao, “Teaching laboratory optimization construction promotes the construction of “double first-class” in colleges and universities,” *New Campus*, no. 7, pp. 47-48, 2017.
- [2] H. Zhang, “Research on construction of first-class laboratories under “Double world-class” background,” *Experimental Technology and Management*, vol. 34, no. 12, pp. 6-10, 2017.
- [3] H. Liu and D. Ding, “The strategy of document resources guarantee in local university libraries under the background of “double First-class” — taking Shanghai University Library as an example,” *Journal of Library Science*, no. 3, pp. 9-14, 2019.
- [4] H. Zhang and X. Zheng, “New measures for opening and sharing of university large-scale instruments and equipment under background of “Double first-class”” *Experimental Technology and Management*, vol. 36, no. 6, pp. 8-11, 2019.
- [5] W. Jiang, Y. Zhang, and Y. Su, “Research on establishment and application of experimental teaching platform in “Double first-class” construction,” *Experimental Technology and Management*, vol. 36, no. 6, pp. 16-20, 2019.
- [6] Q. Wu and L. Ma, “An empirical study on the open access of scientific research achievements of domestic “double first class” university libraries,” *Research on Library Science*, no. 12, pp. 72-81, 2019.
- [7] C. Fan, J. Yu, and D. Li, “A study on ladder-type resources construction model of academic libraries under the background of “double first-class,” *Construction Library Work in Colleges and Universities*, no. 4, pp. 62-66, 2019.
- [8] J. Wang, “Study on the construction of electronic resources’ quality evaluation system in university libraries: based on the BP neural network model,” *New Century Library*, no. 3, pp. 30-33, 2017.
- [9] A. Liu and Y. Li, “The recommendation system of university library personalized service based on SOM,” *Library Tribune*, no. 4, pp. 95-102, 2018.
- [10] L. Zhang, X. Zhang, Z. Li, and H. Lu, “Evaluation of think tank’s information dissemination capacity on wechat public platform based on BP neural network,” *Information Studies: Theory & Application*, vol. 41, no. 10, pp. 93-99, 2018.
- [11] X. Zhang, B. Zhao, H. Lu, and Y. Li, “Research on the maturity model and evaluation of university library think-tank service capability,” *Library*, no. 7, pp. 26-33, 2019.
- [12] Y. Zheng and C. Yan, “Research on evaluation model of university teachers’ teaching quality based on BP neural network,” *Journal of Chongqing University of Technology (Natural Science)*, no. 1, pp. 85-90, 2015.
- [13] Y. Fan and L. Ma, “Teaching quality evaluation model of colleges and universities optimized BP neural network,” *Statistics & Decision*, no. 2, pp. 80-82, 2018.
- [14] Q. Zhu and J. Wang, “Research on university scientific research management evaluation based on particle swarm optimization algorithm and BP neural network,” *Modern Electronics Technique*, vol. 42, no. 7, pp. 87-89+94, 2019.

Research Article

A Hybrid Approach Integrating Multiple ICEEMDANs, WOA, and RVFL Networks for Economic and Financial Time Series Forecasting

Jiang Wu , Tengfei Zhou , and Taiyong Li 

School of Economic Information Engineering, Southwestern University of Finance and Economics, Chengdu 611130, China

Correspondence should be addressed to Taiyong Li; litaiyong@gmail.com

Received 8 May 2020; Revised 11 August 2020; Accepted 6 October 2020; Published 22 October 2020

Academic Editor: Lei Xie

Copyright © 2020 Jiang Wu et al. This is an open access article distributed under the Creative Commons Attribution License, which permits unrestricted use, distribution, and reproduction in any medium, provided the original work is properly cited.

The fluctuations of economic and financial time series are influenced by various kinds of factors and usually demonstrate strong nonstationary and high complexity. Therefore, accurately forecasting economic and financial time series is always a challenging research topic. In this study, a novel multidecomposition and self-optimizing hybrid approach integrating multiple improved complete ensemble empirical mode decompositions with adaptive noise (ICEEMDANs), whale optimization algorithm (WOA), and random vector functional link (RVFL) neural networks, namely, MICEEMDAN-WOA-RVFL, is developed to predict economic and financial time series. First, we employ ICEEMDAN with random parameters to separate the original time series into a group of comparatively simple subseries multiple times. Second, we construct RVFL networks to individually forecast each subseries. Considering the complex parameter settings of RVFL networks, we utilize WOA to search the optimal parameters for RVFL networks simultaneously. Then, we aggregate the prediction results of individual decomposed subseries as the prediction results of each decomposition, respectively, and finally integrate these prediction results of all the decompositions as the final ensemble prediction results. The proposed MICEEMDAN-WOA-RVFL remarkably outperforms the compared single and ensemble benchmark models in terms of forecasting accuracy and stability, as demonstrated by the experiments conducted using various economic and financial time series, including West Texas Intermediate (WTI) crude oil prices, US dollar/Euro foreign exchange rate (USD/EUR), US industrial production (IP), and Shanghai stock exchange composite index (SSEC).

1. Introduction

Economic and financial time series, such as price movements, stock market indices, and exchange rate, are usually characterized by strong nonlinearity and high complexity, since they are influenced by a number of extrinsic and intrinsic factors including economic conditions, political events, and even sudden crises [1, 2]. Economic and financial time series forecasting always play a vital role in social and economic development, which is of great economic importance to both individuals and countries. Therefore, economic and financial time series forecasting is always a very active research area.

In extant research, various forecasting methods were proposed to forecast various economic and financial time series. These forecasting methods mainly include statistical

and artificial intelligence (AI) approaches. The frequently used statistical approaches for economic and financial time series forecasting include the error correction model (ECM) [3], hidden Markov model (HMM) [4], random walk (RW) model [5], autoregressive moving average (ARMA) model [6], autoregressive integrated moving average (ARIMA) model [7], and generalized autoregressive conditional heteroskedasticity (GARCH) model [8, 9]. Lanza et al. forecasted the series of crude oil prices in two distinct areas using the ECM [3]. Hassan and Nath developed the HMM approach for forecasting stock price for interrelated markets [4]. Kilian and Taylor analyzed the advantage of RW in exchange rate forecasting [5]. Rout et al. integrated ARMA with differential evolution (DE) to develop a hybrid model for exchange rate forecasting [6]. Mondal et al. conducted a study on the effectiveness of the ARIMA model on the

forecasting of 56 Indian stocks from different sectors [7]. Alberg et al. conducted a comprehensive analysis of the stock indices using various GARCH models, and the experimental results showed that the asymmetric GARCH model enhanced the overall prediction performance [9].

Since most economic and financial time series involve the complex characteristics of strong nonlinearity and nonstationarity, it is difficult to obtain satisfactory forecasting accuracy by statistical approaches. Hence, various AI approaches were proposed for economic and financial time series forecasting. These AI forecasting approaches include the artificial neural network (ANN) [10, 11], support vector machine (SVM) [12, 13], extreme learning machine (ELM) [14], random vector functional link (RVFL) neural network [15], and recurrent neural network (RNN) [16]. Pradhan and Kumar utilized ANN to forecast foreign exchange rate in India, and the experimental results indicated that the ANN could effectively forecast the exchange rate [10]. Das and Padhy forecasted the commodity futures contract index using the SVM, and the empirical analysis showed that the proposed model was effective and achieved the satisfactory prediction performance [12]. Li et al. made stock price prediction using the ELM, and the comparison results showed that the ELM with radial basis function (RBF) kernels achieved better prediction performance with faster speed than back propagation neural networks (BPNNs) [14]. Moudiki et al. employed quasirandomized functional link networks for various time series forecasting, and the proposed approach could generate more robust prediction results [15]. Baek and Kim employed long short-term memory (LSTM) for stock index forecasting, and the results confirmed the LSTM model had excellent prediction accuracy [16].

In order to effectively improve prediction accuracy, various hybrid forecasting models were designed for economic and financial time series forecasting. Babu and Reddy combined ARIMA and nonlinear ANN models to develop a novel hybrid ARIMA-ANN model, and the experiments on electricity price and stock index indicated that the proposed ARIMA-ANN had higher prediction accuracy [17]. Kumar and Thenmozhi compared three different hybrid models for the forecasting of stock index returns and concluded that the ARIMA-SVM model could obtain the highest prediction accuracy [18]. Hsu built a hybrid model based on a back propagation neural network (BPNN) and genetic programming (GP) for stock/futures price forecasting, and the empirical analysis showed that the proposed hybrid model could effectively improve the prediction accuracy [19]. These hybrid models are able to fully take advantage of the potential of single models and, thus, obtain better prediction accuracy than single models.

Due to the complexity of original economic and financial time series, conducting forecasting on original time series is hard to obtain satisfactory prediction accuracy. To reduce the complexity of original time series, a framework of “decomposition and ensemble” is widely utilized in the field of time series forecasting. The framework includes three stages: decomposition, forecasting, and ensemble. The original time series is firstly separated into a sum of

subseries, then a prediction model is used to forecast each subseries, and finally, the predictions of all the subseries are aggregated as the final prediction results. Decomposition, as the first step, is very important for enhancing the performance of the ensemble model. The widely used decomposition approaches include wavelet decomposition (WD), variational mode decomposition (VMD), and empirical mode decomposition (EMD) class methods. Lahmiri combined VMD with a general regression neural network (GRNN) to develop a novel ensemble forecasting model, and the experimental results suggested that VMD outperformed EMD for the prediction of economic and financial time series [20]. Kao et al. integrated WD, support vector regression (SVR), and multivariate adaptive regression splines (Mars) to develop an ensemble forecasting model to forecast stock price, and the proposed model obtained better prediction accuracy [21]. In the second stage of the framework of “decomposition and ensemble,” various optimization approaches were introduced to enhance the performance of predictors. Li et al. proposed a ridge regression (RR) with DE to forecast crude oil prices and obtained excellent forecasting accuracy [22]. Bagheri et al. introduced quantum-behaved particle swarm optimization (QPSO) to tune the adaptive network-based fuzzy inference system (ANFIS) for financial time series forecasting [23]. Wang et al. employed brain storm optimization (BSO) algorithm to optimize SVR, and the results indicated that the developed approach was effective in stock market analysis [24].

In the “decomposition and ensemble” framework, decomposition approaches and prediction approaches influence the final prediction results greatly. Considering the powerful decomposition ability of ICEEMDAN, the excellent search efficiency of WOA, and the accurate forecasting ability of the RVFL network, we develop a novel ensemble prediction model integrating multiple ICEEMDANs, WOA, and the RVFL network, namely, MICEEMDAN-WOA-RVFL, for economic and financial time series forecasting. Firstly, ICEEMDAN with random parameters is utilized to divide the original economic and financial time series into a sum of subseries. Secondly, the RVFL network is applied to forecast each decomposed subseries individually, and WOA is used to optimize the parameter values of the RVFL network simultaneously. Finally, the predictions of all individual subseries are aggregated as the prediction values of one process of decomposition and ensemble. From our observations, we find that the decomposition in the first stage has some disadvantages of the uncertainties with a quite randomness, which can lead to the difference and instability of the prediction results. In addition, extensive literature has shown that combining multiple forecasts can effectively enhance prediction accuracy [25, 26]. Therefore, we randomize the decomposition parameter values of ICEEMDAN in the first stage, repeat the abovementioned processes multiple times, and integrate the results of multiple decompositions and ensembles as the final prediction values. We expect that the multiple decomposition strategy can reduce the randomness of one single decomposition and further improve the ensemble prediction stability and accuracy.

The main contributions of this paper are as follows: (1) we propose a new multidecomposition and self-optimizing ensemble prediction model integrating multiple ICEEMDANs, WOA, and RVFL networks for economic and financial time series forecasting. As far as we know, this is the first time that the novel combination is developed for economic and financial time series forecasting. (2) To further enhance forecasting accuracy and stability, we utilize multiple differentiated ICEEMDANs to decompose original economic and financial time series and, finally, ensemble the predictions of all decompositions as the final predictions. (3) WOA is firstly introduced to optimize various parameters of RVFL networks. (4) The empirical results on four different types of economic and financial time series show that our proposed MICEEMDAN-WOA-RVFL significantly enhances the prediction performance in terms of forecasting accuracy and stability.

The novelty of the proposed MICEEMDAN-WOA-RVFL is three-fold: (1) a novel hybrid model integrating multiple ICEEMDANs, WOA, and RVFL networks is designed for economic and financial time series forecasting; (2) the multiple decomposition strategy is firstly proposed to overcome the randomness of one single decomposition and to improve prediction accuracy and stability; and (3) WOA is first applied to optimizing RVFL networks to improve the performance of individual forecasting.

The remainder of the paper is organized as follows. Section 2 offers a brief introduction to the ICEEMDAN, WOA, and RVFL network. Section 3 provides the architecture and the detailed implementation of the proposed MICEEMDAN-WOA-RVFL. Section 4 analyzes the empirical results on various economic and financial time series forecasting. Section 5 discusses some details of the developed prediction model, and Section 6 concludes this paper.

2. Preliminaries

2.1. Improved Complete Ensemble Empirical Mode Decomposition with Adaptive Noise (ICEEMDAN). Empirical mode decomposition (EMD), an adaptive time-frequency analysis approach for nonstationary signals, was designed by Huang et al. [27]. EMD separates original time series into a sum of “intrinsic mode functions” (IMFs) and one residue, and thus, it can simplify time series analysis. Due to some drawbacks of EMD, such as mode mixing, EEMD [28] and CEEMDAN [29] have been proposed to improve decomposition performance and applied in various fields [30–32]. In spite of that, these decomposition methods still have some new problems. To solve these problems, an improved CEEMDAN (ICEEMDAN) was developed by Colominas et al. [33].

Let $E_k(\cdot)$ be the operator which generates the k th mode using EMD, $M(\cdot)$ be the operator which generates the local mean of the series, and $w_{(i)}$ be a realization of zero mean unit variance noise. When x is the original signal, the detailed decomposition process of ICEEMDAN is as follows:

- (i) Step 1: employ EMD to compute the local means of I realizations $x^{(i)} = x + \beta_0 E_1(w_{(i)})$ to achieve the first residue $r_1 = M(x^{(i)})$, and $\beta_0 > 0$
- (ii) Step 2: calculate the first $IMF_1 = x - r_1$
- (iii) Step 3: calculate the average of local means of the realizations as the second residue: $r_2 = (r_1 + \beta_1 E_2(w^{(i)}))$
- (iv) Step 4: compute the k th residue for $k = 3, \dots, K$: $r_k = M(r_{k-1} + \beta_{k-1} E_k(w^{(i)}))$
- (v) Step 5: go to step 4 for next k

Since ICEEMDAN can effectively decompose the original time series, it has been frequently introduced into various time series forecasting [34–36]. In our study, we employ ICEEMDAN to separate the original economic and financial time series into a sum of simpler subseries for subsequent forecasting.

2.2. Whale Optimization Algorithm (WOA). Whale optimization algorithm (WOA) is a type of optimization method and outperforms particle swarm optimization (PSO), ant colony optimization (ACO), gravitational search algorithm (GSA), and fast evolutionary programming (FEP) in the optimization performance [37, 38]. Simulating the hunting process of whales, WOA includes three main operators: encircling prey, bubble-net foraging, and search for prey. In each iteration, individuals update their positions toward the best individual in the last iteration, which can be formulated as follows:

$$P(t+1) = P_{\text{best}}(t) - A \cdot |C \cdot P_{\text{best}}(t) - P(t)|, \quad (1)$$

where t represents the t th iteration, A and C are two coefficient vectors, P_{best} is the best individual so far, P is the position of an individual, $||$ represents the absolute value, and \cdot indicates an element-by-element multiplication.

In the exploitation (bubble-net foraging) phase, the individual position is updated based on its distance to the best individual by simulating the helix-shaped movement of whales, which is formulated as follows:

$$P(t+1) = D \cdot e^{bl} \cdot \cos(2\pi l) + P_{\text{best}}(t), \quad (2)$$

where $D = |P_{\text{best}}(t) - P(t)|$ represents the distance between the best individual obtained so far and the i th individual, l is a random number in $[-1, 1]$, and b is a constant which is used to define the shape of logarithmic spiral.

In exploration (search for prey) phase, the individual position is updated using a randomly selected individual. The mathematical model is follows:

$$P(t+1) = P_{\text{rand}} - A \cdot |C \cdot P_{\text{rand}} - P(t)|, \quad (3)$$

where P_{rand} represents a randomly selected individual.

The detailed flowchart of WOA is illustrated in Figure 1, where p is a random number in $[0, 1]$. Due to its very competitive search ability, WOA has been widely applied in various fields [39–41]. Therefore, we consider taking advantage of the effective search ability of WOA to seek the optimal parameters for RVFL networks.

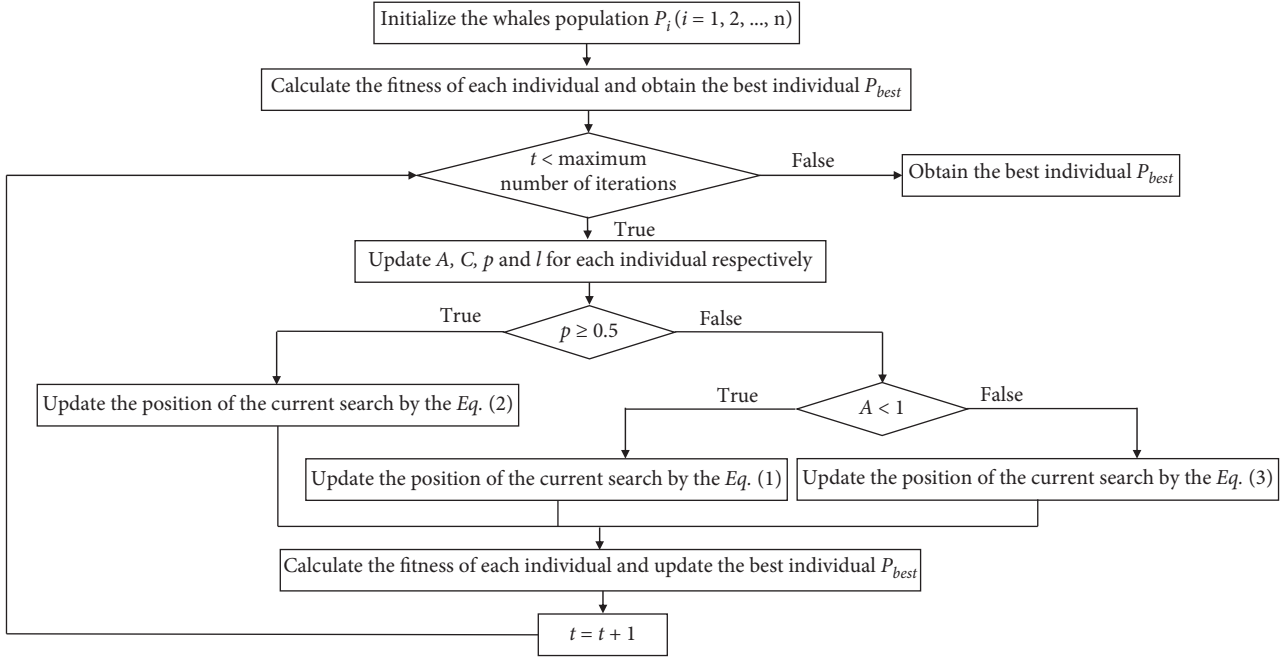


FIGURE 1: The flowchart of whale optimization algorithm (WOA).

2.3. Random Vector Functional Link (RVFL) Neural Network. As a kind of modification of the multilayer perceptron (MLP) model, the random vector functional link (RVFL) neural network was proposed by Pao et al. [42]. The RVFL neural network is able to overcome the slow convergence, overfitting, and local minimum inherently in the traditional gradient-based learning algorithms. Like MLP, the architecture of the RVFL neural network includes three layers, which is illustrated in Figure 2. The main modification in the RVFL network lies in the connection in the network structure. Since the RVFL network has the direct connections from the input layer to the output layer, it can perform better compared to no direct link [43, 44].

The neurons in the hidden layer, known as enhancement nodes, calculate the sum of all the output of the input layer neurons and obtain their output with an activation function:

$$h_m = g\left(\sum_{n=1}^N w_{mn}i_n + b_m\right), \quad (4)$$

where w_{mn} denotes the weight between i_n and h_m , b_m represents the bias of the m th neuron in hidden layer, and $g(\cdot)$ represents an activation function.

The output layer neurons integrate all the output from the hidden layer and input layer neurons, and the final output is

$$o_l = \sum_{m=1}^M w_{ml}h_m + \sum_{n=1}^N w_{nl}i_n, \quad (5)$$

where w_{ml} represents the weight between h_m and o_l and w_{nl} indicates the weight between i_n and o_l .

To enhance the training efficiency, the RVFL neural network utilizes a given distribution to fix the values of w_{mn}

and b_m and obtain the weights of w_{ml} and w_{nl} by minimizing the system error:

$$E = \frac{1}{2P} \sum_{j=1}^P (t^{(j)} - Bd^{(j)})^2, \quad (6)$$

where P indicates the number of training samples and t are the target values, B is the combination of w_{ml} and w_{nl} , and d represents a combined vector.

The RVFL neural network has demonstrated an extremely efficient and fast forecasting ability and has been frequently used in time series forecasting [44, 45].

3. MICEEMDAN-WOA-RVFL: The Proposed Approach for Economic and Financial Time Series Forecasting

Referring to the framework of “decomposition and ensemble,” we design a multidecomposition and self-optimizing hybrid model that integrates multiple ICEEMDANs, WOA, and RVFL networks, termed as MICEEMDAN-WOA-RVFL, to forecast economic and financial time series. The architecture of the proposed hybrid model is illustrated in Figure 3.

Our proposed MICEEMDAN-WOA-RVFL takes advantage of the idea of “divide and conquer” that was frequently used in time series forecasting, image processing, fault diagnosis, and so on [46–53]. A procedure of “decomposition and ensemble” in the MICEEMDAN-WOA-RVFL is as follows:

- (i) Stage 1: decomposition: ICEEMDAN is employed to separate original time series into several subseries (i.e., several IMFs and one residue).

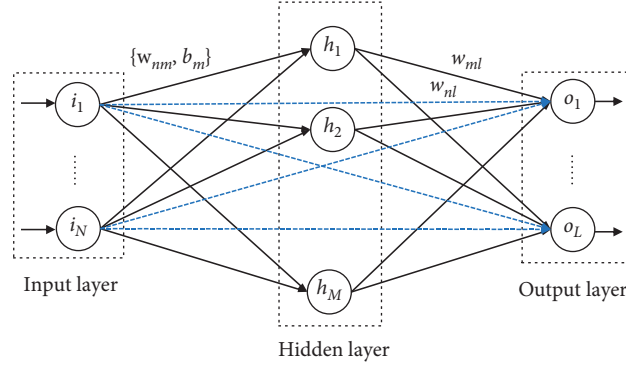


FIGURE 2: The architecture of the random vector functional link (RVFL) neural network.

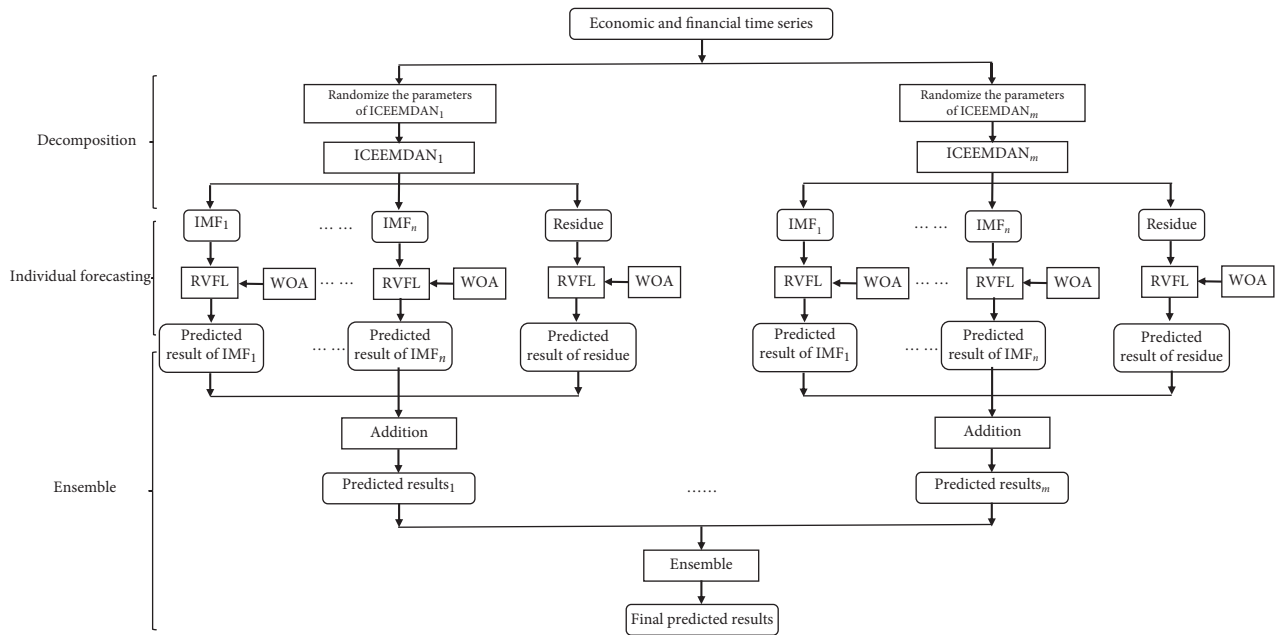


FIGURE 3: The flowchart of the proposed MICEEMDAN-WOA-RVFL.

(ii) Stage 2: individual forecasting. Each decomposed subseries is divided into a training dataset and a testing dataset, then the RVFL network with WOA optimization is developed on each training dataset independently, and finally, the developed RVFL model is used to each testing dataset. The reason why we select the RVFL network as the predictor is its powerful forecasting ability in extant research [15, 34, 44]. Since the parameter setting of the RVFL network plays an important role in the prediction performance, we introduce WOA to seek the optimal parameter values for the RVFL network in the forecasting stage.

(iii) Stage 3: ensemble: the predictions of all the decomposed subseries are aggregated as the final prediction results of one “decomposition and ensemble” using addition aggregation.

In this study, to enhance both accuracy and stability of final prediction, we generate random values for the decomposition parameters of ICEEMDAN in the decomposition stage, including number of realizations (Nr), noise standard deviation (Nsd), and maximum number of sifting iterations (Max_{si}), for each decomposition, and repeat the procedure of “decomposition and ensemble” M times and, finally, combine all the results of multiple “decompositions and ensembles” using the RMSE-weighted method as the final prediction results. The corresponding weight of i th forecasting model is as follows:

$$\text{Weight}_i = \frac{1/\text{RMSE}_i}{\sum_{j=1}^M 1/\text{RMSE}_j}, \quad (7)$$

where M denotes the number of individual models and RMSE_i indicates the RMSE value of the i th forecasting model in the training process.

Although some recent studies also employ the RVFL network for time series forecasting, they obviously differ from the current study in the decomposition technique and network optimization: (1) they divide the original time series using WD or EMD; (2) they construct RVFL networks using the fixed parameter values. Unlike the previous studies, our study decomposes economic and financial time series using ICEEMDAN and searches the optimal parameter values of RVFL networks based on WOA. Furthermore, the previous research mainly focuses on dividing original time series by one single decomposition or dual decomposition [20, 35, 54]. In dual decomposition, the original signal is first decomposed into several components, and then, the high-frequency components continue to be decomposed into other components using the same or different decomposition method. Essentially, the dual decomposition process belongs to one decomposition, just including two different decomposition stages. Unlike the previous research, one main improvement in this study is the multiple decomposition strategy, which can successfully overcome the randomness of one single decomposition and further improve the prediction accuracy and stability of the developed forecasting approach. To our knowledge, it is the first time that the multiple decomposition strategy is developed for the forecasting of economic and financial time series.

4. Experimental Results

4.1. Data Description. As we know, economic and financial time series are influenced by various factors, sometimes raising and dropping down in a short time. The dramatic fluctuations usually lead to the significant nonlinearity and nonstationarity of the time series. To comprehensively evaluate the effectiveness of the proposed MICEEMDAN-WOA-RVFL, we choose four different time series, including the West Texas Intermediate crude oil spot price (WTI), US dollar/Euro foreign exchange rate (USD/EUR), US industrial production (IP), and Shanghai stock exchange composite index (SSEC), as the experimental datasets. The first three datasets can be accessed via the website of St. Louis Fed Research [55], and the last one can be obtained via the website of NetEase [56].

Each time series is separated into two subdatasets: the first 80% for training and the last 20% for testing. Table 1 shows the divided samples of the abovementioned four economic and financial time series.

We utilize ICEEMDAN to decompose these time series into groups of relatively simple subseries. Figure 4 offers an example of the decomposition of the WTI dataset using ICEEMDAN.

4.2. Evaluation Indices. In this study, we use four evaluation metrics, including the mean absolute percent error (MAPE), the root mean squared error (RMSE), the directional statistic (Dstat), and the Diebold–Mariano (DM) test, to assess the performance of the proposed model. Among them, MAPE and RMSE are used to assess the forecasting error, defined as follows:

$$\text{MAPE} = \sum_{t=1}^N \left| \frac{O_t - P_t}{O_t} \right| \times \frac{100}{N}, \quad (8)$$

$$\text{RMSE} = \sqrt{\frac{1}{N} \sum_{t=1}^N (O_t - P_t)^2}, \quad (9)$$

where N is the size of the evaluated samples, O_t denotes the actual values, and P_t represents the predicted values at time t . The lower the values of RMSE and MAPE, the better the prediction models.

The Dstat indicates the performance of direction prediction, which is formulated as follows:

$$D_{\text{stat}} = \frac{1}{N} \sum_{i=1}^N d_i \times 100\%, \quad (10)$$

where $d_i = 1$ if $(P_{t+1} - O_t)(O_{t+1} - O_t) \geq 0$; otherwise, $d_i = 0$. A higher value of D_{stat} indicates a more accurate direction prediction.

Furthermore, to test the significance of the prediction performance of pairs of models, we employ the Diebold–Mariano (DM) test in this study.

4.3. Experimental Settings. In this study, we compare the proposed MICEEMDAN-WOA-RVFL with several state-of-the-art forecasting models, including the single models and the ensemble models. Among all these models, the single models include one popular statistical model, RW, and two popular AI models. BPNN and least square SVR (LSSVR). The ensemble models derive from the combination of the single models and the decomposition method ICEEMDAN.

The detailed parameters of all prediction models, decomposition approach ICEEMDAN, and optimization method WOA in the experiments are shown in Table 2. The parameter values of BPNN, LSSVR, RVFL, and ICEEMDAN refer to the previous literature [22, 34, 45].

All experiments were conducted using Matlab R2019b on a PC with 64 bit Microsoft Windows 10, 8 GB RAM, and 1.8 GHz i7-8565U CPU.

4.4. Results and Analysis. We compare the forecasting performance of six prediction models, including three single models.

(RW, LSSVR, and BPNN) and three ensemble modes (ICEEMDAN-RW, ICEEMDAN-LSSVR, and ICEEMDAN-BPNN) with that of our proposed MICEEMDAN-WOA-RVFL in terms of MAPE, RMSE, and Dstat. Due to the different horizons, we train different forecasting models separately. That is to say, we use the proposed scheme for different horizons to train different models. Tables 3–5 report the experimental results in terms of each evaluation index with 1-, 3-, and 6-horizon, respectively.

From Table 3, we can see that the proposed MICEEMDAN-WOA-RVFL obtains the lowest (the best) MAPE values with all the horizons in all the datasets. RW obtains the best MAPE values with all the horizons in all the datasets among all the compared single models,

TABLE 1: Samples of economic and financial time series.

Dataset	Type	Dataset	Size	Date
WTI	Daily	Sample set	8641	2 January 1986~15 April 2020
		Training set	6912	2 January 1986~24 May 2013
		Testing set	1729	28 May 2013~15 April 2020
USD/EUR	Daily	Sample set	5341	4 January 1999~10 April 2020
		Training set	4272	4 January 1999~30 December 2015
		Testing set	1069	31 December 2015~10 April 2020
IP	Monthly	Sample set	1215	January 1919~March 2020
		Training set	972	January 1919~December 1999
		Testing set	243	January 2000~March 2020
SSEC	Daily	Sample set	7172	19 December 1990~21 April 2020
		Training set	5737	19 December 1990~4 June 2014
		Testing set	1435	5 June 2014~21 April 2020

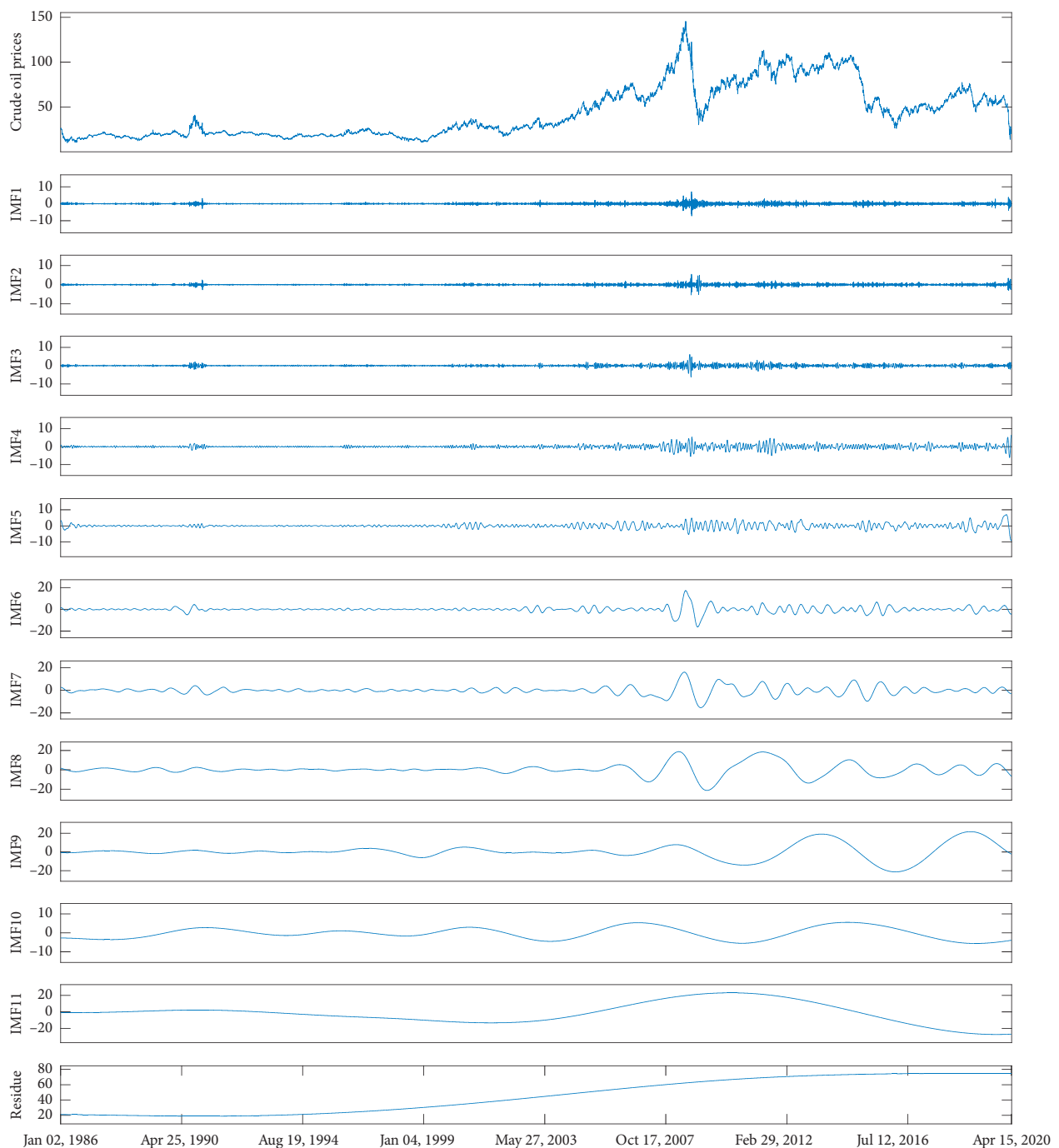


FIGURE 4: The WTI crude oil price series and the corresponding decomposed subseries by ICEEMDAN.

TABLE 2: The settings for the parameters.

Method	Parameters	Description
ICEEMDAN	$Nsd = 0.2$	Noise standard deviation
	$Nr = 100$	Number of realizations
	$Max_{si} = 5000$	Maximum number of sifting iterations
LSSVR	$Rp = 2^{\{-10, -9, \dots, 11, 12\}}$	Regularization parameter
	$Wid_{RBF} = 2^{\{-10, -9, \dots, 11, 12\}}$	Width of the RBF kernel
BPNN	$N_{he} = 10$	Number of hidden neurons
	$Max_{te} = 1000$	Maximum training epochs
	$Lr = 0.0001$	Learning rate
WOA	$Pop = 40$	Population size
	$Max_{gen} = 100$	Maximum generation
MICEEMDAN-WOA-RVFL	$Nsd = [0.01, 0.4]$	Noise standard deviation in ICEEMDAN
	$Nr = [50, 500]$	Number of realizations in ICEEMDAN
	$Max_{si} = [2000, 8000]$	Maximum number of sifting iterations in ICEEMDAN
	$N_{he} = [5, 30]$	Number of hidden neurons in RVFL
	$Func = \{\text{sigmoid, sine, hardlim, tribas, radbas, sign}\}$	Activation function in RVFL
	$Mod = 1$: Regularized least square, 2 : Moore-Penrose pseudoinverse	Mode in RVFL
	$Lag = [3, 20]$	Lag in RVFL
	$Bias = \{\text{true, false}\}$	Bias in RVFL
	$Rand = \{1: \text{Gaussian, } 2: \text{Uniform}\}$	Random type in RVFL
	$Scale = [0.1, 1]$	Scale value in RVFL
	$ScaleMode = \{1$: Scale the features for all neurons, 2 : Scale the features for each hidden neuron, 3 : Scale the range of the randomization for uniform diatribution}	Scale mode in RVFL

TABLE 3: The mean absolute percent error (MAPE) values of different prediction models.

Dataset	Horizon	MICEEMDAN -WOA-RVFL	RW	LSSVR	BPNN	ICEEMDAN -RW	ICEEMDAN -LSSVR	ICEEMDAN -BPNN
WTI	1	0.0036	0.0176	0.0177	0.0182	0.0200	0.0044	0.0055
	3	0.0080	0.0307	0.0309	0.0320	0.0331	0.0092	0.0094
	6	0.0113	0.0441	0.0449	0.0457	0.0458	0.1202	0.0130
USD/EUR	1	0.0006	0.0034	0.0034	0.0034	0.0044	0.0010	0.0010
	3	0.0015	0.0063	0.0063	0.0063	0.0071	0.0020	0.0021
	6	0.0022	0.0087	0.0088	0.0087	0.0094	0.0032	0.0031
IP	1	0.0012	0.0049	0.0057	0.0056	0.0053	0.0024	0.0022
	3	0.0023	0.0102	0.0140	0.0123	0.0104	0.0033	0.0033
	6	0.0032	0.0183	0.0279	0.0235	0.0184	0.0043	0.0049
SSEC	1	0.0020	0.0096	0.0096	0.0097	0.0111	0.0026	0.0026
	3	0.0044	0.0178	0.0178	0.0179	0.0185	0.0047	0.0051
	6	0.0065	0.0259	0.0259	0.0269	0.0268	0.0072	0.0074

demonstrating it is better than LSSVR and BPNN for the forecasting of economic and financial time series. Of all the ensemble models, the ICEEMDAN-LSSVR model and ICEEMDAN-BPNN model obtain the close MAPE values, obviously better than the ICEEMDAN-RW.

The RMSE values of the four time series datasets are listed in Table 4. From this table, we can find that the proposed MICEEMDAN-WOA-RVFL outperforms all the single and ensemble models with all the horizons in all the datasets. The statistical model RW obtains the best RMSE values in 10 out of 12 cases, demonstrating that it is more suitable for economic and financial time series forecasting than LSSVR and BPNN among all the single models. As to the ensemble models, the proposed MICEEMDAN-WOA-RVFL obtains the lower RMSE values than the compared ensemble models,

demonstrating that the former is more effective for economic and financial time series forecasting.

Table 5 shows the directional statistics D_{stat} , and we can see that the MICEEMDAN-WOA-RVFL achieves the highest D_{stat} values in all the 12 cases, indicating that it has better performance of direction forecasting. Amongst the single prediction models, LSSVR and RW obtain the best D_{stat} values in 5 cases, respectively, better than the BPNN. Similarly, the ICEEMDAN-LSSVR model and ICEEMDAN-BPNN model obtain the close D_{stat} values, obviously better than the ICEEMDAN-RW model in all the 12 cases.

From the all prediction results, we can find that all the ensemble prediction models except ICEEMDAN-RW greatly outperform the corresponding single prediction models in all the 12 cases, showing that the framework of decomposition and ensemble is an effective tool for improving the forecasting

TABLE 4: The root mean squared error (RMSE) values of different prediction models.

Dataset	Horizon	MICEEMDAN -WOA-RVFL	RW	LSSVR	BPNN	ICEEMDAN -RW	ICEEMDAN -LSSVR	ICEEMDAN -BPNN
WTI	1	0.2715	1.3196	1.3228	1.3744	1.8134	0.3467	0.4078
	3	0.5953	2.1784	2.1929	2.2867	2.5041	0.6754	0.7620
	6	0.8146	3.0737	3.1271	3.1845	3.2348	0.8692	0.9462
USD/EUR	1	0.0009	0.0051	0.0052	0.0052	0.0099	0.0015	0.0016
	3	0.0022	0.0091	0.0092	0.0092	0.0129	0.0031	0.0031
	6	0.0033	0.0127	0.0128	0.0127	0.0154	0.0047	0.0046
IP	1	0.2114	0.7528	0.8441	0.8230	0.8205	0.3861	0.4175
	3	0.3875	1.4059	1.8553	1.8311	1.4401	0.5533	0.5294
	6	0.5340	2.4459	3.6015	2.8116	2.4569	0.6408	0.8264
SSEC	1	10.8115	50.0742	49.8800	50.8431	63.3951	12.6460	13.7928
	3	22.2983	89.1834	88.5290	89.1781	93.2887	25.2526	29.7784
	6	35.7201	131.6386	131.3487	133.5647	137.2598	40.4357	49.6341

TABLE 5: The directional statistic (D_{stat}) values of different prediction models.

Dataset	Horizon	MICEEMDAN -WOA-RVFL	RW	LSSVR	BPNN	ICEEMDAN -RW	ICEEMDAN -LSSVR	ICEEMDAN -BPNN
WTI	1	0.9381	0.4815	0.5243	0.5191	0.4977	0.9190	0.9097
	3	0.8576	0.4873	0.5087	0.5012	0.4907	0.8300	0.8449
	6	0.7737	0.5116	0.4902	0.4948	0.5185	0.7714	0.7575
USD/EUR	1	0.9410	0.5019	0.4719	0.4897	0.5056	0.8998	0.9026
	3	0.8502	0.4888	0.4897	0.4925	0.4916	0.8118	0.8024
	6	0.7828	0.4991	0.5318	0.5253	0.5047	0.7023	0.7154
IP	1	0.9256	0.5579	0.5909	0.5785	0.5620	0.8636	0.8760
	3	0.8802	0.6983	0.5455	0.4876	0.6529	0.8430	0.8058
	6	0.8141	0.6198	0.5537	0.5661	0.6405	0.7355	0.7645
SSEC	1	0.9156	0.4944	0.5049	0.5098	0.4979	0.9024	0.9002
	3	0.8396	0.5042	0.5021	0.5007	0.4965	0.8222	0.8145
	6	0.7587	0.4833	0.5063	0.4965	0.4805	0.7448	0.7455

performance. Of all the compared models, the proposed MICEEMDAN-WOA-RVFL obtains the highest D_{stat} values and the lowest MAPE and RMSE values in all the time series datasets, showing that it is completely superior to the benchmark prediction models. Furthermore, for each prediction model, the MAPE and RMSE values increase while the D_{stat} values decrease with the horizon. This demonstrates that it is easier to forecast time series with a short horizon than with a long one. It is worth noting that the proposed MICEEMDAN-WOA-RVFL still achieves the relatively good MAPE and RMSE with the increase of horizon among the compared models. For example, when the proposed model obtains 0.7737 D_{stat} with horizon 6 in the WTI dataset, it achieves the relatively low MAPE (0.0113) and RMSE (0.8146), indicating that the prediction values are very close to the real values although the proposed model misses direction about 22.63%. In other words, the proposed MICEEMDAN-WOA-RVFL can still achieve satisfactory forecasting accuracy with a long horizon.

Furthermore, we can find that the multiple decomposition strategy does not improve the forecast for the RW model. One possible explanation is simply that RW infers that the past movement or trend of a time series cannot be used to predict its future movement, and thus, it cannot take advantage of the historical data and the diversity of multiple decomposition to make the future prediction. Therefore, when we aggregate the multiple RW model predictions of all the decomposed subseries, we just integrate several random predictions and, thus, cannot significantly improve the ensemble prediction results. In contrast, the LSSVR and

BPNN, as well as RVFL, can fully use all the historical data and the diversity of multiple decomposition to make the future prediction. Specifically, the multiple decomposition using different parameters generates many groups of different decomposed subseries, and the diversity of decomposition can successfully overcome the randomness of one single decomposition and further improve the prediction accuracy and stability of the developed forecasting approach.

In addition, the Diebold–Mariano (DM) test is utilized to evaluate whether the forecasting accuracy of the proposed MICEEMDAN-WOA-RVFL significantly outperforms those of the other compared models. Table 6 shows the statistics and p values (in brackets).

On one hand, the DM statistical values between the ensemble prediction models and their corresponding single predictors are much lower than zero and the corresponding p values are almost equal to zero with all the horizons except for the RW model, showing that the architecture of “decomposition and ensemble” contributes to greatly improving prediction accuracy and the combination of ICEEMDAN and AI predictors is more effective for economic and financial time series forecasting.

On the other hand, DM test results on the prediction of all the four time series datasets indicate that the MICEEMDAN-WOA-RVFL is significantly better than the single models and the other ensemble models with all the horizons, and the corresponding p values are much lower than 0.01 in all the cases.

In summary, the DM test results demonstrate that the combination of multiple ICEEMDANs, RVFL networks, and

TABLE 6: Results of the Diebold–Mariano (DM) test.

Dataset	Horizon	Tested Model	ICEEMDAN-LSSVR	ICEEMDAN-BPNN	ICEEMDAN-RW	LSSVR	BPNN	RW
WTI	1	MICEEMDAN-WOA-RVFL	-4.9081 (≤ 0.0001)	-7.0030 (≤ 0.0001)	-6.1452 (≤ 0.0001)	-10.7240 (≤ 0.0001)	-10.3980 (≤ 0.0001)	-10.6210 (≤ 0.0001)
		ICEEMDAN-LSSVR		-3.5925 (0.0003)	-6.0620 (≤ 0.0001)	-10.5640 (≤ 0.0001)	-10.3680 (≤ 0.0001)	-10.4660 (≤ 0.0001)
		ICEEMDAN-BPNN			-5.9718 (≤ 0.0001)	-10.2070 (≤ 0.0001)	-9.9529 (≤ 0.0001)	-10.0960 (≤ 0.0001)
		ICEEMDAN-RW			3.0776 (0.0021)		2.7682 (0.0057)	3.0951 (0.0020)
	3	LSSVR					-1.8480 (0.0648)	1.0058 (0.3147)
		BPNN						1.9928 (0.0464)
		MICEEMDAN-WOA-RVFL	-4.9136 (≤ 0.0001)	-3.6146 (0.0003)	-10.8660 (≤ 0.0001)	-16.5990 (≤ 0.0001)	-15.6260 (≤ 0.0001)	-16.6720 (≤ 0.0001)
		ICEEMDAN-LSSVR		-2.1143 (0.0346)	-10.7560 (≤ 0.0001)	-16.7020 (≤ 0.0001)	-15.6780 (≤ 0.0001)	-16.7760 (≤ 0.0001)
	6	ICEEMDAN-BPNN			-10.5250 (≤ 0.0001)	-16.2160 (≤ 0.0001)	-15.3500 (≤ 0.0001)	-16.2430 (≤ 0.0001)
		ICEEMDAN-RW			3.0818 (0.0021)		2.0869 (0.0370)	3.2155 (0.0012)
		LSSVR					-2.7750 (0.0056)	2.3836 (0.0173)
		BPNN						3.0743 (0.0021)
USD/EUR	1	MICEEMDAN-WOA-RVFL	-3.9302 (≤ 0.0001)	-5.1332 (≤ 0.0001)	-18.9130 (≤ 0.0001)	-19.0620 (≤ 0.0001)	-21.9930 (≤ 0.0001)	-19.5080 (≤ 0.0001)
		ICEEMDAN-LSSVR		-3.4653 (0.0005)	-18.9170 (≤ 0.0001)	-19.1680 (≤ 0.0001)	-22.0120 (≤ 0.0001)	-19.5420 (≤ 0.0001)
		ICEEMDAN-BPNN			-18.8380 (≤ 0.0001)	-19.1650 (≤ 0.0001)	-21.9930 (≤ 0.0001)	-19.5200 (≤ 0.0001)
		ICEEMDAN-RW			2.6360 (0.0085)		0.5129 (0.6081)	4.1421 (≤ 0.0001)
	3	LSSVR					-2.2124 (0.0271)	3.9198 (≤ 0.0001)
		BPNN						4.3545 (≤ 0.0001)
		MICEEMDAN-WOA-RVFL	-8.8860 (≤ 0.0001)	-8.6031 (≤ 0.0001)	-4.4893 (≤ 0.0001)	-15.4300 (≤ 0.0001)	-15.4100 (≤ 0.0001)	-15.3440 (≤ 0.0001)
		ICEEMDAN-LSSVR		-0.8819 (0.3780)	-4.4230 (≤ 0.0001)	-14.7210 (≤ 0.0001)	-14.7320 (≤ 0.0001)	-14.6280 (≤ 0.0001)
	6	ICEEMDAN-BPNN			-4.4158 (≤ 0.0001)	-14.6310 (≤ 0.0001)	-14.6440 (≤ 0.0001)	-14.5310 (≤ 0.0001)
		ICEEMDAN-RW			3.3089 (0.0010)		3.2912 (0.0010)	3.3244 (0.0009)
		LSSVR					-1.8732 (0.06132)	2.9472 (0.0033)
		BPNN						3.4378 (0.0006)
3	MICEEMDAN-WOA-RVFL	-10.1370 (≤ 0.0001)	-7.9933 (≤ 0.0001)	-5.7359 (≤ 0.0001)	-18.3380 (≤ 0.0001)	-18.6460 (≤ 0.0001)	-18.2090 (≤ 0.0001)	
	ICEEMDAN-LSSVR		-1.4797 (0.1392)	-5.5972 (≤ 0.0001)	-17.9030 (≤ 0.0001)	-18.1920 (≤ 0.0001)	-17.7730 (≤ 0.0001)	
	ICEEMDAN-BPNN			-5.6039 (≤ 0.0001)	-17.8370 (≤ 0.0001)	-18.1350 (≤ 0.0001)	-17.6910 (≤ 0.0001)	
	ICEEMDAN-RW			3.0048 (0.0027)		2.9552 (0.0032)	3.0206 (0.0026)	
6	LSSVR					-1.4077 (0.1595)	1.5242 (0.1278)	
	BPNN						2.1240 (0.0339)	
	MICEEMDAN-WOA-RVFL	-11.1070 (≤ 0.0001)	-10.0570 (≤ 0.0001)	-7.4594 (≤ 0.0001)	-18.3010 (≤ 0.0001)	-18.4640 (≤ 0.0001)	-18.4940 (≤ 0.0001)	
	ICEEMDAN-LSSVR		1.9379 (0.0529)	-7.0858 (≤ 0.0001)	-17.4490 (≤ 0.0001)	-17.5970 (≤ 0.0001)	-17.6370 (≤ 0.0001)	
6	ICEEMDAN-BPNN			-7.1244 (≤ 0.0001)	-17.5850 (≤ 0.0001)	-17.7340 (≤ 0.0001)	-17.7690 (≤ 0.0001)	
	ICEEMDAN-RW			2.5399 (0.0112)		2.6203 (0.0089)	2.6207 (0.0089)	
	LSSVR					2.2946 (0.0220)	2.5913 (0.0097)	
	BPNN						-0.2090 (0.8345)	

TABLE 6: Continued.

Dataset	Horizon	Tested Model	ICEEMDAN-LSSVR	ICEEMDAN-BPNN	ICEEMDAN-RW	LSSVR	BPNN	RW
IP	1	MICEEMDAN-WOA-RVFL	-3.4304 (0.0007)	-2.4253 (0.0098)	-3.4369 (0.0007)	-3.5180 (0.0005)	-4.1486 (≤ 0.0001)	-3.3215 (0.0015)
		ICEEMDAN-LSSVR		-0.6714 (0.5026)	-3.2572 (0.0013)	-3.3188 (0.0010)	-4.0082 (≤ 0.0001)	-2.9573 (0.0034)
		ICEEMDAN-BPNN			-3.6265 (0.0004)	-3.7455 (0.0002)	-4.6662 (≤ 0.0001)	-3.3790 (0.0008)
		ICEEMDAN-RW				-0.7438 (0.4577)	-0.0502 (0.9600)	2.6089 (0.0096)
	3	LSSVR					0.4094 (0.6826)	3.4803 (0.0006)
		BPNN						1.6021 (0.1104)
		MICEEMDAN-WOA-RVFL	-4.5687 (≤ 0.0001)	-3.7062 (0.0003)	-5.9993 (≤ 0.0001)	-6.8919 (≤ 0.0001)	-5.5008 (≤ 0.0001)	-5.8037 (≤ 0.0001)
		ICEEMDAN-LSSVR		1.1969 (0.2325)	-5.5286 (≤ 0.0001)	-6.6325 (≤ 0.0001)	-5.2260 (≤ 0.0001)	-5.3260 (≤ 0.0001)
	6	ICEEMDAN-BPNN			-5.7199 (≤ 0.0001)	-6.7722 (≤ 0.0001)	-5.2955 (≤ 0.0001)	-5.5099 (≤ 0.0001)
		ICEEMDAN-RW				-5.6536 (≤ 0.0001)	-3.6721 (0.0003)	1.7609 (0.0795)
		LSSVR					0.2479 (0.8044)	6.3126 (≤ 0.0001)
		BPNN						3.9699 (≤ 0.0001)
SSEC	1	MICEEMDAN-WOA-RVFL	-5.9152 (≤ 0.0001)	-3.5717 (0.0004)	-5.9430 (≤ 0.0001)	-7.5672 (≤ 0.0001)	-10.8900 (≤ 0.0001)	-5.8450 (≤ 0.0001)
		ICEEMDAN-LSSVR		-2.5163 (0.0125)	-5.8465 (≤ 0.0001)	-7.5185 (≤ 0.0001)	-10.7140 (≤ 0.0001)	-5.7483 (≤ 0.0001)
		ICEEMDAN-BPNN			-5.6135 (≤ 0.0001)	-7.4370 (≤ 0.0001)	-10.3470 (≤ 0.0001)	-5.5254 (≤ 0.0001)
		ICEEMDAN-RW				-7.6719 (≤ 0.0001)	-2.2903 (0.02287)	0.8079 (0.4200)
	3	LSSVR					3.8137 (0.0002)	7.7861 (≤ 0.0001)
		BPNN						2.3351 (0.0204)
		MICEEMDAN-WOA-RVFL	-4.0255 (≤ 0.0001)	-3.748 (0.0004)	-7.9407 (≤ 0.0001)	-10.8090 (≤ 0.0001)	-10.3070 (≤ 0.0001)	-10.7330 (≤ 0.0001)
		ICEEMDAN-LSSVR		-1.5083 (0.1317)	-7.8406 (≤ 0.0001)	-10.5410 (≤ 0.0001)	-10.0710 (≤ 0.0001)	-10.5020 (≤ 0.0001)
	6	ICEEMDAN-BPNN			-7.7986 (≤ 0.0001)	-10.5470 (≤ 0.0001)	-10.0580 (≤ 0.0001)	-10.5030 (≤ 0.0001)
		ICEEMDAN-RW				3.5571 (0.0004)	3.2632 (0.0011)	3.5150 (0.0005)
		LSSVR					-1.0197 (0.3081)	-0.6740 (0.5004)
		BPNN						0.8078 (0.4193)
3	MICEEMDAN-WOA-RVFL	-3.8915 (0.0001)	-3.7312 (0.0002)	-10.5890 (≤ 0.0001)	-10.5480 (≤ 0.0001)	-10.7470 (≤ 0.0001)	-10.1260 (≤ 0.0001)	
	ICEEMDAN-LSSVR		-2.4145 (0.0159)	-10.5830 (≤ 0.0001)	-10.5240 (≤ 0.0001)	-10.7760 (≤ 0.0001)	-10.1110 (≤ 0.0001)	
	ICEEMDAN-BPNN			-10.2420 (≤ 0.0001)	-10.1860 (≤ 0.0001)	-10.4400 (≤ 0.0001)	-9.7595 (≤ 0.0001)	
	ICEEMDAN-RW				3.4031 (0.0007)	2.3198 (0.0205)	3.1912 (0.0014)	
6	LSSVR					-0.5931 (0.5532)	-1.2284 (0.2194)	
	BPNN						-0.0042 (0.9966)	
	MICEEMDAN-WOA-RVFL	-2.9349 (0.0034)	-3.7544 (0.0002)	-10.2390 (≤ 0.0001)	-10.1970 (≤ 0.0001)	-11.0150 (≤ 0.0001)	-10.1630 (≤ 0.0001)	
	ICEEMDAN-LSSVR		-2.5830 (0.0099)	-10.1390 (≤ 0.0001)	-10.0940 (≤ 0.0001)	-10.9630 (≤ 0.0001)	-10.0690 (≤ 0.0001)	
6	ICEEMDAN-BPNN			-9.6418 (≤ 0.0001)	-9.5562 (≤ 0.0001)	-10.4090 (≤ 0.0001)	-9.5122 (≤ 0.0001)	
	ICEEMDAN-RW				2.3167 (0.0207)	1.3656 (0.1723)	2.2227 (0.02639)	
	LSSVR					-1.9027 (0.05728)	-0.5814 (0.5611)	
	BPNN						1.5707 (0.1165)	

WOA optimization can significantly enhance the prediction accuracy of economic and financial time series forecasting.

5. Discussion

To better investigate the proposed MICEEMDAN-WOA-RVFL, we further discuss the developed prediction model, including the comparison of single decomposition and multiple decompositions, the optimization effectiveness of WOA, and the impact of ensemble size in this subsection.

5.1. Comparison of Single Decomposition and Multiple Decompositions. One of the main novelties of this study is the multiple decomposition strategy, which can successfully overcome the randomness of a single decomposition and improve the prediction accuracy and stability of the developed forecasting model. To evaluate the effectiveness of the multiple decomposition strategy, we compare the prediction results of MICEEMDAN-WOA-RVFL and ICEEMDAN-WOA-RVFL. The former ensembles the prediction results of $M(M=100)$ individual ICEEMDAN decompositions with random parameters, while the latter only employs one ICEEMDAN decomposition. We randomly choose 5 out of these 100 decompositions and execute ICEEMDAN-WOA-RVFL for time series forecasting. Tables 7–9 report the MAPE, RMSE, and D_{stat} values of the MICEEMDAN-WOA-RVFL and the five ICEEMDAN-WOA-RVFL models using single decomposition and the corresponding mean values of these five models using single decomposition.

On one hand, compared with the prediction results of the five single decompositions and the mean prediction results, the proposed MICEEMDAN-WOA-RVFL achieves the lowest MAPE and the highest D_{stat} values in all the 12 cases and the lowest RMSE values in 11 out of all the 12 cases, indicating that the multiple decomposition strategy can successfully overcome the randomness of single decomposition and improve the ensemble prediction accuracy.

On the other hand, we can find that the multiple decomposition strategy can greatly improve the stability of the prediction model. For example, the range of MAPE values of the five single decomposition models with horizon 6 in the IP time series dataset is from 0.0034 to 0.1114, indicating that different single decomposition can produce relatively great difference in prediction results. When we employ the multiple decomposition strategy, we can overcome the randomness of single decomposition and, thus, enhance prediction stability.

In summary, the experimental results suggest that the multiple decomposition strategy and prediction ensemble can effectively enhance prediction accuracy and stability. The main reasons for the prediction improvement lie in three aspects: (1) the multiple decomposition can reduce the

randomness of one single decomposition and simultaneously generate groups of differential subseries; (2) predictions using these groups of differential subseries can achieve diverse prediction results; and (3) the selection and ensemble of these diverse prediction results can ensure both accuracy and diversity and, thus, improve the final ensemble prediction.

5.2. The Optimization Effectiveness of WOA. When we use RVFL networks to construct predictors, a number of parameters need to be set in advance. In this study, WOA is introduced to search the optimal parameter values for RVFL predictors using its powerful optimization ability. To investigate the optimization effectiveness of WOA for parameter search, we compare the proposed MICEEMDAN-WOA-RVFL with MICEEMDAN-RVFL without WOA optimization. According to the literature [45], we fixed the number of hidden neurons $N_{\text{ne}} = 100$, activation function $\text{Func} = \text{sigmoid}$, and random type $\text{Rand} = \text{Gaussian}$ in MICEEMDAN-RVFL. The MAPE, RMSE, and D_{stat} values are reported in Tables 10–12, respectively.

In all the four time series datasets, the prediction performance of the proposed MICEEMDAN-WOA-RVFL model is better than or equal to that of the MICEEMDAN-RVFL model without WOA optimization in all the 12 cases except for the RMSE value with horizon 1 in the SSEC dataset in terms of MAPE and RMSE, as listed in Tables 10 and 11. In addition, the MICEEMDAN-WOA-RVFL obtains the higher D_{stat} values in 10 out of 12 cases, which can be seen in Table 12. The all results indicate that WOA can effectively search the optimal parameter settings for RVFL networks, further improving the overall prediction performance.

5.3. The Impact of Ensemble Size. The previous research has demonstrated that the ensemble strategy of using all individual prediction models is unlikely to work well and the selection of individual prediction models contributes to improving the ensemble prediction performance [57]. In this study, we sort all individual prediction models based on their past performance (RMSE values) and, then, select the top N percent as the ensemble size to construct the ensemble prediction model. To further investigate the impact of ensemble size on ensemble prediction, we use different ensemble sizes ($es = 10\%, 20\%, \dots, 100\%$) to select the top N percent of individual forecasting models to develop the ensemble prediction model and conduct the one-step-ahead forecasting experiment on the four time series datasets. The results are demonstrated in Figure 5.

We can see that the MICEEMDAN-WOA-RVFL obtains the best forecasting performance in the WTI, IP, and SSEC datasets when the ensemble size es is in the range of 20%–40% and in the USD/EUR dataset when the ensemble size es

TABLE 7: The mean absolute percent error (MAPE) values of single decomposition and multiple decompositions.

Dataset	Horizon	MICEEMDAN- WOA-RVFL	ICEEMDAN- WOA-RVFL1	ICEEMDAN- WOA-RVFL2	ICEEMDAN- WOA-RVFL3	ICEEMDAN- WOA-RVFL4	ICEEMDAN- WOA-RVFL5	Mean
WTI	1	0.0036	0.0043	0.0045	0.0045	0.0041	0.0040	0.0043
	3	0.0080	0.0088	0.0084	0.0084	0.0082	0.0083	0.0084
	6	0.0113	0.0132	0.0115	0.0113	0.0118	0.0120	0.0112
USD/ EUR	1	0.0006	0.0011	0.0010	0.0008	0.0010	0.0008	0.0009
	3	0.0015	0.0021	0.0021	0.0015	0.0017	0.0015	0.0018
	6	0.0022	0.0033	0.0022	0.0023	0.0023	0.0024	0.0025
IP	1	0.0012	0.0016	0.0016	0.0017	0.0017	0.0015	0.0016
	3	0.0023	0.0024	0.0026	0.0030	0.0028	0.0024	0.0026
	6	0.0032	0.0036	0.0034	0.1114	0.0036	0.0041	0.0252
SSEC	1	0.0020	0.0024	0.0023	0.0026	0.0023	0.0023	0.0024
	3	0.0044	0.0045	0.0046	0.0052	0.0045	0.0047	0.0047
	6	0.0065	0.0067	0.0070	0.0085	0.0068	0.0075	0.0073

TABLE 8: The root mean squared error (RMSE) values of single decomposition and multiple decompositions.

Dataset	Horizon	MICEEMDAN- WOA-RVFL	ICEEMDAN- WOA-RVFL1	ICEEMDAN- WOA-RVFL2	ICEEMDAN- WOA-RVFL3	ICEEMDAN- WOA-RVFL4	ICEEMDAN- WOA-RVFL5	Mean
WTI	1	0.2715	0.3316	0.3376	0.3352	0.3191	0.3148	0.3277
	3	0.5953	0.6557	0.6214	0.6200	0.6058	0.6133	0.6232
	6	0.8146	0.9490	0.8239	0.8199	0.8508	0.8597	0.8607
USD/ EUR	1	0.0009	0.0017	0.0017	0.0012	0.0015	0.0012	0.0015
	3	0.0022	0.0031	0.0034	0.0023	0.0025	0.0023	0.0027
	6	0.0033	0.0048	0.0033	0.0035	0.0035	0.0036	0.0037
IP	1	0.2114	0.2894	0.3080	0.3656	0.3220	0.2589	0.3088
	3	0.3875	0.4098	0.4507	0.4809	0.4776	0.4027	0.4443
	6	0.5340	0.5502	0.5563	1.0081	0.5697	0.6466	0.6661
SSEC	1	10.8115	11.5515	13.0728	16.7301	12.2465	14.3671	13.5936
	3	22.2983	22.0603	22.8140	33.9937	23.9755	25.8004	25.7288
	6	35.7201	37.0255	41.9033	55.5066	38.6140	48.2131	44.2525

TABLE 9: The directional statistic (D_{stat}) values of single decomposition and multiple decompositions.

Dataset	Horizon	MICEEMDAN- WOA-RVFL	ICEEMDAN- WOA-RVFL1	ICEEMDAN- WOA-RVFL2	ICEEMDAN- WOA-RVFL3	ICEEMDAN- WOA-RVFL4	ICEEMDAN- WOA-RVFL5	Mean
WTI	1	0.9381	0.9201	0.9161	0.9184	0.9323	0.9271	0.9228
	3	0.8576	0.8414	0.8548	0.8385	0.8553	0.8513	0.8483
	6	0.7737	0.7419	0.7703	0.7668	0.7627	0.7616	0.7607
USD/ EUR	1	0.941	0.9008	0.9270	0.9204	0.9073	0.9157	0.9142
	3	0.8502	0.8052	0.8418	0.8399	0.8296	0.8427	0.8318
	6	0.7828	0.6826	0.7809	0.7819	0.7772	0.7706	0.7586
IP	1	0.9256	0.8967	0.8926	0.9132	0.8967	0.9174	0.9033
	3	0.8802	0.8760	0.8430	0.8223	0.8471	0.8802	0.8537
	6	0.8141	0.8017	0.8017	0.7066	0.7851	0.8017	0.7794
SSEC	1	0.9156	0.9052	0.9052	0.9052	0.9087	0.9135	0.9076
	3	0.8396	0.8222	0.8292	0.8208	0.8368	0.8264	0.8271
	6	0.7587	0.7462	0.7441	0.7134	0.7594	0.7448	0.7416

TABLE 10: The mean absolute percent error (MAPE) values with and without WOA optimization.

Dataset	Horizon	MICEEMDAN- WOA-RVFL	MICEEMDAN- RVFL
WTI	1	0.0036	0.0037
	3	0.0080	0.0082
	6	0.0113	0.0118
USD/EUR	1	0.0006	0.0006
	3	0.0015	0.0015
	6	0.0022	0.0023
IP	1	0.0012	0.0013
	3	0.0023	0.0023
	6	0.0032	0.0036
SSEC	1	0.0020	0.0020
	3	0.0044	0.0044
	6	0.0065	0.0066

TABLE 11: The root mean squared error (RMSE) values with and without WOA optimization.

Dataset	Horizon	MICEEMDAN-WOA-RVFL	MICEEMDAN-RVFL
WTI	1	0.2715	0.2824
	3	0.5953	0.6079
	6	0.8146	0.8485
USD/EUR	1	0.0009	0.0010
	3	0.0022	0.0022
	6	0.0033	0.0034
IP	1	0.2114	0.2362
	3	0.3875	0.4033
	6	0.5340	0.5531
SSEC	1	10.8115	10.7616
	3	22.2983	22.7456
	6	35.7201	36.3150

TABLE 12: The directional statistic (D_{stat}) values with and without WOA optimization.

Dataset	Horizon	MICEEMDAN-WOA-RVFL	MICEEMDAN-RVFL
WTI	1	0.9381	0.9358
	3	0.8576	0.8565
	6	0.7737	0.7656
USD/EUR	1	0.941	0.9317
	3	0.8502	0.8455
	6	0.7828	0.7762
IP	1	0.9256	0.9174
	3	0.8802	0.8430
	6	0.8141	0.7893
SSEC	1	0.9156	0.9191
	3	0.8396	0.8351
	6	0.7587	0.7594

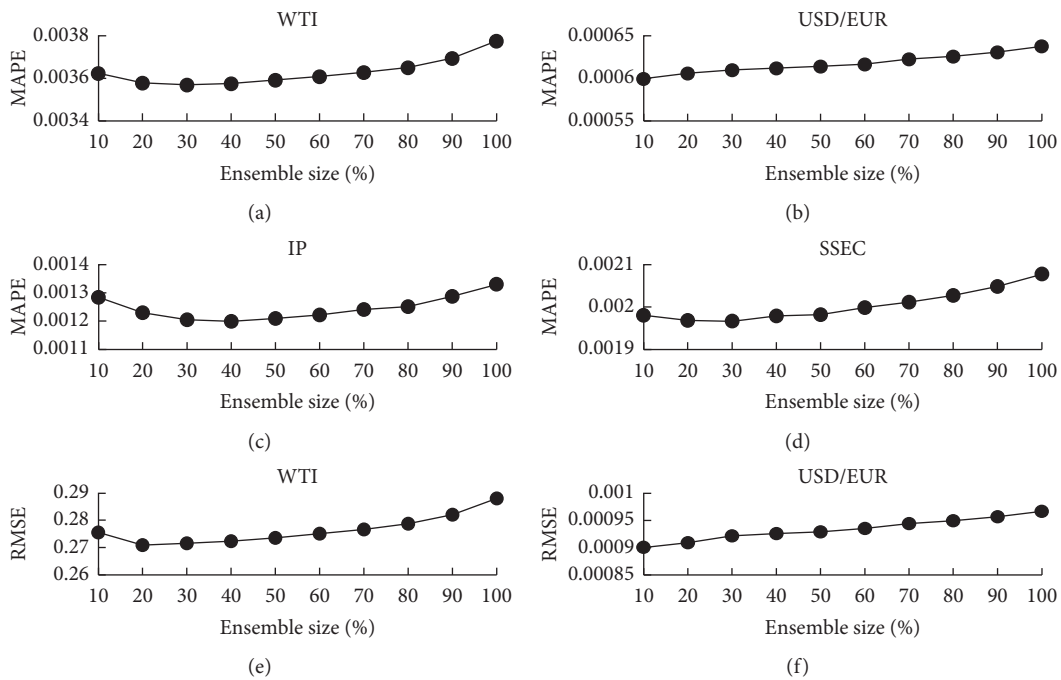


FIGURE 5: Continued.

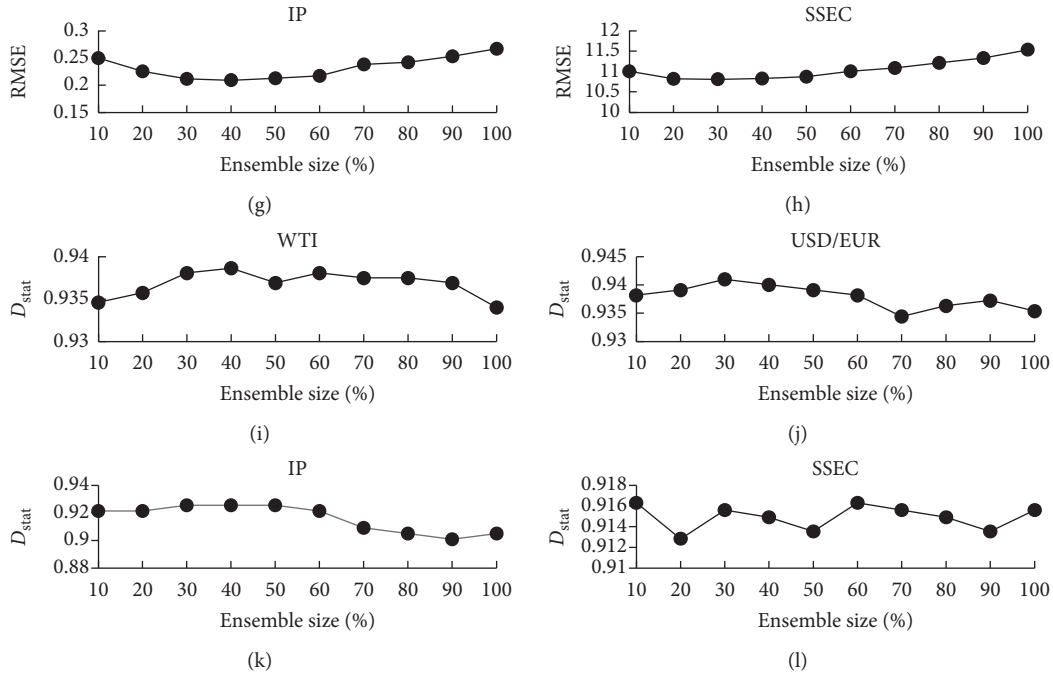


FIGURE 5: The impact of ensemble size with one-step-ahead forecasting.

is in the range of 10%–40% in terms of MAPE, RMSE, and D_{stat} . When the es is greater than 40%, the MAPE and RMSE values continue to worsen and become the worst when the ensemble size grows to 100. The experimental results indicate that the ensemble size has an overall significant impact on ensemble prediction, and an ideal range of ensemble size is about 20% to 40%.

6. Conclusions

To better forecast economic and financial time series, we propose a novel multidecomposition and self-optimizing ensemble prediction model MICEEMDAN-WOA-RVFL combining multiple ICEEMDANs, WOA, and RVFL networks. The MICEEMDAN-WOA-RVFL first uses ICEEMDAN to multiply separate original economic and financial time series into groups of subseries many times, and then, RVFL networks are used to individually forecast the decomposed subseries in each decomposition. Simultaneously, WOA is introduced to optimize RVFL networks to further improve the prediction accuracy. Thirdly, the predictions of subseries in each decomposition are integrated into the forecasting results of each decomposition using addition. Finally, the prediction results of each decomposition are selected based on RMSE values and are combined as the final prediction results.

As far as we know, it is the first time that WOA is employed for the optimal parameter search for RVFL networks and the multiple decomposition strategy is introduced in time series forecasting. The empirical results indicate that

(1) the proposed MICEEMDAN-WOA-RVFL significantly improves prediction accuracy in various economic and financial time series forecasting; (2) WOA can effectively search optimal parameters for RVFL networks and improve prediction performance of economic and financial time series forecasting; and (3) the multiple decomposition strategy can successfully overcome the randomness of a single decomposition and enhance the prediction accuracy and stability of the developed prediction model.

We will extend our study in two aspects in the future: (1) applying the MICEEMDAN-WOA-RVFL to forecast more economic and financial time series and (2) improving the selection and ensemble method of individual forecasting models to further enhance the prediction performance.

Data Availability

The data used to support the findings of this study are included within the article.

Conflicts of Interest

The authors declare that they have no conflicts of interest.

Acknowledgments

This work was supported by the Fundamental Research Funds for the Central Universities (Grant no. JBK2003001), the Ministry of Education of Humanities and Social Science Project (Grant nos. 19YJAZH047 and 16XJAZH002), and

the Scientific Research Fund of Sichuan Provincial Education Department (Grant no. 17ZB0433).

References

- [1] Y. Hui, W.-K. Wong, Z. Bai, and Z.-Z. Zhu, "A new non-linearity test to circumvent the limitation of Volterra expansion with application," *Journal of the Korean Statistical Society*, vol. 46, no. 3, pp. 365–374, 2017.
- [2] R. Adhikari and R. K. Agrawal, "A combination of artificial neural network and random walk models for financial time series forecasting," *Neural Computing and Applications*, vol. 24, no. 6, pp. 1441–1449, 2014.
- [3] A. Lanza, M. Manera, and M. Giovannini, "Modeling and forecasting cointegrated relationships among heavy oil and product prices," *Energy Economics*, vol. 27, no. 6, pp. 831–848, 2005.
- [4] M. R. Hassan and B. Nath, "Stock market forecasting using hidden Markov model: a new approach," in *Proceedings of the 5th International Conference on Intelligent Systems Design and Applications (ISDA'05)*, pp. 192–196, IEEE, Warsaw, Poland, September 2005.
- [5] L. Kilian and M. P. Taylor, "Why is it so difficult to beat the random walk forecast of exchange rates?" *Journal of International Economics*, vol. 60, no. 1, pp. 85–107, 2003.
- [6] M. Rout, B. Majhi, R. Majhi, and G. Panda, "Forecasting of currency exchange rates using an adaptive ARMA model with differential evolution based training," *Journal of King Saud University-Computer and Information Sciences*, vol. 26, no. 1, pp. 7–18, 2014.
- [7] P. Mondal, L. Shit, and S. Goswami, "Study of effectiveness of time series modeling (ARIMA) in forecasting stock prices," *International Journal of Computer Science, Engineering and Applications*, vol. 4, no. 2, pp. 13–29, 2014.
- [8] A. A. Drakos, G. P. Kouretas, and L. P. Zarangas, "Forecasting financial volatility of the Athens stock exchange daily returns: an application of the asymmetric normal mixture GARCH model," *International Journal of Finance & Economics*, vol. 15, pp. 331–350, 2010.
- [9] D. Alberg, H. Shalim, and R. Yosef, "Estimating stock market volatility using asymmetric GARCH models," *Applied Financial Economics*, vol. 18, no. 15, pp. 1201–1208, 2008.
- [10] R. P. Pradhan and R. Kumar, "Forecasting exchange rate in India: an application of artificial neural network model," *Journal of Mathematics Research*, vol. 2, pp. 111–117, 2010.
- [11] S. T. A. Niaki and S. Hoseinzade, "Forecasting S&P 500 index using artificial neural networks and design of experiments," *Journal of Industrial Engineering International*, vol. 9, pp. 1–9, 2013.
- [12] S. P. Das and S. Padhy, "A novel hybrid model using teaching-learning-based optimization and a support vector machine for commodity futures index forecasting," *International Journal of Machine Learning and Cybernetics*, vol. 9, no. 1, pp. 97–111, 2018.
- [13] M. K. Okasha, "Using support vector machines in financial time series forecasting," *International Journal of Statistics and Applications*, vol. 4, pp. 28–39, 2014.
- [14] X. Li, H. Xie, R. Wang et al., "Empirical analysis: stock market prediction via extreme learning machine," *Neural Computing and Applications*, vol. 27, no. 1, pp. 67–78, 2016.
- [15] T. Moudiki, F. Planchet, and A. Cousin, "Multiple time series forecasting using quasi-randomized functional link neural networks," *Risks*, vol. 6, no. 1, pp. 22–42, 2018.
- [16] Y. Baek and H. Y. Kim, "ModAugNet: a new forecasting framework for stock market index value with an overfitting prevention LSTM module and a prediction LSTM module," *Expert Systems with Applications*, vol. 113, pp. 457–480, 2018.
- [17] C. N. Babu and B. E. Reddy, "A moving-average filter based hybrid ARIMA-ANN model for forecasting time series data," *Applied Soft Computing*, vol. 23, pp. 27–38, 2014.
- [18] M. Kumar and M. Thenmozhi, "Forecasting stock index returns using ARIMA-SVM, ARIMA-ANN, and ARIMA-random forest hybrid models," *International Journal of Banking, Accounting and Finance*, vol. 5, no. 3, pp. 284–308, 2014.
- [19] C.-M. Hsu, "A hybrid procedure with feature selection for resolving stock/futures price forecasting problems," *Neural Computing and Applications*, vol. 22, no. 3-4, pp. 651–671, 2013.
- [20] S. Lahmieri, "A variational mode decomposition approach for analysis and forecasting of economic and financial time series," *Expert Systems with Applications*, vol. 55, pp. 268–273, 2016.
- [21] L.-J. Kao, C.-C. Chiu, C.-J. Lu, and C.-H. Chang, "A hybrid approach by integrating wavelet-based feature extraction with MARS and SVR for stock index forecasting," *Decision Support Systems*, vol. 54, no. 3, pp. 1228–1244, 2013.
- [22] T. Li, Y. Zhou, X. Li, J. Wu, and T. He, "Forecasting daily crude oil prices using improved CEEMDAN and ridge regression-based predictors," *Energies*, vol. 12, no. 19, pp. 3603–3628, 2019.
- [23] A. Bagheri, H. Mohammadi Peyhani, and M. Akbari, "Financial forecasting using ANFIS networks with quantum-behaved particle swarm optimization," *Expert Systems with Applications*, vol. 41, no. 14, pp. 6235–6250, 2014.
- [24] J. Wang, R. Hou, C. Wang, and L. Shen, "Improved v-Support vector regression model based on variable selection and brain storm optimization for stock price forecasting," *Applied Soft Computing*, vol. 49, pp. 164–178, 2016.
- [25] G. Claeskens, J. R. Magnus, A. L. Vasnev, and W. Wang, "The forecast combination puzzle: a simple theoretical explanation," *International Journal of Forecasting*, vol. 32, no. 3, pp. 754–762, 2016.
- [26] S. G. Hall and J. Mitchell, "Combining density forecasts," *International Journal of Forecasting*, vol. 23, no. 1, pp. 1–13, 2007.
- [27] N. E. Huang, Z. Shen, S. R. Long et al., "The empirical mode decomposition and the Hilbert spectrum for nonlinear and non-stationary time series analysis," *Proceedings of the Royal Society of London. Series A: Mathematical, Physical and Engineering Sciences*, vol. 454, no. 1971, pp. 903–995, 1998.
- [28] Z. Wu and N. E. Huang, "Ensemble empirical mode decomposition: a noise-assisted data analysis method," *Advances in Adaptive Data Analysis*, vol. 1, no. 1, pp. 1–41, 2009.
- [29] M. E. Torres, M. A. Colominas, G. Schlotthauer, and P. Flandrin, "A complete ensemble empirical mode decomposition with adaptive noise," in *Proceedings of the 2011 IEEE International Conference on Acoustics, Speech and Signal Processing (ICASSP)*, pp. 4144–4147, IEEE, Prague, Czech Republic, May 2011.

- [30] J. Wu, T. Zhou, and T. Li, "Detecting epileptic seizures in EEG signals with complementary ensemble empirical mode decomposition and extreme gradient boosting," *Entropy*, vol. 22, no. 2, pp. 140–165, 2020.
- [31] T. Li, Z. Hu, Y. Jia, J. Wu, and Y. Zhou, "Forecasting crude oil prices using ensemble empirical mode decomposition and sparse Bayesian learning," *Energies*, vol. 11, no. 7, pp. 1882–1905, 2018.
- [32] T. Li, M. Zhou, C. Guo et al., "Forecasting crude oil price using EEMD and RVM with adaptive PSO-based kernels," *Energies*, vol. 9, no. 12, p. 1014, 2016.
- [33] M. A. Colominas, G. Schlotthauer, and M. E. Torres, "Improved complete ensemble EMD: a suitable tool for biomedical signal processing," *Biomedical Signal Processing and Control*, vol. 14, pp. 19–29, 2014.
- [34] J. Wu, F. Miu, and T. Li, "Daily crude oil price forecasting based on improved CEEMDAN, SCA, and RVFL: a case study in WTI oil market," *Energies*, vol. 13, no. 7, pp. 1852–1872, 2020.
- [35] T. Li, Z. Qian, and T. He, "Short-term load forecasting with improved CEEMDAN and GWO-based multiple kernel ELM," *Complexity*, vol. 2020, Article ID 1209547, 20 pages, 2020.
- [36] W. Yang, J. Wang, T. Niu, and P. Du, "A hybrid forecasting system based on a dual decomposition strategy and multi-objective optimization for electricity price forecasting," *Applied Energy*, vol. 235, pp. 1205–1225, 2019.
- [37] W. Deng, J. Xu, Y. Song, and H. Zhao, "An effective improved co-evolution ant colony optimization algorithm with multi-strategies and its application," *International Journal of Bio-Inspired Computation*, vol. 16, pp. 1–10, 2020.
- [38] S. Mirjalili and A. Lewis, "The whale optimization algorithm," *Advances in Engineering Software*, vol. 95, pp. 51–67, 2016.
- [39] I. Aljarah, H. Faris, and S. Mirjalili, "Optimizing connection weights in neural networks using the whale optimization algorithm," *Soft Computing*, vol. 22, no. 1, pp. 1–15, 2018.
- [40] J. Wang, P. Du, T. Niu, and W. Yang, "A novel hybrid system based on a new proposed algorithm-Multi-Objective Whale Optimization Algorithm for wind speed forecasting," *Applied Energy*, vol. 208, pp. 344–360, 2017.
- [41] Z. Alameer, M. A. Elaziz, A. A. Ewees, H. Ye, and Z. Jianhua, "Forecasting gold price fluctuations using improved multi-layer perceptron neural network and whale optimization algorithm," *Resources Policy*, vol. 61, pp. 250–260, 2019.
- [42] Y.-H. Pao, G.-H. Park, and D. J. Sobajic, "Learning and generalization characteristics of the random vector functional-link net," *Neurocomputing*, vol. 6, no. 2, pp. 163–180, 1994.
- [43] L. Zhang and P. N. Suganthan, "A comprehensive evaluation of random vector functional link networks," *Information Sciences*, vol. 367–368, pp. 1094–1105, 2016.
- [44] Y. Ren, P. N. Suganthan, N. Srikanth, and G. Amaratunga, "Random vector functional link network for short-term electricity load demand forecasting," *Information Sciences*, vol. 367–368, pp. 1078–1093, 2016.
- [45] L. Tang, Y. Wu, and L. Yu, "A non-iterative decomposition-ensemble learning paradigm using RVFL network for crude oil price forecasting," *Applied Soft Computing*, vol. 70, pp. 1097–1108, 2018.
- [46] T. Li, J. Shi, X. Li, J. Wu, and F. Pan, "Image encryption based on pixel-level diffusion with dynamic filtering and DNA-level permutation with 3D Latin cubes," *Entropy*, vol. 21, no. 3, pp. 319–340, 2019.
- [47] J. Wu, J. Shi, and T. Li, "A novel image encryption approach based on a hyperchaotic system, pixel-level filtering with variable kernels, and DNA-level diffusion," *Entropy*, vol. 22, pp. 5–24, 2020.
- [48] T. Li, M. Yang, J. Wu, and X. Jing, "A novel image encryption algorithm based on a fractional-order hyperchaotic system and DNA computing," *Complexity*, vol. 2017, Article ID 9010251, 13 pages, 2017.
- [49] H. Zhao, J. Zheng, W. Deng, and Y. Song, "Semi-supervised broad learning system based on manifold regularization and broad network," *IEEE Transactions on Circuits and Systems I: Regular Papers*, vol. 67, no. 3, pp. 983–994, 2020.
- [50] S. Sun, S. Wang, and Y. Wei, "A new multiscale decomposition ensemble approach for forecasting exchange rates," *Economic Modelling*, vol. 81, pp. 49–58, 2019.
- [51] T. Li and M. Zhou, "ECG classification using wavelet packet entropy and random forests," *Entropy*, vol. 18, no. 8, p. 285, 2016.
- [52] H. Zhao, H. Liu, J. Xu, and W. Deng, "Performance prediction using high-order differential mathematical morphology gradient spectrum entropy and extreme learning machine," *IEEE Transactions on Instrumentation and Measurement*, vol. 69, pp. 4165–4172, 2019.
- [53] W. Deng, H. Liu, J. Xu, H. Zhao, and Y. Song, "An improved quantum-inspired differential evolution algorithm for deep belief network," *IEEE Transactions on Instrumentation and Measurement*, vol. 69, no. 10, pp. 7319–7327, 2020.
- [54] H. Liu, Z. Duan, F.-Z. Han, and Y.-F. Li, "Big multi-step wind speed forecasting model based on secondary decomposition, ensemble method and error correction algorithm," *Energy Conversion and Management*, vol. 156, pp. 525–541, 2018.
- [55] Fred Website. <https://fred.stlouisfed.org/>.
- [56] NetEase Website. <http://quotes.money.163.com/service/chddata.html?code=0000001&start=19901219>.
- [57] M. Aiolfi and A. Timmermann, "Persistence in forecasting performance and conditional combination strategies," *Journal of Econometrics*, vol. 135, no. 1–2, pp. 31–53, 2006.

Research Article

An Analytical Optimisation Framework for Airport Terminal Capacity Expansion

Sultan Alodhaibi ¹, Robert L. Burdett,² and Prasad K. D. V. Yarlagadda³

¹Department of Mathematics, College of Sciences and Arts in Al-Rass, Qassim University, Buraidah 51921, Saudi Arabia

²School of Mathematical Science, Science and Engineering Faculty, Queensland University of Technology, Brisbane, QLD 4001, Australia

³School of Mechanical Medical and Process Engineering, Science and Engineering Faculty, Queensland University of Technology, Brisbane, QLD 4001, Australia

Correspondence should be addressed to Sultan Alodhaibi; sathaieby@qu.edu.sa

Received 5 May 2020; Revised 26 June 2020; Accepted 29 July 2020; Published 5 October 2020

Guest Editor: Baogui Xin

Copyright © 2020 Sultan Alodhaibi et al. This is an open access article distributed under the Creative Commons Attribution License, which permits unrestricted use, distribution, and reproduction in any medium, provided the original work is properly cited.

This article considers how to allocate additional physical resources within airport terminals. An optimization model was developed to determine where additional resources should be placed to minimise passenger waiting times. The objective function is stochastic and can only be evaluated using discrete event simulation. As this model is stochastic and nonlinear, a Simulated Annealing (SA) metaheuristic was implemented and tested. The SA algorithm repeatedly perturbs a resource allocation solution using one of two methods. The first method is creating new solution randomly in each iteration, and the second method is local search that is mimicked by any move of the current solution of x solution chosen randomly in its neighborhood. Numerical testing shows that the random approach is best, and solutions that are 12.11% better can be obtained.

1. Introduction

The high growth in passenger numbers in recent years has created considerable strains on airports. Airport terminals are expected to process the increasing passenger numbers efficiently and with minimum delay. At the same time, the required expansion of the airport capacity might be limited by the available resources (e.g., limited available land), environmental impacts, and lengthy approval processes [1]. In addition, extension of the major airport infrastructure is typically time-consuming and costly, which raises the need for the development of smart systems and methods to improve airport performance within the available infrastructure.

Airport terminals are complex systems and are inherently stochastic in nature. Passenger numbers continually change throughout the day, depending on the status of incoming or outgoing flights. It is an integrated system, and operational problems within any of its internal processes can

jeopardise the performance of other elements, creating significant bottlenecks, long passenger queues, congestion, and overall delays [2–4]. For example, disruption, congestion, and uneven passenger inflow into the terminal processing points, caused by the operation of the landside element (including the infrastructure and facilities associated with the arrival of passengers to the airport), could have a significant impact on the performance of the terminal (such as passenger boarding and take-off procedures). It involves multiple stakeholders, and each is responsible for performing particular terminal process such as check-in, security, and immigration [5].

It is conventional to subdivide airport operations into those relevant to the arrival procedures of incoming passengers and departure procedures for outgoing passengers. The arrival processes and facilities include disembarking, immigration, baggage claim, and quarantine procedures [6]. The departure processes and facilities include check-in, security screening, immigration and customs, boarding, and

take-off procedures. It is these departure flow processes that have the greatest impact on the entire operation of passenger terminals and other elements of the airport. According to Neufville and Odoni [7], the departure process requires significantly more time than the arrival process because it sometimes involves services provided to transit passengers. Due to the complex structure of airport terminals, the development of an analytical optimization framework for studying passengers flow in airports under uncertainty of future demand is a difficult task. These difficulties and challenges have led to studies of overall terminal capacity planning problems. Previous studies have generally focused on one element of the terminal or have not accounted for expandability [8]. The general aim of this paper is to propose a mathematical approach for capacity expansion planning. This model will determine where additional resources should be placed within airport terminal processes. Hence, the objective function of the proposed model is to minimise the cost of used resources and the total waiting time. A number of technical constraints exist.

The main contribution of this work is to provide a Capacity Expansion Planning Model (CEPM) for airports. Therefore, this paper has contributed to the body of knowledge by enabling two levels of planning, operational and strategic. In comparison with existing approaches, the new approach is more accurate because real waiting time can be identified and effects of uncertainty can be included. For example, Sun and Schonfeld [9] used mathematical functions, which are more approximate.

2. Related Work

This section analyses existing research conducted to address the issues of passenger flows within airports. The irregular flows occurring in airport terminal areas represent a significant management challenge, for instance, determining the number of service counters to open, and personnel allocation and reallocation issues [5–8, 10, 11]. A significant problem when studying passenger flow is capturing stochastic elements. This is because, as Guizzi et al. [12] argued, passengers behave differently inside airports according to their previous experiences. Thus, in order to assist decision-makers at the airport terminal to address sudden and unforeseen congestion conditions, extensive research has been conducted on uncertainty. Yamada et al. [13] examined links between passenger behavior and facilities and identified several sources of congestion.

Additionally, Alodhaibi et al. [14] conducted their research using a simulation framework developed in [15] to investigate how the arrival pattern of passengers affects international terminal operations. The simulation outcomes provided a better understanding of the behavior of passenger airport access, which could lead to reduced waiting time and possible congestion by increasing the number of working stations (i.e., number of check-in counters) at peak times.

Safety concerns in recent times have caused many changes to security screening procedures and this impacts passenger throughput times. Previous research can be categorized according to related topic areas, including the

significance of the security screening system in airport operations, the capacity of security screening areas, and dynamic system management [16–21]. For instance, Dorton and Liu [21] proposed the application of a DES for the security screening system coupled with a queuing. The aim is to analyze external factors influencing security screening operation efficiency and to identify the effect on throughput and cycle time.

In airport apron areas, a common optimization problem is gate assignment, which considers the minimization of passenger walking distance, from check-in to baggage claim area. Genç et al. [22] applied a heuristic to solve stochastic approaches to minimise the total duration of ungated flight. Similarly, Ding et al. [23] applied a Tabu Search metaheuristic to identify the problem when the number of aircraft exceeds the number of available gates. The two objective functions optimized were number of ungated aircraft and total walking distance. Finally, the research by Mota [24] is noteworthy as a mix of two models was applied to satisfy the different mandatory restricted policies related to airport terminal processing units, such as opening or closing check-in counters for each flight, check-in starting time, and load balance.

Capacity planning problems feature prominently in airport terminal research. For instance, Solak et al. [8] considered terminal operations to be a network system and used a multistage stochastic-integer linear programming model to determine the optimal capacity, taking into account optimal future expansion and desired LOS. The main objective was to minimise the maximum delay of each passageway and processing station by considering the variation in demand as a significant constraint. Also, Sun and Schonfeld [9] investigated uncertainties within the terminal. They found that facility performances are nonlinear functions. These functions are represented by delay level as a function of utilisation rates of capacity and demand fluctuations as indicated by uncertainties in traffic predictions. It is known that passenger departure flow is an important process for any airport facility because of the fixed departure time of flights. The same researchers [25, 26] go further by considering strategic airport facility planning under demand uncertainty and proposed a mixed-integer nonlinear program to determine when and where to adjust process capacity over a number of planning periods. Airport congestion and delay cost are approximated using some appropriate mathematical functions.

The novelty of our work lies in integrating a discrete event simulation to an optimization model for airport terminal capacity planning. Hence, undertaking such research is significant to identify a real waiting time and to know the effect of decision. Other models like Sun and Schonfeld's [9, 27], for instance, use mathematical functions, which are exact. Furthermore, in [26], the same authors used a discrete approximation technique when the model is solved where the mathematical relations in the formulation are accurate. Hence, a simulated annealing metaheuristic was applied to perform airport terminal capacity expansion and this may be the first application of such an approach to this domain.

3. Problem Description and Formulation

This section defines the variables and parameters used in our capacity expansion model. The purpose of the model is to determine where additional resources should be placed in order to reduce the waiting costs. Each resource type has different costs, and a budget for total spending has been provided.

3.1. Model Notation

(i) Indices

p, r, k, t, f : process, resource, passenger types, period, and shift.

(ii) Sets

P, R, K, T, F : processes, resources, passenger types, periods, and shifts.

(iii) Parameters

$\bar{N}_{r,p}, \bar{N}_r$: maximum number of resources of type r in process p and across all processes
 $C_{r,p}$: cost of providing a resource of type r in process p
 $V_{k,p}$: cost incurred per unit of waiting time for passengers of type k in process p
 B : total budget available for capacity expansion
 $n_{r,p}$: current number of resources of type r in process p
 $\tau_{k,p}$: expected time taken to serve passenger k in process p .

(iv) Decision variables

$N_{r,p}$: number of resources to open of type r in process p
 $W_{k,p}$: total waiting time incurred in process p for passengers of type k .

The model is as follows:

$$\text{minimize } \sum_p \sum_r C_{r,p} N_{r,p} + \sum_k \sum_p V_{k,p} W_{k,p} \quad (1)$$

[resource cost + cost of waiting],

subject to

$$N_{r,p} \leq \bar{N}_{r,p}, \quad \forall p \in P; \forall r \in R \quad \text{[upper bound]}, \quad (2)$$

$$\sum_p N_{r,p} \leq \bar{N}_r, \quad \forall r \in R \quad \text{[upper bound]}, \quad (3)$$

$$\sum_r C_{r,p} N_{r,p} \leq B, \quad \forall p \in P \quad \text{[budget constraints]}, \quad (4)$$

$$f_{r,p} \leq F_{r,p}, \quad \forall p \in P; \forall r \in R \quad \text{[shift constraints]}, \quad (5)$$

$$N_{r,p} \geq 0, \quad \forall p \in P; \forall r \in R \quad \text{[positivity]}, \quad (6)$$

$$W_{k,p} = \text{SIMULATE}(N_{r,p}, \tau_{k,p}) \quad (7)$$

[calculation of waiting time via simulation].

The objective function (1) has two components: (i) the cost of purchasing/acquiring additional resources of type r in process p and (ii) the total passenger waiting time converted to a dollar value. Constraints (2) and (3) ensure that the additional resources of type r do not exceed the maximum number of resources. Constraint (4) restricts spending to a particular budget. Constraint (5) restricts the decision variable $N_{r,p}$ to be positive. The waiting time of passengers at different processes is a stochastic auxiliary variable and depends on the number of resources assigned and the processing time, which is a random variable. It is computed using simulation in equation (7) using the simulation model from [11, 15].

3.2. Simulated Annealing. To solve the proposed model, a metaheuristic approach is advocated as constraint (7) cannot be handled using mixed-integer programming, without the application of a simulation model. Of the different metaheuristics, simulated annealing was chosen. It is an effective and computationally fast search algorithm for solving hard optimization problems by Burdett and Kozan [27–29] and is well suited to probabilistic and nonlinear optimization problems. The algorithm is iterative and comprises two nested “for” loops. The outer loop controls and alters the “temperature” parameter T . In the inner loop, a specified number of solution refinements (a.k.a. perturbations) are entertained and evaluated. Refinements are accepted when they are explicitly better; otherwise, they are accepted/rejected probabilistically according to the following function:

$$P(\Delta f) = e^{-1 * (\Delta f / T)}, \quad (8)$$

where $\Delta f = f' - f$ is the difference between the new solution f' and the current solution f . At every temperature, a selected number of perturbations are evaluated. SA requires several parameters (i.e., primary temperature, the cooling rate, the number of function evaluations at every temperature, and the final temperature). At early stages of the search, the temperature is high and many nonimproving moves are accepted. As the search progresses, the temperature is reduced and solutions are only accepted if a strict improvement occurs. With the slow reduction in temperature, worse solutions are accepted with less probability. The SA metaheuristic was implemented in C++ and the simulation model was integrated to evaluate the waiting times. Preliminary numerical testing was performed to identify an appropriate starting temperature (see Figure 1). It is evident from the graph below that the best parameter values of this problem are as follows: temperature (T) = 15000, cooling rate (α) = 0.015, and total number of iterations = 600.

3.2.1. Simulated Annealing Algorithm Description

(1) Phase 1: Create Initial Solution. SA may be initialized with a randomly created solution or via some heuristic/constructive algorithm. However, because of the resource limitation constraints, some of the generated solutions will

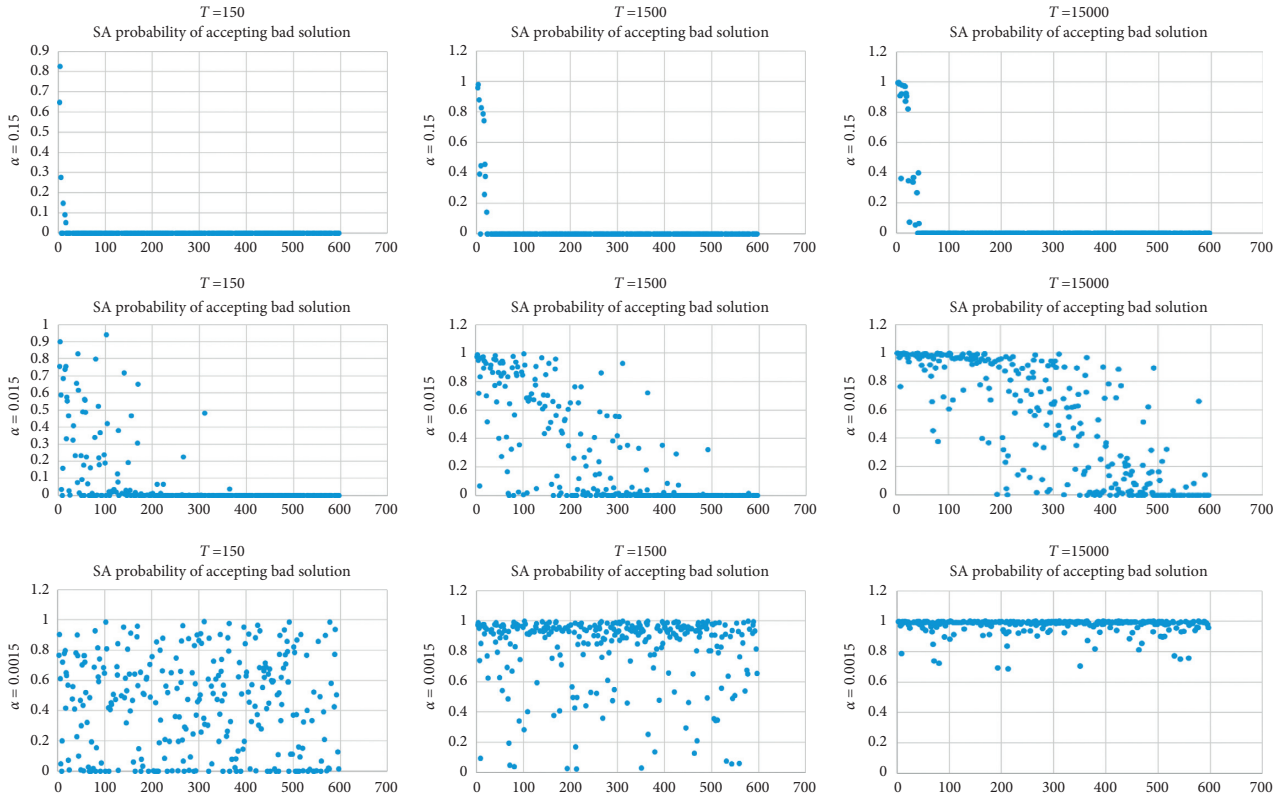


FIGURE 1: Selecting the best initial parameters.

not be feasible. The solution chromosome should simultaneously reflect two main characteristics:

- (i) Number of resources for each process, such as check-in resources (i.e., economy and business counters), security screening resources, and immigration resources (i.e., common counters and SmartGates).
- (ii) The number of assignment resources for each shift.

These solutions should be corrected via a corrective algorithm. Algorithm 1 is used to initialize a set of solutions.

(2) *Phase 2: Perturbing a Solution.* To create a new solution, it is necessary to perturb the current solution. There are many perturbation techniques that can be applied. In this article, a new solution is created by randomly changing the number of resources assigned to a randomly selected airport process. The creation of a new solution is performed by Algorithm 2.

(3) *Phase 3: Assess New Solution.* In this step, the goodness of the new solution is evaluated. Algorithm 3 demonstrates the assessment procedures. The generated solution will be simulated to measure a performance matrix, such as the average waiting time at each processing point. Also, the best cost will be selected by comparing it with the current cost.

(4) *Phase 4: Stop Criteria.* Finally, the condition of stopping the SA algorithm is based on the given maximum number of iterations. Algorithm 4 is an illustration of the main loop of the stopping criteria algorithm.

4. Numerical Testing and Analysis

In this section, the SA metaheuristic approach coupled with discrete event simulation is analyzed. In this numerical investigation, there are three types of process and five types of resources that were considered. Process type 1, the check-in process, has five separate lines, each with eight counters, two for business and six for economy. Process type 2 is security screening with five lanes. Process type 3 is immigration, which has eight common counters and 10 SmartGates. It is assumed that there are three periods during the day to which these processes are assigned to be operated. Figure 2 is a snapshot of the simulation outputs, for instance, the appropriate number of resources that need to be opened, the average waiting time that passengers spent at each process, and the cost of resources ending with the total cost.

The cost of waiting time is considered based on the given policy of acceptable queue time in a particular process. This is named the cost of inconvenience, as it exceeds given acceptable average waiting time. For example, passengers at the check-in process can be classified as business and economy, each with different queue time limits. Kazda and Caves [30] argued that the average waiting time should not be higher than 12 minutes for economy class and 3 minutes for business. The summary of input data used in this study is listed in Table 1.

Two different methods of creating new solutions were used to generate a starting solution. The first is creating a new solution randomly and the second is local search. The

```

(a) For (each Shift);
(2)   For (each process  $p_1$ );
(3)     do
(4)        $N_{r_{1,1},p_1} \leftarrow U(1, r_{1,1})$ ; //Select resources of type 1 in process  $p_1$ 
(5)        $N_{r_{1,2},p_1} \leftarrow U(1, r_{1,2})$ ; //Select resources of type 2 in process  $p_1$ 
(6)        $X \leftarrow N_{r_{1,1},p_1} + N_{r_{1,2},p_1}$ ; economy and business counters;
        } while  $x \leq r_{1,1} + r_{1,2}$ ;
(7)     End
(8)    $N_{r_2,p_2} \leftarrow \text{Uniform}(1, \overline{N}_{r_2,p_2})$ ;
(9)    $N_{r_n,p_n} \leftarrow \text{Uniform}(1, \overline{N}_{r_n,p_n})$ ;
(10)  End

```

ALGORITHM 1: CreateSolution.

```

(1)   If (change in process  $p_1$ );
(3)     while  $x \leq$  number of available  $r_{1,1}$  and  $r_{1,2}$  do
(4)        $N_{r_{1,1},p_1} \leftarrow U(1, r_{1,1})$ ; //Select resources of type 1 in process  $p_1$ 
(5)        $N_{r_{1,2},p_1} \leftarrow U(1, r_{1,2})$ ; //Select resources of type 2 in process  $p_1$ 
(6)        $X \leftarrow N_{r_{1,1},p_1} + N_{r_{1,2},p_1}$ ;
(7)     Else If (change in  $p_2$ )
(8)        $N_{r_2,p_2} \leftarrow U(1, \overline{N}_{r_2,p_2})$ ;
(9)     Else
(10)     $N_{r_n,p_n} \leftarrow U(1, \overline{N}_{r_n,p_n})$ ;

```

ALGORITHM 2: PerturbSolution.

```

(1) Function Local Search();
(2) cost ← Simulate();
(3) If (cost < best);
(4)   Update Best solution;
(5)   best ← cost;
(6) Else
(7)   If (cost < current);
(8)     Update Current solution;
(9)     current ← cost;
(10) Else
(11)    $prob = e^{-1 * ((cost - current) / T)}$ 
(12)   If ( $U(0, 1) > prob$ )
(13)     Reject the new solution;
(14)   Else
(15)     Accept the new solution
(16)

```

ALGORITHM 3: EvaluateSolution.

```

(1) Parameter initialisation
(2) CreateSolution();
(3) Simulate();
(4) do
(5)   PerturbSolution();
(6)   EvaluateSolution();
(7)    $x \leftarrow x + 1$ ;
(8) } while ( $x < max\_iter$ )

```

ALGORITHM 4: Main loop.

random search method initializes SA with a randomly created solution, while the local search initializes SA via constructive algorithm by changing one solution chromosome and then refinement by SA. For each method, 10 runs were repeated with the same parameters. The results of the runs are presented in Tables 2 and 3. The general parameters used for both methods are as follows: temperature (T) = 15000, cooling rate (α) = 0.015, and the maximum number of runs = 1500.

The first column refers to the number of better solutions, where the average number of better solutions obtained by random search approach is 7.9 and the local search approach

is able to find 7.8 better solutions on average. The second column presents the total average waiting time spent in the airport terminal process. It is evident that local search provides lower waiting times compared with the random approach. It also has shorter run-time, with an average of 15.27 minutes compared to 21.05 minutes for the random approach. However, from the results presented in both tables, it can be clearly seen that the random search method reduces the objective function value by 12.11%. The mean μ value of the objective function obtained from the random approach is \$1998.3, whereas μ of objective function value of the local search is \$2256.

From the 10 replications of both random search and local search, solution numbers 4 and 6 from the random search and local search were selected as the best solutions for two reasons. The first reason is that the value of the objective function is closer to the mean value of all the objective values. The second reason is that the chosen simulation runs


```

Line Number      1      2      3      4      5
Class            B  E  B  E  B  E  B  E  B  E
-----|-----|-----|-----|-----|
Shift (1)        1  4  1  2  2  2  2  4  2  2  Screening counters: 5  Immigration counters: 8  SmartGate: 7
Shift (2)        2  3  1  3  1  3  2  3  2  3  Screening counters: 5  Immigration counters: 6  SmartGate: 9
Shift (3)        1  4  2  2  1  1  1  4  1  2  Screening counters: 4  Immigration counters: 2  SmartGate: 3
-----|-----|-----|-----|-----|
                Average WT          WT          Resources
                (minute/Passenger)    cost          cost
check in Avarage WT (B):      1.35863      |      0      |      440
check in Avarage WT (E):      56.0925      |      70      |      840
Screening Avarage WT :      0.359279      |      0      |      210
Immigration Avarage WT :      0.0329785      |      0      |      240
Smart Gate Avarage WT :      0.597841      |      11      |      190
Total Avarage WT:      58.4412  minute/Passenger
Total Cost:      2001  $

```

FIGURE 2: Snapshot of simulated annealing results.

TABLE 1: Summary of the input data.

Domain of the airport	Values
<i>Check-in</i>	
(i) Cost for opening new check-in counter	20\$
(ii) The acceptable average waiting time for economy passengers	12 minutes
(iii) Cost for inconvenience at check-in for economy	15\$
(iv) The acceptable average waiting time for business passengers	3 minutes
(v) Cost for inconvenience at check-in for business	25\$
<i>Security screening</i>	
(i) Cost for opening new security screening desk	15\$
(ii) The acceptable average time that normal passengers should wait	5 minutes
(iii) Cost for inconvenience at security screening for normal passengers	15\$
(iv) The acceptable average time that diplomatic passengers should wait	2 minutes
(v) Cost for inconvenience at security screening for diplomatic passengers	20\$
<i>Immigration</i>	
(i) Cost for opening new immigration desk	15\$
(ii) Cost for opening new SmartGate	10\$
(iii) The acceptable average waiting time at common counter	7 minutes
(iv) Cost for inconvenience at common counters	20 \$
(v) The acceptable average waiting time at SmartGate	0.5 minute
(vi) Cost for inconvenience at SmartGate	10\$

TABLE 2: Summary of simulated annealing results using random search technique.

Run #	# of better solutions	Random search		
		Total average waiting time	Objective function value	Run-time (min)
Run 1	6	118.73	2031	21.05
Run 2	5	58.44	2001	21.16
Run 3	10	126.39	2060	23.48
Run 4	9	39.57	2038	23.43
Run 5	6	64.74	1973	20.24
Run 6	9	148.18	1874	20.55
Run 7	8	112.714	1913	17.36
Run 8	10	86.67	1997	21.55
Run 9	7	127.8	2052	17.36
Run 10	9	131.25	2044	24.36
μ	7.9	101.4484	1998.3	21.054
σ	1.7	34.725498	58.99160957	2.256671

provide the minimum total average waiting time in the airport.

Figure 3 demonstrates the best solution given by the random search for the solution run number 4. The optimal

solution for this simulation run with regard to opening additional resources for check-in is summarized in Table 4. The average waiting time is 1.91 minutes for business-class passengers and 34.5 minutes for economy-class passengers.

TABLE 3: Summary of simulated annealing results using local search technique.

Run #	# of better solutions	Local search		
		Total average waiting time	Objective function value	Run-time (min)
Run 1	7	38.88	2336	13.7
Run 2	10	92.31	2195	14.02
Run 3	9	80.49	2182	15.4
Run 4	10	94.97	2042	15.48
Run 5	8	22.25	2180	17.22
Run 6	8	28.89	2250	22.22
Run 7	8	72.6	1994	12.53
Run 8	8	85.47	2531	17.27
Run 9	4	86.45	2638	12.21
Run 10	6	45.6	2215	13.27
μ	7.8	64.82	2256.3	15.27
σ	1.72	26.45	186.49	2.88

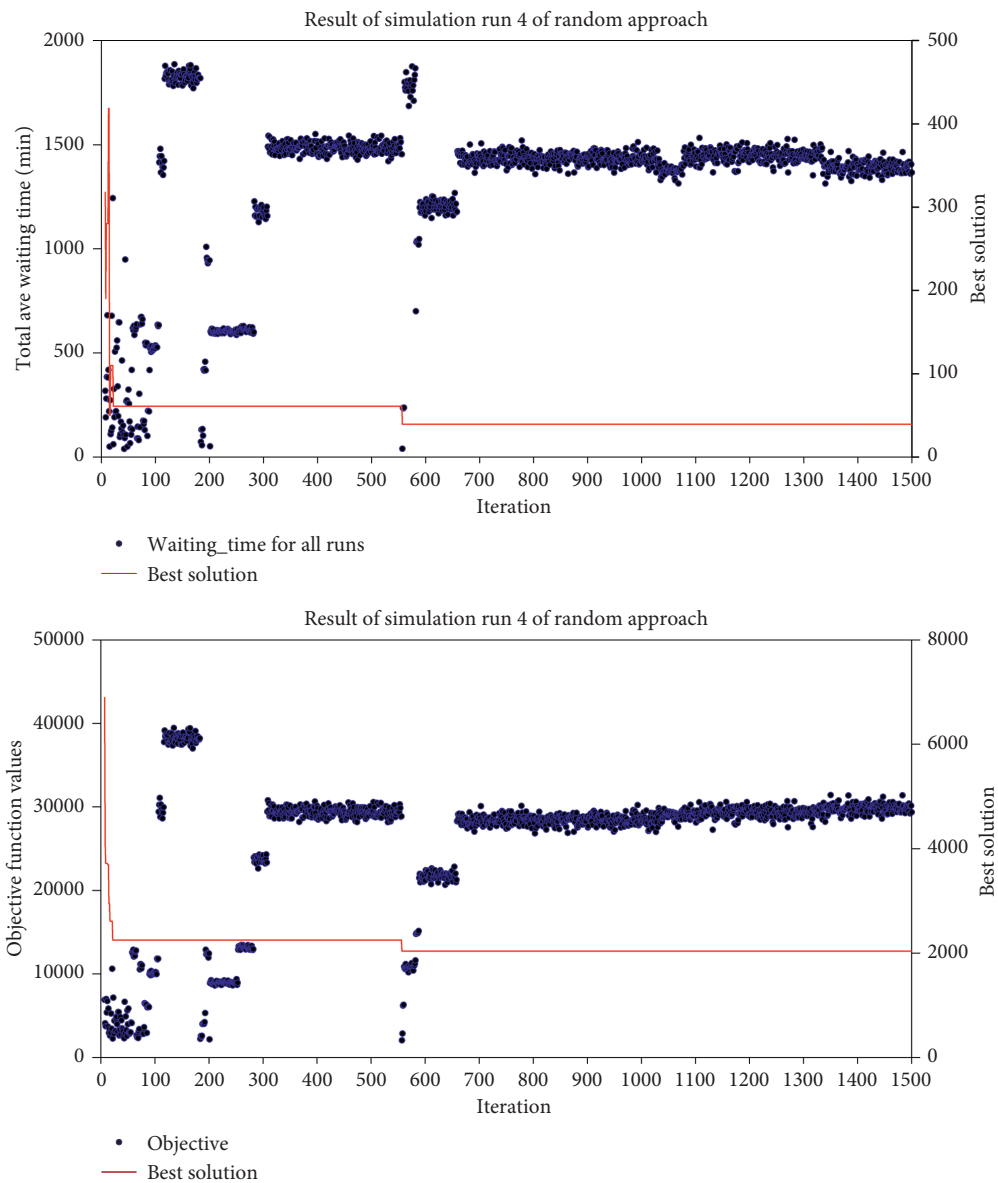


FIGURE 3: SA optimisation results using the random method of creating new solutions.

TABLE 4: Check-in additional resource results using the random technique.

	Line 1		Line 2		Line 3		Line 4		Line 5	
	Business	Economy	Business	Economy	Business	Economy	Business	Economy	Business	Economy
Shift 1	1	4	2	3	2	4	1	4	1	4
Shift 2	2	2	1	1	1	1	1	2	2	4
Shift 3	2	4	1	6	1	6	1	2	2	4

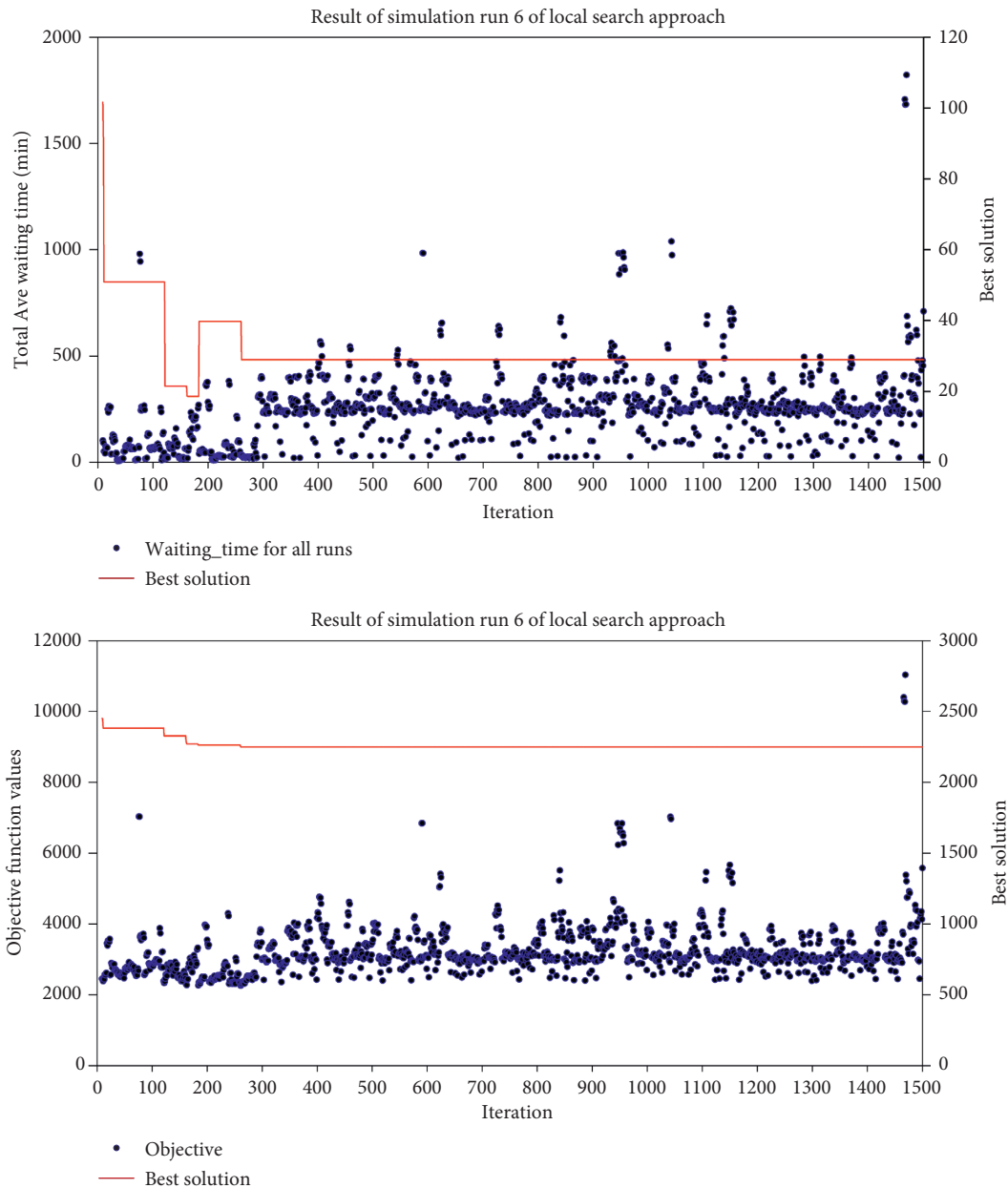


FIGURE 4: Optimisation results using the method of creating new solution using local technique.

For the security screening checkpoints, the opening resources are 5, 2, and 3 control checkpoints for shift 1, shift 2, and shift 3, respectively, having an average waiting time of 3.04 minutes. The opening common immigration process is 4, 3, and 5 counters, while for SmartGates there are 8, 9, and 7 kiosks for the three shifts, having average waiting times of 0.11 and 0.02 minutes for the common immigration desks

and SmartGate kiosk, respectively. The total cost of opening all resources is \$2038 given that the total average time spent in the queues is 39.57 minutes.

Figure 4 illustrates the optimal solution provided by the SA algorithm using local search for creating a new solution. In this simulation run, the solution is characterised from the total cost of \$2250 given that the total average waiting time

TABLE 5: Check-in additional resource results using local technique.

	Line 1		Line 2		Line 3		Line 4		Line 5	
	Business	Economy	Business	Economy	Business	Economy	Business	Economy	Business	Economy
Shift 1	1	4	2	3	3	5	2	5	1	5
Shift 2	2	7	1	2	1	3	4	3	1	4
Shift 3	2	1	2	2	2	2	4	1	2	1

spent in the system is 28.89 minutes. The optimal solution for this simulation run is opening a check-in resource based on the detailed information listed in Table 5. By adding this resource, the average waiting time at the check-in process will be 1.56 minutes for business-class passengers and 7.03 minutes for economy-class passengers, reductions of 20.17% for business-class passengers and 132.29% for economy-class passengers compared with the random search method.

For the process of security screening checkpoints, the best solution can be found when opening 4, 4, and 5 security control checkpoints for shift 1, shift 2, and shift 3, respectively. By opening these numbers of resources at the security screening process, the average waiting time is 7.92 minutes. Finally, the immigration process should open 5, 4, and 3 common immigration counters and 10, 10, and 9 SmartGates for the three shifts, in order to get the optimal solution, having the average waiting of 0.10 minutes and 0.012 minutes for the common counters and SmartGates, respectively.

5. Conclusion

This paper has discussed the development of a mathematical approach to perform capacity planning in airport terminals. The objective of the model is determining where additional resources should be opened to decrease the cost of time spent in the queues of the airport terminal. Since the proposed problem is probabilistic and nonlinear, a meta-heuristic approach is advocated. The waiting times are computed using discrete event simulation and those times are used in the objective function. Two different approaches for creating new solutions were used in this study. The first one is creating a new solution using the random technique and the other is creating a new solution by using the local search technique. The random technique decreased the objective function value by 12.11%. It also has shorter run-times, with average of 15.27 minutes compared to 21.05 minutes for the random approach.

The developed model can be more accurate because the effect of decision can be known and real time can be identified. It also can provide strategic planning, while the proposed simulation model can be used for the operational planning level. This work has contributed to the body of knowledge by enabling two levels of planning, operational and strategic.

On the other hand, the lack of access to the detailed data related to operational facilities due to the recent strict regulations with respect to security issues resulted in some difficulties in developing the modelled passengers' flows within international terminal. Because of these difficulties, this model has been simplified by, firstly, utilizing available

data collected by previous research, and, secondly, making an assumption where needed.

Data Availability

No data were used to support this study.

Conflicts of Interest

The authors declare that they have no conflicts of interest.

Authors' Contributions

Dr. Sultan Alodhaibi mainly undertook this research as a Ph.D. student and formulated and conducted the experimental design. He designed, developed, and tested the simulation models and wrote the main manuscript. Dr. Robert L. Burdett provided necessary guidance for mathematical optimisation of simulation models and interpretation of the simulation results. Professor Prasad K. D. V. Yarlagadda conceived the project and got necessary infrastructure and funding for undertaking this research. He also planned and helped in design of simulation model and related experiments and supervised and oversaw the full project from its inceptual stage to final stages of delivery. All authors reviewed and commented on the manuscript.

Acknowledgments

This research was supported by the Australian Research Council's Linkage Project "Improving Productivity and Efficiency of Australian Airports" (140100282). The authors would like to acknowledge QUT High Performance Computing (HPC) for providing the computational resources for this research.

References

- [1] C. Barnhart, D. Fearing, A. Odoni, and V. Vaze, "Demand and capacity management in air transportation," *EURO Journal on Transportation and Logistics*, vol. 1, no. 1-2, pp. 135-155, 2012.
- [2] R. D. Neufville and A. Odoni, *Airport Systems: Planning, Design and Management*, McGraw-Hill Professional, New York, NY, USA, 2003.
- [3] K. G. Zografos and M. A. Madas, "Development and demonstration of an integrated decision support system for airport performance analysis," *Transportation Research Part C: Emerging Technologies*, vol. 14, no. 1, pp. 1-17, 2006.
- [4] I. E. Manataki and K. G. Zografos, "A generic system dynamics based tool for airport terminal performance analysis," *Transportation Research Part C: Emerging Technologies*, vol. 17, no. 4, pp. 428-443, 2009.

- [5] P. P.-Y. Wu and K. Mengersen, "A review of models and model usage scenarios for an airport complex system," *Transportation Research Part A: Policy and Practice*, vol. 47, pp. 124–140, 2013.
- [6] S. Alodhaibi, R. L. Burdett, and P. K. Yarlagadda, "A model to simulate passenger flow congestion in airport environment," *International Journal of Engineering & Technology*, vol. 7, no. 4, pp. 6943–6946, 2018.
- [7] R. D. Neufville and A. R. Odoni, *Airport Systems: Planning, Design, and Management*, McGraw-Hill Education, New York, NY, USA, 2013.
- [8] S. Solak, J.-P. B. Clarke, and E. L. Johnson, "Airport terminal capacity planning," *Transportation Research Part B: Methodological*, vol. 43, no. 6, pp. 659–676, 2009.
- [9] Y. Sun and P. Schonfeld, "Stochastic capacity expansion models for airport facilities," *Transportation Research Part B: Methodological*, vol. 80, pp. 1–18, 2015.
- [10] P. Fonseca, J. Casanovas, and X. Ferran, "Passenger flow simulation in a hub airport: an application to the Barcelona international airport," *Simulation Modelling Practice and Theory*, vol. 44, pp. 78–94, 2014.
- [11] S. Alodhaibi, R. L. Burdett, and P. K. D. V. Yarlagadda, "A framework for sharing staff between outbound and inbound airport processes," *Mathematics*, vol. 8, no. 6, p. 895, 2020.
- [12] G. Guizzi, T. Murino, and E. Romano, "A discrete event simulation to model passenger flow in the airport terminal," in *Proceedings of the 11th WSEAS International Conference on Mathematical Methods and Computational Techniques in Electrical Engineering (MMACTEE'09)*, Athens, Greece, September 2009.
- [13] H. Yamada, K. Otori, T. Iwao et al., "Modeling and managing airport passenger flow under uncertainty: a case of Fukuoka airport in Japan," in *Social Informatics*, pp. 419–430, Springer-Verlag, Cham, Switzerland, 2017.
- [14] S. Alodhaibi, R. L. Burdett, and P. K. D. V. Yarlagadda, "Impact of passenger-arrival patterns in outbound processes of airports," *Procedia Manufacturing*, vol. 30, pp. 323–330, 2019.
- [15] S. Alodhaibi, R. L. Burdett, and P. K. Yarlagadda, "Framework for airport outbound passenger flow modelling," *Procedia Engineering*, vol. 174, pp. 1100–1109, 2017.
- [16] K. Leone and R. Liu, "Improving airport security screening checkpoint operations in the US via paced system design," *Journal of Air Transport Management*, vol. 17, no. 2, pp. 62–67, 2011.
- [17] J. V. Boekhold, A. Faghri, and M. Li, "Evaluating security screening checkpoints for domestic flights using a general microscopic simulation model," *Journal of Transportation Security*, vol. 7, no. 1, pp. 45–67, 2014.
- [18] A. Kierzkowski and T. Kisiel, "Simulation model of security control system functioning: a case study of the Wrocław airport terminal," *Journal of Air Transport Management*, vol. 64, no. Part B, pp. 173–185, 2016.
- [19] J. Skorupski and P. Uchroński, "Managing the process of passenger security control at an airport using the fuzzy inference system," *Expert Systems with Applications*, vol. 54, pp. 284–293, 2016.
- [20] A. Kierzkowski and T. Kisiel, "Evaluation of a security control lane with the application of fuzzy logic," *Procedia Engineering*, vol. 187, pp. 656–663, 2017.
- [21] S. Dorton and D. Liu, "Effects of baggage volume and alarm rate on airport security screening checkpoint efficiency using queuing networks and discrete event simulation," *Human Factors and Ergonomics in Manufacturing & Service Industries*, vol. 26, no. 1, pp. 95–109, 2016.
- [22] H. M. Genç, O. K. Erol, İ. Eksin, M. F. Berber, and B. O. Güleriyüz, "A stochastic neighborhood search approach for airport gate assignment problem," *Expert Systems with Applications*, vol. 39, no. 1, pp. 316–327, 2012.
- [23] H. Ding, A. Lim, B. Rodrigues, and Y. Zhu, "The over-constrained airport gate assignment problem," *Computers & Operations Research*, vol. 32, no. 7, pp. 1867–1880, 2005.
- [24] M. M. Mota, "Check-in allocation improvements through the use of a simulation–optimization approach," *Transportation Research Part A: Policy and Practice*, vol. 77, pp. 320–335, 2015.
- [25] Y. Sun and P. M. Schonfeld, "Capacity investment model for airport facilities under demand uncertainty," *Journal of Advanced Transportation*, vol. 50, no. 8, pp. 1896–1911, 2016.
- [26] Y. Sun and P. M. Schonfeld, "Coordinated airport facility development under uncertainty," *Transportation Research Record: Journal of the Transportation Research Board*, vol. 2603, no. 1, pp. 78–88, 2017.
- [27] R. L. Burdett and E. Kozan, "Sequencing and scheduling in flowshops with task redistribution," *Journal of the Operational Research Society*, vol. 52, no. 12, pp. 1379–1389, 2001.
- [28] R. L. Burdett and E. Kozan, "An integrated approach for earthwork allocation, sequencing and routing," *European Journal of Operational Research*, vol. 238, no. 3, pp. 741–759, 2014.
- [29] R. L. Burdett, P. Corry, P. K. D. V. Yarlagadda, C. Eustace, and S. Smith, "A flexible job shop scheduling approach with operators for coal export terminals—a mature approach," *Computers and Operational Research*, vol. 104, pp. 15–36, 2019.
- [30] A. Kazda and R. E. Caves, *Airport Design and Operation*, Emerald Group Publishing Limited, Bingley, UK, 2015.

Research Article

Scheduling on a Single Machine and Parallel Machines with Batch Deliveries and Potential Disruption

Hua Gong ^{1,2}, Yuyan Zhang,¹ and Puyu Yuan ¹

¹College of Science, Shenyang Ligong University, Shenyang 110159, China

²Key Laboratory of Data Analytics and Optimization for Smart Industry (Northeastern University), Ministry of Education, Shenyang 110819, China

Correspondence should be addressed to Hua Gong; gonghua@sylu.edu.cn and Puyu Yuan; 452983100@qq.com

Received 8 May 2020; Revised 30 June 2020; Accepted 20 July 2020; Published 14 September 2020

Guest Editor: Baogui Xin

Copyright © 2020 Hua Gong et al. This is an open access article distributed under the Creative Commons Attribution License, which permits unrestricted use, distribution, and reproduction in any medium, provided the original work is properly cited.

In this paper, we study several coordinated production-delivery scheduling problems with potential disruption motivated by a supply chain in the manufacturing industry. Both single-machine environment and identical parallel-machine environment are considered in the production part. The jobs finished on the machines are delivered to the same customer in batches. Each delivery batch has a capacity and incurs a delivery cost. There is a situation that a possible disruption in the production part may occur at some particular time and will last for a period of time with a probability. We consider both resumable case and nonresumable case where a job does not need (needs) to restart if it is disrupted for a resumable (nonresumable) case. The objective is to find a coordinated schedule of production and delivery that minimizes the expected total flow times plus the delivery costs. We first present some properties and analyze the NP-hard complexity for four various problems. For the corresponding single-machine and parallel-machine scheduling problems, pseudo-polynomial-time algorithms and fully polynomial-time approximation schemes (FPTASs) are presented in this paper, respectively.

1. Introduction

Production scheduling and delivery decision are two key operations in the supply chain management. Coordinated production and delivery schedules play an important role in improving optimal operational performance in the supply chain of high energy-consuming manufacturing industry. However, traditionally, the scheduling decisions of coordinated production and delivery in a firm are often made in a certain environment. In a real industry, the production scheduling environment is dynamic and uncertain. Unexpected events may occur from some time point and will last a period. There is a situation that the internal and external factors cause various disruptions since the machines or facilities are disrupted and unavailable for a certain period of time during production, such as material shortages, machine breakdowns, power failures, quality issues, and others. This will lead to affect production efficiency, extra energy consumption, and logistics management in the service system.

For example, in the iron and steel industry, the slabs are first rolled into the coils in the hot rolling mill. The coils are transported by the trucks to the customers or the downstream facilities for further processing. The slabs need high temperature to ensure to be processed on the hot rolling machines. If the disruption occurs on the hot rolling machines, it will lead to the temperature decrease of the slabs. When the disruption time exceeds a limit, the slabs must return to the heating furnaces to re-heat to keep high temperature. This disruption will not only affect the production rhythm and increase the energy consumption in the mill but also influence the delivery decision for the customers. Hence, the reasonable scheduling for the disruption affects the revenue in the iron and steel industry. The inventory level and the total delivery cost are the major concerns for the industry managers. The inventory level is measured by a function of the flow time when the finished coils arrive to the customers. It is well understood that coordinated scheduling of production and delivery can

significantly improve inventory level and reduce delivery cost.

In this paper, we study several coordinated production-delivery scheduling problems with potential disruption motivated by the dynamic and uncertain environment. All the jobs are first finished processing on the machines and then delivered to the customers in batches. A possible disruption in the production part may occur at a particular time and will last for a period of time with a probability. We investigate the optimal strategies on how to deal with disruptions in scheduling in the single-machine environment and identical parallel-machine environment, respectively. The objective is to find a feasible schedule to minimize the expected total flow times and the delivery costs.

Many coordinated scheduling problems with production and delivery in most manufacturing systems consider the balance relationship between the finished products and the transportation or delivery. Chen [1] presented a survey of integrated production and outbound distribution scheduling with batch delivery. Wang et al. [2] provided a survey of the integrated scheduling models of production and distribution. The coordinated scheduling problems of production and transportation with batching decisions in the iron and steel industry are considered in [3–6]. Some researchers addressed production and distribution scheduling of minimizing the sum of the total (weighted) flow time and delivery cost from a batch delivery point of view. This environment is related to batching because all the completed jobs are delivered in batches to the customer. Hall and Potts [7] considered the single-machine or identical parallel-machine scheduling problems in supply chain with batch deliveries. Wang and Cheng [8] considered a parallel-machine scheduling problem with batch delivery cost where the batch delivery date is equal to the completion time of the last job in a batch. Chen and Vairaktarakis [9] considered the single-machine and parallel-machine scheduling problems with distribution scheduling and routing for delivery of completed jobs to the customers. Wan and Zhang [10] studied the extension of the parallel-machine scheduling problem with batch delivery. The above scheduling literatures do not deal with the coordination of production and delivery related to potential disruptions.

The research on machine scheduling with potential disruption has some results in a significant amount of interest in production scheduling research. Lee and Yu [11] considered the single-machine scheduling problems with potential disruptions due to external factors where the objective functions are the expected total weighted completion times and the expected maximum tardiness. Lee and Yu [12] further considered the parallel-machine problems to minimize the expected total weighted completion time. Yin et al. [13] considered the parallel-machine scheduling problems with deterioration in a disruptive environment in which the machines may be unavailable due to potential disruptions. Zheng and Fan [14] studied the parallel-machine scheduling problems with position-dependent processing times under potential disruption. Lee et al. [15] considered a two-machine scheduling problem with disruptions and transportation considerations. In [15], once

one machine undergoes disruption and is unavailable, the jobs can either be moved to other available machines for processing, which consider transportation time and transportation cost, or be processed by the same machine after the disruption.

In this paper, we study coordinated scheduling problems with potential disruption and batch deliveries considering single machine or identical parallel machines. Our problem is an extension of the problem proposed by Gong et al. [6] and Hall and Potts [7], who studied the single-machine and parallel-machine scheduling problems with batch delivery without potential disruption. On the other hand, our problem is a natural extension of the problem proposed by Lee and Yu [12], who studied the parallel-machine problem under potential disruption without production and delivery coordination. We develop coordinated scheduling on the single machine and parallel machines with both batch deliveries and potential disruption in this paper. Both resumable case and nonresumable case are considered in this paper where a job does not need (needs) to restart if it is disrupted for a resumable (nonresumable) case. The objective is to minimize the sum of the expected total flow time and total delivery costs. To the best of our knowledge, the scheduling problems with batch deliveries and potential disruption on the single machine and parallel machines have never been discussed. In this paper, we first pinpoint the difficulty by reducing the problems to be NP-hard. We also present pseudo-polynomial-time algorithms to solve these problems and further show that the problems proposed in this paper are NP-hard in the ordinary sense, respectively. Finally, we provide fully polynomial-time approximation schemes via the scaling and trimming techniques to solve the problems.

For many NP-hard scheduling problems, it will be clearly hard to find optimal schedules in a time-effective manner. The existence of a pseudo-polynomial-time algorithm for a NP-hard problem means that this NP-hard problem is ordinarily NP-hard, but not strongly NP-hard [16]. A fully polynomial-time approximation scheme (FPTAS) for a problem is an approximation scheme with a time complexity that is polynomial in the input size n and in $1/\varepsilon$ for any given $\varepsilon > 0$. With regard to worst-case approximations, an FPTAS is the strongest possible polynomial-time approximation result that one can obtain for an NP-hard problem unless $P = NP$ [17].

The rest of the paper is organized as follows. We introduce the problem description and some properties in Section 2. In Section 3, we provide the algorithms and approximation schemes for the single-machine scheduling problems. Section 4 deals with two-parallel-machine problems and develops the corresponding algorithms and approximation schemes. Section 5 provides a conclusion and some suggestions for future research.

2. Problem Description and Notation

In this section, we describe our problems briefly. There are n jobs $\{J_1, \dots, J_n\}$ to be first processed on either a single machine or m identical parallel machines M_1, \dots, M_m , all to

be delivered in batches to the same customer. Each machine can process at most one job at a time. All the jobs are available for processing at initial time. For job J_j , let a_j and C_j be the processing time and the completion time on the machine, respectively. Preemption may happen for some jobs if potential disruption of some machines happens. We assume that a machine disruption occurs at time point r and will last for α time units ($\alpha = 0, 1, \dots, \gamma$) with a certain probability p_α . The machines are the same for all the disrupted machines once the disruption occurs. Here, p_0 is the probability that the potential disruption will not happen and the machine is always available. Without loss of generality, we assume the machine disruption situation that the disruption may happen simultaneously on the first k machines M_1, \dots, M_k , with $1 \leq k \leq m$. Let $A_j = \sum_{i=1}^j a_i$ represent the total processing time for the first jobs J_1, \dots, J_j . Set $a_{\max} = \max\{a_j : j = 1, \dots, n\}$.

Once the disruption machines have unavailable time intervals $[r, r + \alpha]$, the disrupted jobs need to restart on the machines. We consider two cases: resumable and non-resumable. If a job is disrupted during processing on some disrupted machine, it is called resumable (nonresumable) that the job does not need (needs) to restart when the machine becomes available again. For the resumable case, the remaining part of the disrupted job will continue at time point $r + \alpha$ without any penalty. For the nonresumable case, the disrupted job needs to restart at time point $r + \alpha$.

In the delivery part, a fleet of transporter for delivering the jobs in batches to the same customer will be viewed as a single transporter because they have common departure times and return times. A group of jobs forms a delivery batch B_j if all of these jobs are delivered to the customer simultaneously. The number of jobs in a delivery batch cannot exceed the delivery capacity C . Let y be the number of delivery batches for all jobs in a schedule. Delivering a batch will incur a fixed delivery cost D . The single transporter is located at the production area at initial time. Assume that $T/2$ is the transportation time from the machine to the customers, and the return time from the customer to the machine is $T/2$. There is at least minimum time interval T between any consecutive batches. Let F_j denote the flow time of job J_j when it is delivered to the customer. The objective that we consider is to schedule the jobs for production and delivery such that the sum of the expected total flow times $E[\sum F_j]$ and the delivery costs Dy is minimized. The problems considered in this paper can be expressed as $1|T, \text{disruption}|E[\sum F_j] + Dy$ and $P_m|T, \text{disruption}|E[\sum F_j] + Dy$ by adopting the notation introduced by Hall and Potts [7]. The four various problems can be expressed as follows:

- $P1: 1|T, \text{non-resumable, disruption}|E[\sum F_j] + Dy,$
 - $P2: 1|T, \text{resumable, disruption}|E[\sum F_j] + Dy,$
 - $P3: P_m|T, \text{non-resumable, disruption}|E[\sum F_j] + Dy,$
 - $P4: P_m|T, \text{resumable, disruption}|E[\sum F_j] + Dy.$
- (1)

Next, we analyze the complexity of the problems studied in this paper.

For the single-machine scheduling problem with batch deliveries without delivery capacity, problem $1|T| \sum F_j + Dy$ proposed by Hall and Potts [7] is optimal to sequencing the jobs in SPT rule. Note that a special case of our problem $1|T, \text{disruption}|E[\sum F_j] + Dy$, in which the delivery part is ignored and the objective is to minimize $E[\sum C_j]$, was studied by Lee and Yu [11]. On the other hand, even if $p_0 = 1$ (it means that the disruption will certainly happen in a fixed period), problem $1|\text{disruption}|E[\sum C_j]$ in [11] is ordinarily NP-hard. We extend $1|T| \sum F_j + Dy$ to consider disruption constraint and $1|\text{disruption}|E[\sum C_j]$ to consider delivery coordination. Hence, $P1$ and $P2$ proposed in this paper are NP-hard.

For the parallel-machine scheduling problem with batch deliveries, $P_m|T| \sum F_j + Dy$ is shown NP-hard in the ordinary sense by Gong et al. [6] even if the potential disruption does not happen. Hence, $P_m|T, \text{disruption}|E[\sum F_j] + Dy$ is at least NP-hard even if $p_0 = 0$. If the delivery is ignored, two-parallel-machine scheduling problem with potential disruption is already NP-hard even if $p_0 = 1$ as presented by Lee and Yu [12]. Hence, our problems $P3$ and $P4$ are also NP-hard.

In [6, 7], the goal is to determine the job sequencing on the machines and the job partitioning into delivery batches, but not considering the machine potential disruption. In [11, 12], they made the production scheduling decision on potential disruption according to two sequential decisions at 0 and disruption r . In this paper, we need to not only sequence the jobs on the single machine or parallel machines and reschedule the jobs with disruption consideration in the production part but also partition the jobs into delivery batches in the delivery part. In this paper, we will derive the corresponding pseudo-polynomial-time algorithms for problem $1|T, \text{disruption}|E[\sum F_j] + Dy$ and $P_m|T, \text{disruption}|E[\sum F_j] + Dy$ based on dynamic programming, respectively. Furthermore, the fully polynomial-time approximation schemes are provided for four problems that show that the problems are NP-hard in the ordinary sense.

The following properties hold for both resumable and nonresumable cases.

2.1. General Results

Lemma 1. *For $P1$ – $P4$, there exists an optimal schedule without idle time between jobs for any machine except during the machine disruption time interval.*

Lemma 2. *For $P1$ – $P4$, there exists an optimal schedule that all the departure times of delivery batches are made either at the completion times of jobs or at immediate available times of the transporter.*

Lemma 3. *For $P1$ and $P2$, there exists an optimal schedule that the jobs finished no later than r are sequenced in the shortest processing time (SPT) rule, and the remaining jobs finished after r are also sequenced in the SPT rule.*

Proof. Assume an optimal schedule π^* . If π^* contains jobs that are not sequenced in SPT rule, then J_j is followed by J_i where $a_j > a_i$.

- (1) If J_j and J_i are assigned into the same delivery batch, then the jobs can be sequenced in the SPT rule without affecting the objective cost.
- (2) If J_j is the last job in batch B_{l-1} and J_i is the first job in batch B_l , then form a schedule π with $B_{l-1} \cup \{i\} \setminus \{j\}$ and $B_l \cup \{j\} \setminus \{i\}$ by interchanging J_j and J_i . Before r or after r , $B_{l-1} \cup \{i\} \setminus \{j\}$ in schedule π is delivered at the same time as batch B_{l-1} in schedule π^* , and $B_l \cup \{j\} \setminus \{i\}$ in schedule π is delivered at the same time as batch B_l in schedule π^* . All other delivery batches are identical and delivered at the same time in π as in π^* . Hence, the objective cost associated with π is the same as the objective cost associated with π^* . Repeating the argument can find an optimal schedule with SPT rule.

Lemma 4. For P3 and P4, there exists an optimal schedule in which

- (1) The jobs finished no later than r are sorted in the SPT rule on each disrupted machine $M_{\bar{p}}$, $i = 1, \dots, k$, and sorted in the SPT rule on each nondisrupted machine $M_{\bar{p}}$, $i = k+1, \dots, m$, respectively.
- (2) The remaining jobs finished after r are also sorted in the SPT rule on each disrupted machine $M_{\bar{p}}$, $i = 1, \dots, k$.

Proof. For any given scenario α , Lemma 3 shows that the subproblem is optimal to schedule the jobs finished no later than r or after r in the SPT rule when M_i can be viewed as a single machine. For all possible scenarios α and all the machines, this argument holds when the objective is to minimize $E[\sum F_j] + D_y$.

3. Single-Machine Scheduling

In this section, two pseudo-polynomial-time algorithms to solve two single-machine problems with the nonresumable case (P1) and the resumable case (P2) are developed, respectively. Furthermore, we will convert the dynamic programming algorithms into fully polynomial-time approximation schemes (FPTASs) to solve problems P1 and P2. We will recall the definition of an FPTAS in Section 3.3.

3.1. The Nonresumable Case P1. In this section, a pseudo-polynomial-time algorithm based on dynamic programming is presented to solve P1. At first, re-index jobs in the SPT rule. Fix the following variables: jobs J_1, \dots, J_j are assigned to two sets, S and $\{J_1, \dots, J_j\} \setminus S$, such that $\sum_{i \in S} a_i = q \leq r$ and the jobs in S will be processed consecutively without idle time on the single machine from initial time 0. Define t as the starting time of the first job in $\{J_1, \dots, J_j\} \setminus S$ if the disruption does not happen but the first job will finish after time r . It is clear that t ranges from $\max\{q, r - a_{\max} + 1\}$ to r . Let $F(j, q, t, |B_l|)$ be the

expected objective value of a feasible partial schedule for jobs J_1, \dots, J_j , where $|B_l|$ is the number of jobs assigned into delivery batch B_l and the variable q denotes the total actual processing time of jobs in S finished no later than r on the machine. Let $F_{[l]}$ be the delivery completion time of batch B_l , which is the flow time of each job in B_l delivered to the customer. We provide a dynamic programming to solve problem $1|T, \text{nonresumable, disruption}| E[\sum F_j] + D_y$.

Theorem 1. Algorithm 1 (DP1) can solve problem P1 in time complexity $O(n \log n + r^2 n^2)$.

Proof. We first analyze the possible recursive situations. Suppose that jobs J_1, \dots, J_{j-1} have been assigned optimally, and start to assign J_j . In an optimal schedule, J_j will be either the last job processed no later than t or last in the whole sequence. If J_j is assigned no later than t , then it will be completed at least at time q on the machine. On the other hand, if job J_j is assigned last in the whole sequence, then its completion time on the machine is at least $p_0(t + A_j - q) + \sum_{\alpha=1}^s p_\alpha(r + \alpha + A_j - q)$. Simultaneously, delivery batch B_l at either the completion time of job J_j or the return time of the transporter which has finished the previous batch to the machine. If J_i is assigned into a new batch, then the delivery cost contributes D . Hence, the objective contribution of a new batch is $F_{[l]} + D$. If J_i is assigned into the current batch, the objective contribution is $F_{[l]}$ and the delivery cost does not change. Simultaneously, the number of jobs in each delivery batch cannot exceed the delivery capacity C . The SPT rule needs $O(n \log n)$ time to sequence the jobs in Step 1. By the definition of the recursive relations, we have $j, l \leq n$ and $q, t \leq r$. Hence, the overall complexity is $O(n \log n + r^2 n^2)$.

3.2. The Resumable Case P2. Actually, Algorithm 1 (DP1) can be modified as below to solve problem P2 with resumable consideration.

Theorem 2. Algorithm 2 (DP2) can solve problem P2 in time complexity $O(n \log n + r^2 n^2)$.

Theorem 3. P1 and P2 are NP-hard in the ordinary sense.

3.3. Fully Polynomial-Time Approximation Schemes for P1 and P2. A fully polynomial-time approximation scheme for the single-machine scheduling problems is provided in this section. Let f^* represent the objective value of the optimal schedule and f represent the objective value of the schedule generated by the approximation algorithms. Note that a polynomial-time approximation scheme (PTAS) for a problem is a family of polynomial time $(1 + \epsilon)$ -approximation algorithms if $f \leq (1 + \epsilon)f^*$, where $\epsilon > 0$ is a bound on relative error of the algorithms. Furthermore, a special PTAS is called a fully polynomial-time approximation scheme (FPTAS) if its time complexity is polynomial in $1/\epsilon$. In pure technical sense, an FPTAS is a best one that may tackle to solve an NP-hard optimization problem, unless $P = NP$ [16].

Step 1. Re-index the jobs in the SPT rule.
Step 2. Initial conditions: $F(0, 0, t, 0) = 0$, for $t = \max\{q, r - a_{\max} + 1\}, \dots, r$.
Step 3. Recursive equations:
 For $t = \max\{q, r - a_{\max} + 1\}, \dots, r$, and $j = 1, \dots, n$;
 For $l = 1$ and $j \leq C$, set $F_{[1]} = C_j + T/2$ and $F(j, q, t, |B_1|) = j(C_j + T/2) + D$.
 For $l = 2$ to n do
 If $t + A_j - q \leq r$ and $|B_l| < C$, then set $F_{[l]} = \max\{F_{[l-1]} + (T/2), q\} + (T/2)$
 When $|B_{l-1}| = C$, set $F(j, q, t, |B_l|) \leftarrow F(j-1, q - a_j, t, |B_{l-1}|) + F_{[l]} + D$;
 When $|B_{l-1}| < C$, set $F(j, q, t, |B_l|) \leftarrow \min\{F(j-1, q - a_j, t, |B_{l-1}|) + F_{[l]} + D, F(j-1, q - a_j, t, |B_l|) + F_{[l]}\}$
 Endif
 If $t + A_j - q > r$ and $|B_l| < C$, then set $F_{[l]} = \max\{F_{[l-1]} + (T/2), p_0(t + A_j - q) + \sum_{\alpha=1}^s p_\alpha(r + \alpha + A_j - q)\} + (T/2)$
 When $|B_{l-1}| = C$, set $F(j, q, t, |B_l|) \leftarrow F(j-1, q, t, |B_{l-1}|) + F_{[l]} + D$;
 When $|B_{l-1}| < C$, set $F(j, q, t, |B_l|) \leftarrow \min\{F(j-1, q, t, |B_{l-1}|) + F_{[l]} + D, F(j-1, q, t, |B_l|) + F_{[l]}\}$
 Endfor
 Endfor
Step 4. Optimal solution:
 $\min\{F(j, q, t, |B_l|) : q = 0, \dots, r; t = \max\{0, r - a_{\max} + 1\}, \dots, r; \lceil n/C \rceil \leq l \leq n\}$.

ALGORITHM 1: Algorithm DP1.

Step 1. Perform Step 1-2 of Algorithm 1 (DP1).
Step 2. Recursive equations:
 For $t = \max\{q, r - a_{\max} + 1\}, \dots, r$, $j = 1, \dots, n$;
 For $l = 1$, i.e., $j \leq C$, set $F_{[1]} = C_j + (T/2)$ and $F(j, q, t, |B_1|) = j(C_j + (T/2)) + D$.
 For $l = 2$ to n do
 If $t + A_j - q \leq r$ and $|B_l| < C$, then set $F_{[l]} = \max\{F_{[l-1]} + (T/2), q\} + (T/2)$
 When $|B_{l-1}| = C$, set $F(j, q, t, |B_l|) \leftarrow F(j-1, q - a_j, t, |B_{l-1}|) + F_{[l]} + D$
 When $|B_{l-1}| < C$, set $F(j, q, t, |B_l|) \leftarrow \min\{F(j-1, q - a_j, t, |B_{l-1}|) + F_{[l]} + D, F(j-1, q - a_j, t, |B_l|) + F_{[l]}\}$
 Endif
 If $t + A_j - q > r$ and $|B_l| < C$, then set $F_{[l]} = \max\{F_{[l-1]} + (T/2), \sum_{\alpha=0}^s p_\alpha(t + \alpha + A_j - q)\} + (T/2)$
 When $|B_{l-1}| = C$, set $F(j, q, t, |B_l|) \leftarrow F(j-1, q, t, |B_{l-1}|) + F_{[l]} + D$
 When $|B_{l-1}| < C$, set $F(j, q, t, |B_l|) \leftarrow \min\{F(j-1, q, t, |B_{l-1}|) + F_{[l]} + D, F(j-1, q, t, |B_l|) + F_{[l]}\}$
 Endfor
 Endfor
Step 3. Optimal solution:
 $\min\{F(j, q, t, |B_l|) : q = 0, \dots, r; t = \max\{0, r - a_{\max} + 1\}, \dots, r; \lceil n/C \rceil \leq l \leq n\}$.

ALGORITHM 2: Algorithm DP2.

In the following, we present the general outline of an FPTAS for solving $P1$ and $P2$. This is done by applying the well-known scaling technique to formulate a certain scaled problem for the original problem. The pseudo-polynomial-time algorithm based on dynamic programming for the original problem can generate this scaled problem with its parameter. This algorithm to solve this scaled problem provides a fully polynomial-time approximation scheme for the original problem.

Next, we convert the pseudo-polynomial-time algorithm using the scaling technique into an FPTAS.

3.3.1. FPTAS_S for $P1$ and $P2$

Step 1. Given an arbitrary $\varepsilon > 0$, we define $\delta = \varepsilon r / n(2n\gamma + 3)$.

Step 2. Construct a scaled problem. Define new parameters of each job J_j for the scaled problem:

$$\begin{aligned} a'_j &= \lfloor \frac{a_j}{\delta} \rfloor, \\ T' &= \lfloor \frac{T}{\delta} \rfloor, \\ r' &= \lfloor \frac{r}{\delta} \rfloor, \\ D' &= \lfloor \frac{D}{\delta} \rfloor, \quad j = 1, 2, \dots, n. \end{aligned} \tag{2}$$

Step 3. For the scaled problem, apply Algorithms 1 (DP1) and 2 (DP2) to obtain a schedule π_l with minimal objective value.

Let π_l be an optimal schedule and F' be its objective value for the scaled problem. Suppose that π^* for the

original problem is an optimal schedule and its objective value is F^* . Note that the schedule has at most $n\gamma$ processing operations if the potential disruption occurs. For each state $(i, q, t|B_l)$, increase each processing time by $a_j/\delta - a'_j$ before disruption q or after disruption, which increases C_j by at most $2n\gamma$. Increase each disruption time point by $r/\delta - r'$ and each returning time by $T/\delta - T'$. Increase each delivery cost by $D/\delta - D'$. Further, the total flow time of all n jobs increases at most $n(2n\gamma + 3)$. Now consider $1/\delta$ to be a unit. Then, we obtain a schedule π' with an approximate solution for the original problem, and its objective value can be formulated as

$$\frac{F(\pi')}{\delta \leq F'(\pi')} + n(2n\gamma + 3). \quad (3)$$

We have $F'(\pi') \leq F'(\pi^*)$ due to the definition of π' . It follows that $F'(\pi^*) \leq F^*(\pi^*)/\delta$ from $\lfloor x \rfloor \leq x$ for any number x . We obtain

$$F(\pi') \leq \delta F(\pi^*) + n\delta(2n\gamma + 3) \leq F^*(\pi^*) + \varepsilon r \leq (1 + \varepsilon)F^*(\pi^*). \quad (4)$$

Thus, we can see that the approximate solution is at most a factor of $1 + \varepsilon$ away from the optimum solution.

The time complexity of the approximation scheme is dominated by the step to solve the scaled problem. It is easy to see that $r' \leq (r/\delta) = (n(2n\gamma + 3)/\varepsilon)$. Thus, the running time of the approximation scheme is bounded by

$$\begin{aligned} O(n^2(r')^2 + n \log n) &\leq O\left(n^2\left(\frac{n(2n\gamma + 3)}{\varepsilon}\right)^2\right) \\ &\leq O\left(\frac{n^4(2n\gamma + 3)^2}{\varepsilon^2}\right), \end{aligned} \quad (5)$$

which is polynomial for given γ and $1/\varepsilon$.

Combining the above discussion and the time complexity, we summarize our main result as the following statement.

Theorem 4. *There exists an FPTAS with the running time $O(n^4(2ns + 3)^2/\varepsilon^2)$ for problem P1 or P2.*

4. Parallel-Machine Scheduling

In this paper, we will develop pseudo-polynomial-time algorithms based on dynamic programming to solve problems P3 and P4 with $m = 2$. Then, the algorithms for two parallel machines can be extended to solve general m -parallel-machine problems.

4.1. The Nonresumable Case P3. For a feasible partial schedule $\{J_1, \dots, J_j\}$ where these jobs are divided into two sets, S and $\{J_1, \dots, J_j\}/S$, we first give the following notation:

$$\begin{aligned} S &= S_1 \cup S_2, \\ \sum_{j \in S_i} a_j &= u_i \leq r, \quad i = 1, 2, \end{aligned} \quad (6)$$

where u_1 (u_2): the total actual processing time of jobs finished no later than r on the first machine M_1 (the second machine M_2).

Jobs in $\{J_1, \dots, J_j\}/S$ finish after r . Jobs in $\{J_1, \dots, J_j\}/S$ are divided into two groups: one is assigned to M_1 with the total processing time of the jobs v_1 and the other is assigned to M_2 with the total processing time of the jobs v_2 .

$F_{[l]}$: the completion time of delivery batch B_l .

Let $F(j, u_1, u_2, v_1, v_2|B_l)$ be the expected optimal objective value of a feasible partial schedule for jobs J_1, \dots, J_j , where $|B_l|$ is the number of jobs assigned into delivery batch B_l . Set $F(j, u_1, u_2, v_1, v_2|B_l) = \infty$, if there is no feasible schedule for the problem. The following dynamic programming algorithm (Algorithm 3) is developed to solve P3 with $m = 2$.

Theorem 5. *Problem P3 with $m = 2$ can be solved in time complexity $O(n \log n + r^2 n^2 \cdot A^2)$.*

Proof. We first analyze the possible recursive situations. Suppose that jobs J_1, \dots, J_{j-1} have been assigned optimally, and start to assign J_j . J_j needs to be assigned into machine 1 or machine 2. In an optimal solution, J_j on each machine will be either the last job processed no later than t or last in the whole sequence. If J_j is assigned no later than t , then it will be completed at time u_1 or u_2 on the machine. On the other hand, if J_j is assigned last in the whole sequence, then its completion time on the machine is $\sum_{\alpha=0}^s p_\alpha(r + \alpha + v_1)$ or $\sum_{\alpha=0}^s p_\alpha(r + \alpha + v_2)$. Delivery batch B_l starts at either the completion time of J_j or the return time of the transporter which has finished the previous batch to the machine. Note that if J_i is assigned into a new batch, then the delivery cost contributes D and the objective is $F_{[l]} + D$. If J_i is assigned into the current batch, the objective contribution is $F_{[l]}$. The SPT rule needs $O(n \log n)$ time to sequence the jobs in Step 1. By the definition of the recursive relations, we have $j, l \leq n$, $u_1, u_2 \leq r$ and $v_1, v_2 \leq A$. Hence, the overall complexity is $O(n \log n + r^2 n^2 A^2)$.

4.2. Modified Algorithm DP3. Similar to Algorithm 3 (DP3), denote u_i as the total actual processing time of jobs finished no later than r on the machine M_i , such that $\sum_{j \in S_i} a_j = u_i \leq r$ for $i = 1, \dots, m$. Denote v_i as the total actual processing time of jobs finished after r on the machine M_i , for $i = 1, \dots, m$. Set $F(j, u_1, \dots, u_m, v_1, \dots, v_m, |B_l)$ as the expected optimal objective value of a feasible partial schedule for $\{J_1, \dots, J_j\}$, where $|B_l|$ is the number of jobs assigned into delivery batch B_l . Algorithm 3 (algorithm DP3) can be extended to the m -parallel-machine scheduling problem.

Step 1. Re-index the jobs in the SPT rule.
Step 2. Initial conditions: $F(0, 0, 0, 0, 0) = 0$.
Step 3. Recursive equations:
 For $j = 1, \dots, n; u_1 = 0, 1, \dots, r; u_2 = 0, 1, \dots, \min\{A_j - u_1, r\}; v_1 = 0, 1, \dots, A_j - u_1 - u_2; v_2 = A_j - u_1 - u_2 - v_1$;
 For $l = 1$ and $j \leq C$, set $F_{[1]} = C_j + (T/2)$ and $F(j, u_1, u_2, v_1, v_2, |B_l|) = j(C_j + (T/2)) + D$.
 For $l = 2$ to n do
 /* Schedule job J_j before r on machine M_1
 If $|B_{l-1}| = C$ and $|B_l| < C$, then set $F_{[l]} = \max\{F_{[l-1]} + (T/2), u_1\} + (T/2)$ and
 $F(j, u_1, u_2, v_1, v_2, |B_l|) \leftarrow F(j-1, u_1 - a_j, u_2, v_1, v_2, |B_{l-1}|) + F_{[l]} + D$,
 If $|B_{l-1}| < C$ and $|B_l| < C$, then set $F_{[l]} = \max\{F_{[l-1]} + (T/2), u_1\} + (T/2)$ and
 $F(j, u_1, u_2, v_1, v_2, |B_l|) \leftarrow \min\{F(j-1, u_1 - a_j, u_2, v_1, v_2, |B_{l-1}|) + F_{[l]} + D, F(j-1, u_1 - a_j, u_2, v_1, v_2, |B_l|) + F_{[l]}\}$
 Endif
 /* Schedule job J_j before r on machine M_2
 If $|B_{l-1}| = C$ and $|B_l| < C$, then set $F_{[l]} = \max\{F_{[l-1]} + (T/2), u_2\} + (T/2)$ and
 $F(j, u_1, u_2, v_1, v_2, |B_l|) \leftarrow F(j-1, u_1, u_2 - a_j, v_1, v_2, |B_{l-1}|) + F_{[l]} + D$,
 If $|B_{l-1}| < C$ and $|B_l| < C$, then set $F_{[l]} = \max\{F_{[l-1]} + (T/2), u_2\} + (T/2)$ and
 $F(j, u_1, u_2, v_1, v_2, |B_l|) \leftarrow \min\{j-1, u_1, u_2 - a_j, v_1, v_2, |B_{l-1}| + F_{[l]} + D, F(j-1, u_1, u_2 - a_j, v_1, v_2, |B_l|) + F_{[l]}\}$
 Endif
 /* Schedule job J_j to be finished after r on machine M_1
 If $|B_{l-1}| = C$ and $|B_l| = C$, then set $F_{[l]} = \max\{F_{[l-1]} + (T/2), \sum_{\alpha=0}^s p_\alpha(r + \alpha + v_1)\} + (T/2)$ and
 $F(j, u_1, u_2, v_1, v_2, |B_l|) \leftarrow F(j-1, u_1, u_2, v_1 - a_j, v_2, |B_{l-1}|) + F_{[l]} + D$,
 If $|B_{l-1}| < C$ and $|B_l| < C$, then set $F_{[l]} = \max\{F_{[l-1]} + (T/2), u_1\} + (T/2)$ and
 $F(j, u_1, u_2, v_1, v_2, |B_l|) \leftarrow \min\{F(j-1, u_1, u_2, v_1 - a_j, v_2, |B_{l-1}|) + F_{[l]} + D, F(j-1, u_1, u_2, v_1 - a_j, v_2, |B_l|) + F_{[l]}\}$
 Endif
 /* Schedule job J_j to be finished after r on machine M_2
 If $|B_{l-1}| = C$ and $|B_l| = C$, then set $F_{[l]} = \max\{F_{[l-1]} + (T/2), \sum_{\alpha=0}^s p_\alpha(r + \alpha + v_2)\} + (T/2)$ and
 $F(j, u_1, u_2, v_1, v_2, |B_l|) \leftarrow F(j-1, u_1, u_2, v_1, v_2 - a_j, |B_{l-1}|) + F_{[l]} + D$,
 If $|B_{l-1}| < C$ and $|B_l| < C$, then set $F_{[l]} = \max\{F_{[l-1]} + (T/2), \sum_{\alpha=0}^s p_\alpha(r + \alpha + v_2)\} + (T/2)$ and
 $F(j, u_1, u_2, v_1, v_2, |B_l|) \leftarrow \min\{F(j-1, u_1, u_2, v_1, v_2 - a_j, |B_{l-1}|) + F_{[l]} + D, F(j-1, u_1, u_2, v_1, v_2 - a_j, |B_l|) + F_{[l]}\}$
 Endfor
 Endfor
Step 4. Optimal solution:
 $\min\{F(n, u_1, u_2, v_1, v_2, |B_l|) : \text{for all possible } u_1, u_2, v_1, v_2, l, \lceil n/C \rceil \leq l \leq n\}$.

ALGORITHM 3: Algorithm DP3.

For $l = 1$ and $j \leq C$, set $F(j, u_1, \dots, u_m, v_1, \dots, v_m, |B_l|) = j(C_j + (T/2)) + D$.

For $l = 2$ to n do,

 /* Schedule job J_j to be finished after r on machine M_i ,
 for $i = 1, \dots, k$

 If $|B_{l-1}| = C$ and $|B_l| < C$, then set $F_{[l]} = \max\{F_{[l-1]} + (T/2), u_1\} + (T/2)$ and $F(j, u_1, \dots, u_m, v_1, \dots, v_m, |B_l|) \leftarrow F(j-1, u_1, \dots, u_i - a_j, \dots, u_m, v_1, \dots, v_m, |B_{l-1}|) + F_{[l]} + D$

 If $|B_{l-1}| < C$ and $|B_l| < C$, then set $F_{[l]} = \max\{F_{[l-1]} + (T/2), u_i\} + (T/2)$ and $F(j, u_1, \dots, u_m, v_1, \dots, v_m, |B_l|) \leftarrow \min\{F(j-1, u_1, \dots, u_i - a_j, \dots, u_m, v_1, \dots, v_m, |B_{l-1}|) + F_{[l]} + D, F(j-1, u_1, \dots, u_i - a_j, \dots, u_m, v_1, \dots, v_m, |B_l|) + F_{[l]}\}$

 Endif

 /* Schedule job J_j to be finished after r on machine M_i ,
 for $i = 1, \dots, k$

 If $|B_{l-1}| = C$ and $|B_l| = C$, then set $F_{[l]} = \max\{F_{[l-1]} + (T/2), \sum_{\alpha=0}^s p_\alpha(r + \alpha + v_i)\} + (T/2)$ and $F(j, u_1, \dots, u_m, v_1, \dots, v_m, |B_l|) \leftarrow F(j-1, u_1, \dots, u_m, v_1, \dots, v_i - a_j, \dots, v_m, |B_{l-1}|) + F_{[l]} + D$

 If $|B_{l-1}| < C$ and $|B_l| < C$, then set $F_{[l]} = \max\{F_{[l-1]} + (T/2), \sum_{\alpha=0}^s p_\alpha(r + \alpha + v_i)\} + (T/2)$ and $F(j, u_1, \dots, u_m, v_1, \dots, v_m, |B_l|) \leftarrow \min\{F(j-1, u_1, \dots, u_m, v_1, \dots, v_i - a_j, \dots, v_m, |B_{l-1}|) + F_{[l]} + D, F(j-1, u_1, \dots, u_m, v_1, \dots, v_i - a_j, \dots, v_m, |B_l|) + F_{[l]}\}$

 Endfor

 Optimal solution:

$\min\{F(n, u_1, \dots, u_m, v_1, \dots, v_m, |B_l|) : \text{for all possible } u_1, \dots, u_m, v_1, \dots, v_m, l, \lceil n/C \rceil \leq l \leq n\}$.

Time complexity: the SPT rule needs $O(n \log n)$ time to sequence the jobs. Because $j, l \leq n$, $u_1, \dots, u_m \leq r$, and $v_1, \dots, v_m \leq A$, the overall complexity of modified algorithm DP3 to solve m -parallel-machine problem is $O(n \log n + r^m n^2 \cdot A^m)$.

4.3. The Resumable Case P4. Similar to the nonresumable case P3, a pseudo-polynomial-time algorithm based on dynamic programming is developed for P4 with $m = 2$.

For a feasible partial schedule $\{J_1, \dots, J_j\}$ where these jobs are divided into two sets, S and $\{J_1, \dots, J_j\}/S$, we first give the following notation: $S = S_1 \cup S_2$ and $\sum_{j \in S_i} a_j = u_i \leq r$ for $i = 1, 2$.

Step 1. Re-index the jobs in the SPT rule.
Step 2. Initial conditions: $F(0, 0, 0, 0, 0, 0, 0, 0) = 0$.
Step 3. Recursive equations:
For $j = 1, \dots, n$; $u_1 = 0, 1, \dots, r$; $u_2 = 0, 1, \dots, \min\{A_j - u_1, r\}$; $v_1 = 0, 1, \dots, A_j - u_1 - u_2$; $v_2 = A_j - u_1 - u_2 - v_1$; $q_1 = \max\{u_1, r - a_{\max} + 1\}, \dots, r$; $q_2 = \max\{u_2, r - a_{\max} + 1\}, \dots, r$.
For $l = 1$ and $j \leq C$, then $F(j, u_1, u_2, q_1, q_2, v_1, v_2, |B_l|) = j(C_j + (T/2)) + D$.
For $l = 2$ to n do,
/* schedule job J_j before r on machine M_2
If $|B_{l-1}| = C$ and $|B_l| = C$, then set $F_{[l]} = \max\{F_{[l-1]} + (T/2), u_1\} + (T/2)$ and
 $F(j, u_1, u_2, q_1, q_2, v_1, v_2, |B_l|) \leftarrow F(j-1, u_1 - a_j, u_2, q_1, q_2, v_1, v_2, |B_{l-1}|) + F_{[l]} + D$,
If $|B_{l-1}| < C$ and $|B_l| < C$, then set $F_{[l]} = \max\{F_{[l-1]} + (T/2), u_1\} + (T/2)$ and
 $F(j, u_1, u_2, q_1, q_2, v_1, v_2, |B_l|) \leftarrow \min\{F(j-1, u_1 - a_j, u_2, q_1, q_2, v_1, v_2, |B_{l-1}|) + F_{[l]} + D, F(j-1, u_1 - a_j, u_2, q_1, q_2, v_1, v_2, |B_l|) + F_{[l]}\}$
/* schedule job J_j before r on machine M_2
If $|B_{l-1}| = C$ and $|B_l| = C$, then set $F_{[l]} = \max\{F_{[l-1]} + (T/2), u_2\} + (T/2)$ and
 $F(j, u_1, u_2, q_1, q_2, v_1, v_2, |B_l|) \leftarrow F(j-1, u_1, u_2 - a_j, q_1, q_2, v_1, v_2, |B_{l-1}|) + F_{[l]} + D$,
If $|B_{l-1}| < C$ and $|B_l| < C$, then set $F_{[l]} = \max\{F_{[l-1]} + (T/2), u_2\} + (T/2)$ and
 $F(j, u_1, u_2, q_1, q_2, v_1, v_2, |B_l|) \leftarrow \min\{F(j-1, u_1, u_2 - a_j, q_1, q_2, v_1, v_2, |B_{l-1}|) + F_{[l]} + D, F(j-1, u_1, u_2 - a_j, q_1, q_2, v_1, v_2, |B_l|) + F_{[l]}\}$
Endif
/* schedule job J_j to be finished after r on machine M_1
If $|B_{l-1}| = C$ and $|B_l| = C$, then set $F_{[l]} = \max\{F_{[l-1]} + (T/2), \sum_{\alpha=0}^s P_\alpha(q_1 + \alpha + v_1)\} + (T/2)$ and
 $F(j, u_1, u_2, q_1, q_2, v_1, v_2, |B_l|) \leftarrow F(j-1, u_1, u_2, q_1, q_2, v_1 - a_j, v_2, |B_{l-1}|) + F_{[l]} + D$,
If $|B_{l-1}| < C$ and $|B_l| < C$, then set $F_{[l]} = \max\{F_{[l-1]} + (T/2), \sum_{\alpha=0}^s P_\alpha(q_1 + \alpha + v_1)\} + (T/2)$ and
 $F(j, u_1, u_2, q_1, q_2, v_1, v_2, |B_l|) \leftarrow \min\{F(j-1, u_1, u_2, q_1, q_2, v_1 - a_j, v_2, |B_{l-1}|) + F_{[l]} + D, F(j-1, u_1, u_2, q_1, q_2, v_1 - a_j, v_2, |B_l|) + F_{[l]}\}$
Endif
/* schedule job J_j to be finished after r on machine M_2
If $|B_{l-1}| = C$ and $|B_l| < C$, then set $F_{[l]} = \max\{F_{[l-1]} + (T/2), \sum_{\alpha=0}^s P_\alpha(q_2 + \alpha + v_2)\} + (T/2)$ and
 $F(j, u_1, u_2, q_1, q_2, v_1, v_2, |B_l|) \leftarrow F(j-1, u_1, u_2, q_1, q_2, v_1, v_2 - a_j, |B_{l-1}|) + F_{[l]} + D$,
If $|B_{l-1}| < C$ and $|B_l| < C$, then set $F_{[l]} = \max\{F_{[l-1]} + (T/2), \sum_{\alpha=0}^s P_\alpha(q_2 + \alpha + v_2)\} + (T/2)$ and
 $F(j, u_1, u_2, q_1, q_2, v_1, v_2, |B_l|) \leftarrow \min\{F(j-1, u_1, u_2, q_1, q_2, v_1, v_2 - a_j, |B_{l-1}|) + F_{[l]} + D, F(j-1, u_1, u_2, q_1, q_2, v_1, v_2 - a_j, |B_l|) + F_{[l]}\}$
Endfor
Endfor
Step 4. Optimal solution:
 $\min\{F(n, u_1, u_2, q_1, q_2, v_1, v_2, |B_l|) : \text{for all possible } u_1, u_2, q_1, q_2, v_1, v_2, l, \lceil n/C \rceil \leq l \leq n\}$.

ALGORITHM 4: Algorithm DP4.

Jobs in $\{J_1, \dots, J_j\} \setminus S$ are finished processing after r . And jobs in $\{J_1, \dots, J_j\} \setminus S$ are divided into two groups: one is assigned to M_1 with the total processing time v_1 , and starts at time q_1 , while the other is assigned to M_2 with the total processing time v_2 and starts at time q_2 . If there is no feasible solution for $P4$, then $F(j, u_1, u_2, q_1, q_2, v_1, v_2, |B_l|) = \infty$. Here, q_1 and q_2 represent the state link between the set of jobs finished no later than r and the set of jobs finished after r .

Time complexity: the SPT rule needs $O(n \log n)$ time to sequence the jobs in Step 1. By the definition of the recursive relation, we have $j, l \leq n$, $u_1, u_2, q_1, q_2 \leq r$ and $v_1, v_2 \leq A$. Hence, the overall complexity is $O(n \log n + r^4 n^2 A^2)$.

Theorem 6. Problem $P4$ with $m = 2$ can be solved in time complexity $O(n \log n + r^4 n^2 A^2)$.

Similar to modified algorithm DP3, define $F(n, u_1, \dots, u_m, q_1, \dots, q_m, v_1, \dots, v_m, |B_l|)$ as the objective value for $P4$, and we can extend Algorithm 4 to solve general m -parallel-machine problem with resumable case. The overall time complexity to solve $P4$ is $O(n \log n + r^{2m} n^2 A^m)$.

Theorem 7. $P3$ and $P4$ are NP-hard in the ordinary sense.

4.4. Fully Polynomial-Time Approximation Schemes for $P3$ and $P4$. In this section, the dynamic programming algorithms for $P3$ or $P4$ will be translated into fully polynomial-time approximation schemes. The main framework is to iteratively thin out the state space of the dynamic programming by using the trimming technique. This method is to collapse solutions that are close to each other and decrease the size of the state space down to polynomial.

4.4.1. FPTAS for $P3$. In the dynamic programming DP 3, we will store necessary information for some schedules for the first j jobs: each schedule is indexed by a six-dimensional vector $[u_1, u_2, v_1, v_2, l, F]$. Let the trimming parameter be $\delta = 1 + (\varepsilon/2n)$ for any given $\varepsilon > 0$. The trimming of the state spaces is formulated as the notion of δ -domination: a state $s^j = [u_1^j, u_2^j, v_1^j, v_2^j, l, F^j]$ is δ -dominated by another state $s = [u_1, u_2, v_1, v_2, l, F]$, if and only if

$$\begin{aligned}
\frac{T}{\delta} &\leq T' \leq T\delta, \\
\frac{u_1}{\delta} &\leq u'_1 \leq u_1\delta, \\
\frac{u_2}{\delta} &\leq u'_2 \leq u_2\delta, \\
\frac{v_1}{\delta} &\leq v'_1 \leq v_1\delta, \\
\frac{v_2}{\delta} &\leq v'_2 \leq v_2\delta, \\
\frac{F}{\delta} &\leq F' \leq F\delta.
\end{aligned} \tag{7}$$

If a state s' contained in the state space is δ -dominated by another state s , then the dominated state s' can be removed. The trimming state space forms if the removal procedure eventually stops. When a new state space in the trimmed dynamic programming is computed, the trimmed state space can start instead of the original state space in the original dynamic programming. Next, we will present the time complexity of the trimmed state space.

Note that there are at most r possible values for each of u_1 and u_2 : A possible values for each of v_1 and v_2 and at most $n^2 r^2 A^2$ possible values for F . For any vector $(u_1, u_2, v_1, v_2, l, F)$ of integers, the trimmed state space contains at most one state $[u_1, u_2, v_1, v_2, l, F]$ with $\delta^{f_1} \leq u_1 \leq \delta^{f_1+1}$, $\delta^{f_2} \leq u_2 \leq \delta^{f_2+1}$, $\delta^{g_1} \leq v_1 \leq \delta^{g_1+1}$, and $\delta^{g_2} \leq v_2 \leq \delta^{g_2+1}$. Since $f_1 f_2 \leq \lceil \log_\delta r \rceil$ and $g_1 g_2 \leq \lceil \log_\delta A \rceil$, up to a constant factor the time complexity of a state space is bounded from above by

$$\begin{aligned}
O(n^2 (\log_\delta r)^2 (\log_\delta A)^2 + n \log n) &\leq O\left(n^2 \left(\frac{\log_2 r}{\log_2 \delta}\right)^2 \left(\frac{\log_2 A}{\log_2 \delta}\right)^2\right), \\
&\leq O\left(\frac{n^2 (\log_2 r)^2 (\log_2 A)^2}{(\log_2 \delta)^4}\right) \leq O\left(\frac{n^2 (\log_2 r)^2 (\log_2 A)^2}{(\delta - 1)^4}\right) \leq O\left(\frac{n^6 (\log_2 r)^2 (\log_2 A)^2}{\epsilon^4}\right).
\end{aligned} \tag{8}$$

Here, the inequality $\log_2(1+x) \geq x$ for $0 \leq x \leq 1$ and $\delta = 1 + (\epsilon/2n)$. Hence, the time complexity of the space is polynomial bounded in the input size and in $1/\epsilon$.

Theorem 8. For P3, the best feasible solution for the trimmed problem has an objective value that is at most a factor $1 + \epsilon$ above the objective of the best feasible solution for the original problem.

Proof. Note that the final trimmed state $s' = [u'_1, u'_2, v'_1, v'_2, l, F']$ yields the optimal objective value. The trimmed state space contains a state $s = [u_1, u_2, v_1, v_2, l, F]$ that is δ^n -dominated by s' . Hence, the total cost F is at most a factor $\delta^n = (1 + (\epsilon/2n))^n \leq 1 + \epsilon$ above the optimal cost where the inequality $(1 + (x/n))^n \leq 1 + 2x$ is used for real number x with $0 \leq x \leq 1$ and for integers $n \geq 1$.

4.4.2. FPTAS for P4. Similar to the above discussion for P3, each schedule is indexed by an eight-dimensional vector $[u_1, u_2, v_1, v_2, l, F]$. A state $s' = [u'_1, u'_2, q'_1, q'_2, v'_1, v'_2, l, F']$ is δ -dominated by another state $s = [j, u_1, u_2, q_1, q_2, v_1, v_2, l]$ if and only if

$$\frac{T}{\delta} \leq T' \leq T\delta,$$

$$\frac{u_1}{\delta} \leq u'_1 \leq u_1\delta,$$

$$\frac{u_2}{\delta} \leq u'_2 \leq u_2\delta,$$

$$\frac{q_1}{\delta} \leq q'_1 \leq q_1\delta, \tag{9}$$

$$\frac{q_2}{\delta} \leq q'_2 \leq q_2\delta,$$

$$\frac{v_1}{\delta} \leq v'_1 \leq v_1\delta,$$

$$\frac{v_2}{\delta} \leq v'_2 \leq v_2\delta.$$

The worst-case discussion is similar to Theorem 5. The time complexity of a trimmed state space is bounded from above by

$$\begin{aligned}
& O(n^2 (\log_\delta r)^4 (\log_\delta A)^2 + n \log n) \\
& \leq O\left(n^2 \left(\frac{\log_2 r}{\log_2 \delta}\right)^4 \left(\frac{\log_2 A}{\log_2 \delta}\right)^2\right), \\
& \leq O\left(n^2 \frac{(\log_2 r)^4 (\log_2 A)^2}{(\log_2 \delta)^6}\right) \leq O\left(n^2 \frac{(\log_2 r)^2 (\log_2 A)^2}{(\delta - 1)^6}\right) \\
& \leq O\left(\frac{n^6 (\log_2 r)^2 (\log_2 A)^2}{\varepsilon^6}\right).
\end{aligned} \tag{10}$$

Hence, the time complexity of the trimmed state spaces in the dynamic programming DP 3 or DP 4 can be done within a time polynomial complexity bounded in $1/\varepsilon$. The worst-case ratio guarantees $1 + \varepsilon$. We have the following theorem.

Theorem 9. *Problem P3 and P4 have fully polynomial-time approximation schemes, respectively.*

5. Conclusions

In this paper, we study single-machine and two-parallel-machine scheduling problems with batch deliveries and potential disruption motivated by the iron and steel industry. The objective is to find a coordinated schedule to minimize the total expected flow time plus the total delivery cost. For the four corresponding scheduling problems, pseudo-polynomial-time algorithms and fully polynomial-time approximation schemes are presented in this paper, respectively. Furthermore, the existence of the FPTAS means that the strongest possible polynomial-time approximation result is obtained for a NP-hard problem. In addition, several issues are worthy of future investigations. A future interesting issue is to develop effective heuristics or reinforcement learning algorithm to solve the general problem with stochastic processing times. It would also be interesting to study the problem by taking into account other objective functions.

Data Availability

No data were used to support the study.

Conflicts of Interest

The authors declare that they have no conflicts of interest.

Authors' Contributions

Hua Gong and Puyu Yuan contributed equally to this study.

Acknowledgments

This research was partly supported by the Project of Liaoning BaiQianWan Talents Program (grant no. LR201945-22), the Science and Technology Project of

Educational Department of Liaoning Province (grant no. LG201912), the Major International Joint Research Project of the National Natural Science Foundation of China (71520107004), and the 111 Project (B16009).

References

- [1] Z.-L. Chen, "Integrated production and outbound distribution scheduling: review and extensions," *Operations Research*, vol. 58, no. 1, pp. 130–148, 2010.
- [2] D. Y. Wang, O. Grunder, and A. E. Moudni, "Integrated scheduling of production and distribution operations: a review," *International Journal of Industrial and Systems Engineering*, vol. 19, no. 1, pp. 94–122, 2015.
- [3] F. Li, Z.-L. Chen, and L. Tang, "Integrated production, inventory and delivery problems: complexity and algorithms," *Inform Journal on Computing*, vol. 29, no. 2, pp. 232–250, 2017.
- [4] L. Tang, F. Li, and J. Liu, "Integrated scheduling of loading and transportation with tractors and semitrailers separated," *Naval Research Logistics (NRL)*, vol. 62, no. 5, pp. 416–433, 2015.
- [5] L. Tang, H. Gong, J. Liu, and F. Li, "Bicriteria scheduling on a single batching machine with job transportation and deterioration considerations," *Naval Research Logistics (NRL)*, vol. 61, no. 4, pp. 269–285, 2014.
- [6] H. Gong, L. Tang, and J. Y. T. Leung, "Parallel machine scheduling with batch deliveries to minimize total flow time and delivery cost," *Naval Research Logistics (NRL)*, vol. 63, no. 6, pp. 492–502, 2016.
- [7] N. G. Hall and C. N. Potts, "The coordination of scheduling and batch deliveries," *Annals of Operations Research*, vol. 135, no. 1, pp. 41–64, 2005.
- [8] G. Wang and T. C. E. Cheng, "Parallel machine scheduling with batch delivery costs," *International Journal of Production Economics*, vol. 68, no. 2, pp. 177–183, 2000.
- [9] Z.-L. Chen and G. L. Vairaktarakis, "Integrated scheduling of production and distribution operations," *Management Science*, vol. 51, no. 4, pp. 614–628, 2005.
- [10] L. Wan and A. Zhang, "Coordinated scheduling on parallel machines with batch delivery," *International Journal of Production Economics*, vol. 150, no. 4, pp. 199–203, 2014.
- [11] C.-Y. Lee and G. Yu, "Single machine scheduling under potential disruption," *Operations Research Letters*, vol. 35, no. 4, pp. 541–548, 2007.
- [12] C. Y. Lee and G. Yu, "Parallel-machine scheduling under potential disruption," *Optimization Letters*, vol. 2, no. 1, pp. 27–37, 2008.
- [13] Y. Yin, Y. Wang, T. C. E. Cheng, W. Liu, and J. Li, "Parallel-machine scheduling of deteriorating jobs with potential machine disruptions," *Omega*, vol. 69, no. 6, pp. 17–28, 2017.
- [14] B. Zheng and M. Fan, "Parallel-machine scheduling with potential disruption and positional-dependent processing times," *Journal of Industrial and Management Optimization*, vol. 13, no. 2, pp. 697–711, 2017.
- [15] C.-Y. Lee, J. Y.-T. Leung, and G. Yu, "Two machine scheduling under disruptions with transportation considerations," *Journal of Scheduling*, vol. 9, no. 1, pp. 35–48, 2006.
- [16] M. L. Pinedo, *Scheduling Theory, Algorithms, and Systems*, Springer, New York City, NY, USA, 2010.
- [17] G. J. Woeginger, "When does a dynamic programming formulation guarantee the existence of a fully polynomial time approximation scheme (fptas)?" *INFORMS Journal on Computing*, vol. 12, no. 1, pp. 57–74, 2000.

Research Article

Complex Dynamic Analysis for Game Model under Different Regulatory Levels in China's Housing Rental Market

Lingling Mu,¹ Xiangyu Qin,¹ Yuan Li,¹ and Ping Liu ²

¹School of Economics and Management, Hebei University of Technology, Tianjin 300401, China

²School of Civil and Transportation Engineering, Hebei University of Technology, Tianjin 300401, China

Correspondence should be addressed to Ping Liu; 2002lp@hebut.edu.cn

Received 5 April 2020; Revised 4 June 2020; Accepted 23 June 2020; Published 26 August 2020

Guest Editor: Lei Xie

Copyright © 2020 Lingling Mu et al. This is an open access article distributed under the Creative Commons Attribution License, which permits unrestricted use, distribution, and reproduction in any medium, provided the original work is properly cited.

In this paper, we construct an evolutionary game model of government and real estate operators (long-term apartment rental companies) in the housing rental market in the context of financial institutions and public participation in regulation and analyze the effects of different regulatory levels of financial institutions and the public on the evolutionary results through model solving and numerical simulation. The results show that, under five different levels of supervision, financial institutions and the public have different evolutionary and stable strategies; financial institutions' participation in supervision can effectively reduce the cost of government supervision and promote the government's evolution towards strict supervision. It is difficult for real estate operators to evolve naturally towards keeping their promises when the probability of the social public or financial institutions participating in regulation is low. Only when the probability of social public and financial institutions participating in regulation reaches a certain level will real estate operators be inclined to keep their promises.

1. Introduction

With the advancement of urbanization, the influx of first- and second-tier cities has increased sharply [1]. The "talent policy" in various regions has intensified the demand for urban housing [2]. According to the data in the White Paper on China Housing Leasing in 2018, the current housing rental population is about 168 million, the market size is 1.2 trillion yuan, and the housing lease population will increase by 50% in the next five years, the market size increased by 150% [3], and the demand is gradually increasing. However, due to the rising cost of construction and maintenance of rental housing, the low rental return rate makes it difficult for real estate operators to obtain profit [4], and the government does not pay much attention to the housing rental market [5]. The relevant laws and regulations set are not sound, regulatory policies are inadequate [6], and financial institutions and the public are lacking awareness of regulatory reporting, which results in frequent defaults of real estate operators. Therefore, it is necessary and urgent for the government to establish a multibody common regulatory system to regulate the behavior of real estate operators, in

order to promote the long-term development of the housing rental market. Therefore, the purpose of this study is to determine what level of regulation should be adopted by both financial institutions and public participation in regulation to promote compliance by real estate operators by exploring the impact of regulation on the evolution of the system.

2. Literature Review

It is necessary and urgent to improve the supervision system of China's housing rental market. Wang and Hu analyzed telephone survey data from four cities in Beijing, Shanghai, Guangzhou, and Shenzhen and found that the housing rental market in first-tier cities in China is not mature enough, and the government needs to strengthen the management of the housing rental market [7]. By combing the development history of the US housing rental policy and comparing it with China's current housing rental policy, Cheng believed that the data of subsidized projects such as China's rent monetary subsidy policy are isolated and have not yet achieved open and transparent monitoring feedback

[8]. Dou compared the models of coliving communities in Canada and Japan and believed that improving the public participation planning and community governance mechanism is the key driving force for the development of coliving communities in China [9]. Lou and Zhou analyzed the characteristics and existing problems of the Russian housing rental market. They believed that the Russian housing rental management department had weak supervision and rental information, which suggested that the government could cooperate with relevant organizations to improve the supervision ability [10]. By comparing the basic framework and operation mode of the British credit system, Du found that the credit data acquisition of China's housing rental market was not widespread; the mechanism of publicity, use, and protection was not perfect; the regulation ability was insufficient; and the mechanism of rewards and punishments was not perfect. Therefore, he suggested improving the management of the housing rental market based on personal credit [11].

There are conflicts of interest between the participants in the housing rental market [12]. Real estate operators will choose improper means to sacrifice the interests of other subjects, such as lessees, in the pursuit of their own values [13]. The government supervision and coordination mechanism need to be improved. Relevant research on the current government-regulated housing rental market participants shows that, in the development of the housing rental market, the three parties of the government, consumers, and enterprises finally reach a stable balance in the government's nonregulation, consumers tend to rent houses, and enterprises actively develop rental business. The cost of government regulation and the penalties for companies are the main drivers of tripartite evolution [14]. Qiu has developed an evolutionary game model of social forces and the government to address the problem of excessive participation of social forces in the profit-seeking behavior of housing rental projects, which leads to rent increases; the study shows that it is difficult for social forces to evolve naturally without external forces to not participate in illegal rental projects, and the government needs to implement appropriate institutional norms to regulate the behavior of social forces [15]. Zhou et al. constructed the interest game model between the central government and local government in the process of developing rental housing. The key to the development of the housing rental market is to enlarge the utility proportion shared by the local government, reduce the supervision cost of the central government, and increase the punishment for the inaction of the local government [16]. Chai et al. reduced the social interest adjustment mechanism of collective rental housing to the Pareto improvement of land and housing interest production and distribution and then designed the multicenter game competition and synergy mechanism of government, lessee, rural collective, and interest group. He suggested that government should give autonomy to local government systems and technology choices [17]. Lai established a dynamic Cournot model of bounded rational duopoly to verify the government's influence on real estate developers [18].

Scholars have reached a unified opinion on the urgent need to strengthen the supervision of China's housing rental market and analyzed the feasibility of government regulation

affecting the choice of real estate operators while ignoring the importance of financial institutions and the public to participate in supervision. Financial institutions and the public are the most direct contacts to the housing rental market. Therefore, this paper incorporates financial institutions and the public into the regulatory system, builds an evolutionary game system in which multiparty entities participate in the supervision of real estate operators' behaviors, analyzes the strategy selection of the government and real estate operators with different participation levels of financial institutions and the public, and explores the impact of financial institutions and the public's participation in supervision on the system evolution.

3. Evolutionary Game Model

3.1. Model Description. In the development of the housing rental market, in order to speed up the capital turnover, the long-term apartment rental companies (abbreviated as real estate operators) have the power of illegal operation to earn additional profits and provide houses that do not meet the standards, or use the funds that should be used to serve the lessee for reinvestment, collection of houses, and expansion of income. Financial institutions are providers of funds for real estate operators. In order to prevent real estate operators from using funds in breach of contract, financial institutions regulate real estate operators, which can reduce the cost of supervision by government departments. As beneficiaries of rental housing, the public can have the most direct experience of rental housing provided by real estate operators and understand whether real estate operators are abiding by their contracts. Therefore, it is easier for financial institutions and the public to detect the default of real estate operators, which can effectively reduce the cost of government regulation and expose the default of real estate operators.

In traditional game theory, it is often assumed that participants are bounded rational and that participants are fully informed; however, the problem of incomplete information and bounded rationality is evident due to the complexity of the economic environment [19]. Evolutionary game is studied with a bounded rational group of participants [20–26]. In the continuous dynamic gaming, the low-yield strategy choice is constantly eliminated by the high-yield strategy choice; after repeated gaming, elimination, and choice, the gaming parties achieve stability at the relative maximum benefit [27]. The gaming participants in this model are governments and real estate operators who are assumed to be bounded rational “economic man.” According to evolutionary game theory, under incomplete information conditions, the government's strategy set is (strict supervision, loose supervision) and the real estate operator's strategy set is (keeping promise, default). Because the participation of financial institutions in the regulation of the housing rental market affects the cost of government regulation, and the participation of the public in the regulation of the housing rental market affects the exposure probability of default by real estate operators, the government-enterprise game in the housing rental market is

defined as the dynamic game between the government and real estate operators in the context of different levels of participation of financial institutions and the public in regulation.

3.2. Model Assumptions. To analyze the problem, several assumptions are made.

Assumption 1. As the government has introduced some regulatory policies, but not fully implemented in practice, the regulation of the housing rental market is in a relatively lax state [28], and the cost of regulation is set at c_0 . If the government is to strictly implement the corresponding regulatory policies need to pay the corresponding additional regulatory cost Δc , the involvement of financial institutions in regulation can effectively reduce the cost of regulation when governments adopt a strict regulatory strategy, so the cost of regulation when governments adopt a strict regulatory strategy can be expressed as $c = c_0 + \Delta c - pk$. p is the probability of financial institutions participating in regulation. k , a constant, represents the financial regulatory capacity coefficient. Strict government regulation will enhance the credibility of the government, which can bring benefits to the government as r_1 .

Assumption 2. Real estate operators keeping their promises can enhance social stability, which brings gains to the government as r_2 . Defaults by real estate operators have a negative impact, which brings losses to the government for v .

Assumption 3. If the real estate operator keeps its promise, it will receive the basic benefits d and the benefits h from public opinion exposure and publicity regarding the good conduct of the business [15]. If the real estate operator defaults, it receives an additional gain Δd . However, if the government detects the real estate operator's default, it will have to pay a penalty z and suffer a potential loss δ such as reputational decline.

Assumption 4. The probability of the government identifying default by real estate operator is λ and λ' , respectively, when the government chooses strict and loose regulation, and the probability of real estate operators adopting default strategies with the participation of the public and being identified by the government is $\mu = \lambda + q(1 - \lambda)$ and $\mu_0 = \lambda' + q(1 - \lambda')$, where q is the probability of the public regulating in the housing rental market. When the government adopts a loose regulatory strategy and the public exposes the real estate operator's default, the government's social credibility will be reduced, and the government will suffer a loss of n .

3.3. Model Building. Assume that x, y, p , and q ($0 < x, y, p, q < 1$) are the probability of strict government supervision, real estate operator compliance, financial institutions' participation in supervision, and public participation in supervision, respectively. The payment matrix of government and real estate operators is shown in Table 1.

The expected benefit of the government choosing strict regulation is

$$U_G^1 = y(r_1 - c + r_2) + (1 - y)(r_1 - c - v + \mu z). \quad (1)$$

The expected benefit of the government choosing loose regulation is

$$U_G^2 = y(r_2 - c_0) + (1 - y)(\mu_0 z - qn(1 - \lambda') - c_0 - v). \quad (2)$$

Thus, the average benefit of the government is

$$\bar{U}_G = xU_G^1 + (1 - x)U_G^2. \quad (3)$$

The replicated dynamic equation dynamic of the government is

$$\begin{aligned} F_G &= \frac{dx}{dt} = x(U_G^1 - \bar{U}_G) \\ &= x(1 - x)(c_0 - c + r_1 + qn(1 - \lambda')(1 - y) \\ &\quad + z(1 - y)(\mu - \mu_0)), \end{aligned} \quad (4)$$

$$\begin{aligned} \frac{\partial F_G}{\partial x} &= (1 - 2x)(c_0 - c + r_1 + qn(1 - \lambda')(1 - y) \\ &\quad + z(1 - y)(\mu - \mu_0)). \end{aligned} \quad (5)$$

The expected benefit of the real estate operators choosing to keep their promises is

$$U_R^1 = x(d + h) + (1 - x)(d + h). \quad (6)$$

The expected benefit of the real estate operator choosing to default is

$$U_R^2 = x(d + \Delta d - \mu(z + \delta)) + (1 - x)(d + \Delta d - \mu_0(z + \delta)). \quad (7)$$

Thus, the average benefit of the real estate operator is

$$\bar{U}_R = yU_R^1 + (1 - y)U_R^2. \quad (8)$$

The replicated dynamic equation dynamic of the real estate operator is

$$\begin{aligned} F_R &= \frac{dy}{dt} = y(U_R^1 - \bar{U}_R) \\ &= y(1 - y)(h - \Delta d + \mu(z + \delta)x + \mu_0(z + \delta)(1 - x)), \end{aligned} \quad (9)$$

$$\begin{aligned} \frac{\partial F_R}{\partial y} &= (1 - 2y)(h - \Delta d + \mu(z + \delta)x + \mu_0(z + \delta)(1 - x)). \end{aligned} \quad (10)$$

4. Evolutionary Game Analysis

4.1. Replication Dynamics Analysis of Government Decision-Making Behavior. From the replicated dynamic equations stability theorem and the nature of the evolutionary stability

TABLE 1: Payment matrix of government and real estate operators.

Government	Real estate operator	
	Keep promise	Default
Strict supervision	$\frac{r_1 - c + r_2}{d + h}$	$\frac{r_1 - c - v + \mu z}{d + \Delta d - \mu(z + \delta)}$
Loose supervision	$\frac{r_2 - c_0}{d + h}$	$\frac{\mu_0 z - qn(1 - \lambda) - c_0 - v}{d + \Delta d - \mu_0(z + \delta)}$

strategy, it is known that when the stability strategy x satisfies $F_G = 0$, $(\partial F_G / \partial x) < 0$, x is the evolutionary stability strategy. Calculated by $F_G = 0$, y_0 can be represented by the following equation:

$$y_0 = \frac{c - c_0 - r_1 - qn(1 - \lambda') - z(\mu - \mu_0)}{-qn(1 - \lambda') - z(\mu - \mu_0)}. \quad (11)$$

When $y = y_0$, F_G is constant at zero, which means that the strategies adopted by the government are stable and do not change over time.

If $y_0 < 0$, the probability of financial institutions participating in regulation satisfies the following equation:

$$p < \frac{\Delta c - r_1 - (\mu - \mu_0)z - qn(1 - \lambda')}{k} = p_L. \quad (12)$$

Since $y > y_0$, $x = 0$ is the evolutionary stability strategy. The government's gains from strict regulation are always less than those from loose regulation, so the government will adopt loose regulation regardless of whether real estate operators keep their promises.

If $y_0 > 1$, the probability of financial institutions participating in regulation satisfies the following equation:

$$p > \frac{\Delta c - r_1}{k} = p_H. \quad (13)$$

Since $y < y_0$, $x = 1$ is the evolutionary stability strategy. The government's gains from strict regulation are always more than those from loose regulation, so the government will adopt strict regulation regardless of whether real estate operators keep their promises.

If $0 < y_0 < 1$, the probability of financial institutions participating in regulation satisfies the following equation:

$$\frac{\Delta c - r_1 - (\mu - \mu_0)z - qn(1 - \lambda')}{k} < p < \frac{\Delta c - r_1}{k}. \quad (14)$$

The relationship between y and y_0 needs to be discussed according to different situations. When $y < y_0$, $x = 1$ is the evolutionary stability strategy and at this time the government adopts strict regulatory behavior. When $y > y_0$, $x = 0$ is the evolutionary stability strategy and at this time the government adopts loose regulatory behavior.

In order to vividly understand the dynamic evolution of government decision-making behavior, we give a graph of the evolution of government decision-making behavior under different circumstances, as shown in Figure 1.

4.2. Replication Dynamics Analysis of Real Estate Operators Decision-Making Behavior.

From the replicated dynamic

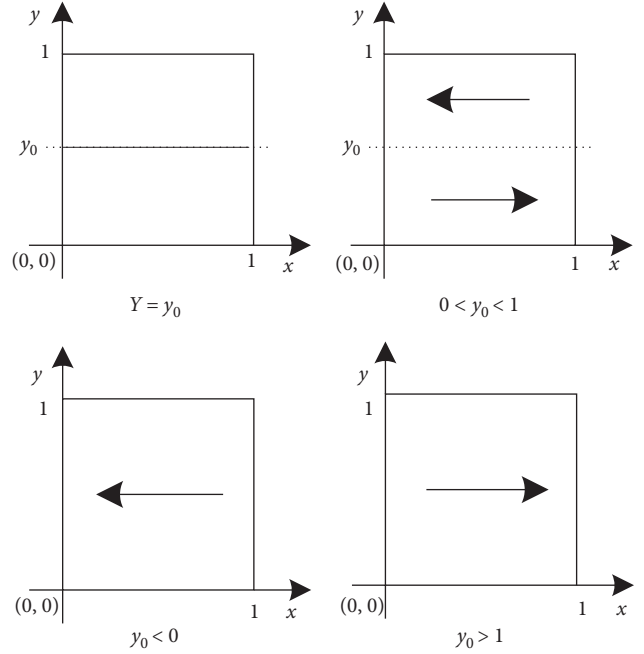


FIGURE 1: Government replication dynamic phase diagram.

equations stability theorem and the nature of the evolutionary stability strategy, it is known that when the stability strategy y satisfies $F_R = 0$, $(\partial F_R / \partial y) < 0$, y is the evolutionary stability strategy. Calculated by $F_R = 0$, x_0 can be represented by the following equation:

$$x_0 = \frac{h - \Delta d + \mu_0(z + \delta)}{(\mu - \mu_0)(z + \delta)}. \quad (15)$$

When $x = x_0$, F_R is constant at zero, which means that the strategies adopted by the real estate operators are stable and do not change over time.

If $x_0 < 0$, the probability of financial institutions participating in regulation satisfies the following equation:

$$q > \frac{\Delta d - h - \lambda'(z + \delta)}{(1 - \lambda)(z + \delta)} = q_H. \quad (16)$$

Since $x > x_0$, $y = 1$ is the evolutionary stability strategy. The real estate operators' gains from keeping their promises are always more than those from default. So, no matter what regulatory actions the government takes, real estate operators keep their promises.

If $x_0 > 1$, the probability of public participation in regulation satisfies the following equation:

$$q < \frac{\Delta d - h - \lambda'(z + \delta)}{(1 - \lambda')(z + \delta)} = q_L. \quad (17)$$

Since $x < x_0$, $y = 0$ is the evolutionary stability strategy. The real estate operators' gains from keeping their promises are always less than those from default. So, no matter what regulatory actions the government takes, real estate operators are in default.

If $0 < x_0 < 1$, the probability of public participation in regulation satisfies the following equation:

$$\frac{\Delta d - h - \lambda'(z + \delta)}{(1 - \lambda')(z + \delta)} < q < \frac{\Delta d - h - \lambda(z + \delta)}{(1 - \lambda)(z + \delta)}. \quad (18)$$

The relationship between x and x_0 needs to be discussed according to different situations. When $x < x_0$, $y = 0$ is the evolutionary stability strategy and at this time real estate operators adopt default behaviors. When $x > x_0$, $y = 1$ is the evolutionary stability strategy and at this time real estate operators keep their promises.

In order to vividly understand the dynamic evolution of government decision-making behavior, we give a graph of the evolution of government decision-making behavior under different circumstances, as shown in Figure 2.

4.3. Stability Analysis of Equilibrium Point. Since the above equilibrium point is not necessarily the system's evolutionary stability strategy (ESS), according to the computational differential equations proposed by Friedman to form the dynamics of the dynamic system, the stability analysis of the equilibrium point can be analyzed by analyzing the local stability of the Jacobian matrix of the system. Solving the partial derivatives of x and y for the differential equations (4) and (9) sequentially, the Jacobian matrix can be obtained as

$$J = \begin{bmatrix} \frac{\partial F_G}{\partial x} & \frac{\partial F_G}{\partial y} \\ \frac{\partial F_R}{\partial x} & \frac{\partial F_R}{\partial y} \end{bmatrix} = \begin{bmatrix} J_{11} & J_{12} \\ J_{21} & J_{22} \end{bmatrix}, \quad (19)$$

$$\begin{aligned} J_{11} &= (1 - 2x)(c_0 - c + r_1 + (qn(1 - \lambda') + z(\mu - \mu_0))(1 - y)), \\ J_{12} &= x(x - 1)(qn(1 - \lambda') + z(\mu - \mu_0)), \\ J_{21} &= y(1 - y)(\mu - \mu_0)(z + \delta), \\ J_{22} &= (1 - 2y)(h - \Delta d + (z + \delta)(\mu x + \mu_0(1 - x))). \end{aligned} \quad (20)$$

The calculation process of the determinant $\det J$ and the $\text{tr} J$ trace of the Jacobian matrix is as follows:

$$\begin{aligned} \det J &= x(1 - x)(qn(1 - \lambda') + z(\mu - \mu_0))y(1 - y)(\mu - \mu_0) \\ &\quad \cdot (z + \delta) + (1 - 2x)c_0 - c + r_1 + (qn(1 - \lambda') + z(\mu - \mu_0)) \\ &\quad \cdot (1 - 2y)(h - \Delta d + (z + \delta)(\mu x + \mu_0(1 - x))), \\ \text{tr} J &= (1 - 2x)c_0 - c + r_1 + (qn(1 - \lambda') + z(\mu - \mu_0)) \\ &\quad \cdot (1 - y) + (1 - 2y)(h - \Delta d + (z + \delta)(\mu x + \mu_0(1 - x))). \end{aligned} \quad (21)$$

If the equilibrium point satisfies $\det J > 0$ and $\text{tr} J < 0$, the equilibrium point is the local asymptotic stability point of the evolutionary dynamic process. In this paper, we discuss the parameter conditions from the evolutionary path of the government and the real estate operator, combined with the mathematical point of view and practical significance, and conclude that the dynamic system needs to analyze the local stability under the following nine parameter conditions, as shown in Tables 2–6.

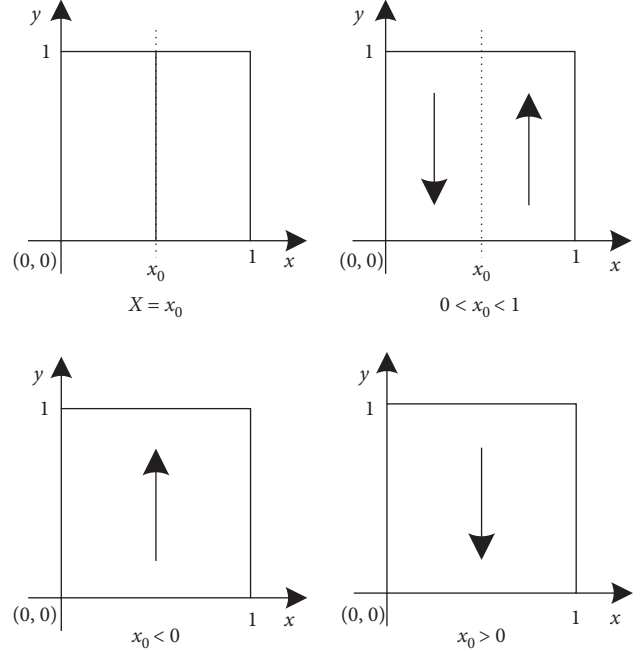


FIGURE 2: Replication dynamic phase diagram of the real estate operator.

4.4. Result Analysis

4.4.1. Scenario 1. When the probability of financial institutions and the public participating in supervision is $p < p_L$ and $q < q_H$, respectively, and the government benefits less than the regulatory cost by adopting a strict regulatory strategy, the government tends to adopt a loose supervision strategy. The low probability of public participation in regulation makes defaults by real estate operators less susceptible to detection, and the damage to the operator's reputation and government penalties are less than the gains in the event of default, so real estate operators tend to choose default. In this case, the evolutionary equilibrium strategy is $(0, 0)$.

4.4.2. Scenario 2. When the probability of financial institutions and the public participating in supervision is $p_L < p$ and $q < q_L$, respectively, the participation of financial institutions in regulation can reduce the cost of government regulation and therefore the government tends to adopt strict regulatory measures. However, the probability of public participation in regulation is low, and the investigation and punishment of real estate operators' defaults mainly rely on government regulation. Real estate operators choose to default because the penalty for default is less than the proceeds they would have received if they had defaulted. So in this case, the evolutionary equilibrium strategy is $(1, 0)$.

4.4.3. Scenario 3. When the probability of financial institutions and the public participating in supervision is $p < p_H$ and $q > q_H$, respectively, the high probability of social public

TABLE 2: Equilibrium point local stability.

Equilibrium	$P < P_L, Q > Q_H$			$P < P_L, Q < Q_L$		
	$\det J$	$\text{tr } j$	Stability	$\det J$	$\text{tr } j$	Stability
(0, 0)	-	Uncertain	Saddle point	+	-	ESS
(0, 1)	+	-	ESS	-	Uncertain	Saddle point
(1, 0)	+	+	Unstable	-	Uncertain	Saddle point
(1, 1)	-	Uncertain	Saddle point	+	+	Unstable

TABLE 3: Equilibrium point local stability.

Equilibrium	$P < P_L, Q_L < Q < Q_H$			$P_L < P < P_H, Q > Q_H$		
	$\det J$	$\text{tr } j$	Stability	$\det J$	$\text{tr } j$	Stability
(0, 0)	+	-	ESS	+	+	Unstable
(0, 1)	-	Uncertain	Saddle point	+	-	ESS
(1, 0)	+	+	Unstable	-	Uncertain	Saddle point
(1, 1)	-	Uncertain	Saddle point	-	Uncertain	Saddle point

TABLE 4: Equilibrium point local stability.

Equilibrium	$P_L < P < P_H, Q < Q_L$			$P > P_H, Q > Q_H$		
	$\det J$	$\text{tr } j$	Stability	$\det J$	$\text{tr } j$	Stability
(0, 0)	-	Uncertain	Saddle point	+	+	Unstable
(0, 1)	-	Uncertain	Saddle point	-	Uncertain	Saddle point
(1, 0)	+	-	ESS	-	Uncertain	Saddle point
(1, 1)	+	+	Unstable	+	-	ESS

TABLE 5: Equilibrium point local stability.

Equilibrium	$P > P_H, Q < Q_L$			$P > P_H, Q_L < Q < Q_H$		
	$\det J$	$\text{tr } j$	Stability	$\det J$	$\text{tr } j$	Stability
(0, 0)	-	Uncertain	Saddle point	-	Uncertain	Saddle point
(0, 1)	+	+	Unstable	+	+	Unstable
(1, 0)	+	-	ESS	-	Uncertain	Saddle point
(1, 1)	-	Uncertain	Saddle point	+	-	ESS

TABLE 6: Equilibrium point local stability.

Equilibrium	$P_L < P < P_H, Q_L < Q < Q_H$		
	$\det J$	$\text{tr } j$	Stability
(0, 0)	-	Unstable	Saddle point
(0, 1)	-	Unstable	Saddle point
(1, 0)	-	Unstable	Saddle point
(1, 1)	-	Unstable	Saddle point
(X_0, Y_0)	0	0	Saddle point

participation in regulation leads to a higher probability of exposure of the real estate operator to default, and therefore it is more likely to be penalized by the government and to suffer reputational damage. The real estate operator's gains when keeping its promise are greater than those when it defaults, so real estate operator tends to keep its promise. The increased probability of default exposure makes it easier for

the government to detect defaults by real estate operators, so the government tends to choose lax regulation. In this case, the evolutionary equilibrium strategy is (0, 1).

4.4.4. *Scenario 4.* When the probability of financial institutions and the public participating in supervision is $p > p_H$

and $q_L < q$, respectively, financial institution participation reduces the expected costs that governments adopt strict regulation, so governments tend to adopt strict regulation strategies. The high probability of financial institutions participating in regulation enhances government enforcement against real estate operators, so when public participation in regulation is at a superior level, the government penalties for default and reputational damage to real estate operators will outweigh the gains from compliance. So, in this case, the evolutionary equilibrium strategy of the game is (1, 1).

4.4.5. Scenario 5. When the probability of financial institutions and the public participating in supervision is $p_L < p < p_H$ and $q_L < q < q_H$, respectively, the probability of financial institutions and the public participating in regulation is low, which has limited impact on the strategic choices of governments and real estate operators. As a result, the government and real estate operators have not reached the stability strategy, and the evolutionary result is a cyclical random state that belongs to the chaotic period of government and real estate operator strategy selection.

4.5. Numerical Simulation. In this section we use numerical simulations to illustrate in detail the impact of different levels of financial institutions and social public participation in regulation on the decisions of governments and real estate operators. This paper assumes that $r_1 = 0.2$, $r_2 = 1$, $v = 1$, $z = 1$, $n = 1$, $\lambda = 0.5$, $\lambda' = 0.3$, $d = 1$, $\Delta d = 2.5$, $\delta = 1$, $\Delta c = 1$, $k = 1$. Due to the lack of recognizing the behavior of real estate operator awareness, the government adopts a more relaxed regulatory strategy, which leads to frequent defaults of real estate operators. Therefore, this paper assumes that the initial values of x and y are $x = 0.2$ and $y = 0.2$, respectively.

A schematic of the strategy evolution when the government and real estate operator strategies are $p = 0.3$, $q = 0.55$, respectively, is shown in Figure 3(a), which validates the analysis results of Scenario 1. The figure shows that the final evolutionary strategy of the government and real estate operators is (0, 0) when financial regulation is at a low level and public participation is at a medium to low level. The probability of financial institutions participating in regulation increases in comparison Scenario 1, that is, $p = 0.7$, $q = 0.55$, and the government's behavior tends to choose a strict regulatory strategy. However, due to the moderate level of regulation of financial institutions and public participation in society, the game between the government and real estate operator shows a cyclical state and the evolutionary results can be seen in Figure 3(b). The probability of social public participation in regulation increases to a high level in comparison to Scenario 5, that is, $p = 0.7$, $q = 0.7$, and the increase in the exposure of default leads the real estate operator to choose to keep its promise. The evolutionary results can be seen in Figure 3(c). The probability of social public participation in regulation is reduced to a low level in comparative Scenario 5, that is, $p = 0.7$, $q = 0.4$. The

reduction in the exposure to default causes the real estate operator to choose to default, and the evolutionary results can be seen in Figure 3(d). The probability of financial institutions participating in the regulation increased to a high level, that is, $p = 0.81$, $q = 0.55$, which can effectively reduce the pressure of government regulation, the government tends to choose strict regulation. At this point, real estate operator tends to keep its promise under strict government regulation and a higher level of social public regulation, and the evolutionary results can be seen in Figure 3(e).

5. Discussion

Through the analysis and simulation of evolutionary results, the article illustrates the impact of different levels of financial institutions and social public participation in regulation on the decision-making behavior of governments and real estate operators. The strong regulatory awareness of financial institutions or the public will lead real estate operator to keep its promise, but if the regulatory awareness of the public is weak, the public will be less exposed to the operators' violations, and thus the strong regulatory awareness of financial institutions will not lead real estate operators to keep their promises. However, the public with a high level of supervision will expose the real estate operator's default to a great extent, which results in significant default costs for real estate operators, including government penalties and reputational damage. Therefore, the real estate operator must choose to keep its promise. Public participation in regulation is particularly important for the governance of China's housing rental market. The combination of financial institutions and the public is important for maximizing regulatory effectiveness.

There are four types of regulatory subjects involved in our study, including the government, financial institutions, and the public in the housing rental market. However, Qiu [15] and Zheng and Xu [14] argue that the government is the only entity involved in regulation in the housing rental market. Their study found that different government regulation behaviors is the key to guide firms to produce different decision behaviors, and that changes in government incentives and penalties can have an impact on the evolutionary path of firms' behavior. Zhou et al. [16] also found that reducing the cost of regulation can change the evolutionary path of the regulated behavior. Based on previous studies involving government incentives and penalties, we also set incentives and penalties in our study. However, today is the age of information technology. The popularity of mobile devices, the development of network technology, and the construction of big data provide new ways and means for the public and financial institutions to participate in regulation. The multidominant participatory regulatory model becomes an important way of regulatory governance. In contrast to related research, our study finds that in the case of multiagency regulation, real estate operators can choose to keep their promises even if the government does not need to change its regulatory measures.

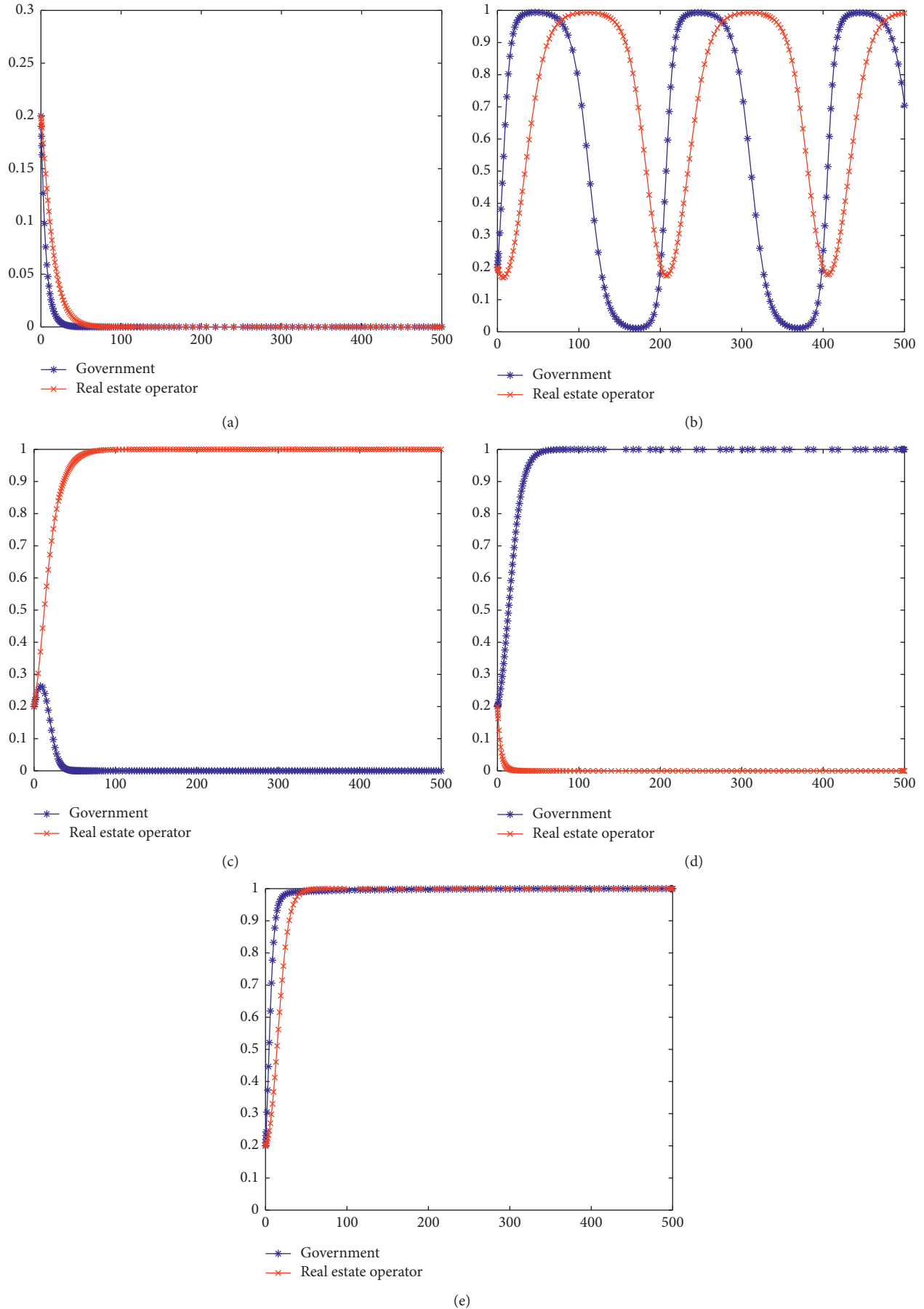


FIGURE 3: Government's and real estate operators' strategic evolutionary roadmaps with different levels of financial institutions and public involvement in regulation.

6. Implications

In this paper, we construct an evolutionary game system in which multiple subjects are involved in monitoring the behavior of real estate operators and analyze the strategic choices of government and real estate operators with different levels of participation by financial institutions and the public in society. This paper draws conclusions from both theoretical and practical perspectives.

From a theoretical perspective, the implications are as follows. We find that the level of regulatory involvement of financial institutions and the public at large is complex in its impact on the strategies of governments and real estate operators. If one of the financial institutions and the public is involved in regulation at a low level, the real estate operator will default. If the probability of public participation in regulation is high, regardless of the level of financial institutions' participation in regulation, real estate operators will ultimately choose to keep their promises. However, real estate operators will only choose to be compliant if the probability of financial institutions participating in regulation is high and the probability of requiring community participation in regulation is at a medium level and above.

From a practical perspective, we propose several conclusions. In contrast to the involvement of financial institutions in regulation, social and public participation in regulation is essential for the healthy development of China's housing rental market. Therefore, in order to strengthen public participation in regulation, the government can simplify the process of reporting violations in the housing rental market, broaden the reporting channels, and strictly scrutinize reports from the public once received. In order to facilitate public participation, the government can build a platform for information disclosure and sharing and regularly check public messages and provide timely responses. In contrast to a single public regulation, the participation of financial institutions and the public in regulation is conducive to a higher level of regulation. Therefore, in order to improve the level of regulation, the government can reduce the default risk for real estate operators by requiring companies to hand over their pools to third-party banks for management.

Data Availability

All data used have been included in this article and are also available from the corresponding author upon request.

Conflicts of Interest

The authors declare no conflicts of interest.

Acknowledgments

This research was supported by the National Natural Science Foundation of China (no. 71904042). The authors would like to thank Shihao Zhou who helped them in using MATLAB software and Masese Duke for correcting grammar mistakes in this paper.

References

- [1] L. Bi, Y. Fan, M. Gao, C. L. Lee, and G. Yin, "Spatial mismatch, enclave effects and employment outcomes for rural migrant workers: empirical evidence from Yunnan Province, China," *Habitat International*, vol. 86, pp. 48–60, 2019.
- [2] S. Zheng, Y. Cheng, and Y. Ju, "Understanding the intention and behavior of renting houses among the young generation: evidence from jinan, China," *Sustainability*, vol. 11, no. 6, p. 1507, 2019.
- [3] Shell institute, "A white paper on housing rental in china in 2018," 2018, <https://www.useit.com.cn/thread-20115-1-1.html>.
- [4] R. Collinson, "Rental housing affordability dynamics, 1990–2009," *Cityscape*, vol. 13, no. 2, pp. 71–103, 2011.
- [5] J. Shi, K. Duan, S. Wen, and R. Zhang, "Investment valuation model of public rental housing PPP project for private sector: a real option perspective," *Sustainability*, vol. 11, no. 7, p. 1857, 2019.
- [6] X. Yi and L. Zheng, "The major theoretical issues of the sustainable development of China's residential housing rental market," *Exploration and Free Views*, vol. 2, pp. 117–144, 2019.
- [7] W. Wang and Y. Hu, "Research on housing rental market in first-tier cities," *The World of Survey and Research*, vol. 4, pp. 25–30, 2019.
- [8] C. Lv, "Research on the "market priority" rental policy in the United States," *On Economic Problems*, vol. 2, pp. 19–26, 2019.
- [9] R. Dou, "A comparative study between Canadian and Japanese cohousing modes and related experience: based on the features of system building, space arrangement, and operations management," *City Planning Review*, vol. 42, no. 11, pp. 111–123, 2018.
- [10] W. Lou and H. Zhou, "Experience of Russian housing rental market reform and reference," *Price: Theory & Practice*, vol. 11, pp. 58–61, 2018.
- [11] L. Du, "Learning from the credit mechanism of the British housing leasing market," *Frontiers*, vol. 19, pp. 70–78, 2018.
- [12] J. Yuan, W. Li, X. Zheng, and M. J. Skibniewski, "Improving operation performance of public rental housing delivery by PPPs in China," *Journal of Management in Engineering*, vol. 34, no. 4, Article ID 04018015, 2018.
- [13] T. Yu, X. Liang, G. Q. Shen, Q. Shi, and G. Wang, "An optimization model for managing stakeholder conflicts in urban redevelopment projects in China," *Journal of Cleaner Production*, vol. 212, pp. 537–547, 2019.
- [14] S. Zheng and S. Xu, "Co-evolutionary simulation analysis of multiple stakeholders in the housing rental market based on system dynamics," *Journal of Engineering Management*, vol. 32, no. 6, pp. 149–154, 2018.
- [15] J. Qiu, "The game of social forces participating in the evolution of the housing rental market and government regulation," *American Journal of Industrial and Business Management*, vol. 10, no. 01, pp. 99–109, 2020.
- [16] J. Zhou, Y. Zhao, and F. Jv, "The static game and solution strategy in the development of housing rental market and its solution strategy," *Seeker*, vol. 3, pp. 72–76, 2016.
- [17] D. Chai, M. Lin, and H. Fan, "The benefit impacts and multi-center governance mechanism of rental-housing in collective land," *Economic Geography*, vol. 38, no. 8, pp. 152–161, 2018.
- [18] C. Lai and X. Chen, "Complex dynamic analysis for a real-estate oligopoly game model with bounded rationality," *Journal of Systems Engineering*, vol. 28, no. 3, pp. 285–296, 2013.

- [19] B. Xin, F. Cao, W. Peng, and A. A. Elsadany, "A bertrand duopoly game with long-memory effects," *Complexity*, vol. 2020, Article ID 2924169, , 2020.
- [20] B. Xin and M. Sun, "A differential oligopoly game for optimal production planning and water savings," *European Journal of Operational Research*, vol. 269, no. 1, pp. 206–217, 2018.
- [21] J. Ma, F. Zhang, and B. Bao, "Dynamic game and coordination strategy of multichannel supply chain based on brand competition," *Complexity*, vol. 2019, pp. 1–26, 2019.
- [22] Z. Guo, "Complexity and implications on channel conflict under the uncertain impacts of online customer reviews," *Nonlinear Dynamics*, vol. 96, no. 3, pp. 1971–1987, 2019.
- [23] A. A. Elsadany, "Competition analysis of a triopoly game with bounded rationality," *Chaos, Solitons & Fractals*, vol. 45, no. 11, pp. 1343–1348, 2012.
- [24] F. Tramontana and A. E. A. Elsadany, "Heterogeneous triopoly game with isoelastic demand function," *Nonlinear Dynamics*, vol. 68, no. 1-2, pp. 187–193, 2011.
- [25] R. K. Ghaziani, W. Govaerts, and C. Sonck, "Resonance and bifurcation in a discrete-time predator-prey system with Holling functional response," *Nonlinear Analysis: Real World Applications*, vol. 13, no. 3, pp. 1451–1465, 2012.
- [26] W. Govaerts and R. Khoshsiar Ghaziani, "Stable cycles in a cournot duopoly model of kopel," *Journal of Computational and Applied Mathematics*, vol. 218, no. 2, pp. 247–258, 2008.
- [27] R. Liao, "Customs supervision based on evolutionary game of heterogeneous groups in super-network," *System Engineering*, vol. 36, no. 8, pp. 140–147, 2018.
- [28] L. Li and S. Chen, "An analysis of the policy structure of nurturing and developing the housing rental market - based on a dual perspective of policy instruments and industry chains," *Fujian Forum (Humanities and Social Sciences Edition)*, vol. 8, pp. 28–37, 2018.

Research Article

A New Method for Interindustry Linkage Analysis Based on Demand-Driven and Multisector Input-Output Model and Its Application in China's Manufacturing and Producer Services

Xiao Liu ^{1,2} and Jinchuan Shi ¹

¹School of Economics, Zhejiang University, Hangzhou 310007, China

²Zhejiang Economic Information Center, Hangzhou 310006, China

Correspondence should be addressed to Jinchuan Shi; jinchuan_shi@163.com

Received 24 April 2020; Revised 23 June 2020; Accepted 13 July 2020; Published 20 August 2020

Guest Editor: Baogui Xin

Copyright © 2020 Xiao Liu and Jinchuan Shi. This is an open access article distributed under the Creative Commons Attribution License, which permits unrestricted use, distribution, and reproduction in any medium, provided the original work is properly cited.

Interindustry linkage analysis is an important interdisciplinary research field of technical economic and complex systems, and the results can be used as critical bases for making strategies and policies of economic development. This study reviews the previous methods for measuring interindustry linkages and their disadvantages and puts forward a new method for interindustry linkage analysis in a complex economic system on the basis of demand-driven and multisector input-output model. Firstly, it makes a further decomposition of the Leontief inverse matrix in the economic sense and decomposes the gross output of one industrial sector or its sub-industries into three components. Then, it analyzes the structural features of output and measures the interindustry linkages between two industrial sectors with three indices: interindustry linkage effect, interindustry linkage contribution, and interindustry linkage coefficient. Compared with the previous measurements, the method in this study has three obvious advantages: it integrates the sectoral internal effect and external linkage effect at the same time; it can not only measure the interindustry linkage effects between two given industrial sectors but also clearly describe the composition ratio of the direct and indirect interindustry linkage effects; and it adopts, respectively, the absolute flow value, relative flow value, and unit relative value to measure the linkages comprehensively. Finally, this study takes China's input and output in 2017 as an application case to analyze the structural features of output of its manufacturing and producer services and measure the interindustry linkages between them.

1. Introduction

National economy is a large and complex system, and the industries in it interact with and impact each other. Interindustry linkage is a kind of technical and economic link existing extensively among the industries and the concept was first introduced by Hirschman in 1958 based on the theory of unbalanced development [1]. Since the 1950s, with the acceleration of industrialization in developing countries, interindustry linkages have gained extensive attention from academia circle, industrial field, and policy-makers and are used to measure the relative importance of industries in order to identify the key industries which are central for economic development and can drive economic high-speed

growth. Therefore, an applicable and reasonable method to measure the interindustry linkages is helpful to recognize the relationship between or among industries, promote the level of balanced development of the entire economic system, and even optimize the industrial structure of the national economy. Over the years, the previous scholars have conducted many research studies on the analysis of interindustry linkages from different perspectives. In general, the traditional econometric analysis and input-output analysis are two main and common kinds of methods which can be used to well describe the interrelatedness of industries.

The former is a relatively indirect method which generally first puts forward hypotheses and then usually adopts the econometric model such as the panel data regression

model or the vector autoregressive (VAR) model to search the supporting empirical evidences based on the macro-statistics data of the economy system: e.g., Banga and Golder use regression analysis model to research the contribution of services to manufacturing output growth and productivity on the basis of Indian panel data [2]; Francois and Woerz use regression analysis model to research the interaction between production services and manufacturing on the basis of the panel data on goods and services trade of Organization for Economic Co-operation and Development (OECD) during 1994–2004 [3]; Ke et al. conduct a panel data analysis of Chinese cities and construct a simultaneous equation model of co-agglomeration of producer services and manufacturing that highlights the synergy effects of the two sectors located in the same cities or neighboring cities [4]; Kong and Liang use VAR model to analyze the interaction between producer services and manufacturing in Shaanxi Province, China [5].

The latter is a relatively direct method which is first introduced by Leontief in 1936 [6], and it quantitatively analyzes or computes the interindustry linkages or relationships through the input-output data and a series of linear equations: e.g., Guerrieri and Meliciani study empirically the interindustry linkages between producer service and three major industries on the basis of the input-output data of Denmark, the UK, Germany, France, Japan, and the US [7]; through measuring the backward and forward linkages of one certain industry, Chiu and Lin investigate the role and influence of the maritime sector on the national economy of Taiwan [8]; Mattioli and Lamonica evaluate the information and communications technology (ICT) role in the world economy [9]; Khanal et al. study the significance of economic linkages between the tourism sector and the rest of the economy in Lao People's Democratic Republic (Lao PDR) [10]; Guerra and Sancho measure the role of energy and non-energy efficiency gains in an interconnected and multisector economy with the hypothetical extraction method [11], which is a powerful input-output analysis tool and will be discussed later; Sajid et al. conduct a serial of researches on carbon linkages via hypothetical extraction method or its modification [12, 13]; Wang et al. employ the hypothetical extraction method to map flows of embodied air pollutant emission from economic sectors in China [14] and even conduct an analysis on interregional and sectoral linkages of air pollutant emissions in Beijing-Tianjin-Hebei region of China [15]; Ali et al. use the Asian Development Bank input-output database to analyze and compare the performance of the construction sector in some south Asian countries [16].

Comparing the two kinds of methods mentioned above, although the latter is insufficient in terms of data immediacy and availability due to the fact that input-output data usually are only issued by the official statistics department every few years, it can provide a more convictive and micro-view perspective to describe the interrelatedness of industries, and overcome the disadvantages of the former that it is difficult to obtain high quality economic statistics data and reflect promptly when the economic structure changes greatly. What is more, due to an apparent intimate tie between the

interdependencies studied in input-output analysis and the causal relations expressed in Hirschman's interindustry linkages, Hirschman's interindustry linkages have been embraced by input-output economists [17].

Therefore, on the foundation of the theory of input-output analysis, this study designs a new method for interindustry linkage analysis based on demand-driven and multisector input-output model and applies it in the scenario of China's Manufacturing and Producer Services. Since its obvious advantages, compared with the previous measurements of interindustry linkages specifically discussed later, the authors hold that it is a helpful tool for analyzing the interrelatedness between two industrial sectors and identifying the key weak links.

Section 2 reviews the theory of input-output and interindustry linkages and summarizes the features and disadvantages of different attempts to measure the interindustry linkages. In Section 3, demand-driven and multisector input-output model is carried out, in which the output and Leontief inverse matrix are structurally decomposed in economic sense; it also presents the ways to analyze the output structural features of an industrial sector and its sub-industries and measure the interindustry linkages between two different industrial sectors; in particular, this study takes China as an example to emphatically analyze the interindustry linkages between its manufacturing and producer services in a framework of multisector economic system. Section 4 presents the results of the application in China, and then the specific discussion and policy implication are presented in Section 5. The paper ends up with a discussion of the value of this method in analyzing the interindustry linkages in multisector economic system.

2. Theoretical Background

According to the view of Hirschman [1], any nonprimary activity which does not only produce for final demand exerts two distinct effects by means of its demand for and supply of intermediate inputs, respectively, so the interindustry linkage has two different types. The demand stimulates other sectors to satisfy its intermediate requirements, which is named backward linkage; the supply also stimulates sectors because its output is also taken as an input in new activities, which is named forward linkage. Chenery and Watanable's work firstly attracts the scholars' attention [18], which is conducted on the basis of the input coefficient matrix and considered to be the earliest measurement of Hirschman's interindustry linkages. However, the analysis based on the input coefficient matrix only considers the first round of consumption in the entire economic system, ignoring the interrelatedness of indirect transfer; namely, the measurement is incomplete. Rasmussen's dispersion indices on the basis of Leontief inverse matrix (also called total requirements matrix) is another attempt to measure interindustry linkages [19], and it has been widely used because it can be credited with including indirect effects and distinguishing between backward linkage and forward linkage, despite the fact that Rasmussen's original research is before Hirschman introduced the concept of interindustry linkages. Based on

the pioneering work of Hirschman, Chenery and Watanabe, and Rasmussen, the theoretical and applied researches on the measurement of interindustry linkages have been conducted widely, and the later scholars have put forward various schemes to refine the measurement of interindustry linkages.

Jones questions the use of Rasmussen's index of sensitivity of dispersion as a measurement of forward linkage, then puts forward a new method to measure the forward linkage on the basis of Ghosh inverse matrix instead of Leontief inverse matrix, and elaborates its value in detail [20]. Cuello et al. refine Rasmussen's measurement through introducing a serial of parameters which are used in weighting the coefficients in Leontief inverse matrix, in order to take the relative importance of different industries into consideration [21]. Referring to the research of Cuello et al., Drejer even introduces knowledge as a weight in terms of knowledge intensive industries [17]. Hazari and Laumas discuss whether the weighting of different industries should be considered in the measurement of interindustry linkages, although their viewpoints are not the same; Hazari holds that weighting or not weighting depends on the purpose of analysis [22], while Laumas is more inclined to adopt the measurement in the weighted form [23].

Since Rasmussen's dispersion indices and the modified methods evaluate the two types of linkages separately, hypothetical extraction method is proposed as a new and more practical method [24, 25]. In this method, the importance of a sector, also called its total linkage, is measured by comparing numerically the output levels of economy before and after the hypothetical extraction, in which the row and column input-output data of this sector are deleted. (Instead of physically deleting them, they can simply be replaced by zeros.) Cella modifies the method, and the measure of total linkage in his research not only excludes feedback processes which are purely internal to the selected industry, but also is decomposable into additive components measuring backward and forward linkages, respectively [26]. Duarte et al. further modify Cella's method and decompose the total linkage into four components, internal effect, mixed effect, net backward linkage, and net forward linkage, when studying the behavior of the productive sectors of the Spanish economy as direct and indirect consumers of water [27]. Different from the studies that have mostly calculated both backward and forward linkages using only demand-driven Leontief inverse model, Sajid et al. estimate the linkages from both demand and supply with Leontief inverse matrix and Ghosh inverse matrix, when studying the intersectoral carbon linkages of Turkey [28].

The measure methods on the foundation of the research of Chenery and Watanabe and Rasmussen are all based on classical input-output analysis model. When using these classical measurements of interindustry linkages, scholars firstly may face two difficult problems: which coefficient matrix should be chosen; whether and how the researchers weight the different industries according to their scales and importance. Furthermore, Leontief inverse matrix or Ghosh

inverse matrix based on the row balance or column balance in the input-output tables can only represent the overall interrelatedness, which contains not only direct and indirect interrelatedness but also internal effect and external linkage. Finally, the classical measurements only describe the interrelatedness between a given industry and the entire economic system, rather than that between two given industries. As for the hypothetical extraction method, though many scholars have been improving and modifying it in order to better and more accurately measure the importance of the sector, it still has some drawbacks. First of all, its underlying hypothetical deviates somewhat from the economic reality. In the scenario of hypothetical extraction, the row and the column referring to the selected industry in input coefficient matrix are replaced by zeros, while the rest remain the same. In fact, as mentioned, the industries in the economic system interact with and impact each other. The interrelatedness among the rest of the industries may change even dramatically when an industry is removed. So the difference between the output levels before and after the hypothetical extraction probably should not be equated with the real impact of the interindustry linkages. What is more, hypothetical extraction method provides a very practical and simple measure for interindustry linkages between a given industry and the entire economy system; however, the measure for interindustry linkages between two given industries is still inexplicit. In addition, with mounting evidence favoring simultaneous application of both Ghosh supply and Leontief demand for forward and backward linkages, the researches on hypothetical extraction method which only adopts Leontief inverse matrix may provide erroneous evidence or biased suggestions.

With the continuous progress of the input-output theoretical model, now the researchers have many new choices to analyze the interindustry linkages, e.g., the dynamic input-output model aiming to overcome the static analysis disadvantages of the classical input-output model [29, 30], the input-output optimization model that combines optimization theory and input-output theory [31, 32], and the spatial input-output model aiming to analyze the interregional input-output relationships [33, 34]. Now the inter-country input-output tables which are regularly published in the world mainly include the World Input-output Table (WIOT), OECD Inter-Country Input-Output (ICIO) Table, and the Asian International Input-Output Table (AIIOT). Miller first adopted the input-output theory to study the economic impacts between different regions and constructed a two-region input-output model to measure the interregional feedback effect, but it does not involve the concept and measurement of interindustry spillover effect [35]. Later scholars, e.g., Round, Sonis, and Dietzenbacher, distinguish the interindustry spillover effect and interindustry feedback effect between different regions, study the relationship between them and their multiplier effect, and conduct the empirical researches [36–38].

According to the research of Round, the output as well as Leontief inverse matrix can be multiplicatively decomposed into three components: the separate effects of multipliers

wholly within a group of accounts, the effect of an exogenous injection which feeds back upon itself but via other parts of the system, and the effect an increase in income in one group of accounts has upon another. In many kinds of analysis involving multipliers, it is convenient to formulate them so that their sum rather than their sequential multiplication yields the total multipliers. The output as well as Leontief inverse matrix also can be additively decomposed, which is equivalent to Round's multiplicative decomposition. On the foundation of Miller and Round's two-region input-output analysis, this study regards different industrial sectors in the entire economic system as different regions in the spatial scope and constructs a demand-driven and multisector input-output model, focusing on the output structural analysis and the measurement of interindustry linkages between two given industrial sectors in a multisector economic system.

In demand-driven and multisector input-output model, the gross output can be decomposed into three components, intraindustry multiplier effect, interindustry spillover effect, and interindustry feedback effect. Intraindustry multiplier effect is a kind of sectoral internal effect, and an industrial sector's intraindustry multiplier effect refers to the output induced by the increase of its final demand in an input-output system which only contains this industrial sector, and it indicates the viability of this industrial sector. Interindustry spillover effect is a kind of external linkage effect, and an industrial sector's spillover effect refers to the rest of the industrial sectors' output induced by the increase of its final demand, which indicates the impacting capacity of this industrial sector. In this study, the conception of interindustry incoming spillover effect is introduced in order to analyze the output structure easily, which is precisely opposite to that of interindustry spillover effect. An industrial sector's interindustry incoming spillover effect refers to the output induced by the increase of the rest of the industrial sectors' final demand. Interindustry feedback effect is also a kind of external linkage effect, and an industrial sector's interindustry feedback effect refers to the output induced by the increase of its final demand after the multiplier effect, namely, the transfer of the technology, products, or services from this industrial sector to the other industrial sectors and then back to itself. So, the gross output of an industrial sector or its subindustry is the total sum of its intraindustry multiplier effect, interindustry incoming spillover effect, and interindustry feedback effect.

3. Materials and Methods

3.1. Demand-Driven and Multisector Input-Output Model. Suppose that the entire economic system contains n ($n \geq 2$) industrial sectors and each industrial sector contains one or more subindustries. Denote the industrial sector as Ind with superscript, such as Ind^p ($p \in \{1, 2, \dots, n\}$) and the subindustry in it with subscript, such as Ind_u^p ($u \in \{1, 2, \dots, m_p\}$), where m_p is the number of subindustries in Ind^p . X represents the gross output of the entire economic system, X^p represents the gross output of Ind^p , and X_u^p represents the

gross output of Ind_u^p . Similarly, Y represents the final demand of the entire economic system, Y^p represents the final demand of Ind^p , and Y_u^p represents the final demand of Ind_u^p . It is worth mentioning that the final demand in this study also contains the part of net exports if the system is an open economy. Both of X and Y are column vectors consisting of the industrial sectors' gross output or final demand, and both of X^p and Y^p are also column vectors consisting of the subindustries' gross output or final demand, e.g., $X = [X^1, X^2, \dots, X^n]^T$, $Y = [Y^1, Y^2, \dots, Y^n]^T$, $X^p = [X_1^p, X_2^p, \dots, X_{m_p}^p]^T$, $Y^p = [Y_1^p, Y_2^p, \dots, Y_{m_p}^p]^T$.

According to the classical demand-driven input-output theory, the quantitative relationship between the gross output and final demand can be expressed as follows:

$$AX + Y = X. \quad (1)$$

In a multisector input-output scenario, equation (1) can be written specifically as follows:

$$\begin{bmatrix} A^{11} & A^{12} & \dots & A^{1n} \\ A^{21} & A^{22} & \dots & A^{2n} \\ \dots & \dots & \dots & \dots \\ A^{n1} & A^{n2} & \dots & A^{nn} \end{bmatrix} \begin{bmatrix} X^1 \\ X^2 \\ \dots \\ X^n \end{bmatrix} + \begin{bmatrix} Y^1 \\ Y^2 \\ \dots \\ Y^n \end{bmatrix} = \begin{bmatrix} X^1 \\ X^2 \\ \dots \\ X^n \end{bmatrix}, \quad (2)$$

where A is the input coefficient matrix of the entire economic system, A^{pq} is a submatrix in A , and A^{pq} consists of the element a_{uv}^{pq} which represents the direct consumption of Ind_u^p per unit of output of Ind_v^q ($q \in \{1, 2, \dots, n\}$); ($v \in \{1, 2, \dots, m_q\}$). After series of mathematical derivation, equation (2) can be transformed as follows:

$$X = \begin{bmatrix} X^1 \\ X^2 \\ \dots \\ X^n \end{bmatrix} = (I - A)^{-1}Y = BY = \begin{bmatrix} B^{11} & B^{12} & \dots & B^{1n} \\ B^{21} & B^{22} & \dots & B^{2n} \\ \dots & \dots & \dots & \dots \\ B^{n1} & B^{n2} & \dots & B^{nn} \end{bmatrix} \begin{bmatrix} Y^1 \\ Y^2 \\ \dots \\ Y^n \end{bmatrix}, \quad (3)$$

where B is the Leontief inverse matrix of the entire economic system and B^{pq} is its submatrix. B is the so-called multiplier in the demand-driven input-output model, which represents the multiplicative relationship between the gross output and final demand.

Referring to the research on interregional input-output model, the gross output or the Leontief inverse matrix B of the entire economic system can be decomposed into three components, intraregional multiplier effect, interregional spillover effect, and interregional feedback effect. When regarding the industrial sectors as regions, the gross output or the Leontief inverse matrix B of the entire economic system can be also similarly decomposed into three components, intraindustry multiplier effect, interindustry spillover effect, and interindustry feedback effect. For the sake of specific distinction, this study names the components in the gross output as intraindustry multiplier effect, interindustry spillover effect, and interindustry feedback effect, and the components in the Leontief inverse matrix B as

intraindustry multiplier effect coefficient matrix, interindustry spillover effect coefficient matrix, and interindustry feedback effect coefficient matrix, labeled as M , S , and F .

Leontief inverse matrix B has two different kinds of decompositions, multiplicative decomposition and additive

decomposition, in which three components are labeled as M_m, S_m, F_m and M_a, S_a, F_a , respectively. The decompositions are presented as follows [39]:

$$B = F_m S_m M_m = \begin{bmatrix} F^{11} & 0 & \dots & 0 \\ 0 & F^{22} & \dots & 0 \\ \dots & \dots & \dots & \dots \\ 0 & 0 & \dots & F^{nn} \end{bmatrix} \begin{bmatrix} I & S^{12} & \dots & S^{1n} \\ S^{21} & I & \dots & S^{2n} \\ \dots & \dots & \dots & \dots \\ S^{n1} & S^{n2} & \dots & I \end{bmatrix} \begin{bmatrix} M^{11} & 0 & \dots & 0 \\ 0 & M^{22} & \dots & 0 \\ \dots & \dots & \dots & \dots \\ 0 & 0 & \dots & M^{nn} \end{bmatrix}, \quad (4)$$

$$B = M_a + S_a + F_a = \begin{bmatrix} M^{11} & 0 & \dots & 0 \\ 0 & M^{22} & \dots & 0 \\ \dots & \dots & \dots & \dots \\ 0 & 0 & \dots & M^{nn} \end{bmatrix} + \begin{bmatrix} 0 & F^{11} S^{12} M^{22} & \dots & F^{11} S^{1n} M^{nn} \\ F^{22} S^{21} M^{11} & 0 & \dots & F^{22} S^{2n} M^{nn} \\ \dots & \dots & \dots & \dots \\ F^{nn} S^{n1} M^{11} & F^{nn} S^{n2} M^{22} & \dots & 0 \end{bmatrix} + \begin{bmatrix} (F^{11} - I)M^{11} & 0 & \dots & 0 \\ 0 & (F^{22} - I)M^{22} & \dots & 0 \\ \dots & \dots & \dots & \dots \\ 0 & 0 & \dots & (F^{nn} - I)M^{nn} \end{bmatrix}, \quad (5)$$

where M^{PP} , S^{Pq} , and F^{PP} are defined in equations (6)–(8):

$$M^{PP} = (I - A^{PP})^{-1}, \quad (6)$$

$$F^{PP} = B^{PP} (I - A^{PP}), \quad (7)$$

$$S^{Pq} = (B^{PP} - B^{PP} A^{PP})^{-1} B^{Pq} (I - A^{qq}), \quad (p \neq q). \quad (8)$$

Since the additive decomposition is easier to understand in economic sense and more intuitive for output analysis, this study just adopts it instead of the multiplicative decomposition; namely, M , S , and F in the following content are represented by M_a, S_a, F_a in equation (5), shown as follows:

$$M = \begin{bmatrix} M^{11} & 0 & \dots & 0 \\ 0 & M^{22} & \dots & 0 \\ \dots & \dots & \dots & \dots \\ 0 & 0 & \dots & M^{nn} \end{bmatrix},$$

$$S = \begin{bmatrix} 0 & F^{11} S^{12} M^{22} & \dots & F^{11} S^{1n} M^{nn} \\ F^{22} S^{21} M^{11} & 0 & \dots & F^{22} S^{2n} M^{nn} \\ \dots & \dots & \dots & \dots \\ F^{nn} S^{n1} M^{11} & F^{nn} S^{n2} M^{22} & \dots & 0 \end{bmatrix},$$

$$F = \begin{bmatrix} (F^{11} - I)M^{11} & 0 & \dots & 0 \\ 0 & (F^{22} - I)M^{22} & \dots & 0 \\ \dots & \dots & \dots & \dots \\ 0 & 0 & \dots & (F^{nn} - I)M^{nn} \end{bmatrix}. \quad (9)$$

Interindustry spillover effect coefficient matrix S can be further decomposed into two parts which, respectively, represent the impacts on the output in the first round and the rest of the rounds. In this study, the two parts are named as direct interindustry spillover effect coefficient matrix S_d and indirect interindustry spillover effect coefficient matrix S_i , presented as follows:

$$S = S_d + S_i = \begin{bmatrix} 0 & S^{12} M^{22} & \dots & S^{1n} M^{nn} \\ S^{21} M^{11} & 0 & \dots & S^{2n} M^{nn} \\ \dots & \dots & \dots & \dots \\ S^{n1} M^{11} & S^{n2} M^{22} & \dots & 0 \end{bmatrix} + \begin{bmatrix} 0 & (F^{11} - I)S^{12} M^{22} & \dots & (F^{11} - I)S^{1n} M^{nn} \\ (F^{22} - I)S^{21} M^{11} & 0 & \dots & (F^{22} - I)S^{2n} M^{nn} \\ \dots & \dots & \dots & \dots \\ (F^{nn} - I)S^{n1} M^{11} & (F^{nn} - I)S^{n2} M^{22} & \dots & 0 \end{bmatrix}. \quad (10)$$

So, the Leontief inverse matrix B of the entire economic system in multisector input-output model can be decomposed as follows:

$$B = \begin{bmatrix} F^{11} M^{11} & F^{11} S^{12} M^{22} & \dots & F^{11} S^{1n} M^{nn} \\ F^{22} S^{21} M^{11} & F^{22} M^{22} & \dots & F^{22} S^{2n} M^{nn} \\ \dots & \dots & \dots & \dots \\ F^{nn} S^{n1} M^{11} & F^{nn} S^{n2} M^{22} & \dots & F^{nn} M^{nn} \end{bmatrix} = M + S + F. \quad (11)$$

On the basis of this kind of decomposition, the relationship of gross output and final demand shown in equation (3) can be rewritten as follows:

$$\begin{bmatrix} X^1 \\ X^2 \\ \dots \\ X^n \end{bmatrix} = M \times \begin{bmatrix} Y^1 \\ Y^2 \\ \dots \\ Y^n \end{bmatrix} + S \times \begin{bmatrix} Y^1 \\ Y^2 \\ \dots \\ Y^n \end{bmatrix} + F \times \begin{bmatrix} Y^1 \\ Y^2 \\ \dots \\ Y^n \end{bmatrix}. \quad (12)$$

Equation (12) can be also briefly presented as follows:

$$X^p = M^{pp}Y^p + \sum_q F^{pp}S^{pq}M^{qq}Y^q + (F^{pp} - I)M^{pp}Y^p, \quad (q \neq p). \quad (13)$$

Since equation (13) is a kind of matrix expression, when defining $\overline{X^p}$ as the total sum of the elements in X^p , the gross output of Ind^p in algebraic expression can be presented as follows:

$$\begin{aligned} \overline{X^p} = eX^p = eM^{pp}Y^p + e \sum_q F^{pp}S^{pq}M^{qq}Y^q \\ + e(F^{pp} - I)M^{pp}Y^p, \quad (q \neq p), \end{aligned} \quad (14)$$

where e is a column summation operator, e.g., $e = [1, 1, \dots, 1]$. The gross output of Ind_u^p , namely, X_u^p , in algebraic expression can be also written as follows:

$$\begin{aligned} X_u^p = e_u X^p = e_u M^{pp}Y^p + e_u \sum_q F^{pp}S^{pq}M^{qq}Y^q \\ + e_u (F^{pp} - I)M^{pp}Y^p, \quad (q \neq p), \end{aligned} \quad (15)$$

where e_u is a row vector containing m_p elements and the responding element of Ind_u^p is 1 while the rest are 0, e.g., $e_u = [0, \dots, 1, \dots, 0]$.

According to the additive decompositions in equations (14) and (15), the intraindustry multiplier effect, interindustry incoming spillover effect, and interindustry feedback effect of industrial sector Ind^p and its subindustry Ind_u^p in algebraic expression are presented in Table 1.

3.2. Interindustry Linkage Analysis. Denote $M(Z)$, $S(Z)$, and $F(Z)$ as the intraindustry multiplier effect, interindustry incoming spillover effect, and interindustry feedback effect of Z (Z is Ind^p or Ind_u^p), respectively. This study adopts $M(Z)$ to represent the sectoral internal effect of Z , and $S(Z) + F(Z)$ to represent the external linkage effect of Z . $S(Z)$ refers to the output totally induced by the final demand of other industrial sectors, called external linkage effect I in this study; $F(Z)$ refers to the difference between output induced by the final demand of this industrial sector in an economy only containing it and that in the actual economy containing multi-industrial sectors, called external linkage effect II in this study.

This study adopts the proportions of the sectoral internal effect and external linkage effect in the gross output to describe the output structural features of an industrial sector or its subindustries. The proportion of $M(Z)$ in the gross output indicates the contribution of the industrial sector (if Z is Ind^p) or the industrial sector to which the subindustry belongs (if Z is Ind_u^p) on the gross output of Z , and the higher value refers to the greater viability of Z . The proportion of S

(Z) + $F(Z)$ in the gross output indicates the contribution of the external industrial sectors to the gross output of Z , and the higher value refers to the greater dependence of Z for the other industrial sectors. The sectoral internal effect and external linkage effect of Z in demand-driven and multi-sector input-output model are presented in Table 2.

Denote $S(\text{Ind}^q, Z)$ as the interindustry incoming spillover effect from Ind^q to Z ($q \neq p$), and this study adopts $S(\text{Ind}^q, Z)$ to measure the interindustry linkage effect from Ind^q to Z . As mentioned above, $S(\text{Ind}^q, Z)$ can be further decomposed into two parts, which, respectively, represent the direct and indirect interindustry linkage effect from Ind^q to Z and are presented as follows:

$$\begin{aligned} S(\text{Ind}^q, \text{Ind}^p) &= eF^{pp}S^{pq}M^{qq}Y^q = eS^{pq}M^{qq}Y^q \\ &\quad + e(F^{pp} - I)S^{pq}M^{qq}Y^q, \\ S(\text{Ind}^q, \text{Ind}_u^p) &= e_u F^{pp}S^{pq}M^{qq}Y^q = e_u S^{pq}M^{qq}Y^q \\ &\quad + e_u (F^{pp} - I)S^{pq}M^{qq}Y^q. \end{aligned} \quad (16)$$

This study adopts the proportion of $S(\text{Ind}^q, Z)$ in the gross output of Z to measure the contribution of the interindustry linkage effect, named as interindustry linkage contribution and labeled as $\text{LinkC}(\text{Ind}^q, Z)$, and adopts the ratio of $S(\text{Ind}^q, Z)$ and the final demand of Ind^q to measure the efficiency of the interindustry linkage effect, named as interindustry linkage coefficient and labeled as $\text{LinkE}(\text{Ind}^q, Z)$. $\text{LinkC}(\text{Ind}^q, Z)$ and $\text{LinkE}(\text{Ind}^q, Z)$ can be written as follows:

$$\begin{aligned} \text{LinkC}(\text{Ind}^q, \text{Ind}^p) &= \frac{S(\text{Ind}^q, \text{Ind}^p)}{\overline{X^p}}, \\ \text{LinkC}(\text{Ind}^q, \text{Ind}_u^p) &= \frac{S(\text{Ind}^q, \text{Ind}_u^p)}{X_u^p}, \\ \text{LinkE}(\text{Ind}^q, \text{Ind}^p) &= \frac{S(\text{Ind}^q, \text{Ind}^p)}{eY^q}, \\ \text{LinkE}(\text{Ind}^q, \text{Ind}_u^p) &= \frac{S(\text{Ind}^q, \text{Ind}_u^p)}{e_u Y^q}. \end{aligned} \quad (17)$$

Interindustry linkage effect indicates the scale of the absolute flow value from one given industrial sector to the other industrial sector or its subindustries; interindustry linkage contribution indicates the contribution of the interindustry linkage effect on the gross output, namely, the scale of the relative flow value from one given industrial sector to the other industrial sector or its subindustries; interindustry linkage coefficient indicates the efficiency of the interindustry linkage effect, namely, the scale of the unit flow value from one given industrial sector to the other industrial sector or its subindustries. The higher value of them refers to the greater absolute flow value, contribution, or efficiency.

3.3. Input-Output Data in China 2017. In this subsection, this study takes the input-output data in China 2017 as example and adopts the method mentioned above to analyze the structural features of output and measure the

TABLE 1: Decomposition components of gross output in demand-driven and multisector input-output model.

Industrial sector or subindustry	Gross output	Intraindustry multiplier effect	Interindustry incoming spillover effect	Interindustry incoming spillover effect from Ind ^q	Interindustry feedback effect
Ind ^p	\bar{X}^p	$e_u M^{PPY^p}$	$e \sum_q F^{PPS^p q} M^{qqY^q}, (p \neq q)$	$e F^{PPS^p q} M^{qqY^q}, (p \neq q)$	$e(F^{PP} - I)M^{PPY^p}$
Ind ^p _u	X_u^p	$e_u M^{PPY^p}$	$e_u \sum_q F^{PPS^p q} M^{qqY^q}, (p \neq q)$	$e_u F^{PPS^p q} M^{qqY^q}, (p \neq q)$	$e_u (F^{PP} - I)M^{PPY^p}$

TABLE 2: The sectoral internal effect and external linkage effect in demand-driven and multisector input-output model.

Industrial sector or subindustry	Sectoral internal effect	External linkage effect
Ind ^p	$e M^{PPY^p}$	$\bar{X}^p - e M^{PPY^p}$
Ind ^p _u	$e_u M^{PPY^p}$	$X_u^p - e_u M^{PPY^p}$

interindustry linkages between two industrial sectors. Since China's authority and the industry policy-makers have almost regarded manufacturing and producer services as the most critical industrial sectors for industrial transformation and upgrading and have successively introduced a series of industrial policies to promote the integration level of the two industrial sectors, this application case mainly focuses on the interindustry linkages between them.

Firstly, the entire economic system of China is divided into three industrial sectors: manufacturing, producer services, and the rest of the industries, and each of them has some subindustries. In China Input-Output Table in Year 2017, manufacturing has many subindustries. Since the scale of some subindustries of manufacturing is too small, manufacturing is only further divided into three components, low-tech manufacturing, mid-tech manufacturing, and high-tech manufacturing in this study according to the Industrial Classification for National Economic Activities (ICNEA) issued in 2017. The six subindustries of producer services are wholesale service, logistic service, information service, finance service, business service, and technology service. The three subindustries of the rest of the industries are the primary industry, the second industry excluding manufacturing labeled as the rest second industry in brief, and the tertiary industry excluding producer services labeled as the rest of the tertiary industry in brief. The classification of the entire economic system is specifically presented in Appendix A, and the rearranged China Input-Output Table in Year 2017 is shown in Appendix B.

Label manufacturing, producer services, and the rest of the industries as Ind¹, Ind², and Ind³, respectively; the low-tech manufacturing, mid-tech manufacturing, and high-tech manufacturing in Ind¹ as Ind¹₁, Ind¹₂, and Ind¹₃; the wholesale service, logistic service, information service, finance service, business service, and technology service in Ind² as Ind²₁, Ind²₂, Ind²₃, Ind²₄, Ind²₅, and Ind²₆; and the primary industry, the rest of the second industry, and the rest of the tertiary industry in Ind³ as Ind³₁, Ind³₂, and Ind³₃. The gross input vector X , final demand vector Y , input coefficient matrix A , Leontief inverse matrix B , intraindustry multiplier effect coefficient matrix M , interindustry spillover effect coefficient matrix S , direct interindustry spillover effect coefficient matrix S_d , indirect interindustry spillover effect coefficient matrix S_i , and interindustry feedback effect coefficient matrix F are presented in Appendix C.

4. Results

On the basis of the method mentioned in Section 3.1, the decomposition components of gross output of manufacturing, producer services, and their subindustries in China 2017 are presented in Table 3.

Further, combining the data in Table 3 and the method mentioned in Section 3.2, the output structural features of the two industrial sectors and their subindustries, namely, the proportions of sectoral internal effect and external linkage effect, are presented in Table 4; the interindustry linkages from manufacturing to producer services are presented in Table 5, and those from producer services to manufacturing are presented in Table 6.

Through data observation and comparison in Tables 4–6, this study finds the following results on manufacturing and producer services.

As for manufacturing in China 2017, (1) its viability, namely, intraindustry multiplier effect or sectoral internal effect, contributes 48.96% of the gross output of itself, and the external linkage effect, namely, the total sum of interindustry spillover effect and interindustry feedback effect, contributes 51.04% of the gross output of itself, in which the interindustry linkage effect from the rest of the industrial sector accounts for 35.51%, shown in Table 4; (2) the interindustry linkage effect, direct interindustry linkage effect, and indirect interindustry linkage effect from producer services to manufacturing are 7.16, 6.04, and 1.12 Trillion Yuan, respectively, shown in Table 6; (3) the interindustry linkage contribution and coefficient from producer services to manufacturing are 7.09% and 0.5129, respectively, shown in Table 6.

As for producer services in China 2017, (1) its viability contributes 38.06% of the gross output of itself, and the external linkages contribute 61.94% of the gross output of itself, in which the interindustry linkage effect from the rest of the industrial sector accounts for 35.79%, shown in Table 4; (2) the interindustry linkage effect, direct interindustry linkage effect, and indirect interindustry linkage effect from manufacturing to producer services are 11.09, 10.12, and 0.97 Trillion Yuan, respectively, shown in Table 5; (3) the interindustry linkage contribution and coefficient from manufacturing to producer services are 22.53% and 0.4625, respectively, shown in Table 5.

TABLE 3: Decomposition components of gross output of manufacturing, producer services, and their subindustries.

Industrial sector or subindustry	Gross output	Intraindustry multiplier effect	Interindustry incoming spillover effect	Interindustry incoming spillover effect from manufacturing	Interindustry incoming spillover effect from producer services	Interindustry incoming spillover effect from the rest of the industries	Interindustry feedback effect
Manufacturing	100.89	49.40	42.99	—	7.16	35.83	8.51
Low-tech manufacturing	26.70	16.91	8.00	—	1.50	6.50	1.79
Mid-tech manufacturing	26.19	6.65	16.58	—	2.01	14.58	2.95
High-tech manufacturing	48.00	25.83	18.40	—	3.65	14.75	3.76
Producer services	49.22	18.73	28.70	11.09	—	17.61	1.78
Wholesale service	11.59	4.23	6.91	3.30	—	3.60	0.45
Logistic service	10.26	3.33	6.50	2.79	—	3.71	0.42
Information service	5.65	3.68	1.85	0.56	—	1.29	0.11
Finance service	9.43	3.13	5.94	1.85	—	4.09	0.36
Business service	7.18	1.94	4.92	1.95	—	2.98	0.32
Technology service	5.10	2.41	2.58	0.64	-	1.94	0.11

The unit of the data expressed is Trillion Yuan.

TABLE 4: Output structural features of manufacturing, producer services, and their subindustries.

Industrial sector or subindustry	Gross output	Proportion of sectoral internal effect	Proportion of external linkage effect	Interindustry linkage contribution from the rest of the industries
Manufacturing	100.00	48.96	51.04	35.51
Low-tech manufacturing	100.00	63.35	36.65	24.35
Mid-tech manufacturing	100.00	25.41	74.59	55.65
High-tech manufacturing	100.00	53.82	46.18	30.73
Producer services	100.00	38.06	61.94	35.79
Wholesale service	100.00	36.53	63.47	31.09
Logistic service	100.00	32.49	67.51	36.21
Information service	100.00	65.15	34.85	22.90
Finance service	100.00	33.21	66.79	43.36
Business service	100.00	26.98	73.02	41.46
Technology service	100.00	47.30	52.70	37.92

The unit of all the data expressed is %.

TABLE 5: Interindustry linkages from manufacturing to producer services and its subindustries.

Industrial sector or subindustry	Interindustry linkage effect (Trillion Yuan)	Direct interindustry linkage effect (Trillion Yuan)	Indirect interindustry linkage effect (Trillion Yuan)	Interindustry linkage contribution (%)	Interindustry linkage coefficient
Producer services	11.09	10.12	0.97	22.53	0.4625
Wholesale service	3.30	3.06	0.24	28.50	0.1378
Logistic service	2.79	2.56	0.23	27.19	0.1163
Information service	0.56	0.50	0.06	9.91	0.0234
Finance service	1.85	1.65	0.20	19.59	0.0771
Business service	1.95	1.77	0.17	27.11	0.0812
Technology service	0.64	0.58	0.06	12.60	0.0268

TABLE 6: Interindustry linkages from producer services to manufacturing and its subindustries.

Industrial sector or subindustry	Interindustry linkage effect (Trillion Yuan)	Direct interindustry linkage effect (Trillion Yuan)	Indirect interindustry linkage effect (Trillion Yuan)	Interindustry linkage contribution (%)	Interindustry linkage coefficient
Manufacturing	7.16	6.04	1.12	7.09	0.5129
Low-tech manufacturing	1.50	1.29	0.20	5.60	0.1072
Mid-tech manufacturing	2.01	1.57	0.44	7.67	0.1439
High-tech manufacturing	3.65	3.18	0.47	7.61	0.2617

Similarly, the results of the subindustries of manufacturing or producer services can also be summarized according to Tables 4–6, which are not presented for brevity.

Compared with the previous measurements of interindustry linkages based on Leontief inverse matrix or similar coefficient matrix, this study further decomposes Leontief inverse matrix into three components based on demand-driven and multisector input-output model, in which the different industrial sectors in the entire economic system are regarded as different regions in the spatial scope. The method in this study has three obvious advantages.

Firstly, the method takes multiplier effect as sectoral internal effect and takes the total sum of spillover effect and feedback effect as external linkage effect. When analyzing the structural features of the gross output, it integrates the sectoral internal effect and external linkage effect at the same time, which can make it easy to understand the driving mechanism of industrial development.

Secondly, the classical measurements of interindustry linkages based on Leontief inverse matrix or similar coefficient matrix generally only reflect the overall interrelatedness, namely, the interindustry linkages between the given industry and the entire economic system, while the method in this study can not only measure the interindustry linkage effects between two given industrial sectors, but also clearly describe the composition ratio of the direct and indirect interindustry linkage effects through the further decomposition of spillover effect.

Thirdly, the method adopts, respectively, the absolute flow value, relative flow value, and unit relative value of the input-output relationship as the measurement of interindustry linkage effect, interindustry linkage contribution, and interindustry linkage coefficient, which can comprehensively reflect and evaluate the degree of industry linkages.

5. Discussion and Policy Implication

In accordance with the above results, four viewpoints in agreement with the cognitive patterns have been tested again by the empirical evidence from China. Firstly, compared with the indirect interindustry linkage effects, the direct interindustry linkage effects between manufacturing and producer services are overwhelmingly dominant, accounting for about 80%–90% of the total interindustry linkage effects (see Tables 5 and 6). Secondly, the viability of manufacturing is overall significantly stronger than that of producer services;

namely, the proportion of sectoral internal effect on the gross output of manufacturing is significantly greater than that of producer services (see Table 4). Thirdly, among the interindustry linkages from producer services to the subindustries of manufacturing, the interindustry linkages to mid-tech or high-tech manufacturing are significantly stronger than those to low-tech manufacturing (see Table 6). Fourthly, the output of manufacturing induced by per unit final demand of producer services is larger than that of producer services induced by per unit final demand of manufacturing; namely, the interindustry linkage coefficient from producer services to manufacturing is higher than that from manufacturing to producer services (see Tables 5 and 6).

What is more, some unique local features of manufacturing and producer services in China can be also drawn as follows, and in this study we think they are helpful for the policymakers and economists to better evaluate the development status of two critical industrial sectors in China.

- (1) Whether it is the manufacturing or producer services, the total sum of interindustry spillover effect and interindustry feedback effect is higher than intraindustry multiplier effect (see Table 4), indicating that the external linkage effect is the main driving force for the output of these two industrial sectors, and the viability of them is secondary. In addition, compared with the intraindustry multiplier effect, the interindustry feedback has a certain scale, which means that the estimation error will be obvious when a single-sector model is used instead of multisector model. This is different from some researches on multiregional input-output model [40, 41], in which the interregional feedback effect is usually neglected for the very small scale compared with the intraregional multiplier effect. One reasonable explanation is that the interdependence of different industrial sectors is much stronger than that of different regions, for goods' or services' transfer barriers of the former are significantly less than that of the latter.
- (2) The interindustry linkage effects and contributions between manufacturing and producer services in China are not strong overall, compared with those from the rest of the industries to manufacturing or producer service (see Tables 4–6). In 2017, the interindustry linkage effect and proportion from

TABLE 7: The classification of the entire economic system of China.

Industrial sectors	Subindustries	Corresponding industries in China ICNEA
Manufacturing	Low-tech manufacturing	Processing of food from agricultural products, manufacture of foods, manufacture of alcohol/beverages/refined tea, manufacture of tobacco, manufacture of textiles, manufacture of textiles/clothing/apparel industry, manufacture of leather/fur/feather/related products and footwear industry, processing of timber and manufacture of wood/bamboo/rattan/palm/straw products, manufacture of furniture, manufacture of paper and paper prod, printing and recorded media, manufacture of articles for culture/education/art/sports/entertainment
	Mid-tech manufacturing	Processing of petroleum/coking/processing of nuclear fuel, manufacturing of nonmetallic minerals products, smelting and processing of ferrous metals, smelting and processing of nonferrous metals, manufacture of metal products, other manufacturing, comprehensive use of waste resources, repair of metal products/machinery/equipment
	High-tech manufacturing	Manufacture of chemical raw materials and chemical products, manufacture of medicines, manufacture of chemical fibers, manufacturing of rubber and plastics, manufacture of general purpose machinery, manufacture of special purpose machinery, manufacture of automobiles, manufacture of railway/ships/aerospace/other transportation equipment, manufacture of electrical machinery/equipment, manufacture of computers/communication/other electronic equipment, manufacturing of measuring instruments
Producer services	Wholesale service	Wholesale and retail trades
	Logistic service	Transport, storage, and postal services
	Information service	Information transfer, software, and information technology services
	Finance service	Finance
	Business service	Leasing and commercial services
	Technology service	Scientific research and polytechnic services
The rest of the industries	The primary industry	Agriculture
	The rest of the second industry	Mining and quarrying, utilities, and construction
	The rest of the tertiary industry	Accommodation and catering, real estate, administrate of water/environment/public facilities, resident/repair/other services, education, health care and social work, culture/sports/entertainment, public administration/social insurance/social organizations, international organizations

producer services to manufacturing are 7.16 trillion Yuan and 7.09%, and both of them are far smaller than those from the rest of the industries to manufacturing, which are 35.83 trillion Yuan and 35.51%. In spite of the fact that the interindustry linkage proportion from manufacturing to producer services is higher than that from producer services to manufacturing and the interindustry linkage effect from manufacturing to producer services is also higher than that from producer services to manufacturing, they are still smaller than those from the rest of the industries to producer services. The empirical results show that the impact of the rest of the industries in China on manufacturing or producer services is very significant, accounting for the major or overwhelming major of the external linkage effect. If analyzing the interindustry linkages between manufacturing and producer services only with the two-sector model and ignoring the role of the rest of the industries, it will greatly weaken the applicability of the conclusions.

- (3) Interindustry linkages from manufacturing to wholesale service and logistic service are relatively strong, while those from manufacturing to information service and technology service are relatively

weak. Among the interindustry linkages from manufacturing to the subindustries of producer services, the linkage to wholesale service is the highest, followed by logistic service, business service, financial service, and technology service, and the lowest is to information service (see Table 5). Since the labor productivities of information service and technology service are usually higher than those of wholesale service and logistic service, the empirical results show that in China the pull force from manufacturing is more significant in the field of low-level producer services instead of high-level services and the evolution of interindustry linkages between manufacturing and producer services is still in the primary stage.

After the analysis and evaluation of the output structural features and interindustry linkages in Chinese three-sector economic system, in the perspective of improving the current weak links, this study puts forward the following three policy suggestions aiming to promote the integration level of manufacturing and producer services in China.

First of all, the policy-makers in China should pay great attention to the fact that the interindustry linkages between manufacturing and producer services are not strong overall and the interindustry linkage effect from producer services to manufacturing is weaker than that from manufacturing to

TABLE 8: The rearranged China input-output table in year 2017.

Input/output	Low-tech manufacturing	Mid-tech manufacturing	High-tech manufacturing	Wholesale service	Logistic service	Information service	Finance service	Business service	Technology service	The primary industry	The rest of the second industry	The rest of the tertiary industry	Final demand	Gross output
Low-tech manufacturing	8570.65	431.49	1121.97	115.54	139.46	197.62	336.74	807.92	130.31	968.79	757.57	2350.60	10769.80	26698.46
Mid-tech manufacturing	679.78	8395.67	5840.35	35.64	839.76	13.75	30.39	417.47	261.79	71.56	8428.48	229.44	947.66	26191.75
High-tech manufacturing	1855.21	1614.27	22273.82	182.76	1040.60	442.85	59.08	642.04	895.56	1026.88	3240.54	2466.20	12258.21	47998.02
Wholesale service	1549.47	767.84	2333.58	73.63	251.15	81.05	60.57	240.88	117.57	236.66	1225.90	719.93	3931.11	11589.36
Logistic service	908.80	784.20	1430.63	723.60	1104.33	85.64	165.63	450.98	232.75	250.33	936.06	816.30	2366.07	10255.33
Information service	63.27	36.37	291.76	69.37	176.57	925.69	306.41	68.59	61.44	15.91	329.36	460.22	2847.83	5652.80
Finance service	220.97	571.45	671.38	477.29	1105.40	116.95	791.20	488.66	140.81	145.11	1352.42	1290.09	2062.31	9434.05
Business service	515.64	264.19	922.68	1088.66	209.57	372.34	841.23	724.08	206.59	26.88	520.43	831.95	656.30	7180.55
Technology service	55.36	76.54	347.53	84.05	24.52	17.64	11.04	0.84	573.84	78.43	1718.69	27.16	2088.97	5104.60
The primary industry	5736.01	25.29	515.11	0.12	1.01	3.65	0.91	51.53	29.18	1468.38	192.74	482.74	2505.72	11012.40
The rest of the second industry	446.59	6089.86	1548.79	123.18	274.74	68.64	84.86	34.83	52.19	114.09	5029.42	551.91	20227.97	34647.09
The rest of the tertiary industry	256.72	253.01	550.12	909.20	442.44	374.07	1342.65	900.91	356.54	64.15	516.78	2382.75	21659.60	30008.94
Value added	5839.97	6881.57	10150.31	7706.30	4645.76	2952.91	5403.32	2351.83	2046.02	6545.24	10398.69	17399.65		
Gross input	26698.46	26191.75	47998.02	11589.36	10255.33	5652.80	9434.05	7180.55	5104.60	11012.40	34647.09	30008.94		

The original input-output table in 2017 has totally 149 industries, and it can be downloaded through <http://data.stats.gov.cn/files/html/quickSearch/trcc/trcc01.html>; the final demand in this table contains the part of net exports. The unit of the data expressed is Billion Yuan.

producer services. It means that the producer services are a more obvious weak link compared with manufacturing, so it is necessary to further strengthen the supporting of producer services for manufacturing and take measures such as promoting the industrial clustering degree or improving the serviceability of producer services.

Secondly, in view of the fact that low-tech manufacturing is the key weak link among the subindustries of manufacturing, it is necessary to accelerate the transformation of traditional low-tech manufacturing through the universal application and integration of producer services, in response to the trends of industrialization upgrading in China.

Finally, in view of the fact that information service is the key weak link among the subindustries of producer service, it is necessary to speed up the pace of manufacturing servitization, especially manufacturing digitization, and promote the widespread application of information technology in the field of manufacturing.

6. Conclusions

This study puts forward a new method for interindustry linkage analysis in a complex economic system on the basis of demand-driven and multisector input-output model, in which the output as well as Leontief inverse matrix is decomposed into three components and interindustry linkage effect, interindustry linkage contribution, and interindustry linkage coefficient are adopted as the measuring indices. Compared with the previous measurements of interindustry linkages based on Leontief inverse matrix or similar coefficient matrix, the method in this study has some obvious advantages. As a whole, this method is a refinement of Hirschman's backward linkage, which is critical in the perspective of output structure in demand side.

Based on the method and input-output data, this study also conducts an empirical study on the interindustry linkages between China's manufacturing and producer services, and the results show that the external linkage effect is the main driving force for the output of these two industrial sectors, and the viability of them is secondary; the interindustry linkage effects and contributions between manufacturing and producer services in China are not strong overall, compared with those from the rest of the industries to manufacturing or producer service; interindustry linkages from manufacturing to wholesale service and logistic service are relatively strong, while those from manufacturing to information service and technology service are relatively weak. The authors hold that the method in this study is helpful for policy-makers and relevant stakeholders to better understand the interrelatedness between two industrial sectors in a complex economic system and identify the key weak links which guide them to promote balanced development of economy.

Finally, it is worth mentioning that this study only discusses Hirschman's backward linkage on the basis of Leontief inverse matrix, mainly due to the fact that the output structure on the demand side generally is paid more

attention. Further research may focus on the forward linkage on the basis of Ghosh inverse matrix and explore the structural features of output on the supply side, or some other important economic factors, such as value added, employment, and resource utilization.

Appendix

A. The Classification of the Entire Economic System of China

The classification of the entire economic system of China is shown in Table 7

B. The Rearranged China Input-Output Table in Year 2017 (Unit: Billion Yuan)

The rearranged China input-output table in year 2017 is shown in Table 8

C. Some Critical Vectors and Matrices of the Application Case in China 2017

$$X = \begin{bmatrix} X^1 \\ X^2 \\ X^3 \end{bmatrix} = \begin{bmatrix} X_1^1 \\ X_2^1 \\ X_3^1 \\ X_1^2 \\ X_2^2 \\ X_3^2 \\ X_1^3 \\ X_2^3 \\ X_3^3 \end{bmatrix} = \begin{bmatrix} 26.70 \\ 26.19 \\ 48.00 \\ 11.59 \\ 10.26 \\ 5.65 \\ 9.43 \\ 7.18 \\ 5.10 \\ 11.01 \\ 34.65 \\ 30.01 \end{bmatrix}, \quad (\text{C.1})$$

$$Y = \begin{bmatrix} Y^1 \\ Y^2 \\ Y^3 \end{bmatrix} = \begin{bmatrix} Y_1^1 \\ Y_2^1 \\ Y_3^1 \\ Y_1^2 \\ Y_2^2 \\ Y_3^2 \\ Y_1^3 \\ Y_2^3 \\ Y_3^3 \end{bmatrix} = \begin{bmatrix} 10.77 \\ 0.95 \\ 12.26 \\ 3.93 \\ 2.37 \\ 2.85 \\ 2.06 \\ 0.66 \\ 2.09 \\ 2.51 \\ 20.23 \\ 21.66 \end{bmatrix}. \quad (\text{C.2})$$

Note: the unit of the elements in X and Y is Trillion Yuan.

$$A = \begin{bmatrix} A^{11} & A^{12} & A^{13} \\ A^{21} & A^{22} & A^{23} \\ A^{31} & A^{32} & A^{33} \end{bmatrix} = \begin{bmatrix} 0.32 & 0.02 & 0.02 & 0.01 & 0.01 & 0.03 & 0.04 & 0.11 & 0.03 & 0.09 & 0.02 & 0.08 \\ 0.03 & 0.32 & 0.12 & 0.00 & 0.08 & 0.00 & 0.00 & 0.06 & 0.05 & 0.01 & 0.24 & 0.01 \\ 0.07 & 0.06 & 0.46 & 0.02 & 0.10 & 0.08 & 0.01 & 0.09 & 0.18 & 0.09 & 0.09 & 0.08 \\ 0.06 & 0.03 & 0.05 & 0.01 & 0.02 & 0.01 & 0.01 & 0.03 & 0.02 & 0.02 & 0.04 & 0.02 \\ 0.03 & 0.03 & 0.03 & 0.06 & 0.11 & 0.02 & 0.02 & 0.06 & 0.05 & 0.02 & 0.03 & 0.03 \\ 0.00 & 0.00 & 0.01 & 0.01 & 0.02 & 0.16 & 0.03 & 0.01 & 0.01 & 0.00 & 0.01 & 0.02 \\ 0.01 & 0.02 & 0.01 & 0.04 & 0.11 & 0.02 & 0.08 & 0.07 & 0.03 & 0.01 & 0.04 & 0.04 \\ 0.02 & 0.01 & 0.02 & 0.09 & 0.02 & 0.07 & 0.09 & 0.10 & 0.04 & 0.00 & 0.02 & 0.03 \\ 0.00 & 0.00 & 0.01 & 0.01 & 0.00 & 0.00 & 0.00 & 0.00 & 0.11 & 0.01 & 0.05 & 0.00 \\ 0.21 & 0.00 & 0.01 & 0.00 & 0.00 & 0.00 & 0.00 & 0.01 & 0.01 & 0.13 & 0.01 & 0.02 \\ 0.02 & 0.23 & 0.03 & 0.01 & 0.03 & 0.01 & 0.01 & 0.00 & 0.01 & 0.01 & 0.15 & 0.02 \\ 0.01 & 0.01 & 0.01 & 0.08 & 0.04 & 0.07 & 0.14 & 0.13 & 0.07 & 0.01 & 0.01 & 0.08 \end{bmatrix}, \quad (C.3)$$

$$B = \begin{bmatrix} 1.57 & 0.11 & 0.13 & 0.07 & 0.09 & 0.12 & 0.12 & 0.26 & 0.12 & 0.19 & 0.11 & 0.17 \\ 0.19 & 1.75 & 0.48 & 0.07 & 0.26 & 0.10 & 0.07 & 0.23 & 0.25 & 0.10 & 0.59 & 0.11 \\ 0.37 & 0.37 & 2.06 & 0.13 & 0.33 & 0.28 & 0.13 & 0.36 & 0.51 & 0.29 & 0.41 & 0.27 \\ 0.14 & 0.10 & 0.14 & 1.03 & 0.07 & 0.05 & 0.04 & 0.09 & 0.08 & 0.06 & 0.10 & 0.06 \\ 0.11 & 0.11 & 0.12 & 0.10 & 1.17 & 0.06 & 0.06 & 0.13 & 0.11 & 0.06 & 0.10 & 0.07 \\ 0.02 & 0.02 & 0.03 & 0.02 & 0.04 & 1.21 & 0.05 & 0.03 & 0.03 & 0.01 & 0.03 & 0.03 \\ 0.06 & 0.10 & 0.09 & 0.08 & 0.17 & 0.06 & 1.13 & 0.14 & 0.09 & 0.04 & 0.11 & 0.08 \\ 0.07 & 0.07 & 0.09 & 0.13 & 0.07 & 0.12 & 0.13 & 1.17 & 0.10 & 0.03 & 0.07 & 0.07 \\ 0.02 & 0.04 & 0.03 & 0.01 & 0.02 & 0.01 & 0.01 & 0.01 & 1.14 & 0.02 & 0.08 & 0.01 \\ 0.40 & 0.04 & 0.06 & 0.02 & 0.03 & 0.04 & 0.04 & 0.08 & 0.05 & 1.20 & 0.05 & 0.07 \\ 0.11 & 0.50 & 0.22 & 0.05 & 0.13 & 0.07 & 0.05 & 0.10 & 0.11 & 0.06 & 1.36 & 0.07 \\ 0.07 & 0.08 & 0.08 & 0.13 & 0.11 & 0.13 & 0.21 & 0.21 & 0.14 & 0.04 & 0.08 & 1.13 \end{bmatrix}, \quad (C.4)$$

$$M = \begin{bmatrix} 1.48 & 0.04 & 0.07 & 0 & 0 & 0 & 0 & 0 & 0 & 0 & 0 & 0 \\ 0.09 & 1.51 & 0.35 & 0 & 0 & 0 & 0 & 0 & 0 & 0 & 0 & 0 \\ 0.20 & 0.18 & 1.92 & 0 & 0 & 0 & 0 & 0 & 0 & 0 & 0 & 0 \\ 0 & 0 & 0 & 1.01 & 0.03 & 0.02 & 0.01 & 0.04 & 0.03 & 0 & 0 & 0 \\ 0 & 0 & 0 & 0.08 & 1.13 & 0.03 & 0.03 & 0.08 & 0.07 & 0 & 0 & 0 \\ 0 & 0 & 0 & 0.01 & 0.03 & 1.20 & 0.05 & 0.02 & 0.02 & 0 & 0 & 0 \\ 0 & 0 & 0 & 0.06 & 0.14 & 0.04 & 1.11 & 0.10 & 0.05 & 0 & 0 & 0 \\ 0 & 0 & 0 & 0.12 & 0.04 & 0.09 & 0.12 & 1.13 & 0.06 & 0 & 0 & 0 \\ 0 & 0 & 0 & 0.01 & 0.00 & 0.00 & 0.00 & 0.00 & 1.13 & 0 & 0 & 0 \\ 0 & 0 & 0 & 0 & 0 & 0 & 0 & 0 & 0 & 1.15 & 0.01 & 0.02 \\ 0 & 0 & 0 & 0 & 0 & 0 & 0 & 0 & 0 & 0.01 & 1.17 & 0.02 \\ 0 & 0 & 0 & 0 & 0 & 0 & 0 & 0 & 0 & 0.01 & 0.02 & 1.09 \end{bmatrix}, \quad (C.5)$$

$$S = \begin{bmatrix} 0 & 0 & 0 & 0.07 & 0.09 & 0.12 & 0.12 & 0.26 & 0.12 & 0.19 & 0.11 & 0.17 \\ 0 & 0 & 0 & 0.07 & 0.26 & 0.10 & 0.07 & 0.23 & 0.25 & 0.10 & 0.59 & 0.11 \\ 0 & 0 & 0 & 0.13 & 0.33 & 0.28 & 0.13 & 0.36 & 0.51 & 0.29 & 0.41 & 0.27 \\ 0.14 & 0.10 & 0.14 & 0 & 0 & 0 & 0 & 0 & 0 & 0.06 & 0.10 & 0.06 \\ 0.11 & 0.11 & 0.12 & 0 & 0 & 0 & 0 & 0 & 0 & 0.06 & 0.10 & 0.07 \\ 0.02 & 0.02 & 0.03 & 0 & 0 & 0 & 0 & 0 & 0 & 0.01 & 0.03 & 0.03 \\ 0.06 & 0.10 & 0.09 & 0 & 0 & 0 & 0 & 0 & 0 & 0.04 & 0.11 & 0.08 \\ 0.07 & 0.07 & 0.09 & 0 & 0 & 0 & 0 & 0 & 0 & 0.03 & 0.07 & 0.07 \\ 0.02 & 0.04 & 0.03 & 0 & 0 & 0 & 0 & 0 & 0 & 0.02 & 0.08 & 0.01 \\ 0.40 & 0.04 & 0.06 & 0.02 & 0.03 & 0.04 & 0.04 & 0.08 & 0.05 & 0 & 0 & 0 \\ 0.11 & 0.50 & 0.22 & 0.05 & 0.13 & 0.07 & 0.05 & 0.10 & 0.11 & 0 & 0 & 0 \\ 0.07 & 0.08 & 0.08 & 0.13 & 0.11 & 0.13 & 0.21 & 0.21 & 0.14 & 0 & 0 & 0 \end{bmatrix}, \quad (C.6)$$

$$S_d = \begin{bmatrix} 0 & 0 & 0 & 0.06 & 0.07 & 0.11 & 0.11 & 0.24 & 0.09 & 0.17 & 0.08 & 0.16 \\ 0 & 0 & 0 & 0.06 & 0.21 & 0.08 & 0.05 & 0.18 & 0.19 & 0.07 & 0.50 & 0.08 \\ 0 & 0 & 0 & 0.11 & 0.29 & 0.25 & 0.11 & 0.30 & 0.46 & 0.25 & 0.32 & 0.23 \\ 0.13 & 0.09 & 0.13 & 0 & 0 & 0 & 0 & 0 & 0 & 0.06 & 0.09 & 0.06 \\ 0.10 & 0.10 & 0.11 & 0 & 0 & 0 & 0 & 0 & 0 & 0.06 & 0.09 & 0.06 \\ 0.02 & 0.02 & 0.03 & 0 & 0 & 0 & 0 & 0 & 0 & 0.01 & 0.03 & 0.03 \\ 0.06 & 0.09 & 0.08 & 0 & 0 & 0 & 0 & 0 & 0 & 0.04 & 0.10 & 0.08 \\ 0.07 & 0.06 & 0.08 & 0 & 0 & 0 & 0 & 0 & 0 & 0.03 & 0.06 & 0.06 \\ 0.02 & 0.04 & 0.03 & 0 & 0 & 0 & 0 & 0 & 0 & 0.02 & 0.08 & 0.01 \\ 0.38 & 0.02 & 0.05 & 0.02 & 0.02 & 0.03 & 0.03 & 0.07 & 0.04 & 0 & 0 & 0 \\ 0.08 & 0.43 & 0.19 & 0.04 & 0.11 & 0.05 & 0.03 & 0.08 & 0.09 & 0 & 0 & 0 \\ 0.05 & 0.05 & 0.07 & 0.12 & 0.10 & 0.12 & 0.20 & 0.20 & 0.13 & 0 & 0 & 0 \end{bmatrix}, \quad (C.7)$$

$$S_i = \begin{bmatrix} 0 & 0 & 0 & 0.01 & 0.02 & 0.01 & 0.01 & 0.03 & 0.02 & 0.02 & 0.03 & 0.02 \\ 0 & 0 & 0 & 0.02 & 0.05 & 0.03 & 0.02 & 0.05 & 0.05 & 0.03 & 0.09 & 0.03 \\ 0 & 0 & 0 & 0.02 & 0.05 & 0.03 & 0.02 & 0.06 & 0.06 & 0.04 & 0.08 & 0.04 \\ 0.01 & 0.01 & 0.01 & 0 & 0 & 0 & 0 & 0 & 0 & 0.00 & 0.01 & 0.01 \\ 0.01 & 0.01 & 0.01 & 0 & 0 & 0 & 0 & 0 & 0 & 0.00 & 0.01 & 0.01 \\ 0.00 & 0.00 & 0.00 & 0 & 0 & 0 & 0 & 0 & 0 & 0.00 & 0.00 & 0.00 \\ 0.01 & 0.01 & 0.01 & 0 & 0 & 0 & 0 & 0 & 0 & 0.00 & 0.01 & 0.01 \\ 0.01 & 0.01 & 0.01 & 0 & 0 & 0 & 0 & 0 & 0 & 0.00 & 0.01 & 0.01 \\ 0.00 & 0.00 & 0.00 & 0 & 0 & 0 & 0 & 0 & 0 & 0.00 & 0.00 & 0.00 \\ 0.02 & 0.02 & 0.01 & 0.01 & 0.01 & 0.01 & 0.01 & 0.01 & 0.01 & 0 & 0 & 0 \\ 0.03 & 0.07 & 0.03 & 0.01 & 0.02 & 0.01 & 0.01 & 0.02 & 0.02 & 0 & 0 & 0 \\ 0.02 & 0.03 & 0.01 & 0.01 & 0.01 & 0.01 & 0.01 & 0.01 & 0.01 & 0 & 0 & 0 \end{bmatrix}, \quad (C.8)$$

$$F = \begin{bmatrix} 0.09 & 0.06 & 0.06 & 0 & 0 & 0 & 0 & 0 & 0 & 0 & 0 & 0 \\ 0.10 & 0.24 & 0.13 & 0 & 0 & 0 & 0 & 0 & 0 & 0 & 0 & 0 \\ 0.17 & 0.19 & 0.14 & 0 & 0 & 0 & 0 & 0 & 0 & 0 & 0 & 0 \\ 0 & 0 & 0 & 0.02 & 0.04 & 0.03 & 0.02 & 0.05 & 0.05 & 0 & 0 & 0 \\ 0 & 0 & 0 & 0.02 & 0.04 & 0.03 & 0.02 & 0.05 & 0.05 & 0 & 0 & 0 \\ 0 & 0 & 0 & 0.01 & 0.01 & 0.01 & 0.01 & 0.01 & 0.01 & 0 & 0 & 0 \\ 0 & 0 & 0 & 0.02 & 0.03 & 0.02 & 0.02 & 0.04 & 0.04 & 0 & 0 & 0 \\ 0 & 0 & 0 & 0.01 & 0.03 & 0.02 & 0.02 & 0.04 & 0.03 & 0 & 0 & 0 \\ 0 & 0 & 0 & 0.00 & 0.01 & 0.01 & 0.01 & 0.01 & 0.01 & 0 & 0 & 0 \\ 0 & 0 & 0 & 0 & 0 & 0 & 0 & 0 & 0 & 0.05 & 0.04 & 0.05 \\ 0 & 0 & 0 & 0 & 0 & 0 & 0 & 0 & 0 & 0.05 & 0.19 & 0.05 \\ 0 & 0 & 0 & 0 & 0 & 0 & 0 & 0 & 0 & 0.03 & 0.06 & 0.04 \end{bmatrix}. \quad (\text{C.9})$$

Data Availability

The data used to support the findings of this study are included within the article.

Conflicts of Interest

The authors declare that they have no conflicts of interest.

Acknowledgments

The authors would like to thank the research team on economic systems engineering in Zhejiang Economic Information Center for their great and sincere help. This work was supported by the Project in 2020 of Zhejiang Provincial Soft Science Research of China (2020C35009) and the Project in 2019 of Zhejiang Provincial Social Science Foundation of China (19NDQN368YB).


References

- [1] A. Hirschman, *The Strategy of Economic Development*, Yale University Press, New Haven, CT, USA, 1958.
- [2] R. Banga and B. Goldar, "Contribution of services to output growth and productivity in Indian manufacturing: pre-and post-reforms," *Economic and Political Weekly*, vol. 42, no. 26, pp. 2769–2777, 2007.
- [3] J. Francois and J. Woerz, "Producer services, manufacturing linkages, and trade," *Journal of Industry, Competition and Trade*, vol. 8, no. 3-4, pp. 199–229, 2008.
- [4] S. Ke, M. He, and C. Yuan, "Synergy and co-agglomeration of producer services and manufacturing: a panel data analysis of Chinese cities," *Regional Studies*, vol. 48, no. 11, pp. 1829–1841, 2014.
- [5] L. Kong and X. Liang, "Research on the interaction between producer services and manufacturing industry in Shaanxi Province," *American Journal of Industrial and Business Management*, vol. 8, no. 5, pp. 1277–1289, 2018.
- [6] W. W. Leontief, "Quantitative input and output relations in the economic systems of the United States," *The Review of Economics and Statistics*, vol. 18, no. 3, pp. 105–125, 1936.
- [7] P. Guerrieri and V. Meliciani, "Technology and international competitiveness: the interdependence between manufacturing and producer services," *Structural Change and Economic Dynamics*, vol. 16, no. 4, pp. 489–502, 2005.
- [8] R.-H. Chiu and Y.-C. Lin, "The inter-industrial linkage of maritime sector in Taiwan: an input-output analysis," *Applied Economics Letters*, vol. 19, no. 4, pp. 337–343, 2012.
- [9] E. Mattioli and G. R. Lamonica, "The ICT role in the World economy: an input-output analysis," *Journal of World Economic Research*, vol. 2, no. 2, pp. 20–25, 2013.
- [10] B. R. Khanal, C. Gan, and S. Becken, "Tourism inter-industry linkages in the Lao PDR economy: an input-output analysis," *Tourism Economics*, vol. 20, no. 1, pp. 171–194, 2014.
- [11] A.-I. Guerra and F. Sancho, "Measuring energy linkages with the hypothetical extraction method: an application to Spain," *Energy Economics*, vol. 32, no. 4, pp. 831–837, 2010.
- [12] M. J. Sajid, N. Shahni, and M. Ali, "Calculating inter-sectoral carbon flows of a mining sector via hypothetical extraction method," *Journal of Mining and Environment*, vol. 10, no. 4, pp. 853–867, 2019.
- [13] M. J. Sajid, Q. Cao, and W. Kang, "Transport sector carbon linkages of EU's top seven emitters," *Transport Policy*, vol. 80, pp. 24–38, May 2019.
- [14] Y. Wang, N. Lai, G. Mao et al., "Air pollutant emissions from economic sectors in China: a linkage analysis," *Ecological Indicators*, vol. 77, pp. 250–260, 2017.
- [15] Y. Wang, H. Liu, G. Mao, J. Zuo, and J. Ma, "Inter-regional and sectoral linkage analysis of air pollution in Beijing-Tianjin-Hebei (Jing-Jin-Ji) urban agglomeration of China," *Journal of Cleaner Production*, vol. 165, pp. 1436–1444, 2017.
- [16] Y. Ali, M. Sabir, and N. Muhammad, "A comparative input-output analysis of the construction sector in three developing economies of South Asia," *Construction Management and Economics*, vol. 37, no. 11, pp. 643–658, 2019.
- [17] I. Drejer, "Input-Output based measures of interindustry linkages revisited—A survey and discussion," in *Proceedings of the 14th International Conference on Input-Output Techniques*, Montreal, Canada, October 2002.
- [18] H. B. Chenery and T. Watanabe, "International comparisons of the structure of production," *Econometrica*, vol. 26, no. 4, pp. 487–521, 1958.
- [19] P. N. Rasmussen, *Studies in Inter-sectoral Relations*, E. Harck, Copenhagen, Denmark, 1956.
- [20] L. P. Jones, "The measurement of hirschmanian linkages," *The Quarterly Journal of Economics*, vol. 90, no. 2, pp. 323–333, 1976.

- [21] F. A. Cuello, F. Mansouri, and G. J. D. Hewings, "The identification of structure at the sectoral level: a reformulation of the hirschman-rasmussen key sector indices," *Economic Systems Research*, vol. 4, no. 4, pp. 285–296, 1992.
- [22] B. R. Hazari, "Empirical identification of key sectors in the Indian economy," *The Review of Economics and Statistics*, vol. 52, no. 3, pp. 301–305, 1970.
- [23] P. S. Laumas, "An international comparison of the structure of production," *Economia Internazionale*, vol. 29, no. 1–2, pp. 2–13, 1976.
- [24] G. Strassert, "Zur bestimmung strategischer sektoren mit hilfe von input-output modellen," *Jahrbücher für Nationalökonomie und Statistik*, vol. 182, pp. 211–215, 1968, (In German).
- [25] S. Schultz, "Approaches to identifying key sectors empirically by means of input-output analysis," *The Journal of Development Studies*, vol. 14, no. 1, pp. 77–96, 1977.
- [26] G. Cella, "The input-output measurement of interindustry linkages," *Oxford Bulletin of Economics and Statistics*, vol. 46, no. 1, pp. 73–84, 1984.
- [27] R. Duarte, J. Sánchez-Chóliz, and J. Bielsa, "Water use in the Spanish economy: an input-output approach," *Ecological Economics*, vol. 43, no. 1, pp. 71–85, 2002.
- [28] M. J. Sajid, X. Li, and Q. Cao, "Demand and supply-side carbon linkages of Turkish economy using hypothetical extraction method," *Journal of Cleaner Production*, vol. 228, pp. 264–275, 2019.
- [29] M. S. Silva and T. P. de Lima, "Looking for nonnegative solutions of a Leontief dynamic model," *Linear Algebra and Its Applications*, vol. 364, pp. 281–316, 2003.
- [30] H. D. Kurz and N. Salvadori, "The dynamic Leontief model and the theory of endogenous growth," *Economic Systems Research*, vol. 12, no. 2, pp. 255–265, 2010.
- [31] A. Rose, "Input-output economics and computable general equilibrium models," *Structural Change and Economic Dynamics*, vol. 6, no. 3, pp. 295–304, 1995.
- [32] Q.-X. Li and S.-F. Liu, "The foundation of the grey matrix and the grey input-output analysis," *Applied Mathematical Modelling*, vol. 32, no. 3, pp. 267–291, 2008.
- [33] A. Tukker and E. Dietzenbacher, "Global multiregional input-output frameworks: an introduction and outlook," *Economic Systems Research*, vol. 25, no. 1, pp. 1–19, 2013.
- [34] G. E. Halkos and K. D. Tsilika, "A new vision of classical multi-regional input-output models," *Computational Economics*, vol. 51, no. 3, pp. 1–24, 2018.
- [35] R. E. Miller, "Interregional feedback effects in input-output models: some preliminary results," *Papers of the Regional Science Association*, vol. 17, no. 1, pp. 105–125, 1966.
- [36] J. I. Round, "Decomposing multipliers for economic systems involving regional and world trade," *The Economic Journal*, vol. 95, no. 378, pp. 383–399, 1985.
- [37] M. Sonis, J. Oosterhaven, and G. J. D. Hewings, "Spatial economic structure and structural changes in the EC: feedback loop input-output analysis," *Economic Systems Research*, vol. 5, no. 2, pp. 173–184, 1993.
- [38] E. Dietzenbacher, "Interregional multipliers: looking backward, looking forward," *Regional Studies*, vol. 36, no. 2, pp. 125–136, 2002.
- [39] R. E. Miller and P. D. Blair, *Input-Output Analysis: Foundation and Extension*, Cambridge University Press, Cambridge, UK, 2nd edition, 2009.
- [40] B. Meng and C. Qu, "Application of the input-output decomposition technique to China's regional economics," *IDE Discussion Papers*, vol. 102, 2007.
- [41] J. Oosterhaven, D. Stelder, and S. Inomata, "Evaluation of non-survey international IO construction methods with the asian-pacific input-output table," *IDE Discussion Papers*, vol. 114, 2007.

Research Article

A Dynamic Duopoly Cournot Model with R&D Efforts and Its Dynamic Behavior Analysis

Wei Zhou ^{1,2}, Jie Zhou,¹ Tong Chu,³ and Hui Li^{1,2}

¹School of Mathematics and Physics, Lanzhou Jiaotong University, Lanzhou, Gansu 730070, China

²Research Centre of Game Theory and Economics Mathematics, Lanzhou Jiaotong University, Lanzhou, Gansu 730070, China

³School of Law, Zhejiang University of Finance and Economics, Hangzhou 310018, China

Correspondence should be addressed to Wei Zhou; wei_zhou@vip.126.com

Received 7 May 2020; Accepted 15 June 2020; Published 11 August 2020

Guest Editor: Lei Xie

Copyright © 2020 Wei Zhou et al. This is an open access article distributed under the Creative Commons Attribution License, which permits unrestricted use, distribution, and reproduction in any medium, provided the original work is properly cited.

In this paper, a dynamic two-stage Cournot duopoly game with R&D efforts is built. Then, the local stability of the equilibrium points are discussed, and the stability condition of the Nash equilibrium point is also deduced through Jury criterion. The complex dynamical behaviors of the built model are investigated by numerical simulations. We found that the unique route to chaos is flip bifurcation, and the increase of adjusting speed will cause the system to lose stability and produce more complex dynamic behavior. In addition, we also found the phenomenon of multistability in the given model. Several kinds of coexistence of attractors are shown. In particular, we found that boundary attractors can coexist with internal attractors, which also aggravates the complexity of the system. At last, the chaotic state in the built system has been successfully controlled.

1. Introduction

In recent years, the market competition mode among firms are no longer subjected to price or quantity, but more towards soft power, including technical level, talent resources, and corporate culture. With more and more systematic and mature development of the organization management for a great quantity of large firms, R&D (the abbreviation of Research and Development) is becoming more and more important for them. The visionary entrepreneurs will spend a lot of money to build their own exclusive R&D team. It may be risky for the capitalists who pursue maximum profits to do such things which may be harmful to their revenues. However, the reasons for these firms that lay much stress on R&D activity can be listed as follows: on the one hand, R&D activities can improve production efficiency, reduce production costs, and then the entrepreneurs can gain surplus value proliferation; on the other hand, R&D activities can also improve quality of products so as to increase advantage competitiveness of firms in the market. Hence, R&D activity gradually attracts a lot of attentions of economists.

In the process of carrying out R&D activities, due to the flow of technical talents, information diffusion, and other factors, R&D spillover effect may emerge among firms [1, 2]. Numerous scholars studied and advanced this problem. Zhou et al. [3] studied the types of bifurcation, intermittent chaos, and coexistences in a dynamical two-stage Cournot duopoly game with R&D spillover effect. Zhou and Wang [4] studied the stability and multistability of a duopoly game model with R&D spillover. While in the case that the firms take highly confidential measures for its R&D achievements, the positive effects of R&D achievements only promote the firms that carry out R&D activities, but not the competitors. In other words, there is no spillover effect. Based on this assumption, D'Aspremont and Jacquemin [5] built the foundation of the performance of R&D cooperation in the product differentiation market. Luckraz [6] established a Cournot duopoly game model with isoelastic demand function and also considered the case without R&D spillovers. The work of Chatterjee [7] showed that the firms in the market undertake R&D activity and studied that R&D incentive may depend on the information structures they

had. In addition, Ferreira et al. [8] constructed myopic optimal discrete and continuous R&D dynamics.

The most extensive research on spillover effect is technology spillover. AJ Model [5] and KMZ model [9] are the most representative ones. In both cases, they are both two-stage game models. Also, the two-stage game presents good adaptability in dealing with problems about uncertainty of R&D market and mutuality of competitive strategies. That is to say, on the first stage, both these two firms conduct R&D activities to reduce their production costs. And on the second stage, they compete in market in term of the price or the quantity. The investigations on the two-stage model have gradually become the focus of economists. While at the beginning of the study, many scholars were limited in studying the properties of the static model [10–12]. All the investigations about the static model just illustrated the equilibrium solutions under different R&D strategies. No one can deny that the static model does have some limitations. One limitation is that it can only analyze the single supply and demand balance between firms. Once the supply and demand factors change, the corresponding supply relationship will shift.

In this research, we introduce nonlinear dynamics theory to discuss evolution process among firms' games. Many scholars had carried out some studies about this issue. Bischi and Lamantia [13, 14] revealed the local and global dynamical properties of the two-stage oligopoly game model with adaptive dynamic mechanism and described its complex evolutionary behaviors. Askar et al. [15] investigated the properties in a dynamic Cournot duopoly game model with nonlinear demand function. A homogeneous Cournot duopoly market possessing two different mechanisms was proposed by Elettrey [16]. Most of the similar works can be seen in [17–19]. Additionally, the dynamical two-stage game has raised much interest in the economic dynamical system. For instance, Zhang et al. [20] proposed a two-stage Cournot duopoly game of semicollusion in production and analyzed its complex dynamics, such as local stabilities and existence. Ma et al. [21, 22] have focused the analysis of complex dynamical behaviors of the two-stage dynamic games.

Furthermore, although in the electronic information world, the corresponding channels for firms to obtain market information have proliferated. However, it cannot be ignored that if the firms want to get complete information, they still need to pay its costs. That is to say, few firms are willing to pay high cost to obtain all the information about market demand and consumer preferences. So, most firms have incomplete information about the market, so they could be regarded to be bounded rational [23] when making decisions. In fact, compared with those having complete information of demand function, it is much easier to obtain the existing information, such as local estimation of marginal profit. That is, gradient adjustment mechanism which has attracted many scholars to carry out deep research studies on this topic (see e.g., [23–26]). Cavalli and Naimzada [27] took the factors such as rationality and information set into consideration and adopted a traditional dynamical adjustment mechanism based on classical best reply function. Elsadany [28] interpreted a Cournot duopoly

dynamics model with different strategies including bounded rationality. Fanti and Gori [29] put forward a Bertrand duopoly game model with heterogeneous product expectations and further studied the properties of the model. And Naimzada and Sbragia [30] dealt with an oligopoly game model with nonlinear demand function and bounded rationality.

Additionally, other topics worth studying in nonlinear dynamics are global dynamics, synchronization, and multistability. In recent years, great deals of scholars have deepened the study of these topics. Askar [31] dealt with the dynamical characteristics with log-concave demand of equilibrium points, such as stability, bifurcation, and chaos. Andaluz and Jarne [32] analyzed the dynamics of not only quantity-setting competition but also price-setting competition. Agliari et al. [19] observed that some bifurcations can lead to changes in the structure of attractors and their basins. And a higher degree of production differentiation tends to reduce competition. Tu and Wang [33] built a dynamical R&D two-stage input competition triopoly game model with bounded rationality and further analyzed the dynamics properties of this model. Bischi et al. [34, 35] had studied the phenomena of dynamic properties, such as synchronization, intermittency, coexisting attractors, and complex basins. Fanti et al. [36] provided local and global dynamic characteristics in a duopoly game model with price-setting competition and market share delegation.

Basing on the above analyses, the behaviors including dynamic evolution, intermittency, and multistability are exploited to interpret the complexity of competition. We take use of a Cournot duopoly model with differentiated products to consider the impact of adjustment speeds. And the influence of firm's adjustment speed on the development of firms is studied through combining a two-stage dynamic game with the method of numerical simulation and the properties of nonlinear dynamics. It is worth to focus on whether the firm will gain more advantages at a lower adjustment speed.

Furthermore, another noticed feature is chaos control. Since chaos could increase the disorder and unpredictability of the established model. In the sense of economics, if actual economic market is in a chaotic state, then the resources of firms will not be controlled by market supply, demand relationship, and the government macrocontrol to some extent. This may disrupt the development of market economy. However, as for firms in the market, they prefer to pursue a long-term and stable development, which can raise their accumulation of capitals to expand themselves industrial scale. Hence, it is necessary to control chaos. A large number of scholars have carried out relevant research studies and achieved some results. For instance, feedback control was given by Elsadany et al. [37, 38]. Ma and Ji [39] studied the dynamical repeated Cournot model by using the chaos control method with feedback control. Parameters adjustment was provided to control chaos by Askar and Al-khedhairi [40].

The main purpose of this research is to investigate the influence of continuous change of system parameters on the eventual dynamical scenarios of the dynamic duopoly model with R&D efforts. The local stability of boundary equilibrium and Nash equilibrium is provided by Jury stability criterion and

numerical simulation to obtain the internal complexity of the model. We show that the successive change of system parameters not only causes the system to lose its stability but also causes the high complexity of eventual behaviors of the system, such as the number of coexisting attractors, the critical bifurcation of attractors, and the global bifurcation of attracting domain.

This research is organized as follows. In Section 2, a two-stage dynamical game model without R&D efforts is established, where these two firms' products are of the same kind but different products. In addition, its stability and the conditions of stability of equilibrium points are discussed. In Section 3, the complex evolution law based on speed of adjustment is discussed in details. Through numerical simulation, the complexity of bifurcations, evolution of strange attractors, intermittent chaos, multistability, and control of chaos are studied. At last, the impacts of adjustment speeds on built model are concluded in Section 4.

2. The model

Assume that there are two technology-based firms operating in the market, labeled by i ($i = 1, 2$), and they supply homogeneous products to the same market. Research and Development (R&D) is a kind of creative behavior for the firms to increase production efficiency and decrease costs so as to gain more market share. While in the actual economics environment, R&D activity is always carried out in a stepwise manner: research phase and development phase. The process of competition between two R&D firms can be simulated by a two-stage game. On the first stage, these two firms conduct R&D activities to reduce their production costs. And on the second stage, they compete in the market in terms of the price or the quantity. The difference between the R&D levels of the firms can result the difference of goods in quality, function, and externalization. Hence, the inverse demand function can be written as

$$p_i(q_i, q_{3-i}) = a - q_i - bq_{3-i}, \quad i = 1, 2, \quad (1)$$

where p_i is the price of firm i ($i = 1, 2$), q_i and q_{3-i} represents the outputs of firm i and its rival, respectively, $a > 0$ denotes the maximum scale of this market, b is defined as the differentiating degree of the products of two firms, and $b \in [0, 1]$. Moreover, if $b = 0$, it means that the products of firm 1 and firm 2 are mutually independent, and the oligopoly market will be degenerated into two completely independent monopoly markets. If $0 < b < 1$, it indicates that the products of these two firms can replace each other. And if $b = 1$, it means that there is no difference between the products of these two firms. In other words, the products of firm 1 and firm 2 are totally identical.

Consider now the R&D efforts of firm i ($i = 1, 2$) labeled by x_i . Then, the effective marginal cost of firm i can be represented as

$$C_i(x_i) = c - x_i, \quad i = 1, 2, \quad (2)$$

where c represents the marginal cost of two firms without presence of R&D activities and $a > c > 0$. Equation (2) states

that technology is totally confidential and there is no R&D spillover. The investments of firm i ($i = 1, 2$) can be seen as a quadratic function with respect to its R&D efforts, which can be expressed as $I(x_i) = \gamma x_i^2/2$ ($i = 1, 2$), where γ is a parameter about the technical innovation cost of firm i . The innovation ability of firm i is stronger when the technical innovation cost parameter γ is tinny. Therefore, by following the above assumptions, the profits of firm 1 and firm 2 can be represented as follows:

$$\begin{cases} \pi_1(q_1, q_2, x_1, x_2) = [p_1(q_1, q_2) - C_1(x_1, x_2)]q_1 - \frac{\gamma x_1^2}{2}, \\ \pi_2(q_1, q_2, x_1, x_2) = [p_2(q_1, q_2) - C_2(x_1, x_2)]q_2 - \frac{\gamma x_2^2}{2}. \end{cases} \quad (3)$$

Substituting equations (1) and (2) into equation (3), we can get the specific expression of profit function, which could be given as

$$\begin{cases} \pi_1(q_1, q_2, x_1, x_2) = [(a - q_1 - bq_2) - (c - x_1)]q_1 - \frac{\gamma x_1^2}{2}, \\ \pi_2(q_1, q_2, x_1, x_2) = [(a - q_2 - bq_1) - (c - x_2)]q_2 - \frac{\gamma x_2^2}{2}. \end{cases} \quad (4)$$

The marginal profits of these two firms captured by taking the derivative of (4) with respect to q_i ($i = 1, 2$) are given as

$$\begin{cases} \frac{\partial \pi_1}{\partial q_1} = a - 2q_1 - bq_2 - c + x_1, \\ \frac{\partial \pi_2}{\partial q_2} = a - 2q_2 - bq_1 - c + x_2. \end{cases} \quad (5)$$

Letting $\partial \pi_i / \partial q_i = 0$ ($i = 1, 2$), the subgame perfect Nash equilibrium (SPNE) of firm i ($i = 1, 2$) in the second stage can be obtained as

$$\begin{cases} q_1^* = \frac{(a - c)(2 - b) + 2x_1 - bx_2}{4 - b^2}, \\ q_2^* = \frac{(a - c)(2 - b) + 2x_2 - bx_1}{4 - b^2}. \end{cases} \quad (6)$$

The profit function about R&D efforts x_i captured by taking equation (6) into equation (4) in reverse order can be obtained as

$$\begin{cases} \pi_1(x_1, x_2) = \frac{[(a - c)(2 - b) + 2x_1 - bx_2]^2}{(4 - b^2)^2} - \frac{\gamma x_1^2}{2}, \\ \pi_2(x_1, x_2) = \frac{[(a - c)(2 - b) + 2x_2 - bx_1]^2}{(4 - b^2)^2} - \frac{\gamma x_2^2}{2}. \end{cases} \quad (7)$$

Computing the derivative of equation (7) with respect to x_i ($i = 1, 2$), the local marginal profits about the R&D efforts of two firms are given as

$$\begin{cases} \frac{\partial \pi_1}{\partial x_1} = \frac{4[(a-c)(2-b) + 2x_1 - bx_2]}{(4-b^2)^2} - \gamma x_1, \\ \frac{\partial \pi_1}{\partial x_2} = \frac{4[(a-c)(2-b) + 2x_2 - bx_1]}{(4-b^2)^2} - \gamma x_2. \end{cases} \quad (8)$$

Actually, it is impossible to make perfect rational decision with incomplete market information, such as incomplete demand information, the investments of their competitors, and the level of technical innovation. These incomplete elements make the firms “myopic” in some aspects. These “myopic” firms can only adjust their strategies through continuous “trial and error.” That is, the output at the next period is decided according to their own experience, so these firms can be seen as bounded rational. The firm shall

have a decision on its R&D effort x_i at $t + 1$ period by using a local estimate of marginal profit $\partial \pi_i / \partial x_i$ at t period. More in detail, if $\partial \pi_i / \partial x_i > 0$, the firm i will increase its R&D investment in the next period. And the firm will keep invariant outputs in next period if the local estimate of marginal profit meets $\partial \pi_i / \partial x_i = 0$. Then, if $\partial \pi_i / \partial x_i < 0$, the R&D investment of the firm i in the next period will be reduced. On the basis of the above thoughts, a dynamical gradient adjustment mechanism is introduced [20]; then, the dynamic model can be constructed as

$$\begin{cases} x_1(t+1) = x_1(t) + \alpha_1 x_1(t) \frac{\partial \pi_1}{\partial x_1}, \\ x_2(t+1) = x_2(t) + \alpha_2 x_2(t) \frac{\partial \pi_2}{\partial x_2}. \end{cases} \quad (9)$$

Taking equation (8) into equation (9), the two-dimensional nonlinear discrete-time evolution of dynamic system (9) is as follows:

$$\begin{cases} x_1(t+1) = x_1(t) + \alpha_1 x_1(t) \left\{ \frac{4[(a-c)(2-b) + 2x_1(t) - bx_2(t)]}{(4-b^2)^2} - \gamma x_1(t) \right\}, \\ x_2(t+1) = x_2(t) + \alpha_2 x_2(t) \left\{ \frac{4[(a-c)(2-b) + 2x_2(t) - bx_1(t)]}{(4-b^2)^2} - \gamma x_2(t) \right\}, \end{cases} \quad (10)$$

where $\alpha_i > 0$ denotes the adjustment speed, which determines the variation ratio of R&D efforts x_i of firm i in the next period.

2.1. Stability Analysis of the Equilibrium Points. System (10) is a two-dimensional noninvertible map whose iteration decides the trajectory of R&D effort. In order to discuss local qualitative behaviors of the solutions of system (10), we need to find equilibrium points of the game between these two firms. Let $x_i(t+1) = x_i(t)$ ($i = 1, 2$); then, we can get the nonlinear equations as follows:

$$\begin{cases} \alpha_1 x_1(t) \left\{ \frac{4[(a-c)(2-b) + 2x_1(t) - bx_2(t)]}{(4-b^2)^2} - \gamma x_1(t) \right\} = 0, \\ \alpha_2 x_2(t) \left\{ \frac{4[(a-c)(2-b) + 2x_2(t) - bx_1(t)]}{(4-b^2)^2} - \gamma x_2(t) \right\} = 0. \end{cases} \quad (11)$$

By solving these nonlinear equations, four equilibrium points of system (10) can be obtained. They are

$$\begin{aligned} E_1(0, 0), \\ E_2\left(0, -\frac{4(2-b)(a-c)}{8-\gamma(4-b^2)^2}\right), \\ E_3\left(-\frac{4(2-b)(a-c)}{8-\gamma(4-b^2)^2}, 0\right), \\ E_4(x^*, x^*), \end{aligned} \quad (12)$$

where $x^* = -(4(2-b)(a-c)/8 - 4b - \gamma(4-b^2)^2)$. The fixed points E_1 , E_2 , and E_3 are boundary equilibrium points. And the fixed point E_4 is a unique Nash equilibrium point. In the sense of economy, the inequalities $a > c$ and $0 \leq b \leq 1$ should be satisfied. And if the other parameters satisfy the condition

$$\gamma > \frac{8}{(4-b^2)^2}, \quad (13)$$

all the four equilibrium points of system (10) will be non-negative. The corresponding Jacobian matrix of system (10) at any point (x_1, x_2) has the form

$$J = \begin{bmatrix} 1 + \alpha_1 \left[\frac{4(2-b)(a-c) + 2(8-\gamma(4-b^2)^2)x_1 - 4bx_2}{(4-b^2)^2} - \frac{4\alpha_1 b}{(4-b^2)^2} x_1 \right] & \\ -\frac{4\alpha_2 b}{(4-b^2)^2} x_2 & 1 + \alpha_2 \left[\frac{4(2-b)(a-c) + 2(8-\gamma(4-b^2)^2)x_2 - 4bx_1}{(4-b^2)^2} \right] \end{bmatrix}. \quad (14)$$

In addition, the local stability of equilibrium points of system (10) depends on the eigenvalues of Jacobian matrix at the given equilibrium point.

Proposition 1. *The boundary equilibrium point E_1 is an unstable node.*

Proof. The Jacobian matrix at $E_1 = (0, 0)$ is given as follows:

$$J(E_1) = \begin{bmatrix} 1 + \frac{4\alpha_1(2-b)(a-c)}{(4-b^2)^2} & 0 \\ 0 & 1 + \frac{4\alpha_2(2-b)(a-c)}{(4-b^2)^2} \end{bmatrix}. \quad (15)$$

Obviously, the Jacobian matrix $J(E_1)$ is a diagonal matrix; thus, its corresponding distinct eigenvalues are

$$\begin{aligned} \lambda_1 &= 1 + \frac{4\alpha_1(2-b)(a-c)}{(4-b^2)^2}, \\ \lambda_2 &= 1 + \frac{4\alpha_2(2-b)(a-c)}{(4-b^2)^2}. \end{aligned} \quad (16)$$

With the constricts $a > c$ and $0 \leq b \leq 1$, $\lambda_{1,2} > 1$ is satisfied, then we can get that the equilibrium point $E_1(0, 0)$ is an unstable node. \square

Proposition 2. *The types of local stability of the equilibrium point E_2 can be classified as follows:*

- (1) *If the condition $(8 + 4b - \gamma(4 - b^2)^2) < 0$ meets, the equilibrium point E_2 is an unstable node*
- (2) *If the conditions $(8 + 4b - \gamma(4 - b^2)^2) > 0$, $0 < \alpha_1 < (((4 - b^2)^2(8 - \gamma(4 - b^2)^2))/(2(2 - b)(a - c)(8 + 4b - \gamma(4 - b^2)^2)))$, and $\alpha_2 > (((4 - b^2)^2)/(2(2 - b)(a - c)))$ meet, then the equilibrium point E_2 is an unstable saddle*
- (3) *If the conditions $(8 + 4b - \gamma(4 - b^2)^2) > 0$, $0 < \alpha_1 < (((4 - b^2)^2(8 - \gamma(4 - b^2)^2))/(2(2 - b)(a - c)(8 + 4b - \gamma(4 - b^2)^2)))$, and $\alpha_2 < (4 - b^2)^2/2(2 - b)(a - c)$ meet, then the equilibrium point E_2 is a stable node*
- (4) *Else if $(8 + 4b - \gamma(4 - b^2)^2) > 0$ and $\alpha_1 > (((4 - b^2)^2(8 - \gamma(4 - b^2)^2))/(2(2 - b)(a - c)(8 + 4b - \gamma(4 - b^2)^2)))$ are satisfied, then the equilibrium point E_2 is an unstable point*

Proof. The Jacobian matrix at E_2 is

$$J(E_2) = \begin{bmatrix} 1 + \frac{4\alpha_1(2-b)(a-c)(8+4b-\gamma(4-b^2)^2)}{(4-b^2)^2(8-\gamma(4-b^2)^2)} & 0 \\ \frac{16\alpha_2b(2-b)(a-c)}{(4-b^2)^2(8-\gamma(4-b^2)^2)} & 1 - \frac{4\alpha_2(2-b)(a-c)}{(4-b^2)^2} \end{bmatrix}, \quad (17)$$

where $J(E_2)$ is a lower triangular matrix; thus, its eigenvalues are main diagonal elements, that is,

$$\begin{aligned} \lambda_1 &= 1 + \frac{4\alpha_1(2-b)(a-c)(8+4b-\gamma(4-b^2)^2)}{(4-b^2)^2(8-\gamma(4-b^2)^2)}, \\ \lambda_2 &= 1 - \frac{4\alpha_2(2-b)(a-c)}{(4-b^2)^2}. \end{aligned} \quad (18)$$

The type of local stability of this boundary equilibrium point E_2 is determined by different values of the parameters:

- (1) If $(8 + 4b - \gamma(4 - b^2)^2) < 0$, then $\lambda_1 = 1 + (((4\alpha_1(2 - b)(a - c)(8 + 4b - \gamma(4 - b^2)^2))/((4 - b^2)^2(8 - \gamma(4 - b^2)^2))) > 1$; thus, the equilibrium point E_2 is an unstable node.
- (2) If $(8 + 4b - \gamma(4 - b^2)^2) > 0$ and $0 < \alpha_1 < (((4 - b^2)^2(8 - \gamma(4 - b^2)^2))/(2(2 - b)(a - c)(8 + 4b - \gamma(4 - b^2)^2)))$ are satisfied, then $\lambda_1 = |1 + (((4\alpha_1(2 - b)(a - c)(8 + 4b - \gamma(4 - b^2)^2))/((4 - b^2)^2(8 - \gamma(4 - b^2)^2)))| < 1$ meets. And if $\alpha_2 > (4 - b^2)^2/2(2 - b)(a - c)$, then

$\lambda_2 = |1 + (4\alpha_2(2 - b)(a - c)/(4 - b^2)^2)| > 1$ meets; hence, the equilibrium point E_2 is an unstable saddle.

- (3) If $(8 + 4b - \gamma(4 - b^2)^2) > 0$ and $0 < \alpha_1 < (((4 - b^2)^2(8 - \gamma(4 - b^2)^2))/(2(2 - b)(a - c)(8 + 4b - \gamma(4 - b^2)^2)))$, then $\lambda_1 = |1 + (((4\alpha_1(2 - b)(a - c)(8 + 4b - \gamma(4 - b^2)^2))/((4 - b^2)^2(8 - \gamma(4 - b^2)^2)))| < 1$. And if $\alpha_2 < (4 - b^2)^2/2(2 - b)(a - c)$, then $\lambda_2 = |1 - (4\alpha_2(2 - b)(a - c)/(4 - b^2)^2)| < 1$, so the equilibrium point E_2 is a stable node.
- (4) If the parameters meet with $(8 + 4b - \gamma(4 - b^2)^2) > 0$ and $\alpha_1 > (((4 - b^2)^2(8 - \gamma(4 - b^2)^2))/(2(2 - b)(a - c)(8 + 4b - \gamma(4 - b^2)^2)))$, then $\lambda_1 = |1 + (((4\alpha_1(2 - b)(a - c)(8 + 4b - \gamma(4 - b^2)^2))/((4 - b^2)^2(8 - \gamma(4 - b^2)^2)))| > 1$; thus, the equilibrium point E_2 is an unstable point. \square

Proposition 3. *The types of equilibrium point E_3 are similar to the boundary equilibrium point E_2 .*

Proof. The Jacobian matrix at E_3 can be written as follows:

$$J(E_3) = \begin{bmatrix} 1 - \frac{4\alpha_1(2-b)(a-c)}{(4-b^2)^2} & \frac{16\alpha_1 b(2-b)(a-c)}{(4-b^2)^2(8-\gamma(4-b^2)^2)} \\ 0 & 1 + \frac{4\alpha_2(2-b)(a-c)(8+4b-\gamma(4-b^2)^2)}{(4-b^2)^2(8-\gamma(4-b^2)^2)} \end{bmatrix}. \quad (19)$$

Matrix (19) is an upper triangular matrix and the corresponding eigenvalues are

$$\begin{aligned} \lambda_1 &= 1 - \frac{4\alpha_1(2-b)(a-c)}{(4-b^2)^2}, \\ \lambda_2 &= 1 + \frac{4\alpha_2(2-b)(a-c)(8+4b-\gamma(4-b^2)^2)}{(4-b^2)^2(8-\gamma(4-b^2)^2)}. \end{aligned} \quad (20)$$

In addition, the boundary equilibrium points E_2 and E_3 are symmetrically located around the diagonal line in the plane R^2 . And the local stability conditions of E_3 are symmetrical to the conditions of E_2 listed in Proposition 2, so the conclusions of E_3 are no longer repeated here.

In sense of economics, the boundary equilibrium points interpret a situation that one of these two firms has

withdrawn from the market. The equilibrium points E_2 and E_3 can be regarded as the situation that one of these two firms takes the lead in the market. That is to say, the oligopoly market becomes the monopoly market, and the local stability of equilibrium points implies the stability of economic market in a short term. Actually, neither of the above two market situations is expected, only when these two companies restrict each other can they be conducive to the stable development of the market and the country. That is, the game between firms reaches an equilibrium, named ‘‘Nash equilibrium.’’ Nash equilibrium [41] is on the premise of maximizing its own profits. Meanwhile, it also ensures the stable development of the market.

The Jacobian matrix at the Nash equilibrium E_4 of system (10) is formulated as

$$J(E_4) = \begin{bmatrix} 1 + \frac{4\alpha_1(2-b)(a-c) + 2(8-2b-\gamma(4-b^2)^2)x^*}{(4-b^2)^2} & \frac{4\alpha_1 b x^*}{(4-b^2)^2} \\ \frac{4\alpha_2 b x^*}{(4-b^2)^2} & 1 + \frac{4\alpha_2(2-b)(a-c) + 2(8-4b-\gamma(4-b^2)^2)x^*}{(4-b^2)^2} \end{bmatrix}, \quad (21)$$

where $x^* = -((4(2-b)(a-c))/(8-4b-\gamma(4-b^2)^2))$. To simplify the process of analyses, the auxiliary variables $A = 4(2-b)(a-c)/(4-b^2)^2 > 0$, $B = (8-\gamma(4-b^2)^2)/(4-b^2)^2 < 0$, and $C = 4b/(4-b^2)^2 > 0$ are introduced. Thus, the matrix $J(E_4)$ can be rewritten as follows:

$$J(E_4) = \begin{bmatrix} 1 + \alpha_1(A + (2B - C)x^*) & \alpha_1 x^* C \\ \alpha_2 x^* C & 1 + \alpha_2(A + (2B - C)x^*) \end{bmatrix}. \quad (22)$$

The characteristic polynomial of matrix (22) is

$$P(\lambda) = \lambda^2 - \text{Tr}(J) + \text{Det}(J) = 0, \quad (23)$$

where $\text{Tr}(J)$ and $\text{Det}(J)$ denote the trace and the determinant of matrix (22) at Nash equilibrium point E_4 . And the specific formulation of $\text{Tr}(J)$ and $\text{Det}(J)$ are given as

$$\begin{aligned} \text{Tr}(J) &= 2 + (\alpha_1 + \alpha_2)(A + (2B - C)x^*), \\ \text{Det}(J) &= [1 + \alpha_1(A + (2B - C)x^*)][1 + \alpha_2(A + (2B - C)x^*)] - \alpha_1\alpha_2 C^2 x^{*2} \\ &= 1 + (\alpha_1 + \alpha_2)(A + (2B - C)x^*) + \alpha_1\alpha_2[A^2 + 2A(2B - C)x^* + 4B(B - C)x^{*2}]. \end{aligned} \quad (24)$$

Proposition 4. *Neimark–Sacker bifurcation will not occur at the Nash equilibrium point E_4 .*

Proof. The corresponding discriminant of roots of characteristic polynomial (23) is given as □

$$\Delta = (\alpha_1 - \alpha_2)^2 (A + (2B - C)x^*)^2 + 4\alpha_1\alpha_2 C^2 x^{*2} > 0, \quad (25)$$

which means that the dynamical system (10) will not generate complex eigenvalues at the Nash equilibrium point E_4 ; hence, the Neimark–Sacker bifurcation will not occur at the Nash equilibrium point E_4 .

On the basis of canonical stability analysis, the sufficient condition of local asymptotical stability of Nash equilibrium point E_4 is that the eigenvalues of corresponding Jacobian matrix of E_4 is within the unit cycle. According to Jury criterion [15], the condition of local asymptotical stability of Nash equilibrium point E_4 can be expressed in detail as

- (i) $1 + \text{Tr}(J) + \text{Det}(J) = 4 + (\alpha_1 + \alpha_2)(A + (2B - C)x^*) + \alpha_1\alpha_2[A^2 + 2A(2B - C)x^* + 4B(B - C)x^{*2}] > 0$
- (ii) $1 - \text{Tr}(J) + \text{Det}(J) = \alpha_1\alpha_2[A^2 + 2A(2B - C)x^* + 4B(B - C)x^{*2}] > 0$
- (iii) $1 - \text{Det}(J) = -(\alpha_1 + \alpha_2)(A + (2B - C)x^*) - \alpha_1\alpha_2[A^2 + 2A(2B - C)x^* + 4B(B - C)x^{*2}] > 0$ \square

Proposition 5. *When $B + C < 0$ is satisfied, the second condition of Jury criterion holds. That is,*

$$1 - \text{Tr}(J) + \text{Det}(J) = \alpha_1\alpha_2[A^2 + 2A(2B - C)x^* + 4B(B - C)x^{*2}] > 0. \quad (26)$$

Proof. First, let $y = A^2 + 2B(2B - C)x + 4B(B - C)x^2$, and then its roots can be computed as $x_1 = -A/2(B - C)$ and $x_2 = -A/2B$. We recall that $A = ((4(2 - b)(a - c))/(4 - b^2)^2) > 0$, $B = (8 - \gamma(4 - b^2)^2)/(4 - b^2)^2 < 0$, and $C = 4b/(4 - b^2)^2 > 0$; then, we can obtain

$$B - C = \frac{8 - 4b - \gamma(4 - b^2)^2}{(4 - b^2)^2} < 0. \quad (27)$$

The numerical relationship between x_1 and x_2 is that $x_1 = -A/2(B - C) < x_2 = -A/2B$. If the condition $A^2 + 2B(2B - C)x^* + 4B(B - C)x^{*2} > 0$ holds, then x^* satisfies the condition $x^* < x_1$ or $x^* > x_2$. Following the constriction $x^* = ((-4(2 - b)(a - c))/(8 - \gamma(4 - b^2)^2)) = -A/2(B - C)$, $x^* = (-A/(B - C)) > x_1 = (-A/2(B - C))$ can be captured. Hence, $x^* < x_1$ does not hold. Only when the condition $x^* > x_2$ meets, the second condition of Jury criterion holds. The corner case is

$$x^* - x_2 = \frac{-A}{B - C} + \frac{A}{2B} = \frac{-A(B + C)}{2B(B - C)}. \quad (28)$$

Hence, when $B + C < 0$ and $x^* > x_2$ meet, the second condition of Jury criterion holds. \square

Proposition 6. *If the first condition of Jury criterion holds, the third condition of Jury criterion will certainly hold.*

Proof. Let $\alpha_1 = 0$ of first condition of Jury criterion, and we can get $4 + (\alpha_1 + \alpha_2)(A + (2B - C)x^*) > 0$. As for $A > 0$, $B < 0$, $C > 0$, $B - C < 0$, and $x^* = -A/(B - C)$, we have

$$(A + (2B - C)x^*) = A + \frac{-A(2B - C)}{B - C} = \frac{-AB}{B - C} < 0. \quad (29)$$

After this, we can deduce that $\alpha_2 < (-2/(A + (2B - C)x^*))$.

Let $\Delta = A^2 + 2B(2B - C)x^* + 4B(B - C)x^{*2} > 0$, if $0 < \alpha_2 \leq (-(A + (2B - C)x^*)/\Delta)$, the third condition of Jury criterion will hold. That is,

$$\begin{aligned} &4 + (\alpha_1 + \alpha_2)(A + (2B - C)x^*) + \alpha_1\alpha_2\Delta \\ &= \alpha_2(A + (2B - C)x^*) + \alpha_1(A + (2B - C)x^* + \alpha_2\Delta) < 0, \end{aligned} \quad (30)$$

In the same time, it can be easily proved that

$$(A + (2B - C)x^*)\Delta\alpha_2^2 + 4\Delta\alpha_2 + 4(A + (2B - C)x^*) < 0. \quad (31)$$

which is satisfied for any value of α_2 . Following the above formulations, we can get $(-2/(A + (2B - C)x^*)) < (-2(A + (2B - C)x^*)/\Delta)$. The inequalities $(-(A + (2B - C)x^*)/\Delta) < \alpha_2 < (-2/(A + (2B - C)x^*))$ and

$$\alpha_1 < \frac{-4 - 2\alpha_2(A + (2B - C)x^*)}{2(A + (2B - C)x^*) + \alpha_2\Delta} < \frac{-\alpha_2(A + (2B - C)x^*)}{2(A + (2B - C)x^*) + \alpha_2\Delta}, \quad (32)$$

can be captured through jury criterion and inequality (31). Then, we can deduce the conclusion that if the first condition of Jury criterion holds, the third condition of Jury criterion will certainly hold. In summary, system (10) has a unique Nash equilibrium point E_4 . When $B + C < 0$ and $\alpha_1 < ((-4 - 2\alpha_2(A + (2B - C)x^*)) / (2(A + (2B - C)x^*) + \alpha_2\Delta))$, system (10) is local asymptotical stable at Nash equilibrium point E_4 . Under the above constrictions of the system parameters, these two firms will reach equilibrium state and get a maximum value for total profit after several games. Then, the market will keep stable development. \square

3. Analysis of Complex Evolution Law Based on Speed of Adjustment

The local stability of boundary equilibrium points and Nash equilibrium point are discussed by the way of analytics. In this part, in order to investigate the intrinsic laws of evolution of system (10) and to mainly analyze its local and global properties, the method of numerical simulation through two-dimensional bifurcation diagram, one-dimensional bifurcation diagram, two-dimensional largest Lyapunov exponent, and basin of attraction is used.

3.1. The Routes to Chaos. Firstly, the parameters a, c, b , and γ are fixed as $a = 61$, $c = 51.5$, $b = 0.85$, and $\gamma = 2$, and then the speeds of adjustment α_1 and α_2 are chosen as the bifurcation parameters. The global bifurcation route with respect to speed of adjustment (α_1, α_2) is illustrated in Figure 1, where Figure 1(a) is a two-dimensional bifurcation and Figure 1(b) is a two-dimensional largest Lyapunov exponent corresponding to Figure 1(a).

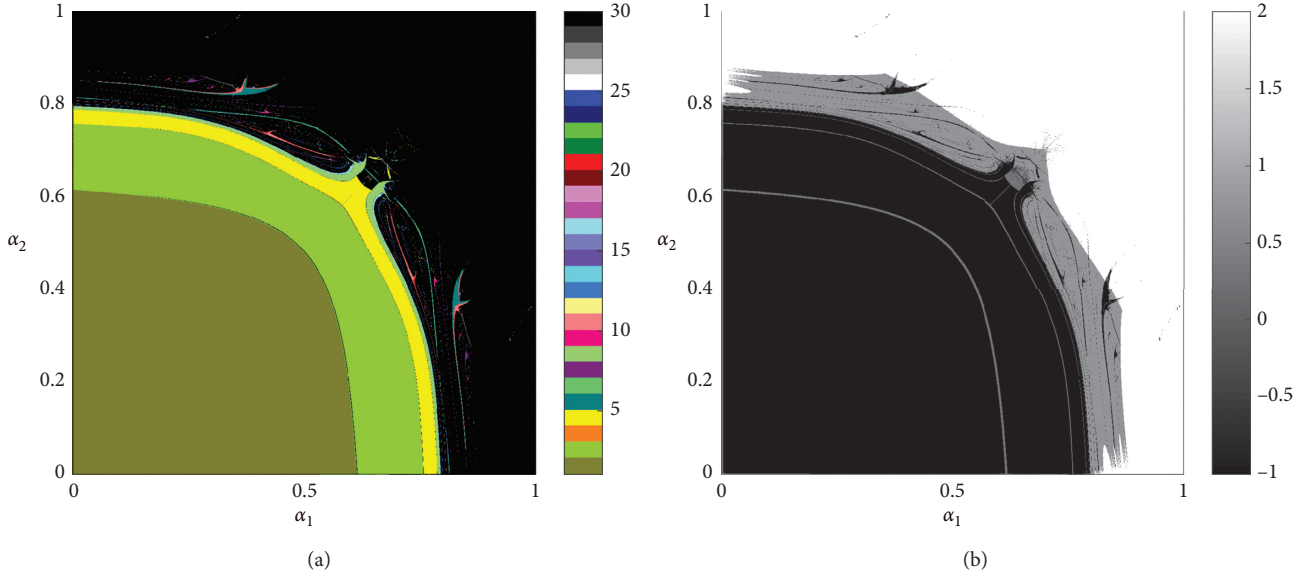


FIGURE 1: (a) The two-dimensional bifurcation with respect to (α_1, α_2) of system (10). (b) The two-dimensional largest Lyapunov exponent corresponding to Figure 1(a).

In the right of Figure 1(a) is a color bar with different colors, that is to say, these different colors represent different periods. Specifically speaking, the brown area denotes the stable area of Nash equilibrium point, i.e., period-1. The green area denotes period-2, the orange area denotes period-3, the yellow area denotes period-4, and so on; the color of deep black denotes period more than 30. As a result of the constraints of algorithm, the states of quasi-period, chaotic, and escaping of system (10) cannot be classified clearly, so all three states are marked by dark black in Figure 1(a). In addition, when the largest Lyapunov exponent is equal to zero then the corresponding state of system (10) is quasi-period, and when the largest Lyapunov exponent is greater than zero and less than 2, then the state of system (10) is chaotic. The last situation is when the largest Lyapunov exponent is greater than 2, and the corresponding state of system (10) is escaping area. So, the three states mentioned above can be distinguished by this method displayed in Figure 1(b), where the color bar in the right of this figure represents the largest Lyapunov exponent.

The Nash equilibrium point corresponding to Figure 2(a) is $E_4(2.59, 2.59)$. With the increase of α_2 , the corresponding eigenvalues at the Nash equilibrium point will increase to $\lambda_1 = 0.97376$ and $\lambda_2 = -0.69956$. Then, we can deduce that this Nash equilibrium point E_4 is a stable node. And more in detail, when the speed of adjustment $\alpha_2 < 0.608$, then the state of system (10) is at the Nash equilibrium and will keep stable. While if the speed of adjustment satisfy that $\alpha_2 = 0.608$, then the stability of this Nash equilibrium will change and a flip bifurcation will occur. Once the speed of adjustment α_2 meets the condition that $\alpha_2 > 0.791$, system (10) will enter into a chaotic state. And in the corresponding largest Lyapunov exponent to Figure 2(a), when the largest Lyapunov exponent is less than zero, the state of system (10) is stable, and system (10) enters into the chaotic state when the largest Lyapunov exponent is

greater than zero. And when the largest Lyapunov exponent is equal to zero, a bifurcation takes place in system (10).

As it is known to all, the flip bifurcation is a classical trajectory for economic system to change the state from stable into chaotic. A new way of development for firms will generate when the economy develops to a certain stage, and there is only one way for firms to further develop the economy and they will face a dilemma in the choice of the new and old way. As a result, the route of period-doubling is generated in constant choice between firms in dilemma. When the speeds of adjustment of these two firms are relatively small, then the two firms will be in the Nash equilibrium state and maintain its profit maximizing, respectively. In the same time, these two firms mutually hold each other back. Once the speed of adjustment exceeds the threshold value, the stability of Nash equilibrium point will be destroyed and then the period-doubling will occur. Finally, the constant choice of the firms leads to the disorder state of the market.

3.2. The Evolution of Strange Attractor. In the case of a nonlinear dynamic system, its final state inflects the eventual behavior of system because it is a key point to focus on. Furthermore, the final state of the nonlinear system can be indicated by the attractors representing asymptotical behaviors of the nonlinear system if the number of iteration times tends to infinite. In this research, we discuss the impact of adjustment speed of firm 2 α_2 on eventual behavior of system (10) by investigating the evolution of attractors, where the parameters are chosen as the same as in Figure 1(a), and the adjustment speed of firm 1 is fixed as $\alpha_1 = 0.63$. The attractor is a period-4 focus with rough selvedge when the parameter equals to 0.625, which can be seen in Figure 3(a). As shown in Figures 3(b) and 3(c), as the adjustment speed of firm 2 increases, this period-4 focus is

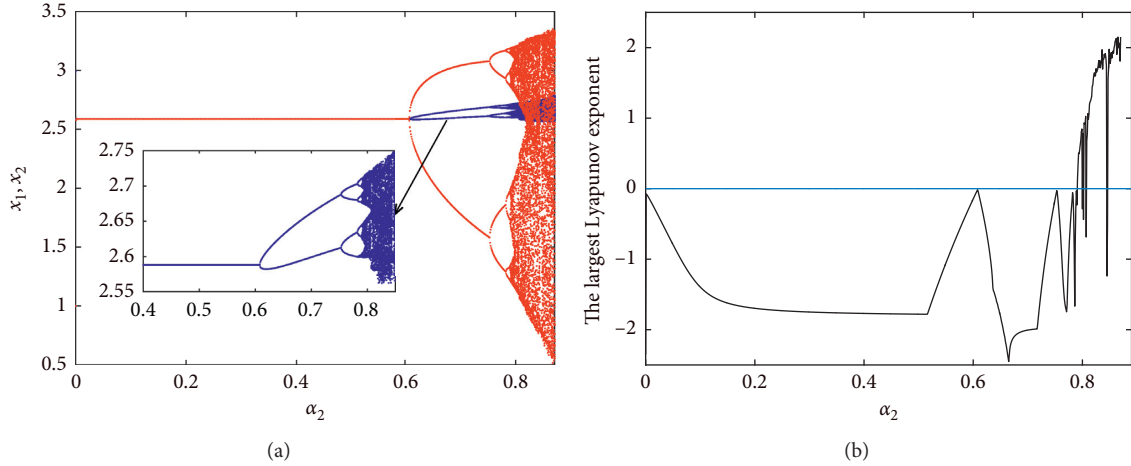


FIGURE 2: (a) The one-dimensional bifurcation with respect to α_2 of system (10). (b) The corresponding largest Lyapunov exponent of Figure 2(a).

transformed to four invariant cycles with selvedge via a Neimark–Sacker bifurcation, and these four invariant cycles become more and more larger and the rough selvedge disappears simultaneously. While when the parameter α_2 further grows up to 0.657, these four invariant cycles break to form the attractor shown in Figure 3(d); system (10) enters into “periodic window.” And the broken attractor continues to spread then recombine to form four chaotic attractors, which can be seen in Figure 3(e). When the adjustment speed of firm 2 α_2 continues to increase until $\alpha_2 = 0.7$, the four chaotic attractors mentioned above conduct the dynamic behaviors that spread and merge and finally form a piece of chaotic attractor, see Figure 3(f).

The increase of adjustment speed leads to the complexity of eventual behavior of system (10). This process of evolution presents the properties of “certainty” and “irregular development,” where “certainty” means that the way of bifurcation, that is to say, period-4 Neimark–Sacker bifurcation, and “irregular development” means that the interior structure of the attractors, as well as complexity of interior structure of the chaotic attractor, as shown in Figures 3(e) and 3(f). No matter if from phenomenon development or interior mechanism, system (10) presents a high of certainty and complexity. That means the economic system makes mistakes in predicting, and due to the influence of external condition the development of economy cannot be forecasted anymore.

3.3. Multistability. In the process of studying the nonlinear dynamic system, we can observe that the stability of equilibrium points may vary with the change of parameters and initial conditions by numerical simulation. This variety can cause single-level or multilevel bifurcation so as to lead to the system displaying complex dynamical behaviors, such as coexistence of attractor, fractal, and chaos. The coexistence of the attractor implies the motion of multistability of system. That is to say, the bifurcation of the nonlinear system varies with the change of the parameters and initial

conditions, which will lead to the change of number of solution. And the number of bifurcation solution varies raised a phenomenon of coexistence of multiattractors, so there is a close relationship between the motion of multistability and bifurcation. In addition, the phenomenon of coexistence of the attractor also indicates that the global bifurcation behavior of the system and the discussion of global bifurcation behavior are mainly reflected in two aspects. One is about the variation of the structure, shape, and amount of attractors with parameters, and another is about the variation of the structure and shape of basin of attraction with parameters.

Then, we fixed the values of parameters as $a = 50$, $c = 38$, $b = 0.45$, $\gamma = 2.3$, and $\alpha_1 = 0.4925$. This set of parameters has a case that the Nash equilibrium point $E_4(2.759, 2.759)$ is an unstable node, and the corresponding eigenvalues, respectively, are $\lambda_1 = 1.526$ and $\lambda_2 = 1.1877$. As shown in Figure 4, with the increase of the adjustment speed α_2 of system (10) can lead to the phenomenon about the global bifurcation of structure, shape, and amount of attractors.

When the adjustment speed α_2 is equal to 0.4865, the chaotic attractor coexists with a period-2 attractor, see Figure 4(a), where the red area denotes the escaping area. The initial value $(x_1, x_2) = (2, 3.3)$ corresponds to two Lyapunov exponents, $\lambda_{LE1} = -0.06358486$ and $\lambda_{LE2} = -\infty$; the corresponding attractor is period-2 attractor and its attracting area is the light blue area. The initial value $(x_1, x_2) = (2, 2.4)$ corresponds to two Lyapunov exponents, $\lambda_{LE1} = 0.04076098$ and $\lambda_{LE2} = -0.10188996$; the corresponding attractor is the chaotic attractor and its attracting area is the white area.

When the adjustment speed α_2 increases to $\alpha_2 = 0.489$, the period-4 attractor suddenly adds into the basin of attraction, which can be seen in Figure 4(b). The increase of parameter raises the change of the structure of the chaotic attractor and the number of the attractor, at the same time, also gives rise to the change of corresponding largest Lyapunov exponent of attractor. The initial value $(x_1, x_2) = (2, 3.3)$ corresponds to two Lyapunov exponents,

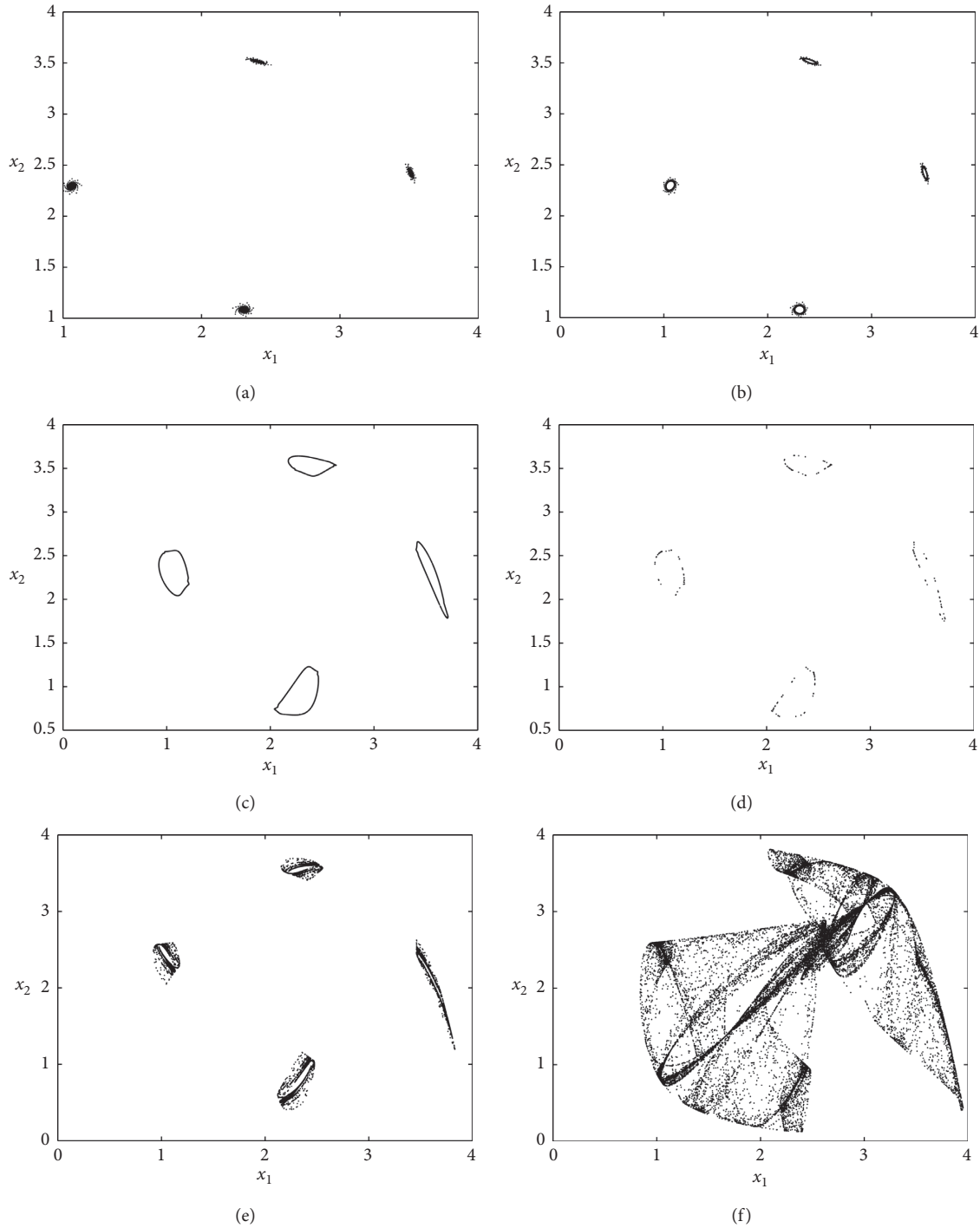


FIGURE 3: The process of evolution of attractors in system (10). (a) $\alpha_2 = 0.625$; (b) $\alpha_2 = 0.626$; (c) $\alpha_2 = 0.656$; (d) $\alpha_2 = 0.658$; (e) $\alpha_2 = 0.679$; (f) $\alpha_2 = 0.7$.

$\lambda_{LE1} = -0.18013771$ and $\lambda_{LE2} = -\infty$; the corresponding attractor is a period-2 attractor. The initial value $(x_1, x_2) = (2, 2)$ corresponds to two Lyapunov exponents, $\lambda_{LE1} = -0.04197454$ and $\lambda_{LE2} = -0.06106757$; the corresponding attractor is period-4 attractor. The initial value $(x_1, x_2) = (2, 2.4)$ corresponds to two Lyapunov exponents, $\lambda_{LE1} = 0.06520552$ and $\lambda_{LE2} = 0.00617542$; the corresponding chaotic attractor becomes a hyperchaotic attractor. From

Figure 4(b), it is easy to know that the attracting area of period-2 attractors is the light blue area, the attracting area of period-4 attractors is the blue area, and the attracting area of super-chaotic attractor is the white area.

And if we further increase the value of parameter α_2 to $\alpha_2 = 0.496$, then we can get an interesting phenomenon that the period-4 attractors become the period-8 attractors via the period-doubling bifurcation, and the chaotic attractors

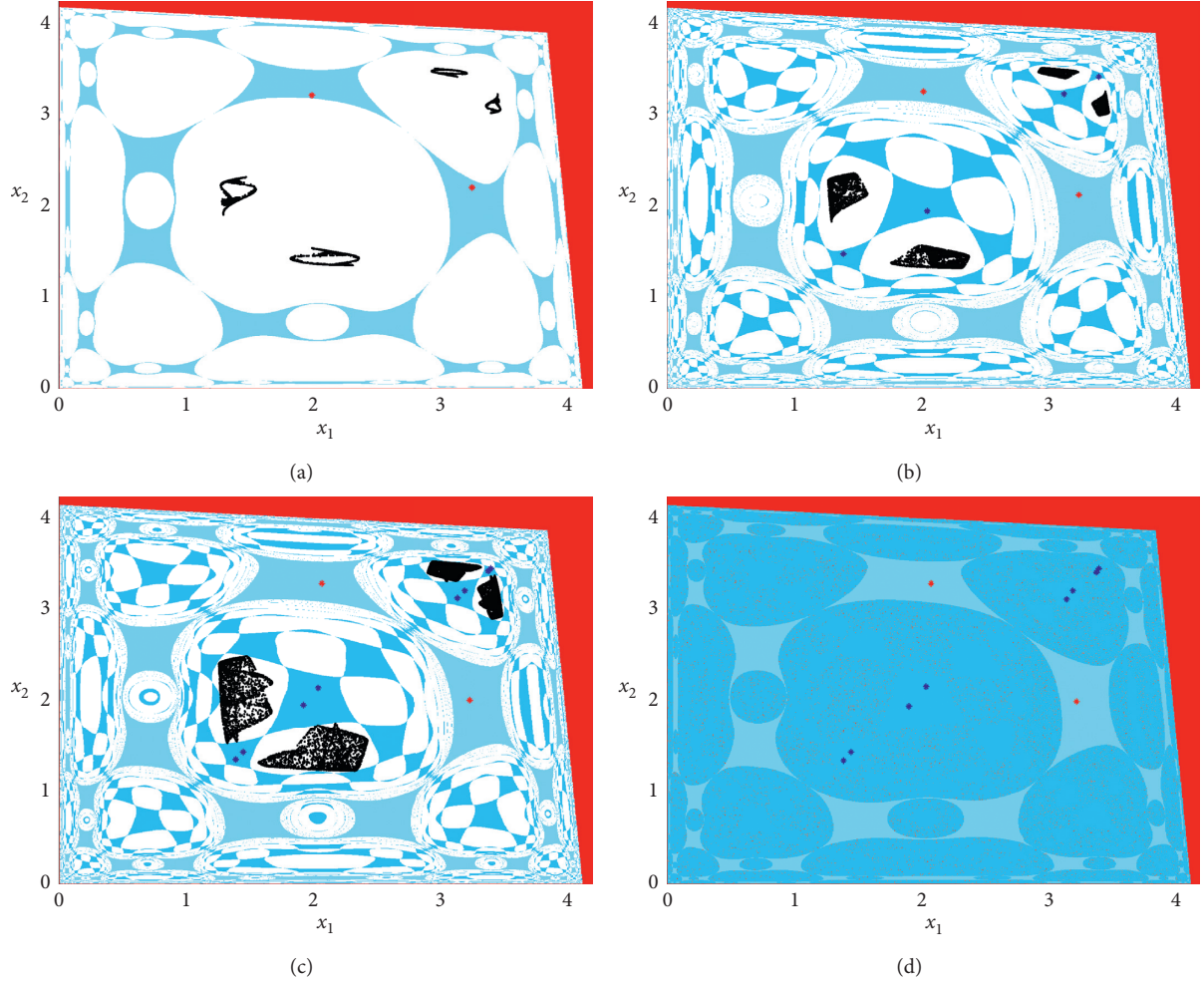


FIGURE 4: The evolution of attracting basin of system (10) with respect to the parameter α_2 . (a) $\alpha_2 = 0.4865$; (b) $\alpha_2 = 0.489$; (c) $\alpha_2 = 0.496$; (d) $\alpha_2 = 0.497$.

constantly enlarge so the scenario of coexistence, as shown in Figure 4(c). The initial value $(x_1, x_2) = (2, 3.3)$ corresponds to two Lyapunov exponents, $\lambda_{LE1} = -0.26726652$ and $\lambda_{LE2} = -0.26726652$; the corresponding attractor is period-2 attractor and its attracting area is the light blue area. The initial value $(x_1, x_2) = (2, 2)$ corresponds to two Lyapunov exponents, $\lambda_{LE1} = -0.19091335$ and $\lambda_{LE2} = -0.29042750$; the corresponding attractor is period-4 attractor and its attracting area is the blue area. The initial value $(x_1, x_2) = (2, 2.4)$ corresponds to two Lyapunov exponents, $\lambda_{LE1} = 0.11730683$ and $\lambda_{LE2} = 0.05142154$; the corresponding attractor is still hyperchaotic attractor and its attracting area is the white area.

And then if we continue to increase the value of parameter α_2 , the chaotic attractor will contact with the boundary of the blue area and a “contact bifurcation” will occur, which can be seen in Figure 4(c). As shown in Figure 4(d), this “contact bifurcation” can lead to the chaotic attractor burst and then form a “ghost” existing in the former attracting area. Based on above analysis, it is obvious that, with the increase of the parameter α_2 , the largest Lyapunov exponent of period-2 decreases but the

corresponding attracting area is the light blue area keeping invariantly, while the largest Lyapunov exponent of the chaotic attractor increases, where the attractor becomes hyperchaotic from chaotic, and its attracting area is the white area. This white area is constantly occupied by the blue attracting area so as to shrink with the presence of period-4 attractors. In addition, the number of attractors has increased from two to three and the structure of the attractor changes. The last bifurcation form of the chaotic attractor is the “critical bifurcation,” when this chaotic attractor contacts the boundary of its basin of attraction.

The parameters are given as $a = 48.344$, $c = 43.965$, $b = 0.936$, $\gamma = 1.202$, and $\alpha_1 = 1.557$. A series of special phenomena about the coexistence are discussed in Figure 5, which indicates the one-dimensional bifurcation of different initial values of the adjustment speed ... The initial value corresponds to Figure 5(a) which is $(x_1, x_2) = (1, 4)$, and the initial values corresponds to Figure 5(c) which is $(x_1, x_2) = (3, 0.5)$, where the blue curve represents the R&D effort x_1 of the firm 1 and the red curve represents the R&D effort x_2 of the firm 2. The diagrams in Figures 5(b) and 5(d) are the largest Lyapunov exponent corresponding to

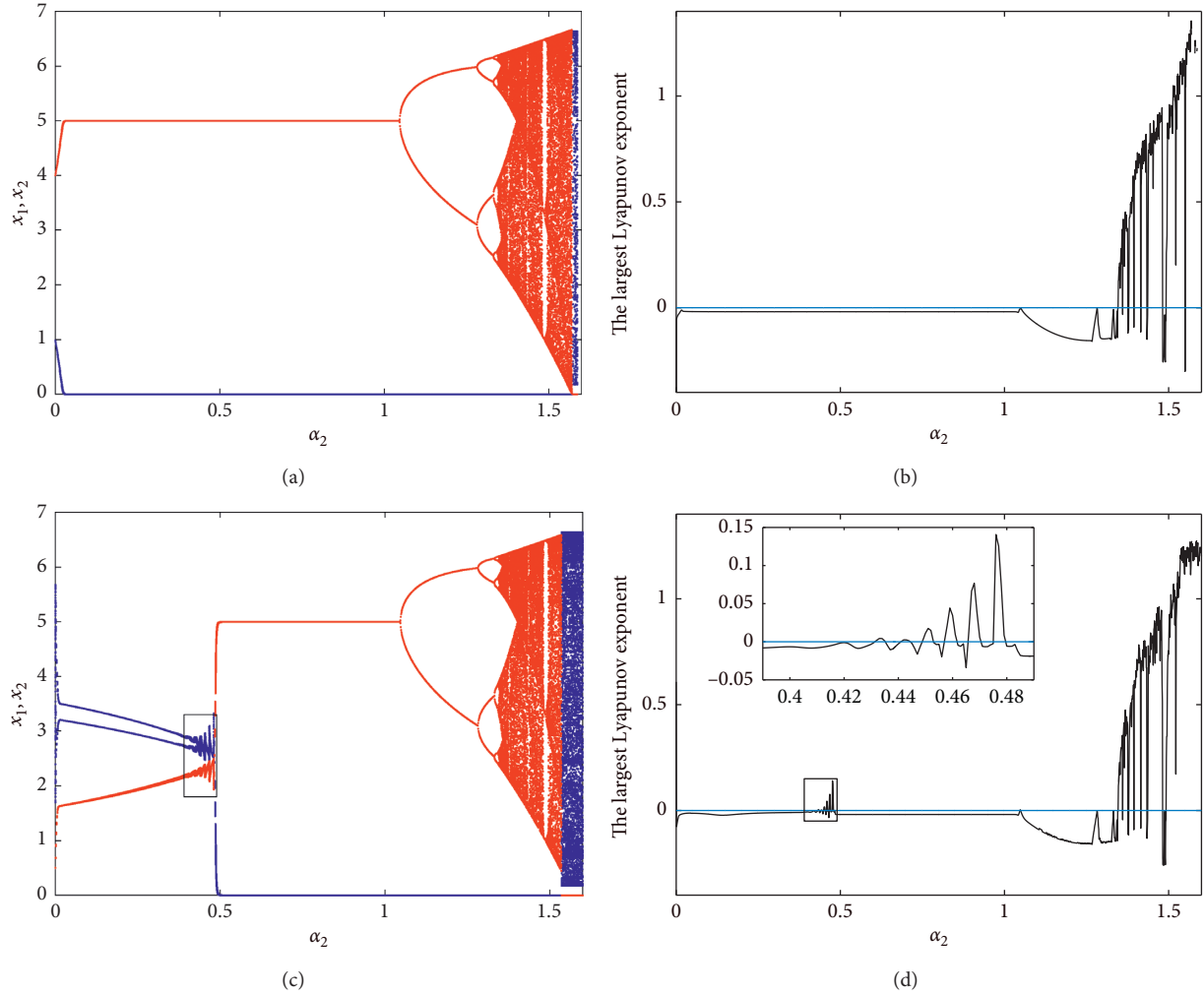


FIGURE 5: The bifurcation of system (10) with respect to parameter α_2 . (a) The initial value is given as $(x_1, x_2) = (1, 4)$. (b) The corresponding largest Lyapunov exponent to Figure 5(a). (c) The initial value is given as $(x_1, x_2) = (3, 0.5)$. (d) The corresponding largest Lyapunov exponent to Figure 5(c).

Figures 5(a) and 5(c), respectively. Let us compare the one-dimensional bifurcation Figure 5(a) with Figure 5(c), and we can draw a result that these two bifurcating diagrams have an obvious difference between them when the adjustment speed α_2 satisfies this condition as $\alpha_2 \in (0, 0.5) \cup (1.536, 1.6)$, which means that due to the different choices of initial values, a huge difference of the eventual state of the system will arise. And if we constantly increase the value of the parameter, α_2 tends to a relative large number; then, firm 1 and firm 2 will withdraw from the market in turn. Especially, the way of bifurcation of system (10) is a nonnormal bifurcation in Figure 5(c) when parameter α_2 belongs to the interval $(0.4, 0.5)$. As shown in the local enlargement of Figure 5(d), the corresponding largest Lyapunov will present a form of oscillation in this interval and the detailed discussion is shown in Figure 6.

In the case of this group of parameters, the boundary equilibrium point $E_2 = (0, 4.99)$ is a stable node and the corresponding eigenvalues are $\lambda_1 = 0.98888$ and $\lambda_2 = 0.1788$, respectively. When the parameter α_2 is

$\alpha_2 = 0.43$, the phenomenon of period-2 attractors coexisting with the stable boundary equilibrium E_2 is shown in Figure 6(a), where the red area represents the escaping area. And the attractor corresponding to the initial values $(x_1, x_2) = (1, 4)$ is this boundary equilibrium point E_2 , and its attracting area is the white area. The attractor corresponding to the initial values $(x_1, x_2) = (3, 0.5)$ is the period-2 attractor, and its attracting area is the light blue area, where the diagram in right upper corner of Figure 6(a) is the enlargement of period-2 attractors.

When the parameter α_2 is $\alpha_2 = 0.468$, the period-2 attractors become the chaotic attractors through a non-normal bifurcation, see Figure 6(b), where the corresponding largest Lyapunov exponents are $\lambda_{LE1} = 0.0251229$ and $\lambda_{LE2} = -0.3369075$. From the enlargement diagram in the right upper corner of Figure 6(b), we can clearly see these chaotic attractors have an obvious level of structure, by using the colors of green, red, and black separately represent the inner, middle, and outer layers of the attractor. Each layer is surrounded by numerous points, and the outer layer is not

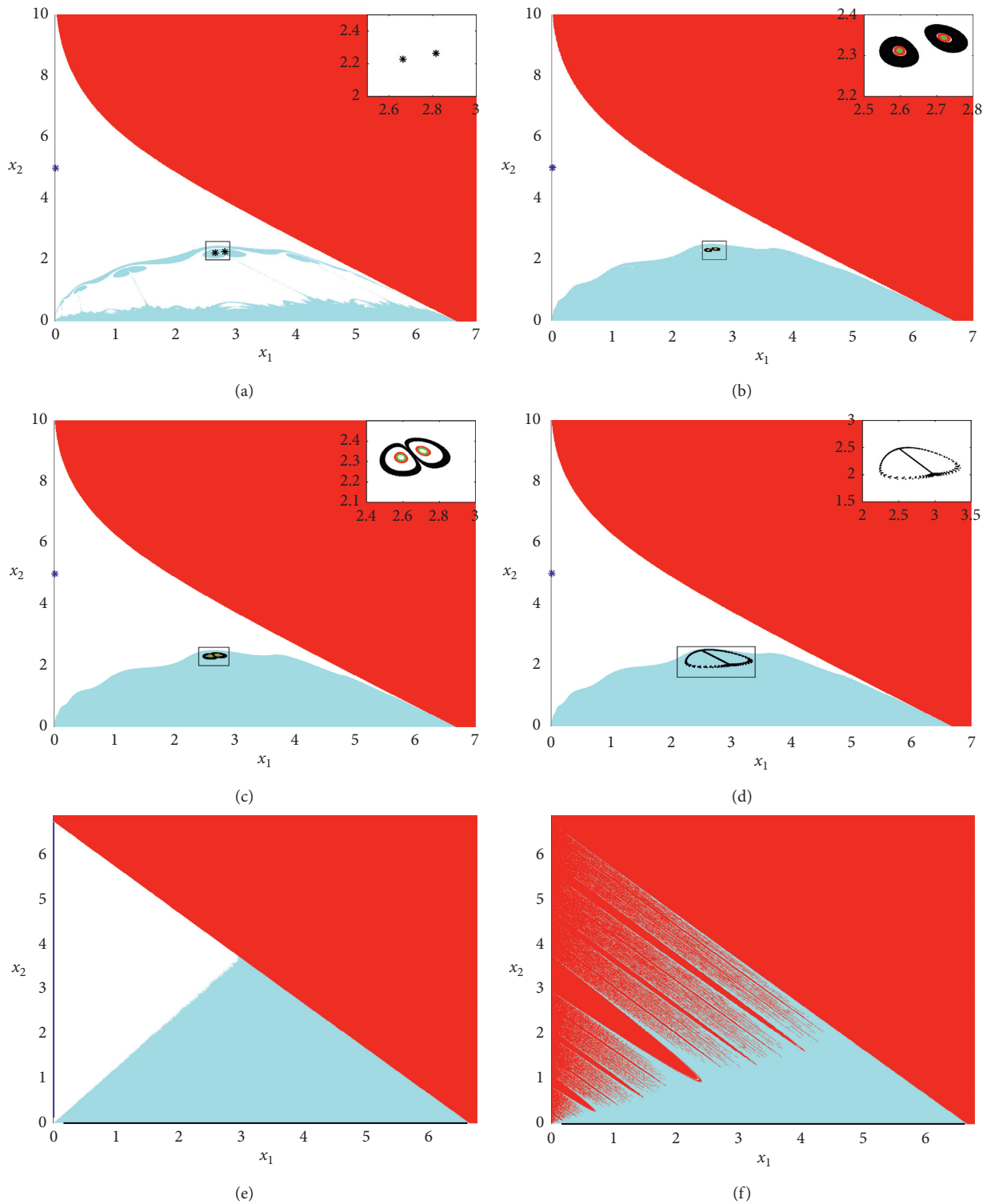


FIGURE 6: The evolution of basin of attraction of system (10) with respect to parameter α_2 . (a) $\alpha_2 = 0.43$; (b) $\alpha_2 = 0.468$; (c) $\alpha_2 = 0.472$; (d) $\alpha_2 = 0.48$; (e) $\alpha_2 = 1.56$; (f) $\alpha_2 = 1.6$.

connected with the inner layer and the middle layer, but the boundary of the inner layer and the inner layer is nested. In addition, with increase of the adjustment speed α_2 , the white attracting area corresponding to the boundary equilibrium point E_2 shrinks much more smaller, while the light blue

attracting area expands more and more larger. When the value of adjustment speed α_2 grows up to 0.472, the three layers of chaotic attractors split from each other and then the outer expands outward continuously to form the attractor, as shown in Figure 5(c). In this case, the attractors are

periodic attractors, and the corresponding largest Lyapunov exponent are $\lambda_{LE1} = -0.00826758$ and $\lambda_{LE2} = -0.05828646$. And let the value of parameter α_2 further increase, then the inner and middle layers of the periodic attractors vanish. Finally, the outer layer constantly expands outward and mutually merge into the periodic attractors, as shown in Figure 6(c), where the corresponding largest Lyapunov exponent are $\lambda_{LE1} = -0.00731851$ and $\lambda_{LE2} = -0.0565693$.

With the increase of adjustment speed α_2 , the periodic attractor will contact its attracting area so as that "critical bifurcation" occurs. And until the value of adjustment speed α_2 increases to 1.56, the boundary equilibrium point E_2 becomes the boundary chaotic attractor represented by the blue straight line via flip bifurcation, as shown in Figure 6(e). In the same time, the periodic attractor undergoes the "critical bifurcation" and then reforms the boundary chaotic attractor represented by the black straight line, where the attracting area corresponding to the chaotic attractor represented by the blue straight line is the white area, and the attracting area of another boundary chaotic attractor is the light blue area. In addition, these two different attracting areas locate symmetric along the diagonal. If the value of parameter α_2 continues to increase, then the basin of attraction will go through a bifurcation, named "global bifurcation," and the chaotic attractor represented by blue line disappears, forming a "hole," as shown in Figure 6(f) in the light blue attracting area.

From the study above, we can deduce that there is no relationship between the bifurcation of changing qualitative property of basin of attraction and the bifurcation of

changing qualitative property of the attractor. After the local bifurcation, the game between the firms will not converge to Nash equilibrium point representing the global optimal strategy anymore. Even though this game starting near Nash equilibrium point, system (10) will also tend to different attractors, and these attractors may be periodic or aperiodic. Furthermore, these bifurcations may also lead to the lack of predictabilities of system (10). The global bifurcation with respect to the boundary of basin of attraction increases the uncertainty of the game fate of the firms as given in the initial strategy. Hence, a slight variation in initial condition of the firms or a small external disturbance in the process of adjustment, will cause a huge influence on the evolution behaviors of the firms in the long run.

3.4. The Control of Chaos. With the increase of the speed of adjustment, the oligopoly market will enter into the disorder and chaotic state, and the nonlinear dynamic system is at the chaotic state. It is harmful to the development of the firms when this kind of fierce economic fluctuation serves in the market. For the sake of maintaining the longrun and stable development of two firms in this market, we can take control of system (10), aiming at expanding the stable range at Nash equilibrium of system (10) by introducing a control factor. Based on the opinions above, we exploit the method of state feedback and parameter variable control [40] to take control of system (10). And then the form of system (10) after conducting the control factor can be written as follows:

$$\begin{cases} x_1(t+1) = (1-\mu_1) \left\{ x_1(t) + \alpha_1 x_1(t) \left[\frac{4[(a-c)(2-b) + 2x_1(t) - bx_2(t)]}{(4-b^2)^2} - \gamma x_1(t) \right] \right\} + \mu_1 x_1(t), \\ x_2(t+1) = (1-\mu_1) \left\{ x_2(t) + \alpha_2 x_2(t) \left[\frac{4[(a-c)(2-b) + 2x_2(t) - bx_1(t)]}{(4-b^2)^2} - \gamma x_2(t) \right] \right\} + \mu_2 x_2(t), \end{cases} \quad (33)$$

where the parameters μ_1 and μ_2 are control factors and the restrictive condition is $(\mu_1, \mu_2) \in (0, 1)$.

Firstly, the parameters are given as $a = 61$, $c = 51.5$, $b = 0.85$, $\gamma = 2$, $\alpha_1 = 0.87$, and $\alpha_2 = 0.87$, and we choose the control factors μ_1 and μ_2 as the parameters of bifurcation. The route of global bifurcation with respect to the control parameters (μ_1, μ_2) is indicated in Figure 7, where Figure 7(a) is a two-dimensional bifurcation and Figure 7(b) is the largest Lyapunov exponent corresponding to Figure 7(a).

It can be observed from Figure 7(a) that there is only one route for system (33) which leads to the Nash equilibrium from chaotic, that is, inverse flip bifurcation. The control parameters μ_1 and μ_2 successively pass through the dark black area, yellow area, green area, and eventually enter into brown area, which implies that system (33) changes from chaotic to period-4, period-2, and other period-halving and finally reaches the Nash equilibrium. Figure 7(b) is a

diagram of the largest Lyapunov exponent corresponding to Figure 7(a), where the color bar in the right of this figure represents the largest Lyapunov exponent. When the largest Lyapunov exponent is equal to zero then the corresponding state of system (33) is quasi-period, that is, the dark grey area. And when the largest Lyapunov exponent is greater than zero and less than 2, then the state of system (33) is the chaotic state, that is, grey area. The last situation is when the largest Lyapunov exponent is greater than 2, and the corresponding state of system (33) is escaping trajectories, that is, the white area. Fix the control factor as $\mu_1 = 0.4$ and $\mu_2 = 0.65$; then, the one-dimensional bifurcation and the corresponding largest Lyapunov exponent are displayed in Figures 8(a) and 8(b), respectively, where the red curve represents the R&D effort x_1 of firm 1, the blue curve represents the R&D effort x_2 of firm 2, and the black curve represents the largest Lyapunov exponent (abbreviated as Lyp).

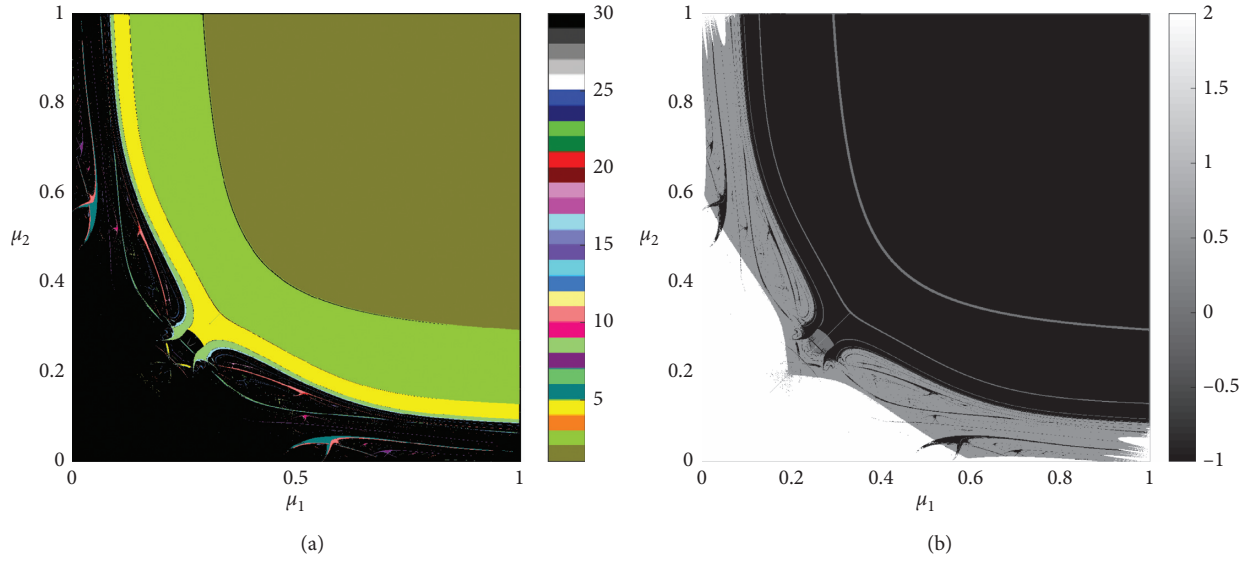


FIGURE 7: (a) The two-dimensional bifurcation of system (33) with respect to a pair of parameters (μ_1, μ_2) . (b) The corresponding two-dimensional largest Lyapunov exponent to Figure 7(a).

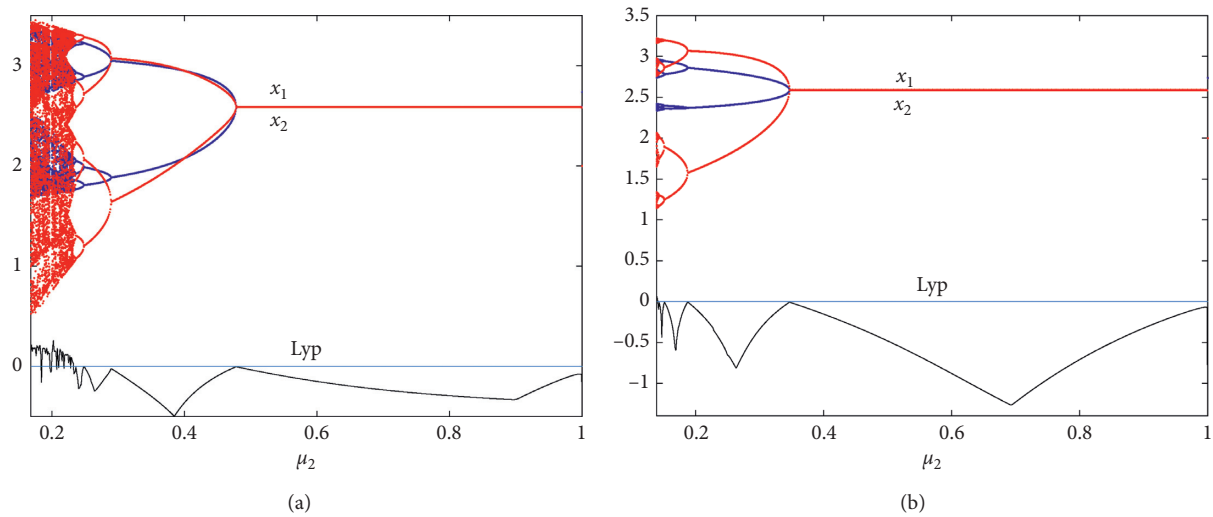


FIGURE 8: The bifurcation and the largest Lyapunov exponent of system (33) with respect to the parameter μ_2 . (a) $\mu_1 = 0.4$ and (b) $\mu_1 = 0.65$.

From Figure 8, we can observe that when control factor μ_1 is fixed as $\mu_1 = 0.4$, and if another control factor satisfies the condition that $0 < \mu_2 < 0.168$, then system (33) is at the escaping state, that is, the market disappears. If the value of μ_2 meets $0.168 < \mu_2 < 0.232$, then system (33) is at the chaotic state. If the value of μ_2 meets $0.232 < \mu_2 < 0.478$, then system (33) conducts an inverse flip bifurcation. And if $\mu_2 > 0.478$ is met, then system (33) will enter into the Nash equilibrium. And with regards to the corresponding largest Lyapunov exponent, when the value of μ_2 meets $0.168 < \mu_2 < 0.232$, then $Lyp > 0$. The corresponding largest Lyapunov exponent is less than zero when $\mu_2 > 0.232$. When the corresponding largest Lyapunov exponent is equal to zero, then system (33) takes place a bifurcation. Another case is that the control factor μ_1 increases to 0.65. In this case, when the condition $0 < \mu_2 < 0.139$ is met, then system (33) is at the escaping state.

When the condition $0.139 < \mu_2 < 0.141$ is met, then system (33) is at the chaotic state. When the condition $0.141 < \mu_2 < 0.347$ is satisfied, then system (33) conducts an inverse flip bifurcation. And if $\mu_2 > 0.347$ is met, then system (33) will enter into the Nash equilibrium. And with regards to the corresponding largest Lyapunov exponent, when the value of μ_2 meets $0.168 < \mu_2 < 0.141$ then $Lyp > 0$. The corresponding largest Lyapunov exponent is less than zero when $\mu_2 > 0.141$. When the corresponding largest Lyapunov exponent is equal to zero, then system (33) takes place at bifurcation. In addition, we can also know that the larger the control factor μ_2 is, the faster system (33) enters into Nash equilibrium.

For sake of eliminating or slowing down the speed of system (10) entering into chaos, the control factors are introduced and play a stabilizing role in system (33). We will

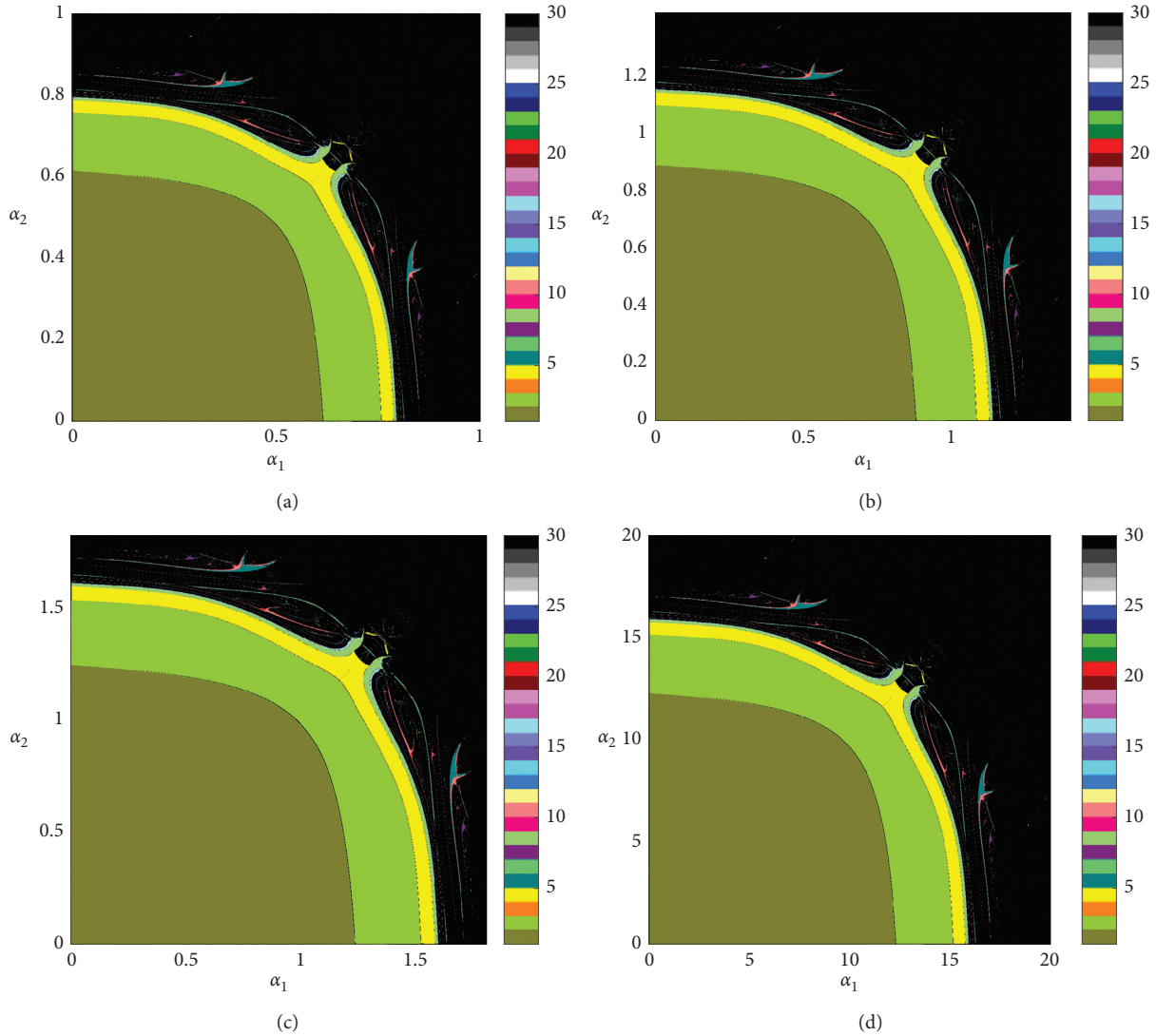


FIGURE 9: The two-dimensional bifurcation of system (33) with respect to a pair of parameters (α_1, α_2) . (a) $\mu_1 = \mu_2 = 0$; (b) $\mu_1 = \mu_2 = 0.3$; (c) $\mu_1 = \mu_2 = 0.5$; (d) $\mu_1 = \mu_2 = 0.95$.

illustrate how they affect the behavior of system (10) entering into chaos through the control factors and the influence on the adjustment speeds α_1 and α_2 . As shown in Figure 9, a two-dimensional bifurcation with respect to adjustment speeds (α_1, α_2) when the parameters are fixed as $a = 61$, $c = 51.5$, $b = 0.85$, and $\gamma = 2$.

In this group of parameters, the Nash equilibrium point is $E_4(2.59, 2.59)$. The increase of control factors and adjustment speeds have no impacts on Nash equilibrium point E_4 . It can be seen from Figure 9 that the stability region with respect to (α_1, α_2) gradually expands at the increase of control factors. However, it does not affect the global shape of two-dimensional bifurcation with respect to (α_1, α_2) , but increases the stability region of the Nash equilibrium. The purpose of introducing the control factor is to expand the region of the Nash equilibrium point attracting area, so as to further delay the speed of system (10) to enter into chaos with increasing of parameters, so as to keep the market stable as long as possible.

Furthermore, we will illustrate the influence of control factors on local bifurcation of system (33). Under the action of control factors, the one-dimensional bifurcation and the corresponding largest Lyapunov exponent about adjustment speed α_2 are shown in Figure 10, where the parameters are the same as in Figure 9, and the adjustment speed of firm 1 is fixed as $\alpha_1 = 0.8$. In Figure 10, the blue curve represents R&D effort x_1 of firm 1, the red curve represents R&D effort x_2 of firm 2, and the local enlargement is the one-dimensional bifurcation of R&D effort x_1 with respect to adjustment speed α_2 . When the control factors are chosen as $\mu_1 = \mu_2 = 0$, system (33) is equivalent to system (10). At present, if the adjustment speed of firm 2 is less than 0.465, that is, $\alpha_2 < 0.465$, then system (33) will enter into the chaotic state and the market enters into a disorder state. And if $\alpha_2 > 0.465$, then system is at escaping state, and the corresponding largest Lyapunov exponent is greater than zero, that is, $\text{Lyp} > 0$. If the largest Lyapunov exponent is less than zero, that is, $\text{Lyp} < 0$, then system (33) is at the period state,

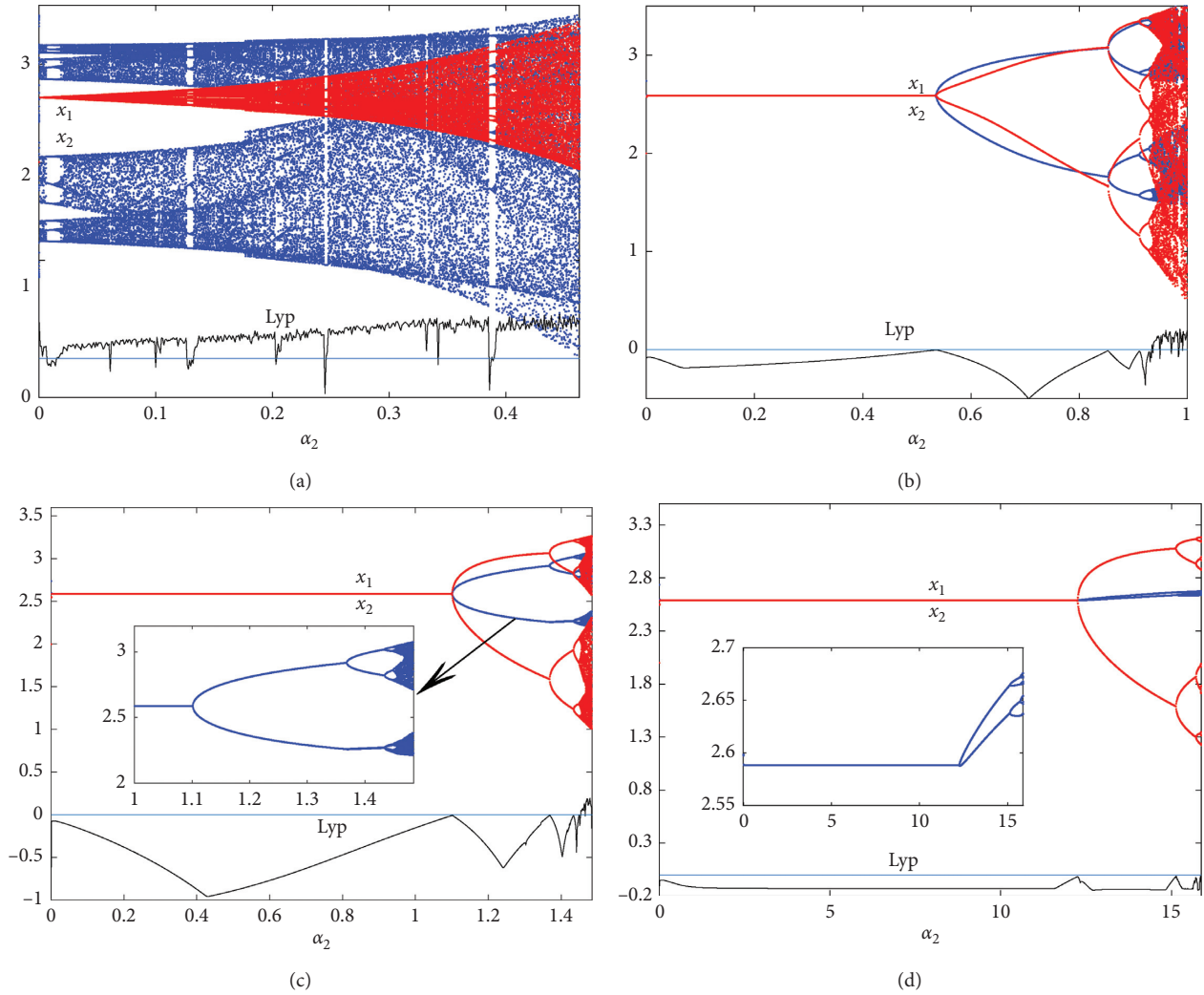


FIGURE 10: The bifurcation and the largest Lyapunov exponent of system (33) with respect to parameter α_2 . (a) $\mu_1 = \mu_2 = 0$; (b) $\mu_1 = \mu_2 = 0.3$; (c) $\mu_1 = \mu_2 = 0.5$; (d) $\mu_1 = \mu_2 = 0.95$.

see Figure 10(a) for more details. When the control factors are chosen as $\mu_1 = \mu_2 = 0.3$, and the adjustment speed of firm 2 is chosen in the interval that $0 < \alpha_2 < 0.534$, then system (33) is at the Nash equilibrium state, see Figure 10(b). System (33) will take place a bifurcation, i.e., flip bifurcation, when the adjustment speed of firm 2 is chosen in the interval that $0.534 < \alpha_2 < 0.934$. When the condition $0.934 < \alpha_2 < 1.05$ is satisfied, system (33) enters into chaos. Lastly, when the condition $\alpha_2 > 1.05$ is met, system (33) is at the escaping state. The corresponding largest Lyapunov exponent is negative when $0 < \alpha_2 < 0.934$. And when $\alpha_2 > 0.934$, the corresponding largest Lyapunov exponent is positive, that is, $Lyp > 0$. In addition, if we further increase the value of control factors to 0.5 (that is, $\mu_1 = \mu_2 = 0.5$), then we can get the results as follows. System (33) is at the Nash equilibrium when $0 < \alpha_2 < 1.1$. When $1.1 < \alpha_2 < 1.453$, system (33) takes place at bifurcation. When $1.453 < \alpha_2 < 1.49$, then system (33) will enter into chaos. And when $\alpha_2 > 1.49$, then system (33) is at the escaping state. If $0 < \alpha_2 < 1.453$, then the corresponding largest Lyapunov

exponent is negative, that is, $Lyp < 0$. If $\alpha_2 > 1.453$, then the corresponding largest Lyapunov exponent is positive, that is, $Lyp > 0$. The detailed dynamical behaviors under $\mu_1 = \mu_2 = 0.5$ are shown in Figure 10(c). While when $0 < \alpha_2 < 12.34$ and $\mu_1 = \mu_2 = 0.95$, system (33) is in a stable period-1 state, see Figure 10(d). From Figure 10(d), we find that system (33) takes place at a series of bifurcations when $12.24 < \alpha_2 < 15.88$. And when $\alpha_2 > 15.88$, then system (33) is at the escaping state. If $0 < \alpha_2 < 15.88$, then the corresponding largest Lyapunov exponent is negative, that is, $Lyp < 0$. The control factors are increased from 0 to 0.95, the stability of system (33) gradually gets stronger and the local bifurcation point is increased from 0.534 to 12.34. It means that the increase of control factors are more beneficial for system (33) to maintain stability, delay the bifurcation point, and keep local stability of the Nash equilibrium point in the long run. However, as for the firms, any slight change of parameters may lead to a huge fluctuation in the market, which makes it difficult for the firms to keep pace with or catch the changing trend of the market. While this

fluctuation can be eliminated or slowed down by introducing a control strategy, it is a benefit to a long-term stable development for the market.

4. Conclusion

In this research, a nonlinear game model of the R&D competition between duopoly firms is studied in detail. The game between these two firms is mainly described by the way of a two-stage game. In the first stage, all of firms determine the level of their R&D efforts to reduce the production cost. And in the second stage, supposing that all firms compete in the market with a Cournot form and determine the outputs to maximize themselves profits, respectively, the local and global properties are discussed by theoretical analysis and numerical simulation. Theoretically, the local stability condition of the equilibrium points and the kind of local bifurcation are analyzed through stability theory and the Jury criterion.

In numerical simulation, we choose the adjusting speeds of these two firms as bifurcation parameters. The evolution law of internal complexity of the nonlinear economic system can be explained by the tools as one-dimensional bifurcation, two-dimensional bifurcation, the one-dimensional largest Lyapunov exponent, the two-dimensional largest Lyapunov exponent, and the basin of attraction. The system will transform from the stable Nash equilibrium state to the chaotic state via a flip bifurcation, which can be verified by the diagrams of one-dimensional bifurcation and the corresponding largest Lyapunov exponent. As it is known to all, the flip bifurcation is a classical route for the economic system to change the state from stable into chaotic. A new way of development for firms will generate when the economy develops to a certain stage, and there is only one way for firms to further develop the economy and they will face a dilemma in the choice of the new and old way. As a result, the route of period-doubling is generated in constant choice between firms in dilemma.

The increase of adjusting speed leads to the complexity of eventual behavior of system (10). This process of evolution presents the properties of “certainty” and “irregular development,” where “certainty” means that the way of bifurcation, that is to say, period-4 Neimark–Sacker bifurcation, and “irregular development” means that the interior structure of strange attractors. No matter from phenomenon development or interior mechanism, system (10) presents a high of certainty and complexity. That means the economic system makes mistakes in predicting, due to the influence of external condition, the development of economy cannot be forecasted anymore. Both the variation of parameters and the choice of initial condition will cause system (10) to generate multistability. With the increase of adjustment speed of firms, the properties of multistability are mainly reflected in the number and structure of coexisting attractors and global bifurcation of the system. There are four distinct coexisting phenomena displayed here, that is, periodic attractors coexist with periodic attractors, boundary equilibrium points coexist with strange attractors, periodic attractors coexist with chaotic attractors, and multiboundary

chaotic attractors coexist. In the case of the boundary attractors coexisting with strange attractors with the layered structure, the largest Lyapunov exponent corresponds to strange attractors displaying a fluctuating and oscillating phenomenon as adjusting speed increases. This is a special phenomenon of coexistence and seldom reported by other researchers. As we all know, the boundary attractor corresponds to the fact that the duopoly market has degenerated into a monopoly market. That is, one of these two firms was forced out of the market. Therefore, the coexistence of the boundary attractor and internal attractor implies that not only the parameters can affect the market structure but also the initial state of market can affect the market structure.

The increase of the adjustment speed will lead to change of multistability, and at the same time, it will also cause “critical bifurcation” so as to form “ghost,” as well as the “global bifurcation” of attracting basin so as to form “hole.” The increasing of control factors are more beneficial for system (33) to maintain stability, delay the bifurcation point, and keep local stability of the Nash equilibrium point in the long run. However, as for the firms, any slight change of parameters may lead to a huge fluctuation in the market, which makes it difficult for the firms to keep pace with or catch the changing trend of the market. While this fluctuation can be eliminated or slowed down by introducing a control strategy, it is a benefit to a long-term stable development for the market.

Data Availability

No data were used to support this study.

Conflicts of Interest

The authors declare that there are no conflicts of interest.

Acknowledgments

This investigation was funded by the National Natural Science Foundation of China (Project no. 61463027), Young Scholars Science Foundation of Lanzhou Jiaotong University (Project no. 2015029), and Foundation of Humanities and Social Sciences from the Ministry of Education of China (Project no. 15YJC82007).

References

- [1] Z. Griliches, “The search for R&D spillovers,” *The Scandinavian Journal of Economics*, vol. 94, 1992.
- [2] K. Kultti and T. Takalo, “R&D spillovers and information exchange,” *Economics Letters*, vol. 61, no. 1, pp. 121–123, 1998.
- [3] J. Zhou, W. Zhou, T. Chu, Y.-x. Chang, and M.-j. Huang, “Bifurcation, intermittent chaos and multi-stability in a two-stage Cournot game with R&D spillover and product differentiation,” *Applied Mathematics and Computation*, vol. 341, pp. 358–378, 2019.
- [4] W. Zhou and X.-X. Wang, “On the stability and multistability in a duopoly game with R&D spillover and price competition,” *Discrete Dynamics in Nature and Society*, vol. 2019, Article ID 2369898, 20 pages, 2019.

- [5] C. D'Aspremont and A. Jacquemin, "Cooperative and non-cooperative R & D in duopoly with spillovers," *The American Economic Review*, vol. 78, no. 5, pp. 1133–1137, 1988.
- [6] S. Luckraz, "R&D games in a Cournot duopoly with isoelastic demand functions: a comment," *Economic Modelling*, vol. 28, no. 6, pp. 2873–2876, 2011.
- [7] R. Chatterjee, S. Chattopadhyay, and T. Kabiraj, "R&D in a duopoly under incomplete information," *International Journal of Economic Theory*, vol. 15, no. 4, pp. 341–359, 2019.
- [8] M. Ferreira, I. P. Figueiredo, B. M. P. M. Oliveira, and A. A. Pinto, "Strategic optimization in R&D investment," *Optimization*, vol. 61, no. 8, pp. 1013–1023, 2012.
- [9] M. I. Kamien, E. Muller, and I. Zang, "Research joint ventures and R&D cartels," *The American Economic Review*, vol. 82, no. 5, pp. 1293–1306, 1992.
- [10] R. Amir and J. Wooders, "Effects of one-way spillovers on market shares, industry price, welfare, and R & D cooperation," *Journal of Economics*, vol. 8, no. 2, pp. 223–249, 1999.
- [11] S. Banerjee and P. Lin, "Vertical research joint ventures," *International Journal of Industrial Organization*, vol. 19, no. 1–2, pp. 285–302, 2001.
- [12] A. Stepanova and A. Tesoriere, "R&D with spillovers: monopoly versus noncooperative and cooperative duopoly," *The Manchester School*, vol. 79, no. 1, pp. 125–144, 2011.
- [13] G. I. Bischi and F. Lamantia, "A dynamic model of oligopoly with R&D externalities along networks. Part I," *Mathematics and Computers in Simulation*, vol. 84, pp. 51–65, 2012.
- [14] G. I. Bischi, U. Merlone, and E. Pruscini, "Evolutionary dynamics in club goods binary games," *Journal of Economic Dynamics and Control*, vol. 91, pp. 104–119, 2018.
- [15] S. S. Askar, A. M. Alshamrani, and K. Alnowibet, "Dynamic Cournot duopoly games with nonlinear demand function," *Applied Mathematics and Computation*, vol. 259, pp. 427–437, 2015.
- [16] M. F. Elettrey, "Dynamical analysis of a Cournot duopoly model," *Journal of the Egyptian Mathematical Society*, vol. 24, no. 4, pp. 681–686, 2016.
- [17] G. I. Bischi, F. Lamantia, and D. Radi, "An evolutionary Cournot model with limited market knowledge," *Journal of Economic Behavior & Organization*, vol. 116, pp. 219–239, 2015.
- [18] A. A. Elsadany, "Dynamics of a Cournot duopoly game with bounded rationality based on relative profit maximization," *Applied Mathematics and Computation*, vol. 294, pp. 253–263, 2017.
- [19] A. Agliari, A. K. Naimzada, and N. Pecora, "Nonlinear dynamics of a Cournot duopoly game with differentiated products," *Applied Mathematics and Computation*, vol. 281, pp. 1–15, 2016.
- [20] Y. Zhang, W. Zhou, T. Chu, Y. Chu, and J. Yu, "Complex dynamics analysis for a two-stage Cournot duopoly game of semi-collusion in production," *Nonlinear Dynamics*, vol. 91, no. 2, pp. 819–835, 2018.
- [21] J. Ma and Z. Guo, "The parameter basin and complex of dynamic game with estimation and two-stage consideration," *Applied Mathematics and Computation*, vol. 248, pp. 131–142, 2014.
- [22] J. Ma and H. Ren, "The impact of variable cost on a dynamic Cournot–Stackelberg game with two decision-making stages," *Communications in Nonlinear Science and Numerical Simulation*, vol. 62, pp. 184–201, 2018.
- [23] H. A. Simon, "Bounded rationality and organizational learning," *Organization Science*, vol. 1, no. 2, pp. 17–27, 1991.
- [24] D. Furth, "Stability and instability in oligopoly," *Journal of Economic Theory*, vol. 40, no. 2, pp. 197–228, 1986.
- [25] C. Tuge and M. Daba, "Stability analysis of delayed cournot model in the sense of Lyapunov," *Ethiopian Journal of Education and Sciences*, vol. 12, no. 2, pp. 67–80, 2017.
- [26] G. I. Bischi and A. Naimzada, "Global analysis of a dynamic duopoly game with bounded rationality," in *Advances in Dynamic Games and Applications*, pp. 361–385, Springer, Berlin, Germany, 2000.
- [27] F. Cavalli and A. Naimzada, "A cournot duopoly game with heterogeneous players: nonlinear dynamics of the gradient rule versus local monopolistic approach," *Applied Mathematics and Computation*, vol. 249, pp. 382–388, 2014.
- [28] A. A. Elsadany, "A dynamic Cournot duopoly model with different strategies," *Journal of the Egyptian Mathematical Society*, vol. 23, no. 1, pp. 56–61, 2015.
- [29] L. Fanti and L. Gori, "Stability analysis in a Bertrand duopoly with different product quality and heterogeneous expectations," *Journal of Industry, Competition and Trade*, vol. 13, no. 4, pp. 481–501, 2013.
- [30] A. K. Naimzada and L. Sbragia, "Oligopoly games with nonlinear demand and cost functions: two boundedly rational adjustment processes," *Chaos, Solitons & Fractals*, vol. 29, no. 3, pp. 707–722, 2006.
- [31] S. S. Askar, "Complex dynamic properties of Cournot duopoly games with convex and log-concave demand function," *Operations Research Letters*, vol. 42, no. 1, pp. 85–90, 2014.
- [32] J. Andaluz and G. Jarne, "On the dynamics of economic games based on product differentiation," *Mathematics and Computers in Simulation*, vol. 113, pp. 16–27, 2015.
- [33] H. Tu and X. Wang, "Complex dynamics and control of a dynamic R&D Bertrand triopoly game model with bounded rational rule," *Nonlinear Dynamics*, vol. 88, no. 1, pp. 703–714, 2017.
- [34] G.-I. Bischi, L. Stefanini, and L. Gardini, "Synchronization, intermittency and critical curves in a duopoly game," *Mathematics and Computers in Simulation*, vol. 44, no. 6, pp. 559–585, 1998.
- [35] G. I. Bischi and F. Lamantia, "Coexisting attractors and complex basins in discrete-time economic models," in *Nonlinear Dynamical Systems in Economics*, pp. 187–231, Springer Vienna, Vienna, Austria, 2005.
- [36] L. Fanti, L. Gori, C. Mamma, and E. Michetti, "Local and global dynamics in a duopoly with price competition and market share delegation," *Chaos, Solitons & Fractals*, vol. 69, pp. 253–270, 2014.
- [37] A. A. Elsadany and A. M. Awad, "Dynamical analysis and chaos control in a heterogeneous Kopel duopoly game," *Indian Journal of Pure and Applied Mathematics*, vol. 47, no. 4, pp. 617–639, 2016.
- [38] A. A. Elsadany, H. N. Agiza, and E. M. Elabbasy, "Complex dynamics and chaos control of heterogeneous quadropoly game," *Applied Mathematics and Computation*, vol. 219, no. 24, pp. 11110–11118, 2013.
- [39] J. Ma and W. Ji, "Chaos control on the repeated game model in electric power duopoly," *International Journal of Computer Mathematics*, vol. 85, no. 6, pp. 961–967, 2008.
- [40] S. S. Askar and A. Al-khedhairi, "Analysis of nonlinear duopoly games with product differentiation: stability, global dynamics, and control," *Discrete Dynamics in Nature and Society*, vol. 2017, Article ID 2585708, 13 pages, 2017.
- [41] J. Nash, "Non-cooperative games," *The Annals of Mathematics*, vol. 54, no. 2, p. 286, 1951.

Research Article

Numerical Solutions to Optimal Portfolio Selection and Consumption Strategies under Stochastic Volatility

Lei Ge ¹ and Qiang Zhang²

¹*School of Finance, Southwestern University of Finance and Economics, Chengdu, China*

²*Department of Mathematics, City University of Hong Kong, Hong Kong*

Correspondence should be addressed to Lei Ge; leige365@outlook.com

Received 23 April 2020; Revised 30 June 2020; Accepted 13 July 2020; Published 30 July 2020

Guest Editor: Lei Xie

Copyright © 2020 Lei Ge and Qiang Zhang. This is an open access article distributed under the Creative Commons Attribution License, which permits unrestricted use, distribution, and reproduction in any medium, provided the original work is properly cited.

Based on the method of dynamic programming, this paper uses analysis methods governed by the nonlinear and inhomogeneous partial differential equation to study modern portfolio management problems with stochastic volatility, incomplete markets, limited investment scope, and constant relative risk aversion (CRRA). In this paper, a three-level Crank–Nicolson finite difference scheme is used to determine numerical solutions under this general setting. One of the main contributions of this paper is to apply this three-level technology to solve the portfolio selection problem. In addition, we have used a technique to deal with the nonlinear term, which is another novelty in performing the Crank–Nicolson algorithm. The Crank–Nicolson algorithm has also been extended to third-order accuracy by performing Richardson’s extrapolation. The accuracy of the proposed algorithm is much higher than the traditional finite difference method. Lastly, experiments are conducted to show the performance of the proposed algorithm.

1. Introduction

How to optimally allocate assets and optimally consume are extremely important and difficult topics in portfolio management [1–3]. These topics are important not only for theoretical consideration but also for applications in the financial industry. Early studies usually assumed the volatility of the risky asset to be a constant. However, in recent years, researchers found that volatility should be modeled as stochastic rather than deterministic [4–7]. This adds further complication to the problem. The optimal asset allocation and optimal consumption strategies are governed by the Hamilton–Jacobi–Bellman (HJB) equation. Due to the nonlinearity and inhomogeneity of this partial differential equation, no exact solution has been found. Furthermore, even numerical solutions are not available. In this paper, we present an accurate and efficient numerical method for solving this equation and generate the first set of accurate numerical solutions for this problem.

Due to the importance of portfolio selection under stochastic volatilities, several important theoretical works have been carried out, and exact solutions have been obtained under certain special settings, such as no consumption [8–10], complete markets which means that the stock movement and the volatility movement are either perfectly correlated or perfectly anticorrelated [9–12], or when investors have unit elasticity of intertemporal substitution of consumption [13].

In this paper, we consider this optimal stochastic control problem under a general setting: stochastic volatility, incomplete markets, finite investment horizons, and CRRA utility. Our numerical method combines a three-level Crank–Nicolson scheme and Richardson’s extrapolation technique. The Crank–Nicolson scheme has second-order accuracy in terms of discretization error, and Richardson’s extrapolation technique further improves the accuracy. We verify that our numerical method is accurate and efficient.

This paper is organized as follows. In Section 2, we describe the model for financial market, the stochastic control optimization procedure, and the governing HJB equation for the optimal asset allocation and consumption strategies. In Section 3, we present our numerical method for solving the HJB equation. In Section 4, we verify the accuracy and the efficiency of our numerical method and present accurate numerical solutions for the optimal asset allocation strategy and the optimal consumption strategy. In the last section, we present our conclusions.

2. Financial Market and Stochastic Control

We consider a market consisting of one riskless asset B_t , whose price is governed by

$$dB_t = rB_t dt, \quad (1)$$

with a constant risk-free interest rate r and a risky asset S_t modeled as

$$dS_t = S_t [\mu(v_t) + \sigma(v_t) dW_t^S]. \quad (2)$$

In (2), $\mu(v_t)$ and $\sigma(v_t)$ are the return and the stochastic volatility of the stock price S_t , respectively. $v_t = \sigma_t^2$ is the stochastic variance of S_t . Empirical studies show presence of mean reversion in the stock movements [14]. Heston model [5] is selected for v_t , namely,

$$dv_t = \kappa(\theta - v_t)dt + \xi\sqrt{v_t}dW_t^v. \quad (3)$$

Here, dW_t^v and dW_t^S are the increments of the Wiener processes under a probability P . The correlation between dW_t^v and dW_t^S is ρ , namely, $\text{Corr}((dv_t/v_t), (dS_t/S_t)) = \rho dt$. We assume ρ is a constant. In (3), θ is the long-run average variance (i.e., as t tends to infinity, the expected value of v_t tends to θ), κ is the rate at which v_t reverts to θ , and ξ is the volatility of the stock variance v_t . The parameters κ, θ, ξ are positive constants and need to satisfy the Feller condition, $2\kappa\theta > \xi^2$, to ensure that v_t is strictly positive. The risk premia is defined as

$$A = \frac{\mu_t - r}{\sigma_t^2} \equiv \frac{\mu_t - r}{v_t}. \quad (4)$$

Following [1, 5, 15–17], we assume A is a constant. This means the stock excess return is proportional to the stock variance.

Consider an investor who has an initial wealth w_0 and needs to determine strategies for asset allocation and consumption over an investment horizon $[0, T]$. Let w_t be the investor's wealth at time t . The strategies consist of an asset allocation rate φ_t and a consumption rate c_t , which mean he/she allocates $\varphi_t w_t$ to the risky asset and $(1 - \varphi_t)w_t$ to the riskless asset at time t and consumes $c_t dt$ over the time interval $[t, t + dt]$. Thus, under the strategies φ_t and c_t , the wealth process is governed by

$$dw_t = \frac{\varphi_t w_t}{S_t} dS_t + (1 - \varphi_t)w_t r dt - c_t dt. \quad (5)$$

The goal is to maximize the expected utilities over the investment horizon, namely,

$$\sup_{\varphi_t, c_t} E \left[\int_0^T \alpha e^{-\beta t} u_1(c_t) dt + (1 - \alpha) e^{-\beta T} u_2(w_T) \right]. \quad (6)$$

In (6), φ_t and c_t are control variables for this optimization problem. E is the expectation operator under the probability P . β is the subjective discount rate, namely, the time preference of the investor. The larger β is, the more weight the investor puts on the present than on the future. The parameter α determines the relative importance between intertemporal consumption and the terminal wealth. $u_1(\cdot)$ and $u_2(\cdot)$ are the investor's utility functions which measure the investor's degree of satisfaction with the outcomes from intertemporal consumption and terminal wealth, respectively.

CRRA utility functions have been widely adopted for modeling investors' behavior. Therefore, we adopt the CRRA utility function for $u_1(\cdot)$ and $u_2(\cdot)$:

$$\begin{cases} u_1(c_t) = \frac{a_c c_t^{1-\gamma}}{1-\gamma}, & \text{for } \gamma \neq 1, \\ a_c \log(c_t), & \text{for } \gamma = 1, \end{cases} \quad (7)$$

$$\begin{cases} u_2(w_T) = \frac{a_w w_T^{1-\gamma}}{1-\gamma}, & \text{for } \gamma \neq 1, \\ a_w \log(w_T), & \text{for } \gamma = 1, \end{cases}$$

where γ, a_c , and a_w are positive constants. Since $u_1(\cdot)$ and $u_2(\cdot)$ stand for the intertemporal consumption utility and the terminal wealth utility of the same investor, we use the same γ in $u_1(\cdot)$ and $u_2(\cdot)$. However, a_c and a_w can be different since c and w have different dimensions.

Let $V(t, w, v)$ be the value function of problem (6), which is given by

$$V(t, w, v) = \sup_{\varphi_t, c_t} E \left[\int_t^T \alpha e^{-\beta t'} u_1(c_t') dt' + (1 - \alpha) e^{-\beta T} u_2(w_T) \mid \mathcal{F}_t \right], \quad (8)$$

where \mathcal{F}_T is the filtration associated to the stochastic processes in this problem. The terminal condition is obtained by setting $t = T$ in (8):

$$V(T, w_T, v_T) = (1 - \alpha) e^{-\beta T} u_2(w_T). \quad (9)$$

Based on the HJB dynamic programming procedure, V is governed by

$$0 = \sup_{\varphi, c} \left[\alpha e^{-\beta t} u_1(c) + V_t + (r w + \varphi w A v - c) V_w + \kappa(\theta - v) V_v + \frac{1}{2} \varphi^2 w^2 v V_{ww} + \varphi w \rho \xi v V_{wv} + \frac{1}{2} \xi^2 v V_{vv} \right], \quad (10)$$

with the optimal strategies φ^* and c^* determined by

$$\varphi^* = -\frac{AV_w + \rho\xi V_{wv}}{wV_{ww}}, \quad (11)$$

$$c^* = \left(\frac{V_w}{a_c \alpha e^{-\beta t}} \right)^{-(1/\gamma)}. \quad (12)$$

After substituting expressions (11) and (12) into (10), one obtains an equation for the value function V :

$$\begin{aligned} & \frac{\gamma}{1-\gamma} (a_c \alpha e^{-\beta t})^{(1/\gamma)} V_w^{(1-\gamma/\gamma)} + r w V_w + V_t + \kappa(\theta - v) V_v \\ & + \frac{1}{2} \xi^2 v V_{vv} - \frac{1}{2} v \frac{(AV_w + \rho\xi V_{wv})^2}{V_{ww}} = 0. \end{aligned} \quad (13)$$

Based on the terminal condition and the scaling property of (13), it is reasonable to guess that

$$V(\tau, w, v) = e^{-\beta(T-\tau)} \frac{a_w w^{1-\gamma}}{1-\gamma} f(\tau, v)^\gamma, \quad (14)$$

where $\tau = T - t$, (13) becomes

$$\begin{aligned} 0 = & -f_\tau + \frac{1}{2} \xi^2 v f_{vv} + \left(\kappa(\theta - v) + \frac{1-\gamma}{\gamma} A \rho \xi v \right) f_v \\ & - \frac{1}{2} (1-\gamma)(1-\rho^2) \xi^2 v \frac{f_v^2}{f} \\ & + \left(\frac{(1-\gamma)A^2}{2\gamma^2} v + \frac{(1-\gamma)r}{\gamma} - \frac{\beta}{\gamma} \right) f + \left(\frac{\alpha a_c}{a_w} \right)^{(1/\gamma)}, \end{aligned} \quad (15)$$

with

$$f(0, v) = (1-\alpha)^{(1/\gamma)}, \quad (16)$$

and (11) and (12) become

$$\varphi^* = \frac{A}{\gamma} + \rho \xi \frac{f_v}{f}, \quad (17)$$

$$\frac{c^*}{w} = \left(\frac{\alpha a_c}{a_w} \right)^{(1/\gamma)} f^{-1}. \quad (18)$$

Equation (15) is a nonlinear and inhomogeneous partial differential equation. Since no closed-form solution is available for this equation, numerical computation plays a critical role for studying this important practical problem in modern finance. However, there are even no numerical solutions available in the literature.

3. Numerical Method

In this section, we develop a numerical method for solving (15). For the sake of conciseness of our expressions, we rewrite (15) as

$$\begin{aligned} & -f_\tau + a_1 v f_{vv} + (a_2 v + a_3) f_v + a_4 v \frac{f_v^2}{f} + (a_5 v + a_6) f \\ & + \alpha^{(1/\gamma)} a_7 = 0, \end{aligned} \quad (19)$$

with the initial condition $f(0, v) = (1-\alpha)^{(1/\gamma)}$, where

$$\begin{aligned} a_1 &= \frac{1}{2} \xi^2, \\ a_2 &= \frac{1-\gamma}{\gamma} A \rho \xi - \kappa, \\ a_3 &= \kappa \theta, \\ a_4 &= \frac{1}{2} (1-\gamma) \xi^2 (1-\rho^2), \\ a_5 &= \frac{1-\gamma}{2\gamma^2} A^2, \\ a_6 &= \frac{(1-\gamma)r}{\gamma} - \frac{\beta}{\gamma}, \\ a_7 &= \left(\frac{a_c}{a_w} \right)^{(1/\gamma)}. \end{aligned} \quad (20)$$

3.1. Crank–Nicolson Scheme and Richardson’s Extrapolation. We use a three-level Crank–Nicolson scheme (see [18–21]) of second-order accuracy to solve the nonlinear and inhomogeneous partial differential equation given by (19) and use Richardson’s extrapolation technique for further improving accuracy. Numerically, one can only solve (19) over a finite domain $v \in [0, v_{\max}]$. Since the boundary conditions at $v = 0$ and at $v = v_{\max}$ are not known, we use one-sided difference method at these two numerical boundaries. Step sizes $\Delta\tau$ and Δv are used to discretize τ and v , respectively. Thus, $\tau = n\Delta\tau$ and $v = m\Delta v$. We adopt the standard notation $f_m^n = f(n\Delta\tau, m\Delta v)$.

The three-level Crank–Nicolson scheme involves the levels $n-1$, n , and $n+1$. It is straightforward to discretize all linear terms in (19) with second-order errors, namely,

$$\begin{aligned} (f_\tau)_m^n &= \frac{f_m^{n+1} - f_m^{n-1}}{2\Delta\tau} + O(\Delta\tau^2), \\ (f_v)_m^n &= \frac{1}{2} \left(\frac{f_{m+1}^{n+1} - f_{m-1}^{n+1}}{2\Delta v} + \frac{f_{m+1}^{n-1} - f_{m-1}^{n-1}}{2\Delta v} \right) + O(\Delta\tau^2) \\ &+ O(\Delta v^2), \\ (f_{vv})_m^n &= \frac{1}{2} \left(\frac{f_{m+1}^{n+1} - 2f_m^{n+1} + f_{m-1}^{n+1}}{\Delta v^2} + \frac{f_{m+1}^{n-1} - 2f_m^{n-1} + f_{m-1}^{n-1}}{\Delta v^2} \right) \\ &+ O(\Delta\tau^2) + O(\Delta v^2). \end{aligned} \quad (21)$$

The nonlinear term f_v^2/f has two factors f_v/f and f_v . We discretize the factor f_v/f at level n and approximate the factor f_v as an average between f_v at level $n-1$ and that at level $n+1$, namely,

$$\begin{aligned} \left(\frac{f_v^2}{f}\right)_m^n &= \left(\frac{f_v}{f}\right)_m^n \frac{1}{2} \left((f_v)_m^{n+1} + (f_v)_m^{n-1} \right) + O(\Delta\tau^2) \\ &= \frac{f_{m+1}^n - f_{m-1}^n}{4\Delta v f_m^n} \left(\frac{f_{m+1}^{n+1} - f_{m-1}^{n+1}}{2\Delta v} + \frac{f_{m+1}^{n-1} - f_{m-1}^{n-1}}{2\Delta v} \right) \\ &\quad + O(\Delta\tau^2) + O(\Delta v^2). \end{aligned} \quad (22)$$

This discretization scheme leads to a set of linear equations. Based on the expressions given by (21) and (22), equation (19) can be discretized as

$$\begin{aligned} e_1(m)f_{m-1}^{n+1} + e_2(m)f_m^{n+1} + e_3(m)f_{m+1}^{n+1} &= e_4(m) + O(\Delta\tau^2) \\ &\quad + O(\Delta v^2), \end{aligned} \quad (23)$$

for $0 < m < M$ and $n \geq 2$, where M is the maximal value of m and

$$\begin{aligned} e_1(m) &= \frac{a_1 m}{\Delta v} - \frac{\lambda(m)}{2\Delta v}, \\ e_2(m) &= \frac{-2a_1 m}{\Delta v} - \frac{1}{\Delta\tau} + a_5 m \Delta v + a_6, \\ e_3(m) &= \frac{a_1 m}{\Delta v} + \frac{\lambda(m)}{2\Delta v}, \\ e_4(m) &= -\frac{1}{\Delta\tau} f_m^{n-1} - 2\alpha^{(1/\gamma)} a_7 - \frac{a_1 m}{\Delta v} (f_{m+1}^{n-1} - 2f_m^{n-1} + f_{m-1}^{n-1}) \\ &\quad - \frac{\lambda(m)}{2\Delta v} (f_{m+1}^{n-1} - f_{m-1}^{n-1}) - (a_5 m \Delta v + a_6) f_m^{n-1}, \end{aligned} \quad (24)$$

with

$$\lambda(m) = a_2 m \Delta v + a_3 + \frac{a_4 m (f_{m+1}^n - f_{m-1}^n)}{2f_m^n}. \quad (25)$$

Since (23) is not applicable to the boundaries at $m=0$ and $m=M$, we used one-sided difference technique to discretize (19) and obtained the boundary equations in the following. It is straightforward to show that, at $m=0$, we have

$$\begin{aligned} f_v(0, \tau) &= \frac{1}{4\Delta v} (-3f_0^{n+1} + 4f_1^{n+1} - f_2^{n+1} - 3f_0^{n-1} + 4f_1^{n-1} - f_2^{n-1}) + O(\Delta\tau^2) + O(\Delta v^2), \\ f_{vv}(0, \tau) &= \frac{1}{2\Delta v^2} (2f_0^{n+1} - 5f_1^{n+1} + 4f_2^{n+1} - f_3^{n+1} + 2f_0^{n-1} - 5f_1^{n-1} + 4f_2^{n-1} - f_3^{n-1}) + O(\Delta\tau^2) + O(\Delta v^2), \\ \frac{f_v^2}{f}(0, \tau) &= \frac{-3f_0^n + 4f_1^n - f_2^n}{8\Delta v^2 f_0^n} (-3f_0^{n+1} + 4f_1^{n+1} - f_2^{n+1} - 3f_0^{n-1} + 4f_1^{n-1} - f_2^{n-1}) + O(\Delta\tau^2) + O(\Delta v^2), \end{aligned} \quad (26)$$

and at $m=M$, we have

$$\begin{aligned} f_v(v_{\max}, \tau) &= \frac{1}{4\Delta v} (3f_M^{n+1} - 4f_{M-1}^{n+1} + f_{M-2}^{n+1} + 3f_M^{n-1} - 4f_{M-1}^{n-1} + f_{M-2}^{n-1}) + O(\Delta\tau^2) + O(\Delta v^2), \\ f_{vv}(v_{\max}, \tau) &= \frac{1}{2\Delta v^2} (2f_M^{n+1} - 5f_{M-1}^{n+1} + 4f_{M-2}^{n+1} - f_{M-3}^{n+1} + 2f_M^{n-1} - 5f_{M-1}^{n-1} + 4f_{M-2}^{n-1} - f_{M-3}^{n-1}) + O(\Delta\tau^2) + O(\Delta v^2), \\ \frac{f_v^2}{f}(v_{\max}, \tau) &= \frac{3f_M^n - 4f_{M-1}^n + f_{M-2}^n}{8\Delta v^2 f_M^n} (3f_M^{n+1} - 4f_{M-1}^{n+1} + f_{M-2}^{n+1} + 3f_M^{n-1} - 4f_{M-1}^{n-1} + f_{M-2}^{n-1}) + O(\Delta\tau^2) + O(\Delta v^2). \end{aligned} \quad (27)$$

By substituting these expressions into (19), we have

$$d_1(0)f_0^{n+1} + d_2(0)f_1^{n+1} + d_3(0)f_2^{n+1} + d_4(0)f_3^{n+1} = d_5(0) + O(\Delta\tau^2) + O(\Delta v^2), \quad (28)$$

$$d_4(M)f_{M-3}^{n+1} + d_3(M)f_{M-2}^{n+1} + d_2(M)f_{M-1}^{n+1} + d_1(M)f_M^{n+1} = d_5(M) + O(\Delta\tau^2) + O(\Delta v^2), \quad (29)$$

where

$$\begin{aligned}
d_1(0) &= -\frac{3\lambda(0)}{2\Delta v} - \frac{1}{\Delta\tau} + a_6, \\
d_2(0) &= \frac{2\lambda(0)}{\Delta v}, \\
d_3(0) &= \frac{\lambda(0)}{2\Delta v}, \\
d_4(0) &= 0, \\
d_5(0) &= -\frac{1}{\Delta\tau}f_0^{n-1} - 2\alpha^{\frac{1}{\gamma}}a_7 - \frac{\lambda(0)}{2\Delta v}(-3f_0^{n-1} + 4f_1^{n-1} - f_2^{n-1}) - a_6f_0^{n-1}, \\
d_1(M) &= \frac{2a_1M}{\Delta v} + \frac{3\lambda(M)}{2\Delta v} - \frac{1}{\Delta\tau} + a_5M\Delta v + a_6, \\
d_2(M) &= \frac{-5a_1M}{\Delta v} - \frac{2\lambda(M)}{\Delta v}, \\
d_3(M) &= \frac{4a_1M}{\Delta v} + \frac{\lambda(M)}{2\Delta v}, \\
d_4(M) &= \frac{-a_1M}{\Delta v}, \\
d_5(M) &= -\frac{1}{\Delta\tau}f_M^{n-1} - 2\alpha^{(1/\gamma)}a_7 - \frac{a_1M}{\Delta v}(2f_M^{n-1} - 5f_{M-1}^{n-1} + 4f_{M-2}^{n-1} - f_{M-3}^{n-1}) \\
&\quad - \frac{\lambda(M)}{2\Delta v}(3f_M^{n-1} - 4f_{M-1}^{n-1} + f_{M-2}^{n-1}) - (a_5M\Delta v + a_6)f_M^{n-1},
\end{aligned} \tag{30}$$

with

$$\lambda(0) = a_3,$$

$$\lambda(M) = a_2M\Delta v + a_3 + \frac{a_4M(3f_M^n - 4f_{M-1}^n + f_{M-2}^n)}{2f_M^n}. \tag{32}$$

From (23), (28), and (29), the numerical solution of (19) for $n \geq 2$ is determined by the following system of linear equations:

$$\begin{bmatrix}
d_1(0) & d_2(0) & d_3(0) & d_4(0) \\
e_1(1) & e_2(1) & e_3(1) & \\
& e_1(2) & e_2(2) & e_3(2) \\
& & \ddots & \ddots & \ddots \\
& & & e_1(M-1) & e_2(M-1) & e_3(M-1) \\
& & & d_4(M) & d_3(M) & d_2(M) & d_1(M)
\end{bmatrix}
\begin{bmatrix}
f_0^{n+1} \\
f_1^{n+1} \\
f_2^{n+1} \\
\vdots \\
f_{M-1}^{n+1} \\
f_M^{n+1}
\end{bmatrix}
=
\begin{bmatrix}
d_5(0) \\
e_4(1) \\
e_4(2) \\
\vdots \\
e_4(M-1) \\
d_5(M)
\end{bmatrix}. \tag{33}$$

The details of derivations for $f_\tau(0, v)$, $f_{\tau\tau}(0, v)$, and $f_{\tau\tau\tau}(0, v)$ are given in Appendix A. From (36), f_m^1 is given by

$$f_m^1 = f_m^0 + f_\tau(0, m\Delta v)\Delta\tau + \frac{1}{2}f_{\tau\tau}(0, m\Delta v)\Delta\tau^2 + \frac{1}{6}f_{\tau\tau\tau}(0, m\Delta v)\Delta\tau^3, \quad (38)$$

with an error of $O(\Delta\tau^4)$.

Knowing f , the numerical solutions of optimal portfolio and consumption rules can be obtained from (17) and (18):

$$\varphi_m^{n*} = \frac{A}{\gamma} + \rho\xi \frac{(f_v)_m^n}{f_m^n}, \quad (39)$$

$$\frac{c_m^{n*}}{w} = \left(\frac{\alpha a_c}{a_w}\right)^{(1/\gamma)} (f_m^n)^{-1}, \quad (40)$$

for $0 \leq m \leq M$, where f_m^n is given by (34) and $(f_v)_m^n$ is given by

$$(f_v)_m^n = \begin{cases} \frac{-3f_0^n + 4f_1^n - f_2^n}{2\Delta v}, & \text{for } m = 0, \\ \frac{f_{m+1}^n - f_{m-1}^n}{2\Delta v}, & \text{for } 0 < m < M, \\ \frac{3f_M^n - 4f_{M-1}^n + f_{M-2}^n}{2\Delta v}, & \text{for } m = M. \end{cases} \quad (41)$$

In summary, our numerical solutions for f_m^0 and f_m^1 are determined by (16) and (38), respectively, and the numerical solutions for f_m^n with $n \geq 2$ are determined by (34). The numerical solution of f obtained by the three-level Crank–Nicolson scheme has an accuracy of $O(\Delta\tau^2) + O(\Delta v^2)$.

3.2. Performing Richardson's Extrapolation. To further improve the accuracy of the numerical method, we apply Richardson's extrapolation technique to f . We will choose Δv proportional to $\Delta\tau$. Let $f(\tau_n, v_m, \Delta\tau)$ represent f_m^n obtained by (34) with a step size $\Delta\tau$. Then,

$$f(\tau_n, v_m, \Delta\tau) = f_{\text{exact}}(\tau, v) + C_1\Delta\tau^2 + C_2\Delta\tau^3 + O(\Delta\tau^4), \quad (42)$$

where f_{exact} is the exact value. We perform two computations with the step sizes $\Delta\tau$ and $\Delta\tau/2$, respectively. Then, we have the following two equations:

$$f(\tau_n, v_m, \Delta\tau) = f_{\text{exact}}(\tau, v) + C_1\Delta\tau^2 + C_2\Delta\tau^3 + O(\Delta\tau^4), \quad (43)$$

$$f\left(\tau_{2n}, v_{2m}, \frac{\Delta\tau}{2}\right) = f_{\text{exact}}(\tau, v) + \frac{C_1}{2^2}(\Delta\tau^2) + \frac{C_2}{2^3}\Delta\tau^3 + O(\Delta\tau^4). \quad (44)$$

From (43) and (44), we solve f_{exact} and obtain an expression based on Richardson's extrapolation technique:

$$f_{\text{extrpl.}}(n\Delta\tau, m\Delta v) = \frac{4}{3}f\left(\tau_{2n}, v_{2m}, \frac{\Delta\tau}{2}\right) - \frac{1}{3}f(\tau_n, v_m, \Delta\tau) = f_{\text{exact}} + O(\Delta\tau^3). \quad (45)$$

After substituting $f_{\text{extrpl.}}$ into (39) and (40), we obtain the expressions for φ^* and c^*/w with an accuracy of $O(\Delta\tau^3)$:

$$\varphi_{\text{extrpl.}}^* = \frac{A}{\gamma} + \rho\xi \frac{(f_{\text{extrpl.}})_v}{f_{\text{extrpl.}}}, \quad (46)$$

$$\frac{c_{\text{extrpl.}}^*}{w} = \left(\frac{\alpha a_c}{a_w}\right)^{(1/\gamma)} (f_{\text{extrpl.}})^{-1}, \quad (47)$$

where $f_{\text{extrpl.}}$ is given by (45) and $(f_{\text{extrpl.}})_v$ is given by

$$((f_{\text{extrpl.}})_v)_m^n = \begin{cases} \frac{1}{6\Delta v} [-9(f_{\text{extrpl.}})_m^n + 16(f_{\text{extrpl.}})_{m+1}^n - 8(f_{\text{extrpl.}})_{m+2}^n + (f_{\text{extrpl.}})_{m+4}^n], & \text{for } m \leq 1, \\ \frac{1}{6\Delta v} [(f_{\text{extrpl.}})_{m-2}^n - 4(f_{\text{extrpl.}})_{m-1}^n + 4(f_{\text{extrpl.}})_{m+1}^n - (f_{\text{extrpl.}})_{m+2}^n], & \text{for } 1 < m < M-1, \\ \frac{1}{6\Delta v} [9(f_{\text{extrpl.}})_m^n - 16(f_{\text{extrpl.}})_{m-1}^n + 8(f_{\text{extrpl.}})_{m-2}^n - (f_{\text{extrpl.}})_{m-4}^n], & \text{for } m \geq M-1. \end{cases} \quad (48)$$

For the purpose of giving a quick understanding of our method, Figure 1 presents a flowchart of the algorithm for solving (19). We also summarize the procedure in words in the following for obtaining the numerical solutions of f , φ^* , c^* , $f_{\text{extrpl.}}$, $\varphi_{\text{extrpl.}}^*$, and $c_{\text{extrpl.}}^*$. Here, we choose $\Delta v = \Delta\tau$.

(i) Step 1: initialize f by initial condition (16), namely, $f_m^0 = (1 - \alpha)^{(1/\gamma)}$, for $0 \leq m \leq M$.

(ii) Step 2: initialize f_m^1 by (38) for $0 \leq m \leq M$.

(iii) Step 3: for $n > 2$, knowing f_m^{n-1} and f_m^n , for $0 \leq m \leq M$, f_m^{n+1} can be determined from (34), which is in a tridiagonal form and can be easily and efficiently solved. f_m^n has an accuracy of $O(\Delta\tau^2)$.

(iv) Step 4: to obtain φ^* and c^* , we substitute f_m^n from Steps 1–3 into (39) and (40). This provides the

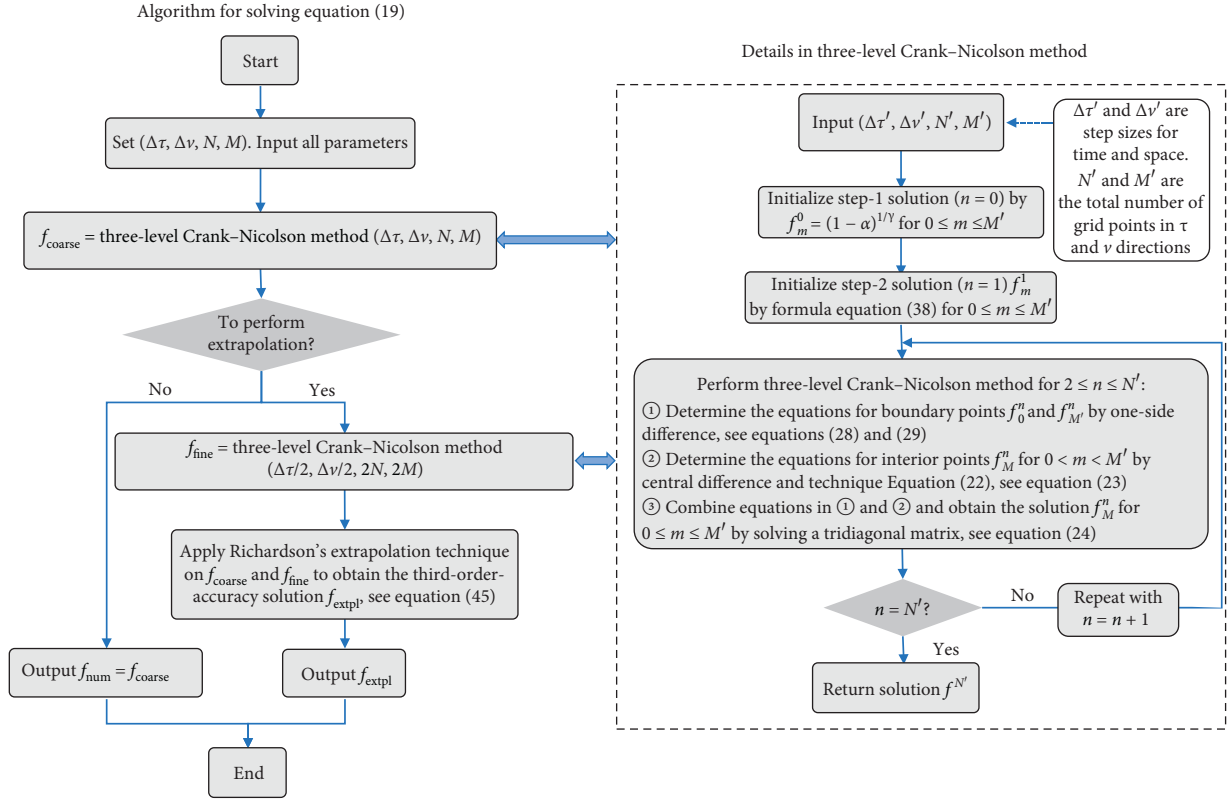


FIGURE 1: Flowchart of the algorithm.

numerical solutions for optimal strategies φ_m^{*n} and c_m^{*n} without extrapolation, which have accuracy of $O(\Delta\tau^2)$.

- (v) Step 5: to obtain f_{extpl} , φ_{extpl}^* , and c_{extpl}^* , we repeat Steps 1–3 with the step size $\Delta\tau/2$ to obtain $f(\tau_{2n}, v_{2m}, (\Delta\tau/2))$. Then, from (45), (46), and (47), we obtain f_{extpl} , φ_{extpl}^* , and c_{extpl}^* , all of which have accuracy of $O(\Delta\tau^3)$.

In the next section, we will verify the accuracy of the numerical solutions without extrapolation and those with extrapolation.

4. Validation Study of the Numerical Method

Equation (19) is an inhomogeneous equation. However, since the inhomogeneous term $\alpha^{(1/\gamma)}a_7$ affects neither the stability nor the accuracy of the three-level Crank–Nicolson method, it is sufficient to conduct validation studies for the corresponding homogeneous equation, namely, for the case

of $\alpha = 0$. Let \hat{f} be the solution of the homogeneous equation of (19), namely, the case of $\alpha = 0$. Then, \hat{f} satisfies

$$\begin{aligned}
 -(\hat{f})_\tau + a_1 v (\hat{f})_{vv} + (a_2 v + a_3)(\hat{f})_v + a_4 v \frac{(\hat{f})_v^2}{\hat{f}} \\
 + (a_5 v + a_6)\hat{f} = 0,
 \end{aligned} \tag{49}$$

with the initial condition $\hat{f}(0, v) = 1$. Following the procedure outlined in [10], the exact solution for \hat{f} can be obtained. After expressing $\hat{f}(\tau, v)$ as

$$\hat{f}(\tau, v) = e^{h_1(\tau)v + h_2(\tau)}, \tag{50}$$

from (49), $h_1(\tau)$ and $h_2(\tau)$ are governed by

$$\begin{aligned}
 h_1'(\tau) - (a_1 + a_4)h_1(\tau)^2 - a_2 h_1(\tau) - a_5 &= 0, & \text{with } h_1(0) &= 0, \\
 h_2'(\tau) - a_3 h_1(\tau) - a_6 &= 0, & \text{with } h_2(0) &= 0,
 \end{aligned} \tag{51}$$

and the solutions are

$$h_1(\tau) = \begin{cases} \frac{2a_5(e^{\sqrt{\Delta}\tau} - 1)}{a_2 + \sqrt{\Delta} - (a_2 - \sqrt{\Delta})e^{\sqrt{\Delta}\tau}}, & \text{for } \Delta > 0, \\ -\frac{2a_5\tau}{a_2\tau - 2}, & \text{for } \Delta = 0, \\ \frac{2a_5}{\sqrt{-\Delta}(\cot(\sqrt{-\Delta}\tau/2) - (a_2/\sqrt{-\Delta}))}, & \text{for } \Delta < 0, \end{cases} \quad (52)$$

$$h_2(\tau) = \begin{cases} -\frac{a_3}{a_8} \log \left| \frac{(a_2 + \sqrt{\Delta})e^{-\sqrt{\Delta}\tau} - a_2 + \sqrt{\Delta}}{2\sqrt{\Delta}} \right| + \left(a_6 - \frac{a_3\sqrt{\Delta}}{2a_8} - \frac{a_2a_3}{2a_8} \right) \tau, & \text{for } \Delta > 0, \\ -\frac{a_3}{a_8} \log \left| 1 - \frac{a_2\tau}{2} \right| + \left(a_6 - \frac{a_2a_3}{2a_8} \right) \tau, & \text{for } \Delta = 0, \\ -\frac{a_3}{a_8} \log \left| \cos \left(\frac{\sqrt{-\Delta}\tau}{2} \right) - \frac{a_2}{\sqrt{-\Delta}} \sin \left(\frac{\sqrt{-\Delta}\tau}{2} \right) \right| + \left(a_6 - \frac{a_2a_3}{2a_8} \right) \tau, & \text{for } \Delta < 0, \end{cases} \quad (53)$$

where $a_8 = a_1 + a_4$ and $\Delta = a_2^2 - 4a_5a_8$. From (17) and (18), we obtain the exact solutions of optimal strategies $\hat{\varphi}^*$ and \hat{c}^* for the case of $\alpha = 0$:

$$\hat{\varphi}_{\text{exact}}^* = \frac{A}{\gamma} + \rho\xi h_1(\tau), \quad (54)$$

$$\frac{\hat{c}_{\text{exact}}^*}{w} = 0, \quad (55)$$

where $h_1(\tau)$ is given by (52).

The exact solutions \hat{f}_{exact} , $\hat{\varphi}_{\text{exact}}^*$, and \hat{c}_{exact}^* for the case of $\alpha = 0$ given by (50), (54), and (55) offer a benchmark for testing the accuracy of our numerical solutions. We show that our numerical solutions are accurate and efficient for $\alpha = 0$. Since neither the inhomogeneous term $\alpha^{(1/\gamma)}a_7$ nor the constant initial condition $(1 - \alpha)^{(1/\gamma)}$ affects the stability or the accuracy of a numerical method, the accuracy and the stability of the method remain valid for $\alpha \neq 0$. The numerical results for $\alpha \neq 0$ are presented at the end of this section.

4.1. Numerical Validation. To set parameters for numerical validation, we use the estimation values of the parameters $\kappa, \theta, \xi, \rho, A, \beta$, and γ given in [4, 15, 22, 23] and the historical records of r . These values are listed in Table 1.

We note that since a_w determines the wealth scale and a_w/a_c determines the temporal scale, without loss of generality, we choose $a_c = a_w = 1$ in this study.

For the range of the state variables t and v , we consider $T \leq 100$. Based on the historical records of the Chicago Board Options Exchange Volatility Index, a popular measure of the implied volatility of S&P 500 index options, we examine the numerical solutions for the instantaneous volatility $\sigma_t = \sqrt{v_t}$ in the interval $[0.1, 0.8]$ (to eliminate possible influence from the numerical boundary, the authors choose $v_{\max} = 2$ in their numerical computations). Since wealth w does not appear in (19), (17), and (18), its value is irrelevant in our study.

In Table 2, we show the comparison between \hat{f}_{exact} , \hat{f}_{num} , and \hat{f}_{extpl} . \hat{f}_{exact} is the exact solution of (49). When $\alpha = 0$, \hat{f}_{num} given by (34) is the numerical solution of (49) without performing Richardson's extrapolation and \hat{f}_{extpl} given by (45) is the numerical solution of (49) after performing Richardson's extrapolation. The relative errors in \hat{f}_{num} and \hat{f}_{extpl} , namely, $|(\hat{f}_{\text{num}} - \hat{f}_{\text{exact}})/\hat{f}_{\text{exact}}|$ and $|(\hat{f}_{\text{extpl}} - \hat{f}_{\text{exact}})/\hat{f}_{\text{exact}}|$, are shown in the last two columns of Table 2.

In Table 3, we show the comparison between the exact solution $\hat{\varphi}_{\text{exact}}^*$ given by (54), the numerical solution $\hat{\varphi}_{\text{num}}^*$ determined from (39) without performing Richardson's extrapolation, and $\hat{\varphi}_{\text{extpl}}^*$ determined from (46) after performing Richardson's extrapolation. The relative errors in $\hat{\varphi}_{\text{num}}^*$ and $\hat{\varphi}_{\text{extpl}}^*$, namely, $|(\hat{\varphi}_{\text{num}}^* - \hat{\varphi}_{\text{exact}}^*)/\hat{\varphi}_{\text{exact}}^*|$ and $|(\hat{\varphi}_{\text{extpl}}^* - \hat{\varphi}_{\text{exact}}^*)/\hat{\varphi}_{\text{exact}}^*|$, are shown in the last two columns of Table 3.

There is no error in c^* since both numerical and theoretical values of c^* are zero.

In Table 4, we show the global relative errors and the computational times of \hat{f}_{num} and \hat{f}_{extpl} for different values of $\Delta\tau$ and Δv . The global relative error in \hat{f}_{num} is defined as the maximum of the local relative errors between \hat{f}_{exact} and \hat{f}_{num} in the domain $0 \leq \tau \leq 100$ and $0 \leq \sqrt{v} = \sigma \leq 0.8$. The global relative error in \hat{f}_{extpl} is defined in the same way.

Table 4 confirms that our numerical solutions \hat{f}_{num} and $\hat{\varphi}_{\text{num}}^*$ have accuracy at orders of $\Delta\tau^2$ and that \hat{f}_{extpl} and $\hat{\varphi}_{\text{extpl}}^*$ have accuracy at orders of $\Delta\tau^3$. Therefore, the extrapolation technique does improve the accuracy. For the same order of accuracy, the application of Richardson's extrapolation technique significantly saves the computational time.

4.2. Extensive Sets of Parameters. In this section, some extensive sets of parameters are used to further validate the proposed method. Since this system contains several

TABLE 1: Values for the parameters $\kappa, \theta, \xi, \rho, A, r, \beta, \gamma, a_c,$ and a_w .

Parameter	κ	θ	ξ	ρ	A	r	β	γ	a_c	a_w
Value	1.6048	0.0464	0.3796	-76.70%	1.55	1%	0.06	2	1	1

TABLE 2: Comparison between the exact solution \hat{f}_{exact} , the numerical solution without Richardson's extrapolation $\hat{f}_{\text{num.}}$, and the numerical solution after Richardson's extrapolation $\hat{f}_{\text{extrpl.}}$. The relative errors in numerical solutions are shown in the last two columns. Here, the numerical solutions are obtained with $\Delta\tau = \Delta\nu = 0.01$.

τ	$\sigma = \sqrt{\nu}$	\hat{f}_{exact}	$\hat{f}_{\text{num.}}$	$\hat{f}_{\text{extrpl.}}$	$ (\hat{f}_{\text{num.}} - \hat{f}_{\text{exact}})/\hat{f}_{\text{exact}} $	$ (\hat{f}_{\text{extrpl.}} - \hat{f}_{\text{exact}})/\hat{f}_{\text{exact}} $
0.1	0.1	0.9961202112	0.9961202904	0.9961202112	7.9×10^{-8}	2.1×10^{-12}
0.1	0.4	0.9919378844	0.9919376809	0.9919378844	2.1×10^{-7}	6.2×10^{-12}
0.1	0.8	0.9786720788	0.9786706845	0.9786720789	1.4×10^{-6}	8.1×10^{-11}
1	0.1	0.9569365332	0.9569367514	0.9569365330	2.3×10^{-7}	1.3×10^{-10}
1	0.4	0.9339516557	0.9339511052	0.9339516557	5.9×10^{-7}	1.4×10^{-11}
1	0.8	0.8640451414	0.8640421623	0.8640451415	3.4×10^{-6}	8.9×10^{-11}
10	0.1	0.6062531863	0.6062531702	0.6062531839	2.6×10^{-8}	4.0×10^{-9}
10	0.4	0.5870696178	0.5870696136	0.5870696159	7.1×10^{-9}	3.2×10^{-9}
10	0.8	0.5296676303	0.5296676662	0.5296676288	6.8×10^{-8}	2.7×10^{-9}
100	0.1	0.0061763000	0.0061762986	0.0061762997	2.2×10^{-7}	4.2×10^{-8}
100	0.4	0.0059808642	0.0059808630	0.0059808640	2.0×10^{-7}	4.1×10^{-8}
100	0.8	0.0053960721	0.0053960714	0.0053960718	1.3×10^{-7}	4.0×10^{-8}

TABLE 3: Comparison between the exact solution $\hat{\varphi}_{\text{exact}}^*$, the numerical solution without Richardson's extrapolation $\hat{\varphi}_{\text{num.}}^*$, and the numerical solution after Richardson's extrapolation $\hat{\varphi}_{\text{extrpl.}}^*$. The relative errors in numerical solutions are shown in the last two columns. Here, the numerical solutions are obtained with $\Delta\tau = \Delta\nu = 0.01$.

τ	$\sigma = \sqrt{\nu}$	$\hat{\varphi}_{\text{exact}}^*$	$\hat{\varphi}_{\text{num.}}^*$	$\hat{\varphi}_{\text{extrpl.}}^*$	$ (\hat{\varphi}_{\text{num.}}^* - \hat{\varphi}_{\text{exact}}^*)/\hat{\varphi}_{\text{exact}}^* $	$ (\hat{\varphi}_{\text{extrpl.}}^* - \hat{\varphi}_{\text{exact}}^*)/\hat{\varphi}_{\text{exact}}^* $
0.1	0.1	0.7831667609	0.7831672706	0.7831667609	6.5×10^{-7}	1.5×10^{-11}
0.1	0.4	0.7831667609	0.7831673568	0.7831667609	7.6×10^{-7}	2.8×10^{-11}
0.1	0.8	0.7831667609	0.7831676487	0.7831667608	1.1×10^{-6}	9.1×10^{-11}
1	0.1	0.8221908761	0.8221924687	0.8221908741	1.9×10^{-6}	2.4×10^{-9}
1	0.4	0.8221908761	0.8221925174	0.8221908760	2.0×10^{-6}	6.6×10^{-11}
1	0.8	0.8221908761	0.8221927448	0.8221908760	2.3×10^{-6}	5.8×10^{-11}
10	0.1	0.8374121549	0.8374122233	0.8374121478	8.2×10^{-8}	8.6×10^{-9}
10	0.4	0.8374121549	0.8374121589	0.8374121544	4.8×10^{-9}	6.4×10^{-10}
10	0.8	0.8374121549	0.8374121565	0.8374121548	1.9×10^{-9}	1.6×10^{-10}
100	0.1	0.8374121969	0.8374122652	0.8374121897	8.2×10^{-8}	8.6×10^{-9}
100	0.4	0.8374121969	0.8374122009	0.8374121964	4.7×10^{-9}	6.4×10^{-10}
100	0.8	0.8374121969	0.8374121985	0.8374121968	1.9×10^{-9}	1.6×10^{-10}

TABLE 4: Maximum relative errors and computational times of $\hat{f}_{\text{num.}}$ and $\hat{f}_{\text{extrpl.}}$ in the domain $0 \leq \tau \leq 100$ and $0 \leq \sqrt{\nu} = \sigma \leq 0.8$.

Step size		$\hat{f}_{\text{num.}}$		$\hat{f}_{\text{extrpl.}}$	
$\Delta\tau$	$\Delta\nu$	Max. rel. err.	Comp. time	Max. rel. err.	Comp. time
0.02	0.02	1.5×10^{-5}	0.39	3.3×10^{-7}	0.84
0.01	0.01	3.8×10^{-6}	1.52	4.2×10^{-8}	3.31
0.005	0.005	9.6×10^{-7}	6.02	5.2×10^{-9}	13.18
0.0025	0.0025	2.4×10^{-7}	24.02	6.3×10^{-10}	52.54

parameters, we vary only one of the parameters at a time and keep other parameters at their benchmark values as shown in Table 1. Extensive sets are given in Table 5.

By choosing the step size $\Delta\tau = 0.01$ and $\Delta\nu = 0.01$, the proposed algorithm is conducted, and the relative errors are recorded both before and after performing the extrapolation technique. In Tables 6 and 7, we show the maximum relative

errors of the proposed algorithm before and after performing the extrapolation technique, respectively, in the domain $0 \leq \tau \leq 100$ and $0 \leq \sqrt{\nu} = \sigma \leq 0.8$. It can be found that the extrapolation technique does improve one-order accuracy for the ten sets of parameters in Table 5.

By taking half of the step size above, namely, choosing $\Delta\tau = 0.005$ and $\Delta\nu = 0.005$, the proposed algorithm is

TABLE 5: Values for the parameters $\kappa, \theta, \xi, \rho, A, r, \beta, \gamma, a_c,$ and a_w .

Parameter	κ	θ	ξ	ρ	A	r	β	γ	a_c	a_w
Set 1	2.5	0.0464	0.3796	-76.70%	1.55	1%	0.06	2	1	1
Set 2	1.6048	0.08	0.3796	-76.70%	1.55	1%	0.06	2	1	1
Set 3	1.6048	0.0464	0.6	-76.70%	1.55	1%	0.06	2	1	1
Set 4	1.6048	0.0464	0.3796	-50%	1.55	1%	0.06	2	1	1
Set 5	1.6048	0.0464	0.3796	-76.70%	1.25	1%	0.06	2	1	1
Set 6	1.6048	0.0464	0.3796	-76.70%	1.55	5%	0.06	2	1	1
Set 7	1.6048	0.0464	0.3796	-76.70%	1.55	1%	0.15	2	1	1
Set 8	1.6048	0.0464	0.3796	-76.70%	1.55	1%	0.06	5	1	1
Set 9	1.6048	0.0464	0.3796	-76.70%	1.55	1%	0.06	2	2	1
Set 10	1.6048	0.0464	0.3796	-76.70%	1.55	1%	0.06	2	1	2

TABLE 6: Maximum relative error for $\hat{f}_{\text{num.}}$ and $\hat{\varphi}_{\text{num.}}$ with $\Delta\tau = 0.01$ and $\Delta\nu = 0.01$.

Set	Maximum relative error	
	$\hat{f}_{\text{num.}}$	$\hat{\varphi}_{\text{num.}}$
Set 1	5.8×10^{-6}	3.9×10^{-6}
Set 2	3.6×10^{-6}	2.7×10^{-6}
Set 3	3.6×10^{-6}	3.9×10^{-6}
Set 4	4.0×10^{-6}	1.8×10^{-6}
Set 5	2.4×10^{-6}	2.0×10^{-6}
Set 6	4.0×10^{-6}	2.8×10^{-6}
Set 7	4.2×10^{-6}	2.9×10^{-6}
Set 8	2.1×10^{-6}	1.4×10^{-6}
Set 9	3.8×10^{-6}	2.7×10^{-6}
Set 10	3.8×10^{-6}	2.7×10^{-6}

TABLE 7: Maximum relative error for $\hat{f}_{\text{expl.}}$ and $\hat{\varphi}_{\text{expl.}}$ with $\Delta\tau = 0.01$ and $\Delta\nu = 0.01$.

Set	Maximum relative error	
	$\hat{f}_{\text{expl.}}$	$\hat{\varphi}_{\text{expl.}}$
Set 1	1.2×10^{-7}	9.3×10^{-8}
Set 2	5.0×10^{-8}	4.3×10^{-8}
Set 3	9.5×10^{-8}	5.9×10^{-8}
Set 4	5.9×10^{-8}	3.1×10^{-8}
Set 5	3.3×10^{-8}	3.1×10^{-8}
Set 6	5.6×10^{-8}	4.5×10^{-8}
Set 7	5.8×10^{-8}	4.7×10^{-8}
Set 8	2.5×10^{-8}	2.02×10^{-8}
Set 9	5.4×10^{-8}	4.4×10^{-8}
Set 10	5.4×10^{-8}	4.4×10^{-8}

TABLE 8: Maximum relative error for $\hat{f}_{\text{num.}}$ and $\hat{\varphi}_{\text{num.}}$ with $\Delta\tau = 0.005$ and $\Delta\nu = 0.005$.

Set	Maximum relative error	
	$\hat{f}_{\text{num.}}$	$\hat{\varphi}_{\text{num.}}$
Set 1	1.4×10^{-6}	9.7×10^{-7}
Set 2	9.1×10^{-7}	6.7×10^{-7}
Set 3	9.0×10^{-7}	9.8×10^{-7}
Set 4	1.0×10^{-6}	4.6×10^{-7}
Set 5	6.0×10^{-7}	5.0×10^{-7}
Set 6	10.0×10^{-7}	6.9×10^{-7}
Set 7	1.0×10^{-6}	7.2×10^{-7}
Set 8	5.1×10^{-7}	3.5×10^{-7}
Set 9	9.6×10^{-7}	6.7×10^{-7}
Set 10	9.6×10^{-7}	6.7×10^{-7}

TABLE 9: Maximum relative error for $\hat{f}_{\text{expl.}}$ and $\hat{\varphi}_{\text{expl.}}$ with $\Delta\tau = 0.005$ and $\Delta\nu = 0.005$.

Set	Maximum relative error	
	$\hat{f}_{\text{expl.}}$	$\hat{\varphi}_{\text{expl.}}$
Set 1	1.6×10^{-8}	1.2×10^{-8}
Set 2	6.4×10^{-9}	7.5×10^{-9}
Set 3	2.1×10^{-8}	7.6×10^{-9}
Set 4	7.6×10^{-9}	4.0×10^{-9}
Set 5	4.2×10^{-9}	4.0×10^{-9}
Set 6	7.1×10^{-9}	5.8×10^{-9}
Set 7	7.4×10^{-9}	6.0×10^{-9}
Set 8	3.2×10^{-9}	2.5×10^{-9}
Set 9	6.9×10^{-9}	5.6×10^{-9}
Set 10	6.9×10^{-9}	5.6×10^{-9}

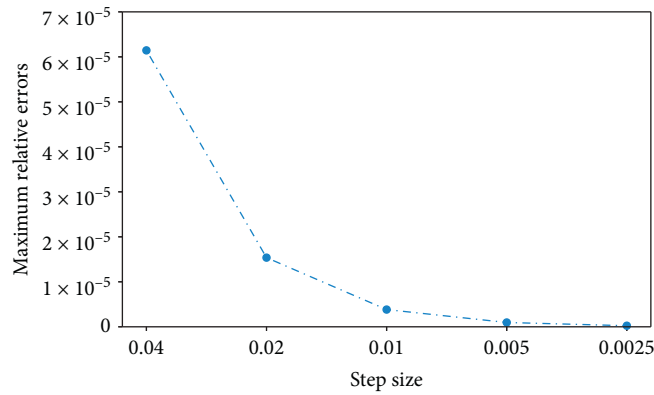


FIGURE 2: Maximum relative errors for decreasing step size.

TABLE 10: Maximum relative errors and convergence orders of $\hat{f}_{\text{num.}}$ in the domain $0 \leq \tau \leq 100$ and $0 \leq \sqrt{\nu} = \sigma \leq 0.8$.

Step size		Maximum relative errors	Convergence order
$\Delta\tau$	$\Delta\nu$		
0.02	0.02	1.53×10^{-5}	2.0
0.01	0.01	3.83×10^{-6}	2.0
0.005	0.005	9.58×10^{-7}	2.0
0.0025	0.0025	2.40×10^{-7}	2.0

conducted, and the relative errors are recorded both before and after performing the extrapolation technique. In Tables 8 and 9, we show the maximum relative errors of the proposed algorithm before and after performing the extrapolation technique, respectively, in the domain $0 \leq \tau \leq 100$ and $0 \leq \sqrt{\nu} = \sigma \leq 0.8$. Tables 6–9 show that the proposed algorithm before and after performing the extrapolation technique has second-order accuracy and third-order accuracy, respectively, for the extensive sets of parameters.

4.3. Evidence for Stability and Convergence. To provide the evidence for stability, we calculate the maximum relative errors of $\hat{f}_{\text{num.}}$ for $\Delta\tau = \Delta\nu = 0.04, 0.02, 0.01, 0.005, 0.0025$, respectively. The results are shown in Figure 2. One can see

that, as the step size goes to zero, the maximum relative errors tend to zero, which numerically verifies the stability of the proposed algorithm.

To provide the evidence for convergence, let $e(\Delta\tau, \Delta\nu)$ be the maximum relative error; then, the convergence order is given by

$$\text{convergence order} = \log_2 \left(\frac{e(\Delta\tau, \Delta\nu)}{e((\Delta\tau/2), (\Delta\nu/2))} \right). \quad (56)$$

In Table 10, the maximum relative errors and convergence orders of $\hat{f}_{\text{num.}}$ for different values of $\Delta\tau$ and $\Delta\nu$ are given. It shows that the convergence orders are always equal to 2.0 as $\Delta\tau$ and $\Delta\nu$ go to zero, which numerically verifies the convergence of the proposed algorithm.

TABLE 11: Numerical solutions for f , φ^* , and c^*/w after performing Richardson's extrapolation. Here, $\alpha = 0.1$ and $\Delta\tau = \Delta\nu = 0.001$. Other parameter values are the same as those in Table 1.

τ	$\sigma = \sqrt{\nu}$	$f_{\text{extrpl.}}$	$\varphi_{\text{extrpl.}}^*$	$c_{\text{extrpl.}}^*/w$
0.1	0.1	0.976564446	0.783037744	0.323816587
0.1	0.4	0.972528955	0.783037394	0.325160258
0.1	0.8	0.959728271	0.783036268	0.329497187
1	0.1	1.217443571	0.817505616	0.259747370
1	0.4	1.191090583	0.817448428	0.265494305
1	0.8	1.110757357	0.817260409	0.284695630
10	0.1	3.073495770	0.833010306	0.102888629
10	0.4	2.983046823	0.832947671	0.106008315
10	0.8	2.711715965	0.832739549	0.116615372
100	0.1	6.227692985	0.835240145	0.050777674
100	0.4	6.037435062	0.835206694	0.052377833
100	0.8	5.467451073	0.835095101	0.057838243

TABLE 12: Numerical solutions for f , φ^* , and c^*/w after performing Richardson's extrapolation. Here, $\alpha = 0.5$ and $\Delta\tau = \Delta\nu = 0.001$. Other parameter values are the same as those in Table 1.

τ	$\sigma = \sqrt{\nu}$	$f_{\text{extrpl.}}$	$\varphi_{\text{extrpl.}}^*$	$c_{\text{extrpl.}}^*/w$
0.1	0.1	0.774937774	0.782803210	0.912469110
0.1	0.4	0.771828844	0.782802269	0.916144540
0.1	0.8	0.761966328	0.782799238	0.928002663
1	0.1	1.368974100	0.812872895	0.516523126
1	0.4	1.342553293	0.812781707	0.526688054
1	0.8	1.261787768	0.812484452	0.560400726
10	0.1	6.015181176	0.832382642	0.117553696
10	0.4	5.840061390	0.832312731	0.121078656
10	0.8	5.314527422	0.832080689	0.133051676
100	0.1	13.916810422	0.835238781	0.050809543
100	0.4	13.491657157	0.835205311	0.052410669
100	0.8	12.217961221	0.835093653	0.057874368

TABLE 13: Numerical solutions for f , φ^* , and c^*/w after performing Richardson's extrapolation. Here, $\alpha = 0.9$ and $\Delta\tau = \Delta\nu = 0.001$. Other parameter values are the same as those in Table 1.

τ	$\sigma = \sqrt{\nu}$	$f_{\text{extrpl.}}$	$\varphi_{\text{extrpl.}}^*$	$c_{\text{extrpl.}}^*/w$
0.1	0.1	0.409686387	0.782244153	2.315632955
0.1	0.4	0.408160455	0.782242030	2.324290085
0.1	0.8	0.403318534	0.782235205	2.352193658
1	0.1	1.231451909	0.808291630	0.770377869
1	0.4	1.210542696	0.808188721	0.783684294
1	0.8	1.146400499	0.807855696	0.827532175
10	0.1	7.686789813	0.832131657	0.123417359
10	0.4	7.463974966	0.832058953	0.127101618
10	0.8	6.795202083	0.831817743	0.139610756
100	0.1	18.667454349	0.835238326	0.050820175
100	0.4	18.097174990	0.835204850	0.052421624
100	0.8	16.388702420	0.835093170	0.057886419

4.4. *Numerical Results for $\alpha \neq 0$.* We have confirmed the accuracy of our numerical solutions for $\alpha = 0$. This guarantees that our numerical solution $f_{\text{extrpl.}}$ for $\alpha \neq 0$ will also have an accuracy of $O(\Delta\tau^3)$. In Tables 11–13, we present the numerical solutions of $f_{\text{extrpl.}}$, $\varphi_{\text{extrpl.}}^*$, and $c_{\text{extrpl.}}^*/w$ for $\alpha = 0.1, 0.5$, and 0.9 with step sizes $\Delta\tau = \Delta\nu = 0.001$. In

Tables 14 and 15, we show the results for $\gamma = 1$ and 10 with $\alpha = 0.5$ and $\Delta\tau = \Delta\nu = 0.001$. All other parameter values in Tables 11–15 are the same as the ones in Table 1. All digits shown in Tables 11–15 are exact, in the sense that they do not change when we further refine the values of $\Delta\tau$ and $\Delta\nu$. Therefore, we have provided the first set of exact numerical

TABLE 14: Numerical solutions for f , φ^* , and c^*/w after performing Richardson's extrapolation. Here, $\alpha = 0.5$, $\gamma = 1$, and $\Delta\tau = \Delta\nu = 0.001$. Other parameter values are the same as those in Table 1.

τ	$\sigma = \sqrt{\nu}$	$f_{\text{extrpl.}}$	$\varphi_{\text{extrpl.}}^*$	$c_{\text{extrpl.}}^*/w$
0.1	0.1	0.546859282	1.550000000	0.914311994
0.1	0.4	0.546859282	1.550000000	0.914311994
0.1	0.8	0.546859282	1.550000000	0.914311994
1	0.1	0.956177820	1.550000000	0.522915288
1	0.4	0.956177820	1.550000000	0.522915288
1	0.8	0.956177820	1.550000000	0.522915288
10	0.1	4.034308851	1.550000000	0.123936966
10	0.4	4.034308851	1.550000000	0.123936966
10	0.8	4.034308851	1.550000000	0.123936966
100	0.1	8.313916441	1.550000000	0.060140128
100	0.4	8.313916441	1.550000000	0.060140128
100	0.8	8.313916441	1.550000000	0.060140128

TABLE 15: Numerical solutions for f , φ^* , and c^*/w after performing Richardson's extrapolation. Here, $\alpha = 0.5$, $\gamma = 10$, and $\Delta\tau = \Delta\nu = 0.001$. Other parameter values are the same as those in Table 1.

τ	$\sigma = \sqrt{\nu}$	$f_{\text{extrpl.}}$	$\varphi_{\text{extrpl.}}^*$	$c_{\text{extrpl.}}^*/w$
0.1	0.1	1.024730849	0.157833805	0.910515178
0.1	0.4	1.023235912	0.157833681	0.911845432
0.1	0.8	1.018467192	0.157833282	0.916114922
1	0.1	1.840789858	0.169544364	0.506865565
1	0.4	1.827054636	0.169530453	0.510676021
1	0.8	1.783873146	0.169485620	0.523037747
10	0.1	9.182254704	0.178575988	0.101612624
10	0.4	9.071426914	0.178564461	0.102854049
10	0.8	8.726039146	0.178527017	0.106925144
100	0.1	38.546073475	0.180136006	0.024205656
100	0.4	38.050155049	0.180132872	0.024521135
100	0.8	36.506088964	0.180122662	0.025558284

data for optimal asset allocation and consumption strategies.

5. Conclusion

In this paper, we study the portfolio selection problem in a general setting under CRRA utility functions: stochastic volatility, incomplete markets, finite investment horizons, and consumption choice. To the best of our knowledge, no explicit solution or numerical result is available in the literature for this setting. We present an accurate and efficient numerical method for optimal asset allocation and optimal consumption strategies. The optimal strategies are depended on a solution to a nonlinear and inhomogeneous partial differential equation which is derived from the portfolio selection problem. A three-level Crank–Nicolson finite difference scheme, which has second-order accuracy, is used to determine numerical solutions. In addition, we have used a technique to deal with the nonlinear term, which is one of our main contributions. We believe that the technique to deal with the nonlinear term could be applied to other similar numerical problems. The Crank–Nicolson algorithm also has been extended to third-order accuracy by performing Richardson's extrapolation. Some experiments are conducted to verify the performance of the proposed algorithm. Based on this algorithm, we present the first set of

accurate numerical solutions of optimal strategies. Since the portfolio selection problem under stochastic volatility is an important issue in modern finance, the proposed algorithm will be useful for further theoretical research and for applications in the financial industry.

Appendix

A. Derivations for $f_\tau(0, \nu)$, $f_{\tau\tau}(0, \nu)$, and $f_{\tau\tau\tau}(0, \nu)$

From (19), we obtain

$$f_\tau = a_1\nu f_{\nu\nu} + (a_2\nu + a_3)f_\nu + a_4\nu \frac{f_\nu^2}{f} + (a_5\nu + a_6)f + \alpha^{(1/\gamma)}a_7. \quad (\text{A.1})$$

By taking the derivative of (A.1) with respect to τ , we obtain

$$f_{\tau\tau} = a_1\nu f_{\nu\nu\tau} + (a_2\nu + a_3)f_{\nu\tau} + a_4\nu \frac{2f_\nu f_{\nu\tau}}{f} - a_4\nu \frac{f_\nu^2}{f^2} f_\tau + (a_5\nu + a_6)f_\tau. \quad (\text{A.2})$$

By taking the derivative of (A.2) with respect to τ , we obtain

$$\begin{aligned} f_{\tau\tau\tau} = & a_1 v f_{v\tau\tau} + (a_2 v + a_3) f_{v\tau\tau} + a_4 v \frac{2f_{v\tau}^2}{f} + a_4 v \frac{2f_v f_{v\tau\tau}}{f} \\ & - 4a_4 v \frac{f_v f_{v\tau}}{f^2} f_\tau + 2a_4 v \frac{f_v^2}{f^3} f_\tau^2 - a_4 v \frac{f_v^2}{f^2} f_{\tau\tau} \\ & + (a_5 v + a_6) f_{\tau\tau}. \end{aligned} \quad (\text{A.3})$$

By setting $\tau = 0$ in (A.1) and using the initial condition $f(0, v) = (1 - \alpha)^{(1/\gamma)}$, we obtain

$$f_\tau(0, v) = (a_5 v + a_6) f(0, v) + \alpha^{(1/\gamma)} a_7. \quad (\text{A.4})$$

By setting $\tau = 0$ in (A.2) and using the initial condition $f(0, v) = (1 - \alpha)^{(1/\gamma)}$ and (A.4), we obtain

$$\begin{aligned} f_{\tau\tau}(0, v) = & (a_5^2 v^2 + (a_2 a_5 + 2a_5 a_6) v + a_3 a_5 + a_6^2) f(0, v) \\ & + (a_5 v + a_6) \alpha^{(1/\gamma)} a_7. \end{aligned} \quad (\text{A.5})$$

By setting $\tau = 0$ in (A.3) and using the initial condition $f(0, v) = (1 - \alpha)^{(1/\gamma)}$, (A.4), and (A.5), we obtain

$$f_{\tau\tau\tau}(0, v) = a_5^3 v^3 + a_2 a_3 a_5 + 3a_3 a_6 a_5 + a_6^3. \quad (\text{A.6})$$

B. HARA Utility Setting

In this appendix, the portfolio selection problem under HARA utility setting is considered. We would like to show that the proposed method could also be applied to this problem under HARA utility setting.

We assume that HARA utility functions $u_1(\cdot)$ and $u_2(\cdot)$ are used for consumption utility and terminal wealth utility, respectively:

$$\begin{aligned} u_1(c_t) &= \frac{a_c(1-\gamma)}{\gamma} \left(\frac{c_t}{1-\gamma} + b_c \right)^\gamma, \\ u_2(w_T) &= \frac{a_w(1-\gamma)}{\gamma} \left(\frac{w_T}{1-\gamma} + b_w \right)^\gamma. \end{aligned} \quad (\text{B.1})$$

The market setting and investors' objective are the same as before which are given by (2)–(6). Following the procedure in this paper, the value function satisfies the following equation:

$$\begin{aligned} 0 = & \frac{(1-\gamma)^2}{\gamma} (a_c \alpha e^{-\beta t})^{(1/(1-\gamma))} V_w^{(\gamma/(1-\gamma))} + ((1-\gamma)b_c + r w) V_w \\ & + V_t + \kappa(\theta - v) V_v + \frac{1}{2} \xi^2 v V_{vv} - \frac{1}{2} v \frac{(AV_w + \rho \xi V_{wv})^2}{V_{ww}}, \end{aligned} \quad (\text{B.2})$$

and optimal strategies are given by

$$\begin{aligned} \varphi^* &= -\frac{AV_w + \rho \xi V_{wv}}{w V_{ww}}, \\ c^* &= (1-\gamma) \left[\left(\frac{V_w}{a_c \alpha e^{-\beta t}} \right)^{(1/\gamma-1)} - b_c \right]. \end{aligned} \quad (\text{B.3})$$

Based on the terminal condition and the scaling property of this problem, a reasonable trial solution form for V is assumed:

$$V(\tau, w, v) = e^{-\beta(T-\tau)} \frac{a_w(1-\gamma)}{\gamma} \left(\frac{w}{1-\gamma} + g(\tau) \right)^\gamma f(\tau, v)^{1-\gamma}, \quad (\text{B.4})$$

where $g(\tau)$ and $f(\tau, v)$ need to be determined and $\tau = T - t$. The initial conditions of g and f are

$$\begin{aligned} g(0) &= b_w, \\ f(0, v) &= (1-\alpha)^{(1/(1-\gamma))}. \end{aligned} \quad (\text{B.5})$$

To determine f and g , we substitute expression (B.4) into (B.2) and obtain

$$\begin{aligned} -f_\tau + \frac{1}{2} \xi^2 v f_{vv} + \left(\kappa(\theta - v) + \frac{\gamma}{1-\gamma} A \rho \xi v \right) f_v \\ - \frac{1}{2} \gamma (1-\rho^2) \xi^2 v \frac{f_v^2}{f} \\ + \left(\frac{A^2 \gamma}{2(1-\gamma)^2} v + \frac{\gamma r}{1-\gamma} - \frac{\beta}{1-\gamma} \right) f + \left(\frac{\alpha a_c}{a_w} \right)^{(1/(1-\gamma))} \\ - \frac{\gamma}{1-\gamma} \left(\frac{g'(\tau) + r g(\tau) - b_c}{(w/(1-\gamma) + g)} \right) f = 0. \end{aligned} \quad (\text{B.6})$$

By setting

$$g'(\tau) + r g(\tau) - b_c = 0, \quad (\text{B.7})$$

equation (B.6) becomes an equation involving f only, namely,

$$\begin{aligned} -f_\tau + \frac{1}{2} \xi^2 v f_{vv} + \left(\kappa(\theta - v) + \frac{\gamma}{1-\gamma} A \rho \xi v \right) f_v \\ - \frac{1}{2} \gamma (1-\rho^2) \xi^2 v \frac{f_v^2}{f} \\ + \left(\frac{A^2 \gamma}{2(1-\gamma)^2} v + \frac{\gamma r}{1-\gamma} - \frac{\beta}{1-\gamma} \right) f + \left(\frac{\alpha a_c}{a_w} \right)^{(1/(1-\gamma))} = 0. \end{aligned} \quad (\text{B.8})$$

Thus, we have achieved dimension reduction by removing w dependence in (B.2). The solution of g is obtained from (B.7) and (B.5):

$$g(\tau) = b_w e^{-r\tau} + \frac{b_c}{r} (1 - e^{-r\tau}). \quad (\text{B.9})$$

Equation (B.8) has the same form as (19), which could be solved numerically by applying the proposed algorithm the same as that in Section 3. Then, the optimal strategies could be obtained:

$$\varphi^* = \left(1 + \frac{1-\gamma}{w} g(\tau)\right) \left(\frac{A}{1-\gamma} + \rho\xi \frac{f_v}{f}\right),$$

$$\frac{c^*}{w} = \left(\frac{\alpha a_c}{a_w}\right)^{(1/(1-\gamma))} f^{-1} + \frac{1-\gamma}{w} \left(\left(\frac{\alpha a_c}{a_w}\right)^{(1/(1-\gamma))} g(\tau) f^{-1} - b_c\right). \quad (\text{B.10})$$

Data Availability

The data used to support the findings of this study are available from the corresponding author upon request.

Conflicts of Interest

The authors declare that they have no conflicts of interest.

Acknowledgments

The work of L. Ge was supported by the Fundamental Research Funds for the Central Universities (220110004005040120 and 220110001002020043). The work of Q. Zhang was supported by the Research Grants Council of the Hong Kong Special Administrative Region, China (project CityU 11335816).

References

- [1] A. Buraschi, P. Porchia, and F. Trojani, "Correlation risk and optimal portfolio choice," *The Journal of Finance*, vol. 65, no. 1, pp. 393–420, 2010.
- [2] Š. Raudys, A. Raudys, and Ž. Pabarškaitė, "Sustainable economy inspired large-scale feed-forward portfolio construction," *Technological and Economic Development of Economy*, vol. 20, no. 1, pp. 79–96, 2014.
- [3] J. Kallsen and J. Muhle-Karbe, "Utility maximization in affine stochastic volatility models," *International Journal of Theoretical and Applied Finance*, vol. 13, no. 3, pp. 459–477, 2010.
- [4] P. Christoffersen, S. Heston, and K. Jacobs, "The shape and term structure of the index option smirk: why multifactor stochastic volatility models work so well," *Management Science*, vol. 55, no. 12, pp. 1914–1932, 2009.
- [5] S. L. Heston, "A closed-form solution for options with stochastic volatility with applications to bond and currency options," *Review of Financial Studies*, vol. 6, no. 2, pp. 327–343, 1993.
- [6] S. Li, Y. Zhou, Y. Wu, and X. Ge, "Equilibrium approach of asset and option pricing under Lévy process and stochastic volatility," *Australian Journal of Management*, vol. 42, no. 2, pp. 276–295, 2017.
- [7] S. Liu, Y. Zhou, Y. Wu, and X. Ge, "Option pricing under the jump diffusion and multifactor stochastic processes," *Journal of Function Spaces*, vol. 2019, Article ID 9754679, 12 pages, 2019.
- [8] T. S. Kim and E. Omberg, "Dynamic nonmyopic portfolio behavior," *Review of Financial Studies*, vol. 9, no. 1, pp. 141–161, 1996.
- [9] J. A. Wachter, "Portfolio and consumption decisions under mean-reverting returns: an exact solution for complete markets," *The Journal of Financial and Quantitative Analysis*, vol. 37, no. 1, pp. 63–91, 2002.
- [10] J. Liu, "Portfolio selection in stochastic environments," *Review of Financial Studies*, vol. 20, no. 1, pp. 1–39, 2007.
- [11] Y. Xia, "Learning about predictability: the effects of parameter uncertainty on dynamic asset allocation," *The Journal of Finance*, vol. 56, no. 1, pp. 205–246, 2001.
- [12] M. Schroder and C. Skiadas, "Optimal consumption and portfolio selection with stochastic differential utility," *Journal of Economic Theory*, vol. 89, no. 1, pp. 68–126, 1999.
- [13] G. Chacko and L. M. Viceira, "Dynamic consumption and portfolio choice with stochastic volatility in incomplete markets," *Review of Financial Studies*, vol. 18, no. 4, pp. 1369–1402, 2005.
- [14] R. I. Palwasha, N. Ahmad, R. R. Ahmed, J. Vveinhardt, and D. Štreimikienė, "Speed of mean reversion: an empirical analysis of kse, lse and ise indices," *Technological and Economic Development of Economy*, vol. 24, no. 4, pp. 1435–1452, 2018.
- [15] R. C. Merton, "On estimating the expected return on the market," *Journal of Financial Economics*, vol. 8, no. 4, pp. 323–361, 1980.
- [16] K. R. French, G. W. Schwert, and R. F. Stambaugh, "Expected stock returns and volatility," *Journal of Financial Economics*, vol. 19, no. 1, pp. 3–29, 1987.
- [17] H. Kraft, "Optimal portfolios and Heston's stochastic volatility model: an explicit solution for power utility," *Quantitative Finance*, vol. 5, no. 3, pp. 303–313, 2005.
- [18] D. He, "On the L_∞-norm convergence of a three-level linearly implicit finite difference method for the extended Fisher-Kolmogorov equation in both 1D and 2D," *Computers & Mathematics with Applications*, vol. 71, no. 12, pp. 2594–2607, 2016.
- [19] B. Wongsaijai and K. Poochinapan, "A three-level average implicit finite difference scheme to solve equation obtained by coupling the Rosenau-KdV equation and the Rosenau-RLW equation," *Applied Mathematics and Computation*, vol. 245, pp. 289–304, 2014.
- [20] D. He, "Exact solitary solution and a three-level linearly implicit conservative finite difference method for the generalized Rosenau-Kawahara-RLW equation with generalized Novikov type perturbation," *Nonlinear Dynamics*, vol. 85, no. 1, pp. 479–498, 2016.
- [21] H.-Y. Cao, Z.-Z. Sun, and G.-H. Gao, "A three-level linearized finite difference scheme for the camassa-holm equation," *Numerical Methods for Partial Differential Equations*, vol. 30, no. 2, pp. 451–471, 2014.
- [22] S. Frederick, G. Loewenstein, and T. O'donoghue, "Time discounting and time preference: a critical review," *Journal of Economic Literature*, vol. 40, no. 2, pp. 351–401, 2002.
- [23] C. Munk, *Financial Asset Pricing Theory*, Oxford University Press, Oxford, UK, 2013.

Research Article

Adaptive Finite-Time Congestion Control for Uncertain TCP/AQM Network with Unknown Hysteresis

Weimin Zheng, Yanxin Li , Xiaowen Jing, and Shangkun Liu

College of Computer Science and Engineering, Shandong University of Science and Technology, Qingdao 266590, China

Correspondence should be addressed to Yanxin Li; lyx94lyx@126.com

Received 8 May 2020; Revised 24 June 2020; Accepted 6 July 2020; Published 27 July 2020

Guest Editor: Lei Xie

Copyright © 2020 Weimin Zheng et al. This is an open access article distributed under the Creative Commons Attribution License, which permits unrestricted use, distribution, and reproduction in any medium, provided the original work is properly cited.

The issue of adaptive practical finite-time (FT) congestion control for the transmission control protocol/active queue management (TCP/AQM) network with unknown hysteresis and external disturbance is considered in this paper. A finite-time congestion controller is designed by the backstepping technique and the adaptive neural control method. This controller guarantees that the queue length tracks the desired queue in finite-time, and it is semiglobally practical finite-time stable (SGPFS) for all the signals of the closed-loop system. At last, the simulation results show that the control strategy is effective.

1. Introduction

Recently, the communication network based on TCP has been rapidly developed and widely used. However, the congestion of network traffic has become a critical problem in network control. TCP congestion control can not only ward off network collapse and avert locking behavior, but also effectively reduce the probability of control loop synchronization [1]. It is of great significance to maintain the stability and robustness of the TCP network. Since Jacobson proposed the end-to-end TCP congestion control algorithm in 1988 [2], many scholars have conducted more in-depth and detailed research, such as Vegas [3], Sack [4], and New Reno [5], and they all concentrate on end-to-end congestion control based on the end system. However, with the increasing demand of application and the improvement of service quality, the TCP congestion control mechanism of end-to-end is no longer suitable. After that, some scholars have proposed a solution called AQM [6], which is one of the most widely studied congestion solutions at present. It can drop or mark some packets before the router generates a full queue state, so that the TCP source can timely sense the network congestion state and take corresponding measures. The first algorithm is named as random early detection (RED) [7], but RED and its improved algorithms [8, 9]

are too complicated for parameter configuration. Based on fluid flow theory, Misra et al. proposed a nonlinear model of TCP/AQM in 2000 [10]. Based on the above model, many researchers have combined control theory to design several congestion schemes, such as P and PI [11], PD [12], and PID [13]. An AQM algorithm is presented on the strength of the fuzzy sliding-mode control method in the nonlinear control method in [14], which improves the control effect of the system. In [15], considering the limited input of the TCP network system, an AQM algorithm is presented on the strength of the sliding-mode control method, which makes the system obtain better asymptotic stability. Tan et al. [16] proposed a congestion control scheme composed of source and link algorithms. Zhang et al. [17] analyzed the TCP/RED model from a time-delay control theory standpoint, and the time-delayed control analyzing techniques explored can be extended to other AQM or AQM-based schemes for their stability analysis. The primal-dual algorithm has been analyzed from the multivariable time-delay control theory standpoint in [18]. The stability analysis can be applied to various TCP/AQM systems other than FAST TCP/DropTail and TCP/AVQ. The AQM controller with specified performance is designed by the backstepping method considering the interference of UDP flow [19]. Due to the complex environment and continuous

application of the network [20–22], congestion algorithms need to further improve network performance and achieve better congestion control effects.

Nowadays, many scholars have noticed the hysteresis phenomenon widely existing in the nonlinear system. In the process of practical application, the tracking performance of the system has been limited by the hysteresis, which even makes the system unstable [23, 24]. To reduce the impact of nonlinear system control on the unknown hysteresis in the actuator, more and more scholars have studied the design of the controller in [25–28]. Zhou et al. [25] not only first proposed a new Bouc–Wen hysteresis model, but also put forward an adaptive control method to ensure a good tracking performance by constructing an inverse of compensating hysteresis nonlinearity. For the sake of the stability of the controlled system, Su et al. [26] designed an adaptive control scheme based on the backlash-like hysteresis model. Wang et al. [28] discussed the adaptive stabilization of pure-feedback nonlinear systems, and it not only solved the unknown direction hysteresis, but also eliminated the constraint assumption that the nonlinear function needs to satisfy the linear growth condition by using the characteristic of the Nussbaum function and introducing a virtual controller. Up to now, there are no literature studies for the congestion control of TCP/AQM networks with unknown hysteresis.

On the other hand, some scholars pay more attention to the FT control because the FT stability has more meaning than infinite-time stability in practical application [29–31]. In practice, the control goal is promising to be realized in a limited time, and the control scheme of infinite time cannot achieve such a goal because they will lead to a long time transient response. The FT stability is different from the asymptotic stability of infinite time, its control method will enable the system to achieve the transient performance quickly, and in FT, the system state variables can be converged in equilibrium. Dorato conducted a comprehensive study on the problem of FT stability and elaborated on the differences between FT stability and asymptotic stability [29]. The Lyapunov theory of FT stability was first put forward in [30, 32]. The authors in [33, 34] proposed some FT control schemes for the nonlinear systems via the Lyapunov stability theory. However, in practice, these FT control strategies cannot satisfy the actual control system with unknown nonlinearity. Wang et al. [34] studied the FT tracking problem with unknown functions. A criterion of SGPFs is set up for the first time by the fuzzy logic system (FLS), and a novel adaptive fuzzy control strategy based on it is presented.

To sum up, this manuscript researches FT congestion control for the TCP/AQM network with unknown hysteresis and external disturbance. The main works are summarized as follows:

- (1) Inspired from [35], a newfangled model of TCP is established, which considers the effects of hysteresis input and exogenous disturbance. The model in this work is more general and more exact.
- (2) An adaptive FT congestion controller is constructed by combining the backstepping technique and the

radial basis function neural networks (RBFNNs) in this paper. This controller guarantees that the queue length tracks the desired queue in FT, and all the signals of the closed-loop system are SGPFs.

- (3) The classical FT control strategy requires that the nonlinear function of the controlled system must satisfy the linear growth condition or matching condition [30, 36–38]. In this article, as the nonlinear function is unknown, the studied system cannot satisfy the linear growth condition. Therefore, in the new congestion control strategy, continuity is the only requirement for nonlinear functions. Hence, this scheme is more general.

The surplus of the manuscript is summarized as follows. A network model and advance preliminaries are recommended in Section 2. The main result is shown in Section 3. Section 4 gives a simulation example. Finally, Section 5 draws a conclusion.

2. Model and Preliminaries

2.1. TCP/AQM System Model. This article, based on [35], considers the following TCP/AQM network, in which the authors takes account of external interference, and in contrast, the time-delay is neglected:

$$\left\{ \begin{array}{l} \dot{W}(t) = \frac{1}{R(t)} (1 - p(t)) - \frac{W(t)}{2} \frac{W(t - R(t))}{R(t - R(t))} p(t - R(t)), \\ \dot{q}(t) = \left\{ \begin{array}{l} -C(t) + \frac{N(t)}{R(t)} W(t) + \omega(t), q > 0 \\ \max \left\{ 0, -C(t) + \frac{N(t)}{R(t)} W(t) + \omega(t) \right\}, q = 0 \end{array} \right\}, \\ R(t) = \frac{q(t)}{C(t)} + T_p, \end{array} \right. \quad (1)$$

where $W(t) \in [0, W_{\max}]$ is the TCP window size, $q(t) \in (0, q_{\max}]$ is the queue length of the router, $R(t)$ is the round-trip time, $C(t)$, $N(t)$, and T_p are the available link capacity, the number of TCP sessions, and the propagation delay, respectively, $p \in [0, 1]$ is the probability of packet loss, and $\omega(t)$ is the external disturbance, which can be thought of as unresponsive flows.

Assumption 1. In fact, most Internet routing scenarios change over time slowly. Therefore, we suppose that the parameters $N(t)$ and $C(t)$ are fixed values [13, 39]. $N(t)$, $C(t)$, and $R(t)$ can be simply rewritten as N , C , and R .

Assumption 2. It is bounded for the external disturbance $\omega(t)$ and its derivative.

According to [40], the rate model is adopted by

$$\dot{r}(t) = \frac{\dot{\omega}(t) - r(t)\dot{R}}{R}, \quad (2)$$

with $r(t) = W(t)/R$. It is not hard to conclude that, based on (1) and (2),

$$\begin{cases} \dot{r}(t) = \frac{1}{R^2} - \frac{1}{R^2}P(t) - \frac{r^2(t)}{2}P(t) + \frac{r(t)}{R} - \frac{Nr^2(t)}{RC} - \frac{r(t)\omega(t)}{RC}, \\ \dot{q}(t) = -C + Nr(t) + \omega(t). \end{cases} \quad (3)$$

Set $x_1 = q(t)$, $x_2 = r(t)$, and $u(t) = p(t)$, and the above model can be converted to

$$\begin{cases} \dot{x}_1 = Nx_2 + \omega(t) - C, \\ \dot{x}_2 = f(x) + g(x)u(t) + \psi(x)\omega(t), \\ y = x_1, \end{cases} \quad (4)$$

where $x(t) = [x_1(t), x_2(t)]^T$ and $f(x)$ and $g(x)$ are as follows:

$$\begin{aligned} f(x) &= \frac{1}{R^2} - \frac{N}{RC}x_2 + \frac{x_2}{R}, \\ g(x) &= -\frac{1}{R^2} - \frac{1}{2}x_2^2, \\ \psi(x) &= -\frac{x_2}{RC}. \end{aligned} \quad (5)$$

2.2. Hysteresis Nonlinearity. Consider a modified Bouc–Wen hysteresis in the form of

$$H(u) = \mu_1 u + \mu_2 \iota. \quad (6)$$

It is assumed that $\text{sign}(\mu_1) = \text{sign}(\mu_2)$ and

$$\dot{\iota} = \dot{u} - \omega|\dot{u}||\iota|^{\vartheta-1} - \xi\dot{u}|\iota|^{\vartheta} = \dot{u}f(\iota, \dot{u}), \iota(t_0) = 0, \quad (7)$$

where $\omega > |\xi|$, $n > 1$, $|\iota| \leq \bar{\iota} = \sqrt[n]{1/(\omega + \xi)}$, ω is the shape and amplitude of the hysteresis, and ϑ represents the smoothness from the initial slope to the asymptote's slope. Define $f(\iota, \dot{u})$ as

$$f(\iota, \dot{u}) = 1 - \text{sign}(\dot{u})\vartheta|\iota|^{\vartheta-1}\iota - \xi|\iota|^{\vartheta}. \quad (8)$$

Remark 1. The sign of μ_1 determines the direction of hysteresis.

Assumption 3. Without losing generality, assume that $\text{sign}(\mu_1) > 0$.

Remark 2. In the process of practical application, the tracking performance of the system has been limited by the hysteresis, which even makes the system unstable. For the TCP/AQM system model (4), the authors take account of the hysteresis nonlinearity in the control system to reduce the influence of the hysteresis input on the system and realize the stability of the controlled system.

2.3. RBFNNs. RBFNNs are applied to identify the unknown nonlinear functions. The RBFNNs can be written as

$$f_m(\varsigma) = Y^T \mathbf{h}(\varsigma), \quad (9)$$

where $\varsigma \in \Omega_\varsigma \subset \mathcal{R}^q$ is the input vector, $Y = (Y_1, Y_2, \dots, Y_N)^T \in \mathcal{R}^N$ is the weight vector, $N > 1$ represents the number of RBFNNs nodes, and $\mathbf{h}(\varsigma) = [\mathbf{h}_1(\varsigma), \mathbf{h}_2(\varsigma), \dots, \mathbf{h}_N(\varsigma)]^T \in \mathcal{R}^N$ denotes the basis function vector. Select the Gaussian basis function $\mathbf{h}_i(\varsigma)$ as follows:

$$\mathbf{h}_i(\varsigma) = \exp\left[-\frac{(\varsigma - \kappa_i)^T(\varsigma - \kappa_i)}{\nu^2}\right], \quad i = 1, 2, \dots, N, \quad (10)$$

where ν is the width of the Gaussian function and $\kappa_i = [\kappa_{i1}, \dots, \kappa_{iq}]$ is the center of the receptive field.

Lemma 1 (see [41]). *Define a continuous function $f(\varsigma)$ on a compact set Ω . Then, for $\forall \varepsilon > 0$, the following holds:*

$$f(\varsigma) = Y^*{}^T \mathbf{h}(\varsigma) + \varepsilon(\varsigma), \quad (11)$$

where

$$\Phi = \arg \min_Y \left[\sup_{\varsigma \in \Omega} |f(\bar{\varsigma}) - Y^T \mathbf{h}(\varsigma)| \right], \quad \varepsilon(\varsigma) \leq \varepsilon. \quad (12)$$

Definition 1 (see [42]). Consider the following system:

$$\dot{\varphi} = f(\varphi), \quad (13)$$

where φ represents the state vector. The origin of system (13) is SGPFS if all $\varphi(t_0) = \varphi_0$, and there exist $\delta > 0$ and a setting time $0 < T(\varphi_0, \delta) < \infty$ such that $\|\varphi(t)\| \leq \delta$ when $t \geq t_0 + T$.

Assumption 4. There exists an unknown constant $b_2 > 0$ such that

$$b_2 \leq |g(x)|. \quad (14)$$

Lemma 2 (see [43]). *For any real variables x_0 and y_0 and constants $\iota > 0$, $\xi > 0$, and $\mu > 0$, the following inequality is satisfied:*

$$|\phi|^\xi |\psi|^\xi \leq \frac{1}{1+\xi} \mu |\phi|^{1+\xi} + \frac{\xi}{1+\xi} \mu^{1/\mu} |\psi|^{1+\xi}. \quad (15)$$

Lemma 3 (see [41]). *For any real number $l_i, i = 1, 2, \dots, n$, when $\zeta \in (0, 1)$ and $\lambda \in (0, 2)$, it holds*

$$\begin{aligned} (|l_1| + \dots + |l_n|)^\zeta &\leq |l_1|^\zeta + \dots + |l_n|^\zeta, \\ (|l_1|^2 + \dots + |l_n|^2)^\lambda &\leq (|l_1|^\lambda + \dots + |l_n|^\lambda)^2. \end{aligned} \quad (16)$$

Lemma 4 (see [44]). *Consider system (13), and suppose that there is a C^1 function $V(\varphi)$ and $V(\varphi)$ with $V(0) = 0$ is positive definite on D , one has*

$$\dot{V}(\varphi) \leq -\tau V^\zeta(\varphi) + \varrho, \quad (17)$$

where $\tau > 0, 0 < \zeta < 1$, and $0 < \varrho < \infty$. Then, the trajectory of system $\dot{\varphi} = f(\varphi)$ is SGPFs.

Proof. According to equation (17), for $0 < \vartheta < 1$, the following inequality holds:

$$\dot{V}(\varphi) \leq -\vartheta \tau V^\zeta(\varphi) - (1 - \vartheta) \tau V^\zeta(\varphi) + \varrho. \quad (18)$$

Let $\Gamma_\varphi = \{\varphi \mid V^\zeta(\varphi) \leq \varrho / (1 - \vartheta) \tau\}$ and $\tilde{\Gamma}_\varphi = \{\varphi \mid V^\zeta(\varphi) > \varrho / (1 - \vartheta) \tau\}$. Discuss the following two cases:

(1) If the initial value satisfies $\varphi(t) \in \tilde{\Gamma}_\varphi$, then one has

$$\dot{V}(\varphi) \leq -\vartheta \tau V^\zeta(\varphi). \quad (19)$$

According to equation (19), it holds that

$$\int_{t_0}^T \frac{\dot{V}(\varphi)}{V^\zeta} dt \leq \int_{t_0}^T \vartheta \tau dt. \quad (20)$$

Then, we can get the following inequality:

$$\frac{1}{1 - \zeta} V^{1-\zeta}(\varphi(T)) - \frac{1}{1 - \zeta} V^{1-\zeta}(\varphi(t_0)) \leq -\vartheta \tau T. \quad (21)$$

Let

$$T_r = \frac{1}{(1 - \zeta) \vartheta \tau} \left[V^{1-\zeta}(\varphi(t_0)) - \left(\frac{\varrho}{(1 - \vartheta) \tau} \right)^{1-\zeta/\zeta} \right]. \quad (22)$$

Then, for $\forall t \geq T$, combining equations (21) and (22) can be expressed as

$$\varphi(t) \in \Gamma_\varphi. \quad (23)$$

(2) If the initial value satisfies $\varphi(t) \in \Gamma_\varphi$, then according to the first case, the trajectory of $\varphi(t)$ does not exceed Γ_φ . Then, it can be obtained that there exists $T_r < \infty$, $\forall t \geq T$, such that $\varphi(t) \in \Gamma_\varphi$. That is, the solution of the nonlinear system $\dot{\varphi} = f(\varphi)$ is SGPFs. \square

3. Main Results

3.1. Adaptive RBFNN Controller Design. Before we begin designing, coordinate transformation is introduced as follows:

$$z_1 = x_1 - q_d, z_2 = x_2 - \alpha_1, \quad (24)$$

where α_1 is a virtual controller defined as

$$\alpha_1 = \frac{b_1}{N} \left(-\frac{1}{2a_i^2} z_i \hat{\theta}_i \hat{h}_i(Z_i)^T \hat{h}_i(Z_i) - \frac{1}{2} z_i - k_i z_i^{2\zeta-1} \right), \quad (25)$$

where $\zeta > 0, k_i > 0$, and $a_i > 0$ are design parameters and the i th RBFNN $\hat{h}_i(Z_i)$ can identify the unknown nonlinear function in the design process. Define the unknown constant $\theta_i = \|\Upsilon_i^*\|^2 / b_i$, where $\hat{\theta}_i$ is the estimation of θ_i and the estimation error is $\tilde{\theta}_i = \theta_i - \hat{\theta}_i$.

Choose the control law u , the auxiliary controller \bar{u} , and the adaptive law as follows:

$$u = \hat{e} \bar{u}, \quad (26)$$

$$\bar{u} = -\frac{1}{2a_i^2} z_i \hat{\theta}_i \hat{h}_i(Z_i)^T \hat{h}_i(Z_i) - \frac{1}{2} z_i - k_i z_i^{2\zeta-1}, \quad (27)$$

$$\dot{\hat{\theta}}_i = \frac{r_i}{2a_i^2} z_i^2 \hat{h}_i(Z_i)^T \hat{h}_i(Z_i) - \beta_i \hat{\theta}_i, \quad (28)$$

where $r_i > 0$ and $\sigma_i > 0$. We assume that $\hat{\theta}_i(t) \geq 0$ in this article, $\hat{e} = 1/\hat{\mu}_1$ is the estimation of $\hat{e} = 1/\mu_1$, and $\tilde{e} = e - \hat{e}$ is the estimated error. Select \hat{e} as

$$\dot{\hat{e}} = -\varrho z_n b_n \bar{u} - \varrho_0 \hat{e}, \quad (29)$$

where ϱ and ϱ_0 are the design constants.

Step 1: Lyapunov function candidate will be chosen as follows:

$$V_1 = \frac{1}{2} z_1^2 + \frac{b_1}{2r_1} \tilde{\theta}_1^2. \quad (30)$$

Differentiating V_1 yields

$$\dot{V}_1 = z_1 (N x_2 + \omega(t) - C - q_d) - \frac{b_1}{r_1} \tilde{\theta}_1 \dot{\hat{\theta}}_1. \quad (31)$$

Choose the function $\hat{f}_1(Z_1)$ defined by

$$\hat{f}_1(Z_1) = -C + \omega(t) - \dot{y}_d + k_1 z_1^{2\zeta-1}, \quad (32)$$

then equation (29) can be rewritten as

$$\dot{V}_1 = z_1 (\hat{f}_1 + N x_2) - \frac{b_1}{r_1} \tilde{\theta}_1 \dot{\hat{\theta}}_1 - k_1 z_1^{2\zeta}. \quad (33)$$

According to Lemma 1, RBFNN $\Upsilon_1^* \hat{h}_1(Z_1)$ can be applied to identify the unknown function $\hat{f}_1(Z_1)$. For any given $\varepsilon_1 > 0$,

$$\hat{f}_1(Z_1) = \Upsilon_1^* \hat{h}_1(Z_1) + \varepsilon_1(Z_1), |\varepsilon_1(Z_1)| \leq \varepsilon_1, \quad (34)$$

where $\varepsilon_1(Z_1)$ is the approximation error. Consequently, let $\theta_1 = \|\Upsilon_1^*\|^2 / b_1$, and one can obtain

$$\begin{aligned}
z_1 \hat{f}_1(Z_1) &= z_1 \frac{Y_1^{*T}}{\|Y_1^*\|} \|Y_1^*\| \hat{h}_1 - z_1 \delta_1 \leq \frac{b_1 z_1^2}{2a_1^2} \frac{\|Y_1^*\|^2}{b_1} \hat{h}_1^T \hat{h}_1 \\
&\quad + \frac{1}{2} a_1^2 + \frac{1}{2} b_1 z_1^2 + \frac{1}{2b_1} \varepsilon_1^2 \\
&= \frac{b_1}{2a_1^2} z_1^2 \theta_1 \hat{h}_1^T \hat{h}_1 + \frac{1}{2} a_1^2 + \frac{1}{2} b_1 z_1^2 + \frac{1}{2b_1} \varepsilon_1^2.
\end{aligned} \tag{35}$$

Combining equations (31) and (33) gives

$$\begin{aligned}
\dot{V}_1 &\leq z_1 \left(\frac{b_1}{2a_1^2} z_1^2 \theta_1 \hat{h}_1^T \hat{h}_1 + N \alpha_1 \right) + N z_1 z_2 - \frac{b_1}{r_1} \dot{\theta} \hat{\theta}_1 \\
&\quad - k_1 z_1^{2\zeta} + \frac{1}{2} a_1^2 + \frac{1}{2} b_1 z_1^2 + \frac{1}{2b_1} \varepsilon_1^2.
\end{aligned} \tag{36}$$

According to equation (24) and Assumption 4, it holds that

$$z_1 N \alpha_1 \leq -\frac{b_1}{2a_1^2} z_1^2 \tilde{\theta}_1 \hat{h}_1^T \hat{h}_1 - k_1 b_1 z_1^{2\zeta} - \frac{1}{2} b_1 z_1^2. \tag{37}$$

Combining (36) with (37) gives

$$\begin{aligned}
\dot{V}_1 &\leq \frac{b_1}{2a_1^2} z_1^2 \theta_1 \hat{h}_1^T \hat{h}_1 - \frac{b_1}{2a_1^2} z_1^2 \tilde{\theta}_1 \hat{h}_1^T \hat{h}_1 - k_1 (1 + b_1) z_1^{2\zeta} \\
&\quad + N z_1 z_2 - \frac{b_1}{r_1} \dot{\theta} \hat{\theta}_1 + \frac{1}{2} a_1^2 + \frac{1}{2b_1} \varepsilon_1^2.
\end{aligned} \tag{38}$$

Choose the adaptation law as

$$\dot{\hat{\theta}}_1 = \frac{r_1}{2a_1^2} z_1^2 \hat{h}_1(Z_1)^T \hat{h}_1(Z_1) - \beta_i \hat{\theta}_1. \tag{39}$$

According to equation (37), it holds that

$$\frac{b_1}{r_1} \dot{\theta} \hat{\theta}_1 = \frac{b_1}{2a_1^2} z_1^2 \tilde{\theta}_1 \hat{h}_1^T \hat{h}_1 - \frac{b_1 \beta_i}{r_1} \tilde{\theta}_1 \hat{\theta}_1. \tag{40}$$

It is noted that

$$\frac{b_1 \beta_i}{r_1} \tilde{\theta}_1 \hat{\theta}_1 \leq -\frac{b_1 \beta_i}{2r_1} \tilde{\theta}_1^2 + \frac{b_1 \beta_i}{2r_1} \theta_1^2. \tag{41}$$

Therefore, combining equations (38), (40), and (41) can be expressed as

$$\dot{V}_1 \leq \ell_1 + N z_1 z_2, \tag{42}$$

where

$$\ell_1 = -k_1 (1 + b_1) z_1^{2\zeta} + \frac{b_1 \beta_i}{2r_1} (-\tilde{\theta}_1^2 + \theta_1^2) + \frac{1}{2} a_1^2 + \frac{1}{2b_1} \varepsilon_1^2. \tag{43}$$

Step 2: choose a Lyapunov function candidate as

$$V_2 = V_1 + \frac{1}{2} z_2^2 + \frac{b_2}{2r_2} \tilde{\theta}_2^2 + \frac{\mu_1}{2\varrho} \tilde{e}^2. \tag{44}$$

It is that

$$\begin{aligned}
\dot{V}_2 &= \ell_1 + N z_1 z_2 - \frac{b_2}{r_2} \tilde{\theta}_2 \dot{\theta}_2 \\
&\quad - \frac{\mu_1}{\varrho} \tilde{e} \dot{\tilde{e}} + z_2 (f(x) + g(x)H(\bar{u}) + \psi(x)\omega(t) - \dot{\alpha}_1).
\end{aligned} \tag{45}$$

Establish the actual controller as

$$\bar{u} = -\frac{1}{2a_2^2} z_2 \hat{\theta}_2 \hat{h}_2(Z_2)^T \hat{h}_2(Z_2) - \frac{1}{2} z_2 - k_2 z_2^{2\zeta-1}. \tag{46}$$

According to equations and Assumption 4, one has

$$\begin{aligned}
z_2 g(x)H(\bar{u}) - \frac{\mu}{\varrho} \tilde{e} \dot{\tilde{e}} &\leq z_2 b_2 \bar{u} - z_2 b_2 \mu_1 \tilde{e} \bar{u} + z_2 b_2 \mu_2 \iota \\
&\quad - \frac{\mu_1}{\varrho} \tilde{e} (-\varrho z_2 b_2 \bar{u} - \varrho_0 \tilde{e}) \\
&\leq z_2 b_2 \bar{u} + z_2 b_2 \mu_2 \iota + \frac{\mu_1}{\varrho} \tilde{e} \tilde{e} \leq -\frac{1}{2a_2^2} z_2^2 b_2 \hat{\theta}_2 \hat{h}_2^T \hat{h}_2 \\
&\quad - \frac{1}{2} b_2 z_2^2 - k_2 b_2 z_2^{2\zeta} + \frac{1}{2} (b_2 z_2)^2 + \frac{1}{2} (\mu_2 \bar{i})^2 + \frac{\varrho_0}{2\varrho \mu_1},
\end{aligned} \tag{47}$$

where $\bar{i} = \sqrt{[n]}1/(\vartheta + \xi)$.

Now, substituting inequalities (47) into (45) results in

$$\begin{aligned}
\dot{V}_2 &\leq \ell_1 + z_2 \hat{f}_2 - \frac{1}{2a_2^2} z_2^2 b_2 \hat{\theta}_2 \hat{h}_2^T \hat{h}_2 - \frac{1}{2} b_2 z_2^2 - k_2 b_2 z_2^{2\zeta} \\
&\quad - k_2 z_2^{2\zeta} + \frac{1}{2} (\mu_2 \bar{i})^2 + \frac{\varrho_0}{2\varrho \mu_1} - \frac{b_2}{r_2} \tilde{\theta}_2 \dot{\theta}_2,
\end{aligned} \tag{48}$$

where $\hat{f}_2 = f(x) + k_2 z_2^{2\zeta} + N z_1 + \psi(x)\omega(t) + (1/2)b_2^2 z_2^2 - \dot{\alpha}_1$, which can be estimated by RBFNN $Y_2^{*T} \hat{h}_2(Z_2)$ for any given positive constant ε_2 . Similarly, let $\theta_2 = \|Y_2^*\|^2/b_2$, and one easily obtains

$$\begin{aligned}
z_2 \hat{f}_2(Z_2) &= z_2 \frac{Y_2^{*T}}{\|Y_2^*\|} \|Y_2^*\| \hat{h}_2 - z_1 \delta_2 \leq \frac{b_2 z_2^2}{2a_2^2} \frac{\|Y_2^*\|^2}{b_1} \hat{h}_2^T \hat{h}_2 \\
&\quad + \frac{1}{2} a_2^2 + \frac{1}{2} b_2 z_2^2 + \frac{1}{2b_2} \varepsilon_2^2 \\
&= \frac{b_2}{2a_2^2} z_2^2 \theta_2 \hat{h}_2^T \hat{h}_2 + \frac{1}{2} a_2^2 + \frac{1}{2} b_1 z_2^2 + \frac{1}{2b_2} \varepsilon_2^2.
\end{aligned} \tag{49}$$

Then, equation (46) can be rewritten as

$$\begin{aligned}
\dot{V}_2 \leq & \ell_1 + \frac{b_2}{2a_2^2} z_2^2 \theta_2 \hat{h}_2^T \hat{h}_2 - \frac{1}{2a_2^2} z_2^2 \hat{\theta}_2 \hat{h}_2^T \hat{h}_2 \\
& - k_2 (1 + b_2) z_2^{2\zeta} + \frac{1}{2} a_2^2 + \frac{1}{2b_2} \varepsilon_2^2 + \frac{1}{2} (\mu_2 \bar{t})^2 + \frac{\varrho_0}{2\varrho\mu_1} - \frac{b_2 \hat{\theta}_2 \dot{\hat{\theta}}_2}{r_2}.
\end{aligned} \tag{50}$$

3.2. Stability Analysis

Theorem 1. Consider system (4). Suppose Assumptions 2–4 hold, then all the signals are SGPFs, under any bounded initial conditions when controller (25) and adaptive law (28) are employed.

Proof. Choose the adaptation law as

$$\dot{\hat{\theta}}_2 = \frac{r_2}{2a_2^2} z_2^2 \hat{h}_1(Z_2)^T \hat{h}_1(Z_2) - \beta_i \hat{\theta}_2. \tag{51}$$

According to equation (49), it holds that

$$\frac{b_2}{r_2} \tilde{\theta} \hat{\theta}_2 = \frac{b_2}{2a_2^2} z_2^2 \tilde{\theta}_2 \hat{h}_2^T \hat{h}_2 - \frac{b_2 \beta_2}{r_2} \tilde{\theta}_2 \hat{\theta}_2. \tag{52}$$

It is noted that

$$\frac{b_2 \beta_2}{r_2} \tilde{\theta}_2 \hat{\theta}_2 \leq -\frac{b_2 \beta_2}{2r_2} \tilde{\theta}_2^2 + \frac{b_2 \beta_2}{2r_2} \theta_2^2. \tag{53}$$

Substituting (52) and (53) into (50), it gives

$$\begin{aligned}
\dot{V}_2 \leq & \ell_1 + \frac{b_2 \beta_2}{r_2} \tilde{\theta}_2 \hat{\theta}_2 - k_2 b_2 z_2^{2\zeta} - k_2 z_2^{2\zeta} + \frac{1}{2} (\mu_2 \bar{t})^2 \\
& + \frac{\varrho_0}{2\varrho\mu_1} + \frac{1}{2} a_2^2 + \frac{1}{2b_2} \varepsilon_2^2.
\end{aligned} \tag{54}$$

Then, we can get

$$\begin{aligned}
\dot{V}_2 \leq & -\sum_{i=1}^2 k_i (1 + b_i) z_i^{2\zeta} + \frac{b_1 \beta_1}{2r_1} (-\tilde{\theta}_1^2 + \theta_1^2) \\
& + \frac{b_2 \beta_2}{2r_2} (-\tilde{\theta}_2^2 + \theta_2^2) + \frac{1}{2} \left(a_1^2 + \frac{1}{b_1} \varepsilon_1^2 \right) \\
& + \frac{1}{2} \left(a_2^2 + \frac{1}{b_2} \varepsilon_2^2 \right) + \frac{1}{2} (\mu_2 \bar{t})^2 + \frac{\varrho_0}{2\varrho\mu_1}.
\end{aligned} \tag{55}$$

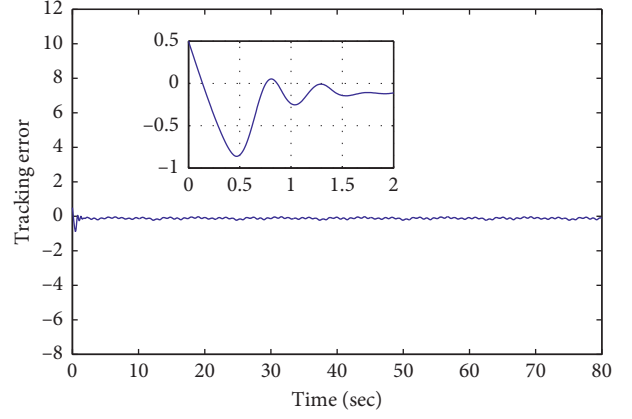


FIGURE 1: Tracking error $q(t) - q_d$.

Let $k_{\min} = \min_{1 \leq i \leq 2} \{k_i (1 + b_i)\}$, and by Lemma 3, it is deduced that

$$-\sum_{i=1}^2 k_i (1 + b_i) z_i^{2\zeta} \leq -k_{\min} \sum_{i=1}^2 z_i^{2\zeta} \leq -\bar{K} \left(\frac{1}{2} \sum_{i=1}^2 z_i^2 \right)^\zeta, \tag{56}$$

where $\bar{K} = 2^\zeta k_{\min}$.

Let $\beta_{\min} = \min_{1 \leq i \leq 2} \{\beta_i\}$, and by taking equation (54) into account, inequality (55) can be rewritten as

$$\begin{aligned}
\dot{V}_2 \leq & -\bar{K} \left(\frac{1}{2} \sum_{i=1}^2 z_i^2 \right)^\zeta - \beta_{\min}^\zeta \left(\sum_{i=1}^2 \frac{b_i}{2r_i} \tilde{\theta}_i^2 \right)^\zeta + \left(\sum_{i=1}^2 \frac{b_i \beta_i}{2r_i} \tilde{\theta}_i^2 \right)^\zeta \\
& + \frac{b_1 \beta_1}{2r_1} (-\tilde{\theta}_1^2 + \theta_1^2) + \frac{b_2 \beta_2}{2r_2} (-\tilde{\theta}_2^2 + \theta_2^2) \\
& + \frac{1}{2} \left(a_1^2 + \frac{1}{b_1} \varepsilon_1^2 \right) + \frac{1}{2} \left(a_2^2 + \frac{1}{b_2} \varepsilon_2^2 \right) + \frac{1}{2} (\mu_2 \bar{t})^2 + \frac{\varrho_0}{2\varrho\mu_1} \leq -\lambda V^\zeta \\
& + \left(\sum_{i=1}^2 \frac{b_i \beta_i}{2r_i} \tilde{\theta}_i^2 \right)^\zeta + \frac{b_1 \beta_1}{2r_1} (-\tilde{\theta}_1^2 + \theta_1^2) + \frac{b_2 \beta_2}{2r_2} (-\tilde{\theta}_2^2 + \theta_2^2) \\
& + \frac{1}{2} \left(a_1^2 + \frac{1}{b_1} \varepsilon_1^2 \right) \\
& + \frac{1}{2} \left(a_2^2 + \frac{1}{b_2} \varepsilon_2^2 \right) + \frac{1}{2} (\mu_2 \bar{t})^2 + \frac{\varrho_0}{2\varrho\mu_1},
\end{aligned} \tag{57}$$

where $\lambda = \min\{\bar{K}, \beta_{\min}^\zeta\}$.

By Lemma 2, let $\mu = \zeta, \rho = 1 - \zeta, \lambda = \zeta^{-1}, \phi = \sum_{i=1}^2 b_i \beta_i / 2r_i \tilde{\theta}_i^2$, and $\psi = 1$, then we get

$$\left(\sum_{i=1}^2 \frac{b_i \beta_i}{2r_i} \tilde{\theta}_i^2 \right)^\zeta \leq \sum_{i=1}^2 \frac{b_i \beta_i}{2r_i} \tilde{\theta}_i^2 + (1 - \zeta) \zeta^{\zeta/(1-\zeta)}. \tag{58}$$

Then, equation (55) becomes

$$\dot{V}_2 \leq -\lambda V^\zeta + \varrho, \tag{59}$$

where $\varrho = (1 - \zeta) \zeta^{\zeta/(1-\zeta)} + \sum_{i=1}^2 b_i \beta_i / 2r_i \theta_i^2 + (1/2) (a_1^2 + (1/b_1) \varepsilon_1^2) + (1/2) (a_2^2 + (1/b_2) \varepsilon_2^2) + (1/2) (\mu_2 \bar{t})^2 + \varrho_0 / 2\varrho\mu_1$.

Define a positive constant ϑ as follows:

$$\vartheta = \frac{\varrho}{(1 - \theta_0)\lambda}. \quad (60)$$

Equation (57) can be expressed as

$$V^\zeta(z(t), \bar{\theta}(t)) \leq \frac{\varrho}{(1 - \theta_0)\lambda}. \quad (61)$$

For $t \geq T_{\text{reach}}$, let

$$T_{\text{reach}} = \frac{1}{(1 - \theta_0)\lambda} \left[V^{1-\zeta}(z(0), \bar{\theta}(0)) - \left(\frac{\varrho}{(1 - \theta_0)\lambda} \right)^{1-\zeta/\zeta} \right], \quad (62)$$

with $z(0) = [z_1(0), z_2(0)]^T$ and $\bar{\theta}(0) = [\theta_1(0), \theta_2(0)]^T$.

Therefore, all the signals are SGPFs.

Then, for $t \geq T_{\text{reach}}$, we can obtain that

$$|y - q_d| \leq 2 \left(\frac{\varrho}{(1 - \theta_0)\lambda} \right)^{1/2\zeta}. \quad (63)$$

Then, the proof is completed. \square

4. Simulation Example

In this section, to certify the feasibility of the strategy presented in this work, a simulation example is given by MATLAB.

Select the system parameters and external disturbance in system (4) as

$$\begin{aligned} N &= 1, R = 6s, C = 2.5 \text{ packets/s}, \\ a_1 &= 0.3, a_2 = 2, k_1 = k_2 = 0.1, \\ r_1 &= r_2 = 20, \beta_1 = 0.08, \beta_2 = 0.2, \\ \omega &= 0.5e^{-0.5t} \sin(6t). \end{aligned} \quad (64)$$

Define the hysteresis $H(u)$ as follows:

$$H(u) = \mu_1 u + \mu_2 \iota, \quad (65)$$

where $\mu_1 = 10$ and $\mu_2 = 0.5$. ι is selected as equation (8). The function $f(\iota, \dot{\iota})$ is selected as equation (7).

The initial values of the state are $\vartheta = 2$, $\xi = 1$, and $n = 3$; $y(0) = 0.5$.

The results of simulation are shown in Figures 1–6. Figure 1 shows the tracking error of $q(t)$ and q_d . It is clear that the queue can track the desired queue within the allowable error. Figure 2 introduces the hysteresis output $H(u)$. Besides, Figures 3 and 4 show the trajectory of the adaptive law, from which we can obtain that all the adaptive laws are SGPFs. Figure 5 shows the trajectory of the rate $r(t)$. As a result, the proposed strategy is effective.

In addition, in order to illustrate the advantages of this algorithm, the simulation comparisons are made between the method in this paper and the random early detection (RED) algorithm. The comparison result is shown in Figure 6, in which the preset properties with respect to $q(t) - q_d$ are obtained. Moreover, it should be pointed out that the maximum overshoot of $q(t) - q_d$ is less than 0.8. Further, it

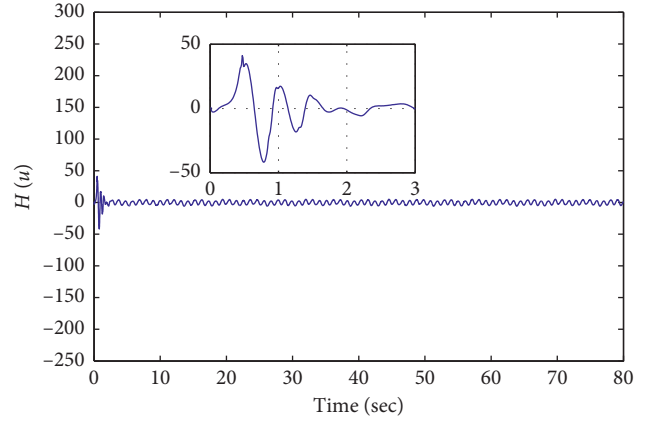


FIGURE 2: The hysteresis output $H(u)$.

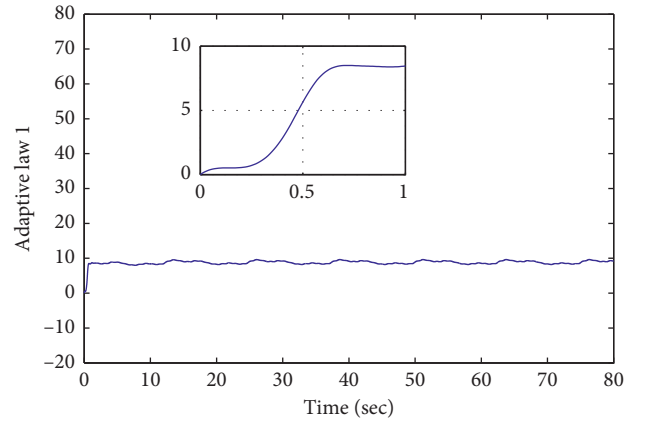


FIGURE 3: The trajectory of the adaptive law 1.

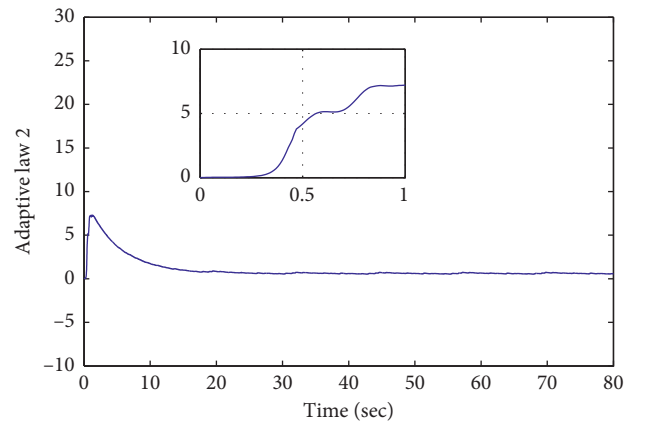


FIGURE 4: The trajectory of the adaptive law 2.

is easy to observe from Figure 6 that the smaller overshoot and the less chattering are achieved comparing with RED algorithm. As a result, the proposed method has the better performances.

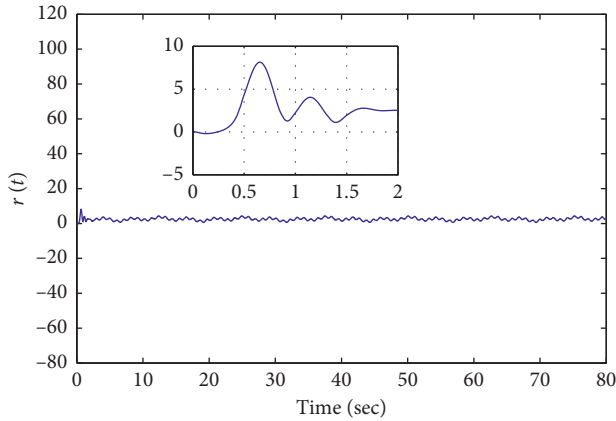


FIGURE 5: The sending rate $r(t)$.

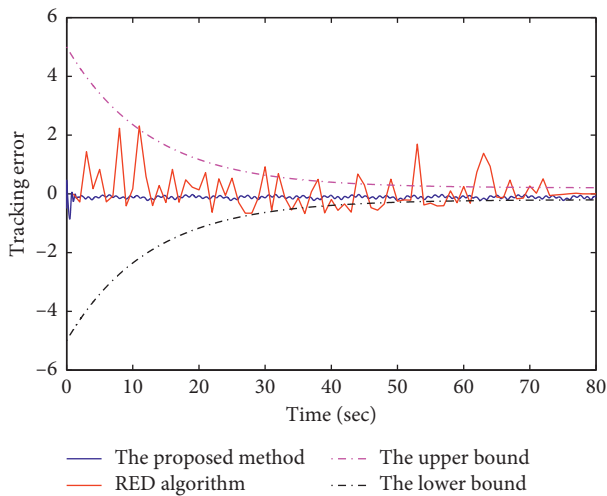


FIGURE 6: The comparison results with the tracking error.

5. Conclusion

In this manuscript, an adaptive FT control is considered for TCP/AQM networks. The finite-time controller by using the backstepping technique and the adaptive neural control method ensures that the queue length tracks the desired queue length and the tracking error converges to the prescribed area. Besides, the controller can not only reduce the influence of the disturbance, but also shorten the impression of uncertainty. Finally, an example is offered to verify the superiority and effectiveness.

Data Availability

The raw data supporting the conclusions of this article will be made available by the authors, without undue reservation, to any qualified researcher.

Conflicts of Interest

The authors declare that there are no conflicts of interest regarding the publication of this paper.

Acknowledgments

This research work was supported financially by the National Natural Science Foundation of China (Grant no. 11974373).

References

- [1] K. Wang, Y. Liu, X. Liu, Y. Jing, and G. M. Dimirovski, "Study on TCP/AQM network congestion with adaptive neural network and barrier Lyapunov function," *Neurocomputing*, vol. 363, pp. 27–34, 2019.
- [2] V. Jacobson, "Congestion avoidance and control," *ACM SIGCOMM Computer Communication Review*, vol. 18, no. 4, pp. 314–329, 1988.
- [3] B.-M. Laps and L. Larry, "TCP Vegas: end-to-end congestion avoidance on a global Internet," *IEEE Journal on Selected Areas in Communications*, vol. 13, pp. 1465–1480, 1995.
- [4] M. Mathis, J. Mahdavi, S. Floyd et al., "TCP selective acknowledgment options," *RFC*, vol. 2018, 1996.
- [5] S. Floyd and T. Henderson, "The new reno modification to TCPs fast recovery algorithm," *RFC*, vol. 2582, 1999.
- [6] B. Braden and D. Clark, "Recommendations on queue management and congestion avoidance in the Internet," *RFC*, vol. 2309, 1998.
- [7] S. Floyd and V. Jacobson, "Random early detection gateways for congestion avoidance," *IEEE/ACM Transactions on Networking*, vol. 1, no. 4, pp. 397–413, 1993.
- [8] G. Feng, A. K. Agarwal, A. Jayaraman, and C. K. Siew, "Modified RED gateways under bursty traffic," *IEEE Communications Letters*, vol. 8, no. 5, pp. 323–325, 2004.
- [9] F. Anjum and L. Tassiulas, "Fair bandwidth sharing among adaptive and non-adaptive flows in the internet," *IEEE*, vol. 8, pp. 1412–1420, 1999.
- [10] V. Misra, W. B. Gong, and D. Towsley, "Fluid-based analysis of a network of AQM routers supporting TCP flows with an application to RED," *IEEE*, vol. 51, pp. 151–160, 2000.
- [11] L. Tan, W. Zhang, G. Peng, and G. Chen, "Stability of TCP/RED systems in AQM routers," *IEEE Transactions on Automatic Control*, vol. 51, pp. 393–1398, 2006.
- [12] J. Sun, K. Ko, G. Chen, S. Chan, and M. Zukerman, "PD-RED: to improve the performance of RED," *IEEE Communications Letters*, vol. 7, pp. 406–408, 2003.
- [13] C. Holot, V. Misra, D. Towsley, and W. Gong, *On Designing Improved Controllers for AQM Routers Supporting TCP Flows*, pp. 1726–1734, Springer, Anchorage, AK, USA, 2001.
- [14] T. Wei and S. Zhang, "AQM algorithm based on nonlinear control method," *Journal of Communication*, vol. 30, pp. 58–67, 2009.
- [15] C.-K. Chen, Y.-C. Hung, T.-L. Liao, and J.-J. Yan, "Design of robust active queue management controllers for a class of TCP communication networks," *Information Sciences*, vol. 177, no. 19, pp. 4059–4071, 2007.
- [16] L.-S. Tan, C. Yuan, and M. Zukerman, "A price-based Internet congestion control scheme," *IEEE Communications Letters*, vol. 12, pp. 331–333, 2008.
- [17] W. Zhang, L. Tan, and G. Peng, "Dynamic queue level control of TCP/RED systems in AQM routers," *Computers & Electrical Engineering*, vol. 35, no. 1, pp. 59–70, 2009.
- [18] W. Zhang, L. Tan, C. Yuan, G. Chen, and F. Ge, "Internet primal-dual congestion control: stability and applications," *Control Engineering Practice*, vol. 21, no. 1, pp. 87–95, 2013.
- [19] Y. Liu, X. Liu, Y. Jing, and S. Zhou, "Adaptive backstepping H ∞ tracking control with prescribed performance for internet congestion," *ISA Transactions*, vol. 72, pp. 92–99, 2018.

- [20] D. Ghosh, K. Jagannathan, and G. Raina, "Right buffer sizing matters: some dynamical and statistical studies on Compound TCP," *Performance Evaluation*, vol. 139, p. 102095, 2020.
- [21] R. K. Chaturvedi and S. Chand, "Optimal load balancing linked increased algorithm for multipath TCP," *Wireless Personal Communications*, vol. 111, no. 3, pp. 1505–1524, 2019.
- [22] J. Zhao, J.-C. Liu, H.-Y. Wang, and C. Xu, "Measurement, analysis, and enhancement of multipath TCP energy efficiency for datacenters," *IEEE Transactions on Automatic Control*, vol. 28, pp. 57–70, 2019.
- [23] G. Tao and P. V. Kokotovic, "Adaptive control of plants with unknown hystereses," *IEEE Transactions on Automatic Control*, vol. 40, no. 2, pp. 200–212, 1995.
- [24] J.-S. Pan, C.-Y. Lee, A. Sghaier, M. Zeghid, and J. Xie, "Novel systolization of subquadratic space complexity multipliers based on toeplitz matrix-vector product approach," *IEEE Transactions on Very Large Scale Integration (VLSI) Systems*, vol. 27, no. 7, pp. 1614–1622, 2019.
- [25] J. Zhou, C. Wen, and T. Li, "Adaptive output feedback control of uncertain nonlinear systems with hysteresis nonlinearity," *IEEE Transactions on Automatic Control*, vol. 57, no. 10, pp. 2627–2633, 2012.
- [26] C.-Y. Su, Y. Stepanenko, J. Svoboda, and T. P. Leung, "Robust adaptive control of a class of nonlinear systems with unknown backlash-like hysteresis," *IEEE Transactions on Automatic Control*, vol. 45, no. 12, pp. 2427–2432, 2000.
- [27] X. Liu, Y. Li, and Y. Li, "Adaptive tracking control for a class of uncertain switched stochastic nonlinear systems," *IEEE Transactions on Automatic Control*, vol. 2019, p. 33, 2019.
- [28] F. Wang, Z. Liu, Y. Zhang, and C. L. P. Chen, "Adaptive fuzzy control for a class of stochastic pure-feedback nonlinear systems with unknown hysteresis," *IEEE Transactions on Fuzzy Systems*, vol. 24, no. 1, pp. 140–152, 2016.
- [29] P. Dorato, *An Overview of Finite-Time Stability*, pp. 185–194, Springer, Boston, MA, USA, 2006.
- [30] S. P. Bhat and D. S. Bernstein, "Finite-time stability of continuous autonomous systems," *SIAM Journal on Control and Optimization*, vol. 38, no. 3, pp. 751–766, 2000.
- [31] W. Lv, F. Wang, and Y. Li, "Finite-time adaptive fuzzy output-feedback control of MIMO nonlinear systems with hysteresis," *Neurocomputing*, vol. 296, pp. 74–81, 2018.
- [32] S. P. Bhat and D. S. Bernstein, "Continuous finite-time stabilization of the translational and rotational double integrators," *IEEE Transactions on Automatic Control*, vol. 43, no. 5, pp. 678–682, 1998.
- [33] L. Zou, Z. Wang, H. Gao, and F. E. Alsaadi, "Finite-horizon consensus control of time-varying multiagent systems with stochastic communication protocol," *IEEE Transactions on Cybernetics*, vol. 47, no. 8, pp. 1830–1840, 2017.
- [34] F. Wang, B. Chen, X. Liu, and C. Lin, "Finite-time adaptive fuzzy tracking control design for nonlinear systems," *IEEE Transactions on Fuzzy Systems*, vol. 26, no. 3, pp. 1207–1216, 2018.
- [35] A. Elham and S. M. Vahid, *Robust Congestion Control for TCP/AQM Using Integral Backstepping Control*, pp. 1840–1844, IEEE, New York, NY, USA, 2015.
- [36] V. Nekoukar and A. Erfanian, "Adaptive fuzzy terminal sliding mode control for a class of MIMO uncertain nonlinear systems," *Fuzzy Sets and Systems*, vol. 179, no. 1, pp. 34–49, 2011.
- [37] H. Liu and T. Zhang, "Neural network-based robust finite-time control for robotic manipulators considering actuator dynamics," *Robotics and Computer-Integrated Manufacturing*, vol. 29, no. 2, pp. 301–308, 2013.
- [38] H. Liu and T. Zhang, "Adaptive neural network finite-time control for uncertain robotic manipulators," *Journal of Intelligent & Robotic Systems*, vol. 75, no. 3–4, pp. 363–377, 2014.
- [39] Y. Cui, M. Fei, and D. Du, "Design of a robust observer-based memoryless H_∞ control for internet congestion," *International Journal of Robust and Nonlinear Control*, vol. 26, no. 8, pp. 1732–1747, 2016.
- [40] L.-X. Wang and J. M. Mendel, "Fuzzy basis functions, universal approximation, and orthogonal least-squares learning," *IEEE Transactions on Neural Networks*, vol. 3, no. 5, pp. 807–814, 1992.
- [41] C. Qian and W. Lin, "Non-Lipschitz continuous stabilizers for nonlinear systems with uncontrollable unstable linearization," *Systems & Control Letters*, vol. 42, no. 3, pp. 185–200, 2001.
- [42] Z. Zhu, Y. Xia, and M. Fu, "Attitude stabilization of rigid spacecraft with finite-time convergence," *International Journal of Robust and Nonlinear Control*, vol. 21, no. 6, pp. 686–702, 2011.
- [43] S. Yu, X. Yu, B. Shirinzadeh, and Z. Man, "Continuous finite-time control for robotic manipulators with terminal sliding mode," *Automatica*, vol. 41, no. 11, pp. 1957–1964, 2005.
- [44] W.-S. Lv and F. Wang, "Finite-time adaptive fuzzy tracking control for a class of nonlinear systems with unknown hysteresis," *International Journal of Robust and Nonlinear Control*, vol. 2, pp. 1–9, 2017.

Research Article

Decisions and Coordination in a Capacity Sharing Supply Chain considering Production Cost Misreporting

Daozhi Zhao  and Hongshuai Han 

College of Management and Economics, Tianjin University, Tianjin, China

Correspondence should be addressed to Hongshuai Han; hshan@tju.edu.cn

Received 23 April 2020; Revised 10 June 2020; Accepted 22 June 2020; Published 27 July 2020

Guest Editor: Baogui Xin

Copyright © 2020 Daozhi Zhao and Hongshuai Han. This is an open access article distributed under the Creative Commons Attribution License, which permits unrestricted use, distribution, and reproduction in any medium, provided the original work is properly cited.

In the manufacturing capacity sharing platform, considering the manufacturing capacity provider's cost misreporting behavior and the collusion behavior of the platform operator, this paper built a supply chain consisting of a platform operator, a capacity provider with surplus capacity, and a manufacturer with insufficient capacity. This paper studied the influence of the cost misreporting behavior on the supply chain members' decisions and profits. By use of the game theory, in the scenarios including the supplier misreporting to other supply chain members and the supplier colluding with the platform, the paper analyzed the optimal pricing decision, misreporting coefficient decision, and platform's service fee decision and further compared the profits of the supply chain and its members. The results show that the capacity provider tends to overstate the production cost for gaining more profits, which exerts negative effects on profits of other members and the supply chain. Compared with the case of misreporting to both the manufacturer with insufficient capacity and the platform, the case of colluding with platform is more favorable to the profits of the manufacturer, the platform, and the supply chain, while the supplier prefers to choose the former situation. When the sales revenue-sharing proportion, cost-sharing proportion, and service fee satisfy certain conditions, the sales revenue-sharing and cost-sharing contract can avoid the capacity provider's cost misreporting behavior and coordinate the supply chain.

1. Introduction

In recent years, with the development of the Internet of Things (IoT), big data, cloud computing, and other technologies, sharing economy has attracted extensive attention. The manufacturing industry is also undergoing a radical transformation driven by the IoT-related technologies and business innovation. An increasing number of intermediary manufacturing capacity sharing platforms have arisen to integrate fragmented manufacturing capacity from enterprises with surplus capacities in a sharable resource pool and provide manufacturing services to manufacturers or retailers with inadequate capacity, for example, Thomas platform in the United States, CASICloud platform, and Tao factory in China. The intermediary manufacturing capacity sharing platform offers an effective manufacturing solution to facilitate the match between capacity supply and demand,

improving the utilization rate of capacities and expediting transaction processes. Participants of the platform are able to easily provide or obtain manufacturing service through online sharing platforms. In this paper, we consider a supply chain (SC) composed of a platform operator, a capacity provider with surplus capacity, and a manufacturer with insufficient capacity. We focus on investigating the influence of manufacturing cost misreporting behavior of the capacity provider on the SC members' decisions and profits and further strive to propose a contract to avoid the cost misreporting behavior and coordinate the SC.

It is worth noting that the intermediary manufacturing capacity platform has dual attributes, i.e., the attribute of marketplace and the attribute of enterprise. On the one hand, the platform, as the online trading place of capacity sharing transactions and the maker of trading rules, should be safe, fair, and stable. The platform operator should

regulate the participants' operations to ensure orderly and fair competition in the platform and facilitate the sharing transaction. However, since the number of participants in the platform is continuously increasing, it is difficult for the platform to grasp all the information on capacities of participants. There is an opportunity for participants to take advantage of their information for seeking more benefits. For example, in the Tao Factory platform of China, although the platform's in-depth factory inspection service can enable the manufacturing capacity requestor have a comprehensive understanding of the production line, warehousing, and quality control capabilities of the capacity provider, the capacity requestor still cannot accurately grasp the manufacturing cost information of the capacity provider due to the difficulty in real-time supervision of the whole manufacturing process. Since many suppliers misreport their cost to charge an excessively high price, the Alibaba group takes measures to punish suppliers for their false quotation, according to the rules of the website. In the platform, the capacity provider may have three choices on the cost information: disclosing the real cost information, misreporting the cost information, or hiding the cost information. In this paper, we consider the scenario that the capacity provider misreports the cost information and examine its influence on the decision-making process.

On the other hand, the platform is also a profit-oriented enterprise. It may conceal certain information or collude with participating companies for the purpose of pursuing benefits. With the rapid expansion of the capacity sharing platform, the highly clustered platform is more likely to breed opportunistic behavior such as misreporting information. For example, the Tao factory platform will offer the order supervision service to the capacity requestor that orders a quantity of more than 100 pieces. The order supervisor will help the requestor find a more appropriate capacity provider and monitor the production process to guarantee the product quality and delivery time. Since order supervisors from different places know well the capacity providers in their nearby regions, respectively, the platform will assign a proper order supervisor for the capacity requestor according to their requirements on the location of the capacity provider. Order supervisors may help the capacity providers misreport information to attain more benefits because they usually have long-term cooperative relationships with capacity providers in their vicinity. If this collusion behavior can also bring higher benefits to the platform, the platform may also connive at this behavior. This will cause potential loss for the capacity requestor and disturb the orderly and fair transaction in the platform.

Therefore, we consider three scenarios in this paper, i.e., the capacity provider reporting real cost information; the capacity provider misreporting cost information without being noticed by both the capacity provider and the platform operator; the capacity provider misreporting cost information with the acquiescence of the platform operator. We investigate the pricing decisions and profits of SC members under each scenario. Through comprehensive analysis on the equilibrium results, we analyze the impact of the capacity provider's cost misreporting and the platform operator's

acquiescence. Finally, we propose the contract to incentivize the capacity provider to disclose the real cost information and coordinate the SC. The contributions of this research are threefold. First, we take the cost misreporting behavior into account in the context of capacity sharing through platform. Second, we investigate the impact of the platform operator's acquiescence on decisions and provide insights on platform governance. Third, we propose a coordination contract for the capacity sharing SC to avoid the cost misreporting behavior.

The remainder of this paper is organized as follows. Section 2 reviews the literature. Section 3 formulates the models and derives and compares the equilibrium outcomes. Section 4 proposes the coordination contracts for the SC. Section 5 gives numerical analysis. Section 6 presents conclusions.

2. Literature Review

This research is highly related to three areas of literature: manufacturing capacity sharing platform, cost information asymmetry and SC coordination. We review them in the following sections.

2.1. Manufacturing Capacity Sharing Platform. Although great attention has been paid on capacity sharing between enterprises, most previous studies have focused on capacity sharing among enterprises without the online platform. For example, Renna and Argoneto [1] studied the cooperation mechanism of capacity sharing among factories based on game theory and evaluated the benefits of this mechanism under different market conditions and capacity conditions. With the goal of cost minimization, Moghaddam and Nof [2] proposed an optimal matching mechanism for sharing demand and capabilities among enterprises in the supply network. Moghaddam and Nof [3] further proposed a real-time optimization and control mechanism for demand and capacity sharing among enterprises. Yu et al. [4] studied the circumstances under which capacity sharing among independent companies is advantageous and proposed a cost-sharing mechanism to ensure the stability of the capacity sharing alliance in the queuing system. Guo and Wu [5] studied capacity sharing among competitors under contracts considering before and after the decision-making on capacity sharing prices. Qin et al. [6] studied the design of revenue-sharing contract under capacity sharing between two companies with horizontal competition. Zeng et al. [7] studied the cooperation of service providers based on capability sharing in the queuing system and proposed a cost-sharing mechanism that can encourage providers to reach cooperation based on the principles of fairness and easy implementation. Although these studies investigate matching mechanisms, cost-sharing mechanisms, and cooperative game between manufacturers, their researches pay attention to the game problems between the supply and demand sides of the manufacturing capacity, without incorporating the decision-making process of platform operators and opportunistic behaviors of capacity providers.

With the vigorous development of the sharing economy, an increasing number of scholars began to pay attention to sharing platforms, such as housing sharing platform [8], vehicle sharing platform [9], car-hailing platform [10], and personal to personal product sharing platform [11–13]. Although these platforms are similar to manufacturing capacity sharing platforms in the nature of sharing, manufacturing capacity sharing platforms connects manufacturing enterprises with relatively greater complexity than individuals. This puts forward higher requirements for analyzing the behaviors and decisions of the platform operator. The intermediary manufacturing capacity platform highlighted in our paper can gather scattered manufacturing resources and reduce the difficulties for firms in finding sufficient manufacturing capacity or utilizing the idle capacities. Moreover, the platform has mastered a large amount of transaction data, enabling the platform to take advantage of big data to increase the added value of participants. For example, it can help the factory to integrate upstream and downstream resources and provide more flexible services. The platform offers the order processing supervision services to ensure the product quality and the timely delivery. In contrast, the traditional capacity sharing among enterprises suffers the lack of assistance and supervision in capacity transaction. However, the platform, as an enterprise, has the nature of pursuing profits, in which opportunistic behaviors may occur.

In terms of research on manufacturing capacity sharing platforms, Aloui and Jebli [14] studied the optimal capacity sharing strategy between two different but interdependent consumers on the platform, pointing out that the optimal strategy depends on the level of bilateral participation and externalities between them. Li et al. [15] studied the sharing and scheduling problem of decentralized manufacturing resources and proposed an optimization algorithm based on multiagent. As a kind of manufacturing capacity sharing platform, i.e., cloud manufacturing platform has attracted the attention of many scholars. Ren et al. [16], Adamson et al. [17], and Yang et al. [18] have deeply discussed the concept, characteristics, and industry applications of cloud manufacturing platforms. These studies conceptually explained the functional characteristics of the cloud manufacturing platform. Argoneto and Renna [19] proposed a cloud manufacturing capacity sharing framework based on cooperative games and fuzzy theory, which showed that this allocation strategy can enable enterprises to faithfully report their demand information. Tao et al. [20] proposed a manufacturing service supply and demand matching system in the cloud environment. Based on cloud design and cloud computing, Thekinen and Panchal [21] provide matching services for providers and demanders including services and products.

Most of the abovementioned studies on the capacity sharing platform have focused on the capacities and resources matching and optimization in the manufacturing platform, considering the intermediary role of the platform. Some studies explain the role of the capacity sharing platform from a theoretical framework. Few studies have considered the opportunistic behavior of participating

companies and the platform operator. This paper focuses on the influence of capacity providers' misreporting of cost information and collusion with the platform operator on decisions and profits of SC members.

2.2. Cost Information Asymmetry. In the traditional supply chain without the consideration of sharing platform, the problem of cost information asymmetry has been studied by many scholars. Scholars mainly focus on how to design contracts to encourage SC members to share real information when the owner conceals the cost information or discloses the false cost information. For example, Xu et al. [22] studied the impact of the emergency supplier with private cost information on the performance of primary suppliers and manufacturers and pointed out that a combined contract including lead time and transfer payment can encourage emergency suppliers to report real cost information. Çakanyildirim et al. [23] investigated how retailers design profit-sharing contracts to achieve supply chain coordination when the production cost is private information. Cao et al. [24] studied the design of the optimal wholesale price contract considering the private cost information of retailers in the dual-channel supply chain. Kayış et al. [25] discussed whether the manufacturer directly purchases from the second-level supplier or delegates the first-level supplier to purchase under cost information asymmetry. Lei et al. [26] explored the game between suppliers with private production cost information and retailers facing inventory inaccuracy issues and designed a revenue-sharing contract to coordinate the supply chain.

Ma et al. [27] investigated decisions and profits of supply chain members under the wholesale price contract and the two-part tariff contract when the cost of social responsibility input is private information. Wang et al. [28] studied the production and pricing decisions of an assembly system composed of a single manufacturer and two complementary suppliers and analyzed the value of production cost information sharing. Dai et al. [29] focused on the information-sharing strategies of manufacturers with private production cost information when facing competitive retailers in different market competition environments and found that the optimal strategy is related to the degree of competition, the return cost, and the relationship between the retailer's estimated and real production costs. In these literature, most researchers considered that other members of the supply chain will predict the cost information or offer different contracts to identify high or low-cost types. Yan et al. [30] studied the impact of manufacturers' misreporting cost information on decision-making and profits when there is a competition between two manufacturers and between manufacturers and retailers.

They analyzed the value of cost information sharing, the impact of cost misreporting, and further studied the design of incentive mechanisms for gaining real information, which provides insights into the mechanism design to avoid cost misreporting in this paper. Since they do not involve the participation of the capacity sharing platform, they do not consider the impact of misreporting on platform operator's

service fee decision and profits and not involve in the situation where the platform may acquiesce to the cost misreporting. Thereby, mechanism design with the participation of platform operator is not discussed.

2.3. SC Coordination. A large number of researches have been done on SC coordination. Revenue-sharing or revenue and cost-sharing contract has been widely adopted by many researchers. To cite a few in recent years, Hu and Feng [31] investigate the optimization of a supply chain under both supply and demand uncertainty and propose the revenue-sharing contract and service requirement to coordinate the supply chain and further give conditions of achieving coordination. Xie et al. [32] propose the revenue and cost-sharing contract to coordinate a dual-channel closed-loop supply chain and increase the retailer's efforts regarding servicing and recycling. Su et al. [33] propose a cost profit-sharing contract to coordinate a closed-loop supply chain with third-party recycling, taking environmental protection factors into account. Jian et al. [34] design a revenue-sharing contract to coordinate a supply chain with competing manufacturers, considering the manufacturer's peer-induced fairness concern model and the manufacturer's distributional fairness concern model.

Coordination of SC under cost information asymmetry has also attracted the attention of researchers. For example, Wang et al. [35] propose an innovative coordination contract including the trading quantity, the transfer payment, and the profit allocation rules to coordinate a supply chain under asymmetric information on manufacturing cost and degree of risk aversion. Wang et al. [36] propose the collaboration mechanism consisting of the order quantity and the innovative transfer payment under production cost information asymmetry. Liu et al. [37] propose a coordination mechanism for a corporate social responsibility-sensitive supply chain to inspire the supplier to reveal the true corporate social responsibility cost information and to improve the performance of the supply chain.

The abovementioned literature on SC coordination mostly focuses on the supply chain without the third-party platform. They provide guidance for us to design coordination contracts as well as the avoidance mechanism of cost misreporting behavior. The main difference of this paper with them is in that the incorporation of the service fee decision and the possible acquiescence of the platform in our decision-making and coordination models. This paper investigates the cost of misreporting behavior in a capacity sharing SC. Like the previous study such as Xin and Sun [38], we also investigate equilibrium results under different scenarios. Specifically, we built models of disclosing real cost information, misreporting cost without being noticed, and misreporting cost with the platform operator's acquiescence. We try to analyze the influence of the misreporting behavior on decisions and profits of SC members and further design the contract to enable the capacity provider to report the real cost information and achieve SC coordination.

3. Models

3.1. Model Description. In a supply chain consisting of a capacity provider (M_1), a capacity demand side (M_2), and a capacity sharing platform operator (P), M_2 purchases the manufacturing service of a single product from M_1 . The paper considers a platform at a mature stage, i.e., the platform has a large number of participants. P has strong market power and is the leader of the SC. The dominant power of the leader in this paper refers to the priority of pricing. All SC members are risk-neutral and completely rational, that is, they make decisions based on the principle of maximizing their own profits. M_1 is a small and medium-sized manufacturing company with surplus capacity, and it is not directly oriented to the end market. M_2 is a more comprehensive manufacturing and sales-oriented manufacturing company with a market power higher than M_1 . P charges a service fee for M_1 , for example, the Tao Factory platform charges a service fee for capacity providers but does not charge a fee for capacity requestors in the current stage. Based on the service fee, M_2 determines the sales margin and M_1 determines its wholesale price.

The market demand D of the product is a linear function of the market price p , i.e., $D = a - bp$, where a is the potential market size. We assume that a is large enough to avoid meaningless situations. b is the price sensitivity coefficient, and a and b are both positive values. p is the sales price of M_2 . $p = w + r$, where M_1 decides the wholesale price w and M_2 decides the sales margin r . Suppose the real unit product production cost of M_1 is c , and M_1 may lie about the production cost for its own benefit. We denote the cost reported to M_2 as kc , and k is the cost misreporting coefficient of M_1 , $k > 0$. M_1 will determine k with the goal of profit maximization. M_1 may understate the production cost (i.e., $0 < k < 1$) to attract M_2 in order to win the contract, or M_1 may overstate the production cost (i.e., $k > 1$) to charge a higher wholesale price. We will investigate the optimal decision of k for M_1 in this paper. P charges M_1 a service fee s for the transaction, $s > 0$, and s is the decision variable of P . Since the fixed investment at the platform's start stage exerts no effect on our analytical results, the marginal service cost of processing online transactions is relatively low, and we normalize the platform's cost to zero. We consider that M_1 can completely meet the capacity demand of M_2 . In addition, to simplify the calculation and highlight the focus on production cost misreporting, we also normalize the unit inventory cost and the sales cost to zero. The notations in this paper are summarized in Table 1, and the supply chain structure of this article is shown in Figure 1. In this article, subscripts s , m , p , and sc represent M_1 , M_2 , P , and the entire SC; the subscript r represents the reaction function of a member's decision or profit to a certain decision variable.

3.2. Decentralized Model with Real Cost Information (Model DR). In this section, we first analyze decisions and profits of SC members when M_1 reports real production costs. Profit functions of M_2 , M_1 , and P are as follows:

TABLE 1: List of notations.

Notation	Definition
D	Market demand
M_1	Capacity provider
M_2	Capacity requestor
P	Manufacturing capacity sharing platform
a	Potential market size
b	Price sensitivity coefficient
c	Real unit product production cost of M_1
k	Cost misreporting coefficient, decision variable of M_1
p	Unit sales price of the product
r	Unit sales margin, decision variable of M_2
s	Unit service fee, decision variable of P
w	Unit wholesale price, decision variable of M_1
λ	Ratio of sales revenue shared by M_1 , $0 < \lambda < 1$
ϕ	Proportion of production cost shared by M_1 , $0 < \phi < 1$
ρ	Service fee proportion, $0 < \rho < 1$
π_s	Profit of M_1
π_m	Profit of M_2
π_p	Profit of P
π_{sc}	Profit of the entire SC

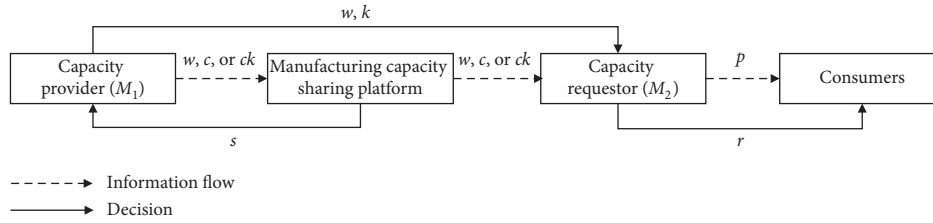


FIGURE 1: Supply chain structure.

$$\pi_m^{DR} = r(a - b(w + r)); \quad (1)$$

$$\pi_s^{DR} = (a - b(r + w))(w - c - s); \quad (2)$$

$$\pi_p^{DR} = s(a - b(w + r)). \quad (3)$$

Since this paper assumes that P is the leader of the SC and the channel power of M_2 is higher than that of M_1 , the decision-making process of SC members in this section is as follows. P first decides the service fee s ; then M_2 determines the sales margin by r , and during this period, M_2 should consider the reaction of M_1 , and then M_1 decides the wholesale price w . We adopt the backward induction to solve this Stackelberg game and derive the Proposition 1. Please refer to the Appendix for proofs of all propositions.

Proposition 1. When M_1 discloses real cost information, equilibrium solutions and profits are given as follows: $w^{DR} = (5a + 3bc)/(8b)$; $r^{DR} = (a - bc)/(4b)$; $s^{DR} = (a - bc)/(2b)$. $\pi_s^{DR} = (a - bc)^2/(64b)$; $\pi_m^{DR} = (a - bc)^2/(32b)$; $\pi_p^{DR} = (a - bc)^2/(16b)$; $\pi_{sc}^{DR} = 7(a - bc)^2/(64b)$.

Proposition 1 shows that the profits of all SC members under the model DR increase with the market size and

decrease with the price sensitivity and the production cost. And, it is easy to get that the platform operator's profit is the highest compared with the profits of other SC members. It implies that changes in exogenous variables such as an increase in market size, a decrease in the cost of M_1 , and a decrease in the sensitivity of consumers to product prices are beneficial to all SC members, while these changes benefit P the most.

3.3. Decentralized Model with Cost Misreporting to M_2 and P (Model DH). In this section, we consider that M_1 deliberately misreports its production cost information to both M_2 and P and construct a decentralized decision-making game model. For example, Tao Factory platform in China provides in-depth factory inspection services. The capacity provider may deliberately misrepresent the production capacity information to the platform during the factory inspection or misreport the cost of raw materials and processing costs when making quotations. In this case, the profit function of M_2 is the same as equation (1), the profit function of P is the same as equation (3), and the profit function of M_1 thought by M_2 and P is

$$\pi_s^{DH} = (a - b(r + w))(w - ck - s). \quad (4)$$

The real profit function of M_1 is equal to equation (2). In model DH, M_1 decides the optimal k to maximize its own

profit and then announces its own production cost as kc . M_2 and the platform believe that kc is its true cost; similar to the sequence of decisions under the model DR, the platform first decides s and M_2 , then decides r , and then M_1 decides the wholesale price w . It is notable that when deciding w , the objective function of M_1 is to maximize the profit function with cost misreporting, i.e., equation (4) instead of its real profit function equation (2). It is because that each of SC members can predict others' reactions to a certain decision under information disclosure. M_1 's pricing decision should coincide with its misreporting behavior [30].

Proposition 2. *The optimal response function of each SC member to the k under model DH: $w_r^{DH} = (5a + 3bck)/(8b)$; $r_r^{DH} = (a - bck)/(4b)$; $s_r^{DH} = (a - bck)/(2b)$, where $0 < k < \bar{k} = a/(bc)$.*

Proposition 2 shows that the wholesale price increases with the cost misreporting coefficient, the sales margin decreases with the cost misreporting coefficient, and the service fee decreases with the cost misreporting coefficient. By simple calculation, we can further know that the sales price increases with the cost misreporting coefficient. The service fee will also decrease with the cost misreporting coefficient. This shows that when M_1 overstates cost information, its wholesale price will increase, and manufacturers will reduce sales margins in order to avoid excessively high sales prices that will affect sales volume. Since the sales price increases with the cost misreporting coefficient, the increase in the wholesale price has a greater impact on the sales price than the decrease of sales margin. Overstatement of cost information will adversely affect the customers' benefit. Based on the reaction functions in Proposition 2, we can derive the reaction function of M_1 's profit:

$$\pi_{sr}^D = \frac{(a - bck)(a + bc(-8 + 7k))}{64b}. \quad (5)$$

Taking the first derivative of π_{sr}^D with respect to k , we get $\partial \pi_{sr}^D / \partial k = (1/32)c(3a + bc(4 - 7k))$. Taking the second derivative of π_{sr}^D to k yields $\partial^2 \pi_{sr}^D / \partial k^2 = -(1/32)(7bc^2) < 0$. Therefore, the optimal k can be obtained by solving the first-order condition and we can get the optimal cost misreporting coefficient as follows:

$$k^{DH} = \frac{3a + 4bc}{7bc}. \quad (6)$$

When $0 < k < (3a + 4bc)/(7bc)$, π_{sr}^D is an increasing function of k ; when $(3a + 4bc)/(7bc) < k < \bar{k}$, π_{sr}^D is a decreasing function of k . Due to $a > bc$, it is easy to get $k^{DH} > 1$. Therefore, M_1 's optimal strategy is to overstate the production cost to k^{DH} . M_1 's excessively overstatement on production cost information will damage its profit, since the excessively high production cost information will exert negative impacts on sales volumes which will be greater than the positive impact on wholesale prices with the increasing k .

Bringing the optimal cost misreporting coefficient k^{DH} into each reaction function in Proposition 2, we can obtain $w^{DH} = (11a + 3bc)/(14b)$, $r^{DH} = (a - bc)/(7b)$, $s^{DH} = (2(a - bc))/(7b)$. $\pi_s^D = (a - bc)^2/(28b)$, $\pi_m^{DH} = (a - bc)^2/$

(98b), $\pi_p^{DH} = (a - bc)^2/(49b)$, and $\pi_{sc}^{DH} = 13(a - bc)^2/(196b)$. Comparing the profits of SC members and the entire SC under model DH and model DR yields the results in Proposition 3.

Proposition 3. $\pi_s^D > \pi_p^{DH} > \pi_m^{DH}$, $\pi_s^D > \pi_s^{DR}$, $\pi_m^{DH} < \pi_m^{DR}$, $\pi_p^{DH} < \pi_p^{DR}$, and $\pi_{sc}^{DH} < \pi_{sc}^{DR}$.

Proposition 3 indicates that the profit of M_1 among the profits of SC members under model DH is the highest, and the profit of M_2 is the lowest. In comparison to the model DR, the profit of M_1 jumps from the lowest to the highest with cost misreporting. Proposition 3 shows that M_1 will benefit from misreporting the production cost, which is unfavorable to both M_2 's profit and P 's profit. The reason is that overstating the cost will increase the sales price and reduce the sales volume, the sales margin, and the service fee, leading to the decrease in profits of M_2 and P . Thereby, it is advisable for M_2 and P to propose a contract for avoiding the cost misreporting behavior. Moreover, Proposition 3 also implies that the cost misreporting will cause losses to the entire SC, which shows the necessity of a hedging mechanism. As the rule maker of the platform and the leader of SC, P should actively inspire SC members to reach an agreement for SC coordination.

3.4. Decentralized Model under Cost Misreporting with the Platform Operator's Acquiescence (Model DC). In this section, we consider that M_1 misrepresents the cost information. P is aware of M_1 's cost misreporting behavior and colludes with M_1 by acquiescing in cost misreporting behavior to gain more profits. Specifically, the sequence of the Stackelberg game in model DC is as follows. P determines the service fee s with the knowledge of the real cost information c , and M_1 determines k and M_1 lies to M_2 about the production cost information. Regarding kc as the real production cost, M_2 decides the sales margin r . M_1 then determines the wholesale price w to maximize its profits and ensure consistency with the misreporting behavior.

The profit function of M_2 is the same as equation (1), and the profit function of P is the same as equation (3). The M_1 's profit function thought by M_2 is equal to equation (4), and the M_1 's real profit function is the same as equation (2). Similar to the model DR, we adopt backward induction to solve this Stackelberg game and show the equilibrium solutions and profits in Proposition 4.

Proposition 4. *Under model DC, equilibrium solutions and profits are given as follows: $k^{DC} = (1/6)((a/bc) + 5)$, $w^{DC} = (3a + bc)/(4b)$, $r^{DC} = (a - bc)/(6b)$, $s^{DC} = (a - bc)/(2b)$. $\pi_s^{DC} = (a - bc)^2/(48b)$, $\pi_m^{DC} = (a - bc)^2/(72b)$, $\pi_p^{DC} = (a - bc)^2/(24b)$, and $\pi_{sc}^{DC} = 11(a - bc)^2/(144b)$.*

We can learn that the profit of P under model DC is the highest, and the profit of M_2 is the lowest. It implies that after misreporting M_2 's profit became the lowest among the three SC members in both model DH and model DC, and after collision with M_1 , the proportion of the P 's profit in the profit of entire SC turns back to the highest. We further

compare the equilibrium results of model DR, model DH, and model DC and obtain Proposition 5.

Proposition 5. (1) $1 < k^{DC} < k^{DH}$, $s^{DR} = s^{DC} > s^{DH}$, $r^{DR} > r^{DC} > r^{DH}$, $w^{DR} < w^{DC} < w^{DH}$, $p^{DR} < p^{DC} < p^{DH}$. (2) $\pi_m^{DR} > \pi_m^{DC} > \pi_m^{DH}$, $\pi_s^{DR} < \pi_s^{DC} < \pi_s^D$, $\pi_p^{DR} > \pi_p^{DC} > \pi_p^{DH}$, and $\pi_{sc}^{DR} > \pi_{sc}^{DC} > \pi_{sc}^{DH}$.

Proposition 5 points out that compared with misreporting costs to both M_2 and P , the cost misreporting coefficient under collusion is lower, the platform service fee is higher, the sales margin is higher, the wholesale price is lower, and the final sales price is lower. Although the P 's profits in model DH and model DC are lower than those in model DR, P can gain more profits when colluding with M_1 in comparison to model DH. The same applies to the profit of the entire SC. It implies that, under cost misreporting behavior, P 's collusion with M_1 is conducive to both M_2 and P . In contrast, misreporting to both M_2 and the P is the most favorable to M_1 . Therefore, it is easy for M_1 to exaggerate production costs, which will be detrimental to M_2 , P , and the entire SC. Furthermore, for gaining more profits than that M_1 can earn in model DR, M_1 may be willing to pay a transfer payment which is up to the difference between M_1 's profit in model DC and M_1 's profit in model DR to P for persuading P to acquiesce in the cost misreporting behavior. M_2 has a big motivation to initiate the coordination contract to avoid the cost misreporting behavior.

At present, many capacity sharing platforms are actively advocating the manufacturing enterprise's digital transformation, which can improve the visualization of the whole production process and strengthen real-time data interaction. It can help the capacity requestor and the platform operator monitor the operations of capacity provider to reduce the misstatement of information. However, the digitalization of SC is still in the early stage in China. For example, a small number of manufacturers have finished the digital transformation in the Tao factory platform. In this paper, we tried to use the coordination mechanism to avoid cost misreporting and improve the performance of SC.

4. Coordination Contract for the SC

In this section, we first investigate the centralized decision model of the SC to find out the SC performance gap between decentralized and centralized settings and take the centralized model as the benchmark of SC coordination. Under centralized decision-making, SC members make decisions as an integrated entity, and their profit function is

$$\pi_{sc}^C = (p - c)(a - bp). \quad (7)$$

It is easy to derive the optimal sales price $p^C = (a + bc)/(2b)$. The optimal profit of the entire SC is given by $\pi_{sc}^C = (a - bc)^2/(4b)$. By comparing the decisions and profits under centralized and decentralized models, we can get Proposition 6.

Proposition 6. $p^C < p^{DR} < p^{DC} < p^{DH}$ and $\pi_{sc}^C > \pi_{sc}^{DR} > \pi_{sc}^{DC} > \pi_{sc}^{DH}$.

Proposition 6 shows that the sales price under a centralized setting is lower than that under a decentralized setting. The profit of the entire SC is the highest under centralized setting, due to the double marginal effect and information misreporting in the decentralized setting.

Based on the equilibrium results in SC under a centralized setting, we explore the role of sales revenue-sharing and cost-sharing contracts in avoiding the cost of misreporting behavior and coordinating the SC. In this contract, M_2 sells products directly to consumers at the wholesale price of M_1 and shares part of the production cost of M_1 . At the end of the sales season, M_1 and M_2 share sales revenue. For example, in the Tao Factory platform in China, the capacity requestor can choose to provide the raw materials of the product and bear the corresponding cost. Let λ denote the ratio of sales revenue shared by M_1 , $0 < \lambda < 1$; let ϕ represent the proportion of production cost-shared by M_1 , $0 < \phi < 1$. Thus, the proportion of sales revenue shared by M_2 is $1 - \lambda$, and the proportion of production cost borne by M_2 is $1 - \phi$. We assume the unit service fee charged by P is proportional to the wholesale price, which is denoted by $s = \rho w$, where ρ is the service fee proportion. On this basis, the profit functions of M_1 , M_2 , and P under the sales-revenue-sharing and cost-sharing contract are as follows:

$$\pi_s^{RS} = (a - bw)(-ck\phi + \lambda w - \rho w); \quad (8)$$

$$\pi_m^{RS} = (1 - \lambda)w(a - bw) - ck(1 - \phi)(a - bw); \quad (9)$$

$$\pi_p^{RS} = \rho w(a - bw). \quad (10)$$

When $k = 1$, equations (7) and (8) are, respectively, the profits of M_1 and M_2 when M_1 reports real production cost. Under the sales revenue-sharing and cost-sharing contract, M_1 and M_2 negotiate on the value of λ and ϕ . On this basis, the decision-making sequence is as follows: P determines the proportion ρ , and then M_1 decides the cost misreporting coefficient k and the wholesale prices w . Using backward induction, we get the sales revenue-sharing and cost-sharing contract as shown in Proposition 7.

Proposition 7

(1) In the sales revenue-sharing and cost-sharing contract, $\rho = \lambda - \phi$; $k^{RS} = 1$, $w^{RS} = (a + bc)/(2b) = p^C$, $\pi_s^{RS} = (\phi(a - bc)^2)/(4b)$, $\pi_m^{RS} = (bc - a)(a(\lambda - 1) + bc(\lambda - 2\phi + 1))/(4b)$, $\pi_p^{RS} = (\lambda - \phi)(a - bc)(a + bc)/(4b)$, and $\pi_{sc}^{RS} = (a - bc)^2/(4b) = \pi_{sc}^C$.

(2) When $1/7 \leq \phi \leq 5/8$ and $(4a\phi + a + bc(4\phi - 1))/(4(a + bc)) \leq \lambda \leq (7a + bc(16\phi - 7))/(8(a + bc))$, we can ensure $0 < \rho < 1$ and $\pi_s^{RS} \geq \max\{\pi_s^{DR}, \pi_s^D, \pi_s^{DC}\}$, $\pi_m^{RS} \geq \max\{\pi_m^{DR}, \pi_m^{DH}, \pi_m^{DC}\}$, and $\pi_p^{RS} \geq \max\{\pi_p^{DR}, \pi_p^{DH}, \pi_p^{DC}\}$.

Proposition 7 shows that, under the sales revenue-sharing and cost-sharing contract, the supplier will choose to report the true cost. Thereby, this contract can effectively avoid the cost misreporting behavior of M_1 . The profit of the entire SC has also reached the profit of SC under a

centralized setting. Under the conditions of the parameters given in Proposition 7, the profit of each SC member is not lower than their respective profit under a decentralized setting. Therefore, the sales revenue-sharing and cost-sharing contract can coordinate the SC.

The platform should act as the coordinator in the capacity sharing transaction and be committed to improving the performance of the entire SC rather than focusing solely on its own profits. Although P 's profit increases with the service fee proportion, P should set the proportion with a moderate value, i.e., $\lambda - \phi$, to facilitate the coordination of SC. When P offers order processing supervision service, the order supervisor is suggested to actively facilitate the coordination contract in the SC. For example, in Tao factory platform, instead of punishing the supplier which misreports cost information and offers false quotation as mentioned in Introduction, the platform operator can utilize the coordination contract to address the essential drive of the misreporting behavior.

On the premise of guaranteeing that each SC member's profit with coordination contract is no less than that without coordination contract, M_2 can properly concede to M_1 in the bargaining of λ and ϕ , so as to encourage M_1 's acceptance of the coordination contract. It is advisable for M_1 to sign the coordination contract to improve its own profit and benefit the entire SC. It is worth noting that the wise strategy for the M_1 in reaching the coordination contract is to struggle for a higher production cost-sharing ratio.

5. Numerical Analysis

On the manufacturing capacity sharing platform, the market demand faced by M_2 is given by $D = 10 - 0.5p$, i.e., the potential market size $a = 10$, and the customers' price sensitivity coefficient for the product $b = 0.5$; M_2 seeks product processing capacity through the platform, and M_1 on the platform reached a processing agreement with it. The actual product production cost of M_1 is $c = 0.2$. Bringing these parameter values into Proposition 7, we can get the range of λ and ϕ that can coordinate the SC, as shown in Figure 2. When λ and ϕ lie within the range of triangle ABC (including three sides and vertices) in Figure 2, the contract can effectively coordinate the SC.

To visually show the coordination effect of this contract, Table 2 gives profits of SC members and the entire SC before and after coordination. First, we can derive the optimal sales price of the SC is $p = 10.1$ under centralized setting, and the profit of entire SC is $\pi_{sc}^C = 49$. Table 2 shows that the relationship between the profits of SC members and the entire SC under a decentralized setting before coordination verifies Proposition 5. The profit of the entire SC under each decentralized model is much lower than that under the centralized setting, which demonstrates the Proposition 6. With the coordination of sales revenue-sharing and cost-sharing contracts, the profit of the entire SC can reach the level of centralized setting, which verifies Proposition 7. Table 1 also shows that if parameters λ and ϕ are defined as point A in Figure 2, M_1 is the biggest beneficiary after coordination. Similarly, M_2 benefits the most from the

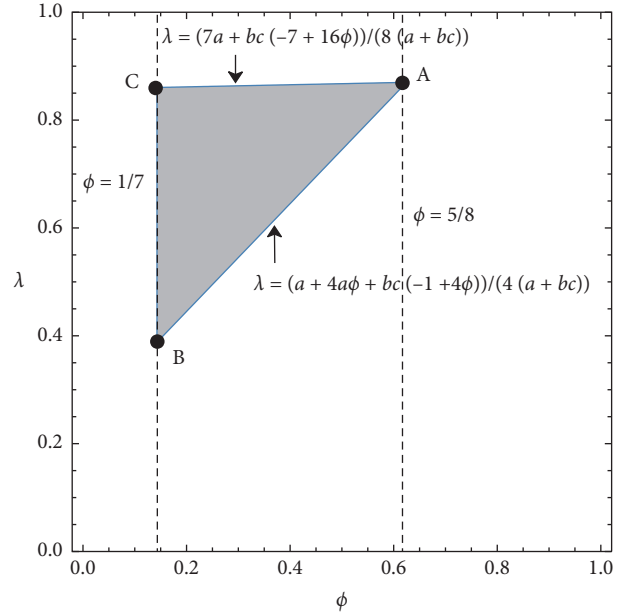


FIGURE 2: The range of λ and ϕ when achieving SC coordination.

TABLE 2: Effect of the coordination contract on profits of SC members and the entire SC.

	λ	ϕ	π_s	π_m	π_p	π_{sc}
Model DR	—	—	3.06	6.13	12.25	21.44
Model DH	—	—	7	2	4	13
Model DC	—	—	4.08	2.72	8.17	14.97
Figure 2, point A	0.87	0.625	30.63	6.13	12.25	49
Figure 2, point B	0.39	0.14	7	29.75	12.25	49
Figure 2, point C	0.86	0.14	7	6.15	35.85	49

coordination contract when λ and ϕ are defined as point B in Figure 2; the platform operator's profit is improved to the largest extent under the coordination contract if λ and ϕ are defined as point C in Figure 2. The values of λ and ϕ reflect the negotiation power of M_1 and M_2 .

The sales revenue-sharing and cost-sharing contract designed in this paper serve as guidance for P to inspire the collaboration among SC members. A moderate service fee, which equals to the difference between the revenue-sharing ratio and the cost-sharing proportion, is critical to facilitate the coordination. The ranges of the revenue-sharing ratio and production cost-sharing proportion derived in this paper provide references for M_1 and M_2 in their negotiation. It is wise for M_2 to assume a greater share of production cost in the meantime of struggling for a higher share of sales revenue, in order to achieve profit maximization. Under the service fee charged by P , M_1 is prone to share a large ratio of the production cost, since the service fee proportion in the coordination contract decreases with the production cost-sharing ratio.

6. Conclusions

In the manufacturing capacity sharing platform, the transactions between capacity requestors and capacity

providers are often short-term and flexible. Although the platform can conduct qualification supervision on participants, the platform cannot fully control the production capacity information disclosed by participants due to limitations of current technology and management capacity. Capacity providers can easily use their information advantages to generate opportunistic behavior. And, the platform may collude with it for the purpose of profit-seeking and acquiesce in the opportunistic behavior, which will affect the interests of capacity requestors and even damage the overall performance of the SC. This paper investigates a SC consisting of a capacity requestor, a capacity provider, and a platform operator. Taking the cost misreporting behavior of capacity providers into account, we use game theory to analyze the decisions and profits of SC members in models of disclosing the real cost information, misreporting cost information to both the capacity requestor and the platform operator and misreporting cost to the capacity requestor with the acquiescence of the platform operator. By comprehensive comparisons between decisions and profits in different models, we examine the influence of cost misreporting and the platform's collusion. Finally, we propose the coordination contract for the SC to avoid the cost misreporting behavior and improve the performance of the SC. The main findings are as follows.

In the manufacturing capacity sharing platform, capacity providers have the incentive to overstate the production cost, and they can set higher wholesale prices by misrepresenting their production costs. Exaggerating production cost within a certain range can help capacity providers gain more profits, while the excessive exaggeration will be detrimental to their own interests. When the capacity provider overstates the cost information, the sales price will increase, profits of the capacity requestor and the platform operator will be damaged, and the profit of the entire SC will also decline. Compared with misreporting to both the platform operator and the capacity requestor, the platform operator's collusion with the capacity provider is favorable to the capacity requestor and the platform operator. However, the capacity provider will be inclined to lie to both of them. The sales revenue-sharing and cost-sharing contract can effectively avoid cost misreporting behavior of the capacity provider, and when the revenue-sharing ratio and cost-sharing proportion are within a certain range, the contract can improve the supply chain members' profit and achieve the SC coordination.

Theoretically, this paper enriches the literature on production cost information asymmetry and capacity sharing SC by investigating the cost of misreporting behavior in the context of capacity sharing SC and by considering the service fee decision and the possible acquiescence behavior of the capacity sharing platform. Besides, the sales revenue-sharing and cost-sharing contracts proposed in this paper throw lights on supply chain coordination under cost information asymmetry. In practice, the platform operator is suggested to facilitate the coordination contract designed in this paper when handling the capacity transaction between the capacity provider and the capacity requestor.

This paper has conducted research on the capacity provider's cost misreporting behavior in the capacity sharing SC. This paper provides a reference for the future research on opportunistic behavior in capacity sharing transaction. However, we made some assumptions to simplify the calculation such as the linear demand function. Relaxing these assumptions may generate different results. In the future, we can further explore other opportunistic behaviors such as falsely reporting production capacity. And, the problem of joint supply under capacity insufficiency of a single capacity provider under the impact of opportunistic behavior is also an interesting direction. Exploring how the government can govern the platform is also one of future research directions.

Appendix

Proof of Proposition 1

Taking the second derivative of π_s^{DR} with respect to w , we can get $\pi_s^{DR''} = -2b < 0$. It implies that there exists the optimal w to maximize π_s^{DR} , which satisfies $\pi_s^{DR'} = 0$. Solving $\pi_s^{DR'} = a - b(-c + w - s) - b(r + w) = 0$ yields $w_r^{DR} = (a + b(c - r + s))/(2b)$. Substituting w_r^{DR} into π_m^{DR} , we can get that $\pi_m^{DR} = -(1/2)r(b(c + r + s) - a)$. Similarly, taking the second derivative of π_m^{DR} with respect to r , we can get $\pi_m^{DR''} = -b < 0$. Solving the first-order condition, we can get that $r_r^{DR} = (a - b(c + s))/(2b)$. Substituting w_r^{DR} and r_r^{DR} into π_p^{DR} , we can get $\pi_p^{DR} = -(1/4)s(b(c + s) - a)$. Taking the second derivative of π_p^{DR} with respect to s , we can get $\pi_p^{DR''} = -(b/2) < 0$. Solving the first-order condition, we can get that $s^{DR} = (a - bc)/(2b)$. On the basis of s^{DR} , w_r^{DR} , and r_r^{DR} , we can derive the optimal w^{DR} and r^{DR} . Bringing w^{DR} , r^{DR} , and s^{DR} back to the profit functions, we can get π_s^{DR} , π_m^{DR} , π_p^{DR} , and π_{sc}^{DR} .

Proof of Proposition 2

Taking the second derivative of π_s^{DH} with respect to w , we can get $\pi_s^{DH''} = -2b < 0$. It implies that there exists the optimal w to maximize π_s^{DH} . Solving $\pi_s^{DH'} = a - b(-ck + w - s) - b(r + w) = 0$ yields $w_r^{DH} = (a + b(ck - r + s))/(2b)$. Substituting w_r^{DH} into π_m^{DH} , we can get $\pi_m^{DH} = -(1/2)r(b(ck + r + s) - a)$. Similarly, taking the second derivative of π_m^{DH} with respect to r , we can derive $\pi_m^{DH''} = -b < 0$. Solving the first-order condition yields $r_r^{DH} = (a - b(ck + s))/(2b)$. Substituting w_r^{DH} and r_r^{DH} into π_p^{DH} , we can get $\pi_p^{DH} = -(1/4)s(b(ck + s) - a)$. Taking the second derivative of π_p^{DH} with respect to s , we can get $\pi_p^{DH''} = -(b/2) < 0$. Thus, we solve the first-order condition and derive that $s^{DH} = (a - bck)/(2b)$. To ensure all decisions are positive, k should satisfy $k < a/(bc)$, and let $\bar{k} = a/(bc)$.

Proof of Proposition 3

$\pi_s^D - \pi_p^{DH} = (3(a - bc)^2)/(196b) > 0$. $\pi_p^{DH} - \pi_m^{DH} = (a - bc)^2/(98b) > 0$. $\pi_s^D - \pi_s^{DR} = 9(a - bc)^2/(448b) > 0$. $\pi_m^{DH} - \pi_m^{DR} = -33(a - bc)^2/(1568b) < 0$. $\pi_p^{DH} - \pi_p^{DR} = -33(a - bc)^2/(784b) < 0$. $\pi_{sc}^{DH} - \pi_{sc}^{DR} = -135(a - bc)^2/(3136b) < 0$.

Proof of Proposition 4

Since $\partial^2 \pi_s / \partial w^2 = -2b < 0$, we can get $w_r^{DC} = (a + b(ck + s - r)) / (2b)$ by solving the first-order condition; Substituting w_r^{DC} into π_m^{DC} , we can get $\partial^2 \pi_m / \partial r^2 = -b < 0$. Solving the first-order condition, we can get $r = (a - b(s + ck)) / (2b)$, since the objective function of M_1 when deciding the optimal k is its real profit function with the real production cost. Since $\partial^2 \pi_s' / \partial k^2 = -1/8(3bc^2)$, we can get the optimal reaction function $k = (a + 2bc - bs) / (3bc)$ by solving the first-order condition. Finally, substituting w_r^{DC} , r_r^{DC} , and k_r^{DC} into π_p^{DC} and taking the second derivative, we can get $\partial^2 \pi_p / \partial s^2 = -b/3 < 0$. Then, solving the first-order condition yields $s = (a - bc) / (2b)$. Substituting the optimal s into the abovementioned reaction functions, we can get the optimal decisions and profits, respectively.

Proof of Proposition 5

- (1) Since $k^{DH} - k^{DC} = (11(a - bc)) / (42bc) > 0$ and $k^{DC} = 1/6((a/bc) + 5) > 1$, we can get $1 < k^{CC} < k^{CH}$. Since $s^{DR} = s^{DC}$ and $s^{DC} - s^{DH} = 3(a - bc) / (14b) > 0$, we have $s^{DR} = s^{DC} > s^{DH}$. Since $r^{DR} - r^{DC} = (a - bc) / (12b) > 0$ and $r^{DC} - r^{DH} = (a - bc) / (42b) > 0$, we can get $r^{DR} > r^{DC} > r^{DH}$. Since $w^{DR} - w^{DC} = -(a - bc) / (8b) < 0$ and $w^{DC} - w^{DH} = -(a - bc) / (28b) < 0$, we derive $w^{DR} < w^{DC} < w^{DH}$. Since $p^{DC} - p^{DH} = -(a - bc) / (84b) < 0$ and $p^{DC} - p^{DR} = (a - bc) / (24b) > 0$, we have $p^{DR} < p^{DC} < p^{DH}$.
- (2) Since $\pi_m^{DR} - \pi_m^{DC} = 5(a - bc)^2 / (288b) > 0$ and $\pi_m^{DC} - \pi_m^{DH} = 13(a - bc)^2 / (3528b) > 0$, we get $\pi_m^{DR} > \pi_m^{DC} > \pi_m^{DH}$. Since $\pi_s^{DR} - \pi_s^{DC} = -(a - bc)^2 / (192b) < 0$ and $\pi_s^{DC} - \pi_s^D = -5(a - bc)^2 / (336b) < 0$, we have $\pi_s^{DR} < \pi_s^{DC} < \pi_s^D$. Since $\pi_p^{DR} - \pi_p^{DC} = (a - bc)^2 / (48b) > 0$ and $\pi_p^{DC} - \pi_p^{DH} = 25(a - bc)^2 / (1176b) > 0$, we can get $\pi_p^{DR} > \pi_p^{DC} > \pi_p^{DH}$. Since $\pi_{sc}^{DR} - \pi_{sc}^{DC} = 19(a - bc)^2 / (576b) > 0$ and $\pi_{sc}^{DC} - \pi_{sc}^{DH} = 163(a - bc)^2 / (3528b) > 0$, we have $\pi_{sc}^{DR} > \pi_{sc}^{DC} > \pi_{sc}^{DH}$.

Proof of Proposition 6

Since $p^C - p^{DR} = -3(a - bc) / (8b) < 0$, we have $p^C < p^{DR}$. Since $p^C - p^{DH} = -3(a - bc) / (7b) < 0$, we get $p^C < p^{DH}$. Considering $p^{DR} < p^{DC} < p^{DH}$ in Proposition 5, we can get $p^C < p^{DR} < p^{DC} < p^{DH}$. Since $\pi_{sc}^C - \pi_{sc}^{DR} = 9(a - bc)^2 / (64b) > 0$, we can get $\pi_{sc}^C > \pi_{sc}^{DR}$. Considering $\pi_{sc}^{DH} < \pi_{sc}^{DC} < \pi_{sc}^{DR}$ in Proposition 5, we have $\pi_{sc}^C > \pi_{sc}^{DR} > \pi_{sc}^{DC} > \pi_{sc}^{DH}$.

Proof of Proposition 7

- (1) Taking the second derivative of π_s with respect to w , we can get $\partial^2 \pi_s / \partial w^2 = 2b(\rho - \lambda)$. Since $\rho < \lambda$, we have $\partial^2 \pi_s / \partial w^2 < 0$ and there exists the optimal w to maximize π_s^{DR} . $w_r^{RS} = (-a\lambda + a\rho - bck\phi) / (2b\rho - 2b\lambda)$. The w_r^{RS} predicted by M_2 and the platform operator is given by $w_r^{RS} = (-a\lambda + a\rho - bck\phi) / (2b\rho - 2b\lambda)$.

Substituting the w_r^{RS} into M_1 's product function with real cost information, we can get that $\pi_s = ((a(\lambda - \rho) + bc(k - 2)\phi) / (a(\rho - \lambda) + bck\phi)) / (4b(\rho - \lambda))$. Taking the second derivative of π_s with respect to k yields $\partial^2 \pi_s / \partial k^2 = bc^2\phi^2 / (2\rho - 2\lambda) < 0$. And thus, there exists the optimal k to maximize π_s . Solving the first-order condition $\partial \pi_s / \partial k = (bc^2(k - 1)\phi^2) / (2(\rho - \lambda)) = 0$ yields $k^{RS} = 1$. Therefore, the optimal strategy of M_1 is to disclose the real cost information and thus $w_r^{RS} = (-a\lambda + a\rho - bc\phi) / (2b\rho - 2b\lambda)$. To achieve the SC coordination, the sales price in the coordination contract should be equal to that in SC under decentralized setting, i.e., $(-a\lambda + a\rho - bc\phi) / (2b\rho - 2b\lambda) = (a + bc) / (2b)$. To facilitate the coordination contract, the platform operator should set the service fee proportion as $\rho = \lambda - \phi$.

To ensure $\rho > 0$, $\lambda > \phi$ should be satisfied. Therefore, in the coordination contract, $k = 1$, $\rho = \lambda - \phi$, and $w^{RS} = (a + bc) / 2b = p^C$. The profits of SC members can be given by $\pi_s^{RS} = \phi(a - bc)^2 / (4b)$, $\pi_m^{RS} = ((bc - a)(a(\lambda - 1) + bc(\lambda - 2\phi + 1))) / (4b)$, and $\pi_p^{RS} = ((\lambda - \phi)(a - bc)(a + bc)) / (2b)$. The profit of entire SC is $\pi_{sc}^{RS} = (a - bc)^2 / (4b)$.

- (2) Since $\max\{\pi_s^{DR}, \pi_s^D, \pi_s^{DC}\} = \pi_s^D$, $\max\{\pi_m^{DR}, \pi_m^{DH}, \pi_m^{DC}\} = \pi_m^{DR}$, and $\max\{\pi_p^{DR}, \pi_p^{DH}, \pi_p^{DC}\} = \pi_p^{DR}$, we can get $\phi \geq (1/7)$ by solving $\pi_s^{RS} \geq \pi_s^D$. Solving $\pi_m^{RS} \geq \pi_m^{DR}$ yields $\lambda \leq (7a + bc(16\phi - 7)) / (8(a + bc))$. Solving $\pi_p^{RS} \geq \pi_p^{DR}$, we can get $\lambda \geq (4a\phi + a + bc(4\phi - 1)) / (4(a + bc))$. Taking the intersection of these three range, we can derive the conditions that λ and ϕ should satisfy.

Comparing $(7a + bc(16\phi - 7)) / (8(a + bc))$ with 0 and 1, we know that $0 < (7a + bc(16\phi - 7)) / (8(a + bc)) < 1$. Similarly, comparing $(4a\phi + a + bc(4\phi - 1)) / (4(a + bc))$ with 0 and 1, we get that $(4a\phi + a + bc(4\phi - 1)) / (4(a + bc)) > 0$; when $\phi < (3a + 5bc) / (4a + 4bc)$, $(4a\phi + a + bc(4\phi - 1)) / (4(a + bc)) < 1$. Comparing $(7a + bc(16\phi - 7)) / (8(a + bc))$ and $(4a\phi + a + bc(4\phi - 1)) / (4(a + bc))$, we know that when $\phi > (5/8)$, $(7a + bc(16\phi - 7)) / (8(a + bc)) < (4a\phi + a + bc(4\phi - 1)) / (4(a + bc))$. Under such situation, $\lambda \leq (7a + bc(16\phi - 7)) / (8(a + bc))$ and $\lambda \geq (4a\phi + a + bc(4\phi - 1)) / (4(a + bc))$ have no intersection. When $\phi \leq (5/8)$, $(7a + bc(16\phi - 7)) / (8(a + bc)) \geq (4a\phi + a + bc(4\phi - 1)) / (4(a + bc))$. Since $\phi \leq (5/8)$ also satisfies $\phi < (3a + 5bc) / (4a + 4bc)$, and $\lambda \geq (4a\phi + a + bc(4\phi - 1)) / (4(a + bc))$ satisfies $\lambda > \phi$; therefore, $(4a\phi + a + bc(4\phi - 1)) / (4(a + bc)) \leq \lambda \leq (7a + bc(16\phi - 7)) / (8(a + bc))$. The conditions that the parameters should satisfy are given by $1/7 \leq \phi \leq 5/8$ and $(4a\phi + a + bc(4\phi - 1)) / (4(a + bc)) \leq \lambda \leq (7a + bc(16\phi - 7)) / (8(a + bc))$.

Data Availability

The data used to support the findings of our paper have been included within the article.

Conflicts of Interest

The authors declare that they have no conflicts of interest.

Acknowledgments

The research was supported by the National Natural Science Foundation of China (Grant number 71472134).

References

- [1] P. Renna and P. Argoneto, "Capacity sharing in a network of independent factories: a cooperative game theory approach," *Robotics and Computer-Integrated Manufacturing*, vol. 27, no. 2, pp. 405–417, 2011.
- [2] M. Moghaddam and S. Y. Nof, "Combined demand and capacity sharing with best matching decisions in enterprise collaboration," *International Journal of Production Economics*, vol. 148, pp. 93–109, 2014.
- [3] M. Moghaddam and S. Y. Nof, "Real-time optimization and control mechanisms for collaborative demand and capacity sharing," *International Journal of Production Economics*, vol. 171, pp. 495–506, 2016.
- [4] Y. Yu, S. Benjaafar, and Y. Gerchak, "Capacity sharing and cost allocation among independent firms with congestion," *Production and Operations Management*, vol. 24, no. 8, pp. 1285–1310, 2015.
- [5] L. Guo and X. Wu, "Capacity sharing between competitors," *Management Science*, vol. 64, no. 8, pp. 3554–3573, 2018.
- [6] J. Qin, K. Wang, Z. Wang et al., "Revenue sharing contracts for horizontal capacity sharing under competition," *Annals of Operations Research*, 2018.
- [7] Y. Zeng, L. Zhang, X. Cai, and J. Li, "Cost sharing for capacity transfer in cooperating queueing systems," *Production and Operations Management*, vol. 27, no. 4, pp. 644–662, 2018.
- [8] T. A. Weber, "Intermediation in a sharing economy: insurance, moral hazard, and rent extraction," *Journal of Management Information Systems*, vol. 31, no. 3, pp. 35–71, 2014.
- [9] I. Bellos, M. Ferguson, and L. B. Toktay, "The car sharing economy: interaction of business model choice and product line design," *Manufacturing & Service Operations Management*, vol. 19, no. 2, pp. 185–201, 2017.
- [10] G. P. Cachon, K. M. Daniels, and R. Lobel, "The role of surge pricing on a service platform with self-scheduling capacity," *Manufacturing & Service Operations Management*, vol. 19, no. 3, pp. 368–384, 2017.
- [11] L. Tian and B. Jiang, "Effects of consumer-to-consumer product sharing on distribution channel," *Production and Operations Management*, vol. 27, no. 2, pp. 350–367, 2018.
- [12] B. Jiang and L. Tian, "Collaborative consumption: strategic and economic implications of product sharing," *Management Science*, vol. 64, no. 3, pp. 1171–1188, 2018.
- [13] S. Benjaafar, G. Kong, X. Li, and C. Courcoubetis, "Peer-to-peer product sharing: implications for ownership, usage, and social welfare in the sharing economy," *Management Science*, vol. 65, no. 2, pp. 477–493, 2019.
- [14] C. Aloui and K. Jebbsi, "Platform optimal capacity sharing: willing to pay more does not guarantee a larger capacity share," *Economic Modelling*, vol. 54, pp. 276–288, 2016.
- [15] K. Li, T. Zhou, B.-h. Liu, and H. Li, "A multi-agent system for sharing distributed manufacturing resources," *Expert Systems with Applications*, vol. 99, pp. 32–43, 2018.
- [16] L. Ren, L. Zhang, F. Tao, C. Zhao, X. Chai, and X. Zhao, "Cloud manufacturing: from concept to practice," *Enterprise Information Systems*, vol. 9, no. 2, pp. 186–209, 2015.
- [17] G. Adamson, L. Wang, M. Holm et al., "Cloud manufacturing—a critical review of recent development and future trends," *International Journal of Computer Integrated Manufacturing*, vol. 30, no. 4–5, pp. 347–380, 2017.
- [18] X. Yang, G. Shi, and Z. Zhang, "Collaboration of large equipment complete service under cloud manufacturing mode," *International Journal of Production Research*, vol. 52, no. 2, pp. 326–336, 2014.
- [19] P. Argoneto and P. Renna, "Supporting capacity sharing in the cloud manufacturing environment based on game theory and fuzzy logic," *Enterprise Information Systems*, vol. 10, no. 2, pp. 193–210, 2016.
- [20] F. Tao, J. Cheng, Y. Cheng, S. Gu, T. Zheng, and H. Yang, "SDMSim: a manufacturing service supply-demand matching simulator under cloud environment," *Robotics and Computer-Integrated Manufacturing*, vol. 45, pp. 34–46, 2017.
- [21] J. Thekinen and J. H. Panchal, "Resource allocation in cloud-based design and manufacturing: a mechanism design approach," *Journal of Manufacturing Systems*, vol. 43, pp. 327–338, 2017.
- [22] H. Xu, N. Shi, S.-h. Ma, and K. K. Lai, "Contracting with an urgent supplier under cost information asymmetry," *European Journal of Operational Research*, vol. 206, no. 2, pp. 374–383, 2010.
- [23] M. Çakanyildirim, Q. Feng, X. Gan et al., "Contracting and coordination under asymmetric production cost information," *Production and Operations Management*, vol. 21, no. 2, pp. 345–360, 2012.
- [24] E. Cao, Y. Ma, C. Wan, and M. Lai, "Contracting with asymmetric cost information in a dual-channel supply chain," *Operations Research Letters*, vol. 41, no. 4, pp. 410–414, 2013.
- [25] E. Kayış, F. Erhun, and E. L. Plambeck, "Delegation vs. control of component procurement under asymmetric cost information and simple contracts," *Manufacturing & Service Operations Management*, vol. 15, no. 1, pp. 45–56, 2013.
- [26] Q. Lei, J. Chen, X. Wei, and S. Lu, "Supply chain coordination under asymmetric production cost information and inventory inaccuracy," *International Journal of Production Economics*, vol. 170, pp. 204–218, 2015.
- [27] P. Ma, J. Shang, and H. Wang, "Enhancing corporate social responsibility: contract design under information asymmetry," *Omega*, vol. 67, pp. 19–30, 2017.
- [28] X. Wang, X. Lu, G. Xu et al., "Research on pricing and supply strategies in assembly system under asymmetric cost information," *Systems Engineering-Theory & Practice*, vol. 35, no. 7, pp. 1689–1697, 2015.
- [29] B. Dai, Y. Pi, and J. Li, "Production cost information sharing strategies under various market competition," *Systems Engineering-Theory & Practice*, vol. 37, no. 6, pp. 1452–1466, 2017.
- [30] B. Yan, T. Wang, Y.-p. Liu, and Y. Liu, "Decision analysis of retailer-dominated dual-channel supply chain considering cost misreporting," *International Journal of Production Economics*, vol. 178, pp. 34–41, 2016.
- [31] B. Hu and Y. Feng, "Optimization and coordination of supply chain with revenue sharing contracts and service requirement under supply and demand uncertainty," *International Journal of Production Economics*, vol. 183, pp. 185–193, 2017.
- [32] J. Xie, W. Zhang, L. Liang, Y. Xia, J. Yin, and G. Yang, "The revenue and cost sharing contract of pricing and servicing policies in a dual-channel closed-loop supply chain," *Journal of Cleaner Production*, vol. 191, pp. 361–383, 2018.

- [33] J. Su, C. Li, Q. Zeng et al., "A green closed-loop supply chain coordination mechanism based on third-party recycling," *Sustainability*, vol. 11, no. 19, pp. 1–14, 2019.
- [34] J. Jian, Y. Zhang, L. Jiang et al., "Coordination of supply chains with competing manufacturers considering fairness concerns," *Complexity*, vol. 2020, Article ID 4372603, 15 pages, 2020.
- [35] X. Wang, H. Guo, and X. Wang, "Supply chain contract mechanism under bilateral information asymmetry," *Computers & Industrial Engineering*, vol. 113, pp. 356–368, 2017.
- [36] X. Wang, H. Guo, R. Yan, and X. Wang, "Achieving optimal performance of supply chain under cost information asymmetry," *Applied Mathematical Modelling*, vol. 53, pp. 523–539, 2018.
- [37] Y. Liu, J. Li, B.-t. Quan, and J.-b. Yang, "Decision analysis and coordination of two-stage supply chain considering cost information asymmetry of corporate social responsibility," *Journal of Cleaner Production*, vol. 228, pp. 1073–1087, 2019.
- [38] B. Xin and M. Sun, "A differential oligopoly game for optimal production planning and water savings," *European Journal of Operational Research*, vol. 269, no. 1, pp. 206–217, 2018.

Research Article

Supply Chain Decision-Making and Coordination considering Anticipated Regret under Price Discount

Jie Jian ¹, Huipeng Li,¹ Nian Zhang ¹ and Jiafu Su ^{2,3}

¹School of Economics and Management, Chongqing University of Posts and Telecommunications, Chongqing, China

²Research Center for Economy of Upper Reaches of the Yangtze River, Chongqing Technology and Business University, Chongqing, China

³National Research Base of Intelligent Manufacturing Service, Chongqing Technology and Business University, Chongqing, China

Correspondence should be addressed to Jiafu Su; jiafu.su@hotmail.com

Received 4 April 2020; Revised 3 June 2020; Accepted 24 June 2020; Published 24 July 2020

Guest Editor: Baogui Xin

Copyright © 2020 Jie Jian et al. This is an open access article distributed under the Creative Commons Attribution License, which permits unrestricted use, distribution, and reproduction in any medium, provided the original work is properly cited.

The increasing homogeneous product market has made more competition among companies to focus on improving customers' experience. In order to get more competitive advantages, companies often launch discount products to attract consumers. However, stimulated by discount products, the perception of anticipated regret is becoming stronger, which is an inevitable issue in front of companies with price discount strategy. Considering the impact of anticipated regret for discount products, this paper quantitatively describes the utility functions and deduces the demand functions of original price products and discount products. The theoretical analysis and numerical simulation are used to analyze centralized and decentralized models of supply chain for discount products. On its basis, the revenue-sharing contract is designed to optimize the profits of supply chain. This paper finds that the price of products increases first and then decreases with the increase of regret sensitivity coefficient and consumer heterogeneity. When the regret sensitivity coefficient and consumer heterogeneity are lower, companies in the supply chain can adopt the "skimming pricing" strategy in order to obtain more profits. When the regret sensitivity coefficient and consumer heterogeneity increase, companies in the supply chain can adopt "penetrating pricing" strategies to stimulate market demand. For high regret consumers, manufacturers can adopt a "commitment advertising" strategy to promise price and quality, and retailers can adopt a "prestige pricing" strategy to reduce consumer perception of regret. In response to products with higher differences in consumer acceptance, manufacturers can adopt a "differentiated customization" strategy to meet different types of consumer demand and retailers can adopt a "differential pricing" strategy for precise marketing.

1. Introduction

In the increasingly fierce market competition, companies generally like to implement discount products to acquire more market advantages and attract more customers, such as Amazon Black Friday, Tmall Double Eleven, and other national carnival shopping discount festivals. On the day of Double Eleven in 2019, the entire network generated 1.337 billion parcels, but the return rate after discount products was as high as 30%. The high return cost caused the original meager profits in the supply chain to disappear [1, 2]. Stimulated by discount products, consumers often expect the current original price products and the future discount products separately. When they realize that their current

choices may regret in the future, the negative emotions shown are anticipated regret. The anticipated regret will not only reduce the shopping experience of consumers but also inevitably produce various resource waste and cost losses [3, 4]. Modern business management has attached great importance to this issue. Like Amazon, AliExpress, and JD.com, many physical malls have promised consumers to enjoy the "right to regret" and implemented offline shopping service with no reason to return and exchange. This measure reduces the risk of consumer anticipated regret and improves corporate reputation [5]. On the other hand, affected by the anticipated regret stimulated by discount products, the product returns will be seriously damaged during the return process. If the supply chain member companies only

consider their own interests and disregard the decisions of other members, it will lead to supply chain coordination problems [6]. The circulation is particularly tricky, specifically manifested as the profits of the members of the supply chain are not guaranteed, and the profit distribution of the supply chain system is uneven. Revenue-sharing contract is a new profit-based form of profit, and its flexible distribution mechanism is particularly suitable for competitive supply chains whose demand depends on price [7]. Therefore, this article considers the revenue-sharing contract as a coordination mechanism.

The “discount products” has become the most common promotion method for enterprises. This promotion strategy brings a surge in transaction volume for the enterprises but also makes consumers face shopping difficulties during the promotion period when the product is out of stock and codes. Consumers need to make choices about the uncertain future promotion environment or do not understand the real values of original price products and discount products before they buy them. Once uncertainty disappears, consumers regret when they know they could have made better choices. With frequent “discount products” promotion strategy, the anticipated regret from consumers will become more common. This phenomenon greatly affects the promotion decisions of enterprises and makes the supply chain evolve new characteristics and laws. Aiming at the behavior of anticipated regret for discount product, this paper introduces the negative utility formula of anticipated regret to derive the demand functions of the original price products and the discount products. After analyzing the impact of regret sensitivity coefficient and consumer heterogeneity on supply chain members, the revenue-sharing contract was introduced to optimize the supply chain.

In summary, in the face of discount product strategies that companies often adopt, what is the impact of anticipated regret on decision-making for consumers? How to guarantee the profits of the member companies of the supply chain under the consumers’ anticipated regret? How should the supply chain choose the appropriate coordination mechanism to achieve the improvement of channel utility? The above has become a new problem in theoretical research and practical management. Revenue-sharing contract is widely used in real life as the most applicable and flexible contract in the supply chain coordination mechanism. The article not only enriches the behavioral economic theory related to consumer anticipated regret but also provides practical basis for companies’ discount product strategies.

2. Literature Review

Aiming at the impact of anticipated regret on the supply chain stimulated by price discounts, this paper designed the revenue-sharing contract to optimize the supply chain profits. So, the following issues are closely related to discount products supply chain, anticipated regret, and revenue-sharing contract. In the following section, the paper reviews studies relevant to discount products supply chain and anticipated regret and highlights the revenue-sharing contract in this situation.

Discount product in supply chain is not only an important topic in everyday society but also receives significant attention in academia. The most representative was that by Monahan [8] who proposed that sellers can attract consumers to increase order volume through discount products, thereby creating more profits. Raju [9] first discovered that the increase of discounts strength will increase the variability of category sales. Davis and Millner [10] used case analysis to demonstrate the impact of different discounts on consumer purchasing behavior, indicating that lower discounts were not favored by consumers. Chan and Lee [11] studied the realization of coordination and incentives for a single coordination model of a single supplier multibuyer supply chain based on discount products of buyer order intervals, finding that the discount products which guaranteed the buyer’s overall related coordination costs were reduced. Andrews et al. [12] studied the relationship between marketing and discount products and found that the influence of marketing on sales purchases follows an inverted U-shape relationship under the moderating effect of price discounts. When the discounts are moderate, it is the strongest. Xia [13] studied a supply chain with only one retailer and supplier and addressed how retailers should use their ordering and price decisions to respond to temporary price discounts from their suppliers. Gao et al. [14] established a dual-channel supply chain model, studied the impact of price discounts on the bullwhip effect in e-commerce, and found that price discounts in online retail markets generally amplify the bullwhip effect in the retail supply chain. Shaikh et al. [15] study two different inventory models, namely, (a) inventory model for zero-ending case and (b) inventory model for shortages case. The demand for both models is considered as price and stock dependent, whereas shortages are partially backlogged at a rate with the length of the waiting time to the arrivals of the next lot. Most of the literature about price discount is based on the assumption that consumers complete rationality. In the actual purchase process, consumers are extremely susceptible to discount products and may have anticipated regrets in purchasing decisions.

Anticipated regret is more common and the discount product strategy becomes more frequent, so more research studies focus on anticipated regret. Most of the existing literature analyzed purchasing behavior from the perspective of consumers. Loomes and Sugden [16] proposed and studied the theory of anticipated regret for the first time. Simonson’s [17] research found that they would buy products that are guaranteed and free from regrets in future choices after consumers learn that they have made wrong decisions. In contrast, it is less likely to buy more risk products (cheaper products; lesser-known brands). Larrick and Boles [18] found that anticipated regret can make people more risk-seeking than risk-averse. Zeelenberg [19] through empirical research found that anticipated regret promoted risk-aversion and risk-seeking options. Bjälkebring et al. [20] conducted research based on the network day and law and found that anticipated regret was relatively common in daily life decision-making. Anticipated regret was less frequent than predicted regret, so controlling and preventing regrets

is an important strategy in our daily decision-making. Syam et al. [21] studied the relationship between anticipated regret and product standardization. By establishing a game model, it was found that the higher the anticipated regret coefficient, the more inclined to purchase standardized products, and this relationship will weaken as the number of products increases; Yin and Yu [22] analyzed the impact of anticipated regret on consumers' impulse purchase behavior through a 2×2 experimental design and found that anticipated regret had a mediation effect in the impact of impulse traits and shopping situations on impulse purchases. Nasiry and Popescu [23] considered two "regrets for action" and "abandon regrets" and analyzed the impact of these two types of anticipated regret on consumers' early purchase decisions. On this basis, Jiang et al. [24] studied the consumer utility formulas with these two types of anticipated regret and analyzed the impact of the sensitivity coefficient of anticipated regret and consumer heterogeneity on the company's new product development strategies. Liu and Zhang [25] analyzed the two-stage dynamic game between retail enterprises and consumers under the symbiotic replacement strategy and single product replacement strategy and found that anticipated regret has a significant impact on consumers' own purchase decisions. Sarangee et al. [26] use anticipated regret theory to develop a model and demonstrate how forward-looking emotions can lead decision-makers to continue failing NPD projects in business-to-business (B2B) markets. The results suggest that anticipated drop regret plays a significant role in commitment to a failing course of action, whereas anticipated keep regret actually reduces commitment. Zhang et al. [27] studied the impact of consumer's anticipated regret on the product innovation supply chain and proposed a continuous replacement product plan. Enterprises should adopt a "moderate innovation strategy" for long-term development. When the attribute exceeds the threshold, the "skimming pricing strategy" is adopted for innovative products; when the product depreciates rapidly, the "skimming pricing strategy" is adopted for incumbent products, and the "penetrating pricing strategy" is adopted for innovative products. The above researches show that anticipated regret has a significant impact on the decisions of supply chain member companies but does not study the impact of anticipated regret caused by "discount products" on supply chain member companies.

In recent years, research on supply chain contract has been quite rich. Starting from Cachon and Lariviere's [28] classic study on supply chain coordination contracts, various contract forms are widely used in a variety of scenarios. Such option contracts were used to solve supply chain financing decisions [29], and wholesale price contracts were used to coordinate retailers' loss-averse supply chains [30]. Revenue-sharing contracts were used to resolve channel conflicts in dual-channel supply chains [31]. Jian et al. [32] examined the contract coordination between manufacturers with peer-induced and distributional fairness concerns and found that there is a revenue-sharing contract parameter in both the peer-induced and distributional fairness concerns of manufacturers. The repurchase contract is suitable for

coordination when the retail price is unchanged, but the revenue-sharing contract can also play a good coordination effect under the variable retail price. Compared with the traditional wholesale price contract, the revenue-sharing contract has greater flexibility and practicality. The actual situation of the article is directed to the "price discount promotion" strategy; the most typical feature is that the retail price is variable, so it is more appropriate to choose the revenue-sharing contract.

The existing literature on discount products is mostly based on the assumption of "consumer complete rationality." But in the actual purchase process, consumers are extremely susceptible to price discounts and are not very clear about the actual utility of discounted products. This has led many consumers to regret after purchasing discounted products [33, 34]. Therefore, it is particularly important to cross-integrate the anticipated regret under discount products with the research on supply chain operations management. Based on this, this paper combines discount products and anticipated regret theory to build three models of centralized decision, decentralized decision, and revenue-sharing decision and analyzes the influence of regret sensitivity coefficient and consumer heterogeneity.

3. Problem Description and Demand Function

3.1. Problem Description. Suppose that consumer wants to buy a product that has just hit the market early. Based on the past shopping experience, the product will be sold at a discount in the future. At this time, consumers are faced with two choices. If they purchase the current original price products, they may regret the expensive purchase. If they buy future discount products, he may face uncertain factors such as product out of stock and code, which may lead to regret for missing the purchase opportunity. The performance of this kind of consumer anticipating future risks before making decisions is called anticipated regret. This paper uses p_n and p_d to denote the selling price of the original price product and the discount product per unit, respectively, and $p_d = \delta \cdot p_n$ (δ is the discount level per unit of product).

Considering a supply chain consisting of a manufacturer (represented by the subscript M) and a retailer (represented by the subscript R), the original price products existing in the market will be discounted at a certain time in the future. p_n represents the price of each unit of original price products. p_d represents the discount price products. $p_d = \delta \cdot p_n$ (δ is the discount level per unit product). At this time, the consumer's valuation for the original price products is v and obeys the uniform distribution on $[0, 1]$. According to consumers' preference for discount products, they are divided into two types: higher preference (type θ_H) and lower preference (type θ_L). θ_H and θ_L , respectively, indicate acceptance of discounted products by two types of consumers. Set $\theta_H = 1$, $\theta_L = 1 - \gamma$. This article uses $\gamma = \theta_H - \theta_L$ to represent consumer heterogeneity. That is the difference in acceptance of discount products between θ_H and θ_L consumers, because consumers do not know the discount time and discount information of discount products. They are not

sure of their true preferences before buying, and they do not know the expected utility that can be obtained by purchasing discount products. They only know whether to choose the original price products or the discount products; there are 1/2 possibilities to regret; that is, the probability of belonging to both θ_H and θ_L is 1/2. The consumer's expected utility in purchasing discounted product can be expressed as $((\theta_H + \theta_L)/2)v$. Because consumers have a certain fear of anticipated regret, the anticipated regret generated before the purchase decision will have certain side effects on the consumer's utility. According to research by Jiang et al. [24], the formula for calculating the anticipated regret side effects is as follows:

$$\text{A.R.} = -\lambda_i \cdot \text{prob}(U_f > U_c) \cdot (U_f - U_c). \quad (1)$$

When the consumer chooses to purchase the original price products, the consumer of type θ_H may regret. The net utility of type θ_H consumers who give up buying original

price products and buying discount products is $U_f = \theta_H v - p_d = v - \delta p_n$. The actual net utility of type θ_H consumers who continue to choose to purchase original priced products is $U_c = v - p_n$.

When the consumer chooses to purchase the discount products, the consumer of type θ_L may regret. The net utility of type θ_L consumers who give up buying discount products and buying original price products is $\bar{U}_f = v - p_n$. The actual net utility of type θ_L consumers who continue to choose to purchase discount products is $\bar{U}_c = \theta_L v - p_d = (1 - \gamma)v - \delta p_n$.

3.2. Demand Function. According to the above-mentioned analysis, the expressions of the anticipated regret net utility of consumers who purchase of the original products and the discount products are as follows:

$$\begin{aligned} U_n &= v - p_n - \frac{\lambda}{2} ((v - \delta p_n) - (v - p_n)) = v + \frac{p_n}{2} (-2 + (\delta - 1)\lambda), \\ U_d &= \frac{(v - \delta p_n) + ((1 - \gamma)v - \delta p_n)}{2} - \frac{\lambda}{2} (v - p_n - ((1 - \gamma)v - \delta p_n)) \\ &= \frac{\gamma}{2} (2 - \gamma - \lambda\gamma) + \frac{p_n}{2} (\lambda - 2\delta - \lambda\delta). \end{aligned} \quad (2)$$

Similar to the description of Örsdemir et al. and Chiang et al. [35, 36], consumers purchase the original price products when $U_n > U_d$ and $U_n > 0$ are satisfied. Consumers purchase discount products when $U_n < U_d$ and $U_d > 0$ are satisfied. The critical payment points are $v_1 = -(2p_n(\delta - 1)/\gamma)$, $v_2 = (p_n(2 + \lambda - \delta\lambda)/2)$, and

$v_3 = (p_n(\lambda - \delta(2 + \lambda))/-2 + \gamma + \gamma\lambda)$ derived from $U_n = U_d$, $U_n = 0$, and $U_d = 0$. Comparing these three critical payment points can obtain the demand function of the original price product and discounted product in the supply chain at this time:

$$\begin{aligned} D_n &= \int_{U_n > U_d, U_n > 0} f(v)dv = \begin{cases} 1 - \frac{p_n(2 + \lambda - \delta\lambda)}{2}, & \text{if } p_n \leq 0, \\ 1 + \frac{2p_n(\delta - 1)}{\gamma}, & \text{if } 0 \leq p_n \leq \frac{\gamma}{2 - 2\delta}, \\ 0, & \text{if } p_n \geq \frac{\gamma}{2 - 2\delta}, \end{cases} \\ D_d &= \int_{U_d > U_n, U_d > 0} f(v)dv = \begin{cases} 0, & \text{if } p_n \leq 0, \\ \frac{2p_n(\delta - 1)}{\gamma} - \frac{p_n(\lambda - \delta(2 + \lambda))}{-2 + \gamma + \gamma\lambda}, & \text{if } 0 \leq p_n \leq \frac{\gamma}{2 - 2\delta}, \\ 1 - \frac{p_n(\lambda - \delta(2 + \lambda))}{-2 + \gamma + \gamma\lambda}, & \text{if } p_n \geq \frac{\gamma}{2 - 2\delta}. \end{cases} \end{aligned} \quad (3)$$

In the game model, the unprofitable situation of the companies in the supply chain is not considered. The price of the products needs to satisfy the inequality: $0 \leq p_n \leq (\gamma/2 - 2\delta)$. At this time, the demand functions of the original price products and the discount products are as follows:

$$\begin{aligned} D_n &= 1 + 2p_n A, \\ D_d &= (-2A - B)p_n. \end{aligned} \quad (4)$$

Among them,

$$\begin{aligned} A &= \frac{\delta - 1}{\gamma}, \\ B &= \frac{\lambda - \delta(2 + \lambda)}{\gamma + \gamma\lambda - 2}. \end{aligned} \quad (5)$$

4. Models of Different Power Structures

When manufacturers and retailers play a game in the supply chain, the manufacturers determine the wholesale price of the products, and the retailers determine the retail price of the products. According to the demand function of original price products and discount products, the profit expressions of manufacturers and retailers are as follows:

$$\pi_M(w) = (w - c)(1 + 2p_n A) + (w - c)(-2p_n A - p_n B), \quad (6)$$

$$\pi_R(p_n) = (p_n - w)(1 + 2p_n A) + (\delta p_n - w)(-2p_n A - p_n B). \quad (7)$$

4.1. Centralized Decision-Making Model. In the case of centralized decision-making situation (CL), manufacturers and retailers form a unified decision-making body. They start from maximizing the overall total profits of the supply chain. The total profit π^{CL} of the entire supply chain under centralized decision-making is as follows:

$$\begin{aligned} \pi^{CL} &= (w - c)(1 - p_n B) + (p_n - w)(1 + 2p_n A) \\ &\quad + (\delta p_n - w)(-2p_n A - p_n B). \end{aligned} \quad (8)$$

Since $\pi_{ALL}^{CL*} > 0$ needs to be satisfied, $8A(-1 + \delta) + 4B\delta > 0$ and $(\partial^2 \pi^{CL} / \partial p_n^2) = 4A - 4A\delta - 2B\delta < 0$ are satisfied. So, the stagnation point is the point where the profit of the unconstrained equilibrium model is maximized. Derivate p_n in (8), and obtain the equilibrium expression of retail price p_n :

$$p_n^{CL*} = \frac{1 + Bc}{-4A + 4A\delta + 2B\delta} \quad (9)$$

Substituting the above expression, the total profits of the supply chain in the case of centralized decision-making situation can be obtained:

$$\pi_{ALL}^{CL*} = \frac{(1 + Bc)^2}{8A(-1 + \delta) + 4B\delta} - c. \quad (10)$$

4.2. Decentralized Decision-Making Model. Decentralized decision (DL) situation studies traditional manufacturers-dominated supply chains, where manufacturers have a dominant role in the pricing process. For example, the vehicle manufacturing company Toyota Motor has completed the preliminary research and development, procurement, manufacturing, logistics (shipping), and 4S store management mode on the basis of the original manufacturer. Other upstream and downstream supply chains are supporting enterprises [37]. In the entire supply chain, Toyota car manufacturers have the leading power. Solved by the inverse induction method, the retailers' profits function formula (7) finds the first derivative of p_n and gets the response function of product retail price p_n to wholesale price w :

$$p_n = \frac{1 + Bw}{4A(-1 + \delta) + 2B\delta}. \quad (11)$$

Substituting (11) into (6) gives the manufacturers' profits function expression for w :

$$\pi_M(w) = (w - c) \left(1 - \frac{1 + Bw}{4A(-1 + \delta) + 2B\delta} B \right). \quad (12)$$

Since $\pi_M^{DL*} > 0$ needs to be satisfied, $2A(-1 + \delta) + B\delta > 0$ is derived. $(\partial^2 \pi_M / \partial w^2) = -(B^2/2A(-1 + \delta) + B\delta) < 0$ is proved. The stagnation point is the point where the profit of the unconstrained equilibrium model is maximized. Find the first-order partial derivative of w in (12) to obtain the equilibrium expression of the wholesale price w . Replace the reaction function (11) to obtain the equation of equilibrium p_n :

$$w^{DL*} = \frac{4A(\delta - 1) + B(Bc + 2\delta - 1)}{2B^2}, \quad (13)$$

$$p_n^{DL*} = \frac{1}{4} \left(\frac{2}{B} + \frac{1 + Bc}{2A(\delta - 1) + B\delta} \right).$$

By substituting the above expressions back, we can obtain the demand functions for the original price products and discount products and the profits of manufacturers and retailers in the case of decentralized decision-making situation:

$$\begin{aligned}
D_n^{DL*} &= 1 + \frac{A}{B} + \frac{A + ABc}{4A(\delta - 1) + 2B\delta}, \\
D_d^{DL*} &= \frac{1}{4}(2A + B) \left(-\frac{2}{B} - \frac{1 + Bc}{2A(\delta - 1) + B\delta} \right), \\
\pi_M^{DL*} &= \frac{(4A + B + B^2c - 2(2A + B)\delta)^2}{8B^2(2A(\delta - 1) + B\delta)}, \\
\pi_R^{DL*} &= \frac{-48A^2(\delta - 1)^2 - 8AB(\delta - 1)(Bc + 6\delta - 3) + B^2((1 + Bc)^2 - 4(Bc - 3)\delta - 12\delta^2)}{16B^2(2A(\delta - 1) + B\delta)}.
\end{aligned} \tag{14}$$

4.3. Model Analysis

Proposition 1. λ has an inflection point. When λ is smaller than the inflection point, p_n is positively correlated with λ , and w is positively correlated with λ ; when λ is greater than the inflection point, p_n is negatively correlated with λ , and w is negatively correlated with λ .

Proposition 1 shows that, as the regret sensitive coefficient increases, the wholesale price and retail price increase first and then decrease. This is because the regret sensitive coefficient is smaller, companies in the supply chain adopt a “skimming pricing” strategy to increase customer perceived value. When the regret sensitive coefficient increases, the reduction of wholesale and retail prices will stimulate more market demands and obtain more supply chain profits. At this time, enterprises should increase the supply of products to meet market demands, increase product promotion efforts, and attract potential customers to expand consumer groups.

Proposition 2. γ has an inflection point. When γ is smaller than the inflection point, w is positively correlated with γ ; when γ is greater than the inflection point, w is negatively correlated with γ .

Proposition 2 shows that, with the consumer heterogeneity increases, the wholesale price of a product increases first and then decreases. This is because when consumer heterogeneity is lower, supply chain companies gain market profits by increasing product prices. But when consumer heterogeneity is higher, supply chain companies stimulate market demand by reducing the wholesale price of products. At this time, enterprises adopt customized service strategies for consumers with different market preferences and provide professional, one-to-one services.

Proposition 3. Compare and analyze the total profits of the supply chain under different decision-making situations, and find that $\pi_{ALL}^{DL*} < \pi_{ALL}^{CL*}$.

Proposition 3 shows that the total profits of the supply chain in the case of centralized decision-making are always greater than that in the case of decentralized decision-making. This is because the centralized situation is based on maximizing the overall total profit of the supply chain.

Centralized decision-making can make manufacturers, retailers, and consumers benefit.

The above proposition proof process is detailed in Appendix. Because derivative result of profits formula is too complicated, the results will be discussed in the numerical analysis section.

5. Revenue-Sharing Contract

The supply chain collaboration incentive mechanism based on the revenue-sharing contract is that the manufacturer wholesales the product to the retailer at a lower wholesale price w in the early stage of the sale. After the sales cycle ends, the retailers receive φ ($0 < \varphi < 1$) proportion of revenue and share $1 - \varphi$ proportion of sales revenue to the manufacturers. The profits of the manufacturers and the retailers after being coordinated by the revenue-sharing contract (the coordinated expression is marked with “CO”) are as follows:

$$\pi_M^{CO}(w) = (w - c)(1 - p_n B) + (1 - \phi)(p_n(1 + 2p_n A) - \delta p_n((2A + B)p_n)), \tag{15}$$

$$\pi_R^{CO}(p_n) = (\phi p_n - w)(1 + 2p_n A) + (\phi \delta p_n - w)((-2A - B)p_n). \tag{16}$$

The purpose of the revenue-sharing mechanism is to make the optimal retail price under the decentralized decision equal the sales price when the expected profit of the supply chain is maximized; that is, $p_n^{CO} = p_n^{CL}$. The optimal retail price after deriving the retailers’ profit (16) from p_n can be calculated:

$$p_n^{CO} = \frac{Bw + \varphi}{2(-2A + 2A\delta + B\delta)\varphi}. \tag{17}$$

Therefore, as long as (17) is equal to (9), the purpose of incentives is achieved:

$$w^{CO} = c\varphi. \tag{18}$$

Take formulas (17) and (18) into formulas (15) and (16), respectively, and the total profits of the manufacturers, retailers, and supply chain after the revenue-sharing contract are as follows:

$$\begin{aligned}\pi_M^{\text{CO}} &= \frac{((1+Bc)^2 - 8Ac(\delta-1) - 4Bc\delta)(1-\varphi)}{8A(\delta-1) + 4B\delta}, \\ \pi_R^{\text{CO}} &= \frac{((1+Bc)^2 - 8Ac(\delta-1) - 4Bc\delta)\varphi}{8A(\delta-1) + 4B\delta}, \\ \pi_{\text{ALL}}^{\text{CO}} &= \frac{(1+Bc)^2}{8A(\delta-1) + 4B\delta} - c.\end{aligned}\quad (19)$$

The revenue-sharing contract needs to meet the principle of individual rational people; that is, the profits of the manufacturers and the retailers must not be less than the profits of the noncooperation:

$$\pi_M^{\text{CO}} \geq \pi_M^{\text{DL}}, \quad (20)$$

$$\pi_R^{\text{CO}} \geq \pi_R^{\text{DL}}. \quad (21)$$

From (20) and (21), we can get

$$\frac{-48A^2(\delta-1)^2 - 8AB(\delta-1)(Bc+6\delta-3) + B^2((1+Bc)^2 - 4(Bc-3)\delta - 12\delta^2)}{4B^2((1+Bc)^2 - 8Ac(\delta-1) - 4Bc\delta)} \leq \varphi \leq 1 - \frac{(4A+B+B^2c-2(2A+B)\delta)^2}{2B^2((1+Bc)^2 - 8Ac(\delta-1) - 4Bc\delta)}. \quad (22)$$

Proposition 4. *Under the role of the supply chain collaboration mechanism of revenue-sharing contract, the wholesale price should satisfy $w = c\varphi$, and*

$$\frac{-48A^2(\delta-1)^2 - 8AB(\delta-1)(Bc+6\delta-3) + B^2((1+Bc)^2 - 4(Bc-3)\delta - 12\delta^2)}{4B^2((1+Bc)^2 - 8Ac(\delta-1) - 4Bc\delta)} \leq \varphi \leq 1 - \frac{(4A+B+B^2c-2(2A+B)\delta)^2}{2B^2((1+Bc)^2 - 8Ac(\delta-1) - 4Bc\delta)}. \quad (23)$$

Proposition 4 shows that when the revenue-sharing contract is introduced for coordination, the revenue-sharing ratio φ is an increasing function of the wholesale price w . This means that, in the case of decentralized decision-making, when the wholesale price agreed between the manufacturers and the retailers is higher, the retailers will enjoy the higher proportion of the φ benefit, and the proportion of the $1-\varphi$ benefit to the manufacturers is smaller. Because when the wholesale price is higher, the retailers' purchase costs paid by the retailers at the beginning of the sales season are higher. At the end of the sales season, the smaller the profit realized by the retailers is, the smaller the proportion of profits shared with the manufacturers will be.

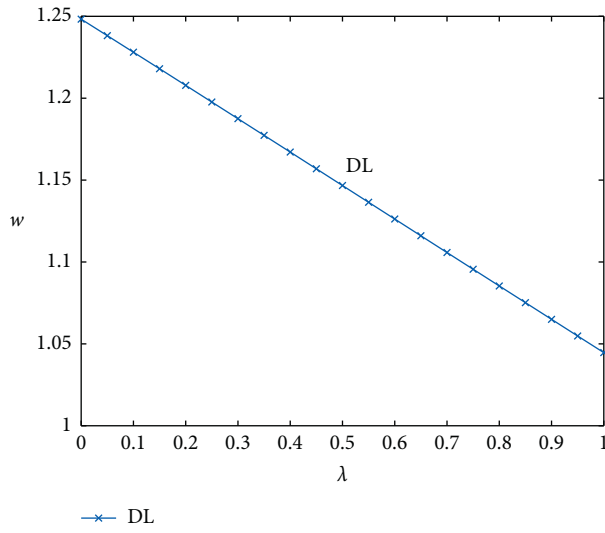
6. Numerical Analysis

On the basis of theoretical analysis, in order to further visually inspect, this part uses the method of numerical simulation to study the influence of regret sensitivity coefficient and consumer heterogeneity on the pricing decisions of various enterprises in the supply chain. According to the past experience, a cup with cost of two dollars will be discounted by 0.8% during the promotion period. Suppose that such consumers who prefer discounted cup are $\theta_H = 1$, and those who prefer original price cup are $\theta_L = 0.1$. Consumer heterogeneity $\gamma = \theta_H - \theta_L = 0.9$ indicates the difference in the acceptance of discounted cup between these two types of consumers. Consumers' sensitivity to anticipated regret is $\lambda = 0.7$. Therefore, the parameters of numerical simulation are set as $\delta = 0.8$, $\gamma = 0.9$, $\lambda = 0.7$, and $c = 2$.

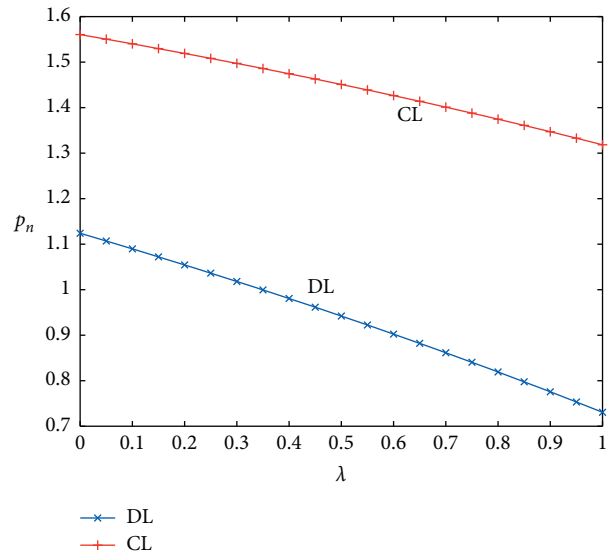
6.1. Sensitivity Analysis of Regret Sensitive Coefficient. Because anticipated regret affects consumers' acceptance of the cup, it has an important impact on the supply chain. For further visual inspection, the change curves of retail price, wholesale price, and system profits in the supply chain are plotted. It can be shown in Figures 1 and 2.

It can be seen from Figure 1 that the wholesale price (Figure 1(a)) and retail price (Figure 1(b)) of products will decrease with the increase of the regret sensitivity coefficient. And the retail price in the case of centralized decision-making is much higher than that of decentralized decision-making. This shows anticipated regret expanding the uncertainty of cups' market transactions, so companies can adopt "penetration pricing" strategies to stimulate market demands.

It can be seen from Figure 2 that, with the increased regret sensitivity coefficient, manufacturers' profits (Figure 2(a)), retailers' profits (Figure 2(b)), and the total profits of supply chain (Figure 2(c)) will increase. This shows "penetration pricing" strategy adopted by companies in the supply chain, which has stimulated market demands and achieved a surge in corporate profits. At this time, manufacturers and retailers should especially strengthen the quality and commitment of cups to consumers with high levels of anticipated regret and reduce the level of consumer regret perception. In the case of centralized decision-making, the total profit of the supply chain is much higher than that in the case of decentralized decision-making. The decentralized decision-making situation needs to be coordinated to achieve the optimal decision of the supply chain.

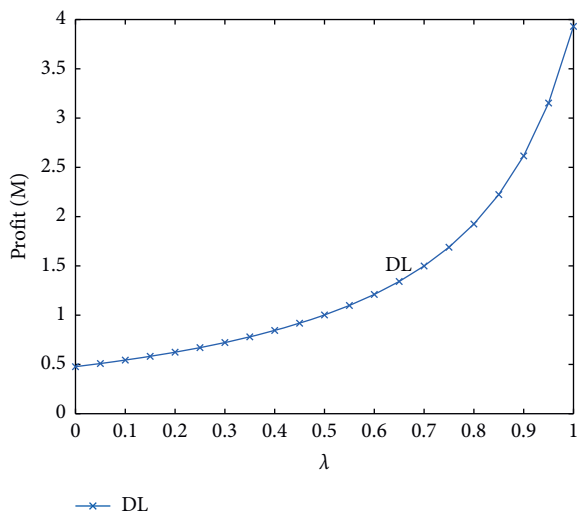


(a)

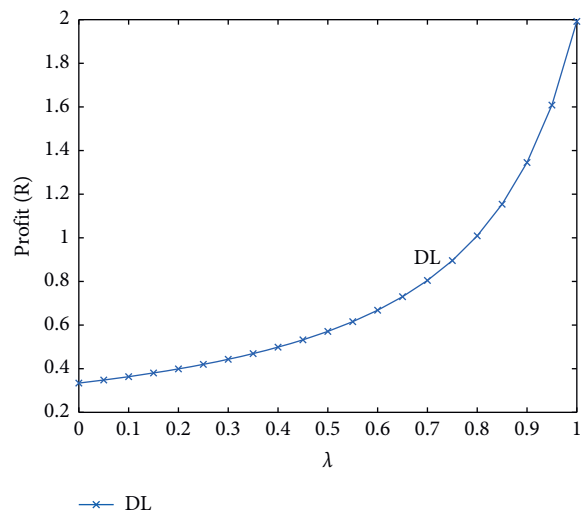


(b)

FIGURE 1: The impact of regret sensitivity coefficient on wholesale price and retail price: (a) wholesale price and (b) retail prices.

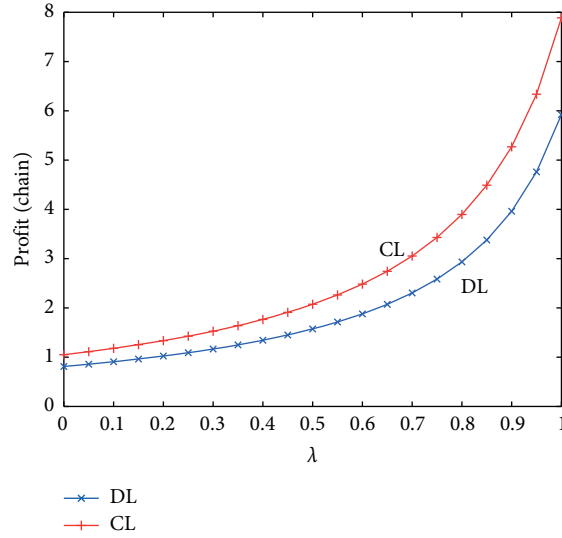


(a)



(b)

FIGURE 2: Continued.



(c)

FIGURE 2: The impact of regret sensitivity coefficient on profits in the supply chain: (a) manufacturers' profits, (b) retailers' profits, and (c) the total profits of supply chain.

6.2. *Sensitivity Analysis of Consumer Heterogeneity.* Because different types of consumers have different acceptance levels of discount cups, the paper uses γ to indicate consumer heterogeneity. This article studies the impact of consumer heterogeneity on cups' prices and the profits of both parties. It can be shown in Figures 3 and 4.

As can be seen from Figure 3, with consumer heterogeneity increases, the wholesale price (Figure 3(a)) of the product decreases, and the retail price (Figure 3(b)) increases first and then decreases. This is because the heterogeneity of consumers increases the uncertainty of the cup's market. Manufacturers adopt the "low-cost strategy" to obtain more market demands. Retailers first increase the perceived price of customers by increasing the retail price of cups. The "low-price strategy" attracts high-preference (θ_H type) consumers. At this time, the supply chain companies can understand the different shopping preferences of consumers through market research and adopt a "commitment-based advertising strategy" to make quality and price commitments to consumers, reducing the uncertainty of consumer perception. In the centralized decision-making situation, the retail price in this case is higher than the decentralized decision, which shows that market leaders often adopt price competition strategies to obtain supply chain profits. When $\gamma \rightarrow 0$, the retail price in the case of decentralized decision-making was greater than that in centralized decision-making. Because there are no infinitely small cognitive differences in the product market, this case is not considered in the paper.

As can be seen from Figure 4, as consumer heterogeneity increases, manufacturers' profits (Figure 4(a)) increase first and then decrease and retailers' profits (Figure 4(b)) and the total profits of the supply chain (Figure 4(c)) all increase. This shows that, in the face of consumers with different cup demands, companies adopt "customized services" and "low-

price competition" strategies to stimulate enterprises to obtain more profits. The profit in the case of centralized decision-making is always higher than the profit in the case of decentralized decision-making. Therefore, this paper designs a contract coordination mechanism for decentralized decision-making situations to achieve optimal decision-making in the supply chain.

6.3. *Optimal Results and Comparison of Different Decision Models.* First, by comparing the optimal results under the decentralized decision and centralized decision and revenue-sharing mechanism, it can be seen in Table 1 that, compared with decentralized decisions, centralized decision-making reduces the retail price of products and increases the total profit of the supply chain. In other words, decentralized decisions reduce the overall profit of the supply chain and therefore need to be coordinated. After introducing the revenue-sharing contract to coordinate decentralized decision-making, we can know that when the revenue-sharing coefficient satisfies $0.26 < \varphi < 0.51$ (derived from Proposition 4), there are always $\pi_M^{CO} \geq \pi_M^{DL}$, $\pi_R^{CO} \geq \pi_R^{DL}$, and $\pi_{ALL}^{CO} \geq \pi_{ALL}^{DL}$. This proves that the design of the revenue-sharing contract increases the profits of both the manufacturer and the retailer, and the overall profit of the supply chain reaches the total profit of the centralized decision-making supply chain. The revenue-sharing contract mechanism coordinated the decentralized supply chain, achieved Pareto improvement, and achieved a "win-win" situation in the supply chain.

Figure 5 shows that any value is within the range of $0.26 < \varphi < 0.51$, manufacturers' profits (Figure 5(a)) under the revenue-sharing mechanism gradually increase, and retailers' profits (Figure 5(b)) gradually decline with φ increase. The profits that manufacturers and retailers can distribute in any proportion are greater than the profits

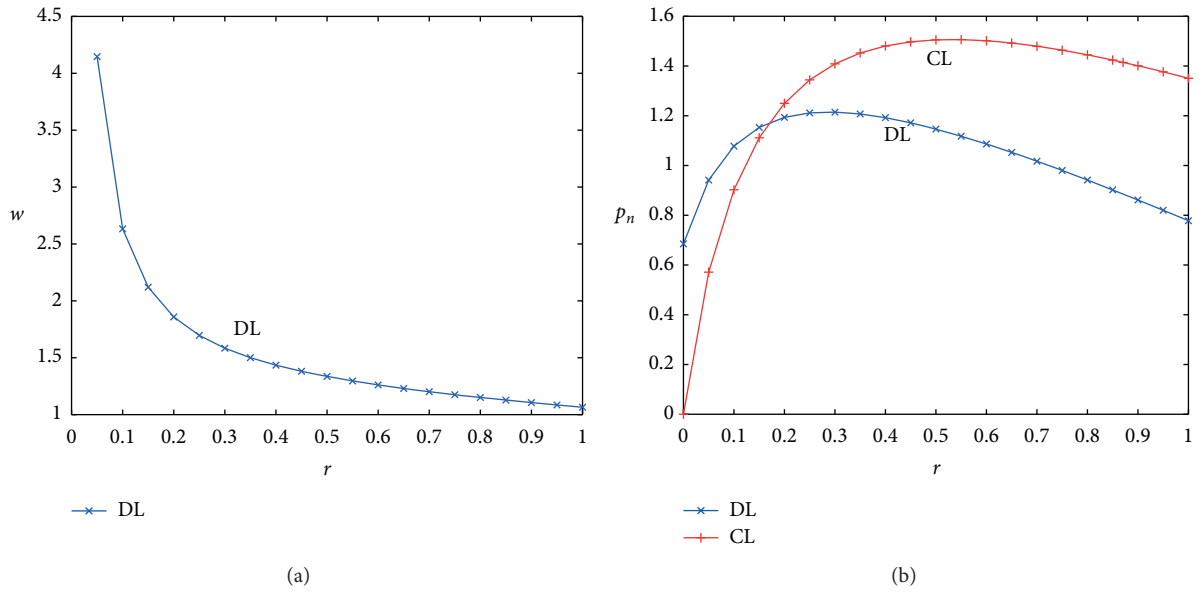


FIGURE 3: The impact of consumer heterogeneity on wholesale price and retail price: (a) wholesale price and (b) retail price.

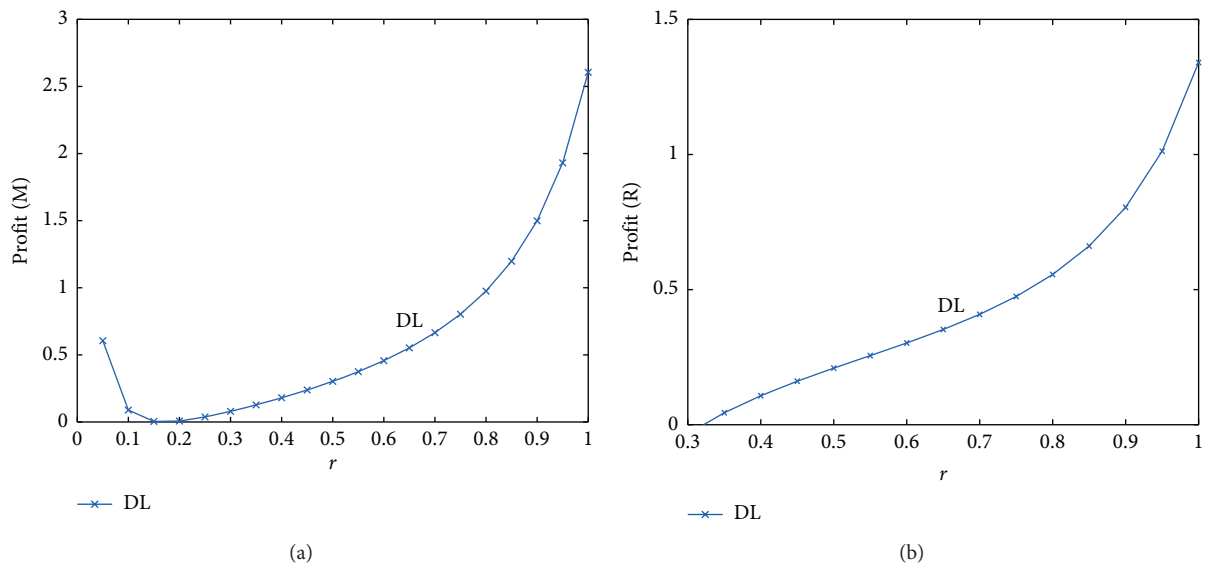
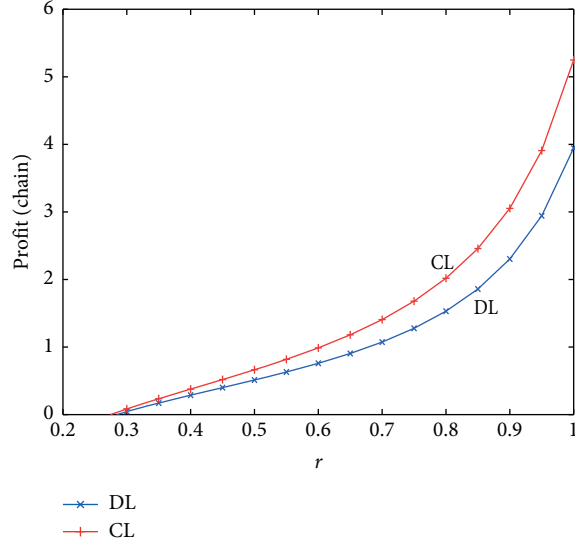


FIGURE 4: Continued.

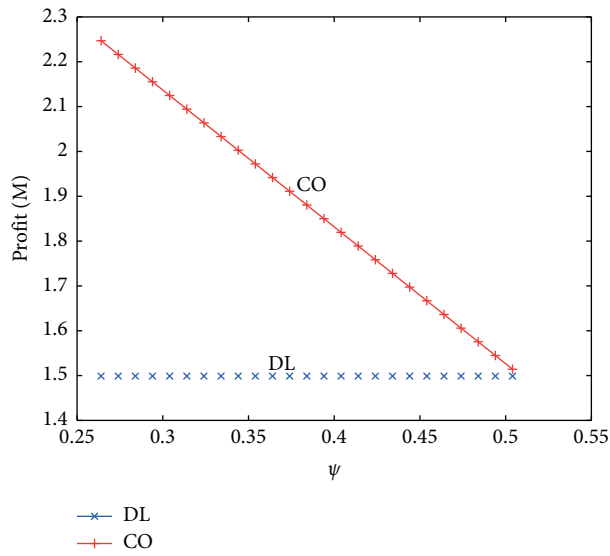


(c)

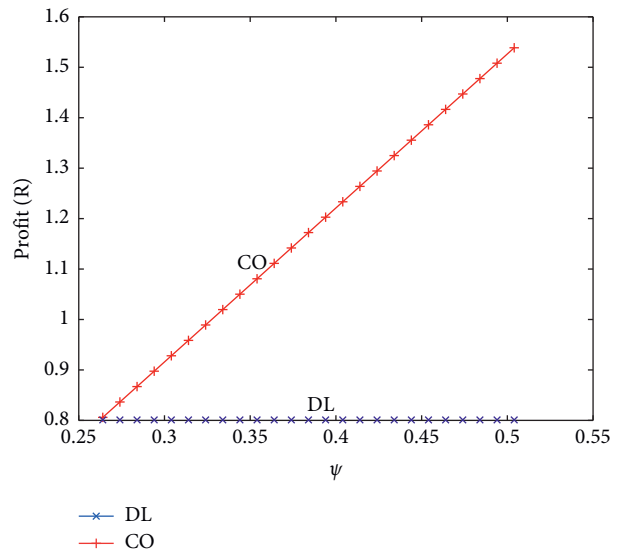
FIGURE 4: The impact of consumer heterogeneity on profits in the supply chain: (a) manufacturers' profits, (b) retailers' profits, and (c) the total profits of supply chain.

TABLE 1: Profit comparison of members under decentralized decision, centralized decision, and coordination mechanism.

	$0.26 < \varphi < 0.51$	Manufacturer profit	Retailer profit	Total supply chain profit
Centralized decision				$\pi_{ALL}^{DL*} = 3.05$
Decentralized decision		$\pi_M^{CL*} = 1.5$	$\pi_R^{CL*} = 0.8$	$\pi_{ALL}^{CL*} = 2.3$
Revenue-sharing contract	$\varphi = 0.3$	$\pi_M^{CO*} = 2.14$	$\pi_R^{CO*} = 0.91$	$\pi_{ALL}^{CO*} = 3.05$
	$\varphi = 0.35$	$\pi_M^{CO*} = 1.98$	$\pi_R^{CO*} = 1.07$	$\pi_{ALL}^{CO*} = 3.05$
	$\varphi = 0.4$	$\pi_M^{CO*} = 1.83$	$\pi_R^{CO*} = 1.22$	$\pi_{ALL}^{CO*} = 3.05$
	$\varphi = 0.45$	$\pi_M^{CO*} = 1.68$	$\pi_R^{CO*} = 1.37$	$\pi_{ALL}^{CO*} = 3.05$



(a)



(b)

FIGURE 5: The impact of different contract parameters on supply chain profits under the revenue-sharing mechanism: (a) manufacturers' profits and (b) retailers' profits.

TABLE 2: Explanation of major symbols and hypothesis.

Variable symbol	Variable description	Assumptions
p_n	The selling price of the original product per unit	
p_d	The selling price of the discount product per unit	
w	Wholesale price product per unit	
δ	Discount level of product per unit	$0 < \delta < 1$
v	The consumer valuation of buying original price products	$0 < v < 1$
θ_H	Consumers who have a higher preference for discount products	$\theta_H = 1$
θ_L	Consumers who have a lower preference for discount products	$\theta_L = 1 - \gamma$
$\lambda_i (i \in \{f, c\})$	Regret sensitivity coefficient, used to measure how sensitive consumers are to anticipated regret	$0 < \lambda < 1, \lambda_c = \lambda_f = \lambda$
$\text{prob}(U_f > U_c)$	The possibility of anticipated regret	$\text{prob}(U_f > U_c) = (1/2)$
γ	Consumer heterogeneity	
U_f	Net effect of forgotten products	
U_c	Net effect of chosen products	
c	Manufacturer's production costs	

when the two parties do not cooperate. When the two parties agree on the parameters of the revenue-sharing contract, the parameters can choose any value in the area. At this time, the profits of both parties are greater than or equal to the profits when they do not cooperate.

7. Conclusions

This article considers consumer anticipated regret caused by the “price discount” strategy, constructs centralized decision-making, and decentralizes decision-making models. By examining the effects of regret sensitivity coefficient and consumer heterogeneity on the pricing decisions of supply chain member companies, this paper studies the company's promotion strategies.

As the regret sensitivity coefficient and consumer heterogeneity increase, the price of the product first increases and then decreases. When the regret sensitivity coefficient and consumer heterogeneity are lower, companies in the supply chain can adopt the “skimming pricing” strategy in order to obtain more profits; as the regret sensitivity coefficient and consumer heterogeneity increase, market transactions uncertainty has expanded, so companies in the supply chain can adopt “penetrating pricing” strategies to stimulate market demand. Through numerical simulations, it has been found that low-price strategies cause manufacturers in the supply chain to bear more profit losses. For high regret consumers, manufacturers can adopt a “commitment advertising” strategy to promise price and quality, and retailers can adopt a “prestige pricing” strategy to reduce

consumer perception of regret. In response to products with higher differences in consumer acceptance, manufacturers can adopt a “differentiated customization” strategy to meet different types of consumer demand, and retailers can adopt a “differential pricing” strategy for precise marketing.

This article analyzes the impact of anticipated regret under the stimulation of discount products and designs a revenue-sharing contract to achieve a win-win situation for manufacturers and retailers. Although our research addresses some issues, there are still some limitations. For example, this article does not consider the impact on the supply chain when there is a competition between original price products and discount products, nor does it consider the impact of regrets on the retailer-led supply chain at the same time.

Appendix

A. Sign Convention

In the model constructed in this paper, the definition and assumptions of specific parameter symbols are shown in Table 2.

B. Proof Process of Propositions

The first proposition: the expressions of decentralized decision-making (DL) w and p_n , respectively, find the first-order partial derivative of λ and get

$$\frac{\partial w^{\text{DL}}}{\partial \lambda} = \frac{(-2 + \gamma + (2 + \gamma)\delta)(-16(-1 + \delta)^2 + \gamma(8 + 7\lambda + \delta(-14 - 13\lambda + \delta(4 + 6\lambda))))}{2\gamma(-\lambda + \delta(2 + \lambda))^3}, \quad (\text{B.1})$$

$$\frac{\partial p_n^{\text{DL}}}{\partial \lambda} = \frac{-2 + \gamma + (2 + \gamma)\delta}{4} \left(\frac{\gamma(2c(-1 + \delta)^2 - \gamma\delta)}{(-4(-1 + \delta)^2 + \gamma(2(1 + \lambda) + \delta(-4 + (-3 + \delta)\lambda)))^2} - \frac{2}{(\lambda - \delta(2 + \lambda))^2} \right).$$

It can be seen that λ has an inflection point. When λ is smaller than the inflection point, $(\partial w^{\text{DL}}/\partial \lambda) > 0$, $(\partial p_n^{\text{DL}}/\partial \lambda) > 0$.

When λ is greater than the inflection point, $(\partial w^{\text{DL}}/\partial \lambda) < 0$, $(\partial p_n^{\text{DL}}/\partial \lambda) < 0$. Therefore, Proposition 1 is

proved. The specific proof process of the centralized decision case (CL) is similar to the decentralized decision case (DL) and is omitted here for the sake of space.

The second proposition: in the case of decentralized decision-making, the expression w finds the first partial derivative of γ :

$$\frac{\partial w^{DL}}{\partial \gamma} = \frac{-16(-1 + \delta)^2 + \gamma^2(1 + \lambda)(4 + 3\lambda + \delta(-6 + (-5 + 2\delta)\lambda))}{2(2\gamma\delta + \gamma(-1 + \delta)\lambda)^2}. \quad (\text{B.2})$$

It can be seen that γ has an inflection point. When γ is smaller than the inflection point, $(\partial p_n^{DL}/\partial \gamma) > 0$. When γ is greater than the inflection point, $(\partial p_n^{DL}/\partial \gamma) < 0$. Therefore, Proposition 2 is proved. The specific proof process of the centralized decision case (CL) is similar to the decentralized decision case (DL) and is omitted here for the sake of space.

The third proposition: subtract the total profit of the supply chain in different situations:

$$\pi_{ALL}^{DL*} - \pi_{ALL}^{CL*} = -\frac{(4A + B + B^2c - 2(2A + B)\delta)^2}{16B^2(-2A + 2A\delta + B\delta)} < 0. \quad (\text{B.3})$$

Since $-2A + 2A\delta + B\delta > 0$, $\pi_{ALL}^{DL*} - \pi_{ALL}^{CL*} < 0$ is always true, so Proposition 3 is proved.

Data Availability

The data used to support the findings of this study are included within the article.

Conflicts of Interest

The authors declare that they have no conflicts of interest.

Acknowledgments

The authors are grateful to the support of Team of Trade Circulation Funding Project (CJSYTD201701), Chongqing Municipal Education Commission humanities and Social Sciences Research Project (17SKG065), E-commerce and modern logistics Chongqing university municipal key laboratory open fund project (ECML202002), Chongqing Social Science Planning Doctoral Program, China(2018BS71), and the Humanities & Social Science Foundation of Chongqing Municipal Education Commission, China(18SKGH045).

References

- [1] Y. Su and W. Sun, "Analyzing a closed-loop supply chain considering environmental pollution using the NSGA-II," *IEEE Transactions on Fuzzy Systems*, vol. 27, no. 5, pp. 1066–1074, 2019.
- [2] J. Jian, Y. Guo, L. Jiang, Y. An, and J. Su, "A multi-objective optimization model for green supply chain considering environmental benefits," *Sustainability*, vol. 11, no. 21, p. 5911, 2019.
- [3] G. Y. Ke and J. H. Bookbinder, "Coordinating the discount policies for retailer, wholesaler, and less-than-truckload carrier under price-sensitive demand: a tri-level optimization approach," *International Journal of Production Economics*, vol. 196, no. 1, pp. 82–100, 2018.
- [4] M. Mourali, Z. Yang, F. Pons, and D. Hassay, "Consumer power and choice deferral: the role of anticipated regret," *International Journal of Research in Marketing*, vol. 35, no. 1, pp. 81–99, 2018.
- [5] J. Su, Q. Bai, S. Sindakis, X. Zhang, and T. Yang, "Vulnerability of multinational corporation knowledge network facing resource loss," *Management Decision*, 2020, In press.
- [6] R. Levi, G. Perakis, C. Shi, and W. Sun, "Strategic capacity planning problems in revenue-sharing joint ventures," *Production and Operations Management*, vol. 29, no. 3, pp. 1–24, 2020.
- [7] J. A. Niederhoff and P. Kouvelis, "Effective and necessary: individual supplier behavior in revenue sharing and wholesale contracts," *European Journal of Operational Research*, vol. 277, no. 3, pp. 1061–1070, 2019.
- [8] J. P. Monahan, "A quantity discount pricing model to increase vendor profits," *Management Science*, vol. 32, no. 11, pp. 1513–1517, 1986.
- [9] J. S. Raju, "The effect of price promotions on variability in product category sales," *Marketing Science*, vol. 11, no. 3, pp. 207–220, 1992.
- [10] D. D. Davis and E. L. Millner, "Rebates, matches, and consumer behavior," *Southern Economic Journal*, vol. 72, no. 2, pp. 410–421, 2005.
- [11] C. K. Chan and Y. C. E. Lee, "A co-ordination model combining incentive scheme and co-ordination policy for a single-vendor-multi-buyer supply chain," *International Journal of Production Economics*, vol. 135, no. 1, pp. 136–143, 2012.
- [12] M. Andrews, X. Luo, Z. Fang, and J. Aspara, "Cause marketing effectiveness and the moderating role of price discounts," *Journal of Marketing*, vol. 78, no. 6, pp. 120–142, 2014.
- [13] Y. Xia, "Responding to supplier temporary price discounts in a supply chain through ordering and pricing decisions," *International Journal of Production Research*, vol. 54, no. 7, pp. 1938–1950, 2016.
- [14] D. Gao, N. Wang, Z. He, and T. Jia, "The bullwhip effect in an online retail supply chain: a perspective of price-sensitive demand based on the price discount in E-commerce," *IEEE Transactions on Engineering Management*, vol. 64, no. 2, pp. 134–148, 2017.
- [15] A. A. Shaikh, M. A.-A. Khan, G. C. Panda, and I. Konstantaras, "Price discount facility in an EOQ model for deteriorating items with stock-dependent demand and partial backlogging," *International Transactions in Operational Research*, vol. 26, no. 4, pp. 1365–1395, 2019.
- [16] G. Loomes and R. Sugden, "Regret theory: an alternative theory of rational choice under uncertainty," *The Economic Journal*, vol. 92, no. 368, pp. 805–824, 1982.
- [17] I. Simonson, "The influence of anticipating regret and responsibility on purchase decisions," *Journal of Consumer Research*, vol. 19, no. 1, pp. 105–118, 1992.
- [18] R. P. Larrick and T. L. Boles, "Avoiding regret in decisions with feedback: a negotiation example," *Organizational Behavior and Human Decision Processes*, vol. 63, no. 1, pp. 87–97, 1995.
- [19] M. Zeelenberg, "Anticipated regret, expected feedback and behavioral decision making," *Journal of Behavioral Decision Making*, vol. 12, no. 2, pp. 93–106, 1999.
- [20] P. Bjälkebring, D. Västfjäll, O. Svenson, and P. Slovic, "Regulation of experienced and anticipated regret in daily decision making," *Emotion*, vol. 16, no. 3, pp. 381–386, 2015.
- [21] N. Syam, P. Krishnamurthy, and J. D. Hess, "That's what I thought I wanted? miswanting and regret for a standard good

- in a mass-customized world,” *Marketing Science*, vol. 27, no. 3, pp. 379–397, 2008.
- [22] C. Yin and H. Yu, “Research on the impact of expected regret on consumer impulse buying behavior,” *Business Review*, vol. 21, no. 12, pp. 71–79, 2009.
- [23] J. Nasiry and I. Popescu, “Advance selling when consumers regret,” *Management Science*, vol. 58, no. 6, pp. 1160–1177, 2012.
- [24] B. J. Jiang, C. Narasimhan, and O. Turut, “Anticipated regret and product innovation,” *Social Science Electronic Publishing*, vol. 1, no. 1, pp. 1–32, 2015.
- [25] W. Q. Liu and J. J. Zhang, “Research on price discrimination strategy considering consumers’ expectations of regret,” *Chinese Journal of Management Science*, vol. 26, no. 5, pp. 1–8, 2018.
- [26] K. R. Sarangee, J. B. Schmidt, and R. J. Calantone, “Anticipated regret and escalation of commitment to failing, new product development projects in business markets,” *Industrial Marketing Management*, vol. 76, pp. 157–168, 2019.
- [27] N. Zhang, S. Y. Li, L. Jiang, and J. Jian, “Research on the leadership structure of innovative product supply chain considering expected regret,” *Industrial Engineering Journal*, vol. 22, no. 5, pp. 32–42, 2019.
- [28] G. P. Cachon and M. A. Lariviere, “Supply chain coordination with revenue-sharing contracts: strengths and limitations,” *Management Science*, vol. 51, no. 1, pp. 30–44, 2005.
- [29] L. H. Zhang, Y. J. Wu, and Y. J. Li, “Research on optimal retailer financing strategy based on option contract,” *Management Review*, vol. 26, no. 10, pp. 197–208, 2014.
- [30] P. Zhang, J. Zhang, and J. Ma, “Supply chain contract and coordination considering expected loss aversion,” *Management Review*, vol. 27, no. 4, pp. 177–186, 2015.
- [31] L. Q. Zhao, J. W. Xu, and J. M. Wang, “Contract design of dual channel conflict and coordination in supply chain based on electronic market,” *China Management Science*, vol. 22, no. 5, pp. 61–68, 2014.
- [32] J. Jian, Y. Zhang, L. Jiang, and J. Su, “Coordination of supply chains with competing manufacturers considering fairness concerns,” *Complexity*, vol. 2020, Article ID 4372603, 15 pages, 2020.
- [33] B. Zeng, X. Ma, and J. Shi, “Modeling method of the grey GM (1, 1) model with interval grey action quantity and its application,” *Complexity*, vol. 2020, Article ID 6514236, 10 pages, 2020.
- [34] J. Su, C. Li, Q. Zeng, J. Yang, and J. Zhang, “A green closed-loop supply chain coordination mechanism based on third-party recycling,” *Sustainability*, vol. 11, no. 19, p. 5335, 2019.
- [35] W.-y. K. Chiang, D. Chhajed, and J. D. Hess, “Direct marketing, indirect profits: a strategic analysis of dual-channel supply-chain design,” *Management Science*, vol. 49, no. 1, pp. 1–20, 2003.
- [36] A. Örsdemir, E. Kemahlioğlu-Ziya, and A. K. Parlaktürk, “Competitive quality choice and remanufacturing,” *Production and Operations Management*, vol. 23, no. 1, pp. 48–64, 2014.
- [37] S. Jiafu, Y. Yang, and X. Zhang, “Knowledge transfer efficiency measurement with application for open innovation networks,” *International Journal of Technology Management*, vol. 81, no. 1-2, pp. 118–142, 2019.

Research Article

Digital Twin Driven Green Performance Evaluation Methodology of Intelligent Manufacturing: Hybrid Model Based on Fuzzy Rough-Sets AHP, Multistage Weight Synthesis, and PROMETHEE II

Lianhui Li ^{1,2,3}, Chunlei Mao,⁴ Hongxia Sun,¹ Yiping Yuan ⁵, and Bingbing Lei ^{2,6}

¹College of Mechatronic Engineering, North Minzu University, Yinchuan 750021, China

²Ningxia Key Laboratory of Intelligent Information and Big Data Processing, North Minzu University, Yinchuan 750021, China

³Institute of Physical Internet, Jinan University, Zhuhai 519070, China

⁴Nanjing Automation Institute of Water Conservancy and Hydrology, Nanjing 210012, China

⁵School of Mechanical Engineering, Xinjiang University, Urumqi 830046, China

⁶School of Computer Science and Engineering, North Minzu University, Yinchuan 750021, China

Correspondence should be addressed to Bingbing Lei; x_generation@126.com

Received 24 March 2020; Accepted 22 June 2020; Published 16 July 2020

Guest Editor: Baogui Xin

Copyright © 2020 Lianhui Li et al. This is an open access article distributed under the Creative Commons Attribution License, which permits unrestricted use, distribution, and reproduction in any medium, provided the original work is properly cited.

The design, planning, and implementation of intelligent manufacturing are mainly carried out from the perspectives of meeting the needs of mass customization, improving manufacturing capacity, and innovating business pattern currently. Environmental and social factors should be systematically integrated into the life cycle of intelligent manufacturing. In view of this, a green performance evaluation methodology of intelligent manufacturing driven by digital twin is proposed in this paper. Digital twin framework, which constructs the bidirectional mapping and real-time data interaction between physical entity and digital model, provides the green performance evaluation with a total factor virtual image of the whole life cycle to meet the monitoring and simulation requirements of the evaluation information source and demand. Driven by the digital twin framework, a novel hybrid MCDM model based on fuzzy rough-sets AHP, multistage weight synthesis, and PROMETHEE II is proposed as the methodology for the green performance evaluation of intelligent manufacturing. The model is tested and validated on a study of the green performance evaluation of remote operation and maintenance service project evaluation for an air conditioning enterprise. Testing demonstrates that the proposed hybrid model driven by digital twin can enable a stable and reasonable evaluation result. A sensitivity analysis was carried out by means of 27 scenarios, the results of which showed a high degree of stability.

1. Introduction

The concept of intelligent manufacturing rose in the 1980s. Its emergence and development are closely related to the four industrial revolutions and the development of related technologies and industries. First of all, the first and second industrial revolutions brought manufacturing industry into the era of mechanization and electrification. With the invention and application of atomic energy and electronic computer technology, the third industrial revolution appeared. In the same period, terms representing new

manufacturing paradigms such as flexible manufacturing cells (FMCs) [1], flexible manufacturing systems (FMSs) [2], computer integrated manufacturing (CIM) [3], and intelligent manufacturing system (IMS) [4] are emerging gradually. After more than 40 years of development and progress, intelligent manufacturing has gradually evolved from concept to industrialization and integrated into the emerging fourth industrial revolution.

At present, the design and implementation of intelligent manufacturing are mainly carried out from the perspectives of meeting the needs of mass customization, improving

manufacturing capacity, and innovating business pattern. In some theoretical research and practice, green or even sustainability has also been brought into the intelligent manufacturing paradigm. But most of them focus on the optimization of energy consumption in the manufacturing process. For example, cloud platform is used for promoting resource sharing and improving application efficiency of manufacturing system [5]; combining big data technology in the product life cycle to achieve sustainable intelligent manufacturing is proposed [6]; big data method was used for energy efficiency optimization [7], anomaly detection [8], and energy consumption monitoring [9] in intelligent manufacturing process; and through the analysis of relevant literature, it can be seen that there is no clear definition of green intelligent manufacturing in the current academic circle, and few research studies systematically integrated environmental and social factors into the design, planning, and implementation of intelligent manufacturing [10, 11]. On the one hand, the current research and practice pay more attention to the core business and competitive elements (for example, productivity improvement, personalized customization, and intelligent services). On the other hand, the improvement of the environment and social impact of intelligent manufacturing may conflict with the realization of other elements and even may bring a lot of investment costs. The research on the green of intelligent manufacturing is still in the exploratory stage.

At present, there are many researches on performance evaluation of intelligent manufacturing, focusing on the following aspects.

The first aspect is overall performance evaluation of intelligent manufacturing enterprises. Gong [12] introduced a three-tier index system to evaluate the performance of enterprise intelligent manufacturing by using the comprehensive scoring method of experts, which covers many aspects of enterprise performance, but does not involve environmental performance, and only uses an overall satisfaction degree for the evaluation of employees. Jia and Shi [13] use the DEA model of cross efficiency to measure the performance of some listed intelligent manufacturing enterprises, which can evaluate the overall economic performance of enterprises, but cannot pay attention to the details of intelligent manufacturing itself, and does not consider the environmental factors.

In the second aspect, enterprise's intelligent manufacturing capability is assessed. Yi et al. [14] established the evaluation model of enterprise intelligent manufacturing capability based on tensor analysis and measured the enterprise intelligent manufacturing capability from three dimensions of life cycle, system level, and intelligent function. Similarly, Ding et al. [15] put forward the intelligent manufacturing capability maturity model from three dimensions of manufacturing resources, manufacturing assurance, and intelligent promotion, which can support enterprises to describe their comprehensive level of intelligent manufacturing. Qu et al. [16] used Douglas production function and seemingly unrelated regression (SUA) analysis to evaluate the production capacity of intelligent manufacturing enterprises, so as to compare its advantages

and disadvantages with traditional manufacturing capacity. Schumacher et al. [17] proposed an empirical model to evaluate the industry 4.0 maturity of discrete manufacturing enterprise, in which nine dimensions and sixty-two indicators were established for evaluation, including the items of the impact on employees and products.

The third aspect is environment and social impact assessment of intelligent manufacturing. There are few research studies on intelligent manufacturing environment and social impact assessment. The above two aspects or part of the performance assurance research of intelligent manufacturing involved environmental and social dimensions, but it was often described as a macromethod only including environmental or social factors as a macro-indicator [18].

In addition, Mashhadi and Behdad [19] summarized the shortcomings of traditional life cycle assessment (LCA) in the assessment of the environment impact of intelligent manufacturing, combined with the characteristics of intelligent manufacturing, and put forward the assessment concept based on product characteristics data. It is mainly a scheme of data collection and real-time assessment by using the new generation of information technology, rather than studying specific assessment methods. Peruzzini et al. [20] used social life cycle assessment (SLCA) to evaluate the impact of the implementation of intelligent manufacturing on the society, but it only focuses on the general social impact, not the special impact of intelligent manufacturing on employees or users.

By creating the virtual model of physical entity in a digital way and simulating the behavior of physical entity by means of data, digital twin has the characteristics of real-time synchronization, faithful mapping and high fidelity through the means of virtual real interaction feedback, data fusion analysis, and decision iteration selection optimization [21]. Digital twin can promote the interaction and integration of physical world and information world and increase or expand new capabilities for physical entity [22]. In this study, digital twin mainly focuses on obtaining the virtual image of all factors in the whole life cycle of intelligent manufacturing project to meet the monitoring and simulation requirements of the evaluation information source and demand for the green evaluation of intelligent manufacturing. Based on digital twin technology [21, 22], the complete and dynamic mapping interaction between physical entity and digital model in green performance evaluation of intelligent manufacturing can be realized. And then, how to comprehensively master the multidimensional influencing factors and their coupling relationship for comparative analysis is the key problem in green performance evaluation of intelligent manufacturing.

Multicriteria decision-making (MCDM) [23, 24] by using the experience and wisdom of experts is a feasible method to comprehensively consider the multidimensional influencing factors and their coupling relationship that affect the green performance evaluation. In the existing similar evaluation problem and its solution, the value or importance of a factor is usually evaluated by one expert in numerical number form, which is unreasonable due to the preferences

of individual expert and the fuzziness of expert judgment [25, 26]. Additionally, the green performance evaluation of intelligent manufacturing includes multidimensional influencing factors with complex coupling relationship, and these factors and their relationship are dynamic evolution. Therefore, it is difficult for a single expert to achieve accurate judgment with the numerical number form as the judgment opinion, while integrating the fuzzy number form judgment of multiple experts is more reasonable. Trapezoid fuzzy number, which is a key definition in fuzzy theory, can reflect the internal uncertainty of expert's judgment [27, 28]. To express the expert judgment value about the value or importance of the index, using trapezoid fuzzy number can better describe the uncertainty. The single weight method cannot fully reflect the weight information. The weights obtained by the multiple weight method should be synthesized.

To sum up, there is a lack of special, systematic, and objective research to evaluate the green performance of intelligent manufacturing. The existing studies prove the necessity of green performance evaluation of intelligent manufacturing and provide reference for the study of this paper. Additionally, digital twin can provide an overall information framework for this study. In view of this, this paper constructs an overall information framework driven by digital twin for the green performance of intelligent manufacturing. In this framework, the digital twin system is formed by mapping and interacting between intelligent manufacturing entity and intelligent manufacturing model. All activities in the life cycle of intelligent manufacturing entity interact with the model in real time, and both physical entity and digital model provide a source of digital twin data. With the full mastery of digital twin data by multiple experts, a novel hybrid MCDM model based on fuzzy rough-sets AHP, multistage weight synthesis, and PROMETHEE II (FRSA-MSWS-PII) is proposed as the methodology for the green performance evaluation of intelligent manufacturing.

The rest of this work is arranged as follows: overall framework driven by digital twin is stated in Section 2; Section 3 builds the novel hybrid MCDM model (FRSA-MSWS-PII) for the green performance evaluation of intelligent manufacturing, which include three phases: multi-expert judgment integration based on fuzzy rough-sets AHP, multistage weight synthesis, and intelligent manufacturing project evaluation by PROMETHEE II; case study is given in Section 4 by an application of remote operation and maintenance service project evaluation for an air conditioning enterprise; Section 5 presents a discussion of the results and validation of the FRSA-MSWS-PII model; finally, Section 6 summarizes the conclusion.

2. Overall Framework

On the basis of digital twin technology [21, 22], the bidirectional mapping and real-time data interaction are constructed between physical entity and digital model. Therefore, the comprehensive data integration and fusion of physical entity and digital model can be realized and form the digital twin data that can support and drive the green

performance evaluation methodology. In addition, the green performance evaluation methodology results in an optimal project alternative selection, which can interact with the physical entity and digital model and provide the physical entity and digital model with the support of decision-making. The overall framework built in this paper is driven by digital twin. As shown in Figure 1, it consists of three layers, which are the digital twin concept layer, information layer, and methodology layer.

The bidirectional mapping and real-time data interaction between physical entity and digital model are defined theoretically in the digital twin concept layer. In the design stage of intelligent manufacturing project, multiple project alternatives are produced in general. All of them meet the actual demands. After that, in the test running stage, the original intelligent manufacturing project will be adjusted and optimized iteratively. Finally, an optimal alternative is determined and put into formal running stage. Additionally, the data of formal running stage will also be fed back to assist in the selection optimization of design stage.

Intelligent manufacturing project entity really exists in the physical world, while intelligent manufacturing project model is a real and complete digital mirror image of intelligent manufacturing project entity. Intelligent manufacturing project model can integrate all influencing factors related to green performance evaluation of intelligent manufacturing project. At the same time, it is a dynamic model, which can describe the dynamic evolution of the whole life cycle including but not limited to the design, test running, and formal running stages.

3. Hybrid MCDM Model (FRSA-MSWS-PII)

3.1. Fundamental Concepts. The fundamental concepts in the proposed hybrid model mainly include two aspects: trapezoid fuzzy number (TFN) related to fuzzy mathematics, rough approximation set (RAS), and rough boundary interval (RBI) related to rough-sets theory [27, 28].

3.1.1. Trapezoid Fuzzy Number (TFN). A TFN is defined as follows:

$$\tilde{a} = (\alpha, \chi, \delta, \beta). \quad (1)$$

Its membership function $f_{\tilde{a}}(x): R \rightarrow [0, 1]$ is defined as follows:

$$f_{\tilde{a}}(x) = \begin{cases} \frac{x - \alpha}{\chi - \alpha}, & \alpha \leq x \leq \chi, \\ 1, & \chi \leq x \leq \delta, \\ \frac{x - \beta}{\delta - \beta}, & \delta \leq x \leq \beta, \\ 0, & x < \alpha \text{ or } x > \beta, \end{cases} \quad (2)$$

where $x \in R$, $\alpha \leq \chi \leq \delta \leq \beta$, and α and β are the lower bound and upper bound of \tilde{a} , respectively. Especially, when $\chi = \delta$, \tilde{a}

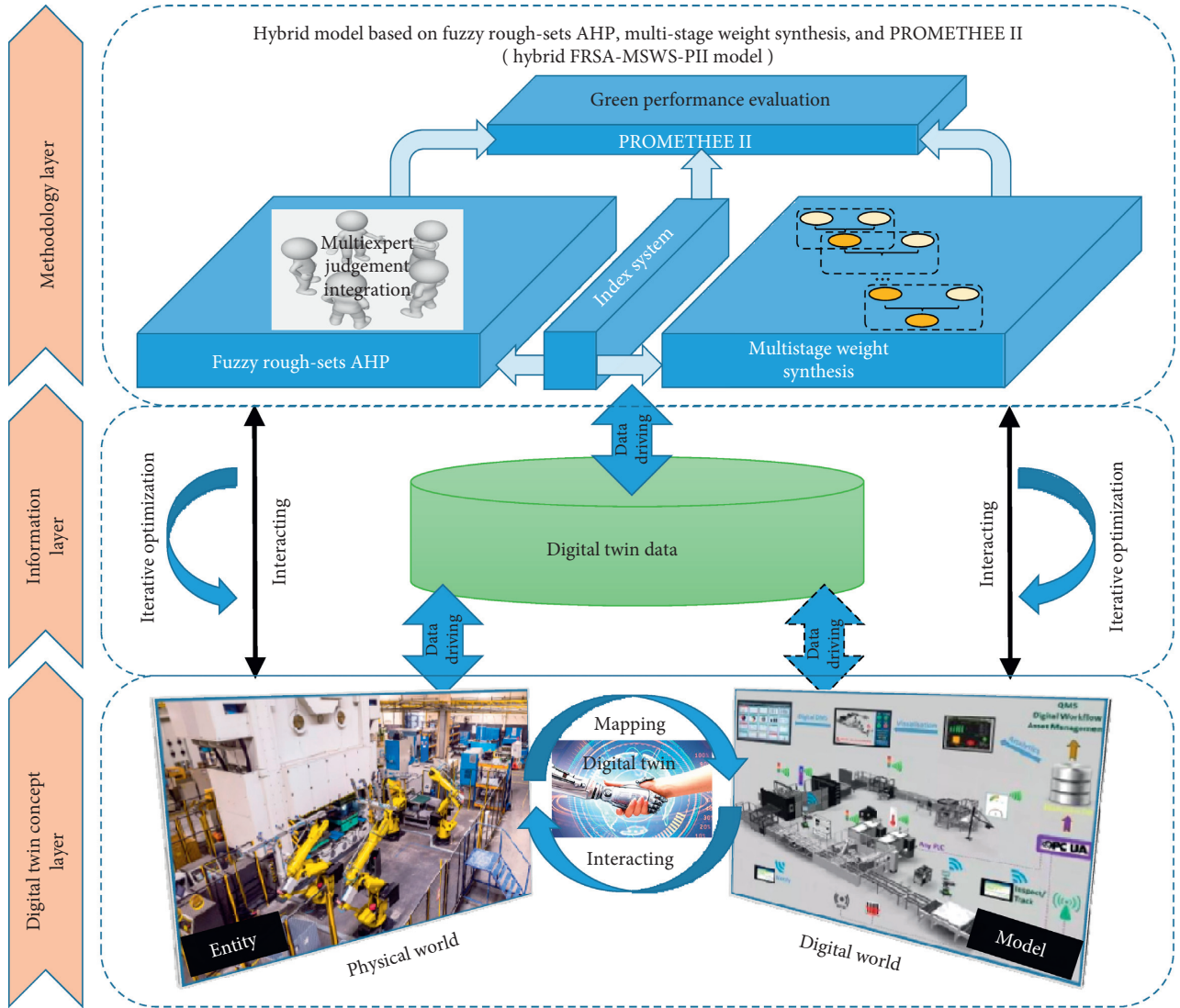


FIGURE 1: Green performance evaluation framework of intelligent manufacturing driven by digital twin.

degenerates into a triangular fuzzy number; when $\alpha = \chi = \delta = \beta$, \tilde{a} degenerates into a real number.

The graph of function $f_{\tilde{a}}(x)$ is shown in Figure 2.

The TFN is characterized by specific arithmetic operations that differ from those dealing with typical real numbers. The arithmetic operations between two TFNs $\tilde{a}_1 = (\alpha_1, \chi_1, \delta_1, \beta_1)$ and $\tilde{a}_2 = (\alpha_2, \chi_2, \delta_2, \beta_2)$ ($\alpha_1, \chi_1, \delta_1, \beta_1, \alpha_2, \chi_2, \delta_2, \beta_2 \in R^+, \lambda > 0$) are carried out using the following expressions:

(1) Addition of two TFNs “ \oplus ”:

$$\tilde{a}_1 \oplus \tilde{a}_2 = (\alpha_1 + \alpha_2, \chi_1 + \chi_2, \delta_1 + \delta_2, \beta_1 + \beta_2). \quad (3)$$

(2) Multiplication of two TFNs “ \otimes ”:

$$\tilde{a}_1 \otimes \tilde{a}_2 = (\alpha_1 \cdot \alpha_2, \chi_1 \cdot \chi_2, \delta_1 \cdot \delta_2, \beta_1 \cdot \beta_2). \quad (4)$$

(3) Multiplication of a real number and a TFN “ \odot ”:

$$\lambda \otimes \tilde{a}_1 = (\lambda \cdot \alpha_1, \lambda \cdot \chi_1, \lambda \cdot \delta_1, \lambda \cdot \beta_1). \quad (5)$$

(4) Reciprocal of a TFN “ -1 ”:

$$(\tilde{a}_1)^{-1} = (\beta_1^{-1}, \delta_1^{-1}, \chi_1^{-1}, \alpha_1^{-1}) \quad (6)$$

(5) Division of two TFNs “ $/$ ”:

$$\frac{\tilde{a}_1}{\tilde{a}_2} = \left(\frac{\alpha_1}{\beta_2}, \frac{\chi_1}{\delta_2}, \frac{\delta_1}{\chi_2}, \frac{\beta_1}{\alpha_2} \right). \quad (7)$$

(6) Barycenter of a TFN “ \odot ”:

$$\odot \tilde{a}_1 = \frac{(\delta_1^2 + \beta_1^2 - \alpha_1^2 - \chi_1^2) + (\delta_1 \cdot \beta_1 - \alpha_1 \cdot \chi_1)}{3(\delta_1 + \beta_1 - \alpha_1 - \chi_1)}. \quad (8)$$

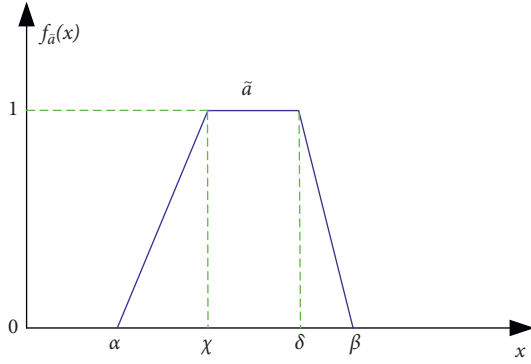


FIGURE 2: The membership function graph of triangular fuzzy number.

On the basis of the membership function of trapezoid fuzzy number shown by formula (2), a real number a can be converted to trapezoid fuzzy number \tilde{a} [27, 28]. For example, $\tilde{2}=(1, 3/2, 5/2, 3)$. For trapezoid fuzzy number \tilde{a} , its membership function $f_{\tilde{a}}(x)$ is shown in Figure 3. The commonly used nine-level scale assessment comments are extremely superior (ES), strongly superior (SS), obviously superior (OS), weakly superior (WS), equal (E), weakly inferior (WI), obviously inferior (OI), strongly inferior (SI), and extremely inferior (EI). The corresponding assessment values are 9, 7, 5, 3, 1, 1/3, 1/5, 1/7, and 1/9 in order. The commonly used nine-level scale assessment comments and corresponding assessment values are converted to the trapezoid fuzzy number form as ES: $\tilde{9}/1$, SS: $\tilde{8}/2$, OS: $\tilde{7}/3$, WS: $\tilde{6}/4$, E: $\tilde{5}/5$, WI: $\tilde{4}/6$, OI: $\tilde{3}/7$, SI: $\tilde{2}/8$, and EI: $\tilde{1}/9$. The membership functions of nine-level trapezoid fuzzy number scales are shown in Figure 4.

According to the arithmetic rules of trapezoid fuzzy number shown by formulas (3)–(8), the trapezoid fuzzy number values of nine-level scales are shown in Table 1.

3.1.2. Rough Approximation Set (RAS) and Rough Boundary Interval (RBI). According to rough-sets theory, the definitions of RAS and RBI are given as follows:

- (1) Rough approximation set (RAS).

The domain φ which is a nonempty finite set contains all objects. All objects in φ belong to n divisions, i.e., D_1, D_2, \dots, D_n . The set of divisions in φ is as follows:

$$D = \{D_1, D_2, \dots, D_n\}. \quad (9)$$

Here, D_1, D_2, \dots, D_n have an order relationship as $D_1 < D_2 < \dots < D_n$.

For a division $D_w (1 \leq w \leq n)$, its upper RAS (URAS) is defined as follows:

$$\text{URAS}(S_w) = \{Y \in K \mid K \in D \wedge K \geq D_w\}. \quad (10)$$

And its lower RAS (LRAS) is defined as follows:

$$\text{LRAS}(S_w) = \{Y \in K \mid K \in D \wedge K \leq D_w\}, \quad (11)$$

where Y is any object in φ .

- (2) Rough boundary interval (RBI).

The mathematical characteristics of division S_w can be embodied by its RBI, which is composed of lower rough limit (LRL) and upper rough limit (URL). So, RBI of S_w is defined as follows:

$$\text{RBI}(S_w) = [\text{LRL}(S_w), \text{URL}(S_w)]. \quad (12)$$

LRL(S_w) and URL(S_w) are expressed as follows:

$$\text{LRL}(S_w) = \frac{1}{\text{Num}(\text{LRAS}(S_w))} \sum_{Y \in \text{LRAS}(S_w)} Y, \quad (13)$$

$$\text{URL}(S_w) = \frac{1}{\text{Num}(\text{URAS}(S_w))} \sum_{Y \in \text{URAS}(S_w)} Y, \quad (14)$$

where $\text{Num}(\text{LRAS}(S_w))$ and $\text{Num}(\text{URAS}(S_w))$ are the numbers of objects contained in the LRAS and URAS of S_w , respectively.

The arithmetic operations between two RBIs $\text{RBI}(S_w) = [\text{LRL}(S_w), \text{URL}(S_w)]$ and $\text{RBI}(S_u) = [\text{LRL}(S_u), \text{URL}(S_u)]$ ($\text{LRL}(S_w), \text{URL}(S_w), \text{LRL}(S_u),$ and $\text{URL}(S_u) \in R^+, \lambda > 0$) are carried out using the following expressions:

- (1) Addition of two RBIs “ \oplus ”:

$$\text{RBI}(S_w) \oplus \text{RBI}(S_u) = [\text{LRL}(S_w) + \text{LRL}(S_u), \text{URL}(S_w) + \text{URL}(S_u)]. \quad (15)$$

- (2) Multiplication of two RBIs “ \otimes ”:

$$\text{RBI}(S_w) \otimes \text{RBI}(S_u) = [\text{LRL}(S_w) \cdot \text{LRL}(S_u), \text{URL}(S_w) \cdot \text{URL}(S_u)] \quad (16)$$

- (3) Multiplication of a real number and an RBI “ \otimes ”:

$$\lambda \otimes \text{RBI}(S_w) = [\lambda \cdot \text{LRL}(S_w), \lambda \cdot \text{URL}(S_w)]. \quad (17)$$

3.2. Evaluation Index System. Considering the typical environmental problems and the special influence of main stakeholders of intelligent manufacturing, the index system of green performance evaluation of intelligent manufacturing is constructed through the summary of the existing research, as shown in Figure 5. By integrating the target, dimension, and index of the green performance evaluation of intelligent manufacturing, the index system in this paper mainly constructs the three-level standardized framework.

In Figure 5, the target level is green performance evaluation of intelligent manufacturing; the dimension level has three elements: general environmental effect (dimension 1), social effect on employees (dimension 2), and social effect on users (dimension 3); the index level has nine indexes.

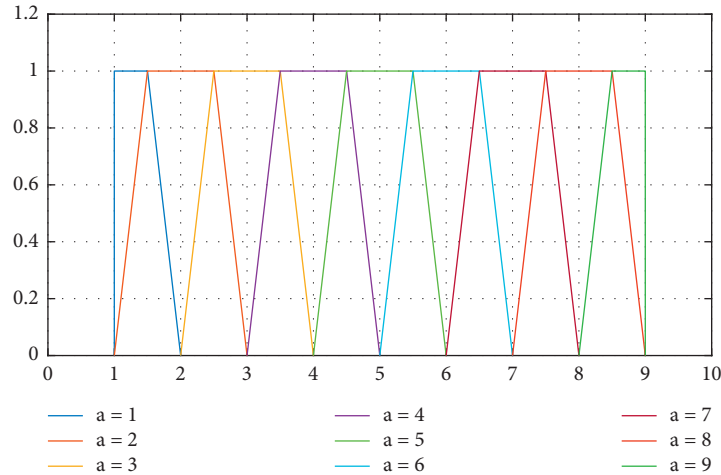


FIGURE 3: Membership functions of trapezoid fuzzy numbers \bar{a} ($a=1-9$).

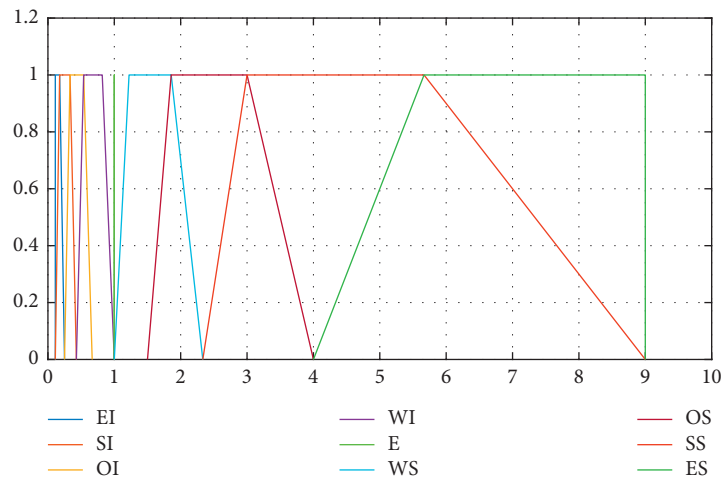


FIGURE 4: Membership functions of nine-level trapezoid fuzzy number scales (EI-ES).

TABLE 1: The trapezoid fuzzy number values of nine-level scales.

Nine-level scale	Trapezoid fuzzy number value
EI	(0.1111, 0.1111, 0.1765, 0.2500)
SI	(0.1111, 0.1765, 0.3333, 0.4286)
OI	(0.2500, 0.3333, 0.5385, 0.6667)
WI	(0.4286, 0.5385, 0.8182, 1.0000)
E	(1.0000, 1.0000, 1.0000, 1.0000)
WS	(1.0000, 1.2222, 1.8571, 2.3333)
OS	(1.5000, 1.8571, 3.0000, 4.0000)
SS	(2.3333, 3.0000, 5.6667, 9.0000)
ES	(4.0000, 5.6667, 9.0000, 9.0000)

Furthermore, in the index level, exhaustion of resources and energy (index 1), destruction of ecological environment (index 2), and hazards to human health (index 3) belong to dimension 1; physical health effects (index 4), mental health effects (index 5), and impact on employee development (index 6) belong to dimension 2; physical health effects

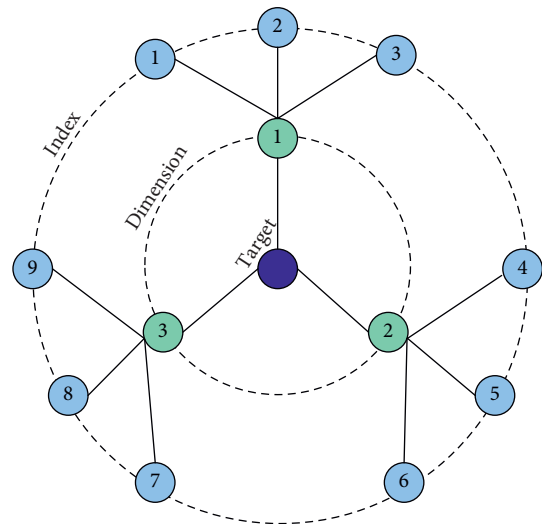


FIGURE 5: Three-level standardized framework for the index system.

(index 7), mental health effects (index 8), and impact on user development (index 9) belong to dimension 1.

3.3. The Process of Proposed Hybrid Model. This paper presents a digital twin driven green performance evaluation methodology of intelligent manufacturing by introducing the hybrid model (FRSA-MSWS-PII), as shown in Figure 6. Fuzzy numbers are used to deal with uncertainty of expert judgment in the group decision-making process, while RBI is used to integrate the judgments of multiple experts. Phase 1 includes the expert judgment of assessment index value by applying the fuzzy rough-sets AHP model, which results in the creation of input data required for the multistage weight synthesis model (phase 2) and PROMETHEE II model (phase 3). In phase 2, the multiple objective weights are based on the assessment index values from phase 1, while the multiple subjective weights are based on experts' judgment about the importance of assessment index. The output data of phase 2 are the final synthesized weights which are the input data of phase 3.

The FRSA-MSWS-PII model, which is the subject matter of this paper, represents a novel approach for dealing with uncertainty in green performance evaluation of intelligent manufacturing based on fuzzy rough-sets AHP, multistage weight synthesis, and PROMETHEE II. For defining the final rank of intelligent manufacturing project alternatives, the FRSA-MSWS-PII method is used. The following three sections deal with the algorithms for the FRSA-MSWS-PII model.

3.3.1. Multiexpert Judgment Integration Based on Fuzzy Rough-Sets AHP. To achieve multiexpert judgment integration, there are two preconditions: (1) there are N indexes: index 1, index 2, . . . , index N , which constitute the index set is I . Here, $N=9$ and index 1, index 2, . . . , index N represent the indexes shown in Figure 5. (2) There are q experts to assess the sustainable performance of l intelligent manufacturing project alternatives. As shown in Figure 6, the fuzzy rough-sets AHP for multiexpert judgment integration, which is phase 1 of the hybrid model, is to obtain the index value of intelligent manufacturing project alternatives. Its process is as follows.

Experts judge the performance of all intelligent manufacturing project alternatives on any index based on their experiences and wisdom. On index t ($t = 1, 2, \dots, N$), the fuzzy reciprocal judgment matrix given by expert k ($k = 1, 2, \dots, q$) is as follows:

$$\tilde{\Phi}^{k,t} = \begin{bmatrix} \tilde{\phi}_{1,1}^{k,t} & \tilde{\phi}_{1,2}^{k,t} & \cdots & \tilde{\phi}_{1,l}^{k,t} \\ \tilde{\phi}_{2,1}^{k,t} & \tilde{\phi}_{2,2}^{k,t} & \cdots & \tilde{\phi}_{2,l}^{k,t} \\ \vdots & \vdots & & \vdots \\ \tilde{\phi}_{l,1}^{k,t} & \tilde{\phi}_{l,2}^{k,t} & \cdots & \tilde{\phi}_{l,l}^{k,t} \end{bmatrix}, \quad (18)$$

where $\tilde{\phi}_{i,j}^{k,t}$ is the fuzzy score of intelligent manufacturing project alternative i relative to intelligent manufacturing

project alternative j given by expert k on index t and $\tilde{\phi}_{j,i}^{k,t} = 1/\tilde{\phi}_{i,j}^{k,t}$.

According to the table, the set of the nine-level scales is $SCA = \{EI, SI, OI, WI, E, WS, OS, SS, ES\}$ and the set of trapezoid fuzzy number values of nine-level scales is $TFN-SCA = \{(0.1111, 0.1111, 0.1765, 0.2500), (0.1111, 0.1765, 0.3333, 0.4286), (0.2500, 0.3333, 0.5385, 0.6667), (0.4286, 0.5385, 0.8182, 1.0000), (1.0000, 1.0000, 1.0000, 1.0000), (1.0000, 1.2222, 1.8571, 2.3333), (1.0000, 1.2222, 1.8571, 2.3333), (2.3333, 3.0000, 5.6667, 9.0000), (4.0000, 5.6667, 9.0000, 9.0000)\}$.

From the perspective of judgment comment, $\tilde{\phi}_{i,j}^{k,t} \in SCA$, which represents the evaluation of performance of intelligent manufacturing project alternative i relative to intelligent manufacturing project alternative j given by expert k on index t , while from the perspective of judgment value, $\tilde{\phi}_{i,j}^{k,t} \in TFN-SCA$, which is a trapezoid fuzzy number, and can be represented as follows:

$$\tilde{\phi}_{i,j}^{k,t} = (\alpha_{i,j}^{k,t}, \lambda_{i,j}^{k,t}, \delta_{i,j}^{k,t}, \beta_{i,j}^{k,t}). \quad (19)$$

Especially, when $i=j$, $\tilde{\phi}_{i,i}^{k,t} = (1, 1, 1, 1)$.

Consistency inspection is carried out after all experts finish their judgment. If any fuzzy reciprocal judgment matrix fails to pass the consistency inspection, the corresponding expert should adjust his judgment matrix. The basic idea of consistency inspection for fuzzy reciprocal judgment matrix is using formula (8) to convert trapezoid fuzzy number to real number, and then, fuzzy reciprocal judgment matrix $\tilde{\Phi}^{k,t}$ could be transformed into general judgment matrix $\Phi^{k,t}$ as follows:

$$\Phi^{k,t} = \begin{bmatrix} \phi_{1,1}^{k,t} & \phi_{1,2}^{k,t} & \cdots & \phi_{1,l}^{k,t} \\ \phi_{2,1}^{k,t} & \phi_{2,2}^{k,t} & \cdots & \phi_{2,l}^{k,t} \\ \vdots & \vdots & & \vdots \\ \phi_{l,1}^{k,t} & \phi_{l,2}^{k,t} & \cdots & \phi_{l,l}^{k,t} \end{bmatrix}. \quad (20)$$

Consistency index (CI) of $\Phi^{k,t}$ is represented as follows:

$$CI^{k,t} = \frac{(\lambda_{\max}^{k,t})^{k,t} - l}{l - 1}, \quad (21)$$

where $(\lambda_{\max}^{k,t})^{k,t}$ is the maximum eigenvalue of $\Phi^{k,t}$.

Usually, consistency ratio (CR) is used to evaluate the consistency of reciprocal judgment matrix. For $\Phi^{k,t}$, its CR is represented as follows:

$$CR^{k,t} = \frac{CI^{k,t}}{RI^{k,t}}, \quad (22)$$

where $RI^{k,t}$ is a random index (RI) that depends on the dimension l of $\Phi^{k,t}$. The specific value of RI is shown in Table 2.

When $CR^{k,t} > 0.1$, the judgment logic of expert k on index I_t is inconsistent and $\Phi^{k,t}$ fails to pass the consistency inspection. As a result, expert k should adjust his judgment process and give a new judgment matrix.

Ultimately, the group judgment matrix is constructed as follows:

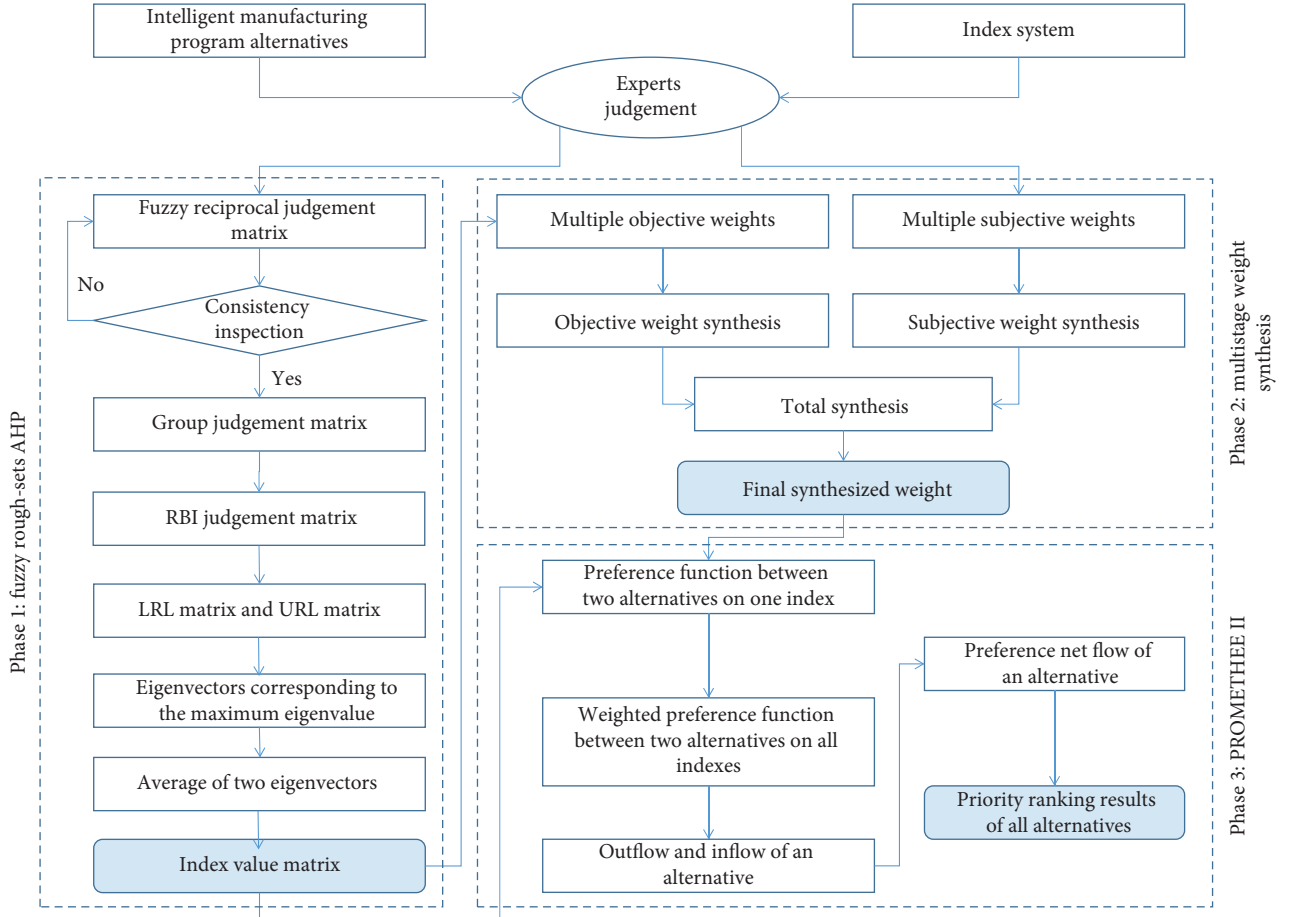


FIGURE 6: The process of the proposed FRSA-MSWS-PII model.

TABLE 2: The specific value of RI.

Dimension l	1	2	3	4	5	6	7	8	9
RI	0.00	0.00	0.58	0.90	1.12	1.24	1.32	1.41	1.45

$$\tilde{\Theta}^t = \begin{bmatrix} \tilde{\rho}_{1,1}^t & \tilde{\rho}_{1,2}^t & \cdots & \tilde{\rho}_{1,l}^t \\ \tilde{\rho}_{2,1}^t & \tilde{\rho}_{2,2}^t & \cdots & \tilde{\rho}_{2,l}^t \\ \vdots & \vdots & \ddots & \vdots \\ \tilde{\rho}_{l,1}^t & \tilde{\rho}_{l,2}^t & \cdots & \tilde{\rho}_{l,l}^t \end{bmatrix}. \quad (23)$$

Element $\tilde{\rho}_{i,j}^t$ is a set, which can be represented as follows:

$$\tilde{\rho}_{i,j}^t = \left\{ \tilde{\phi}_{i,j}^{1,t}, \tilde{\phi}_{i,j}^{2,t}, \dots, \tilde{\phi}_{i,j}^{q,t} \right\}, \quad (24)$$

In $\tilde{\rho}_{i,j}^t$, the fuzzy RBI of $\tilde{\phi}_{i,j}^{k,t}$ is obtained according to related concepts given by formulas (8)–(13) as follows:

$$\begin{aligned} \text{RBI}(\tilde{\phi}_{i,j}^{k,t}) &= \left[\text{LRL}(\tilde{\phi}_{i,j}^{k,t}), \text{URL}(\tilde{\phi}_{i,j}^{k,t}) \right] \\ &= \left[\frac{1}{\text{Num}(\text{LRAS}(\tilde{\phi}_{i,j}^{k,t}))} \sum_{\substack{Y \in \tilde{\rho}_{i,j}^t \\ Y \leq \tilde{\phi}_{i,j}^{k,t}}} Y, \frac{1}{\text{Num}(\text{URAS}(\tilde{\phi}_{i,j}^{k,t}))} \sum_{\substack{Y \in \tilde{\rho}_{i,j}^t \\ Y \geq \tilde{\phi}_{i,j}^{k,t}}} Y \right]. \end{aligned} \quad (25)$$

Based on the arithmetic operation rule of RBI shown by formulas (16)–(18), RBI of $\tilde{\rho}_{i,j}^t$ is obtained as follows:

$$\begin{aligned} \text{RBI}(\tilde{\rho}_{i,j}^t) &= [\text{LRL}(\tilde{\rho}_{i,j}^t), \text{URL}(\tilde{\rho}_{i,j}^t)] \\ &= \left[\frac{1}{q} \sum_{k=1}^q \text{LRL}(\tilde{\phi}_{i,j}^{k,t}), \frac{1}{q} \sum_{k=1}^q \text{URL}(\tilde{\phi}_{i,j}^{k,t}) \right]. \end{aligned} \quad (26)$$

Then, the RBI judgment matrix is constructed as follows:

$$\tilde{\Lambda}^t = \begin{bmatrix} \text{RBI}(\tilde{\rho}_{1,1}^t) & \text{RBI}(\tilde{\rho}_{1,2}^t) & \cdots & \text{RBI}(\tilde{\rho}_{1,l}^t) \\ \text{RBI}(\tilde{\rho}_{2,1}^t) & \text{RBI}(\tilde{\rho}_{2,2}^t) & \cdots & \text{RBI}(\tilde{\rho}_{2,l}^t) \\ \vdots & \vdots & & \vdots \\ \text{RBI}(\tilde{\rho}_{l,1}^t) & \text{RBI}(\tilde{\rho}_{l,2}^t) & \cdots & \text{RBI}(\tilde{\rho}_{l,l}^t) \end{bmatrix}. \quad (27)$$

$\tilde{\Lambda}^t$ is decomposed into LRL matrix and URL matrix as follows:

$$\tilde{\Lambda}_{\text{LRL}}^t = \begin{bmatrix} \text{LRL}(\tilde{\rho}_{1,1}^t) & \text{LRL}(\tilde{\rho}_{1,2}^t) & \cdots & \text{LRL}(\tilde{\rho}_{1,l}^t) \\ \text{LRL}(\tilde{\rho}_{2,1}^t) & \text{LRL}(\tilde{\rho}_{2,2}^t) & \cdots & \text{LRL}(\tilde{\rho}_{2,l}^t) \\ \vdots & \vdots & & \vdots \\ \text{LRL}(\tilde{\rho}_{l,1}^t) & \text{LRL}(\tilde{\rho}_{l,2}^t) & \cdots & \text{LRL}(\tilde{\rho}_{l,l}^t) \end{bmatrix}, \quad (28)$$

$$\tilde{\Lambda}_{\text{URL}}^t = \begin{bmatrix} \text{URL}(\tilde{\rho}_{1,1}^t) & \text{URL}(\tilde{\rho}_{1,2}^t) & \cdots & \text{URL}(\tilde{\rho}_{1,l}^t) \\ \text{URL}(\tilde{\rho}_{2,1}^t) & \text{URL}(\tilde{\rho}_{2,2}^t) & \cdots & \text{URL}(\tilde{\rho}_{2,l}^t) \\ \vdots & \vdots & & \vdots \\ \text{URL}(\tilde{\rho}_{l,1}^t) & \text{URL}(\tilde{\rho}_{l,2}^t) & \cdots & \text{URL}(\tilde{\rho}_{l,l}^t) \end{bmatrix}. \quad (29)$$

Based on the barycenter operation shown by formula (8), $\tilde{\Lambda}_{\text{LRL}}^t$ and $\tilde{\Lambda}_{\text{URL}}^t$ are converted into real number forms: Λ_{LRL}^t and Λ_{URL}^t . The eigenvectors of Λ_{LRL}^t and Λ_{URL}^t corresponding to the maximum eigenvalue are obtained, respectively, as follows:

$$\text{Eig}(\Lambda_{\text{LRL}}^t) = [\text{Eig}_1(\Lambda_{\text{LRL}}^t), \text{Eig}_2(\Lambda_{\text{LRL}}^t), \dots, \text{Eig}_l(\Lambda_{\text{LRL}}^t)], \quad (30)$$

$$\text{Eig}(\Lambda_{\text{URL}}^t) = [\text{Eig}_1(\Lambda_{\text{URL}}^t), \text{Eig}_2(\Lambda_{\text{URL}}^t), \dots, \text{Eig}_l(\Lambda_{\text{URL}}^t)]. \quad (31)$$

After averaging the two eigenvectors shown in formulas (29) and (30), an average vector is obtained as follows:

$$\text{Eig}(\Lambda_{\text{Aver}}^t) = [\text{Eig}_1(\Lambda_{\text{Aver}}^t), \text{Eig}_2(\Lambda_{\text{Aver}}^t), \dots, \text{Eig}_l(\Lambda_{\text{Aver}}^t)], \quad (32)$$

where $\text{Eig}_i(\Lambda_{\text{Aver}}^t) = (1/2)(\text{Eig}_i(\Lambda_{\text{LRL}}^t) + \text{Eig}_i(\Lambda_{\text{URL}}^t))$.

The index value of alternate intelligent manufacturing project i on index t is obtained as $\text{Eig}_i(\Lambda_{\text{Aver}}^t)$. After solving the index values of l intelligent manufacturing project alternates on other indexes by similar way, the index value matrix of l intelligent manufacturing project alternates on all indexes is obtained as $X = [x_{i,t}]_{l \times N}$, where $x_{i,t} = \text{Eig}_i(\Lambda_{\text{Aver}}^t)$.

3.3.2. Multistage Weight Synthesis. Solving index weight is the key step of comprehensive decision of green

performance evaluation of intelligent manufacturing. Generally, there are three methods to determine index weight: subjective weight method, objective weight method, and synthesis weight method. The subjective weight method generally uses the knowledge and experience of experts, but the evaluation results are not scientific because of subjectivity; the objective weight method determines the weight according to the degree of difference between indexes but often ignores the importance of the indexes themselves; the synthesis weight method is usually composed of a variety of subjective and objective weight methods, which can offset the shortcomings of different weight methods.

In the aspect of index weight solving for green performance evaluation of intelligent manufacturing, in order to avoid the instability of assessment result caused by single weight and make the weight setting of assessment index more fair and reasonable, a multistage synthesis weight method is proposed to solve index weight. The proposed method has three stages of weight synthesis, and there are several substages in each stage of weight synthesis.

As shown in Figure 7, the proposed multistage weight synthesis method has a detailed process as follows:

(1) Stage 1: subjective weight synthesis.

Subjective weight methods mainly include complex networks method, ANP method, and Delphi method. The principle and solution process of these methods are as follows:

(i) Complex networks method. By complex networks method, the determination of index weight is regarded as the evaluation of node importance in complex networks. The index can be treated as node in complex networks, and the network attributes (degree centrality, betweenness centrality, and closeness centrality) of a node describe its importance in the network from different aspects (local attribute, propagation attribute, and global attribute). Therefore, we use expert evaluation to determine whether there is a relationship between two indexes, regardless of the direction of the relationship. Based on this, an undirected network with index as node is established. Then, the degree centrality, betweenness centrality, and closeness centrality of each node are computed. Taking the network attributes of index as criterion, the net flow of each index is calculated by the Preference Ranking Organization Method for Enrichment Evaluations II (PROMETHEE II) method. The relative net flow of an index is obtained by calculating the relative difference between its net flow and the minimum net flow, and then, the relative net flow of all indexes is normalized to get the index weight. The process of complex networks method is shown in Figure 8.

(ii) ANP method. The ANP structure of determining the subjective weight of green performance evaluation of intelligent manufacturing is

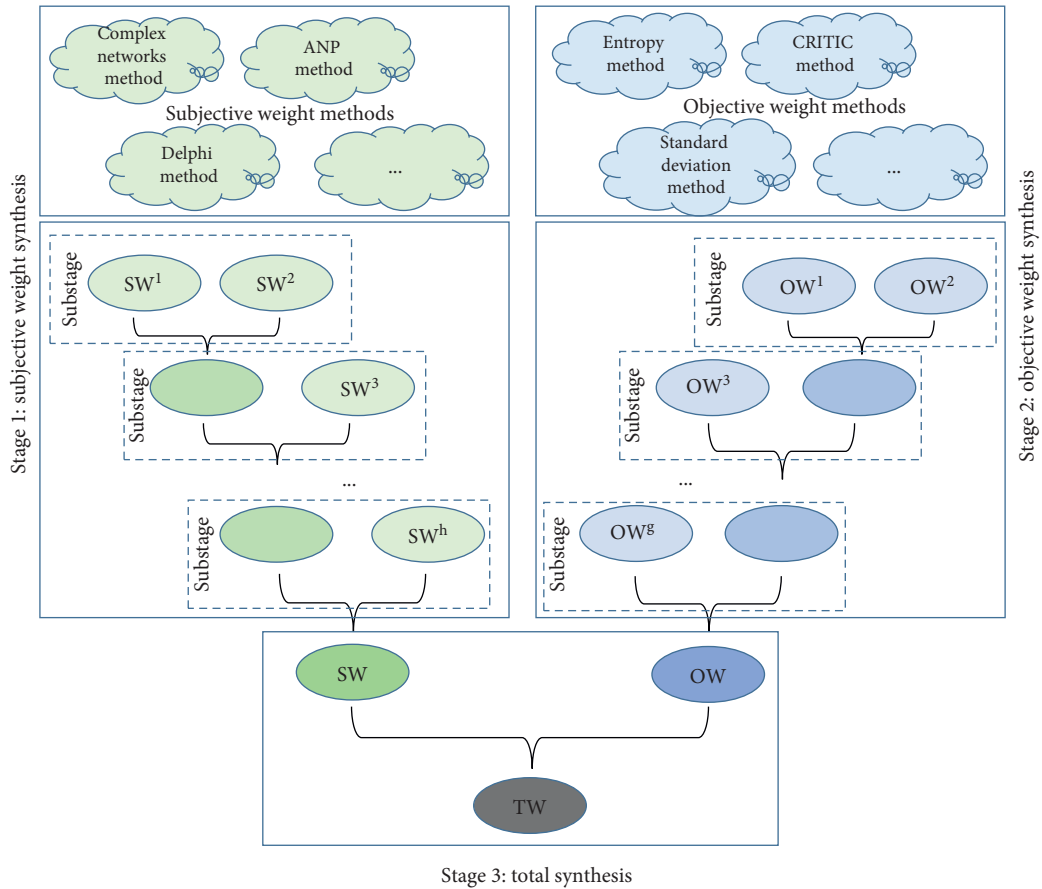


FIGURE 7: The process of multistage weight synthesis.

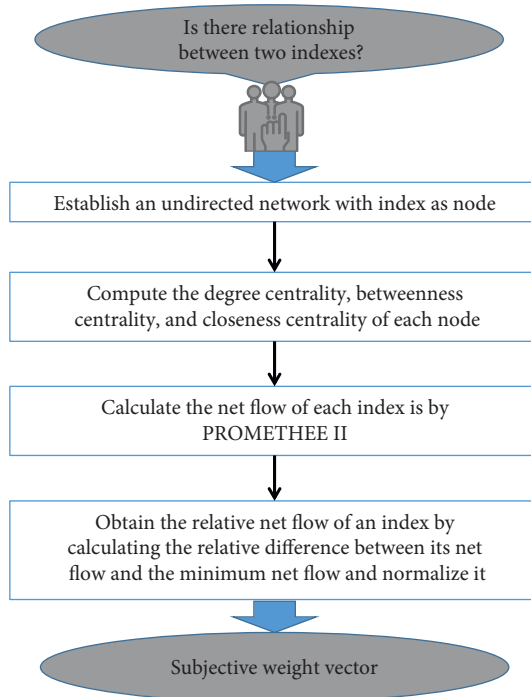


FIGURE 8: The process of obtaining subjective weight by complex networks method.

set up, as shown in Figure 9. The control layer only has one element: the overall goal (green performance evaluation of intelligent manufacturing), and the network layer has three element groups corresponding to three performance dimensions. Each element group affects each other and contains different elements. The elements in the same element group also affect each other. Based on the experts' evaluation of the importance and influence among the indexes, the weights of the indexes are determined by the classical ANP method.

- (iii) Delphi method. It usually relies on the knowledge, experience, and specialty of experts to score the indexes of the evaluation object separately and generally adopts the percentage grading system and then takes the average value of all experts' scores as the weight of the evaluation index. This method has convenient operation, easy investigation procedure, and simple calculation.

It is assumed that the subjective weight vectors obtained by h different methods are as follows:

$$\begin{aligned} SW^1 &= [sw_1^1, sw_2^1, \dots, sw_N^1]^T, \\ SW^2 &= [sw_1^2, sw_2^2, \dots, sw_N^2]^T, \\ &\dots \\ SW^h &= [sw_1^h, sw_2^h, \dots, sw_N^h]^T. \end{aligned} \quad (33)$$

In the subjective weight synthesis stage, there are $h - 1$ substages, and each substage corresponds to a synthesis. Taking the synthesis of SW^1 and SW^2 as an example, their synthesized weight vector $SW^{1 \circ 2} = [sw_1^{1 \circ 2}, sw_2^{1 \circ 2}, \dots, sw_N^{1 \circ 2}]^T$ is defined as follows:

$$SW^{1 \circ 2} = \tau_1 SW^1 + \tau_2 SW^2, \quad (34)$$

where τ_1 and τ_2 are the synthesis coefficients corresponding to SW^1 and SW^2 and $\tau_1 \geq 0$, $\tau_2 \geq 0$, and $\tau_1 + \tau_2 = 1$.

According to index value matrix $X = [x_{i,t}]_{l \times N}$, the weight contribution difference degree of SW^1 and SW^2 is defined as follows:

$$\xi^{1 \circ 2} = \sum_{i=1}^l \sum_{t=1}^N (\tau_1 sw_t^1 x_{i,t} - \tau_2 sw_t^2 x_{i,t})^2. \quad (35)$$

Therefore, a weight synthesis optimization model is established to balance the weight contribution of SW^1 and SW^2 as follows:

$$\begin{aligned} \min \quad & \xi^{1 \circ 2}, \\ \text{s.t.} \quad & \tau_1 \geq 0, \tau_2 \geq 0, \tau_1 + \tau_2 = 1. \end{aligned} \quad (36)$$

Two synthesis coefficients are solved as follows:

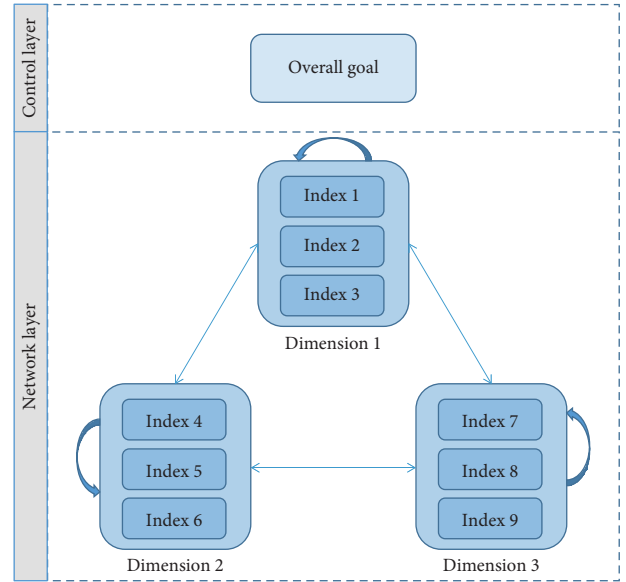


FIGURE 9: The ANP structure.

$$\tau_1 = \frac{\sum_{i=1}^l \sum_{t=1}^N (x_{i,t})^2 sw_t^2 (sw_t^1 + sw_t^2)}{\sum_{i=1}^l \sum_{t=1}^N (x_{i,t})^2 (sw_t^1 + sw_t^2)}, \quad (37)$$

$$\tau_2 = 1 - \tau_1.$$

$SW^{1 \circ 2}$ and SW^3 are synthesized in the same way, and their synthesized weight vector is obtained as $SW^{1 \circ 2 \circ 3}$. According to the process of subjective weight synthesis stage shown in Figure 1, the synthesized subjective weight vector can be obtained in the end as follows:

$$SW^{1 \circ 2 \circ \dots \circ h} = [sw_1^{1 \circ 2 \circ \dots \circ h}, sw_2^{1 \circ 2 \circ \dots \circ h}, \dots, sw_N^{1 \circ 2 \circ \dots \circ h}]^T. \quad (38)$$

(2) Stage 2: objective weight synthesis.

Objective weight methods mainly include entropy method, CRITIC method, and standard deviation method. The principle and solution process of these methods are as follows:

- (i) Entropy method. In information theory, entropy is a measure of uncertainty, which determines the weight according to the variation in index. Generally, the smaller the entropy of an index, the greater the variation degree in the index, the more the information it provides, and the greater its weight; on the contrary, the larger the entropy of an index, the smaller the variation degree of the index, the less information it provides, and the smaller its weight. Entropy method calculates the weight of an index based on its information quantity.
- (ii) CRITIC method. Its basic idea is to comprehensively measure the weight of the index through the contrast intensity within the index and the conflict between the indexes. Contrast

intensity is presented in the form of standard deviation, while conflict is determined by the correlation between indexes.

- (iii) Standard deviation method. This method uses the standard deviation of an index to determine its weight. If an index has a larger standard deviation, which means that the index is more different in value, its weight will be larger. By normalizing the standard deviations of all indexes, the weights of indexes can be obtained. According to the process of objective weight synthesis stage shown in Figure 1, by the same way with the solving process of synthesized subjective weight vector, the synthesized objective weight vector also can be obtained in the end as follows:

$$OW^{1 \circ 2 \circ \dots \circ g} = [ow_1^{1 \circ 2 \circ \dots \circ g}, ow_2^{1 \circ 2 \circ \dots \circ g}, \dots, ow_N^{1 \circ 2 \circ \dots \circ g}]^T. \quad (39)$$

- (3) Stage 3: total synthesis.

Under the premise of obtaining synthesized subjective weight $SW^{1 \circ 2 \circ \dots \circ h}$ and synthesized objective weight $OW^{1 \circ 2 \circ \dots \circ g}$, total synthesis of subjective and objective weight is carried out using the same weight synthesis optimization model shown by formula (35), and the vector $TW = [tw_1, tw_2, \dots, tw_N]^T$ is obtained as follows:

$$TW = \tau_{sw} SW^{1 \circ 2 \circ \dots \circ h} + \tau_{ow} OW^{1 \circ 2 \circ \dots \circ g}, \quad (40)$$

where τ_{sw} and τ_{ow} are the subjective synthesis coefficient and objective synthesis coefficient, and they are corresponding to $SW^{1 \circ 2 \circ \dots \circ h}$ and $OW^{1 \circ 2 \circ \dots \circ g}$, respectively. Here, $\tau_{sw} \geq 0$, $\tau_{ow} \geq 0$, and $\tau_{sw} + \tau_{ow} = 1$.

3.3.3. Intelligent Manufacturing Project Evaluation by PROMETHEE II. Traditional object assessment methods include TOPSIS (Technique for Order Preference by Similarity to an Ideal Solution) [28], VIKOR (VlseKriterijumska Optimizacija I Kompromisnoresenje) [29], AHP, and other mixed-model MCDM methods. These methods have decision compensation in the assessment and decision-making process; that is, the high value of one index can remedy the low value of other indexes. In this part, PROMETHEE II [30] is used to assess the green performance and sort several intelligent manufacturing projects. The core idea of this method is that the level is not lower than the relationship. By PROMETHEE II, the priority function is used to compare the intelligent manufacturing projects one by one to determine the priority sequence of all intelligent manufacturing projects, which can avoid the influence of decision compensation on the assessment results of intelligent manufacturing projects. This method fully considers the objective facts of the existence of the preference of the decision-maker, making the decision-making results more convincing.

In PROMETHEE II, there are many common criteria to determine the preference function. Compared with others, the Gaussian preference function has nonlinear characteristics, which is more in line with the actual decision-making environment. Therefore, this paper chooses the preference function in the form of Gaussian criteria. The index values of intelligent manufacturing projects i and m ($i, m = 1, 2, \dots, l$ and $i \neq m$) in index t are $x_{i,t}$ and $x_{m,t}$, respectively. On index t , the preference function of intelligent manufacturing project i compared with intelligent manufacturing project m is defined as follows:

$$p_t(i, m) = \begin{cases} 0, & x_{i,t} - x_{m,t} \leq 0, \\ 1 - e^{-(x_{i,t} - x_{m,t})/2\eta^2}, & x_{i,t} - x_{m,t} > 0, \end{cases} \quad (41)$$

where the value of parameter η is 0.2.

Under the condition of considering all indexes, the weighted preference degree of intelligent manufacturing project i compared with intelligent manufacturing project m is expressed as follows:

$$p(i, m) = \sum_{t=1}^N w_t \cdot p_t(i, m). \quad (42)$$

The outflow Ω_i^+ and inflow Ω_i^- of intelligent manufacturing project i can be obtained as follows:

$$\Omega_i^+ = \sum_{m=1, m \neq i}^l p(i, m), \quad (43)$$

$$\Omega_i^- = \sum_{m=1, m \neq i}^l p(m, i),$$

where $p(m, i)$ represents the weighted preference degree of intelligent manufacturing project m compared with intelligent manufacturing project i under the condition of considering all indexes.

The degree of intelligent manufacturing project i superior to other projects can be represented by outflow Ω_i^+ , and the degree of intelligent manufacturing project i inferior to other projects can be represented by inflow Ω_i^- . Therefore, the preference net flow of intelligent manufacturing project i is represented as follows:

$$\Omega_i = \Omega_i^+ - \Omega_i^-. \quad (44)$$

The net flow is the main basis for the PROMETHEE II method to measure the advantages and disadvantages of the intelligent manufacturing projects. The priority ranking results of all intelligent manufacturing projects can be obtained by comparing the net flow values.

4. Case Study: Application of the FRSA-MSWS-P II Model for Green Performance Evaluation of Intelligent Manufacturing Project for an Air Conditioning Enterprise Driven by Digital Twin

The remote operation and maintenance service project is a key component of the intelligent manufacturing strategy for an air conditioning enterprise. This section will evaluate the

green performance of the remote operation and maintenance service project alternatives to obtain the optimal one from multiple alternatives. The enterprise has built the digital twin system of its intelligent manufacturing project, which can provide the digital twin data of whole life cycle for green performance evaluation. There are ten alternatives of intelligent manufacturing project of remote operation and maintenance service, which are Alter. 1, Alter. 2, . . . , Alter. 10. Three experts participate in the index value calculation of intelligent manufacturing project alternatives. For index 1, the fuzzy reciprocal assessment matrices given by three experts are $\tilde{\Phi}^{1,1} = [\tilde{\phi}_{i,j}^{1,1}]_{10 \times 10}$, $\tilde{\Phi}^{2,1} = [\tilde{\phi}_{i,j}^{2,1}]_{10 \times 10}$, and $\tilde{\Phi}^{3,1} = [\tilde{\phi}_{i,j}^{3,1}]_{10 \times 10}$. Due to limited space and without losing generality, only $\tilde{\Phi}^{1,1}$ is given as follows:

$$\tilde{\Phi}^{1,1} = \begin{bmatrix} E & OS & E & WS & OS & E & ES & WS & OS & E \\ OI & E & OI & WI & E & E & SI & OI & WI & WI \\ E & OS & E & WS & E & OS & WS & SS & E & OS \\ WI & WS & WI & E & WS & OS & E & WS & E & SS \\ OI & E & OI & WI & E & EI & E & SI & WI & WI \\ E & E & OI & OI & ES & E & E & SI & SI & EI \\ EI & SS & WI & E & SS & E & E & SS & OS & E \\ WI & OS & SI & WI & SS & SS & SI & E & WI & WS \\ OI & WS & E & E & WS & SS & OI & WS & E & SI \\ E & WS & OI & SI & WS & ES & E & WI & SS & E \end{bmatrix}. \quad (45)$$

Through consistency inspection, three matrices $\tilde{\Phi}^{1,1}$, $\tilde{\Phi}^{2,1}$, and $\tilde{\Phi}^{3,1}$ can pass the inspection. Then, the group judgment matrix $\tilde{\Theta}^1 = [\tilde{\rho}_{i,j}^1]_{10 \times 10}$ is constructed based on $\tilde{\Phi}^{1,1}$, $\tilde{\Phi}^{2,1}$, and $\tilde{\Phi}^{3,1}$ and $\tilde{\rho}_{i,j}^1 = \{\tilde{\phi}_{i,j}^{1,1}, \tilde{\phi}_{i,j}^{2,1}, \tilde{\phi}_{i,j}^{3,1}\}$. For example, $\tilde{\rho}_{1,2}^1 = \{\tilde{\phi}_{1,2}^{1,1}, \tilde{\phi}_{1,2}^{2,1}, \tilde{\phi}_{1,2}^{3,1}\} = \{OS, E, OS\} = \{(1.0000, 1.2222, 1.8571, 2.3333), (1.0000, 1.0000, 1.0000, 1.0000), (1.0000, 1.2222, 1.8571, 2.3333)\}$. Based on formulas (11)–(13), the rough boundary interval of $\tilde{\phi}_{1,2}^{1,1} = OS$ in $\tilde{\rho}_{1,2}^1 = \{\tilde{\phi}_{1,2}^{1,1}, \tilde{\phi}_{1,2}^{2,1}, \tilde{\phi}_{1,2}^{3,1}\}$ is obtained as $RBI(\tilde{\phi}_{1,2}^{1,1}) = [LRL(\tilde{\phi}_{1,2}^{1,1}), URL(\tilde{\phi}_{1,2}^{1,1})] = [(1.0000, 1.1481, 1.5714, 1.8889), (1.0000, 1.2222, 1.8571, 2.3333)]$, while $RBI(\tilde{\phi}_{1,2}^{2,1}) = [LRL(\tilde{\phi}_{1,2}^{2,1}), URL(\tilde{\phi}_{1,2}^{2,1})] = [(1.0000, 1.0000, 1.0000, 1.0000), (1.0000, 1.1481, 1.5714, 1.8889)]$ and $RBI(\tilde{\phi}_{1,2}^{3,1}) = [LRL(\tilde{\phi}_{1,2}^{3,1}), URL(\tilde{\phi}_{1,2}^{3,1})] = [(1.0000, 1.1481, 1.5714, 1.8889), (1.0000, 1.2222, 1.8571, 2.3333)]$. According to the arithmetic operation rules shown in formulas (14)–(16), the rough boundary interval of $\tilde{\rho}_{1,2}^1 = \{\tilde{\phi}_{1,2}^{1,1}, \tilde{\phi}_{1,2}^{2,1}, \tilde{\phi}_{1,2}^{3,1}\}$ can be obtained as $RBI(\tilde{\rho}_{1,2}^1) = [(1.0000, 1.0988, 1.3809, 1.5926), (1.0000, 1.1975, 1.7619, 2.1852)]$.

The rough boundary intervals of other elements in $\tilde{\Theta}^1 = [\tilde{\rho}_{i,j}^1]_{10 \times 10}$ can be obtained by the same way. The RBI judgment matrix is constructed as $\tilde{\Lambda}^1 = [RBI(\tilde{\rho}_{i,j}^1)]_{10 \times 10}$. Then, $\tilde{\Lambda}^1$ is decomposed into LRL matrix $\tilde{\Lambda}_{LRL}^1$ and URL matrix $\tilde{\Lambda}_{URL}^1$. $\tilde{\Lambda}_{LRL}^1$ is shown in Tables 3 and 4, while $\tilde{\Lambda}_{URL}^1$ is shown in Tables 5 and 6.

According to formula (8), $\tilde{\Lambda}_{LRL}^1$ and $\tilde{\Lambda}_{URL}^1$ are converted into real number forms Λ_{LRL}^1 , shown in Table 7, and Λ_{URL}^1 shown in Table 8.

The eigenvectors of Λ_{LRL}^1 and Λ_{URL}^1 corresponding to the maximum eigenvalue are obtained, respectively, as $Eig(\Lambda_{LRL}^1)$ and $Eig(\Lambda_{URL}^1)$. After averaging the two eigenvectors, an average vector is obtained as $Eig(\Lambda_{Aver}^1) = [0.3353, 0.3039, 0.3235, 0.3009, 0.3108, 0.3354, 0.2915, 0.3100, 0.3234, 0.3214]^T$.

The index value of ten intelligent manufacturing project alternatives on index 1 is obtained as $Eig(\Lambda_{Aver}^1)$. After solving the index values of ten intelligent manufacturing project alternatives on other indexes by the same way, the index value matrix of ten intelligent manufacturing project alternatives on all indexes is obtained as $X = [x_{i,t}]_{10 \times 9}$, as shown in Table 9.

Subjective weight solved by the complex networks method, ANP method, and Delphi method is shown in Table 10, while objective weight solved by the entropy method, CRITIC method, and standard deviation method is shown in Table 11.

As shown in Figure 10, the weight synthesis has three stages. Stage 1 and stage 2 have two substages, respectively.

The synthesized weight obtained in each stage is shown in Table 12.

According to formulas (40) and (41), the weighted preference degree matrix is obtained, as shown in Table 13.

According to formulas (42) and (43), the outflow, inflow, net flow, and final rank are obtained, as shown in Table 14.

5. Discussion of the Results

In order to make a final selection of the optimal alternatives, it is necessary to assess the reliability of the results obtained by the initial model. The most common means of assessing the reliability of the results is to compare them with other MCDM techniques. The discussion of the results is presented using the comparison of three MCDM methods (PROMETHEE II, TOPSIS, and VIKOR). These methods were chosen because they have so far given stable and reliable results [27–30]. TOPSIS and VIKOR methods were modified using fuzzy rough-sets AHP and multistage weight synthesis techniques proposed in this paper, which are called FRSA-MSWS-TOPSIS and FRSA-MSWS-VIKOR. These two modified models are compared with the proposed FRSA-MSWS-PII. Additionally, the models for comparison (FRSA-MSWS-TOPSIS and FRSA-MSWS-VIKOR) are divided into multiple submodels which are with synthesis of different quantity weights. In the second part of this section, a sensitivity analysis [31, 32] of the proposed FRSA-MSWS-PII model was carried out through 27 scenarios.

TABLE 3: LRL matrix $\tilde{\Lambda}_{LRL}^1$ (part 1: columns 1–5).

Alter.	1	2	3	4	5
1	(1, 1, 1, 1)	(1.0000, 1.0988, 1.3809, 1.5926)	(1.1037, 1.6779, 1.8694, 1.9372)	(0.6468, 1.7128, 1.8540, 1.8657)	(0.9951, 1.3021, 1.3572, 1.7378)
2	(0.5336, 0.5676, 1.0397, 1.3301)	(1, 1, 1, 1)	(0.4684, 0.9725, 1.1776, 1.3317)	(0.8246, 1.0541, 1.0761, 1.6594)	(0.5427, 0.8139, 0.9974, 1.3416)
3	(1.1489, 1.4540, 1.4561, 1.5842)	(0.4953, 0.5825, 0.8568, 1.6916)	(1, 1, 1, 1)	(0.8178, 1.1612, 1.2975, 1.9428)	(1.0195, 1.0630, 1.5027, 1.9814)
4	(0.7188, 1.0560, 1.6952, 1.7386)	(0.9026, 1.1191, 1.4234, 1.4681)	(0.7571, 0.9762, 1.0272, 1.2090)	(1, 1, 1, 1)	(0.5961, 1.1055, 1.1799, 1.3777)
5	(0.5566, 0.9454, 1.2728, 1.4644)	(0.6137, 0.9540, 1.2736, 1.3970)	(1.4355, 1.4538, 1.5025, 1.9150)	(1.1477, 1.1610, 1.3913, 1.4760)	(1, 1, 1, 1)
6	(0.8475, 1.4009, 1.7410, 1.7550)	(1.0563, 1.1164, 1.7237, 1.8260)	(0.7848, 1.0350, 1.6751, 1.9214)	(0.7092, 1.6417, 1.7861, 1.9843)	(0.4996, 1.3061, 1.4028, 1.4263)
7	(0.6408, 0.6771, 0.7431, 0.7685)	(1.1400, 1.2236, 1.2805, 1.5275)	(0.5379, 0.7261, 1.0074, 1.2589)	(0.6112, 1.1761, 1.4969, 1.8638)	(0.6579, 0.7795, 0.9149, 1.3757)
8	(0.5216, 0.6006, 0.8792, 1.7264)	(1.0414, 1.1301, 1.6366, 1.6826)	(0.8778, 1.5035, 1.5495, 1.6198)	(0.6862, 0.8049, 1.7300, 1.8657)	(0.4572, 0.6153, 1.6511, 1.9409)
9	(1.1202, 1.2001, 1.3715, 1.3804)	(0.9248, 1.1256, 1.1425, 1.2045)	(1.0368, 1.2759, 1.4487, 1.7079)	(0.7720, 0.9169, 1.3599, 1.4148)	(1.2160, 1.5583, 1.6575, 1.8508)
10	(0.4973, 1.1939, 1.2250, 1.6033)	(0.7335, 0.8219, 1.3439, 1.6985)	(1.2856, 1.4828, 1.4831, 1.5321)	(0.5005, 1.3199, 1.4872, 1.8169)	(0.6924, 1.0332, 1.4494, 1.7761)

TABLE 4: LRL matrix $\tilde{\Lambda}_{LRL}^1$ (part 2: columns 6–10).

Alter.	6	7	8	9	10
1	(0.8231, 1.4384, 1.4980, 1.9344)	(0.7973, 0.8449, 1.4851, 1.7588)	(0.4518, 1.0495, 1.3834, 1.8698)	(1.0328, 1.0413, 1.0671, 1.2811)	(1.0170, 1.0771, 1.1450, 1.6334)
2	(0.5954, 0.6653, 0.7476, 1.5292)	(0.6231, 0.6613, 1.2175, 1.5019)	(1.3189, 1.5298, 1.7686, 1.8909)	(0.4508, 1.3995, 1.7914, 1.9844)	(0.6138, 0.6702, 0.7080, 1.4125)
3	(0.5483, 1.5937, 1.7837, 1.8983)	(0.4979, 0.6576, 0.7253, 1.0678)	(0.5462, 0.9109, 0.9647, 1.9929)	(0.5753, 0.5893, 1.4282, 1.6547)	(0.4660, 0.9057, 0.9741, 1.6068)
4	(0.7969, 0.9776, 1.3572, 1.9376)	(0.6649, 1.2982, 1.8309, 1.9369)	(0.8275, 0.9925, 1.7121, 1.8904)	(0.6747, 1.3023, 1.3485, 1.7974)	(0.5677, 0.6411, 0.8219, 1.0728)
5	(1.2083, 1.2108, 1.8492, 1.9144)	(0.7146, 0.8002, 0.8029, 1.1253)	(0.6222, 1.1302, 1.8526, 1.9686)	(0.6320, 0.7937, 1.3844, 1.5524)	(0.8933, 0.9312, 1.1001, 2.3003)
6	(1, 1, 1, 1)	(0.5999, 1.2586, 1.7172, 1.7181)	(1.1534, 1.4559, 1.6905, 1.9581)	(0.8006, 1.0462, 1.3536, 1.3637)	(0.9830, 1.5819, 1.7278, 1.9731)
7	(0.4849, 0.8541, 1.3713, 1.7175)	(1, 1, 1, 1)	(0.5054, 0.9498, 1.1806, 1.6663)	(0.7472, 0.9787, 1.3915, 1.5946)	(0.5912, 0.7424, 0.8956, 1.3431)
8	(1.0599, 1.2561, 1.4907, 1.5989)	(0.5189, 0.8263, 1.1357, 1.6201)	(1, 1, 1, 1)	(0.4803, 1.1356, 1.5093, 1.5413)	(1.2220, 1.3407, 1.7600, 1.8463)
9	(0.5794, 1.4202, 1.4745, 1.5811)	(0.4763, 0.6373, 1.3491, 1.8889)	(0.4891, 1.1740, 1.4547, 1.7554)	(1, 1, 1, 1)	(0.5341, 0.7245, 0.9628, 1.4774)
10	(0.8962, 1.0925, 1.5457, 1.9992)	(0.8964, 1.5462, 1.5810, 1.6611)	(0.9733, 1.3922, 1.5989, 1.6593)	(0.5296, 1.5882, 1.6884, 1.8302)	(1, 1, 1, 1)

5.1. Comparing the Ranks of Different Models. FRSA-MSWS-TOPSIS model and FRSA-MSWS-TOPSIS model are divided into multiple submodels. All models including the proposed model (model 1) are as follows:

- (1) Model 1: proposed model (FRSA-MSWS-PII) with synthesis of six weights ($SW^1, SW^2, SW^3 + OW^1, OW^2, OW^3$)
- (2) Model 2: FRSA-MSWS-TOPSIS with synthesis of two weights
 - Model 2.1: $SW^1 + OW^1$
 - Model 2.2: $SW^1 + OW^2$

- Model 2.3: $SW^2 + OW^2$
- Model 2.4: $SW^2 + OW^3$
- Model 2.5: $SW^3 + OW^1$
- Model 2.6: $SW^3 + OW^3$

(3) Model 3: FRSA-MSWS-VIKOR with synthesis of two weights

- Model 3.1: $SW^1 + OW^1$
- Model 3.2: $SW^1 + OW^2$
- Model 3.3: $SW^2 + OW^2$
- Model 3.4: $SW^2 + OW^3$
- Model 3.5: $SW^3 + OW^1$
- Model 3.6: $SW^3 + OW^3$

TABLE 5: URL matrix $\tilde{\Lambda}_{\text{URL}}^1$ (part 1: columns 1–5).

Alter.	1	2	3	4	5
1	(1, 1, 1, 1)	(1.0000, 1.1975, 1.7619, 2.1852)	(1.3959, 1.8678, 2.5606, 2.9058)	(0.8786, 2.2426, 2.6681, 4.7228)	(1.4288, 2.4658, 2.8178, 3.9657)
2	(1.3456, 1.9678, 2.5142, 2.8548)	(1, 1, 1, 1)	(1.1568, 1.4847, 2.5474, 3.0198)	(1.0122, 1.0903, 2.8725, 4.8158)	(0.8339, 0.8947, 1.5098, 2.6066)
3	(1.4519, 1.5936, 2.0034, 2.4383)	(1.8749, 2.4067, 2.8435, 3.2298)	(1, 1, 1, 1)	(1.3095, 1.8756, 1.9465, 3.4211)	(0.8830, 2.7474, 2.8092, 4.1440)
4	(0.9330, 1.6784, 1.9591, 2.5506)	(0.8341, 1.1678, 1.2461, 2.9649)	(0.9159, 2.8247, 2.8936, 3.8990)	(1, 1, 1, 1)	(0.9411, 2.2048, 2.3311, 2.3398)
5	(1.6968, 2.3804, 2.6040, 4.8683)	(0.9998, 1.7316, 1.9192, 2.5134)	(1.2597, 1.3015, 1.3197, 2.3604)	(1.5705, 2.2564, 2.4946, 2.5479)	(1, 1, 1, 1)
6	(1.9121, 1.9896, 2.0809, 2.7139)	(1.6729, 2.4921, 2.5787, 3.9713)	(1.5206, 1.7650, 2.2768, 4.3007)	(1.4500, 1.9317, 2.0937, 2.7454)	(0.9090, 1.5973, 1.6085, 1.8771)
7	(0.8938, 1.4201, 2.1974, 3.0621)	(1.0727, 1.8788, 2.6766, 4.4705)	(1.1865, 1.2597, 1.5389, 4.6016)	(1.5736, 2.0361, 2.4198, 2.4402)	(0.9572, 1.0258, 1.3335, 2.7689)
8	(0.9447, 1.4976, 2.3286, 2.8905)	(1.2111, 1.7803, 1.8775, 3.5145)	(1.0618, 1.1577, 2.2412, 2.8931)	(0.9720, 1.9844, 2.6592, 2.9915)	(0.9858, 2.4791, 2.5981, 2.7111)
9	(0.8528, 1.1187, 1.6901, 1.8615)	(1.9187, 1.9237, 2.5988, 4.1383)	(1.5716, 2.7271, 2.8658, 3.1107)	(1.3071, 1.6180, 1.8360, 2.6575)	(1.5352, 1.6308, 2.3372, 2.7600)
10	(2.1417, 2.1589, 2.7904, 4.4097)	(0.8631, 1.5053, 1.8778, 2.7503)	(1.0816, 1.1919, 1.5187, 2.9980)	(1.2190, 1.6116, 1.8136, 4.9229)	(1.2200, 1.3066, 1.7422, 1.8604)

TABLE 6: URL matrix $\tilde{\Lambda}_{\text{URL}}^1$ (part 2: columns 6–10).

Alter.	6	7	8	9	10
1	(1.0856, 1.4359, 2.2780, 2.3293)	(0.8282, 1.5578, 2.2857, 2.5171)	(1.7336, 1.8140, 1.8174, 4.0347)	(1.2599, 1.2930, 1.5676, 2.9902)	(2.1814, 2.4984, 2.8523, 4.8855)
2	(1.9559, 1.9668, 2.6945, 2.8364)	(1.0309, 1.1247, 1.2174, 1.8890)	(2.0821, 2.5939, 2.7338, 4.9534)	(1.7569, 1.8550, 1.9609, 2.5630)	(0.9146, 2.0622, 2.8486, 3.8604)
3	(2.5282, 2.6897, 2.9562, 2.9657)	(1.4502, 1.4629, 2.1983, 2.8661)	(0.9020, 1.4561, 1.9119, 3.9980)	(1.0401, 1.9743, 2.7913, 4.2684)	(0.9066, 2.1276, 2.2694, 3.0096)
4	(1.3612, 1.9131, 2.4528, 3.7361)	(1.1284, 1.3665, 1.8680, 2.6496)	(1.2325, 1.3524, 2.1553, 2.7878)	(1.5721, 2.1685, 2.6767, 2.9556)	(1.0085, 1.2046, 1.3279, 1.7180)
5	(1.2671, 1.5430, 1.6123, 2.7801)	(1.4844, 1.5762, 1.7465, 2.8314)	(1.3677, 1.6992, 1.9013, 2.1088)	(1.4527, 1.5013, 1.7332, 2.9330)	(1.1802, 1.2257, 1.5547, 1.9670)
6	(1, 1, 1, 1)	(1.1297, 2.2511, 2.3894, 2.9781)	(0.9836, 1.3593, 1.7513, 2.6157)	(1.3540, 1.4390, 1.9142, 2.1576)	(1.0371, 2.0850, 2.7939, 4.4945)
7	(1.1553, 1.4880, 1.5508, 1.7356)	(1, 1, 1, 1)	(1.1869, 1.4414, 1.8417, 2.3879)	(1.3343, 1.3919, 2.8183, 4.0151)	(1.7366, 2.0025, 2.3034, 3.5067)
8	(1.1300, 1.5650, 1.9010, 2.0894)	(1.5903, 2.3132, 2.4199, 2.4578)	(1, 1, 1, 1)	(1.3946, 1.5279, 1.6276, 1.7335)	(1.3428, 2.0892, 2.4250, 3.5989)
9	(2.4919, 2.7597, 2.9611, 3.2421)	(1.6795, 1.8655, 2.6587, 2.6980)	(1.5653, 2.0299, 2.6733, 2.6790)	(1, 1, 1, 1)	(1.0599, 2.7767, 2.9745, 3.0679)
10	(1.2209, 1.8226, 2.4807, 2.6000)	(1.0587, 1.6723, 2.0247, 2.3236)	(1.0306, 1.0814, 2.0090, 2.8380)	(0.9603, 0.9948, 2.5564, 4.7606)	(1, 1, 1, 1)

TABLE 7: Real number form matrix Λ_{LRL}^1 .

Alter.	1	2	3	4	5	6	7	8	9	10
1	1	1.5314	1.6206	1.4502	1.3533	1.4101	1.2253	1.1829	1.1195	1.2467
2	0.8732	1	0.9696	1.1815	0.9277	0.9341	1.0056	1.6240	1.3692	0.9003
3	1.3962	0.9456	1	1.3245	1.4052	1.3976	0.7491	1.1550	1.0641	1.0024
4	1.2965	1.2240	0.9899	1	1.0433	1.2840	1.4147	1.3558	1.2670	0.7829
5	1.0521	1.0520	1.6035	1.2950	1	1.5459	0.8802	1.3835	1.0907	1.3823
6	1.4157	1.4310	1.3540	1.4816	1.1058	1	1.3005	1.5629	1.1353	1.5446
7	0.7071	1.3030	0.8849	1.2772	0.9513	1.1062	1	1.0778	1.1772	0.9094
8	0.9719	1.3723	1.3468	1.2719	1.1681	1.3485	1.0335	1	1.1417	1.5417
9	1.2668	1.0891	1.3683	1.1145	1.5616	1.2089	1.0983	1.1979	1	0.9408
10	1.1048	1.1561	1.4336	1.2495	1.2373	1.3923	1.3778	1.3899	1.3436	1

TABLE 8: Real number form matrix Λ_{URL}^1 .

Alter.	1	2	3	4	5	6	7	8	9	10
1	1	1.9481	2.1786	2.6741	2.6765	1.7774	1.7807	2.5275	1.8617	3.2143
2	2.1596	1	2.0555	2.5039	1.5031	2.3644	1.3543	3.2199	2.0662	2.4149
3	1.8819	2.5825	1	2.2090	2.6034	2.7819	2.0116	2.1619	2.5455	2.0433
4	1.7712	1.6605	2.5614	1	1.8669	2.4042	1.7760	1.8956	2.3310	1.3261
5	3.0017	1.7821	1.6409	2.1853	1	1.8684	1.9738	1.7633	1.9750	1.4944
6	2.2110	2.7231	2.5680	2.0662	1.4638	1	2.1489	1.7024	1.7196	2.6385
7	1.9067	2.5757	2.3581	2.1032	1.6022	1.4725	1	1.7266	2.4189	2.4427
8	1.9157	2.1776	1.8503	2.1235	2.0933	1.6615	2.1507	1	1.5697	2.3904
9	1.3786	2.7131	2.5055	1.8854	2.0731	2.8643	2.2239	2.2266	1	2.3587
10	2.9505	1.7620	1.7784	2.5948	1.5328	2.0168	1.7550	1.7606	2.3935	1

TABLE 9: Index value matrix $X = [x_{i,t}]_{10 \times 9}$.

	Index 1	Index 2	Index 3	Index 4	Index 5	Index 6	Index 7	Index 8	Index 9
Alter. 1	0.3353	0.8333	0.9152	0.2143	0.9220	0.6691	0.1878	0.3506	0.5922
Alter. 2	0.3039	0.9618	0.9684	0.2419	0.9735	0.9615	0.5368	0.8203	0.2277
Alter. 3	0.3235	0.4796	0.9242	0.8130	0.9635	0.6902	0.1321	0.8642	0.9406
Alter. 4	0.3009	0.7109	0.7820	0.7688	0.4530	0.6899	0.2541	0.7354	0.1286
Alter. 5	0.3108	0.3492	0.1416	0.1874	0.8411	0.7253	0.3854	0.9552	0.1310
Alter. 6	0.3354	0.4949	0.4434	0.7890	0.8157	0.2682	0.5408	0.5010	0.6817
Alter. 7	0.2915	0.7384	0.7792	0.3484	0.7117	0.6896	0.2464	0.2071	0.5485
Alter. 8	0.3100	0.9638	0.4063	0.6267	0.3014	0.7761	0.3296	0.5554	0.7292
Alter. 9	0.3234	0.9018	0.9634	0.5925	0.2248	0.2344	0.3318	0.8566	0.3289
Alter. 10	0.3214	0.8329	0.3192	0.9363	0.4150	0.2769	0.3260	0.3260	0.5260

TABLE 10: Subjective weight.

	Index 1	Index 2	Index 3	Index 4	Index 5	Index 6	Index 7	Index 8	Index 9
Complex networks method (SW^1)	0.0685	0.0309	0.1646	0.0656	0.0258	0.1591	0.1396	0.2425	0.1034
ANP method (SW^2)	0.0284	0.0913	0.0711	0.1715	0.1104	0.1162	0.1852	0.1049	0.1209
Delphi method (SW^3)	0.0830	0.0497	0.0607	0.0970	0.1141	0.1530	0.1323	0.0875	0.2226

TABLE 11: Objective weight.

	Index 1	Index 2	Index 3	Index 4	Index 5	Index 6	Index 7	Index 8	Index 9
Entropy method (SW^1)	0.1154	0.1133	0.1099	0.1091	0.1108	0.1111	0.1117	0.1110	0.1077
CRITIC method (SW^2)	0.1077	0.1153	0.1024	0.1189	0.1066	0.1143	0.1163	0.1116	0.1069
Standard deviation method (SW^3)	0.0072	0.1070	0.1515	0.1388	0.1416	0.1226	0.0663	0.1306	0.1344

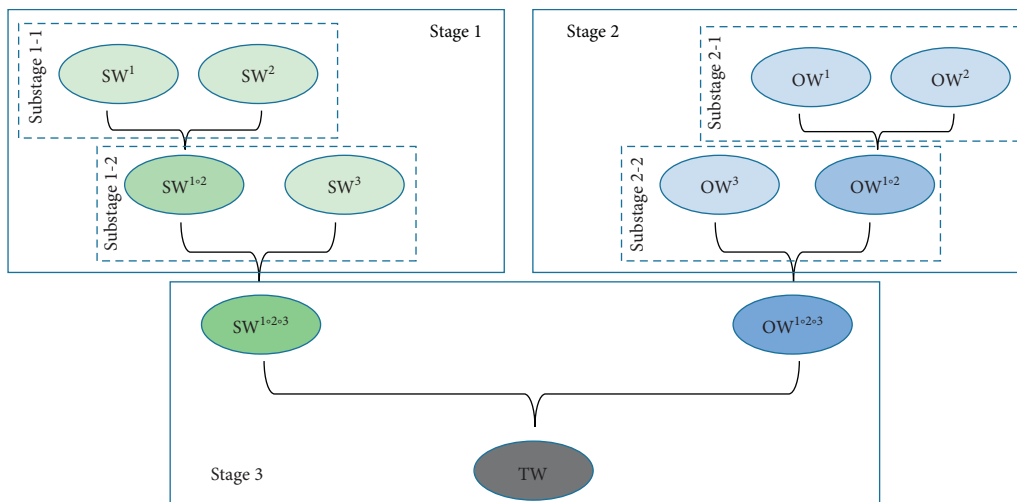


FIGURE 10: The weight synthesis process.

TABLE 12: The synthesized weight obtained in each stage.

	Synthesis coefficients	Index 1	Index 2	Index 3	Index 4	Index 5	Index 6	Index 7	Index 8	Index 9
Substage 1-1: $SW^{1\circ 2}$	0.3131 and 0.6869	0.0409	0.0724	0.1004	0.1384	0.0839	0.1296	0.1709	0.1480	0.1154
Substage 1-2: $SW^{1\circ 2\circ 3}$	0.6181 and 0.3819	0.0570	0.0638	0.0852	0.1226	0.0954	0.1385	0.1562	0.1249	0.1564
Substage 2-1: $OW^{1\circ 2}$	0.7110 and 0.2890	0.1132	0.1139	0.1077	0.1119	0.1096	0.1120	0.1130	0.1111	0.1075
Substage 2-2: $OW^{1\circ 2\circ 3}$	0.4289 and 0.5711	0.0527	0.1100	0.1327	0.1273	0.1279	0.1181	0.0864	0.1222	0.1228
Stage 3: TW	0.3509 and 0.6491	0.0542	0.0937	0.1161	0.1256	0.1165	0.1252	0.1108	0.1232	0.1346

TABLE 13: The weighted preference degree matrix.

	Alter. 1	Alter. 2	Alter. 3	Alter. 4	Alter. 5	Alter. 6	Alter. 7	Alter. 8	Alter. 9	Alter. 10
Alter. 1	0	0.1097	0.0784	0.2744	0.3406	0.3040	0.1158	0.2275	0.3077	0.3417
Alter. 2	0.3107	0	0.2633	0.3761	0.3417	0.4448	0.4223	0.3916	0.2909	0.5367
Alter. 3	0.3512	0.2610	0	0.2990	0.4132	0.4260	0.4460	0.4158	0.4229	0.5779
Alter. 4	0.2334	0.1217	0.0645	0	0.3146	0.3027	0.2314	0.1943	0.2120	0.3286
Alter. 5	0.1696	0.0251	0.0751	0.1781	0	0.2308	0.1711	0.2242	0.2525	0.3466
Alter. 6	0.2542	0.2477	0.0974	0.2982	0.3858	0	0.3120	0.1972	0.3178	0.2443
Alter. 7	0.0306	0.1140	0.0698	0.1867	0.3491	0.2484	0	0.1980	0.2872	0.2967
Alter. 8	0.2483	0.2347	0.1425	0.2035	0.4120	0.2161	0.2838	0	0.2529	0.2619
Alter. 9	0.2567	0.1170	0.1293	0.1556	0.3694	0.2919	0.2656	0.1974	0	0.2404
Alter. 10	0.1489	0.2158	0.1373	0.1762	0.3675	0.1012	0.1628	0.1051	0.1939	0

TABLE 14: The outflow, inflow, net flow, and final rank.

	Outflow	Inflow	Net flow	Final rank
Alter. 1	2.0998	2.0036	0.0962	4
Alter. 2	3.3781	1.4468	1.9313	2
Alter. 3	3.6129	1.0577	2.5552	1
Alter. 4	2.0032	2.1477	-0.1445	5
Alter. 5	1.6731	3.2940	-1.6208	10
Alter. 6	2.3546	2.5657	-0.2111	6
Alter. 7	1.7805	2.4108	-0.6302	8
Alter. 8	2.2557	2.1512	0.1045	3
Alter. 9	2.0233	2.5379	-0.5145	7
Alter. 10	1.6088	3.1748	-1.5660	9

(4) Model 4: FRSA-MSWS-TOPSIS with synthesis of three weights

- Model 4.1: $SW^1, SW^2 + OW^1$
- Model 4.2: $SW^2, SW^3 + OW^2$
- Model 4.3: $SW^1, SW^3 + OW^3$
- Model 4.4: $SW^1 + OW^1, OW^2$
- Model 4.5: $SW^2 + OW^2, OW^3$
- Model 4.6: $SW^3 + OW^1, OW^3$

(5) Model 5: FRSA-MSWS-VIKOR with synthesis of three weights

- Model 5.1: $SW^1, SW^2 + OW^1$
- Model 5.2: $SW^2, SW^3 + OW^2$
- Model 5.3: $SW^1, SW^3 + OW^3$
- Model 5.4: $SW^1 + OW^1, OW^2$
- Model 5.5: $SW^2 + OW^2, OW^3$
- Model 5.6: $SW^3 + OW^1, OW^3$

(6) Model 6: FRSA-MSWS-TOPSIS with synthesis of four weights

- Model 6.1: $SW^1, SW^2 + OW^1, OW^2$
- Model 6.2: $SW^1, SW^2 + OW^2, OW^3$

- Model 6.3: $SW^2, SW^3 + OW^1, OW^3$
- Model 6.4: $SW^2, SW^3 + OW^1, OW^2$
- Model 6.5: $SW^1, SW^3 + OW^2, OW^3$
- Model 6.6: $SW^1, SW^3 + OW^1, OW^3$

(7) Model 7: FRSA-MSWS-VIKOR with synthesis of four weights

- Model 7.1: $SW^1, SW^2 + OW^1, OW^2$
- Model 7.2: $SW^1, SW^2 + OW^2, OW^3$
- Model 7.3: $SW^2, SW^3 + OW^1, OW^3$
- Model 7.4: $SW^2, SW^3 + OW^1, OW^2$
- Model 7.5: $SW^1, SW^3 + OW^2, OW^3$
- Model 7.6: $SW^1, SW^3 + OW^1, OW^3$

(8) Model 8: FRSA-MSWS-TOPSIS with synthesis of five weights

- Model 8.1: $SW^1, SW^2, SW^3 + OW^1, OW^2$
- Model 8.2: $SW^1, SW^2, SW^3 + OW^2, OW^3$
- Model 8.3: $SW^1, SW^2, SW^3 + OW^1, OW^3$
- Model 8.4: $SW^1, SW^2 + OW^1, OW^2, OW^3$
- Model 8.5: $SW^2, SW^3 + OW^1, OW^2, OW^3$
- Model 8.6: $SW^1, SW^3 + OW^1, OW^2, OW^3$

TABLE 15: Comparison of the ranks of alternatives according to models 1, 2, and 3.

	Model 1	Model 2						Model 3					
		2.1	2.2	2.3	2.4	2.5	2.6	3.1	3.2	3.3	3.4	3.5	3.6
Alter. 1	4	6	6	6	6	4	4	7	7	9	8	2	2
Alter. 2	2	2	2	2	2	3	2	1	1	3	4	3	3
Alter. 3	1	1	1	1	1	1	1	2	2	6	1	1	1
Alter. 4	5	3	3	5	5	7	7	3	3	2	3	9	9
Alter. 5	10	7	7	10	10	10	10	9	9	10	10	10	10
Alter. 6	6	8	8	3	3	5	5	5	6	1	2	4	4
Alter. 7	8	9	9	9	9	6	6	10	10	8	7	6	5
Alter. 8	3	5	5	4	4	2	3	6	5	4	6	5	6
Alter. 9	7	4	4	8	7	9	8	4	4	7	9	8	8
Alter. 10	9	10	10	7	8	8	9	8	8	5	5	7	7

TABLE 16: Comparison of the ranks of alternatives according to models 1, 4, and 5.

	Model 1	Model 4						Model 5					
		2.1	2.2	2.3	2.4	2.5	2.6	3.1	3.2	3.3	3.4	3.5	3.6
Alter. 1	4	7	5	4	6	6	3	7	4	4	7	7	3
Alter. 2	2	2	3	2	2	2	2	1	1	2	1	2	2
Alter. 3	1	1	1	1	1	1	1	3	6	1	2	1	1
Alter. 4	5	3	7	5	3	5	7	2	9	6	3	4	8
Alter. 5	10	8	10	9	8	10	10	9	10	10	9	10	10
Alter. 6	6	6	4	7	7	3	5	5	2	5	5	3	4
Alter. 7	8	9	6	8	9	8	6	10	5	9	10	8	6
Alter. 8	3	4	2	3	5	4	4	4	3	3	4	6	5
Alter. 9	7	5	9	6	4	7	8	6	8	7	6	9	9
Alter. 10	9	10	8	10	10	9	9	8	7	8	8	5	7

(9) Model 9: FRSA-MSWS-VIKOR with synthesis of five weights

- Model 9.1: $SW^1, SW^2, SW^3 + OW^1, OW^2$
- Model 9.2: $SW^1, SW^2, SW^3 + OW^2, OW^3$
- Model 9.3: $SW^1, SW^2, SW^3 + OW^1, OW^3$
- Model 9.4: $SW^1, SW^2 + OW^1, OW^2, OW^3$
- Model 9.5: $SW^2, SW^3 + OW^1, OW^2, OW^3$
- Model 9.6: $SW^1, SW^3 + OW^1, OW^2, OW^3$

(10) Model 10: FRSA-MSWS-TOPSIS with synthesis of six weights ($SW^1, SW^2, SW^3 + OW^1, OW^2, OW^3$)

(11) Model 11: FRSA-MSWS-VIKOR with synthesis of six weights ($SW^1, SW^2, SW^3 + OW^1, OW^2, OW^3$)

Ranking of the alternatives according to the models used in order to assess the reliability of the results shows that alternative 3 remained in the first place for the majority of the models (Tables 15–19). There was a change in the ranking of alternative 3 using the FRSA-MSWS-TOPSIS model and FRSA-MSWS-TOPSIS model, whereby alternatives 3 and 2 changed places for the majority of the models.

In order to establish the connection between the results obtained using 51 different models (Tables 15–19), Spearman’s correlation coefficient (SCC) was used. SCC of ranks is a useful and important indicator for determining the link between the results obtained by different models [31–33]. Additionally, the case in this study has ordinal variables or ranked variables, while SCC is suitable for use in this situation. In this paper, SCC was used to define the statistical

significance of the difference between the ranks obtained by different models. The results of the comparison of ranks using SCC are shown in Tables 20–24.

The SCC values from Tables 20–24, which are with the average values of 0.64, 0.74, 0.77, 0.90, and 0.92 (all greater than 0.60), show a high correlation between the ranks among the models examined. In addition, the average value of SCC tends to increase when the number of synthesized weights increases, which reveals that the model tends to be stable when more weights are synthesized. Based on recommendations by Ghorabae et al. [33], when all SCC values are greater than 0.8, an extremely high correlation is shown. In our case, when the number of synthesized weights is 6, all of the SCC values are significantly greater than 0.8 (Table 24) and the average value is 0.92; when the number of synthesized weights is 5, most of the SCC values are significantly greater than 0.8 (Table 23) and the average value is 0.90; when the number of synthesized weights is 4, most of the SCC values are also significantly greater than 0.8 (Table 22) and the average value is 0.77 (slightly less than 0.8). Therefore, we can conclude that there is a very high correlation (closeness) between the proposed FRSA-MSWS-PII model and the other models for the treatment of uncertainty (fuzzy and rough), especially when the number of synthesized weights is more than 4.

5.2. Sensitivity Analysis. Since the results of MCDM models depend to a great extent on the values of the weight coefficients of the assessment index, this section shows

TABLE 17: Comparison of the ranks of alternatives according to models 1, 6, and 7.

	Model 1	Model 6						Model 7					
		2.1	2.2	2.3	2.4	2.5	2.6	3.1	3.2	3.3	3.4	3.5	3.6
Alter. 1	4	7	6	5	5	4	4	7	7	4	3	4	4
Alter. 2	2	2	2	2	2	2	2	1	1	1	1	1	2
Alter. 3	1	1	1	1	1	1	1	4	2	2	5	2	1
Alter. 4	5	3	3	7	6	5	5	2	3	8	8	6	6
Alter. 5	10	8	9	10	10	9	9	9	10	9	9	10	10
Alter. 6	6	6	7	4	4	7	7	5	5	3	2	5	5
Alter. 7	8	9	8	6	7	8	8	10	9	6	7	9	9
Alter. 8	3	4	4	3	3	3	3	3	4	7	4	3	3
Alter. 9	7	5	5	8	9	6	6	6	6	10	10	7	7
Alter. 10	9	10	10	9	8	10	10	8	8	5	6	8	8

TABLE 18: Comparison of the ranks of alternatives according to models 1, 8, and 9.

	Model 1	Model 8						Model 9					
		2.1	2.2	2.3	2.4	2.5	2.6	3.1	3.2	3.3	3.4	3.5	3.6
Alter. 1	4	5	4	4	6	5	4	4	4	4	6	4	4
Alter. 2	2	2	2	2	2	2	2	1	1	1	1	1	1
Alter. 3	1	1	1	1	1	1	1	3	2	2	2	2	2
Alter. 4	5	6	6	6	3	6	5	6	6	6	3	7	6
Alter. 5	10	9	9	9	9	10	9	9	10	10	10	10	10
Alter. 6	6	4	5	5	7	4	6	5	5	5	5	3	5
Alter. 7	8	8	8	8	8	7	8	10	9	9	9	8	9
Alter. 8	3	3	3	3	4	3	3	2	3	3	4	6	3
Alter. 9	7	7	7	7	5	8	7	7	7	7	7	9	7
Alter. 10	9	10	10	10	10	9	10	8	8	8	8	5	8

TABLE 19: Comparison of the ranks of alternatives according to models 1, 10, and 11.

	Model 1	Model 10	Model 11
Alter. 1	4	4	3
Alter. 2	2	2	2
Alter. 3	1	1	1
Alter. 4	5	6	5
Alter. 5	10	10	10
Alter. 6	6	5	4
Alter. 7	8	8	9
Alter. 8	3	3	6
Alter. 9	7	7	8
Alter. 10	9	9	7

TABLE 20: Correlation of the ranks in the models 1, 2, and 3.

	Model 1	Model 2.1	Model 2.2	Model 2.3	Model 2.4	Model 2.5	Model 2.6	Model 3.1	Model 3.2	Model 3.3	Model 3.4	Model 3.5	Model 3.6
Model 1	1	0.78	0.78	0.88	0.90	0.90	0.94	0.76	0.79	0.38	0.58	0.77	0.71
Model 2.1	—	1	1	0.61	0.68	0.48	0.59	0.87	0.90	0.21	0.35	0.32	0.27
Model 2.2	—	—	1	0.61	0.68	0.48	0.59	0.87	0.90	0.21	0.35	0.32	0.27
Model 2.3	—	—	—	1	0.99	0.83	0.84	0.79	0.78	0.67	0.84	0.73	0.67
Model 2.4	—	—	—	—	1	0.82	0.85	0.84	0.83	0.65	0.79	0.72	0.66

TABLE 20: Continued.

	Model 1	Model 2.1	Model 2.2	Model 2.3	Model 2.4	Model 2.5	Model 2.6	Model 3.1	Model 3.2	Model 3.3	Model 3.4	Model 3.5	Model 3.6
Model 2.5	—	—	—	—	—	1	0.98	0.47	0.50	0.32	0.59	0.88	0.83
Model 2.6	—	—	—	—	—	—	1	0.58	0.60	0.31	0.56	0.89	0.85
Model 3.1	—	—	—	—	—	—	—	1	0.99	0.59	0.61	0.38	0.33
Model 3.2	—	—	—	—	—	—	—	—	1	0.55	0.56	0.37	0.31
Model 3.3	—	—	—	—	—	—	—	—	—	1	0.77	0.14	0.09
Model 3.4	—	—	—	—	—	—	—	—	—	—	1	0.49	0.48
Model 3.5	—	—	—	—	—	—	—	—	—	—	—	1	0.99
Model 3.6	—	—	—	—	—	—	—	—	—	—	—	—	1

TABLE 21: Correlation of the ranks in the models 1, 4, and 5.

	Model 1	Model 4.1	Model 4.2	Model 4.3	Model 4.4	Model 4.5	Model 4.6	Model 5.1	Model 5.2	Model 5.3	Model 5.4	Model 5.5	Model 5.6
Model 1	1	0.85	0.88	0.98	0.83	0.92	0.93	0.81	0.56	0.98	0.85	0.71	0.82
Model 4.1	—	1	0.62	0.89	0.98	0.85	0.66	0.92	0.24	0.81	0.94	0.64	0.49
Model 4.2	—	—	1	0.79	0.53	0.88	0.93	0.59	0.75	0.89	0.66	0.73	0.90
Model 4.3	—	—	—	1	0.89	0.85	0.88	0.78	0.45	0.93	0.83	0.58	0.72
Model 4.4	—	—	—	—	1	0.78	0.64	0.87	0.15	0.77	0.89	0.55	0.45
Model 4.5	—	—	—	—	—	1	0.87	0.84	0.62	0.93	0.89	0.84	0.81
Model 4.6	—	—	—	—	—	—	1	0.59	0.72	0.92	0.66	0.67	0.95
Model 5.1	—	—	—	—	—	—	—	1	0.35	0.79	0.99	0.76	0.48
Model 5.2	—	—	—	—	—	—	—	—	1	0.62	0.38	0.49	0.77
Model 5.3	—	—	—	—	—	—	—	—	—	1	0.85	0.76	0.85
Model 5.4	—	—	—	—	—	—	—	—	—	—	1	0.79	0.56
Model 5.5	—	—	—	—	—	—	—	—	—	—	—	1	0.75
Model 5.6	—	—	—	—	—	—	—	—	—	—	—	—	1

sensitivity analysis of the results when there is a change in the weights of the assessment index.

Sometimes the ranks of the alternatives change as a result of very small changes in the weight coefficients. Therefore, the results of MCDM models as a rule are accompanied by an analysis of their sensitivity to these changes. This section presents a sensitivity analysis of the ranking of the alternatives to changes in the weight coefficients of the assessment index carried out through 27 scenarios (Tables 25–27).

The scenarios for the sensitivity analysis were grouped into three phases. In each phase of the sensitivity analysis,

the weight coefficients of the assessment index are increased, respectively, by 25%, 50%, and 75%. One assessment index is favoured per scenario for each of nine scenarios in the phase, and its weight coefficient is increased by the given values. In the same scenario, the weight coefficients of the remaining assessment index were each reduced by the corresponding ratios. Changes in the ranking of the alternatives for the scenarios are shown in Tables 25–27.

The results (Tables 25–27) show that the allocation of different weights to the assessment index through the scenarios leads to a change in the ranking of the alternatives,

TABLE 24: Correlation of the ranks in the models 1, 10, and 11.

	Model 1	Model 10	Model 11
Model 1	1	0.99	0.88
Model 10	—	1	0.89
Model 11	—	—	1

TABLE 25: Scenarios for the sensitivity analysis (phase I, 25%).

	$tw_1 * 1.25$	$tw_2 * 1.25$	$tw_3 * 1.25$	$tw_4 * 1.25$	$tw_5 * 1.25$	$tw_6 * 1.25$	$tw_7 * 1.25$	$tw_8 * 1.25$	$tw_9 * 1.25$
Alter. 1	4	4	3	8	3	3	5	7	4
Alter. 2	2	2	2	3	2	1	1	1	2
Alter. 3	1	1	1	1	1	2	2	2	1
Alter. 4	5	5	4	5	8	5	4	3	7
Alter. 5	10	10	9	10	6	7	10	5	10
Alter. 6	6	7	5	2	4	8	3	8	5
Alter. 7	8	8	7	9	5	6	7	9	6
Alter. 8	3	3	8	4	7	4	6	6	3
Alter. 9	7	6	6	7	9	9	8	4	8
Alter. 10	9	9	10	6	10	10	9	10	9

TABLE 26: Scenarios for the sensitivity analysis (phase I, 50%).

	$tw_1 * 1.50$	$tw_2 * 1.50$	$tw_3 * 1.50$	$tw_4 * 1.50$	$tw_5 * 1.50$	$tw_6 * 1.50$	$tw_7 * 1.50$	$tw_8 * 1.50$	$tw_9 * 1.50$
Alter. 1	4	4	3	8	3	4	6	7	4
Alter. 2	2	1	2	5	2	1	1	1	2
Alter. 3	1	2	1	1	1	2	2	2	1
Alter. 4	5	5	4	4	7	5	4	3	7
Alter. 5	10	10	9	10	5	7	10	5	10
Alter. 6	6	8	7	2	4	8	3	8	5
Alter. 7	8	7	6	9	6	6	7	9	6
Alter. 8	3	3	8	3	8	3	5	6	3
Alter. 9	7	6	5	7	9	9	8	4	8
Alter. 10	9	9	10	6	10	10	9	10	9

TABLE 27: Scenarios for the sensitivity analysis (phase I, 75%).

	$tw_1 * 1.75$	$tw_2 * 1.75$	$tw_3 * 1.75$	$tw_4 * 1.75$	$tw_5 * 1.75$	$tw_6 * 1.75$	$tw_7 * 1.75$	$tw_8 * 1.75$	$tw_9 * 1.75$
Alter. 1	4	4	3	8	3	4	6	8	4
Alter. 2	2	1	2	6	2	1	1	1	2
Alter. 3	1	2	1	1	1	2	2	2	1
Alter. 4	5	6	4	3	7	5	5	3	8
Alter. 5	10	10	9	10	5	7	10	5	10
Alter. 6	6	8	7	2	4	8	3	7	5
Alter. 7	8	7	6	9	6	6	8	9	6
Alter. 8	3	3	8	4	8	3	4	6	3
Alter. 9	7	5	5	7	9	9	7	4	7
Alter. 10	9	9	10	5	10	10	9	10	9

TABLE 28: Correlations in the ranking of 27 scenarios.

Scenario	SCC	Scenario	SCC	Scenario	SCC
S1	1.00	S10	1.00	S19	1.00
S2	0.99	S11	0.95	S20	0.93
S3	0.81	S12	0.77	S21	0.77
S4	0.73	S13	0.68	S22	0.58
S5	0.64	S14	0.59	S23	0.59
S6	0.84	S15	0.85	S24	0.85
S7	0.85	S16	0.87	S25	0.90
S8	0.61	S17	0.61	S26	0.59
S9	0.94	S18	0.94	S27	0.92

which confirms that the model is sensitive to changes in the weight coefficients. By comparing the alternatives which are ranked first (Alter. 3 and Alter. 2) in scenarios 1–27 with the initial ranking (Table 14), it can be seen that the rank of the highest ranked alternative is confirmed. Analyzing the ranking through 27 scenarios also shows that alternative Alter. 3 holds its rank in 16 scenarios, while in 11 scenarios, it is ranked second. The alternative ranked second (Alter. 2) holds its rank in 13 scenarios, while it is ranked first in 11 scenarios. Changing the weights of the assessment indexes through the scenarios leads to changes in the ranking of the remaining alternatives. However, these changes were not drastic, which also confirms the correlation of the ranks through the scenarios (Table 28).

The SCC values were obtained by comparing the initial ranks of the FRSA-MSWS-PII model (Table 14) with those obtained through the scenarios (Tables 25–27). By analyzing the results (Table 28), we can conclude that there is a high correlation of the ranks, since in 15 scenarios, the value of SCC is greater than 0.80, while in the remaining scenarios, it is greater than 0.55. The average value of SCC through all the scenarios is 0.81, which indicates a high average correlation. On this basis, we can conclude that there is satisfactory closeness of the ranks and that the proposed ranking is confirmed and credible.

6. Conclusions

In future manufacturing industry, there is no doubt about that green intelligent manufacturing is the target direction of sustainable development. The key point of green intelligent manufacturing is to achieve a reasonable balance of environmental, social, and economic performance of manufacturing system and a sustainable development of consumption and production. Obviously, some technical and policy support are required. Driven by digital twin system, this paper focuses on the methodology from the perspective of green performance evaluation of intelligent manufacturing to promote the transformation of manufacturing industry to green intelligent manufacturing.

Because the contribution in this paper is just a pilot study on the social influence evaluation for intelligent manufacturing, there are many future works that should be carried out in the future. It is only a performance evaluation model based on MCDM, and the mechanism that how multiple factors affect the green performance of intelligent manufacturing has not been studied deeply. In addition, the development of intelligent manufacturing will pay more attention to the impact on people in the future. In the final analysis, whether intelligent manufacturing can provide human with a well-being work and comfortable life will be explored. Human-oriented green performance evaluation methodology of intelligent manufacturing is necessary to study in the future. For example, the long-term and cumulative impact of intelligent manufacturing on human beings should be evaluated with the coordination of intelligence and economy of intelligent manufacturing. Then, a green maturity model of intelligent manufacturing in the whole life cycle can be

built based on the decision-making support from the green performance evaluation.

Data Availability

The data used to support the findings of this study are available from the corresponding author upon request.

Conflicts of Interest

The authors declare that there are no conflicts of interest.

Authors' Contributions

Lianhui Li and Bingbing Lei are the principal investigators of the study. Bingbing Lei assisted Lianhui Li to propose the novel hybrid model. Chunlei Mao and Hongxia Sun designed the case study and checked the manuscript. Yiping Yuan processed the data and did the data analysis work in the case study.

Acknowledgments

The authors thank assistant editor for the useful suggestions which improve the quality of this research. This research was funded by The Third Batch of Ningxia Youth Talents Supporting Project (TGJC2018048), Ningxia Natural Science Foundation (NZ17111 and 2020AAC03202), National Natural Science Foundation of China (51875251), Guangdong Special Support Talent Program-Innovation and Entrepreneurship Leading Team (2019BT02S593), National Key Research and Development Plan (2019YFB2102000), and Youth Project with Special Fund for Basic Scientific Research Business Expenses of Central Level Public Welfare Scientific Research Institutes (Y919008).

References

- [1] H. Feng, L. Xi, L. Xiao, T. Xia, and E. Pan, "Imperfect preventive maintenance optimization for flexible flowshop manufacturing cells considering sequence-dependent group scheduling," *Reliability Engineering & System Safety*, vol. 176, pp. 218–229, 2018.
- [2] G. Mejía and J. Pereira, "Multiobjective scheduling algorithm for flexible manufacturing systems with Petri nets," *Journal of Manufacturing Systems*, vol. 54, pp. 272–284, 2020.
- [3] J. Delaram and O. F. Valilai, "An architectural solution for virtual computer integrated manufacturing systems using ISO standards," *Scientia Iranica*, vol. 26, no. 6, pp. 3712–3727, 2018.
- [4] Q. Guo and M. Zhang, "A novel approach for multi-agent-based Intelligent Manufacturing System," *Information Sciences*, vol. 179, no. 18, pp. 3079–3090, 2009.
- [5] A. Simeone, "Resource efficiency optimization engine in smart production networks via intelligent cloud manufacturing platforms," *Procedia Cirp*, vol. 78, pp. 19–24, 2018.
- [6] S. Ren, Y. Zhang, Y. Liu, T. Sakao, D. Huisingsh, and C. M. V. B. Almeida, "A comprehensive review of big data analytics throughout product lifecycle to support sustainable smart manufacturing: a framework, challenges and future research directions," *Journal of Cleaner Production*, vol. 210, pp. 1343–1365, 2019.

- [7] S. Wang, W. D. Liang, and X. T. Cai, "Big data enabled intelligent immune system for energy efficient manufacturing management," *Journal of Cleaner Production*, vol. 195, no. 9, pp. 507–520, 2018.
- [8] T. F. Edgar and E. N. Pistikopoulos, "Smart manufacturing and energy systems," *Computers & Chemical Engineering*, vol. 114, pp. 130–144, 2018.
- [9] S. Jia, R. Tang, and J. Lv, "Therblig-based energy demand modeling methodology of machining process to support intelligent manufacturing," *Journal of Intelligent Manufacturing*, vol. 25, no. 5, 2014.
- [10] K.-D. Thoben, S. Wiesner, and S. T. Wiesner, "Industrie 4.0 and smart manufacturing—a review of research issues and application examples," *International Journal of Automation Technology*, vol. 11, no. 1, pp. 4–16, 2017.
- [11] A. Wuest, "Fundamentals of smart manufacturing: a multi-thread perspective," *Annual Reviews in Control*, vol. 47, pp. 214–220, 2019.
- [12] B. Gong, "The discussion on evaluation index and the assessment method of intelligent manufacturing," *Application of Electronic Technique*, vol. 41, no. 11, pp. 6–8, 2015.
- [13] J. Y. Jia and J. Shi, "Review on middle managers performance appraisal," in *Proceedings of the International Conference on Education, Management, Arts, Economics and Social Science*, vol. 1, Atlantis Press, Paris, France, pp. 695–700, 2016.
- [14] W. Yi, Pe. Dong, and J. Wang, "Research on evaluation model of enterpri es intelligent manufacturing capacity based on high order tensor analysis," *Industrial Technology & Economy*, vol. 37, no. 1, pp. 11–16, 2018.
- [15] D. Xue-hong, S. Li, L. I. Min et al., "Research on intelligent manufacturing capability maturity evaluation based on BP neural network," *Journal of Qingdao University (Natural Science Edition)*, vol. 32, no. 3, pp. 20–25, 2019.
- [16] Y. Qu, Y. Shi, K. Guo, and Y. Zheng, "Has "intelligent manufacturing" promoted the productivity of manufacturing sector?—evidence from China's listed firms," *Procedia Computer Science*, vol. 139, pp. 299–305, 2018.
- [17] A. Schumacher, W. S. Erol, and W. Sihm, "A maturity model for assessing industry 4.0 readiness and maturity of manufacturing enterprises," *Procedia CIRP*, vol. 52, pp. 161–166, 2016.
- [18] K. Jung, K. W. Morris, S. Leong, and H. Cho, "Mapping strategic goals and operational performance metrics for smart manufacturing systems," *Procedia Computer Science*, vol. 44, pp. 184–193, 2015.
- [19] A. R. Mashhadi and S. Behdad, "Ubiquitous life cycle assessment (U-LCA): a proposed concept for environmental and social impact assessment of industry 4.0," *Manufacturing Letters*, vol. 15, pp. 93–96, 2018.
- [20] M. Peruzzini, F. Gregori, A. Luzi, M. Mengarelli, and M. Germani, "A social life cycle assessment methodology for smart manufacturing: the case of study of a kitchen sink," *Journal of Industrial Information Integration*, vol. 7, pp. 24–32, 2017.
- [21] K. Zhang, T. Qu, D. Zhou, H. Jiang, and Y. Lin, "Digital twin-based opti-state control method for a synchronized production operation system," *Robotics and Computer-Integrated Manufacturing*, vol. 63, no. 11, pp. 1–15, 2019.
- [22] J. Leng, D. Yan, Q. Liu* et al., "Digital twin-driven joint optimization of packing and storage assignment in large-scale automated high-rise warehouse," *International Journal of Computer Integrated Manufacturing*, vol. 21, no. 8, pp. 2490–2509, 2019.
- [23] F. Meng, H. J. Tang, and H. Fujita, "Linguistic intuitionistic fuzzy preference relations and their application to multi-criteria decision making," *Information Fusion*, vol. 46, pp. 77–90, 2019.
- [24] Y. Qin, X. Cui, M. Huang et al., "Archimedean muirhead aggregation operators of q-rung orthopair fuzzy numbers for multicriteria group decision making," *Complexity*, vol. 2019, Article ID 3103741, 33 pages, 2019.
- [25] F. Meng and X. Chen, "Interval-valued intuitionistic fuzzy multi-criteria group decision making based on cross entropy and 2-additive measures," *Soft Computing*, vol. 19, no. 7, pp. 2071–2082, 2015.
- [26] T.-L. Nguyen, "Methods in ranking fuzzy numbers: a unified index and comparative reviews," *Complexity*, vol. 2017, Article ID 3083745, 13 pages, 2017.
- [27] L.-Y. Li, J.-C. Hang, Y. Gao, and C. Y. Mu, "Using an integrated group decision method based on SVM, TFN-RS-AHP, and TOPSIS-CD for cloud service supplier selection," *Mathematical Problems in Engineering*, vol. 2017, Article ID 3143502, 14 pages, 2017.
- [28] L. H. Li, J. C. Hang, H. X. Sun, and L. Wang, "A conjunctive multiple-criteria decision-making approach for cloud service supplier selection of manufacturing enterprise," *Advances in Mechanical Engineering*, vol. 9, no. 3, pp. 1–15, 2017.
- [29] W. Yang and Y. Pang, "Hesitant interval-valued pythagorean fuzzy VIKOR method," *International Journal of Intelligent Systems*, vol. 34, no. 5, pp. 754–789, 2019.
- [30] H. J. Zhang, Y. Zhou, and Q. H. Gan, "An extended PROMETHEE-II-based risk prioritization method for equipment failures in the geothermal power plant," *International Journal of Fuzzy Systems*, vol. 2, no. 8, pp. 2490–2509, 2019.
- [31] Pamučar, "Novel approach to group multi-criteria decision making based on interval rough numbers: hybrid DEMATEL-ANP-MAIRCA model," *Expert Systems with Application*, vol. 88, pp. 58–80, 2017.
- [32] D. Pamučar, I. Petrovic, and G. Cirovic, "Modification of the Best-Worst and MABAC methods: a novel approach based on interval-valued fuzzy-rough numbers," *Expert Systems with Application*, vol. 91, pp. 89–106, 2018.
- [33] M. K. Ghorabae, E. K. Zavadskas, Z. Turskis et al., "A new combinative distance-based assessment(codas) method for multi-criteria decision-making," *Economic Computation and Economic Cybernetics Studies and Research*, vol. 50, no. 3, pp. 25–44, 2016.

Research Article

Stock Market Temporal Complex Networks Construction, Robustness Analysis, and Systematic Risk Identification: A Case of CSI 300 Index

Xiaole Wan ¹, Zhen Zhang,² Chi Zhang,³ and Qingchun Meng ⁴

¹Management College, Ocean University of China, Qingdao 266100, China

²Department of Statistics, The Chinese University of Hong Kong, Hong Kong, China

³School of Mathematics, Shandong University, Jinan 250100, China

⁴School of Management, Shandong University, Jinan 250100, China

Correspondence should be addressed to Xiaole Wan; waxiaole@ouc.edu.cn and Qingchun Meng; meqich@163.com

Received 7 May 2020; Revised 18 June 2020; Accepted 23 June 2020; Published 15 July 2020

Guest Editor: Baogui Xin

Copyright © 2020 Xiaole Wan et al. This is an open access article distributed under the Creative Commons Attribution License, which permits unrestricted use, distribution, and reproduction in any medium, provided the original work is properly cited.

The Chinese stock 300 index (CSI 300) is widely accepted as an overall reflection of the general movements and trends of the Chinese A-share markets. Among the methodologies used in stock market research, the complex network as the extension of graph theory presents an edged tool for analyzing internal structure and dynamic involutions. So, the stock data of the CSI 300 were chosen and divided into two time series, prepared for analysis via network theory. After stationary test and coefficients calculated for daily amplitudes of stock, two “year-round” complex networks were constructed, respectively. Furthermore, the network indexes, including out degree centrality, in degree centrality, and betweenness centrality, were analyzed by taking negative correlations among stocks into account. The first 20 stocks in the market networks, termed “major players,” “gatekeeper,” and “vulnerable players,” were explored. On this basis, temporal networks were constructed and the algorithm to test robustness was designed. In addition, quantitative indexes of robustness and evaluation standards of network robustness were introduced and the systematic risks of the stock market were analyzed. This paper enriches the theory on temporal network robustness and provides an effective tool to prevent systematic stock market risks.

1. Introduction

Following its rapid growth and development, the Chinese economy has become the second largest economy in the world. However, the functionality of the underdeveloped financial market in China still contains room for improvement compared with the financial markets in other countries [1]. The stock market provides the most active window of capital in the financial system because of the more frequent events than Gaussian fluctuations, which reflect the features of loss, namely, initiating systemic financial risk [2–4].

Some scholars have investigated stock index futures with regard to three aspects, so as to evaluate market risks [5]. First of all, due to the high liquidity, high leverage, and

bidirectional operation of futures markets, stock index futures are believed to improve the volatility of the spot market [6]. Secondly, stock index futures can help to enhance the depth and efficiency of the market, thus decreasing its volatility [7, 8]. Finally, the stability of the stock market is not very likely to be affected by transactions [9, 10]. By introducing the CSI 300 futures market on April 16, 2010, China attempted to enhance its financial system. In the CSI 300 futures market, investors can take short positions on futures to hedge against the risk in the Chinese stock market. It is generally believed that the futures market can signal a new era for China’s financial market. Through the CSI 300 stock index, the performance and price fluctuation of the A-share index in China can be reflected. The index is designed to be a performance benchmark and a base for derivatives

innovation. At present, the CSI 300 stock index has been widely used to reflect the trends and movements in the Chinese A-share markets [11]. Increasing attention has been paid to the influence of the CSI 300 index futures on the underlying stock market. For instance, Cao et al. [5] investigated the correlation between the CSI 300 markets and the China securities index 300 (CSI 300) futures according to high-frequency data, using MF-DCCA. Suo et al. [12] used the recurrence interval analysis method to explore the risk estimation, memory effects, and scaling behavior of the CSI 300 in China. Qu et al. [13] carried out a comprehensive analysis of some popular time-series models to predict the RMVHR for the CSI 300 futures. Moreover, the out-of-sample dynamic hedging performance was evaluated by comparing this with the conventional hedging models through daily prices and the vector heterogeneous autoregressive model through intraday prices.

To date, the stock index has been widely studied through the theory of the complex network. There exist interactive individuals in technological, physical, biological, and social networks [14–16]. Therefore, the extension of graph theory, the complex network, and the edged tool have been used to analyze the dynamic involutions and internal structure of these networks [17–19].

Multilayer network theory is a development tool based on single network research, which provides a new perspective for grasping information within a colorful structure. A key aspect of multilayer network theory is that the underlying network structure can significantly influence the dynamic processes mediated by the edges [20]. Moreover, the authors adapted the implicit null model to fit the layered network, the main idea being to represent every layer through a slice [21–23]. A temporal network is a special multiplex network constructed on a timeline basis, which is of great importance to the process of risk dissemination. In the network, electronic or biological viruses and information or rumors are transmitted through electronic connections, social ties, and physical contact edges. The speed and extent of spreading are affected by the network structure owing to features such as degree correlations [24], degree distribution [25, 26], short path lengths [27], and community.

On this basis, this paper purposes two research questions: (i) what complex network indexes characterize the special stock in the market? (ii) How to quantify the risk or to say robustness in the stock market?

The contributions of this article to the existing research can be classified into the following aspects: first of all, the study establishes directed weighted stock networks using the CSI 300 index, considering the negative correlation between stocks; a multilayer time-series network was constructed. Secondly, the paper analyzes the systematic stock market risk according to the temporal network and designs an algorithm for measuring robustness. In addition, a quantitative index is provided. Finally, this article provides an effective tool for a systematic approach to risk in the stock market.

The remainder of this article is structured as follows: in Section 2, the literature pertaining to stock market risks and the application of temporal networks are reviewed; Section 3

details the data processing and the corresponding time-series tests; in Section 4, the complex network models are established, and their statistical characteristics are analyzed; Section 5 discusses the rationality criterion of stock market robustness in the context of the time complex network; finally, Section 6 concludes this paper. Figure 1 presents an overview of the research conducted for this study.

2. Literature Review

2.1. Stock Market Risk. Stock market risks are generally discussed from the perspectives of the correlations of individual stocks, or whole sectors and changes in the volatility of stock prices [28, 29], or in the context of financial restrictions [30, 31]. There are also some studies that explore technological risks, policy risks, and the social factors and economic policy behind stock risk. Apergis [32] studied the effect of policy and technological risks on US stock returns and emphasized the impact of economic policy uncertainty on stock returns, which rose to an all-time high after the 2007–2009 recession. Tsai [33] revealed the impact of economic policy uncertainty in China, Japan, Europe, and the United States on the risk of contagion in global stock market investments. Cao et al. [34] used a sample of A-shares listed in China from 2001 to 2012 to study the relationship between social trust and the risk of stock price collapse, finding that social trust as a social and economic factor is related to the latter risk. Regarding social factors, Li et al. [35] pointed out a correlation between stock price crash risks and social trust, based on the data of listed firms in China from 2001 to 2015.

In recent years, the distress risk anomaly in emerging markets has been investigated in many studies. For example, Gao et al. [36] investigated the significance of book-to-market, size, and momentum factors in capturing the financial distress risks of the stock market in China. Lai et al. [37] explained stock returns in the stock markets of Australia, Thailand, Singapore, Malaysia, Korea, Indonesia, and Hong Kong, finding that the four-factor financial crisis risk asset pricing model has received extensive empirical support in these markets. Eisdorfer et al. [38] studied several potential drivers of stock returns for distressed companies in 34 different countries and documented the exclusive risk anomalies in developed countries. Distress anomaly is more serious in countries with higher information transparency, lower arbitrage barriers, and stronger acquisition legislation. These findings demonstrate that all aspects of shareholder risk are of great importance to shape the stock returns of distressed firms. Gao et al. [39] studied the abnormal risk of distress in 38 countries over the past 20 years, finding this anomaly to be highly concentrated in low-market stocks in developed countries such as North America and Europe, instead of 17 emerging markets. The existing research predicts the stock return or the national attribute in order to explain the abnormal risk of distress, none of which studies the factors that capture the risk of stock financial distress.

The abovementioned research was mainly conducted using traditional measurement methods, such as the VAR model and the GARCH model, which have yielded different results without multifractality.

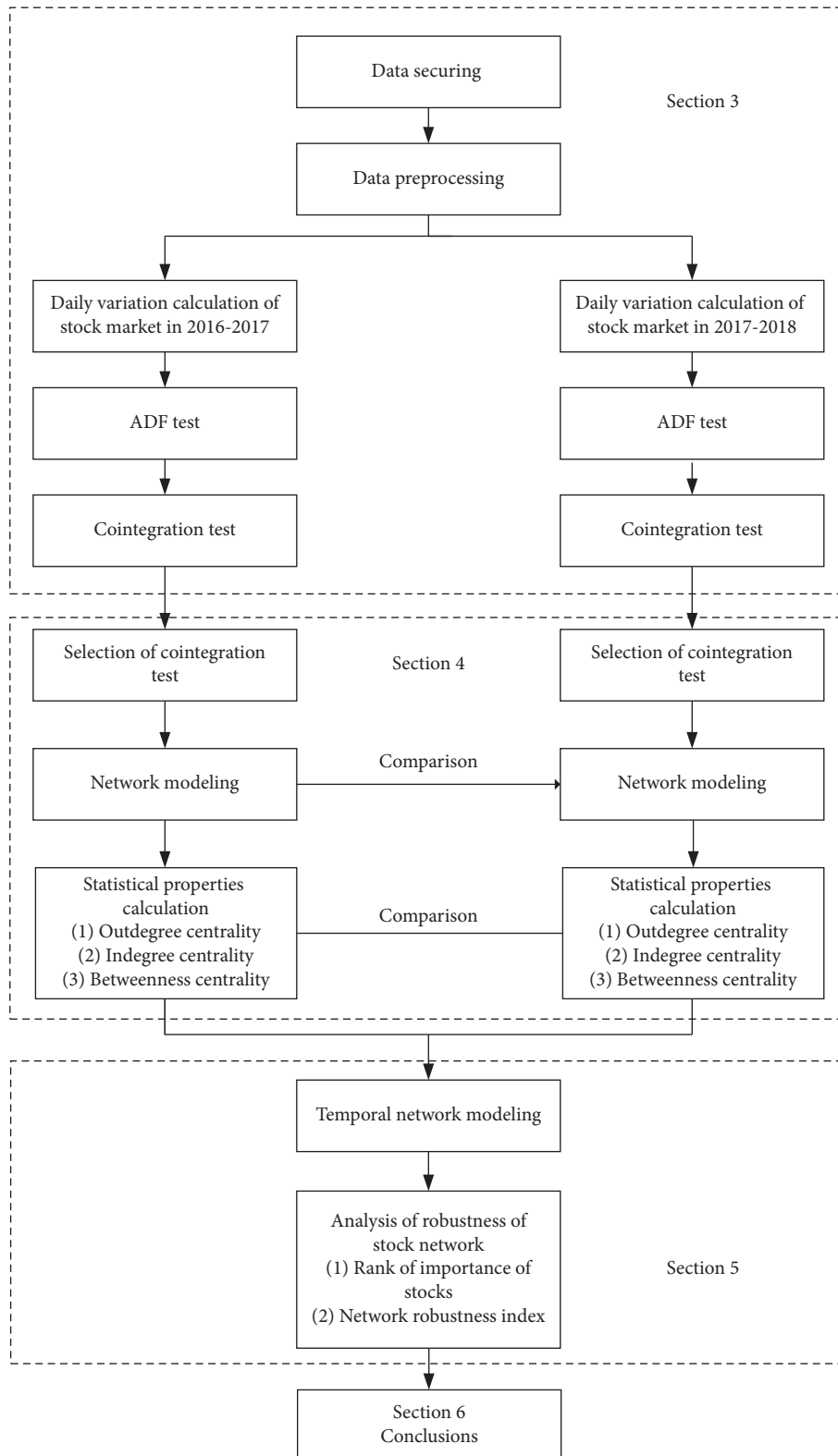


FIGURE 1: Research overview.

2.2. *Temporal Network.* Artificial intelligence generates data in a new form of complexity, bringing about the new era of big data [40], which is a huge challenge for researchers from different shielding agencies involved in extracting new

structures or patterns from data with a large volume, high variety, and high speed. Over the past ten years, there have emerged increasing studies describing dynamic systems through complex networks based on time series [41].

In recent years, most studies have projected the time dimension by aggregating the connection between vertices and edges, even when the information about the time series of contacts or interactions was available [42]. This method, temporal network, is to split the data into adjacent time windows in which contacts gather into edges. For instance, Karimi and Holme [43] explained the consequences of social influence, such as the spread of opinions and fads, in a temporal network by establishing threshold models. By exploring the diffusion of a supermarket, Deng et al. [44] found that the system evolves in a certain order that is not completely random. Moreover, the nodes are classified according to certain rules. Flores and Romance [45] recognized the nodes connected to a given complex network to be main topics in complex network analysis. Therefore, an eigenvector concentration model of a time network that evolves on a continuous time scale and sorts the nodes was proposed, according to the correlation of the nodes in the process of their occurrence in the network. For example, Everett et al. [46] used two-mode temporal data to measure the experience and knowledge held in social temporal networks. Li et al. [47] used the decision tree to find the node-level features that have a general impact on node transition over the temporal network.

In recent years, the temporal network method has been used to investigate the stock market in terms of stock risks. Huang et al. [48] put forward an algorithm—namely, a backward temporal diffusion process—to calculate the shortest temporal distance to the transmission source. Zhao et al. [49] characterized the time-evolving correlation-based networks of stock markets through the temporal network framework, in order to highlight the instability of the underlying market by portfolio selection in the evolution of the topology structure of the financial networks. Qu et al. [13] investigated the dynamic hedging performance of the high-frequency data of the CSI 300 index futures by designing the minimum-variance hedge ratio (RMVHR) approach. Lyócsa et al. [50] studied the connectedness of a sample of 40 stock markets across five continents using daily closing prices and return spillovers based on Granger causality based on the network model. Zhao et al. [51] utilized the temporal network framework to characterize the time-evolving correlation-based networks of stock markets.

All these studies focus on the critical value of the volatility, ignoring mechanism of the detail structure of the network influencing the risk propagation. This is the exact starting point of this paper.

3. Temporal Data Processing and Complex Networks Modeling

Stock data have a temporal property, which is mainly manifested on top price, floor price, closing price, and turnover. Annual cross section data also have a temporal property. Hence, the complex network established in the following subsections is a temporal complex one. Stocks on the CSI 300 index are those that are performing well in China's stock markets. They are thus not only a barometer of the stock market but also a symbol of economic status.

Therefore, studying stocks in the CSI 300 index may be seen as significant.

Previous studies have generally constructed undirected networks with positive weights based on fluctuating stock data in a certain period. However, the influences among stocks are causal, to some extent. In this paper, directed networks were constructed to depict the collaborative relationships between stocks, and a multilayer temporal network was constructed based on several time series to describe the network's influential stocks from a long-term perspective.

3.1. Data Processing. In this paper, data from the CSI 300 index over 488 trading days from October 15, 2016, to October 15, 2018, were output from the "Choice Financial Terminals," including the opening price, top price, floor price, closing price, turnover, and volume of transaction of each stock during each trading day.

Two types of data anomalies were found during the data examination: missing data and zero transaction volume (or turnover). The missing data were due to the fact that the stock was not issued on the day or may have been issued but was not listed. For example, Merchants Highway was listed on December 25, 2017 [52], and data before were missing. Similarly, Huaneng Hydropower was listed on December 15, 2017 [53], and data before were missing. Caitong Security was listed on October 24, 2017 [54], and data before were missing. Zero transaction volume (or turnover) was caused by the suspension of stocks for major assets restructuring, the planning of nonpublic issue shares, major decision planning, and major cooperative projects. For example, the Midea Group planned an asset restructuring with the Cygnet Subsidiary and was suspended from September 10, 2018 [55]. Perfect World was planning to issue nonpublic shares and applied this to the Shenzhen Stock Exchange, so it was suspended as of June 4, 2018 [56]. Donghua Software and Tencent Cloud Computing were in the process of discussing key issues and planning to carry out extensive cooperation in the fields of medicine, the intelligent city, finance, and electricity, according to the latest communication, further promoting the update of strategic cooperation between the two parties. In addition, the dominant stockholder of Donghua Software was discussing with capital cooperation with Tencent-related companies, but this capital cooperation involved no changes to corporate control [57]. Donghua Software was suspended since May 14, 2018, after its application to the Shenzhen Stock Exchange [58]. Hence, this type of data exerted a certain disturbance and was deleted from the dataset. In the end, a total of 169 stocks were retained for the present study.

The CSI 300 index stocks can be discussed from multiple aspects, such as daily closing price, daily price change ratio, historical volatility, daily amplitude, and weekly amplitude of stocks. Among them, stock amplitude reflects the stock activity, denoting not only the industrial development of the stock market but also indicating the investment orientation and investors' attitudes. The amplitude analysis of stocks covers the daily, weekly, and monthly amplitude analyses. In

this paper, the daily amplitude (DA) of stocks was applied [59]. A low DA represents poor stock activity on the given day, the contrasting scenario indicating that the stocks are active.

If p_i^t is the share price of stock i on day t , therefore, $\max(p_i^t)$ “denotes the top price of stock i ” on day t , and $\min(p_i^t)$ is the floor price of stock i on day t . If p_{si}^{t-1} is the closing price of stock i on the previous day, the calculation formula of its amplitude on day t (DA_i^t) is as follows:

$$DA_i^t = \frac{\max(p_i^t) - \min(p_i^t)}{p_{si}^{t-1}}. \quad (1)$$

The daily amplitude data of each stock can be derived from equation (1). The DA data of certain stocks during 2016-2017 and 2017-2018 are shown in Figure 2.

In short, the data may be seen as stationary from the perspective of the sequence chart. The data were also tested using ADF in terms of the quantity angle.

3.2. ADF Test and Cointegration Test. With an unsteady time series, the traditional analysis method cannot assure the validity of the data. Conversely, the unit root test can create conditions for an unsteady time series. There are many unit root test methods, of which ADF was applied in the current study. If the DA data were to be deemed steady, they needed to meet the following condition:

- (1) The mean, $E[DA_i^t] = \mu$, is a constant unrelated with time t
- (2) The variance, $D[DA_i^t] = \sigma^2$, is a constant unrelated with time t
- (3) The covariance, $\text{Cov}[DA_i^{t1}, DA_i^{t2}]$, is a constant related with the time interval only, but it is unrelated with time t

The ADF test was applied to verify whether the DA met the above conditions. The verification results are shown in Table 1, obtained using Matlab 2017b.

The DA of other stocks also underwent the ADF test. In other words, the data of these 169 stocks in the study period were found to be steady sequences.

On this basis, the DA of all of the stocks could be seen as steady sequences and thereby meet the same-order conditions of the cointegration test. Hence, the correlation coefficient between two stocks was gained through the cointegration test.

Cointegration theory plays a vital role in economic circles. It is an econometric analysis method created by Johansen and is mainly applied to study the long-term equilibrium relationship among economic variables based on an unsteady time series [59]. The higher the absolute value of the cointegration coefficient, the stronger the correlation between two stocks; otherwise, the correlation is weaker. Selected cointegration coefficients are listed based on two stocks in the following section (as listed in Tables 2 and 3).

The program results show that the cointegration coefficients between the different pairs of stocks all passed the

test. The following sections detail the construction of the complex networks based on the cointegration coefficient.

4. Complex Networks Modeling and Statistical Analysis

In this paper, stocks were denoted as nodes and the cointegration coefficients used as the weights of edges. Out degree centrality, in degree centrality, and betweenness centrality were chosen for the correlation analysis of network characteristics.

4.1. Stock Market Complex Networks Modeling. The above selected 169 stocks were viewed as nodes in the complex networks, and the cointegration relationships among the stocks were used as edges. The cointegration relationships between stocks i and j were determined in Section 3.2. The cointegration coefficient (a_{ij}) using stock i as a dependent variable and stock j as an independent variable was obtained, which corresponds to one directed side from node i to node j , with a weight of a_{ij} . In this way, a weighted directed graph $G(V, E, W)$ was plotted, where V represents the set of stocks, E the set of edges, and W the set of weights corresponding to the edges. This was determined by the following method. Since the cointegration coefficients a_{ij} and a_{ji} may not be equal, the rule for retaining edges was such that all directed edges of a_{ij} were retained if $|a_{ij}| > |a_{ji}|$; otherwise, all directed edges of a_{ji} were retained. The histograms of the frequency distribution of $|a_{ij}|$ after screening are shown in Figure 3.

It can be seen from Figure 3 that the absolute value of the cointegration coefficient during 2016-2017 is mainly concentrated in a relatively small region and generally presents a power-low distribution. The absolute value of the cointegration coefficient during 2017-2018 presents an approximately clock-shaped distribution pattern. There is no large frequency in regions with low and high absolute cointegration coefficient values. The number and proportions of the intervals corresponding to the two distribution tables are shown in Table 4.

Due to the positive relationship between the correlation of the pairs of stocks and the cointegration coefficient, the weight was determined as follows:

$$w_{ij} = \begin{cases} a_{ij} \left(|a_{ij}| > \text{Con} \right), \\ 0 \left(|a_{ij}| \leq \text{Con} \right), \end{cases} \quad (2)$$

where Con is the screened threshold. In Table 4, there are significantly different numbers of cointegration coefficients at different intervals. Here, the 70% quantile of two networks was selected as the screening base, according to the histogram results, and only 30% of the edges with great weights was retained. Finally, the threshold of absolute values of the cointegration coefficient during 2016-2017 was $\text{Con} = 0.3117$, and the threshold of the absolute value of the cointegration coefficient during 2017-2018 was $\text{Con} = 0.4284$. Stocks with strong correlations were chosen by this

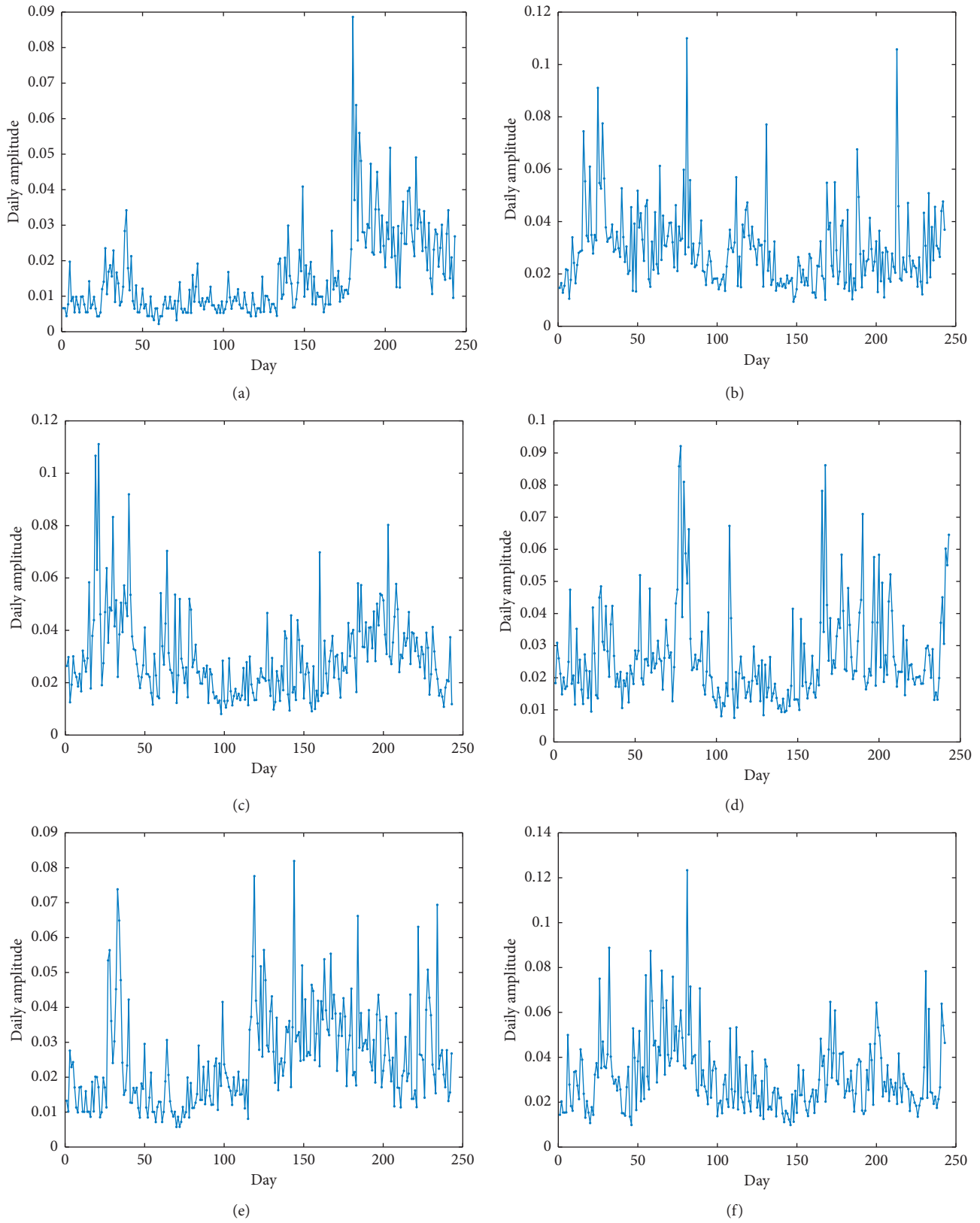


FIGURE 2: Display of daily amplitude of some stocks: (a) Ping An Bank during 2016-2017; (b) Ping An Bank during 2017-2018; (c) Shenzhen Zhongjin Lingnan Nonfemet during 2016-2017; (d) Shenzhen Zhongjin Lingnan Nonfemet during 2017-2018; (e) Overseas China Town A during 2016-2017; (f) Overseas China Town A during 2017-2018.

TABLE 1: ADF test of selected stocks during 2016-2017 and 2017-2018.

2016-2017			2017-2018		
Stock	D-F	<i>P</i> value	Stock	D-F	<i>P</i> value
Ping An Bank	25.2817	0.001	Ping An Bank	23.5691	0.001
Shenzhen Zhongjin Lingnan Nonfemet	27.0890	0.001	Shenzhen Zhongjin Lingnan Nonfemet	27.8371	0.001
Overseas China Town A	28.0743	0.001	Overseas China Town A	25.6870	0.001
Zoomlion Heavy Industry Science & Technology	22.0906	0.001	Zoomlion Heavy Industry Science & Technology	21.3686	0.001
Wei Chai Power	24.7719	0.001	Wei Chai Power	26.5893	0.001
Financial Street Holding	25.8204	0.001	Financial Street Holding	24.5114	0.001
Shandong Dong-Ee Jiao	26.0686	0.001	Shandong Dong-Ee Jiao	31.4732	0.001
Luzhou Lao Jiao	29.0036	0.001	Luzhou Lao Jiao	33.0492	0.001
Jilin Aodong Pharmaceutical	24.4411	0.001	Jilin Aodong Pharmaceutical	21.6696	0.001
Chongqing Changan Automobile	26.6082	0.001	Chongqing Changan Automobile	16.9782	0.001
Hubei Biocause Pharmaceutical	23.4925	0.001	Hubei Biocause Pharmaceutical	24.1930	0.001
Tongling Nonferrous Metals	24.5328	0.001	Tongling Nonferrous Metals	22.8132	0.001
HESTEEL	24.6379	0.001	HESTEEL	22.2333	0.001
BOE Technology	19.2278	0.001	BOE Technology	21.5965	0.001
Guoyuan Securities	20.5826	0.001	Guoyuan Securities	20.5943	0.001
Avic Aircraft	22.8011	0.001	Avic Aircraft	26.0381	0.001
GF Securities	22.7073	0.001	GF Securities	21.6436	0.001
Changjiang Securities	19.5375	0.001	Changjiang Securities	18.6640	0.001
CITIC Guoan Information Industry	20.3464	0.001	CITIC Guoan Information Industry	23.1893	0.001
Wuliangye	26.6843	0.001	Wuliangye	32.7552	0.001

TABLE 2: Cointegration coefficient of Ping An Bank with other selected stocks during 2016-2017.

Taking Ping An Bank as an independent variable	Cointegration coefficient	<i>P</i> value	Taking Ping An Bank as a dependent variable	Cointegration coefficient	<i>P</i> value
Shenzhen Zhongjin Lingnan Nonfemet	0.3800	0.001	Shenzhen Zhongjin Lingnan Nonfemet	0.2069	0.001
Overseas China Town A	0.2845	0.001	Overseas China Town A	0.1990	0.001
Zoomlion Heavy Industry Science & Technology	-0.0263	0.001	Zoomlion Heavy Industry Science & Technology	-0.0332	0.001
Wei Chai Power	0.1911	0.001	Wei Chai Power	0.1913	0.001
Financial Street Holding	0.0388	0.001	Financial Street Holding	0.0175	0.001
Shandong Dong-Ee Jiao	-0.0735	0.001	Shandong Dong-Ee Jiao	-0.0921	0.001
Luzhou Lao Jiao	0.0951	0.001	Luzhou Lao Jiao	0.0774	0.001
Jilin Aodong Pharmaceutical	0.0484	0.001	Jilin Aodong Pharmaceutical	0.0408	0.001
Chongqing Changan Automobile	0.0592	0.001	Chongqing Changan Automobile	0.1228	0.001
Hubei Biocause Pharmaceutical	0.9468	0.001	Hubei Biocause Pharmaceutical	0.2885	0.001
Tongling Nonferrous Metals	0.1386	0.001	Tongling Nonferrous Metals	0.0697	0.001
HESTEEL	0.1649	0.001	HESTEEL	0.0468	0.001
BOE Technology	-0.0866	0.001	BOE Technology	-0.0384	0.001
Guoyuan Securities	0.3485	0.001	Guoyuan Securities	0.1364	0.001
Avic Aircraft	0.0701	0.001	Avic Aircraft	0.0379	0.001
GF Securities	0.2499	0.001	GF Securities	0.3116	0.001
Changjiang Securities	0.1883	0.001	Changjiang Securities	0.1466	0.001
CITIC Guoan Information Industry	0.1263	0.001	CITIC Guoan Information Industry	0.0431	0.001
Wuliangye	0.1396	0.001	Wuliangye	0.1530	0.001
Henan Shuanghui Investment & Development	0.1728	0.001	Henan Shuanghui Investment & Development	0.3226	0.001

method to establish directed complex networks, thus enabling more accurate and explicit results. The two complex networks constructed are shown in Figures 4 and 5, respectively.

The size of the points (or names) in Figures 4 and 5 reflects the out degree of the points, that is, the influencing strength of the stock on other stocks. The different colors

represent different communities. Both networks are divided into three respective communities: the bank security community, the industrial infrastructure community, and others. On the one hand, such a stable community division reflects the equilibrium state of economic relationships, which indirectly proves the certain coordinated relationships among stocks, to some extent. On the other hand, the

TABLE 3: Cointegration coefficient of Ping An Bank with other selected stocks during 2017-2018.

Taking Ping an bank as an independent variable	Cointegration coefficient	P value	Taking Ping an bank as a dependent variable	Cointegration coefficient	P value
Shenzhen Zhongjin Lingnan Nonfemet	0.2256	0.001	Shenzhen Zhongjin Lingnan Nonfemet	0.2370	0.001
Overseas China Town A	0.4112	0.001	Overseas China Town A	0.3500	0.001
Zoomlion Heavy Industry Science & Technology	0.1531	0.001	Zoomlion Heavy Industry Science & Technology	0.3943	0.001
Wei Chai Power	0.2849	0.001	Wei Chai Power	0.3529	0.001
Financial Street Holding	0.2593	0.001	Financial Street Holding	0.3746	0.001
Shandong Dong-Ee Jiao	0.0358	0.001	Shandong Dong-Ee Jiao	0.0966	0.001
Luzhou Lao Jiao	0.3454	0.001	Luzhou Lao Jiao	0.4204	0.001
Jilin Aodong Pharmaceutical	0.2238	0.001	Jilin Aodong Pharmaceutical	0.4819	0.001
Chongqing Changan Automobile	0.1454	0.001	Chongqing Changan Automobile	0.2494	0.001
Hubei Biocause Pharmaceutical	0.3767	0.001	Hubei Biocause Pharmaceutical	0.3035	0.001
Tongling Nonferrous Metals	0.1702	0.001	Tongling Nonferrous Metals	0.3043	0.001
HESTEEL	0.1881	0.001	HESTEEL	0.2488	0.001
BOE Technology	0.3214	0.001	BOE Technology	0.2195	0.001
Guoyuan Securities	0.2821	0.001	Guoyuan Securities	0.3623	0.001
Avic Aircraft	0.2119	0.001	Avic Aircraft	0.1579	0.001
GF Securities	0.3065	0.001	GF Securities	0.5227	0.001
Changjiang Securities	0.2526	0.001	Changjiang Securities	0.3744	0.001
CITIC Guoan Information Industry	0.2956	0.001	CITIC Guoan Information Industry	0.1725	0.001
Wuliangye	0.3000	0.001	Wuliangye	0.4482	0.001
Henan Shuanghui Investment & development	0.1772	0.001	Henan Shuanghui Investment & development	0.2126	0.001

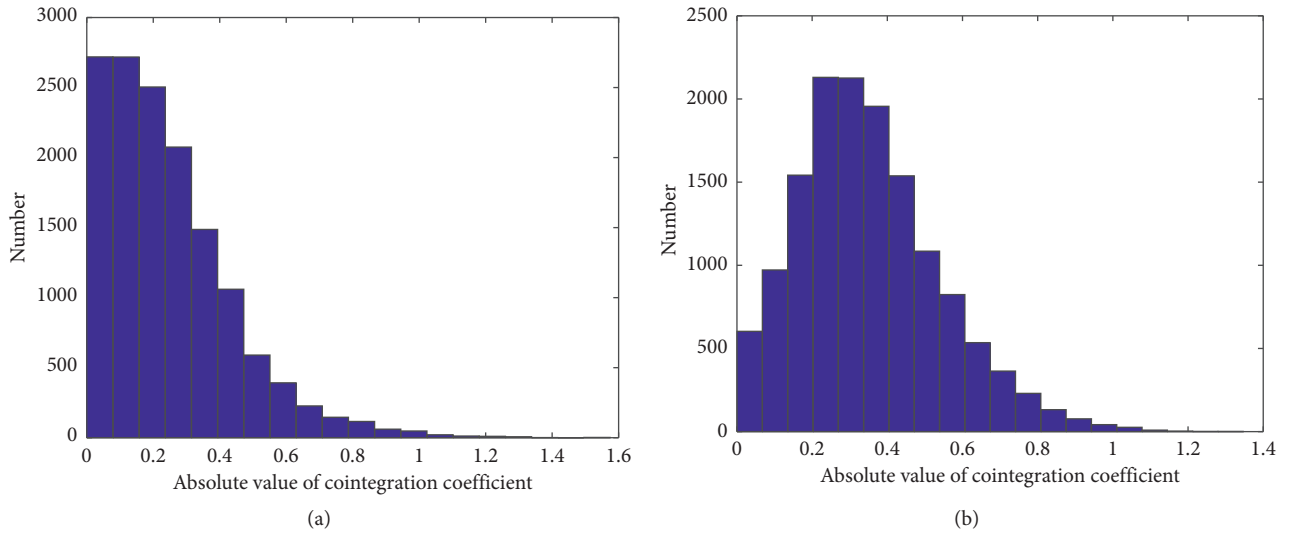


FIGURE 3: Distribution diagram of the absolute value of the cointegration coefficient during 2016-2017 (a) and 2017-2018 (b).

density of the edges is similar in the three communities of the complex CSI 300 network during 2016-2017. However, most edges in the complex CSI 300 network during 2017-2018 are concentrated in the bank security and industrial infrastructure communities, indicating the locally disharmonious correlations among the other industries during 2017-2018. The overall network situation is illustrated through network indexes in the following section.

4.2. Out Degree Centrality. Out degree centrality (k_i^{out}) was used to depict the number of sides from point i in the

network to other nodes. In this paper, k_i^{out} reflects the influencing strength of stock i on other stocks, which is called “major players” in the stock market and can be calculated as follows:

$$k_i^{\text{out}} = \sum_{j=1}^n \varphi(|a_{ij}|), \quad (3)$$

where $\varphi(|a_{ij}|) = 1$ if $|a_{ij}| \neq 0$ or otherwise $\varphi(|a_{ij}|) = 0$. This index depicts the influence of each node in the network. The distribution of the out degree centrality reflects the overall

TABLE 4: Statistical chart of the absolute value of the cointegration coefficient during 2016-2017 and 2017-2018.

2016-2017			2017-2018		
Interval	Number	Frequency (%)	Interval	Number	Frequency (%)
[0.0000, 0.0788)	2719	19.15	[0.0000, 0.0679)	603	4.25
[0.0788, 0.1575)	2718	19.15	[0.0679, 0.1357)	972	6.85
[0.1575, 0.2363)	2504	17.64	[0.1357, 0.2036)	1542	10.86
[0.2363, 0.3150)	2075	14.62	[0.2036, 0.2714)	2130	15.00
[0.3150, 0.3938)	1487	10.47	[0.2714, 0.3393)	2126	14.98
[0.3938, 0.4726)	1060	7.47	[0.3393, 0.4071)	1956	13.78
[0.4726, 0.5513)	590	4.16	[0.4071, 0.4750)	1538	10.83
[0.5513, 0.6301)	392	2.76	[0.4750, 0.5429)	1085	7.64
[0.6301, 0.7089)	227	1.60	[0.5429, 0.6107)	824	5.80
[0.7089, 0.7876)	146	1.03	[0.6107, 0.6786)	535	3.77
[0.7876, 0.8664)	116	0.82	[0.6786, 0.7464)	364	2.56
[0.8664, 0.9451)	61	0.43	[0.7464, 0.8143)	230	1.62
[0.9451, 1.0239)	48	0.34	[0.8143, 0.8821)	132	0.93
[1.0239, 1.1027)	21	0.15	[0.8821, 0.9500)	77	0.54
[1.1027, 1.1814)	12	0.08	[0.9500, 1.0179)	42	0.30
[1.1814, 1.2602)	10	0.07	[1.0179, 1.0857)	26	0.18
[1.2602, 1.3389)	7	0.05	[1.0857, 1.1536)	9	0.06
[1.3389, 1.4177)	1	0.01	[1.1536, 1.2214)	3	0.02
[1.4177, 1.4965)	0	0.00	[1.2214, 1.2893)	1	0.01
[1.4965, 1.5752]	2	0.01	[1.2893, 1.3571]	1	0.01

characteristics of the networks. The distribution diagrams of the out degree centrality during 2016-2017 and 2017-2018 were obtained using Matlab 2017b, as shown in Figure 6.

As can be seen from Figure 6, a high density occurs in a small degree region (degree centrality from 0 to 20) in the two distribution diagrams, indicating that significant stocks in the network occupy important positions. In order to mine out these special nodes, the top 20 stocks with a high out degree are listed in Table 5.

As can be seen from Table 5, most of the top 20 stocks located in the out degree centrality during the study period are financial securities, indicating that financial security stocks significantly influenced other stocks and the fluctuation of the stock market. The fluctuation of nodes with a high out degree centrality was quickly transmitted to most nodes in the network. Hence, this index measures the indicators that can influence other stocks, whereby stocks with a high out degree centrality are the sources of potential large-scale network risks.

4.3. In Degree Centrality. In degree centrality (k_j^{in}) was applied to depict the number of sides from node j in the network to other nodes. Here, k_j^{in} reflects the influences of other stocks on the stock j , which is called “vulnerable players,” and can be calculated as follows:

$$k_j^{\text{in}} = \sum_{i=1}^n \varphi(|a_{ij}|), \quad (4)$$

where $\varphi(|a_{ij}|)$ in equation (4) is the same as above and describes the vulnerability of the stocks. A higher in degree centrality reflects a stronger vulnerability of the stock to most stocks. The distribution of the in degree centrality reflects the overall characteristics of the networks. The distribution diagrams of in degree centrality during 2016-

2017 and 2017-2018 were obtained using Matlab 2017b (Figure 7).

Figure 7 indicates a high density occurring in a small degree region (degree centrality from 0 to 40) in the two distribution diagrams, indicating that significant stocks in the network occupy important positions. This is similar to the distribution diagrams of the out degree centrality. To specify these nodes, the top 20 stocks that had a high in degree are listed in Table 6.

Tables 5 and 6 show that the top 20 stocks in both the in degree and out degree centrality rankings during 2016-2017 and 2017-2018 are financial security stocks. This reflects the notion that financial security stocks influence other stocks and are, in turn, controlled by other stocks. However, some stocks are completely passive. For instance, the out degree centrality of Rongsheng Development and CITIC Guoan was 0 during 2017-2018. These stocks are at the margins of the stock network and their fluctuation at the occurrence of systematic network risks may not influence other stocks. Thus, these stocks can be said to be significantly controlled by other stocks, which are terminal bearers of network risks. The corresponding company thus has to pay attention to risk dispersion during the loss reduction brought about by network risks in daily management.

4.4. Betweenness Centrality. Betweenness centrality can indicate how many shortest paths cross a certain node. The current paper demonstrates that different stocks act as “moderators” or “gatekeepers” of information (and, correspondingly, may be unwilling to develop a requested feature).

If g_{st} is the number of shortest paths from node s to node t , n_{st}^i is the number of paths that pass node i in g_{st} . The betweenness centrality of node i can be expressed as follows:

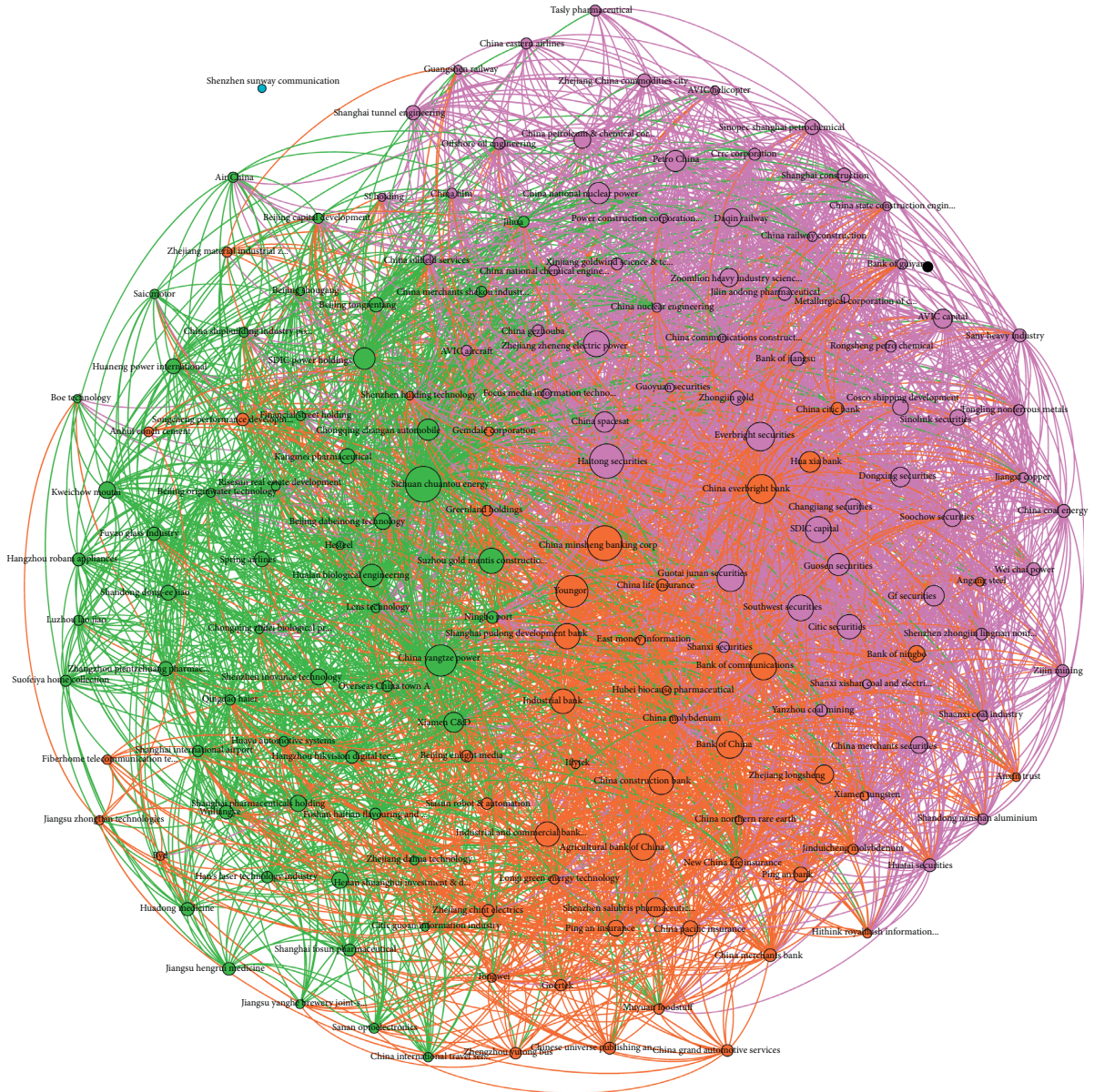


FIGURE 4: Complex network of CSI 300 during 2016-2017.

$$BC_i = \sum_{s \neq i \neq t} \frac{n_{st}^i}{g_{st}} \quad (5)$$

A higher BC_i (equation (5)) reflects a stronger bridging effect of node i in the network. In this paper, weight represents the closeness between points. The higher the closeness between nodes i and j , the lower the weight between them for calculating the betweenness centrality. Hence, the following conversion becomes necessary:

$$\widetilde{w}_{ij} = 2 - \frac{w_{ij} - \min(w_{ij})}{\max(w_{ij}) - \min(w_{ij})}, \quad (6)$$

where $\max(w_{ij})$ is the maximum weight of edges in the network, $\min(w_{ij})$ is the minimum weight of edges, and \widetilde{w}_{ij} reflects the weights after conversion. The value of \widetilde{w}_{ij} is

negatively related with the correlation between two stocks. Such a conversion assures the weight in the interval of $[1, 2]$ and protects the significance of the betweenness calculation. Moreover, the data involved in this paper contain negative weights. The shortest path describes the shortest travelling path of fluctuation of one stock to another stock. Upon the occurrence of network risks, the government or other organizations should protect these stocks in a timely manner, which could then prevent the global loss of networks in the evolution of network risks. It shows different stocks act as moderators or gatekeepers of information. The relevant top 20 stocks with the highest betweenness centrality are listed in Table 7.

The top 20 stocks in terms of betweenness centrality shown in Table 7, including Jianfa Share, Overseas China Town A, and China Satellite, remained basically stable

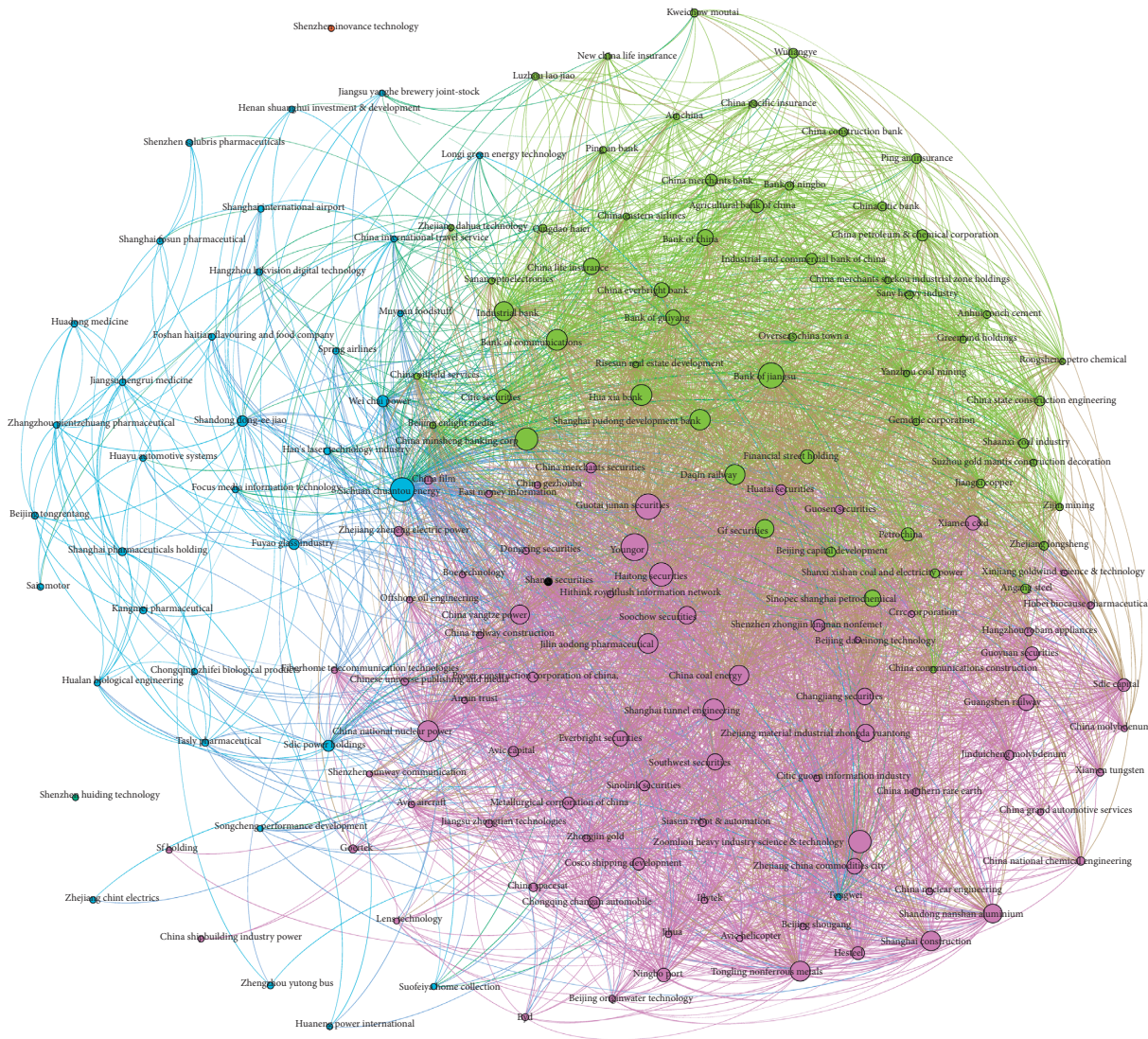


FIGURE 5: Complex network of CSI 300 during 2017-2018.

throughout the study period. Hence, they played a more prominent gatekeeper role in the financial network.

According to the results of the out degree centrality, in degree centrality, and betweenness centrality, some conclusions can be drawn:

- (a) At the occurrence of collapse, the in-edges of nodes with a large out degree centrality and in degree centrality failed, exerting a domino effect on the outgoing edges. Based on the algorithmic principle, this paper finds that weights of the outgoing edges of nodes with a large out degree centrality and in degree centrality were mainly positive, meaning that the network collapsed in a short period. These findings prove that financial stocks are the backbone forces of stock networks, and that they are more important than other stocks to maintain the stability of the economic market. Any threats to these key financial stocks may spread over the whole network.
- (b) The betweenness centrality results emerged as similar to algorithm principle, with a domino effect of

collapse of the top 20 stocks. For instance, the intersection of SDIC Power Holdings, East Money, and Shanxi Securities reflected their role as bridges in the stock network. These stocks connect influential neighbouring nodes. Therefore, cutting the loss in time of these stocks at the point of network collapse could effectively prevent a follow-up loss. This may thus be termed the “defense force” of the stock network.

As a result, it is recommended that stock regulation departments, enterprises, and shareholders pay attention to the governance of the “major players,” “gatekeepers,” and “vulnerable players” in the stock network and prevent systematic stock market risks being incurred by these stocks.

5. Temporal Network and Robustness Analysis

5.1. Temporal Network Modeling. The out degree centrality, in degree centrality, and betweenness centrality of stocks during 2016-2017 and 2017-2018 were analyzed in this paper,

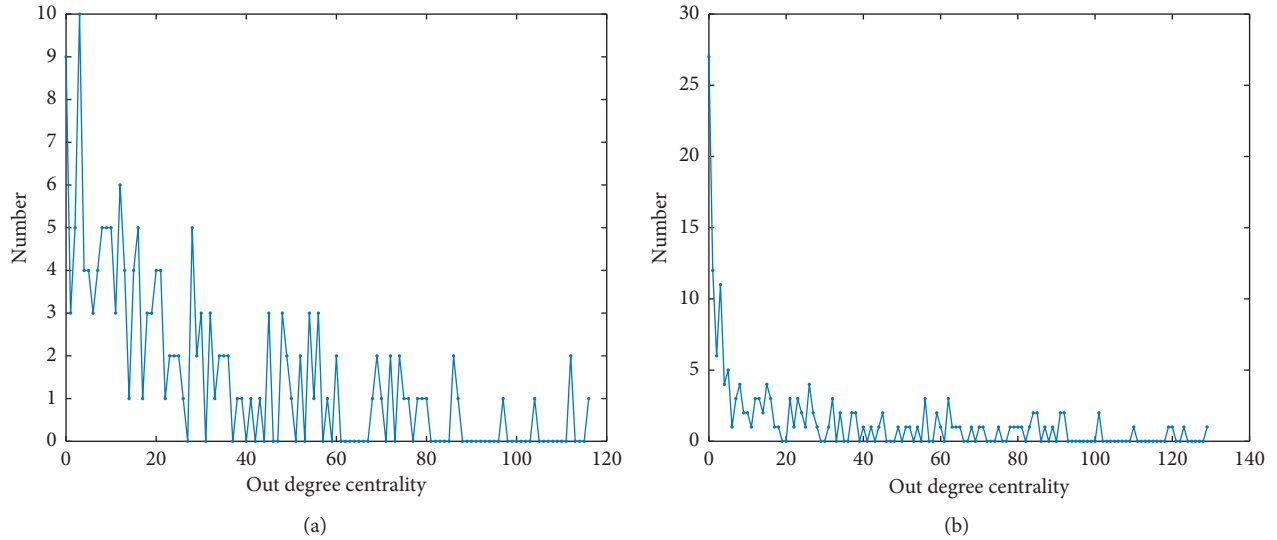


FIGURE 6: Distribution diagram of out degree centrality of CSI 300 network in 2016-2017 (a) and 2017-2018 (b).

TABLE 5: Top 20 out degree centrality stocks of CSI 300 network in 2016-2017 and 2017-2018.

2016-2017			2017-2018		
Id	Stock	Out degree centrality	Id	Stock	Out degree centrality
108	Sichuan Chuantou Energy	116	81	Youngor	129
63	China Minsheng Banking Corp	112	117	Haitong Securities	123
117	Haitong Securities	112	132	Guotai Junan Securities	120
81	Youngor	104	120	Bank of Jiangsu	119
119	China Yangtze Power	97	108	Sichuan Chuantou Energy	110
154	China Everbright Bank	87	4	Zoomlion Heavy Industry Science & Technology	101
30	Suzhou Gold Mantis Construction Decoration	86	63	China Minsheng Banking Corp	101
151	Everbright Securities	86	116	Shanghai Tunnel Engineering	92
136	Bank of Communications	80	136	Bank of Communications	92
132	Guotai Junan Securities	79	62	Hua Xia Bank	91
164	Bank of China	78	163	China national Nuclear Power	91
134	Agricultural Bank of China	76	59	Shanghai Pudong development Bank	89
70	SDIC Capital	75	123	Daqin railway	87
64	Zhejiang Zheneng Electric Power	74	6	Financial Street Holding	85
89	Southwest Securities	74	12	Tongling Nonferrous Metals	85
59	Shanghai Pudong development Bank	72	9	Jilin Aodong Pharmaceutical	84
76	China Northern rare Earth	72	159	China Coal Energy	84
161	China Construction Bank	70	80	Shanghai Construction	83
129	Industrial Bank	69	129	Industrial Bank	81
139	Industrial and Commercial Bank of China	69	119	China Yangtze Power	80

with certain differences found in terms of the stock ranking. Boccaletti et al. [60] introduced a basic multilayer network model and integrated structural characteristics of the multiplex network. Thus, two networks were effectively overlapped for a systematic analysis of stock importance. The temporal network was then analyzed from the multiplex perspective.

Firstly, a multiplex network was designed as follows: the upper layer was taken as the stock network during 2016-2017

and the lower layer as the stock network during 2017-2018. The same topics between adjacent layers were connected by lines. The multiplex network constructed is shown in Figure 8.

5.2. Robustness Analysis of Temporal Network. This section analyzes the potential “avalanche effect” in the temporal network according to the robustness of the network, with the

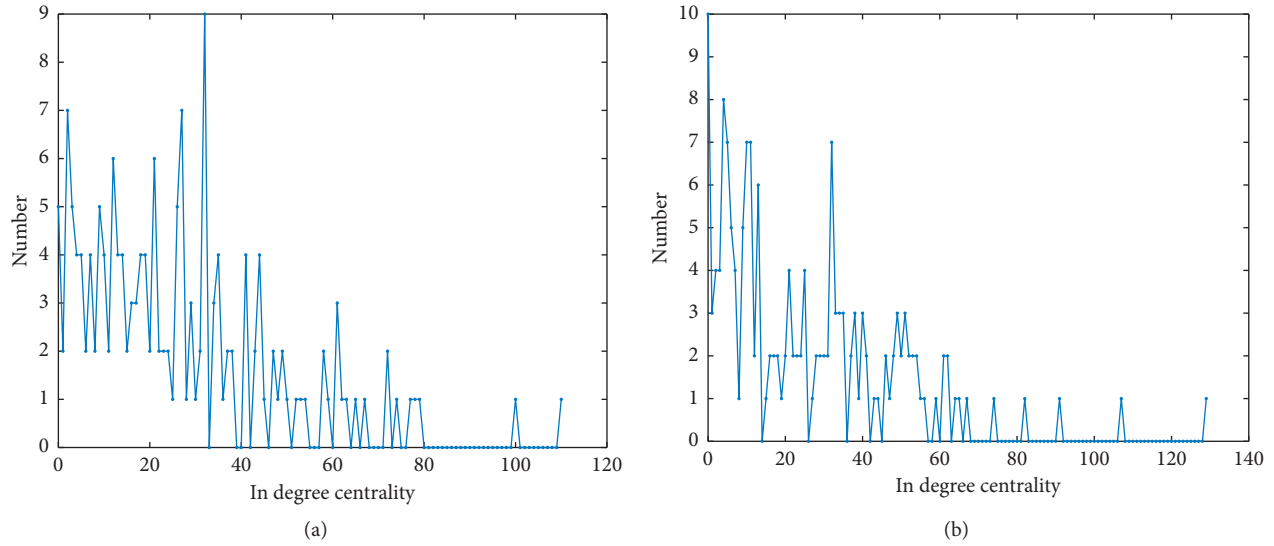


FIGURE 7: Distribution diagrams of in degree centrality of CSI 300 network in 2016-2017 (a) and 2017-2018 (b).

TABLE 6: Top 20 in degree centrality stocks of CSI 300 network during 2016-2017 and 2017-2018.

2016-2017			2017-2018		
Id	Stock	In degree centrality	Id	Stock	In degree centrality
117	Haitong Securities	110	81	Youngor	129
81	Youngor	100	117	Haitong Securities	107
15	Guoyuan Securities	79	136	Bank of Communications	91
51	East Money Information	78	32	Risesun Real Estate development	82
136	Bank of Communications	77	82	Yanzhou Coal mining	74
43	Shanxi Securities	74	131	Dongxing Securities	67
11	Hubei Biocause Pharmaceutical	72	19	CITIC Guoan Information Industry	65
30	Suzhou Gold Mantis Construction Decoration	72	92	Gemdale Corporation	64
143	China Nuclear Engineering	67	2	Shenzhen Zhongjin Lingnan Nonfemet	62
169	China Molybdenum	65	3	Overseas China Town A	62
152	China Communications Construction	63	26	China Merchants Shekou Industrial Zone Holdings	61
144	Metallurgical Corporation of China	62	43	Shanxi Securities	61
25	Shanxi Xishan Coal And Electricity Power	61	48	Guosen Securities	59
34	Iflytek	61	106	Greenland Holdings	56
130	China railway Construction	61	91	Beijing Capital development	55
147	Power Construction Corporation of China,	59	11	Hubei Biocause Pharmaceutical	54
58	Lens Technology	58	57	Beijing Enlight Media	54
103	Xiamen Tungsten	58	51	East Money Information	53
13	HESTEEL	54	88	Jiangxi Copper	53
149	Jihua	53	25	Shanxi Xishan Coal And Electricity Power	52

overall robustness of the network also investigated. The robustness analysis of the temporal network was based on a series of domino effects brought about by the reduction of nodes. If a stock network is rousting, the overall loss of the stock network caused by the disappearance of some seriously influenced stocks in the network is not very large. This reflects

that the stock network is robust and has a strong resistance to interference, if the proportion of network loss after the node elimination is lower than 50% and such nodes account for 50% or higher of the total nodes. Otherwise, this stock network is vulnerable. However, the fluctuation of one node can never be transmitted to other nodes under extreme conditions

TABLE 7: Top 20 betweenness centrality stocks of CSI 300 network during 2016-2017 and 2017-2018.

2016-2017			2017-2018		
Id	Stock	Betweenness centrality	Id	Stock	Betweenness centrality
79	Xiamen C&D	479.7774	2	Shenzhen Zhongjin Lingnan Nonfemet	365.0909
89	Southwest Securities	249.2328	79	Xiamen C&D	287.7911
3	Overseas China Town A	229.713	78	China Spacesat	250.327
78	China Spacesat	223.3947	5	Wei Chai Power	236.3662
18	Changjiang Securities	212.8275	66	CITIC Securities	234.1923
168	Foshan Haitian Flavouring and Food Company	199.758	91	Beijing Capital development	170.5163
149	Jihua	161.4737	122	China Merchants Securities	143.3816
43	Shanxi Securities	160.9054	147	Power Construction Corporation of China,	138.1491
138	New China Life Insurance	157.7938	110	Qingdao Haier	136.6742
1	Ping An Bank	150.8605	140	Soochow Securities	98.52948
41	Hangzhou Hikvision Digital Technology	143.871	159	China Coal Energy	96.61944
132	Guotai Junan Securities	142.1785	148	Huatai Securities	95.98428
57	Beijing Enlight Media	135.3603	11	Hubei Biocause Pharmaceutical	94.59229
16	Avic Aircraft	127.645	3	Overseas China Town A	89.39425
141	China Pacific Insurance	126.0323	88	Jiangxi Copper	89.02667
82	Yanzhou Coal mining	125.4607	116	Shanghai Tunnel Engineering	80.96572
51	East Money Information	106.8625	75	Sinolink Securities	75.92961
9	Jilin Aodong Pharmaceutical	106.3568	15	Guoyuan Securities	74.45371
70	SDIC Capital	102.3938	135	Ping An Insurance	73.94458
130	China railway Construction	102.3834	18	Changjiang Securities	72.65543

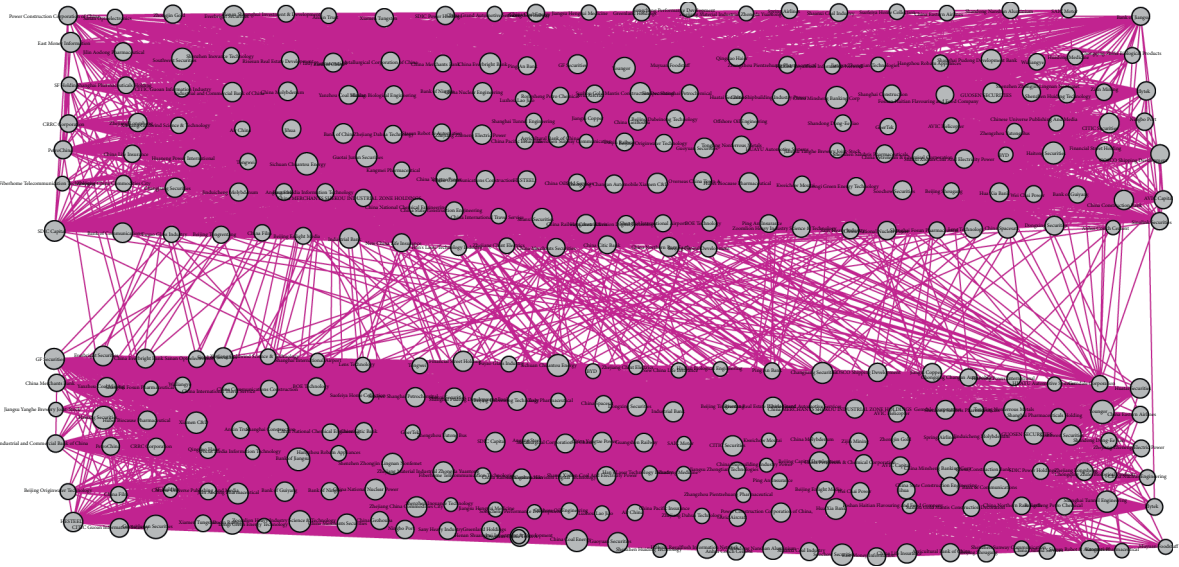


FIGURE 8: Temporal complex network.

because all of the nodes are isolated. Therefore, the robustness coefficient (ρ) of the network was defined as follows:

$$\rho = \frac{n_{\text{secure}} - n_{\text{isolated}}}{n - n_{\text{isolated}} + 1} = \frac{(n_{\text{secure}} - n_{\text{isolated}})/n}{1 - n_{\text{isolated}}/n + 1/n} = \frac{\rho_{\text{secure}} - \rho_{\text{isolated}}}{1 - \rho_{\text{isolated}} + (1/n)}, \quad (7)$$

where n_{isolated} denotes the number of isolated nodes, ρ_{secure} is the proportion of nodes with less than 50% of a destructive effect, and the corresponding ρ_{isolated} denotes the density of

isolated nodes [61]. 1 exists for adjustment purposes, to prevent the denominator of 0. This definition integrates the network connection into the robustness coefficient well. The probability of controlling network loss that is lower than 50% upon a random attack is ρ .

Different from the traditional monolayer network, the multilayer network model applied in Section 4 considers the stock relationships in the study period from a time series perspective.

The following domino spreading algorithm was designed based on the ordinary spreading model:

Step 1: initialize the spreading time vector, t , and the spreading proportion vector, percent.

Step 2: choose the starting node, i (i circulates from 1 to n). The spreading set, $S_i = \{i\}$, the termination set $D_i = \{\emptyset\}$, and the healthy set, $H_i = \{j \mid 1 \leq j \leq n, j \neq i\}$, are established. The spreading time and spreading proportion are also determined at $t_i = 1$ and $\text{percent}_i = 1/n$, respectively.

Step 3: search the starting point of all nodes in S which are connected to node i in each layer of the network and the neighbouring set, $(S_{\text{neighbour}}^i)$, with positive weights of connecting sides. $D_i = D_i + S_i$.

Step 4: if $S_{\text{neighbour}}^i \subseteq D_i$ and $|H_i| = 0$, go to Step 6; otherwise, go to Step 5.

Step 5: for $\forall j \in S_{\text{neighbour}}^i$, search the starting point of the connecting sides of node j in each layer of network and the neighbouring set, $(S_{\text{neighbour}}^{i(j)})$, with positive weights of connecting sides. If $S_{\text{neighbour}}^{i(j)} \subseteq D_i$, then $D_i = D_i + \{j\}$; otherwise, $S_i = S_i + \{j\} - \{i\}$. After all of the elements in $S_{\text{neighbour}}^i$ have been circulated, set $t_i = t_i + 1$ and $\text{percent}_i = (|S_i| + |D_i| - 1)/n$. $H_i = H_i - D_i - S_i$ and return to Step 3.

Step 6: if $S_{\text{neighbour}}^i = \emptyset$ and $t_i = 1$, let $t_i = n + 1$; otherwise, go to Step 7.

Step 7: $\text{percent}(i) = \text{percent}_i$ and $t(i) = t_i$. If $i \leq n$, go to Step 2.

Step 8: output the spreading time, t , and the spreading proportion, percent.

In Steps 3 and 5, a Boolean retrieve was applied to search the neighbouring nodes of each node in the set S and $S_{\text{neighbour}}^i$ and to determine the potential communication target. Step 6 examines whether the spreading nodes in the initial state are isolated or have no positive weights on the outgoing edges. Under this circumstance, the passive nodes that are isolated in the initial state, or have no outgoing edges with a positive weight, cannot influence other nodes. Therefore, the nodes with the longest time are directly omitted from the algorithm. The simulated process of risk spreading based on a stock temporal network in Figure 9 is introduced in the following section.

The above algorithm considers two characteristics of stock networks: (1) the development of one stock is closely related with the amplitudes of other stocks; (2) the network collapse exerts a domino effect, as reflected by the spreading time and spreading proportion in the algorithm.

An example of a stock temporal network can be seen in Figure 9, and the process of spreading network risk is shown in Figures 10(a)–10(d), with the starting point at node 1.

The spreading set, (S_1) , under each spreading time, (t_1) , termination set (D_1) , and the healthy set (H_1) and the spreading proportion of the final network (percent_1) after node 1 chosen as the risk spreading source in the network are shown in Table 8.

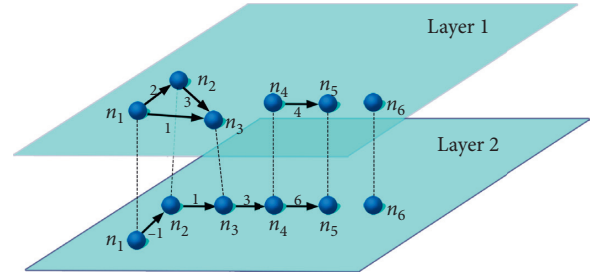


FIGURE 9: Initial status of 6 nodes in multiplex network with 2 layers.

As shown in Figures 9 and 10, if risk spreading was only to occur in layer 1, the process would end with $S_1 = \{2, 3\}$, $D_1 = \{\emptyset, 1\}$, and $H_1 = \{4, 5, 6\}$. However, layer 2 provides more information; namely, that in some cases, node 3 is linked with node 4. If that happens, the single layer (layer 1) cannot capture this chance of risk process. Similarly, due to the negative weight of the edge between nodes 1 and 2, that is, -1 , without information from layer 1, the spreading process would end with $S_1 = \{1\}$, $D_1 = \{\emptyset\}$, and $H_1 = \{2, 3, 4, 5, 6\}$.

In short, the algorithm takes the worst network collapse into account. If the connecting side of two nodes in one layer is positive and the starting point of the side is collapsed (infected), the node at the other end will also, ultimately, be infected.

The Matlab simulation results are shown in Figure 11.

The red line in Figure 11 reflects that the collapse time of the network caused by most nodes is relatively small, indicating that these nodes might lie at the edges or core of the network. This has to be further determined according to the collapse proportion because the core nodes of the network would cause a more extensive collapse at the same time. Moreover, the collapse time of a few nodes is relatively high, and most of these nodes are isolated or powerless. The statistics on the top 20 stocks in terms of the collapse proportion are presented in Table 9.

Table 9 reveals that the top 20 stocks in terms of the collapse proportion fluctuate, essentially, at the same time. On the one hand, this explains the fact that these stocks can influence over 80% of the network's stocks in a short period. On the other hand, the importance of these stocks in the network varies to some extent. The difference in importance between China Yangtze Power in the first position and Shandong Dong-Ee Jiao in the 20th position reaches as high as 20%. In conclusion, the nodes in the stock market are significantly different, and the global stability of the network is almost controlled by a few stocks.

It finds from comparison of out degree centrality, in degree centrality, and betweenness centrality that the large-scale collapse of stock networks is mainly caused by financial stocks with a high out degree centrality and in degree centrality, such as those of the China Minsheng Banking Co., Ltd., Shanghai Pudong Development Bank, and Industrial Bank. Stocks with a high out degree centrality are more likely to establish positive correlations with other stocks. However, the in-sides of these stocks become ineffective when they are

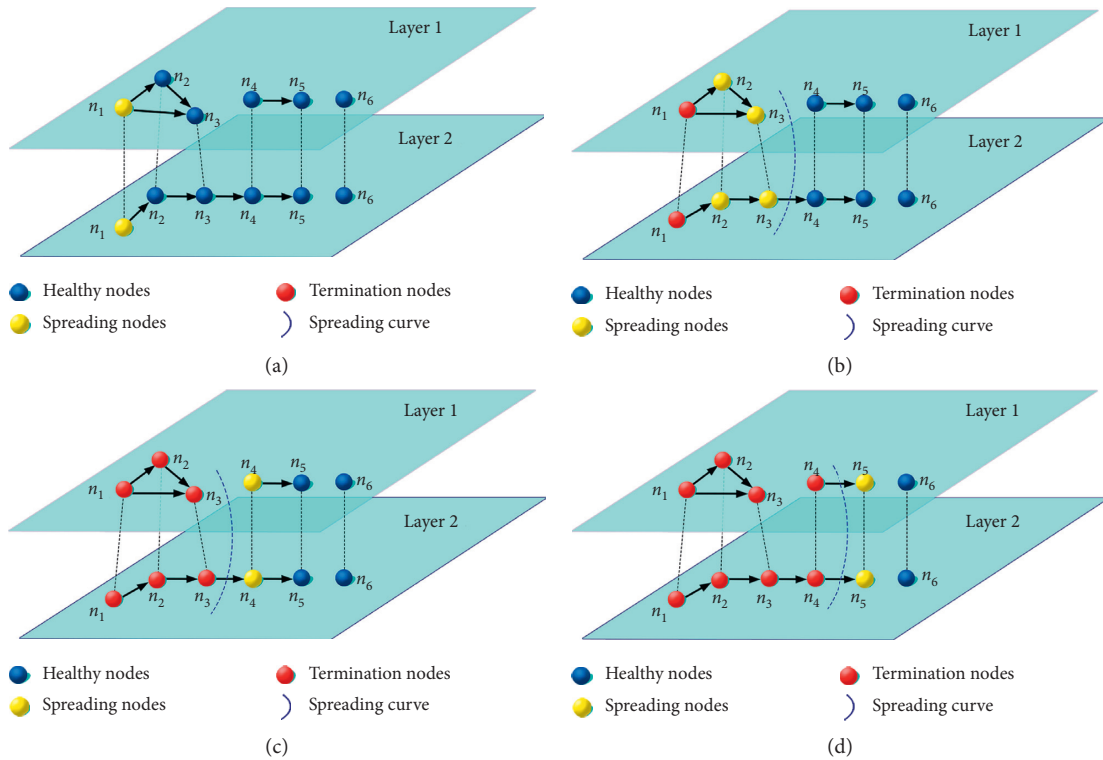


FIGURE 10: Example of risk spreading from node 1 with domino spreading algorithm: (a) spreading status with $t = 1$; (b) spreading status with $t = 2$; (c) spreading status with $t = 3$; (d) spreading status with $t = 4$.

TABLE 8: Risk spreading process from node 1.

	$t_1 = 1$	$t_1 = 2$	$t_1 = 3$	$t_1 = 4$
S_1	{1}	{2, 3}	{4}	{5}
D_1	{ \emptyset }	{ $\emptyset, 1$ }	{ $\emptyset, 1, 2, 3$ }	{ $\emptyset, 1, 2, 3, 4$ }
H_1	{2, 3, 4, 5, 6}	{4, 5, 6}	{5, 6}	{6}
percent ₁	1/6	1/2	2/3	5/6

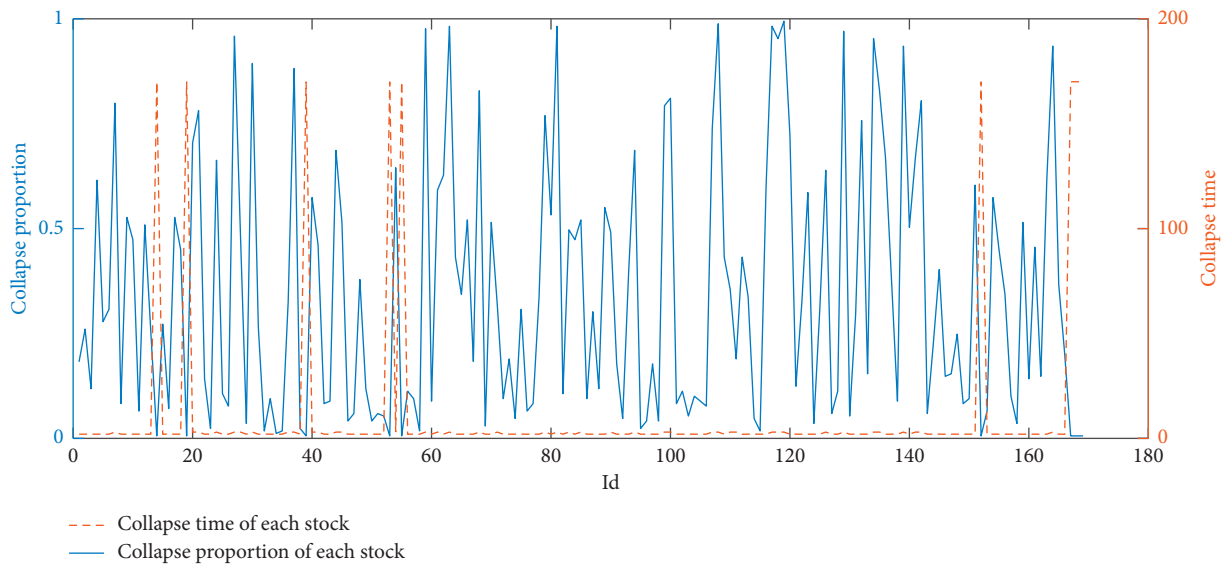


FIGURE 11: Collapse proportion and time originated from each stock.

TABLE 9: Top 20 stocks with disturbance power in collapse process.

Id	Stock	Collapse proportion	Collapse time
119	China Yangtze Power	0.9941	3
108	Sichuan Chuantou Energy	0.9882	3
63	China Minsheng Banking Corp	0.9822	3
81	Youngor	0.9822	3
117	Haitong Securities	0.9822	3
59	Shanghai Pudong development Bank	0.9763	3
129	Industrial Bank	0.9704	3
27	Hualan Biological Engineering	0.9586	3
118	SDIC Power Holdings	0.9527	3
134	Agricultural Bank of China	0.9527	3
139	Industrial and Commercial Bank of China	0.9349	3
164	Bank of China	0.9349	3
30	Suzhou Gold Mantis Construction Decoration	0.8935	3
37	Shenzhen Salubris Pharmaceuticals	0.8817	3
68	China Merchants Bank	0.8284	3
135	Ping An Insurance	0.8284	3
100	Kweichow Moutai	0.8107	3
142	Shanghai Pharmaceuticals Holding	0.8047	3
7	Shandong Dong-Ee Jiao	0.7988	3

collapsed, and the major domino effect occurs on the out-sides. Based on the algorithmic principle, the weights of the out-sides of these stocks are mainly positive, so that they can induce a network collapse in a short period. Therefore, financial stocks can be seen as the core of the stock network, making it more important to maintain their stability in the economic market. In the worst-case scenario, any threats to these important financial stocks may spread over the whole network.

Moreover, the betweenness centrality and eigenvector centrality emerged as similar in the top 20 stocks, to some extent. For instance, the intersection of SDIC Power Holdings, East Money and Shanxi Securities reflects their role as bridges in the stock network. These stocks connect influential neighbouring nodes. Therefore, cutting the loss in time of these stocks at the point of network collapse can effectively prevent a follow-up loss. This may thus be termed the “defense force” of the stock network.

Finally, 116 nodes were seen to cause a collapse effect smaller than 50%, given that a two-layer temporal network was constructed in the current study, and the inner layer covered 0 isolated nodes. Therefore, $\rho_{\text{isolated}} = 0$, and the stability index of the network was $\rho = 0.6824 > 0.5$, indicating the high stability of the stock network.

Based on above analysis, the new algorithm developed here is arguably superior to the traditional infection model of complex networks in actual networks. Moreover, the situation of the negative weights of the sides between nodes in the stock network is here taken into account. The domino effect of collapse among different stocks was simulated from a multiplex perspective, thus obtaining the network loss caused by the collapse of each node. Finally, the backbone force and defense force of stock networks were analyzed, based on the data in previous sections.

6. Conclusions

In this paper, selected stock data drawn from the CSI 300 index were divided into two time series.

Next, the daily amplitudes of stock samples were calculated. The stationarity of the calculated data of each stock was tested using the ADF method. Finally, the cointegration coefficients between any two stocks were obtained by applying a cointegration test. The thresholds of the cointegration coefficients were acquired by combining the frequency distribution. Meanwhile, edges with a high weight were chosen in order to establish a weighted directed graph, which considered the negative correlations among stocks.

Distributions of out degree centrality and in degree centrality reflected the scale-free characteristics of the network. Only a few stocks were found to play important roles in the network and to control the stability of the stock network. The top 20 node stocks in the stock network, such as “major players,” “gatekeeper,” and “vulnerable players,” were explored by analyzing the out degree centrality, in degree centrality, and betweenness centrality of the complex network.

On this basis, the temporal complex networks were constructed and an algorithm to test the robustness of these networks was designed. The quantitative indexes and evaluation standards of robustness were then proposed, and the systematic risk of the stock market was analyzed.

In summary, this paper has the following highlights:

- (i) A robustness test algorithm for network stableness is designed
- (ii) Quantitative indexes and evaluation standards of robustness are introduced
- (iii) The methodology can be applied in other situations like social networks, to specify the strength among people or global supply chain networks

Apart from this research, some guidance is given for other situations for researchers to follow:

- (i) The time slice is the year unit. It is chosen as the “year-round” feature of the stock market. In other situations, the features can be chosen as others like “month-round” and “season-round”.
- (ii) Generally, time series should be firstly stationary. ADF test is done for this. If the criterion is not fulfilled, the data should be differenced, and then the left jobs could be executed in the stream of Figure 1. Furthermore, the data can be analyzed in more than two layers of network, just replications of downstream of the single layer.

Also, US stock market or EU stock market could be done in the future for justifying the usage of methodology, and if real system risk dispersion data is obtained, the research could be enriched.

So, the research conclusions not only enrich the robustness theory of temporal networks but also provide an effective tool to prevent systematic stock market risks.

Data Availability

All data, the models used during the study that appear in the submitted article, and the original data used to support the findings of this study are available from the corresponding author upon request.

Conflicts of Interest

The authors declare that there are no conflicts of interest regarding the publication of this paper.

Acknowledgments

This study was supported by the National Natural Science Foundation of China (nos. 71901199, 71974115, 71874167, and 71804170), China Postdoctoral Science Foundation (no. 2019M660170), Fundamental Research Funds for the Central Universities (no. 201913015), Shandong Social Science Planning Project (no. 19CHYJ10), Postdoctoral Innovation Project of Shandong Province (no. 201902019), Special Funds of Taishan Scholars Project of Shandong Province (no. tsqn20171205), and Major Program of National Social Science Foundation of China (no. 18ZDA055).

References

- [1] L. Wei, W. Zhang, X. Xiong, and L. Shi, “Position limit for the CSI 300 stock index futures market,” *Economic Systems*, vol. 39, no. 3, pp. 369–389, 2015.
- [2] A. Bunde, J. Kropp, Schellnhuber, and H. Joachim, *The Science of Disasters*, Springer, Berlin, Germany, 2002.
- [3] B. Derrida, V. Hakim, and R. Zeitak, “Persistent spins in the linear diffusion approximation of phase ordering and zeros of stationary Gaussian processes,” *Physical Review Letters*, vol. 77, no. 14, pp. 2871–2874, 1996.
- [4] D. Sornette, *Why Stock Markets Crash: Critical Events in Complex Financial*, Princeton University Press, Princeton, NJ, USA, 2003.
- [5] G. Cao, Y. Han, W. Cui, and Y. Guo, “Multifractal detrended cross-correlations between the CSI 300 index futures and the spot markets based on high-frequency data,” *Physica A: Statistical Mechanics and Its Applications*, vol. 414, pp. 308–320, 2014.
- [6] C. J. Green and E. Joujon, “Unified tests of causality and cost of carry: the pricing of the French stock index futures contract,” *International Journal of Finance & Economics*, vol. 5, no. 2, pp. 121–140, 2000.
- [7] H. Choh and A. Subrahmanyam, “Using intraday data to test for effects of index futures on the underlying stock markets,” *Journal of Futures Markets*, vol. 14, no. 3, pp. 293–322, 1994.
- [8] D. Butterworth, “The impact of futures trading on underlying stock index volatility: the case of the FTSE Mid 250 contract,” *Applied Economics Letters*, vol. 7, no. 7, pp. 439–442, 2000.
- [9] A. C. N. Kan, “The effect of index futures trading on volatility of HSI constituent stocks: a note,” *Pacific-Basin Finance Journal*, vol. 5, no. 1, pp. 105–114, 1997.
- [10] M. Ibrahim, “Macroeconomic variables and stock prices in Malaysia: an empirical analysis,” *Asian Economic Journal*, vol. 13, no. 2, pp. 219–231, 1999.
- [11] J. Yang, Z. Yang, and Y. Zhou, “Intraday price discovery and volatility transmission in stock index and stock index futures markets: evidence from China,” *Journal of Futures Markets*, vol. 32, no. 2, pp. 99–121, 2012.
- [12] Y.-Y. Suo, D.-H. Wang, and S.-P. Li, “Risk estimation of CSI 300 index spot and futures in China from a new perspective,” *Economic Modelling*, vol. 49, pp. 344–353, 2015.
- [13] H. Qu, T. Wang, Y. Zhang, and P. Sun, “Dynamic hedging using the realized minimum-variance hedge ratio approach—examination of the CSI 300 index futures,” *Pacific-Basin Finance Journal*, vol. 57, Article ID 101048, 2019, In press.
- [14] T. Toulouse, A. Ping, I. Shmulevich, and S. Kauffman, “Noise in a small genetic circuit that undergoes bifurcation,” *Complexity*, vol. 11, no. 1, pp. 45–51, 2005.
- [15] S. Dealy, S. Kauffman, and J. Socolar, “Modeling pathways of differentiation in genetic regulatory networks with boolean networks,” *Complexity*, vol. 11, no. 1, pp. 52–60, 2010.
- [16] M. Gherardi and P. Rotondo, “Measuring logic complexity can guide pattern discovery in empirical systems,” *Complexity*, vol. 21, no. 2, pp. 397–408, 2016.
- [17] S. Boccaletti, V. Latora, Y. Moreno, M. Chavez, and D. Hwang, “Complex networks: structure and dynamics,” *Physics Reports*, vol. 424, no. 4-5, pp. 175–308, 2006.
- [18] M. E. J. Newman, “The structure and function of complex networks,” *SIAM Review*, vol. 45, no. 2, pp. 167–256, 2003.
- [19] M. E. J. Newman, *Networks: An Introduction*, Oxford University Press, Oxford, UK, 2010.
- [20] S. H. Lee and P. Holme, “Navigating temporal networks,” *Physica A: Statistical Mechanics and Its Applications*, vol. 513, pp. 288–296, 2019.
- [21] B. Guerra, J. Poncela, J. Gómez-Gardeñes, V. Latora, and Y. Moreno, “Dynamical organization towards consensus in the Axelrod model on complex networks,” *Physical Review E*, vol. 81, no. 5, Article ID 056105, 2010.
- [22] C. D. Brummitt, K.-M. Lee, and K.-I. Goh, “Multiplexity-facilitated cascades in networks,” *Physical Review E*, vol. 85, no. 4, Article ID 045102, 2012.

Research Article

Research on Dynamic and Complexity of Energy-Saving Investment about Multichannel and Multienergy Supply Chain

Fang Wu ^{1,2}

¹College of Computer and Information Engineering, Tianjin Agricultural College, Tianjin 300384, China

²Complex Dynamics Research Group, College of Management and Economics, Tianjin University, Tianjin, 300072, China

Correspondence should be addressed to Fang Wu; w-fang@hotmail.com

Received 7 May 2020; Accepted 27 June 2020; Published 15 July 2020

Academic Editor: Abdelalim A. Elsadany

Copyright © 2020 Fang Wu. This is an open access article distributed under the Creative Commons Attribution License, which permits unrestricted use, distribution, and reproduction in any medium, provided the original work is properly cited.

Considering the multienergy structure of the electricity market and supply-side competition reform in China, a dual-channel and multiproduct supply chain model is constructed. There are three players in the game model: new energy company and traditional energy company provide energy for the market and the State Grid at the same time. The State Grid is a retailer who buys electricity from two companies and supplies to the market after converting and transmitting the power. Three companies can invest in grid management for saving energy and reducing losses. The energy loss rate is an exponential function of line loss investment. Through the bifurcation graph, Lyapunov exponent, and the basin of parameter, the complex characteristics of the investment market are analyzed. It is interesting to find the Grazing–Hopf bifurcation which usually occurs in nonlinear circuits. The mixed expectation of bounded rationality and the naive expectation is conducive to suppressing the bifurcation and chaos of the market. When external shocks occur, the control model has good robustness.

1. Introduction

Supply-side reform has been continuously implemented in Chinese power industry [1]. The huge power market has gradually opened up, and customer can purchase electricity directly from the State Grid or power companies. Multienergy can be connected to the State Grid on a large scale. The electricity market shows a complex competition with multiple energy sources and multiple channels. Energy saving and low-carbon development are urgent tasks for the world. For power enterprises, the loss in processes of transmission, substation, and distribution is the main power supply costs [2]. Reducing electricity loss is an important measure to ensure energy security and sustainable development.

Therefore, considering electricity reform of China, co-existence of macrocontrol and market competition, this study builds a dual-channel supply framework for multi-energy supply. Based on the goals of saving energy strategy, a line loss investment model of multichannel supply chain is proposed, and the complex characteristics of investment market in line loss are analyzed.

2. Related Research

Considering economic practice, there are two types of research related to this article: electricity market reform and dual-channel supply chain.

2.1. Electricity Market Reform. The electricity market reform has always been a hot issue in the world. In regions with abundant energy supply, it was believed that encouraging competition was conducive to introducing new energy and lowering prices. In 1996, the European electricity market began to introduce liberalization and agreed that introducing competition could promote efficiency and reduce electricity price [3]. Zhang et al. [4] believed that electricity price reform and electricity trading were conducive to promoting the integration of renewable energy with the traditional power industry. In the Russian power industry, the combination of government regulation and appropriate market mechanisms was considered a suitable development strategy [5].

If energy was not available locally, some researchers thought that market-oriented reforms may be harmful. Australian scholars discovered [6] that power reform would bring hidden dangers to the power supply security. Woo et al. [7] found that competition in the electricity market could not bring stable prices and reliable services, and market-oriented reforms may bring great risks or even catastrophic consequences to the United Kingdom, Norway, Alberta (Canada), and California (United States).

Other scholars focused on how to introduce sustainable electricity through reform. Tian et al. [8] built a dynamic game model to analyze the promotion of natural gas reform. It was found that relaxing natural gas prices, levying carbon taxes, and choosing environmental subsidies could promote the market penetration of natural gas power. Taking Yunnan province of China as an example, Liu et al. [9] systematically analyzed a series of policies for introducing new energy.

At present, the reform of China's power market mainly focusses on two aspects: the introduction of new energy and trying to encourage competition. Those lead to multienergy and multichannel. This paper will build such a power supply structure model for analyzing this situation.

2.2. The Dual-Channel Supply Chain. Some scholars believed that the dual-channel supply chain structure could promote the green level of the product [10]. Rahmani et al. [11] built a dual-channel supply chain of green products by a mathematical method, solved the model by Invasive Weed Optimization algorithm (IWO), and verified the abovementioned result by Genetic algorithms considering the nonlinear characteristic. Rahmani and Yavari [12] built a dual-channel supply chain consisting of a green product manufacturer and a retailer, analyzed demand management in Stackelberg game, and found that reducing green costs can increase product's green level. Yang et al. [10] believed that environmental responsibility of green products led to dual channels choice and proposed a dual-channel structure strategy that considered behavioural characteristics.

Some scholars discovered that the dual-channel master-slave supply chain shows nonlinear dynamic characteristics and further explored its complex features [13, 14]. Zhang and Wang [13] analyzed the dynamic pricing strategy of the dual-channel supply chain, studied the impact of service value decisions on price, discussed the complex characteristics of the model, such as period and chaos, and further investigated the bullwhip effect. Lou and Ma [14] analyzed the dynamic characteristics of household appliances' supply chain considering energy saving and emission reduction. The optimal solutions of Nash equilibrium and Stackelberg were studied. The conditions for bifurcation and chaos were discussed, and a new phenomenon from cycle 2 to cycle 6 was discovered. However, according to the current competitive reform orientation of the Chinese power market, competitive games are more suitable for practice than master-slave games.

Therefore, based on the current power industry reform of China, this study will construct a dual-channel supply model with multienergy products, as Figure 1 shows, based

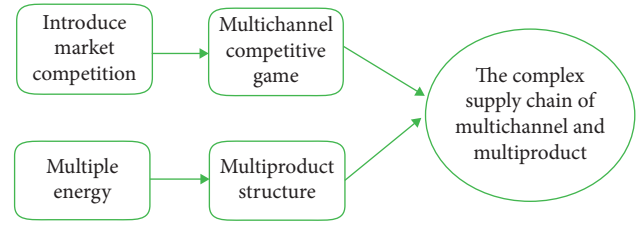


FIGURE 1: The structure of the supply chain.

on the goal of saving energy, building the line loss investment model, and analyzing its complex characteristics.

The structure of the article is arranged as follows. Section 3 includes the assumption, functions, and the model. Section 4 is the complexity simulation. Section 5 is the chaos control. Section 6 is the robustness analysis, and the last section is a conclusion.

3. The Model

3.1. Assumptions

- (1) There are three types of enterprises in the Chinese electrical energy market: new energy enterprises, traditional enterprises based on coal burning, and the State Grid. Consumers can buy electricity from three companies.
- (2) The State Grid established basic facilities for electric energy transmission and management. New energy company and traditional energy company supply power for the market at retail prices or for the State Grid at wholesale prices.
- (3) Line loss occurs during energy transmission. In order to establish an energy-saving grid, new energy company, traditional energy company, and the State Grid are permitted to invest in line loss management.

The system structure diagram is shown in Figure 2.

In Figure 2, new energy companies, traditional energy companies, and the State Grid can provide electricity products to the market directly, and the market prices are p_1 , p_2 , and p_g , respectively. New energy company and traditional energy company provide electricity products for the State Grid, and the wholesale prices are p_s and p_c , respectively. The State Grid purchases electric energy from two companies in proportion. The proportion from the traditional energy company is ω , and the proportion from the new energy company is $1 - \omega$. In order to promote the overall operating efficiency of the power grid, three companies can invest in grid management to reduce management line losses. Their investments are x , y , and z .

3.2. Variables and Functions

3.2.1. Line Loss Rate. Line loss occurs in energy transmission. The loss of electrical energy is divided into two parts [15, 16]: fixed line loss and management line loss. As long as the power transmission equipment is running, a fixed line loss will occur and is related to the power grid equipment,

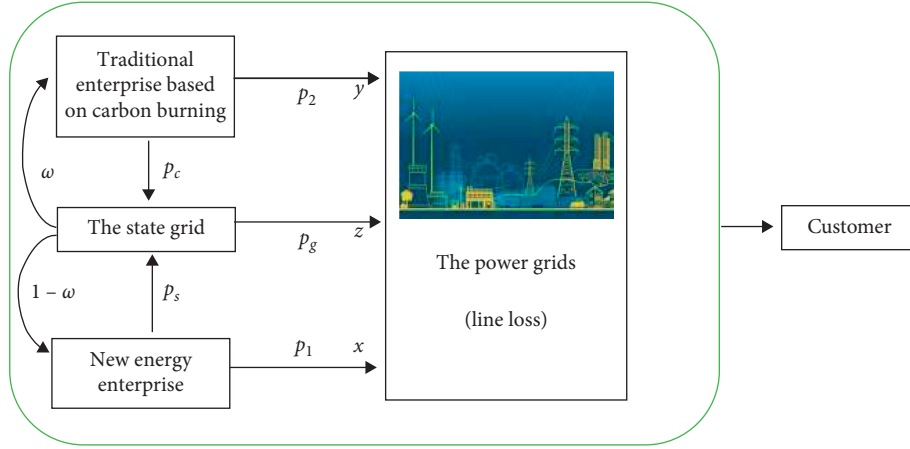


FIGURE 2: The model structure.

such as circuits, resistors, and network structure. It is not easy to change in the short term. Management line loss is related to electricity theft, management intensity, and the transmission paths planning. The increase in the management investment can reduce the management line loss. Some scholars have used an exponential function to build investment and decaying product models. Chung and Kwon [17] used an exponential investment model to study the impact of advertising investment on prices, and Guo and Ma [18] used an exponential model to study the output of decaying products. The exponential advertising investment model is introduced into the management line loss investment, and the decaying model was changed according to the composition of electric power line losses.

Three power companies invest in line loss management, and investments are represented by x , y , and z . The line loss investment function is

$$L = (1 - A) + Ae^{-\sigma_1 x - \sigma_2 y - \sigma_3 z - \sigma_4 xyz}. \quad (1)$$

The line loss composition is shown in Figure 3.

In equation (1) and Figure 3, $1 - A$ means the fixed line loss rate, which is related to the network architecture and hardware, and will not change in the short term; $Ae^{-\sigma_1 x - \sigma_2 y - \sigma_3 z - \sigma_4 xyz}$ is the variable line loss rate which is related to the management intensity. $\sigma_1 \sim \sigma_4$ are constants and represent degrees of influence.

3.2.2. Investment Model for Line Loss Management

The State Grid: q_g is the output of the State Grid to the market. d is the potential demand of electric energy in the market, $\theta_1 d$ is the market's potential demand for the Station Grid, and θ_1 is the proportional constant. a , a_1 , and a_2 are influence parameters.

$$q_g = \theta_1 d - a p_g + a_1 p_1 + a_2 p_2. \quad (2)$$

The State Grid should carry out transmission, distribution, voltage transformation, and other operations for traditional energy and new energy before providing them to the market. It is a dual-product production

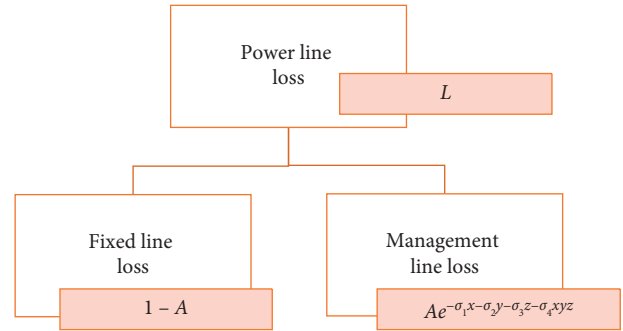


FIGURE 3: The line loss structure.

process that embodies the enterprise's flexible manufacturing [19, 20]. The dual-product cost function is as follows:

$$C_g = k + s + \{q_g w c_r + q_g (1 - w) [c_r + r(1 - d_0)]\}. \quad (3)$$

The working cost of traditional carbon-fired electricity is k , and the marginal cost is c_r . $q_g w$ is the purchase amount from the traditional enterprise, and $q_g (1 - w)$ is the purchase amount from the new energy enterprise. w is the purchase share from the traditional enterprise by the State Grid.

The State Grid handles new energy through flexible manufacturing technology. The conversion cost of switching from one variety to another is s , and the marginal cost of processing new energy is $c_r + r(1 - d_0)$.

$r(1 - d_0)$ is the increase in the cost of changing. The greater the gap between the processing of traditional energy and new energy, the greater the cost of changing.

The profit function of the State Grid is

$$\prod_g = q_g p_g L - p_s q_g (1 - w) - p_c q_g w - c_g q_g - z. \quad (4)$$

New energy enterprise: the power provided by new energy companies for the market is q_1 , the total output of new energy enterprise is q_s . c_1 is the marginal cost, and the profit function is Π_s .

$$\begin{aligned} q_1 &= (1 - \theta_1)(1 - \theta_2)d - ap_1 + a_1p_g + a_2p_2, \\ q_s &= q_1 + q_g(1 - w), \\ \Pi_s &= p_1q_1L + p_sq_g(1 - w) - c_1q_s - x. \end{aligned} \quad (5)$$

Traditional power enterprises based on carbon burning: the power provided by the traditional energy company for the market is q_2 , and the total output of traditional enterprise is q_c . c_2 is the marginal cost, and the profit function is Π_c .

$$\begin{aligned} q_2 &= (1 - \theta_1)\theta_2d - ap_2 + a_1p_1 + a_2p_g, \\ q_c &= q_2 + q_gw, \\ \Pi_c &= p_2q_2L + p_cq_gw - c_2q_c - y. \end{aligned} \quad (6)$$

θ_1 and θ_2 are the proportional coefficients about the potential demand.

3.3. *The Model.* Assuming that line loss investments of three companies follow the rule of bounded rational expectation, that is, adjusting the investment of the current period according to the marginal profit of the previous period, the discrete dynamic equations of the system can be obtained as follows:

$$\begin{cases} x' = x + \varepsilon x \frac{\partial \Pi_s}{\partial x}, \\ y' = y + \phi y \frac{\partial \Pi_c}{\partial y}, \\ z' = z + \eta z \frac{\partial \Pi_g}{\partial z}, \end{cases} \quad (7)$$

' means unite time advancement of the variable.

Namely,

$$\begin{cases} x' = x + \varepsilon x \{ Ap_1(\sigma_1 + yz\sigma_4)[a_2p_2 - ap_1 + a_1p_g + d(\theta_1 - 1)(\theta_2 - 1)]e^{-x\sigma_1 - y\sigma_2 - z\sigma_3 - xyz\sigma_4} + 1 \}, \\ y' = y + \phi y \{ Ap_2(\sigma_2 + xz\sigma_4)[ap_2 - a_1p_1 - a_2p_g + d\theta_2(\theta_1 - 1)]e^{-x\sigma_1 - y\sigma_2 - z\sigma_3 - xyz\sigma_4} - 1 \}, \\ z' = z + \eta z \{ Ap_g(\sigma_3 + xy\sigma_4)(a_1p_1 + a_2p_2 - ap_g + d\theta_1)e^{-x\sigma_1 - y\sigma_2 - z\sigma_3 - xyz\sigma_4} + 1 \}. \end{cases} \quad (8)$$

Let

$$\begin{cases} x' = x, \\ y' = y, \\ z' = z. \end{cases} \quad (9)$$

$$\begin{cases} \frac{\partial \Pi_s}{\partial x} = 0, \\ \frac{\partial \Pi_c}{\partial y} = 0, \\ \frac{\partial \Pi_g}{\partial z} = 0. \end{cases} \quad (10)$$

Namely,

The Nash equilibrium point (x^*, y^*, z^*) can be obtained as follows:

$$\begin{cases} x^* = - \left\{ \ln \left\{ \frac{1}{Ap_1(\sigma_1 + yz\sigma_4)[a_2p_2 - ap_1 + a_1p_g + d(\theta_1 - 1)(\theta_2 - 1)]} \right\} + y\sigma_2 + z\sigma_3 \right\} \left(\frac{1}{\sigma_1 + yz\sigma_4} \right), \\ y^* = - \frac{1}{\sigma_2 + xz\sigma_4} \left\{ \ln \left[\frac{1}{Ap_2(\sigma_2 + xz\sigma_4)(ap_2 - a_1p_1 - a_2p_g + d\theta_2\theta_1 - d\theta_2)} \right] + x\sigma_1 + z\sigma_3 + xz\sigma_4 \right\}, \\ z^* = - \frac{1}{\sigma_3 + xy\sigma_4} \left\{ \ln \left[\frac{1}{Ap_g(\sigma_3 + xy\sigma_4)(a_1p_1 + a_2p_2 - ap_g + d\theta_1)} \right] + x\sigma_1 + y\sigma_2 \right\}. \end{cases} \quad (11)$$

In existing research [21, 22], according to the jury [23] conditions, the stability of the system equilibrium point can be obtained through calculating the Jacobian matrix of the

model and its eigenvalues. But in this model, the complex exponential line loss function and multiproduct structure make the calculation amount huge, and the results cannot be

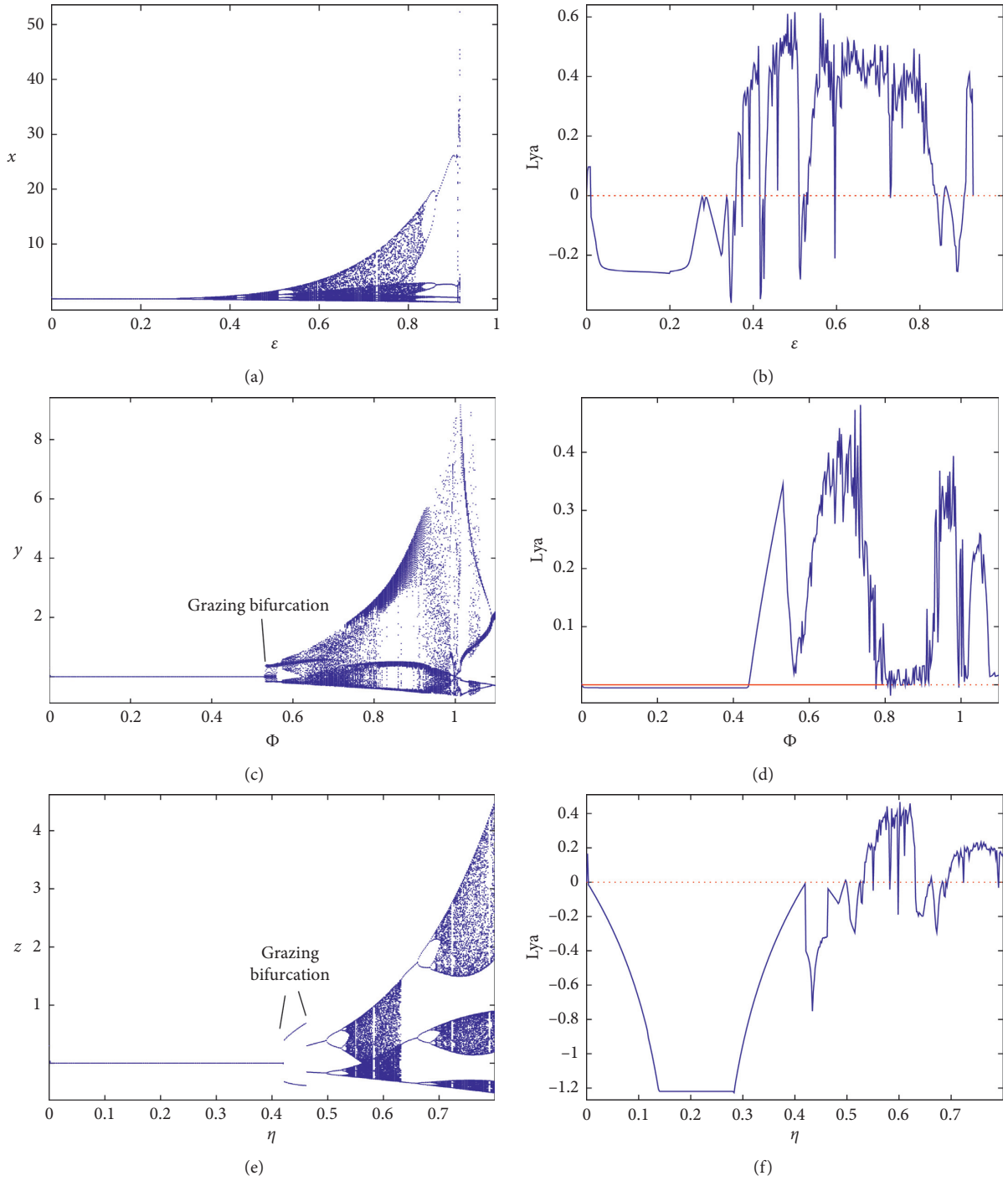


FIGURE 4: Bifurcation diagrams and Lyapunov exponents. (a) $\eta = 0.3, \phi = 0.3$. (b) $\eta = 0.3, \phi = 0.3$. (c) $\varepsilon = 0.3, \eta = 0.3$. (d) $\varepsilon = 0.3, \eta = 0.3$. (e) $\varepsilon = 0.35, \phi = 0.35$. (f) $\varepsilon = 0.35, \phi = 0.35$.

expressed by the mathematical analysis method. Therefore, this study turns to the numerical simulation to explore the period, chaos, and stability characteristics.

4. The Simulation

4.1. The Bifurcation and Lyapunov. In order to explore the complex characteristics of the model through numerical simulation, parameter values are set as follows:

$$\begin{aligned}
 c_1 &= 0.2; c_2 = 0.3; \theta_1 = 0.8; \theta_2 = 0.9; \\
 A &= 0.7; \sigma_1 = 3; \sigma_2 = 2; \sigma_3 = 3; \sigma_4 = 2; s = 0.3; a = 1; \\
 a_1 &= 1; a_2 = 1; w = 0.5; d_0 = 0.1; \\
 r &= 0.5; k = 0.5; d = 1.2; c_r = 0.1.
 \end{aligned}$$

Figure 4 shows the bifurcation diagrams and Lyapunov exponents with changing ε , ϕ , and η . In (a) and (b), the model enters chaos through Hopf bifurcation. (c) and (e)

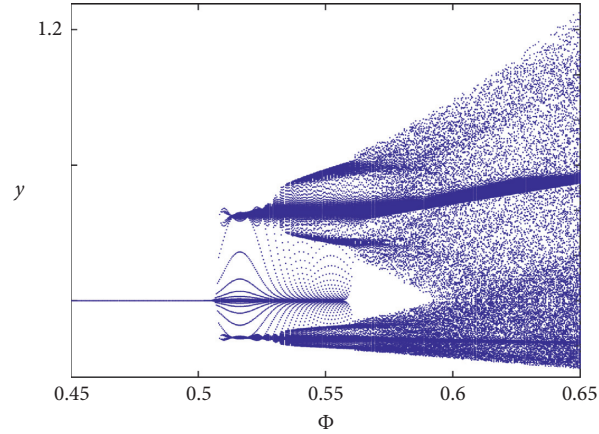


FIGURE 5: Detailed view of the grazing bifurcation.

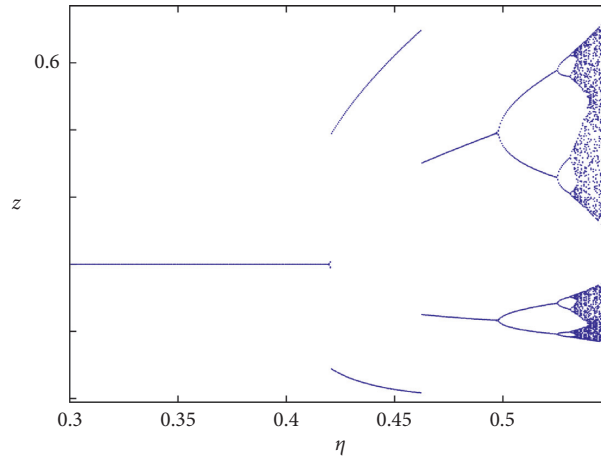


FIGURE 6: The Grazing-Hopf bifurcation.

show mutations: Grazing bifurcations appear, and it often occurred in nonlinear circuit theory [24]. As in (c), the investment of new energy enterprise enters chaos after Grazing bifurcation. Figure 5 is a detailed view of the process. As in (e), the system enters the two-cycle orbit from the steady state through the Grazing bifurcation mutation. In the two-period orbit, the Grazing bifurcation mutation occurs again, and then enters chaos through the Hopf bifurcation, as Figure 6 detailed.

4.2. The Basin of Parameter. In this section, basins of parameter in Figure 7 show the model's complex character. Orange represents stable equilibrium, green represents the two-period orbit, brown represents three-period, dark green represents the 4-period orbit, blue means the 6-period orbit,

and magenta represents the 8-period orbit, white represents nonconvergence and yellow-green represent divergence.

5. Chaos Control Based on Mixed Expectation

In the existing differential economic system, there are three types of expectation rules [25, 26, 27]: the bounded rational expectation, the naive expectation, and the adaptive expectation. The bounded rational expectation has the strongest complex characteristics, followed by adaptive expectations, and the last is naive expectations which do not have complex characteristics when used alone. This section will study the impact of the mixed expectation rule (the combination of the bounded rationality and naive expectation) on the complexity of the economic system.

The mixed expectation model is as follows:

$$\begin{cases} x = (1 - \text{Con}_1)\{x + \varepsilon x\{Ap_1(\sigma_1 + yz\sigma_4)[a_2p_2 - ap_1 + a_1p_g + d(\theta_1 - 1)(\theta_2 - 1)]e^{-x\sigma_1 - y\sigma_2 - z\sigma_3 - xyz\sigma_4} + 1\}\} + \text{Con}_1x, \\ y = (1 - \text{Con}_2)\{y + \phi y\{Ap_2(\sigma_2 + xz\sigma_4)[ap_2 - a_1p_1 - a_2p_g + d\theta_2(\theta_1 - 1)]e^{-x\sigma_1 - y\sigma_2 - z\sigma_3 - xyz\sigma_4} - 1\}\} + \text{Con}_2y, \\ z = (1 - \text{Con}_3)\{z + \eta z\{Ap_g(\sigma_3 + xy\sigma_4)(a_1p_1 + a_2p_2 - ap_g + d\theta_1)e^{-x\sigma_1 - y\sigma_2 - z\sigma_3 - xyz\sigma_4} + 1\}\} + \text{Con}_3z. \end{cases} \quad (12)$$

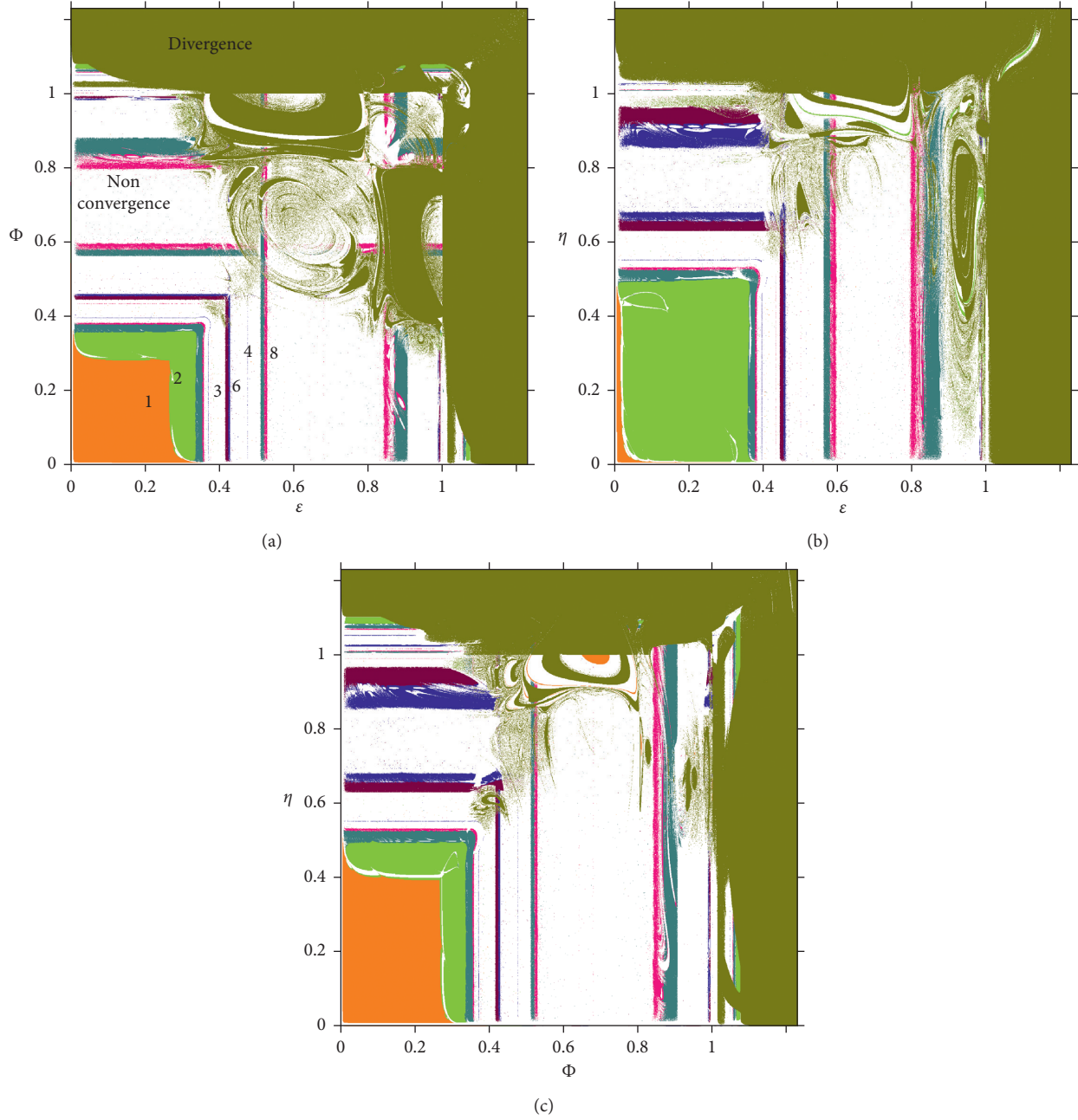


FIGURE 7: The basin of parameter. (a) The basin of ϵ and ϕ . (b) The basin of ϵ and η . (c) The basin of ϕ and η .

$Con_i (i = 1, 2, 3)$ is the weight for choosing the naive expectation, and $1 - Con_i$ is the weight for choosing the bounded rational expectation. For research convenience, let $Con_1 = Con_2 = Con_3 = Con$. Looking at the parameter base diagram in Figure 8, we can find that even if the investment adjustment speed parameter increases, the system's stable region is still gradually expanding with increasing Con .

6. Robustness Analysis

External shocks such as natural disasters, epidemic outbreaks, and financial crises will directly affect power grid investment. When the shock occurs, the investment is interrupted. When the emergency disappears, the investment rebounds. The drastic changes of investment shock the stability of the market. In this section, we study the

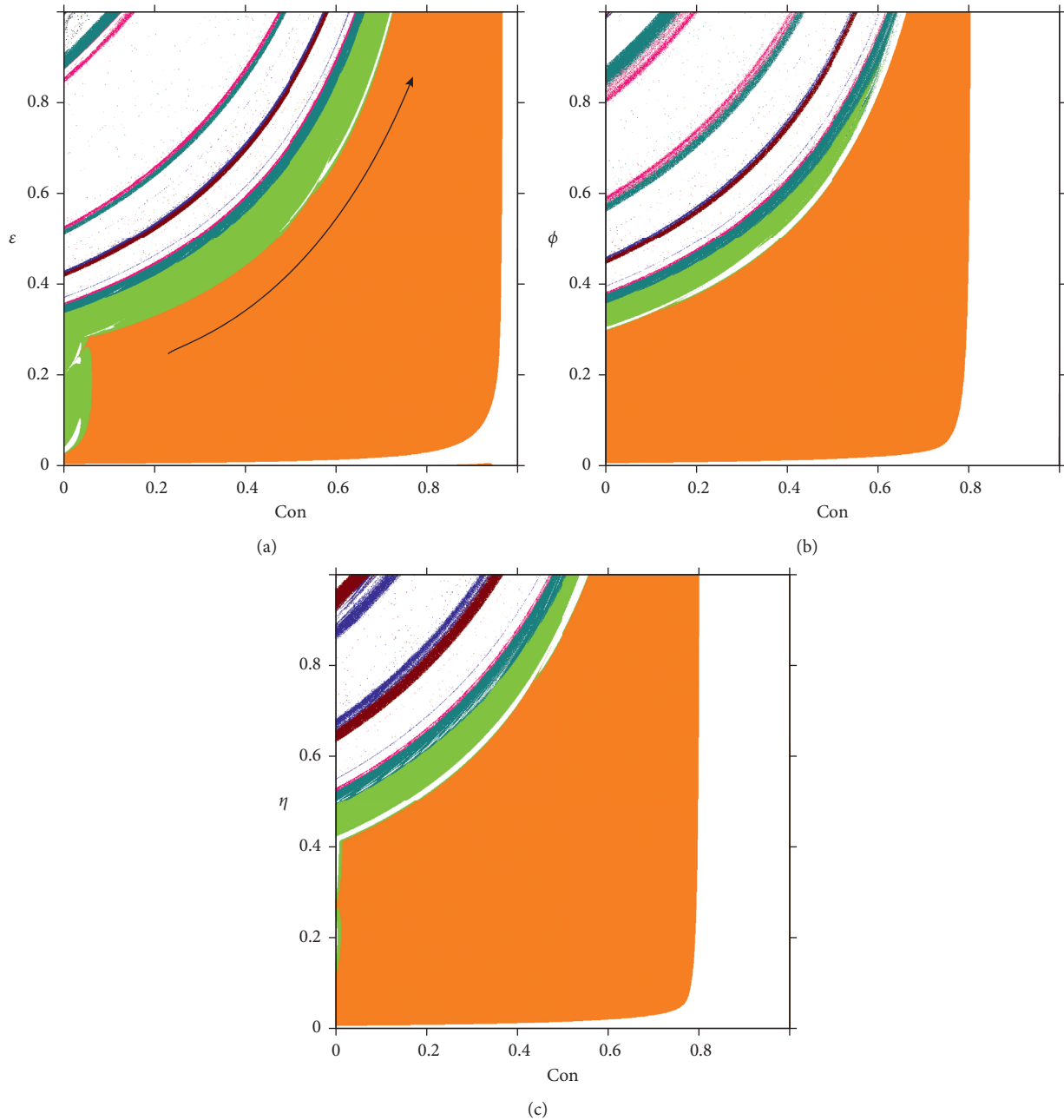


FIGURE 8: The basin of parameter under control. (a) The basin of Con and ε . (b) The basin of Con and ϕ . (c) The basin of Con and η .

robustness of the mixed expectation control method under severe fluctuations in investment.

In Figure 9(a), there is no control ($\eta = 0.3$). As shown in Figure 9(b), the investment rate η suddenly increases to 0.9 from 0.3, the steady state disappears, and the cycle bifurcation and chaos interlace occur. After adopting the mixed

expectation control strategy, when the control coefficient is 0.6, the same external mutation occurs, and the parameter base diagram is shown in (c): equilibrium appears. If the control coefficient is increased to 0.9, even if the outside world suddenly changes, the system will be in Nash equilibrium with great probability, as (d) shows.

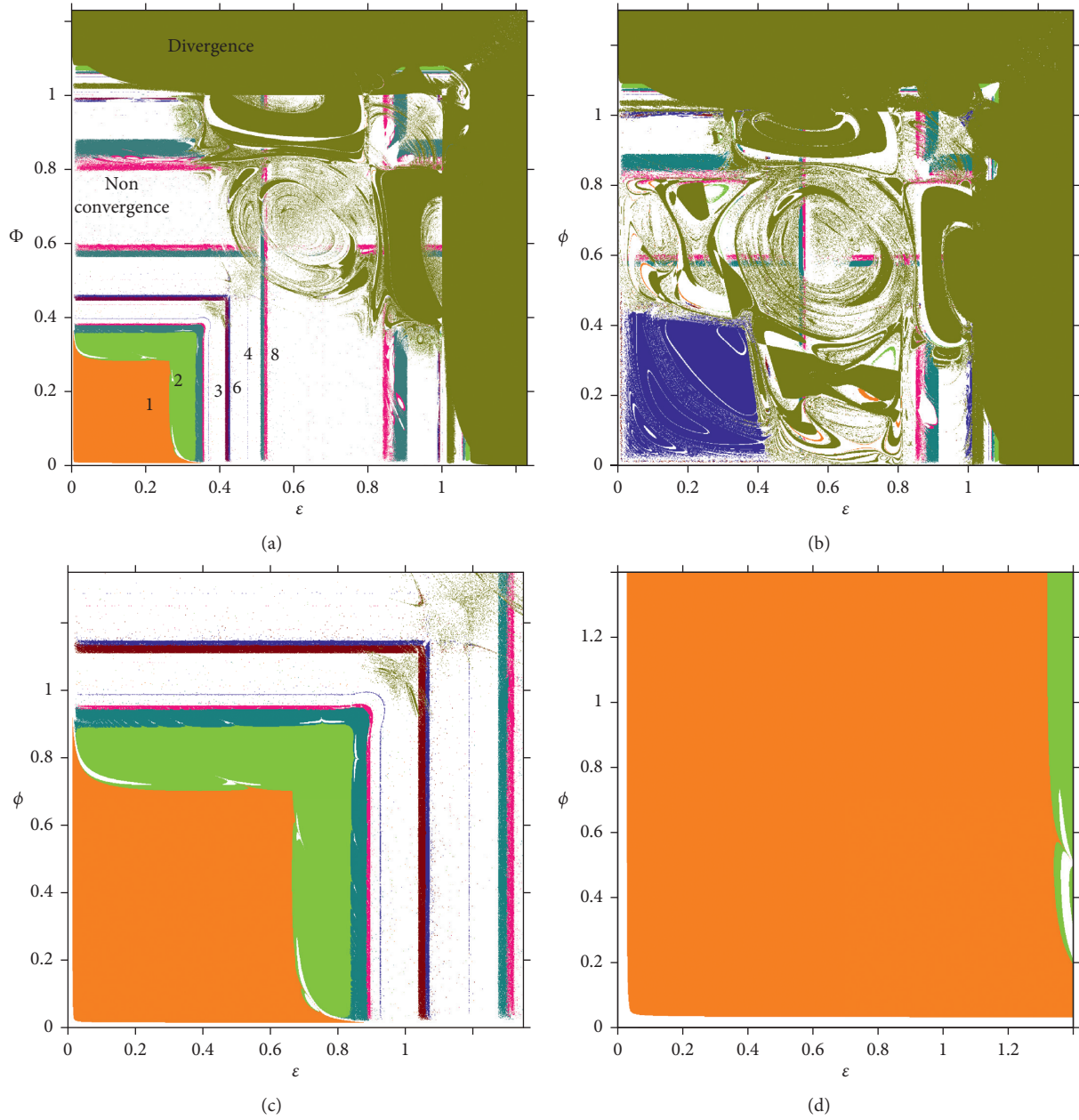


FIGURE 9: The parameter basin of robustness. (a) $\text{Con} = 0$, $\eta = 0.3$. (b) $\eta = 0.9 = 0.9$. (c) $\eta = 0.9 =$, $\text{Con} = 0.6$. (d) $\eta = 0.9$, $\text{Con} = 0.8$.

7. Conclusions

For supply-side reform of China, multiple energy production companies enter the market, and the competition between multienergy enterprises and the State Grid appears. At this time, the State Grid deals with multiple energy sources from power enterprises and retails them. Based on the abovementioned realities, a dual-channel and multiproduct supply chain model is constructed, in which energy companies conduct dual-channel sales and the State Grid corporation processes multiple power. For saving energy, all companies are permitted to invest in reducing line loss, and

the energy loss rate is an exponential function of investments. The bifurcation graph, Lyapunov exponent, parameter basin, and other techniques are used to analyze the complex characteristics of the system. In this economic model, besides the double-cycle bifurcation, a Grazing-Hopf bifurcation is found, which usually occurs in nonlinear circuits. The study finds that the mixed strategy that is combined by bounded rationality and naive expectation can suppress bifurcation and chaos. Also, the parameter basin technique is used to analyze the robustness of the control method. This paper enriches the issue about complex dynamics of economics.

Data Availability

The data used to support the findings of this study are included within the article.

Conflicts of Interest

The author declares that there are no conflicts of interest regarding the publication of this paper.

Acknowledgments

This research was supported by the Philosophy and Social Science Planning Project of Tianjin, China (No. TJGL19-027).

References

- [1] Z. Yu, "Beyond the state market dichotomy: institutional innovations in China's electricity industry reform," *Journal of Environmental Management*, vol. 264, no. 15, Article ID 110306, 2020.
- [2] M. A. Sayed and T. Takeshita, "Line loss minimization in isolated substations and multiple loop distribution systems using the UPFC," *IEEE Transactions on Power Electronics*, vol. 29, no. 11, pp. 5813–5822, 2014.
- [3] A. Kaller, S. Bielen, and W. Marneffe, "The impact of regulatory quality and corruption on residential electricity prices in the context of electricity market reforms," *Energy Policy*, vol. 123, pp. 514–524, 2018.
- [4] S. Zhang, P. Andrews-Speed, and S. Li, "To what extent will China's ongoing electricity market reforms assist the integration of renewable energy?" *Energy Policy*, vol. 114, pp. 165–172, 2018.
- [5] K. Letova, R. Yao, M. Davidson, and E. Afanasyeva, "A review of electricity markets and reforms in Russia," *Utilities Policy*, vol. 53, pp. 84–93, 2018.
- [6] M. Abbott and B. Cohen, "Finding a way forward: policy reform of the Australian national electricity market," *The Electricity Journal*, vol. 31, no. 6, pp. 65–72, 2018.
- [7] C.-K. Woo, D. Lloyd, and A. Tishler, "Electricity market reform failures: UK, Norway, Alberta and California," *Energy Policy*, vol. 31, no. 11, pp. 1103–1115, 2003.
- [8] R. Tian, Q. Zhang, G. Wang et al., "Study on the promotion of natural gas-fired electricity with energy market reform in China using a dynamic game-theoretic model," *Applied Energy*, vol. 185, pp. 1832–1839, 2017.
- [9] S. Liu, Q. Yang, H. Cai et al., "Market reform of Yunnan electricity in southwestern China: practice challenges and implications," *Renewable and Sustainable Energy Reviews*, vol. 113, Article ID 109265, 2019.
- [10] D. Yang, T. Xiao, and J. Huang, "Dual-channel structure choice of an environmental responsibility supply chain with green investment," *Journal of Cleaner Production*, vol. 210, pp. 134–145, 2019.
- [11] D. Rahmani, M. Q. Hasan Abadi, and S. J. Hosseini-zhad, "Joint decision on product greenness strategies and pricing in a dual-channel supply chain: a robust possibilistic approach," *Journal of Cleaner Production*, vol. 256, Article ID 120437, 2020.
- [12] K. Rahmani and M. Yavari, "Pricing policies for a dual-channel green supply chain under demand disruptions," *Computers & Industrial Engineering*, vol. 127, pp. 493–510, 2019.
- [13] F. Zhang and C. Wang, "Dynamic pricing strategy and co-ordination in a dual-channel supply chain considering service value," *Applied Mathematical Modelling*, vol. 54, pp. 722–742, 2018.
- [14] W. Lou and J. Ma, "Complexity of sales effort and carbon emission reduction effort in a two-parallel household appliance supply chain model," *Applied Mathematical Modelling*, vol. 64, pp. 398–425, 2018.
- [15] P. Raj and S. Senthilkumar, "Optimization of distributed generation capacity for line loss reduction and voltage profile improvement using PSO," *Journal of Electrical Engineering*, vol. 2, 2018.
- [16] N. Inayoshi, M. A. Sayed, T. Takeshita, N. Izuhara, and F. Ueda, "Construction method of loop distribution system for line loss minimization," *IEEE Transactions on Power & Energy*, vol. 128, no. 6, pp. 893–894, 2018.
- [17] S. H. Chung and C. Kwon, "Integrated supply chain management for perishable products: dynamics and oligopolistic competition perspectives with application to pharmaceuticals," *International Journal of Production Economics*, vol. 179, pp. 117–129, 2016.
- [18] Z. Guo and J. Ma, "Dynamics and implications on a cooperative advertising model in the supply chain," *Communications in Nonlinear Science and Numerical Simulation*, vol. 64, pp. 198–212, 2018.
- [19] D. C. Chisholm and G. Norman, "Market access and competition in product lines," *International Journal of Industrial Organization*, vol. 30, no. 5, pp. 429–435, 2012.
- [20] A. Garcia-Gallego and N. Georgantzis, "Multiproduct activity in an experimental differentiated oligopoly," *International Journal of Industrial Organization*, vol. 19, no. 3-4, pp. 493–518, 2001.
- [21] A. A. Elsadany and A. M. Awad, "Dynamics and chaos control of a duopolistic Bertrand competitions under environmental taxes," *Annals of Operations Research*, vol. 274, no. 1-2, pp. 211–240, 2019.
- [22] F. Wu and J. Ma, "The equilibrium, complexity analysis and control in epiphytic supply chain with product horizontal diversification," *Nonlinear Dynamics*, vol. 93, no. 4, pp. 2145–2158, 2018.
- [23] L. E. Eshet, *Mathematical Models in Biology*, Random House, New York, NY, USA, 1992.
- [24] S. Yin, G. Wen, H. Xu, and X. Wu, "Higher order zero time discontinuity mapping for analysis of degenerate grazing bifurcations of impacting oscillators," *Journal of Sound and Vibration*, vol. 437, pp. 209–222, 2018.
- [25] C. Hommes, *Behavioral Rationality and Heterogeneous Expectations in Complex Economic Systems*, Cambridge University Press, Cambridge, United Kingdom, 2013.
- [26] B. Xin, J. Ma, and Q. Gao, "Complex dynamics of an adnascent-type game model," *Discrete Dynamics in Nature and Society*, vol. 2008, Article ID 467972, pp. 1–12, 2008.
- [27] J. Ma, W. Lou, and Y. Tian, "Bullwhip effect and complexity analysis in a multi-channel supply chain considering price game with discount sensitivity," *International Journal of Production Research*, vol. 57, no. 17, pp. 5432–5452, 2019.

Research Article

Complexity Analysis of Pricing in a Multichannel Supply Chain with Spillovers from Online to Offline Sales

Fengxia Mai,^{1,2} Jianxiong Zhang ,¹ Rui Yang,¹ and Xiaojie Sun ^{1,3}

¹College of Management and Economics, Tianjin University, Tianjin 300072, China

²School of Science, Tianjin University of Commerce, Tianjin 300134, China

³Rowe School of Business, Dalhousie University, Halifax, NS B3H 4R2, Canada

Correspondence should be addressed to Xiaojie Sun; xj933918@dal.ca

Received 20 March 2020; Revised 31 May 2020; Accepted 18 June 2020; Published 14 July 2020

Academic Editor: Abdelalim A. Elsadany

Copyright © 2020 Fengxia Mai et al. This is an open access article distributed under the Creative Commons Attribution License, which permits unrestricted use, distribution, and reproduction in any medium, provided the original work is properly cited.

In recent years, many manufacturers have been selling their products to online consumers through e-tailers by adopting reselling mode and agency selling mode simultaneously. The sales from the online channels inevitably incur spillover effect to the traditional offline channels. This paper develops a dynamic pricing game model on the basis of a long-term gradient adjustment mechanism for a multichannel supply chain that consists of a manufacturer and an e-tailer and focuses on examining the impacts of spillover effect, agency fee, and adjustment speed on the stability and complexity of the dynamic game system. The results show that both a greater spillover effect and a higher agency fee can make the dynamic game system more stable, and a higher adjustment speed can destabilize the dynamic game system through period doubling bifurcation. Furthermore, it is interesting to find that the destabilization of the game system benefits the e-tailer and the supply chain while having little influence on the manufacturer, and thus the dynamic adjustment strategy may improve the supply chain efficiency.

1. Introduction

E-commerce has witnessed rapid growth in the past decade and has been occupying market share previously dominated by physical stores, making up 10.2% of the global retail sales in 2017 [1]. According to reports, the sales of online retailing reached \$2.304 trillion in 2017, with a 24.8% increase over the previous year [1]. With the increasing prevalence of online retailing and the implementation of platform opening plan (POP), e-tailers have begun to allow manufacturers to directly access online consumers with charging a commission fee for providing this platform. This agency selling mode has been embraced by some prominent online retailers, such as Taobao and JD [2] in China, Amazon in the US, and Flipkart in India [3]. In addition to agency selling, manufacturers also have an alternative selling mode in practice, i.e., the reselling mode, where e-tailers who act as conventional merchants wholesale from manufacturers and resell to consumers. As one of the largest online retailers in China, JD adopted the two online selling modes

simultaneously and significantly benefited from this retail structure, according to the financial report in 2018 (<https://www.chyxx.com/industry/201807/661976.html>).

The boom of online retailing has raised the concern about whether brick-and-mortar stores will give way to e-commerce. “Online-only will not survive, all businesses need to integrate online and offline resources,” Jianlin Wang, the chairman of Dalian Wanda Group said [4]. Nowadays, more and more manufacturers are able to sell their products in a multichannel supply chain, i.e., they sell not only through physical stores but also through e-tailers’ channels in the reselling mode and the agency selling mode; for instance, manufacturers, including Huawei, Gree, Haier, Midea, and Xiaomi, sell their products via multichannel selling to improve their performance. Particularly, Xiaomi, who is a major Chinese smart phone vendor, sells through a large online retail platform JD and also sells through physical stores to offline consumers directly, in a bid to make its products more accessible [5]. Such an offline expansion strategy appears to be paying off, since Xiaomi bounces back

with a 70% increase in shipments as compared with the previous quarter [6]. Therefore, how the cooperation between supply chain members and the interactions between online selling and offline selling affect the pricing strategy of firms has become a critical problem to be addressed in multichannel supply chain management.

Spillover effect usually arises in a multichannel supply chain and gives rise to complex effects in which the sales of offline selling are influenced by that of online selling. There are several studies taking spillover effect into consideration and exploring the interactions between online selling and offline selling. Abhishek et al. [7] investigated the interactions between online selling and traditional selling and suggested two competitive and homogeneous e-tailers' preferences for reselling mode and agency selling mode in the presence of spillover effect. They also found that if there is negative spillover effect, e-tailers prefer the agency selling channel; otherwise, they prefer the reselling channel. By measuring the combined impacts of the online spillover effect, the platform fee, and the manufacturer's inefficiency in selling, Yan et al. [8] focused on whether and under what conditions the marketplace channel should be introduced. However, all the above researches are based on the assumption that the decision makers know full information about the market and can make pricing decisions accurately. That is, the decision makers are fully rational and make pricing decisions on the basis of a static one-shot pricing game model. In practice, due to limited opportunities to learn the market information, the decision makers are usually boundedly rational and have to make decisions based on the limited information, which will lead to a dynamic repeated game process for the players. That is, the decision makers can adjust pricing decisions through a long-term gradient adjustment mechanism to achieve their maximum profits. In consideration of the players' bounded rationality, it is still unclear how spillover effect influences the interactions between online selling and offline selling, which deserves further investigation.

When players with bounded rationality implement dynamic pricing strategy, it is important to identify how spillover effect affects the dynamic evolution, system stability, and players' profits when e-tailers have more exact information. In the context of dynamic game, there are an increasing number of studies investigating a multichannel supply chain or marketing competition. For instance, considering the service value in a dual-channel supply chain, Zhang and Wang [9] developed two dynamic pricing strategies and examined the effect of service value on players' decisions. Ma and Xie [10] developed the dynamic game models in a dual-channel supply chain consisting of a manufacturer and a retailer, considering two scenarios in which the manufacturer holds either asymmetric or symmetric channel power to the retailer, and compared the complex behavior under different channel power structures via numerical simulation. Guo [11] explored channel conflict taking into consideration the impacts of online consumer reviews in a dual-channel supply chain from a dynamic perspective and analyzed the stability of the equilibrium point and complexity of channel conflict.

Taking the input of a retailing service into account, Ma et al. [12] investigated a dual-channel dynamic game and explored the stability of the equilibrium point and further made a discussion about the effects of the adjustment speed on the complexity of the game system and the market performance. In addition, for dynamic analysis, Naimzada and Pireddu [13] explored the dynamic behavior of the fashion cycle by investigating the asymptotic heterogeneity among agents and found that the global dynamics may differ according to the chosen functional form for the attractiveness. Naimzada and Pireddu [14] also examined the globally educative stability of a Muthian cobweb model in a profit-based evolutionary setting, assuming that agents face heterogeneous information costs. Baiardi and Naimzada [15] investigated the stability properties of a dynamic model of a linear Cournot oligopoly considering rational agents and indicated that the heterogeneities among players influence the stability of the Cournot-Nash equilibrium. Baiardi et al. [16] also studied the stability properties of a Minskyan type model formulated in a discrete time framework and showed that its stability and complexity depend on either a subcritical flip or a supercritical Neimark–Sacker bifurcation. Different from the above existing literatures, our paper focuses on the dynamic repeated pricing game in a multichannel supply chain, especially on the impact of spillover effect from online to offline on the complexity and dynamics of the game system.

In addition, it is necessary to explore the different profit distributions among participants if e-tailers allow manufacturers to directly have an access to their online consumers, which is related to the topic of supply chain coordination, and this topic has attracted significant academic interest (e.g., [17–23]). Players can coordinate the supply chain through a variety of mechanisms, such as two-part tariff contract, rebate contract, quantity discounts contract, and revenue-sharing contract, among which revenue-sharing contract has been universally applied in industries and widely explored by researchers. For instance, Zhang et al. [23] considered a two-echelon deteriorating item supply chain with a manufacturer and a retailer over an infinite time horizon, where a revenue-sharing and cooperative investment contract is designed to coordinate the supply chain. Yan [22] found that although differentiated branding effectively alleviates channel competition and conflict, it is not sufficient to achieve full channel coordination, and a profit sharing mechanism is necessary. Note that agency selling works as a revenue-sharing mechanism to some extent. However, in a long-term dynamic pricing process, the effects of agency selling on the evolution features of the game system and the supply chain members' profits are still indistinct, which is worth to be further studied.

In this paper, we develop a dynamic pricing model for a multichannel supply chain where a manufacturer sells through not only the traditional offline stores but also e-tailers' online channels in both the reselling mode and the agency selling mode under a static one-shot game and a dynamic repeated game, respectively. We focus on the dynamic game in which the manufacturer with bounded rationality employs a long-term gradient adjustment

mechanism to adjust the pricing decisions for improving profitability. We aim to investigate the impacts of spillover effect from online sales to offline sales, adjustment speed, and agency fee on the stability and complexity of the dynamic game system. By resorting to a large number of numerical studies with depicting the stability region, bifurcation diagrams, basin of attraction, and critical curve, we obtain some meaningful results for the multichannel supply chain. The results show that both a greater spillover effect and a higher agency fee can make the dynamic game system more stable, and a higher adjustment speed can destabilize the dynamic game system through period doubling bifurcation. Furthermore, it is interesting to find that the destabilization of the game system benefits the e-tailer and the supply chain while having little influence on the manufacturer, and thus the dynamic adjustment strategy may improve the supply chain efficiency.

In summary, the main contributions of the paper are presented as follows. First, our work extends the existing literatures considering the impacts of spillover effect and dealing with reselling and agency selling in a platform-based retailing market with rational decisions to the case of decision-making under bounded rationality, where the supply chain members cannot obtain complete market information which prevents them from making perfect decisions. Specifically, we make a leading effort to present a dynamic game for the multichannel supply chain in which the manufacturer changes the prices dynamically with the impacts of spillover effect. Second, we analyze the complex changes in the prices and profits of the supply chain members in the long-term pricing decision strategy. In particular, we investigate the impacts of the agency fee and spillover effect on the static game and also on the stability and complexity in the long-term dynamic game and obtain some interesting managerial insights.

The remainder of the paper is organized as follows. Section 2 presents the problem description and model setup. Section 3 gives the static game model and the dynamic game model (the repeated game) and conducts complexity analysis for the dynamic game, focusing on the impacts of key system parameters on the players' profits and the stability of the game equilibria. Finally, Section 4 concludes the paper.

2. Problem Description and Model Setup

2.1. Online Channel Structure. We consider a supply chain consisting of a manufacturer (she, denoted by subscript m) and an e-tailer (he, denoted by subscript r). The manufacturer cooperates with the e-tailer to sell her product on the electronic channel (e-channel, E) to online consumers. They cooperate through the reselling mode in which the e-tailer buys the product from the manufacturer at a unit wholesale price w and then sells to online consumers at price p_r . In addition, the agency selling mode is also applied, in which the e-tailer offers the manufacturer direct access to his consumers with charging an agency fee for providing this service. The manufacturer sells to online consumers directly via the e-tailer's platform at price p_m with paying a fraction δ of the profit as the agency fee to the e-tailer. In this paper, we

assume a constant linear agency fee contract used by the e-tailer, as it is widely adopted in the literature on platform (e.g., [7, 24] and is generally applied in practice such as Taobao, JD, and Amazon.

2.2. Online Demand Specification. Note that online consumers can choose from one of the available options: (i) buying through the reselling channel and (ii) buying through the agency selling channel. For example, when consumers choose products from the JD platform, they can find self-run products from JD and direct selling products from direct sale stores. Similar to Abhishek et al. [7] and Lu et al. [25], we assume that the products sold through the two e-channels are symmetric substitutes, i.e., the substitution degree of the agency selling product (the e-tailer's product) over the reselling product (the manufacturer's product) equals that of the latter over the former. Then, the consumer demand for the product can be captured by a linear and downward-sloping inverse demand function, $q_k = \alpha_k - p_k + \gamma p_l$, $k, l \in \{m, r\}$ and $k \neq l$, where p_k and q_k represent the market clearing price and the product quantity for the e-tailer or the manufacturer, respectively, and the parameter α_k denotes product k 's market potential. The parameter $\gamma \in [0, 1]$ measures the substitution degree between the two e-channels' products, and the products become more homogeneous and the retail market is more competitive as γ increases. Note that the two retail products turn out to be perfect substitutes when γ approaches 1 and independent when γ approaches 0. We normalize the slope of this inverse demand function to be -1 , which is widely used in the modelling literatures on online selling [7, 26–28].

2.3. Online Spillover Effect. To incorporate the spillover effect, similar to Abhishek et al. [7] and Yan et al. [8], we assume that there already exists a brick-and-mortar retail channel (i.e., traditional channel) where the manufacturer sells the product at a unit price normalized to 1 with a base demand \tilde{Q} , which represents the general demand of the traditional channel when the manufacturer does not sell online. The sales of traditional channel are influenced by the sales through the e-channels. Note that it is assumed that the manufacturer sells her product through e-channels only by a single e-tailer with the total demand for the manufacturer in the e-channels given by $q_E = q_e + q_m$. We formulate the spillover effect by assuming that the sales in the traditional channel are $\tilde{Q} + \tau q_E$, where the parameter τ represents the net overall cross-channel effect that the e-channels place on the sales of the traditional channel.

More specifically, the parameter τ captures the quantity change in traditional sales brought by per unit sold through the e-channels. In our work, we restrict $\tau \in [-1, 1]$. This model formulates an increase with $\tau > 0$, a decrease with $\tau < 0$, or no effect when $\tau = 0$ in traditional channel sales for per unit sold by the e-channels. Note that the online sales will have a negative cross-influence on sales in the traditional channel if $\tau < 0$. This could be due to cannibalization, i.e., consumers who have bought from online are less likely to purchase the same products from the physical stores. This

negative effect is widespread in reality, especially for durable goods that will not be purchased again in the near period. However, various studies also report that spillover effect can sometimes stimulate offline sales and has a positive cross effect, i.e., $\tau > 0$, under which per unit sold through the e-channels can result in τ units increased sales in the traditional channel. One reason for this increase could be word-of-mouth effect; for example, if a consumer who has been recommended e-book through push service or bought an e-book on Apple's iBook store or Amazon Kindle discusses the book to her/his acquaintances, then they may buy the physical book from a bookstore. Moreover, consumers who have very high regard for certain pieces of music or books often buy print editions to collect, commemorate, and display. This is in line with previous studies that cross effect can be negative or positive in different cases [29].

In addition, we assume that the product price in the traditional channel takes a constant value, which can be driven by two reasons. First, there exists operational difficulty in adjusting the product price in the traditional channel. In practice, the prices of physical books have not been affected by the e-book pricing. Moreover, prices are marked on books or special goods and cannot be changed as frequently as the prices in the e-channels. Second, the baseline demand \bar{Q} is sufficiently high as compared to the small-scale demand from the cross-channel effect, since online sales account for 11% of the total sales at most [30]. From this point of view, the product price in the traditional channel is not influenced. Besides, Abhishek et al. [7] further extended their model to consider endogenous consumer choice across the electronic and traditional channels and reported that the results remain unchanged qualitatively. Thus, we concern the qualitative nature of spillover effect in the multichannel supply chain and consider this model in absence of the endogenous consumer choice across the electronic and traditional channels. For brevity, we normalize the product price in the traditional channel to 1.

3. Game Models and Analysis

In this section, we first consider the case where the participants of the game are fully rational, which will lead to a static one-shot game. For convenience, we name this case as the static game model. And then, we focus on the case in which the participants with bounded rationality are involved in a dynamic repeated game, which is referred to as the dynamic game model.

3.1. Static Game. Consider a product distribution system in which a manufacturer cooperates with an e-tailer to sell her product to online consumers through two e-channels: the reselling channel and the agency selling channel. The manufacturer also sells her product through a traditional brick-and-mortar channel, which is either positively or negatively affected by the online sales volume. The e-tailer chooses to sell the product as a reseller (we name this as the wholesale configuration) and also enters into an agency selling arrangement with the manufacturer where the

e-tailer acts as an agency seller (we name this as the agency configuration). This model also characterizes the asymmetry in sales efficiency between the e-tailer and the manufacturer by normalizing the e-tailer's unit selling cost to zero but denoting $c (>0)$ as the manufacturer's unit direct selling cost. This assumption is widely applied in the literature [8, 31, 32] and is also reasonable in practice because e-tailers often have an advantage in the sales process as compared to the manufacturer. The retailer's advantage may stem from superior knowledge of customer preferences and more direct contact with customers or from economies of scope with other retailing activities and logistics [31]. Particularly, in the e-commerce environment, economies of scale in logistics are increasingly significant. For example, JD's self-logistic network has operated for 9 years and covers 98% of consumers in China; this powerful logistics network and the continuous technological innovation will provide substantial economies of scale for JD. As common in the literature, we further normalize the production cost of the manufacturer to zero due to her production advantage. This assumption aims to simplify the mathematical derivations of the model while preserving the fundamental qualitative results in the problem.

Given the above considerations, the manufacturer's profit is related to the profit from the e-channels, sales in the traditional channel, and the spillover effect from the e-channels to the traditional channel and is given as

$$\pi_M = 1 \cdot (\bar{Q} + \tau Q_E) + w q_r + (1 - \delta)(p_m - c)q_m, \quad (1)$$

where δ denotes the agency fee from the manufacturer to the agency e-tailer and is assumed to be an exogenous factor since the platform fee is generally a longer-term and larger-scale decision as compared to the pricing strategy. Besides, the agency fee charged by the e-tailer is mainly related to the product category, which means that it will not be adjusted for one specific manufacturer or one specific type of product. For instance, JD charges 7% for clothes and shoes and 10% for audiovisual products; Amazon charges 12% to 30% for e-book [33]. Considering the revenue from the agent fee and combining the sales revenue from the reselling channel, the profit function of the e-tailer can be formulated as

$$\pi_E = q_r(p_r - w) + \delta(p_m - c)q_m. \quad (2)$$

Then, the profit of the supply chain is given by

$$\pi_T = \pi_E + \pi_M = (p_m - c)q_m + p_r q_r + 1 \cdot (\bar{Q} + \tau Q_E). \quad (3)$$

For most cases in the multichannel supply chain, the manufacturer usually holds more market power than the e-tailer, because the manufacturer produces and owns the products, and first decides the wholesale price in the reselling channel and the retail price in the agency selling channel. Thus, the manufacturer is the leader, and the e-tailer is the follower, which constitutes a typical Stackelberg game. The sequence of events is as follows: first, the manufacturer determines the wholesale price w under a wholesale contract and the retail price p_m under an agency contract simultaneously; then, given the manufacturer's wholesale price w and retail price p_m , the e-tailer sets his

retail price p_r in the reselling channel; and finally, the profits of the manufacturer and the e-tailer are realized.

By backward induction, the e-tailer's response function to the manufacturer's announcement of w and p_m can be obtained by setting $(\partial\pi_E/\partial p_r) = 0$ and is given as

$$p_r = \frac{1}{2}(\alpha_r + w + \gamma p_m + \delta\gamma p_m - \delta\gamma c). \quad (4)$$

$$\begin{aligned} \pi_M(w, p_m) = & \bar{Q} + \tau\left(\frac{1}{2}\gamma(\delta(1-\gamma)(c-p_m) + p_m(1+\gamma) + w + \alpha_r) - p_m + \frac{1}{2}(\alpha_r - w) + \alpha_m\right) \\ & + \frac{1}{2}(\gamma p_r(1-\delta) + c\delta\gamma + \alpha_r - w)w + (1-\delta)\left(\frac{1}{2}\gamma\left(\gamma p_m(1+\delta) + w + \alpha_r - c\delta\gamma\right)\right) \\ & - p_m + \alpha_m)(p_m - c). \end{aligned} \quad (5)$$

Then, the manufacturer decides the optimal wholesale price w and the retail price p_m . Before maximizing the profit, we should assure that the function in (5) is concave in w and p_m . The Hessian matrix of (5) is

$$H_{\pi_M}(w, p_m) = \begin{pmatrix} -1 & (1-\delta)\gamma \\ (1-\delta)\gamma & (1-\delta)(\gamma^2(1+\delta) - 2) \end{pmatrix}. \quad (6)$$

The first-order principal minor of matrix H_{π_M} in (6) is -1 , and the second-order one is $2(1-\delta)(1-\gamma^2)$. Because $0 < \delta < 1$ and $0 < \gamma < 1$, it is clear that $2(1-\delta)(1-\gamma^2) > 0$. Therefore, the matrix H_{π_M} is negative definite, meaning that the profit function of the manufacturer is concave and has a unique maximum solution. The marginal profit can be calculated as

$$\frac{\partial\pi_M}{\partial w} = (1-\delta)\gamma p_m - w + A_1, \quad (7)$$

$$\frac{\partial\pi_M}{\partial p_m} = (1-\delta)(\gamma^2(1+\delta) - 2)p_m + (1-\delta)\gamma w + A_2,$$

where $A_1 = (1/2)(\alpha_r + 2c\delta\gamma - \gamma c - \tau(1-\gamma))$ and $A_2 = (\tau/2)(\gamma^2(1+\delta) + \gamma(1-\delta) - 2) + (1-\delta)(\gamma/2$

The manufacturer makes decisions based on the response function. We substitute (4) into the manufacturer's profit function in (1) and obtain

$(\alpha_r - c\delta\gamma) + \alpha_m - (\gamma^2/2(1+\delta) - 1)c$. Then, the manufacturer's equilibrium can be obtained via the first-order conditions and is given as

$$w^* = \frac{A_1(2 - \gamma^2(1+\delta)) + A_2\gamma}{2(1-\gamma^2)}, \quad (8)$$

$$p_m^* = \frac{A_2 + A_1\gamma(1-\delta)}{2(1-\delta)(1-\gamma^2)}. \quad (9)$$

Substituting (8) and (9) into (4), the e-tailer's optimal retail price can be generated and is presented as

$$p_r^* = \frac{(c\delta^2\gamma + \alpha_r)(1-\gamma^2) + \delta(c\gamma^3 + \alpha_r(1-\gamma^2) - c\gamma - A_1) + A_1 + A_2\gamma}{2(1-\delta)(1-\gamma^2)}. \quad (10)$$

Then, we can obtain the profits of the manufacturer, the e-tailer, and the supply chain in this unique static equilibrium by substituting (8) and (10) into the profit functions in (1)–(3), which are given as

$$\begin{aligned} \pi_M = & 1 * \left(\bar{Q} + \tau(\alpha_r - p_r^* + \gamma p_m^* + \alpha_m - p_m^* + \gamma p_r^*) \right) + w^* (\alpha_r - p_r^* + \gamma p_m^*) \\ & + (1-\delta)(p_m^* - c)(\alpha_m - p_m^* + \gamma p_r^*), \\ \pi_E = & (p_r^* - w^*)(\alpha_r - p_r^* + \gamma p_m^*) + \delta(p_m^* - c)(\alpha_m - p_m^* + \gamma p_r^*), \\ \pi_T = & (p_m^* - c)(\alpha_m - p_m^* + \gamma p_r^*) + p_r^* (\alpha_r - p_r^* + \gamma p_m^*) \\ & + 1 * \left(\bar{Q} + \tau(\alpha_r - p_r^* + \gamma p_m^* + \alpha_m - p_m^* + \gamma p_r^*) \right). \end{aligned} \quad (11)$$

Corollary 1. *The wholesale price w and the retail prices p_m and p_r all decrease with the spillover effect τ .*

Proof. Since $(\partial w/\partial \tau) = -(1/2)$, $(\partial p_m/\partial \tau) = -(2 - \gamma^2/4(1-\delta)(1-\gamma^2))$, and $(\partial p_r/\partial \tau) = -((\gamma(2-\gamma-\gamma^2 + \gamma\delta(1-$

$\delta)) + (1-\gamma)(1-\delta))/(4(1-\delta)(1-\gamma^2)))$, one can obtain the results of Corollary 1. The proof is complete.

Corollary 1 depicts the impacts of spillover effect on the optimal decisions of both the manufacturer and the e-tailer under the framework of static game. Results show that the manufacturer's optimal wholesale price w decreases with the

spillover effect τ . Besides, as spillover effect increases, the manufacturer will markedly increase the sale quantities through the e-channels to simulate the offline sales. The intuition is that as the wholesale price w and the retail prices decrease, the e-tailer will be more motivated to sell through online selling. \square

3.2. Dynamic Game. In this section, we focus on the dynamic game which captures the practical background that the manufacturer is boundedly rational and cannot know full information about the market. In this scenario, the bounded rationality will prevent the manufacturer from immediately reaching the Nash equilibrium in (8) and (9). Instead, the manufacturer will obtain the local maximum profit and reach the Nash equilibrium over time. Thus, the manufacturer updates her output next time $t + 1$ on the basis of the expected marginal profit of the current period t . This means that the manufacturer will increase (decrease) her output in the next period if the marginal profit in the current period is positive (negative). This captures that the manufacturer will adjust her pricing decisions based on the local knowledge and estimation for the marginal profit in discrete time periods. Note that as compared to the manufacturer, the e-tailer often has more selling advantage and information. Thus, it is assumed that the e-tailer is fully rational.

And at each period t , once the manufacturer makes decisions on the prices $w(t)$ and $p_m(t)$, the e-tailer can optimally determine the retail price $p_r(t)$ under a static expectation to maximize his profit. Therefore, the optimal retail price can be identified as

$$p_r(t + 1) = \frac{1}{2} (\alpha_r + w(t) + \gamma p_m(t) + \delta \gamma (p_m(t) - c)). \quad (12)$$

At each time period t , the manufacturer adopts the myopic adjustment mechanism (e.g., [34, 35]); that is,

$$\begin{aligned} w(t + 1) &= w(t) + \kappa_w w(t) \frac{\partial \Pi_m(t)}{\partial w(t)}, \\ p_m(t + 1) &= p_m(t) + \kappa_p p_m(t) \frac{\partial \Pi_m(t)}{\partial p_m(t)}, \end{aligned} \quad (13)$$

where κ_w and κ_p , respectively, denote the adjustment speeds of wholesale price and retail price and also represent the manufacturer's management behaviors. $\partial \Pi_m(t) / \partial w(t)$ and $\partial \Pi_m(t) / \partial p_m(t)$ are the marginal profits of the manufacturer at current period. If the marginal profits are equal to 0, the prices $w(t + 1)$ and $p_m(t + 1)$ will not be modified further.

From (8)–(12), the dynamics of this game can be described by the following nonlinear dynamical system T :

$$T: \begin{cases} w(t + 1) = w(t) + \kappa_w w(t) ((1 - \delta) \gamma p_m(t) - w(t) + A_1), \\ p_m(t + 1) = p_m(t) + \kappa_p p_m(t) ((1 - \delta) (\gamma^2 (1 + \delta) - 2) p_m(t) + (1 - \delta) \gamma w(t) + A_2), \end{cases} \quad (14)$$

where $A_1 = (1/2) (\alpha_r + 2c\delta\gamma - \gamma c - \tau(1 - \gamma))$ and $A_2 = (\tau/2) (\gamma^2 (1 + \delta) + \gamma(1 - \delta) - 2) + (1 - \delta) ((\gamma/2) (\alpha_r - c\delta\gamma) + \alpha_m - ((\gamma^2/2) (1 + \delta) - 1)c)$.

In the following sections, we will analyze the dynamic behaviors of dynamic game system (14).

3.3. Equilibrium Points and Stability. The equilibrium of system (14) can be obtained as $w(t + 1) = w(t)$ and $p_m(t + 1) = p_m(t)$. The system has four equilibrium points as follows: $E_0 = (0, 0)$, $E_1 = (A_1, 0)$, $E_2 = (0, (A_2 / ((1 - \delta) (2 - \delta\gamma^2 - \gamma^2))))$, and $E^* = (w^*, p_m^*) = (((A_1 (2 - \gamma^2 (1 +$

$\delta)) + A_2\gamma) / (2(1 - \gamma^2)))$, $((A_2 + A_1\gamma(1 - \delta)) / (2(1 - \delta)(1 - \gamma^2)))$. Note that E_0 , E_1 , and E_2 are boundary equilibria, which is not in line with reality since the manufacturer will never adopt a zero price on w or p_m . As a result, we only focus on E^* , which is the unique interior equilibrium of the two-dimensional dynamic system (14) and is also the static game equilibrium in the previous section. Next, we will explore the local stability of the fixed point E^* by introducing the Jacobian matrix of the mapping (14) at the point E^* , which is given as

$$J(E^*) := J(w^*, p_m^*) = \begin{pmatrix} 1 - \kappa_w w^* & (1 - \delta) \gamma \kappa_w w^* \\ (1 - \delta) \gamma \kappa_p p_m^* & 1 + (1 - \delta) (\gamma^2 (1 + \delta) - 2) \kappa_p p_m^* \end{pmatrix}. \quad (15)$$

We further analyze the conditions for the local stability of the dynamic game equilibrium point E^* , which are shown in Proposition 1.

Proposition 1. *The equilibrium E^* is locally asymptotically stable, when*

$$\begin{cases} \kappa_p (1 - \delta) p_m^* (\gamma^2 (1 + \delta) + (1 - \gamma^2) \kappa_w w^* - 2) - \kappa_w w^* + 2 > 0, \\ (1 - \delta) \kappa_p p_m^* ((2 - \gamma^2 - \delta\gamma^2) - 2\kappa_w (1 - \gamma^2) w^*) + \kappa_w w^* > 0. \end{cases} \quad (16)$$

Proof. The characteristic equation of the Jacobian matrix at E^* is

$$\lambda^2 - \text{Tr}(J(E^*))\lambda + \text{Det}(J(E^*)) = 0, \quad (17)$$

where $\text{Tr}(J(E^*))$ and $\text{Det}(J(E^*))$, respectively, denote the trace and determinant of $J(E^*)$ and are given as

$$\begin{aligned} \text{Tr}(J) &= 2 - \kappa_w w^* + \kappa_p (1 - \delta) (\gamma^2 (1 + \delta) - 2) p_m^*, \\ \text{Det}(J) &= \kappa_p p_m (2\kappa_w (1 - \gamma^2) w - (2 - \gamma^2 - \delta\gamma^2)) - \kappa_w w + 1, \\ \Delta &= \text{Tr}(J(E^*))^2 - 4\text{Det}(J(E^*)). \end{aligned} \quad (18)$$

Moreover, the eigenvalues of the Jacobian matrix at $E^*(w^*, p_m^*)$ are $\lambda_{1,2} = (-\text{Tr}(J(E^*)) \pm \sqrt{\Delta})/2$ when $\Delta \geq 0$ or $\lambda_{1,2} = (-\text{Tr}(J(E^*)) \pm i\sqrt{-\Delta})/2$ when $\Delta < 0$. Next, we examine the conditions under which the local asymptotical stability of the equilibrium E^* can be guaranteed. According to Jury's stability criterion [36], the equilibrium is locally stable when the eigenvalues of $J(E^*)$ are inside the unit circle. Then, the coefficients of the characteristic polynomial of (17) satisfy the following conditions:

$$\begin{cases} 1 - \text{Tr}(J) + \text{Det}(J) > 0, \\ 1 + \text{Tr}(J) + \text{Det}(J) > 0, \\ 1 - \text{Det}(J) > 0. \end{cases} \quad (19)$$

Note that the first condition $1 - \text{Tr}(J) + \text{Det}(J) = 2\kappa_p \kappa_w p_m w (1 - \delta) (1 - \gamma^2) > 0$ can be naturally satisfied since $\gamma < 1$ and $\delta < 1$. The second condition is equivalent to $2(\kappa_p (1 - \delta) p_m (\gamma^2 (1 + \delta) + (1 - \gamma^2) \kappa_w w - 2) - \kappa_w w + 2) > 0$. For the third condition, it can be transformed into $(1 - \delta) \kappa_p p_m ((2 - \gamma^2 - \delta\gamma^2) - 2\kappa_w (1 - \gamma^2) w) + \kappa_w w > 0$. The proof is complete.

As mentioned above, the equilibrium E^* is locally asymptotically stable only when the three inequalities in (19) hold simultaneously. According to the nonlinear dynamic system theory, the equilibrium will lose its stability if any one of them changes from an inequality to an equality with the other two remaining unchanged [37, 38]. Therefore, these bifurcations exist: the system represents a transcritical, a fold (saddle-node), or a pitchfork bifurcation if $1 - \text{Tr}(J) + \text{Det}(J) = 0$, which is excluded from the system parameter values in this paper; the stability is lost through a flip bifurcation if $1 + \text{Tr}(J) + \text{Det}(J) = 0$; otherwise, the stability is lost through a Neimark–Sacker bifurcation if $1 - \text{Det}(J) = 0$. In other words, the three conditions, respectively, point to a transcritical, a fold (saddle-node), or a pitchfork bifurcation curve, flip bifurcation curve, and Neimark–Sacker bifurcation curve. Theoretically, the Neimark–Sacker bifurcation will destabilize the equilibrium, which essentially means that the stability of the system changes via a pair of complex eigenvalues within unit modulus. That also implies that both conditions $1 - \text{Det}(J) = 0$ and $\Delta < 0$ should be met together. In our model, the main parameters κ_w , κ_p , and τ are in the following region $\mathcal{P} = \{(\kappa_w, \kappa_p, \tau) : 0 < \kappa_w < 1, 0 < \kappa_p < 1, -1 < \tau < 1\}$, since empirical studies show that realistic values are in this range (see, e.g., [7, 10, 39]). In the simulation, the points $p \in \mathcal{P}$ which satisfy $1 - \text{Det}(J) = 0$ but cannot meet $\Delta < 0$. Thus, the Neimark–Sacker bifurcation is also excluded

by the system parameter values in this work (e.g., [40, 41]). \square

3.4. Dynamics Analysis. In this section, we plot the stability region, bifurcation diagrams, basin of attraction, and critical curve to investigate the dynamic behavior of system (14). We provide numerical evidences for the complex dynamical behaviors of system (14) when losing stability and show how the system evolves when the model parameters (mainly the adjustment speed κ_w , κ_p , agency fee δ , and spillover parameter τ) adopt different values. We set the basic parameters as follows: $\alpha_r = \alpha_m = 10$, $\gamma = 0.2$, $w(0) = 6.02$, $p_m(0) = 6.75$, and $c = 1$. The simulated data used for carrying out the study are assumed to represent the real-world conditions as close as possible. Additionally, the data can ensure the existence of the equilibrium solution under full rationality.

First, we analyze the impacts of spillover effect on the stability. According to the Jury stability condition in (19), the 2D and 3D stable regions are depicted in Figure 1. If one of the four adjustment parameters is fixed, the stable condition can be plotted in a 3D space. Figure 1(a) shows the 3D stability region of the adjustment speeds (κ_w, κ_p) and τ when $\delta = 0.2$. If the values of (κ_w, κ_p , and τ) are in this region, system (14) will be stable at a fixed point; if any values of (κ_w, κ_p , and τ) do not belong to the 3D region, the system will lose its stability. In addition, Figure 1(b) reports the impacts of spillover effect on the system stability with τ taking various values and other parameter values remaining constant. As shown in Figure 1 that as τ increases, the intersection of the bifurcation curve with κ_w -axis moves rightwards and that with κ_p -axis moves upwards, which indicates that the size of the stability region increases in τ . This implies that the increase in τ benefits the local stability of the dynamic system, and from a practical view, a greater spillover effect from online to offline sales pushes the “competition” business alliance towards a more coordinated outcome.

Furthermore, we analyze the effects of the agency fee on the stability. Similar to the spillover effect, the increase in the agency fee δ is more beneficial to the local stability of the dynamic system, as shown in Figure 2. The results show that the stable range of δ changes more in δ than that of τ , which means that the agency fee has more influence on the stability than spillover effect. To show the dynamic behavior of this deterministic system when the equilibrium point loses its stability, we simulate the evolution process with respect to the wholesale price adjustment speed.

Figures 3 and 4 help to find the reciprocal effect of the wholesale price adjustment speed, spillover effect, and agency fee. Figure 3 shows the bifurcation phenomenon of pricing strategy in a 3D space with respect to the wholesale price adjustment speed κ_w and τ . The bifurcation graphs in red, green, and blue represent $\tau = -0.2$, $\tau = -0.1$, and $\tau = 0.1$, respectively. With the increase of τ , the value of κ_w where the dynamic system (14) exhibits a period doubling bifurcation increases, which will give rise to a chaotic dynamic state. The increase of spillover effect expands the

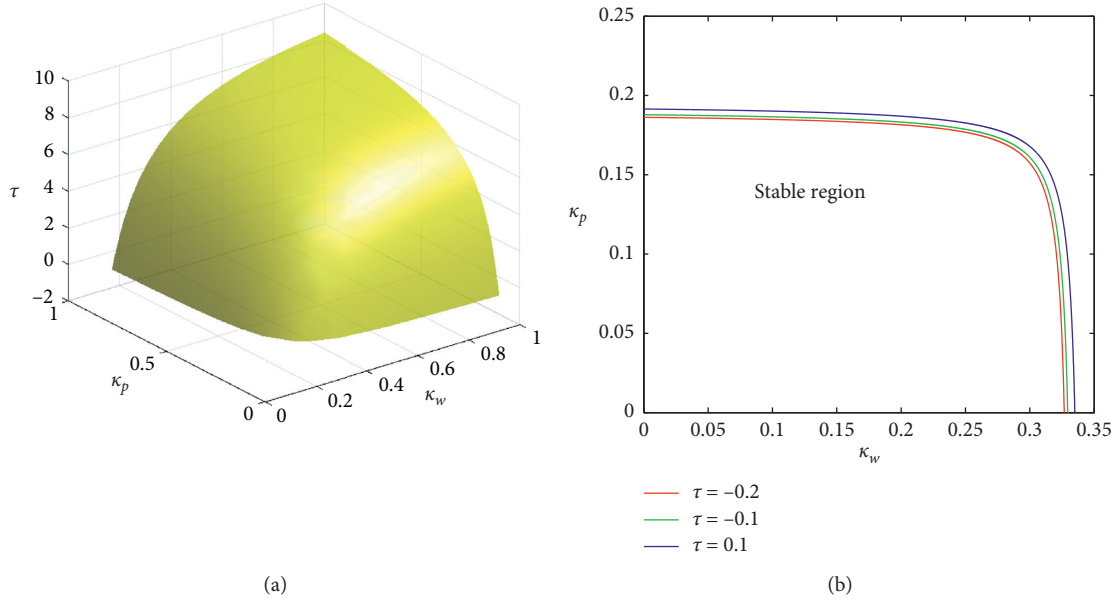


FIGURE 1: Stable region for adjustment speeds and τ . (a) 3D stable region for κ_w , κ_p , and τ , when $\delta = 0.2$. (b) 2D stable region for κ_w and κ_p , when $\delta = 0.2$.

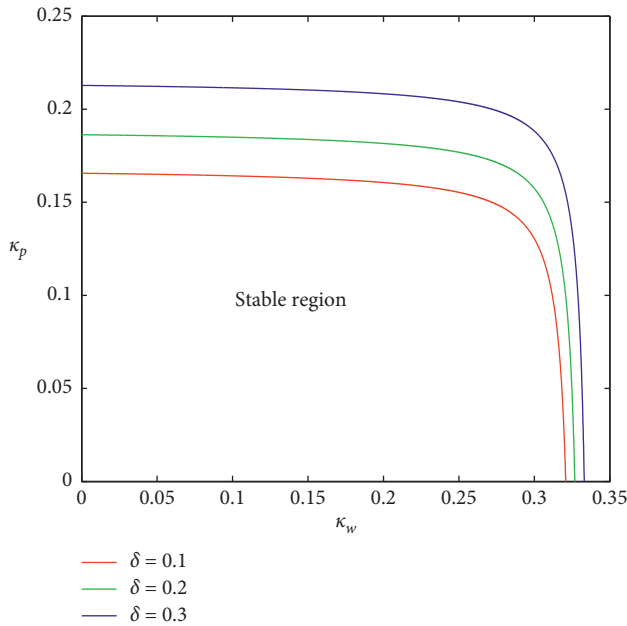


FIGURE 2: 2D stable region for κ_w and κ_p , when $\tau = -0.2$.

stable range of the manufacturer's price adjustment speed, and the pricing decision system will enter into bifurcation and chaos later. This effect is mutual for the wholesale price and the agency selling price. Figure 4 also shows the bifurcation phenomenon in a 3D space with respect to the wholesale price adjustment speed κ_w and δ . The bifurcation graphs in red, green, and blue represent $\delta = 0.1$, $\delta = 0.2$, and $\delta = 0.3$, respectively. Similarly, with the increase of δ , the value of κ_w where chaos occurs also increases. It can be concluded that the increase of the agency fee enlarges the stable range of the manufacturer's price

adjustment speed, and the pricing decision system will lose its stability later.

In order to further study the impacts of the adjustment speeds on the system, the overall system decision-making situation is shown through 2D bifurcation diagram as in Figure 5. In Figure 5, different colors are used to represent stable cycles of different periods. We assign different colors to stable steady states (red); stable cycles of periods 2 (blue), 4 (purple), and 3 (green); chaos (white); and divergence (black). The stable region in Figure 5 is the same as that in Figure 1(b), where the manufacturer's decisions have the same stable region according to Proposition 1. Besides, with the adjustment speeds increasing, the system goes into chaos through period doubling and finally disappears. Over high adjustment speeds for the manufacturer do not benefit the system's stability, which is shown clearly in the figures. By comparing the sizes of stable regions, we can see the different capacity of the models for maintaining the system stability. Figures 5(a)–5(d) all show that spillover effect benefits the system's stability.

The above analysis of bifurcation and chaos provides some managerial insights into pricing, spillover effect, and agency fee. The increase of any adjustment speed may make the system from a stable state to a periodic state or a chaotic state, causing the decision variables to suffer from a large fluctuation. However, a higher agency fee and higher spillover effect bring more price adjustment space.

3.5. Global Analysis. In the previous section, we limit the scope of local analysis to a small neighborhood near the equilibrium point. Nevertheless, because of the manufacturer's subjective judgement of the market under limited information at the beginning of the game, the initial values of the state variables (i.e., the initial pricing strategies) may not belong to such a neighborhood. As a result, it is

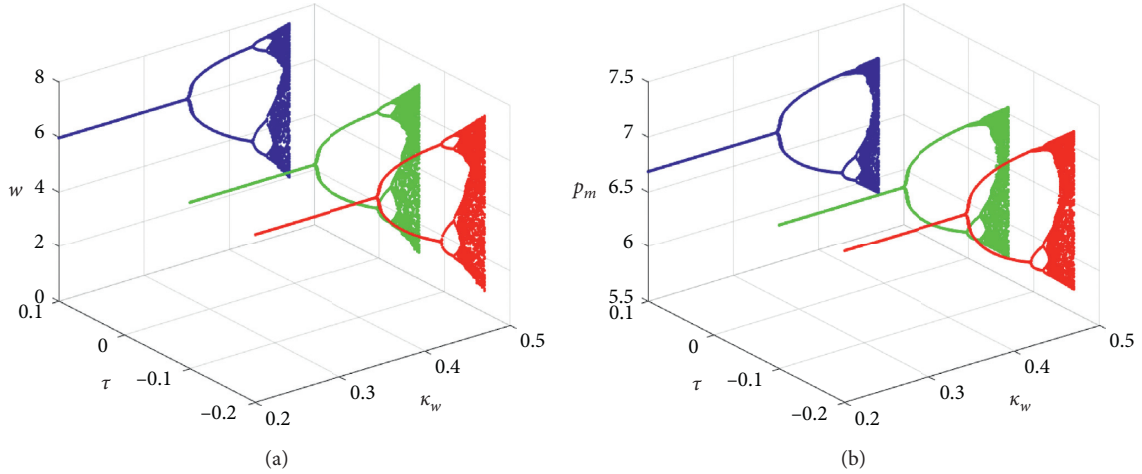


FIGURE 3: 3D bifurcation diagrams of w in (a) and p_m in (b) with respect to κ_w and τ , when $\kappa_p = 0.14$ and $\delta = 0.2$.

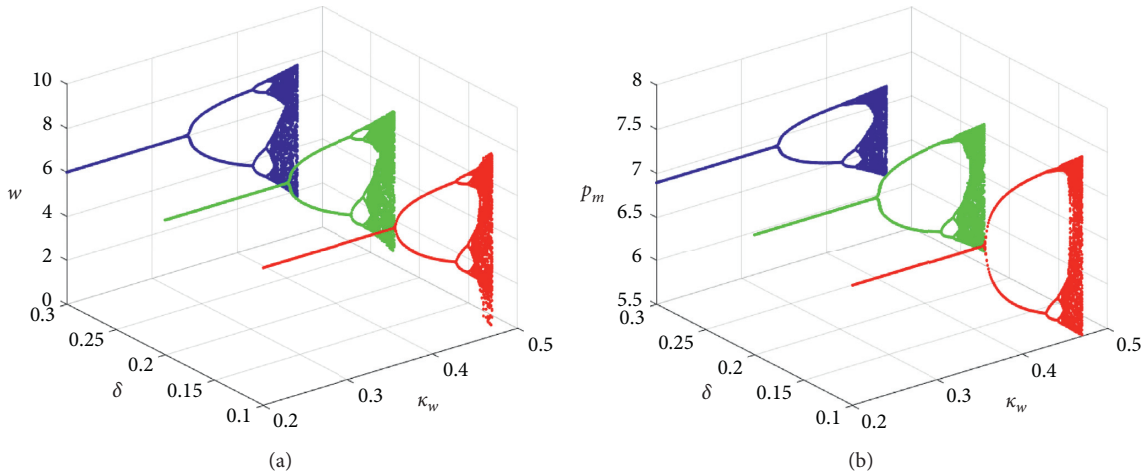


FIGURE 4: 3D bifurcation diagrams of w in (a) and p_m in (b) with respect to κ_w and δ , when $\kappa_p = 0.14$ and $\tau = -0.2$.

significant to apply the global analysis method, which has been widely proposed by some previous researches, such as Mira et al. [42]; Agliari et al. [43]; Andaluz and Jarne [44]; Bischi and Kopel [45]; and Bischi et al. [46] to explore the long-run behaviors of the dynamic game system (14). In this study, a flip (period doubling) bifurcation will destabilize the equilibrium, which essentially means that the stability of the system changes via a real eigenvalue -1 . Thus, there is a flip-type bifurcation that can produce periodic and chaotic attractors around the unstable equilibrium. In the following, we will focus on three important concepts belonging to the global dynamics in a two-dimensional noninvertible mapping, i.e., attractors, critical curves, and basins of attraction, to analyze the equilibrium from the perspective of global dynamics.

The role of a basin of attraction is to serve as a guideline, which can ensure that the initial pricing strategies belonging to the domain of the attraction converge to the same attractor. For better illustration, Figure 6 shows the basin of attraction for the dynamic game system (14). Note that the dynamic process has practical significance only when the

condition $S = \{(w, p_m) \in \mathbb{R}^2: w > 0, p_m > 0\}$ is satisfied, and this is worth further studying. If we define system (14) as a mapping T , which is noninvertible, then the rank-1 preimage may not exist or may be multivalued for a given $(w(t+1), p_m(t+1))$. As the point $(w(t+1), p_m(t+1))$ varies in the plane S , the number of solutions of system (14), i.e., the number of the rank-one preimages of $(w(t+1), p_m(t+1))$, changes. Pairs of real preimages appear or disappear as the points $(w(t+1), p_m(t+1))$ cross the boundary separating regions whose points have a different number of preimages. Such boundaries generally characterized by the presence of two merging preimages are called critical curves. The critical curves are defined as the locus of points having two or more coincident rank-1 preimages. LC is the two-dimensional generalization of the notion of critical value (local minimum of maximum value), which means that critical curves may be used in order to bound chaotic attractors or in order to detect global bifurcations that cause a qualitative change in the topological structure of basins of attraction, such as the creation of nonconnected basins (e.g., [42, 45, 47, 48]). To be specific,

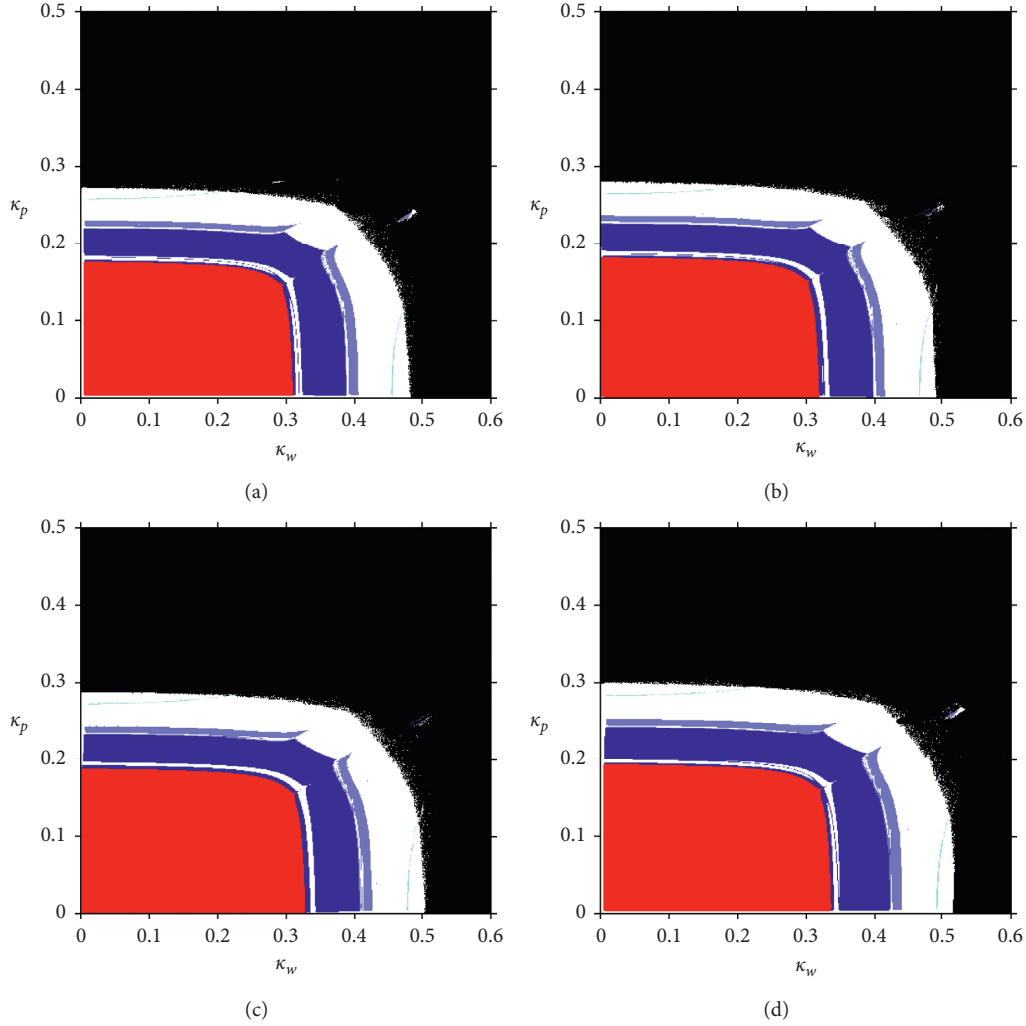


FIGURE 5: 2D bifurcation diagrams with respect to κ_w and κ_p , under different τ . (a) $\tau = -0.5$. (b) $\tau = -0.2$. (c) $\tau = 0.1$. (d) $\tau = 0.5$.

due to the binary quadratic character of the system, there is a fourth-degree algebraic equation with no, two, or four solutions when we solve $(w(t), p_m(t))$ by means of $(w(t+1), p_m(t+1))$ in the mapping T . The direct result is that the space of R^2 is divided into different regions, which are represented by Z_i (i being the number of rank-1 preimages) and are specified by some boundaries composed of at least two preimages. For instance, $(w(t), p_m(t))$ in region Z_2 has 2 preimages $(w(t-1), p_m(t-1))$. In Figure 6, the symbols Z_0 , Z_2 , and Z_4 refer to the 0-, 2-, and 4-solution regions, respectively. It is intuitive to find that the region is divided into three parts with two critical curves $LC^{(a)}$ and $LC^{(b)}$. Next, we will introduce another curve represented by LC_{-1} , which is the rank-1 preimage of LC under T , i.e., $T(LC_{-1}) = LC$, to obtain the critical curve LC . When the Jacobian determinant of T vanishes, the curve LC_{-1} generally belongs to the locus of points; that is,

$$LC_{-1} \subseteq \{(w, p_m) : \text{Det}(J)(w, p_m) = 0\}. \quad (20)$$

Note that the curve LC_{-1} can be defined as a function of (w, p_m) when the parameters κ_w , κ_p , and δ are fixed. We find that LC_{-1} is a hyperbola with two branches represented by

LC_{-1}^a and LC_{-1}^b , respectively. And LC is the union of two branches denoted as $LC^a = T(LC_{-1}^a)$ and $LC^b = T(LC_{-1}^b)$.

Figure 6 depicts the evolution process of the attractors (red dot) and basins of attractors (green region), where the red dotted curves and blue solid curves stand for LC_{-1} and LC , respectively. Some conclusions can be obtained by comparing Figures 6(a)–6(d). First of all, it is obvious to observe that when the wholesale price adjustment speed gets larger, the attractor becomes more complex and its basins shrink. Besides, the system will be more easier to collapse as the wholesale price adjustment speed increases. To be more specific, with a relatively small wholesale price adjustment speed as shown in Figure 6(a), the attractor is a single point set, which corresponds to a global asymptotically stable equilibrium. As the wholesale price adjustment speed increases as shown in Figure 6(b), the attractor turns to be the set with only two elements, corresponding to a two-period cycle. When the wholesale price adjustment speed is large enough, as depicted in Figures 6(c) and 6(d), the sets with uncountable elements which correspond to chaotic attractors will occur. From Figure 6, we can observe that the LC curves constitute the boundary (or the envelope) of the attractor.

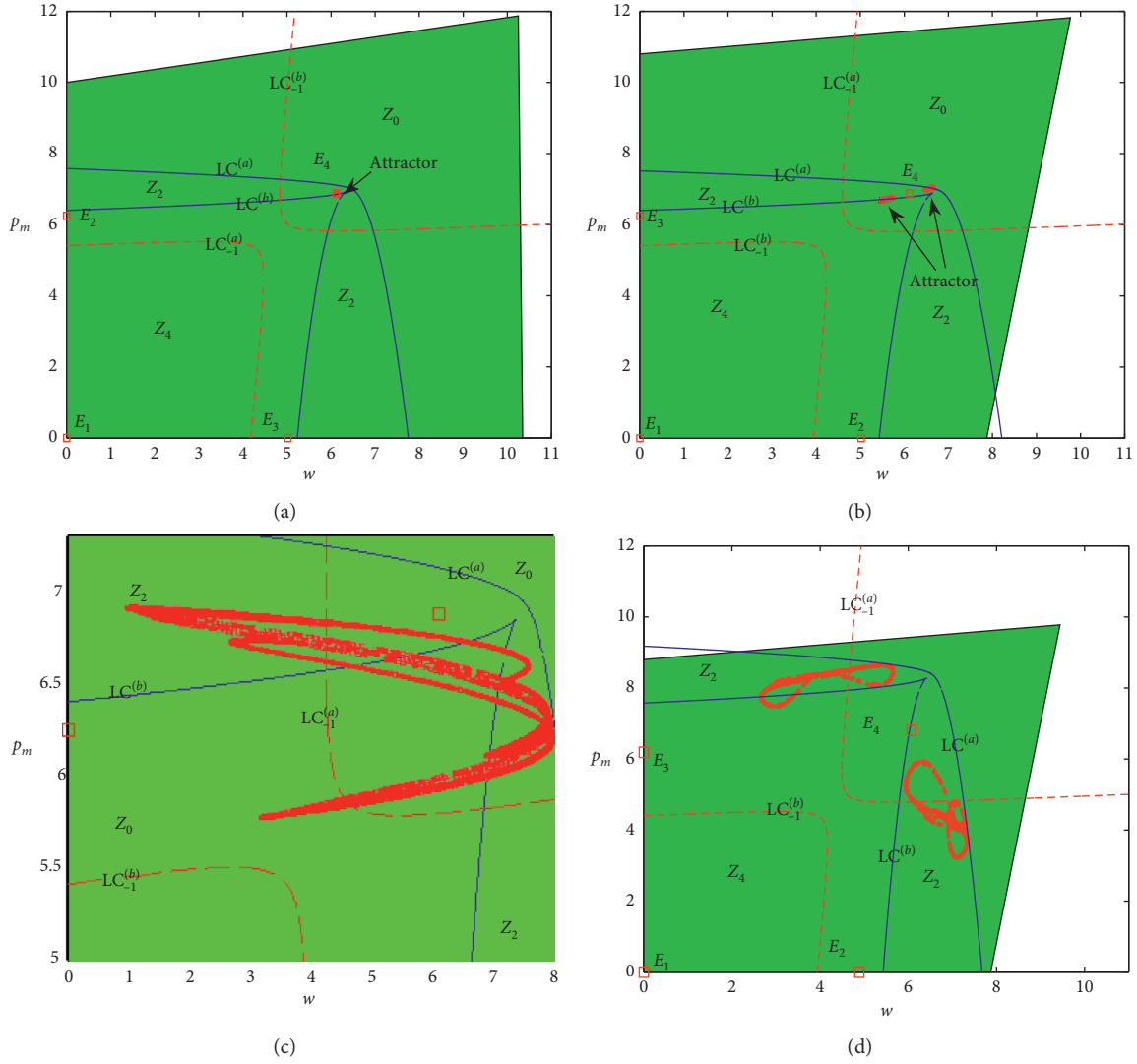


FIGURE 6: Attractors (red dot) and basins of attractors (green region) where LC^a and LC^b are represented by blue solid line, and LC_{-1}^a and LC_{-1}^b are represented by red dotted line when $\delta = 0.2$. These curves of LC separate the plane into three regions, denoted by Z_4 , Z_2 , and Z_0 whose points have four, two, and no rank-1 preimages, respectively. (a) $\kappa_w = 0.3, \kappa_p = 0.14, \tau = -0.2$. (b) $\kappa_w = 0.35, \kappa_p = 0.14, \tau = -0.2$. (c) $\kappa_w = 0.455, \kappa_p = 0.14, \tau = -0.2$. (d) $\kappa_w = 0.35, \kappa_p = 0.25, \tau = -0.1$.

To verify that an observable chaos occurs for such values of κ_w and κ_p in Figures 6(c) and 6(d). We plot the Largest Lyapunov Exponent (LLE) in the interval $\kappa_w \in [0.454, 0.4555]$. As $LLE > 0$, the mapping exhibits an observable chaos in the sense that it has attractors. That means that the system is in chaotic state. From Figure 7, it can be seen that $LLE > 0$ when $\kappa_w = 0.455$. This means that the red attractors in Figure 6(c) are chaotic attractors. For the attractors in Figure 6(d), we have made a verification similar to Figure 6(c), and thus the details are omitted here.

The time series corresponding to Figure 6 are described in Figure 8, where the blue series and the red series stand for retail price p_m and wholesale price w , respectively. As shown in Figure 8(a), the system converges to the equilibrium point after a few periods when the adjustment speed is relatively low. In other words, the pricing strategies of the dynamic

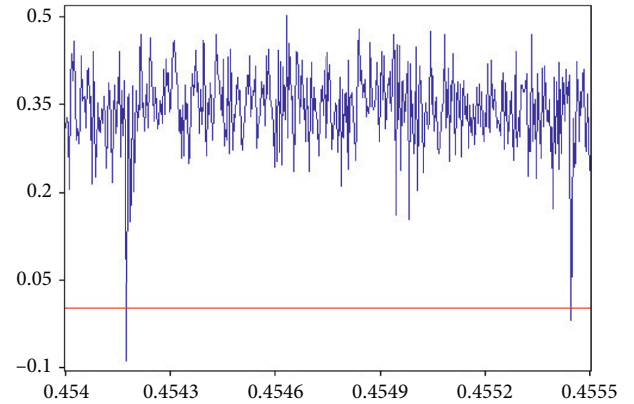


FIGURE 7: LLE with respect to κ_w in $[0.454, 0.4555]$, with $\kappa = 0.14$ and $\tau = -0.2$.

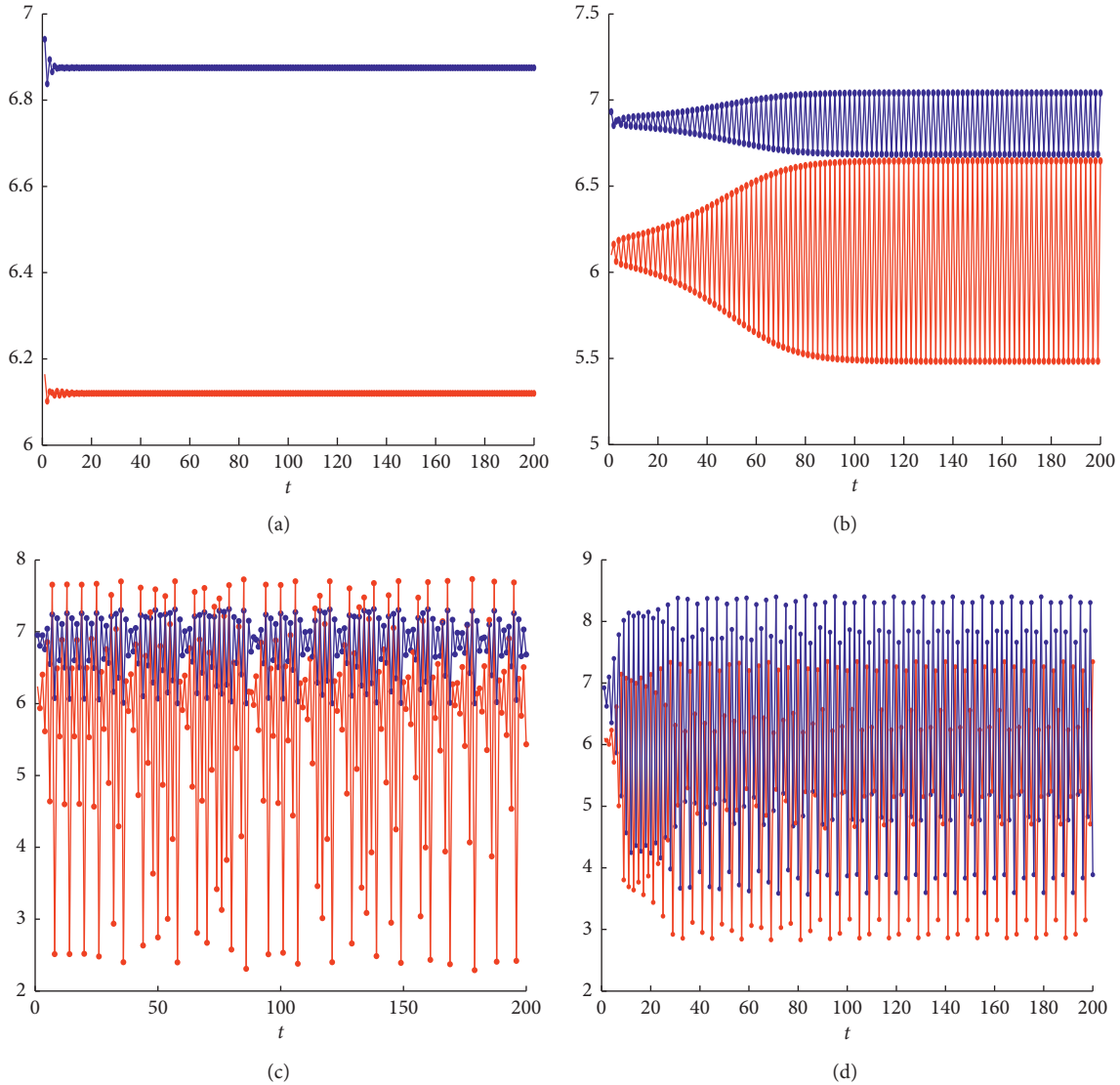


FIGURE 8: Time series of w (red dot) and p_m (blue dot) corresponding to Figure 6. (a) $\kappa_w = 0.3, \kappa_p = 0.14, \tau = -0.2$. (b) $\kappa_w = 0.35, \kappa_p = 0.14, \tau = -0.2$. (c) $\kappa_w = 0.445, \kappa_p = 0.14, \tau = -0.2$. (d) $\kappa_w = 0.35, \kappa_p = 0.25, \tau = -0.1$.

repeated game will eventually converge to the same equilibrium state as that of the static one-shot game. As shown in Figure 8(b), the evolution trajectory becomes periodic as the wholesale price adjustment speed increases, meaning that the prices are adjusted periodically. Furthermore, as shown in Figures 8(c) and 8(d), the chaos will occur when the wholesale price adjustment speed gets even higher. Under this situation, the prices over time are irregular, which rely on the initial strategy values sensitively. As a consequence, it is difficult for the manufacturer to implement stable long-term pricing strategies, indicating that the manufacturer should set the wholesale price adjustment speed carefully. Note that in the case of chaos, the manufacturer takes irregular and unpredictable pricing strategies with the wholesale price w being “randomly” larger or smaller than the agency selling price p_m , which leads to a “randomly” larger or smaller retail price p_r as compared to the agency selling price p_m .

3.6. Performance Comparison. This section investigates the effects of critical parameters on the supply chain members’ profits and further compares the performance of the dynamic game with that of the static game. It should be noted that the game process may evolve to complex dynamics including periodic or chaotic state under the dynamic game, meaning that the profits of the supply chain members are generally unpredictable. As a consequence, we need to calculate the average profits to make a further comparison. To reach the goal, we adopt 10^3 game outcomes (strategy points) in the chaotic attractor and set the initial strategies randomly. The initial strategies should ensure the existence of the game equilibria under full rationality, and we find this initial strategy values will not essentially affect the members’ profits. Figures 9 and 10 depict the performances of the dynamic repeated game and the static one-shot game intuitively, which are denoted by the solid curves and the dotted lines, respectively. Besides, in both figures, the profits

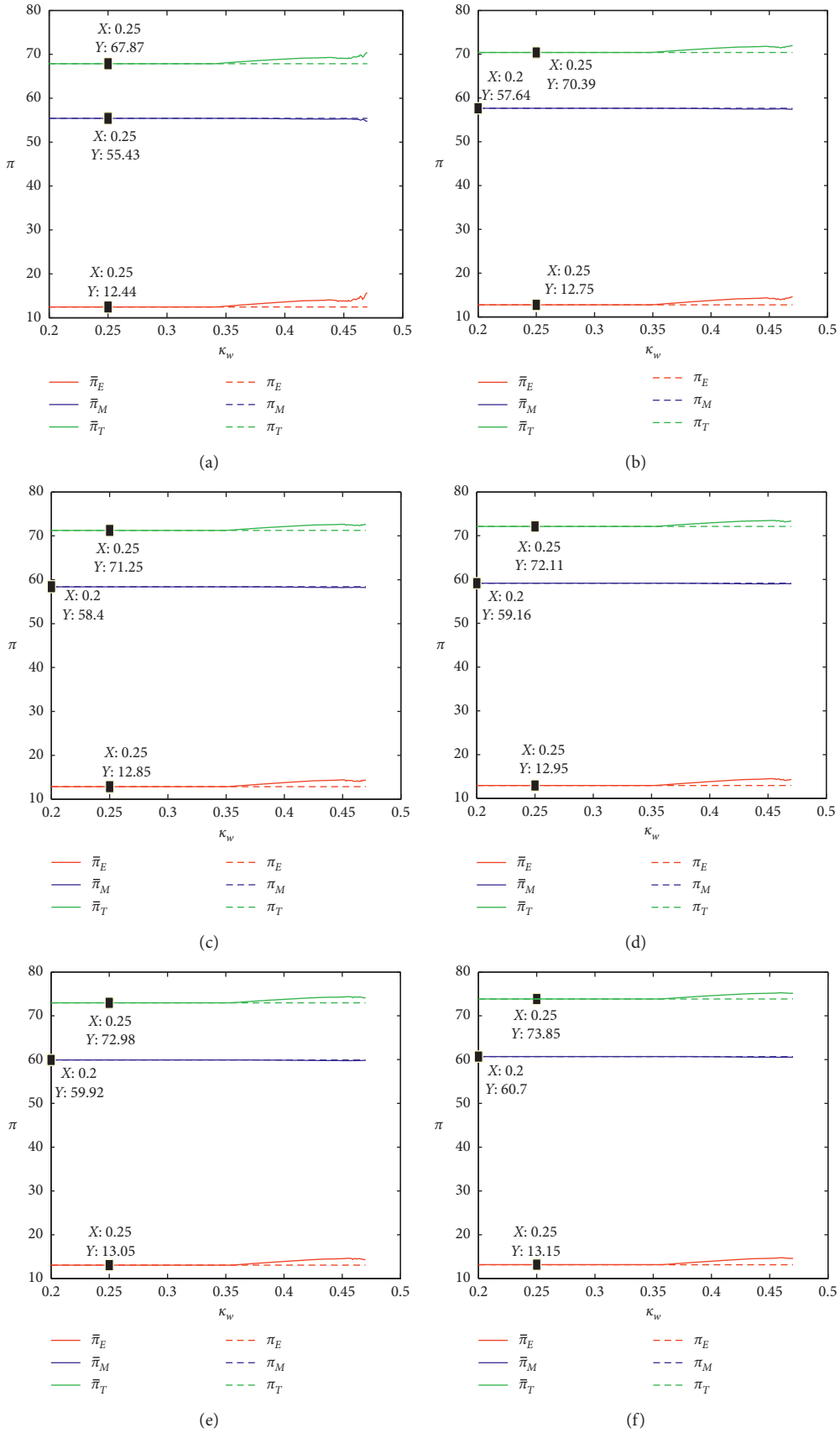


FIGURE 9: Supply chain members' average profits via κ_w under different τ . (a) $\tau = -0.4$. (b) $\tau = -0.1$. (c) $\tau = 0$. (d) $\tau = 0.1$. (e) $\tau = 0.2$. (f) $\tau = 0.3$.

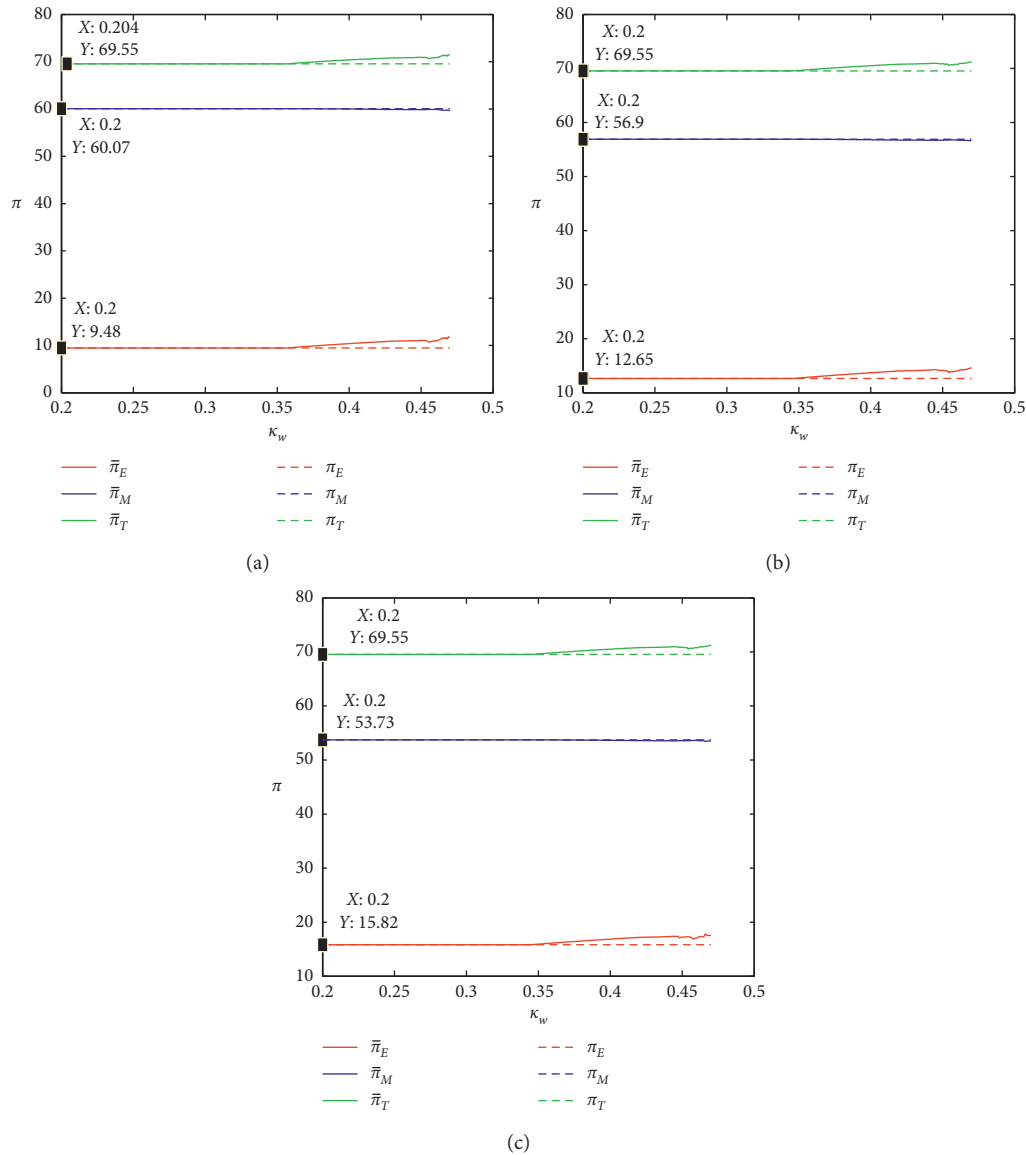


FIGURE 10: Supply chain members' average profits via κ_w under different δ . (a) $\delta = 0.1$. (b) $\delta = 0.2$. (c) $\delta = 0.3$.

of the total supply chain, the manufacturer, and the e-tailer are represented by the green lines, blue lines, and red lines, respectively. Note that we have carried out a large number of numerical examples to verify that the main results would not be influenced qualitatively by the various values of the parameters, which demonstrates that the results are robust.

Figure 9 shows the effects of the manufacturer's wholesale price adjustment speed on the members' and the supply chain's profits for different spillover effect levels. When the system converges to the equilibrium point, the total average profits of the members in the dynamic game are not sensitive to the wholesale price adjustment speed and are the same as those in the static one-shot game. However, when the system is in periodic or chaotic state, the total average profits of the manufacturer and the e-tailer will change. To be specific, as the wholesale price adjustment speed increases, the average profit of the manufacturer in the

dynamic game is almost the same as that in the static game. While for the e-tailer, his average profit will climb up as the wholesale price adjustment speed increases. From the perspective of the whole supply chain, the average profit in the dynamic game increases with the wholesale price adjustment speed and is higher than the profit in the static game. Moreover, by comparing Figures 9(a)–9(f), it is clearly observed that spillover effect has a significant effect on the total average profit, i.e., a higher spillover effect makes the average profits of the members and the whole supply chain increase in the dynamic game, which demonstrates that spillover effect benefits the supply chain performance.

Figure 10 characterizes the effects of the agency fee δ on the profits of the members and the supply chain under both the dynamic and static games. First, the effect of the adjustment speed κ_w on average profits in Figure 10 is similar to that in Figure 9, and thus we will not repeat it. By

comparing Figures 10(a)–10(c), we find that a higher agency fee will harm the manufacturer but benefit the e-tailer. From the perspective of the whole supply chain, its efficiency will not essentially change with the agency fee.

The joint observations of Figures 9 and 10 show that as compared to the outcomes under the equilibrium strategy in the static game, the e-tailer's profit in the repeated game is always higher, and the manufacturer's profit is identical. This implies that bounded rationality can mitigate the competition between the two members and encourage the e-tailer to introduce the agency selling channel. Particularly, a win-win outcome occurs in a certain interval of κ_w as presented where the whole supply chain's profit in the dynamic game is higher than the equilibrium profit in the static game. This dynamic pricing process provided by the manufacturer can effectively encourage the e-tailer to participate in multi-channel selling, which is different from the common conclusion that the equilibrium profit in the static game is the first-best outcome (e.g., [10]).

4. Conclusion

With the rapid development of e-commerce, upstream manufacturers often cooperate with e-tailers to sell their products in two online modes (reselling and agency selling modes) in addition to the traditional offline channel (i.e., the brick-and-mortar channel), and the multichannel supply chain structure is a common setting in practice. The introduction of multi-online channels is inevitably accompanied by spillover effect; that is, the sales in the offline channel are affected by the sales in the online channels. The spillover effect which can stimulate offline demand or decrease offline demand (the cannibalization effect) will significantly affect pricing strategies in the supply chain. This paper incorporates the spillover effect from online to offline sales into the pricing game in a multichannel supply chain. In this study, combined with the spillover effect, we mainly focus on a dynamic repeated game process for the decision makers with bounded rationality, which is different from the existing researches with the assumption of fully rational players. By virtue of the nonlinear system theory, we investigate the impacts of critical system parameters (such as the level of spillover effect, the adjustment speed, and the agency fee) on the stability, complexity, and efficiency of the dynamic game system.

Some meaningful conclusions emerge after solving and analyzing the model. First, the stability of the dynamic system depends on the wholesale price adjustment speed. When this adjustment speed is relatively low, the dynamic strategies will converge to a static equilibrium point under certain conditions. While as the adjustment speed increases, the attractor of the game system becomes more complex, leading to chaos eventually. Besides, although an excessively high adjustment speed can destabilize the dynamic system, the e-tailer can benefit from this instability, and so as the whole supply chain. The agency fee and the spillover effect have similar effects on the dynamic system, and the system will become more stable if either of them increases. Furthermore, the spillover effect has less

impact on the stability of the dynamic system than the agency fee.

Although some important findings and interesting managerial insights are provided in the paper, there are also some limitations as follows. In this study, we only consider that the manufacturer is a local profit maximizer (bounded rationality) but the e-tailer acts as a global profit maximizer (full rationality). In some practical cases, the e-tailer may also be a local profit maximizer with bounded rationality. Thus, it is of great significance to further explore firms' dynamic pricing strategies considering both chain members' actions under bounded rationality and provide more reasonable operational decisions for firms. In addition, we only focus on the pricing policy in a supply chain and omit the other operational or marketing policies. It may be interesting to include quality improvement or retail service investment policies into the research.

Data Availability

The data used to support the findings of this study are included within the article.

Conflicts of Interest

The authors declare that there are no conflicts of interest regarding the publication of this paper.

Acknowledgments

This work was supported by the National Natural Science Foundation of China (no. 71971152).

References

- [1] eMarketer, *Worldwide Retail and Ecommerce Sales: Emarketer's Updated Forecast and New Mcommerce Estimates for 2016–2021*, eMarketer, New York City, NY, USA, 2018, <https://www.emarketer.com/Report/Worldwide-Retail-Ecommerce-Sales-eMarketers-Updated-Forecast-New-Mcommerce-Estimates-20162021/2002182>.
- [2] M. Bonfils, "Taobao SEO: a guide to one of the world's largest consumer marketplaces," 2012, <http://searchenginewatch.com/article/2200749/Taobao-SEO-A-Guide-to-One-of-the-Worlds-Largest-Consumer-Marketplaces>.
- [3] A. Tiwari, "Flipkart to grow marketplace to compete with amazon. DNA India," 2014, <http://www.dnaindia.com/money/report-?ipkart-to-grow-marketplace-to-compete-with-amazon-1979084>.
- [4] CKGSB, *Will Ecommerce Replace Brick-ortar-hinese-etilers?*, CKGSB, Beijing, China, 2017, <http://knowledge.ckgsb.edu.cn/2017/02/27/retail/will-ecommerce-replace-brick-mortar-chinese-retailers/>.
- [5] C. Daily, "Xiaomi releases mi 6, speeds up offline expansion," 2017, http://m.chinadaily.com.cn/en/2017-04/19/content_28999144.htm.
- [6] CNET, *Xiaomi's Move into Brick-and-Mortar Stores has Paid Off*, CNET, San Francisco, CA, USA, 2017, <https://www.cnet.com/news/xiaomi-hits-its-highest-ever-phone-shipments-for-q2/>.
- [7] V. Abhishek, K. Jerath, and Z. J. Zhang, "Agency selling or reselling? Channel structures in electronic retailing," *Management Science*, vol. 62, no. 8, pp. 2259–2280, 2015.

- [8] Y. Yan, R. Zhao, and T. Xing, "Strategic introduction of the marketplace channel under dual upstream disadvantages in sales efficiency and demand information," *European Journal of Operational Research*, vol. 273, no. 3, pp. 968–982, 2019.
- [9] F. Zhang and C. Wang, "Dynamic pricing strategy and coordination in a dual-channel supply chain considering service value," *Applied Mathematical Modelling*, vol. 54, pp. 722–742, 2018.
- [10] J. Ma and L. Xie, "The comparison and complex analysis on dual-channel supply chain under different channel power structures and uncertain demand," *Nonlinear Dynamics*, vol. 83, no. 3, pp. 1379–1393, 2016.
- [11] Z. Guo, "Complexity and implications on channel conflict under the uncertain impacts of online customer reviews," *Nonlinear Dynamics*, vol. 96, no. 3, pp. 1971–1987, 2019.
- [12] J. Ma, T. Li, and W. Ren, "Research on the complexity of dual-channel supply chain model in competitive retailing service market," *International Journal of Bifurcation and Chaos*, vol. 27, no. 7, Article ID 1750098, 2017.
- [13] A. Naimzada and M. Pireddu, "Fashion cycle dynamics induced by agents' heterogeneity for generic bell-shaped attractiveness functions," *Journal of Difference Equations and Applications*, vol. 25, no. 7, pp. 942–968, 2019.
- [14] A. Naimzada and M. Pireddu, "Eductive stability may not imply evolutionary stability in the presence of information costs," *Economics Letters*, vol. 186, Article ID 108513, 2020.
- [15] L. C. Baiardi and A. K. Naimzada, "An oligopoly model with rational and imitation rules," *Mathematics and Computers in Simulation*, vol. 156, pp. 254–278, 2019.
- [16] L. C. Baiardi, A. K. Naimzada, and A. Panchuk, "Endogenous desired debt in a Minskyan business model," *Chaos, Solitons and Fractals*, vol. 131, Article ID 109470, 2020.
- [17] G. P. Cachon, "The allocation of inventory risk in a supply chain: push, pull, and advance-purchase discount contracts," *Management Science*, vol. 50, no. 2, pp. 222–238, 2004.
- [18] G. Cai, "Channel selection and coordination in dual-channel supply chains," *Journal of Retailing*, vol. 86, no. 1, pp. 22–36, 2010.
- [19] L. Dai, X. Wang, X. Liu, and L. Wei, "Pricing strategies in dual-channel supply chain with a fair caring retailer," *Complexity*, vol. 2019, Article ID 1484372, 23 pages, 2019.
- [20] J. Raju and Z. J. Zhang, "Channel coordination in the presence of a dominant retailer," *Marketing Science*, vol. 24, no. 2, pp. 254–262, 2005.
- [21] Y. Wang and X. Sun, "Dynamic vs. static wholesale pricing strategies in a dual-channel green supply chain," *Complexity*, vol. 2019, Article ID 8497070, 14 pages, 2019.
- [22] R. Yan, "Managing channel coordination in a multi-channel manufacturer-retailer supply chain," *Industrial Marketing Management*, vol. 40, no. 4, pp. 636–642, 2011.
- [23] J. Zhang, G. Liu, Q. Zhang, and Z. Bai, "Coordinating a supply chain for deteriorating items with a revenue sharing and cooperative investment contract," *Omega*, vol. 56, pp. 37–49, 2015.
- [24] S. Zhang and J. Zhang, "Agency selling or reselling: E-tailer information sharing with supplier offline entry," *European Journal of Operational Research*, vol. 280, no. 1, pp. 134–151, 2020.
- [25] Q. Lu, V. Shi, and J. Huang, "Who benefit from agency model: a strategic analysis of pricing models in distribution channels of physical books and e-books," *European Journal of Operational Research*, vol. 264, no. 3, pp. 1074–1091, 2018.
- [26] D. C. Dantas, S. Taboubi, and G. Zaccour, "Which business model for e-book pricing?" *Economics Letters*, vol. 125, no. 1, pp. 126–129, 2014.
- [27] N. Singh and X. Vives, "Price and quantity competition in a differentiated duopoly," *The RAND Journal of Economics*, vol. 15, no. 4, pp. 546–554, 1984.
- [28] C. Chang and Z. Yao, "Comparison between the agency and wholesale model under the e-book duopoly market," *Electronic Commerce Research*, vol. 18, no. 2, pp. 313–337, 2018.
- [29] M. D. Smith and R. Telang, "Piracy or promotion? The impact of broadband internet penetration on DVD sales," *Information Economics and Policy*, vol. 22, no. 4, pp. 289–298, 2010.
- [30] B. Sun, "Online retail sales of China continue to win the first place all over the world in 2015," 2016, <http://finance.people.com.cn/n1/2016/0223/c1004-28143131>.
- [31] A. Arya, B. Mittendorf, and D. E. M. Sappington, "The bright side of supplier encroachment," *Marketing Science*, vol. 26, no. 5, pp. 651–659, 2007.
- [32] Z. Li, S. M. Gilbert, and G. Lai, "Supplier encroachment as an enhancement or a hindrance to nonlinear pricing," *Production and Operations Management*, vol. 24, no. 1, pp. 89–109, 2015.
- [33] R. Wischenbart, "The global ebook report 2015: a report on market trends and developments," Rdiger Wischenbart Content and Consulting, Vienna, Austria, 2015.
- [34] S. S. Askar and K. Alnowibet, "Nonlinear oligopolistic game with isoelastic demand function: rationality and local monopolistic approximation," *Chaos, Solitons & Fractals*, vol. 84, pp. 15–22, 2016.
- [35] A. K. Naimzada and L. Sbragia, "Oligopoly games with nonlinear demand and cost functions: two boundedly rational adjustment processes," *Chaos, Solitons & Fractals*, vol. 29, no. 3, pp. 707–722, 2006.
- [36] T. Puu, *Attractors, Bifurcations and Chaos: Nonlinear Phenomena in Economics, Seconded*, Springer, Berlin, Germany, 2003.
- [37] R. L. Devaney, *An Introduction to Chaotic Dynamical Systems*, Benjamin-Cummings, Menlo Park, CA, USA, 2nd edition, 1989.
- [38] H. W. Lorenz, *Nonlinear Dynamical Economics and Chaotic Motion*, Springer-Verlag, Berlin, Germany, 1989.
- [39] J. Zhou, W. Zhou, T. Chu, Y.-X. Chang, and M.-J. Huang, "Bifurcation, intermittent chaos and multi-stability in a two-stage Cournot game with R&D spillover and product differentiation," *Applied Mathematics and Computation*, vol. 341, pp. 358–378, 2019.
- [40] A. E. Matouk, A. A. Elsadany, and B. Xin, "Neimark-Sacker bifurcation analysis and complex nonlinear dynamics in a heterogeneous quadropoly game with an isoelastic demand function," *Nonlinear Dynamics*, vol. 89, no. 4, pp. 2533–2552, 2015.
- [41] B. Xin and Z. Wu, "Neimark-Sacker bifurcation analysis and 0-1 chaos test of an interactions model between industrial production and environmental quality in a closed area," *Sustainability*, vol. 7, no. 8, pp. 10191–10209, 2015.
- [42] C. Mira, L. Gardini, A. Barugola, and J. C. Cathala, *Chaotic Dynamics in Two-Dimensional Noninvertible Maps*, World Scientific, Singapore, 1996.
- [43] A. Agliari, G.-I. Bischi, R. Dieci, and L. Gardini, "Global bifurcations of closed invariant curves in two-dimensional maps: a computer assisted study," *International Journal of Bifurcation and Chaos*, vol. 15, no. 4, pp. 1285–1328, 2005.
- [44] J. Andaluz and G. Jarne, "Stability of vertically differentiated Cournot and Bertrand-type models when firms are boundedly rational," *Annals of Operations Research*, vol. 238, no. 1–2, pp. 1–25, 2016.

- [45] G. I. Bischi and M. Kopel, "Equilibrium selection in a non-linear duopoly game with adaptive expectations," *Journal of Economic Behavior & Organization*, vol. 46, no. 1, pp. 73–100, 2001.
- [46] G. I. Bischi, C. Chiarella, and I. Sushko, *Global Analysis of Dynamic Models in Economics and Finance: Essays in Honour of Laura Gardini*, Springer-Verlag, Berlin, Germany, 2013.
- [47] A. Gardini, G. I. Bischi, and L. Gardini, "Some methods for the global analysis of dynamic games represented by iterated noninvertible maps," in *Oligopoly Dynamics: Models and Tools*, pp. 31–83, Springer, Berlin, Heidelberg, 2002.
- [48] G. I. Bischi, L. Gardini, and M. Kopel, "Analysis of global bifurcations in a market share attraction model," *Journal of Economic Dynamics and Control*, vol. 24, no. 5–7, pp. 855–879, 2000.

Research Article

Dynamic Investigation in Green Supply Chain considering Channel Service

Qiuxiang Li ¹, Mengmeng Li,² and Yimin Huang ³

¹Institute of Management Science and Engineering, Henan University, Kaifeng 475004, China

²School of Business, Henan University, Kaifeng 475004, China

³School of Management & Economics, North China University of Water Resources and Electric Power, Zhengzhou 450046, China

Correspondence should be addressed to Yimin Huang; huang800526@163.com

Received 7 May 2020; Revised 14 June 2020; Accepted 17 June 2020; Published 14 July 2020

Guest Editor: Lei Xie

Copyright © 2020 Qiuxiang Li et al. This is an open access article distributed under the Creative Commons Attribution License, which permits unrestricted use, distribution, and reproduction in any medium, provided the original work is properly cited.

Considering firm's innovation input of green products and channel service, this paper, in dynamic environment, studies a dynamic price game model in a dual-channel green supply chain and focuses on the effect of parameter changing on the pricing strategies and complexity of the dynamic system. Using dynamic theory, the complex behaviors of the dynamic system are discussed; besides, the parameter adaptation method is adopted to restrain the chaos phenomenon. The conclusions are as follows: the stable scope of the green supply chain system enlarges with decision makers' risk-aversion level increasing and decreases with service value increasing; excessive adjustment of price parameters will make the green supply chain system fall into chaos with a large entropy value; the attraction domain of initial prices shrinks with price adjustment speed increasing and enlarges with the channel service values raising. As the dynamic game model system is in a chaotic state, the profit of the manufacturer will be damaged, while the efficiency of the retailer will be improved. The system would be kept at a stable state and casts off chaos by the parameter adaptation method. Results are significant for the manager to make reasonable price decision.

1. Introduction

At present, China is the largest producer and consumer of household appliances in the world. The development of the home appliance industry has made great contribution to the economic development. According to the relevant report of China's home appliance market in 2019, the scale of China's home appliance market still keeps rapid growth [1, 2]. However, with people's living standard improving, consumers are no longer satisfied with the low level of retail services but also put forward higher requirements for the environmental performance and technology of products. For household appliance enterprises, increasing their research and development (R&D) investment for green product can not only meet the market demand for intelligent safety products but also improve their independent innovation ability and market competitiveness. In this environment, the dynamic price game of enterprises considering technological innovation and channel service has attracted wide attention from business and academia.

In recent years, many scholars have conducted extensive research on technological innovation for green product in various ways [3–6]. Apte and Viswanathan [7] reviewed the role of strategy and innovation in manufacturing and specifically discussed technology innovation in product and information flow management. Using system dynamic approach, Li and Ma [8] investigated the mechanism of the innovation level on the stability of the dynamic game. By the differential game approach, considering knowledge spillovers are endogenously caused by the R&D process, Lee et al. [9] collected and analyzed data from 133 companies in Malaysia and showed that there is a certain connection between technology innovation input and supply chain practice in manufacturing firms. In three different contract situations, Wang and Shin [10] explored the influence of different contracts with endogenous upstream innovation and found that supply chain decisions (e.g., the innovation input) could be coordinated by the profit-sharing contract considering investment in innovation, whereas the other two contracts would lead to insufficient investment in

innovation of supply chains. Verma et al. [11] considered the effects of three factors (e.g., SMAC capabilities, innovation, and advantage in competition) on supply chain performance and showed how three factors improve supply chain revenue. Considering fairness contract and power structure, Kim et al. [12] examined the innovation performance of the supplier in an innovative supply chain. In addition, Song et al. [13] integrated the technological innovation and advertising strategies of firms into a two-level supply chain and found that the influence of technological innovation investment and advertising level on market demand and optimal marketing decision is more sensitive. In terms of innovation cooperation, Yoon and Jeong [14] put forward the technological innovation coordinative strategies and studied the differences among them in the reverse supply chain. Yan et al. [15] paid attention to the innovation cooperation of construction industry and discussed the influence of profit distribution and spillover effect on game evolution. Based on the consumer market demand, Aydin and Parker [16] set up a game model and analyzed innovation and technology diffusion in competitive supply chains.

The previous literature has elaborated the influence of innovation factors on the supply chain from various angles in detail, and the conclusions have important reference value for society and enterprises. However, the complexity degree of the supply chain based on the impact of product innovation input on market demand is rarely explored.

In recent years, the supply chain-related problems considering channel service factors have become the focus of the industry and academia [17–20]. Pei and Yan [21] thought that retail service can not only coordinate the conflict between channels but also improve the relationship between channel members. Introducing RLS to substitute naive estimation, Ma and Guo [22] explored the complex dynamic behavior of the game model with service factors. Protappa-Sieke et al. [23] put forward a two-stage inventory strategy based on multiple service contracts. Jena and Sarma [24] explored the price and service competition between two firms, which competed on price and service level and provided retail service directly to customers by a common retailer. In the omni-channel environment, Chen et al. [25] introduce service cooperation into mixed channels with different power structures. Under the two game structures of centralization and decentralization, Kong et al. [26] paid attention to the pricing and service level decision of the low-carbon closed-loop supply chain and researched the role of related parameters in the system. Zhang and Wang [27] put forward two kinds of dynamic pricing strategies based on the changing market and focused on the mechanism of service factors on pricing. In addition, Zhou et al. [28] found that the retailer's service input is easy to lead to the free-riding effect and further discussed the best service strategy of the supply chain under the free-riding effect. Considering the sensitive factors of consumers to service, Ghosh [29] explored the price and service level strategy of a supply chain including one manufacturer and two retailers. Yang et al. [30] studied the impact of quick response service on supply chain performance with a strategic customer in various

supply chain structures and showed that the size of the extra service cost affected the decision-making right structure of the supply chain. Tu et al. [31] studied the effect of coefficient of services on a hybrid supply chains.

Scholars have done some research on price game issues. Xin and Sun [32] studied a differential oligopoly game in which a production-planning single-decision problem is extended to a production-planning and water-saving dual-decision problem, and the decisions are affected simultaneously by both the product and the water right prices. Li et al. [33] studied a Stackelberg game model in a dual-channel supply chain, in which the manufacturer and retailer all considered fairness concern in the price game. Li et al. [34] constructed a dual-channel valued chain in which the manufacturer made green innovation input and the retailer provided channel service, and they make the dynamic price game in decentralized and centralized decisions.

This paper establishes a price game model considering the factors of green innovation input and channel service in decentralized decision scenario. Using game theory and nonlinear dynamics theory, we discuss the equilibrium points and the complex dynamic behaviors of the dynamic system and study the effects of channel service level and risk-aversion level on optimal pricing, stability, and utility of the dual-channel value chain system. The global stability and chaos phenomenon of the dynamic system are analyzed.

Our theoretical contribution is as follows: the first contribution is to the construct dynamic dual-channel supply chain model considering innovation investment and channel service. The second contribution is to analyze the effects of the key parameters on the stability and profitability of the dynamic dual-channel supply chain model.

The rest of this paper is arranged as follows: in Section 2, we present the problem basic description and related hypothesis. Section 3 constructs the static game model and dynamic game model; besides, their stability and the equilibrium solutions are analyzed. Section 4 analyzes the stability characteristics of the dynamic game model. The global stability analysis of the system is given by basins of attraction in Section 5. The control of the chaos phenomenon is made in Section 6. Section 7 presents the conclusions.

2. Model Construction

2.1. Problem Description and Model Assumptions. In a dual-channel green supply chain, to satisfy consumers' demand for intelligent and personalized green products, the manufacturer makes innovative investment in green products, and I_m stands for the amount of innovation input. Two sales channels exist in the dual-channel green supply chain, and one is a traditional channel where the retailer gets green products from the manufacturer and the retailer sells green products to consumers at price p_2 ; the other is the direct marketing channel where the manufacturer also sells the same green products to the consumer at price p_1 directly. The manufacturer and retailer provide sales services (v_1 and v_2) to win more customer demand, respectively. The manufacturer and the retailer compete for retail prices in the

same market. The dual-channel green supply chain system is structured in Figure 1.

To support this research, the following assumptions are made in this paper:

- (1) We assume that the participants all show risk-aversion behaviors facing the changing market demand.
- (2) In a game cycle, because of difficulty that decision makers grasp the perfect market information through their own abilities, therefore, this paper assumes that the manufacturer and retailer are both bounded rationality and they will make the next decision based on the current marginal utility; as the current marginal utility is more than zero, they would improve selling price in the next period; otherwise, they would reduce selling price.
- (3) For the convenience of research, this paper assumes that the unit distribution cost of participants is zero [29] and only considers innovation cost and service cost.

The notations of parameters and its meanings employed in this paper are listed in Table 1.

2.2. Dynamic Game Model. In the market competition, market demand is not only affected by retail price but also by the manufacturer's investment in technological innovation and channel services provided by the participant. In this paper, considering the above factors and relevant literature [29], the market demands from the direct channel and traditional channel can be expressed as follows:

$$\begin{cases} D_m = \theta a - b_1(p_1 - v_1) + \beta_1(p_2 - v_2) + \theta Q, \\ D_r = (1 - \theta)a - b_2(p_2 - v_2) + \beta_2(p_1 - v_1) + (1 - \theta)Q, \end{cases} \quad (1)$$

where $b_i > \beta_i$ ($i = 1, 2$), means that the influence of product price on demand in each channel is greater than that in a competitive channel; $Q = (1/\sqrt{\varepsilon})\sqrt{I_m}$ is the increased market demand for technological innovation investment, and the slowdown of demand growth caused by the increase of technological innovation input is in line with the actual situation of the market.

The connection between service value and service cost of unit product satisfies

$$c_i = \frac{\eta_i v_i^2}{2}, \quad i = 1, 2. \quad (2)$$

Therefore, service cost and service value change in the same direction.

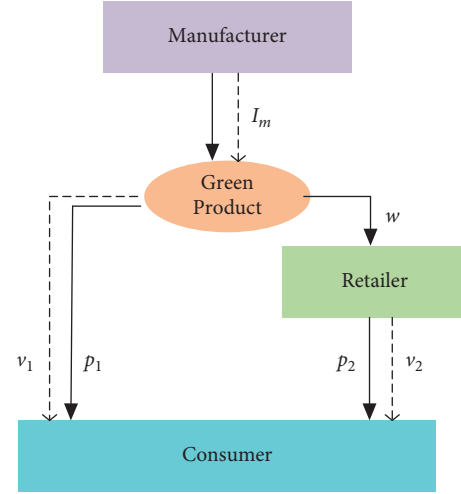


FIGURE 1: The dual-channel green supply chain system.

TABLE 1: Notations and their meanings.

a	The basic market scale
\bar{a}	The mean of basic market scale
θ	Consumer's preference for direct channel ($0 < \theta < 1$)
w	The wholesale price of product
c	Manufacturing cost per unit product
p_1	Retail price of product in direct channel
p_2	Retail price of product in traditional channel
b_i	Price-sensitive coefficient ($i = 1, 2$)
β_i	Cross-price-sensitive coefficient ($0 < \beta_i \leq 1, i = 1, 2$)
I_m	The scale of innovation input
v_1	Service value of unit product of the manufacturer
v_2	Service value of unit product of the retailer
η_1	Service cost coefficient of the manufacturer
η_2	Service cost coefficient of the retailer
c_1	Service cost of unit product for manufacturer
c_2	Service cost of unit product for the retailer
σ_i	Market demand variance ($i = 1, 2$)
Q	Customer demand created by innovation input
ε	Innovation input coefficient
R_1	Risk attitude of the manufacturer
R_2	Risk attitude of the retailer

Based on the features of this paper, the parameters should satisfy

$$\begin{cases} 0 < c + c_1 < p_1, \\ w + c_2 < p_2, \\ D_m > 0, D_r > 0. \end{cases} \quad (3)$$

According to inequality (3), the following conditions can be obtained:

$$\begin{cases} 0 < c < w < p_1 < \frac{\theta a b_2 + (1 - \theta) a \beta_1 + (1 - \theta) (\beta_1 / \sqrt{\varepsilon}) \sqrt{I_m} + \theta (b_2 / \sqrt{\varepsilon}) \sqrt{I_m}}{b_1 b_2 (1 - \beta_1 \beta_2)}, \\ 0 < w + c_2 < p_2 < \frac{(1 - \theta) a b_1 + \theta a \beta_2 + \theta (\beta_2 / \sqrt{\varepsilon}) \sqrt{I_m} + (1 - \theta) (b_1 / \sqrt{\varepsilon}) \sqrt{I_m}}{b_1 b_2 (1 - \beta_1 \beta_2)} + v_2. \end{cases} \quad (4)$$

The profit functions of firms are as follows:

$$\left\{ \begin{array}{l} \pi_m = (w - c) \left[(1 - \theta)a - b_2(p_2 - v_2) + \beta_2(p_1 - v_1) + (1 - \theta) \frac{1}{\sqrt{\varepsilon}} \sqrt{I_m} \right] \\ + (p_1 - c - c_1) \left[\theta a - b_1(p_1 - v_1) + \beta_1(p_2 - v_2) + \theta \frac{1}{\sqrt{\varepsilon}} \sqrt{I_m} \right] - I_m, \\ \pi_r = (p_2 - w - c_2) \left[(1 - \theta)a - b_2(p_2 - v_2) + \beta_2(p_1 - v_1) + (1 - \theta) \frac{1}{\sqrt{\varepsilon}} \sqrt{I_m} \right]. \end{array} \right. \quad (5)$$

In the face of the uncertain demand, the manufacturer and the retailer have financial risks for their product sales [35]. Therefore, this paper will consider the effect of the risk attitudes of firms on variable decision and the exponential utility is used to express the utility function:

$$U(\pi_i) = -e^{-\pi_i/R_i}, \quad (6)$$

where R_i , ($i = 1, 2$) are the risk-aversion levels of the participant and e is the exponential constant; π_i is the profit of

the manufacturer and retailer and follows a normal distribution; $E(\pi_i)$ is the mean of π_i , and $\text{Var}(\pi_i)$ is the variance of π_i . The expected utility is as follows:

$$E(U_{\pi_i}) = E(\pi_i) - \frac{\text{Var}(\pi_i)}{2R_i}. \quad (7)$$

The expected utilities of participants are as follows:

$$\left\{ \begin{array}{l} E_m(U_{\pi_m}) = (w - c) \left[(1 - \theta)\bar{a} - b_2(p_2 - v_2) + \beta_2(p_1 - v_1) + (1 - \theta) \frac{1}{\sqrt{\varepsilon}} \sqrt{I_m} \right] \\ + (p_1 - c - c_1) \left[\theta\bar{a} - b_1(p_1 - v_1) + \beta_1(p_2 - v_2) + \theta \frac{1}{\sqrt{\varepsilon}} \sqrt{I_m} \right] - I_m - \frac{(p_1 - c - c_1)^2 \sigma_1^2}{2R_1} - \frac{(w - c)^2 \sigma_2^2}{2R_2}, \\ E_r(U_{\pi_r}) = (p_2 - w - c_2) \left[(1 - \theta)\bar{a} - b_2(p_2 - v_2) + \beta_2(p_1 - v_1) + (1 - \theta) \frac{1}{\sqrt{\varepsilon}} \sqrt{I_m} \right] - \frac{(p_2 - w - c_2)^2 \sigma_2^2}{2R_2}. \end{array} \right. \quad (8)$$

Making first-order derivatives of $E_m(U_{\pi_m})$ with respect to $\sqrt{I_m}$,

$$\frac{\partial E_m(U_{\pi_m})}{\partial \sqrt{I_m}} = \frac{(w - c)(1 - \theta)}{\sqrt{\varepsilon}} + \frac{(p_1 - c - c_1)\theta}{\sqrt{\varepsilon}} - 2\sqrt{I_m}. \quad (9)$$

Making second-order derivatives of $E_m(U_{\pi_m})$ in $\sqrt{I_m}$,

$$\frac{\partial^2 E_m(U_{\pi_m})}{\partial (\sqrt{I_m})^2} = -2. \quad (10)$$

From the above analysis, the manufacturer's utility function $E_m(U_{\pi_m})$ is concave and only has a maximum

value. Solving $(\partial E_m(U_{\pi_m})/\partial \sqrt{I_m}) = 0$, the optimal technological innovation input is expressed as follows:

$$I_m^* = \frac{[\theta(p_1 - w - c_1) + w - c]^2}{4\varepsilon}. \quad (11)$$

From (11), it is clear that the greater the innovation cost coefficient is, the smaller the optimal technological innovation input is, and it shows that the high innovation cost coefficient has a restraining effect on the technology innovation investment enthusiasm of the manufacturer.

Substituting (11) into (8), the expected utility functions of participants under optimal technological innovation input are obtained:

$$\left\{ \begin{array}{l} E_m(U_{\pi_m}) = (p_1 - c - c_1) \left[\begin{array}{l} \theta \bar{a} - b_1(p_1 - v_1) + \beta_1(p_2 - v_2) + \frac{\theta[(p_1 - c_1 - w)\theta + w - c]}{2\varepsilon} \\ + (w - c) \left[(1 - \theta)\bar{a} - b_2(p_2 - v_2) + \beta_1(p_1 - v_1) + \frac{(1 - \theta)[(p_1 - c_1 - w)\theta + w - c]}{2\varepsilon} \right] \end{array} \right], \\ E_r(U_{\pi_r}) = (p_2 - w - c_2) \left[(1 - \theta)\bar{a} - b_2(p_2 - v_2) + \beta_1(p_1 - v_1) \right] - \frac{(p_2 - w - c_2)^2 \sigma_2^2}{2R_2} \\ + (p_2 - w - c_2) \left[\frac{(1 - \theta)[(p_1 - c_1 - w)\theta + w - c]}{2\varepsilon} \right]. \end{array} \right. \quad (12)$$

Considering the first-order partial derivatives of $E_m(U_{\pi_m})$ and $E_r(U_{\pi_r})$ in p_1 and p_2 , respectively, we can get the related equations in the following equation:

$$\left\{ \begin{array}{l} \frac{\partial E_m(U_{\pi_m})}{\partial p_1} = G_1 + X_1 p_1 + \beta_1 p_2, \\ \frac{\partial E_r(U_{\pi_r})}{\partial p_2} = G_2 + X_2 p_2 + X_3 p_1, \end{array} \right. \quad (13)$$

where

$$\begin{aligned} G_1 &= \theta \bar{a} + b_1 v_1 - \beta_1 v_2 + \frac{\theta[(-c_1 - w)\theta + w - c]}{2\varepsilon} + b_1(c + c_1) - \frac{\theta^2(c + c_1)}{2\varepsilon} \\ &\quad + \beta_2(w - c) + (w - c) \frac{\theta(1 - \theta)}{2\varepsilon} - \frac{-\theta c + \theta w - \theta^2 c_1 - \theta^2 w}{2\varepsilon} + \frac{\sigma_1^2(c + c_1)}{R_1}, \\ G_2 &= (1 - \theta)\bar{a} + b_2 v_2 - v_1 \beta_2 + (1 - \theta) \frac{(-c_1 - w)\theta + w - c}{2\varepsilon} + b_2(w + c_2) + \frac{(w + c)\sigma_2^2}{R_2}, \\ X_1 &= -2b_1 + \frac{\theta^2}{2\varepsilon} - \frac{\sigma_1^2}{R_1}, \\ X_2 &= -2b_2 - \frac{\sigma_2^2}{R_2}, \\ X_3 &= \beta_2 + (1 - \theta) \frac{\theta}{2\varepsilon}. \end{aligned} \quad (14)$$

In multistage game process, participants cannot grasp the perfect market information of the current market, and the grey forecasting model is a good way for the nonlinear system [36], but in this paper, we make price forecasting by bounded rational expectations to obtain profit

maximization. As the current marginal utility is more than zero, decision makers would improve price p_i ($i = 1, 2$) in the next period; otherwise, they would reduce them. Then, the dynamic decision-making process of participants can be expressed as follows:

$$\begin{cases} p_1(t+1) = p_1(t) + \delta_1 p_1(t)(G_1 + X_1 p_1(t) + \beta_1 p_2(t)), \\ p_2(t+1) = p_2(t) + \delta_2 p_2(t)(G_2 + X_2 p_2(t) + X_3 p_1(t)), \end{cases} \quad (15)$$

where δ_1 and δ_2 represent the price adjustment speeds of decision makers.

3. Equilibrium Points, Conditions for Existence, and Local Stability

For the system disturbed by weak noise, its variation can be seen as the random factors around the deterministic system and transformation between them [33]. When interference factors are very small, the motion state of the system would not be affected by the disturbance term; when interference factors are very large, the state of the system would be changed. Therefore, we first explore the Nash equilibrium solution and the local stability of dynamic system (15).

Based on the theory of the fixed point [37], letting $p_i(t+1) = p_i(t)$, the four possible Nash equilibrium points are obtained as follows:

$$\begin{aligned} \rho_1 &= (0, 0), \\ \rho_2 &= \left(0, -\frac{G_2}{X_2}\right), \\ \rho_3 &= \left(-\frac{G_1}{X_1}, 0\right), \\ \rho_4 &= (S_1^*, S_2^*), \end{aligned} \quad (16)$$

where $S_1^* = (\beta_1 G_2 - G_1 X_2 / X_1 X_2 - \beta_1 X_3)$ and $S_2^* = -(X_1 G_2 - G_1 X_3 / X_1 X_2 - \beta_1 X_3)$.

Proposition 1. *Nash equilibrium point ρ_1 is an unstable equilibrium point.*

Proof. See Appendix.

Proposition 2. *Nash equilibrium point ρ_2 and ρ_3 are unstable saddle points.*

Proof. See Appendix.

Economically, zero price means nothing to manufacturers and retailers. Next, we will study the stability characteristics of equilibrium solutions (ρ_4).

The Jacobian matrix of dynamic system (15) at ρ_4 can be written as follows:

$$J(S_1^*, S_2^*) = \begin{pmatrix} 1 + \delta_1(G_1 + 2Y_1 S_1^* + \beta_1 S_2^*) & \beta_1 \delta_1 S_1^* \\ Y_3 \delta_2 S_2^* & 1 + \delta_2(G_2 + 2Y_2 S_2^* + Y_3 S_1^*) \end{pmatrix}. \quad (17)$$

The feature equation of the Jacobian matrix can be written as follows:

$$F(\lambda) = \lambda^2 - \text{tr}(J)\lambda + \det(J), \quad (18)$$

where $\text{tr}(J)\lambda = \delta_1(G_1 + 2S_1^* Y_1 + \beta_1 S_2^*) + \delta_2(G_2 + S_1^* Y_3 + 2S_2^* Y_2) + 2$; $\det(J) = [\delta_1(G_1 + 2S_1^* Y_1 + \beta_1 S_2^*) + 1] [\delta_2(G_2 + S_1^* Y_3 + 2S_2^* Y_2) + 1] - \beta_1 S_1^* S_2^* Y_3 \delta_1 \delta_2$, $\Delta = (\text{tr}(J))^2 - 4\det(J)$ be its discriminant.

In (18), setting $\lambda = 1$, we can get $F(1) = 1 - \text{tr}(J) + \det(J)$. Therefore, Lemma 1 can be employed to study the eigenvalues of $J(S_1^*, S_2^*)$.

Lemma 1 (see [38]). *Suppose that $F(1) > 0$ and λ_1 and λ_2 are two roots of $F(\lambda) = 0$. Then,*

- (1) $|\lambda_1| < 1$ and $|\lambda_2| < 1$ if and only if $F(-1) > 0$ and $\det(J) < 1$
- (2) $|\lambda_1| < 1$ and $|\lambda_2| > 1$ (or $|\lambda_1| > 1$ and $|\lambda_2| < 1$) if and only if $F(-1) < 0$
- (3) $|\lambda_1| > 1$ and $|\lambda_2| > 1$ if and only if $F(-1) > 0$ and $\det(J) > 1$
- (4) $|\lambda_1| = -1$ and $|\lambda_2| \neq 1$ if and only if $F(-1) = 0$ and $\det(J) \neq 0, 2$
- (5) λ_1 and λ_2 are complex and $|\lambda_1| = |\lambda_2| = 1$ if and only if $\Delta < 0$ and $\det(J) = 1$

If all eigenvalues of $J(S_1^, S_2^*)$ are less than one in the modulus, dynamic system (15) will run stably at this equilibrium point. If not, the bifurcation behavior or chaos phenomenon appears in dynamic system (15). Concretely, that flip bifurcation happens as a single characteristic root is equal to -1 , while Neimark–Sacker (N–S) bifurcation emerges as two characteristic roots equal one.*

4. The Stable Region of Dynamic System (15)

Next, we adopt numerical simulation to indicate how key factors affect the complex dynamical behaviors of dynamic system (15). Taking the current situation and distinguishing the feature of the dual-channel green supply chain into account, parameter values are set as follows: $a = 120, \theta = 0.4, b_1 = 3, b_2 = 3.5, \beta_1 = 1, \beta_2 = 1, \varepsilon = 1.2, \nu_1 = 1.5, \nu_2 = 2, \eta_1 = 0.6, \eta_2 = 0.5, c = 6, w = 10, R_1 = 70, R_2 = 60, \sigma_1 = 0.05$, and $\sigma_2 = 0.05$. Thus, the Nash equilibrium solution is $\rho_4 = (15.3102, 18.8588)$ and the optimal innovation input is 7.553.

4.1. The Influence of Key Parameters on Stable Region of Dynamic System (15). In dynamic system (15), price adjustment speed is regarded as a key factor, which can reflect the type of a decision maker. Radical players prefer to exert a larger adjustment speed to get more benefits in a short time. However, prudent players prefer to choose smaller adjustment speed to avoid risks and obtain stable profits.

Figure 2 shows the stable range of dynamic system (15) as the parameters take the above values; as the adjustment speed is within the light purple scope, dynamic system (15) will return to the Nash equilibrium point after several game cycles. If $\delta_1 > 0.0212$ or $\delta_2 > 0.01483$, dynamic system (15) would enter a bifurcation or chaotic state, and it means that the manufacturer or retailer would face the risk of withdrawing from the market.

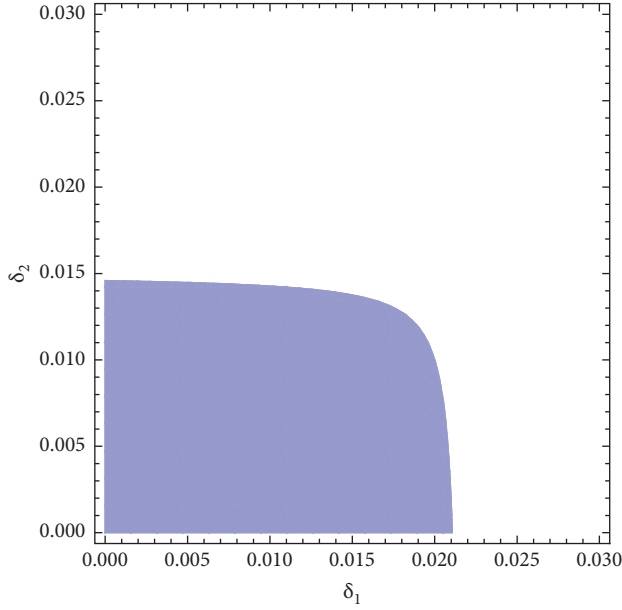


FIGURE 2: The stable region of dynamic system (15).

Figure 3(a) shows the stable regions of dynamic system (15) when $R_2 = 60$ with $R_1 = 10, 35, 60$, respectively, it can be seen that, as $R_1 = 10$, the range of price adjustment speed on the x -axis is $0 < \delta_1 < 0.01948$; when $R_1 = 35$, the range of the price adjustment parameter on the X -axis is $0 < \delta_1 < 0.0204$; when $R_1 = 60$, the range of price adjustment speeds on the X -axis is $0 < \delta_1 < 0.02121$. We conclude that the larger the risk-aversion level of the manufacturer is, the larger the stable range of the price adjustment of the manufacturer is, and the stable range of the price adjustment of the retailer remains unchanged. That is to say, the increase of the manufacturer's risk-aversion level has no effect on the stable range of the retailer's price adjustment but enlarges the stable scope of the retailer's price adjustment.

Figure 3(b) shows that the stability regions of dynamic system (15) decrease gradually in the direction of δ_1 , while the stability regions hardly change in the direction of δ_2 when ν_1 takes different values. Figure 3(c) shows that the stability scope of dynamic system (15) decreases in the direction of δ_2 . However, the stability regions hardly change in the direction of δ_2 . That is to say, the service values of the manufacturer and retailer only affect the stable ranges of price adjustment of their own channels but have no effect on other channels.

For understanding better the change process of dynamic system (15), Figure 4 displays the 2D diagram of dynamic system (15) using the parameter basin, which indicates the route of dynamic system (15) to chaos. In Figure 4, different periods are represented by different colors: for a single-cycle state, period-1 (green), period-3 (red), period-5 (purplish red), and period-7 (orange); for a period-doubling state, period-2 (pink), period-4 (blue), period-8 (purple), chaos (grey), and divergence (white). We can see that dynamic system (15) goes through period-doubling bifurcation and goes into a chaotic state. The stable region in Figure 4 is consistent with that in Figure 2.

Figures 5(a)–5(c) show the change process of dynamic system (15) in the (δ_1, δ_2) plane with R_2 having different values, and green areas represent the stable regions of dynamic system (15). The stable scope of dynamic system (15) enlarged with the direction of δ_2 in the increase of risk-aversion level of retailers and almost unchanged in the direction of δ_1 . Figures 6(a)–6(c) show the change process of dynamic system (15) in the (ν_1, ν_2) plane with δ_1 and δ_2 having different values, and areas represent the stable regions of dynamic system (15). We can see that the stable regions of dynamic system (15) shrink in the direction of ν_1 and ν_2 with price adjustment speeds of participants increasing; that is to say, as the price adjustment speeds are relatively large, the manufacturer and the retailer can choose a smaller service level to make dynamic system (15) stable.

From the above analysis, a conclusion can be drawn that the stability region of dynamic system (15) shrinks with the increase of service values, enlarges in risk-aversion level, when the price adjustment speeds are relatively large. Participants can choose a smaller service level to keep dynamic system (15) stable.

If participants improve their service levels in order to obtain the best utilities, they will consume a lot of manpower and material resources of the dual-channel green supply chain. At this time, the ability of the dual-channel green supply chain system to resist risks will be weakened, which will lead to the decrease of system stability and the increase of vulnerability. Therefore, from the point of view of the supply chain, decision makers should make their own service decisions and price adjustment decisions prudently to make the dynamic system stable.

4.2. Global Stability of Dynamic System (15). The variation of the key parameter affects the stability of system (15). The influence of parameter variation on global stability can be analyzed by the basins of attraction, which includes the attraction domain and escaping area. If the initial values of parameters are set in attraction scope, dynamic system (15) will appear the same attractor after several iterations. If the initial values of parameters are not in the basins of attraction, which is marked by red, dynamic system (15) will evolve from a stable state to a divergent state.

With the same values for parameters, the basins of attraction about initial price p_1 and p_2 are showed in Figure 7, where the red range represents the stable domain of attraction and the white range represents the escape area. We find that the attraction range shrinks as δ_1 and δ_2 increase. Figure 8 indicates the basins of attraction of dynamic system (15) with ν_1 and ν_2 changing as $\delta_1 = 0.005$ and $\delta_2 = 0.005$. Compared with Figure 7, the stable attraction domain of initial value of p_1 enlarges with ν_1 increasing and that of p_2 enlarges with ν_2 increasing. If the initial values of p_1 and p_2 are taken in the attraction scope, dynamic system (15) will appear the chaotic attractor after several iterations. Otherwise, dynamic system (15) will fall into divergence at last. From economic perspective, the participant should choose the initial prices in basins of attraction to ensure that the market enters a stable state.

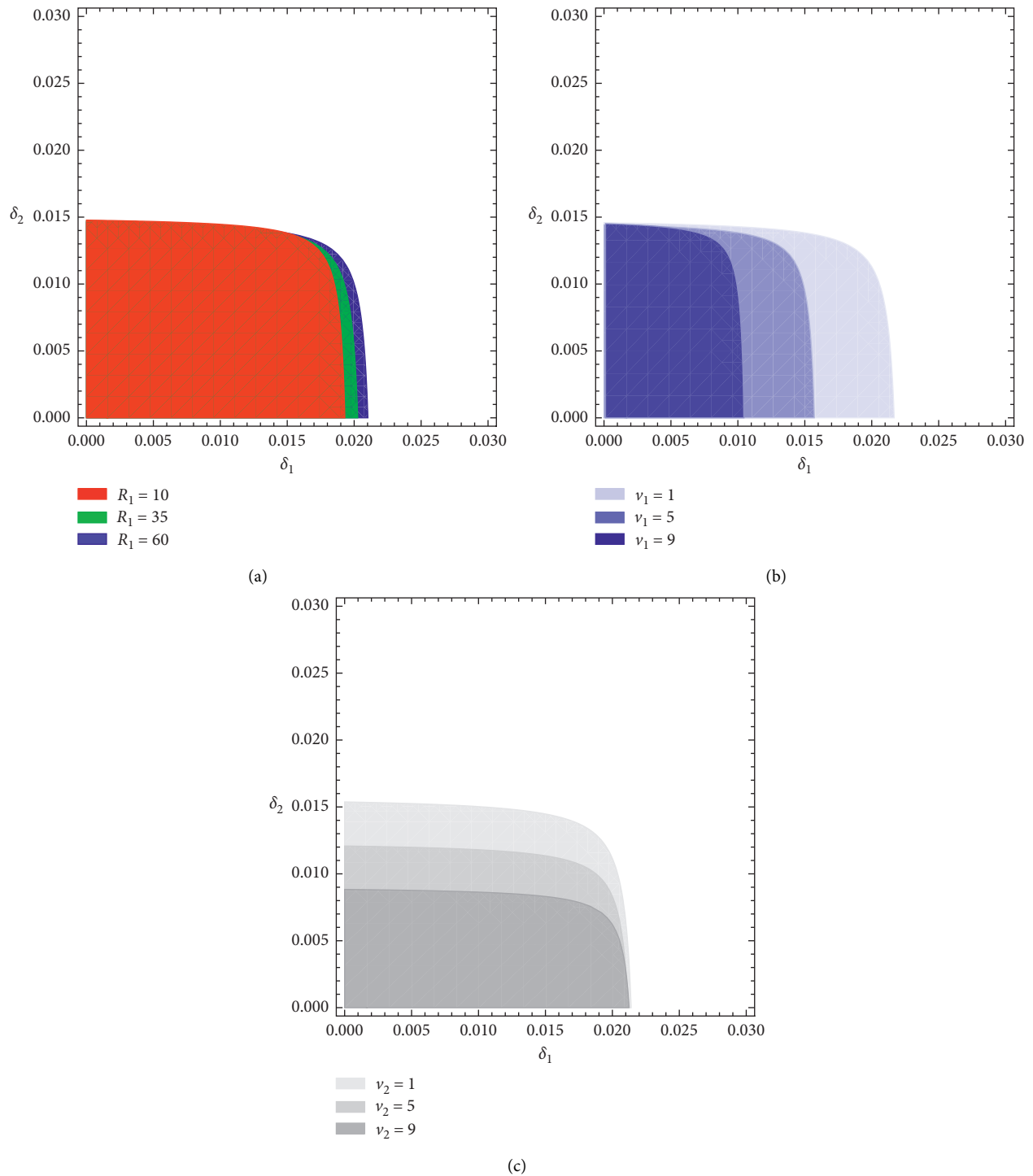


FIGURE 3: The stable regions of dynamic system (15) with R_1 , v_1 , and v_2 having different values. (a) R_1 . (b) v_1 . (c) v_2 .

5. The Effect of Parameters on Dynamic System (15)

5.1. The Effect of Price Change on Dynamic System (15). Since the influence of the price adjustment parameters of participants on system behavior is similar, the evolution of system behavior is discussed by taking the price adjustment

parameter of the manufacturer as an example. Figure 9(a) shows the effect of δ_1 on price evolution of dynamic system (15) when $\delta_2 = 0.005$. When $\delta_1 < 0.0207$, dynamic system (15) returns to the Nash equilibrium point after several games from the initial state; as $\delta_1 = 0.0207$, dynamic system (15) appears the first bifurcation; after that, dynamic system (15) appears four periodic bifurcations and eight periodic

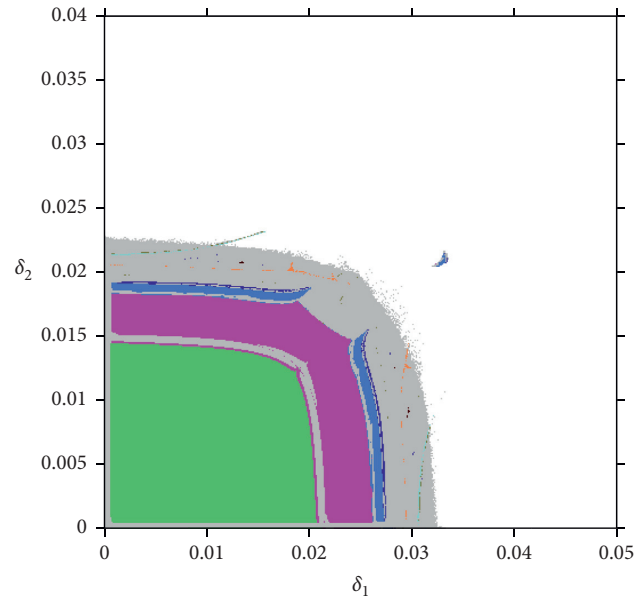


FIGURE 4: The 2D bifurcation diagram of dynamic system (15) in the (δ_1, δ_2) plane.

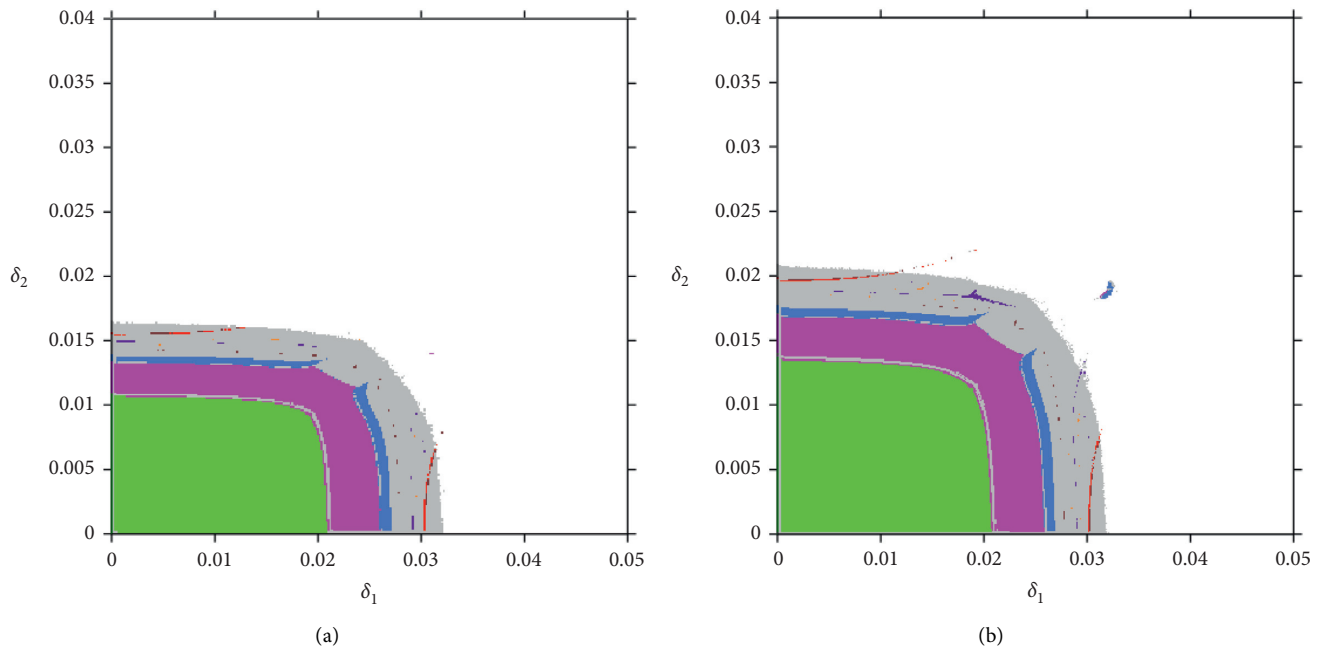


FIGURE 5: Continued.

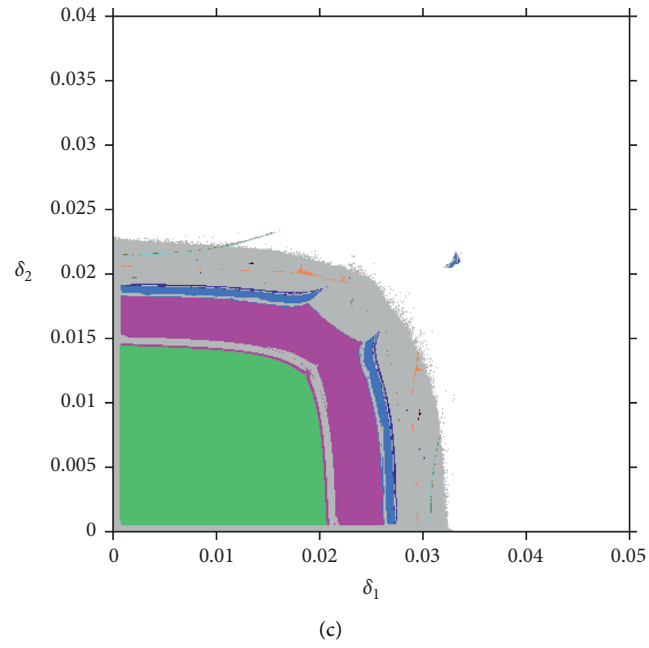


FIGURE 5: The 2D bifurcation diagrams in the (δ_1, δ_2) plane with R_r changing. (a) $R_2 = 5$. (b) $R_2 = 30$. (c) $R_2 = 60$.

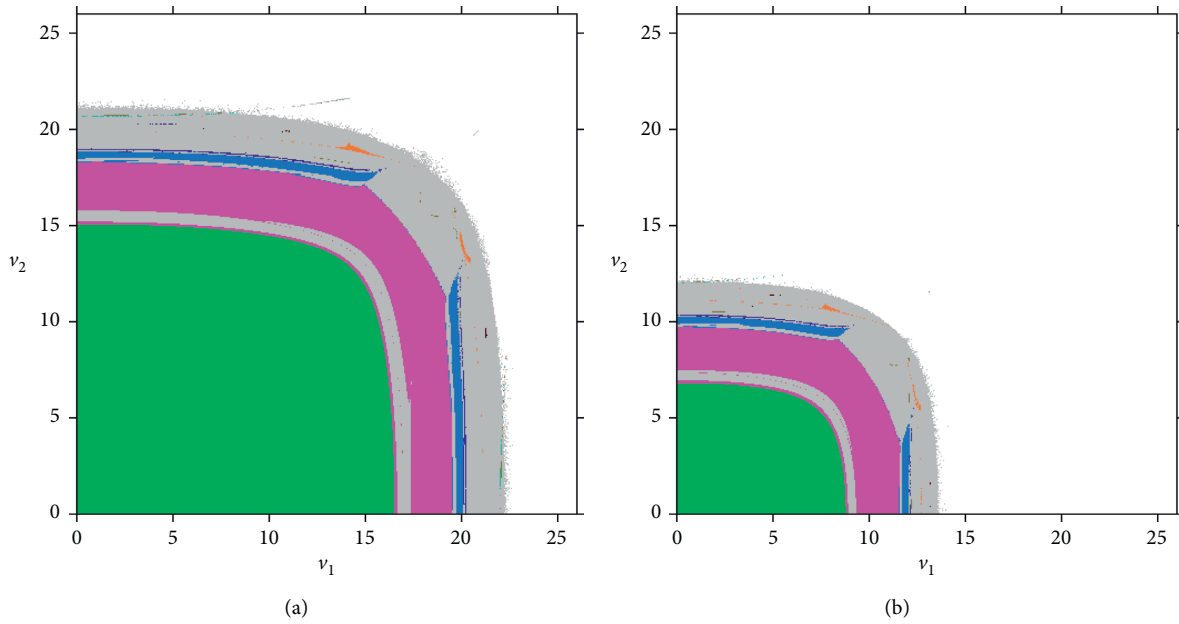


FIGURE 6: Continued.

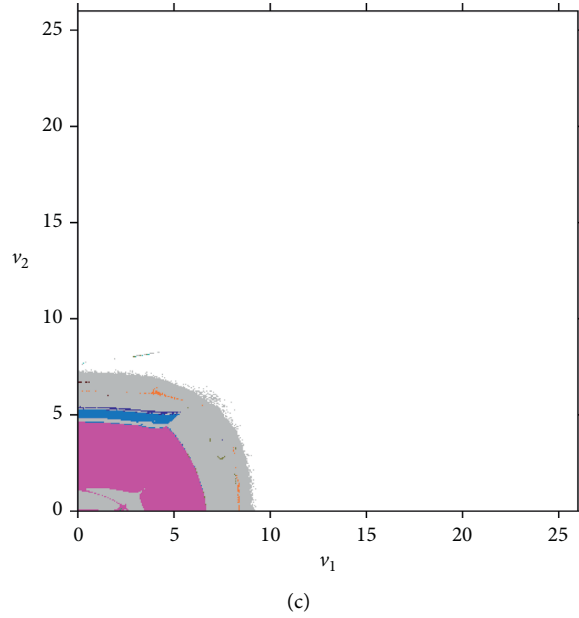


FIGURE 6: The 2D bifurcation diagrams in the (v_1, v_2) plane with δ_1 and δ_2 changing. (a) $\delta_1 = 0.005$ and $\delta_2 = 0.005$. (b) $\delta_1 = 0.01$ and $\delta_2 = 0.01$. (c) $\delta_1 = 0.015$ and $\delta_2 = 0.015$.

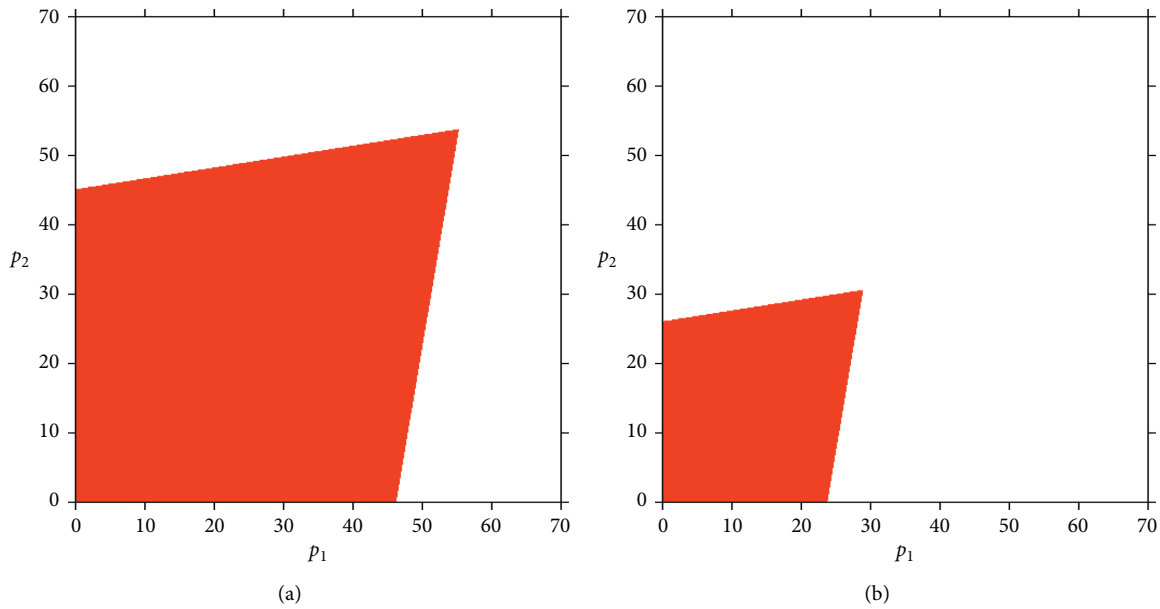


FIGURE 7: Basins of attraction of dynamic system (15) with δ_1 and δ_2 changing. (a) $\delta_1 = 0.005$ and $\delta_2 = 0.005$. (b) $\delta_1 = 0.015$ and $\delta_2 = 0.015$.

bifurcations and then gradually falls into chaos with δ_1 increasing.

Figure 9(b) shows the entropy change of dynamic system (15) with δ_1 increasing. When the system entropy equals to zero, dynamic system (15) is in the stable state; when the system entropy is greater than zero, dynamic system (15) is in the unstable state.

In order to visually show the effect of service values on the behavior of the system, Figures 10(a)–10(c) indicate that the system evolution process as v_1 has different values. From Figure 10, we can see that, with v_1 varying, the Nash

equilibrium value increases, the stability of dynamic system (15) decreases, and market spillover effect appears ahead of time, which is consistent with Figure 3(b).

Figure 11 shows the forming process of the chaotic attractor as dynamic system (15) is in the chaotic state. Figure 11(a) shows the chaotic state of dynamic system (15) in its initial stage, and the orbit of dynamic system (15) is composed of scattered points. When the adjustment parameter increases, the trajectory of the system in the chaotic state presents a preliminary outline shown in Figure 11(b) when $\delta_1 = 0.0285$. From Figure 11(c), it can be found that

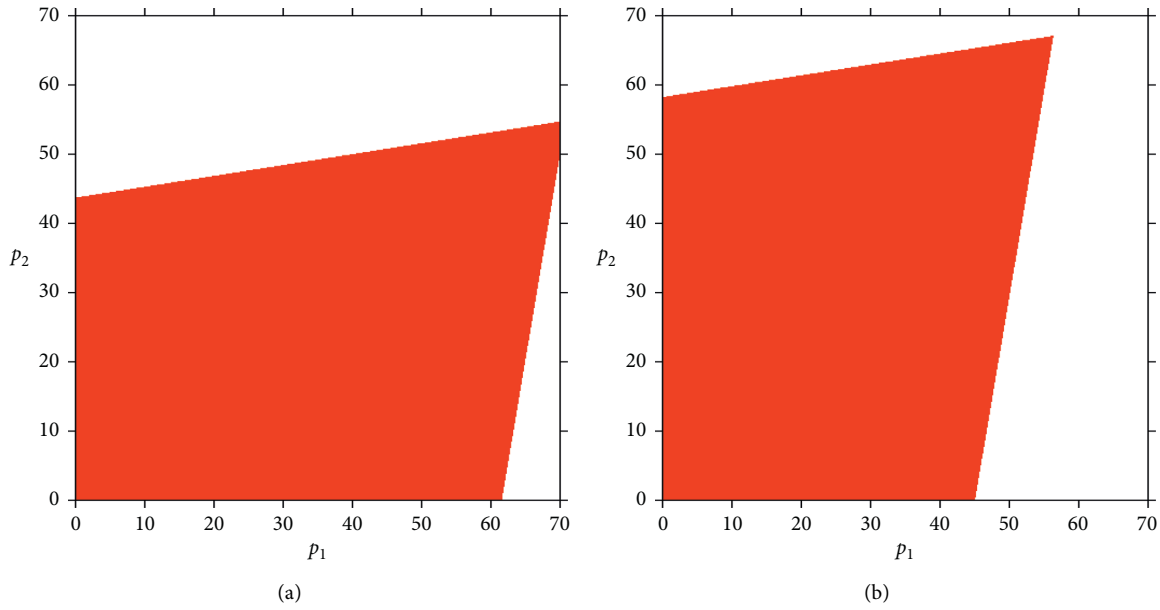


FIGURE 8: Basins of attraction with v_1 and v_2 changing. (a) $v_1 = 9$. (b) $v_2 = 9$.

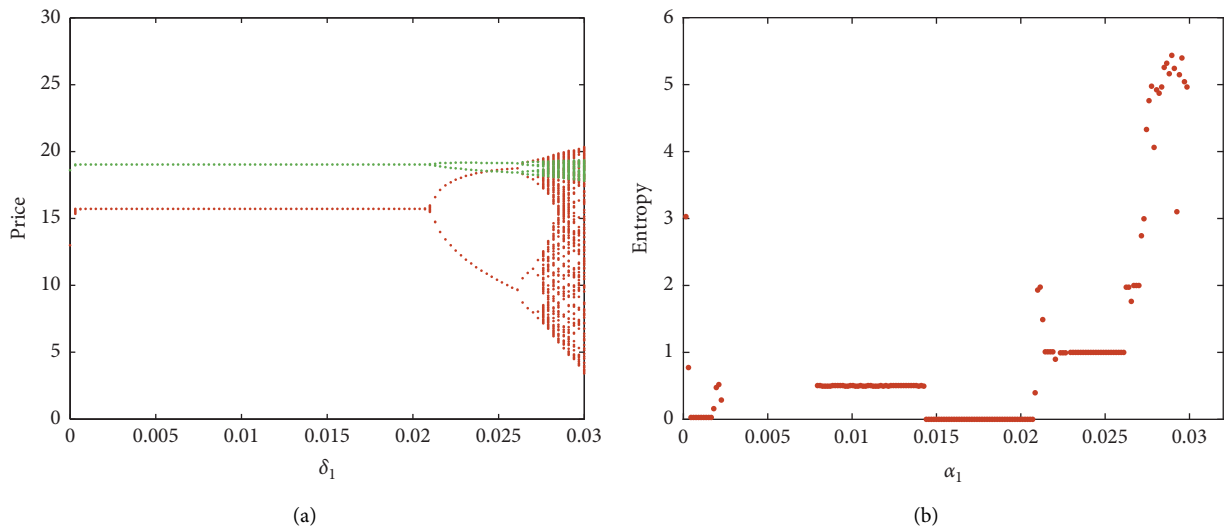


FIGURE 9: The price bifurcation and entropy with δ_1 varying. (a) The price bifurcation. (b) Entropy.

when $\delta_1 = 0.03$, there are countless points in the trajectory of dynamic system (15), and the distribution of countless points is attracted to a certain region.

Figure 11(a) shows the path of the initial chaotic system in phase space. With δ_1 increasing, in Figures 11(c) and 11(b), the chaos degree of dynamic system (15) increases, which can be called as the chaotic attractor.

Sensitivity to the initial value is also an important characteristic of chaotic systems. Figure 12(a) shows the running trend of dynamic system (15) as the initial value of p_1 only changes 0.001. Figure 12(b) shows the running trend of dynamic system (15) as the initial value of p_2 only changes 0.001. We can see that there is almost no difference in the retail prices between participants before 20 time iterations. After 20 time iterations, retail prices began to fluctuate

sharply, which indicates that the small difference in the initial value will lead to system instability.

From this, it can be drawn that the sensitivity of the dynamic system in the unstable state is just like the butterfly effect. With the small change of initial conditions, the chaotic system will fluctuate violently with time. In formulating market strategies, decision makers should choose the initial values carefully.

Thus, the excessive price adjustment parameter and larger service value can easily make dynamic system (15) enter the chaotic state and cause disorderly fluctuations. Therefore, managers should reasonably formulate market price strategies in the market competition and should not adjust prices too quickly in order to maximize short-term utility.

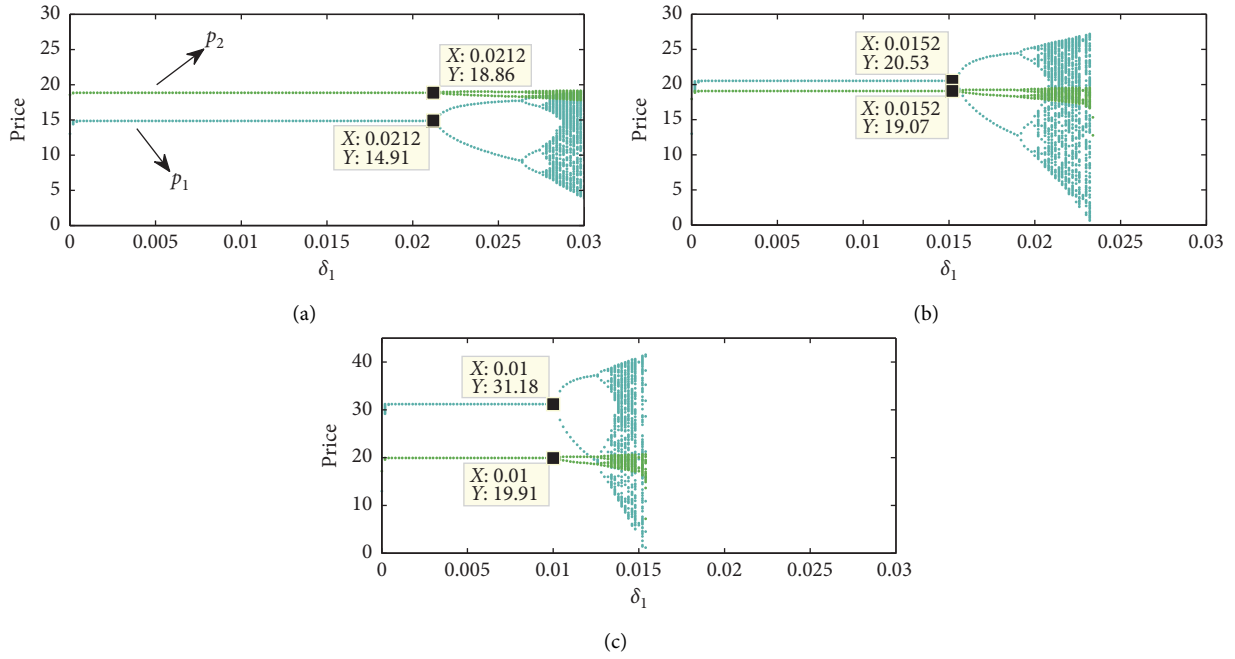


FIGURE 10: The bifurcation diagrams of dynamic system (15) with δ_1 increasing. (a) $\nu_1 = 1$. (b) $\nu_1 = 5$. (c) $\nu_1 = 9$.

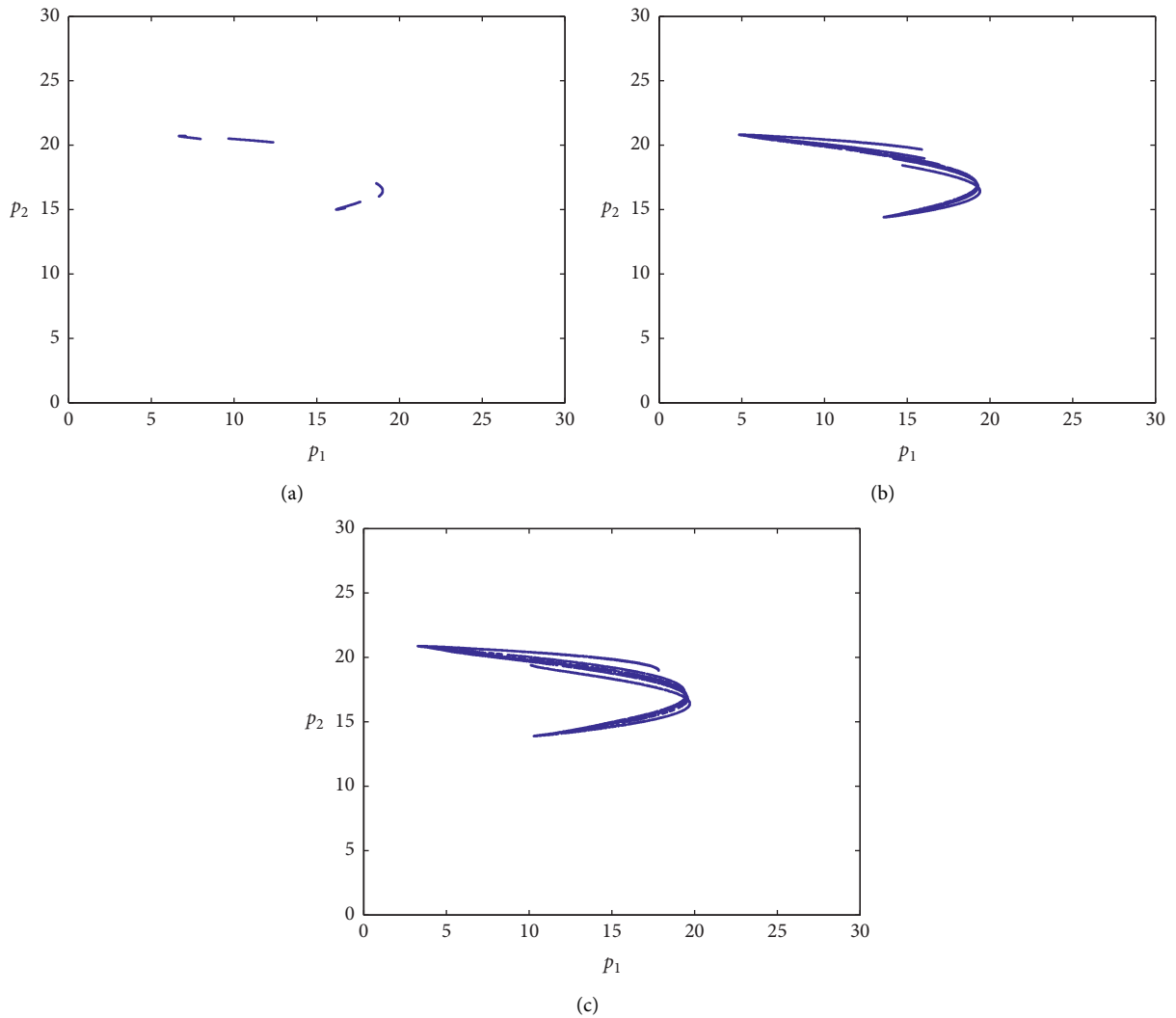


FIGURE 11: The chaotic attractor of dynamic system (15). (a) $\delta_1 = 0.027$. (b) $\delta_1 = 0.0285$. (c) $\delta_1 = 0.03$.

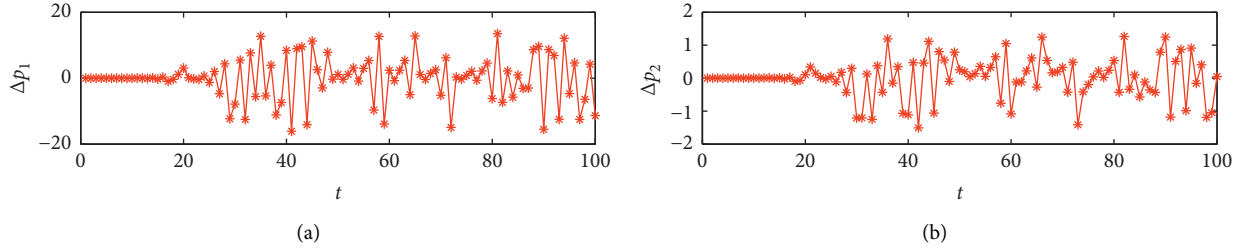


FIGURE 12: Sensitivity of dynamic system (15) to initial price values. (a) Δp_1 . (b) Δp_2 .

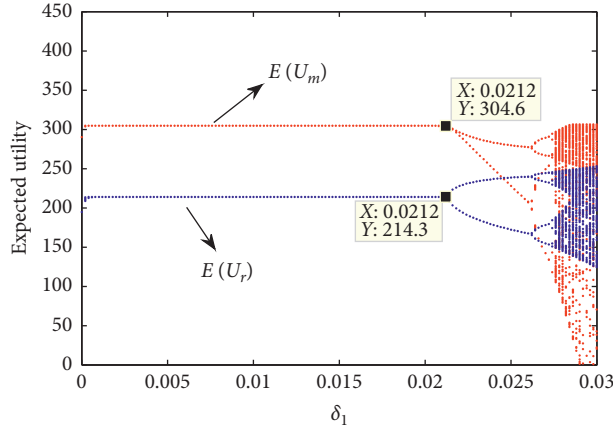


FIGURE 13: The expected utility of dynamic system (15) with δ_1 increasing.

5.2. The Effect of Chaos on the System Efficiency. Figure 13 shows the expected utility of dynamic system (15) and goes into the chaotic state with δ_1 increasing, which is similar to the price evolution process. Figure 14 shows the utility changing of participants over time. As $\delta_1 = 0.005$, the expected utility of the system is a fixed value with time; when $\delta_1 = 0.024$, the expected utility of the system changes periodically; when $\delta_1 = 0.029$, the expected utility fluctuates sharply in Figure 14(c). The expected utility of the system fluctuates in the doubling period and chaotic state, which makes it impossible for two firms to make the next decision according to the current expected utility. In the chaotic state, the expected utility of dynamic system (15) is difficult to measure.

In Figure 15, the red points denote the manufacturer's the expected average utility and the blue line indicates the retailer's expected average utility. With the increase of δ_1 , it can be seen intuitively that the average utility of the manufacturer in the unstable state is significantly less than that in the stable state, which means that chaos destroys the effectiveness of the manufacturer; on the contrary, the average efficiency of the retailer in the unstable state is higher than that in the stable state. So, chaos is beneficial for the retailer to achieve high expected utility.

6. Chaos Control

The above research states clearly that the average utility of the manufacturer is higher than that in the stable state, and the one of the retailer is lower than that in the unstable state.

In this uncertain situation, it brings great suffering to the participants in making the next price decision. If the chaos phenomenon is not controlled, it will lead to a vicious circle in the market and even lead to the withdrawal of participants from the market competition. In order to restore market stability, it is necessary to control the chaotic market effectively.

Some chaos control methods have been applied to the supply chain, such as modified straight-line stabilization method [39], time-delayed feedback method [40], OGY method [41], and the parameter adaptation method [42]. In this section, the parameter adaptation method is adopted to control the market prices of participants. Based on dynamic system (15), the controlled system can be expressed as follows:

$$\begin{cases} p_1(t+1) = (1-\alpha)\delta_1 p_1(t)(G_1 + X_1 p_1 + \beta_1 p_2) + \alpha p_1(t), \\ p_2(t+1) = \delta_2 p_2(t)(G_2 + X_2 p_2 + X_3 p_1) + p_2(t). \end{cases} \quad (19)$$

Figures 16(a) and 16(b) show the dynamic process of control system (19) with the adjustment parameter δ_1 increasing when $\alpha = 0.1$ and $\alpha = 0.4$, respectively. It can be seen that controlled system (19) appears the first bifurcation at $\delta_1 = 0.024$ when $\alpha = 0.1$; and the first bifurcation of controlled system (19) is delayed again when $\alpha = 0.4$.

When $\delta_1 = 0.03$ and $\delta_2 = 0.005$, the market is in a chaotic state. As α increases, the game evolution of controlled system (19) is shown in Figure 17(a). When $\alpha = 0$, controlled system (19) is chaos; as $0 < \alpha \leq 0.31$, controlled

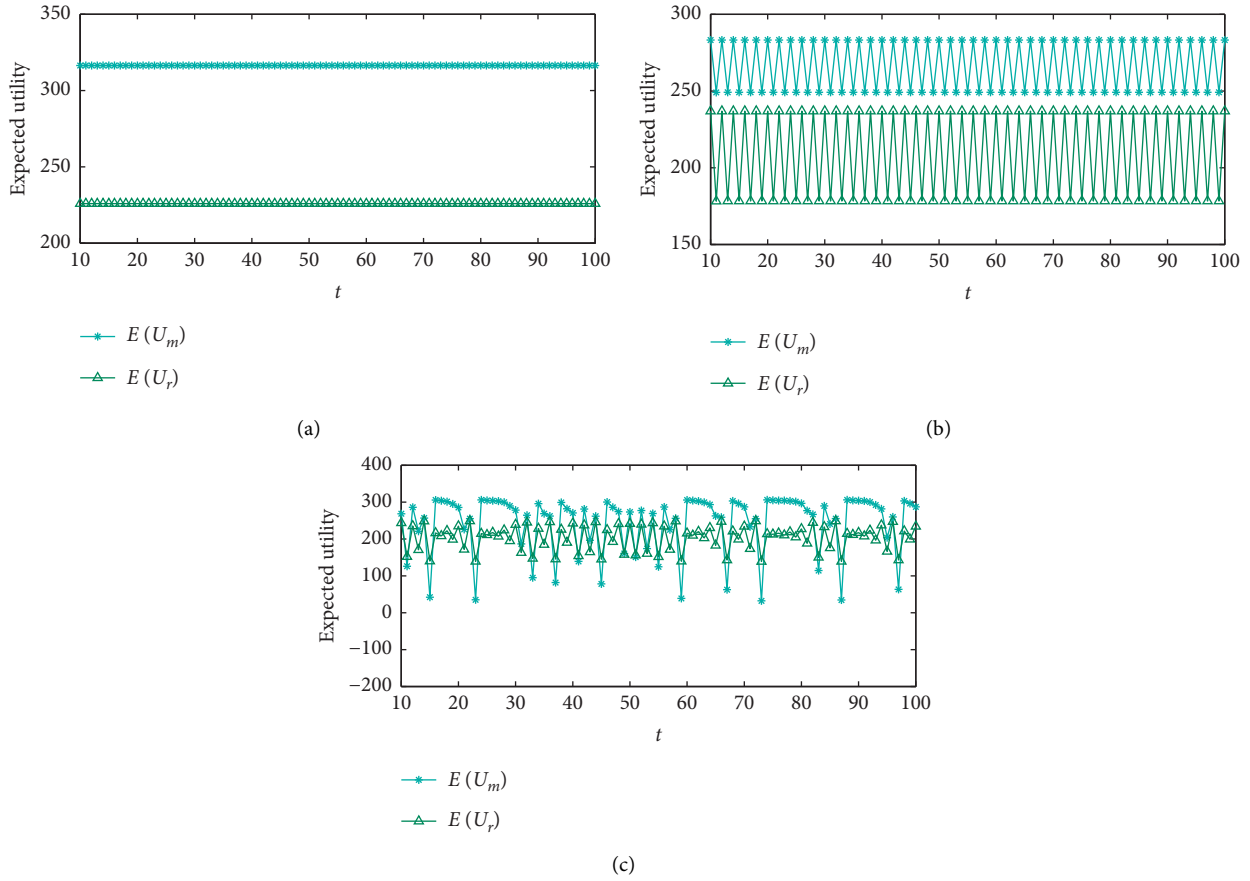


FIGURE 14: The evolution of expected utility over time in different periods. (a) $\delta_1 = 0.005$. (b) $\delta_1 = 0.024$. (c) $\delta_1 = 0.029$.

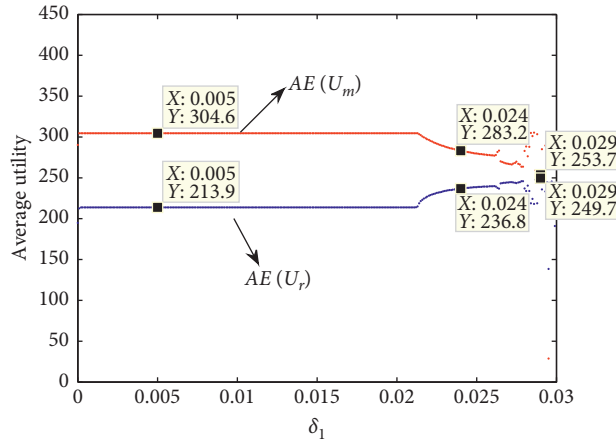


FIGURE 15: The average utility diagram with δ_1 varying.

system (19) gets rid of the chaotic state and enters a period-doubling bifurcation state; as $\alpha > 0.31$, the dynamic system is completely controlled in the stable period. Correspondingly, Figure 17(b) indicates the entropy of system (19); as $0 < \alpha \leq 0.31$, the entropy value is larger than one and system (19) is in the state of chaos and periodic doubling state; when $\alpha > 0.31$, the entropy value is equal to 0.5 or 0 and controlled system (19) is in the stable state.

In market competition, chaos has an important effect on the utility of participants. However, due to the market complexity and the difference of decision makers, the behavior of the decision makers may make the stable market into a bifurcation state or even chaotic state in pursuit of maximizing their utilities. At this time, it is necessary for participants to cooperate and coordinate to hold the system in a stable state, or for the government to

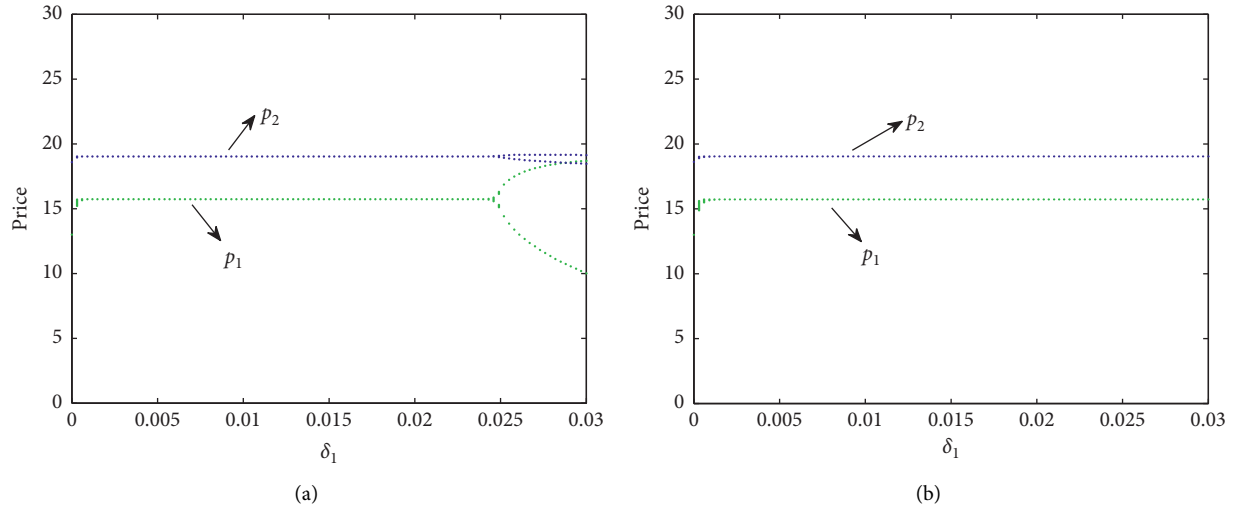


FIGURE 16: The bifurcation diagram of controlled system (19) with δ_1 varying. (a) $\alpha = 0.1$. (b) $\alpha = 0.4$.

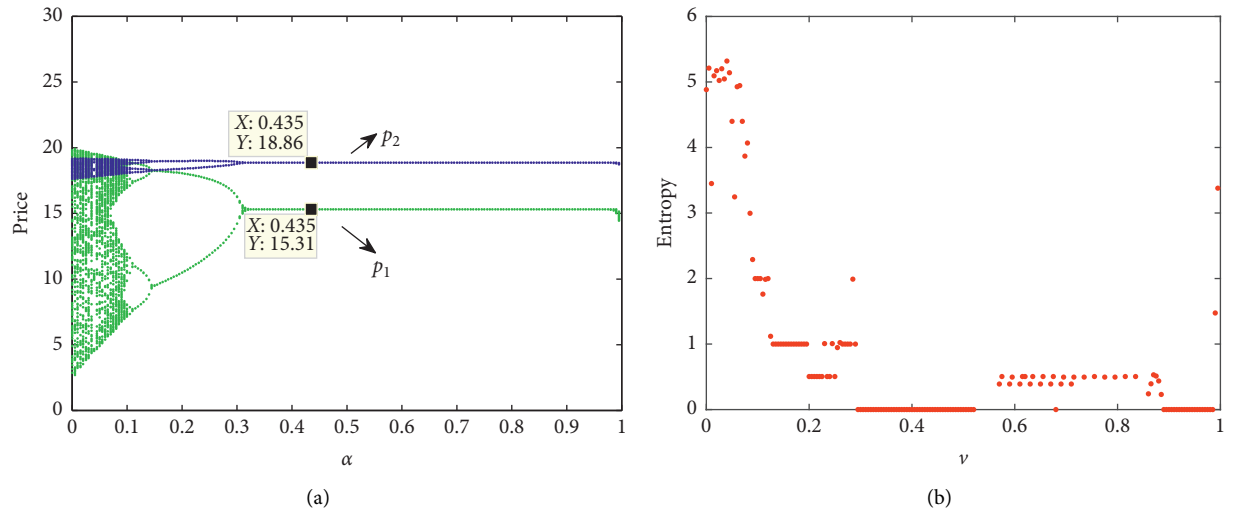


FIGURE 17: The price bifurcation diagram and entropy of controlled system (19) with α varying. (a) The price bifurcation diagram. (b) Entropy.

control the chaotic market and create a good market competition environment.

7. Conclusions

Considering the innovation input for green products and channel service, this article establishes a dynamic game model under the optimal innovation input and focuses on the influence of key factors on the pricing decisions and complexity of the dynamic system. Firstly, equilibrium points, conditions for existence, and local stability of the dynamic system are discussed. Secondly, the complexity dynamics of the dynamic system (the influence of parameters on prices, utilities, and global stability of the dynamic system) are studied by employing dynamic theory. Finally, the parameter adaptation method is employed to restrain chaos of the system. The results are summarized as follows:

- (1) The stable range of the dynamic dual-channel green supply chain system enlarges with the increase of risk-aversion levels of participants, shrinks with service value increasing. In addition, the retailer's channel service will only decrease the stable scope of its own channel price adjustment speed and brings no influence on the manufacturer's decision range of channel price adjustment speed.
- (2) The dynamic system experiences flip bifurcation and enters into chaos as the adjustment speed increasing. In stable range, the retail prices and the utilities of participants are fixed values, and the entropy value of the dynamic dual-channel green supply chain system is low. In the chaotic state, the average utility of the manufacturer declines and that of the retailer improves. The entropy value of the dynamic dual-channel green supply chain system is high. So, chaos

is beneficial for the retailer and is harmful to the manufacturer to achieve high expected utility.

- (3) The attraction domain of initial prices shrinks with price adjustment speed increasing and enlarges with the channel service values increasing. The dynamic system, from chaos, can run to a stable state again using the parameter adaptation method.

There are some shortcomings in this paper, and we can study from the following aspects in the future: (1) one can

consider the nonlinearity of market demand, which is more in line with the market competition environment. (2) One can consider the cost sharing of innovation input based on the cooperation of participants.

Appendix

Proof of Proposition 1. the Jacobian matrix of dynamic system (15) can be expressed as follows:

$$J(p_1, p_2) = \begin{pmatrix} 1 + \delta_1(G_1 + 2X_1p_1 + \beta_1p_2) & \beta_1\delta_1p_1 \\ X_3\delta_2p_2 & 1 + \delta_2(G_2 + 2X_2p_2 + X_3p_1) \end{pmatrix}. \quad (\text{A.1})$$

Substituting the values of ρ_1 into the Jacobian matrix, the two eigenvalues of the Jacobian matrix of dynamic system (15) are $\lambda_1 = 1 + \delta_1G_1$ and $\lambda_2 = 1 + \delta_2G_2$. Because $G_1 > 0$ and $G_2 > 0$, we can verify that all the eigenvalues of the Jacobian matrix are more than 1, so ρ_1 is an unstable equilibrium point.

The proof of Proposition 2. substituting $\rho_2 = (0, -(G_2/X_2))$ and $\rho_3 = (-(G_1/X_1), 0)$ into the Jacobian matrix, the Jacobian matrix of dynamic system (15) can be expressed, respectively, as follows:

$$J(\rho_2) = \begin{pmatrix} 1 + \delta_1\left(G_1 - \beta_1\frac{G_2}{X_2}\right) & 0 \\ \frac{X_3\delta_2G_2}{X_2} & 1 - \delta_2G_2 \end{pmatrix}, \quad (\text{A.2})$$

$$J(\rho_3) = \begin{pmatrix} 1 - \delta_1G_1 & \frac{\beta_1\delta_1G_1}{X_1} \\ 0 & 1 + \delta_2\left(G_2 - \frac{X_3G_1}{X_1}\right) \end{pmatrix}.$$

The eigenvalues of the matrix $J(\rho_2)$ are $\lambda'_1 = 1 - \delta_2G_2$ and $\lambda'_2 = 1 + \delta_1G_1 - (\beta_1G_2\delta_1/X_2)$. The eigenvalues of the matrix $J(\rho_3)$ are $\lambda''_1 = 1 - \delta_1G_1$ and $\lambda''_2 = 1 + \delta_2G_2 - (\beta_1G_1X_3/X_1)$.

According to the previous restrictions on the parameters, it can deduce that $\lambda'_1 < 1$, $\lambda'_2 > 1$, $\lambda''_1 < 1$, and $\lambda''_2 > 1$. The eigenvalues of the Jacobian matrix $J(\rho_2)$ and $J(\rho_3)$ are not less than 1. So, ρ_2 and ρ_3 are unstable saddle points.

Data Availability

The data used to support the findings of this study are available from the corresponding author upon request.

Conflicts of Interest

The authors declare no conflicts of interest.

Authors' Contributions

Li Qiuxiang provided research methods, Huang Yimin wrote the original draft, and Li Mengmeng revised the paper.

Acknowledgments

The research was supported by the National Social Science Foundation of China (no. 19FGLB067) and Henan Province Soft Science Research Plan Project (no. 192400410088).

References

- [1] <http://www.cheari.org/index.php/Show/cid/14/aid/335>.
- [2] W. Liu, D. Qin, N. Shen et al., "Optimal pricing for a multi-echelon closed loop supply chain with different power structures and product dual differences," *Journal of Cleaner Production*, vol. 257, no. 1, Article ID 120281, 2020.
- [3] B. Kim, "Coordinating an innovation in supply chain management," *European Journal of Operational Research*, vol. 123, no. 3, pp. 568–584, 2000.
- [4] O. Toivanen, P. Stoneman, and D. Bosworth, "Innovation and the market value of UK firms, 1989–1995," *Oxford Bulletin of Economics & Statistics*, vol. 64, no. 1, pp. 39–61, 2010.
- [5] T. S. Genc and P. D. Giovanni, "Trade-in and save: a two-period closed-loop supply chain game with price and technology dependent returns," *International Journal of Production Economics*, vol. 183, pp. 514–527, 2017.
- [6] B. Xin, J. Ma, and Q. Gao, "The complexity of an investment competition dynamical model with imperfect information in a security market," *Chaos, Solitons & Fractals*, vol. 42, no. 4, pp. 2425–2438, 2009.
- [7] U. M. Apte and S. Viswanathan, "Strategic and technological innovations in supply chain management," *International Journal of Manufacturing Technology and Management*, vol. 4, no. 3/4, pp. 264–282, 2002.
- [8] T. Li and J. H. Ma, "The complex dynamics of R&D competition models of three oligarchs with heterogeneous players," *Nonlinear Dynamics*, vol. 74, no. 1–2, pp. 45–54, 2013.
- [9] V.-H. Lee, K.-B. Ooi, A. Y.-L. Chong, and C. Seow, "Creating technological innovation via green supply chain management: an empirical analysis," *Expert Systems with Applications*, vol. 41, no. 16, pp. 6983–6994, 2014.

- [10] J. Wang and H. Shin, "The impact of contracts and competition on upstream innovation in a supply chain," *Production and Operations Management*, vol. 24, no. 1, pp. 134–146, 2015.
- [11] P. Verma, V. Kumar, and R. R. K. Sharma, "Role of SMAC stack on competitive advantage and innovation with supply chain performance," in *Proceedings of the International Conference on Business Management*, Social Science Electronic Publishing, Taj Samudra, Colombo, December 2017.
- [12] K. T. Kim, J. S. Lee, and S. Y. Lee, "The effects of supply chain fairness and the buyer's power sources on the innovation performance of the supplier: a mediating role of social capital accumulation," *Journal of Business & Industrial Marketing*, vol. 32, no. 7, pp. 987–997, 2017.
- [13] J. Song, F. Li, D. D. Wu, L. Liang, and A. Dolgui, "Supply chain coordination through integration of innovation effort and advertising support," *Applied Mathematical Modelling*, vol. 49, pp. 108–123, 2017.
- [14] S. Yoon and S. Jeong, "Effects to implement the open-innovation coordinative strategies between manufacturer and retailer in reverse supply chain," *Journal of Open Innovation: Technology, Market, and Complexity*, vol. 3, no. 1, p. 2, 2017.
- [15] W. Y. Yan, R. Hong, and J. F. Rong, "Cooperative innovation evolutionary game analysis of industrialized building supply chain," *Applied Mechanics and Materials*, vol. 878, pp. 213–218, 2018.
- [16] A. Aydin and R. P. Parker, "Innovation and technology diffusion in competitive supply chains," *European Journal of Operational Research*, vol. 265, no. 3, 2018.
- [17] A. Dumrongsiri, M. Fan, A. Jain, and K. Moinsadeh, "A supply chain model with direct and retail channels," *European Journal of Operational Research*, vol. 187, no. 3, pp. 691–718, 2008.
- [18] D.-Q. Yao, X. Yue, and J. Liu, "Vertical cost information sharing in a supply chain with value-adding retailers," *Omega*, vol. 36, no. 5, pp. 838–851, 2008.
- [19] B. Dan, G. Xu, and C. Liu, "Pricing policies in a dual-channel supply chain with retail services," *International Journal of Production Economics*, vol. 139, no. 1, pp. 312–320, 2012.
- [20] F. Ding and J.-Z. Huo, "A feasibility of service level coordination of dual channel supply chain effect of dual-channel supply chain," *Chinese Journal of Management Science*, vol. S1, pp. 485–490, 2014.
- [21] Z. Pei and R. Yan, "Do channel members value supportive retail services? Why?" *Journal of Business Research*, vol. 68, no. 6, pp. 1350–1358, 2015.
- [22] J. Ma and Z. Guo, "Research on the complex dynamic characteristics and RLS estimation's influence based on price and service game," *Mathematical Problems in Engineering*, vol. 2015, Article ID 302506, 13 pages, 2015.
- [23] M. Protopappa-Sieke, M. A. Sieke, and U. W. Thonemann, "Optimal two-period inventory allocation under multiple service level contracts," *European Journal of Operational Research*, vol. 252, no. 1, pp. 145–155, 2016.
- [24] S. K. Jena and S. P. Sarmah, "Price and service co-opetition under uncertain demand and condition of used items in a remanufacturing system," *International Journal of Production Economics*, vol. 173, pp. 1–21, 2016.
- [25] X. Chen, X. Wang, and X. Jiang, "The impact of power structure on the retail service supply chain with an O2O mixed channel," *Journal of the Operational Research Society*, vol. 67, no. 2, pp. 294–301, 2016.
- [26] L. C. Kong, Z. Y. Liu, Y. F. Pan, J. P. Xie, and G. Yang, "Pricing and service decision of dual-channel operations in an O2O closed-loop supply chain," *Industrial Management & Data Systems*, vol. 117, no. 8, pp. 1567–1588, 2017.
- [27] F. Zhang and C. Wang, "Dynamic pricing strategy and coordination in a dual-channel supply chain considering service value," *Applied Mathematical Modelling*, vol. 54, pp. 722–742, 2017.
- [28] Y. W. Zhou, J. S. Guo, and W. H. Zhou, "Pricing/service strategies for a dual-channel supply chain with free riding and service-cost sharing," *International Journal of Production Economics*, vol. 196, pp. 198–210, 2018.
- [29] S. K. Ghosh, "Optimal pricing strategy of a two-echelon supply chain consisting of one manufacturer and two retailers with price and service sensitive demand," *International Journal of Applied & Computational Mathematics*, vol. 4, p. 1, 2018.
- [30] D. Yang, E. Qi, and Y. Li, "Quick response and supply chain structure with strategic consumers," *Omega*, vol. 52, pp. 1–14, 2015.
- [31] H. Tu, X. Mao, and X. Wang, "Complexity of a dynamic hybrid supply chain game model with a service factor," *Nonlinear Dynamics*, vol. 97, no. 4, pp. 2055–2066, 2019.
- [32] B. Xin and M. Sun, "A differential oligopoly game for optimal production planning and water savings," *European Journal of Operational Research*, vol. 269, no. 1, pp. 206–217, 2018.
- [33] Q. X. Li, Y. H. Zhang, and Y. M. Huang, "The impacts of fairness concern and different business objectives on the complexity of dual-channel value chains," *Complexity*, vol. 2020, Article ID 1716084, 15 pages, 2020.
- [34] Q. X. Li, X. L. Chen, Y. M. Huang, H. Gui, and S. Liu, "The impacts of green innovation input and channel service in a dual-channel value chain," *International Journal Of Environmental Research And Public Health*, vol. 16, no. 22, p. 4566, 2019.
- [35] K. Guo, J. Jiang, and Y. Xu, "Semi-analytical expression of stochastic closed curve attractors in nonlinear dynamical systems under weak noise," *Communications in Nonlinear Science and Numerical Simulation*, vol. 38, pp. 91–101, 2016.
- [36] X. Liu and N. Xie, "A nonlinear grey forecasting model with double shape parameters and its application," *Applied Mathematics and Computation*, vol. 360, pp. 203–212, 2019.
- [37] O. Galor, "Discrete dynamical systems," *Ge Growth Math Methods*, vol. 11, no. 4, pp. 438–447, 2005.
- [38] X. Liu and D. Xiao, "Complex dynamic behaviors of a discrete-time predator-prey system," *Chaos, Solitons & Fractals*, vol. 32, no. 1, pp. 80–94, 2007.
- [39] J. A. Holyst and K. Urbanowicz, "Chaos control in economical model by time-delayed feedback method," *Physica A: Statistical Mechanics and Its Applications*, vol. 287, no. 3–4, pp. 587–598, 2000.
- [40] J.-g. Du, T. Huang, and Z. Sheng, "Analysis of decision-making in economic chaos control," *Nonlinear Analysis: Real World Applications*, vol. 10, no. 4, pp. 2493–2501, 2009.
- [41] A. Matsumoto, "Controlling the cournot-nash chaos," *Journal of Optimization Theory and Applications*, vol. 128, no. 2, pp. 379–392, 2006.
- [42] T. Li, D. Yan, and X. Ma, "Stability analysis and chaos control of recycling price game model for manufacturers and retailers," *Complexity*, vol. 2019, Article ID 3157407, 13 pages, 2019.

Research Article

Forecasting CDS Term Structure Based on Nelson–Siegel Model and Machine Learning

Won Joong Kim,¹ Gunho Jung,² and Sun-Yong Choi ²

¹Department of Industrial and Management Engineering, POSTECH, Gyeongbuk 37673, Republic of Korea

²Department of Financial Mathematics, Gachon University, Gyeonggi 13120, Republic of Korea

Correspondence should be addressed to Sun-Yong Choi; sunyongchoi@gachon.ac.kr

Received 18 March 2020; Revised 18 May 2020; Accepted 20 June 2020; Published 14 July 2020

Guest Editor: Baogui Xin

Copyright © 2020 Won Joong Kim et al. This is an open access article distributed under the Creative Commons Attribution License, which permits unrestricted use, distribution, and reproduction in any medium, provided the original work is properly cited.

In this study, we analyze the term structure of credit default swaps (CDSs) and predict future term structures using the Nelson–Siegel model, recurrent neural network (RNN), support vector regression (SVR), long short-term memory (LSTM), and group method of data handling (GMDH) using CDS term structure data from 2008 to 2019. Furthermore, we evaluate the change in the forecasting performance of the models through a subperiod analysis. According to the empirical results, we confirm that the Nelson–Siegel model can be used to predict not only the interest rate term structure but also the CDS term structure. Additionally, we demonstrate that machine-learning models, namely, SVR, RNN, LSTM, and GMDH, outperform the model-driven methods (in this case, the Nelson–Siegel model). Among the machine learning approaches, GMDH demonstrates the best performance in forecasting the CDS term structure. According to the subperiod analysis, the performance of all models was inconsistent with the data period. All the models were less predictable in highly volatile data periods than in less volatile periods. This study will enable traders and policymakers to invest efficiently and make policy decisions based on the current and future risk factors of a company or country.

1. Introduction

A credit default swap (CDS) is a credit derivative based on credit risk, similar to a bond. The prices of both CDSs and bonds change depending on the risk of the reference entity. If the reference entity has a higher risk, then the CDS spread is set higher. To manage credit risk, we can use a CDS contract. The CDS seller (protection seller) insures the protection buyer's risk in the event of a credit default, such as bankruptcy of the reference entity, debt repudiation, or, in the case of a sovereign bond, a moratorium. There are two ways for a protection seller to compensate the protection buyer's loss. The first is to buy the underlying asset at face value; the second is to pay the difference between the remaining value and the face value. In this way, the protection buyer can hedge his or her credit risk and give the CDS spread to the protection seller.

A CDS spread is an insurance fee that a protection buyer pays to the protection seller, often quarterly. Its value is

determined by factors such as the probability of credit default and recovery rate. The recovery rate is the percentage of the bond value that the reference entity offers to the protection buyer when a credit default happens. Therefore, if the recovery rate is high, the CDS spread will be low. The CDS spread will be high if the default rate is high, which indicates a high probability of credit default. Because the CDS spread indicates the bankruptcy risk of institutions or countries, it is an important economic index that is being actively traded. According to the Bank for International Settlements, the total outstanding notional amount of CDS contracts was \$7809 billion in the first half of 2019.

To date, numerous studies have been conducted on the prediction of financial asset values. For example, Li and Tam [1] forecasted stock price movements of different volatilities using a recurrent neural network (RNN) and support vector machine (SVM). Chen et al. [2] predicted the movement of the Chinese stock market using a long short-term memory- (LSTM-) based model. Gao et al. [3] also used LSTM to

predict stock prices. However, few studies have been conducted on forecasting the CDS term structure. Shaw et al. [4] used the Nelson–Siegel model to make 1-, 5-, and 10-day forecasts of the CDS curve and compared its efficiency with that of the random-walk method. They showed that, although the 1-day forecast was not very effective, the accuracy of the 5- and 10-day forecasts outperformed those of the random-walk model. Avino and Nneji [5] predicted daily quotes of iTraxx Europe CDS indices using linear and nonlinear forecasting models, such as autoregressive (AR) and Markov switching AR models. They found that the AR model often outperforms Markov switching models, but Markov switching models offer a good in-sample fit for iTraxx index data. Sensoy et al. [6] used permutation entropy to test the weak-form efficiency of CDS markets in some countries. They found that CDS markets could be efficient during crisis periods, which implies that the impact of a crisis on CDS market efficiency is limited, and Asian markets outperformed the other tested markets in terms of efficiency. In addition, they showed a negative linear correlation between a country’s CDS efficiency and daily CDS levels. Neftci et al. [7] asserted that CDS markets provide unique information on default probability. They showed that the information provided by a CDS regarding the default risk of a sovereign bond is more accurate than the information from a bond spread provided by the corresponding treasury using a stochastic differential equation based on the Markov process. Duyvesteyn and Martens [8] used the structural model for a sovereign bond from Gray et al. [9] to predict how exchange rate returns and volatility changes affect market CDS spread movements. The model results, such as default probability and spreads, were strongly correlated with CDS spreads. Their results also rejected their hypothesis that changes in sovereign credit spreads are correlated to changes in sovereign market spreads.

As mentioned above, several studies have attempted to predict various financial market indices with machine-learning methods; however, research on CDS term structure is limited. CDS term structure reflects the conditions for monetary policy and companies’ future risk expectations. CDS spread can be classified into two types. The first one is sovereign CDS, which has a country as its reference entity. Sovereign CDS spreads reflect the creditworthiness of a country. That is, the sovereign CDS spread can be considered as a measure of the sovereign credit risk [10]. Furthermore, the sovereign CDS spreads contain some components that are attributed to global risk, according to Pan and Singleton [11] and Longstaff et al. [12]. Studies on sovereign CDS include Pan and Singleton [11], Longstaff et al. [12], Blommestein et al. [10], Galarionis et al. [13], Srivastava et al. [14], Ho [15], and Augustin [16]. The other type of CDS is written with respect to one single reference entity, the so-called single-name CDS. In addition, CDS sector indices are based on the most liquid 5-year term, are equally weighted, and reflect an average midspread calculation of the given index’s constituents. However, single-name CDS spreads are much less liquid than indices [17–19]. In several studies, the creditworthiness of individual industries was investigated using CDS sector data [19–22].

The CDS term structure is important because it integrates the future risk expectations of both markets and companies by offering CDS spreads over time. Thus, we can confirm various types of information from the CDS term structure, such as firm leverage and volatility, as shown by Han and Zhou [23]. Furthermore, understanding the implications of the term structure also provides us with a method of extracting this information and predicting the effect of financial events and risk on it. Despite the large number of studies on CDS, studies that attempt to forecast its term structure remain few.

In this study, we analyze the CDS term structure, particularly sovereign CDS, forecast it using machine-learning models, and identify the most suitable model for predicting CDS term structure. We consider model-driven and data-driven methods: the Nelson–Siegel model, RNN, SVR, LSTM, and GMDH. The Nelson–Siegel model, as a model-driven method, was devised to fit the yield term structure; however, in this study, it was fitted to the CDS term structure to extract the term structure parameters and forecast the CDS term structure with the AR(1) model. RNN, SVR, LSTM, and GMDH are machine-learning models that specialize in predicting time-series data. RNN memorizes previous information and uses it to predict future information. LSTM is basically the same as RNN; however, it memorizes only significant information based on some calculations. SVR is derived from the structural risk minimization principle [24] and has been used for prediction in many fields [25–27]. Among the machine-learning methods, a GMDH network is a system identification method that has been used in various fields of engineering to model and forecast the nature of unknown or complex systems based on a given set of multi-input-single-output data pairs [28–30].

Machine learning is widely used in various fields to analyze data and forecast future flow. For example, Yan and Ouyang [31] compared the efficiency of the LSTM model in predicting financial time-series data with that of other machine-learning models, such as SVM and K-nearest neighbor. Baek and Kim [32], Yan and Ouyang [31], Cao et al. [33], and Fischer and Krauss [34] also analyzed and forecasted financial data using machine learning. Machine learning is widely used in medical research. Thottakkara et al. [35], Motka et al. [36], Boyko et al. [37], and Tighe et al. [38] studied and predicted various illnesses and clinical data with machine-learning models. Many studies have also been performed to predict weather conditions using machine learning. Choi et al. [39], Haupt and Kosovic [40], Rhee and Im [41], and James et al. [42] conducted research on forecasting weather conditions. Ma et al. [43] and Li et al. [44] used a convolutional neural network (CNN) to predict a transportation network. Furthermore, GMDH has been widely used for time-series prediction [45–47]. As in these studies, we will apply machine-learning methods to forecast the CDS term structure and identify the most efficient method. There are not many studies on financial data using machine-learning methods compared to other

areas, and to the best of our knowledge, this work is the first to present a forecasting model for CDS data. Therefore, although there are many prediction methods, we especially focus on methods which are generally used in the prediction of time-series data, such as LSTM, RNN, SVR, and GMDH.

Methodologically, we adopt Nelson–Siegel as a model-driven method and RNN, LSTM, SVR, and GMDH as data-driven methods to predict the CDS term structure for the period (2008–2019). We optimize the data-driven models using a grid search algorithm with the Python technological stack. Furthermore, these tests are explored using subperiod analyses to investigate changes in the model performances over the experimental period. Specifically, we split the entire sample period into two subperiods: January 2008–December 2011 (subperiod 1) and January 2012–December 2019 (subperiod 2), because subperiod 1 contains financial market turbulence due to the global financial crisis and European debt crisis. Through this subperiod analysis, we investigate the change in the forecasting performance of all methods in both high-variance and relatively low-variance data. This kind of subperiod analysis is common in other studies [48–51].

In time-series forecasting, sequence models, either RNN, LSTM, or a combination of both, are frequently used owing to considerations of time. The sequence model recognizes time as an order and can check how it changes according to the order; therefore, it can be applied to data, such as weather and finance. According to Siami-Namini and Namin [52] and McNally et al. [53], neural network (NN) models, such as RNN and LSTM, outperformed conventional algorithms, as measured by their autoregressive integrated moving averages (ARIMAs), when using financial data or bitcoin prices. McNally et al. [53] also evaluated the performance of LSTM using volatile Bitcoin data, and Cortez et al. [54] used data from the Republic of Guatemala to predict emergency events. Furthermore, LSTM is known to be better than RNN because it is modified to correct the disadvantages of RNN; however, it appears to depend on the dataset. For example, Samarawickrama and Fernando [55] demonstrated that LSTM exhibited higher accuracy than RNN when predicting stock prices. However, Selvin et al. [56] also compared RNN with LSTM in forecasting stock prices and found that RNN outperformed LSTM. Therefore, in this study, we used both RNN and LSTM to confirm whether LSTM outperforms RNN when forecasting CDS spreads. Ultimately, the motivation for conducting this study is to compare the CDS forecasting performance between the Nelson–Siegel model and the RNN, LSTM, SVR, and GMDH models, to determine the difference between model-driven and data-driven methods.

This paper is organized as follows: in the next section, we review our dataset and present a statistical summary of the CDS term structure; we describe our methods: Nelson–Siegel, RNN, SVR, LSTM, and GMDH, and we explain hyperparameter optimization and its application to the CDS term structure; Section 3 presents our forecasting results on CDS term structure with various error estimates and demonstrates the performance of each model; and Section 4 provides a summary and concluding remarks.

2. Data Description and Methods

2.1. Data Description. The CDS spread can be classified into several categories. The classification method usually depends on the frame of the credit event. The full restructuring clause is the standard term. Under this condition, any restructuring event could be a credit event. The modified restructuring clause limits the scope of opportunistic behavior by sellers when restructuring agreements do not result in a loss. While restructuring agreements are still considered as credit events, the clause limits the deliverable obligations to those with a maturity of less than 30 months after the termination date of the CDS contract. Under the modified contract option, any restructuring event, except the restructuring of bilateral loans, could be a credit event. Additionally, the modified-modified restructuring term is introduced because modified restructuring has been too severe in its limitation of deliverable obligations. Under this term, the remaining maturity of deliverable assets must be less than 60 months for restructured obligations and 30 months for all other obligations. Under the no restructuring contract option, all restructuring events are excluded under the contract as “trigger events.”

For this type of CDS, we will use a full restructuring sovereign CDS spread dataset because other datasets are unavailable for long periods. Sovereign CDS spread reflects the market participants’ perceptions of a country’s credit ratings. Our data cover the period from October 2008 to October 2019 and maturities of six months and 1, 2, 3, 4, 5, 7, 10, 20, and 30 years. All data were sourced from Datastream and correspond to the daily closing price of the CDS spread. The term structure of the CDS spread normally shows upward sloping curves, as seen in Figure 1. Furthermore, CDS spreads seem to be lower as they get closer to the current date with no exceptions. Table 1 provides summary statistics of the CDS data. We can also verify that spreads with longer maturities have higher prices in terms of both mean and percentile. It is interesting to note that the standard deviation is also higher when the maturity is longer, which implies that the market predictions are highly unstable for longer periods.

2.2. Nelson–Siegel Model. Nelson and Siegel [57] proposed a parsimonious model, and it is widely used to predict the interest rate term structure. The formula is as follows:

$$f_t(\tau) = \beta_{1t} + \beta_{2t} \frac{1 - e^{-\lambda_t \tau}}{\lambda_t \tau} + \beta_{3t} \left(\frac{1 - e^{-\lambda_t \tau}}{\lambda_t \tau} - e^{-\lambda_t \tau} \right), \quad (1)$$

where λ_t is the time-decay parameter; τ is the maturity; and β_{1t} , β_{2t} , and β_{3t} are the three Nelson–Siegel parameters. β_{1t} is the long-term component of the yield curve as it does not decay to 0 and remains constant for all maturities. β_{2t} is the short-term factor, which starts at 1 but quickly decays to 0. Finally, β_{3t} starts at 0 and increases before decaying back to 0; hence, it is medium term, which creates a hump in the yield curve.

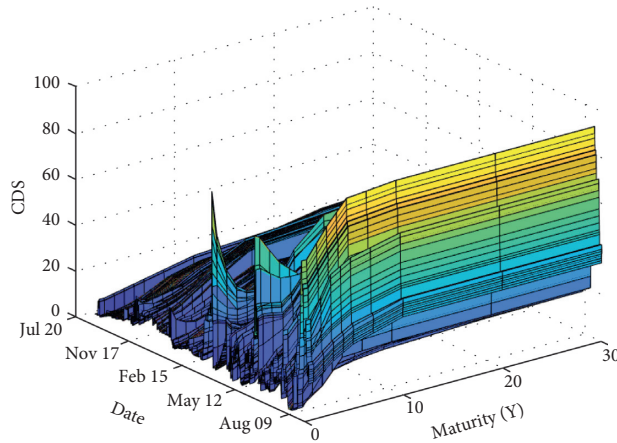


FIGURE 1: CDS term structure from 2008 to 2019.

TABLE 1: Summary statistics for the historical CDS term structure.

Index	Mean	Std. dev.	1st per.	10th per.	25th per.	Median	75th per.	90th per.	99th per.
CDS6M	12.081	9.995	1	4.745	6.263	9.122	13.688	22.98	58
CDS1Y	12.305	9.718	2	4.84	6.54	9.715	14.158	23.39	57.43
CDS2Y	14.117	10.126	4.02	6.21	7.5	11.406	16.49	23.54	62
CDS3Y	16.083	10.838	5.2	7.29	9.063	13.35	19.48	26.57	68
CDS4Y	19.038	11.557	6.29	8.57	11.33	16.005	23.04	30.743	73
CDS5Y	22.154	12.35	7.91	10.38	13.88	19.16	27.783	35.561	78
CDS7Y	26.715	11.819	11.95	14.95	18.8	23.57	32.499	40.731	78
CDS10Y	31.02	11.813	14.12	17.695	23.790	27.963	36.783	44.774	80
CDS20Y	33.903	11.986	17.83	18.77	24.33	34.01	39.597	47.952	80
CDS30Y	34.709	12.214	16.788	19.04	24.159	35.485	40.493	49.265	80

per.: percentile.

The Nelson–Siegel model is a simple but effective method for modeling a term structure, and various studies have used the model to predict the yield curve or other term structures. For example, Shaw et al. [4] forecasted CDS using the Nelson–Siegel model to fit the CDS curve. Guo et al. [58] used the Nelson–Siegel model to model the term structure of implied volatility. GrØnborg and Lunde [59] used it to model the term structure of future oil contracts and forecast the prices of these contracts, while West [60] determined the future price of agricultural commodities. In particular, the CDS term structure has a strong relationship with the interest rate term structure. For example, Chen et al. [61] found that interest rate factors not only affected credit-spread movements but also forecasted future credit risk dynamics. They claimed that the different frequency components of interest rate movements affected the CDS term structure in various industrial sectors and credit rating classes. Specifically, worsening credit conditions tend to lead to future easing of monetary policy, leading to lower current forward interest rate curves. On the contrary, positive shocks to the interest rate narrow the credit spread at long maturities. Tsuruta [62] tried to decompose the yield and CDS term structure into risk and nonrisk structures and found that credit risk components have a negative relationship to the local equity market.

In this study, we attempted to fit the CDS curve to the Nelson–Siegel model by estimating the time-decay parameter λ_t and Nelson–Siegel parameters β_{1t} , β_{2t} , and β_{3t} . We can estimate Nelson–Siegel parameters using various models, such as autoregressive-moving-average (ARMA) and ARIMA, and select the most accurate model. For example, Shaw et al. [4] used the AR(1) process to estimate β_{1t} , β_{2t} , and β_{3t} . Here, we used the AR(1) process to estimate Nelson–Siegel parameters and time-decay parameters. The error measures mean squared error (MSE), root MSE (RMSE), mean percentage error (MPE), mean absolute percentage error (MAPE), and mean absolute error (MAE) to compare the efficiency of this method with that of other methods, such as RNN or LSTM.

2.3. SVR. SVR is a field of machine-learning models derived from SVM. SVM is an algorithm that returns a hyperplane that separates the training samples into two labels, positive and negative. We refer to the distance between the closest point and the hyperplane as the “margin,” and the goal of SVM is to identify the hyperplane that maximizes the margin. There are two types of margin. The first type is a hard margin, which is for linearly separable datasets, meaning that every point does not violate its label. In other

words, all the points can be classified into their labels with a hyperplane. The second one is a soft margin, which is for nonseparable cases. In this case, some points in the dataset, called “outliers,” are incorrectly classified. There are two ways to select a soft margin hyperplane. On the one hand, we can make the margin larger and take more errors (outliers). This is usually used for datasets that have only a small number of outliers. On the other hand, we can choose a hyperplane that has a small margin and minimize the empirical errors. This is useful for datasets with dense point distributions, where it is difficult to separate the data explicitly.

Additionally, the kernel trick can be used for linearly nonseparable datasets. Kernel represents a function that maps origin data points to a higher dimensional dataset that is separable. The reason it is called the “kernel trick” is that, although the dimension of the dataset is increased, the cost of the algorithm does not increase much.

SVM originated from the statistical learning theory introduced by Vapnik and Chervonenkis. The characteristic idea of SVM is to minimize the structural risk, while artificial neural networks (ANNs) minimize the empirical risk. Furthermore, SVM theoretically demonstrates better forecasting than articular neural networks, according to Gunn et al. [63] and Haykin [64].

SVR is derived from SVM. It is a nonlinear kernel-based approach, and the main idea is to identify a function whose deviation from the actual data is located within the pre-determined scale. SVR is applied to a given dataset

$\{(x_i, y_i)\}_{i=1}^n$, where x_i is the input vector, y_i is the output, and n is the total number of data points. The following formulation was introduced by Pérez-Cruz et al. [65]. SVR assumes that the function is a nonlinear function of the form $f(x) = (w^T \phi(x) + b)$, where w and b are the weight and constant, respectively. $\phi(x)$ denotes a mapping function in the feature space. Then, weight vector w and the constant b are estimated by minimizing the following optimization problem:

$$\min_{w, b, \zeta_i, \zeta_i^*} \left\{ \frac{1}{2} \|w\|^2 + C \sum_{i=1}^n (\zeta_i + \zeta_i^*) \right\}, \quad (2)$$

$$\text{subject to } y_i - (w^T \phi(x_i) + b) \leq \epsilon + \zeta_i, \quad (3)$$

$$\begin{aligned} (w^T \phi(x_i) + b) - y_i &\leq \epsilon + \zeta_i^*, \\ \zeta_i, \zeta_i^* &\geq 0, \end{aligned} \quad (4)$$

where $C > 0$ is the prespecified value and ζ_i and ζ_i^* are slack variables indicating the upper and lower constraints, respectively. Setting $\zeta_i = 0$ and $\zeta_i^* = 0$, equations (3) and (4) become the ϵ -loss function introduced by Vapnik. C is the regularization parameter, and $\phi(\cdot)$ is a nonlinear transformation to a higher dimensional space, also known as feature space.

Using Lagrange multipliers and the Karush–Kuhn–Tucker condition, the dual problem for the optimization problem (2)–(4) can be obtained:

$$\begin{aligned} \text{maximize : } L_d &= \epsilon \sum_{i=1}^n (\alpha_i + \alpha_i^*) - \sum_{i=1}^n \sum_{j=1}^n (\alpha_i - \alpha_i^*) (\alpha_j - \alpha_j^*) \phi^T(x_i) \phi(x_j), \\ \text{subject to} & \\ \sum_{i=1}^n (\alpha_i - \alpha_i^*) &= 0, 0 \leq \alpha_i, \alpha_i^* \leq C. \end{aligned} \quad (5)$$

To solve the above problem, we do not identify the nonlinear function $\phi(\cdot)$. The solution can be obtained as

$$f(x) = \sum_{i=1}^n (\alpha_i - \alpha_i^*) K(x, x_i) + b, \quad (6)$$

where $K(x, x_i)$ is called the kernel function, defined as $K(x_i, x_j) = (\phi(x_i) \cdot \phi(x_j))$. Any kernel function satisfying Mercer’s condition can be used as the kernel function (see Mohri et al. [66]).

The selection of the kernel has a significant impact on its forecasting performance. It is a common practice to estimate a range of potential settings and use cross-validation over the training set to determine the best one. In this research, we use three kernel functions: polynomial, Gaussian, and Sigmoid, as presented in Table 2.

Cao and Tay [67] provided a sensitivity of SVMs to the parameters C and ϵ . C and ϵ play an important role in the performance of SVR. Therefore, it is necessary to choose these parameters properly.

2.4. RNN. An ANN is a classification or prediction process that imitates human neurons. The output of a simple ANN model is generated by multiplying weights assigned to input data. After comparing the output data and the real values to be predicted, we create new weights adjusted according to the error. The step in which weights are multiplied by the input data is called forward propagation, and the step in which the error is calculated and weights are adjusted is called backpropagation. The final goal of the ANN model is to determine the weights that minimize the error between the predicted and target values.

A CNN is a machine-learning method that uses a neural network algorithm. It consists of convolution layers, pooling layers, and neural network layers. A convolution layer uses a “filter” to analyze data, typically vectorized image data. The filter analyses small sections while moving over the entire dataset, and each section expresses a “feature” of the data with pooling layers.

TABLE 2: Summary of kernels.

Types of kernel	Kernel $K(u, v)$
Polynomial kernel	$(u \cdot v)^d$
Gaussian kernel	$\exp(-\ u - v\ ^2/2\sigma^2)$
Sigmoid kernel	$\tanh(\eta u \cdot v + \gamma)$

An RNN is another representative neural network model that has a special hidden layer. While a simple neural network has a backpropagation algorithm and adjusts its weights to reduce prediction errors, the RNN has a hidden layer that is modified by the hidden layer of the previous state. Each time the algorithm operates, the RNN hidden layer affects the next hidden layer of the algorithm. Because of its characteristics, RNN is an optimized method to analyze and predict nonlinear time-series data, such as stock prices. It is an algorithm operating in sequence with input and output data. It can return a single output from one or more input data and return more than one output from one or more input data. One of its characteristics is that it returns the output in every hidden time-step layer and simultaneously sends it as input data to the next layer; we demonstrate the simplified structure in Figure 2. RNN has a memory cell in the hidden layer, which returns the output through various activation functions, such as the sigmoid and softmax functions. The memory cell memorizes the output from the previous time-step and uses it as input data recurrently. For instance, at a specific time t , the output of the previous time-step $t - 1$ and input of time-step t are used as input data, and the output is among the input data of the next time-step $t + 1$.

The greatest difference between RNN and CNN or multilayer perceptron (MLP) is that CNN and MLP do not consider previous state data in later steps, but RNN considers both the output of the previous state and the input of the present state. Furthermore, as it is optimized to deal with sequential data, it is used in text, audio, and visual data processing.

However, RNN has a vanishing gradient problem in long backpropagation processes. The algorithm of an RNN is based on gradient descent and modifies its weights in each time-step after one forward propagation process. Weights are modified with error differentials so that these rapidly converge to zero with repetitive backpropagation—this is called the vanishing gradient problem. To solve this problem in long-term time-series data, LSTM is widely used.

2.5. LSTM. To solve the vanishing gradient problem of RNN, Hochreiter and Schmidhuber [68] proposed LSTM, while Gers and Schmidhuber [69] added a forget gate to improve it. RNN considers all previous time-step memories, whereas LSTM chooses only the necessary memories to convey to the next time-step, using an algorithm in a special cell called the LSTM cell. Each of the cells has a forget gate, input gate, output gate, and long short-term memory (c_t, h_t) that pass these cells, as shown in Figure 3.

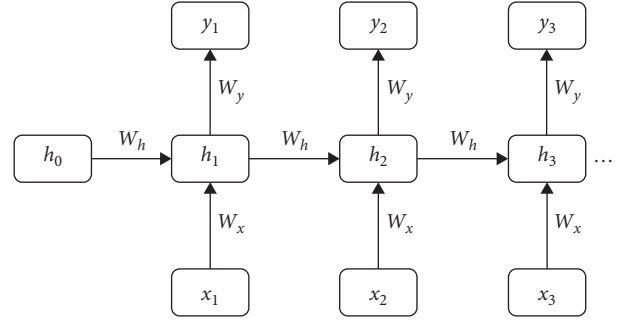


FIGURE 2: RNN cell.

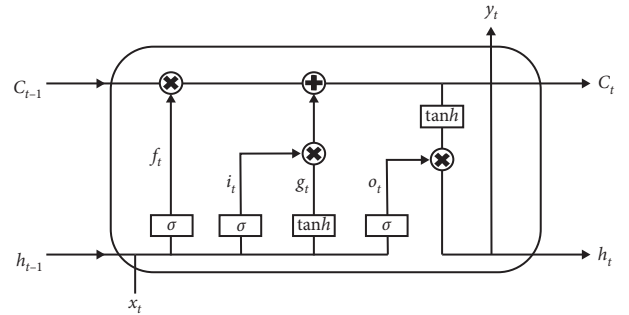


FIGURE 3: LSTM cell.

Input data x_t are deleted, filtered, and added to the long-term memory in the forget gate. The forget gate generally uses a sigmoid function as an activation function that transposes input data and short-term memory into numbers ranging from zero to one. This implies that if the output of the forget gate is close to zero, then most of the information will not pass through; if the output is close to one, then most of the information will pass to the next cell. Next, the input gates decide which data from input x_t and short-term memory must be added after substitution to g_t and i_t .

g_t generates new candidate vectors that could be added to the present cell state, and i_t decides the amount of the information that g_t generated to save. i_t uses the sigmoid function in the same way as the forget gate with the same meaning, i.e., if the value of i_t is close to one, then most of g_t will pass through, and if it is close to zero, then most g_t would not be taken in this cell. c_t is computed with the input gate value and forget gate value. By multiplying f_t with c_{t-1} , the amount of information from the previous time-step cell that will be memorized is determined. Finally, the output gate decides which data will be the output y_t of each cell, considering the memory term and o_t .

The processes performed by each gate are expressed as follows:

$$\text{Input activation : } a_t = \tanh(W_a \cdot x_t + U_a \cdot \text{out}_{t-1} + b_a)$$

$$\text{Input gate : } i_t = \sigma(W_i \cdot x_t + U_i \cdot \text{out}_{t-1} + b_i)$$

$$\text{Forget gate : } f_t = \sigma(W_f \cdot x_t + U_f \cdot \text{out}_{t-1} + b_f)$$

$$\text{Output gate : } o_t = \sigma(W_o \cdot x_t + U_o \cdot \text{out}_{t-1} + b_o)$$

W and U are the weights of x and out, respectively. For example, W_i is the weight of input data x to input gate i .

To develop an LSTM model, we must assign the initial values of c_t and h_t . As mentioned by Zimmermann et al. [70], we set both initial memory term values as zero. LSTM is broadly applied to forecast time-series data; however, owing to its complexity, Chung et al. [71] designed a simpler model called a gated recurrent unit (GRU) while adopting the advantages of LSTM. GRU consists of a reset gate, which decides how to add new input data to the previous cell memory, and an update gate, which decides the amount of memory of the previous cell to save. However, as our dataset is not very large, we used the LSTM model and compared its performance in forecasting the CDS term structure with RNN.

2.6. GMDH. GMDH is a machine-learning method based on the principle of heuristic self-organizing, proposed by Ivakhnenko [72]. The advantage of GMDH is that various considerations, including the number of layers, neurons in hidden layers, and optimal model structure, are determined automatically. In other words, we can apply GMDH to model complex systems without a priori knowledge of the systems.

Suppose that there is a set of n variables consisting of x_1, x_2, \dots, x_n and one y variable. The GMDH algorithm represents a model as a set of neurons in which different pairs in each layer are connected via quadratic polynomials, and they generate new neurons in the next layer [28, 73]. Figure 4 shows the simplified structure. The formal identification problem of the GMDH algorithm is to identify a function \hat{f} that can be used to forecast the output \hat{y} for a given input vector $X = (x_1, x_2, \dots, x_n)$ as close as possible to its actual output y instead of actual function f . Therefore, we can describe the M observations of multi-input and single output data pairs as follows:

$$y_i = f(x_{i1}, x_{i2}, \dots, x_{in}), \quad i = 1, 2, \dots, M. \quad (7)$$

We train a GMDH network to predict the output \hat{y} for any given input vector $X = (x_{i1}, x_{i2}, \dots, x_{in})$, which is given as

$$\hat{y}_i = \hat{f}(x_{i1}, x_{i2}, \dots, x_{in}), \quad i = 1, 2, \dots, M. \quad (8)$$

Now, the GMDH network is determined by minimizing the squared sum of differences between sample outputs and model predictions, that is,

$$\min \sum_{i=1}^M [\hat{f}(x_{i1}, x_{i2}, \dots, x_{in}) - y_i]^2. \quad (9)$$

The general connection between input and output variables can be expressed by a series of Volterra functions:

$$y = w_0 + \sum_{i=1}^n a_i x_i + \sum_{i=1}^n \sum_{j=1}^n w_{ij} x_i x_j + \sum_{i=1}^n \sum_{j=1}^n \sum_{k=1}^n w_{ijk} x_i x_j x_k + \dots, \quad (10)$$

where $X = (x_1, x_2, \dots, x_n)$ is the input variable vector and $A = (w_1, w_2, \dots, w_n)$ is the weight vector. Equation (10) is

known as the Kolmogorov–Gabor polynomial [28, 45, 72, 74, 75].

In this study, we use the second-order polynomial function of two variables, which is written as

$$\hat{y} = G(x_i, x_j) = w_0 + w_1 x_i + w_2 x_j + w_3 x_i x_j + w_4 x_i^2 + w_5 x_j^2. \quad (11)$$

The main objective of the GMDH network is to build the general mathematical relation between the inputs and output variables given in equation (10). The weights a_i in equation (11) are estimated using regression techniques so that the difference between actual output (y) and the calculated output (y_i) is minimized, described as

$$e = \sum_{i=1}^n (\hat{y}_i - y_i) \longrightarrow \min. \quad (12)$$

These parameters can be obtained from multiple regression using the least squares method, and we can compute them by solving some matrix equations. Refer to [28, 29, 46, 76] for a detailed description of the parameter estimation process. The GMDH network can be associated with various algorithms, such as the genetic algorithm [77, 78], singular value decomposition [28], and back-propagation [29, 46, 73, 79–81]. We also improved the GMDH network using backpropagation.

2.7. Hyperparameter Optimization. Hyperparameter optimization refers to the problem of determining the optimal values of hyperparameters that must be set up in advance to perform training and that can complete the generalized performance of the training model to the highest level. In the deep-learning model, for example, the learning rate, batch size, etc. can be regarded as hyperparameters, and in some cases, they can be added as targets for exploration as hyperparameters that determine the structure of the deep-learning model, such as the number of layers and the convolution filter size. Hyperparameter optimization typically includes manual search, grid search, and random search.

Manual search is a way for users to set hyperparameters individually and compare performances according to their intuition. After selecting the candidate hyperparameter values and performing training using them, the performance results measured against the verification dataset are recorded, and this process is repeated several times to select the hyperparameter values that demonstrate the highest performance. This is the most intuitive method; however, it has some problems. First, it is relatively difficult to ensure that the optimal hyperparameter value to be determined is actually optimal because the process of determining the optimal hyperparameter is influenced by the user's selections. Second, the problem becomes more complicated when attempting to search for several types of hyperparameters at once. Because there are some types of hyperparameters that have mutually affecting relationships with others, it is difficult to apply an existing intuition to each single hyperparameter.

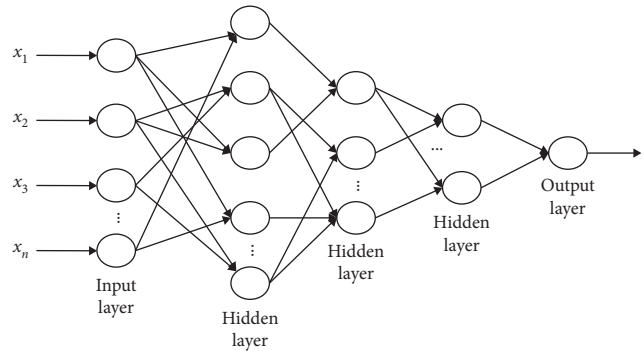


FIGURE 4: GMDH cell.

Grid search is a method of selecting candidate hyperparameter values within a specific section to be searched at regular intervals, recording the performance results measured for each of them, and selecting the hyperparameter values that demonstrated the highest performance (see Hsu et al. [82]). The user determines the search target, length of the section, interval, etc., but more uniform and global search is possible than in the previous manual search. On the contrary, the more the hyperparameters to be searched that are set at one time, the longer the overall search time, and it increases exponentially.

Random search (see Bergstra and Bengio [83]) is similar to grid search but differs in that the candidate hyperparameter values are selected through random sampling. This method can reduce the number of unnecessary repetitions and simultaneously search for values located between predetermined intervals so that the optimal hyperparameter value can be determined more quickly. Random search has the disadvantage that unexpected results can be obtained by testing various combinations other than the values set by the user.

The grid search and random search algorithms are illustrated in Figure 5. In this study, we use the grid search algorithm because it is the simplest and is most widely used for determining optimal hyperparameters [84]. Although a random search can perform much better than grid search for high-dimensional problems, according to Hutter et al. [85], our data are simple time-series data, and the candidate parameter set is limited; thus, we use the grid search algorithm [86, 87]. The Python technological stack was used for experiments. We implemented the machine-learning algorithms and grid search via “Keras,” “TensorFlow,” and “GmdhPy.”

3. Empirical Results

We used 2886 daily time-series data points on CDS term structure from October 2008 to October 2019. Because international financial markets from 2008 to 2011 were unstable, we divided these data into two subperiods, and we measured the forecasting performance of the five methods we used in both high-variance and relatively low-variance data. The first training dataset is from 1st October 2008 to 22nd January 2019 (full period), the second one is from 1st

October 2008 to 9th September 9th 2011 (subperiod 1), and the third one is from 2nd January 2012 to 22nd January 2019 (subperiod 2). We selected our test dataset as the last 200 days (from 23rd January 2019 to 29th October 2019, test dataset 1) for each maturity in the full period, the subperiod 2, and last 80 days (from 12th September 2011 to 30th December 2011, test dataset 2) for the subperiod 1. There is a gap between subperiod 1 and subperiod 2 because of the test dataset 2 for subperiod 1 training set. These all cases are summarized in Table 3. Summary statistics for the test dataset are provided in Tables 4 and 5. Test dataset 2 has higher standard deviations than test dataset 1. Through this subperiod analysis, we compared the prediction power of the models in a relatively volatile period (subperiod 2) and a less volatile period (subperiod 1). We used grid search to optimize the parameters in RNN, LSTM, SVR, and GMDH and calculated the RMSE, MSE, MAPE, MPE, and MAE to compare the performance of these five models. Figures 6–11 show the performance of the Nelson–Siegel, RNN, LSTM, SVR, and GMDH models with the test datasets for each maturity.

Our main findings can be summarized as follows: first, as shown in Figures 6–11, every model provides accurate predictions of CDS term structure. Figures 12–14 also show that machine-learning methods have similar accuracy and outperformed the Nelson–Siegel with AR(1) model. This proves that machine-learning models can be applied to forecasting CDS time-series data and that the Nelson–Siegel model fits both the interest rate term structure and CDS term structure. Furthermore, GMDH, SVR, and RNN have very similar accuracies in all periods and maturities. Second, comparing the Nelson–Siegel model with the four machine-learning methods in predictive power, the Nelson–Siegel model shows the poorest performance for all test sets. That is, machine-learning algorithms are more effective in predicting CDS spread than the Nelson–Siegel model, based on interest rate term structures, which play an important role in determining CDS spread levels. Third, among the machine-learning methods, GMDH presents the best prediction results. The error of the GMDH was found to be the lowest among the five methods, as shown in Tables 6–8. In addition, we expected LSTM to outperform RNN, but the RNN model slightly outperformed the LSTM model. However, this result remains debatable, as mentioned in Introduction.

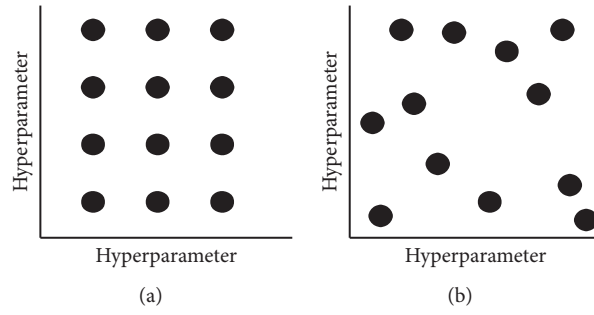


FIGURE 5: Comparison between (a) grid search and (b) random search.

TABLE 3: Descriptions of the training and test datasets.

Case	Training set	Test dataset
Case 1	Full period (2008/10/01–2019/01/22)	Test dataset 1 (2019/01/23–2019/10/29)
Case 2	Subperiod 1 (2008/10/01–2011/09/09)	Test dataset 2 (2011/09/12–2011/12/30)
Case 3	Subperiod 2 (2012/01/02–2019/01/22)	Test dataset 1 (2019/01/23–2019/10/29)

TABLE 4: Summary statistics for test dataset 1 for the full period and subperiod 2 training sets.

	CDS6M	CDS1Y	CDS2Y	CDS3Y	CDS4Y	CDS5Y	CDS7Y	CDS10Y	CDS20Y	CDS30Y
Mean	5.18	5.07	5.42	6.32	7.52	9.25	13.22	15.93	18.39	18.76
Std. dev.	1.84	1.85	1.92	1.86	1.78	1.56	1.21	1.52	1.43	1.89

TABLE 5: Summary statistics for test dataset 2 for the subperiod 1 training set.

	CDS6M	CDS1Y	CDS2Y	CDS3Y	CDS4Y	CDS5Y	CDS7Y	CDS10Y	CDS20Y	CDS30Y
Mean	13.99	14.44	19.74	25.55	30.83	35.83	40.10	44.76	48.17	49.23
Std. dev.	3.77	4.02	3.85	3.73	3.79	4.44	4.98	4.63	3.42	3.20

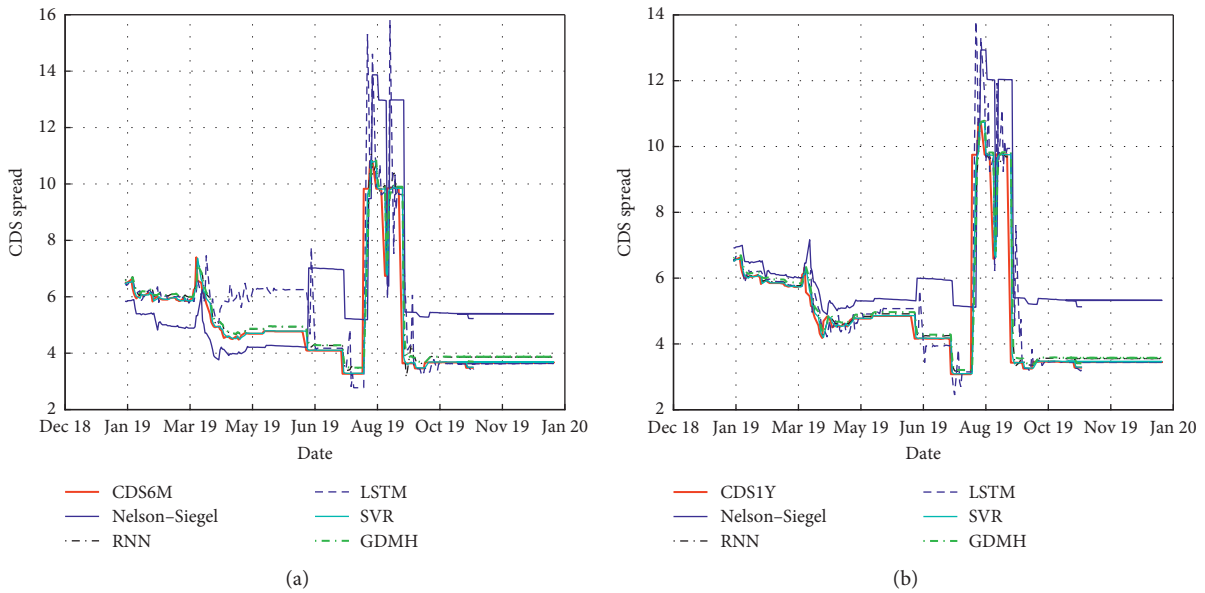


FIGURE 6: Continued.

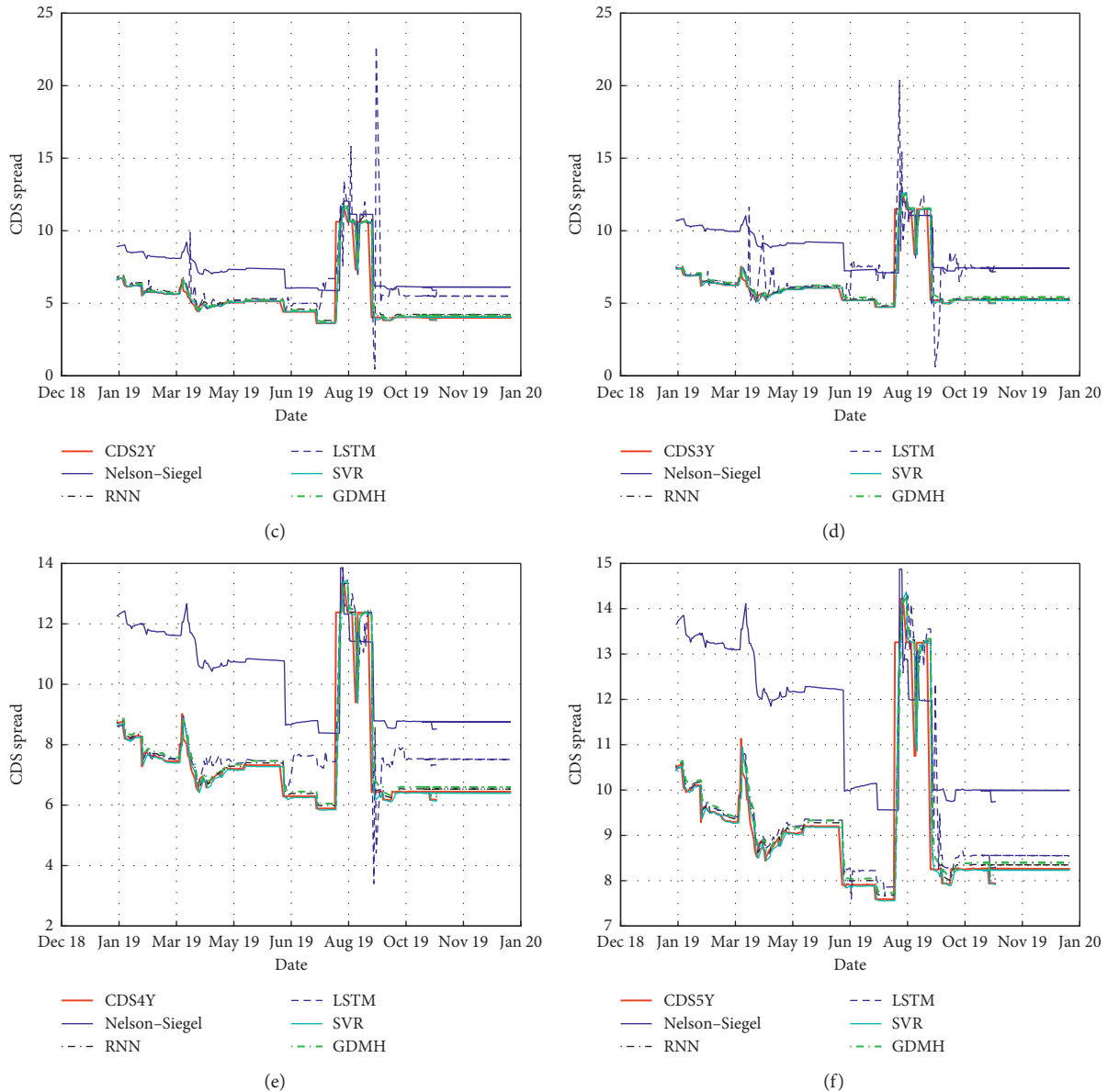


FIGURE 6: Predictions of each model and target CDS term structure from six months to five years maturity for test dataset 1 with the full period training set (case 1).

Performance comparisons between machine-learning algorithms are finding different conclusions in different studies [55, 56, 88–91]. Fourth, the periods with higher standard deviations are generally harder to predict accurately, as seen in Tables 7 and 8. Additionally, the maturities with higher standard deviations are generally harder to predict accurately, as seen in Figures 12–14. The changes in the standard deviation and in the forecasting error are similar for most error measures except MAPE and MPE, as shown in Figure 13.

4. Summary and Concluding Remarks

The purpose of this study is to compare the prediction of CDS term structure between the Nelson-Siegel, RNN,

LSTM, SVR, and GMDH models. We determined the most suitable model to predict time-series data, especially the CDS term structure. The CDS spread is a default risk index for a country or company; hence, this study is useful because it not only offers the best time-series forecasting model but also predicts future risk.

Existing studies on the prediction of CDS term structure and other risk indicators using machine-learning models remain few; most focus on stock price prediction. This study is significant because it demonstrated that various machine-learning models can be applied to other time-series data, and further research on various time-series data using machine-learning models is expected. This study also confirmed that data-driven methods, such as RNN, LSTM, SVR, and GMDH,

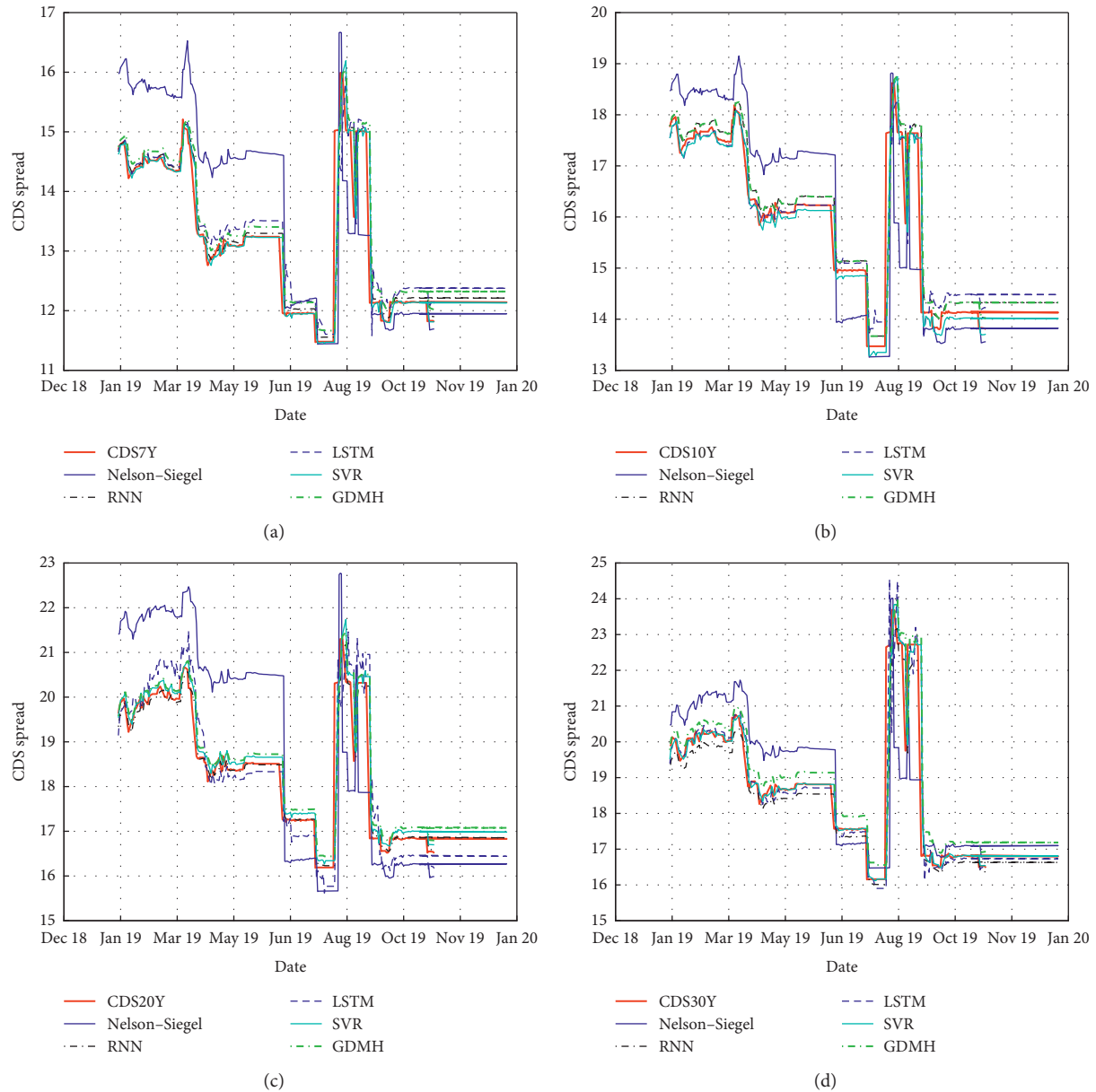


FIGURE 7: Predictions of each model and target CDS term structure from seven years to 30 years maturity for test dataset 1 with the full period training set (case 1).

outperform the model-driven Nelson–Siegel method, which is usually used in analyzing the CDS term structure. The performance of model-driven methods could decline if the data have a significant number of outliers because it is dependent on the assumption that the dataset can be formalized on a specific formula. In our dataset, the presence of outliers made it difficult to make predictions with model-driven methods. On the contrary, data-driven methods were not affected by outliers (see Solomatine et al. [92]), as these consider only datasets that include outliers. As most data available today have many outliers, it is not surprising that data-driven methods outperform model-driven ones.

Some studies show that linear models such as AR are better than ANNs [93–95] for forecasting time series. However, CDS series data are not persistent and volatile, as shown in Figure 1, so Nelson–Siegel based on the AR process performs more poorly than the machine-learning methods. In other words, because of the nonlinearity, machine-learning techniques can be successfully used for modeling and forecasting time series [96–100].

Based on the empirical findings given in Section 3, we have three implications. The first is that the data-driven method is more effective in predictive power than the theoretical model consisting of theoretical variables that influence a financial asset’s price. Of course, the data-driven

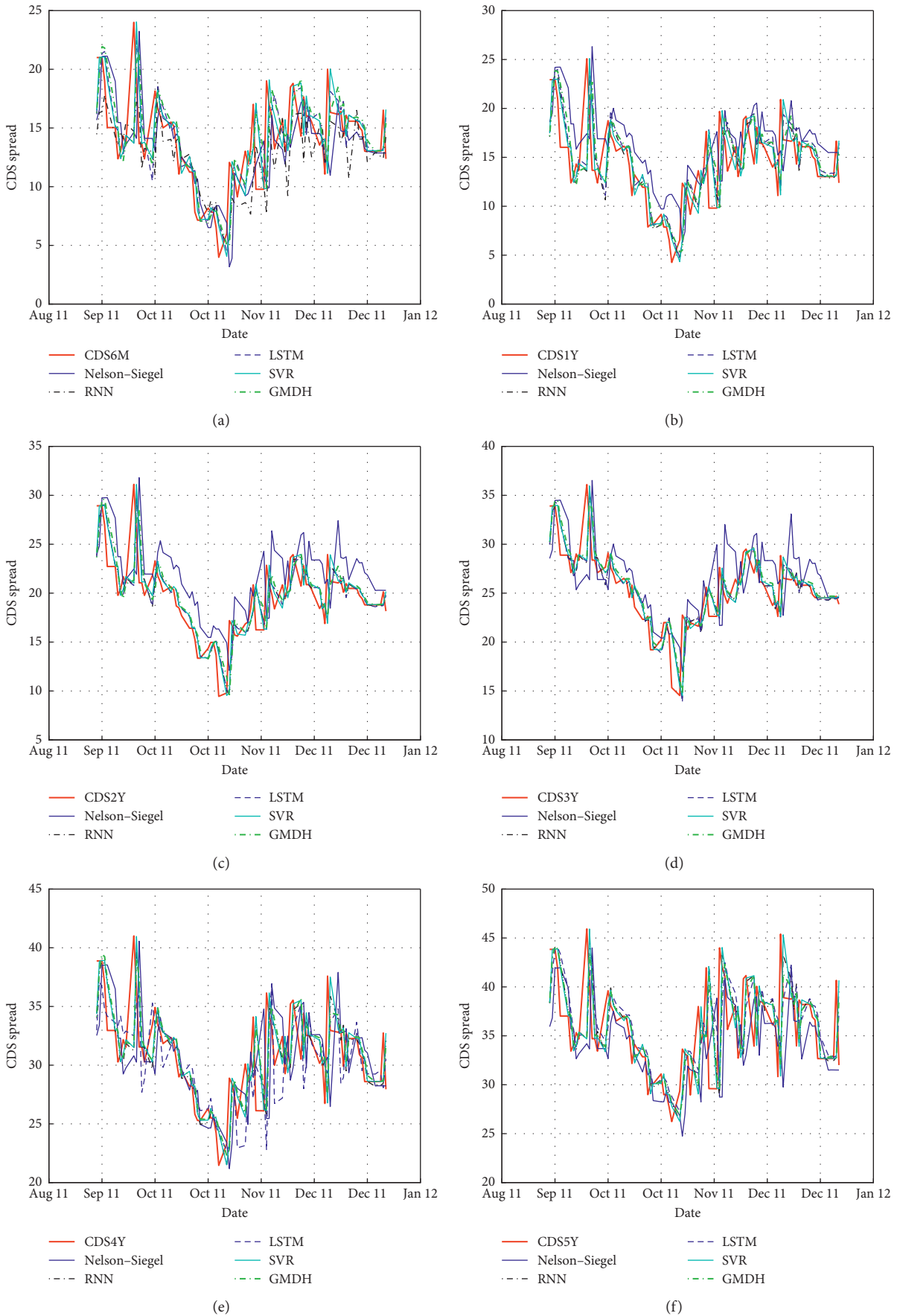


FIGURE 8: Predictions of each model and target CDS term structure from six months to five years maturity for test dataset 2 with the subperiod 1 training set (case 2).

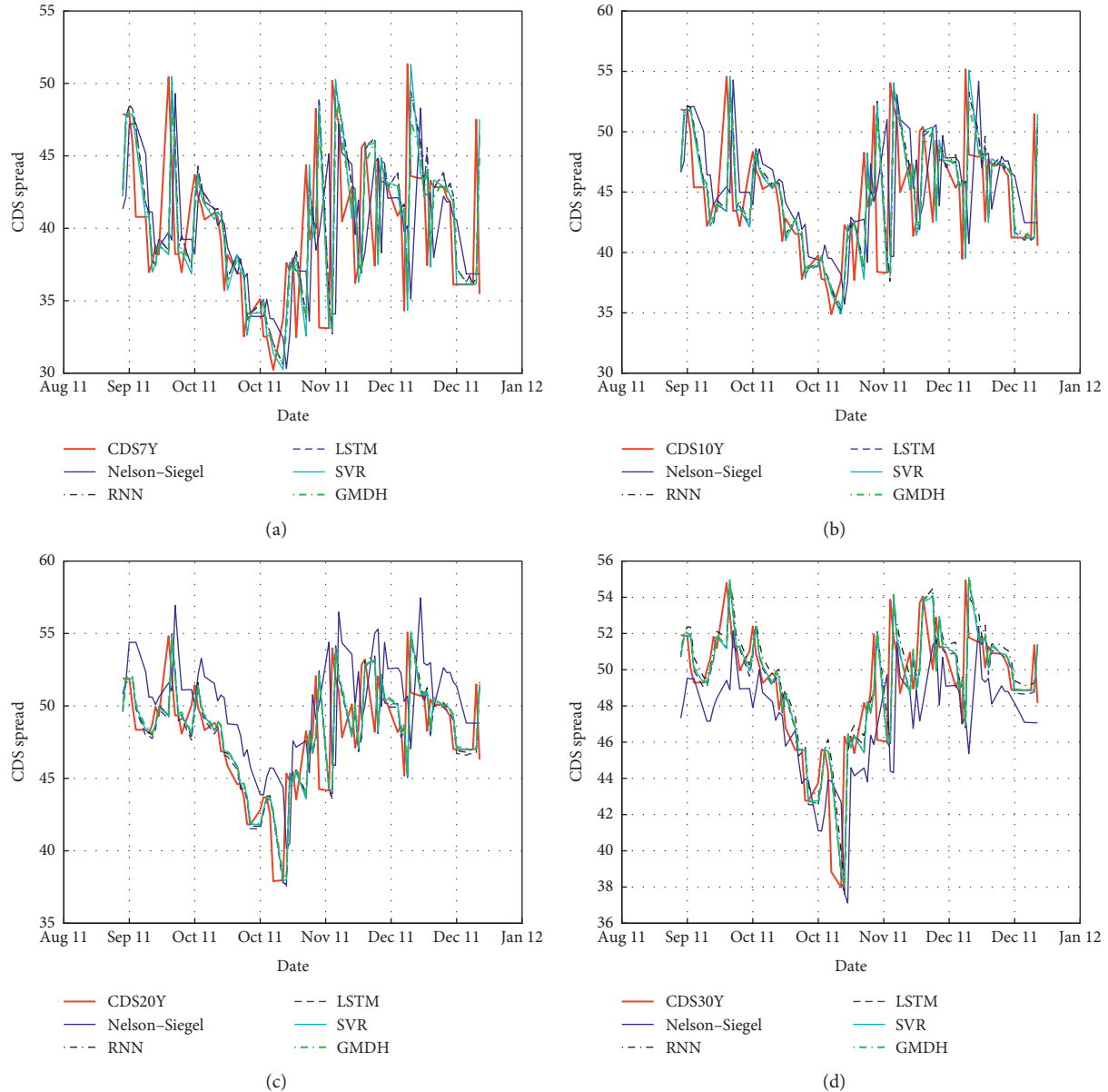


FIGURE 9: Predictions of each model and target CDS term structure from seven years to 30 years maturity for test dataset 2 with the subperiod 1 training set (case 2).

method has a much larger number of parameters than the model-driven method and a much slower implementation speed. However, it is acceptable to use a machine-learning algorithm without the need for prior knowledge, such as interest rate period structure, to predict CDS term structure more accurately. Second, we need to improve the existing Nelson-Siegel model. We showed that the machine-learning models outperform the Nelson-Siegel model for all three cases, which implies both that the machine-learning methodologies excel at this task and that there is a factor in the CDS term structure that the Nelson-Siegel model does not reflect. Nelson-Siegel still has room for improvement in its performance, especially in forecasting applications. Third, the performance of all models was inconsistent depending

on the data period. In the highly volatile data period (subperiod 1), all models were less predictable than in the less volatile data period (subperiod 2). In both approaches, the model performance is not stable when the data are highly volatile. Figure 1 shows that the CDS term structure from 2012 to 2019 seems regular but has some unpredictable points related to the financial turbulence from 2008 to 2011. This unusual volatility is one of the things that reduced the forecasting performance of all models. Therefore, it is necessary to consider a new approach that can achieve solid forecasting performance regardless of the volatility of the data.

Our findings can help investors and policymakers analyze the risk of companies or countries. The CDS spread is

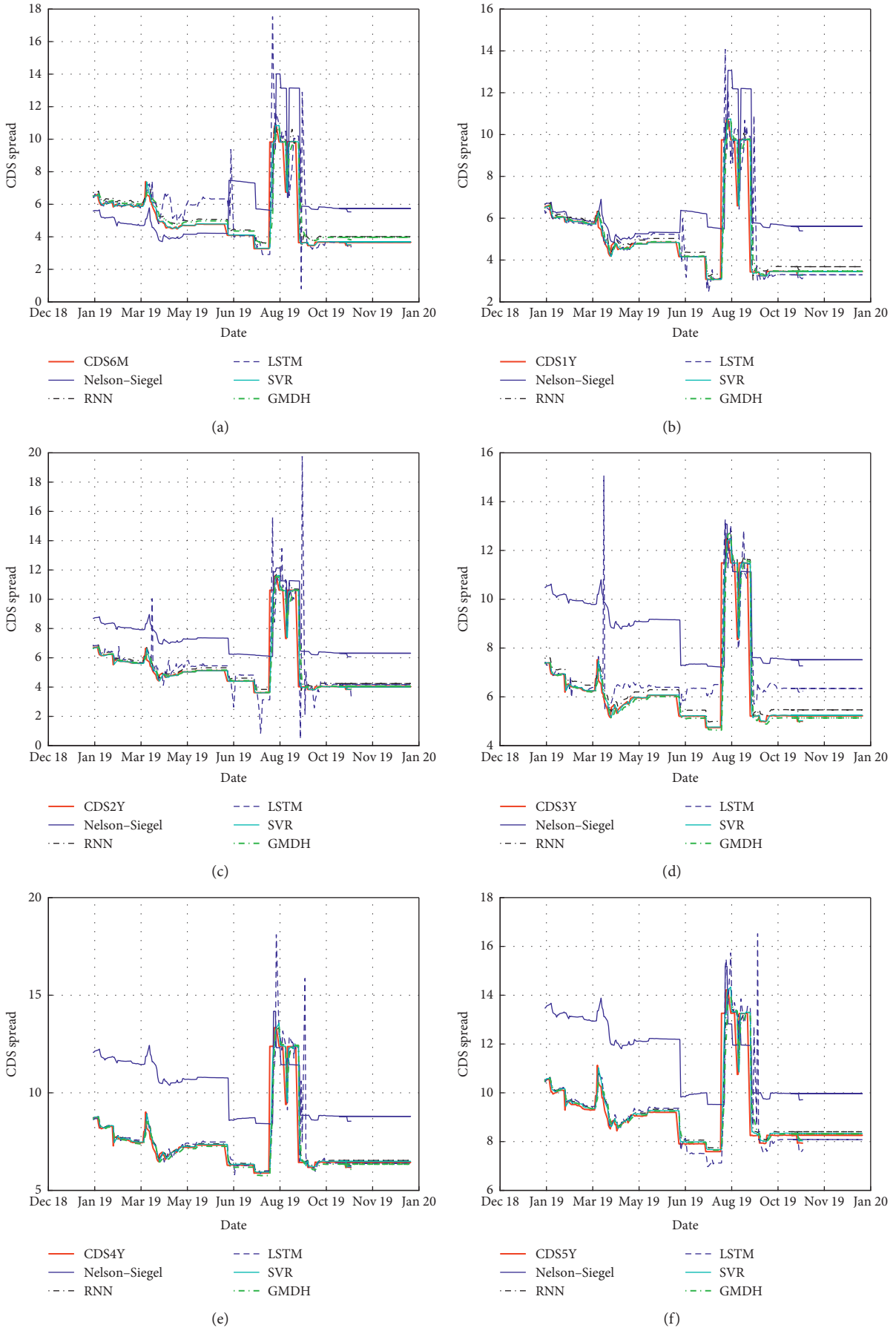


FIGURE 10: Predictions of each model and target CDS term structure from six months to five years maturity for test dataset 1 with the subperiod 2 training set (case 3).

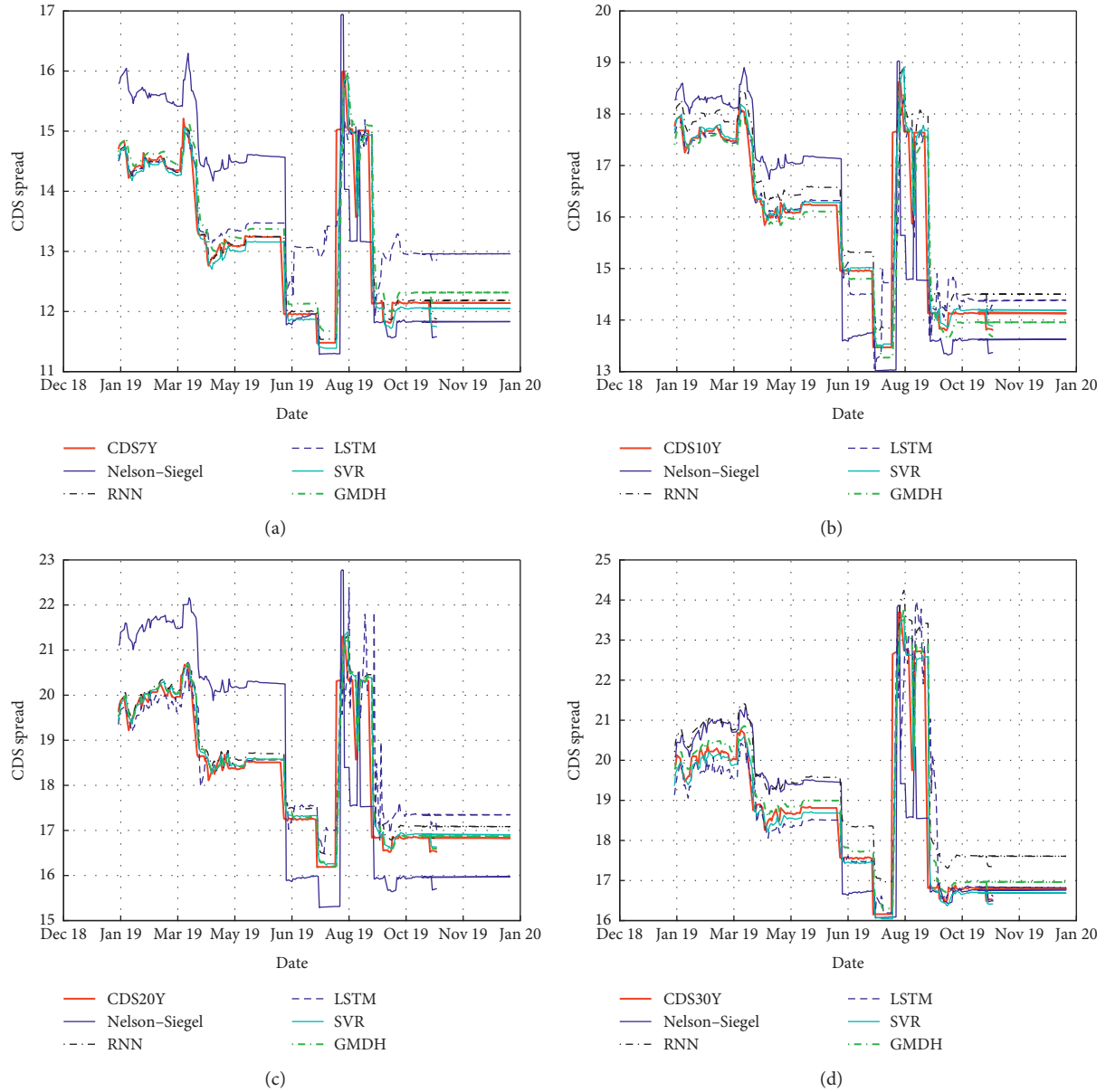


FIGURE 11: Predictions of each model and target CDS term structure from seven years to 30 years maturity for test dataset 1 with the subperiod 2 training set (case 3).

an index that represents the probability of credit default; thus, this study offers a measure to predict future risk. For instance, Zghal et al. [101] showed that CDS can function as a strong hedging mechanism against European stock market fluctuations, and Ratner and Chiu [19] confirmed the hedging and safe-haven characteristics of CDS against stock risks in the U.S. Researchers can also apply machine-learning models to forecast financial risk time-series data.

Future studies should apply this same experiment to datasets other than CDS data for comparing the forecasting performance of model-driven and data-driven methods, such as the implied volatility surface. The implied volatility surface is a fundamental concept for pricing various financial derivatives. Therefore, for a long time, many

researchers have been working on it, and various models have been developed [102–106]. Because it is a key part of the evaluation of financial derivatives, comparisons of performance between existing volatility models and data-driven models in predicting implied volatility should draw attention from academics and practitioners. GMDH showed the best predictive performance for the CDS term structure used in this study. It is now necessary to ensure that GMDH performs best for other term structures as well, such as for volatility term structures and yield curves, or other CDS contracts, for example, corporate CDS and CDS index. As a possible future study, extended Nelson–Siegel models can be used, such as regime-switching [107] and the Nelson–Siegel–Svensson model [108], to forecast CDS term

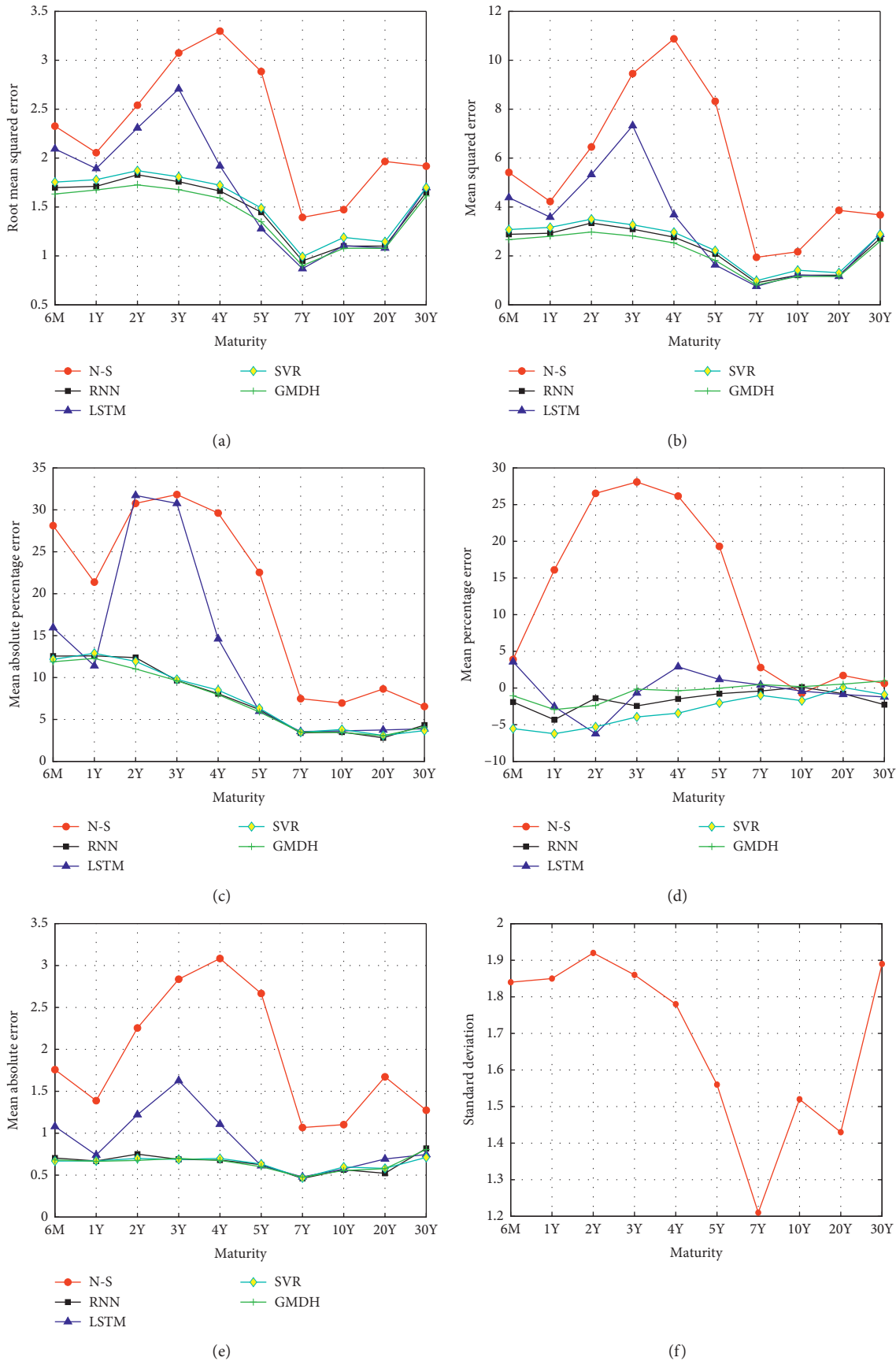
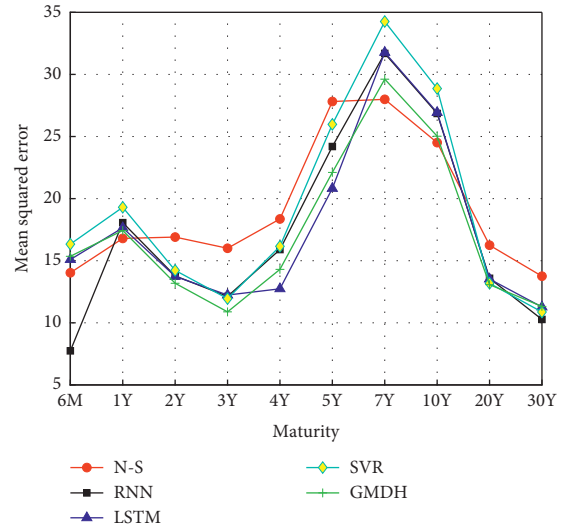
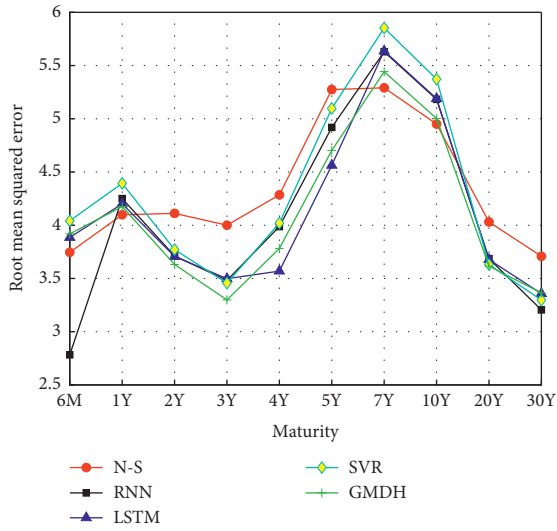
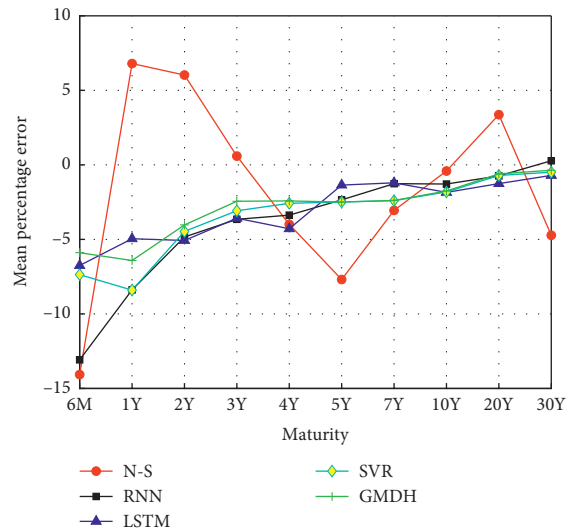
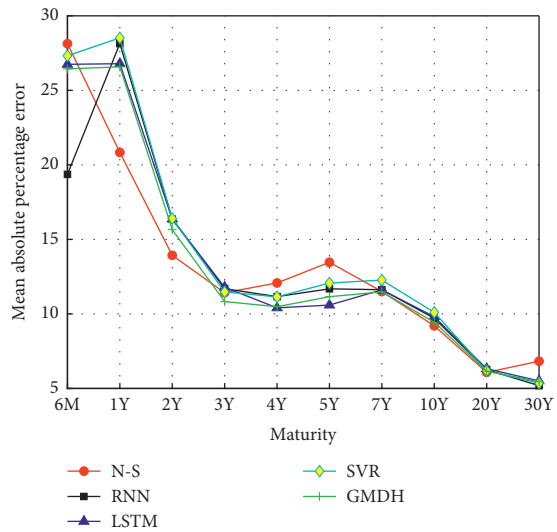


FIGURE 12: Error of each method for all maturities from Table 6 and standard deviations for all maturities (case 1): (a) RMSE (full period training set); (b) MSE (full period training set); (c) MAPE (full period training set); (d) MPE (full period training set); (e) MAE (full period training set); (f) test dataset 1.



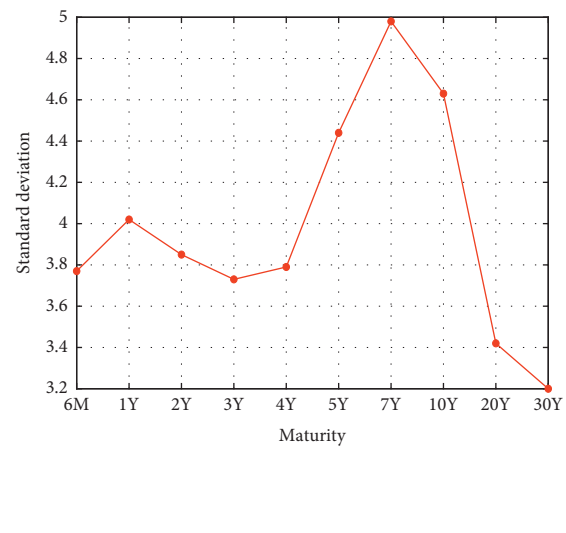
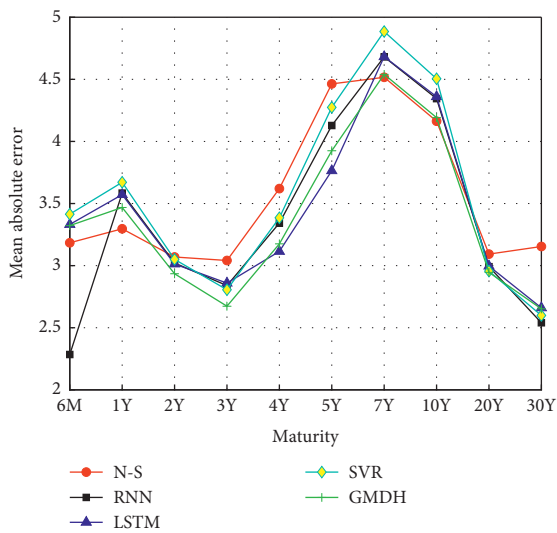
(a)

(b)



(c)

(d)



(e)

(f)

FIGURE 13: Error of each method for all maturities from Table 7 and standard deviations for all maturities (case 2): (a) RMSE (subperiod 1 training set); (b) MSE (subperiod 1 training set); (c) MAPE (subperiod 1 training set); (d) MPE (subperiod 1 training set); (e) MAE (subperiod 1 training set); (f) test dataset 2.

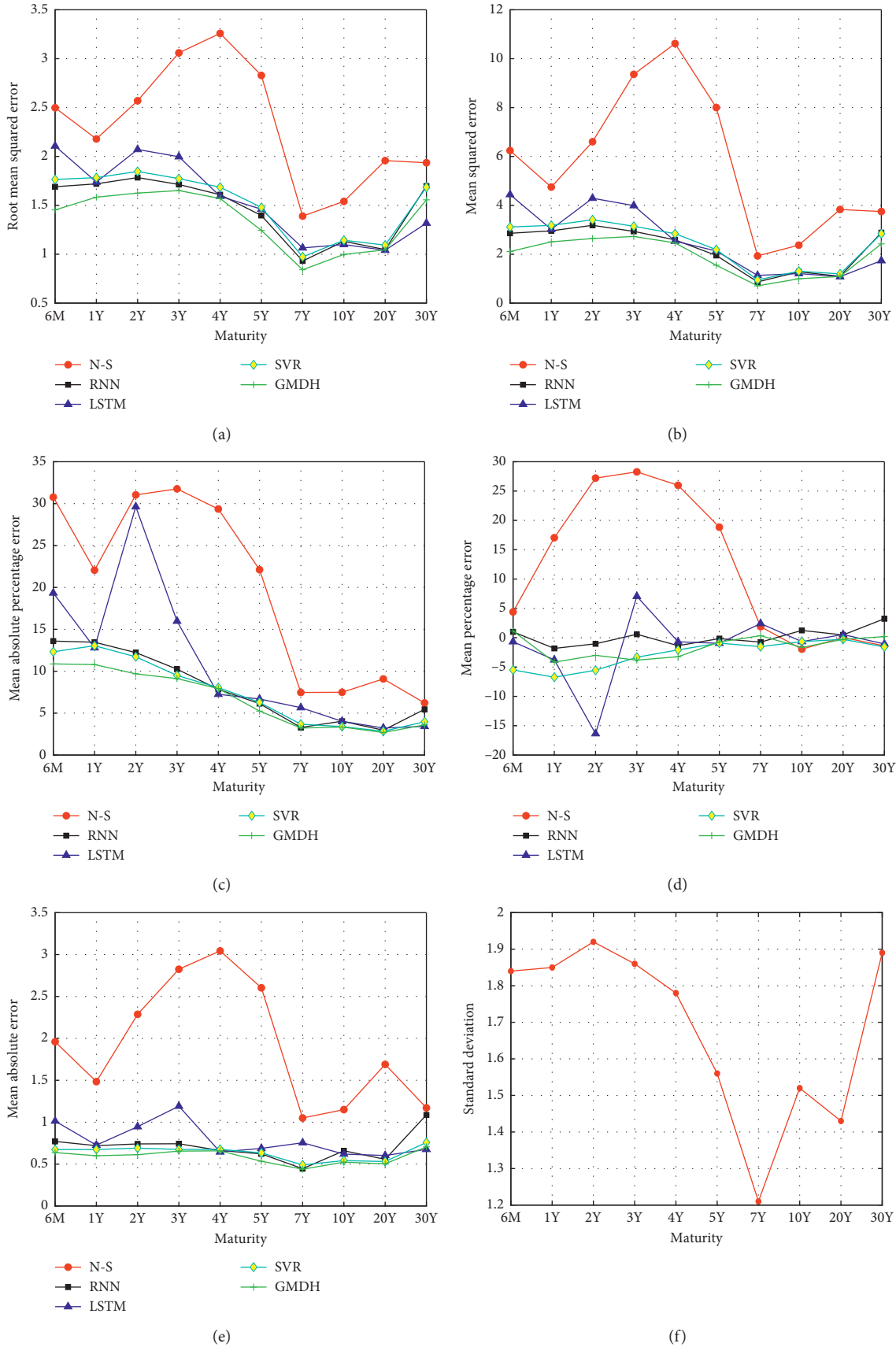


FIGURE 14: Error of each method for all maturities from Table 8 and standard deviations for all maturities (case 3): (a) RMSE (subperiod 2 training set); (b) MSE (subperiod 2 training set); (c) MAPE (subperiod 2 training set); (d) MPE (subperiod 2 training set); (e) MAE (subperiod 2 training set); (f) test dataset 1.

TABLE 6: Error statistics of each method for all maturities for test dataset 1 with the full period training set (case 1).

Type	Method	6M	1Y	2Y	3Y	4Y	5Y	7Y	10Y	20Y	30Y	Average
RMSE	N-S	2.33	2.06	2.54	3.07	3.30	2.88	1.39	1.47	1.97	1.92	2.29
	RNN	1.70	1.71	1.83	1.76	1.66	1.45	0.95	1.10	1.10	1.64	1.49
	LSTM	2.09	1.89	2.31	2.71	1.91	1.28	0.87	1.10	1.08	1.70	1.69
	SVR	1.75	1.78	1.87	1.81	1.72	1.49	0.99	1.19	1.15	1.70	1.55
	GMDH	1.63	1.67	1.73	1.68	1.59	1.35	0.90	1.08	1.08	1.61	1.43
MSE	N-S	5.41	4.22	6.45	9.45	10.88	8.32	1.94	2.17	3.86	3.68	5.64
	RNN	2.88	2.93	3.34	3.09	2.77	2.09	0.90	1.21	1.21	2.71	2.31
	LSTM	4.38	3.58	5.33	7.33	3.68	1.63	0.76	1.22	1.17	2.89	3.20
	SVR	3.08	3.17	3.50	3.27	2.97	2.22	0.99	1.41	1.31	2.89	2.48
	GMDH	2.67	2.80	2.98	2.81	2.53	1.82	0.81	1.16	1.16	2.60	2.13
MAPE (%)	N-S	37.30	32.47	46.24	48.08	43.09	29.50	7.89	6.82	8.95	6.51	26.69
	RNN	12.56	12.59	12.38	9.65	8.07	6.18	3.40	3.50	2.81	4.33	7.55
	LSTM	15.94	11.40	31.72	30.77	14.62	5.98	3.56	3.64	3.75	3.89	12.53
	SVR	12.18	12.89	11.93	9.78	8.50	6.34	3.47	3.81	3.09	3.67	7.57
	GMDH	11.88	12.28	11.03	9.63	7.96	5.90	3.48	3.44	3.06	4.11	7.28
MPE (%)	N-S	-19.03	-29.26	-43.62	-45.40	-40.38	-26.86	-3.79	-0.13	-2.76	-1.55	-21.28
	RNN	-1.91	-4.32	-1.39	-2.44	-1.49	-0.77	-0.41	0.13	-0.77	-2.26	-1.56
	LSTM	3.57	-2.54	-6.23	-0.68	2.90	1.16	0.43	-0.42	-0.87	-1.22	-0.39
	SVR	-5.53	-6.23	-5.29	-3.94	-3.43	-2.04	-0.99	-1.72	0.08	-0.90	-3.00
	GMDH	-1.05	-2.94	-2.38	-0.15	-0.37	-0.02	0.47	0.19	0.54	0.98	-0.47
MAE	N-S	1.76	1.39	2.26	2.84	3.08	2.67	1.07	1.10	1.67	1.27	1.91
	RNN	0.70	0.67	0.75	0.69	0.68	0.62	0.46	0.56	0.52	0.82	0.65
	LSTM	1.08	0.74	1.22	1.63	1.11	0.61	0.48	0.57	0.69	0.75	0.89
	SVR	0.67	0.67	0.70	0.69	0.70	0.63	0.47	0.60	0.58	0.71	0.64
	GMDH	0.68	0.66	0.68	0.70	0.68	0.60	0.48	0.56	0.58	0.81	0.64

N-S: Nelson-Siegel.

TABLE 7: Error statistics of each method for all maturities for test dataset 2 with the subperiod 1 training set (case 2).

Type	Method	6M	1Y	2Y	3Y	4Y	5Y	7Y	10Y	20Y	30Y	Average
RMSE	N-S	3.75	4.10	4.11	4.00	4.29	5.27	5.29	4.95	4.03	3.71	4.35
	RNN	2.78	4.25	3.71	3.48	3.99	4.92	5.63	5.18	3.69	3.20	4.08
	LSTM	3.89	4.20	3.71	3.50	3.57	4.56	5.64	5.19	3.68	3.36	4.13
	SVR	4.04	4.39	3.77	3.46	4.02	5.10	5.85	5.37	3.63	3.30	4.29
	GMDH	3.92	4.18	3.63	3.30	3.78	4.70	5.44	5.00	3.62	3.36	4.09
MSE	N-S	14.03	16.80	16.90	16.00	18.36	27.82	27.99	24.51	16.25	13.75	19.24
	RNN	7.74	18.07	13.78	12.13	15.90	24.20	31.69	26.86	13.59	10.27	17.42
	LSTM	15.10	17.65	13.74	12.24	12.74	20.82	31.77	26.93	13.53	11.27	17.58
	SVR	16.33	19.30	14.22	11.95	16.16	25.98	34.26	28.86	13.18	10.87	19.11
	GMDH	15.36	17.43	13.19	10.88	14.30	22.11	29.62	25.03	13.07	11.32	17.23
MAPE (%)	N-S	28.13	20.83	13.93	11.42	12.08	13.47	11.50	9.20	6.08	6.83	13.35
	RNN	19.36	28.14	16.36	11.69	11.16	11.68	11.62	9.71	6.26	5.19	13.11
	LSTM	26.75	26.79	16.36	11.79	10.41	10.59	11.61	9.82	6.32	5.51	13.60
	SVR	27.32	28.52	16.40	11.48	11.14	12.07	12.27	10.11	6.19	5.36	14.09
	GMDH	26.44	26.58	15.65	10.83	10.48	11.16	11.48	9.44	6.16	5.46	13.37
MPE (%)	N-S	-14.07	6.80	6.03	0.59	-3.99	-7.69	-3.05	-0.41	3.37	-4.72	-1.72
	RNN	-13.08	-8.39	-4.84	-3.65	-3.37	-2.35	-1.26	-1.28	-0.74	0.27	-3.87
	LSTM	-6.75	-4.96	-5.07	-3.58	-4.29	-1.35	-1.20	-1.85	-1.26	-0.71	-3.10
	SVR	-7.37	-8.40	-4.46	-3.08	-2.58	-2.49	-2.40	-1.82	-0.71	-0.49	-3.38
	GMDH	-5.89	-6.42	-4.03	-2.44	-2.42	-2.49	-2.38	-1.75	-0.60	-0.36	-2.88
MAE	N-S	3.18	3.30	3.07	3.04	3.62	4.46	4.52	4.16	3.09	3.15	3.56
	RNN	2.28	3.58	3.02	2.84	3.34	4.13	4.68	4.34	2.99	2.54	3.37
	LSTM	3.33	3.57	3.01	2.86	3.11	3.76	4.68	4.36	3.00	2.66	3.43
	SVR	3.41	3.67	3.05	2.81	3.39	4.27	4.88	4.50	2.96	2.60	3.55
	GMDH	3.32	3.47	2.93	2.67	3.18	3.92	4.54	4.19	2.95	2.65	3.38

TABLE 8: Error statistics of each method for all maturities for test dataset 1 with the subperiod 2 training set (case 3).

Type	Method	6M	1Y	2Y	3Y	4Y	5Y	7Y	10Y	20Y	30Y	Average
RMSE	N-S	2.50	2.18	2.57	3.06	3.26	2.83	1.39	1.54	1.96	1.94	2.32
	RNN	1.69	1.72	1.78	1.71	1.61	1.40	0.93	1.13	1.05	1.70	1.47
	LSTM	2.11	1.74	2.07	2.00	1.59	1.46	1.06	1.10	1.04	1.32	1.55
	SVR	1.76	1.78	1.84	1.77	1.69	1.48	0.97	1.14	1.09	1.68	1.52
	GMDH	1.45	1.58	1.63	1.65	1.57	1.24	0.84	1.00	1.04	1.56	1.36
MSE	N-S	6.24	4.75	6.60	9.36	10.62	8.00	1.93	2.37	3.83	3.75	5.74
	RNN	2.86	2.96	3.18	2.94	2.59	1.95	0.87	1.28	1.10	2.88	2.26
	LSTM	4.44	3.02	4.29	3.99	2.54	2.13	1.13	1.21	1.08	1.74	2.56
	SVR	3.11	3.18	3.41	3.14	2.84	2.19	0.95	1.31	1.20	2.84	2.42
	GMDH	2.11	2.51	2.64	2.73	2.47	1.55	0.71	1.00	1.09	2.42	1.92
MAPE (%)	N-S	30.77	22.06	31.04	31.76	29.36	22.11	7.47	7.49	9.08	6.22	19.74
	RNN	13.60	13.46	12.23	10.25	7.84	6.14	3.29	4.04	2.96	5.45	7.93
	LSTM	19.34	12.80	29.63	15.97	7.25	6.69	5.65	4.03	3.23	3.42	10.80
	SVR	12.32	13.05	11.73	9.49	8.05	6.28	3.68	3.39	2.84	3.97	7.48
	GMDH	10.88	10.80	9.69	9.11	7.94	5.25	3.22	3.34	2.69	3.60	6.65
MPE (%)	N-S	4.40	17.04	27.21	28.27	25.98	18.84	1.88	-1.95	0.03	-1.39	12.03
	RNN	1.00	-1.82	-1.04	0.59	-1.36	-0.15	-0.75	1.24	0.47	3.23	0.14
	LSTM	-0.68	-3.77	-16.35	7.06	-0.69	-0.96	2.42	-0.66	0.54	-1.07	-1.42
	SVR	-5.49	-6.74	-5.55	-3.33	-2.07	-0.92	-1.52	-0.66	-0.28	-1.56	-2.81
	GMDH	1.14	-4.17	-3.01	-3.82	-3.24	-0.73	0.34	-1.66	-0.29	0.19	-1.53
MAE	N-S	1.96	1.48	2.29	2.82	3.04	2.60	1.05	1.15	1.69	1.17	1.93
	RNN	0.77	0.72	0.74	0.74	0.66	0.62	0.45	0.66	0.56	1.09	0.70
	LSTM	1.01	0.73	0.95	1.19	0.64	0.69	0.75	0.62	0.60	0.68	0.79
	SVR	0.67	0.67	0.69	0.68	0.68	0.63	0.49	0.54	0.53	0.76	0.63
	GMDH	0.64	0.60	0.61	0.66	0.66	0.53	0.44	0.52	0.50	0.71	0.59

structure. Optimized through grid search for machine-learning algorithms, we expect to increase the forecasting power of the Nelson–Siegel model using extended models rather than by optimizing parameters for the Nelson–Siegel model.

Data Availability

The data used to support the findings of this study are available from the corresponding author upon request.

Conflicts of Interest

The authors declare that there are no conflicts of interest regarding the publication of this paper.

Acknowledgments

The authors are grateful to the editor Baogui Xin for the valuable comments which helped to significantly improve this paper. This work was supported by the Gachon University Research Fund of 2018 (GCU-2018-0295) and by the National Research Foundation of Korea (NRF) grant funded by the Korean government (MSIT) (no. 2019R1G1A1010278).

References

- [1] Z. Li and V. Tam, “A comparative study of a recurrent neural network and support vector machine for predicting price movements of stocks of different volatilities,” in *Proceedings of the 2017 IEEE Symposium Series on Computational Intelligence (SSCI)*, IEEE, Paris, France, pp. 1–8, June 2017.
- [2] K. Chen, Y. Zhou, and F. Dai, “A LSTM-based method for stock returns prediction: a case study of China stock market,” in *Proceedings of the 2015 IEEE international conference on big data (big data)*, IEEE, Santa Clara, CA, USA, pp. 2823–2824, 2015.
- [3] T. Gao, Y. Chai, and Yi Liu, “Applying long short term memory neural networks for predicting stock closing price,” in *Proceedings of the 2017 8th IEEE International Conference on Software Engineering and Service Science (ICSESS)*, IEEE, Beijing, China, pp. 575–578, November 2017.
- [4] F. Shaw, F. Murphy, and F. O’Brien, “The forecasting efficiency of the dynamic Nelson-Siegel model on credit default swaps,” *Research in International Business and Finance*, vol. 30, pp. 348–368, 2014.
- [5] D. Avino and O. Nneji, “Are CDS spreads predictable? an analysis of linear and non-linear forecasting models,” *International Review of Financial Analysis*, vol. 34, pp. 262–274, 2014.
- [6] A. Sensoy, F. J. Fabozzi, and V. Eraslan, “Predictability dynamics of emerging sovereign CDS markets,” *Economics Letters*, vol. 161, pp. 5–9, 2017.
- [7] S. Neftci, A. Oliveira Santos, and Y. Lu, *Credit Default Swaps and Financial Crisis Prediction*, Technical Report, Working Paper Series, 2005.
- [8] J. Duyvesteyn and M. Martens, “Forecasting sovereign default risk with Merton’s model,” *The Journal of Fixed Income*, vol. 25, no. 2, pp. 58–71, 2015.
- [9] D. F. Gray, R. C. Merton, and Z. Bodie, “Contingent claims approach to measuring and managing sovereign credit risk,” *Journal of Investment Management*, vol. 5, no. 4, p. 5, 2007.

- [10] H. Blommestein, S. Eijffinger, and Z. Qian, "Regime-dependent determinants of euro area sovereign CDS spreads," *Journal of Financial Stability*, vol. 22, pp. 10–21, 2016.
- [11] J. Pan and K. J. Singleton, "Default and recovery implicit in the term structure of sovereign CDS spreads," *The Journal of Finance*, vol. 63, no. 5, pp. 2345–2384, 2008.
- [12] F. A. Longstaff, J. Pan, L. H. Pedersen, and K. J. Singleton, "How sovereign is sovereign credit risk?" *American Economic Journal: Macroeconomics*, vol. 3, no. 2, pp. 75–103, 2011.
- [13] E. C. Galariotis, P. Makrchoriti, and S. Spyrou, "Sovereign CDS spread determinants and spill-over effects during financial crisis: a panel var approach," *Journal of Financial Stability*, vol. 26, pp. 62–77, 2016.
- [14] S. Srivastava, H. Lin, I. M. Premachandra, and H. Roberts, "Global risk spillover and the predictability of sovereign CDS spread: International evidence," *International Review of Economics & Finance*, vol. 41, pp. 371–390, 2016.
- [15] S. H. Ho, "Long and short-runs determinants of the sovereign CDS spread in emerging countries," *Research in International Business and Finance*, vol. 36, pp. 579–590, 2016.
- [16] P. Augustin, "The term structure of CDS spreads and sovereign credit risk," *Journal of Monetary Economics*, vol. 96, pp. 53–76, 2018.
- [17] E. Bouri, S. J. H. Shahzad, N. Raza, and D. Roubaud, "Oil volatility and sovereign risk of BRICS," *Energy Economics*, vol. 70, pp. 258–269, 2018.
- [18] E. Bouri, N. Jalkh, and D. Roubaud, "Commodity volatility shocks and BRIC sovereign risk: a GARCH-quantile approach," *Resources Policy*, vol. 61, pp. 385–392, 2019.
- [19] M. Ratner and C.-C. Chiu, "Hedging stock sector risk with credit default swaps," *International Review of Financial Analysis*, vol. 30, pp. 18–25, 2013.
- [20] S. Hammoudeh, T. Liu, C.-L. Chang, and M. McAleer, "Risk spillovers in oil-related cds, stock and credit markets," *Energy Economics*, vol. 36, pp. 526–535, 2013.
- [21] S. J. Hussain Shahzad, E. Bouri, J. Arreola-Hernandez, D. Roubaud, and S. Bekiros, "Spillover across eurozone credit market sectors and determinants," *Applied Economics*, vol. 51, no. 59, pp. 6333–6349, 2019.
- [22] S. J. H. Shahzad, S. M. Nor, R. Ferrer, and S. Hammoudeh, "Asymmetric determinants of CDS spreads: U.S. industry-level evidence through the NARDL approach," *Economic Modelling*, vol. 60, pp. 211–230, 2017.
- [23] B. Han and Y. Zhou, "Understanding the term structure of credit default swap spreads," *Journal of Empirical Finance*, vol. 31, pp. 18–35, 2015.
- [24] W. Huang, Y. Nakamori, and S.-Y. Wang, "Forecasting stock market movement direction with support vector machine," *Computers & Operations Research*, vol. 32, no. 10, pp. 2513–2522, 2005.
- [25] K.-j. Kim, "Financial time series forecasting using support vector machines," *Neurocomputing*, vol. 55, no. 1-2, pp. 307–319, 2003.
- [26] C.-J. Lu, T.-S. Lee, and C.-C. Chiu, "Financial time series forecasting using independent component analysis and support vector regression," *Decision Support Systems*, vol. 47, no. 2, pp. 115–125, 2009.
- [27] P.-F. Pai and C.-S. Lin, "A hybrid arima and support vector machines model in stock price forecasting," *Omega*, vol. 33, no. 6, pp. 497–505, 2005.
- [28] N. Amanifard, N. Nariman-Zadeh, M. H. Farahani, and A. Khalkhali, "Modelling of multiple short-length-scale stall cells in an axial compressor using evolved gmdh neural networks," *Energy Conversion and Management*, vol. 49, no. 10, pp. 2588–2594, 2008.
- [29] M. Najafzadeh and G.-A. Barani, "Comparison of group method of data handling based genetic programming and back propagation systems to predict scour depth around bridge piers," *Scientia Iranica*, vol. 18, no. 6, pp. 1207–1213, 2011.
- [30] M. Witczak, J. Korbicz, M. Mrugalski, and R. J. Patton, "A GMDH neural network-based approach to robust fault diagnosis: application to the damadics benchmark problem," *Control Engineering Practice*, vol. 14, no. 6, pp. 671–683, 2006.
- [31] H. Yan and H. Ouyang, "Financial time series prediction based on deep learning," *Wireless Personal Communications*, vol. 102, no. 2, pp. 683–700, 2018.
- [32] Y. Baek and H. Y. Kim, "Modaugnet: a new forecasting framework for stock market index value with an overfitting prevention lstm module and a prediction lstm module," *Expert Systems with Applications*, vol. 113, pp. 457–480, 2018.
- [33] J. Cao, Z. Li, and J. Li, "Financial time series forecasting model based on ceemdan and lstm," *Physica A: Statistical Mechanics and its Applications*, vol. 519, pp. 127–139, 2019.
- [34] T. Fischer and C. Krauss, "Deep learning with long short-term memory networks for financial market predictions," *European Journal of Operational Research*, vol. 270, no. 2, pp. 654–669, 2018.
- [35] P. Thottakkara, T. Ozrazgat-Baslanti, B. B. Hupf et al., "Application of machine learning techniques to high-dimensional clinical data to forecast postoperative complications," *PloS One*, vol. 11, no. 5, Article ID e0155705, 2016.
- [36] R. Motka, V. Parmarl, B. Kumar, and A. R. Verma, "Diabetes mellitus forecast using different data mining techniques," in *Proceedings of the 2013 4th International Conference on Computer and Communication Technology (ICCCCT)*, IEEE, Allahabad, India, pp. 99–103, 2013.
- [37] N. Boyko, T. Sviridova, and N. Shakhovska, "Use of machine learning in the forecast of clinical consequences of cancer diseases," in *Proceedings of the 2018 7th Mediterranean Conference on Embedded Computing (MECO)*, IEEE, Budva, Montenegro, pp. 1–6, 2018.
- [38] P. J. Tighe, C. A. Harle, R. W. Hurley, H. Aytug, A. P. Boezaart, and R. B. Fillingim, "Teaching a machine to feel postoperative pain: combining high-dimensional clinical data with machine learning algorithms to forecast acute postoperative pain," *Pain Medicine*, vol. 16, no. 7, pp. 1386–1401, 2015.
- [39] S. Choi, Y. J. Kim, B. Simon, and D. Mavris, "Prediction of weather-induced airline delays based on machine learning algorithms," in *Proceedings of the 2016 IEEE/AIAA 35th Digital Avionics Systems Conference (DASC)*, IEEE, Sacramento, CA, USA, pp. 1–6, September 2016.
- [40] S. E. Haupt and B. Kosovic, "Big data and machine learning for applied weather forecasts: forecasting solar power for utility operations," in *Proceedings of the 2015 IEEE Symposium Series on Computational Intelligence*, IEEE, Cape Town, South Africa, pp. 496–501, December 2015.
- [41] J. Rhee and J. Im, "Meteorological drought forecasting for ungauged areas based on machine learning: using long-range climate forecast and remote sensing data," *Agricultural and Forest Meteorology*, vol. 237–238, pp. 105–122, 2017.
- [42] S. C. James, Y. Zhang, and F. O'Donncha, "A machine learning framework to forecast wave conditions," *Coastal Engineering*, vol. 137, pp. 1–10, 2018.
- [43] X. Ma, Z. Dai, Z. He, J. Ma, Y. Wang, and Y. Wang, "Learning traffic as images: a deep convolutional neural network for

- large-scale transportation network speed prediction,” *Sensors*, vol. 17, no. 4, p. 818, 2017.
- [44] Y. Li, R. Yu, C. Shahabi, and Y. Liu, “Diffusion convolutional recurrent neural network: data-driven traffic forecasting,” 2017, <http://arxiv.org/abs/1707.01926>.
- [45] S. J. Farlow, *Self-Organizing Methods in Modeling: GMDH Type Algorithms*, Vol. 54, CRC Press, Boca Raton, FL, USA, 1984.
- [46] M. Najafzadeh and H. M. Azamathulla, “Group method of data handling to predict scour depth around bridge piers,” *Neural Computing and Applications*, vol. 23, no. 7-8, pp. 2107–2112, 2013.
- [47] N. Nariman-Zadeh, A. Darvizeh, and G. R. Ahmad-Zadeh, “Hybrid genetic design of GMDH-type neural networks using singular value decomposition for modelling and prediction of the explosive cutting process,” *Proceedings of the Institution of Mechanical Engineers, Part B: Journal of Engineering Manufacture*, vol. 217, no. 6, pp. 779–790, 2003.
- [48] S.-Y. Choi and C. Hong, “Relationship between uncertainty in the oil and stock markets before and after the shale gas revolution: evidence from the OVX, VIX, and VKOSPI volatility indices,” *PloS One*, vol. 15, no. 5, Article ID e0232508, 2020.
- [49] R. Y. M. Li, S. Fong, and K. W. S. Chong, “Forecasting the reits and stock indices: group method of data handling neural network approach,” *Pacific Rim Property Research Journal*, vol. 23, no. 2, pp. 123–160, 2017.
- [50] I. Pavlova, M. E. de Boyrie, and A. M. Parhizgari, “A dynamic spillover analysis of crude oil effects on the sovereign credit risk of exporting countries,” *The Quarterly Review of Economics and Finance*, vol. 68, pp. 10–22, 2018.
- [51] R. Ramezani, A. Peymanfar, and S. B. Ebrahimi, “An integrated framework of genetic network programming and multi-layer perceptron neural network for prediction of daily stock return: an application in tehran stock exchange market,” *Applied Soft Computing*, vol. 82, Article ID 105551, 2019.
- [52] S. Siami-Namini and A. S. Namin, *Forecasting Economics and Financial Time Series: ARIMA vs. LSTM*, <http://arxiv.org/abs/1803.06386>, 2018.
- [53] S. McNally, J. Roche, and S. Caton, “Predicting the price of bitcoin using machine learning,” in *Proceedings of the 2018 26th Euromicro International Conference on Parallel, Distributed and Network-based Processing (PDP)*, pp. 339–343, Cambridge, UK, 2018.
- [54] B. Cortez, B. Carrera, Y.-J. Kim, and J.-Y. Jung, “An architecture for emergency event prediction using LSTM recurrent neural networks,” *Expert Systems with Applications*, vol. 97, pp. 315–324, 2018.
- [55] J. Samarawickrama and T. G. I. Fernando, *A Recurrent Neural Network Approach in Predicting Daily Stock Prices: An Application to the Sri Lankan Stock Market*, IEEE, Peradeniya, Sri Lanka, 2017.
- [56] S. Selvin, R. Vinayakumar, E. A. Gopalakrishnan, V. K. Menon, and K. P. Soman, “Stock price prediction using LSTM, RNN and CNN-sliding window model,” in *Proceedings of the 2017 International Conference on Advances in Computing, Communications and Informatics (ICACCI)*, IEEE, Udipi, India, pp. 1643–1647, September 2017.
- [57] C. R. Nelson and A. F. Siegel, “Parsimonious modeling of yield curves,” *Journal of Business*, vol. 60, no. 4, pp. 473–489, 1987.
- [58] B. Guo, Q. Han, and B. Zhao, “The nelson-siegel model of the term structure of option implied volatility and volatility components,” *Journal of Futures Markets*, vol. 34, no. 8, pp. 788–806, 2014.
- [59] N. S. GrØnborg and A. Lunde, “Analyzing oil futures with a dynamic Nelson-Siegel model,” *Journal of Futures Markets*, vol. 36, no. 2, pp. 153–173, 2016.
- [60] J. West, “Long-dated agricultural futures price estimates using the seasonal Nelson-Siegel model,” *International Journal of Business and Management*, vol. 7, no. 3, pp. 78–93, 2012.
- [61] R.-R. Chen, X. Cheng, and L. Wu, “Dynamic interactions between interest-rate and credit risk: theory and evidence on the credit default swap term structure,” *Review of Finance*, vol. 17, no. 1, pp. 403–441, 2011.
- [62] M. Tsuruta, “Decomposing the term structures of local currency sovereign bond yields and sovereign credit default swap spreads,” *The North American Journal of Economics and Finance*, vol. 51, Article ID 101072, 2020.
- [63] S. R. Gunn, “Support vector machines for classification and regression,” *ISIS Technical Report*, vol. 14, no. 1, pp. 5–16, 1998.
- [64] S. Haykin, *Neural Networks: A Comprehensive Foundation*, Prentice Hall PTR, Upper Saddle River, NJ, USA, 1994.
- [65] F. Pérez-cruz, J. A. Afonso-rodriguez, J. Giner et al., “Estimating GARCH models using support vector machines,” *Quantitative Finance*, vol. 3, no. 3, pp. 163–172, 2003.
- [66] M. Mohri, A. Rostamizadeh, and A. Talwalkar, *Foundations of Machine Learning*, MIT Press, Cambridge, MA, USA, 2018.
- [67] L. Cao and F. E. H. Tay, “Financial forecasting using support vector machines,” *Neural Computing & Applications*, vol. 10, no. 2, pp. 184–192, 2001.
- [68] S. Hochreiter and J. Schmidhuber, “LSTM can solve hard long time lag problems,” in *Proceedings of the 10th Annual Conference on Neural Information Processing Systems (NIPS 1996)*, pp. 473–479, Denver, CO, USA, December 1996.
- [69] F. A. Gers and J. . Schmidhuber, “Recurrent nets that time and count,” in *Proceedings of the IEEE-INNS-ENNS International Joint Conference on Neural Networks (IJCNN 2000)*, IEEE, Como, Italy, pp. 189–194, July 2000.
- [70] H.-G. Zimmermann, C. Tietz, and R. Grothmann, “Forecasting with recurrent neural networks: 12 tricks,” in *Neural Networks: Tricks of the Trade*, Springer, Berlin, Germany, 2012.
- [71] J. Chung, C. Gulcehre, K.H. Cho, and Y. Bengio, “Empirical evaluation of gated recurrent neural networks on sequence modeling,” 2014, <http://arxiv.org/abs/1412.3555>.
- [72] A. G. Ivakhnenko, “Polynomial theory of complex systems,” *IEEE Transactions on Systems, Man, and Cybernetics*, vol. SMC-1, no. 4, pp. 364–378, 1971.
- [73] M. Najafzadeh, G.-A. Barani, and H. M. Azamathulla, “GMDH to predict scour depth around a pier in cohesive soils,” *Applied Ocean Research*, vol. 40, pp. 35–41, 2013.
- [74] G. P. Liu and V. Kadirkamanathan, “Multiobjective criteria for neural network structure selection and identification of nonlinear systems using genetic algorithms,” *IEE Proceedings-Control Theory and Applications*, vol. 146, no. 5, pp. 373–382, 1999.
- [75] E. Sanchez, T. Shibata, and L. Asker Zadeh, *Genetic Algorithms and Fuzzy Logic Systems: Soft Computing Perspectives*, World Scientific, Singapore, 1997.
- [76] A. M. Ghaedi, M. M. Baneshi, A. Vafaei et al., “Comparison of multiple linear regression and group method of data handling models for predicting sunset yellow dye removal

- onto activated carbon from oak tree wood," *Environmental Technology & Innovation*, vol. 11, pp. 262–275, 2018.
- [77] I. Ebtehaj, H. Bonakdari, F. Khoshbin, and H. Azimi, "Pareto genetic design of group method of data handling type neural network for prediction discharge coefficient in rectangular side orifices," *Flow Measurement and Instrumentation*, vol. 41, pp. 67–74, 2015.
- [78] R. Shirmohammadi, B. Ghorbani, M. Hamed, M.-H. Hamed, and L. M. Romeo, "Optimization of mixed refrigerant systems in low temperature applications by means of group method of data handling (GMDH)," *Journal of Natural Gas Science and Engineering*, vol. 26, pp. 303–312, 2015.
- [79] M. Najafzadeh, G.-A. Barani, and H. M. Azamathulla, "Prediction of pipeline scour depth in clear-water and live-bed conditions using group method of data handling," *Neural Computing and Applications*, vol. 24, no. 3-4, pp. 629–635, 2014.
- [80] A. Sakaguchi and T. Yamamoto, "A gmdh network using backpropagation and its application to a controller design," in *Proceedings of the 2000 IEEE International Conference on Systems, Man and Cybernetics' Cybernetics Evolving to Systems, Humans, Organizations, and their Complex Interactions*, IEEE, Nashville, TN, USA, pp. 2691–2696, 2000.
- [81] D. Srinivasan, "Energy demand prediction using GMDH networks," *Neurocomputing*, vol. 72, no. 1–3, pp. 625–629, 2008.
- [82] C.-W. Hsu, C.-C. Chang, C.-J. Lin et al., *A Practical Guide to Support Vector Classification*, National Taiwan University, Taipei, Taiwan, 2003.
- [83] J. Bergstra and Y. Bengio, "Random search for hyperparameter optimization," *Journal of Machine Learning Research*, vol. 13, pp. 281–305, 2012.
- [84] N. Schilling, M. Wistuba, L. Drumond, and L. Schmidt-Thieme, "Hyperparameter optimization with factorized multilayer perceptrons," *Machine Learning and Knowledge Discovery in Databases*, Springer, Berlin, Germany, 2015.
- [85] F. Hutter, J. Lücke, and L. Schmidt-Thieme, "Beyond manual tuning of hyperparameters," *KI-Künstliche Intelligenz*, vol. 29, no. 4, pp. 329–337, 2015.
- [86] J. Sun, C. Zheng, X. Li, and Y. Zhou, "Analysis of the distance between two classes for tuning SVM hyperparameters," *IEEE Transactions on Neural Networks*, vol. 21, no. 2, pp. 305–318, 2010.
- [87] C. Thornton, F. Hutter, H. H. Hoos, and K. Leyton-Brown, "Auto-weka: combined selection and hyperparameter optimization of classification algorithms," in *Proceedings of the 19th ACM SIGKDD International Conference on Knowledge Discovery and Data Mining*, pp. 847–855, Chicago, IL, USA, August 2013.
- [88] N. K. Ahmed, A. F. Atiya, N. El Gayar, and H. El-Shishiny, "An empirical comparison of machine learning models for time series forecasting," *Econometric Reviews*, vol. 29, no. 5-6, pp. 594–621, 2010.
- [89] A. Khosravi, L. Machado, and R. O. Nunes, "Time-series prediction of wind speed using machine learning algorithms: a case study osorio wind farm, Brazil," *Applied Energy*, vol. 224, pp. 550–566, 2018.
- [90] X. Qiu, L. Zhang, Y. Ren, P. N. Suganthan, and G. Amaratunga, "Ensemble deep learning for regression and time series forecasting," in *Proceedings of the 2014 IEEE symposium on computational intelligence in ensemble learning (CIEL)*, IEEE, Orlando, FL, USA, pp. 1–6, 2014.
- [91] A. V. Seliverstova, D. A. Pavlova, S. A. Tonoyan, and Y. E. Gapanyuk, "The time series forecasting of the company's electric power consumption," *Advances in Neural Computation, Machine Learning, and Cognitive Research II*, Springer, Berlin, Germany, 2018.
- [92] D. Solomatine, L. M. See, and R. J. Abrahart, "Data-driven modelling: concepts, approaches and experiences," in *Practical Hydroinformatics*, Springer, Berlin, Germany, 2009.
- [93] S. Aras and İ. D. Kocakoç, "A new model selection strategy in time series forecasting with artificial neural networks: IHTS," *Neurocomputing*, vol. 174, pp. 974–987, 2016.
- [94] M. C. Brace, J. Schmidt, and M. Hadlin, "Comparison of the forecasting accuracy of neural networks with other established techniques," in *Proceedings of the First International Forum on Applications of Neural Networks to Power Systems*, IEEE, Seattle, WA, USA, pp. 31–35, 1991.
- [95] W. R. Foster, F. Collopy, and L. H. Ungar, "Neural network forecasting of short, noisy time series," *Computers & Chemical Engineering*, vol. 16, no. 4, pp. 293–297, 1992.
- [96] Ü. Ç. Büyüksahin and Ş. Ertekin, "Improving forecasting accuracy of time series data using a new ARIMA-ANN hybrid method and empirical mode decomposition," *Neurocomputing*, vol. 361, pp. 151–163, 2019.
- [97] A. Lapedes and R. Farber, "Nonlinear signal processing using neural networks: prediction and system modelling," Technical Report, 1987.
- [98] M. C. Medeiros, A. Veiga, and C. E. Pedreira, "Modeling exchange rates: smooth transitions, neural networks, and linear models," *IEEE Transactions on Neural Networks*, vol. 12, no. 4, pp. 755–764, 2001.
- [99] K. Rasouli, W. W. Hsieh, and A. J. Cannon, "Daily streamflow forecasting by machine learning methods with weather and climate inputs," *Journal of Hydrology*, vol. 414-415, pp. 284–293, 2012.
- [100] J. C. Reboredo, J. M. Matias, and R. Garcia-Rubio, "Non-linearity in forecasting of high-frequency stock returns," *Computational Economics*, vol. 40, no. 3, pp. 245–264, 2012.
- [101] R. Zghal, A. Ghorbel, and M. Triki, "Dynamic model for hedging of the european stock sector with credit default swaps and euro STOXX 50 volatility index futures," *Borsa Istanbul Review*, vol. 18, no. 4, pp. 312–328, 2018.
- [102] S.-Y. Choi, J.-P. Fouque, and J.-H. Kim, "Option pricing under hybrid stochastic and local volatility," *Quantitative Finance*, vol. 13, no. 8, pp. 1157–1165, 2013.
- [103] B. Dupire, "Pricing with a smile," *Risk*, vol. 7, no. 1, pp. 18–20, 1994.
- [104] J. Gatheral and A. Jacquier, "Arbitrage-free SVI volatility surfaces," *Quantitative Finance*, vol. 14, no. 1, pp. 59–71, 2014.
- [105] P. S. Hagan, Deep Kumar, A. S. Lesniewski, and D. E. Woodward, "Managing smile risk," *The Best of Wilmott*, vol. 1, pp. 249–296, 2002.
- [106] S. L. Heston, "A closed-form solution for options with stochastic volatility with applications to bond and currency options," *Review of Financial Studies*, vol. 6, no. 2, pp. 327–343, 1993.
- [107] J. Xiang and X. Zhu, "A regime-switching nelson-siegel term structure model and Interest rate forecasts," *Journal of Financial Econometrics*, vol. 11, no. 3, pp. 522–555, 2013.
- [108] R. B. De Rezende and M. S. Ferreira, "Modeling and forecasting the yield curve by an extended nelson-siegel class of models: a quantile autoregression approach," *Journal of Forecasting*, vol. 32, no. 2, pp. 111–123, 2013.

Research Article

Evolutionary Game Model of Integrating Health and Care Services for Elder People

Tingqiang Chen , Jinnan Pan, Yuanping He , and Jining Wang 

School of Economic and Management, Nanjing Tech University, Nanjing 211816, China

Correspondence should be addressed to Yuanping He; heyp0913@njtech.edu.cn

Received 8 May 2020; Accepted 29 May 2020; Published 7 July 2020

Guest Editor: Baogui Xin

Copyright © 2020 Tingqiang Chen et al. This is an open access article distributed under the Creative Commons Attribution License, which permits unrestricted use, distribution, and reproduction in any medium, provided the original work is properly cited.

With the background of aging, ensuring the deep integration of pension and medical services and effectively integrating pension resources and medical resources are hot issues that must be addressed in the current mode of integrating health and care services for older people. Thus, we use game theory to construct the utility model of resource allocation between pension and medical institutions. We apply this model to explore how pension institutions and medical institutions invest resources into the integration of health and care services, analysis of influencing factors, and conducting incentive mechanism research by using MATLAB 2016b software. Through theoretical deduction and experimental analysis, the following conclusions are drawn. First, the income distribution coefficient of pension institutions is positively correlated with the level of labor input, and its growth rate has a marginal diminishing effect on the level of labor. Second, in early investment, the income distribution coefficient of pension institutions is positively correlated with fixed asset investment regardless of the different effort coefficients between medical institutions and pension institutions. With a high income distribution coefficient, pension institutions are negatively correlated and marginally decrease. Third, in early investment, the income distribution coefficient of pension institutions is positively correlated with medical institutions' labor input level. When the income distribution coefficient of pension institutions reaches a certain value, it is negatively correlated with the labor input level of medical institutions, thereby showing a marginal diminishing effect.

1. Introduction

China has become an aging society since 2000, and its population is rapidly aging and becoming disabled. According to the Statistical Communique on National Economic and Social Development in 2017, the number of people aged 60 and over has reached 241 million, accounting for 17.3% of the total population. Among them, the number of people aged 65 and above reached 158 million, accounting for 11.4% of the total population. China's aging population is expected to reach 487 million in 2050, accounting for about one-third of the total population. The number of elderly people and the proportion of the total population will reach a peak. With the background of aging, the number of disabled elderly is bound to increase, and their dual demands for life care and medical

rehabilitation are increasingly becoming prominent. At present, China's old-age care work is facing the problem of serious separation of medical care and old-age resources, and the pension service system cannot meet the medical service needs of the elderly. Most pension institutions are only responsible for the daily life care and cannot meet the elderly's need for medical and health services. On the contrary, medical institutions mainly aim to provide medical and health services for residents, which prevent them from also giving elderly care services. Therefore, health and care service integration was born. How to ensure the deep integration of elderly care services and medical services and how to effectively integrate elderly care resources with medical resources are hot issues that need to be solved urgently in the current situation of integrated elderly care services.

Theoretical exploration about health and care service integration started late in China, and it needs further understanding. The integrating of health and care services for elder people is a new concept with Chinese characteristics for a new era. It refers to the integration of medical resources and old-age care resources, which can not only meet the basic care needs of the elderly but also meet certain medical needs of the elderly, so as to maximize the utilization of social resources. Health services include medical rehabilitation services, health consultation and examination services, disease diagnosis and care services, serious illness rehabilitation services, and hospice care services. Old-age care service refers to housing, life care, rehabilitation nursing, spiritual comfort, and cultural entertainment services. The health and care service integration is a new type of health and old-age care service mode, which is based on the basic old-age care service. This mode provides good life care, spiritual comfort, and other services for the elderly, and it focuses on improving the quality of medical services such as disease diagnosis, treatment and nursing, health examination, serious illness rehabilitation, and hospice care [1]. To achieve this purpose, the government actively promotes the combination of medical and old-age care services and advocates multiple integrations of medical and old-age care resources to solve the current problem about the separation of health and care. At present, the main problems in the elderly care work are that the number of beds and professional staff are far less than the demand. In addition, the elderly care service projects and facilities are relatively simple and cannot meet the diversified medical and care needs of the elderly. Therefore, realizing the integration of medical care and old-age care services and fully utilizing separated medical and old-age care resources are the focus of old-age care work.

Upon reviewing extensive literature, the findings show that traditional family care resources are gradually reduced with the acceleration of aging, thereby resulting in the increasing contradiction between supply and demand of long-term care services. In recent years, the population of elderly with disabilities, chronic diseases, and terminal diseases has increased rapidly. China's population is aging seriously, and the social pension security burden is heavy [2, 3]. From the perspective of big health, the goal of integrating health and care services is to develop and maintain the healthy life of the elderly and realize healthy aging [4, 5]. Hence, long-term care services have become an important part of medical and care services. Jacobzone and Jenson [6] mentioned that long-term care services rely on a partnership among formal care institutions, the state, and families. Ikegami and Campbell [7] believed that an effective long-term care system should be public, comprehensive, independent, primarily community-based, and separate from medical and social services. The model of integrated health and care services for the aged was an important measure to solve the global pension problem and improve the level of social services in the new era. Hartgerink et al. [8] compared the situational awareness, nursing coordination, and integrated care in different hospitals in the Netherlands and proved that integrated care could improve the care quality and health status of elderly

patients. Fabbri et al. [9] used a quasi-experimental method to evaluate the effect of combined medical and nursing services on the improvement of the quality of life and medical effects of frail elderly people. Bao et al. [10] used 13 nursing homes in Wuhan, China, as an example to explore the influence of medical-nursing combined care on the health status and service satisfaction of the elderly. Reuben [11] said that providing health care to older patients alone is unlikely to produce good results. Wendy et al. [12] argued that focusing on the daily care of elderly patients is more important than curing the disease itself.

The first countries to realize the presence of an aging population were the Western industrialized nations. Therefore, foreign scholars began to study pension problems early on, and the Western pension model gradually emerged. Powell [13] believed that social pension services should be personalized to meet the living needs of different elderly people. This kind of personalized pension service will increase the participation of elderly people and promote pension service that fits the actual situation to eliminate the cost of social pension service. After controlling for age, gender, years of education, and other factors, Zunzunegui et al. [14] found that emotional and material support from children were significantly correlated with self-rated health. People who live with their children after the death of a spouse are in better health than those who live alone after. Hughes and Waite [15] argued that a clear correlation exists between pension patterns and self-reported health, mortality, and depression. Lund et al. [16] found that older adults who lived with other people had significantly lower death rates than those who lived alone. Therefore, the health and longevity of the elderly can only improve by combining the government, children, and the elderly.

Since the 1980s, many countries began to carry out theoretical research and practice of integrated care for the elderly. Britain first put forward the concept of "integrated care." Glendinning [17] combined two integrated care promotion plans about the integration of family doctors with community medical institutions and integration of social services and medical institutions; he concluded that structural integration helps transform the decentralized system into a service planning and supply system with synergistic amplification effect. Michel [18] believed that integrated care aimed to provide multidimensional, comprehensive, and detailed care services for the elderly with similar problems or needs. Many scholars have also carried out numerous analyses on policy implementation and its effects. Leichsenring and Alaszewski [19] summed up the general situation of the nine EU member states' integration care and pointed out that horizontal integration is the most extensive practical idea. Reed et al. [20] divided the integrated care into system, institution, and individual levels. The system level was the overall integration of different regions and management departments. The institutional level was the division of labor and cooperation within or between pension service institutions. The individual level involves enhancing the comprehensiveness of the individual's care. Fisher and Elnitsky [21] pointed out that integrated care aimed to take the elderly as the center and family

and community as the carrier and integrate health, service, and social care resources to provide care, assessment, and supervision for the elderly in life, physiology, and psychology. The development of elderly care services in the United States could be divided into three stages, namely, preparatory, development, and mature stages. Sultz [22] introduced the basic situation of these three stages. The preparatory phase was the establishment of Medicare and Medicaid in 1965. The development period was from 1965 to 1990, whereas the maturity period was from 1990 to present. In the research on the model of medical and nursing care, Carson et al. [23] pointed out that LTAC was the typical representative of the new nursing mode that combines medical treatment and nursing in America. Long-term acute-care hospitals, which provide care to patients suffering from prolonged critical illness, are exempted from the Medicare prospective payment system. The PACE (Program of All Inclusive Care for the Elderly) proposed by the United States aims to provide the elderly with a full range of services, including daily life care, medical rehabilitation, spiritual comfort, and emergency rescue. Chatterji et al. [24] found that PACE can effectively reduce the frequency and time of hospitalization in the long run, and it can help improve the elderly's physical and mental state and quality of life in the short run. Laura and Gadsby [25] also thought that individuals must be at least 55 years old, state-eligible for nursing home care, and living in the program's geographical catchment area. Segelman et al. [26] pointed out that PACE provides continuous services, including primary care, diagnosis, treatment, nursing, and daily care. Integrating the financial resources for Medicare and Medicaid, the entrusted unit must achieve a certain quality of service under a fixed amount of per-person billing and bear its own financial losses. Fretwell et al. [27] found that 104 PACE service centers had opened in 31 states by the end of 2013. Polska [28] pointed out that PACE is directly managed by the government, based on community, guaranteed by public finance and commercial resources, and characterized by integration of medical and nursing care. It aims to provide continuous elderly care services to the frail and high-risk elderly. In Germany, the mode of integrated care for the elderly is provided by social institutions. According to Geraedts et al. [29], older people receive financial compensation by buying long-term care insurance. The new models of choice of care have recently been introduced in Sweden's health care. Ahgren [30] stated that citizens act as purchasers; they can choose the primary care center or family physician they want to be treated by, which in turn generates a capitation payment to the chosen unit.

According to the abovementioned research, it can be found that the theoretical research on the mode of integrating health and care services is mostly limited to economics, management, sociology, and demography. Scholars tend to make more qualitative analysis, while there are few researches on quantitative analysis. The new pension mode combines medical and pension resources. In the process of mutual cooperation between pension and medical institutions, their own benefits and costs will be involved. Both are driven by their own interests and form the game theory of

intersecting interests among subjects. Maruthappu et al. [31] proposed that integrated care projects can achieve the intensification of health resources and the maximization of service efficiency, but the allocation, management, and use of funds as well as service personnel need to be further improved. Shimizutani [32] also studied the cost-effectiveness and incentive mechanism of combining medical care with old-age care. Game theory is an important subject of operational research and can study the multisubject interest in the mode of integrating health and care services for elder people. In existing studies, scholars used game theory to explore the competition and cooperation between economic entities. Ji et al. [33] proposed that suppliers and manufacturers are multistakeholders. They should establish a long-term green purchasing relationship. In addition, they established the evolutionary game model to observe the trend of multistakeholder cooperation to guide stakeholders in making better choices in the future. Li et al. [34] established the cooperative game model of benefit distribution in the supply chain to enhance the stability of partners in the VMI model. The high inventory cost of VMI members will lead to increasing the surplus value of other members under fair distribution. Alavi and Zhou [35] mentioned that cooperative game theory can be applied to positive frequency division multiple access network to realize fair allocation of resources.

Resource integration is also very important in integrating care. Through literature review, we found that resource integration researchers often start from the perspective of social resource integration. They then integrate and innovate information, technology, products, and other resources while creating value together and realizing the maximization of social benefits. Zhang et al. [36] studied the service system of bilateral resource integration by combining the service of providers with the personalized needs of customers; this work aimed to transform the servitization of real resources into service resources by studying service resources. Wan and Zhang [37] explored how the resource integrators cocreate value closely under the rubric of S-D logic and systems and further proposed a conceptual model for deeply understanding the roles of focal actors and others in a service ecosystem. Siltaloppi and Vargo [38] provided that reconciling resource integration and value propositions is the dynamics of value cocreation and propositions as the cocreated forms of shared resources and understanding, which constitutes service systems. Singaraju et al. [39] mentioned that actor interaction is the basis of value cocreation through resource integration. Information transforms social media platform's technological functions into resources, and the social media platform is a "systems resource integrator." Guan et al. [40] studied the resource integration of virtual industry cluster; he used the complex network model to analyze the virtual industrial cluster and promote its resource integration and development. To realize value cocreation, Koskela-Huotari et al. [41] proposed to innovate and reform the rules of resource integration in the service ecosystem based on service-dominant logic and institutional theory. Based on the study of China's express market, Wang et al. [42] found that the express industry was

fragmented, and the service quality was poor. He then proposed the service network cooperation model of horizontal resource integration to maximize the benefits of the network cooperation model.

Literature review also showed that existing scholars have explored the mode of integrating health and care services and its operation mechanism. However, only a few of them have applied quantitative methods to study the resource allocation problem under this mode. Therefore, we use game theory to construct the utility model of resource allocation between pension and medical institutions and explore how pension institutions and medical institutions invest resources in the integration of health and care services. We also analyze the influencing factors and conduct incentive mechanism research and solve the dilemma in the current pension problem. This is also the innovation and motivation of this article.

The remainder of this work is organized as follows. Section 2 builds the utility model of resource allocation between pension and medical institutions. Section 3 analyzes the influencing factors and conducts incentive mechanism research on pension institutions and medical institutions via simulation. Section 4 summarizes and concludes the research.

2. Constructing the Utility Model of Resource Allocation between Pension and Medical Institutions

2.1. Model Assumption. The resource input in integrating health and care services for older people mainly involves intangible human resources, tangible monetary capital, and fixed assets. Effective integration of these resources can result in high level of pension services. We make the following assumptions so that the model is more realistic:

Assumption 1. Pension institutions and medical institutions cooperate to provide integrating health and care services. Pension institutions are the dominant provider of integrating health and care services, whereas medical institutions are the suppliers.

Assumption 2. In the process of providing integrating health and care services for older people, a certain number of elderly users will continue to purchase this new type of pension services.

Assumption 3. In the process of providing integrating health and care services for older people, pension institutions invest in staff and infrastructure equipment, while medical institutions only invest in staff.

Assumption 4. There is a quadratic function relationship between the service effort cost and the level of staff input between the pension institution and medical institution.

Assumption 5. Both pension institutions and medical institutions aim to maximize their own income.

The notations for variables and parameters are given in Table 1.

2.2. Model Construction. Cobb–Douglas production function is used to build the input and output model, which is about the cooperation between pension institutions and medical institutions to build a new type of pension service combining health and care for older people:

$$Y = A(L_1 + L_2)^\alpha K^\beta, \quad (1)$$

where L_1 mainly reflects the professional ability and working time input of nursing staff in pension institutions; L_2 mainly reflects the professional ability and working time of the medical staff involved in the integrating health and care services; K mainly reflects their capital investment in nursing beds, basic medical facilities, and equipment; and $\alpha + \beta = 1$.

In income distribution, pension institutions and medical institutions aim to maximize their own income, and the absolute income functions of pension institutions and medical institutions are as follows:

$$P_1 = \lambda_1 Y - \frac{1}{2} a_1 L_1^2 - K, \quad (2)$$

$$P_2 = \lambda_2 Y - \frac{1}{2} a_2 L_2^2, \quad (3)$$

where $\lambda_1 + \lambda_2 = 1$. The effort cost of nursing staff invested in pension institutions is $(1/2)a_1 L_1^2$, whereas the effort cost of medical institutions' staff participating in integrating health and care services is $(1/2)a_2 L_2^2$. The medical staff invested in medical institutions have professional medical aid skills, and the nursing staff invested in pension institutions need to undergo certain medical organization training. Thus, the medical staff in medical institutions can provide nearly the same service value as the nursing staff in pension institutions with less effort. Hence, assume that $a_1 > a_2$.

To explore the relationship among absolute benefits, labor force, and fixed asset investment of pension and medical institutions, two types of economic actors are considered. The first partial derivative of formula (2) on the labor level of pension institutions can be obtained as follows:

$$\frac{\partial P_1}{\partial L_1} = \lambda_1 A \alpha (\lambda_1 + \lambda_2)^{\alpha-1} K^\beta - a_1 L_1. \quad (4)$$

The first partial derivative of formula (2) on the fixed asset investment of pension institutions can be obtained as follows:

$$\frac{\partial P_1}{\partial K} = \lambda_1 A (\lambda_1 + \lambda_2)^\alpha \beta K^{\beta-1} - 1. \quad (5)$$

The first partial derivative of formula (3) on the labor level of medical institutions can be obtained as follows:

$$\frac{\partial P_2}{\partial L_2} = \lambda_2 A \alpha (\lambda_1 + \lambda_2)^{\alpha-1} K^\beta - a_2 L_2. \quad (6)$$

2.3. Model Analysis. To find the optimal value of resource input when the absolute benefits of the two types of economic actors about the pension and medical institutions

TABLE 1: Variables and notations.

Notations	Meaning
Y	The total revenue from integrating health and care services
P_1	The absolute income functions of pension institutions
P_2	The absolute income functions of medical institutions
L_1	The labor input level of pension institutions in the cooperation between pension and medical institutions
L_2	The labor input level of medical institutions in the cooperation between pension and medical institutions
K	The asset input level of pension institutions
α	The output elasticity of labor input
β	The output elasticity of fixed asset input
A	The profitability or marginal output efficiency of the integrating health and care services
λ_1	The income distribution coefficient of pension institutions
λ_2	The income distribution coefficient of medical institutions
a_1	The effort coefficients of pension institutions
a_2	The effort coefficients of medical institutions

reach the maximum value, set formulas (4)–(6), which can be solved as follows:

$$L_1^* = \lambda_1^{1/\alpha} A^{1/\alpha} \frac{1}{a_1} \frac{\alpha}{\beta} \beta^{1/\alpha}, \quad (7)$$

$$K^* = \left(1 + \frac{\lambda_2 a_1}{\lambda_1 a_2}\right) \lambda_1^{2/\alpha} A^{2/\alpha} \frac{1}{a_1} \frac{\alpha}{\beta} \beta^{2/\alpha}, \quad (8)$$

$$L_2^* = \lambda_2 \lambda_1^{\beta/\alpha} A^{\beta/\alpha} \frac{1}{a_2} \frac{\alpha}{\beta} \beta^{\beta/\alpha}. \quad (9)$$

Formulas (7)–(9) show that a certain correlation exists between the income distribution coefficient of pension and medical institutions and their investment. To a certain extent, the income distribution coefficient has a positive incentive and constraint effect on the resource investment of the two types of economic actors. Under the mode of integrating health and care services for older people, pension institutions are the leading providers and operators of the pension services, whereas medical institutions are the providers of medical services. Therefore, this work mainly explores the incentive relationship between income distribution coefficient of pension institutions, labor level of pension institutions, fixed asset investment level of pension institutions, and labor level of medical institutions.

2.3.1. The Effect of Income Distribution Coefficient on the Level of Labor in Pension Institutions. According to formula (7), the first partial derivative of λ_1 with respect to L_1 can be obtained as follows:

$$\frac{\partial \lambda_1}{\partial L_1} = \frac{a_1^\alpha}{A} \left(\frac{\alpha}{\beta}\right)^\beta L_1^{\alpha-1} > 0. \quad (10)$$

Formula (10) reflects the impact of pension institutions' labor input level on the income distribution coefficient of pension service institutions. $(\partial \lambda_1 / \partial L_1) > 0$ shows that the income distribution coefficient of pension institutions will increase along with the labor input level. According to formula (10), the second partial derivative of λ_1 with respect to L_1 can be obtained as follows:

$$\frac{\partial^2 \lambda_1}{\partial L_1^2} = \frac{a_1^\alpha}{A} \left(\frac{\alpha}{\beta}\right)^\beta (\alpha - 1) L_1^{\alpha-2} < 0. \quad (11)$$

Formula (11) reflects the influence of labor input level on the growth rate of pension institutions' income distribution coefficient. $(\partial^2 \lambda_1 / \partial L_1^2) < 0$ shows that the income distribution coefficient of pension institutions decreases marginally with the change of labor level.

Theorem 1. *When the benefits of pension institutions are maximized, the income distribution coefficient of pension institutions increases with the improvement of labor input level, and the growth rate decreases marginally with the improvement of labor input level.*

Therefore, pension institutions can recruit more professionals, carry out vocational training for nursing staff, cooperate with medical institutions to learn, improve the treatment of nursing staff, and stimulate work enthusiasm to improve the quantity and quality of labor level. Medical institutions reduce the income distribution coefficient when the pension institutions' income distribution coefficient increases because the sum of income distribution coefficient of pension and medical institutions is 1. Hence, to prevent medical institutions from having a low income distribution coefficient and refusing medical cooperation, pension institutions' labor input needs relaxation and not blindly.

2.3.2. The Effect of Income Distribution Coefficient on the Level of Fixed Assets Investment in Pension Institutions. According to formula (8), the first partial derivative of λ_1 with respect to K can be obtained as follows:

$$\frac{\partial \lambda_1}{\partial K} = A^{-(2/\alpha)} a_2 \beta^{1-(2/\alpha)} \lambda_1^{-(2\beta/\alpha)} \left[2 \left(\frac{a_2}{a_1} - 1\right) \lambda_1 + 1 + \beta \right]^{-1}. \quad (12)$$

Formula (12) reflects the influence of pension institutions' fixed assets investment on the income distribution coefficient of pension institutions. According to formula (12), the second partial derivative of λ_1 with respect to K can be obtained as follows:

$$\frac{\partial^2 \lambda_1}{\partial K^2} = -2A^{-(4/\alpha)} a_2^2 \beta^{2-(2/\alpha)} \frac{1+\beta}{\alpha} \lambda_1^{-(4\beta/\alpha)-1} \left[2 \left(\frac{a_2}{a_1} - 1 \right) \lambda_1 + 1 + \beta \right]^{-3} \left[\left(\frac{a_2}{a_1} - 1 \right) \lambda_1 + \beta \right]. \quad (13)$$

Formula (13) reflects the influence of fixed asset investment level on the growth rate of the income distribution coefficient of pension institutions. According to formulas (12) and (13), the incentive relationship between the income distribution coefficient of pension institutions and the level of fixed assets investment of pension institutions is related to the value of the effort coefficient about pension and medical institutions.

To study the influence of fixed asset investment level on the income distribution coefficient of pension institutions, according to formula (12), let $2((a_2/a_1) - 1)\lambda_1 + 1 + \beta = 0$, and we obtain $\lambda_1' = (1 + \beta)a_1/2(a_1 - a_2)$.

According to formula (13), let $((a_2/a_1) - 1)\lambda_1 + \beta = 0$, and we obtain $\lambda_1'' = \beta a_1/a_1 - a_2$.

The results show that $\lambda_1'' < \lambda_1'$. Because $0 \leq \lambda_1 \leq 1$ and the size of λ_1' and λ_1'' cannot be determined, compare λ_1' , λ_1'' and 1, then discuss them separately. The following three cases emerge:

Case 1. When $\lambda_1'' < \lambda_1' < 1$, that means $(1 + \beta)a_1/2(a_1 - a_2) < 1$. Hence, we obtain $0 < a_2 < (\alpha/2)a_1$.

- ① When $0 < \lambda_1 < \lambda_1''$, $(\partial\lambda_1/\partial K) > 0$ can be obtained from formula (12). Thus, the income distribution coefficient of pension institutions will increase with increasing pension institutions' fixed assets investment. According to formula (13), $(\partial^2\lambda_1/\partial K^2) < 0$ can be obtained. Hence, the income distribution coefficient of pension institutions decreases marginally with increasing fixed asset investment.
- ② When $\lambda_1'' < \lambda_1 < \lambda_1'$, $(\partial\lambda_1/\partial K) > 0$ can be obtained from formula (12). Hence, the income distribution coefficient of pension institutions will increase with increasing pension institutions' fixed assets investment. According to formula (13), $(\partial^2\lambda_1/\partial K^2) < 0$ can be obtained. Thus, the income distribution coefficient of pension institutions increases marginally with increasing fixed asset investment.
- ③ When $\lambda_1' < \lambda_1 < 1$, $(\partial\lambda_1/\partial K) < 0$ can be obtained from formula (12). Therefore, the income distribution coefficient of pension institutions will decrease with increasing pension institutions' fixed assets investment. According to formula (13), $(\partial^2\lambda_1/\partial K^2) < 0$ can be obtained. Hence, the income distribution coefficient of pension institutions decreases marginally with increasing fixed asset investment.

Case 2. When $\lambda_1'' < 1 < \lambda_1'$, that means $\begin{cases} (\beta a_1/a_1 - a_2) < 1 \\ (1 + \beta)a_1/2(a_1 - a_2) > 1 \end{cases}$. Hence, we obtain $(\alpha/2)a_1 < a_2 < \alpha a_1$.

- ① When $0 < \lambda_1 < \lambda_1''$, $(\partial\lambda_1/\partial K) > 0$ can be obtained from formula (12). Therefore, the income distribution coefficient of pension institutions will increase with increasing pension institutions' fixed assets investment. According to formula (13), $(\partial^2\lambda_1/\partial K^2) < 0$ can be obtained. Thus, the income distribution coefficient of pension institutions decreases marginally with increasing fixed asset investment.
- ② When $\lambda_1'' < \lambda_1 < 1$, $(\partial\lambda_1/\partial K) > 0$ can be obtained from formula (12). Therefore, the income distribution coefficient of pension institutions will increase with increasing pension institutions' fixed assets investment. According to formula (13), $(\partial^2\lambda_1/\partial K^2) < 0$ can be obtained. Thus, the income distribution coefficient of pension institutions increases marginally with increasing fixed asset investment.

Case 3. When $1 < \lambda_1'' < \lambda_1'$, that means $(\beta a_1/a_1 - a_2) > 1$. Hence, we can obtain $\alpha a_1 < a_2 < a_1$.

- ① $(\partial\lambda_1/\partial K) > 0$ can be obtained from formula (12). Therefore, the income distribution coefficient of pension institutions will increase with increasing pension institutions' fixed assets investment. According to formula (13), $(\partial^2\lambda_1/\partial K^2) < 0$ can be obtained. Thus, the income distribution coefficient of pension institutions decreases marginally with increasing fixed asset investment.

Theorem 2. *The effort coefficient of pension institutions and medical institutions is significantly different for pension institutions in the early stage of the cooperation. Thus, as pension institutions increased fixed assets investment, pension institutions will have bigger income distribution coefficient, which reaches a certain value. Pension institutions' income distribution coefficient will decrease with increasing fixed asset investment. When the difference of the effort coefficient between pension and medical institutions decreases gradually, the income distribution coefficient of pension institutions increases with increasing fixed asset investment.*

Therefore, pension institutions can increase their income distribution coefficient by expanding the fixed assets investment regardless of the difference between the effort coefficient of medical and pension institutions. When the effort coefficient of medical institutions is relatively low, then medical institutions are not highly motivated to participate in integrating health and care services. Therefore, if pension institutions want to continue to obtain increased income distribution after their income distribution coefficient reaches a certain value, then they need to appropriately reduce the fixed assets investment.

2.3.3. *The Effect of Income Distribution Coefficient on the Level of Labor in Medical Institutions.* According to formula (9), the first partial derivative of λ_1 with respect to L_2 can be obtained as follows:

$$\frac{\partial \lambda_1}{\partial L_2} = -a_2 A^{-(1/\alpha)} \alpha^{-1} \beta^{-(\beta/\alpha)} \lambda_1^{-(\beta/\alpha)} \frac{\alpha \lambda_1}{\lambda_1 - \beta}. \quad (14)$$

Formula (14) reflects the influence of medical institutions' labor input level on the pension institutions' income distribution coefficient. According to formula (14), the second partial derivative of λ_1 with respect to L_2 can be obtained as follows:

$$\frac{\partial^2 \lambda_1}{\partial L_2^2} = -a_2^2 A^{-(2/\alpha)} \left(\frac{\beta}{\alpha}\right)^3 \beta^{-(2/\alpha)} \lambda_1^{-(2/\alpha)} \left(\frac{\alpha \lambda_1}{\lambda_1 - \beta}\right)^3 \left(\frac{\lambda_1}{\alpha} + \frac{\alpha - \beta}{\alpha}\right). \quad (15)$$

Formula (15) reflects the influence of medical institutions' labor input level on the growth rate of pension institutions' income distribution coefficient.

Formulas (14) and (15) show that the incentive relationship between the distribution income coefficient of pension institutions and the labor level of medical institutions is directly related to the size relationship between α and β . Therefore, the value of pension institutions' distribution income coefficient is discussed below in the two cases of $\beta - \alpha < 0$ and $\beta - \alpha > 0$:

Case 1. When $\beta - \alpha < 0$, $0 < \beta < 0.5$, $0.5 < \alpha < 1$. Thus, the input of labor has a greater influence on the total output than the input of fixed assets.

- ① When $0 < \lambda_1 < \beta < 0.5$, $(\partial \lambda_1 / \partial L_2) > 0$ can be obtained from formula (14). Therefore, the income distribution coefficient of pension institutions will increase with increasing medical institutions' labor input level. According to formula (15), $(\partial^2 \lambda_1 / \partial L_2^2) > 0$ can be obtained. Thus, the income distribution coefficient of pension institutions increases marginally with increasing medical institutions' labor input level.
- ② When $\beta < \lambda_1 < 1$, $(\partial \lambda_1 / \partial L_2) < 0$ can be obtained from formula (14), and $(\partial^2 \lambda_1 / \partial L_2^2) < 0$ can be obtained from formula (15). Therefore, the pension institutions' income distribution coefficient and its growth rate decrease with increasing medical institutions' labor level.

Case 2. When $\beta - \alpha > 0$, $0 < \alpha < 0.5$, $0.5 < \beta < 1$. Thus, the input of fixed assets has a greater influence on the total output than the input of labor.

- ① When $0 < \lambda_1 < \beta - \alpha$, $(\partial \lambda_1 / \partial L_2) > 0$ can be obtained from formula (14). Therefore, the income distribution coefficient of pension institutions will increase with increasing medical institutions' labor input level. According to formula (15), $(\partial^2 \lambda_1 / \partial L_2^2) < 0$ can be obtained. Thus, the income distribution coefficient of pension institutions decreases marginally with increasing medical institutions' labor input level.

- ② When $\beta - \alpha < \lambda_1 < \beta$, $(\partial \lambda_1 / \partial L_2) > 0$ can be obtained from formula (14) and $(\partial^2 \lambda_1 / \partial L_2^2) > 0$ can be obtained from formula (15). Thus, the pension institutions' income distribution coefficient and its growth rate increase with increasing medical institutions' labor level.
- ③ When $\beta < \lambda_1 < 1$, $(\partial \lambda_1 / \partial L_2) < 0$ can be obtained from formula (14) and $(\partial^2 \lambda_1 / \partial L_2^2) < 0$ can be obtained from formula (15). Thus, the pension institutions' income distribution coefficient and its growth rate decrease with increasing medical institutions' labor level.

Theorem 3. *Even if the labor level input or fixed asset input has a greater impact on the total output, the impact will increase with increasing labor input in medical institutions when the income distribution coefficient of pension institutions is relatively low. However, when the income distribution coefficient of pension service institutions increases to a certain high value, it will decrease with the improvement of the medical institutions' labor level.*

To obtain a high income distribution coefficient, pension service institutions can actively negotiate and cooperate with medical institutions and formulate detailed cooperation rules when the income distribution coefficient of pension institutions is low, thereby encouraging medical institutions to improve their labor level. When pension institutions' income distribution coefficient is high, medical institutions accounted for a relatively low income distribution coefficient. Pension institutions' income distribution coefficient is then negatively related to labor input levels of medical institutions. Therefore, medical institutions can increase the labor input level to reduce the pension institutions' income distribution coefficient and increase their own income distribution coefficient to obtain additional profits.

3. Analogue Simulation

Numerical simulation analysis is the most effective way to test real-time dynamic data without numerous empirical validations. Hence, we analyze the impact of factors, such as the effort coefficient, the output elasticity of labor input, and fixed asset input on cooperative production input through simulation. We then study the incentive mechanism of labor level input and fixed asset input on income distribution of institutions.

3.1. *The Effect of Labor Input Level on Income Distribution Coefficient of Pension Institutions under the Integrating Health and Care Services.* In studying the effect of labor input level on the income distribution coefficient of pension institutions, we found that the output elasticity of labor input and fixed asset input and the profitability of the integrating health and care services have certain influence on the labor input of pension institutions. Let $\alpha = 0.3$, $\beta = 0.7$, $\alpha = 0.5$, $\beta = 0.5$, and $\alpha = 0.7$, $\beta = 0.3$. On this basis, let $A = 5$, $a_1 = 2$, $A = 8$, $a_1 = 2$, and $A = 10$, $a_1 = 2$. The simulation results are shown in Figure 1.

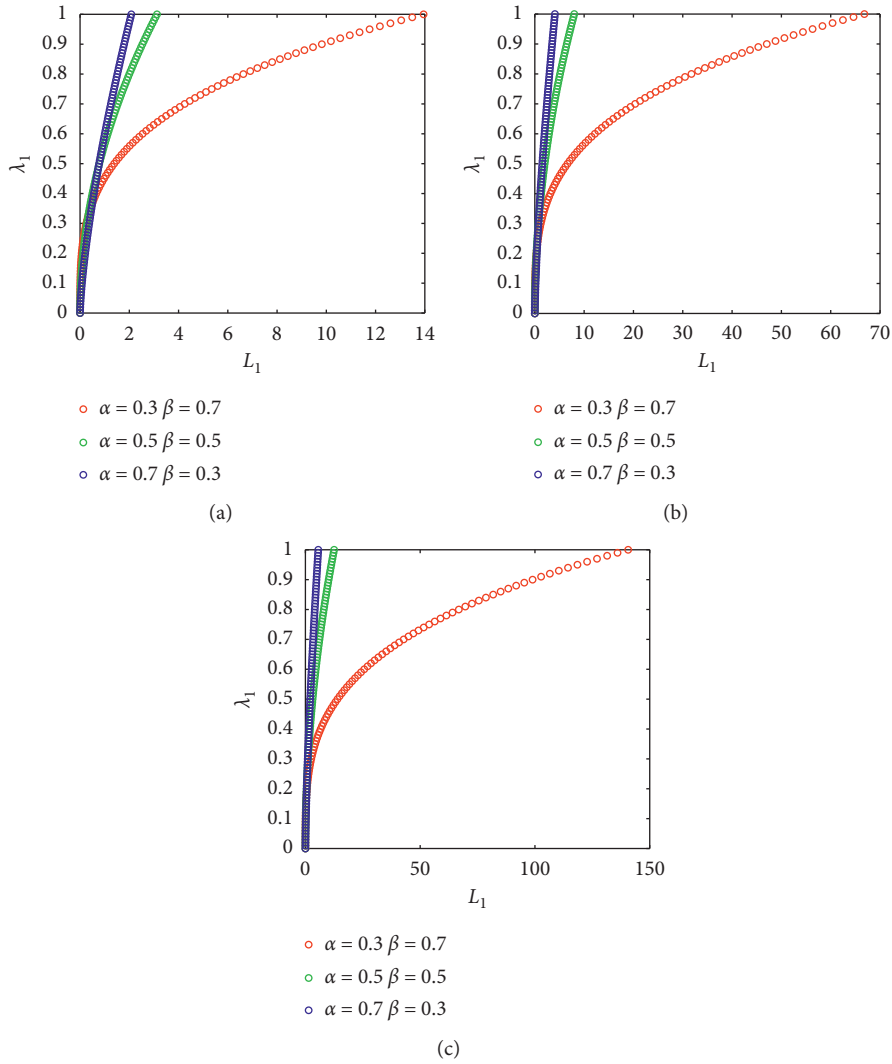


FIGURE 1: The influence mechanism of labor input level on the income distribution coefficient of pension institutions. (a) $A = 5, a_1 = 2$. (b) $A = 8, a_1 = 2$. (c) $A = 10, a_1 = 2$.

As shown in Figure 1, pension institutions' income distribution coefficient will increase when the labor level of pension institutions is improved. Thus, the elderly groups who need integrating health and care services will pay increased attention to daily care, spiritual comfort, and so on. In addition, the income distribution coefficient of pension institutions will increase. By comparing Figures 1(a)–1(c), we found that the profitability of the integrating health and care services has little impact on the labor input level of pension institutions when the input of labor has greater influence on the total output than the input of fixed assets. However, when the input of fixed assets has a greater influence on the total output than the input of labor, the profitability of the integrating health and care services is better, and the more labor must be input for pension institutions to achieve a high income distribution coefficient.

3.2. The Effect of Fixed Assets Level on Income Distribution Coefficient of Pension Institutions under the Integrating Health and Care Services. In studying the effect of fixed assets level on the income distribution coefficient of pension institutions, we found that the effort coefficient of pension institutions and medical institutions, the output elasticity of labor input and fixed asset input, and the profitability of the integrating health and care services have certain influence on the fixed assets input of pension institutions. The numerical simulation is carried out under the different value relations of a_1 and a_2 , which mainly include the following cases:

Case 1. When $0 < a_2 < (\alpha/2)a_1$, analyze the effect of fixed assets investment on the income distribution coefficient of pension institutions.

When $\alpha > \beta$, the input of labor has a greater influence on the total output than the input of fixed assets. Let

$\alpha = 0.7, \beta = 0.3, A = 5$. The simulation result is shown in Figure 2(a). When $\alpha < \beta$, the input of fixed assets has a greater influence on the total output than the input of labor. Let $\alpha = 0.3, \beta = 0.7, A = 5$. The simulation result is shown in Figure 2(b).

As shown in Figure 2, in early investment, the income distribution coefficient of pension institutions is positively correlated with their fixed assets investment. When the pension institutions' income distribution coefficient reaches a certain high value, it is negatively correlated with their fixed assets investment. When the fixed assets investment of pension institutions is certain and the effort coefficient of pension institutions and medical institutions is higher, the income distribution of pension institutions will increase. By comparing Figures 2(a) and 2(b), we found that the fixed assets input of pension institutions is relatively low when the input of fixed assets has a greater influence on the total output than the input of labor. The income distribution coefficient of pension institutions will then increase fast. As the fixed assets investment continues to increase, the income distribution coefficient will gradually slow down. In addition, under the condition that the profitability of the integrating health and care services remains unchanged and the input of fixed assets has a greater influence on the total output than the input of labor, pension institutions should invest additional fixed assets to obtain a high income distribution coefficient.

Case 2. When $(\alpha/2)a_1 < a_2 < a_1$, analyze the effect of fixed assets investment on the income distribution coefficient of pension institutions.

- ① If $(\alpha/2)a_1 < a_2 < \alpha a_1$, when $\alpha > \beta$, then the input of labor has greater influence on the total output than the input of fixed assets. Let $\alpha = 0.7, \beta = 0.3, A = 5$. The simulation result is shown in Figure 3(a). When $\alpha < \beta$, the input of fixed assets has a greater influence on the total output than the input of labor. Let $\alpha = 0.3, \beta = 0.7, A = 5$. The simulation result is shown in Figure 3(b).
- ② If $\alpha a_1 < a_2 < a_1$, when $\alpha > \beta$, the input of labor has a greater influence on the total output than the input of fixed assets. Let $\alpha = 0.7, \beta = 0.3, A = 5$. The simulation result is shown in Figure 3(c). When $\alpha < \beta$, the input of fixed assets has a greater influence on the total output than the input of labor. Let $\alpha = 0.3, \beta = 0.7, A = 5$. The simulation result is shown in Figure 3(d).

As shown in Figure 3, the income distribution coefficient of pension institutions is positively correlated with their fixed assets investment. If the fixed assets investment of pension institutions is certain and the effort coefficient of pension institutions and medical institutions is high, then the income distribution of pension institutions will increase. In comparing Figures 3(a)–3(d), we found that the input of fixed assets has a greater influence on the total output than the input of labor. In addition, the fixed assets input of pension institutions is relatively low, and the income distribution coefficient of

pension institutions increases at a faster speed. As the fixed assets investment continues to increase, the income distribution coefficient gradually slows down. Under the condition that the profitability of the integrating health and care services remains unchanged and the input of fixed assets has a greater influence on the total output than the input of labor, pension institutions need to invest more fixed assets.

3.3. The Effect of Labor Input Level of Medical Institutions on Income Distribution Coefficient of Pension Institutions under the Integrating Health and Care Services. In studying the effect of labor input level of medical institutions on the income distribution coefficient of pension institutions, we found that the output elasticity of labor input and fixed asset input and the profitability of the integrating health and care services have certain influence on the fixed assets input of pension institutions. The numerical simulation is carried out under the two cases about $\beta < \alpha$ and $\beta > \alpha$. When $\beta < \alpha$, the input of labor has a greater influence on the total output than the input of fixed assets. Let $\alpha = 0.7, \beta = 0.3, a_2 = 1$. The simulation result is shown in Figure 4(a). When $\beta > \alpha$, the input of fixed assets has a greater influence on the total output than the input of labor. Let $\alpha = 0.3, \beta = 0.7, a_2 = 1$. The simulation result is shown in Figure 4(b).

As shown in Figure 4, the income distribution coefficient of pension institutions will increase with increasing labor input level in medical institutions. When the labor input level of medical institutions reaches the maximum, the income distribution coefficient of pension service institutions is negatively correlated with the labor level of medical institutions. By comparing Figures 4(a) and 4(b), we found that the maximum value of labor input in medical institutions increases if the profitability of the integrating health and care services is good. In addition, when the input of fixed assets has a greater influence on the total output than the input of labor, the maximum value of labor input in medical institutions is greater, and the income distribution coefficient of pension institutions is relatively higher when the labor level of medical institutions reaches the maximum value. However, when the input of labor has a greater influence on the total output than the input of fixed assets, the income distribution coefficient of pension institutions is relatively lower when the labor input level of medical institutions reaches its peak.

4. Conclusion

Considering the increasing aging problem, pension has become a hot topic of social concern. By using game theory and on the premise of the maximization about pension and medical institutions' own benefits, we constructed the utility model of resource allocation between pension and medical institutions under the integrating health and care services. We also explored the mutual incentive relationship between resource input and income distribution coefficient of pension and medical institutions. We then used computer numerical simulation technology to analyze and draw the following conclusions:

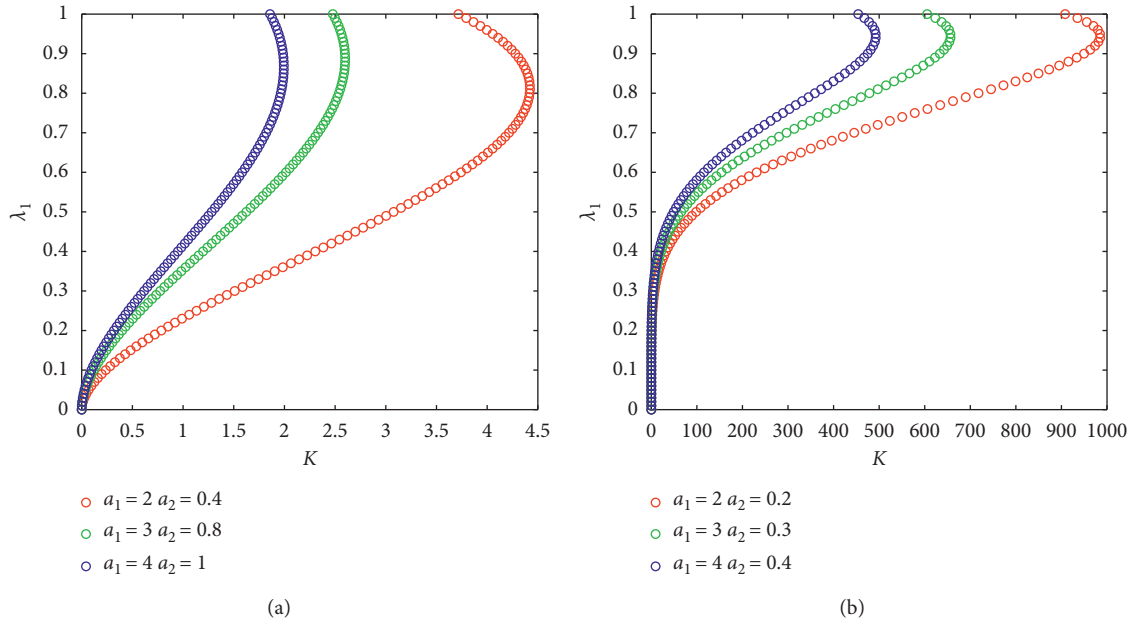


FIGURE 2: When $0 < a_2 < (\alpha/2)a_1$, the influence mechanism of fixed asset investment on the income distribution coefficient of pension institutions. (a) $\alpha > \beta$. (b) $\alpha < \beta$.

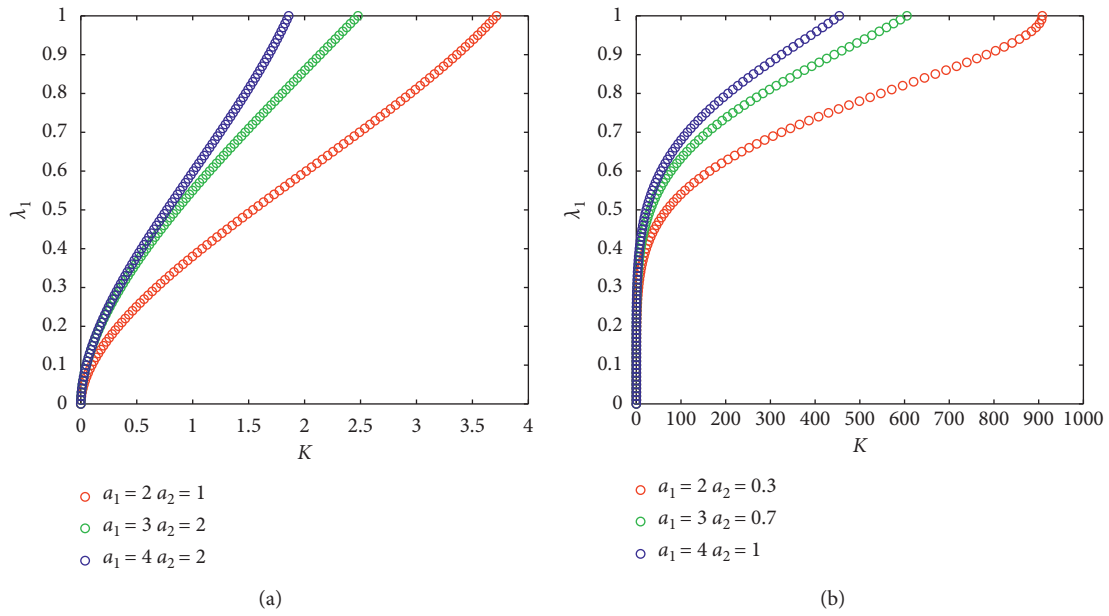


FIGURE 3: Continued.

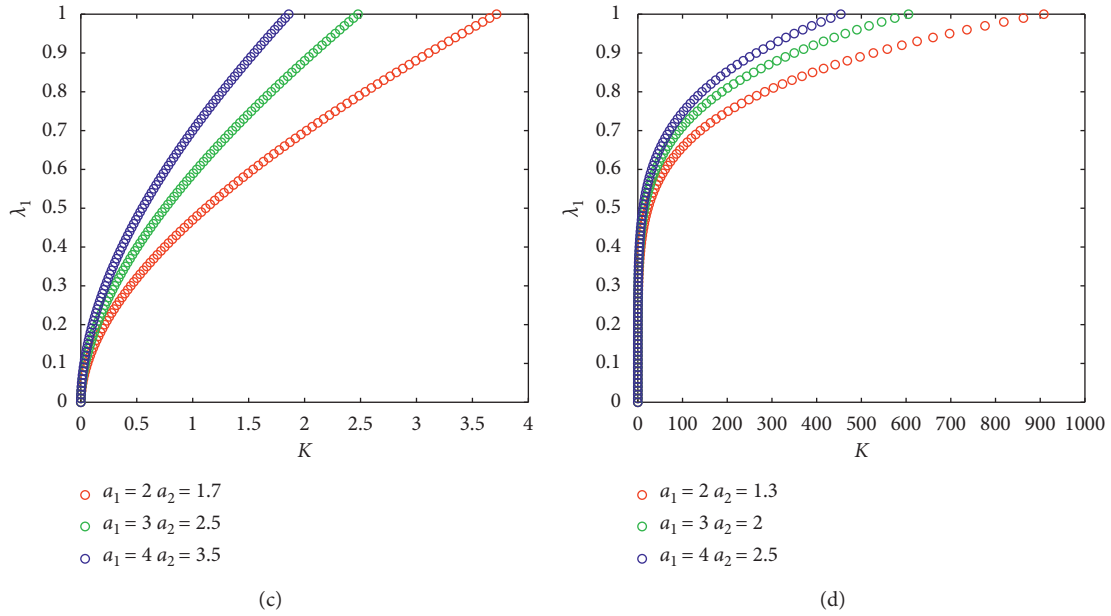


FIGURE 3: When $(\alpha/2)a_1 < a_2 < a_1$, the influence mechanism of fixed asset investment on the income distribution coefficient of pension institutions. (a) $(\alpha/2)a_1 < a_2 < \alpha a_1$ and $\alpha > \beta$. (b) $(\alpha/2)a_1 < a_2 < \alpha a_1$ and $\alpha < \beta$. (c) $\alpha a_1 < a_2 < a_1$ and $\alpha > \beta$. (d) $\alpha a_1 < a_2 < a_1$ and $\alpha < \beta$.

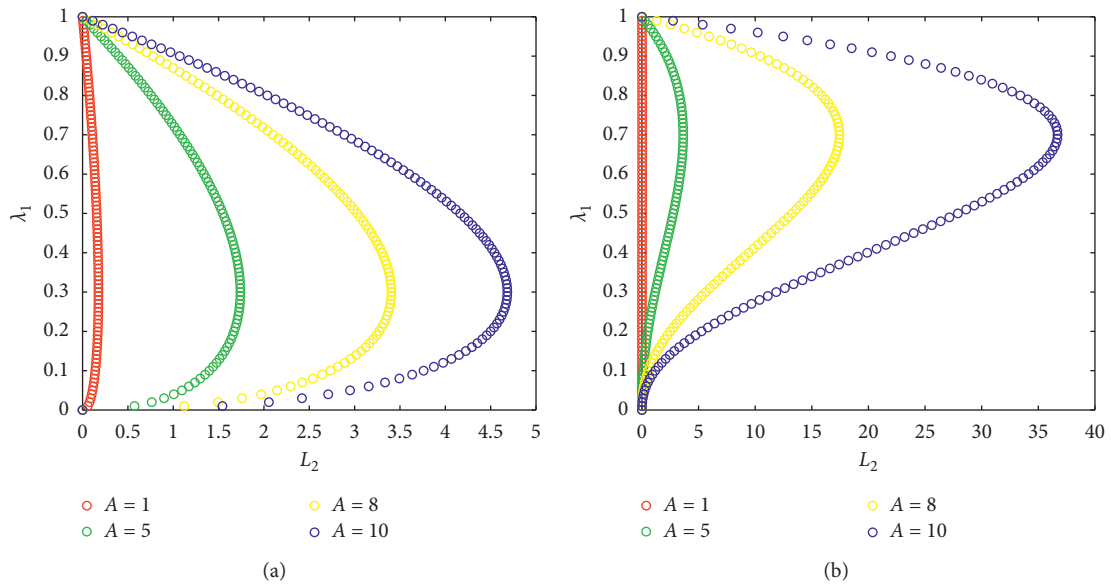


FIGURE 4: The influence mechanism of labor input level in medical institutions on the income distribution coefficient of pension institutions. (a) $\beta < \alpha$. (b) $\beta > \alpha$.

(1) As can be seen from the relationship between the labor input level of pension institutions and the income distribution coefficient of pension institutions, due to the mutual influence of pension institutions and medical institutions, the income distribution coefficient of medical institutions decreases with increasing income distribution coefficient of pension institutions. To prevent medical institutions from refusing medical cooperation due to the low income distribution coefficient, the labor

input of pension institutions should be relaxed and not be increased blindly.
 (2) The relationship between the fixed asset investment and the income distribution coefficient of pension institutions shows that pension institutions can increase the income distribution coefficient by expanding their investment in fixed assets. If the elderly who need the integrating medical and care services prefer more nursing beds, basic medical facilities, and other medical equipment, then pension

institutions should invest in fixed assets. However, when elderly population shows an increased dependence on services, such as daily life care and spiritual comfort, the income distribution coefficient of pension institutions can be greatly affected by the fixed assets invested less.

- (3) As can be seen from the relationship between the labor input level in medical institutions and the income distribution coefficient of pension institutions, when medical institutions account for a relatively low income distribution coefficient, they increase the labor input to reduce the income distribution coefficient of pension institutions and to improve their income distribution and obtain additional benefits. In addition, medical institutions are short on excellent doctors and nurses. If some medical staff were allocated to take care of the elderly, then their workload will increase significantly, and the service quality of medical institutions will decrease. Hence, pension institutions can actively negotiate, cooperate, and formulate detailed cooperation rules with medical institutions to encourage the latter to improve the labor level input when they offer integrating health and care services.

The main contribution of this paper is that we use game theory to construct the utility model of resource allocation between pension and medical institutions to explore how pension institutions and medical institutions invest resources into the integration of health and care services. However, there are still some limitations in our work. For example, the elderly service industry covers medical treatment, health, education, finance, tourism, etc., with a wide range of related branches and few relevant data, which is difficult to conduct in-depth research. Moreover, the relationship between the service demand of the elderly and the resource input of pension institutions and medical institutions has not been studied in depth. These questions can be topics of further research in the future. Through the study of time series, we further explore the relationship between each subject and each variable.

Data Availability

No data were used to support the findings of this study.

Disclosure

Tingqiang Chen, Jinnan Pan, Yuanping He, and Jining Wang are the co-first authors.

Conflicts of Interest

The authors declare that they have no conflicts of interest.

Authors' Contributions

Tingqiang Chen, Jinnan Pan, Yuanping He, and Jining Wang contributed equally to this work.

Acknowledgments

This work was supported by the National Natural Science Foundation of China (nos. 71871115, 71501094, and 71971111), the Major Project of Philosophy and Social Science Research in Colleges and Universities in Jiangsu Province (no. 2019SJZDA035), and the Innovation Team Project of Philosophy and Social Sciences in Colleges and Universities in Jiangsu Province (no. 2017ZSTD005).

References

- [1] D. Szalewska, P. Niedoszytko, and K. Gierat-Haponiuk, "The impact of professional status on the effects of and adherence to the outpatient followed by home-based telemonitored cardiac rehabilitation in patients referred by a social insurance institution," *International Journal of Occupational Medicine and Environmental Health*, vol. 28, no. 4, pp. 761–770, 2015.
- [2] E. R. McGrattan and E. C. Prescott, "On financing retirement with an aging population," *Quantitative Economics*, vol. 8, no. 1, pp. 75–115, 2017.
- [3] A. C. Lyons, J. E. Grable, and S.-H. Joo, "A cross-country analysis of population aging and financial security," *The Journal of the Economics of Ageing*, vol. 12, pp. 96–117, 2018.
- [4] T. Gorrindo, S. Chatterji, P. Kowal, Z. Epstein, and M. Weinstein, "A cross-country comparison of sociodemographic correlates of depression in the WHO study of global aging and adult health (SAGE)," *Applied Demography and Public Health*, vol. 3, pp. 45–60, 2013.
- [5] E. Apodoulaniaki, M. V. Tilborg, and H. S. M. Kort, "Visual functioning of aging care professionals and the influence of light, a brief literature study," *Studies in Health Technology & Informatics*, vol. 217, no. 4, pp. 405–410, 2015.
- [6] B. S. Jacobzone and J. Jenson, "Care allowances for the frail elderly and their impact on women care-givers," *Oecd Labour Market & Social Policy Occasional Papers*, vol. 65, no. 65, pp. 532–539, 2000.
- [7] N. Ikegami and J. C. Campbell, "Choices, policy logics and problems in the design of long-term care systems," *Social Policy & Administration*, vol. 36, no. 7, pp. 719–734, 2003.
- [8] J. M. Hartgerink, J. M. Cramm, A. J. D. Vos et al., "Situational awareness, relational coordination and integrated care delivery to hospitalized elderly in the Netherlands: a comparison between hospitals," *BMC Geriatrics*, vol. 14, no. 1, p. 3, 2014.
- [9] I. N. Fabbricotti, B. Janse, W. M. Looman et al., "Integrated care for frail elderly compared to usual care: a study protocol of a quasi-experiment on the effects on the frail elderly, their caregivers, health professionals and health care costs," *BMC Geriatrics*, vol. 13, no. 1, p. 31, 2013.
- [10] J. Bao, X. J. Wang, Y. Yang, R.-Q. Dong, and Z.-F. Mao, "Can the medical-nursing combined care promote the accessibility of health services for the elderly in nursing home? A study protocol of analysis of the effectiveness regarding health service utilization, health status and satisfaction with care," *West Indian Medical Journal*, vol. 64, no. 5, pp. 514–520, 2015.
- [11] D. B. Reuben, "Making hospitals better places for sick older persons," *Journal of the American Geriatrics Society*, vol. 48, no. 12, pp. 1728–1729, 2000.
- [12] M. Wendy, B. Sally, W. Marianne, R. Olorenshaw, and N. Gracia, "Acute care management of older people with dementia: a qualitative perspective," *Journal of Clinical Nursing*, vol. 20, no. 3–4, pp. 420–428, 2011.

- [13] J. L. Powell, "Personalization and community care: a case study of the British system," *Ageing International*, vol. 37, no. 1, pp. 16–24, 2012.
- [14] M. Zunzunegui, F. Béland, and A. Otero, "Support from children, living arrangements, self-rated health and depressive symptoms of older people in Spain," *International Journal of Epidemiology*, vol. 30, no. 5, pp. 1090–1099, 2001.
- [15] M. E. Hughes and L. J. Waite, "Health in household context: living arrangements and health in late middle age," *Journal of Health and Social Behavior*, vol. 43, no. 1, pp. 1–21, 2002.
- [16] R. Lund, P. Due, J. Modvig, B. E. Holstein, M. T. Damsgaard, and P. K. Andersen, "Cohabitation and marital status as predictors of mortality—an eight year follow-up study," *Social Science & Medicine*, vol. 55, no. 4, pp. 673–679, 2002.
- [17] C. Glendinning, "Breaking down barriers: integrating health and care services for older people in England," *Health Policy*, vol. 65, no. 2, pp. 139–151, 2003.
- [18] T. Michel, "Integrating services for older people: a resource book for managers," *International Journal of Integrated Care*, vol. 5, no. 2, p. e19, 2005.
- [19] K. Leichsenring and A. M. Alaszewski, *Providing Integrated Health and Social Care for Older Persons: A European Overview of Issues at Stake*, Ashgate Publishing Ltd., Aldershot, England, 2004.
- [20] J. Reed, G. Cook, S. Childs, and B. McCormack, "A literature review to explore integrated care for older people," *International Journal of Integrated Care*, vol. 5, no. 1, p. e17, 2005.
- [21] M. P. Fisher and C. Elnitsky, "Health and social services integration: a review of concepts and models," *Social Work in Public Health*, vol. 27, no. 5, pp. 441–468, 2012.
- [22] H. A. Sultz, *Health Care USA*, Jones and Barlett Publishers, Burlington, MA, USA, 2006.
- [23] S. S. Carson, P. B. Bach, L. Brzozowski, and A. Leff, "Outcomes after long-term acute care," *American Journal of Respiratory and Critical Care Medicine*, vol. 159, no. 5, pp. 1568–1573, 1999.
- [24] P. Chatterji, N. Burstein, D. Kidder et al., *Evaluation of the Program of All-Inclusive Care for the Elderly (PACE) Demonstration: The Impact of PACE on Participant Outcomes*, Abt Associates, New York, NY, USA, 1998.
- [25] R. Laura and B. A. Gadsby, *PACE-Program of All Inclusive Care for the Elderly*, Vol. 4, Age in Action, Cape Town, South Africa, 2007.
- [26] M. Segelman, J. Szydlowski, B. Kinoshian et al., "Hospitalizations in the program of all-inclusive care for the elderly," *Journal of the American Geriatrics Society*, vol. 62, no. 2, pp. 320–324, 2014.
- [27] M. D. Fretwell, J. S. Old, K. Zwan, and K. Simhadri, "The elderhaus program of all-inclusive care for the elderly in North Carolina: improving functional outcomes and reducing cost of care: preliminary data," *Journal of the American Geriatrics Society*, vol. 63, no. 3, pp. 578–583, 2015.
- [28] U. Polska, "The program of all-inclusive care for the elderly (PACE): the innovative and economically viable model of American geriatric care," *Pielegniarstwo XXI Wieku/Nursing in the 21st Century*, vol. 16, no. 1, pp. 51–61, 2017.
- [29] M. Geraedts, G. V. Heller, and C. A. Harrington, "Germany's long-term-care insurance: putting a social insurance model into practice," *The Milbank Quarterly*, vol. 78, no. 3, pp. 375–401, 2000.
- [30] B. Ahgren, "Patient choice and health care integration: a review of the consistency between two Swedish policy concepts," *International Journal of Integrated Care*, vol. 10, no. 6, p. e63, 2010.
- [31] M. Maruthappu, A. Hasan, and T. Zeltner, "Enablers and barriers in implementing integrated care," *Health Systems & Reform*, vol. 1, no. 4, pp. 250–256, 2015.
- [32] S. Shimizutani, "The future of long-term care in Japan," *Asia-Pacific Review*, vol. 21, no. 1, pp. 88–119, 2014.
- [33] P. Ji, X. Ma, and G. Li, "Developing green purchasing relationships for the manufacturing industry: an evolutionary game theory perspective," *International Journal of Production Economics*, vol. 166, pp. 155–162, 2015.
- [34] S. Li, Z. Yu, and M. Dong, "Construct the stable vendor managed inventory partnership through a profit-sharing approach," *International Journal of Systems Science*, vol. 46, no. 2, pp. 271–283, 2015.
- [35] S. M. Alavi and C. Zhou, "Resource allocation scheme for orthogonal frequency division multiple access networks based on cooperative game theory," *International Journal of Communication Systems*, vol. 27, no. 8, pp. 1105–1125, 2015.
- [36] D. Zhang, N. Wu, and X. Li, "The bilateral resource integration service system," in *Proceedings of the Fourth International Conference on Computational & Information Sciences*, Chongqing, China, August 2012.
- [37] Z. H. Wan and M. L. Zhang, "Value cocreation through resource integration: new insights into container inspection ecosystems the lens of service dominant logic and systems," in *Proceedings of the IEEE International Conference on Service Operations & Logistics*, Dongguan, China, July 2013.
- [38] J. Siltaloppi and S. L. Vargo, "Reconciling resource integration and value propositions—the dynamics of value co-creation," in *Proceedings of the 47th Hawaii International Conference on System Sciences*, Waikoloa, HI, USA, January 2014.
- [39] S. P. Singaraju, Q. A. Nguyen, O. Niininen, and G. Sullivan-Mort, "Social media and value co-creation in multi-stakeholder systems: a resource integration approach," *Industrial Marketing Management*, vol. 54, pp. 44–55, 2016.
- [40] X. Guan, M. Li, and Y. Li, "Research on the resource integration of virtual industry cluster based on the complex network theory," in *Proceedings of the International Conference on Industrial Economics System & Industrial Security Engineering*, Sydney, Australia, July 2016.
- [41] K. Koskela-Huotari, B. Edvardsson, J. M. Jonas, D. Sörhammar, and L. Witell, "Innovation in service ecosystems—breaking, making, and maintaining institutionalized rules of resource integration," *Journal of Business Research*, vol. 69, no. 8, pp. 2964–2971, 2016.
- [42] Q. Wang, K. Zhang, and D. Mu, "Research on the collaboration of express service network based on resource integration," in *Proceedings of the 2016 International Conference on Logistics, Informatics and Service Sciences (LISS)*, Sydney, Australia, July 2016.

Research Article

Dynamic Green Innovation Decision of the Supply Chain with Innovating and Free-Riding Manufacturers: Cooperation and Spillover

Feifei Zhang,¹ Zaixu Zhang,^{1,2} Yawei Xue,³ Jian Zhang ,⁴ and Yang Che⁴

¹School of Economics and Management, China University of Petroleum (East China), Qingdao, Shandong 266520, China

²School of Literature, Law and Business, Shengli College China University of Petroleum, Dongying, Shandong 257061, China

³School of Management, Qingdao University of Technology, Qingdao, Shandong 266520, China

⁴School of Government, Central University of Finance and Economics, Beijing 100081, China

Correspondence should be addressed to Jian Zhang; zjpolicy@163.com

Received 6 May 2020; Accepted 16 June 2020; Published 4 July 2020

Guest Editor: Baogui Xin

Copyright © 2020 Feifei Zhang et al. This is an open access article distributed under the Creative Commons Attribution License, which permits unrestricted use, distribution, and reproduction in any medium, provided the original work is properly cited.

Green innovation for supply chain has attracted much academic attention. Yet, there is no adequate understanding of how spillover and cooperation can impact the enterprises' green innovation decisions in the presence of free-rider. Besides, the dynamic impact of green innovation on emission is still lack of attention. We develop a differential game model that explicitly considers a supply chain with two types of manufacturers (i.e., green innovation and free-riding) to examine the dynamics of green innovation. The analysis reveals that under the noncooperation mode, the emissions and profits of free-riding manufacturers are found to be lower than that of innovating manufacturers, but technology spillovers will narrow the gap between them. Under the cooperation mode, there would be greater innovation efforts of green manufacturers and lesser efforts of green suppliers. Moreover, technology spillovers will have less impact on optimal decision changes. The profit of free-riding manufacturers is higher than that of innovating manufacturers, but the initial market power will affect the changes in their sales and profits. Meanwhile, cooperation will increase the total emission amount and long-term profits of the green supply chain, and technology spillovers of green manufacturers will help narrow the emission gap and broaden the profit gap, while that of the suppliers will have the opposite effect. The present study provides a new perspective for research on green innovation decisions for supply chain.

1. Introduction

With rapid industrialization, innumerable resources are leading to insurmountable pollution generated by human activities, in particular, fossil fuel combustion producing greenhouse gases, which leads to global warming and thus seriously threatening the global natural ecological balance [1]. Owing to the devastating effects of enterprise behavior on the environment, cleaner production has garnered much attention [2]. To reduce emissions arising from the production process, clean manufacturers will also compel upstream suppliers to reduce emissions by mandating disclosure of green development information and to organize green information for the full product life cycle. In this

case, the entire supply chain has an incentive to implement the green strategy.

Evolution of green technology is vital for improving the enterprises' environmental performance without sacrificing economic benefits [3, 4]. Therefore, more and more enterprises invest in green technology to address the growing environmental needs. In addition, green technology innovation is more dependent than other types of technology innovation on external sources of knowledge and information [5]. Innovation cooperation [6, 7] and technology spillovers [8] are two important means of acquiring technical capacity (knowledge capital). The internal access to more knowledge draws out green innovation [9, 10], which can ease the vulnerability under the demands

of new environmental regulations [11], as well as respond to the market's green demands [12]. Therefore, several researchers analyzed the impact of enterprises' green innovation [13, 14].

Supply chain enterprises recognize that the innovation cooperation between upstream and downstream enterprises favors integration of internal and external innovation resources to earn greater profit margins. As majority of enterprises are still without green innovation, technology spillovers will improve the influence of innovation within the green chain but would undermine the effect outside. In other words, when the free-riding enterprises suffer from both horizontal and vertical technology spillovers, they will also reduce pollution emission. So, we call these enterprises that do not innovate free-riders, whose existence severely hinders the reform of green management [15]. Cappelli [16] empirically analyzed the impact of the source of technology spillover on innovation and found that technology spillovers from companies in the same industry are easy to induce competitors to imitate, and the transfer of innovation advantages has a negative impact on the innovating manufacturers. Therefore, the free-riders' consequent on technology spillovers are very unfavorable to innovating enterprises.

However, the existing research shows that free-riding enterprises are rarely considered within the research framework. The research on technology spillover focuses on the bidirectional (or unidirectional) spillover of the participants in innovation decision-making, disregarding the free-ride behavior, and the spillover consequences for competitors are disregarded in the decision model. Therefore, the present study, assuming that technology spillovers (one-way flow) exist in free-riding manufacturers, complements the existing research by addressing the following issues:

- (1) Whether the enterprise will transform from free-riding to innovation based on the impact on the optimal innovation decision of green manufacturers and green suppliers and by comparing the emissions and profits of the two types of manufacturers.
- (2) Whether chain innovation cooperation will lead manufacturers to switch from free-riding to innovation when the green manufacturer and green supplier engage in innovation cooperation based on the impact on their optimal innovation decision and by comparing the emissions and profits of green innovation manufacturers before and after cooperation.
- (3) Whether innovation cooperation in the green supply chain can improve supply chain profits and reduce emissions.

To address these issues, a supply chain model with two types of manufacturers (green innovation and free-riding) and a shared green supplier was established. The green manufacturer and the green supplier reduced emissions in the production process. The demand for products produced by these manufacturers is determined by the

amount of emissions, and their products compete in the same product market. In the case of vertical innovation noncooperation and cooperation in the green supply chain, the impact of asymmetric technology spillover on the optimal innovation decision of the green manufacturer and the green supplier is considered. In the profit-maximizing decision, the cost of innovation as well as that of the emission treatment is considered in the present study, which makes it unique from other studies. Given that the long-term impact of corporate innovation input on emissions, the static analysis framework is extended to dynamic situations. We use differential game theory to describe the dynamic characteristic. The essence of this theory is to solve the optimal control problem of two or more participants, which can better address the dynamic game problem between supply chain members, such as supply chain cooperation advertising [17], the coordination mechanism of supply chain cooperation [18], and supply chain emission reduction strategy [19]. Using the emissions of supply chain enterprises as state variables to build a differential game model, the dynamic trend of emissions and corporate profits over time are examined, and conclusions are offered from a long-term steady-state perspective.

This study is presented as follows. Section 2 presents the literature, and Section 3 provides a differential game model as well as an explanation of some parameters and assumptions to examine the optimal innovation decision and steady-state equilibrium of green supply chain enterprises under noncooperation and cooperation. Section 4 indicates the impact of innovation cooperation and technology spillovers on enterprise innovation decisions, and Section 5 compares the two situations through numerical analysis. Finally, Section 6 presents the results and conclusions.

2. Literature Review

Green supply chain innovation has been extensively studied. This field is basically an intersection of two research fields: green supply chain management and technological innovation. Some empirical studies have found that green innovation has a favorable influence on the supply chain. For example, Lee et al. [20] used data from 133 Malaysian manufacturing enterprises to confirm that technological innovation not only improves the environment but also favors eco-design, investment recovery, and technological innovation. De Marchi [21] used the data of Spanish manufacturing enterprises to study the relationship between corporate innovation cooperation and green innovation and argued that the focus should be more on external cooperation, such as suppliers and universities, than on other innovations. It also found that there is a substitution effect between cooperation and internal R&D efforts. Green innovation cooperation with upstream suppliers can lead to higher environmental performance [22]. When enterprises need to change their inputs to create new products, establishing a strong cooperative relationship with suppliers

may be the best strategic choice [23, 24]. Dai et al. [25] studied the R&D cooperation behavior of upstream and downstream enterprises in the green supply chain, compared the three scenarios of cartelization, cost-sharing contract, and a benchmark of noncooperation, and introduced the technical differences between the members of the supply chain and consumers' green awareness as well as the influence of government subsidy parameters on cooperative behavior. The results showed that upstream enterprises are always likely to adopt cartel rather than noncooperation models, which favors the cartel. The downstream enterprises generally prefer the cooperation model. However, if the market is more sensitive to green and government subsidies which are strong, downstream enterprises can earn more revenue through a cartel. From the perspective of the overall supply chain, cooperation has more benefits than noncooperation. Upstream suppliers are the best partners for green innovation in supply chain enterprises. However, majority of studies have focused on the cooperation problem of green innovation enterprises in the chain and rarely included innovative enterprises. Therefore, the present study addresses this gap and considers the enterprises that do not include green innovation into the decision-making framework.

Several studies have examined the impact of technology spillovers [26, 27]; D'Aspremont and Jacquemin [28] first studied the duopoly two-stage game model (AJ model). They highlighted that the spillover effect favors improved social welfare and increased research and development (R&D) investment of enterprises. Several other researchers extended the study on this model and applied it to multiple fields. Steurs [29] combined different technology spillover parameters within and between industries to achieve effective R&D investment levels. From the perspective of increasing sales, vertical spillovers between industries can increase product output more than horizontal spillovers within industries that can increase social welfare. From the technological innovation perspective, Ge et al. [9] discussed vertical innovation and cooperation behavior of supply chain enterprises that can reduce the production cost based on endogenizing technology spillover and cartelization as two means of cooperation. Considering the impact of spillovers on production costs, Shibata [30] studied the issue of innovation investment in different market structures and found that, in a duopoly market, noncooperation innovation investment, in contrast with innovation cooperation, is likely to exhibit less technology spillover. When the market tends to be perfectly competitive, technology spillover has no effect regardless of cooperation. Several studies contend that technology spillovers can improve supplier's reliability [31].

The common factor in the aforementioned studies is the positive externality to economic activities. However, the supply chain decisions resulting from various manifestations also differ. Green innovation results in

emission reduction through technology spillovers, thereby increasing the demand in green-sensitive markets and increasing revenues. Besides, unlike other spillovers, owing to the external impact on the environment, the cost of emission treatment for enterprises reduces. Therefore, this spillover effect is affected by the type of market and the extent of environmental regulation. Therefore, the present study considers the two aspects of the spillover of green innovation technology, which provides an accurate reference for enterprises to make green innovation decisions.

Extant literature analyzes the horizontal and vertical technology spillovers of supply chain enterprises, and it is inevitably associated with innovation cooperation to examine the impact of technology spillovers on the cooperation model. However, from the supply chain structure perspective, majority of extant literature focuses on a "one-to-one" type supply chain, and a "one-to-many" or "many-to-one" type supply chain is more consistent with the real situation. Results of past research are combined to examine the "one-to-two" (i.e., one supplier and two manufacturers) supply chain, of which, two manufacturers (green innovation and free-riding) constitute a duopoly market. For a green manufacturer, the technology spillover with suppliers is bidirectional and that with free-riding manufacturers is unidirectional. A free-riding manufacturer enjoys both vertical and horizontal technology spillovers. In this case, technology spillovers are asymmetrical. Therefore, it is important to analyze the green innovation decisions and cooperation strategies of enterprises.

3. The Model

A model that contains a green manufacturer (H), a free-riding manufacturer (L), and a shared green supplier (S) which is considered in the present study. The green manufacturer and the green supplier reduce pollutant emissions in the production process through green innovation activities. At the same time, the green supplier has provided green raw materials or components for undertaking technology spillovers to the downstream, assuming similarities between the manufacturers. The green manufacturer also spills over technology to the supplier and the free-riding manufacturer. For convenience, it is also assumed that there is no difference in the extent of spillovers. Because of the technology spillover, the pollutant emissions from the free-riding manufacturer will also be impacted by the innovation activities of the upstream supplier and the green manufacturer. The game participants (i.e., the green manufacturer and the green supplier) make green innovation decisions in time $t \in [0, +\infty)$; $z(t)$ and $u(t)$ are the degree of green innovation efforts at the moment t , assuming the green innovation efforts are all positive. The amount of pollutant emissions can be altered periodically by adjusting the degree of green innovation efforts $e_i(t)$ [32] at the moment t , where $i = H, L, S$, $e_i(0) = e_{i0}$:

$$\frac{de_H(t)}{dt} = q_H(t) - z(t) - \beta u(t) - \eta e_H(t), \quad (1)$$

$$\frac{de_L(t)}{dt} = q_L(t) - \alpha z(t) - \beta u(t) - \eta e_L(t), \quad (2)$$

$$\frac{de_S(t)}{dt} = Q - \alpha z(t) - u(t) - \eta e_S(t), \quad (3)$$

where $\alpha \in [0, 1]$ and $\beta \in [0, 1]$ are the technology spillovers of the green manufacturer and the supplier. $\eta > 0$ denotes the natural mitigation rate, which implies that when there is no green innovation, the emission is reduced because of the technological progress, assuming that the three enterprises are at the same level of technological progress. q_H and q_L are denoted as the manufacturer's production volume, assuming that one unit of parts can produce one unit of final products; therefore, the total number of components ordered from retailers is $Q = q_H + q_L$. Assuming that the total market to maintain a certain Q is given constant, the manufacturer does not have inventory, that is, sell as much as you produce. The products by both the green and the free-riding manufacturer are homogeneous and can be partially substituted. Given that the production process of both the products yield varying pollutant emissions, consumers could identify them through green labels, etc., which will affect the demand for green products. Therefore, the production volume of the two manufacturers can be assumed to be

$$\begin{aligned} q_H &= \theta Q + s[e_L(t) - e_H(t)], \\ q_L &= (1 - \theta)Q + s[e_H(t) - e_L(t)], \end{aligned} \quad (4)$$

where $\theta \in (0, 1)$ is the initial market share of green manufacturers. $s \in (0, 1)$ denotes the green-sensitive coefficient. In the perfectly competitive market, the total sales volume of an enterprise often depends on its market share and the sales scale of similar products in the market. Therefore, under a duopoly game model, we propose that the sales of two types of manufacturers are affected by market share and competitor emissions, and the green sensitivity coefficient regulates the relationship between market demand and product emissions differences.

Through the aforementioned assumption, the profit margin of the green supply chain members $\rho_i > 0$ is given, $i = H, L, S$, and the instantaneous profit is given by

$$\begin{aligned} \pi_H(t) &= \rho_H q_H(t) - \frac{\varphi_H z(t)^2}{2} - g e_H(t), \\ \pi_L(t) &= \rho_L q_L(t) - g e_L(t), \end{aligned} \quad (5)$$

$$\pi_S(t) = \rho_S Q - \frac{\varphi_S u(t)^2}{2} - g e_S(t).$$

Among them, the square of the green innovation effort is the cost of innovation [28], g is the processing cost per unit of emissions, considering the processing costs of pollutant emissions, which implies that enterprises must examine the targets of minimizing impact on the environment as well when making a green innovation decision.

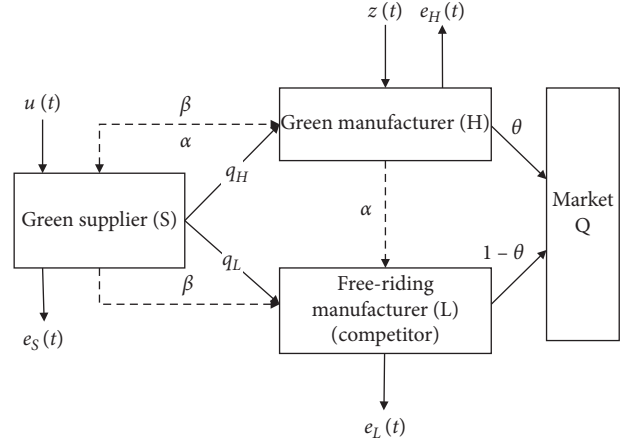


FIGURE 1: Supply chain structure.

Within an unlimited time frame, the manufacturer and the supplier have the same discount factor $r > 0$ at any time. The long-term profits of the green manufacturers, the free-riding manufacturer, and the green supplier are as follows:

$$\begin{aligned} J_H &= \int_0^{\infty} e^{-rt} \pi_H(t) dt, \\ J_L &= \int_0^{\infty} e^{-rt} \pi_L(t) dt, \\ J_S &= \int_0^{\infty} e^{-rt} \pi_S(t) dt. \end{aligned} \quad (6)$$

Figure 1 illustrates the logic framework of this study. The parameters in the model are independent of time and are constant. For the convenience of writing, the time t is not listed below.

Notations and definitions are explained in Table 1.

4. Equilibrium Analysis

4.1. Noncooperation Innovation Mode (N). In this model, the green manufacturer and the green supplier make decisions on optimal green innovation efforts to maximize long-term profits, and the decision process is distinguished by superscript N. Therefore, the decision-making problems of the green manufacturer and the green supplier are as follows:

$$\max_z J_H^N = \int_0^{\infty} e^{-rt} \left[\rho_H (\theta Q + s e_L - s e_H) - \frac{\varphi_H z^2}{2} - g e_H \right] dt, \quad (7)$$

$$\max_u J_S^N = \int_0^{\infty} e^{-rt} \left[\rho_S Q - \frac{\varphi_S u^2}{2} - g e_S \right] dt. \quad (8)$$

In order to have unique continuous solutions $e_H(t)$ and $e_S(t)$ for (1) and (3), a set of bounded, continuous, and differentiable value functions $V_H^N(e_H, e_L)$ and $V_S^N(e_S)$ should be constructed first to maximize (7) and (8), that is, to solve the equilibrium solution of the noncooperation innovation game. Then, Proposition 1 can be obtained.

TABLE 1: Notations and definitions.

Notations	Definitions
Decision variables	
$z(t)$	Green innovation effort of the green manufacturer
$u(t)$	Green innovation effort of the green supplier
Parameters and other variables	
$e_H(t), e_L(t), e_S(t)$	Pollutant emissions of green manufacturer, free-rider, and green supplier at time t , with initial emissions $e_i(0) = e_{i0}, i = H, L, S$
α, β	Technology spillovers of the green manufacturer and the supplier, $\alpha \in [0, 1]$ and $\beta \in [0, 1]$
η	Natural mitigation rate, $\eta > 0$
Q	Market capacity
q_H, q_L	Production volume
θ	Initial market share of green manufacturer, $\theta \in (0, 1)$
s	Green -sensitive coefficient, $s \in (0, 1)$
ρ_H, ρ_L, ρ_S	Profit margin of green manufacturer, free-rider, and green supplier
φ_H, φ_S	Cost parameter associated with green innovation efforts by green manufacturer and supplier, $\varphi_H > 0$ and $\varphi_S > 0$
g	Processing cost per unit of emissions
r	Discount factor, $r > 0$
$\pi_H(t), \pi_L(t), \pi_S(t)$	Instantaneous profit of green manufacturer, free-rider, and green supplier for $t \in [0, +\infty)$

Proposition 1. Under the noncooperation innovation mode, the steady-state equilibrium of the green manufacturer and the green supplier is $(z^{N*}, u^{N*}, e_H^{N*}, e_L^N, e_S^{N*})$:

$$\left\{ \begin{array}{l} z^{N*} = \frac{g(\eta + r + s + \alpha s) + \rho_H s(1 - \alpha)(\eta + r)}{\varphi_H(\eta + r)(\eta + r + 2s)}, \\ u^{N*} = \frac{\eta + g}{\varphi_S r}, \\ e_H^{N*} = \frac{1}{\eta^2} \left\{ (s - \eta - \alpha s) \left[\frac{g(\eta + r + s + \alpha s) + \rho_H s(1 - \alpha)(\eta + r)}{\varphi_H(\eta + r)(\eta + r + 2s)} \right] - \frac{\beta \eta(\eta + g)}{\varphi_S r} + Q(s + \eta\theta - 2s\theta) \right\}, \\ e_L^N = \frac{1}{\eta^2} \left\{ (s - \alpha\eta - \alpha s) \left[\frac{g(\eta + r + s + \alpha s) + \rho_H s(1 - \alpha)(\eta + r)}{\varphi_H(\eta + r)(\eta + r + 2s)} \right] - \frac{\beta \eta(\eta + g)}{\varphi_S r} + Q(s + \eta - \eta\theta - 2s\theta) \right\}, \\ e_S^{N*} = \frac{1}{\eta} \left[Q - \frac{\eta + g}{\varphi_S r} - \frac{\alpha g(\eta + r + s + \alpha s) + \alpha \rho_H s(1 - \alpha)(\eta + r)}{\varphi_H(\eta + r)(\eta + r + 2s)} \right]. \end{array} \right. \quad (9)$$

Proof. According to the optimal control theory, $V_H^N(e_H, e_L)$ and $V_S^N(e_S)$, for any $e_H \geq 0$, $e_L \geq 0$, and $e_S \geq 0$, would satisfy

the Hamilton–Jacobi–Bellman (HJB) equation; let $V'_{ij} = \partial V_i / \partial e_j$, $i, j = H, L, S$,

$$rV_H^N(e_H, e_L) = \max_z \left[\rho_H(\theta Q + se_L - se_H) - \frac{\varphi_H z^2}{2} - ge_H + V_{HH}^{N'} \frac{de_H(t)}{dt} + V_{HL}^{N'} \frac{de_L(t)}{dt} \right], \quad (10)$$

$$rV_S^N(e_S) = \max_u \left[\rho_S Q - \frac{\varphi_S u^2}{2} - ge_S + V_{SS}^{N'} \frac{de_S(t)}{dt} \right]. \quad (11)$$

Consider the first-order partial derivative of (10) and (11) with respect to z and u and make them equal to zero to derive

$$\begin{cases} z = -\frac{V_{HH}^{N'} + \alpha V_{HL}^{N'}}{\varphi_H}, \\ u = -\frac{V_{SS}^{N'}}{\varphi_S}. \end{cases} \quad (12)$$

Substitute (12) into (10) and (11) and simplify to derive

$$\begin{aligned} rV_H^N(e_H, e_L) = & \left(-\rho_H s - g - sV_{HH}^{N'} - \eta V_{HH}^{N'} + sV_{HL}^{N'}\right)e_H + \left(\rho_H s + sV_{HH}^{N'} - sV_{HL}^{N'} - \eta V_{HL}^{N'}\right)e_L + Q\left(\rho_H \theta + V_{HL}^{N'} - \theta V_{HL}^{N'} + \theta V_{HH}^{N'}\right) \\ & + \frac{(V_{HH}^{N'} + \alpha V_{HL}^{N'})^2}{2\varphi_H} + \frac{\beta V_{SS}^{N'}(V_{HH}^{N'} + V_{HL}^{N'})}{\varphi_S}, \end{aligned} \quad (13)$$

$$rV_S^N(e_S) = -(\eta + g)e_S + \rho_S Q + V_{SS}^{N'} Q + \frac{V_{SS}^{N'2}}{2\varphi_S} + \frac{\alpha V_{SS}^{N'}(V_{HH}^{N'} + \alpha V_{HL}^{N'})}{\varphi_H}. \quad (14)$$

According to the structure of (13) and (14), it can be assumed that the linear analytical formulas of the optimal value function $rV_S^N(e_S) = -(\eta + g)e_S + \rho_S Q + V_{SS}^{N'} Q + (V_{SS}^{N'2}/2\varphi_S) + (\alpha V_{SS}^{N'}(V_{HH}^{N'} + \alpha V_{HL}^{N'})/\varphi_H)$, $V_S^N(e_S)$ with respect to e_H and e_L are, respectively,

$$\begin{cases} V_H^N(e_H, e_L) = a_1 e_H + a_2 e_L + a_3, \\ V_S^N(e_S) = b_1 e_S + b_2, \end{cases} \quad (15)$$

where $a_1, a_2, a_3, b_1,$ and b_2 are the constants; substitute (20) and its first-order partial derivative with respect to $e_H, e_L,$ and e_S into fd18(13) and (14)fd19 to obtain

$$\begin{cases} a_1^* = \frac{\rho_H s + g + (gs)(r + \eta)}{r + \eta + 2s}, \\ a_2^* = \frac{s(\rho_H \eta - g + \rho_H r)}{(r + \eta)(r + \eta + 2s)}, \\ a_3^* = \frac{1}{r} \left[Q(\rho_H \theta + a_2^* - \theta a_2^* + \theta a_1^*) + \frac{(a_1^* + \alpha a_2^*)^2}{2\varphi_H} - \frac{\beta(\eta + g)(a_1^* + a_2^*)}{\varphi_S r} \right], \end{cases} \quad (16)$$

$$\begin{cases} b_1^* = -\frac{\eta + g}{r}, \\ b_2^* = \frac{Q(\rho_S + b_1^*)}{r} + \frac{b_1^{*2}}{2r\varphi_S} + \frac{\alpha b_1^*(a_1^* + \alpha a_2^*)}{r\varphi_H}. \end{cases} \quad (17)$$

Substituting fd21(16) and (17)fd22 into (12) can derive the optimal innovation efforts of the green manufacturer and the supplier under the independent innovation model. Meanwhile, into fd1(2)–(3), invoking the steady-state conditions $(d/dt) \begin{pmatrix} e_H \\ e_L \\ e_S \end{pmatrix} = 0$, solve the linear equations to obtain the stable value of pollutant emissions, that is,

$t \rightarrow \infty$. Suppose the market capacity is very large to ensure that the stability of pollution emissions is positive, QED.

Furthermore, the optimal profit function of the green manufacturer and the green supplier under R&D noncooperation mode and the profit function of free-riding manufacturers are obtained: $J_H^{N*}(e_H, e_L) = e^{-rt} V_H^{N*}(e_H, e_L)$, $J_S^{N*}(e_S) = e^{-rt} V_S^{N*}(e_S)$, and $J_L^N(e_H, e_L) = e^{-rt} V_L^N(e_H, e_L)$, where

$$\begin{aligned}
V_L^N(e_H, e_L) &= l_1 e_L + l_2 e_H + l_3, \\
\left\{ \begin{aligned}
l_1 &= \frac{(\eta + r)(g + \rho_L s) + gs}{(s + \eta)^2 + s^2 - r^2}, \\
l_2 &= \frac{s(g + \rho_L \eta - \rho_L r + 2\rho_L s)}{(s + \eta)^2 + s^2 - r^2}, \\
l_3 &= \frac{1}{r} \left[Q(1 - \theta)(\rho_L \theta + l_1) + Q\theta l_2 - (\alpha l_1 + l_2)z^{N*} \right. \\
&\quad \left. - (l_1 + l_2)\beta u^{N*} \right].
\end{aligned} \right.
\end{aligned} \tag{18}$$

The calculation of the profit function of the free-riding manufacturer is consistent with the proof derived earlier, and the profit under the situation of noncooperation innovation of the green manufacturer and the green supplier can be obtained by bringing in the optimal control variable. From the value function, a_1^* , a_2^* , and b_1^* are in fact the profit margins of the green manufacturer and the supplier in terms of pollution emissions. $a_1^* < 0$ explains that pollution emissions have a negative impact on the green manufacturer's profit, while the positive and negative judgments of a_2^* are related to $\rho_H(\eta + r) - g$. If $\rho_H(\eta + r) > g$, increasing emissions from the free-riding manufacturer can increase profits for the green manufacturer, while decreasing emissions can decrease the profits. a_3^* and b_2^* are the profits when the pollutant emissions are 0. The expression of green innovation efforts shows that optimal innovation efforts are guaranteed to be larger than zero. Static optimal control can be obtained by solving the HJB equation, which is the result of solving the linear value function. Such a strategy is more functional in enterprise innovation practice, and the optimal strategy in the continuous time range is not related to time, fairly demonstrating the management significance of the model.

According to Proposition 1, Propositions 2 and 3 can be obtained by analyzing the influence of related factors on the equilibrium strategy. \square

Proposition 2

- (1) Under the noncooperation innovation mode, the optimal innovation efforts of green suppliers are positively related to the treatment cost per unit of emissions, negatively related to the cost coefficient and discount factor, and not related to technology spillovers.
- (2) Under the noncooperation innovation mode, the optimal innovation efforts of green manufacturers is independent of the initial market share and are positively related to the marginal revenue per unit product and emission treatment cost per unit.
- (3) Under the noncooperation innovation mode, when $\rho_H(\eta + r) > g$, $(\partial z^{N*}/\partial \alpha) < 0$ and $(\partial z^{N*}/\partial s) > 0$, and when $\rho_H(\eta + r) < g$, $(\partial z^{N*}/\partial \alpha) > 0$ and $(\partial z^{N*}/\partial s) < 0$.

Proposition 2 (1) and (2) illustrate the relationship between optimal innovation efforts and parameters of green suppliers and manufacturers under the noncooperation innovation mode. Proposition 2 (3) explains that the impact of technology spillovers and green sensitivity coefficients on green manufacturers' innovation efforts is related to unit marginal revenue and unit emission process cost. The unit marginal revenue considering the natural emission reduction rate and the discount factor is still greater than the unit emission process cost; the greater the horizontal technological spillover of green manufacturers to free-riders is, the lower the innovation efforts would be. As technology spillover will weaken the difference between the emissions of the two types, it is not conducive to green manufacturers' exclusively extracting the high profits of innovation, due to lower motivation to innovation. In this case, most green manufacturers will file for patent application and other technical blockades to raise technical barriers and reduce technology spillovers as possible. Meanwhile, the greater the green sensitivity of the market is, the higher the innovation efforts would be because the increased sensitivity will increase the sales of innovation products, and consumers are willing to pay for low-emission products even for higher prices, which will stimulate green manufacturers increase the level of green innovation efforts, increase the green difference between alternatives, and thus increase revenue.

When the unit product revenue is lower than the unit emission process cost, the greater the horizontal technology spillover of green manufacturers to free riders is, the higher the innovation efforts would be. This is because the innovation result of green manufacturers is to be less economical than ecological. To reduce emissions and the cost of treatment, it is more likely to set new innovation standards in the same industry and encourage enterprises to become setters. From the government's point of view, the manufacturer's unit processing cost can be regarded as the government's environmental regulation measures. When the government promotes a certain green technology, it can promote the enterprise's technological exchange by increasing the regulation cost. Meanwhile, the greater the green sensitivity of the market is, the lower the innovation efforts would be. Because the profits of green products are smaller, consumers are reluctant to pay for green innovation. The increasing sales owing to the improvement of green sensitivity cannot compensate for the additional cost, so innovation efforts for green manufacturing cannot have a positive impact.

Proposition 3. As the technological spillovers of green manufacturers increase, the gap between the steady emission of green manufacturers and free-riding manufacturers gradually narrows, and when $\rho_H(\eta + r) > g$, the rate of shrinkage slows down; when $\rho_H(\eta + r) < g$, the rate of shrinkage increases.

Proposition 3 shows that when the margin revenue far outweighs the treatment cost of unit emissions, in the long term, a smaller technology spillover can reduce the eventual emissions of free-riding manufacturers significantly. However, when the margin revenue per unit product is

significantly lesser than the treatment cost of unit emission, a large technology spillover can reduce the final emission of free-riding manufacturers. In contrast with the conclusion of Proposition 2, in the initial stage of the green technology innovation, the government can reduce the cost of emission treatment, such as relaxing regulations and encouraging green enterprises to strengthen innovation, while the lateral technology spillover to the competitors is small. However, in the long term, the amount of pollutants discharged by competitors will also significantly narrow the gap between green enterprises and competitors. When the green technology is in the mature stage, the government can enhance the treatment cost by imposing a more stringent environmental protection tax and encouraging enterprises to increase the spillover. After long-term stability, the amount of emission discharged by free-riding manufacturers will be almost similar to that of green manufacturers.

Proof. Let $f(\alpha) = e_L^{N*} - e_H^{N*}$ and $\partial f(\alpha)/\partial \alpha = -(\eta g + r g + 2\alpha g s + 2s\rho_H(1-\alpha)(\eta+r))/(\eta\varphi_H(\eta+r)(r+\eta+2s)) < 0$; $f(\alpha)$ is judged to be monotonically decreasing, and $(\partial^2 f(\alpha)/\partial \alpha^2) = ((2s(\rho_H\eta + \rho_H r - g))/(\eta\varphi_H(\eta+r)(r+\eta+2s)))$; when $\rho_H(\eta+r) > g$, $f(\alpha)$ is convex; when $\rho_H(\eta+r) < g$, $f(\alpha)$ is concave.

The calculation of the trajectories of pollutant emissions of both the green and the free-riding manufacturer can refer to Proposition 1, take derivative of formula (1) with respect to time to obtain $(d^2 e_H/dt^2) = s(de_L/dt) - (s+\eta)(de_H/dt)$ and combine it with (2) to obtain $e_L(t)$, and then substitute (1) and resolve to obtain the second-order differential equation: $-(1/(s+\eta))(d^2 e_H/dt^2) + 2(de_H/dt) + (s+\eta - (s^2/(s+\eta)))e_H = \theta Q - z_N^* - \beta u_N^*$; according to the boundary conditions $e_H(0) = e_0$ and $e_H(\infty) = e_H^{N*}$, the green manufacturer's optimal emission trajectory can be obtained:

$$e_H^N(t) = e_H^{N*} + (e_0 - A)e^{-(s+\eta)\left(\sqrt{2-(s^2/(s+\eta)^2)}t-1\right)} - (e_H^{N*} - A)e^{-2(s+\eta)\left(\sqrt{2-(s^2/(s+\eta)^2)}t\right)}, \quad (19)$$

where $A = ((s+\eta)(\theta Q - z_N^* - \beta u_N^*)) / ((s+\eta)^2 - s^2)$. Furthermore, the emission trajectory of the free-riding manufacturer can be solved as follows:

$$e_L^N(t) = \frac{B}{\eta+s} + e^{-(\eta+s)t} \left[e_0 - \frac{B}{\eta+s} \right] + \frac{s}{\eta+s} \left[e_H^{N*} + (e_0 - A)e^{-(s+\eta)\left(\sqrt{2-(s^2/(s+\eta)^2)}t-1\right)} - (e_H^{N*} - A)e^{-2(s+\eta)\left(\sqrt{2-(s^2/(s+\eta)^2)}t\right)} \right] (1 - e^{-(\eta+s)t}), \quad (20)$$

where $B = (1-\theta)Q - \alpha z_N^* - \beta u_N^*$. Similarly, the trajectory of pollutant emissions from the green supplier can be obtained as follows: $e_S^V(t) = e_S^{V*} + (e_0 - e_S^{V*})e^{-\eta t}$. \square

green supply chain at time t is $\pi_g(t) = \pi_H(t) + \pi_s(t)$, and the innovation decision of the green supply chain is

$$\max_{z,u} J_G^V = \int_0^\infty e^{-rt} \pi_G dt. \quad (21)$$

4.2. Green Supply Chain Cooperation Mode (V). The green manufacturer and supplier cooperate in innovation and jointly determine the extent of green innovation efforts to maximize the profit of the green supply chain, which is indicated by the superscript V. At this time, the profit of the

Proposition 4. Under the green supply chain cooperation mode, the steady-state equilibrium existing in the green supply chain is $(z^{V*}, u^{V*}, e_H^{V*}, e_L^V, e_S^{V*})$:

$$\begin{cases} z^{V*} = \frac{g(\eta+r+s+\alpha\eta+\alpha r+3\alpha s) + \rho_H s(1-\alpha)(\eta+r)}{\varphi_H(\eta+r)(\eta+r+2s)}, \\ u^{V*} = \frac{g(\alpha+\beta)}{\varphi_S(\eta+r)}, \\ e_H^{V*} = \frac{1}{\eta^2} \left\{ (s-\eta-\alpha s) \left[\frac{g(\eta+r+s+\alpha\eta+\alpha r+3\alpha s) + \rho_H s(1-\alpha)(\eta+r)}{\varphi_H(\eta+r)(\eta+r+2s)} \right] - \frac{\beta\eta g(\alpha+\beta)}{\varphi_S(\eta+r)} + Q(s+\eta\theta-2s\theta) \right\}, \\ e_L^V = \frac{1}{\eta^2} \left\{ (s-\alpha\eta-\alpha s) \left[\frac{g(\eta+r+s+\alpha\eta+\alpha r+3\alpha s) + \rho_H s(1-\alpha)(\eta+r)}{\varphi_H(\eta+r)(\eta+r+2s)} \right] - \frac{\beta\eta g(\alpha+\beta)}{\varphi_S(\eta+r)} + Q(s+\eta-\eta\theta-2s\theta) \right\}, \\ e_S^{V*} = \frac{1}{\eta} \left[Q - \frac{g(\alpha+\beta)}{\varphi_S(\eta+r)} - \frac{\alpha g(\eta+r+s+\alpha\eta+\alpha r+3\alpha s) + \alpha\rho_H s(1-\alpha)(\eta+r)}{\varphi_H(\eta+r)(\eta+r+2s)} \right]. \end{cases} \quad (22)$$

The proof is the same as Proposition 1 and hence omitted.

Furthermore, the optimal value function of the profit of the green manufacturer and the green supplier and the profit function of the free-riding manufacturer can be obtained:

$$\begin{aligned}
 J_G^V(e_H, e_L, e_S) &= e^{-rt} V_G^{V*}(e_H, e_L, e_S), \\
 V_G^{V*}(e_H, e_L) &= c_1 e_H + c_2 e_L + c_3 e_S + c_4, \\
 \left\{ \begin{array}{l}
 c_1 = \frac{\eta g + gr + gs + \eta \rho_H s + r \rho_H s}{(\eta + r)(\eta + r + 2s)}, \\
 c_2 = \frac{\rho_H s(\eta + r) - gs}{(\eta + r)(\eta + r + 2s)}, \\
 c_3 = -\frac{g}{\eta + r}, \\
 c_4 = \frac{1}{r} \left[\rho_S Q + \rho_H \theta Q - \frac{\varphi_H z^{V*2}}{2} - \frac{\varphi_S u^{V*2}}{2} \right. \\
 \quad \left. + (\theta Q - z^{V*} - \beta u^{V*}) c_1 \right. \\
 \quad \left. + (Q - \theta Q - \alpha z^{V*} - \beta u^{V*}) c_2 \right. \\
 \quad \left. + (Q - z^{V*} - u^{V*}) c_3 \right],
 \end{array} \right. \\
 J_L^V(e_H, e_L) &= e^{-rt} V_L^V(e_H, e_L), \\
 V_L^V(e_H, e_L) &= m_1 e_L + m_2 e_H + m_3,
 \end{aligned} \tag{23}$$

where the shadow price of the free-riding manufacturer's unit emissions is not impacted under these two innovation models; therefore, $m_1 = l_1$, $m_2 = l_2$, and $m_3 = (1/r)[Q(1 - \theta)(\rho_L \theta + l_1) + Q\theta l_2 - (\alpha l_1 + l_2)z^{V*} - (l_1 + l_2)\beta u^{V*}]$; substituting the steady-state equilibrium solution of Proposition 2 into the steady-state equation can also find the trajectory of pollution emissions under the cooperation innovation model, $e_H^V(t)$, $e_L^V(t)$, and $e_S^V(t)$, and the formula is identical, except that the best green innovation efforts are replaced, and so it is not repeated here.

5. Comparison and Analysis

Based on the equilibrium analysis of the two models, three problems are solved through a comparative analysis: (1) whether competing in the homogeneous product market can encourage enterprises to change from free-riding to innovation; (2) whether the green supply chain members are willing to innovate and cooperate; and (3) the impact of technology spillover on the enterprise's green innovation decision and cooperation strategy. Owing to the high complexity of the earlier analytical solutions, numerical methods are preferred. The baseline values of parameters are shown in Table 2.

5.1. Green Innovation Decision of a Free-Riding Manufacturer.

The impact on the free-riding manufacturer under the two models is analyzed from the perspective of dynamic emissions, demand, and dynamic profit. Figure 2 shows that, under the benchmark parameter setting, the emission trajectories in both the modes have a time-stable trend, which indicates that even if the emission amount deviates from the stable state because of the interference from factors such as green technology, it would return as time evolves. Meanwhile, the upward trend shows that the emissions of the free-riding manufacturer and the green manufacturer are greater than the initial emissions. A comparison of the emission trajectories of the two types of manufacturers shows that the green manufacturer's emissions are always greater than those of the free-riding manufacturer in the early stage, but quickly stabilize as time evolves, while that of the free-riding manufacturer gradually exceed those of the green manufacturer and gradually stabilize. When the free-riding manufacturer experiences vertical supply chain innovation cooperation, the emissions are higher than that in the noncooperation model. From the perspective of emissions, free-riding manufacturers are encouraged to enhance their issues of emission reduction through technological innovation. The innovative cooperation model of green supply chain is also attractive for innovation for free-riding manufacturers.

Figures 3(a) and 4(a) show that cooperation innovation will reduce sales of the free-riding manufacturer; Figures 3(b) and 4(b) show that cooperation innovation will increase profits. A comparison with the green manufacturer shows that when the free-riding manufacturer dominates the market; the innovation efforts of the green manufacturer is likely to increase the market share of new products, but the effect is insignificant, and they are still not the dominant products in the market. In this case, from the profit perspective, the free-riding manufacturer will choose green innovation when challenged by independent green innovation from competitors and not when confronted by green supply chain cooperation innovation. When the green manufacturer has the same market position as the free-riding manufacturer, the sales volume of the green manufacturer is lower than the latter at the initial stage, but after rapid growth, it eventually surpasses the free-riders. The green manufacturer's profit will be much higher than the free-riding manufacturer's profit to stay abreast with the market changes, and the free-riding manufacturer will choose green innovation. From another perspective, manufacturers who rely on green differences of a product would delay in opening the market, and many short-sighted manufacturers will disregard green production or product R&D activities to earn early profits, while farsighted manufacturers can choose to improve market influence in advance and then promote green innovation strategies to gain competitive advantage for green products.

5.2. Effects of Spillover and Cooperation on the Decision of Green Manufacturers.

Calculate the difference between green innovation efforts in two modes:

TABLE 2: Baseline parameter values.

Q	r	η	s	φ_H	φ_S	ρ_H	ρ_S	ρ_L	e_0	g	β	θ	α
150	0.1	0.5	0.3	2	1	40	30	10	30	4	0.3	0.3	0.3

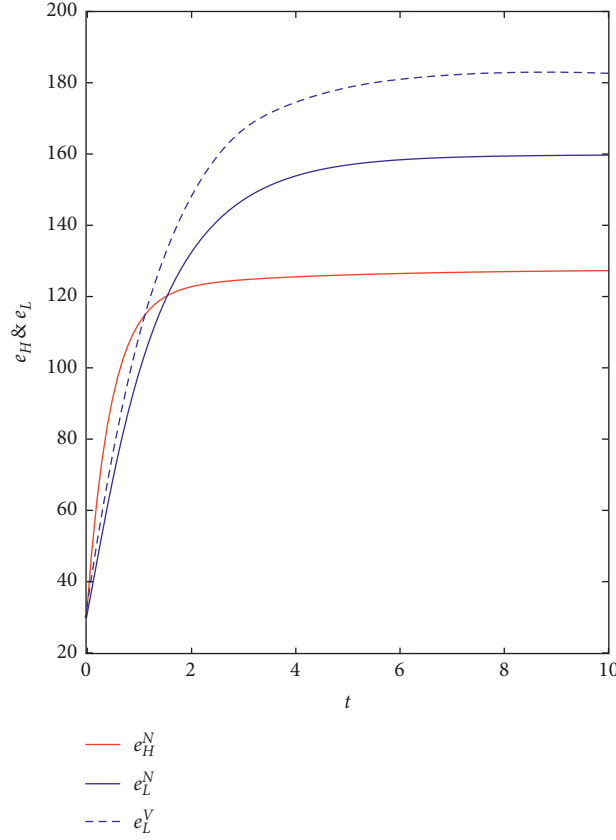


FIGURE 2: Comparison of the trajectories of the free-riding manufacturer and the green manufacturer.

$$\Delta z(t) = z^{V*}(t) - z^{N*}(t) = \frac{\alpha g}{\varphi_H(\eta + r)} > 0,$$

$$\Delta u(t) = u^{V*}(t) - u^{N*}(t) = \frac{gr(\alpha + \beta) - (\eta + r)(\eta + g)}{\varphi_S r(\eta + r)}. \quad (24)$$

The degree of innovation efforts of the green manufacturer in the cooperation mode is higher than that in the noncooperation mode because the discount factor is small, and it can be determined that $\Delta u(t) < 0$; the degree of innovation efforts of the green supplier in innovative cooperation is lesser than that in noncooperation. When maximizing innovation efforts for goal decision-making, the innovation efforts of manufacturers are higher than those of suppliers. Figures 5(a) and 5(b) show that the green manufacturer's innovation efforts decrease with the increase of their own technology spillovers, and the innovation cooperation with suppliers slows down this reduction rate, indicating that, under the cooperation model, if manufacturers are willing to actively share fully technical information

(perfect knowledge share) and still maintain a high degree of innovation efforts and if the green manufacturer does not share technical information with suppliers and competitors, innovation cooperation does not affect the innovation efforts. Under the cooperation mode, green suppliers will increase their innovation efforts with the increase of technology spillovers (including outward spillovers β and inward spillovers α), but there is still a large gap compared with the noncooperation model. This indicates that as the only shared supplier in the product competition market, following innovative cooperation with green manufacturers, and it does not favor suppliers' innovation efforts. This is because suppliers do not need to reduce emissions to increase product sales. There are only two constraints: innovation cost and processing cost. Given the technology spillover from green manufacturers to suppliers, suppliers will pass on the pressure of innovation to manufacturing, which can reduce not only their own emissions but also the cost of innovation.

It is worth noting that the result is the reduction of green innovation spillover on downstream free-riders, and the

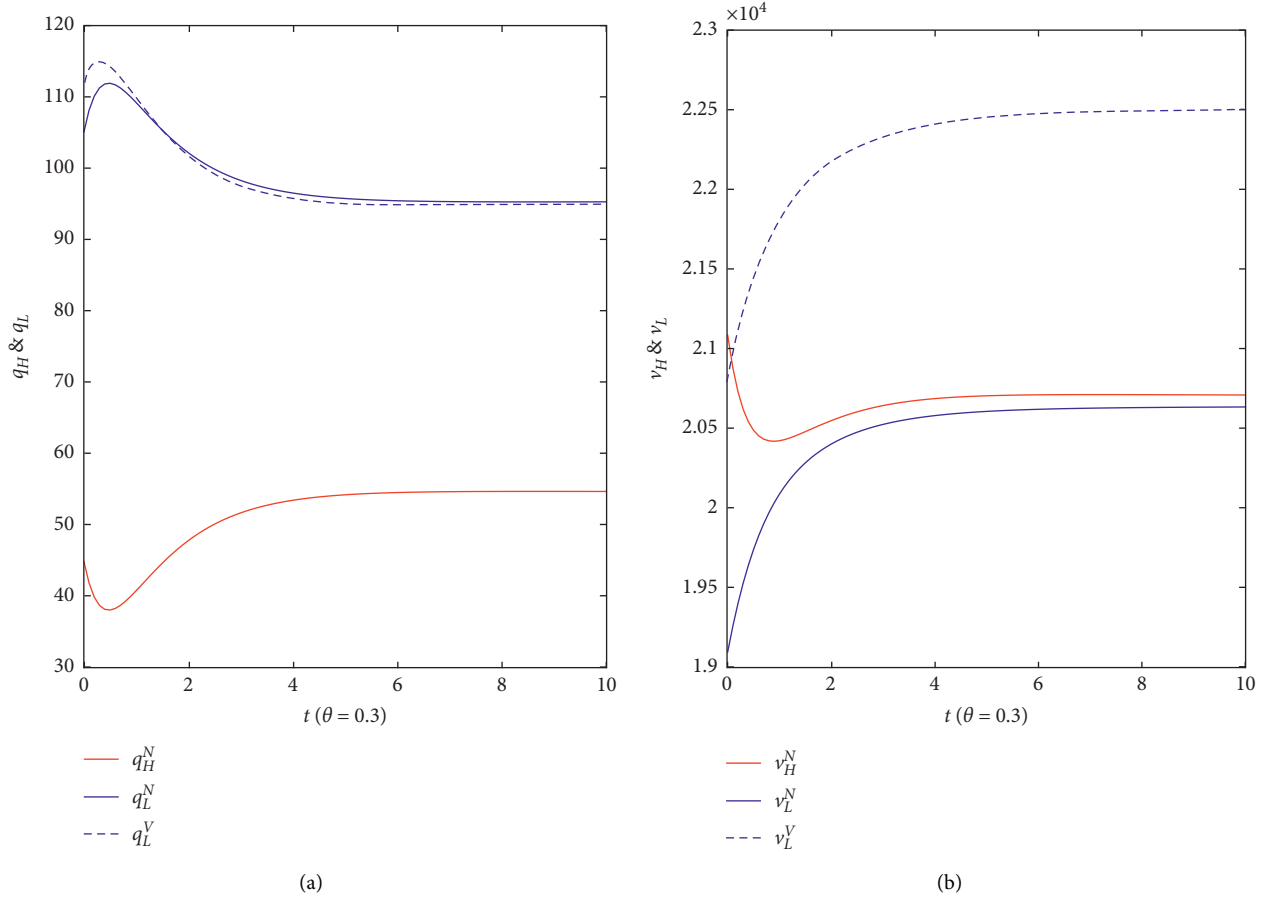


FIGURE 3: (a) Comparison of dynamic sales of the free-riding manufacturer and the green manufacturer under different modes ($\theta=0.3$). (b) Comparison of dynamic profits of the free-riding manufacturer and the green manufacturer under different modes ($\theta=0.3$).

emissions of free-riders are seriously affected, which is consistent with the conclusion of Section 5.1, that is, the emissions of free-riders in the cooperation mode are higher than those in the noncooperation mode.

5.3. Effects of Spillover and Cooperation on the Green Supply Chain Emission and Profit. The impact of cooperation on green supply chain emission reduction and profit is analyzed by comparing the trajectory of emissions and profits before and after the green supply chain cooperation. Let

$$\begin{aligned} \Delta e_G(t) &= e_H^V(t) + e_S^V(t) - e_H^N(t) - e_S^N(t), \\ \Delta V_G(t) &= V_G(t) - V_H^N(t) - V_S^N(t). \end{aligned} \quad (25)$$

$$\Delta e_G^* = \frac{\beta\eta^3\varphi_H g + \beta\eta\varphi_H(\eta g + \eta r - \alpha gr) + \alpha g\varphi_S r(1 - \alpha)(\eta + s) + \beta\eta g\varphi_H r(1 - \beta)}{\eta^2\varphi_H\varphi_S r(\eta + r)}. \quad (26)$$

$\Delta e_G^*(t) > 0$ and $\partial\Delta e_G^*/\partial\beta > 0$ can be intuitively judged, that is, the larger the extent of the technology spillover of green suppliers, the higher the green supply chain emissions after cooperation.

Figure 6 shows that the emissions under the noncooperation model are higher than that under the cooperation model. It will stabilize gradually in about 10 periods, and green suppliers will increase their emissions after cooperation. Figure 7 shows that the degree of technology spillover of green manufacturers and the emissions of the green supply chain after cooperation are inversely proportional. This is the result obtained on the basic parameters set in Table 2, simplified and resolved:

Based on an analysis, the stable emission reduction is closely related to the innovation efforts. Based on earlier conclusion, the innovation efforts of green suppliers under the cooperation mode are observed to have

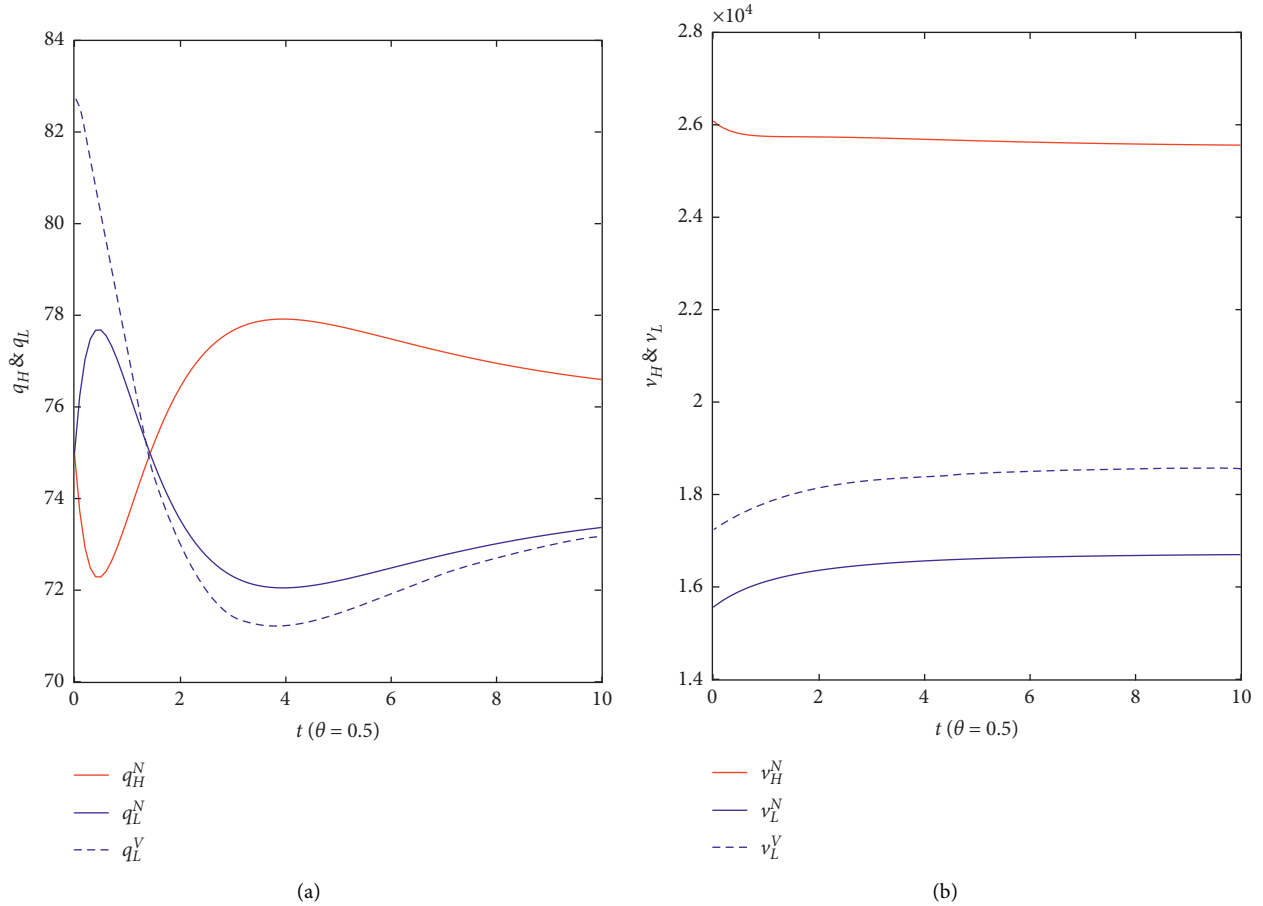


FIGURE 4: (a) Comparison of dynamic sales of the free-riding manufacturer and the green manufacturer under different modes ($\theta = 0.5$). (b) Comparison of dynamic profits of the free-riding manufacturer and the green manufacturer under different modes ($\theta = 0.5$).

dropped sharply, and the increased innovation efforts of green manufacturers are not enough to offset the impact of the sharp reduction of supplier innovation efforts, and the low level of technological spillovers does not favor green suppliers achieving innovation results from manufacturers, so it is reflected in the increase in emissions after cooperation innovation. It is concluded that the existence of green supply chain innovation cooperation with shared suppliers does not reduce emission, and technological spillovers can well compensate for the gap in emissions.

As shown in Figures 8(a) and 8(b), a comparison of the changes in profit of the green supply chain before and after cooperation shows that gradually the profit is greater than that in the noncooperation model and the gap is gradually widened, and finally stabilizes. Technology spillovers from green manufacturers will widen this gap, while that from green suppliers will narrow this gap. This indicates that, in the case of asymmetric technology spillovers, the innovative cooperation model is more inclined to green manufacturers with high technology spillovers and green suppliers with low technology spillovers. When $\alpha = 1$ and $\beta = 0$, a research cartel comprising green manufacturers was formed, that

is, a green supply chain formed a cartel with perfect technology spillovers from manufacturers. This is the organizational form adopted by cooperation innovation trends, which is slightly different from the conclusions by Shibata [30] and Ge et al. [9] on symmetric vertical and horizontal technology spillovers. The research on innovation cooperation on the different roles of technology spillover is extensive.

A comparative analysis of the marginal profit of unit emissions shows that, in the two models of the optimal value function of the supply chain profit, the marginal profit of the emissions of green manufacturers and free-riding manufacturers is equal, while the margin profit of the green suppliers increases ($b_1 < c_3$). It shows that the effect of cooperation and noncooperation on the emissions of the two manufacturers remains unchanged, but under the innovative cooperation model, green suppliers have reduced the profit loss per unit of emissions under the innovative cooperation model. There are fewer constraints, which has reduced innovation efforts and used emissions in exchange for profits. Therefore, green suppliers are more inclined to adopt innovative cooperation models, which is consistent with the conclusion of Dai et al. [25].

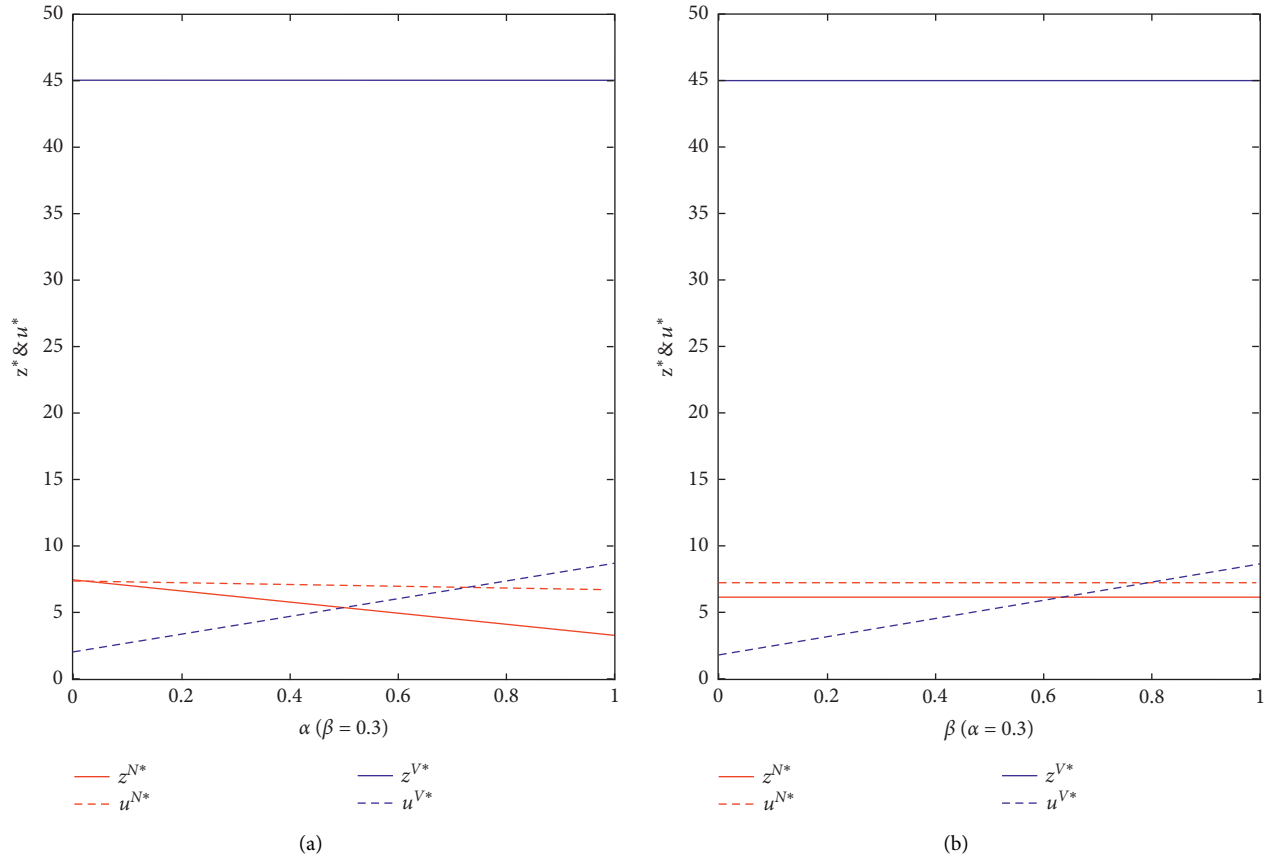


FIGURE 5: (a) The impact of cooperation models and technology spillovers α on optimal innovation decisions. (b) The impact of cooperation models and technology spillovers β on optimal innovation decisions.

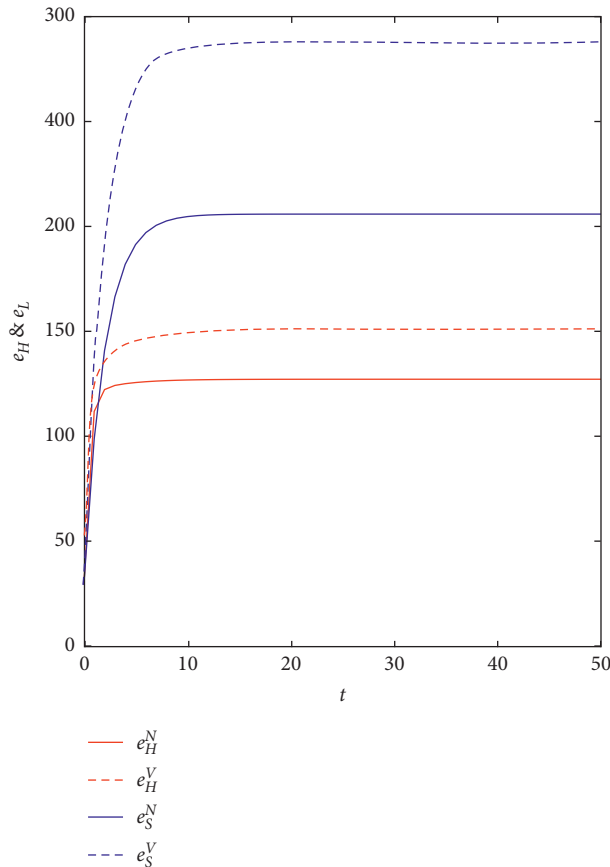


FIGURE 6: Emission trajectories of green manufacturers and suppliers in two modes.

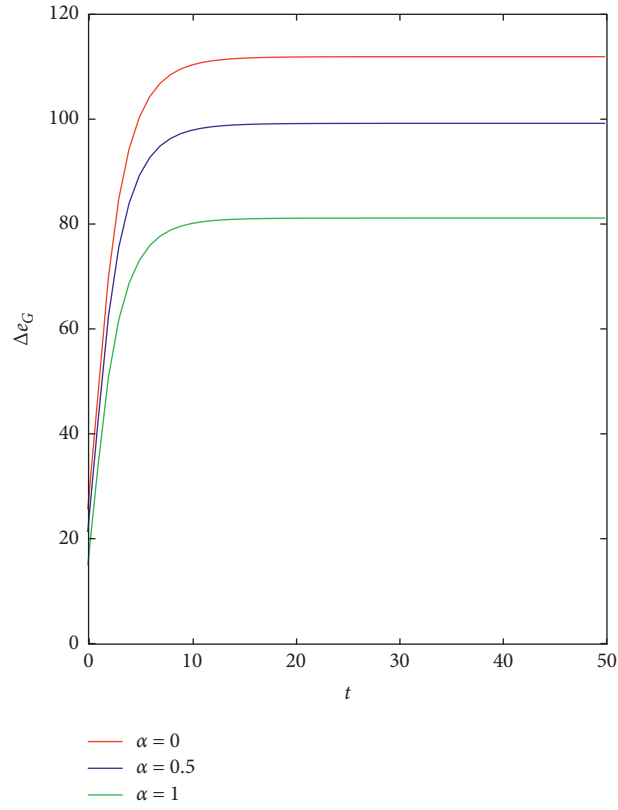


FIGURE 7: Trajectories of $\Delta e_G(t)$.

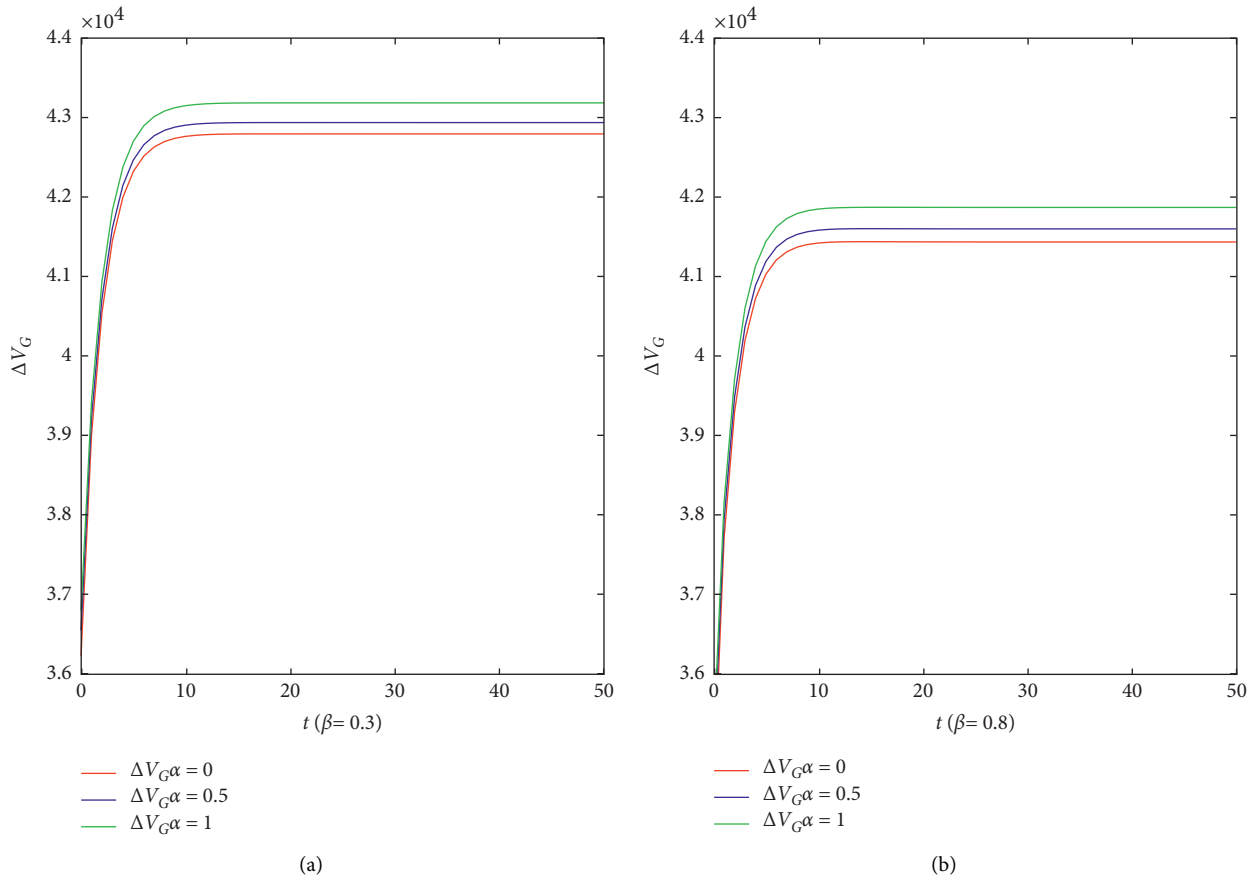


FIGURE 8: (a) Trajectories of $\Delta V_G(t)$ ($\beta = 0.3$). (b) Trajectories of $\Delta V_G(t)$ ($\beta = 0.8$).

6. Conclusion and Discussion

Given those market players that do not implement green strategies, technology spillovers allow such competitors to enjoy innovations at no cost, which will not only disincentive innovation but also weaken the green innovation effect of the enterprise. Meanwhile, the green innovation behavior of the upstream monopoly enterprises will also be passed on to the downstream enterprises, in which case the company's green innovation decision becomes particularly complicated. When enterprises attempt to reduce emissions in the production process through green innovation, two issues must be considered: (1) the impact of green innovation enterprise's technology spillovers on the emissions of different entities and (2) the impact of green innovation efforts on emissions is dynamic, and the innovation efforts the enterprise at various times have different adjustments to emissions. The present study examined the green innovation decision-making problem of green supply chain enterprises under the green innovation noncooperation and cooperation modes when there is an asymmetric technology spillover in the "one-to-two" supply chain structure and obtained the optimal solution and steady-state equilibrium by the differential game model.

The main conclusions are as follows:

- (1) The optimal green innovation efforts of green suppliers and green manufacturers are independent of time. Under the noncooperation mode, the optimal innovation efforts of green suppliers ignore technology spillovers and that of green manufacturers are independent of their technology spillover; the greater the technology spillover, the smaller the gap between emissions from free-riding manufacturers.
- (2) Under the noncooperation model, free-riding manufacturers have the incentive to change to green manufacturers, which cannot only reduce emissions but also increase profits. Under the cooperation model, different choices exist under different initial market forces. When free-riding manufacturers have market advantages, they still have greater profits and will not choose green innovation; when the initial market strengths of the two types of manufacturers are equal, nongreen manufacturers are motivated to change to green manufacturers.
- (3) Under the cooperation model, green manufacturers will increase green innovation efforts, but green suppliers will significantly reduce green innovation efforts, resulting in increased emissions, and lower technological spillovers of green manufacturers will exacerbate this trend. However, the profit of the green supply chain has been greatly improved, and the technology spillovers of green manufacturers have a positive impact on profits, while that of green suppliers have a negative impact.

Existing literature on green innovation always considers profit as the only positive measure, and the impact on the direct results of innovation is always ignored. Yenipazarli

[14] defines the role of eco-efficiency in improving the unit product environmental impact and reduction of production costs. The established objective function only reflects the environmental impact on the sales volume. Chen et al. [33] also only reflect the green innovation efforts on the sales volume. Such assumptions are generally that innovation cannot be distinguished. Therefore, when green innovation is examined, the effect of reducing emissions or the negative impact on the environment must also be considered. The present study draws on the practices of Feichtinger et al. [34] and Ni et al. [35], uses differential game models, and uses emissions as state variables to study the dynamic impact of green supply chain enterprises' innovation decisions and technology spillovers on them to be more targeted to provide green innovation suggestions for enterprises.

This study has certain limitations. It is assumed that green suppliers have the same technology spillovers for both types of manufacturers, and that green manufacturers have the same vertical and horizontal technical spillovers. In fact, the extent of spillover is affected by the company's technical strength, learning ability, or intellectual property protection policies. Therefore, it is necessary to examine the impact of different spillover levels on the stability of innovation cooperation and innovation decisions. In addition, from the perspective of green management in the entire life cycle of the supply chain, green innovation can also be manifested as cost savings (e.g., saving water and energy in green process innovation). However, considering the study focus and simplicity of the solution, the impact on cost is not considered separately. Our analytical framework can be generalized into investigating cooperation among the manufacturer and other stakeholders, such as the retailer, customer, or government. Also, the social welfare and other forms of green innovation should be considered with a holistic modeling framework in the future study.

Data Availability

The data used to support the findings of this study are included within the article.

Disclosure

This article belongs to the Special section on "Complexity in Economics and Business."

Conflicts of Interest

The authors declare that there are no conflicts of interest regarding the publication of this paper.

Authors' Contributions

All authors contributed equally to this work.

Acknowledgments

The paper was funded by the National Key Research and Development Program of China (Grant no. 2016YFA0602500), National Natural Science Foundation of

China (Grant no. 71810107004), Social Sciences project of the Ministry of Education (Grant no. 20YJC790158), and First-class Discipline Construction Project of Central University of Finance and Economics “Research on the theoretical innovation of public sector strategy and performance management in the new era” (Grant no. CUFE2018-005).

References

- [1] A. Goonetilleke, T. Yigitcanlar, P. Egodawatta, and G. Ayoko, *Sustainable Urban Water Environment: Climate, Pollution and Adaptation*, Edward Elgar Publishing, Cheltenham, UK, 2014.
- [2] W. Wu, Y. Liu, Q. Zhang, and B. Yu, “How innovative knowledge assets and firm transparency affect sustainability-friendly practices,” *Journal of Cleaner Production*, vol. 229, pp. 32–43, 2019.
- [3] R. Arbolino, F. Carlucci, L. De Simone, G. Ioppolo, and T. Yigitcanlar, “The policy diffusion of environmental performance in the European countries,” *Ecological Indicators*, vol. 89, no. JUN, pp. 130–138, 2018.
- [4] V. Bosetti, C. Carraro, E. Massetti, and M. Tavoni, “International energy R&D spillovers and the economics of greenhouse gas atmospheric stabilization,” *Energy Economics*, vol. 30, no. 6, pp. 2912–2929, 2008.
- [5] J. Horbach, V. Oltra, and J. Belin, “Determinants and specificities of eco-innovations compared to other innovations—an econometric analysis for the French and German industry based on the community innovation survey,” *Industry and Innovation*, vol. 20, Article ID 833375, 2013.
- [6] P. del Río González, “Analysing the factors influencing clean technology adoption: a study of the Spanish pulp and paper industry,” *Business Strategy and the Environment*, vol. 14, no. 1, pp. 20–37, 2005.
- [7] C. Ghisetti, A. Marzucchi, and S. Montesor, “The open eco-innovation mode. An empirical investigation of eleven European countries,” *Research Policy*, vol. 44, no. 5, pp. 1080–1093, 2015.
- [8] G. Cainelli, V. De Marchi, and R. Grandinetti, “Does the development of environmental innovation require different resources? Evidence from Spanish manufacturing firms,” *Journal of Cleaner Production*, vol. 94, pp. 211–220, 2015.
- [9] Z. Ge, Q. Hu, and Y. Xia, “Firms’ R&D cooperation behavior in a supply chain,” *Production and Operations Management*, vol. 23, no. 4, pp. 599–609, 2014.
- [10] J. Horbach, “Determinants of environmental innovation—New evidence from German panel data sources,” *Research Policy*, vol. 37, no. 1, pp. 163–173, 2008.
- [11] J. Cañón-de-Francia, C. Garcés-Ayerbe, and M. Ramírez-Alesón, “Are more innovative firms less vulnerable to new environmental regulation?” *Environmental and Resource Economics*, vol. 36, no. 3, pp. 295–311, 2007.
- [12] D. Kammerer, “The effects of customer benefit and regulation on environmental product innovation: empirical evidence from appliance manufacturers in Germany,” *Ecological Economics*, vol. 68, no. 8–9, pp. 2285–2295, 2009.
- [13] L. Aldieri, F. Carlucci, C. P. Vinci, and T. Yigitcanlar, “Environmental innovation, knowledge spillovers and policy implications: a systematic review of the economic effects literature,” *Journal of Cleaner Production*, vol. 239, Article ID 118051, 2019.
- [14] A. Yenipazarli, “To collaborate or not to collaborate: prompting upstream eco-efficient innovation in a supply chain,” *European Journal of Operational Research*, vol. 260, no. 2, pp. 571–587, 2017.
- [15] F. de Miranda Ribeiro and I. Kruglianskas, “Critical factors for environmental regulation change management: evidences from an extended producer responsibility case study,” *Journal of Cleaner Production*, vol. 246, pp. 1–14, 2020.
- [16] R. Cappelli, D. Czarnitzki, and K. Kraft, “Sources of spillovers for imitation and innovation,” *Research Policy*, vol. 43, no. 1, pp. 115–120, 2014.
- [17] R. Cellini and L. Lambertini, “Advertising in a differential oligopoly game,” *Journal of Optimization Theory and Applications*, vol. 116, no. 1, pp. 61–81, 2003.
- [18] F. Liu, W.-L. Chen, and D.-B. Fang, “Optimal coordination strategy of dynamic supply chain based on cooperative stochastic differential game model under uncertain conditions,” *Applied Soft Computing*, vol. 56, no. 1, pp. 669–683, 2017.
- [19] Y. Zu, L. Chen, and Y. Fan, “Research on low-carbon strategies in supply chain with environmental regulations based on differential game,” *Journal of Cleaner Production*, vol. 177, no. 6, pp. 527–546, 2018.
- [20] V.-H. Lee, K.-B. Ooi, A. Y.-L. Chong, and C. Seow, “Creating technological innovation via green supply chain management: an empirical analysis,” *Expert Systems With Applications*, vol. 41, no. 16, pp. 6983–6994, 2014.
- [21] V. De Marchi, “Environmental innovation and R&D cooperation: empirical evidence from Spanish manufacturing firms,” *Research Policy*, vol. 41, no. 3, pp. 614–623, 2012.
- [22] C. A. Geffen and S. Rothenberg, “Suppliers and environmental innovation,” *International Journal of Operations & Production Management*, vol. 20, no. 2, pp. 166–186, 2000.
- [23] A. Meyer and P. Hohmann, “Other thoughts; other results? Remei’s bioRe organic cotton on its way to the mass market,” *Greener Management International*, vol. 31, pp. 59–70, 2000.
- [24] M. Goldbach, “Coordinating interaction in supply chains—the example of greening textile chains,” *Strategy and Organization in Supply Chains*, pp. 47–64, Physica-Verlag, Heidelberg, Germany, 2003.
- [25] R. Dai, J. Zhang, and W. Tang, “Cartelization or Cost-sharing? Comparison of cooperation modes in a green supply chain,” *Journal of Cleaner Production*, vol. 156, pp. 159–173, 2017.
- [26] A. Ishii, “Cooperative R&D between vertically related firms with spillovers,” *International Journal of Industrial Organization*, vol. 22, no. 8–9, pp. 1213–1235, 2004.
- [27] B. Hu, M. Hu, and Y. Yang, “Open or closed? Technology sharing, supplier investment, and competition,” *Manufacturing & Service Operations Management*, vol. 19, no. 1, pp. 132–149, 2017.
- [28] C. D’Aspremont and A. Jacquemin, “Cooperative and non-cooperative R&D in duopoly with spillovers,” *American Economic Review*, vol. 78, no. 5, pp. 1133–1137, 1988.
- [29] G. Steurs, “Inter-industry R&D spillovers: what difference do they make?” *International Journal of Industrial Organization*, vol. 13, no. 2, pp. 249–276, 1995.
- [30] T. Shibata, “Market structure and R&D investment spillovers,” *Economic Modelling*, vol. 43, pp. 321–329, 2014.
- [31] Y. Wang, Y. Xiao, and N. Yang, “Improving reliability of a shared supplier with competition and spillovers,” *European Journal of Operational Research*, vol. 236, no. 2, pp. 499–510, 2014.
- [32] L. Lambertini, J. Poyago-Theotoky, and A. Tampieri, “Cournot competition and “green” innovation: an inverted-U relationship,” *Energy Economics*, vol. 68, pp. 116–123, 2017.
- [33] X. Chen, X. Wang, and M. Zhou, “Firms’ green R&D cooperation behaviour in a supply chain: technological spillover,

power and coordination,” *International Journal of Production Economics*, vol. 218, pp. 118–134, 2019.

- [34] G. Feichtinger, L. Lambertini, G. Leitmann, and S. Wrzaczek, “R&D for green technologies in a dynamic oligopoly: schumpeter, arrow and inverted-U’s,” *European Journal of Operational Research*, vol. 249, no. 3, pp. 1131–1138, 2016.
- [35] J. Ni, H. Huang, P. Wang, and W. Zhou, “Capacity investment and green R&D in a dynamic oligopoly under the potential shift in environmental damage,” *Economic Modelling*, vol. 88, pp. 312–319, 2020.

Research Article

Habit or Utility: A Key Choice Point in Promoting the Adoption of Telehealth in China

Yun Fan ^{1,2}, Sifeng Liu,¹ Jun Liu,² Saad Ahmed Javed ³, and Zhigeng Fang ¹

¹College of Economics and Management, Nanjing University of Aeronautics and Astronautics, Nanjing 211106, China

²Nantong University, Nantong 226019, China

³Institute for Grey Systems and Decision Sciences, GreySys Foundation, Lahore, Pakistan

Correspondence should be addressed to Zhigeng Fang; zhigengfang@163.com

Received 25 March 2020; Revised 15 May 2020; Accepted 2 June 2020; Published 4 July 2020

Guest Editor: Lei Xie

Copyright © 2020 Yun Fan et al. This is an open access article distributed under the Creative Commons Attribution License, which permits unrestricted use, distribution, and reproduction in any medium, provided the original work is properly cited.

Telehealth, as an indispensable means of technical support in the Healthy China Strategy, currently has less than 20 percent adoption rate in China despite a great deal of government policies and investments. In the current study, to analyse the influencing factors behind doctors' and patients' adoption of telehealth, an asymmetric dynamic evolutionary game model of doctor-patient behaviour selection was established. Based on the model solution, the evolutionarily stable strategies that emerge in different situations were analysed. The results show that it is difficult for the adoption of telehealth in China to keep pace with coverage due to the "dual low" nature of telehealth: both doctors' utility from telehealth and patients' telehealth cost threshold are too low to incentivize adoption. The strategy to promote the adoption of telehealth in China should include providing adequate training for doctors and patients on the use of telehealth technology, rewarding doctors who provide telehealth services and raising the threshold cost of patient's telehealth adoption.

1. Introduction

Telehealth is the provision of medical services remotely through the internet via mobile phones, smartphones, computers, tablets, or other wireless mobile devices [1, 2]. Telehealth can overcome the limitations of geographical distance and allow the provision of professional technical guidance in situations characterized by a shortage of doctors. It can be used to educate local doctors with limited case exposure and reduce patients' medical expenses by reducing their travel burden. At the same time, internet technology can help link patient data and examination results, thereby avoiding repeated examinations of patients and saving medical resources [3–6].

According to a World Health Organization (WHO) survey in 2015, with the development of information and communication technologies (ICT) and the popularization of mobile Internet technology, approximately 3/4 ($n = 51$; 73%) of countries that participated in the survey reported

including telehealth as a policy or strategic goal [7, 8]. The United States government sees telehealth as an important measure to promote low-cost, high-quality medical system reform [2]. The British and Japanese governments have also adopted telehealth (virtual visits) as part of their health care reforms [9]. The Chinese government has included telehealth in its Healthy China Strategy and expects to achieve win-win outcomes for hospitals and patients in both urban and rural areas through telehealth [10, 11]. Although countries are eagerly developing telehealth, the actual adoption rate of this service is uneven. In 2016, 61 percent of medical institutions and 40 to 50 percent of hospitals in the United States used some form of telehealth [7]. A survey across nine Latin American nations during the same period found that the use of telehealth ranged from 25 percent of hospitals in Colombia to 65 percent of hospitals in Chile [12]. In China, the utilization rate of telehealth was still lower than 20 percent in 2019 [13].

With shortages of doctors and unbalanced medical and health resources in urban and rural areas, the health field in

China is facing new challenges, such as an ageing population and changes in the disease spectrum [14–16]. As an essential strategy to break the deadlock, the Chinese government has fully deployed telehealth while completing the “leap-forward” development of the country’s communications infrastructure [17, 18]. At present, investment in telehealth in China ranks second in the world, and telehealth has been initiated in all first-class hospitals, covering all poor counties [9, 19]. By the end of 2020, all primary medical and health institutions in the medical consortium should be covered [20]. However, despite its inherent advantages, the adoption of telehealth is still not high, although the Chinese government invests a great deal in telehealth policies and funds, with the most obvious challenge being the inability or reluctance of doctors and patients to adopt telehealth.

The literature indicates that telehealth is a complex system [12]. Whether telehealth can be used effectively as an information technology depends on the acceptance and use of this technology by users [21, 22]. The factors influencing the acceptability of telehealth to doctors and patients, primary users, and stakeholders of telehealth, have been widely studied in developed countries and some developing countries by using various theoretical models [23]. However, in countries with a strong traditional medical culture, such as China, the main barrier is the conflict between doctors’ and patients’ established habits and telehealth objectives [5, 24]. The literature that considers the behaviour and evolution of doctor and patient adoption of telehealth from a habit and utility perspective is negligible. The underlying reason doctors and patients have not adopted telehealth is that their individual estimates of telehealth utility are lower than their estimates of the utility of habitual in-person visits. For individuals, due to constraints such as imperfect information, the choice of not adopting telehealth is superficially rational but in fact irrational from the perspective of collective rationality [25, 26]. Therefore, there is a dire need to study the key factors that affect the adoption of telehealth among doctors and patients, specifically with reference to modes of telehealth and in-person visits, the utility of these visit modes, and how doctors and patients choose and evolve between these modes. To this end, evolutionary game theory provides a suitable approach, combining game theory and dynamic evolution to study the stable structure of a game system and the behavioural strategy selection process of a subject in the process of evolution by introducing a dynamic mechanism [27–29]. In this study, we constructed an evolutionary model of doctor-patient behaviour choice to evaluate how to improve the utility of telehealth for doctors and patients, making greater use of the telehealth mode relative to the in-person mode so that doctors and patients can break habits and become telehealth users.

2. Theoretical Background

The existing literature has explored the factors that influence the adoption of telehealth by doctors and patients from different perspectives. Many scholars have approached this question from the perspective of information technology acceptance. Dünnebeil et al. and Liu et al. used the

technology acceptance model (TAM) to study the acceptance of medical information systems by doctors or patients in terms of both perceived ease of use and perceived usefulness [30, 31]. Some scholars have extended the TAM model. Tsai integrated the TAM model, social capital theory, and social cognition theory to develop a comprehensive behavioural model for analysing the telehealth usage intention of elderly people [32]. Rho et al. developed the Telemedicine Service Acceptance (TSA) model based on the TAM model, emphasizing the importance of incentives, and verified the effectiveness of TSA in explaining doctors’ acceptance of telehealth services [33]. Based on the TAM model and combined with contract theory, Wang studied the influencing factors of patient telehealth service quality, price, waiting time, transportation cost, and so on [34]. Zhou et al. used an extended TAM model to verify that medical affordability, waiting time, and information quality are decisive variables affecting acceptance of telehealth among elderly people [9].

In general, the TAM model focuses on extrinsic motivation, such as the user’s perceived ease of use, and involves less consideration of intrinsic motivation [34]. For this reason, Venkatesh et al. integrated eight user acceptance models, including TAM, the motivational model (MM) and the theory of reasoned action (TRA), etc., and constructed their unified theory of acceptance and use of technology (UTAUT) with strong explanatory power [35]. According to the UTAUT, individuals’ behavioural intentions in using technology are jointly determined by performance expectancy, effort expectancy, social influence, and facilitating conditions [36]. Diño et al. and Adenuga et al. used the UTAUT model to determine the effectiveness of behavioural intention for telehealth use among elderly people and doctors and revealed the importance of doctors’ motivation [21, 23].

From the perspective of game theory, Rajan et al. combined a nonatomic game with a queuing model and studied the speed-quality trade-off of medical operations by analysing the doctor’s utility (price, equilibrium arrival rate, etc.) and the patient’s utility (reward from seeking treatment, congestion cost, payment, etc.) [37]. After constructing an evolutionary model of a game between hospitals and patients and analysing factors such as medical expenses, reimbursement ratio of medical insurance, and hospital costs, Wang et al. and Zhan et al. highlighted the importance of improving the utility of patients’ telehealth services and the reimbursement ratio of medical insurance [38, 39].

In light of this literature review and empirical observations, this study underscores that resistance to telehealth is common. Doctors are accustomed to face-to-face visits, and their refusal to use telehealth does not affect their income. Instead, adoption of telehealth consumes their energy and resources, as they need to spend time and energy familiarizing themselves with the new system [5, 22, 40]. Therefore, many scholars have emphasized the importance of motivating doctors to use telehealth [7, 23, 33]. Ordinary patients, influenced by traditional Chinese medicine’s concepts of “looking, smelling, questioning, and cutting,” are used to in-person visits, as intangible telehealth appears

less effective than an in-person visit; moreover, the habitual in-person model also has lower fees [5, 22, 40].

According to the literature, the factors influencing doctors' and patients' adoption of telehealth are summarized in Table 1.

As seen from Table 1, the reward from visits, travel burden, payment, waiting cost, perceived ease of use, and perceived usefulness are the main factors influencing patients' adoption of telehealth. Remuneration, incentives, perceived ease of use, and perceived usefulness are the main factors influencing doctors' adoption of telehealth. Some of these factors, such as perceived ease of use and perceived usefulness, relate to the user's intention to use telehealth systems rather than the utility from actual adoption [32]. To convert intentionality into the utility of adopting telehealth, the cost of patient's telehealth learning and the fixed cost of related equipment are introduced to reflect perceived ease of use and perceived usefulness, because patients are less likely to learn to use telehealth if they are unwilling to avail themselves of telehealth services. Once patients begin to receive telehealth services, they will invest their efforts in learning to verify the ease of use and usefulness of telehealth; this is patients' learning cost of telehealth. When patients find telehealth easy to use and useful, they will take action to pay for the network connection, cameras, or other facilities required for the use of telehealth services, as well as the cost of operation, and thus bear certain amortized costs. Similarly, since Chinese doctors must provide telehealth services due to an administrative order, the usefulness of telehealth has spread among doctors, whereas the government or the hospital bears the cost of related equipment, and thus doctors' learning cost of telehealth is used to reflect the perceived ease of use of the service [19]. Therefore, in this article, the reward from visits, travel burden, payment, telehealth learning cost, amortized costs, and waiting cost are taken as the main influencing factors behind patients' adoption of telehealth, and variables including remuneration, telehealth learning cost, and incentives are taken as the main influencing factors behind doctors' adoption of telehealth.

3. Methods

3.1. Analysis Framework. The basic idea of evolutionary game theory is that in a group of a certain size, both sides of the game are driven by bounded rationality, and it is impossible to find the optimal equilibrium point in every game. Instead, through repeated games, that is, continually imitating the dominant strategies of themselves and others in the past, all players will tend toward a particular stable strategy through long-term improvement [27–29].

In this study, whether doctors and patients adopt telehealth in practice can be regarded as the result of a game between doctors and patients, and the two sides of the game do not benefit symmetrically from the adoption, so it is an asymmetric evolutionary game. In addition, due to this information asymmetry and the bounded rationality of both sides of the game, it is difficult for doctors and patients to know whether their decisions are in line with the

requirements of profit maximization when they make their decisions. Instead, they continually improve by imitating their own and others' dominant strategies in the past. Furthermore, strategy improvements are not adopted by all players at the same time but by gradual adjustment based on differences in the bounded rationality levels of the players. The rate of strategy adjustment can be expressed by the evolutionary dynamic equation of biological evolution—the gene replication dynamic formula [41]. Therefore, the analysis framework of the current study is an asymmetric replication dynamic evolutionary game, that is, a game in which a member is randomly selected from the two groups of doctors and patients repeatedly to assess the behavioural selection.

3.2. Strategy Combinations. Through long-term observation of the behavioural choices of doctors and patients during visits, we summarized four strategy combinations: (1) doctors and patients did not use telehealth but used in-person visits; (2) patients used telehealth, but doctors did not; thus although in-person visits were eventually used, patients paid the learning cost of using telehealth; (3) doctors used telehealth, but patients did not, and although in-person visits were finally used, doctors paid the learning cost of using telehealth; (4) doctors and patients all adopted telehealth, but not all diagnoses and treatments, such as laboratory or in-person clinical examinations, could be performed through telehealth. Therefore, in practice, a combination of both telehealth and in-person visits was mostly adopted. At this point, doctors paid the learning cost of using telehealth, and patients paid both the learning cost and the amortized cost of using telehealth.

3.3. Payoff Matrix of the Doctor-Patient Game. Let i represent in-person visits and t telehealth visits.

In strategy one, when the government set the price per visit based on the level of hospitals and doctors, the utility of each doctor was related to the number of patients treated per unit of time, that is, the doctor's service rate and the commission on each visit fee. The doctor's utility function can be expressed as

$$R_i = \gamma_i P_i \mu. \quad (1)$$

Each patient's utility comprised a reward from the visit, a travel burden, a payment, and a waiting cost. The most significant advantage of telehealth is that patients do not need to travel. To simulate the travel burden of face-to-face visits, we modelled the travel burden $\delta B_{(d)}$ as a function of the distance d between patients and doctors. δ is a random variable related to traffic congestion. The lower the amount of traffic, the smaller is the value of δ , $0 < \delta < 1$. The patient's actual payment is related to the medical insurance rate and the prices charged by the government. The patient's utility function can be expressed as

$$\psi_i = m_i - \delta B_{(d)} - \beta_i P_i - E_i. \quad (2)$$

In strategy two, patients paid the learning cost of using telehealth, and in strategy three, doctors paid the learning

TABLE 1: Factors influencing the adoption of telehealth by doctors and patients.

Author(s) (year)	Influencing factors	Object of study	Model/theory
Dunnebeil et al. (2012) [30], Liu et al. (2013) [31]	Perceived ease of use, perceived usefulness	Doctors/ patients	TAM
Tsai (2014) [32]	Perceived ease of use, perceived usefulness social capital theory, social cognition theory	Elderly people	
Rho et al. (2014) [33]	Perceived incentives, clinical factors, individual factors, perceived ease of use, perceived usefulness	Doctors	Extended TAM
Wang (2016) [34]	Service quality, price, waiting time, transportation cost, etc.	Patients	
Zhou et al. (2019) [9]	Satisfaction with medical services (MSS) (affordability, waiting time), perceived ease of use, information quality	Elderly people	
Diño and de Guzman (2015) [21]	Performance expectancy, effort expectancy, social influence	Elderly people	
Adenuga et al. (2017) [23]	Suitable incentives, performance expectancy, effort expectancy, facilitating condition	Doctors	UTAUT
Wang et al. (2015) [38], Zhan et al. (2017) [39]	Utility of patients' telehealth services, medical expenses, reimbursement ratio of medical insurance, hospital costs, etc.	Hospitals and patients	
Rajan et al. (2019) [37]	Doctor's utility (price, equilibrium arrival rate, etc.), patient's utility (reward from seeking treatment, congestion cost, payment, etc.)	Doctors and patients	Game theory
Xue and Liang (2007) [22], Combi et al. (2016) [5]	Doctor: face-to-face visit habits, extra cost of telehealth, etc. Patient: cost of telehealth, reimbursement, etc.	Doctors and patients	
U.S. Department of Health and Human Services (2016) [7, 22]	Payment, especially more comprehensive coverage by Medicare	Policies	Literature review, survey, report, etc.
Scott Kruse et al. (2018) [40]	Technically challenged staff, resistance to change, cost, reimbursement, etc.	Doctors and patients	

cost of using telehealth. Strategy four, as mentioned earlier, involved the combination of telehealth and in-person visits and was often used in practice. Assuming that the clinical feasibility of telehealth is α , $\alpha \in (0, 1)$, the doctor's utility is the sum of the utility of telehealth and in-person visits. At this time, the doctor's utility function can be expressed as

$$R_t = \alpha\gamma_t p_t \mu + (1 - \alpha)\gamma_i p_i \mu - S_q. \quad (3)$$

Similarly, the patient's utility is the sum of the utility in the two modes. As an advantage of telehealth, patients do not have to travel, so their travel burden is zero. At the same time, patients need to bear the learning cost and amortized cost of using telehealth. The patient's utility function can be expressed as

$$\begin{aligned} \psi_t = & \alpha m_t + (1 - \alpha)(m_i - \delta B_{(d)}) - S_v - C \\ & - \alpha\beta_t p_t - (1 - \alpha)\beta_i p_i - \alpha E_t - (1 - \alpha)E_i. \end{aligned} \quad (4)$$

To study whether to reward doctors for using telehealth, we assumed that doctors would be rewarded for their use of telehealth regardless of whether patients agreed or disagreed to adopt the service. According to equations (1)–(4), we constructed the benefits of the four strategy combinations. The payoff matrix of the two players is shown in Table 2, and the main parameters and their meanings are shown in Table 3.

3.4. Replication Dynamic Equation of the Doctor-Patient Game. It is assumed that the proportion of doctors in the “adoption” game party was x ($0 \leq x \leq 1$), and there were $1 - x$ doctors in the “no adoption” game party. Similarly, the proportion of patients in the “adoption” game party was

y ($0 \leq y \leq 1$), and there were $1 - y$ patients in the “no adoption” game party. According to evolutionary game theory, when the profit of a strategy is higher than the average profit of a mixed strategy, this strategy will develop in the group and be more likely to be adopted. The replication dynamic equation is a dynamic differential equation that describes the frequency at which a particular strategy is adopted in a population [28]. Let U_{11} represent the benefits of doctors choosing to adopt the telehealth strategy, U_{12} the benefits of doctors choosing not to adopt the telehealth strategy, and \bar{U}_1 the average benefits of doctors:

$$\begin{aligned} U_{11} = & y[\alpha\gamma_t p_t \mu + (1 - \alpha)\gamma_i p_i \mu - S_q + w] \\ & + (1 - y)(\gamma_i p_i \mu - S_q + w) \\ = & y\alpha\gamma_t p_t \mu - y\alpha\gamma_i p_i \mu + \gamma_i p_i \mu - S_q + w, \end{aligned} \quad (5)$$

$$\begin{aligned} U_{12} = & y(\gamma_i p_i \mu) + (1 - y)(\gamma_i p_i \mu) \\ = & \gamma_i p_i \mu, \end{aligned} \quad (6)$$

$$\begin{aligned} \bar{U}_1 = & xU_{11} + (1 - x)U_{12} \\ = & x(\alpha\gamma_t p_t \mu - \alpha\gamma_i p_i \mu + \gamma_i p_i \mu - S_q + w) \\ & + (1 - x)(\gamma_i p_i \mu) \\ = & x\alpha\gamma_t p_t \mu - x\alpha\gamma_i p_i \mu - xS_q + xw + \gamma_i p_i \mu. \end{aligned} \quad (7)$$

Let U_{21} represent the benefits of patients choosing to adopt the telehealth strategy, U_{22} the benefits of patients choosing not to adopt the telehealth strategy, and \bar{U}_2 the average benefits of patients:

TABLE 2: Payoff matrix of the doctor-patient game.

		Game party II : patient	
		Adoption	No adoption
Game party I: doctor	Adoption	$\alpha\gamma_t p_t \mu + (1 - \alpha)\gamma_i p_i \mu - S_q + w$ $\alpha m_t + (1 - \alpha)(m_i - \delta B_{(d)}) - S_v - C - \alpha\beta_t p_t - (1 - \alpha)\beta_i p_i - \alpha E_t - (1 - \alpha)E_i$	$\gamma_i p_i \mu - S_q + w$ $m_i - \delta B_{(d)} - \beta_i p_i - E_i$
	No adoption	$\gamma_i p_i \mu$ $m_i - \delta B_{(d)} - S_v - \beta_i p_i - E_i$	$\gamma_i p_i \mu$ $m_i - \delta B_{(d)} - \beta_i p_i - E_i$

TABLE 3: Main parameters and their meanings.

Parameter	Meaning
R	Doctor's utility
ψ	Patient's utility
d	Distance of the patient from the doctor
$\delta B_{(d)}$	Patient's travel burden from distance d to the doctor (δ is a random variable, $0 < \delta < 1$)
m	Patient's reward for each visit
m_i	Patient's reward for each in-person visit
m_t	Patient's reward for each telehealth visit
μ	Doctor's service rate, that is, the number of patients treated per unit of time
P	Price per visit charged by the government
P_i	Price per visit charged by the government for an in-person visit
P_t	Price per visit charged by the government for telehealth
β	Medical insurance rate, $0 \leq \beta \leq 1$
β_i	Medical insurance rate for an in-person visit
β_t	Medical insurance rate for telehealth
γ	Doctor's commission rate on each visit fee
γ_i	Doctor's commission rate on each visit fee for an in-person visit
γ_t	Doctor's commission rate on each visit fee for telehealth
E	Patient's waiting costs for each visit
E_i	Patient's waiting costs for each in-person visit
E_t	Patient's waiting costs for each telehealth visit
α	Clinical feasibility of telehealth
C	Patient's amortized cost of telehealth adoption
S_v	Patient's learning costs of telehealth adoption
S_q	Doctor's learning cost of telehealth adoption
w	Doctor's rewards from telehealth adoption

$$\begin{aligned}
U_{21} &= x \left[\alpha m_t + (1 - \alpha)(m_i - \delta B_{(d)}) - S_v - C - \alpha\beta_t p_t - (1 - \alpha)\beta_i p_i - \alpha E_t - (1 - \alpha)E_i \right] \\
&\quad + (1 - x)(m_i - \delta B_{(d)} - S_v - \beta_i p_i - E_i) \\
&= x\alpha(m_t - m_i + \delta B_{(d)} - \beta_t p_t + \beta_i p_i - E_t + E_i) - xC + m_i - \delta B_{(d)} - S_v - \beta_i p_i - E_i,
\end{aligned} \tag{8}$$

$$\begin{aligned}
U_{22} &= x(m_i - \delta B_{(d)} - \beta_i p_i - E_i) + (1 - x)(m_i - \delta B_{(d)} - \beta_i p_i - E_i) \\
&= m_i - \delta B_{(d)} - \beta_i p_i - E_i,
\end{aligned} \tag{9}$$

$$\begin{aligned}
\bar{U}_2 &= yU_{21} + (1 - y)U_{22} \\
&= y \left[x\alpha(m_t - m_i + \delta B_{(d)} - \beta_t p_t + \beta_i p_i - E_t + E_i) - xC + m_i - \delta B_{(d)} - S_v - \beta_i p_i - E_i \right] \\
&\quad + (1 - y)(m_i - \delta B_{(d)} - \beta_i p_i - E_i) \\
&= xy\alpha(m_t - m_i + \delta B_{(d)} - \beta_t p_t + \beta_i p_i - E_t + E_i) - xyC - yS_v + m_i - \delta B_{(d)} - \beta_i p_i - E_i.
\end{aligned} \tag{10}$$

The gene replication dynamic equation of the doctor groups was

$$\begin{aligned}
 F(x) &= \frac{dx}{dt} = x(U_{11} - \bar{U}_1) \\
 &= x[(y\alpha\gamma_t p_t \mu - y\alpha\gamma_i p_i \mu + \gamma_i p_i \mu - S_q + w) - (xy\alpha\gamma_t p_t \mu - xy\alpha\gamma_i p_i \mu - xS_q + xw + \gamma_i p_i \mu)] \\
 &= x(1-x)(y\alpha\gamma_t p_t \mu - y\alpha\gamma_i p_i \mu - S_q + w).
 \end{aligned} \tag{11}$$

Similarly, the gene replication dynamic equation of patient groups was

$$\begin{aligned}
 F(y) &= \frac{dy}{dt} = y(U_{21} - \bar{U}_2) \\
 &= y[x\alpha(m_t - m_i + \delta B_{(d)} - \beta_t p_t + \beta_i p_i - E_t + E_i) - xC + m_i - \delta B_{(d)} - S_v - \beta_i p_i - E_i \\
 &\quad - xy\alpha(m_t - m_i + \delta B_{(d)} - \beta_t p_t + \beta_i p_i - E_t + E_i) + xyC + yS_v - (m_i - \delta B_{(d)} - \beta_i p_i - E_i)] \\
 &= y(1-y)[x\alpha(m_t - m_i + \delta B_{(d)} - \beta_t p_t + \beta_i p_i - E_t + E_i) - xC - S_v].
 \end{aligned} \tag{12}$$

4. Stability Analysis of the Evolutionary Game

According to gene replication dynamic equations (11) and (12), let $F(x) = 0$ and $F(y) = 0$; five equilibrium points in the system could be obtained, named, in turn, $O(0, 0)$, $A(0, 1)$, $B(1, 0)$, $C(1, 1)$, and $D(x^*, y^*)$. Among them, $x^* = (S_v / (\alpha(m_t - m_i + \delta B_{(d)} - \beta_t p_t + \beta_i p_i - E_t + E_i) - C))$ and

$y^* = ((w - S_q) / (\alpha\mu(\gamma_i p_i - \gamma_t p_t)))$. The equilibrium state is not necessarily stable. According to Friedman's stability theory, the stability of equilibrium points in evolutionary games can be analysed by constructing a Jacobian matrix [42]. According to equations (11) and (12), the Jacobian matrix J could be obtained:

$$\begin{aligned}
 J &= \begin{bmatrix} J_1 & J_2 \\ J_3 & J_4 \end{bmatrix} \\
 &= \begin{bmatrix} (1-2x)(y\alpha\gamma_t p_t \mu - y\alpha\gamma_i p_i \mu - S_q + w) & x(1-x)(\alpha\gamma_t p_t \mu - \alpha\gamma_i p_i \mu) \\ y(1-y)[\alpha(m_t - m_i + \delta B_{(d)} - \beta_t p_t + \beta_i p_i - E_t + E_i) - C] & (1-2y)[x\alpha(m_t - m_i + \delta B_{(d)} - \beta_t p_t + \beta_i p_i - E_t + E_i) - xC - S_v] \end{bmatrix}.
 \end{aligned} \tag{13}$$

According to equation (13), the Jacobian determinant and its trace were obtained:

$$\begin{aligned}
 \text{Det}J &= J_1 J_4 - J_2 J_3 \\
 &= (1-2x)(y\alpha\gamma_t p_t \mu - y\alpha\gamma_i p_i \mu - S_q + w)(1-2y)[x\alpha(m_t - m_i + \delta B_{(d)} - \beta_t p_t + \beta_i p_i - E_t + E_i) - xC - S_v] \\
 &\quad - x(1-x)(\alpha\gamma_t p_t \mu - \alpha\gamma_i p_i \mu)y(1-y)[\alpha(m_t - m_i + \delta B_{(d)} - \beta_t p_t + \beta_i p_i - E_t + E_i) - C],
 \end{aligned} \tag{14}$$

$$\begin{aligned}
 T_r &= J_1 + J_4 \\
 &= (1-2x)(y\alpha\gamma_t p_t \mu - y\alpha\gamma_i p_i \mu - S_q + w) + (1-2y)[x\alpha(m_t - m_i + \delta B_{(d)} - \beta_t p_t + \beta_i p_i - E_t + E_i) - xC - S_v].
 \end{aligned} \tag{15}$$

If and only if both conditions (16) and (17) are met at the same time, it is the equilibrium point of the replicating dynamic equation, and the evolutionary stability strategy (ESS) is given as follows:

$$\det J = J_1 J_4 - J_2 J_3 > 0 \text{ (Jacobian determinant condition),} \quad (16)$$

$$T_r = J_1 + J_4 < 0 \text{ (trace condition).} \quad (17)$$

According to the above-calculated data, $T_r = 0$ at the local equilibrium point $D(x^*, y^*)$, which did not meet the trace condition. Therefore, equilibrium point $D(x^*, y^*)$ was certainly not an evolutionarily stable strategy of the system. For the remaining four equilibrium points, the local stability of the equilibrium points could be judged according to the determinant and trace values of the Jacobian matrix. The results of the local stability analysis are shown in Table 4.

From the local stability analysis, we found that there were three ESSs at five equilibrium points in the following three situations.

Scenario one: when $w < S_q$, $O(0, 0)$ is an ESS. The dynamic phase diagram of the system evolution is illustrated in Figure 1. In this case, from an initial state, the system will converge to $(0, 0)$; that is, neither the doctor nor the patient will adopt telehealth. For doctors, the reward for adopting telehealth is less than their learning cost. For reasons of utility, the probability of doctors adopting telehealth will gradually evolve from 1 to 0. Moreover, since $A(0, 1)$ is not a stable point, once the doctor does not use telehealth, the probability of patients using telehealth will gradually evolve from 1 to 0.

Scenario two: when $w > S_q$ and $\alpha(m_t - m_i + \delta B_{(d)} - \beta_t p_t + \beta_i p_i - E_t + E_i) < C + S_v$, $B(1, 0)$ is an ESS. In this case, from an initial state, the system will converge to $(1, 0)$, and the system evolution dynamic phase diagram is illustrated in Figure 2. Because for doctors, the reward of adopting telehealth is greater than their learning cost; for the consideration of utility, the probability of doctors adopting telehealth will gradually evolve from 0 to 1. At the same time, for patients, if their learning cost and the amortized cost are greater than $\alpha[\delta B_{(d)} + (m_i - m_t) - (\beta_t p_t - \beta_i p_i) - (E_t - E_i)]$, for the sake of utility, the probability of patients adopting telehealth will gradually evolve from 1 to 0.

Scenario three: when $w > S_q + \alpha\mu(\gamma_i p_i - \gamma_t p_t)$ and $\alpha(m_t - m_i + \delta B_{(d)} - \beta_t p_t + \beta_i p_i - E_t + E_i) > C + S_v$, $C(1, 1)$ is an ESS. In this case, from an initial state, the system will converge to $(1, 1)$, and its system evolution dynamic phase diagram is illustrated in Figure 3. In this case, for doctors, the reward from using telehealth is greater than $S_q + \alpha\mu(\gamma_i p_i - \gamma_t p_t)$, and out of utility considerations, the probability of doctors adopting telehealth will gradually evolve from 0 to 1. In scenario two, because the patients do not eventually adopt telehealth, even if the doctors are willing to use it, the visits are ultimately done in face-to-face mode, so $\alpha = 0$, $\alpha\mu(\gamma_i p_i - \gamma_t p_t) = 0$. At the same time, if patients' learning cost and amortized cost are less than c , for the sake of utility, their probability using telehealth will gradually evolve from 0 to 1.

5. Discussion

The study proposes an asymmetric replication dynamic evolutionary game model of telehealth selection between doctors and patients. By analysing the results of the evolutionary game, we obtained evolutionarily stable strategies in different situations. When $w < S_q$, the system is stable at $O(0, 0)$, meaning the utility of telehealth for doctors and patients is lower than that of in-person visits and telehealth projects are relatively difficult to promote. When $w > S_q$ and $C + S_v > \alpha(m_t - m_i + \delta B_{(d)} - \beta_t p_t + \beta_i p_i - E_t + E_i)$, the system is stable at $B(1, 0)$; in this scenario, the utility of doctors from telehealth use is high, while that of patients is low. Although doctors will adopt telehealth, the utilization of telehealth cannot be improved without the participation of patients. When $w > S_q + \alpha\mu(\gamma_i p_i - \gamma_t p_t)$ and $C + S_v < \alpha(m_t - m_i + \delta B_{(d)} - \beta_t p_t + \beta_i p_i - E_t + E_i)$, the system is stable at $c(1, 1)$. At this point, the utility of doctors and patients from telehealth use is higher than that from face-to-face visits; thus, telehealth is adopted by both parties, and the final utilization rate is improved. Here, we discuss how to promote the adoption of telehealth by doctors and patients.

5.1. Provide Adequate Free Training for Doctors and Patients in Telehealth Technology. The literature indicates that the lack of training for doctors and patients is one of the barriers to telehealth adoption [5, 22, 40, 43, 44]. As it is based on a new information technology, telehealth adoption imposes a certain learning cost. In particular, middle-aged and elderly people affected by the digital divide face higher learning costs, regardless of whether they are doctors or patients [21]. The lack of training can increase the time and effort required for doctors and patients to learn, thus further increasing the learning cost. Research shows that telehealth and face-to-face visits are complements rather than substitutes [9]. Faced with complex conditions, doctors and patients, especially doctors, will pay a considerable learning cost to master and apply their knowledge of the relevant technologies, such as when and how to use telehealth. Our study shows that when all else are equal, a high cost of learning can lead directly to doctors or patients abandoning the use of telehealth. To reduce the cost of learning for doctors and patients, adequate, free training on telehealth techniques, for example, guiding doctors and patients in deciding when to use telehealth, is needed [22]. How do doctors and patients use telehealth devices and familiarize themselves with general ICT technologies, such as PC or mobile phone operations, in the first place? Inadequate training of doctors in the use of telehealth may cause medical errors [5].

5.2. Reward Doctors. The current study shows that doctors' use of telehealth is a prerequisite for patients' use of telehealth. As Rho et al. point out, telehealth is a valuable healthcare service only when doctors adopt it proactively [33]. In China, doctors must provide telehealth due to an administrative order, which is guided by a public welfare and assistance motive, without additional remuneration [19]. In the absence of extrinsic motivators, the objective of adopting

TABLE 4: Local stability analysis of the equilibrium point.

Equilibrium point	Det/J	Constraint conditions	Det/J	T_r	Constraint conditions	T_r	Results
O (0, 0)	$S_q(S_q - w)$	$w > S_q$ $w < S_q$	- +	$w - S_q - S_v$	-	Uncertain -	Saddle ESS
A (0, 1)	$S_v[w - S_q - \alpha\mu(\gamma_i P_i - \gamma_t P_t)]$	$w > S_q + \alpha\mu(\gamma_i P_i - \gamma_t P_t)$ $w < S_q + \alpha\mu(\gamma_i P_i - \gamma_t P_t)$	+ -	$w - S_q - \alpha\mu(\gamma_i P_i - \gamma_t P_t) + S_v$	-	+	Unstable Saddle
B (1, 0)	$(S_q - w)[\alpha(m_t - m_i + \delta B_{(d)} - \beta_t P_t + \beta_i P_i - E_t + E_i) - C - S_v]$	$w > S_q$ $w < S_q$	- +	$(S_q - w) + [\alpha(m_t - m_i + \delta B_{(d)} - \beta_t P_t + \beta_i P_i - E_t + E_i) - C - S_v]$	- -	Uncertain +	Saddle ESS Unstable Saddle
C (1, 1)	$[w - S_q - \alpha\mu(\gamma_i P_i - \gamma_t P_t)][\alpha(m_t - m_i + \delta B_{(d)} - \beta_t P_t + \beta_i P_i - E_t + E_i) - C - S_v]$	$w > S_q + \alpha\mu(\gamma_i P_i - \gamma_t P_t)$ $w < S_q + \alpha\mu(\gamma_i P_i - \gamma_t P_t)$	+ -	$-[w - S_q - \alpha\mu(\gamma_i P_i - \gamma_t P_t)]$ $\gamma_t P_t]$ $-[\alpha(m_t - m_i + \delta B_{(d)} - \beta_t P_t + \beta_i P_i - E_t + E_i) - C - S_v]$	- -	Uncertain Uncertain	ESS Saddle Saddle
D (x^*, y^*)	$-x^*(1 - x^*)(\alpha\gamma_t P_t \mu - \alpha\gamma_i P_t \mu)^*(1 - y^*)$ $[\alpha(m_t - m_i + \delta B_{(d)} - \beta_t P_t + \beta_i P_i - E_t + E_i) - C]$	-	-	0	-	-	Unstable

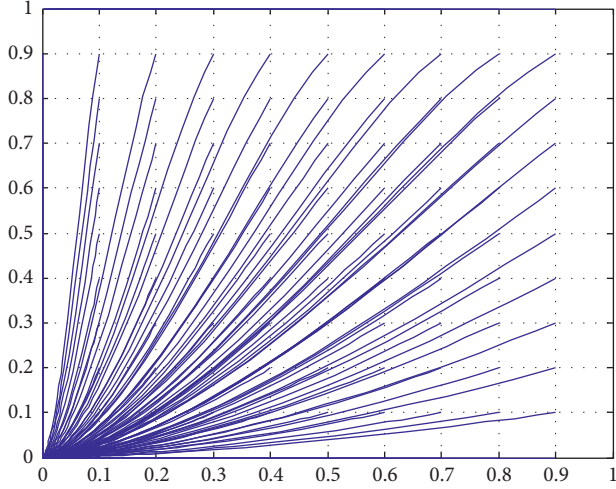


FIGURE 1: Dynamic phase diagram of system evolution in scenario one.

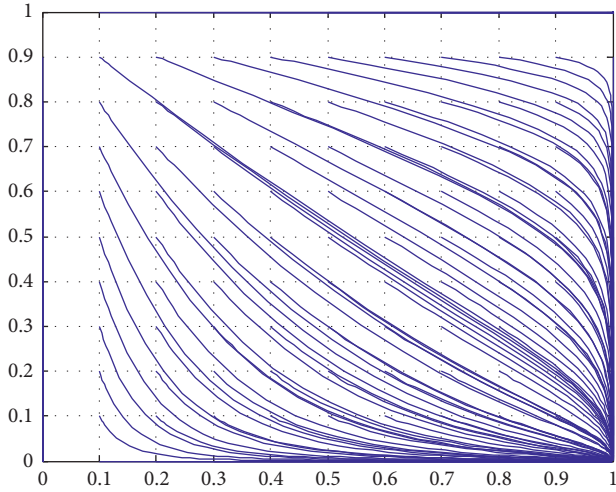


FIGURE 2: Dynamic phase diagram of system evolution in scenario two.

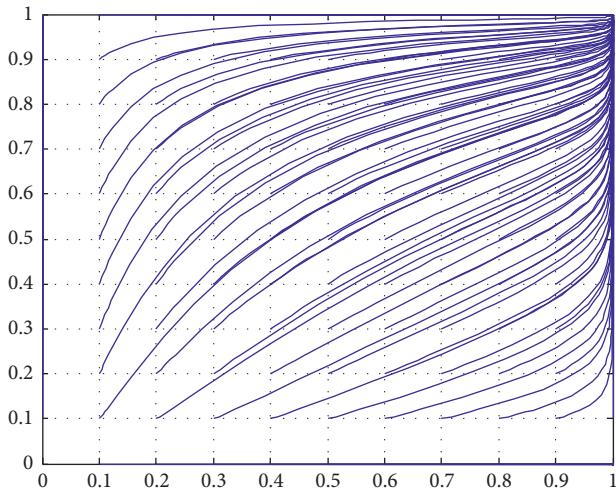


FIGURE 3: Dynamic phase diagram of system evolution in scenario three.

telehealth can be achieved in the short term but may face challenges in the long term. Doctors may eventually abandon telehealth due to the lower utility they derive from it than from in-person visits. Therefore, as the literature suggests, doctors should be rewarded [5, 23, 45]. The current study is pioneering in suggesting that doctors' rewards for adopting telehealth should be greater than $S_q + \alpha\mu(\gamma_i p_i - \gamma_t p_t)$. Further, observing the difference between doctors' face-to-face and telehealth remuneration, many scholars have suggested that doctors who adopt telehealth should be paid the same as those who conduct face-to-face visits [2, 33]. That is, the rewards for doctors should be extended until doctors who use telehealth are paid the same as those who use face-to-face visits and, consequently, no new learning costs are incurred after they receive telehealth training.

5.3. Raise the Cost Threshold for Patient Adoption of Telehealth. The cost of adopting telehealth for patients is composed of a learning cost and an amortized cost, which has a threshold value of $\alpha[\delta B_{(d)} + (m_i - m_t) - (\beta_t p_t - \beta_i p_i) - (E_t - E_i)]$. When the cost of adopting telehealth is above this threshold, patients will abandon it. Therefore, if the threshold value is appropriately raised, the proportion of patients adopting telehealth can be increased. We analyse the threshold composition as follows: first, $m_i - m_t$. Research from the American Telemedicine Association has consistently shown that the quality of telehealth is equal to that provided by in-person visits [46]. However, patients influenced by traditional Chinese medicine usually perceive the effectiveness of telehealth to be lower than that of face-to-face consultations, resulting in a lower threshold. Second, $\delta B_{(d)}$. The closer the patient is to the doctor and the lower the traffic congestion, the smaller is the travel burden of the patient and the lower the threshold. Third, $\beta_t p_t - \beta_i p_i$. Charges for telehealth vary from place to place but are greater than those for face-to-face visits and in most areas not covered by medical insurance [47–49]. In other words, the patient bears more of the cost in the telehealth mode than in the face-to-face mode, resulting in a lower threshold. Finally, $E_t - E_i$. Since telehealth services are still in their infancy, they are coordinated by part-time staff assigned by participating hospitals. The low operating efficiency leads to long waiting times and further lowers the threshold [49, 50]. It is not difficult to see that, by popularizing telehealth knowledge, promoting telehealth in areas far from doctors and with inconvenient transportation, implementing the same fees and medical insurance benefits as for face-to-face services, and improving operational efficiency, the threshold can be further simplified to $\alpha B_{(d)}$. That is, when the right policies and measures are put in place and no new learning costs are incurred after patient training, $S_v = 0$, patients will eventually adopt telehealth if the patient's amortized cost of telehealth is less than the product of the telehealth feasibility and travel burden values.

6. Conclusions

In the context of an intensive push to spread telehealth coverage in China, the adoption rate of telehealth remains

low due to the conflicts between the habits formed by doctors and patients under the influence of the strong traditional Chinese medicine culture and telehealth. The current study analysed the factors influencing doctors' and patients' adoption of telehealth, constructed an asymmetric replication dynamic evolutionary game model, analysed doctors' and patients' visit behaviours, and derived evolutionarily stable strategies in different situations. The results show that doctors' utility from using telehealth is low and the cost threshold of patients using telehealth is also low. This "dual low" nature of telehealth directly leads doctors and patients not to adopt it.

To promote the adoption of telehealth in China, key options include providing adequate training for doctors and patients in telehealth technology, rewarding doctors, and raising patients' cost threshold for adopting telehealth, such that the utility of doctors and patients from adopting telehealth becomes higher than their utility from habitual in-person visits. In addition, doctors adopting telehealth is a prerequisite for patients adopting telehealth. The rewards to doctors should be extended until doctors can obtain the same remuneration from telehealth consultations as from face-to-face visits, and thus no new learning costs are incurred after they are trained in telehealth use. In regards to patients, they will eventually adopt telehealth with the implementation of appropriate policies and measures, such as popularizing telehealth knowledge, promoting telehealth in areas far from doctors and with inconvenient transportation, setting the same fees and medical insurance benefits as those for face-to-face treatment, improving operational efficiency, and ensuring that no additional learning costs are incurred after patients receive telehealth training. Moreover, the patient's amortized cost of telehealth should be less than the product of the telehealth feasibility and travel burden values.

The study is likely to help developing countries solve the problem of conflicts between telehealth and traditional culture and habits in the process of telehealth promotion campaigns by stressing that the failure to adopt telehealth stems from doctors and patients obtaining less utility from telehealth visits than from in-person visits. The study can serve as a reference to help developing countries promote the adoption of telehealth through careful analysis of the factors hampering the promotion and adoption of telehealth.

Data Availability

The data used to support the findings of this study are available from the corresponding author upon reasonable request.

Conflicts of Interest

The authors declare that they have no conflicts of interest.

Acknowledgments

This work was supported by the National Natural Science Foundation of China (Grant nos. 71671091 and 41801119).

References

- [1] E. R. Dorsey and E. J. Topol, "State of telehealth," *New England Journal of Medicine*, vol. 375, no. 2, pp. 154–161, 2016.
- [2] J. Kvedar, M. J. Coye, and W. Everett, "Connected health: a review of technologies and strategies to improve patient care with telemedicine and telehealth," *Health Affairs*, vol. 33, no. 2, pp. 194–199, 2014.
- [3] S. Delaigue, L. Bonnardot, O. Steichen et al., "Seven years of telemedicine in médecins sans frontières demonstrate that offering direct specialist expertise in the frontline brings clinical and educational value," *Journal of Global Health*, vol. 8, no. 2, Article ID 020414, 2018.
- [4] T.-T. Wang, J.-M. Li, C.-R. Zhu et al., "Assessment of utilization and cost-effectiveness of telemedicine program in western regions of China: a 12-year study of 249 hospitals across 112 cities," *Telemedicine and E-Health*, vol. 22, no. 11, pp. 909–920, 2016.
- [5] C. Combi, G. Pozzani, and G. Pozzi, "Telemedicine for developing countries," *Applied Clinical Informatics*, vol. 07, no. 04, pp. 1025–1050, 2016.
- [6] A. G. Ekeland, A. Bowes, and S. Flottorp, "Effectiveness of telemedicine: a systematic review of reviews," *International Journal of Medical Informatics*, vol. 79, no. 11, pp. 736–771, 2010.
- [7] Policy OOH, "Report to congress: e-health and telemedicine," 2016, <https://aspe.hhs.gov/system/files/pdf/206751/TelemedicineE-HealthReport.pdf>.
- [8] WHO, "Global diffusion of eHealth: making universal health coverage achievable: report of the third global survey on eHealth," 2016, https://www.who.int/goe/publications/global_diffusion/en/.
- [9] M. Zhou, L. Zhao, N. Kong, K. S. Campy, S. Qu, and S. Wang, "Factors influencing behavior intentions to telehealth by Chinese elderly: an extended TAM model," *International Journal of Medical Informatics*, vol. 126, pp. 118–127, 2019.
- [10] X. Jinping, "National health conference: put people's health as a priority development strategy and work hard to protect people's health in all aspects," 2016, https://www.who.int/goe/publications/global_diffusion/en/.
- [11] W. Junping, "Making telemedicine fair and efficient," 2019, https://www.who.int/goe/publications/global_diffusion/en/.
- [12] C. M. LeRouge, M. Gupta, G. Corpart, and A. Arrieta, "Health system approaches are needed to expand telemedicine use across nine Latin American nations," *Health Affairs*, vol. 38, no. 2, pp. 212–221, 2019.
- [13] Asia GHFoBFf, "Innovation promotes health, and the future of internet healthcare faces major opportunities," 2019, <http://health.people.com.cn/n1/2019/0611/c14739-31129870.html>.
- [14] H. Li, K. Liu, J. Gu, Y. Zhang, Y. Qiao, and X. Sun, "The development and impact of primary health care in China from 1949 to 2015: a focused review," *The International Journal of Health Planning and Management*, vol. 32, no. 3, pp. 339–350, 2017.
- [15] X. Jinping, "Report delivered at the 19th national congress of the communist party of China," 2017, http://www.xinhuanet.com/english/special/2017-11/03/c_136725942.htm.
- [16] Asia GHFoBFf, "China's medical talent team construction should work hard at the grassroots level," 2019, <http://www.ghfbfa.cn/newsDetail/?id=258>.
- [17] M. Wei, "China's communications infrastructure capacity has grown by leaps and bounds," 2018, <https://baijiahao.baidu.com/s?id=1612678610880277436&wfr=spider&for=pc>.
- [18] China NHaFPCo, "Technical guide for telemedicine information system construction," 2014, <http://www.nhc.gov.cn/guihuaxxs/s10741/201501/e023e2c4e3254f73932f0b0fca99a866.shtml>.

- [19] Y. Jie, "Promote telemedicine and establish industry standards and evaluation systems," 2019, <http://www.jnlc.com/article/20190308236829.shtml>.
- [20] Commission NH, "Statistical communique on the development of China's health undertakings in 2018," 2019, <http://www.nhc.gov.cn/guihuaxxs/s10748/201905/9b8d52727cf346049de8acce25ffcbdd0.shtml>.
- [21] M. J. S. Diño and A. B. de Guzman, "Using partial least squares (PLS) in predicting behavioral intention for telehealth use among Filipino elderly," *Educational Gerontology*, vol. 41, no. 1, pp. 53–68, 2015.
- [22] Y. Xue and H. Liang, "Analysis of telemedicine diffusion: the case of China," *IEEE Transactions on Information Technology in Biomedicine*, vol. 11, no. 2, pp. 231–233, 2007.
- [23] K. I. Adenuga, N. A. Iahad, and S. Miskon, "Towards reinforcing telemedicine adoption amongst clinicians in Nigeria," *International Journal of Medical Informatics*, vol. 104, pp. 84–96, 2017.
- [24] B. Kamsu-Foguem and C. Foguem, "Could telemedicine enhance traditional medicine practices?" *European Research in Telemedicine/La Recherche Européenne en Télémedecine*, vol. 3, no. 3, pp. 117–123, 2014.
- [25] E. Ostrom, J. Burger, C. B. Field et al., "Revisiting the commons: local lessons, global challenges," *Science*, vol. 284, no. 5412, pp. 278–282, 1999.
- [26] E. Fehr and U. Fischbacher, "The nature of human altruism," *Nature*, vol. 425, no. 6960, pp. 785–791, 2003.
- [27] J. Von Neumann and O. Morgenstern, *Theory of Games and Economic Behavior*, Princeton University Press, Princeton, NJ, USA, 1944.
- [28] J. M. Smith, "Evolution and the theory of games," *American Scientist*, vol. 64, pp. 41–45, 1976.
- [29] N. Zhang, X. Zhang, and Y. Yang, "The behavior mechanism of the urban joint distribution alliance under government supervision from the perspective of sustainable development," *Sustainability*, vol. 11, no. 22, p. 6232, 2019.
- [30] S. Dünnebel, A. Sunyaev, I. Blohm, J. M. Leimeister, and H. Krcmar, "Determinants of physicians' technology acceptance for e-health in ambulatory care," *International Journal of Medical Informatics*, vol. 81, no. 11, pp. 746–760, 2012.
- [31] C.-F. Liu, Y.-C. Tsai, and F.-L. Jang, "Patients' acceptance towards a web-based personal health record system: an empirical study in Taiwan," *International Journal of Environmental Research and Public Health*, vol. 10, no. 10, pp. 5191–5208, 2013.
- [32] C.-H. Tsai, "Integrating social capital theory, social cognitive theory, and the technology acceptance model to explore a behavioral model of telehealth systems," *International Journal of Environmental Research and Public Health*, vol. 11, no. 5, pp. 4905–4925, 2014.
- [33] M. J. Rho, I. y. Choi, and J. Lee, "Predictive factors of telemedicine service acceptance and behavioral intention of physicians," *International Journal of Medical Informatics*, vol. 83, no. 8, pp. 559–571, 2014.
- [34] Y. Wang, *Patient Choice of Service Pattern in the Healthcare System*, Southwestern University of Finance and Economics, Chengdu, China, 2016.
- [35] V. Venkatesh, M. G. Morris, G. B. Davis et al., "User acceptance of information technology: toward a unified view," *MIS Quarterly*, vol. 27, no. 13, pp. 425–478, 2003.
- [36] C.-L. Lee, D. C. Yen, K.-C. Peng, and H.-C. Wu, "The influence of change agents' behavioral intention on the usage of the activity based costing/management system and firm performance: the perspective of unified theory of acceptance and use of technology," *Advances in Accounting*, vol. 26, no. 2, pp. 314–324, 2010.
- [37] B. Rajan, T. Tezcan, and A. Seidmann, "Service systems with heterogeneous customers: investigating the effect of telemedicine on chronic care," *Management Science*, vol. 65, no. 3, pp. 1236–1267, 2019.
- [38] X. Wang, R. Du, S. Ai et al., "The evolution analysis of the community hospitals and patients' behavior selection under the background of telemedicine," *Industrial Engineering and Management*, vol. 20, pp. 130–137, 2015.
- [39] X. Zhan, L. Zhou, and X. Sun, "Promoting telemedical services based on evolutionary game theory," *Systems Engineering*, vol. 35, pp. 95–102, 2017.
- [40] C. Scott Kruse, P. Kareem, K. Shifflett, L. Vegi, K. Ravi, and M. Brooks, "Evaluating barriers to adopting telemedicine worldwide: a systematic review," *Journal of Telemedicine and Telecare*, vol. 24, no. 1, pp. 4–12, 2018.
- [41] S. Xie, *Economic Game Theory*, Fudan University Press, Shanghai, China, 2002.
- [42] D. Friedman, "Evolutionary games in economics," *Econometrica*, vol. 59, no. 3, pp. 637–666, 1991.
- [43] C. Ranganathan and S. Balaji, "Key factors affecting the adoption of telemedicine by ambulatory clinics: insights from a statewide survey," *Telemedicine and E-Health*, vol. 26, no. 2, pp. 218–225, 2020.
- [44] J. Moeckli, P. Cram, C. Cunningham, and H. S. Reisinger, "Staff acceptance of a telemedicine intensive care unit program: a qualitative study," *Journal of Critical Care*, vol. 28, no. 6, pp. 890–901, 2013.
- [45] R. Bhatta, K. Aryal, and G. Ellingsen, "Opportunities and challenges of a rural-telemedicine program in Nepal," *Journal of Nepal Health Research Council*, vol. 13, pp. 149–153, 2015.
- [46] Association TAT, "The American telemedicine association reports that telehealth/telemedicine has been growing rapidly because it offers four fundamental benefits," 2020, <http://sctehealth.org/About/>.
- [47] G. J. Chen and L. Yuan, "Jiangsu telemedicine service has standards," 2018, <http://js.people.com.cn/n2/2018/1015/c360306-32158596.html>.
- [48] F. Yao, C. Yunfen, W. Nina et al., "Yesterday, Jiangsu medical reform implemented on the first day, cheap or expensive to see a doctor," 2015, <https://js.qq.com/a/20151101/008541.htm>.
- [49] Asia GHFoBff, "Telemedicine now has a problem of 'applauding or not'," 2019, <http://finance.sina.com.cn/roll/2019-06-11/doc-ihvhiqay4769923.shtml>.
- [50] B. Wang, "How long is the road to popularize 'telemedicine'," 2018, http://www.sohu.com/a/233240219_161795.

Research Article

“Buy Online, Pick Up in Store” under Fit Uncertainty: To Offer or Not to Offer

Huijing Li,^{1,2} Shilei Yang,¹ Haiyan Kang ,^{3,4} and Victor Shi ⁵

¹School of Business Administration, Southwestern University of Finance and Economics, Chengdu, China

²School of Business, Guizhou Education University, Guiyang, China

³Faculty of Business Administration, Jiangxi University of Finance and Economics, Nanchang, China

⁴Faculty of Business Administration, Shanghai Business School, Shanghai 200235, China

⁵Lazaridis School of Business and Economics, Wilfrid Laurier University, N2L 3C5, Waterloo, ON, Canada

Correspondence should be addressed to Haiyan Kang; 21090126@sbs.edu.cn

Received 2 May 2020; Accepted 28 May 2020; Published 4 July 2020

Guest Editor: Lei Xie

Copyright © 2020 Huijing Li et al. This is an open access article distributed under the Creative Commons Attribution License, which permits unrestricted use, distribution, and reproduction in any medium, provided the original work is properly cited.

Retailers offer BOPS (Buy Online, Pick Up in Store) service to improve consumers shopping experience. However, this greatly increases the decision complexity for retailers and consumers. For consumers, whether to purchase online or from a store with the BOPS service is a complex decision. This is especially true when the product has fit uncertainty. That is, consumers are uncertain about product fitness before using it. Also, their store visit cost can be heterogeneous and follows some distribution function. For a retailer, it needs to jointly optimize multiple decisions including the convenience degree of BOPS. To help the retailer develop the jointly optimal decisions, we first build a mathematical model where the retailer sells the product through online and store channel and analyzes the possible effects of BOPS. We find that the retailer should offer BOPS when the channel cost ratio (ratio of shipment fee divided by average store visit cost) is large enough. Through numerical studies, we show that the ratio of profit offering BOPS divided by the benchmark increases with the probability of product fit, shipment fee, and the convenience degree of BOPS. We then consider the case where the convenience degree of BOPS is also a decision itself. We find the optimal convenience degree of BOPS increases along with the average store visit cost and the probability of product fit. When the cost factor of offering the convenience for BOPS is larger than a threshold, the retailer should never offer BOPS.

1. Introduction

Nowadays, consumers can shop over multiple retailing channels, such as brick-and-mortar stores, online stores, mobile stores, and even social network platforms. Different channels have different advantages, and strategic consumers tend to exploit these channels together to buy the right product and enjoy better shopping experience. For instance, about 30% of consumers are willing to use one channel for searching product information and buy at another channel [1]. To make consumers enjoy the seamless shopping experience, omnichannel retailing strategy has been adopted by many retailers. For example, about 40% retailers use three or more channels to sell products and about 42% operate with two channels [2]. Omnichannel retailing is a strategy in

which all of the channels, such as store, online channel, mobile channel, and social networks, are integrated so that the customers can use the channels seamlessly and enjoy a better customer experience [3].

As one way of integrated order fulfillment in the omnichannel, the BOPS (Buy Online, Pick Up in Store) has been offered by the many retailers such as Target, Walmart, and Tesco. Consumers should pay the shipment fee if they choose to buy online and use home delivery service, or pay no fee if picking up in local stores. Some retailers such as Tesco also offer some convenience for the BOPS customers, such as drive-through service where shoppers drive to the store and take the goods without getting out their cars. There is a tendency that consumers adopt the BOPS service due to the free pickup and convenience of BOPS. About 42% of

Internet users respond that the BOPS is appealing [4] and BOPS is used by more consumers, for example, 30% of Target.com's online orders were fulfilled in stores [5]. Recently, there are several studies on the effect of BOPS. The total demand will increase due to cross-selling effect and channel shift effect [6], and the profit will increase under some conditions [7–10]. Meanwhile, BOPS usage will improve the frequency and amount of consumer purchases [11].

However, the existing literature fail to consider different product types, such as books or clothes. Books are more standardized products than clothes, which means consumers need to touch or try on before buying clothes than books due to fit uncertainty. Fit uncertainty is defined as the extent that consumers cannot decide whether the product fits before using it [12]. Fitness is a critical component for consumers shopping experiences, especially for nonstandardized products such as clothes and shoes. To lower the fit uncertainty, consumers prefer making physical purchases to buying online, especially when considering the product returns are costly to both consumers and retailers [13]. Some strategic consumers may visit the physical store first and then shop online and this will bring a new problem which is called search shopping phenomenon [14]. Search shopping phenomenon makes the consumer's search cost higher. The retailers have tried many measures to lower this cost and make better consumer satisfaction, such as virtual try-on [15], free samples [16], and BOPS [6]. For example, Uniqlo, which is a Japanese clothing brand, offers BOPS for the consumers who buy clothes though Alibaba's e-commerce platforms including Taobao and Tmall.

Different product types may affect the consumers' willingness and frequency to use BOPS. According to retail and e-commerce [4], electronics are the most popular goods that respondents were willing to purchase through BOPS, but the fresh prepared meals and groceries stood out as the least appealing categories. How should retailers offer BOPS for different types of products from those with more fit uncertainty to ones with less fit uncertainty? How will fit uncertainty affect the effect of BOPS? Research studies are needed to examine the effect of BOPS on different types of product [7, 17]. Motivated by the above observations, we set out to study the effect of BOPS for the different product types with fit uncertainty. Hence, in this paper, we focus on the following research questions:

- (1) How does the BOPS service affect the demand and profitability for goods with fit uncertainty?
- (2) Should the retailer offer the BOPS service on goods with high fit uncertainty?
- (3) How do the level of fit uncertainty and other shopping cost affect the retailer's performance?

To address these questions, a benchmark model that a retailer who operates dual channels without BOPS service is first constructed. The effect of BOPS from the perspective of the retailer is analyzed. The model is later extended to optimize the convenience degree of BOPS. We show that the retailers should be conscious to offer the BOPS for the goods

with fit uncertainty. We identify that the retailer should offer BOPS when the channel cost ratio (the shipment fee divided by the average store visit cost) is high enough. The total demand will increase due to channel shift effect that consumers switch to BOPS from store channel and generate some new demand. It is interesting to find that the retailer's profit ratio increases with fit uncertainty.

The remainder of this paper is organized as follows. The related literature is reviewed in Section 2. The model of benchmark case without BOPS is introduced in Section 3. In Section 4, the detailed analysis of BOPS service is presented. In Section 5, the optimizing convenience degree of BOPS service is discussed. Finally, the implications and limitations of this research are concluded in Section 6.

2. Relevant Literature

BOPS is related to the integration between online and offline channels, where the online shopping behavior interacts with the offline store picking up experience. Our work is primarily related to three streams of research: dual-channel strategy, BOPS service, and fit uncertainty. We discuss each of these streams as follows.

Research on dual channels focuses on retailers' performance from different aspects such as product availability information [18], channel equilibrium structure [19], production assortment and delivery time design [20], channel integration [21, 22], and fulfillment service contracts [23]. Some studies analyze the dual-channel strategy from manufacturers' perspectives and focus on the channel conflict [24, 25] or channel coordination [26, 27]. The new online channel is used to compete with the independent retailer and improve the profit by the manufacturer [24]. Manufacturer redesigns channel service level to compete with retailers and the dual-channel strategy brings increased competition among the supply chain [25]. To achieve win-win purposes, manufacturers can design the channel coordination contracts to find the channel-adding Pareto zone and contract-implementing Pareto zone [26]. Manufacturers can also design the service-cost sharing contract when manufacturer's online channel free rides the retailer's pre-sales services [27]. Similar to adding a new channel, BOPS service is a new choice for the consumers and may also bring the channel cannibalization problem. But BOPS is a way of integrating the existing channels under the omnichannel strategy [28], and offering BOPS is essentially different from adding a new channel.

Based on the cross-channel integration such as integrated price and assortment [7], BOPS is the most common integrated order fulfillment in the omnichannel strategy [29]. Researchers examine the contributing factors that affect the consumers adopting BOPS [17] and the effects of BOPS on the performance [6–10, 30]. Gallino et al. [6] use sales data and explain why the store demand may increase and the online demand decrease. Mahar et al. [30] optimize a set of pickup and return locations to reduce the cost of the retailer. Gao and Su [8] consider product availability and build a newsvendor model to analyze the effect of BOPS with cross-selling. The authors build a consumer choice model and

conclude that when the operation cost is low enough, the profit of the retailer will increase after offering BOPS, but there exists a channel cannibalization problem. Jin et al. [9] find the BOPS service area and compare the performance of BOPS with the ROPS (Reserve Online Pick Up and Pay in Store) from a retailer's point of view. Shi et al. [10] study the effect of BOPS with preorders when both informed and uninformed consumers exist. As the research progressed, the influence of BOPS on consumers' purchasing behavior has also attracted the attention of scholars. By collecting and analyzing consumers' bulk purchase data, Song et al. [11] find that BOPS usage has a significant impact on increasing the frequency and amount of consumer purchases. However, these researchers consider standardized products without fit uncertainty. Little research has built analytic models to study the effect of BOPS on nonstandardized products with fit uncertainty.

There is much research on the issue of fit uncertainty. As one type of information asymmetry problem, fit uncertainty can result in problems such as customer dissatisfaction [12], product returns [13, 31, 32], and search shopping phenomenon [14, 33, 34]. Retailers can employ fit uncertainty mitigating strategies such as money-back guarantees [35–37], online reviews [38, 39], virtual try-on [15], and free samples [16]. In general, reducing product fit uncertainty will improve consumer's purchase size and loyalty [40]. Some research works study the optimal pricing [41], promotion [42], and retailer shelf layout [43] to deal with the fit uncertainty problem. Our study focuses on the effect of product fit uncertainty on BOPS service.

3. Benchmark Model without Offering BOPS Service

We consider a retailer who sells products through an online channel and a store. Without BOPS, there are only two options: online channel where consumers buy directly online and the product is delivered home, and a store channel where consumers visit the store and purchase the product when it fits. The price p in both channels is the same. Consumers are identical in terms of the product fit uncertainty $1 - \delta$, where δ is called the fit probability where $0 < \delta < 1$. If consumers buy online, they should pay a fixed shipment fee s ; if consumers buy in store, they incur a heterogeneous store visit cost t , which is uniformly distributed between 0 and $2\bar{t}$ with an average positive store visit cost of \bar{t} . v is the product value when it fits and is assumed large enough to ensure the utility of all channels is non-negative. However, the product value is zero while it does not fit.

As shown in Figure 1, consumers may go to the store and buy the product only when it fits. Consumers may also buy directly through the online channel but undertake the shipment fee and the risk of fit uncertainty. The consumer's outcome is given by

$$\begin{cases} v - p - t, & \text{travel to store and find the product fit,} \\ -t, & \text{travel to store and find the product unfit,} \\ v - p - s, & \text{buy online and find the product fit,} \\ -p - s, & \text{buy online and find the product unfit.} \end{cases} \quad (1)$$

Let u_s and u_o denote the expected utility of the store and online channel, respectively. We have $u_s = \delta(v - p) - t$ and $u_o = \delta v - p - s$.

Consumers will buy the product through online channel if $u_o \geq u_s$. Let t_{os} denote the value of t at which a consumer is indifferent between purchasing online or from the store where $t_{os} = (1 - \delta)p + s$. As shown in Figure 2, we can find that consumers who buy online must have higher store visiting cost than those who choose to buy in store. Consumers with a higher t ($2\bar{t} > t \geq t_{os}$) will buy the product online. To make the demand of online channel is nonnegative, it is reasonable to assume t_{os} is lower than $2\bar{t}$, i.e., $p \leq (2\bar{t} - s)/(1 - \delta)$. Consumers with a lower t ($0 < t < t_{os}$) will visit store and buy the product only if it fits. Hence, only δ proportion of store visit consumers will buy the product in store, and $1 - \delta$ proportion of store visit consumers are lost and this part of consumers is called the lost demand.

Let D_o and D_s denote the demand of the online and store channels, respectively. The expect demand of store channel is $D_s = \delta t_{os}/2\bar{t}$, and the demand of online channel is $D_o = (2\bar{t} - t_{os})/2\bar{t}$. The total demand and profit in this benchmark model are expressed as D and π , respectively. The retailer chooses a price p to maximize its profit as follows:

$$\max_p \pi(p) = (D_o + D_s)p. \quad (2)$$

Lemma 1. *In the benchmark model without offering BOPS service, the retailer's optimal price is $\min((2\bar{t} - s)(1 - \delta))/(2(1 - \delta)^2), (2\bar{t} - s)/(1 - \delta)$, and the demand is shown in Table 1.*

Proof. See appendix. \square

4. The Model with BOPS Service

4.1. Consumers' Channel Choice. With the BOPS service available, consumers can make an order online and pick up the product from the store for free. Hence, consumers compare three choices before making a purchase decision: directly buying online, buying in store, or choosing BOPS. Following Cao et al. [7], when consumers adopt the BOPS service, the pickup cost will be less than the store visiting cost due to the convenience that the retailer offers to BOPS adopters. The pickup cost of BOPS and the convenience degree of BOPS are denoted as θt and $1 - \theta$, respectively, where $0 < \theta < 1$. Consumers' realized utility outcome from BOPS is given by

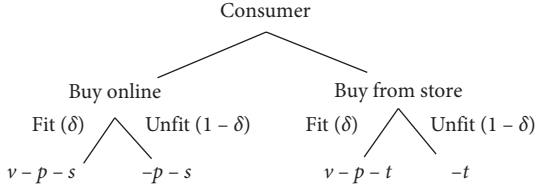


FIGURE 1: Consumers' decision tree and utility in benchmark.

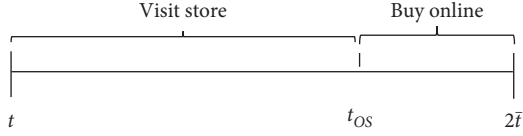


FIGURE 2: Consumers' channel choice in benchmark.

$$\begin{cases} v - p - \theta t, & \text{adopt BOPS and find the product fit,} \\ -p - \theta t, & \text{adopt BOPS and find the product unfit.} \end{cases} \quad (3)$$

Let u_B denote the expected utility of BOPS, then $u_B = \delta v - p - \theta t$. Let t_{BS} and t_{BO} be the value of t at which BOPS service yields the same utility as store and online channel, respectively. These indifference values of t can be shown as follows:

$$\begin{aligned} t_{BS} &= \frac{(1 - \delta)p}{(1 - \theta)}, \\ t_{BO} &= \frac{s}{\theta}. \end{aligned} \quad (4)$$

As shown in Figure 3, consumers with store visit cost between 0 and t_{BS} will visit store and buy only if the product fits. Those with cost between t_{BS} and t_{BO} will adopt BOPS, while consumers whose store visiting cost is higher than t_{BO} will buy from online channel and have the product delivered home.

The following lemma shows the conditions under which consumers choose the BOPS or buy online directly.

Lemma 2. *In the model with BOPS service, (i) consumers choose BOPS service if $p \leq \min(((1 - \theta)s)/((1 - \delta)\theta), (2\bar{t}(1 - \theta))/(1 - \delta))$, and (ii) consumers purchase online directly if $(s/\bar{t}) \leq 2\theta$.*

To understand when consumers choose the BOPS service, we can compare the utilities of store and online channel with BOPS, respectively. When t is smaller than t_{OS} , the store channel is better than online channel. Hence, we compare the expected utility of the store channel with BOPS when $t \leq t_{OS}$. Consumers will adopt BOPS if the saving cost of visiting store $(1 - \theta)t$ is larger than possible loss $(1 - \delta)p$ due to fit uncertainty, which leads to $p \leq (1 - \theta)t/(1 - \delta)$. Since the consumer's possible highest store visit cost is $2\bar{t}$, some consumers buy from BOPS $p \leq 2\bar{t}(1 - \theta)/(1 - \delta)$. We then compare the online channel with the choice of BOPS when $t > t_{OS}$. Consumers will use BOPS if the saved shipment fee s due to adopting BOPS is larger than the picking

up cost θt , which leads to $s/\theta \geq t$. Since the consumer's lowest store visit cost is t_{OS} , some consumers buy through BOPS if $s/\theta \geq t_{OS}$. This is equal to that $p \leq (1 - \theta)s/[(1 - \delta)\theta]$. Hence, consumers adopt BOPS service if $p \leq \min(((1 - \theta)s)/(1 - \delta)\theta, (2\bar{t} - s)/(1 - \delta))$. Consumers will buy from online channel if and only if the picking up cost θt is larger than saving shipping fee s , i.e., $t \geq s/\theta$. Since the highest store visit cost is $2\bar{t}$, some consumers buy online if $s/\bar{t} \leq 2\theta$.

Based on Lemma 2, there are two new scenarios (B-O-S or B-S) compared with the benchmark. When $p \leq \min(((1 - \theta)s)/(1 - \delta)\theta, (2\bar{t} - s)/(1 - \delta))$ and $s/\theta < 2\bar{t}$, all three types of consumers—BOPS shoppers (B), online shoppers (O), and store shoppers (S)—exist, which is called the B-O-S scenario. The consumers who buy directly online or store channel are called online shoppers and store shoppers, respectively. When $p \leq \min(((1 - \theta)s)/(1 - \delta)\theta, (2\bar{t} - s)/(1 - \delta))$ and $s/\theta > 2\bar{t}$, the consumer will not buy online and there are only two kinds of consumers—BOPS (B) and store shopper (S)—existing. This is called the B-S scenario.

4.2. The Equilibrium Solution with BOPS. According to the purchasing behavior of three types of consumers, we can obtain the demand of each type in each scenario. The total demand and profit are expressed as \bar{D} and $\bar{\pi}$ correspondingly. Let D^{B-O-S} , π^{B-O-S} , D^{B-S} , and π^{B-S} denote the total demand and expected profit in scenarios B-O-S and B-S separately. The (expected) demands of store, online channel, and BOPS in scenarios B-O-S and B-S are denoted by D_S^{B-O-S} , D_O^{B-O-S} , D_B^{B-O-S} , D_S^{B-S} , and D_B^{B-S} individually.

The retailer's demand of each channel in the B-O-S scenario is shown as follows: $D_S^{B-O-S} = \delta t_{OS}/(2\bar{t})$, $D_O^{B-O-S} = (2\bar{t} - t_{BO})/(2\bar{t})$, and $D_B^{B-O-S} = (t_{BO} - t_{BS})/(2\bar{t})$. The retailer's demand of BOPS and store channel in the B-S scenario is $D_B^{B-S} = (2\bar{t} - t_{BS})/(2\bar{t})$ and $D_S^{B-S} = \delta t_{BS}/(2\bar{t})$, respectively.

We assume the retailer's cost of offering BOPS service is negligible. Considering the assumption of $p \leq (2\bar{t} - s)/(1 - \delta)$, the condition for consumers to adopt BOPS service can be rewritten as $p \leq \min(((1 - \theta)s)/(1 - \delta)\theta, (2\bar{t} - s)/(1 - \delta))$. Hence, the retailer's objective is to maximize its profit function with a price constraint:

$$\begin{aligned} \max_p \quad & \hat{\pi}(p) = \hat{D}p, \\ \text{s.t.} \quad & p \leq \min\left(\frac{(1 - \theta)s}{(1 - \delta)\theta}, \frac{2\bar{t} - s}{1 - \delta}\right). \end{aligned} \quad (5)$$

Lemma 3. *The optimal scenario, price, and corresponding demand are shown in Table 2.*

According to Lemma 2, for the B-O-S scenario, the price $\bar{t}(1 - \theta)/(1 - \delta)^2$ which makes the first-order derivative of profit function zero must be lower than $\min((1 - \theta)s/[(1 - \delta)\theta], \bar{t}(1 - \theta)/(1 - \delta)^2)$, and s/θ must be smaller than $2\bar{t}$. The validity condition of price $\bar{t}(1 - \theta)/(1 - \delta)^2$ in B-O-S scenario is $\theta/(1 - \delta) < s/\bar{t} < 2\theta$. If the price $\bar{t}(1 - \theta)/(1 - \delta)^2$ is invalid, the optimal price should be the boundary price.

TABLE 1: The optimal price, demand, and profit in the benchmark model.

δ	s/\bar{t}	Optimal price	Total demand
(0, 1/2]	$(0, (2 - 4\delta)/(1 - \delta)]$	$(2\bar{t} - s(1 - \delta))/(2(1 - \delta)^2)$	$(2\bar{t} - s(1 - \delta))/2\bar{t}$
(0, 1/2]	$((2 - 4\delta)/(1 - \delta), 2]$	$(2\bar{t} - s)/(1 - \delta)$	δ
(1/2, 1)	$(0, 2]$	$(2\bar{t} - s)/(1 - \delta)$	δ

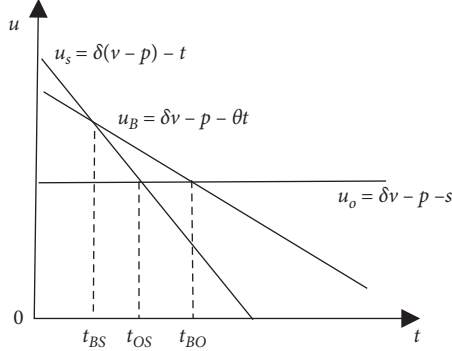


FIGURE 3: Consumers' utility function when offered BOPS.

So, the best prices and the corresponding conditions are shown in Table 2.

According to Balakrishnan et al. [44], the relative cost ratio s/\bar{t} is referred as the channel cost ratio (CCR). Lemma 3 has shown that the optimal channel strategy is determined by the CCR. Low CCR, i.e., $s/\bar{t} < \theta/(1 - \delta)$, implies that the shipment fee is very low compared with the average store visit cost and BOPS service does not have too much advantage. Consumers will buy from the online and store channel but will not adopt BOPS. When CCR is neither low nor high, i.e., $\theta/(1 - \delta) < s/\bar{t} < 2\theta$ for $0 < \delta < 1/2$, the saved shipment fee is relatively high compared with average picking up cost. The advantage of BOPS is so obvious that there are more and more new consumers adopting it. When CCR is high, i.e., $s/\bar{t} > 2\theta$, all of the consumers will not buy from online. Only two options are existing (BOPS and store channel).

In the following sections, we will discuss the effect of BOPS through comparing with the benchmark.

4.3. The Effect of BOPS. Through comparing the profit, demand, and price after offering BOPS with the benchmark, we can get the following proposition.

Proposition 1

- (i) When $0 < \delta \leq (\sqrt{1 - \theta}/2)$, the retailer provides BOPS service to consumers for $(s/\bar{t}) \geq 2(1 - \sqrt{1 - \theta})/(1 - \delta)$
- (ii) When $\sqrt{1 - \theta}/2 < \delta \leq 1/2$, the retailer provides BOPS service to consumers for $s/\bar{t} \geq (4\delta(1 - \delta) - (1 - \theta))/(2\delta(1 - \delta))$
- (iii) When $(1/2) < \delta \leq 1$, the retailer provides BOPS service to consumers for $(s/\bar{t}) \geq 2\theta$

As shown in Figure 4, the retailer should offer BOPS when CCR is higher than a threshold value. Meanwhile, we can also find

the threshold value of CCR increases along with fit probability δ (for the δ smaller than 1/2) and the picking up cost factor θ .

High CCR implies that BOPS is advantageous and more and more new consumers would choose it. As a result, the total demand increases, but the demand of store channel decreases. The profit is higher than that under the benchmark model due to the increased total demand.

Note that there is an important difference between the two purchase processes (buy from store directly vs. BOPS and online channel directly). As shown in Figure 5, when consumers choose to visit store firstly, only δ percent of consumers is translated to the final demand. But all of the consumers who buy online and BOPS are translated into final demand. After offered BOPS, a proportion of consumers who visit the store in the benchmark model is induced to buy though BOPS. The lost demand decreases and the total demand increases compared with the benchmark.

4.4. Numerical Studies

Numerical study 1: we explore the joint impact of shipment fee s and the probability of product fit δ on the profit ratio $\hat{\pi}/\pi$, which is shown in Table 3 and plotted in Figure 6. The following parameters are used: $\bar{t} = 0.6$ and $\theta = 0.4$. From Figure 6, we can find that the profit ratio is bigger than one when the CCR is large enough and the retailer should offer BOPS then. For example, for $\delta = 0.4$, the retailer should offer BOPS if s is bigger than 0.5 and CCR is larger than 5/6. It is interesting to observe that higher fit uncertainty and shipment fee lead to a higher profit ratio.

Numerical study 2: the joint impact of average store visit cost \bar{t} and the picking up cost factor θ on the profit ratio is shown in Table 4 as well as plotted in Figure 7. The following parameters are used: $\delta = 0.9$ and $s = 10$. We can observe from Figure 7 that higher picking up cost factor θ and average store visit cost \bar{t} lead to a lower profit ratio. When picking up cost factor is too high, for example $\theta = 0.9$, the profit ratio is always lower than 1. In this case, the retailer should not offer BOPS.

We will focus on the relationship between the profit ratio and the probability of product fit. As the probability of product fit increases, the lost demand decreases. Therefore, higher probability of product fit leads to lower profit ratio.

The sensitivity of δ , s , \bar{t} , and θ has several important implications. First, everything else being equal, the higher the fit uncertainty and shipping fee, the more likely should the retailer offer BOPS. Second, the retailer can induce the consumers to adopt BOPS by offering more convenience such as drive-through service for BOPS shoppers. That may

TABLE 2: The optimal scenario and the corresponding conditions.

δ	$s\bar{t}$	Scenario	Optimal price	Demand
$(0, 1/2]$	$(0, \theta/(1-\delta)]$	B-O-S	$((1-\theta)s)/((1-\delta)\theta)$	$1 - (s(1-\delta))/(2\theta\bar{t})$
$(0, 1/2]$	$(\theta/(1-\delta), (1-2\delta+\theta)/(1-\delta)]$	B-O-S	$(\bar{t}(1-\theta))/(1-\delta)^2$	$1/2$
$(0, 1/2]$	$((1-2\delta+\theta)/(1-\delta), 2]$	B-S	$(2\bar{t}-s)/(1-\delta)$	$1 - ((2\bar{t}-s)(1-\delta))/(2(1-\theta)\bar{t})$
$(1/2, 1)$	$(0, 2\theta]$	B-O-S	$((1-\theta)s)/((1-\delta)\theta)$	$1 - (s(1-\delta))/2\theta\bar{t}$
$(1/2, 1)$	$(2\theta, 2]$	B-S	$(2\bar{t}-s)/(1-\delta)$	$1 - (((2\bar{t}-s)(1-\delta))/2(1-\theta)\bar{t})$

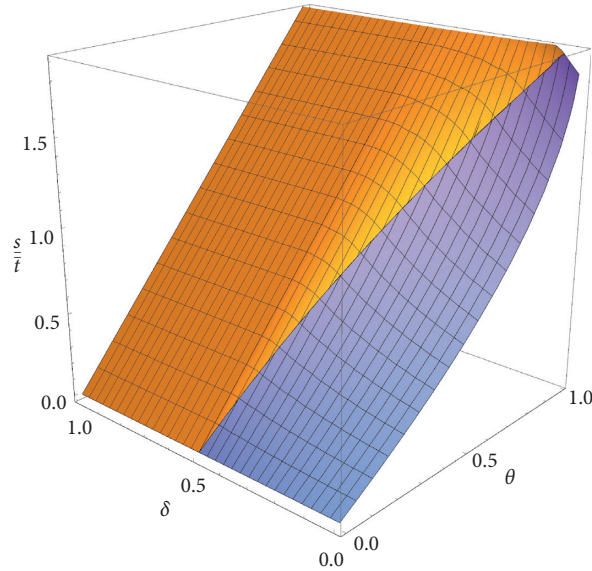


FIGURE 4: The threshold value of CCR above which the retailer should offer BOPS.

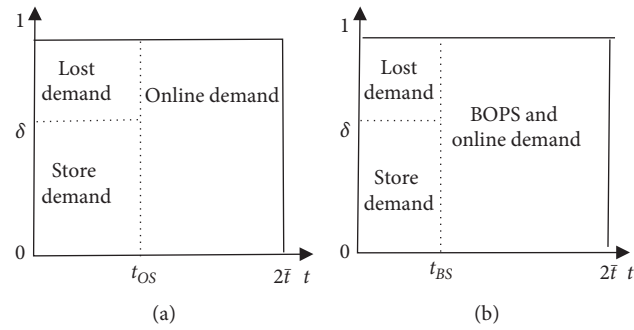


FIGURE 5: The demand allocation of benchmark (a) and the case with BOPS (b).

TABLE 3: The profit ratio $\hat{\pi}/\pi$ given $\bar{t} = 0.6$ and $\theta = 0.4$.

δ	$s = 0.4$	$s = 0.5$	$s = 0.6$	$s = 0.7$	$s = 0.8$
0.1	1.22	1.54	1.98	2.66	3.75
0.2	1.12	1.35	1.67	2.11	2.72
0.3	1.02	1.20	1.42	1.71	2.04
0.4	0.94	1.07	1.25	1.46	1.67
0.5	0.87	1.03	1.17	1.31	1.44
0.6	0.83	1.02	1.11	1.20	1.30
0.7	0.80	1.01	1.07	1.13	1.19
0.8	0.78	1.01	1.04	1.08	1.11
0.9	0.76	1.00	1.02	1.03	1.05

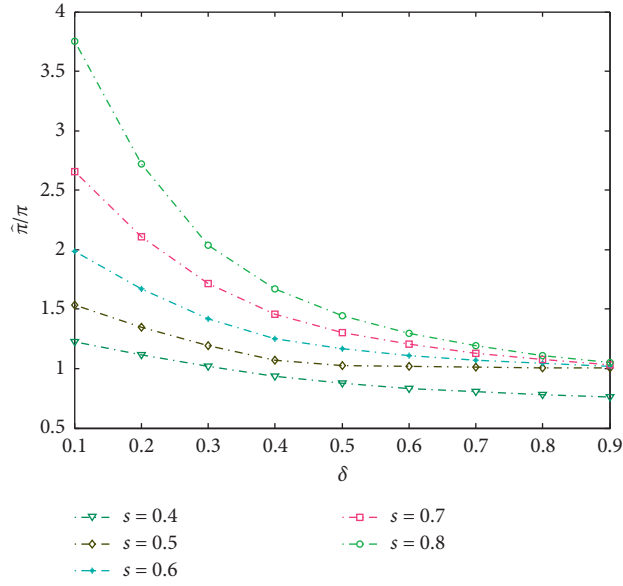


FIGURE 6: The effect of s and δ on the profit ratio $\hat{\pi}/\pi$.

TABLE 4: The profit ratio $\hat{\pi}/\pi$ given $\delta = 0.4$ and $s = 0.3$.

\bar{t}	$\theta = 0.1$	$\theta = 0.3$	$\theta = 0.5$	$\theta = 0.7$	$\theta = 0.9$
0.2	2.08	1.96	1.75	1.25	0.42
0.3	1.67	1.43	1.04	0.61	0.21
0.4	1.46	1.16	0.83	0.50	0.17
0.5	1.33	1.00	0.69	0.34	0.15
0.6	1.25	0.97	0.58	0.28	0.08
0.7	1.19	0.90	0.50	0.24	0.06
0.8	1.14	0.83	0.44	0.21	0.06
0.9	1.11	0.77	0.40	0.18	0.05
1	1.09	0.71	0.36	0.16	0.04

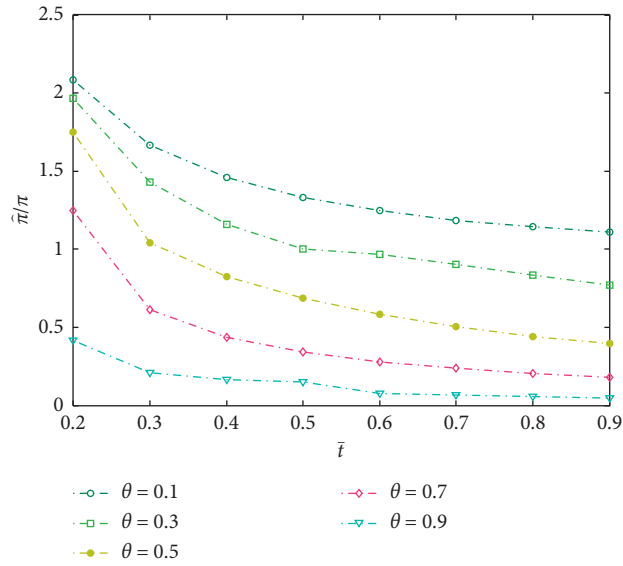


FIGURE 7: The effect of θ and \bar{t} on the profit ratio $\hat{\pi}/\pi$.

TABLE 5: The optimal price and θ .

δ	a	s/\bar{t}	Optimal price and θ
(0, 1/2]	$(0, (4\bar{t}^2(4\bar{t}\delta + s - s\delta - 2\bar{t}))/ (s(2\bar{t} - s)(1 - \delta)))$	$(0, (2 - 4\delta)/(1 - \delta))$	$(\bar{t}^2/(2a(1 - \delta)^4), 1 - \bar{t}/(2a(1 - \delta)^2))$
(0, 1/2]	$(0, (4\bar{t}^2(4\bar{t}\delta + s - s\delta - 2\bar{t}))/ (s(2\bar{t} - s)(1 - \delta)))$	$((2 - 4\delta)/(1 - \delta), 2)$	$((2\bar{t} - s)/(1 - \delta), 1 - ((2\bar{t} - s)^2/2a\bar{t})^{1/3})$
(0, 1/2]	$((4\bar{t}^2(4\bar{t}\delta + s - s\delta - 2\bar{t}))/ (s(2\bar{t} - s)(1 - \delta)), 4\bar{t}^2/(2\bar{t} - s))$	$(0, 2)$	$(\bar{t}^2/(2a(1 - \delta)^4), 1 - \bar{t}/(2a(1 - \delta)^2))$
(0, 1/2]	$(4\bar{t}^2/(2\bar{t} - s), +\infty)$	$(0, 2)$	$((1 - \theta)s/(1 - \delta)\theta, 1)$
(1/2, 1)	$(0, (4\bar{t}^2(4\bar{t}\delta + s - s\delta - 2\bar{t}))/ (s(2\bar{t} - s)(1 - \delta)))$	$(0, 2)$	$((2\bar{t} - s)/(1 - \delta), 1 - ((2\bar{t} - s)^2/2a\bar{t})^{1/3})$
(1/2, 1)	$((4\bar{t}^2(4\bar{t}\delta + s - s\delta - 2\bar{t}))/ (s(2\bar{t} - s)(1 - \delta)), +\infty)$	$(0, 2)$	$((1 - \theta)s/(1 - \delta)\theta, 1)$

TABLE 6: The feasible regions of s/\bar{t} where the retailer should offer BOPS.

Case no.	δ	a	Feasible region of s/\bar{t}
III	(0, 1/2]	$(0, (4\bar{t}^2(4\bar{t}\delta + s - s\delta - 2\bar{t}))/ (s(2\bar{t} - s)(1 - \delta)))$	$((2 - 4\delta)/(1 - \delta), 2)$
III	(0, 1/2]	$((4\bar{t}^2(4\bar{t}\delta + s - s\delta - 2\bar{t}))/ (s(2\bar{t} - s)(1 - \delta)), \bar{t}/(16\delta^2(1 - \delta)^2))$	$(\max((2(1 - \delta) - \sqrt{\bar{t}/a})/(1 - \delta)^2), 0), 2)$
II	(0, 1/2]	$(\bar{t}/(16\delta^2(1 - \delta)^2), 4\bar{t}^2/(2\bar{t} - s))$	$(2 - (\bar{t}/(8a(1 - \delta)^3\delta)), 2)$
II	(0, 1/2]	$(4\bar{t}^2/((2\bar{t} - s)), +\infty)$	\emptyset
I	(1/2, 1)	$(0, 16\bar{t}/27)$	$(0, 2)$
III	(1/2, 1)	$(16\bar{t}/27, (4\bar{t}^2(4\bar{t}\delta + s - s\delta - 2\bar{t}))/ (s(2\bar{t} - s)(1 - \delta)))$	$((\bar{t}(108a - 64\bar{t}))/54a), 2)$
II	(1/2, 1)	$((4\bar{t}^2(4\bar{t}\delta + s - s\delta - 2\bar{t}))/ (s(2\bar{t} - s)(1 - \delta)), +\infty)$	\emptyset

be the main reason why Tesco and other grocery stores offer the drive-through service for BOPS shoppers [45].

5. Extension: The Optimal Convenience Degree

High convenience degree will incentivize more consumers to adopt the BOPS but also lead to higher costs. If we assume the retailer's cost of offering convenience for BOPS users is not negligible, the retailer should jointly determine the price and the convenience degree of BOPS. Then, the profit of the retailer is given by

$$\begin{aligned} \max_{(p, \theta)} \quad & \pi(p, \theta) = Dp - \frac{a(1 - \theta)^2}{2}, \\ \text{s.t.} \quad & p \leq \min\left(\frac{(1 - \theta)s}{(1 - \delta)\theta}, \frac{2\bar{t} - s}{1 - \delta}\right), \end{aligned} \quad (6)$$

where a refers to a positive cost factor. $a(1 - \theta)^2/2$ is the cost of offering convenience for the BOPS adopters, which means the cost becomes higher as the convenience degree $1 - \theta$ increases. Similar approaches to modeling service effort have been used extensively in the literature (see, e.g., Ofek et al. [31]).

5.1. The Profit and Equilibrium Solution with BOPS. Similar to Section 4, there are two scenarios (B-O-S or B-S) with BOPS offering. Setting up Lagrange Functions and using the KKT conditions to discuss each scenario, we can obtain the optimal price and θ .

Lemma 4. *The optimal price and θ are summarized in Table 5.*

5.2. The Effect of BOPS

Proposition 2. *The feasible regions of s/\bar{t} in which the retailer should provide BOPS service to consumers are given in Table 6.*

- (I) *When the cost factor a is sufficiently low, the retailer should always offer BOPS*
- (II) *When the cost factor a is sufficiently high, the retailer should never offer BOPS*
- (III) *Otherwise, the retailer should offer BOPS when CCR is high enough*

6. Conclusion and Future Research

In this paper, we built an analytic model where a retailer sells a product with fit uncertainty through online, store, or BOPS channels. The primary objective of this paper is to examine the effect of BOPS and the strategies of offering BOPS service from a retailer's point of view.

Our main results are as follows. Even if the cost of providing BOPS service is zero, the retailer should not offer BOPS fit when the CCR is low. This is because when the CCR is low, there are fewer consumers who would choose BOPS unless the retailer lowers the price, which leads to a lower profit. When the CCR is high, the total demand and the profit improve but BOPS will cannibalize the store channel. Hence, that retailer should be cautious about offering the BOPS when CCR is under a threshold value. The retailer needs to improve the convenience degree of BOPS and help consumers reduce the picking up cost. Another interesting result is that the higher likelihood of product fit will result in a lower profit ratio $\tilde{\pi}/\pi$. When the cost of offering convenience for BOPS users is not negligible, the retailer should offer BOPS only when the cost factor is not very high but CCR is high enough. It is better to offer a higher convenience degree of BOPS if the average store visit cost and the probability of product fit are high.

There can be multiple directions for future research. First, in our paper, product return is not allowed. As consumer return is an important practice and the majority of retailers do allow consumers to return unfit products, future research might jointly consider the BOPS and product return. Second, in this paper, we limit ourselves to the case of a single retailer. As offering the BOPS service will impact retailer competition, it is worthwhile to investigate how BOPS may affect the competition of multiple retailers and their profits. Third, BOPS can be studied together with issues like manufacturer encroachment [46], supply chain design [47], and corporate social responsibility [48].

Appendix

A. Proof of Lemma 1

From $t_{OS} \leq 2\bar{t}$, we can get $0 < p \leq p_0 = (2\bar{t} - s)/(1 - \delta)$ and $2\bar{t} < s$.

The profit is $\Pi = p(2\bar{t} - p(1 - \delta)^2 + s\delta - s)/2t$.

$\partial^2 \Pi / \partial p^2 = -(1 - \delta)^2 / \bar{t} < 0$; when $\partial \Pi / \partial p = 0$, we can get $p = (2\bar{t} - s(1 - \delta)) / (2(1 - \delta)^2) = p_2$.

So the optimal price $p_0^* = \min(p_2, p_0)$. When $0 < \delta < (1/2)$ and $0 < (s/\bar{t}) < (2 - 4\delta)/(1 - \delta)$, $p_2 < p_0$ and $p_0^* = p_2$. Otherwise, $p_2 < p_0$ and $p_0^* = p_0$. Q.E.D

B. Proof of Lemma 2

We can get that the consumers cost $t_1 < t \leq t_0$ and $t_0 < t \leq t_2$ will adopt the BOPS.

So, the demand of BOPS exists when $t_1 \leq 2\bar{t}$ and $t_1 \leq t_0$ or $t_0 \leq t_2$.

$2\bar{t} - t_1 = (2\bar{t}(1 - \theta) - p(1 - \delta)) / (1 - \theta)$. So when $2\bar{t}(1 - \theta) \geq p(1 - \delta)$, which means $p \leq (2\bar{t}(1 - \theta)) / ((1 - \delta)) \stackrel{\text{def}}{=} p_5$, $t_1 \leq 2\bar{t}$.

$t_0 - t_1 = (s(1 - \theta) - p(1 - \delta)\theta) / (1 - \theta)$; $t_2 - t_0 = (s(1 - \theta) - p(1 - \delta)\theta) / \theta$. So when $s(1 - \theta) \geq p(1 - \delta)\theta$, which means $p \leq (1 - \theta)s / (1 - \delta)\theta \stackrel{\text{def}}{=} p_3$, $t_1 \leq t_0$ and $t_0 \leq t_2$.

The demand of BOPS exists when $t_2 = (s/\theta) \leq 2\bar{t}$, which means $(s/\bar{t}) < 2\theta$, $t_2 \leq 2\bar{t}$. Q.E.D

C. Proof of Lemma 3

The profit is $\pi^S = p - (p^2(1 - \delta)^2) / (2\bar{t}(1 - \theta))$. $\partial^2 \Pi / \partial p^2 = -\bar{t}(1 - \theta) / (1 - \delta)^2 < 0$. When $\partial \Pi / \partial p = 0$, we can get $p = \bar{t}(1 - \theta) / (1 - \delta)^2 = p_4$. When p_4 is the optimal price, the condition of B-O-R scenario is $p_4 \leq p_3$ and $(s/\theta) \leq 2\bar{t}$. And $p_4 - p_3 = (1 - \theta)(s(1 - \delta) - \bar{t}\theta) / (1 - \delta)^2\theta$. Hence, when $s(1 - \delta) - \bar{t}\theta > 0$, which means $s/\bar{t} \geq \theta / (1 - \delta)$, $p_4 \leq p_3$. So the corresponding region of B-O-R scenario is $(\theta / (1 - \delta)) \leq (s/\bar{t}) \leq 2\theta$ and $0 < \delta < (1/2)$.

When $p_4 > p_3$, the optimal price is p_3 . And the corresponding region of B-O-R scenario is $(s/\bar{t}) \leq 2\theta$ when $\delta > (1/2)$ or $(s/\bar{t}) \leq \theta / (1 - \delta)$ when $\delta < (1/2)$.

The condition of O-R scenario can be obtained similarly. Q.E.D

D. Proof of Proposition 1

We prove Proposition 1 by 4 parts according to the value region of δ : $0 < \delta < (1 - \theta) / (2 - \theta)$, $(1 - \theta) / (2 - \theta) < \delta < (2 - \theta) / 4$, $(2 - \theta) / 4 < \delta < (1/2)$, and $(1/2) < \delta < 1$.

Part 1: $0 < \delta < (1 - \theta) / (2 - \theta)$

When $\delta < (1 - \theta) / (2 - \theta)$, we can get $\theta / (1 - \delta) < 2\theta < (2 - 4\delta) / (1 - \delta)$.

We will discuss the changes in profit, demand, and price in turn. First, let us discuss the change in profit. When $0 < \delta < (1 - \theta) / (2 - \theta)$ and $s/\bar{t} \leq \theta / (1 - \delta)$, we should compare $\pi^{\text{BOR}}(p_3)$ with $\pi(p_2)$:

$$\pi^{\text{BOR}}(p_3) - \pi(p_2) = \frac{(s(1 - \delta)(2 - \theta) - 2\bar{t}\theta)^2}{8\bar{t}(1 - \delta)^2\theta^2} < 0. \quad (\text{D.1})$$

When $\theta / (1 - \delta) < (s/\bar{t}) \leq (2 - 4\delta) / (1 - \delta)$, we should compare $\pi^{\text{BOR}}(p_4)$ with $\pi(p_2)$:

$$\pi^{\text{BOR}}(p_4) - \pi(p_2) = \frac{4s\bar{t}(1 - \delta) - s^2(1 - \delta)^2 - 4\bar{t}^2\theta}{8\bar{t}(1 - \delta)^2}. \quad (\text{D.2})$$

When $4s\bar{t}(1 - \delta) - s^2(1 - \delta)^2 - 4\bar{t}^2\theta < 0$, which means $(s/\bar{t}) < 2(1 - \sqrt{1 - \theta}) / (1 - \delta)$, $\pi^{\text{BOR}}(p_4) < \pi(p_2)$.

When $(s/\bar{t}) > 2(1 - \sqrt{1 - \theta}) / (1 - \delta)$, $\pi^{\text{BOR}}(p_4) > \pi(p_2)$.

The change in demand is discussed as follows:

$$\begin{aligned} D^S(p_4) - D_0(p_2) &= \frac{s(1 - \delta)}{4\bar{t}} > 0, \\ D_{S0}(p_2) - D_S^{\text{BOR}}(p_4) &= D_{S0}(p_2) - D_S^{\text{BOR}}(p_4) = \frac{s\delta}{4\bar{t}} > 0, \\ D_{O0}(p_2) - D_O^{\text{BOR}}(p_4) &= \frac{s(1 - \delta)(2 - \theta) - 2\bar{t}\theta}{4\bar{t}(1 - \delta)\theta}. \end{aligned} \quad (\text{D.3})$$

If $s(1 - \delta)(2 - \theta) - 2\bar{t}\theta > 0$, i.e., $2\delta / (1 - \delta)(2 - \theta) < (s/\bar{t})$, we can get $D_{O0}(p_2) > D_O^{\text{BOR}}(p_4)$.

Because $2\delta / (1 - \delta)(2 - \theta) > 2(1 - \sqrt{1 - \theta}) / (1 - \delta)$, the demand of online channel will decrease when $2(1 - \sqrt{1 - \theta}) / (1 - \delta) < (s/\bar{t}) < 2\delta / (1 - \delta)(2 - \theta)$ but increase when $2\delta / (1 - \delta)(2 - \theta) < (s/\bar{t}) < (2 - 4\delta) / (1 - \delta)$.

We will discuss the change in price as follows:

$$p_4 - p_2 = \frac{s(1 - \delta) - 2\bar{t}\theta}{2(1 - \delta)^2}, \quad \text{when } \frac{2\theta}{(1 - \delta)} < \frac{s}{\bar{t}}, p_4 > p_2. \quad (\text{D.4})$$

Because $2\theta / (1 - \delta) > (2(1 - \sqrt{1 - \theta})) / (1 - \delta)$, the price will decrease when $(2(1 - \sqrt{1 - \theta})) / (1 - \delta) < (s/\bar{t}) < 2\theta / (1 - \delta)$ but increase when $2\theta / (1 - \delta) < (s/\bar{t}) < (2 - 4\delta) / (1 - \delta)$.

Similarly, we can get the change in profit, demand, and price when $(2 - 4\delta) / (1 - \delta) < (s/\bar{t}) \leq 2$.

When $0 < \delta < (1 - \theta) / (2 - \theta)$ and $(2 - 4\delta) / (1 - \delta) < (s/\bar{t}) \leq 2$, we should compare $\pi^{\text{BOR}}(p_4)$ with $\pi(p_0)$:

$$\pi^{BOR}(p_4) - \pi(p_0) = \frac{(s(1-\delta) - \bar{t}(1-2\delta + \theta))^2}{2t8(1-\delta)^2(1-\theta)} > 0. \quad (D.5)$$

So, we can get that when $0 < \delta < (1-\theta)/(2-\theta)$, the retailer can get more profit than benchmark with offering BOPS service if $(s/\bar{t}) > 2(1-\sqrt{1-\theta})/(1-\delta)$. Otherwise, the retailer should better not offer BOPS:

$$\begin{aligned} D^S(p_4) - D_0(p_0) &= \frac{1}{2} - \delta > 0, \\ D_{S0}(p_0) - D_S^{BR}(p_4) &= \frac{\delta(1-2\delta)}{2(1-\delta)} > 0, \\ p_4 - p_0 &= \frac{s(1-\delta) + \bar{t}(2\delta - 1 - \theta)}{(1-\delta)^2}, \quad \text{when} \\ &\frac{1-2\delta + \theta}{(1-\delta)} < \frac{s}{\bar{t}}, p_4 > p_2. \end{aligned} \quad (D.6)$$

Because when $(1-\theta)/2 < \delta$, $(1-2\delta + \theta)/(1-\delta) > (2-4\delta)/(1-\delta)$. When $(1-\theta)/2 < \delta < (1-\theta)/(2-\theta)$, the price will decrease if $(2-4\delta)/(1-\delta) < (s/\bar{t}) < (1-2\delta + \theta)/(1-\delta)$ but increase when $(1-2\delta + \theta)/(1-\delta) < (s/\bar{t}) < 2$. When $0 < \delta < (1-\theta)/2$, the price will increase.

The change in profit, demand, and price of other four parts can be obtained similarly.

E. Proof of Lemma 4

$\pi(p'_5, \theta_5) - \pi(p'_3, \theta_3) = (a(2\bar{t} - s)(1-\delta) - 4\bar{t}^2\delta)^2/8a\bar{t}^2(1-\delta)^2 \geq 0$. So, the optimal strategy is (p'_5, θ_5) .
 $\pi(p'_4, \theta_4) - \pi(p_6, \theta_3) = (\bar{t}^2 + a(s-2\bar{t})(1-\delta))^2/(8a\bar{t}^2(1-\delta)^4) \geq 0$. So, the optimal strategy is (p'_4, θ_4) .
 $\pi(p_5, \theta_5) - \pi(p_3, \theta_3) \geq 0$; so, we can get the optimal strategy.

F. Proof of Proposition 2

$$\pi(p'_4, \theta_4) - \pi(p_2) = \frac{\bar{t}^3 - a(2\bar{t} - s(1-\delta))^2(1-\delta)^2}{8a\bar{t}(1-\delta)^4}. \quad (F.1)$$

When $(2(1-\delta) - \sqrt{t/a})/(1-\delta)^2 < (s/\bar{t})$, $\pi(p'_4, \theta_4) > \pi(p_2)$.

When $a < \bar{t}/(16\delta^2(1-\delta)^2)$, $(2(1-\delta) - \sqrt{t/a})/(1-\delta)^2 < (2-4\delta)/(1-\delta)$. The profit will increase for $(2(1-\delta) - \sqrt{t/a})/(1-\delta)^2 < (s/\bar{t})$:

$$\pi(p'_4, \theta_4) - \pi(p_0) = \frac{\bar{t}^2 + 8a\delta(1-\delta)^3(s-2\bar{t})}{8a(1-\delta)^4}. \quad (F.2)$$

When $2 - (\bar{t}/(8a(1-\delta)^3\delta)) < (s/\bar{t})$, $\pi(p'_4, \theta_4) > \pi(p_0)$; the profit will increase for $\max((2(1-\delta) - \sqrt{t/a})/(1-\delta)^2, (2-4\delta)/(1-\delta)) < (s/\bar{t})$:

$$\pi(p'_5, \theta_5) - \pi(p_2) = \frac{16\bar{t}^3\delta^2 - a(2\bar{t} - s(1-\delta))^2}{8a\bar{t}(1-\delta)^2}. \quad (F.3)$$

When $a < (16\bar{t}^3\delta^2)/(2\bar{t} - s(1-\delta))^2$, $\pi(p'_5, \theta_5) > \pi(p_2)$:

$$\pi(p'_5, \theta_5) - \pi(p_0) = \frac{\delta(a(s-2\bar{t})(1-\delta) + 2\bar{t}^2\delta)}{a(1-\delta)^2}. \quad (F.4)$$

When $2 - \bar{t}/(8a(1-\delta)^3\delta) < (s/\bar{t})$, $\pi(p'_5, \theta_5) > \pi(p_0)$:

$$\pi(p'_5, \theta_5) - \pi(p_2) = -\frac{a(s-2\bar{t})^2(1-\delta)^2 + \bar{t}(s-2\bar{t} - s\delta + 4\bar{t}\delta)^2}{8\bar{t}^2(1-\delta)^2} < 0,$$

$$\pi(p'_5, \theta_5) - \pi(p_0) = -\frac{a(s-2\bar{t})^2}{8\bar{t}^2} < 0. \quad (F.5)$$

Data Availability

Data will be available upon request.

Conflicts of Interest

The authors declare that they have no conflicts of interest.

Acknowledgments

This research was supported by the National Natural Science Foundation of China (71871186 and 71471150), the Project for Guizhou Provincial Department of Education (2018qn09), and the Fundamental Research Funds for the Central Universities (JBK18JYT02 and JBK1902009). Kang's research was supported by Application-Oriented Undergraduate Majors of Shanghai Universities (Round 4; #20) and the National Social Science Fund of China (#18BGL115).

References

- [1] B. Yellavali, D. Holt, and A. Jandial, "Retail Multi-Channel Integration, Delivering a Seamless Customer Experience," Infosys Technologies Ltd, Dallas, TX, USA, 2004.
- [2] DMA, "Multichannel Marketing Report," The Direct Marketing Association, New York, NY, USA, 2005.
- [3] D. Rigby, "The future of shopping," *Harvard Business Review*, vol. 89, no. 12, pp. 65–76, 2011.
- [4] Retail & Ecommerce, "Why retailers should offer buy online, pick up in-store," *Retail & Ecommerce*, vol. 8, 2015.
- [5] L. Chao, "Target Says Online Sales Surge Tied to Store Inventories; with Digital Sales up 34% Last Quarter, the Retailer Says in-Store Pickups were Central to Both e Commerce and Store Sales Growth," Wall Street Journal, New York, NY, USA, 2016.
- [6] S. Gallino and A. Moreno, "Integration of online and offline channels in retail: the impact of sharing reliable inventory availability information," *Management Science*, vol. 60, no. 6, pp. 1434–1451, 2014.
- [7] J. Cao, K. C. So, and S. Yin, "Impact of an "online-to-store" channel on demand allocation, pricing and profitability," *European Journal of Operational Research*, vol. 248, no. 1, pp. 234–245, 2016.
- [8] F. Gao and X. Su, "Omni-channel retail operations with buy-online-and-pickup-in-store," *Management Science*, vol. 63, no. 8, pp. 2478–2492, 2016.

- [9] M. Jin, G. Li, and T. C. E. Cheng, "Buy online and pick up in-store: design of the service area," *European Journal of Operational Research*, vol. 268, no. 2, pp. 613–623, 2018.
- [10] X. Shi, C. Dong, and T. C. E. Cheng, "Does the buy-online-and-pick-up-in-store strategy with pre-orders benefit a retailer with the consideration of returns?" *International Journal of Production Economics*, vol. 206, pp. 134–145, 2018.
- [11] P. Song, Q. Wang, H. Liu, and Q. Li, "The value of buy-online-and-pickup-in-store in omni-channel: evidence from customer usage data," *Production and Operations Management*, vol. 29, no. 4, pp. 995–1010, 2019.
- [12] Y. Hong and P. A. Pavlou, "Product fit uncertainty in online markets: nature, effects, and antecedents," *Information Systems Research*, vol. 25, no. 2, pp. 328–344, 2014.
- [13] T. Xiao and J. Shi, "Consumer returns reduction and information revelation mechanism for a supply chain," *Annals of Operations Research*, vol. 240, no. 2, pp. 661–681, 2016.
- [14] J. Shin, "How does free riding on customer service affect competition?" *Marketing Science*, vol. 26, no. 4, pp. 488–503, 2007.
- [15] J. Kim and S. Forsythe, "Adoption of virtual try-on technology for online apparel shopping," *Journal of Interactive Marketing*, vol. 22, no. 2, pp. 45–59, 2008.
- [16] D. R. Bell, S. Gallino, and A. Moreno, "How to win in an Omni-channel world," *Mit Sloan Management Review*, vol. 56, no. 1, pp. 45–53, 2014.
- [17] P. Chatterjee, "Causes and consequences of "order online pick up in-store" shopping behavior," *The International Review of Retail, Distribution and Consumer Research*, vol. 20, no. 4, pp. 431–448, 2010.
- [18] S. Balasubramanian, "Mail versus mall: a strategic analysis of competition between direct marketers and conventional retailers," *Marketing Science*, vol. 17, no. 3, pp. 181–195, 1998.
- [19] F. Bernstein, J.-S. Song, and X. Zheng, "'Bricks-and-mortar' vs. 'clicks-and-mortar': an equilibrium analysis," *European Journal of Operational Research*, vol. 187, no. 3, pp. 671–690, 2008.
- [20] Z. Li, Q. Lu, and M. Talebian, "Online versus bricks-and-mortar retailing: a comparison of price, assortment and delivery time," *International Journal of Production Research*, vol. 53, no. 13, pp. 3823–3835, 2015.
- [21] S. Gallino, A. Moreno, and I. Stamatopoulos, "Channel integration, sales dispersion, and inventory management," *Management Science*, vol. 63, no. 9, pp. 2813–2831, 2017.
- [22] D. R. Bell, S. Gallino, and A. Moreno, "Offline showrooms in omnichannel retail: demand and operational benefits," *Management Science*, vol. 64, no. 4, pp. 1629–1651, 2018.
- [23] R. Zhou, Y. Liao, W. Shen, and S. Yang, "Channel selection and fulfillment service contracts in the presence of asymmetric service information," *International Journal of Production Economics*, vol. 222, Article ID 107504, 2020.
- [24] W.-y. K. Chiang, D. Chhajed, and J. D. Hess, "Direct marketing, indirect profits: a strategic analysis of dual-channel supply-chain design," *Management Science*, vol. 49, no. 1, pp. 1–20, 2003.
- [25] K.-Y. Chen, M. Kaya, and Ö. Özer, "Dual sales channel management with service competition," *Manufacturing & Service Operations Management*, vol. 10, no. 4, pp. 654–675, 2008.
- [26] G. Cai, "Channel selection and coordination in dual-channel supply chains," *Journal of Retailing*, vol. 86, no. 1, pp. 22–36, 2010.
- [27] Y.-W. Zhou, J. Guo, and W. Zhou, "Pricing/service strategies for a dual-channel supply chain with free riding and service-cost sharing," *International Journal of Production Economics*, vol. 196, no. 196, pp. 198–210, 2018.
- [28] L.-B. Oh, H.-H. Teo, and V. Sambamurthy, "The effects of retail channel integration through the use of information technologies on firm performance," *Journal of Operations Management*, vol. 30, no. 5, pp. 368–381, 2012.
- [29] E. Brynjolfsson, Y. J. Hu, and M. S. Rahman, "Competing in the age of Omni-channel retailing," *MIT Sloan Management Review*, vol. 54, no. 4, p. 23, 2013.
- [30] S. Mahar, P. D. Wright, K. M. Bretthauer, and R. P. Hill, "Optimizing marketer costs and consumer benefits across "clicks" and "bricks"," *Journal of the Academy of Marketing Science*, vol. 42, no. 6, pp. 619–641, 2014.
- [31] E. Ofek, Z. Katona, and M. Sarvary, "'Bricks and clicks:" the impact of product returns on the strategies of multichannel retailers," *Marketing Science*, vol. 30, no. 1, pp. 42–60, 2011.
- [32] J. Chen and B. Chen, "Competing with customer returns policies," *International Journal of Production Research*, vol. 54, no. 7, pp. 2093–2107, 2016.
- [33] O. Shy, "Window shopping," 2014.
- [34] B. Jing, "Showrooming and webrooming: information externalities between online and offline sellers," *Marketing Science*, vol. 37, no. 3, pp. 469–483, 2018.
- [35] A. Heiman, B. McWilliams, and D. Zilberman, "Demonstrations and money-back guarantees: market mechanisms to reduce uncertainty," *Journal of Business Research*, vol. 54, no. 1, pp. 71–84, 2001.
- [36] B. McWilliams, "Money-back guarantees: helping the low-quality retailer," *Management Science*, vol. 58, no. 8, pp. 1521–1524, 2012.
- [37] B. Chen and J. Chen, "When to introduce an online channel, and offer money back guarantees and personalized pricing?" *European Journal of Operational Research*, vol. 257, no. 2, pp. 614–624, 2017.
- [38] Y. Chen and J. Xie, "Online consumer review: word-of-mouth as a new element of marketing communication mix," *Management Science*, vol. 54, no. 3, pp. 477–491, 2008.
- [39] H. Risselada, L. De Vries, and M. Verstappen, "The impact of social influence on the perceived helpfulness of online consumer reviews," *European Journal of Marketing*, vol. 52, no. 3/4, pp. 619–636, 2018.
- [40] C. Matt and T. Hess, "Product fit uncertainty and its effects on vendor choice: an experimental study," *Electronic Markets*, vol. 26, no. 1, pp. 1–11, 2016.
- [41] T. Doganoglu, "Switching costs, experience goods and dynamic price competition," *Quantitative Marketing and Economics*, vol. 8, no. 2, pp. 167–205, 2010.
- [42] B. Edelman, S. Jaffe, and S. D. Kominers, "To Groupon or not to Groupon: the profitability of deep discounts," *Marketing Letters*, vol. 27, no. 1, pp. 39–53, 2016.
- [43] Z. Gu and Y. Liu, "Consumer fit search, retailer shelf layout, and channel interaction," *Marketing Science*, vol. 32, no. 4, pp. 652–668, 2013.
- [44] A. Balakrishnan, S. Sundaresan, and B. Zhang, "Browse-and-Switch: retail-online competition under value uncertainty," *Production and Operations Management*, vol. 23, no. 7, pp. 1129–1145, 2014.
- [45] C. Passariello, "In France, a Drive-up Grocery Takes Off—Modifying an Old Model, Online Food Retailer Chrono Drive Drops the Delivery but Keeps the Web Ordering," *Wall Street Journal*, New York, NY, USA, 2010.
- [46] J. Li, L. Yi, V. Shi, and X. Chen, "Supplier encroachment strategy in the presence of retail strategic inventory: centralization or decentralization?" *Omega*, 2020.

- [47] Y. Liao, A. Diabat, C. Alzaman, and Y. Zhang, "Modeling and heuristics for production time crashing in supply chain network design," *Annals of Operations Research*, vol. 288, no. 1, pp. 331–361, 2020.
- [48] J. Bian, Y. Liao, Y. Y. Wang, and F. Tao, "Analysis of firm CSR strategies," *European Journal of Operational Research*, 2020.

Research Article

Risk Evaluation of Sewage Treatment PPPABS Projects Using Combination Weight Method and D-S Evidence Theory

Hui Zhao , Zehui Bu, and Shengbin Ma

School of Management Engineering, Qingdao University of Technology, Qingdao 266520, China

Correspondence should be addressed to Hui Zhao; zhaohui43@126.com

Received 4 May 2020; Accepted 28 May 2020; Published 3 July 2020

Guest Editor: Lei Xie

Copyright © 2020 Hui Zhao et al. This is an open access article distributed under the Creative Commons Attribution License, which permits unrestricted use, distribution, and reproduction in any medium, provided the original work is properly cited.

In order to make up for the shortage of public-private partnership (PPP) model, more and more sewage treatment PPP projects have adopted the asset-backed securitization (ABS) model. To ensure success of sewage treatment PPPABS projects, risk evaluation, which has remained scarcity and unscientific, is becoming an urgent problem to be solved. Firstly, this paper identifies critical risk factors by literature analysis and expert interview. The final risk system is established from the perspectives of macrorisks, basic asset risks, transaction structure risks, operational risks, and other risks, which include 17 second risk factors. Then, the overall risk evaluation method is proposed based on combination weight method and Dempster-Shafer (D-S) evidence theory. Next, Beijing capital Co. Ltd. sewage treatment PPPABS project as a case is employed to verify the feasibility and effectiveness of the proposed method. Finally, awareness of existing risks, suggestions from law risk, quality risk, underwriting and issue risk, and credit enhancement are provided for sewage treatment PPPABS projects. All above studies are expected to provide helpful references for evaluating overall risk of sewage treatment PPPABS projects.

1. Introduction

With the global emphasis on environmental protection and sustainable development, water saving and sewage treatment are becoming necessary and urgent issues [1, 2]. The water environment is the basis for the survival of residents. In addition, the water environment treatment is an important task for the government to build a harmonious society [3]. However, the current capacity for sewage treatment is relatively low. In order to curb the adverse effects of environmental pollution due to the uncontrolled discharge of sewage, effective measures must be taken to ensure that the discharge of sewage meets the required standards [4]. Sewage treatment projects play a key role in environmental protection and sustainable development plans as an effective way to reduce sewage and protect environment [5]. However, such progress is constrained by a shortage of funds. Constructing a sewage treatment project usually costs a large capital investment and has an extensive project period. Only relying on government investment in sewage treatment projects is very difficult if the local government has a high level of debt [6].

The public-private partnership (PPP) model has been adopted and developed rapidly in sewage treatment projects in recent years. As a cooperative mechanism, PPP enables the government and the private sector, with different degrees of rights and responsibilities, to provide more efficient infrastructure products and public services through mutually complementary cooperation. In Germany, one-third of all sewage treatment projects employ the PPP model. During 2013, the White House Council on Environmental Quality held a seminar where various representatives suggested that local government should apply the PPP model to provide financial resources for sewage disposal. From then on, many sewage treatment projects in America have applied the PPP model [7]. Especially in China, a large amount of sewage treatment projects have adopted the PPP model. The number of sewage treatment PPP projects entering project library of China Public Private Partnerships Center (CPPPC) has soared to 951 during 2014–2018. However, in practice, PPP projects have problems such as long operating cycle, large investment, high financing cost, poor liquidity of assets, and unsound exit mechanism, which make the private

participants very cautious, and the actual implementation rate of the project is not high [6]. Taking the 951 sewage treatment PPP projects in China, for example, less than 10 percent of the 951 projects enter the implementation phase.

To overpass these outstanding barriers and further enrich the financing innovation, asset-backed securitization (ABS) mode supported by government policies is widely recognized and rapidly developed in PPP projects [8]. Especially in China, China's National Development and Reform Commission, Ministry of Finance, and other relevant departments have issued a series of documents for encouraging infrastructures with PPP mode to adopt ABS [9]. Until 20 April, 2020, 21 PPP projects, including sewage treatment PPP projects, implemented ABS and the issuance scale exceeded 2.95 billion dollars. Asset-backed securitization of sewage treatment PPP projects is becoming an important channel to solve the development dilemma of sewage treatment projects.

Asset-backed securitization has been used in the capital market for many years, but the combination of asset-backed securitization and PPP model is still a new pattern. What is the PPPABS? It is not until 2016 that PPPABS was first defined in China. Public-private partnership asset-backed securitization (PPPABS) projects usually involve huge capital, exclusive capital, and many participants. Moreover, the PPPABS projects take the project assets and their income as the only or main source of repayment and have the characteristics of nonrecourse or limited recourse. All these characteristics determine the complexity and particularity of the risks in PPPABS projects. However, research on risk evaluation of PPPABS projects is limited and unscientific. Therefore, to ensure the success of sewage treatment PPPABS projects, it is very important and necessary to achieve what risk factors affect sewage treatment PPPABS projects and propose an appropriate method to evaluate overall risk of sewage treatment PPPABS projects.

At present, risk factors and management are the focus research of PPPABS projects by the researchers. Some scholars have focused on the composition of risk factors of PPPABS projects [10–13]. How to eliminate the risk before the occurrence and how to control the risk after the occurrence? Others have made a comprehensive analysis from various aspects or perspectives and put forward some effective preventive measures and risk control theory [13–15]. However, through reviewing the existing literature, it is found that no one has constructed the risk evaluation system for sewage treatment PPPABS projects. It is also found that the management of PPPABS projects is almost qualitative and lacks quantitative research, especially in evaluating the overall risk of sewage treatment PPPABS projects. How to overcome these issues? The present study can fill this research gap.

This paper makes the following practical and academic contributions. Firstly, aiming at the problem of imperfect risk evaluation system for sewage treatment PPPABS projects, we construct a risk evaluation system specially applicable to sewage treatment PPPABS projects through literature review and expert interview. Secondly, in view of the insufficiency of the current methods of determining the

risk factor weight in PPPABS projects, to be more scientific and reasonable, we propose a combination weight method (combining G1 method and the entropy method), which lays a solid foundation for the next scientific risk evaluation. Thirdly, to ensure a more scientific risk evaluation, we put forward an effective quantitative evaluation method based on Dempster–Shafer (D-S) evidence theory, which enriches the research on the overall risk evaluation of sewage treatment PPPABS projects and enables participants to better grasp the overall risk in sewage treatment PPPABS projects. Finally, combined with the case, we present some practical and feasible suggestions which provide a valuable reference for the smooth development of PPPABS projects.

The remainder of this study is organized as follows. The status of risk research in PPPABS projects is reviewed in Section 2. In Section 3, we construct research framework of this work, identify risk factors, determine weights of risk factors using the combination weight method, and propose an approach with D-S evidence theory for the overall risk evaluation of sewage treatment PPPABS projects. In Section 4, the feasibility and effectiveness of the proposed methods are verified by a case study. We discuss the results of the case and put forward some feasible suggestions in Section 5. Finally, the conclusions and further work are presented in Section 6.

2. Literature Review

PPPABS takes the future stable cash flow of PPP projects or specific asset portfolio as the basic assets of asset-backed securitization. Through structural design, financing is realized when the basic assets are turned into liquid securities to flow and transferred in the capital market [9]. PPPABS is a new financing pattern emerging in the area of PPP infrastructure projects. Therefore, there is limited literature on risk research of PPPABS projects.

2.1. Identification of Critical Risk Factors for PPPABS Projects.

Risk factors of PPPABS projects are increasingly concerned by researchers. Several scholars have roughly studied the risk factors in PPPABS projects [10]. For ease of analysis, a few scholars have provided specific risk factors in PPPABS projects. Suleman Baig and Moorad Choudhry collected and analyzed various risk characteristics during the 2007–2008 subprime crisis. The main risk factors of PPPABS projects were found to be the shadow banking system, the lack of effective financial supervision, the moral hazard of speculators, the lack of rationality in the setting of leverage level, the lack of ability of rating agencies, and the lack of risk warning ability [11]. Hou Yufeng, based on the whole process of PPPABS projects, pointed out that the risks mainly included the risk of basic assets, the risk of original stakeholders, the risk related to the guarantor, the risk of rating, the risk of performance of other participating institutions, the risk of market, the risk of information disclosure, and the risk of imperfect policies and laws [12]. Liu et al. constructed the risk evaluation system of PPPABS projects by using the analytic hierarchy process (AHP),

which mainly included four major aspects: environmental risk, credit risk, technical risk, and operational risk [13]. Summarizing the research on risk identification, we find that most of the existing studies identify risks from the perspective of PPPABS projects and no detailed differentiation studies are conducted, such as identifying risk factors for sewage treatment PPPABS projects and for expressway PPPABS projects, which lead to the lack of applicability of the existing evaluation system.

2.2. Risk Management of PPPABS Projects. How to eliminate the risk before the occurrence and how to control the risk after the occurrence? This is another focus of scholars' attention and research. Through a thorough analysis of the financial crisis, Pu Liu and Yingying Shao proposed five improvement measures. Firstly, it was necessary to management comprehensive investment risks. Secondly, the evaluation method of enterprises should be based on marketization. Thirdly, the evaluation, prevention, and control of liquidity risk should keep pace with the time. Fourthly, the rating methods of credit rating agencies should not remain unchanged and timely adjustments should be made. Finally, the information of market participants should be fully disclosed [14]. After analyzing the risks of many PPP financing cases, Terry Lyons believed that it was necessary to analyze the risk that may exist in the process of PPP project asset-backed securitization. In the process of asset-backed securitization, the risk sharing method could better reduce the risk of PPPABS projects [15]. Moreover, as for risk evaluation methods of PPPABS projects, several scholars have proposed a few methods. Liu et al. constructed the risk evaluation system of PPPABS projects by using the analytic hierarchy process (AHP) and also used AHP to evaluate overall risk of PPPABS projects [13]. Taking the asset-backed securities of the parking PPP project in Yanjiang district of China's Ziyang city as an example, Fan Yulin used the fuzzy comprehensive evaluation method to conduct the risk evaluation research. It can be seen from the existing literature that scholars focus on qualitative research and a few scholars have carried out quantitative analysis. However, the AHP method and the fuzzy comprehensive evaluation method are too subjective for evaluation and the evaluation effect is poor [16].

From the literature analysis, current risk research on PPPABS projects is limited. The existing risk evaluation system cannot be fully applied to sewage treatment PPPABS projects. It needed to be rebuilt. Moreover, existing quantitative methods are unscientific. It is also necessary to find an appropriate evaluation method. These are the main contents of this paper.

3. Methodology

In this study, a combination of literature analysis and expert interview is used to generate the critical risk factors for sewage treatment PPPABS projects. With the data collected from a questionnaire, combination weight method (combining G1 method and the entropy method) is applied to determine weight of each critical risk factor. Then, we

evaluate overall risk based on D-S evidence theory. To test the effectiveness and scientificity of the proposed method, a case study of one sewage treatment PPPABS launched in China is used to demonstrate the application. Finally, some suggestions are given based on the results of the case. The research framework is shown in Figure 1. Our purpose is to effectively evaluate the overall risk of sewage treatment PPPABS projects after identifying the critical risk factors affecting sewage treatment PPPABS projects.

3.1. Identification of Critical Risk Factors for Sewage Treatment PPPABS Projects. Literature analysis and expert interview are the main methods used in risk factor identification [17]. Based on the mainstream methodologies, literature analysis and expert interview are adopted to identify the critical risk factors of sewage treatment PPPABS projects. In addition, the introduction of asset-backed securitization into PPP projects is an innovation. Scholars' research in this field is limited. In 2016, China defined PPPABS for the first time and provided policy support. PPPABS projects are developing rapidly in China. In view of the fact that there are many PPPABS projects and also many researchers and practitioners in China, the paper selected experts in China to collect data.

3.1.1. Literature Analysis. In this study, the risk components of PPPABS of sewage treatment project are collected by longitudinal and crosswise designs. Through literature summary, 5 first-level risk factors in the terms of "macro-risks," "basic asset risks," "transaction structure risks," "operational risks," and "other risks" are put forward. A total of 17 second-level risk factors in sewage treatment PPPABS projects are also offered from the existing journal papers as listed in Table 1. After that the initial risk system is further modified in the next expert interview.

3.1.2. Expert Interview. In our study, expert interview method is applied twice. In the first round, we construct an interview guidelines designed for the interview survey. The guidelines consist of 19 columns. The first 18 columns are composed of 18 risk factors in Table 1, while the last 19 columns are blank. Experts can delete these 18 risk factors or add new risks in the blank column according to their own opinions. The final risk system of sewage treatment PPPABS projects is obtained by adding or removing relevant risk factors. In the second round, experts compare and assign the risk factors in the final risk system. In the second round, according to the final risk system obtained in the first round, another interview guidelines are constructed. Experts compare and assign the risk factors in the final risk system.

(1) Select Experts. In order to optimize the selected risk factors and reasonably determine the value of each risk factor of sewage treatment PPPABS projects, the selected experts must satisfy at least one of the following conditions: the professor in a very famous university with more than three years of experience in the PPPABS field; the expert actively participating in PPPABS training for government agencies and private

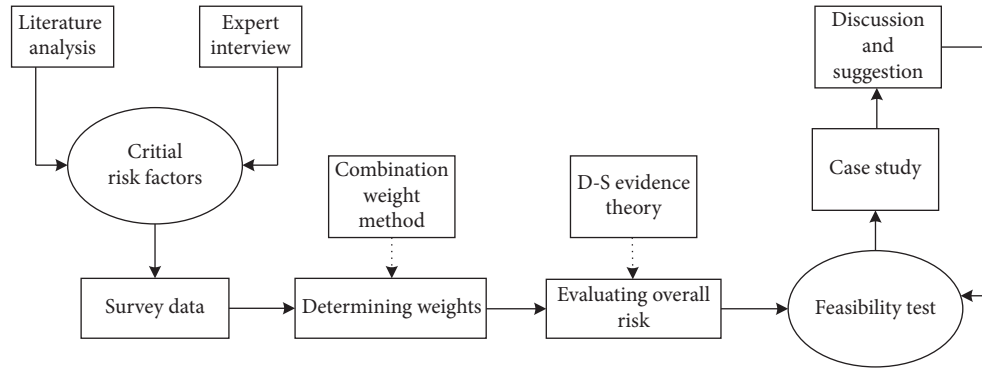


FIGURE 1: Research framework.

TABLE 1: Initial risk system of the sewage treatment PPPABS projects.

First-level risk factors	Second-level risk factors	References
<i>Factor 1: macrorisks</i>		
1	Interest risk	Farooquee [8]
2	Law risk	Austin et al. [10]
3	Inflation risk	Lyons and Martin [15]
4	Political risk	Liu et al. [13]
<i>Factor 2: basic asset risks</i>		
5	Quality risk	Liang [11]
6	Unsold risk	Hou [12]
7	Cash flow prediction deviation risk	Hou [12]
<i>Factor 3: transaction structure risks</i>		
8	Bankruptcy isolation risk	Liu and Shao [14]
9	Transaction structure rationality risk	Austin et al. [10]
10	Prepayment risk	Liu et al. [13]
11	SPV bankruptcy risk	Hou [12]
<i>Factor 4: operational risks</i>		
12	Underwriting and issue risk	Lyons and Martin [15]
13	Service provider risk	Hou [12]
14	Trustee risk	Farooquee [8]
<i>Factor 5: other risks</i>		
15	Government contract fulfillment risk	Liu et al. [13]
16	Ethical risk	Hou [12]
17	Credit enhancement	Lu et al. [9]
18	Credit rating risk	Hou [12]

sectors; the general manager at a large consulting company with multiple PPP or ABS project practical experiences; the experienced professional in a construction management company who has been involved in a number of infrastructure PPP or ABS projects; the lawyer from a famous law firm with the ability to provide the legal advice for PPPABS practice; and the government official in at least the municipal level responsible for facilitating PPPABS projects.

Most of the experts have rich practical experience in PPP or ABS and act as project evaluation experts in the database of China's Ministry of Finance (MOF) and the China asset-backed security (CNABS). Four trained graduate students assist in conducting expert interviews. Finally, according to the selection criteria, ten experts are selected. And work units and related positions are shown in Table 2.

(2) *Experts in the First Round.* In the first round of expert interview, the opinion is put forward that inflation risk can

be ruled out from the initial risk system because the market-oriented economy system is gradually formed. In addition, with public participation, transparent and rigorous governance systems for public infrastructure or services have been established. Ethical risk can also be excluded. Moreover, considering the main content of the special purpose vehicle (SPV) bankruptcy risk overlapping the transaction structure rationality risk's connotation, the transaction structure rationality risk can also be expunged. Additionally, given the long span and preconditions for the securitization of basic asset in sewage treatment PPPABS projects, the majeure risk and basic asset compliance risk should be added. In summary, through expert interviews, three risk factors, "inflation risk," "transaction structure rationality risk," and "ethical risk" are eliminated, and two risk factors, "majeure risk" and "basic asset compliance risk" are added. Combining the literature and opinions of 10 experts, a final risk system of sewage treatment PPPABS projects is provided in Table 3.

TABLE 2: Information of the experts.

No.	Work unit	Position
1	Tsinghua University	Professor
2	Tianjin University	Professor
3	Qingdao Engineering Consulting Institute	Professional advisor
4	China Great Wall Asset Management Co. Ltd.	Professional advisor
5	Qingdao City Financing Department	Official
6	China Construction Eighth Engineering Division Co. Ltd.	General manager
7	Zhong Yin Law Firm	Lawyer
8	China Orient Asset Management Co. Ltd.	Professional advisor
9	Chongqing University	Professor
10	China Cinda Asset Management Co., Ltd.	Professional advisor

TABLE 3: Final risk system of sewage treatment PPPABS projects.

First-level risk factors	Second-level risk factors	References
A_1 : macrorisks	C_1 : interest risk	Farooquee [8]
	C_2 : law risk	Austin et al. [10]
	C_3 : political risk	Liu et al. [13]
A_2 : basic asset risks	C_4 : quality risk	Liang [11]
	C_5 : unsold risk	Hou [12]
	C_6 : cash flow prediction deviation risk	Hou [12]
	C_7 : basic asset compliance risk	Experts
A_3 : transaction structure risks	C_8 : bankruptcy isolation risk	Liu and Shao [14]
	C_9 : prepayment risk	Liu et al. [13]
	C_{10} : SPV bankruptcy risk	Hou [12]
A_4 : operational risks	C_{11} : underwriting and issue risk	Lyons and Martin [15]
	C_{12} : service providers risk	Hou [12]
	C_{13} : trustee risk	Farooquee [8]
A_5 : other risks	C_{14} : government contract fulfillment risk	Liu et al. [13]
	C_{15} : majeure risk	Experts
	C_{16} : credit enhancement	Lu et al. [9]
	C_{17} : credit rating risk	Hou [12]

The main risks are described as follows. (A_1) Macrorisks: at present, laws and policies on PPPABS are mainly industrial regulations and local regulations. The legal and policy documents issued to regulate PPPABS are easily affected by the development of social economy, market changes, and technological progress, thus affecting the issuance of PPP asset securitization. Moreover, in the process of asset securitization, due to the decrease in value or the uncertainty of future returns caused by interest rate changes, such uncertainty will also become interest rate risk. (A_2) Basic asset risks: basic assets of PPPABS must meet certain conditions, or the ABS may have security risks in the first place. The risks related to the basic assets include quality risk (whether it is a high-quality basic asset), unsold risk (are they really for sale?), cash flow prediction deviation risk (whether the cash flow forecast is accurate), and basic asset compliance risk (whether the basic assets are legal). (A_3) Transaction structure risks: the risks in this aspect are mainly analyzed from the aspect of transaction structure. It mainly analyzes whether bankruptcy isolation can be realized, prepayment can be made, and the stability of SPV can be built. (A_4) Operational risks: the risks in this area are mainly in the operational phase. It mainly includes whether the underwriting and issuance can be realized smoothly, the behaviors of service providers that harm the interests of

investors, and whether the management level of the trustee can meet the requirements. (A_5) Other risks: other risks refer to the risks worthy of attention in addition to the above four categories. The risks in this aspect include government contract fulfillment risk, the majeure risk such as war and natural disaster, whether the credit enhancement can be realized at the critical moment and whether the value of assets will be affected due to the credit rating.

(3) *Experts in the Second Round.* In the second round of expert interview, the questionnaire survey of risk factor scores is designed according to the final risk system of sewage treatment PPPABS projects. A questionnaire survey is conducted to obtain the objectives of this study. Based on the need of the research methods in Section 3, experts are required to endow each risk value according to risk degree [1] in Table 4 and also to give the level of each risk so as to calculate occurrence probability of each risk. The professional experience and competence of the experts can guarantee the reliability of the data. The data obtained from the questionnaire survey lay a solid foundation for the overall risk evaluation.

3.2. *Determine Weight of Each Critical Risk Factor with Combination Weight Method.* Common objective weight methods include the entropy method and principal

TABLE 4: Risk evaluation criteria.

Risk level	Corresponding risk value range
Very high (x_1)	[0.8, 1.0]
High (x_2)	[0.6, 0.8]
Moderate (x_3)	[0.4, 0.6]
Low (x_4)	[0.2, 0.4]
Very low (x_5)	[0, 0.2]

component analysis method. However, objective weight methods rely on statistical and mathematical methods and ignore the human factors in the decision-making process, which makes it not close to the reality. Common subjective weight methods include AHP method and Delphi method. However, subjective weight methods depend too much on expert opinions, which are limited by personal knowledge and have certain limitations. Based on the shortcomings of subjective and objective weight methods, some scholars propose the combination weight method. At present, the combination weight method is becoming a trend [18].

Objective weight method: the entropy determines the weight of each factor by the entropy value which reflects the information of each factor. However, this method has the disadvantage of not taking into account the mutual influence of each factor. Subjective weight method: G1 fully considers the mutual influence of each factor and is essentially the analysis of order relation. Therefore, this paper combines G1 method with entropy method, which is not divorced from the subjective reality and based on certain objective data. It not only retains the advantages of the two methods, but also makes up for the shortcomings of each method. In addition, the key step of this combined method is to determine the proportion of the weight determined by G1 and the weight determined by the entropy in the comprehensive weight. The commonly method to determine the subjective and objective weight proportion is the Delphi method. However, the Delphi method has too many human factors to be scientific [18]. This paper is based on Lagrange theory to determine the proportion of subjective and objective weights.

3.2.1. Subjective Weights Based on G1 Method. G1 method is an improved subjective weight method proposed by professor Guo Yajun on the theoretical basis of analytic hierarchy process (AHP) [18]. The G1 method mainly refers to a factor preference method that first sorts the importance of the measurement factors according to the expert opinions, then compares and judges the adjacent measurement factors one by one, and finally quantitatively assigns values on this basis. It can fully reflect the subjective opinions of experts, and its order of importance will not change with the change of factors. Therefore, this paper adopts the G1 method to achieve the subjective weights of risk factors, and the specific steps are as follows:

Step 1. Rank the risks in accordance with their importance. For the risk factor set (c_1, c_2, \dots, c_n) , the unique ordering relationship can be obtained.

Step 2. Determine the relative importance $r_k = \omega_{k-1}/\omega_k$ of adjacent risk factors c_{k-1} and c_k according to Table 5.

TABLE 5: The value of relative importance of criteria.

r_k	Description
1.0	c_{k-1} is the same important as c_k
1.2	c_{k-1} is slightly more important than c_k
1.4	c_{k-1} is more important than c_k
1.6	c_{k-1} is strongly more important than c_k
1.8	c_{k-1} is extremely more important than c_k

Step 3. Calculate the subjective weights of risk factors by

$$\omega_k = \left(1 + \sum_{k=2}^n \prod_{i=k}^n r_i \right), \quad (1)$$

$$\omega_{k-1} = \omega_k * r_k. \quad (2)$$

Considering experts in Table 2 owning the voting right, the final weights are determined by the calculation result and m decision-makers' weights according to

$$\omega'_k = \frac{\omega_{1k} + \omega_{2k} + \dots + \omega_{mk}}{m}. \quad (3)$$

3.2.2. Objective Weights Using the Entropy Method. The concept of entropy, introduced by Shannon in 1948, is mainly used to measure the uncertainty in information. In the decision-making process, the entropy is used to analyze the information quantity provided by data [19]. Therefore, the entropy method can objectively evaluate the importance of risk factors according to the information entropy. The risk factor with higher information entropy should be given higher weight. According to this principle, the specific steps of the entropy method to determine the weights of risk factors are as follows:

Step 1. Construct decision matrix $B = (b_{Lk})_{m \times n}$, where b_{Lk} represent the k th risk weight given by L th expert.

Step 2. Calculate the information entropy of k th risk by

$$\begin{cases} H_k = -\frac{1}{\ln m} \sum_{L=1}^m r_{Lk} \ln r_{Lk}, \\ r_{Lk} = \frac{b_{Lk}}{\sum_{L=1}^m b_{Lk}}. \end{cases} \quad (4)$$

Step 3. Determine the objective weights of k^{th} risk factor by

$$\omega_k^n = \frac{1 - H_k}{n - \sum_{k=1}^n H_k}. \quad (5)$$

3.2.3. Combined Weights on the Basis of Lagrange Theory. Combining the G1 method with the entropy method, the combined weight method integrates professional opinions of experts in the G1 method and uses the entropy objective weight method to avoid subjective errors, which make the final risk factor weight more scientific and reasonable. Under the condition that ω'_k and ω_k are known, this paper builds an optimization model based on Lagrange theory to achieve the

combined weights of risk factors. The combined weight model is shown in

$$w_k^* = \alpha w_k' + \beta w_k'' \quad (6)$$

where α and β , respectively, represent the proportion of subjective and objective weight. Moreover, α and β meet the following conditions in

$$\begin{cases} \max & F(\alpha, \beta) = \sum_{l=1}^m \left(\sum_{k=1}^n (\alpha w_k' + \beta w_k'') \right) \\ \text{s.t.} & \alpha^2 + \beta^2 = 1. \end{cases} \quad (7)$$

Furthermore, α and β can be achieved using Lagrange functions, which are shown in

$$\begin{cases} \alpha = \frac{\sum_{l=1}^m \sum_{k=1}^n w_k' x_{lk}}{\sqrt{(\sum_{l=1}^m \sum_{k=1}^n w_k' x_{lk})^2 + (\sum_{l=1}^m \sum_{k=1}^n w_k'' x_{lk})^2}}, \\ \beta = \frac{\sum_{l=1}^m \sum_{k=1}^n w_k'' x_{lk}}{\sqrt{(\sum_{l=1}^m \sum_{k=1}^n w_k' x_{lk})^2 + (\sum_{l=1}^m \sum_{k=1}^n w_k'' x_{lk})^2}}. \end{cases} \quad (8)$$

4. Risk Evaluation with D-S Evidence Theory

Evidence theory was first proposed by Dempster in 1967 and then further developed by Shafer on the basis of Bayes theory in 1976. This theory can carry out credibility reasoning based on uncertain information, has the ability to directly express “uncertainty” and “don’t know,” and also has strong data fusion ability, which has been widely used in the field of “evaluation” [17, 20, 21]. When D-S evidence theory is used for evaluation, the basic belief degree directly determines the accuracy of the evaluation. Most of the existing research studies take the probability of each of the risk level as the basic belief degree [22]. However, the accuracy of this method to determine the basic belief degree needs to be improved. Due to the existence of uncertain information, the rigor of data can produce a discount effect. The paper believes that it is more reasonable to adjust the data with the discount rate to get the basic belief degree.

Before applying DEST in overall risk level evaluation, we define the discernment frame Θ . $A = \{A_1, A_2, A_3, A_4, A_5\}$ represents 5 first-level risk factors. And n risk evaluation factors in A_1 are expressed as $A_1 = \{c_1, c_2, \dots, c_n\}$. A_2, A_3, A_4 , and A_5 are shown in the same way. The following

operations present risk calculation processes in sewage treatment PPPABS projects:

Step 1: determine the discount rate α_i for the basic belief degree of each risk factor.

Based on the weight vector of each risk factor obtained through the combination weight method mentioned above, $w_{\max}^* = \max\{w_1^*, w_2^*, \dots, w_n^*\}$ and relative weight vector of each risk factor $W' = (w_1^*, w_2^*, \dots, w_n^*)/w_{\max}^*$ are achieved. Then, the discount rate α_i for the basic belief degree of each risk factor is presented in

$$\alpha_i = 1 - \frac{w_i^*}{w_{\max}^*}, \quad i = 1, 2, \dots, n. \quad (9)$$

Step 2: calculate new basic belief degree of each risk factor and improve belief function.

After collecting experts’ distribution of the basic belief degree of each risk factor (namely, $m_i(A_j)$, where m is the number of experts, the basic belief degree of each risk factor is adjusted by using the discount rate α_i . The calculation equations are

$$m_i'(A_j) = (1 - \alpha_i) m_i(A_j), \quad (10)$$

$$m'(\Theta) = (1 - \alpha_i) m(\Theta) + \alpha_i, \quad (11)$$

where $j = 1, 2, \dots, d_i$ and d_i is the number of basic belief degree out of discernment frame Θ .

Then, the improved belief function becomes

$$\text{Bel}'(A) = \sum_{B \subseteq A} m(B), \quad \forall A \subseteq \Theta. \quad (12)$$

Step 3: construct fusion basic belief functions of risk factors.

According to the Dempster combinational rule, there are two fusion patterns:

(1) Fuse two risk factors: if belief functions of two independent risk factors are m_1' and m_2' , respectively, based on the same discernment frame Θ , the basic belief function m' after fusing m_1' and m_2' is expressed as

$$\left\{ \begin{aligned} m'(A) &= m_1'(A) \oplus m_2'(A) = \frac{\sum_{X \cap Y = A} m_1'(X) \times m_2'(Y)}{(1 - \sum_{X \cap Y = \emptyset} m_1'(X) \times m_2'(Y))}, & A \neq \emptyset, A \subseteq \Omega m' \emptyset = 0 \end{aligned} \right. \quad (13)$$

where \oplus is called “direct sum” representing the combinational operation between factors.

(2) Fuse multiple risk factors: if belief functions of p ($p > 2$) independent risk factors are m_1', m_2', \dots, m_p' , respectively, based on the same

discernment frame Θ , the belief function m' after fusing m_1', m_2', \dots, m_p' is expressed as

$$m'(A) = m_1'(A) \oplus m_2'(A) \oplus \dots \oplus m_p'(A), \quad A \neq \emptyset, A \subseteq \Omega m' \emptyset = 0. \quad (14)$$

Because the Dempster combinational rule has commutativity and associativity, $p(p > 2)$ risk factors requires $p - 1$ fusion process according to the fusion formula of two factors, and the final result is independent of the fusion order. It can be understood as

$$m'(A) = \frac{\prod_{i=1}^{m'} m'_i(A_i)}{\sum_{\cap A_i = A} 1 - \sum_{\cap A_i = \emptyset} \prod_{i=1}^{m'} m'_i(A_i)}. \quad (15)$$

Step 4: calculate the adjusted basic belief degree. Using $m'(x_h)$ and fusion basic belief function belief degree of each risk factor, the adjusted basic belief degree is obtained by the following:

$$\text{Bel}'(A) = \sum_{B \subseteq A} m'(B), \quad \forall A \subseteq \Theta. \quad (16)$$

Step 5: calculate the overall risk value by

$$R = \sum_{h=1}^k P x_h \text{Bel}'(x_h), \quad (17)$$

where $P(x_h)$, $h = 1, 2, \dots, k$ is the hazard degree of the risk level x_k , $P(x_h)$ is gained usually by taking its average, and the value range is $0 < P(x_h) < 1$.

5. Case Study

In this section, the proposed method based on the combination weight method and D-S evidence theory is applied to a case study, which is based on a real project. The name of the case is Beijing capital Co. Ltd. sewage treatment PPPABS project in China. Beijing capital Co. Ltd. and CITIC securities officially launched the sale of PPPABS product in Shanghai stock exchange on March 10, 2017. The product name is "CITIC securities-Beijing capital Co. Ltd. charge income right-backed asset special plan for the sewage treatment PPP project." The original stakeholders of the special plan are four water companies in Shandong province which are wholly-owned subsidiaries of Beijing capital Co. Ltd. The basic assets are the sewage treatment charge income rights owned by the four water utilities under the PPP agreement. Beijing capital Co. Ltd. serves as an asset service agency. The special plan for the sewage treatment project is 530 million yuan, of which 500 million yuan is the priority asset-backed securitization and the remaining 30 million yuan is the secondary asset-backed securitization.

The main steps of the proposed method to implement risk evaluation of Beijing capital Co. Ltd sewage treatment PPPABS are divided into two phases. One phase is that weights of first-level risks and second-level risks are determined through the combination weight method. Another phase is that the overall risk evaluation is realized by D-S evidence theory.

Phase 1. Determine weights of first-level risks and second-level risks using the combination weight method.

Firstly, based on their experience and knowledge, 10 experts in Table 2 firstly endow each risk value according to the risk degree in Table 4 and the value of relative importance of criteria in Table 5.

Secondly, to insure the feasibility and effectiveness of the proposed method in the sewage treatment PPPABS project, the data collected from 10 experts are deposed to test reliability. Here, Cronbach's alpha method is applied to test reliability and consistency of the survey data. According to the results and frequencies of data acquisition, three Cronbach's alpha values (0.866, 0.872, and 0.869), all falling between 0.8 and 0.9, manifest that the internal consistency is good [23], that is to say, the data from the questionnaire is deemed consistent and reliable.

Finally, subjective weights are calculated based on the G1 method mentioned above, and objective weights are also obtained using the entropy by equations (1)–(5). Finally, combined weights are achieved by equations (6)–(8). Related results are shown in Table 6.

Phase 2. Evaluate overall risk using D-S evidence theory.

Step 1. Obtain the basic belief degree and Θ .

Through expert voting, the voting results of 10 experts on risk index c_k at risk level x_h ($h = 1, 2, \dots, 5$) is obtained, namely, the basic belief degree of each risk factor $m_{ik}(x_h)$, where Θ expresses that the level of risk indicator is difficult to be determined by experts. The voting results are presented in Table 7.

Step 2. Determine the discount rate for the basic belief degree of each risk factor.

Because some experts believe that the level of some risk factors is not easy to determine, there is a certain "discount" effect on data rigor. The discount rate equation (9) is used to adjust the data. The discount rate of each level is also shown in Table 7.

Step 3. Calculate fusion basic belief degree of risk factors ($m'_i(x_h)$).

Adjusted basic belief degree of risk factors are achieved by using the discount rate equation (9). Then, the fusion basic belief degree of risk factors $m'_i(x_h)$ is obtained by applying equations (13)–(15). The calculating results are displayed in Table 8.

Step 4. Determine the risk level probability of overall risk.

Once again, the belief degree (in Table 8) is adjusted using equations (10) and (11). Then, the adjusted belief degree is fused by equations (13) and (14). Finally, the risk level probability of the overall risk is determined, which is shown in Table 9.

Step 5. Calculate the overall risk value.

TABLE 6: Weights of first-level risks and second-level risks.

First-level risk factors	Weight	Second-level risk factors	Subjective weight	Objective weight	Combined weight
A_1	0.2534	C_1	0.040	0.042	0.0410
		C_2	0.050	0.045	0.0470
		C_3	0.167	0.164	0.1654
A_2	0.1249	C_4	0.045	0.042	0.0434
		C_5	0.031	0.034	0.0327
		C_6	0.022	0.029	0.0259
		C_7	0.019	0.026	0.0229
A_3	0.1867	C_8	0.127	0.125	0.1259
		C_9	0.017	0.016	0.0165
		C_{10}	0.047	0.042	0.0443
A_4	0.1352	C_{11}	0.057	0.059	0.0581
		C_{12}	0.037	0.035	0.0359
		C_{13}	0.044	0.039	0.0413
A_5	0.2998	C_{14}	0.191	0.195	0.1932
		C_{15}	0.036	0.033	0.0344
		C_{16}	0.029	0.028	0.0285
		C_{17}	0.041	0.046	0.0438

TABLE 7: The basic belief degree, Θ , and discount rate.

First-level risk factors	Weight	Second-level risk factors	Combined weight	Basic belief degree					Θ	α_i
				x_1	x_2	x_3	x_4	x_5		
A_1	0.2534	C_1	0.0410	0.2	0.2	0.2	0.1	0.2	0.1	0.7878
		C_2	0.0470	0.1	0.2	0.3	0.1	0.3	0	0.7567
		C_3	0.1654	0.1	0.3	0.3	0.2	0.1	0	0.1439
A_2	0.1249	C_4	0.0434	0.2	0.1	0.3	0.2	0.2	0.1	0.7754
		C_5	0.0327	0.2	0.3	0.2	0.1	0.2	0	0.8307
		C_6	0.0259	0.1	0.1	0.3	0.3	0.2	0.1	0.8659
		C_7	0.0229	0.1	0.1	0.2	0.3	0.4	0	0.8815
A_3	0.1867	C_8	0.1259	0.0	0.2	0.2	0.3	0.2	0	0.3483
		C_9	0.0165	0.2	0.4	0.2	0.1	0.1	0	0.91460
		C_{10}	0.0443	0.1	0.2	0.3	0	0.2	0.2	0.7707
A_4	0.1352	C_{11}	0.0581	0.1	0.2	0.3	0.1	0.3	0	0.6993
		C_{12}	0.0359	0.2	0.2	0.2	0.2	0.1	0.1	0.8142
		C_{13}	0.0413	0	0.1	0.4	0.3	0.2	0	0.7862
A_5	0.2998	C_{14}	0.1932	0.3	0.2	0.1	0.2	0.1	0.1	0
		C_{15}	0.0344	0.1	0.1	0.2	0.5	0.1	0.1	0.8219
		C_{16}	0.0285	0.2	0.1	0.3	0.1	0.3	0	0.8525
		C_{17}	0.0438	0	0.1	0.3	0.4	0.2	0	0.7733

TABLE 8: Fusion basic belief degree of risk factors.

First-level risk factors	A_1	A_2	A_3	A_4	A_5	
Weight	0.2624	0.1928	0.2206	0.2174	0.1069	
$m'_i(x_h)$	x_1	0.0227	0.2990	0.0115	0.0321	0.3981
	x_2	0.5707	0.3657	0.1552	0.0951	0.3611
	x_3	0.3293	0.2161	0.2736	0.5319	0.2408
	x_4	0.0566	0.0397	0.5596	0.3205	0.0000
	x_5	0.0206	0.0794	0.0000	0.0183	0.0000
Θ	0.0000	0.0000	0.0000	0.0021	0.0000	

TABLE 9: Risk level probability of overall risk.

x_1	x_2	x_3	x_4	x_5	Θ
0.0027	0.0066	0.0635	0.5406	0.3861	0.0005

TABLE 10: Risk level hazard degree.

P_{x_1}	P_{x_2}	P_{x_3}	P_{x_4}	P_{x_5}
1	0.77	0.52	0.30	0.15

According to the opinions of 10 experts, the hazard degree of the corresponding risk level is classified, and the values of hazard degree $P(X)$ are given in Table 10.

Then, the overall risk value R is calculated by using equations (16) and (17). The calculating process and result are

$$R = \sum_{h=1}^k P x_h \text{Bel}'(x_h) = 1 * 0.0027 + 0.77 * 0.0066 + 0.52 * 0.0640 + 0.3 * 0.5406 + 0.15 * 0.3861 = 0.2612. \quad (18)$$

6. Discussion and Suggestion

As shown in Table 9, overall risk level probability of uncertainty (0.005) indicates that D-S evidence theory could help to reduce the uncertainty. Moreover, overall risk level probabilities in “Very High,” “High,” “Moderate,” “Low,” and “Very Low” are 0.002, 0.0066, 0.0635, 0.5406, and 0.3861, respectively, which imply few risk factors in “Very High” and “High” and almost risk factors in “Low” and “Very Low.” The final result (0.2612) also confirms the situation and more indicates the overall risk level of Beijing Capital Co. Ltd. sewage treatment PPPABS project is “Low.” The above results are consistent with the actual situation of Beijing Capital Co. Ltd. sewage treatment PPPABS project, which proves that the proposed method is feasible and reliable for the risk evaluation of sewage treatment PPPABS projects, and could play an important role in the risk prediction.

However, 0.2612 shows that Beijing Capital Co. Ltd. sewage treatment PPPABS project still has a certain risk. Based on each risk factor’s combined weight in Table 6 and basic belief degree in Table 7, we provide the following suggestions to ensure sewage treatment PPPABS projects success. Suggestions would be made from low risk, quality risk, underwriting and issue risk, and credit enhancement.

6.1. Law Risk Aspect. Because the current laws and regulations of ABS are not perfect, it is easy to have the risk of contract agreement invalidation, legal uncertainty, and legal clause change. Government sector should take measures as soon as possible from the following. (i) Before special legislation is introduced, the supreme court can be considered to formulate relevant judicial interpretations to solve legal problems. (ii) The supervision subject and principle of ABS should be clarified, and the company law, bankruptcy law, and securities law should be improved as quickly as possible. (iii) We can draw lessons from the successful experience to develop a legal system suitable for PPP project asset-backed securitization.

6.2. Quality Risk Aspect. The basic asset quality of PPPABS projects must meet certain conditions, or it may cause security risks in the beginning of securitization. Basic assets should be rigorously screened. (i) The basic assets should be

subjected to strict examination and approval. Not all public infrastructures have stable cash flow. PPP projects that implement ABS must require the predictability of future cash flow and clearly defined payment patterns. (ii) The project company’s construction quality should meet certain standards. Firstly, the project has continuous safe and stable operation. Secondly, the project has been completed and normal operation for more than 2 years. Finally, the project has established a reasonable return on investment mechanism and moreover has strong performance ability.

6.3. Underwriting and Issuing Risk Aspect. The underwriting and issue of securities are the important links in the process of PPPABS. Some necessary measures should be taken to deal with the underwriting and issue risk. (i) In the design of securities issuance, bonds can be designed with different maturities and currencies, as well as different types of bonds according to the credit rating results, so as to match the risks with the returns. Only after the investigation and analysis of the market can the reasonable price of the stock be determined. (ii) The underwriter should participate in the planning and organization of the issuing securities to ensure that the issuing process complies with the requirements of laws and regulations. At the same time, underwriters are required to expand marketing channels to guarantee the success of the issuing securities. (iii) Based on the market situation and the characteristics of investors’ demand, the underwriting way should be chosen prudently. If the risk is small in the future, we can take the commission. Otherwise, we can choose to underwrite.

6.4. Credit Enhancement. The purpose of credit enhancement is to prevent the credit risk in the process of asset-backed securitization, but it also has own risks. There is a risk that internal credit enhancement will not be fully isolated from the originator’s assets. External credit enhancement may result in a decline in credit rating of the securitization transaction as a result of a reduction in credit rating of the credit enhancement institution itself. For credit enhancement risk, we should take countermeasures. (i) The assets with internal credit enhancement should be estimated by the asset appraisal agency, and the necessary audit also should be conducted to ensure the safety of the assets. (ii) We should choose commercial banks and insurance companies with good reputation and stable operation as external credit enhancement institutions to ensure effective credit enhancement.

7. Conclusion

Sewage treatment PPP projects can play an important role in achieving a clean environment and promoting sustainable development. With the strong support of the government, the ABS mode has been introduced into sewage treatment PPP projects to overcome the imbalance between supply and demand. It is an effective way to attract private capital and improve sewage treatment performance and service. Risk research of sewage treatment PPPABS projects is necessary

to ensure project success and it is important to achieve what risk factors affect the sewage treatment PPPABS projects and how to calculate the overall risk using the scientific method. To solve this problem, this paper establishes a risk identification and evaluation framework for sewage treatment PPPABS projects with the combination weight method and D-S evidence theory. As the results, 17 critical risk factors are selected as the evaluation system by literature review and expert interview. And, we determine risk factors' weights with the combination weight method (the G1 method being combined with the entropy) and evaluate the overall risk of sewage treatment PPPABS projects with D-S evidence theory. Suggestion are put forward to effectively control risks and further to guarantee sewage treatment PPPABS projects success. Risk evaluation of PPPABS projects is the focus of current research and attracts much attention from researchers. As a core part of financing risk management, risk evaluation of sewage treatment PPPABS projects plays an important role though little literature has carried out careful identification of its risk factors and overall risk evaluation. This paper attempts to contribute to this section.

This study also has limitations and shortcomings. Due to inadequate experience in sewage treatment PPPABS projects, risk system cannot be perfect. The availability of collected risk data should be more accurate and feasible. In the next study, identification methods of risk factors can be innovated. Additionally, this study proposed the risk evaluation method using the combination weight method and D-S evidence theory, which is proved to be feasible and reliable. Next, comparative studies based on other risk evaluation methods can be discussed.

Data Availability

No data are used to support this study.

Conflicts of Interest

The authors declare that there are no conflicts of interest regarding the publication of this paper.

Acknowledgments

The authors thank the National Natural Science Foundation of China (Grant no. 71471094).

References

- [1] J. Liu and Q. Wei, "Risk evaluation of electric vehicle charging infrastructure public-private partnership projects in China using fuzzy TOPSIS," *Journal of Cleaner Production*, vol. 189, pp. 211–222, 2018.
- [2] J. Song and L. Zhang, "Study on dynamic income distribution of sewage treatment PPP project," *Construction Economy*, vol. 40, no. 9, pp. 46–51, 2019.
- [3] J. Zhang, Z. Qiu, and L. Fei, "An exploration of comprehensive evaluation method of sewage treatment construction project in small and medium towns: theory and application," *Desalting and Water Treatment*, vol. 118, pp. 70–78, 2018.
- [4] H. Li, L. Ding, C. Li, and H. Wang, "Sponge city construction in China: a survey of the challenges and opportunities," *Water*, vol. 9, no. 9, p. 594, 2017.
- [5] S. Cheng, M. Zhao, X. Zhou, and Z. Li, "Development and application of biogas project for domestic sewage treatment in rural China: opportunities and challenges," *Journal of Water, Sanitation and Hygiene for Development*, vol. 7, no. 4, pp. 576–588, 2017.
- [6] J. Song, L. Chen, and X. Guan, "Research on risk sharing of PPP plus EPC sewage treatment project based on bargaining game mode," *Fresenius Environmental Bulletin*, vol. 29, no. 2, pp. 903–912, 2020.
- [7] L. Qian, Z. Liao, and Q. Guo, "Effects of short-term uncertainties on the revenue estimation of PPP sewage treatment projects," *Water*, vol. 11, no. 6, pp. 1–14, 2019.
- [8] A. A. Farooquee, "Design, structure, and risk assessment of a pre-securitization financing facility for rooftop solar projects in India," *The Journal of Structured Finance*, vol. 23, no. 1, pp. 91–97, 2017.
- [9] Z. Lu, F. Pena-Mora, S. Q. Wang, T. Liu, and D. Wu, "Assessment framework for financing public-private partnership infrastructure projects through asset-backed securitization," *Journal of Management In Engineering*, vol. 35, no. 6, pp. 40–56, 2019.
- [10] J. C. Shenker and A. J. Colletta, "Asset securitization: evolution, current issues and new frontiers," *Texas Law Review*, vol. 69, no. 6, p. 1374, 1991.
- [11] S. Liang, "Chinese credit asset securitization: development status, problems and suggestions," *International Business and Management*, vol. 3, pp. 75–80, 2015.
- [12] Y. Hou, "Risk analysis and evaluation of PPP asset securitization based on the whole process," *Finance and Accounting Monthly*, vol. 9, pp. 79–86, 2018, in Chinese.
- [13] Y. Liu, S. Gan, and S. Zhao, "Research on the construction of risk evaluation system of asset-backed securitization in PPP projects," *Statistics and Decision*, vol. 11, pp. 161–163, 2019, in Chinese.
- [14] P. Liu and Y. Shao, "Small business loan securitization and interstate risk sharing," *Small Business Economics*, vol. 41, no. 2, pp. 449–460, 2013.
- [15] T. Lyons and S. Martin, "Project risk management in the Queensland engineering construction industry: a survey," *International Journal of Project Management*, vol. 22, no. 1, pp. 51–61, 2004.
- [16] F. Y. Meng, J. Tang, S. L. Zhang, and Y. W. Xu, "Public-private partnership decision making based on correlation coefficients of single-valued neutrosophic hesitant fuzzy sets," *Informatica*, vol. 31, no. 2, pp. 359–397, 2020.
- [17] P. Liu and X. Zhang, "Approach to multi-attributes decision making with intuitionistic linguistic information based on Dempster-Shafer evidence theory," *IEEE Access*, vol. 6, pp. 52969–52981, 2018.
- [18] B. Liu and Y. Hu, "Critical factors of effective public participation in sustainable energy projects," *Journal of Management in Engineering*, vol. 34, no. 5, Article ID 04018029, 2018.
- [19] R. Osei-Kyei and A. P. C. Chan, "Review of studies on the critical success factors for public-private partnership (PPP) projects from 1990 to 2013," *International Journal of Project Management*, vol. 33, no. 6, pp. 1335–1346, 2015.
- [20] F. Xu, J. Liu, S. Lin, and J. Yuan, "A VIKOR-based approach for assessing the service performance of electric vehicle sharing programs: a case study in Beijing," *Journal of Cleaner Production*, vol. 148, pp. 254–267, 2017.

- [21] J. W. Godden, F. L. Stahura, and J. Bajorath, "Variability of molecular descriptors in compound databases revealed by Shannon entropy calculations," *Journal of Chemical Information and Computer Sciences*, vol. 40, no. 3, pp. 796–800, 2000.
- [22] L. Wang, G. Zhang, and Q. Hao, "Risk evaluation of cold chain marine logistics based on the dempster-shafer (D-S) evidence theory and radial basis function (RBF) neural network," *Journal of Coastal Research*, vol. 98, no. sp1, pp. 376–380, 2019.
- [23] D. George and M. Mallery, *Using SPSS for Windows Step by Step: A Simple Guide and Reference*, Allyn & Bacon, Boston, MA, USA, 2003.

Research Article

Analysis of Complex Dynamics in Different Bargaining Systems

Xiaogang Ma,¹ Chunyu Bao ,¹ and Lin Su²

¹School of Management, Wuhan Textile University, Hubei 430200, China

²School of Foreign Languages, Shandong Yingcai University, Shandong 250104, China

Correspondence should be addressed to Chunyu Bao; spring_bao.nj@foxmail.com

Received 11 April 2020; Accepted 10 June 2020; Published 1 July 2020

Academic Editor: Abdelalim A. Elsadany

Copyright © 2020 Xiaogang Ma et al. This is an open access article distributed under the Creative Commons Attribution License, which permits unrestricted use, distribution, and reproduction in any medium, provided the original work is properly cited.

This paper focuses on the bargaining behavior of supply chain members and studies the stability of the bargaining system. There are two forms of bargaining in the process of negotiation. One is separate bargaining, and the other is that the automobile manufacturers form an alliance and bargain with the supplier collectively. We explore the influence of bargaining power and adjustment speed on the stability of the dynamic system and find that both of the factors need to be small to maintain the stability of the supply chain. After comparing the two forms of bargaining in terms of profits and stable regions, we find that the collective bargaining is a pattern with the existence of risk and benefit simultaneously. In order to control chaos in collective bargaining to lower the risk, we adopt the delay feedback control method. With the introduction of the control factor, the system tends to be stable finally.

1. Introduction

The bargaining behavior is common in commercial operation and plays a critical role in the whole supply chain performance. Because of the fierce market competition, many manufacturers cannot raise their prices at will but rely more on bargaining to reduce costs to strive for greater profit space. The concept of common parts makes joint procurement possible, and many manufacturers become beneficiaries of collective bargaining. Automobile manufacturers are also one of them. Take the automobile industry as an example; after years of rapid development, the automobile industry has experienced a slowdown recently, which stimulates the fierce competition of the component market. In order to cut costs, most automobile manufacturers choose to purchase parts from external enterprises, while focusing on their core business. In the automobile manufacturing industry, the purchase cost accounts for a high proportion in the whole product cost, while the purchase cost of automobile parts is a large part of the purchase cost. Since that, the bargaining between automobile manufacturers and the supplier is of great significance. Formerly, manufacturers used to purchase components separately. With the prevalence of the supply chain and the win-win concept, many of

them prefer to form an alliance to bargain with the supplier for the sake of a stronger bargaining power. We used the generalized Nash bargaining framework to model the bargaining process and compared separate bargaining and collective bargaining on their performance of maintaining stability in the dynamic system.

Applying nonlinear dynamics theory to an economic system can provide a better understanding of its complex practice, and many scholars had made their attempt in different fields. Fibich and Gavish [1] applied a dynamical system as a new method to analyze the asymmetric first-price auction. The result proved that in the case of two different players, a unique equilibrium strategy exists. Chen et al. [2] analyzed a finite-level dynamic pricing model in which the demand for each period depends on both the current and past price. Chen and Gallego [3] analyzed the influence of dynamic pricing on public welfare and consumer surplus and proposed a dynamic pricing formulation to maximize welfare. Different behaviors of a dynamic system have corresponding explanations in economics. The equilibrium point in a dynamic system represents a stable state in the supply chain, and chaos represents disorder and risk. When variable spillover occurs, it means that in reality, some enterprises go bankrupt and have to withdraw from

the market. In this paper, some methods of nonlinear theory were used to study the dynamic characteristics of separate bargaining and collective bargaining. We analyzed the influence of bargaining power and adjustment speed on the dynamic system and presented some economic explanations for the results.

The inherent randomness of chaos makes the trajectory of a dynamic system difficult to predict. When chaos is beneficial to the system, conditions should be created to guide the system into a specific chaotic orbit. However, when chaos is harmful to the system, it should be controlled. And in most cases, chaos is not desirable and should be controlled via different methods according to its characteristics. Many methods have been proposed by scholars, such as the method of parameter adjustment and the adaptive chaos control method. Later in the paper, we will adopt the delay feedback control method to control the chaos occurred in the bargaining process because of its good tracking ability and stability.

The paper is organized as follows. In Section 2, the related literature is reviewed. We describe the model and compare the two forms of bargaining in Section 3. The delay feedback control method is used to control the chaos occurred in the system in Section 4. And finally, Section 5 draws conclusions.

2. Literature Review

2.1. Bargaining Behavior. One stream of literature that is related to our work is the one which studied bargaining behavior. Feng et al. [4] analyzed a bargaining game and sorted buyers to high type and low type to illustrate the significance of role forecasting accuracy on the supply chain. Aydin and Heese [5] used a bargaining framework to model the assortment selection process. The result showed that the improvements of products from a manufacturer benefit the other parts of the supply chain, even its competitors. Karagözoğlu and Riedl [6] studied the influence of performance information on bargaining and found that the result of bargaining is mainly equal share without performance information. A significant anchoring effect was found by Leider and Lovejoy [7] in their study of sequential bargaining in a two-tier supply chain with competition. Lee [8] introduced a noncooperative multilateral bargaining model for network restricted environment to characterize a significant condition for the efficient equilibrium. Davis and Hyndman [9] studied the bargaining behavior in a supply chain consisting of a retailer and a supplier. They found that when the quantity of orders is included, the efficiency of the supply chain is significantly improved. Haruvy et al. [10] studied the contract performance of bargaining behavior under the allowance of concessions made by the manufacturer. And, the result demonstrated that the contracts are efficient in this instance. Each paper focuses on different points of bargaining, but the ideas on the modeling of bargaining process are interlinked, which is worth learning from. There are also some scholars focusing on the analysis of different forms of bargaining. Guo and Iyer [11] compared two forms of bargaining in the supply chain containing one manufacturer and two retailers. They proved that

when the profitability is similar, simultaneous bargaining is optimal; otherwise, sequential bargaining is better. Hsu et al. [12] analyzed the two forms of leader-based collective bargaining: one is equal price LCB and the other is fixed price LCB. The result showed that the latter had better performance. Melkonyan et al. [13] applied virtual bargaining in competitive interactions to illustrate that it caused collusion in Bertrand instead of Cournot. Most of the above studies focused on a single period to make optimal decision. However, in real life, the manufacturer cannot fully know the information of the opponent, and his own decision-making in each period is not completely independent. Considering the complexity of the economy system in practical, we extend it to a dynamical system and present a multiperiod decision-making process for component bargaining.

2.2. Dynamical System. In recent years, a dynamical system has been widely used. Many researchers integrate nonlinear dynamics theory and complex system theory into the study of an economic system, which greatly enriches the study of long-term game complexity of an economic system. Zhang et al. [14] formulated a finite-level stochastic programming problem as a dynamic chance-constrained program and demonstrated the efficiency of the presented model. Besbes and Zeevi [15] considered a pricing problem with the demand curve unknown and illustrated the sufficiency of the linear model for dynamic pricing with demand learning. Coucheney et al. [16] obtained a new kind of continuous time learning dynamics, which is composed of a class replicator drift with penalty term adjustment in n -person games. Guo et al. [17] applied typical dynamic equilibrium algorithms such as the simplex gravity flow dynamics and the projected dynamical system to study the dynamic traffic equilibrium problem. Kim et al. [18] studied dynamic scheduling in a service system of multilevel. Ajorlou et al. [19] analyzed the optimal dynamical pricing problem in which the information of products can only be spread via words of mouth. By proving that the price fluctuation of nondurable products disappears after a limited time, the critical role of the product type in zero price sales optimization is further revealed. Ma and Xie [20] studied the effects of adjustment speed and loss sensitivity on supply chain stability and found that the supply chain would be stable when the retailer is not sensitive to the loss or adjusts the decision carefully. Camerer et al. [21] studied dynamic unstructured bargaining, which included deadlines and unilateral information about amounts. They used machine learning to prove that the characteristics of bargaining process recorded in the early stage of the game improve the prediction of disagreement. Jin [22] proposed a stable dynamical system for drivers to choose the departure time under a bottleneck. Li et al. [23] considered the issue of fair concern in pricing and discussed the stability of the Nash equilibrium point in the price game. Although the nonlinear dynamics theory has been used in some research studies on the price and quantity game, the market characteristics in different fields are different. Considering the difficulty and cost the manufacturers faced to obtain information about

their competitors, we adopt limited rational hypothesis and set up models under two different bargaining forms, which can further enrich the application of the theory in practice. We analyze the performance of two dynamic bargaining systems in terms of profit and stability and illustrate the different strength of bargaining power in different models. For the chaos appeared in the dynamic system, we not only analyze its influencing factors, but also present a method to control it.

Chaos control is significant since in many cases it may cause fluctuation in the supply chain and is not conducive to decision-making. Many methods have been proposed by scholars and widely used in chaos control. OGY is the earliest proposed method by Ott et al. [24] for chaos control. Askar [25] adopted the feedback control method to return the dynamic Stackelberg game to the stable region. Elsadany and Awad [26] used the feedback control method to control the disordered behaviors of the Bertrand competition market. Li et al. [27] realized effective chaotic control by the application of parameter adaptation method. Besides the above methods, the delay feedback control (DFC) is another method that is effective for chaos control and has been widely used in many other fields. Since DFC has good tracking ability and does not change the structure of the controlled system, we adopted it to stabilize the system in bargaining process.

3. Model Description

We consider a supply chain that consisted of two manufacturers (marked as $i = 1$ and 2) and one supplier. The two manufacturers purchase the common component from the supplier to produce similar products which induces the competition between them. We assume the manufacturer i 's inverse demand function as follows: $p_i = a - q_i - bq_j$, $i, j = 1, 2, i \neq j$, in which p_i is the market price for the products made by the manufacturer i , q_i and q_j represent the quantity of the two products, a is the market capacity, and b is the competition intensity. Similar settings have been used in the supply chain literature (e.g., [12, 28]). Since the price of the manufacturer i is influenced more by his/her own quantity than their competitors [29], b should be in the range of $0 < b < 1$. Here, we normalize a to one and assume the suppliers cost c as zero to simplify calculation. The manufacturers can purchase the component separately or they can form a bargaining alliance and designate the leader to collectively negotiate with the supplier. We used the GNB framework to model the process of the bargaining, which is commonly used in the supply chain in terms of bargaining between buyers and sellers. We assume the bargaining power of the manufacturer i towards the supplier is k_i and the supplier's bargaining power towards the manufacturer i is $1 - k_i$, correspondingly.

3.1. Separate Bargaining. In the case of separate bargaining, the two manufacturers bargain with the supplier separately, and the decision process is as follows: firstly, the manufacturer i decides the procurement quantity q_i and then bargains with the supplier for the wholesale price w . The profit functions of the manufacturer i and the supplier can be described as follows:

$$\begin{aligned}\pi_i(q_i, q_j, w_i) &= (1 - q_i - bq_j - w_i)q_i, \\ \pi_s(q_i, q_j, w_i, w_j) &= w_i q_i + w_j q_j.\end{aligned}\quad (1)$$

We use the GNB framework to solve this case, and this framework has been widely used in the economic system [30]. We assume that two negotiations are carried on at the same time, and no information is shared between manufacturers, so q_j indicates the value estimated by the manufacturer i . Since the supplier has the responsibility to keep business confidential, this assumption is common in practice. Meanwhile, in an order period, renegotiation is not allowed, which in other words means that once the negotiation is failed, the manufacturer cannot launch another negotiation and both sides of the bargaining will gain no profit. Based on the GNB framework, we can formulate the bargaining problem as follows:

$$\max_{w_i} \pi_i(q_i, q_j, w_i)^{k_i} [\pi_s(q_i, q_j, w_i, w_j) - w_j q_j]^{1-k_i}. \quad (2)$$

Lemma 1. *The wholesale price is $w_i(q_i, q_j) = (1 - k_i)(1 - q_i - bq_j)$, and the manufacturer's profit is $\pi_i(q_i, q_j, w_i(q_i, q_j)) = k_i(1 - q_i - bq_j)q_i$.*

As shown in the above formula, the wholesale price is based on manufacturers' procurement quantity and the bargaining power of both. When the bargaining power of the manufacturer is extremely high, the wholesale price is close to zero; in other words, the manufacturer will gain the profit of the whole supply chain as more as possible. This can also be demonstrated in the second formula of profit. On the contrary, when the bargaining power of the manufacturer is rather small, the profit space will be tremendously compressed.

Static analysis is commonly used in the existing literature to analyze the bargaining problem in the supply chain. However, under the complicated environment, bargaining between both sides is a long-term and complex process, which cannot be solved by only one game. Next, we will employ the method of dynamic game to conduct multi-period adjustment to achieve the equilibrium solution and analyze the system stability.

Because of the lack of market information, the manufacturers are not always rational. For a better practical fit, we assume that the manufacturer adopts the adjustment rule called the gradient adjustment mechanism where they decide their procurement quantity based on the counterpart and margin profit in the last period. The application of this mechanism can also be found in other literatures [31, 32]. The mechanism can be formulated as follows:

$$\begin{cases} q_1(t+1) = q_1(t) + \alpha q_1(t) \frac{\partial \pi_1}{\partial q_1(t)}, \\ q_2(t+1) = q_2(t) + \beta q_2(t) \frac{\partial \pi_2}{\partial q_2(t)}. \end{cases} \quad (3)$$

Under this rule, the manufacturers will increase their procurement quantity in period $t + 1$ if the margin profit in period t is positive and will reduce the order quantity on the contrary. The parameters $\alpha > 0$ and $\beta > 0$ are with respect to the decision adjustment speed. The larger the parameters are, the greater change of procurement quantity will be in the next order period.

With the gradient adjustment mechanism, the manufacturers will stop adjusting their procurement quantity when $q_i(t + 1) = q_i(t)$. By solving the equation $q_i(t + 1) = q_i(t)$, we can achieve four equilibrium solutions as follows: $E_0(0, 0)$, $E_1(0, 1/2)$, $E_2(1/2, 0)$, and $E^*(1/(b + 2), t/(b + 2))$, among which E_0 , E_1 , and E_2 are the boundary equilibrium points and E^* is the only Nash equilibrium point.

Equilibrium points' stability is decided by the characteristic roots of the Jacobi matrix. When the absolute values of the characteristic roots are less than one, the equilibrium point tends to be stable, or not, otherwise. And, the Jacobi matrix can be shown as follows:

$$J = \begin{bmatrix} \frac{\partial q_1(t+1)}{\partial q_1(t)} & \frac{\partial q_1(t+1)}{\partial q_2(t)} \\ \frac{\partial q_2(t+1)}{\partial q_1(t)} & \frac{\partial q_2(t+1)}{\partial q_2(t)} \end{bmatrix} = \begin{bmatrix} j_{11} & -bk_1\alpha q_1 \\ -bk_2\beta q_2 & j_{22} \end{bmatrix}, \quad (4)$$

where $j_{11} = 1 + \alpha k_1(1 - 4q_1 - bq_2)$ and $j_{22} = 1 + \beta k_2(1 - 4q_2 - bq_1)$.

Proposition 1. *Equilibrium solutions $E_0(0, 0)$, $E_1(0, 1/2)$, and $E_2(1/2, 0)$ are not stable.*

More detailed proof can be found in Appendix. Lacking of stability implies that the solution cannot return to a fixed position in a certain period, and in this bargaining problem in the supply chain, it means the quantity will not turn to a fixed value after iterations during multiple periods. At these three boundary equilibrium points, at least one of the manufacturers decides not to place order, which signifies abandoning the next bargaining cycle. This will do harm to his/her interests or even force him/her to withdraw from the market in the long term. Therefore, the supply chain is not sustainable and unpredictable, which brings more difficulty to decision-making.

In terms of the Nash equilibrium point, since the characteristic roots of its Jacobi matrix are difficult to compute, we can use the Jury criterion [33] to judge it. And, the two-dimensional Jury criterion can be shown as follows:

$$\begin{cases} 1 + \text{Tr} + \text{Det} > 0, \\ 1 - \text{Tr} + \text{Det} > 0, \\ 1 - \text{Det} > 0, \end{cases} \quad (5)$$

where Tr and Det are the trace and the determinant of the Jacobi matrix, respectively.

Proposition 2. *The conditions for the stability of the supply chain can be described as follows:*

$$\begin{cases} 0 < \alpha k_1 < 2 + b, \\ 0 < \beta k_2 < \frac{4(2 - \alpha k_1 + b)}{4 - \alpha k_1(2 - b)}. \end{cases} \quad (6)$$

Proposition 2 demonstrates that the bargaining power and adjustment speed should be small at the same time to ensure the stability of the system. It is said that when α and β are large, the manufacturers are quite sensitive to the profit they have had in the last period, and a small fluctuation will induce a substantial change in their decision. A strong bargaining power implies a high expectation of profit it can share in a supply chain, following with a high possibility of the failure of negotiation between the supplier and manufacturers, which is not advantageous to the stability of the supply chain.

To better explain the influence of parameters in Proposition 2, we adopt numerical analysis, where we set $b = 0.1$. The 2D bifurcation diagram is shown in Figure 1, using the dual-layer iterative algorithm, which can also be found in [32, 34]. The stable region is marked in blue. When the bargaining power and adjustment of both manufacturers are small, the bargaining system maintains stability. However, the increase of either factor will cause damage to stability, which brings more loss risk and decision-making difficulty to members in the system. Figure 2 focuses on the adjustment speed and depicts the parameter basin with respect to α and β . The system changes from the stable region (marked in green), through the cycle-2 (marked in blue) and the cycle-4 (marked in purple), to the chaotic region (marked in light gray). When the value of adjustment speed is quite big, the system may even enter the divergence region (marked in dark gray) finally.

In Figures 3 and 4, the bifurcation and corresponding LLE diagram show that a manufacturer with a stronger bargaining power will probably induce the system to fall into an unstable region. The formation of chaotic attractors demonstrates the track of the system. We take k_1 for example in Figure 5 and k_2 is similar to it. With the increase of k_1 ($k_1 = 4.465, 6.025, 6.155$, and 6.545), the track tends to be disordered. Strong bargaining power increases the contradiction of negotiation, and sometimes the manufacturers need to sacrifice certain current profit for the sake of long-term benefit.

3.2. Collective Bargaining. Besides separate bargaining, manufacturers can also form an alliance to negotiate with the supplier collectively. Leader-based collective bargaining is one of the most popular forms of collective bargaining in practice. In this case, manufacturers decide their procurement quantity q_i, q_j at first, and then they form an alliance and designate manufacturer i (here, we assume $k_i > k_j$) to negotiate with the supplier with the total quantity $q_i + q_j$ for the wholesale price w . Since the quantity under collective bargaining ($q_i + q_j$) is larger than that under separate one (q_i), we defined k as the new bargaining power and $k > k_i$. No renegotiation is permitted. If succeed, both manufacturers will get the component with the wholesale price; otherwise, none of the three parts in this supply chain will gain profits.

The profit functions of manufacturers and the supplier can be described as follows:

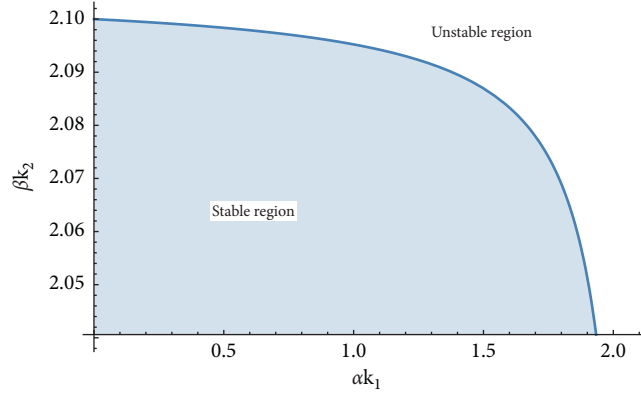
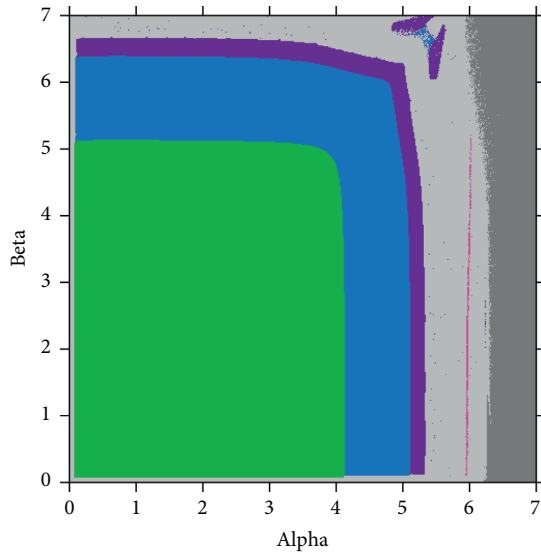


FIGURE 1: The stable region of the separate bargaining system.

FIGURE 2: The parameter basin with respect to α and β .

$$\begin{aligned}\pi_i(q_i, q_j, w_i) &= (1 - q_i - bq_j - w)q_i, \\ \pi_s(q_i, q_j, w_i, w_j) &= w(q_i + q_j).\end{aligned}\quad (7)$$

Based on the GNB framework, the bargaining problem between the leader manufacturer and the supplier can be formulated as

$$\max_w \pi_i(q_i, q_j, w)^k [w(q_i + q_j)]^{1-k}. \quad (8)$$

Lemma 2. The outcomes of the wholesale price is

$$w(q_i, q_j) = (1 - k)(1 - q_i - bq_j), \quad (9)$$

and the manufacturers' profit is

$$\begin{aligned}\pi_1(q_i, q_j) &= k(1 - q_1 - bq_2)q_1, \\ \pi_2(q_i, q_j) &= [k - q_2 - bq_1 + (1 - k)(q_1 + bq_2)]q_2.\end{aligned}\quad (10)$$

Both functions of the wholesale price and the profit have the same form as the counterpart under separate bargaining. But, considering the enhanced bargaining power, it is actually different. Compared with the separate bargaining case, with the stronger bargaining power, the wholesale price is more close to zero and the manufacturer will gain more share of the whole profit in the supply chain. This provides manufacturers with a stand point to form an alliance willingly.

Likewise, under the gradient adjustment mechanism, the system can be formulated as

$$\begin{cases} q_1(t+1) = q_1(t) + \alpha q_1(t)k(1 - 2q_1(t) - bq_2(t)), \\ q_2(t+1) = q_2(t) + \beta q_2(t)(k - 2q_2(t) - bq_1(t) + (1 - k)(q_1(t) + 2bq_2(t))). \end{cases}\quad (11)$$

By solving the equation $q_1(t+1) = q_1(t)$, we can achieve four equilibrium solutions as

$$\begin{aligned}E_0 &(0, 0), \\ E_1 &\left(0, \frac{k}{2 - 2b(1 - k)}\right), \\ E_2 &\left(\frac{1}{2}, 0\right), \\ E^* &\left(\frac{2 - 2b + bk}{4 - b^2 - 3b + 3bk}, \frac{1 - b + k}{4 - b^2 - 3b + 3bk}\right),\end{aligned}\quad (12)$$

in which E_0 , E_1 , and E_2 are the boundary equilibrium points and E^* is the only Nash equilibrium point.

Proposition 3. Equilibrium solutions E_0 , E_1 , and E_2 are not stable.

At least one of the quantity decisions is set to zero in these three boundary equilibrium points, which is the lack of economic significance and is not sustainable. It means that the manufacturer chooses to abandon the next bargaining period, which may cause damage to him/her and may even

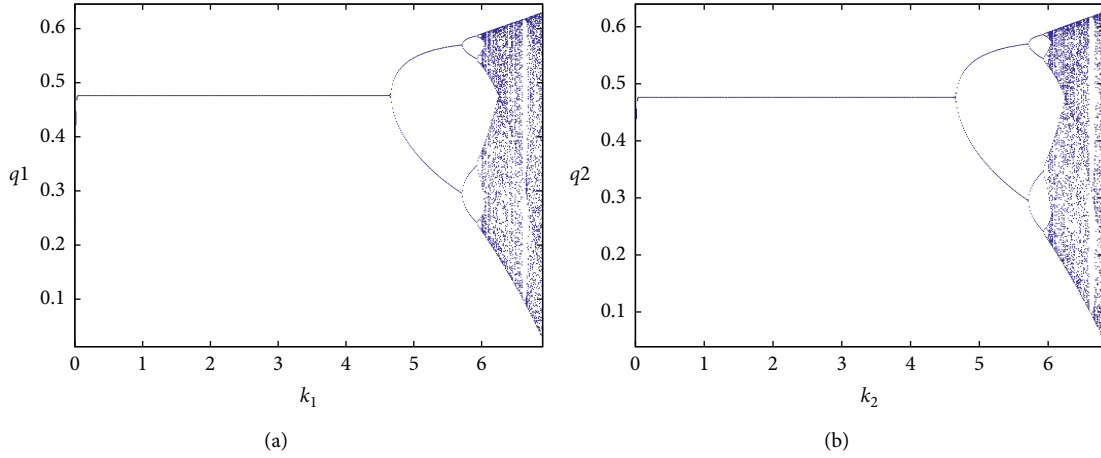


FIGURE 3: The bifurcation diagram of the model with respect to k_1 and k_2 .

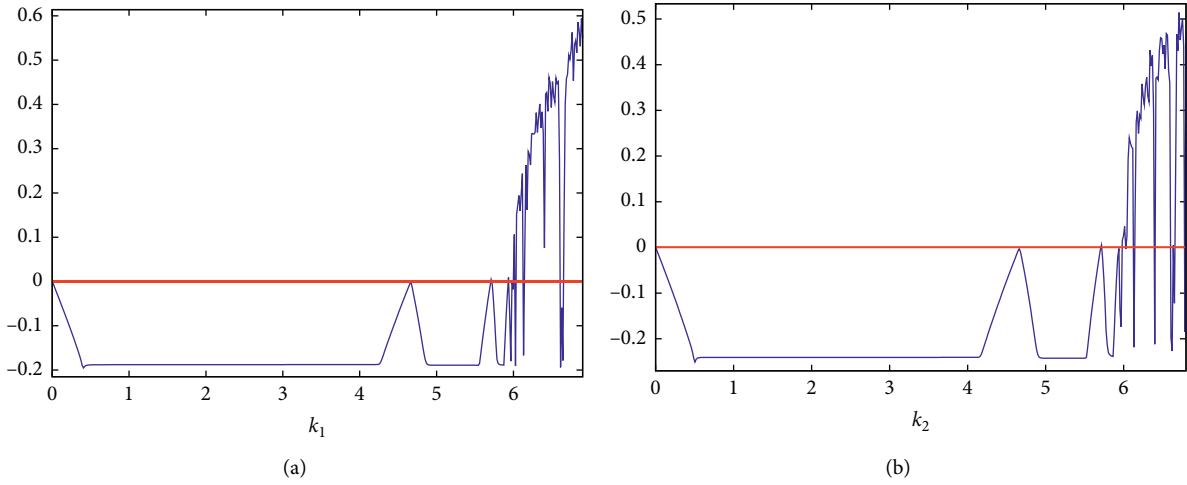


FIGURE 4: LLE diagram of the model with respect to k_1 and k_2 .

be forced out of the market in the long run. Therefore, boundary equilibrium points cannot maintain stability and is not sustainable in reality. Since the absolute values of the characteristic roots are less than one, it means that the three boundary equilibrium points are lacking stability and will approach to chaos after a few iterations. Under these circumstances, the supply chain is in a shambles, and the

economic activities in the supply chain are unpredictable, which add more difficulty for decision-making.

Proposition 4. *In terms of the Nash equilibrium point, the conditions under the Jury criterion for the stability of the supply chain can be described as follows:*

$$\left\{ \begin{array}{l} 0 < \alpha < \frac{4(b(3+b-3k)-4)(4-3b-b^2+3bk+((b-1)b-1)k-(b-1)^2)\beta}{((k-2)b+2)k(4b(3+b-3k)-16+((b-1)^2(4+b)+4(1+b-b^2)k-bk^2)\beta)}, \\ 0 < \beta < \frac{b(3+b-3k)-4}{((b-1)b-1)k-(b-1)^2}. \end{array} \right. \quad (13)$$

Proposition 4 presents that the adjustment speed should be controlled below the threshold so that the stability can be guaranteed. And, the effect of bargaining power is significant

but complex. For the sake of the better explanation of Proposition 4, we picture the stable region of the collective bargaining system in Figure 6.

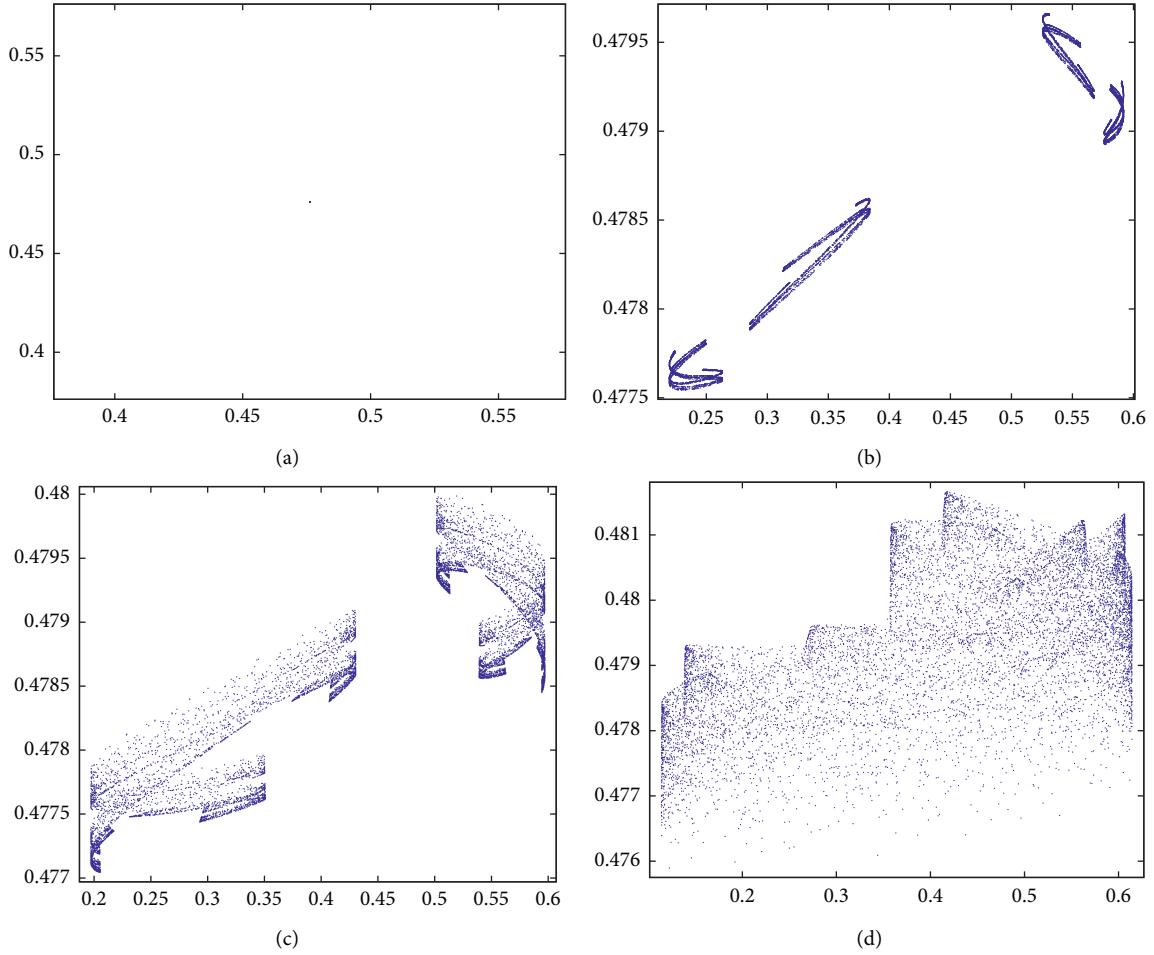


FIGURE 5: The stable region of both bargaining systems.

Just as stated in Proposition 4, the system will stay stable when the bargaining power and adjustment of both manufacturers are small simultaneously. Figures 7 and 8 depict the bifurcation of the model in terms of the adjustment speed. And, Figure 9 shows the track of the system from stable to chaos with the increase of α ($\alpha = 2.594, 3.398, 3.465$, and 3.599). We take α , for example, and β is similar to it. When one of the manufacturers increases the speed of decision adjustment, it means that he/she may make a big change while making the next decision. This change causes the fluctuation of not only ones own decision but also the decision of the others. Due to the sensibility of the dynamical system, the fluctuation will be magnified and lead the system to chaos.

3.3. Performance Comparison. In practice, risk and profit are two key factors emphasized by enterprises. Considering that, we will present the comparisons on these two factors between separate bargaining and collective bargaining in the following.

Proposition 5. *Total profit of the alliance under collective bargaining is greater than that under separate bargaining at the Nash equilibrium point, if $b < b^*$, while chaos will cause damage to profits of both forms.*

According to Lemma 1 and the Nash equilibrium point, the sum of the two manufacturers' profits in the separate bargaining system is $(\pi_1 + \pi_2)^S = (k_1 + k_2)/(2 + b)^2$. Similarly, the gross profit of the alliance formed by these manufacturers in the collective bargaining system is $(\pi_1 + \pi_2)^C = ((1 - b)^3 + (1 - b)^2(6 + b)k + (1 - b)(1 + 6b)k^2 + (b + b^2)k^3)/(4 - b^2 - 3b - 3bk)^2$. Since $k > k_1 > k_2$, the total profit $(\pi_1 + \pi_2)^C$ is greater than $(\pi_1 + \pi_2)^S$ when b satisfies $b < b^*$. More detailed proof can be found in the online appendix. When b is large, the competition intensity between manufacturers is great and the quantity the other manufacturer purchased will lay more influence on one's own sale price. Since the influence is negative, it will diminish the sale price and shrink the profit. Meanwhile, considering the profit expression from above, we can see that profit is closely related to bargaining power. Since bargaining power affects the profit distribution between the supplier and the manufacturer, when the supplier bargains with the powerful buyer, his/her share will be compressed. The enhanced bargaining power has won manufacturers' lower wholesale prices, which means more profit margins. Therefore, the manufacturer will obtain more when his bargaining power is close to one. Especially, when his bargaining power is equal to one, the manufacturer will obtain the whole surplus of the negotiation.

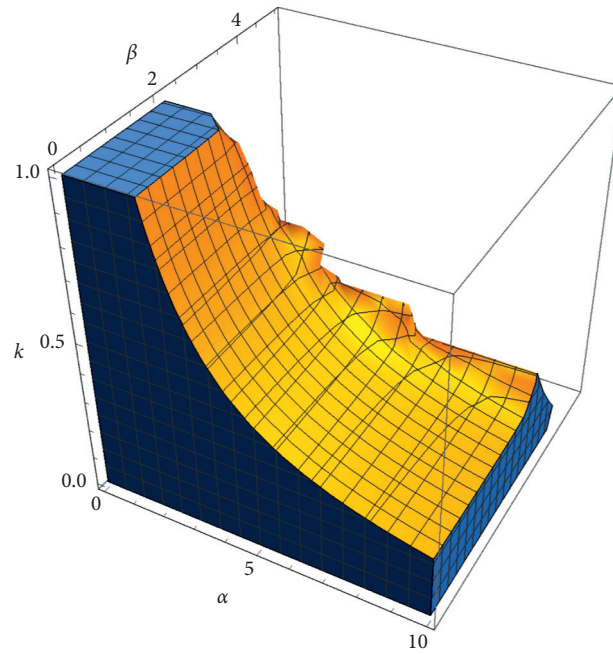


FIGURE 6: The stable region of the collective bargaining system.

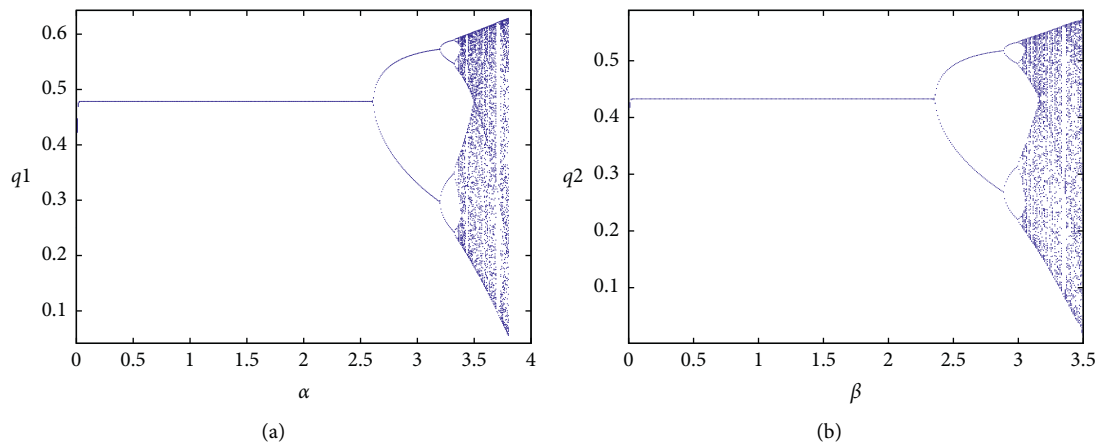


FIGURE 7: The bifurcation diagram of the model with respect to α and β .

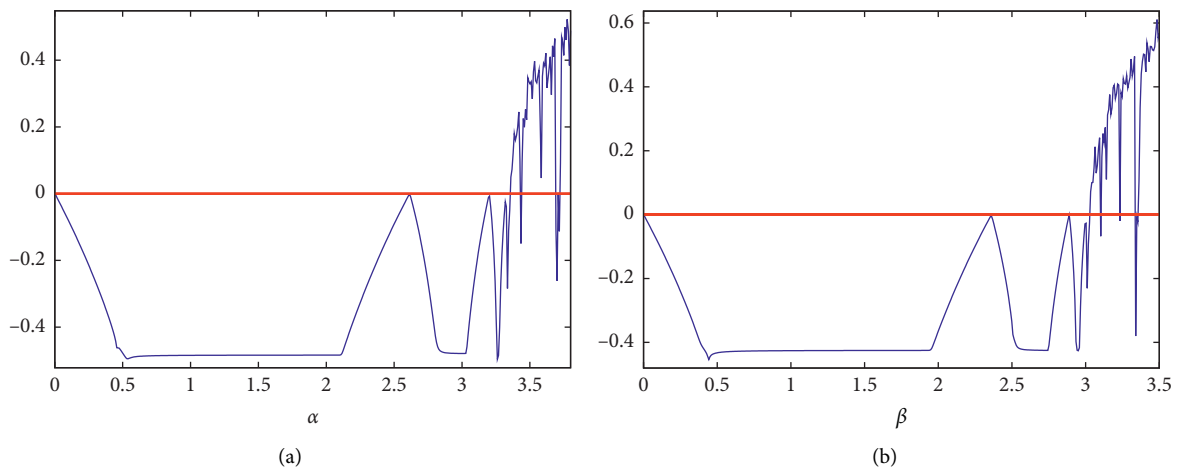


FIGURE 8: LLE diagram of the model with respect to α and β .

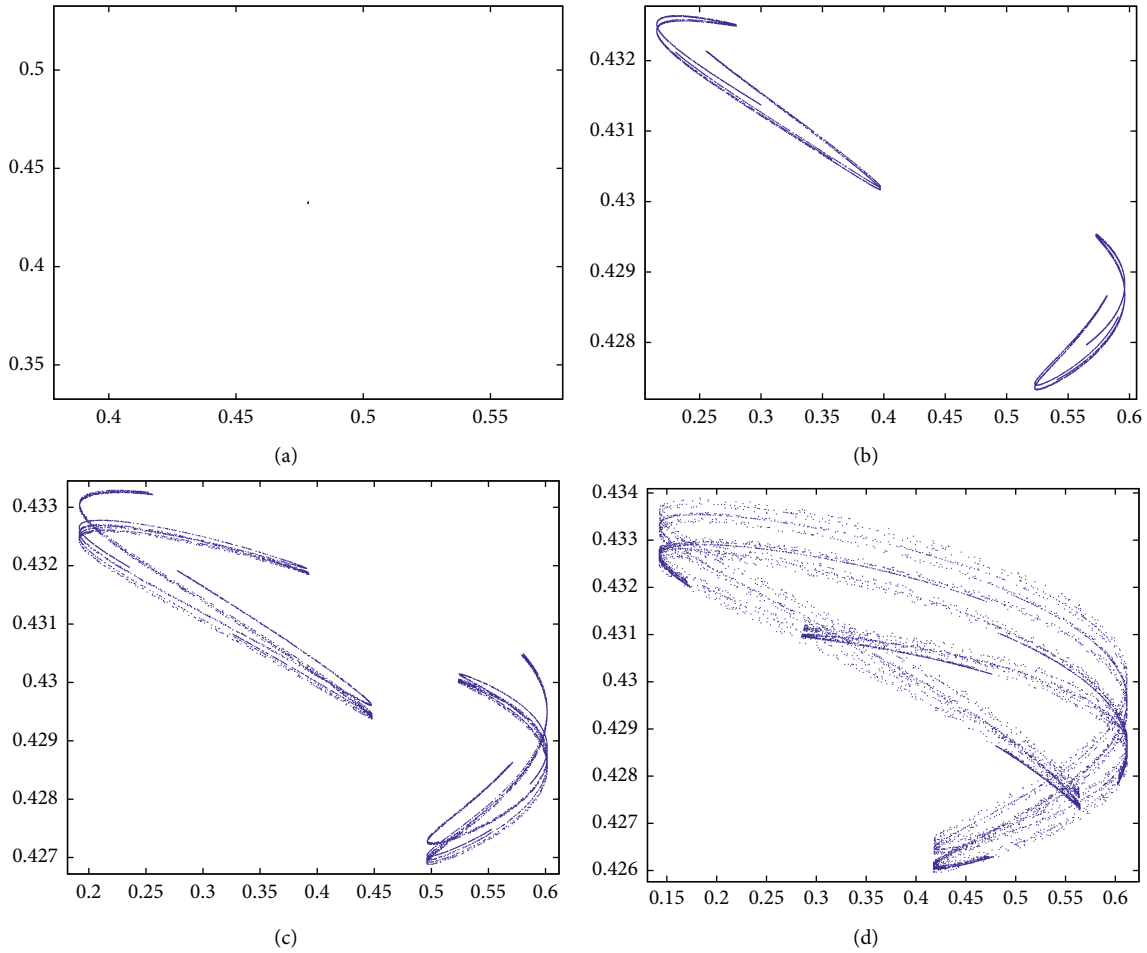


FIGURE 9: The formation of chaotic attractors.

Figure 10 shows the sum of both manufacturers' profits under separate (marked in blue) and collective (marked in red) bargaining. For ease of observation, the profits in the chaotic region are represented by a mean value [35, 36]. With the increase in adjustment speed, the system enters into chaos, and the profits of both forms cut down and eventually become irregular. Chaos will cause the market to fluctuate continuously, and manufacturers will be more sensitive to their current profit to adjust production more frequently and substantially, which adds more difficulty to decision-making. Influenced by both one's own and the opponent's decision, the market price fluctuates greatly, so do the profits of manufacturers.

Proposition 6. *Stability of the supply chain under separate bargaining is better than that under collective bargaining.*

To focus on the common factor, i.e., adjustment speed, we fixed bargaining power as $k = 0.8$, $k_1 = 0.5$, and $k_2 = 0.4$. Based on the above analysis, we can obtain the stable region (marked in green) of both separate bargaining 11(a) and collective bargaining 11(b) in Figure 11. Same as before, the chaotic region and the divergence region are marked in light gray and dark gray, respectively. Obviously, the stable regions of the collective bargaining system shrink a lot compared with the separate bargaining system.

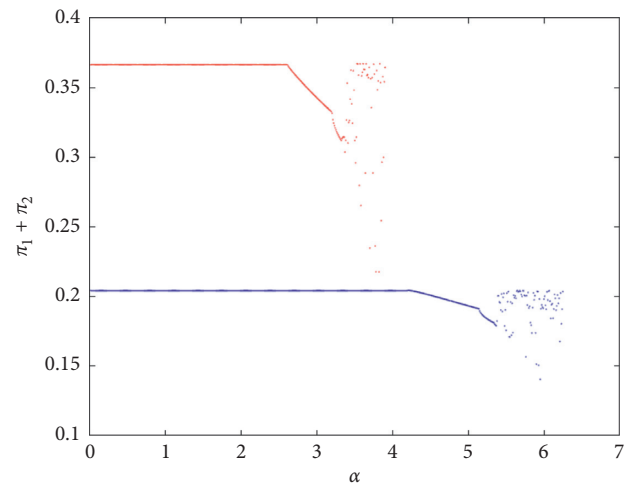


FIGURE 10: The total profit of manufacturers.

In collective bargaining, manufacturers form the alliance designate manufacturer 1 as a leader to negotiate with the supplier. Since the leader pools the quantity of both manufacturers, a slight fluctuation will bring great changes to the system. Therefore, the adjustment speed should be controlled to a smaller extent. Compared with separate

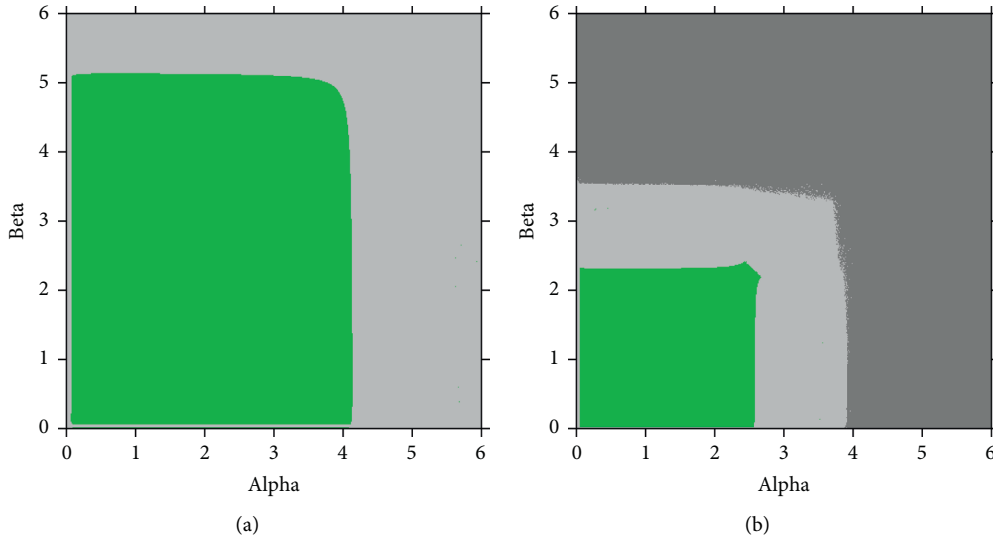


FIGURE 11: The stable region of both bargaining systems.

bargaining, the adjustment speed of the follower not only influences his/her own decision but also has indirect impact on the alliance. With the double influence, the collective bargaining system will be easier to be chaotic if the adjustment speed increased. Meanwhile, according to Proposition 2, the range of the stable region will contract with the enlargement of k . Since $k > k_i$, manufacturer i possesses a stronger bargaining power under collective bargaining and the enhanced bargaining power will also account for the reduction of the stable region.

We depict the bifurcation diagrams of the profit under separate bargaining in Figure 12 and collective bargaining in Figure 13. Profits of manufacturer 1 are marked in blue and pink with respect to α and β . The counterparts of manufacturer 2 are marked in green and red, respectively. Comparing Figure 12 with 13, we also find that though the increase in both adjustment speeds will cause the system to enter into chaos, similarly, the influence of them will be different between separate and collective bargaining systems. For separate bargaining, the bifurcation and chaos appear earlier with the increase in α than β , but in the case of collective bargaining, the situation is reversed.

The transformation of relationship focus between manufacturers, from competition to cooperation, can explain the change of adjustment speed status. In separate bargaining, competition is more emphasized, and the position of the manufacturer determines the influence of his/her adjustment speed. Since we assumed that manufacturer 1 is more powerful than manufacturer 2, his/her adjustment speed has more influence on the system. When two manufacturers form an alliance in collective bargaining, competition is weakened and cooperation plays a more critical role in the bargaining system. Since manufacturer 1 is the representative of the alliance to negotiate with the supplier, the adjustment speed of manufacturer 2 not only influences his/her own decision directly but also has an impact on the alliance. Because the influence of β is double, it has more influence in collective bargaining.

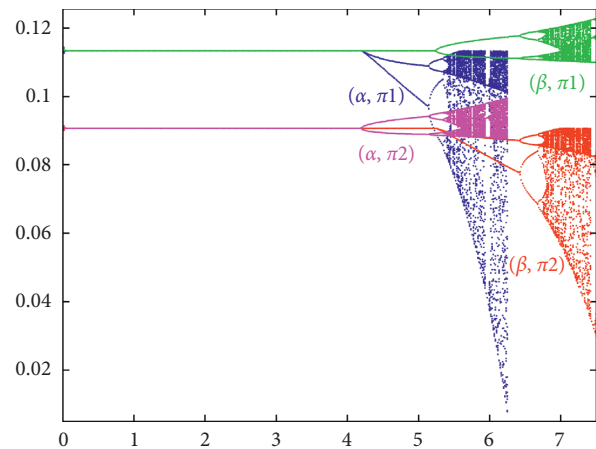


FIGURE 12: The bifurcation diagram of the profit under separate bargaining.

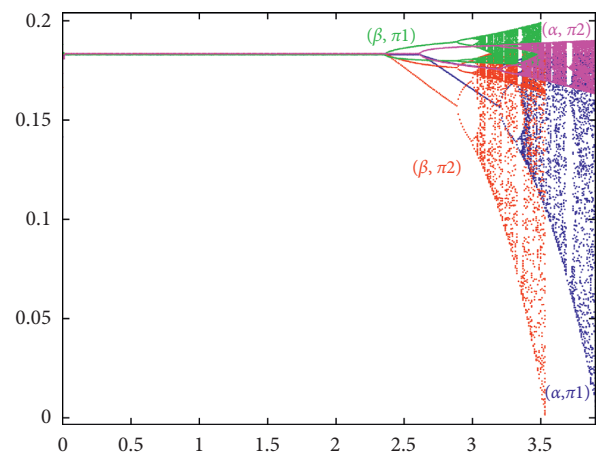


FIGURE 13: The bifurcation diagram of the profit under collective bargaining.

Propositions 5 and 6 imply that the collective bargaining brings more profit and risk at the same time. In order to develop the strength and avoid the weakness, the controlling of the supply chain state is significant. In the following, we will present the chaos controlling method and use it to maintain the stability of the supply chain.

4. Chaos Control

Chaos is inherently random, nonlinear, and sensitive to an initial value. Sometimes, chaos benefits firms [37]. However, in the supply chain and other economic systems, chaos is harmful in many cases. It makes manufacturers difficult to make accurate decisions and causes profit fluctuation. And, for the enterprise, there is even a risk of being forced out of the market in the long run. According to Proposition 5, chaos will cause damage to both the separate bargaining system and the collective bargaining system, which makes profits fall and show irregular fluctuations. In order to maintain profit advantage of collective bargaining, it is very

important to take effective methods according to the characteristics of the system to control the chaos.

As one of the methods of chaos control, the delay feedback control method does not change the structure of the controlled system and has good tracking ability and stability. Its main idea is to feedback partial information of the output signal of the system, instead of the external input, to the control system with delay time. The control system can be described as follows:

$$x_i(t+1) = f(x_i(t), u_i(t)), \quad i = 1, 2, \quad (14)$$

where $x(t)$ is the state variable and $u(t)$ is the control signal. The specific form of the control signal is as follows:

$$u_i(t) = \begin{cases} \delta(x_1(t+1-\tau) - x_1(t+1)), & i = 1, \\ \lambda(x_2(t+1-\tau) - x_2(t+1)), & i = 2, \end{cases} \quad (15)$$

where δ and λ are the controlling factors and $\tau(t > \tau)$ is the length of lag time. Here, we assume τ as one period. The control system can be formulated as

$$\begin{cases} q_1(t+1) = q_1(t) + \frac{\alpha q_1(t)k(1-2q_1-bq_2)}{1+\delta}, \\ q_2(t+1) = q_2(t) + \frac{\beta q_2(t)(k-2q_2-bq_1+(1-k)(q_1+2bq_2))}{1+\lambda}, \end{cases} \quad (16)$$

and the Jacobi matrix of the control system is

$$J = \begin{bmatrix} 1 + \frac{\alpha k(1-4q_1-bq_2)}{1+\delta} & \frac{-\alpha k b q_1}{1+\delta} \\ \frac{\beta q_2(-b+1-k)}{1+\lambda} & 1 + \frac{\beta(k-4q_2-bq_1+(1-k)(q_1+4bq_2))}{1+\lambda} \end{bmatrix}. \quad (17)$$

At the Nash equilibrium point $E^*((2-2b+bk)/(4-b^2-3b+3bk), q(1-b+k)/(4-b^2-3b+3bk))$, the above Jacobi matrix can be formulated as follows:

$$J = \begin{bmatrix} 1 + \frac{\alpha k(4+2b(k-2))}{(1+\delta)(b^2-4-3b(k-1))} & \frac{-\alpha k b(2-2b+bk)}{(1+\delta)(4-b^2-3b+3bk)} \\ \frac{\beta(-b+1-k)(1-b+k)}{(1+\lambda)(4-b^2-3b+3bk)} & 1 + \beta \frac{2(1-b^2(k-1)+k+b(k^2-2))}{(1+\lambda)(b^2-4-3b(k-1))} \end{bmatrix}. \quad (18)$$

From the former numerical analysis, we know that the system is chaotic when $\alpha = 3.5$, $\beta = 3.3$, and $k = 0.8$. But now, the matrix of the control system has the form as

$$J = \begin{bmatrix} 1 - \frac{2.68}{1+\delta} & \frac{-0.13}{1+\delta} \\ \frac{0.14}{1+\lambda} & 1 - \frac{2.80}{1+\lambda} \end{bmatrix}. \quad (19)$$

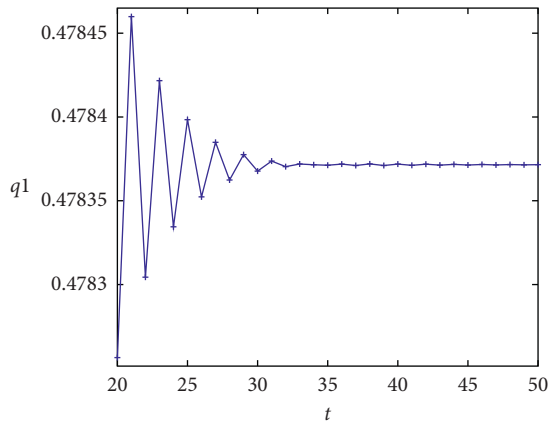


FIGURE 14: The quantity fluctuations of manufacturer 1.

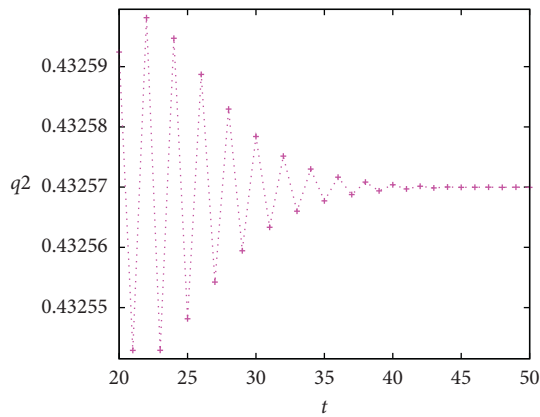


FIGURE 15: The quantity fluctuations of manufacturer 2.

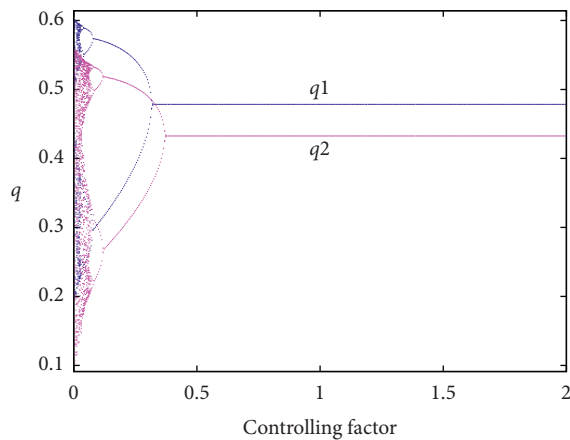


FIGURE 16: The bifurcation diagram of the controlling factors.

The stability is achieved when the Jury criterion is satisfied. Therefore, the control system is stable around the Nash equilibrium point when

$$\begin{cases} 0.14 + \delta(\lambda - 0.40) - 0.34\lambda > 0, \\ 2.80\delta - 2.04 + 2.68\lambda > 0. \end{cases} \quad (20)$$

As shown in Figures 14 and 15, when $\delta = 0.5$ and $\lambda = 0.6$, the quantity tends to the fixed Nash equilibrium value (0.478, 0.433) after several iterations. Obviously, it can also be seen from Figure 16 that the system has changed from chaos to stability with the enhancement of controlling factors δ and λ . The delayed feedback control method is effective for chaos control. Under these circumstances, manufacturers can adjust their decision by not only taking the profit of the last period as the benchmark, but also taking the profit of the previous periods as the reference to improve the stability and effectiveness of decision-making. With the application of controlling factors, manufacturers can guide the system back to stability by increasing the value of controlling factors. Therefore, the manufacturers can make more efficient decision and lower the risk that chaos brought at the same time, which are advantageous for the whole supply chain.

5. Conclusion

This paper analyzed the system of two forms of bargaining: the separate one and the collective one. The boundary equilibrium points of both are unstable. In fact, neither of the manufacturers wants to keep his quantity at zero because that would cost him market share. Therefore, the motivation to change will damage the stability of the bargaining system. The Nash equilibrium point is sensitive to the value of adjustment speed and bargaining power of manufacturers. The result demonstrated that the bargaining power and adjustment speed should be small at the same time to ensure the stability of the system. The adjustment speed reflects the sensitivity of manufacturers to the profits of the last period. When the adjustment speed is large, it will magnify the fluctuation in the system and cause chaos. Meanwhile, the bargaining power should be small to reduce the probability of negotiation failure. Comparing these two forms of bargaining, we found that the collective bargaining brings about more profits and risks at the same time. However, chaos will cause damage to the gross profit of manufacturers, which reduces the profit advantage of collective bargaining. By introducing the controlling factors, the delay feedback method can control the chaos effectively. It means that manufacturers can make their decisions not only based on the information from the last period but also from previous periods to improve decision effectiveness. This result can help manufacturers make decisions accurately and is beneficial for maintaining the stability of the economic system.

Appendix

Proofs for Main Results

Proof of Lemma 1. w can be solved by deriving formula (2), and then π can be described with w as $\pi_i(q_i, q_j, w_i(q_i, q_j)) = k_i(1 - q_i - bq_j)q_i$.

Proof of Proposition 1. The four equilibrium points is the solution of $q_i(t+1) = q_i(t)$ can be specified as follows:

$$\begin{cases} q_1(t) = q_1(t) + \alpha q_1(t)k_1(1 - 2q_1(t) - bq_2(t)), \\ q_2(t) = q_2(t) + \beta q_2(t)k_2(1 - 2q_2(t) - bq_1(t)). \end{cases} \quad (\text{A.1})$$

And, can take $E_0(0, 0)$, $E_1(0, 1/2)$, $E_2(1/2, 0)$, and $E^*(1/(b+2), 1/(b+2))$ into the Jacobi matrix.

The Jacobi matrix of $E_0(0, 0)$ is

$$J(E_0) = \begin{bmatrix} 1 + \alpha k_1 & 0 \\ 0 & 1 + \beta k_2 \end{bmatrix}. \quad (\text{A.2})$$

The characteristic roots of $J(E_0)$ is $\lambda_1 = 1 + \alpha k_1$ and $\lambda_2 = 1 + \beta k_2$. Since $\alpha, \beta > 0$ and $k_1, k_2 \in (0, 1)$, the absolute value of both characteristic roots is more than one, which means that E_0 is unstable. The Jacobi matrix of $E_1(0, 1/2)$ is

$$J(E_1) = \begin{bmatrix} 1 + \frac{1}{2}\alpha k_1(2-b) & 0 \\ -\frac{1}{2}\beta k_2 & 1 - \beta k_2 \end{bmatrix}. \quad (\text{A.3})$$

One of the characteristic roots is $\lambda = 1 + (1/2)\alpha k_1(2-b)$, which is more than one.

E_2 can be proved similarly as E_1 .

Proof of Proposition 2. The Jacobi matrix of $E^*(1/(b+2), 1/(b+2))$ is

$$J(E^*) = \begin{bmatrix} \frac{2 - 2\alpha k_1 + b}{2 + b} & \frac{b\alpha k_1}{2 + b} \\ \frac{b\beta k_2}{2 + b} & \frac{2 - 2\beta k_2 + b}{2 + b} \end{bmatrix}. \quad (\text{A.4})$$

The trace and determinant of $J(E^*)$ is

$$\begin{aligned} \text{Tr}(J(E^*)) &= \frac{2[2 - \alpha k_1 - \beta k_2 + b]}{2 + b}, \\ \text{Det}(E^*) &= \frac{2 + b - 2(\alpha k_1 + \beta k_2) + \alpha k_1 \beta k_2(2 - b)}{2 + b}. \end{aligned} \quad (\text{A.5})$$

Solving three inequalities: $1 + \text{Tr} + \text{Det} > 0$, $1 - \text{Tr} + \text{Det} > 0$, and $1 - \text{Det} > 0$ at the same time and Proposition 2 can be achieved.

Proof of Lemma 2. The proof of Lemma 2 is similar to that of Lemma 1.

Proof of Proposition 3. In terms of collective bargaining, the gradient adjustment mechanism of manufacturer 1 is the same as that in separate bargaining, while the formula of manufacturer 2 is adjusted as

$$q_2(t+1) = q_2(t) + \alpha q_2(t)(k - 2q_2 - bq_1 + (1-k)(q_1 + 2bq_2)). \quad (\text{A.6})$$

When $q_i(t+1) = q_i(t)$ is satisfied, we can obtain four solutions: $(0, 0)$, $(0, k/(2 - 2b(1-k)))$, $(1/2, 0)$, and $((2 - 2b + bk)/(4 - b^2 - 3b + 3bk), (1 - b + k)/(4 - b^2 - 3b + 3bk))$, namely, E_0, E_1, E_2 , and E^* .

The Jacobi matrix of E_0 is

$$J(E_0) = \begin{bmatrix} 1 + \alpha k & 0 \\ 0 & 1 + \beta k \end{bmatrix}. \quad (\text{A.7})$$

The absolute values of both characteristic roots are more than 1, and that means E_0 is unstable.

The Jacobi matrix of E_1 is

$$J(E_1) = \begin{bmatrix} 1 + \frac{\alpha k(2 - 2b + bk)}{2 - 2b(1-k)} & 0 \\ \beta(1 - b - k) \frac{k}{2 - 2b(1-k)} & 1 - \beta k^2 \end{bmatrix}. \quad (\text{A.8})$$

One of the characteristic roots is $\lambda'_1 = 1 + (\alpha k(2 - 2b + bk)/2 - 2b(1-k)) > 1$, so E_1 is unstable.

Similarly, the instability of E_2 can be proved.

Proof of Proposition 4. The Jacobi matrix of $E^*((2 - 2b + bk)/(4 - b^2 - 3b + 3bk), (1 - b + k)/(4 - b^2 - 3b + 3bk))$ is

$$J(E^*) = \begin{bmatrix} 1 + \frac{\alpha k(4b - 4 - 2bk)}{4 - b^2 - 3b + 3bk} & \frac{-b\alpha k(2 - 2b + bk)}{4 - b^2 - 3b + 3bk_1} \\ \frac{\beta(1 - b - k)(1 - b + k)}{4 - b^2 - 3b + 3bk} & 1 + \frac{\beta(-2k + 2b^2k - 2bk - 2 + 4b - 2b^2)}{4 - b^2 - 3b + 3bk} \end{bmatrix}. \quad (\text{A.9})$$

The trace and determinant of $J(E^*)$ is

$$\begin{aligned} \text{Tr}(J(E^*)) &= 2 + \frac{(4b\alpha - 4\alpha + 2b^2\beta - 2\beta - 2b\beta)k - 2b\alpha k^2 - 2\beta + 4b\beta - 2b^2\beta}{4 - b^2 - 3b + 3bk}, \\ \text{Det}(J(E^*)) &= \text{Tr}(J(E^*)) - 1 + \frac{\alpha\beta k(2 - 2b + bk)(4k - 4b^2k + 4bk + 4 - 7b - 6b^2 + b^3 - bk^2)}{(4 - b^2 - 3b + 3bk)^2}. \end{aligned} \quad (\text{A.10})$$

According to the Jury criterion, the following inequalities are solved:

$$\begin{cases} 2\text{Tr} + \frac{\alpha\beta k(2 - 2b + bk)(4k - 4b^2k + 4bk + 4 - 7b - 6b^2 + b^3 - bk^2)}{(4 - b^2 - 3b + 3bk)^2} > 0, \\ \frac{\alpha\beta k(2 - 2b + bk)(4k - 4b^2k + 4bk + 4 - 7b - 6b^2 + b^3 - bk^2)}{(4 - b^2 - 3b + 3bk)^2} > 0, \\ -\text{Tr} - \frac{\alpha\beta k(2 - 2b + bk)(4k - 4b^2k + 4bk + 4 - 7b - 6b^2 + b^3 - bk^2)}{(4 - b^2 - 3b + 3bk)^2} > 0. \end{cases} \quad (\text{A.11})$$

And, Proposition 4 can be obtained.

Proof of Proposition 5. The sum of two manufacturers' profits under separate bargaining is

$$\begin{aligned} (\pi_1 + \pi_2)^S &= k_1 \left(1 - \frac{1+b}{2+b}\right) \frac{1}{2+b} + k_2 \left(1 - \frac{1+b}{2+b}\right) \frac{1}{2+b} \\ &= \frac{k_1 + k_2}{(2+b)^2}. \end{aligned} \quad (\text{A.12})$$

The gross profit of the alliance of these two under collective bargaining is

$$\begin{aligned} (\pi_1 + \pi_2)^C &= k(1 - q_1 - bq_2)q_1 + [k - q_2 - bq_1 + (1 - k)(q_1 + bq_2)]q_2 \\ &= k(1 - q_1 - bq_2)(q_1 + q_2) + q_2(q_1 - q_2)(1 - b) \\ &= \frac{k(2 - 3b + bk + k)(2 - 2b + bk) + (1 - b + k)(1 - b)(1 - b + bk - k)}{(4 - b^2 - 3b - 3bk)^2} \\ &= \frac{(1 - b)^3 + (1 - b)^2(6 + b)k + (1 - b)(1 + 6b)k^2 + (b + b^2)k^3}{(4 - b^2 - 3b - 3bk)^2}. \end{aligned} \quad (\text{A.13})$$

The comparison between $(\pi_1 + \pi_2)^S$ and $(\pi_1 + \pi_2)^C$ is equivalent to that between $(k_1 + k_2)/(2 + b)^2$ and $[(1 - b)^3 + (1 - b)^2(6 + b)k + (1 - b)(1 + 6b)k^2 + (b + b^2)k^3]/(4 - b^2 - 3b - 3bk)^2$.

Since $((k_1 + k_2)/(2 + b)^2) < (2k/(2 + b)^2) < (2k/(4 - b^2 - 3b - 3bk))$, the comparison can be further transformed into the comparison between $2k$ and $(1 - b)^3 + (1 - b)^2(6 + b)k + (1 - b)(1 + 6b)k^2 + (b + b^2)k^3$.

Suppose $f(k) = 2k - (1 - b)^3 - (1 - b)^2(6 + b)k - (1 - b)(1 + 6b)k^2 - (b + b^2)k^3$. Then, the first derivative of $f(k)$ is $f'(k) = 2 - (1 - b)^2(6 + b) - 2k(1 - b)(1 + 6b) - 3k^2(b + b^2)$, and the second derivative of it is $f''(k) = -2(1 - b)(1 + 6b) - 6k(b + b^2)$. $f''(k) < 0$ is always satisfied in the range of $k \in (0, 1)$, which means that $f'(k)$ is monotonically decreasing. $f'(1) = 2 - (1 - b)^2(6 + b) - 2(1 - b)(1 + 6b) - 3(b + b^2)$ is always negative when

$b \in (0, 1)$. And, in this range, $f'(0) = 2 - (1 - b)^2(6 + b)$ continues to increase with the increase in b from negative to positive. There exists a threshold value b^* , smaller than at which $f'(0) \leq 0$. Since $f(0) < 0$, b^* ensures that $f(k) < 0$ is negative when $k \in (0, 1)$. From the above derivation, $(\pi_1 + \pi_2)^S < (\pi_1 + \pi_2)^C$ can be proved.

Data Availability

No data were used to support this study.

Conflicts of Interest

The authors declare that they have no conflicts of interest.

Acknowledgments

This research was supported by the Humanities and Social Science Foundation in the Hubei Provincial Education Department and the Research Center of Enterprise Decision Support, Key Research Institute of Humanities and Social Sciences in Universities of Hubei Province.

References

- [1] G. Fibich and N. Gavish, "Asymmetric first-price auctions-A dynamical-systems approach," *Mathematics of Operations Research*, vol. 37, no. 2, pp. 219–243, 2012.
- [2] X. Chen, P. Hu, and Z. Hu, "Efficient algorithms for the dynamic pricing problem with reference price effect," *Management Science*, vol. 63, no. 12, pp. 4389–4408, 2017.
- [3] N. Chen and G. Gallego, "Welfare analysis of dynamic pricing," *Management Science*, vol. 65, no. 1, pp. 139–151, 2019.
- [4] Q. Feng, G. Lai, and L. X. Lu, "Dynamic bargaining in a supply chain with asymmetric demand information," *Management Science*, vol. 61, no. 2, pp. 301–315, 2015.
- [5] G. Aydin and H. S. Heese, "Bargaining for an assortment," *Management Science*, vol. 61, no. 3, pp. 542–559, 2015.
- [6] E. Karagözoğlu and A. Riedl, "Performance information, production uncertainty, and subjective entitlements in bargaining," *Management Science*, vol. 61, no. 11, pp. 2611–2626, 2015.
- [7] S. Leider and W. S. Lovejoy, "Bargaining in supply chains," *Management Science*, vol. 62, no. 10, pp. 3039–3058, 2016.
- [8] J. Lee, "Multilateral bargaining in networks: on the prevalence of inefficiencies," *Operations Research*, vol. 66, no. 5, pp. 1204–1217, 2018.
- [9] A. M. Davis and K. Hyndman, "Multidimensional bargaining and inventory risk in supply chains: an experimental study," *Management Science*, vol. 65, no. 3, pp. 1286–1304, 2019.
- [10] E. Haruvy, E. Katok, and V. Pavlov, "Bargaining process and channel efficiency," *Management Science*, 2020.
- [11] L. Guo and G. Iyer, "Multilateral bargaining and downstream competition," *Marketing Science*, vol. 32, no. 3, pp. 411–430, 2013.
- [12] V. N. Hsu, G. Lai, B. Niu, and W. Xiao, "Leader-based collective bargaining: cooperation mechanism and incentive analysis," *Manufacturing & Service Operations Management*, vol. 19, no. 1, pp. 72–83, 2017.
- [13] T. Melkonyan, H. Zeitoun, and N. Chater, "Collusion in Bertrand vs. Cournot competition: a virtual bargaining approach," *Management Science*, vol. 64, no. 12, 2017.
- [14] M. Zhang, S. Küçükyavuz, and S. Goel, "A branch-and-cut method for dynamic decision making under joint chance constraints," *Management Science*, vol. 60, no. 5, pp. 1317–1333, 2014.
- [15] O. Besbes and A. Zeevi, "On the (surprising) sufficiency of linear models for dynamic pricing with demand learning," *Management Science*, vol. 61, no. 4, pp. 723–739, 2015.
- [16] P. Coucheney, B. Gaujal, and P. Mertikopoulos, "Penalty-regulated dynamics and robust learning procedures in games," *Mathematics of Operations Research*, vol. 40, no. 3, pp. 611–633, 2015.
- [17] R.-Y. Guo, H. Yang, and H.-J. Huang, "Are we really solving the dynamic traffic equilibrium problem with a departure time choice?" *Transportation Science*, vol. 52, no. 3, pp. 603–620, 2018.
- [18] J. Kim, R. S. Randhawa, and A. R. Ward, "Dynamic scheduling in a many-server, multiclass system: the role of customer impatience in large systems," *Manufacturing & Service Operations Management*, vol. 20, no. 2, pp. 285–301, 2018.
- [19] A. Ajorlou, A. Jadbabaie, and A. Kakhbod, "Dynamic pricing in social networks: the word-of-mouth effect," *Management Science*, vol. 64, no. 2, pp. 971–979, 2018.
- [20] J. Ma and L. Xie, "The impact of loss sensitivity on a mobile phone supply chain system stability based on the chaos theory," *Communications in Nonlinear Science and Numerical Simulation*, vol. 55, pp. 194–205, 2018.
- [21] C. F. Camerer, G. Nave, and A. Smith, "Dynamic unstructured bargaining with private information: theory, experiment, and outcome prediction via machine learning," *Management Science*, vol. 65, no. 4, pp. 1867–1890, 2019.
- [22] W. L. Jin, "Stable day-to-day dynamics for departure time choice," *Transportation Science*, vol. 54, no. 1, pp. 1–20, 2020.
- [23] T. Li, D. Yan, and S. Sui, "Research on the complexity of game model about recovery pricing in reverse supply chain considering fairness concerns," *Complexity*, vol. 2020, Article ID 9621782, 13 pages, 2020.
- [24] E. Ott, C. Grebogi, and J. A. Yorke, "Controlling chaos," *Physical Review Letters*, vol. 64, no. 11, pp. 1196–1199, 1990.
- [25] S. S. Askar, "Duopolistic Stackelberg game: investigation of complex dynamics and chaos control," *Operational Research*, pp. 1–15, 2018.
- [26] A. A. Elsadany and A. M. Awad, "Dynamics and chaos control of a duopolistic Bertrand competitions under environmental taxes," *Annals of Operations Research*, vol. 274, no. 1–2, pp. 211–240, 2019.
- [27] T. Li, D. Yan, and X. Ma, "Stability analysis and chaos control of recycling price game model for manufacturers and retailers," *Complexity*, vol. 2019, Article ID 3157407, 13 pages, 2019.
- [28] G. P. Cachon and P. T. Harker, "Competition and outsourcing with scale economies," *Management Science*, vol. 48, no. 10, pp. 1314–1333, 2002.
- [29] B. Xin and M. Sun, "A differential oligopoly game for optimal production planning and water savings," *European Journal of Operational Research*, vol. 269, no. 1, pp. 206–217, 2018.
- [30] F. Bernstein and M. Nagarajan, "Competition and cooperative bargaining models in supply chains," *Foundations and Trends in Technology, Information and Operations Management*, vol. 5, no. 2, pp. 87–145, 2012.
- [31] Y.-h. Zhang, W. Zhou, T. Chu, Y.-d. Chu, and J.-n. Yu, "Complex dynamics analysis for a two-stage Cournot duopoly game of semi-collusion in production," *Nonlinear Dynamics*, vol. 91, no. 2, pp. 819–835, 2017.

- [32] J. Zhou, W. Zhou, T. Chu, Y.-x. Chang, and M.-j. Huang, "Bifurcation, intermittent chaos and multi-stability in a two-stage Cournot game with R&D spillover and product differentiation," *Applied Mathematics and Computation*, vol. 341, pp. 358–378, 2019.
- [33] E. I. Jury, *Inners and Stability of Dynamic Systems*, Wiley-Interscience, New York, NY, USA, 1974.
- [34] Y. Cao, W. Zhou, T. Chu, and Y. Chang, "Global dynamics and synchronization in a duopoly game with bounded rationality and consumer surplus," *International Journal of Bifurcation and Chaos*, vol. 29, no. 11, Article ID 1930031, 2019.
- [35] T. Li and J. Ma, "Complexity analysis of dual-channel game model with different managers' business objectives," *Communications in Nonlinear Science and Numerical Simulation*, vol. 20, no. 1, pp. 199–208, 2015.
- [36] W. Lou and J. Ma, "Complexity of sales effort and carbon emission reduction effort in a two-parallel household appliance supply chain model," *Applied Mathematical Modelling*, vol. 64, pp. 398–425, 2018.
- [37] W. Zhou and X.-X. Wang, "On the stability and multistability in a duopoly game with R&D spillover and price competition," *Discrete Dynamics in Nature and Society*, vol. 2019, no. 5, pp. 1–20, 2019.

Research Article

Economic Development Forecast of China's General Aviation Industry

Hongqing Liao,¹ Zhigeng Fang ,¹ Chuanhui Wang,² and Xiaqing Liu ^{3,1}

¹College of Economics and Management, Nanjing University of Aeronautics and Astronautics, Nanjing, China

²School of Economics, Qufu Normal University, Jining, China

³College of Foreign Studies, Shandong Technology and Business University, Yantai, China

Correspondence should be addressed to Xiaqing Liu; liuxiaqing111@163.com

Received 14 April 2020; Accepted 5 June 2020; Published 24 June 2020

Academic Editor: Abdelalim A. Elsadany

Copyright © 2020 Hongqing Liao et al. This is an open access article distributed under the Creative Commons Attribution License, which permits unrestricted use, distribution, and reproduction in any medium, provided the original work is properly cited.

Aiming at solving the problem of system external impact on China's general aviation industry, combining functional theory and grey system theory, and applying Bayesian network reasoning technology, a grey Bayesian network reasoning prediction model of system impact and system control is established. Based on the dynamic deduction of the functional analysis factor of system impact evolution, the flight time of general aviation production operation is selected to predict the development trend of the system. Based on the current period information of the general aviation industry, the grey Bayesian network inference prediction model is used to predict the current and future trends, so as to predict the economic development trend of the general aviation industry in China. The prediction results are more accurate than those of other existing models.

1. Introduction

In recent years, China's general aviation industry has been listed as a strategic emerging industry, the development of which has attached great importance by the national high level and the whole society. In November 2010, the State Council and the central military commission issued the Opinions on Deepening the Reform of China's Low-altitude Airspace Management, which made plans for deepening the reform of China's low-altitude airspace management. In November 2014, the National Conference on the Reform of Low-altitude Airspace Management was held, and 10 regions, including Shenyang and Xi'an flight control zone, were listed as pilot areas for airspace reform and planned to be introduced to the whole country in 2015. Therefore, China's low-altitude airspace will gradually open up, general aviation economy will certainly become a new economic growth point to drive the development of national economy, and timely development of general aviation economy has become the general trend of research. In 2016, the State Council issued the Opinions on the Key Work of Deepening Economic Restructuring, in which it proposed to innovate

the operation and supervision mode of emerging general aviation types and introduce relevant policies to promote the development of general aviation. During the 13th five-year plan period, the focus will be on promoting the development of general aviation. More than 500 general airports and more than 5,000 general aircraft will be built, the annual flight capacity will reach 2 million hours, and the overall scale of the industry will exceed 1 trillion Yuan. Although some indicators may not be achieved in the short term, it shows that the state has attached great importance to the development of general aviation, and with the issuance of state council documents, relevant ministries and commissions and local provinces and cities have issued documents, providing a good development condition for the development of China's general aviation industry.

International experience shows that the input-output ratio of the general aviation industry is 1:10 (as a comparison, the ratio of automobile industry is only 1:4), and the employment-driven ratio is 1:12, which has a strong driving effect. In other words, it can gradually create a large market with a scale of 100 billion and employment of millions of people. In the United States, for example, there

are more than 220,000 registered general aviation aircraft, accounting for 96% of the total civil aircraft fleet in the United States. The turnover of general aviation manufacturing industry is about 20 billion US dollars, and the annual output value of related industries is about 150 billion US dollars. In 2015, the general aviation industry contributed US \$219 billion dollars to the US economy, accounting for 14.5% of the aviation economy and 1.26% of US GDP. Mature general aviation and its core industry of manufacturing and operation can drive the development of the entire national economy of different industries. General aviation economy operating in research and development manufacturing and service industry chain, industry chain, and on the basis of related industrial chain to form distinctive industrial clusters promotes the area of modern manufacturing and the coordinated development of high and new technology industries and modern service industry and boost the regional economic growth and transformation and upgrading of the industrial structure.

2. Literature Review

The study of aviation economy in China started relatively late, but the empirical study of aviation economy in China is comprehensive and shows a trend of gradual enrichment. The research mainly focuses on the following three parts, that is, the formation of aviation economy, the impact of aviation economy on regional economic development, and the development of aviation economy and its theoretical research elements.

For the research on the formation of aviation economy, Ou pointed out the classification and spatial layout of aviation city [1], and Cao proposed the cobweb model of the spatial layout of the aviation industry [2]. Lian et al. believe that the aviation economic zone is connected with the central city and hinterland through the flow of production factors and commodities [3]. Kasarda and Wang analyzed the formation of aviation city, and they believed that airport was the most active area in regional development and the growth pole of economic development [4, 5]. Cao and Hu believe that the development of aviation economy has a positive feedback effect on the development of airports [6–8].

In terms of research on the development of aviation economy on regional economy, Kasarda first analyzed the correlation between air transport and the employment rate of the secondary and tertiary industries in the city where the airport is located, and he concluded that the employment rate of air transport and the secondary and tertiary industries showed a positive correlation [9]. On this basis, the Chinese scholar Liu used the input-output model to calculate the impact of capital airport on Beijing's economy [10]. Air passenger linkages and employment growth in US metropolitan areas were studied by Irwin and Kasarda [11]. Goetz found in his research that the increase of urban population and employment level would lead to the increase of air passenger volume, but further empirical evidence showed that this trend would gradually weaken [12]. Ivy et al. showed that the change of urban air service connectivity

would significantly affect the employment level of local core management departments and auxiliary construction [13]. By empirical analysis, Button et al. showed that the presence of hub airports can attract high-tech talents to local employment [14]. Kloukos and Fudalej analyzed the aviation demand in the southwestern United States by assessing the impact of specific economic activities on regional air passenger volume [15]. Kasarda and Green analyzed air passenger and cargo volume and regional GDP, and they pointed out that the reduction of freedom of air service, customs quality, and corruption would increase the positive impact of cargo volume on the economy [16]. Debbage studied the operation of many airports and regional economic structure in Carolina, USA, and showed that while the local economic structure had a significant impact on the operation of airports, it also had a major transformation [17].

In terms of the factors and theoretical research of aviation economy, Yin and Wang, Huang and Cheng, Jaslin et al., and Xiong studied the development status and influencing factors of the aviation economic zone and put forward suggestions on developing their own characteristic aviation industry [18–21]. Haya El Nasser and Lyona introduced the process and experience of developing aviation economy, providing references for other regions to develop aviation economy [22, 23]. Jiang used the DEA window analysis method to investigate the operational efficiency of aviation economy of seven civil airports in Jiangsu province from the perspective of regional integration of resources [24]. Cao and Ma calculated the efficiency of the aviation economic zone in Beijing, Shanghai, Guangzhou, and Zhengzhou, and they concluded that the economic efficiency of airport economy is low, and the industrial development is unbalanced [25, 26]. Moreover, there are other scholars studying general aviation from the perspective of industry chain [27–29].

Through the analysis of domestic and foreign literatures related to the development of the aviation industry, the following problems are found in the current research. At present, people's theoretical research on aviation economy mainly focuses on the concept and connotation of aviation economy. In this paper, the future development of aviation economy is forecasted.

3. General Aviation Industry Development: A Forecast Research

An important symbol of the rapid development of the general aviation industry is the number of flight hours of the general aviation aircraft, the number of aircraft, and the number of general aviation enterprises. The most obvious change of general aviation reform policies and measures introduced in China is the number of flight hours of general aviation, which is an important indicator to remove the institutional obstacles restricting the development of general aviation in China. At the same time, the change of general aviation flight hours also reflects the development trend of the general aviation industry.

Therefore, the index of general aviation production operation flight time is used to study the future development trend of the general aviation industry through various prediction models.

3.1. Design of General Aviation Production Operation Flight Time Functional Bayesian Prediction Algorithm. The establishment of the grey Bayesian network inference prediction model with the system regulation functional analysis factor $\gamma(t)$ can predict the future development trend of the system. The functional analysis factor of system regulation $\gamma(t)$ can comprehensively reflect the influence of factors induced by system regulation and regulation and control factors outside the system and their related influencing factors on the development trend of the system after system regulation. In other words, the development trend of the system after system regulation should be the mapping of the generalized time t , and the Bayesian network reasoning technology is used to establish the Bayesian reasoning network model of the system regulation functional analysis factor $\gamma(t)$, so as to infer and measure the system regulation functional analysis factor.

Grey system theory treats all random quantities as grey numbers, that is, all white numbers that vary within a given range. The processing of grey number is not to find the probability distribution or statistical law but to use the method of data processing to find the law between the data. The method of mining and looking for the regularity of numbers by processing the data in the sequence of numbers and generating new sequences is called generation of numbers. The following is the definition of the accumulation process.

Definition. The process of sequential accumulation of data at each time of sequence x is called the accumulation generation operation, which is denoted by AGO. The new sequence of accumulation is called the cumulative generation sequence. Specifically, the assumed original number column is $x^{(0)} = (x^{(0)}(1), x^{(0)}(2), \dots, x^{(0)}(n))$, and the accumulated generating operation sequence is $x^{(1)} = (x^{(1)}(1), \dots, x^{(1)}(n))$, and $x^{(0)}$ and $x^{(1)}$ satisfy

$$x^{(1)}(k) = \sum_{i=a}^k x^{(0)}(i), \quad k = a, \dots, n, \quad (1)$$

where $a \leq n$ is a positive integer. When $a = 1$, the above AGO is named as a general accumulation generation.

Finally, the prediction data of the grey Bayesian network inference model and the Bayesian network inference data of the system regulation functional analysis factor are used to predict the future development trend of the system after the regulation of the system.

The main problems related to the algorithm step design of the grey functional prediction model are as follows:

Step 1: a prediction source data sequence with the functional analysis factor $\gamma(t)$ is constructed based on $X(n-1) = (x(1), x(2), \dots, x(n-1))$ and $x(n) =$

$A(\otimes)$, and the functional analysis factor data sequence is $X_{A(\otimes)}^{(0)}(k) = (x(1), x(2), \dots, x(n-1), A(\otimes))$

Step 2: the functional analysis factor sequence of system data $X_{A(\otimes)}^{(1)}(k)$ is generated by 1-AGO accumulation of the functional analysis factor data sequence $X_{A(\otimes)}^{(0)}(k)$

Step 3: the adjacent mean value of $X_{A(\otimes)}^{(1)}(k)$ is generated as $z_{A(\otimes)}^{(1)}(k) = 0.5x_{A(\otimes)}^{(1)}(k) + 0.5x_{A(\otimes)}^{(1)}(k-1)$

Step 4: the least square estimation of parameters $\hat{a}(A(\otimes)) = (B(A(\otimes))^T \cdot B(A(\otimes)))^{-1} \cdot B(A(\otimes))^T \cdot Y(A(\otimes))$ is conducted

Step 5: the model and time response formula is determined

Step 6: the prediction sequence of the functional analysis factor data $X_{A(\otimes)}^{(1)}(k)$ is gotten by 1-AGO accumulation

Theorem 1. *The functional analysis factor $\gamma(t)$ is equal to the development coefficient of the aviation industry chain α .*

Proof. Assuming that the aviation industry chain is regulated by government policies, the n^{th} phase value of the aviation industry chain $x(n) = A(\otimes)$ is estimated through the model data processing method. If x_{\min} and x_{\max} represent the most pessimistic and optimistic values of the aviation industry chain, respectively, then there is $A(\otimes) \in [x_{\min}, x_{\max}]$.

Assume that the functional analysis factor is $\gamma(t)$, and equation (2) is obtained in the form of grey number:

$$A(\otimes) = x_{\min} + (x_{\max} - x_{\min}) \cdot \gamma(t). \quad (2)$$

Assuming that the systematic development coefficient of the aviation industry chain is $c(\Delta x) = (c(\Delta x_1), c(\Delta x_2), \dots, c(\Delta x_m))$, the estimated value of the development trend of the aviation industry chain is expressed by equation (3), as is shown as follows:

$$A'(\otimes) = (1 - \alpha)x_{\min} + \alpha x_{\max}. \quad (3)$$

It can be obtained from equation (3) that

$$A'(\otimes) = (1 - \alpha)x_{\min} + \alpha x_{\max} = x_{\min} + (x_{\max} - x_{\min})\alpha. \quad (4)$$

Comparing equations (2) and (4), there is

$$A'(\otimes) = A(\otimes)$$

$$x_{\min} + (x_{\max} - x_{\min}) \cdot \alpha = x_{\min} + (x_{\max} - x_{\min}) \cdot \gamma(t), \quad (5)$$

and then, there is

$$\gamma(t) = \alpha. \quad (6)$$

The probability of optimism and pessimism of the development of the aviation industry chain can be inferred by the Bayesian inference network. The theoretical basis for the inference of the development trend of the control system by the Bayesian inference network is obtained by the conclusion of Theorem 1 $\gamma(t) = \alpha$. In other words, the change of

the development coefficient of the reasoning aviation industry chain α is carried out through the Bayesian reasoning network. With the conclusion of $\gamma(t) = \alpha$, the functional analysis factors $\gamma(t)$ are substituted into $X_{A(\otimes)}^{(1)}(k)$, and the prediction of the future development trend value of the system after the regulation of the grey Bayesian network inference prediction model is obtained finally. \square

3.2. Current Data Inferences of General Aviation Industry Development Policy Regulation. With the regards of estimation of upper bound x_{\max} and lower bound of current data x_{\min} , under the macro-control of the government, the original development trend of the aviation industry has been greatly interfered, which may lead to a severe recession, and may lead to a rapid growth. Therefore, historical statistics from 2015 to 2018 are considered to predict the upper and lower limits of the new policies for the general aviation industry development regulation in 2019.

According to the statistics of flight duration of general aviation's production operations from January to August 2019 (as is shown in Table 1), it should be considered that at the initial stage of the implementation of the new regulation policy in 2019, the policy effect has not yet been fully manifested during the implementation time of the hedging policy for the new regulation of the aviation industry chain. With the time going, these policy effects will be gradually released. Therefore, this paper uses the data from February to August of 2019 to estimate the upper and lower bounds of the flight time length of this year's general aviation production operation. The valuation formulas are shown in the following equations:

$$x_{\min} = 12 \times \min(x_1, x_2, \wedge, x_8) = 4 \quad (100,000 \text{ hours}), \quad (7)$$

$$x_{\max} = 12 \times \max(x_1, x_2, \wedge, x_8) = 12 \quad (100,000 \text{ hours}). \quad (8)$$

On the basis of $x_{\min} = 4$ (100,000 hours) and $x_{\max} = 12$ (100,000 hours), the grey number representation of flight duration interval of general aviation production operation in 2019 can be obtained, as shown in equation (8):

$$x(n = 2019) = A(\otimes) \in [4, 12]. \quad (9)$$

According to equation (9), the grey number in this region is represented as a functional algebraic form, as shown in the following:

$$A(\otimes) = 4 + 8 \cdot \gamma(t). \quad (10)$$

In this way, the prediction problem of the grey Bayesian network inference prediction model for flight duration of

TABLE 1: Flight hours of general aviation production operation in 2019 (10,000 hours).

Index	2	3	4	5	6	7	8
Monthly flight hours	3.5	9.2	9.4	9.9	9.9	10.1	9.6
Monthly growth rate (%)	-33.82	66.89	7.89	9.76	2.22	2.02	-4.95

general aviation production operations in the development of the aviation industry can be divided into the following six steps.

Step 1: sorting out the original initialization sequence.

According to Table 1 and equation (10), the sequence of predicted source data containing the system regulation functional analysis factor $\gamma(t)$ can be sorted out, as shown in

$$[7.4, 7.6, 8.1, 9.4, 11.2, 4 + 8 \cdot \gamma(t)]. \quad (11)$$

Step 2: operator design and data processing.

Considering that after the new regulation of the aviation industry chain, the development mode of the aviation industry chain needs new adjustment, and the weakening buffer operator is constructed as shown in the following equation:

$$x(k)d = \frac{1}{n-k+1} [x(k) + x(k+1) + \dots + x_{A(\otimes)}(n)]; \quad (12)$$

$$k = 1, 2, \dots, n.$$

After processing equation (11) with the weakening operator (as shown in equation (13)), the data sequence can be obtained as follows:

$$X_{A(\otimes)}^{(0)}(k) = [7.95 + 1.33\gamma(t), 8.06 + 1.6\gamma(t), 8.18 + 2\gamma(t), 8.2 + 2.67\gamma(t), 7.6 + 4\gamma(t), 4 + 8\gamma(t)]. \quad (13)$$

Step 3: generating $X_{A(\otimes)}^{(1)}(k)$ by 1-AGO for $X_{A(\otimes)}^{(0)}(k)$. Equation (14) can be obtained by means of 1-AGO from equation (13):

$$X_{A(\otimes)}^{(1)}(k) = [7.95 + 1.33\gamma(t), 16.01 + 2.93\gamma(t), 24.19 + 4.93\gamma(t), 32.39 + 7.6\gamma(t), 39.99 + 11.6\gamma(t), 43.99 + 19.6\gamma(t)]. \quad (14)$$

Step 4: the adjacent mean value is conducted on $X_{A(\otimes)}^{(1)}(k)$.

Formula (15) can be obtained by generating adjacent to the mean value of equation (14), $z_{A(\otimes)}^{(1)}(k) = 0.5x_{A(\otimes)}^{(1)}(k) + 0.5x_{A(\otimes)}^{(1)}(k-1)$:

$$z_{A(\otimes)}^{(1)}(k) = [11.98 + 2.13\gamma(t), 20.1 + 3.93\gamma(t), 28.29 + 6.27\gamma(t), 36.19 + 9.6\gamma(t), 41.99 + 15.6\gamma(t)]. \quad (15)$$

Step 5: perform the least square estimation of parameters for $\hat{a}(A(\otimes)) = (B(A(\otimes))^T \cdot B(A(\otimes)))^{-1} \cdot B(A(\otimes))^T \cdot Y(A(\otimes))$:

$$a(A(\otimes)) = \frac{-2.73 \cdot \gamma(t)^2 - 3.76 \cdot \gamma(t) - 3.14}{5.66 \cdot \gamma(t)^2 + 24.45 \cdot \gamma(t) + 29.08},$$

$$b(B(\otimes)) = \frac{0.17 \cdot \gamma(t)^3 + 26.20 \cdot \gamma(t)^2 + 201.79 \cdot \gamma(t) + 296.46}{5.66 \cdot \gamma(t)^2 + 24.45 \cdot \gamma(t) + 29.08}. \quad (16)$$

Step 6: conduct prediction by means of the grey Bayesian network inference prediction model.

The predicted values of general aviation production flight duration from 2019 to 2021 with the system control functional analysis factor $\gamma(t)$ are shown in equations (17)–(19), respectively.

The functional representation of the transaction value of the aviation industry chain in 2019 is as follows:

$$x(2019) = e^{-(-2.73 \cdot \gamma(t)^2 - 3.76 \cdot \gamma(t) - 3.14/5.66 \cdot \gamma(t)^2 + 24.45 \cdot \gamma(t) + 29.08)} \cdot \left(1 - e^{-(-2.73 \cdot \gamma(t)^2 - 3.76 \cdot \gamma(t) + 3.14/5.66 \cdot \gamma(t)^2 + 24.45 \cdot \gamma(t) + 29.08)}\right) \cdot \left(\frac{3.8\gamma(t)^3 + 52.9\gamma(t)^2 + 227.5\gamma(t) + 271.5}{2.73\gamma(t)^2 + 3.76\gamma(t) - 3.14}\right). \quad (17)$$

The functional representation of the transaction value of the aviation industry chain in 2020 is as follows:

$$x(2020) = e^{-(-5.46 \cdot \gamma(t)^2 - 7.52 \cdot \gamma(t) - 6.28/5.66 \cdot \gamma(t)^2 + 24.45 \cdot \gamma(t) + 29.08)} \cdot \left(1 - e^{-(-2.73 \cdot \gamma(t)^2 - 3.76 \cdot \gamma(t) + 3.14/5.66 \cdot \gamma(t)^2 + 24.45 \cdot \gamma(t) + 29.08)}\right) \cdot \left(\frac{3.8\gamma(t)^3 + 52.9\gamma(t)^2 + 227.5\gamma(t) + 271.5}{2.73\gamma(t)^2 + 3.76\gamma(t) - 3.14}\right). \quad (18)$$

The functional representation of the transaction value of the aviation industry chain in 2021 is as follows:

$$x(2021) = e^{-(-8.19 \cdot \gamma(t)^2 - 11.28 \cdot \gamma(t) - 9.42/5.66 \cdot \gamma(t)^2 + 24.45 \cdot \gamma(t) + 29.08)} \cdot \left(1 - e^{-(-2.73 \cdot \gamma(t)^2 - 3.76 \cdot \gamma(t) + 3.14/5.66 \cdot \gamma(t)^2 + 24.45 \cdot \gamma(t) + 29.08)}\right) \cdot \left(\frac{3.8\gamma(t)^3 + 52.9\gamma(t)^2 + 227.5\gamma(t) + 271.5}{2.73\gamma(t)^2 + 3.76\gamma(t) - 3.14}\right). \quad (19)$$

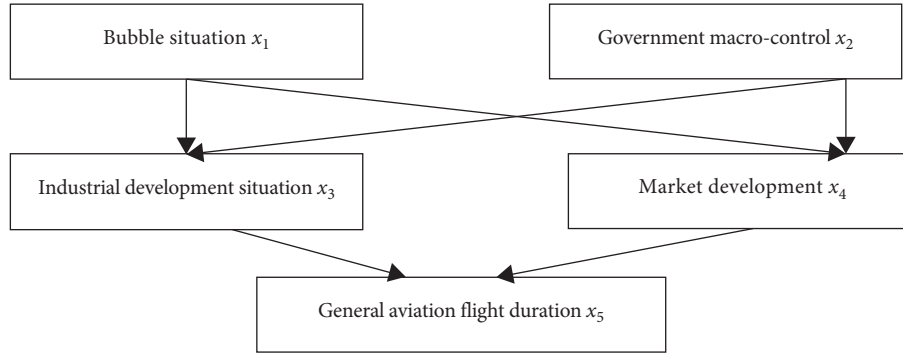


FIGURE 1: Schematic diagram of the Bayesian network correction process of the aviation industry development.

3.3. *Dynamic Prediction Effect Analysis of the Grey Bayesian Network Inference Prediction Model.* Under the influence of the government's macro-control policies and other factors in the development of the aviation industry, they influence each other on the flight duration of general aviation production operations, and a grey Bayesian network reasoning model is established, as shown in Figure 1.

In Figure 1, each node has two states, namely, good (G) and bad (B), and the probabilities of each state are expressed as $P(G)$ and $P(B)$. According to the actual economic development, the experts calculated the conditional probability table, as shown in Tables 2–4.

The chain rule and conditional independence rule of Bayesian network reasoning are used to calculate the relative conditional probability, as follows:

$$\begin{aligned}
 P(x_3 = G) &= P(x_3 = G | x_1 = G, x_2 = G) \\
 &\cdot P(x_1 = G) \cdot P(x_2 = G) \\
 &+ P(x_3 = G | x_1 = B, x_2 = G) \\
 &\cdot P(x_1 = B) \cdot P(x_2 = G) \\
 &+ P(x_3 = G | x_1 = G, x_2 = B) \cdot P(x_1 = G) \\
 &\cdot P(x_2 = B) \\
 &+ P(x_3 = G | x_1 = B, x_2 = B) \cdot P(x_1 = B) \\
 &\cdot P(x_2 = B) = 0.268, \\
 P(x_3 = B) &= 0.732, P(x_4 = G) = 0.254, P(x_4 = B) = 0.746 \\
 \cdot P(x_5 = G) &= P(x_5 = G | x_3 = G, x_4 = G) \cdot P(x_3 = G) \\
 &\cdot P(x_4 = G) \\
 &+ P(x_5 = G | x_3 = B, x_4 = G) \cdot P(x_3 = B) \\
 &\cdot P(x_4 = G) \\
 &+ P(x_5 = G | x_3 = G, x_4 = B) \cdot P(x_3 = G) \\
 &\cdot P(x_4 = B) \\
 &+ P(x_5 = G | x_3 = B, x_4 = B) \cdot P(x_3 = B) \\
 &\cdot P(x_4 = B) = 0.34.
 \end{aligned} \tag{20}$$

TABLE 2: Expert prediction probability table of the economic development and government regulation effect in September 2019.

Bubble situation		Government macro-control	
$P(x_1) = G$	$p(x_1) = B$	$p(x_2) = G$	$p(x_2) = B$
0.2	0.8	0.3	0.7

TABLE 3: Probability table of expert forecast conditions for industrial development and the aviation industry development in September 2019.

Bubble situation x_1	G		B	
Government macro-control x_2	G	B	G	B
$p(x_3) = G$	1	0.8	0.4	0
$p(x_3) = B$	0	0.2	0.6	1
$p(x_4) = G$	1	0.7	0.4	0
$p(x_4) = B$	0	0.3	0.6	1

TABLE 4: Probability table of national economic development experts' forecast conditions in September 2019.

Industrial development situation x_3	G		B	
Development situation of aviation industry chain x_4	G	B	G	B
$p(x_5) = G$	1	0.8	0.6	0
$p(x_5) = B$	0	0.2	0.4	1

TABLE 5: Flight time forecast of the aviation industry production (unit: 10,000 hours).

Methods	Grey Bayesian network inference model	GM (1, 1)	Exponential smoothing model
2019	106.07	103.38	98.62
2020	120.08	114.17	105.68
2021	136.13	126.11	112.75

The system development coefficient of the system is $\alpha = P(x_5 = G)$. According to Theorem 1 $\gamma(t) = \alpha$, the functional analysis factor of system regulation can be obtained, $\gamma(t) = 0.34$.

TABLE 6: Comparison of different prediction models in 2019 (unit: 10,000 hours).

Methods	Actual value	Grey Bayesian network inference model	GM (1, 1)	Exponential smoothing model
Predicted results	112	106.07	103.38	98.62
Deviation from reality	—	5.59%	8.34%	13.57%

By substituting the system control functional analysis factor $\gamma(t) = 0.34$ into the prediction equation, the predicted flight duration of production operations in the aviation industry from 2019 to 2021 is obtained as follows: $x(2019) = 106.07$ (10,000 hours), $x(2020) = 120.08$ (10,000 hours), and $x(2021) = 136.13$ (10,000 hours).

In this paper, the GM (1, 1) model and exponential smoothing model are selected as comparison models. Without considering the impact of the new policies on the production and operation flight time of the aviation industry and according to the statistical data of the production and operation flight time of the aviation industry from 2015 to 2018, the GM (1, 1) model can be used to predict the production and operation flight time of the aviation industry from 2019 to 2020. An exponential smooth regression model was established based on the flight time statistics of the aviation industry from 2015 to 2018. The three models are used to predict the flight time of production operations in the aviation industry in 2019, 2020, and 2021, as shown in Table 5.

These three models are used to compare and analyze the predicted values of flight time in 2019 and their errors in the aviation industry, as shown in Table 6.

According to the above predicted results, the following main conclusions can be drawn:

(1) *Prediction Effect Analysis.* The state shall implement airline industry regulations and control policies, which lead to transformation in the airline industry situation. Forecasting models relying on historical data to predict the future value, and the GM (1, 1) model and the exponential regression model in this case will result in the deviation of the real and estimated values. That is, GM (1, 1) was 8.34%, and exponential regression was 13.57%. The grey forecasting of the Bayesian network inference model based on the current period of economic information to modify the historical trend predicts only 5.59% of the deviation with the actual result, which means the predicted results are more accurate.

(2) *Model Selection Analysis.* The classical GM (1, 1) and exponential regression models are suitable for developing and utilizing the data of the past period to predict the future trend. The grey Bayesian network inference model emphasizes the development and utilization of the recent data, which is suitable for the prediction of the recent development trend of the system.

(3) *Dynamic Prediction Effect Analysis of the Grey Bayesian Network Inference Prediction Model.* Based on the analysis of the current situation of system

regulation, the functional analysis factor of system regulation is determined by the expert group using the Bayesian network reasoning technology. The introduction of the system control functional analysis factor can be sensitive to the current situation of system control and the system development trend of dynamic prediction.

4. Conclusion

The prediction model of grey Bayesian network reasoning was established after the aviation policy was regulated. The model provided a better solution for the prediction problem under the policy control. In theory, a new post-regulation prediction model framework is established, which builds a bridge between social science and system regulation theory. The model inherits the graphical display technology of the system regulation theory, which makes the complex process of economic system regulation and prediction be displayed dynamically and intuitively. This paper, based on the grey system and Bayesian network interference technology, created a grey Bayesian network inference prediction model, which makes full use of the information revealed before and after the system regulation and realizes scientific reasoning and predication under the external regulation environment.

Data Availability

The data used to support the findings of this study are included within the article.

Conflicts of Interest

The authors declare that they have no conflicts of interest.

Acknowledgments

This work was supported by the National Social Science Foundation of China (12AZD102), the National Natural Science Foundation of China (nos. 71671091 and 71701098), the China Scholarship fund, Postgraduate Research and Practice Innovation Program of Jiangsu Province (KYCX18_0233), and the Fundamental Research Funds for Central Universities (NJ20150036).

References

- [1] Y. Ou, "Discussion on the planning and construction of aviation city in China," *Planners*, vol. 4, pp. 30–33, 2005.
- [2] Y. Cao, *Airport Economy—the Growth Space of Speed Economy Era*, Economic Science Press, Beijing, China, 2009.
- [3] Z. Lian, X. Liu, and Z. Xue, "An analysis of the spatial mechanism of airport economy," *Economic Perspective*, vol. 3, pp. 69–71, 2011.
- [4] J. D. Kasara, "From airport city to aerropolis," *Airport World*, vol. 6, no. 4, pp. 42–45, 2001.
- [5] X. Wang, "Analysis and experience of international airport peripheral area development model," *Discussing the Development of Beijing International Airport Nearby Area*, no. 3, pp. 65–68, 2003.

- [6] Y. Cao, Y. Xi, and W. Li, "Analysis of formation of airport economy from the perspective of new economic geography," *Inquiry Into Economic Issues*, vol. 145, no. 2, pp. 49–54, 2009.
- [7] B.o. Sun, L. Jin, and Y. Cao, "Research on the mechanism of airport economy—a case study of capital international airport," *Theoretical Investigation*, vol. 133, no. 6, pp. 93–95, 2006.
- [8] Z. Hu and S. Li, "Spatial development pattern and trend prospect of airport economic zone," *Planner*, vol. 33, no. 11, pp. 5–10, 2014.
- [9] R. Guo and W. Mu, "Planning strategy of airport economic zone from the perspective of regional interaction," *Planner*, vol. 30, no. 11, pp. 23–28, 2014.
- [10] X. Liu, "The assessment of industrial clusters around Beijing international airport," *Soft Science*, vol. 22, no. 3, pp. 41–44, 2008.
- [11] M. D. Irwin and J. D. Kasarda, "Air passenger linkages and employment growth in US metropolitan areas," *American Sociological Review*, vol. 56, pp. 524–537, 1991.
- [12] A. R. Goetz, "Air passenger transportation and growth in the US urban system, 1950-1987," *Growth and Change*, vol. 23, pp. 217–238, 1992.
- [13] R. L. Ivy, T. J. Fik, and E. J. Malecki, "Changes in air service connectivity and employment," *Environment and Planning A: Economy and Space*, vol. 27, no. 2, pp. 165–179, 1995.
- [14] K. Button, S. Lall, R. Stough, and M. Trice, "High-technology employment and hub airports," *Journal of Air Transport Management*, vol. 5, no. 1, pp. 53–59, 1999.
- [15] D. Kloukos, P. Fudalej, P. Sequeira-Byron, and C. Katsaros, "Maxillary distraction osteogenesis versus orthognathic surgery for cleft lip and palate patients an analysis of the determinants of regional air travel demand," *The Cochrane Database of Systematic Reviews*, vol. 8, no. 18, pp. 37–44, 2018.
- [16] J. D. Kasarda and J. D. Green, "Air cargo as an economic development engine: a note on opportunities and constraints," *Journal of Air Transport Management*, vol. 11, no. 6, pp. 459–462, 2005.
- [17] K. G. Debbage, "Air transportation and urban-economic restructuring: competitive advantage in the US Carolinas," *Journal of Air Transport Management*, vol. 5, no. 4, pp. 211–221, 1999.
- [18] J. Yin and Z. Wang, "Research on the development strategy of Beijing airport economy," *Productivity Research*, no. 11, pp. 97–99, 2009.
- [19] J. Huang, Li Cheng et al., "Research on impact of airport economy on regional economy," *Journal of Nanjing University of Aeronautics and Astronautics*, vol. 13, no. 3, pp. 46–49, 2011.
- [20] M. Jaslin, O. Samat, and A. A. Othman, "Upgrading in global value chain of Malaysian aviation industry," *Procedia Economics and Finance*, vol. 31, pp. 839–845, 2015.
- [21] S. Xiong, *Research on the Development Strategy of Wuhan Airport Economic Zone*, Wuhan University, Wuhan, China, 2017.
- [22] H. E. Nasser, "New cities springing up around many U.S. Airports," 2003, <http://www.usatoday.com/travel/news/2003/09/25-airport-cities.htm>.
- [23] D. Lyona and G. Francis, "Managing New Zealand's airports in the face of commercial challenges," *Journal of Air Transport Management*, vol. 12, no. 5, pp. 220–226, 2006.
- [24] P. Shi, K. Jiang, and W. Jieyun, "The efficiency of airport economy from regional integration of resources perspective—empirical study of airport economy zone in Jiangu," *Systems Engineering*, vol. 30, no. 4, pp. 58–66, 2012.
- [25] Y. Cao and D. Shen, "Research on the key elements of constructing aerotropolis with airport as the core," *Port Economy*, no. 1, pp. 42–47, 2013.
- [26] J. Ma, *Evaluation of Economic Efficiency of Zhengzhou Airport Based on the DEA Model*, Zhengzhou University, Zhengzhou, China, 2017.
- [27] F. Liu, *Research on the Development Strategy of Ruijin Airport Economic Zone*, Jiangxi Normal University, Nanchang, China, 2016.
- [28] K. Wang and F. Song, "Construction and development of the general aviation industry chain around Poyang lake city cluster," *Industrial & Science Tribune*, vol. 14, no. 14, pp. 12–14, 2015.
- [29] X. Wang and Yi. Wang, "Research of coordinated development of China general aviation on the view of industry chain," *Journal of Zhengzhou University of Aeronautics*, vol. 34, no. 2, pp. 1–4, 2016.

Research Article

Evaluation and Selection of Manufacturing Suppliers in B2B E-Commerce Environment

Quan Zhang , Zhen Guo , Feiyu Man , and Jiyun Ma 

School of Information Engineering, ShenYang University of Technology, ShenYang 110870, China

Correspondence should be addressed to Quan Zhang; isqzhang@sut.edu.cn

Received 1 May 2020; Revised 24 May 2020; Accepted 1 June 2020; Published 22 June 2020

Guest Editor: Lei Xie

Copyright © 2020 Quan Zhang et al. This is an open access article distributed under the Creative Commons Attribution License, which permits unrestricted use, distribution, and reproduction in any medium, provided the original work is properly cited.

The evaluation and selection of manufacturing suppliers in B2B e-commerce environment is summed up as a multiple-attribute decision-making problem. In B2B E-commerce environment, some performance indicators of manufacturing suppliers present uncertainty and could not be expressed with precise numeric values. Linguistic terms, preference orderings, or interval numbers are commonly used to express the performances of the suppliers accurately instead of crisp values when the available information is uncertain or incomplete. This paper proposes an approach to the selection of manufacturing suppliers in B2B E-commerce environment, where the attribute values in decision matrix are expressed with linguistic terms, preference orderings, and interval numbers. Firstly, the hybrid decision matrix is normalized by calculating the grey correlation coefficients of attribute values with the ideal values of attributes. Secondly, a deviation maximization model is proposed to determine the attribute weights, which is combined with those derived from the entropy method. Thirdly, the overall values of suppliers are calculated and their rankings are obtained. Finally, an example is used to illustrate the proposed approach.

1. Introduction

As important components of the supply chain, suppliers usually play important roles in the manufacturing process [1–3]. The relationships between manufacturers and suppliers are examined by Svensson et al. [2]. The evaluation and selection of suppliers are important steps in the operations of manufacturers and can be modeled as multiple-attribute decision-making (MADM) problems, which involve some qualitative attributes, for example, the quality factor and risk factor of the suppliers.

Traditionally, both the qualitative attributes and the quantitative attributes are adopted in modeling the evaluation and selection of manufacturing suppliers [4]. However, in B2B E-commerce environment, both the qualitative attributes and the quantitative attributes of the suppliers show much more ambiguity and uncertainty than before [5, 6]. Natural language is introduced by Zadeh [7] and can be used to reduce the burden of expressing subjective uncertain judgments in a decision-making process. A linguistic term is one of the easy ways for evaluations in uncertain

environment. Linguistic terms are usually used to assess the qualitative attributes of the suppliers [4, 8]. In the meantime, because the information available is uncertain or incomplete, preference orderings are also likely to be employed to evaluate the qualitative attributes, in addition to linguistic terms. Preference orderings are also the easy ways for evaluating the suppliers by describing their relative positions, i.e., the ranking orders of the suppliers against some qualitative attributes. Preference orderings are used to evaluate the attribute weights in [9].

Furthermore, in the global competitive situations, against the quantitative attributes, the performance of suppliers would be a range of possible values, with the minimum and the maximum of the utility scores [9]. In other words, interval numbers are the ways of evaluating suppliers against some quantitative attributes [9].

It can be seen that, in B2B E-commerce environment, linguistic terms, preference orderings, and interval numbers are the appropriate expressions of the performance indicators (i.e., attribute values) of manufacturing suppliers. In this case, we are facing challenges when evaluating and

selecting the suppliers for the manufacturers in B2B E-commerce environment. It is desirable to propose an approach to the evaluation and selection of manufacturing suppliers in B2B E-commerce environment when their performance indicators are expressed by means of such hybrid information.

However, the research on evaluating the manufacturing suppliers in B2B E-commerce environment is not so common when their performances or attribute values are multiple types of information, such as linguistic terms, preference orderings, and interval numbers. The purpose of this paper is to develop an approach for evaluating and selecting the manufacturing suppliers in B2B E-commerce environment, where their attribute values are expressed with linguistic terms, preference orderings, and interval numbers. Normalizations on the hybrid attribute values are conducted, based on which the attribute weights are determined so that their overall performances (overall values) are obtained for rankings and selections.

2. Current Research and Research Objectives

The approaches of evaluating and selecting suppliers can be classified into three categories, including (i) multiple attribute decision-making approaches [9–12], (ii) mathematical programming approaches [13–15], and (iii) intelligent approaches (e.g., ANN and Grey system theory).

According to the multiple-attribute decision-making approaches, linear weighting methods and TOPSIS are usually utilized. With linear weighting methods, the overall values of every suppliers are calculated by summing up every attribute values multiplied by their corresponding weights. The supplier(s) with the highest overall values would be selected. TOPSIS, i.e., the technique for order preference by similarity to an ideal solution, was first proposed by Hwang and Yoon [16]. The TOPSIS method ranks a limited number of alternatives according to the relative degree of proximity to the idealized alternatives [10–12]. The best the alternative is the smallest degree of proximity to the idealized alternatives. Generally, when applying the linear weighting methods and TOPSIS, attribute weights should be determined beforehand, and the attribute weights can be assigned by decision makers or by using the AHP method subjectively.

According to the mathematical programming approaches, usually, multiple objectives are contained in the objective function, as well as some constraints are considered simultaneously. In [13], in order to determine the best suppliers, AHP is integrated with nonlinear and multi-objective integer programming model, under quantity discounts and capacity and budget constraints, while the objectives of the model are maximizing the total value of purchase (TVP), minimizing the total cost of purchase (TCP), or maximizing TVP and minimizing TCP simultaneously. In [14], a mixed-integer nonlinear program is proposed to solve dynamic supplier selection problems. In [15], the problem of supplier selection and order allocation with multiperiod, multiproduct, multisupplier, and multiobjective is generalized as a mixed integer linear programming model, where the objectives are total inventory cost (i.e., delay, holding and

shortage, ordering, and discounted purchase costs) and the constraints are the budget and capacity limitations for both buyers and suppliers. The model is solved by means of a preemptive fuzzy goal programming approach.

According to the intelligent approaches, artificial neural network (ANN) models [17, 18] and Grey theory [19–21] are usually employed. In [17], an artificial neural network-based predictive model is developed for forecasting the supplier's bid prices in the supplier selection negotiation process, by allowing a demander to foresee the relationship between its alternative bids and corresponding supplier's next bid prices in advance, which decreases the meaningless negotiation times, reduces the procurement cost, improves the negotiation efficiency, or shortens the supplier selection lead-time. In [18], an adaptive neuro-fuzzy inference system is developed by determining the criteria and applied for supplier selections.

In the recent years, grey theory is applied to deal with uncertainty inherent in evaluating the suppliers while the linguistic terms are adopted to express their attribute values [19–21]. Although the proposed approach in [21] does not require any probability distribution or fuzzy membership function, preference orderings and interval numbers are not considered for the attribute values of suppliers.

In [9], the TOPSIS method is extended to the situation by allowing the input attribute values being interval numbers with the minimum and the maximum of the utility scores (a range of possible values for quantitative attributes and a list of possible grades for qualitative attributes). The rank order centroid (ROC) method is used to determine the attribute weights based on the attribute ranking orders [22, 23]. The minimum and the maximum outputs of the extended TOPSIS are obtained, and their averages are adopted as the overall index for selections.

There is rare research on tackling the supplier selection problems with the attribute values being linguistic terms, preference orderings, and interval numbers. The research objective of this paper is to propose a new approach to deal with the qualitative attribute values expressed with linguistic terms and preference orderings and the quantitative attribute values expressed with interval numbers, when evaluating and selecting the manufacturing suppliers in B2B E-commerce environment.

This paper is organized as follows. Section 1 introduces the research background. Section 2 reviews the current research on evaluating and selecting suppliers. Section 3 describes the evaluation and selection of suppliers as a MADM problem. In Section 4, a new approach is proposed to evaluating and selecting the manufacturing suppliers in B2B E-commerce environment, while the attribute values are expressed in linguistic terms, preference orderings, and interval numbers. In Section 5, an example is used to illustrate the proposed approach. Section 6 gives the conclusions and discussions.

3. Problem Descriptions

As stated above, the evaluation and selection of manufacturing suppliers in B2B E-commerce environment is modeled as a MADM problem. The following notations

and assumptions are used to represent the MADM problem of evaluating and selecting manufacturing suppliers.

The alternatives (i.e., the suppliers) are known. Let $S = \{S_1, S_2, \dots, S_m\}$ denote a discrete set of $m (\geq 2)$ possible alternatives. The attributes are known, and let $C = \{C_1, C_2, \dots, C_n\}$ denote a set of $n (\geq 2)$ attributes. In order to distinguish the qualitative and quantitative attributes with different characteristics, the subscript of the attributes is divided into three categories: J_1 for the subscript set of attributes with linguistic assessment values, J_2 for the subscript set of attributes with preference ordering assessment values, and J_3 for the subscript set of attributes with interval number assessment values.

Let $\tilde{A} = [\tilde{a}_{ij}]_{m \times n}$ denote the decision matrix, where \tilde{a}_{ij} are the assessment values for alternative S_i with respect to attribute C_j , $i = 1, \dots, m$, and $j = 1, \dots, n$. In this study, \tilde{a}_{ij} are in the forms of linguistic terms, preference orderings, and interval numbers.

Let $W = (w_1, w_2, \dots, w_n)$ denote the weight vector of $n (\geq 2)$ attributes, where w_j is the weight of attribute C_j , while $\sum_{j=1}^n w_j = 1$ and $w_j > 0$ holds for $j = 1, \dots, n$.

The problem focused in this paper is to select the best supplier(s) for a manufacturer in B2B E-commerce environment, while their performance indicators (i.e., attribute values) are linguistic terms, preference orderings, and interval numbers.

4. The Proposed Approach

The proposed approach to the problem stated in Section 3 is composed of three steps: normalize the attribute values in different formats based on the grey relational degree method, determine the attribute weights, and calculate the overall values of the alternatives (suppliers).

4.1. Normalize the Attribute Values in Different Formats.

Since the attribute values in decision matrix $\tilde{A} = [\tilde{a}_{ij}]_{m \times n}$ are in the formats of linguistic terms, preference orderings, and interval numbers, corresponding methods are developed for transforming them into a comparable format, i.e., the utility value.

4.1.1. Calculate the Grey Correlation Coefficients of Linguistic Attribute Values

Definition 1. A linguistic term \tilde{T} on a real-number set is defined as a triangular fuzzy number (denoted as $(u, \alpha, \text{and } \beta)$), if its membership function $\mu_{\tilde{T}}(R^+ \rightarrow [0, 1])$ is defined as

$$\mu_{\tilde{T}}(x) = \begin{cases} \frac{x - \alpha}{u - \alpha}, & x \in [\alpha, u], \\ \frac{x - \beta}{u - \beta}, & x \in [u, \beta], \\ 0, & \text{otherwise,} \end{cases} \quad (1)$$

where $\alpha \leq u \leq \beta$, u is the model value, and α and β stand for the lower value and the upper value of linguistic term \tilde{T} , respectively.

Given the hybrid decision matrix $\tilde{A} = [\tilde{a}_{ij}]_{m \times n}$, the attributes C_j ($j \in J_1$) with linguistic assessment values may be of different granularities, and different linguistic evaluation sets would be employed [24]. Therefore, a basic linguistic evaluation set TERMSET^B ($\text{TERMSET}^B = \{\text{term}_0^B, \text{term}_1^B, \dots, \text{term}_g^B\}$) is used to transform the linguistic assessment values with different granularities into the comparable form. The triangular fuzzy number $\gamma_l^B = (\mu_l^B, \alpha_l^B, \beta_l^B)$ corresponding to the linguistic term term_l^B is defined as follows:

$$\gamma_l^B = \begin{cases} \alpha_0^B = 0, \\ u_l^B = \frac{l}{g-1}, & 0 \leq l \leq g-1, \\ \alpha_l^B = \frac{l-1}{g-1}, & 1 \leq l \leq g-1, \\ \beta_l^B = \frac{l+1}{g-1}, & 0 \leq l \leq g-2, \\ \beta_{g-1}^B = 1, \end{cases} \quad (2)$$

where μ_l^B is the model value and α_l^B and β_l^B stand for the lower value and the upper value of γ_l^B .

With respect to the attribute values with linguistic assessments \tilde{a}_{ij} ($i = 1, \dots, m, j \in J_1$), denote \tilde{a}_{ij} as ling_{ij} . ling_{ij} can be transformed into the fuzzy set over the basic linguistic evaluation set TERMSET^B (denoted as $F_{ij}(\text{TERMSET}^B)$):

$$\tau: \text{ling}_{ij} \longrightarrow F_{ij}(\text{TERMSET}^B), \quad i = 1, \dots, m, j \in J_1, \quad (3)$$

where, $F_{ij}(\text{TERMSET}^B)$ is the fuzzy set over the basic linguistic evaluation set TERMSET^B , as stated as follows:

$$F_{ij}(\text{TERMSET}^B) = \{(\text{term}_l^B, \gamma_{ij,l}) | l \in [0, g], l = 0, \dots, g\}, \quad (4)$$

where

$$\gamma_{ij,l} = \max_y \min \{ \mu_{\text{ling}_{ij}}(y), \mu_{\text{term}_l^B}(y) \}, \quad (5)$$

where $\mu_{\text{ling}_{ij}}(y)$ and $\mu_{\text{term}_l^B}(y)$ denote the membership functions of ling_{ij} and term_l^B respectively, $i = 1, \dots, m, l = 0, \dots, g, j \in J_1$.

Furthermore, the fuzzy set $F_{ij}(\text{TERMSET}^B)$ can be transformed into a crisp value as follows:

$$\phi(F_{ij}(\text{TERMSET}^B)) = \frac{\sum_{l=0}^g l \times \gamma_{ij,l}}{g \sum_{l=0}^g \gamma_{ij,l}}, \quad i = 1, \dots, m, j \in J_1. \quad (6)$$

Thus, given the linguistic assessment values \tilde{a}_{ij} of attributes C_j ($j \in J_1$), by means of the operations in (3)–(6),

linguistic term \tilde{a}_{ij} is transformed into the form of crisp value, denoted as

$$b_{ij} = \phi(F_{ij}(\text{TERMSET}^B)), \quad i = 1, \dots, m, j \in J_1. \quad (7)$$

In the meantime, the positive ideal attribute value for attribute C_j ($j \in J_1$) is defined as follows:

$$\text{ideal}_j^+ = \max_{1 \leq i \leq m} \{b_{ij}\}, \quad j \in J_1. \quad (8)$$

Therefore, with respect to the attributes C_j ($j \in J_1$) with linguistic assessment values, the grey relational coefficients between their crisp values b_{ij} and the corresponding positive ideal attribute value ideal_j^+ are defined as

$$q_{ij} = \frac{\min_i \min_j \{\text{dis}(b_{ij}, \text{ideal}_j^+)\} + \rho \max_i \max_j \{\text{dis}_1(b_{ij}, \text{ideal}_j^+)\}}{\text{dis}_1(b_{ij}, \text{ideal}_j^+) + \rho \max_i \max_j \{\text{dis}_1(b_{ij}, \text{ideal}_j^+)\}}, \quad i = 1, \dots, m, j \in J_1, \quad (9)$$

where $\text{dis}_1(\cdot)$ is the distance function between b_{ij} and ideal_j^+ and is defined as follows:

$$\text{Dis}_1(b_{ij}, \text{ideal}_j^+) = \text{ideal}_j^+ - b_{ij}, \quad i = 1, \dots, m, j \in J_1. \quad (10)$$

4.1.2. Calculate the Grey Correlation Coefficients of the Attribute Values in the Form of Preference Orderings. With respect to the attributes C_j ($j \in J_2$) with the assessment values in the form of preference orderings, denote \tilde{a}_{ij} ($i = 1, \dots, m, j \in J_2$) as R_{ij} , and R_{ij} is a permutation function over the index set $\{1, \dots, m\}$. Alternatively, R_{ij} represents the position of S_i in the preference ordering. R_{ij} can be transformed into a crisp value b_{ij} as follows:

$$b_{ij} = \frac{m - R_{ij}}{m - 1}, \quad i = 1, \dots, m, j \in J_2. \quad (11)$$

In addition, regarding the attributes C_j ($j \in J_2$) with the assessment values in the form of preference orderings, the positive ideal attribute value for attribute C_j is defined as follows:

$$\text{ideal}_j^\wedge = \max_{1 \leq i \leq m} \{b_{ij}\}, \quad j \in J_2. \quad (12)$$

Furthermore, with respect to the attributes C_j ($j \in J_2$) with the assessment values in the form of preference orderings, the grey relational coefficients between their crisp values b_{ij} and the corresponding positive ideal attribute value ideal_j^\wedge are defined as

$$q_{ij} = \frac{\min_i \min_j \{\text{dis}_2(b_{ij}, \text{ideal}_j^\wedge)\} + \rho \max_i \max_j \{\text{dis}_2(b_{ij}, \text{ideal}_j^\wedge)\}}{\text{dis}_2(b_{ij}, \text{ideal}_j^\wedge) + \rho \max_i \max_j \{\text{dis}_2(b_{ij}, \text{ideal}_j^\wedge)\}}, \quad i = 1, \dots, m, j \in J_2, \quad (13)$$

where $\text{dis}_2(\cdot)$ is the distance function between b_{ij} and ideal_j^\wedge and defined as follows:

$$\text{Dis}_2(b_{ij}, \text{ideal}_j^\wedge) = \text{ideal}_j^\wedge - b_{ij}, \quad i = 1, \dots, m, j \in J_2. \quad (14)$$

4.1.3. Calculate the Grey Correlation Coefficients of the Interval Attribute Values. With respect to the attributes C_j

($j \in J_3$) with interval assessment values, denote \tilde{a}_{ij} as interval numbers $[a_{ij}^L, a_{ij}^U]$ ($i = 1, \dots, m, j \in J_3$). $[a_{ij}^L, a_{ij}^U]$ can be transformed into the benefit type, denoted as $[b_{ij}^L, b_{ij}^U]$ ($i = 1, \dots, m, j \in J_3$).

Definition 2. Given interval attribute values \tilde{b}_{ij} and \tilde{b}_{kj} for C_j , $i, k = 1, \dots, m, j \in J_3$, the distance between \tilde{b}_{ij} and \tilde{b}_{kj} is defined as

$$\text{dis}_3(\tilde{b}_{ij}, \tilde{b}_{kj}) = \frac{\sqrt{2}}{2} \sqrt{(b_{ij}^L - b_{kj}^L)^2 + (b_{ij}^U - b_{kj}^U)^2}, \quad i, k = 1, \dots, m, j \in J_3. \quad (15)$$

Definition 3. With respect to the attributes C_j ($j \in J_3$) with interval assessment values, after the interval attribute values $[a_{ij}^L, a_{ij}^U]$ ($i = 1, \dots, m, j \in J_3$) are transformed into the benefit type $[b_{ij}^L, b_{ij}^U]$, the positive ideal attribute value for attribute C_j is defined as follows:

$$\text{ideal}_j^* = [\text{ideal}_j^{*L}, \text{ideal}_j^{*U}], \quad j \in J_3, \quad (16)$$

where

$$\text{ideal}_j^{*L} = \max_{1 \leq i \leq m} \{b_{ij}^L\}, \quad j \in J_3, \quad (17a)$$

$$\text{ideal}_j^{*U} = \max_{1 \leq i \leq m} \{b_{ij}^U\}, \quad j \in J_3. \quad (17b)$$

Definition 4. Given the hybrid decision matrix $\tilde{A} = [\tilde{a}_{ij}]_{m \times n}$ with respect to the attributes C_j ($j \in J_3$) with interval assessment values, the grey relational coefficients between

$[b_{ij}^L, b_{ij}^U]$ and the corresponding positive ideal attribute value ideal_j^* are defined as

$$q_{ij} = \frac{\min_i \min_j \{ \text{dis}_3(\bar{b}_{ij}, \text{ideal}_j^*) \} + \rho \max_i \max_j \{ \text{dis}_3(\bar{b}_{ij}, \text{ideal}_j^*) \}}{\text{dis}_3(\bar{b}_{ij}, \text{ideal}_j^*) + \rho \max_i \max_j \{ \text{dis}_3(\bar{b}_{ij}, \text{ideal}_j^*) \}}, \quad i = 1, \dots, m, j \in J_3, \quad (18)$$

where $\text{dis}_3(\cdot)$ is the distance function between two interval numbers as defined in (15) and ρ is the parameter which usually has a value of 0.5.

4.2. Determine Attribute Weights. After the hybrid decision matrix $\bar{A} = [\bar{a}_{ij}]_{m \times n}$ is transformed into $Q = [q_{ij}]_{m \times n}$, in this section, a deviation maximization model is proposed firstly to determine the attribute weights and integrate them with those derived by the entropy method.

4.2.1. The Proposed Deviation Maximization Model

Definition 5. Given the normalized and beneficial decision matrix $Q = (q_{ij})_{m \times n}$ for attribute C_j , the weighted distance between alternative S_i and all other alternatives is defined as

$$D_{ij}(W) = \sum_{k=1}^m \text{dev}(q_{ij}, q_{kj}) w_j, \quad i = 1, \dots, m, j = 1, \dots, n, \quad (19)$$

where $W = (w_1, w_2, \dots, w_n)$ is the weight vector of the attributes, and $\text{dev}(\cdot)$ is the difference function between two attribute values and is defined as follows:

$$\text{dev}(q_{ij}, q_{kj}) = |q_{ij} - q_{kj}|, \quad i, k = 1, \dots, m, j = 1, \dots, n. \quad (20)$$

Definition 6. Given the normalized and beneficial decision matrix $Q = (q_{ij})_{m \times n}$ for attribute C_j , the weighted distance between all alternatives and others is defined as

$$D_j(W) = \sum_{i=1}^m D_{ij}(W) = \sum_{i=1}^m \sum_{k=1}^m \text{dev}(q_{ij}, q_{kj}) w_j, \quad j = 1, \dots, n. \quad (21)$$

It can be seen that $D_j(w)$ denotes the weighted distances among all alternatives for attribute C_j , $j = 1, \dots, n$. Assuming that all the alternatives are equally competitive and there is no preference between them, the optimal weight vector $W(W = (w_1, w_2, \dots, w_n))$ of the attributes should maximize the weighted distances among all alternatives across all the attributes. Therefore, the following deviation maximization model is set up to determine the attribute weights:

$$\max D(w) = \sum_{j=1}^n D_j(w) = \sum_{i=1}^m \sum_{j=1}^n \sum_{k=1}^m \text{dev}(q_{ij}, q_{kj}) w_j, \quad (22a)$$

s.t.

$$\sum_{j=1}^n w_j^2 = 1, \quad j = 1, \dots, n, \quad (22b)$$

$$w_j \geq 0, \quad j = 1, \dots, n. \quad (22c)$$

Theorem 1. The optimal solution to model (22a)–(22c) is

$$w_j = \frac{\sum_{i=1}^m \sum_{k=1}^m \text{dev}(q_{ij}, q_{kj})}{\sqrt{\sum_{j=1}^n \left(\sum_{i=1}^m \sum_{k=1}^m \text{dev}(q_{ij}, q_{kj}) \right)^2}}, \quad j = 1, \dots, n. \quad (23)$$

Proof:

The following Lagrange function is constructed:

$$L(W, \lambda) = \sum_{i=1}^m \sum_{j=1}^n \sum_{k=1}^m \text{dev}(q_{ij}, q_{kj}) w_j + \frac{\lambda}{2} \left(\sum_{j=1}^n w_j^2 - 1 \right), \quad (24)$$

where λ is the Lagrange multiplier.

Let $\partial L / \partial w_j = 0$ and $\partial L / \partial \lambda = 0$, the following equation can be obtained:

$$\sum_{i=1}^m \sum_{k=1}^m \text{dev}(q_{ij}, q_{kj}) + \lambda w_j = 0, \quad j = 1, \dots, n, \quad (25a)$$

$$\sum_{j=1}^n w_j^2 = 1. \quad (25b)$$

By solving the equations composed of (25a) and (25b), the following can be obtained:

$$\lambda = - \left[\sum_{j=1}^n \left(\sum_{i=1}^m \sum_{k=1}^m \text{dev}(q_{ij}, q_{kj}) \right) \right]^{1/2}, \quad (26a)$$

$$w_j = \frac{\sum_{i=1}^m \sum_{k=1}^m \text{dev}(q_{ij}, q_{kj})}{\sqrt{\sum_{j=1}^n \left(\sum_{i=1}^m \sum_{k=1}^m \text{dev}(q_{ij}, q_{kj}) \right)^2}}, \quad k = 1, \dots, m. \quad (26b)$$

Furthermore, normalize the weights given by (26b), and the weight of attribute C_j ($j = 1, \dots, n$) is obtained:

$$w_j^1 = \frac{\sum_{i=1}^m \sum_{k=1}^m \text{dev}(q_{ij}, q_{kj})}{\sum_{j=1}^n (\sum_{i=1}^m \sum_{k=1}^m \text{dev}(q_{ij}, q_{kj}))}, \quad j = 1, \dots, n. \quad (27)$$

Thus, weight vector W^1 ($W^1 = (w_1^1, w_2^1, \dots, w_n^1)$) of the attributes can be obtained based on maximizing the weighted distances among all alternatives across the attributes.

4.2.2. Entropy Method. Based on the normalized and beneficial decision matrix $Q = (q_{ij})_{m \times n}$, the attribute weights can be calculated by means of the entropy method [25]:

(a) Calculate the proportions of attributes in matrix Q : Given the normalized and beneficial decision matrix $Q = (q_{ij})_{m \times n}$, for attribute C_j , the ratio of q_{ij} to the sum of all elements in the same column in Q is calculated as

$$Z_{ij} = \frac{q_{ij}}{\sum_{l=1}^n q_{lj}}, \quad i = 1, \dots, m, \quad j = 1, \dots, n. \quad (28)$$

(b) Calculate the information entropy of the attributes: The information entropy of the attributes can be calculated as follows:

$$E_j = -k \sum_{i=1}^m Z_{ij} \ln z_{ij}, \quad j = 1, \dots, n, \quad (29)$$

where k is the adjustment coefficient and $k = 1/\ln n$.

(c) Calculate the redundancy of information entropy:

$$e_j = 1 - E_j, \quad j = 1, \dots, n. \quad (30)$$

(d) Calculate the weights of attributes:

Based on the information entropy of the attributes, their weights can be calculated as follows:

$$W_j = \frac{e_j}{\sum_{j=1}^n e_j}, \quad j = 1, \dots, n. \quad (31)$$

Denote $W^2 = (w_1^2, w_2^2, \dots, w_n^2)$ as the weight vector of the attributes obtained by means of the entropy method.

4.2.3. Determine Comprehensive Attribute Weights. Based on the attribute weight vector W^1 calculated by the deviation maximization model (22a)–(22c) and the attribute weight vector W^2 obtained by the Entropy method, the comprehensive attribute weight vector based on the decision matrix Q is calculated in the following:

$$W^o = 0.5W^1 + 0.5W^2. \quad (32)$$

4.3. Calculate the Overall Values of Suppliers. The overall values of supplier S_i can be obtained by means of the weighted sum method as follows:

$$\text{overall}_i = \sum_{j=1}^n w_j^o q_{ij}, \quad i = 1, \dots, m. \quad (33)$$

All the suppliers can be ranked descendingly according to their overall values calculated in formula (33).

5. Illustrations

In the course of supplier selection, the determination of assessment attributes is the first step. The selection of attributes is reviewed in [9]. In this study, service level (C_1), degree of informatization (C_2), profitability (C_3), level of quality (C_4), and level of risk (C_5) are adopted in evaluating and selecting four suppliers (i.e., S_i , $i = 1, 2, 3$, and 4) in B2B e-commerce environment. Because of the uncertainty and fuzziness in B2B e-commerce environment, for the attributes of service level (C_1) and level of risk (C_5), preference orderings are used.

For the attributes of degree of informatization (C_2) and level of quality (C_4), linguistic terms are used to assess the supplier performances. For the attribute of profitability C_3 , interval numbers are employed. For the sake of simplicity, the linguistic term set {"very poor," "poor," "fair," "good," and "very good"} is employed for both attributes of degree of informatization (C_2) and level of quality (C_4), and is same as the basic linguistic term set TERMSET^B in this study. Details of the assessment information of the suppliers (S_i , $i = 1, 2, 3, 4$) against the attributes are stated in Table 1.

Firstly, with respect to attribute C_1 of the service level, the assessment information of the suppliers in Table 1 is normalized as $(b_{11}, b_{21}, b_{31}, b_{41})^T = (1, 0, 0.3333, 0.6667)^T$ and is further transformed as $(q_{11}, q_{21}, q_{31}, q_{41})^T = (1, 0.3333, 0.4286, 0.6)^T$, by calculating the grey relational coefficients between their crisp values b_{i1} ($i = 1, 2, 3, 4$) and the corresponding positive ideal attribute value.

Secondly, with respect to attribute C_2 of degree of informatization, the linguistic assessment information of the suppliers in Table 1 is normalized as $(b_{12}, b_{22}, b_{32}, b_{42})^T = (0.9167, 0.25, 0.5, 0.75)^T$ and is further transformed as $(q_{12}, q_{22}, q_{32}, q_{42})^T = (1, 0.4, 0.5714, 1)^T$.

Thirdly, with respect to attribute C_3 of profitability, the interval assessment information of the suppliers in Table 1 is normalized as

$$\begin{pmatrix} b_{13}^l & b_{13}^u \\ b_{23}^l & b_{23}^u \\ b_{33}^l & b_{33}^u \\ b_{43}^l & b_{43}^u \end{pmatrix} = \begin{pmatrix} 0.75 & 1 \\ 0 & 0.25 \\ 0.5 & 0.75 \\ 0.25 & 0.5 \end{pmatrix}, \quad (34)$$

and it is further transformed as $(q_{13}, q_{23}, q_{33}, q_{43})^T = (0.5836, 0.5182, 1, 0.6940)^T$.

Fourthly, with respect to attribute C_4 of level of quality, the linguistic assessment information of the suppliers in Table 1 is normalized as $(b_{14}, b_{24}, b_{34}, b_{44})^T = (0.5, 0.0833, 0.75, 0.9167)^T$ and is further transformed as $(q_{14}, q_{24}, q_{34}, q_{44})^T = (0.5, 0.3333, 0.7143, 1)^T$. Fifthly, with respect to attribute C_5 of level of risk, the assessment information of the suppliers in Table 1 is normalized into

TABLE 1: The assessment information of the suppliers.

	Service level C_1	Degree of informatization C_2	Profitability C_3	Level of quality C_4	Level of risk C_5
S_1	1	Poor	[70, 80]	Fair	2
S_2	4	Very poor	[40, 50]	Poor	1
S_3	3	Fair	[60, 70]	Very good	4
S_4	2	Very good	[50, 60]	Good	3

$(b_{15}, b_{25}, b_{35}, b_{45})^T = (0.6667, 1, 0, 0.3333)^T$ and is further transformed as $(q_{15}, q_{25}, q_{35}, q_{45})^T = (0.6, 1, 0.3333, 0.4286)^T$.

Based on the above calculation, the single-point value decision matrix Q is obtained as

$$Q = \begin{pmatrix} 1.0000 & 1.0000 & 0.5836 & 0.5000 & 0.6000 \\ 0.3333 & 0.4000 & 0.5182 & 0.3333 & 1.0000 \\ 0.4286 & 0.5714 & 1.0000 & 0.7143 & 0.3333 \\ 0.6000 & 1.0000 & 0.6940 & 1.0000 & 0.4286 \end{pmatrix}. \quad (35)$$

Furthermore, based on the normalized decision matrix Q , the attribute weight vector can be calculated by the deviation maximization model (22a)–(22c) as $W^1 = (0.2100, 0.2155, 0.1504, 0.2141, \text{ and } 0.2100)$. In the meantime, the attribute weight vector can also be obtained by the entropy weight method as $W^2 = (0.2120, 0.1970, 0.1746, 0.2044, \text{ and } 0.2120)$. Thus, the comprehensive attribute weight vector based on the decision matrix Q is calculated as $W^0 = (0.2110, 0.2062, 0.1625, 0.2092, \text{ and } 0.2110)$. Accordingly, the overall values of the suppliers can be obtained as follows: $\text{overall}_1 = 0.7432$, $\text{overall}_2 = 0.5177$, $\text{overall}_3 = 0.6295$, and $\text{overall}_4 = 0.7452$. Finally, the ranking of the suppliers is $S_4 > S_1 > S_3 > S_2$.

6. Conclusions

This paper proposes an approach to evaluating and selecting the manufacturing suppliers in B2B e-commerce environment, where linguistic terms, preference orderings, and interval numbers are employed to present their fuzzy performances. After the hybrid decision matrix is normalized, the attribute weights are determined by means of proposing the deviation maximization model and the entropy method.

The merits of the proposed approach lie in three aspects. The first one is to express the uncertainty of the suppliers' performances by means of the appropriate and the easiest ways, i.e., linguistic terms, preference orderings, and interval numbers. The second one is to propose the methods of normalizing the hybrid decision matrix by calculating the grey correlation coefficients of attribute values with the ideal values of attributes. The third one is to determine the attribute weights by means of the deviation maximization model and the entropy method based on normalized decision matrix. This paper enables to express the suppliers' performance information in the easiest ways and accurately, especially in fuzzy or uncertain decision environment. Compared with the current research, the proposed approach has more universal significance and practical application prospects.

Data Availability

The data used to support the findings of this study are available from the corresponding author upon request.

Conflicts of Interest

The authors declare that they have no conflicts of interest.

Acknowledgments

This work was supported by the Science and Technology Agency of Liaoning Province under the Grant of the Natural Science Foundation of Liaoning Province (2013020022) "Hybrid multicriteria group decision-making with various forms of information expression."

References

- [1] D. Maffin and P. Braiden, "Manufacturing and supplier roles in product development," *International Journal of Production Economics*, vol. 69, no. 2, pp. 205–213, 2001.
- [2] G. Svensson, T. Mysen, and J. Payan, "Balancing the sequential logic of quality constructs in manufacturing-supplier relationships—causes and outcomes," *Journal of Business Research*, vol. 63, no. 11, pp. 1209–1214, 2010.
- [3] M. J. Sáenz, D. Knoppen, and E. M. Tachizawa, "Building manufacturing flexibility with strategic suppliers and contingent effect of product dynamism on customer satisfaction," *Journal of Purchasing and Supply Management*, vol. 24, no. 3, pp. 238–246, 2018.
- [4] T.-C. Chu and R. Varma, "Evaluating suppliers via a multiple levels multiple criteria decision making method under fuzzy environment," *Computers & Industrial Engineering*, vol. 62, no. 2, pp. 653–660, 2012.
- [5] L. Xie, J. Ma, and H. Han, "Implications of stochastic demand and manufacturers' operational mode on retailer's mixed bundling strategy and its complexity analysis," *Applied Mathematical Modelling*, vol. 55, no. 1, pp. 484–501, 2018.
- [6] J. Ma and L. Xie, "The stability analysis of the dynamic pricing strategy for bundling goods: a comparison between simultaneous and sequential pricing mechanism," *Nonlinear Dynamics*, vol. 95, no. 2, pp. 1147–1164, 2019.
- [7] L. A. Zadeh, "A computational approach to fuzzy quantifiers in natural languages," *Computational Linguistics*, vol. 9, no. 1, pp. 149–184, 1983.
- [8] L. F. D. O. M. Santos, L. Osiro, and R. H. P. Lima, "A model based on 2-tuple fuzzy linguistic representation and Analytic Hierarchy Process for supplier segmentation using qualitative and quantitative criteria," *Expert Systems with Applications*, vol. 79, pp. 53–64, 2017.
- [9] P. Sureeyatanapas, K. Sriwattananusart, T. Niyamosoth, W. Sessomboon, and S. Arunyanart, "Supplier selection towards uncertain and unavailable information: an extension of

- TOPSIS method,” *Operations Research Perspectives*, vol. 5, pp. 69–79, 2018.
- [10] C.-N. Liao and H.-P. Kao, “An integrated fuzzy TOPSIS and MCGP approach to supplier selection in supply chain management,” *Expert Systems with Applications*, vol. 38, no. 9, pp. 10803–10811, 2011.
- [11] F. R. L. Junior, L. Osiro, and L. C. R. Carpinetti, “A comparison between fuzzy AHP and fuzzy TOPSIS methods to supplier selection,” *Applied Soft Computing*, vol. 21, no. 5, pp. 194–209, 2014.
- [12] A. Azizi, D. O. Aikhuele, and F. S. Souleman, “A fuzzy TOPSIS model to rank automotive suppliers,” *Procedia Manufacturing*, vol. 2, pp. 159–164, 2015.
- [13] A. Kokangul and Z. Susuz, “Integrated analytical hierarch process and mathematical programming to supplier selection problem with quantity discount,” *Applied Mathematical Modelling*, vol. 33, no. 3, pp. 1417–1429, 2009.
- [14] N. R. Ware, S. P. Singh, and D. K. Banwet, “A mixed-integer non-linear program to model dynamic supplier selection problem,” *Expert Systems with Applications*, vol. 41, no. 2, pp. 671–678, 2014.
- [15] H. Mirzaee, B. Naderi, and S. H. R. Pasandideh, “A preemptive fuzzy goal programming model for generalized supplier selection and order allocation with incremental discount,” *Computers & Industrial Engineering*, vol. 122, pp. 292–302, 2018.
- [16] C. L. Hwang and K. Yoon, *Multiple Attribute Decision Making: Methods and Applications*, Springer-Verlag, New York, NY, USA, 1981.
- [17] C. C. Lee and C. Ou-Yang, “A neural networks approach for forecasting the supplier’s bid prices in supplier selection negotiation process,” *Expert Systems with Applications*, vol. 36, no. 2, pp. 2961–2970, 2009.
- [18] A. F. Güneri, T. Ertay, and A. Yücel, “An approach based on ANFIS input selection and modeling for supplier selection problem,” *Expert Systems with Applications*, vol. 38, no. 12, pp. 14907–14917, 2011.
- [19] C. Bai and J. Sarkis, “Integrating sustainability into supplier selection with grey system and rough set methodologies,” *International Journal of Production Economics*, vol. 124, no. 1, pp. 252–264, 2010.
- [20] D. Golmohammadi and M. Mellat-Parast, “Developing a grey-based decision-making model for supplier selection,” *International Journal of Production Economics*, vol. 137, no. 2, pp. 191–200, 2012.
- [21] M. S. Memon, Y. H. Lee, and S. I. Mari, “Group multi-criteria supplier selection using combined grey systems theory and uncertainty theory,” *Expert Systems with Applications*, vol. 42, no. 21, pp. 7951–7959, 2015.
- [22] B. S. Ahn and K. S. Park, “Comparing methods for multi-attribute decision making with ordinal weights,” *Computers & Operations Research*, vol. 35, no. 5, pp. 1660–1670, 2008.
- [23] J. Wang and S. Zionts, “Using ordinal data to estimate cardinal values,” *Journal of Multi-Criteria Decision Analysis*, vol. 22, no. 3–4, pp. 185–196, 2015.
- [24] F. Herrera, L. Martínez, and P. J. Sánchez, “Managing non-homogeneous information in group decision making,” *European Journal of Operational Research*, vol. 166, no. 1, pp. 115–132, 2005.
- [25] Y. Ji, G. H. Huang, and W. Sun, “Risk assessment of hydropower stations through an integrated fuzzy entropy-weight multiple criteria decision making method: a case study of the Xiangxi River,” *Expert Systems with Applications*, vol. 42, no. 12, pp. 5380–5389, 2015.

Research Article

A Dynamic Thermal-Allocation Solution to the Complex Economic Benefit for a Data Center

Hui Liu ¹, Wenyu Song,¹ Tianqi Jin,² Zhiyong Wu,³ Fusheng Yan,¹ and Jie Song⁴

¹New Energy Science and Engineering Department, School of Metallurgy, Northeastern University, Shenyang 110819, Liaoning, China

²Thermal Engineering Department, School of Metallurgy, Northeastern University, Shenyang 110819, Liaoning, China

³China Railway Rolling Stock Corporation Zhuzhou Institute Co., Ltd., Zhuzhou 412001, Hunan, China

⁴Software Engineering Department, Software College, Northeastern University, Shenyang 110819, Liaoning, China

Correspondence should be addressed to Hui Liu; liuh@smm.neu.edu.cn

Received 17 March 2020; Revised 5 May 2020; Accepted 15 May 2020; Published 15 June 2020

Guest Editor: Baogui Xin

Copyright © 2020 Hui Liu et al. This is an open access article distributed under the Creative Commons Attribution License, which permits unrestricted use, distribution, and reproduction in any medium, provided the original work is properly cited.

Data centers, which provide computing services and gain profits, are indispensable to every city in the information era. They offer computation and storage while consuming energy and generate thermal discharges. To maximize the economic benefit, the existing research studies on the data center workload management mostly leverage the dynamical power model, i.e., the power-aware workload allocation. Nevertheless, we argue that for the complex relationship between the economic benefit and so many attributes, such as computation, energy consumption, thermal distribution, cooling, and equipment life, the thermal distribution dominates the others. Thus, thermal-aware workload allocation is more efficient. From the perspective of economic benefits, we propose a mathematical model for thermal distribution of a data center and study which workload distribution could determinately change the thermal distribution in the dynamic data center runtime, so as to reduce the cost and improve the economic benefits under the guarantee of service provisioning. By solving the thermal environment evaluation indexes, RHI (Return Heat Index) and RTI (Return Temperature Index), as well as heat dissipation models, we define quantitative models for the economic analysis such as energy consumption model for the busy servers and cooling, energy price model, and the profit model of data centers. Numerical simulation results validate our propositions and show that the average temperature of the data center reaches the best values, and the local hot spots are avoided effectively in various situations. As a conclusion, our studies contribute to the thermal management of the dynamic data center runtime for better economic benefits.

1. Introduction

Data center (DC) is an information service platform with efficient equipment and perfect management mechanisms. Under the background of the high-speed information age, the global demand for Internet business and information services is increasing year by year. According to statistics, the global Internet Data Center (IDC) business market as a whole will exceed 130 billion dollars in 2020, and DCs around the world will consume 8% of the world's electricity and put a heavy environmental burden on society [1].

The huge energy consumption accompanies extremely low resource utilization, which is reported to be between 5% and 25% in typical DCs [2]. The main reason for this is that

DC operators often adopt redundant resource deployment strategies in pursuit of high performance, quality of service, and reliability. Therefore, all servers will be at the highest busy ratio regardless of the load. The low utilization of these multidimensional resources (CPU, storage, memory, and network bandwidth) leads directly to huge resource waste. At the same time, it also increases the cost of other supporting equipment such as cooling system and power distribution unit. Under this development trend, how to reduce the high cost and high energy consumption caused by the high demands has been concerned by scholars.

The key to the cost control of facility operation and maintenance in a DC is the electricity cost of the equipment,

and the main influencing factors are the running time, quantity, and distribution of high-power equipment [3]. In addition, as the main components of a DC, IT equipment and cooling equipment account for about 90% of the energy consumption of the DC, among which the cooling equipment accounts for about 40%–60% [4, 5]. In the optimization scheme, the optimized workload allocation is adopted to improve the cooling capacity and adjust the temperature distribution in the DC, so as to reduce the running time of the air-conditioning equipment and the electricity cost, reduce the hot spot of temperature, and further reduce the possibility of equipment damages and make the effect of full-life cycle cost control of the DC more obvious. Therefore, there is a very complex relationship between economic benefit and calculation, energy consumption, heat distribution, cooling, and equipment life, among which heat distribution dynamically dominates other properties [6].

It is necessary to analyze the economic effects of the improvements in energy efficiency achieved by existing methods. In this paper, the steady and transient numerical simulation is used to seek the switch strategy of energy-saving operation, and the two main problems of improving the airflow organization mode and busy servers distribution mode are studied. To improve the economic performance of the DC cooling strategy from the perspective of dynamic thermal environment, the following research contents are studied:

- (1) A reasonable calculation model and a calculation method are selected, the temperature and velocity distribution of airflow in the DC are simulated, and the temperature distribution and airflow velocity distribution of the specified section of the DC are obtained;
- (2) The influence of power distribution, workload allocation, and overall busy ratio on the thermal environment of the DC is studied, and the optimized switch strategy is analyzed;
- (3) The influence of power and cooling quantity changes on transient temperature rise of busy servers is analyzed, and transient switch strategy analysis is carried out under the condition of dynamic change of switch quantity.
- (4) Based on the heat distribution of the DC, the influence factors and the influence of thermal environment on the economic benefit of the DC are analyzed. The complex economic benefit problem, which is expressed as a nonlinear optimization problem with multiparameters and multiconstraints, is solved.

The rest of the paper is organized as follows. Section 2 introduces the related works about thermal environment and the economic benefit of DCs. Section 3 proposes the mathematical model and thermal evaluation metrics for modeling thermal environment. Section 4 gives workload allocation for servers according to the mathematical thermal model and evaluates the influence of busy ratio. Section 5 discusses the transient analysis of the dynamic switch strategy and Section 6

analyzes the economic effects. Finally, the conclusions and future works are summarized in Section 7.

2. Related Works

In this section, we provide a brief overview of some existing works on two major topics: the first is the thermal optimization for DCs, and the second is the economic benefit optimization for DCs.

The thermal environment of DCs has been studied in existing literature from the aspects of air distribution, construction of hot and cold enclosed aisles, and reduction of inefficiencies of the equipment. In terms of air distribution, many researchers have conducted a lot of studies on air supply methods, perforated tiles, equipment layout, and so on. Chu et al. [7] studied the thermal influence of air intake flow and inlet layout on the DC with the enclosed cold aisle. They found that the uniformity of inlet flow did not improve with the strength of flow, the power consumption increased instead. However, when the inlet direction was deflected to the rack direction, the flow uniformity in the rack was greatly improved. In terms of cold aisles design, Cho and Woo [8] designed the new row-based cooling system, in which the air conditionings, racks, and cold and hot aisles are all enclosed in one line. The cooling efficiency of this model, RHI, and RTI are 20%, 73.2%, and 50% higher than those of the open aisle, respectively. In terms of reducing the energy consumption of equipment, Jin et al. [9] summarized the important influence of the accurate server's power model on the energy saving and reliability of the DCs. In the model, the effects of cooling output, inlet temperature, and energy saving of the server are considered. It is pointed out that the peak power of the server accounts for 40%–50% of the rated power. Energy-saving technology can reduce idle power from 55% of rated power to 15%. With the improvement of heat dissipation requirements, the placement of racks in DC has gradually developed from the extensive form to the orderly form, that is, the racks are arranged in order to naturally form cold aisles and hot aisles [10, 11]. Because the enclosed cold aisles can effectively contain the cold flow loss caused by mixing of cold and hot air in the cold aisles, it has been gradually accepted and popularized in engineering practice [12].

In most studies, the modeling studies focused strictly on steady-state analysis of DCs, and fixed workload allocation and rack powers are imposed. For transient analyzes, the switch coefficient of servers is crucial as it significantly affects the amount of time it takes to reach the steady state [13]. Therefore, in terms of the energy efficiency optimization, we are interested in the thermal impact of various switch strategies [14, 15].

The maximization of economic benefit for DCs is a complex problem because it is with many factors and restrictions. Classic solution only takes one-time investment and operation cost into consideration [16]. The former includes investment on servers, network, accessories, buildings, power generators, and computer room air conditionings (CRAC). Such investment is static and is not

considered in our researches. The latter mainly includes cost of equipment's maintenance and energy. Such cost is dynamic and is considered in our researches. The sophisticated economic benefit models can effectively estimate and even predict the total investment and annual operation cost of a DC. Besides, economic benefit optimization can be reached by several approaches, for example, a model based on a resource management technique and semi-Markov decision process [17], green scheduling for cloud data centers in an economical way by renewable energy trading with the power grid [18], scheduling of data-oriented tasks in geographically distributed cloud data centers [19], transmission cost reduction from the perspective of DC users [20], and replica factor dynamical adjustment to reduce the resource consumption and guarantee the economic profit [21]. However, to the best of our knowledge, there are few researches leveraged the thermal management for economic benefit optimization. There are few researches modeled economic benefit as a maximization problem and took the thermal distribution, profits, energy cost of servers, and cooling system into consideration. Otherwise, the economic benefit models are very challenging to be accurate, quantitative, and efficient. The thermal optimization is mainly associated with energy optimization, for example, MirhoseiniNejad et al. [22] considered thermal effects of server workloads, which in conjunction with control parameters of the cooling unit, save more power than optimizing each of them separately.

3. Mathematical Model and Thermal Evaluation Metrics

In this paper, the airflow distribution model of a DC is "airflow supplied from the lower side and returned from the upper side via the enclosed cold aisle", as shown in Figure 1. Comparing with other airflow modes, our choice has obvious advantages [23, 24]. In Figure 1, all dimensions are listed in $X \times Y \times Z$ order. The size of the DC is $14 \times 12 \times 2.5$ (m), in which there are 4 (columns) \times 11 (racks) with the size of $0.6 \times 1.1 \times 2$ (m). The size of the enclosed cold aisle is 6.6×1.2 (m) and width on each side of hot aisles is 1.4 (m). The size of the server is $0.5 \times 1 \times 0.0495$ (m) and the CRAC is $0.9 \times 1.92 \times 2$ (m). The size of the front rack is $1.82 \times 1.1 \times 2$ (m). In addition, the cooling inlet and outlet of the rack are fully open, and they are in the same size of 0.6×2 (m), and the size of each air conditioner's outlet is 0.8×0.9 (m). The air at 17°C supplied from the floor inlet refrigerates servers through two columns of standard 42 U racks and then returns to the CRAC on top of the hot aisle; the cold aisle is enclosed. There are two air outlets placed on top of each air conditioner. The ambient temperature is set at 20°C . The average temperature difference of return air is predicted to be 10°C . When air flows through the rack, the cooling loss can be considered as sensible heat exchange, which could be calculated by equation (1) to predict the air supply volume in numerical simulation:

$$Q = c_p G \Delta T, \quad (1)$$

where c_p is the specific heat capacity of the fluid at constant pressure (J/kg·K), G is the air volume (kg/s), and ΔT is the average temperature difference of return air ($^\circ\text{C}$).

We design an extreme condition that 20 highly integrated servers (1 U for each) are distributed in each rack in the model. The cooling capacity in this paper depends on the heat conversion rate of IT equipment, which is about 80%. In the numerical simulation model, the rated power of the 1 U server is 200 W/U and the idle power is 20 W/U. Figure 2 shows the heat load of the DC with different busy ratios and the designed cooling flow rate.

In this paper, thermal analysis software IcePak is used for numerical simulation analysis. The finite element volume method is used for the discrete form and the SIMPLE algorithm is used for solution. The minimum cell's size was $3 \text{ mm} \times 1 \text{ mm} \times 6 \text{ mm}$, and the total number of grids was 1.9×10^6 . As for the selection of turbulence models, the zero equation has the advantage of less computation, obtaining more accurate results than other models [25]. The assumed conditions are as the follows:

- (1) The low-speed air in the DC can be regarded as Newtonian fluid, and the dissipation work caused by the viscous force of the fluid can be ignored
- (2) The fluid domain is steady turbulence
- (3) The nonslip boundary condition is applied on the air inside the DC
- (4) The air tightness of the DC is good, and the influence of air leakage is ignored
- (5) According to the Boussinesq hypothesis, the change of fluid density only affects the buoyancy

In this paper, a three-dimensional incompressible fluid model is established, which follows the laws of mass conservation, momentum conservation, and energy conservation. Combined with the Reynolds-averaged Navier-Stokes method, the governing equations are as follows [26]:

- (1) Continuity equation

$$\frac{\partial \rho}{\partial t} + \rho \frac{\partial \bar{v}_i}{\partial x_i} = 0, \quad (2)$$

where t is the time (s), \bar{v}_i , \bar{v}_j are vector speeds (m/s), and x_i , x_j are vector coordinates (m).

- (2) Momentum equation

$$\rho \left(\frac{\partial \bar{v}_i}{\partial t} + \bar{v}_j \frac{\partial \bar{v}_i}{\partial x_j} \right) = \rho f_i - \frac{\partial \bar{p}}{\partial x_i} + \frac{\partial}{\partial x_j} \left(\mu \frac{\partial \bar{v}_j}{\partial x_j} - \rho \overline{v'_i v'_j} \right), \quad (3)$$

where f_i is the body force (N), μ is the dynamic viscosity of the fluid (Pa·s), and ρ is the fluid density (kg/m^3). It is worth noting that $\rho \overline{v'_i v'_j}$ in momentum equation (3) is the turbulent stress. In order to determine its value, it needs to be solved by combining the turbulent zero-equation mode, i.e., equation (4).

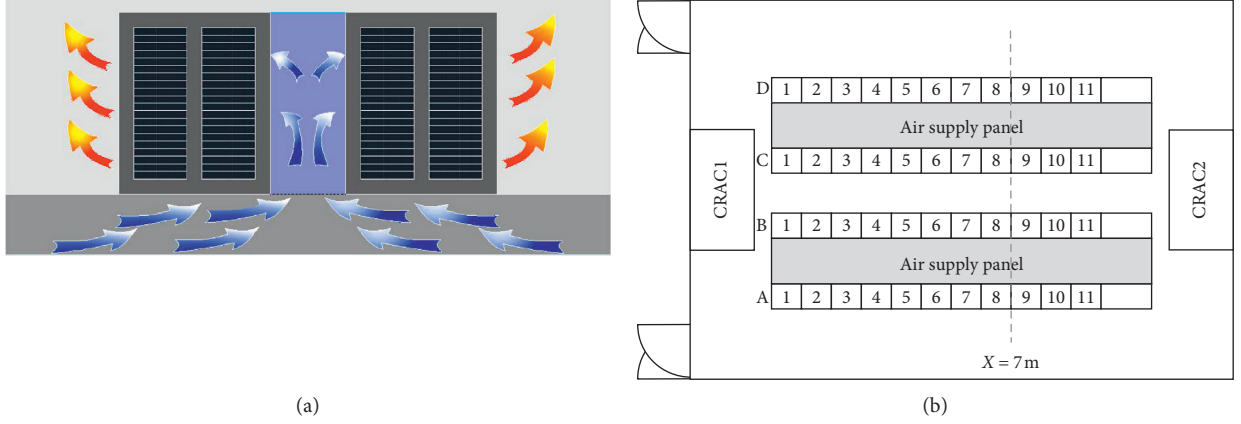


FIGURE 1: Physical model of the DC. (a) Air supply mode. (b) Diagram of the physical mode.

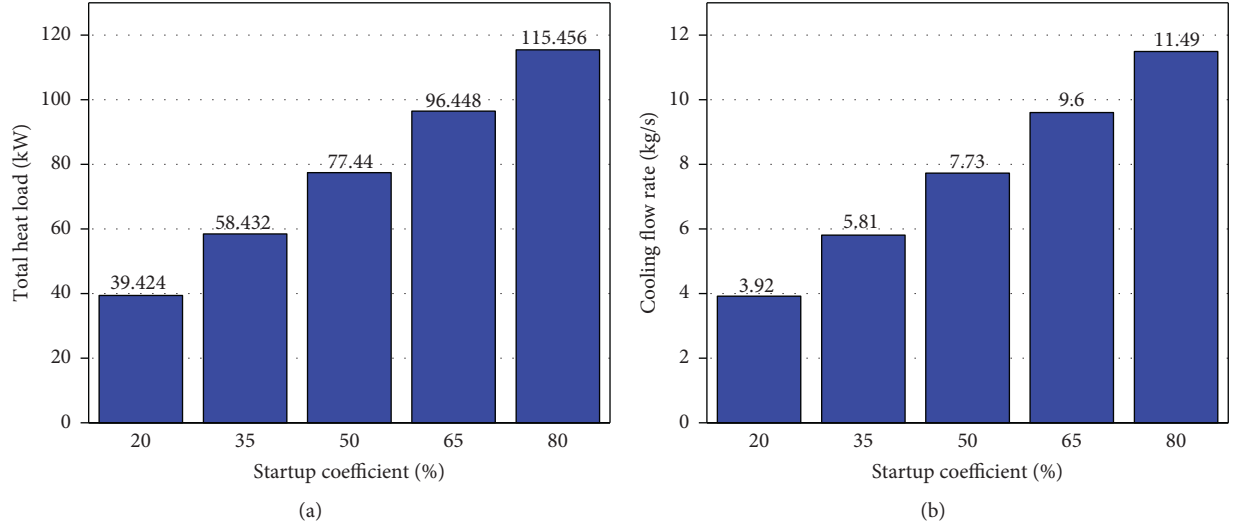


FIGURE 2: Total heat load (a) and cooling flow rate (b) of the DC.

The turbulence model: zero-equation mode

$$\begin{aligned} \tau_t &= -\overline{\rho v_i' v_j'} = v_T \left(\frac{\partial \bar{v}_i}{\partial x_j} + \frac{\partial \bar{v}_j}{\partial x_i} \right) \\ &= \rho l^2 \sqrt{\frac{1}{2} \left(\frac{\partial \bar{v}_i}{\partial x_j} + \frac{\partial \bar{v}_j}{\partial x_i} \right)^2 \left(\frac{\partial \bar{v}_i}{\partial x_j} + \frac{\partial \bar{v}_j}{\partial x_i} \right)}. \end{aligned} \quad (4)$$

(3) Energy conservation equation

$$\frac{\partial(\rho \bar{T})}{\partial t} + \frac{\partial(\rho \bar{v}_i \bar{T})}{\partial x_i} = \frac{\lambda}{c_p} \frac{\partial^2 \bar{T}}{(\partial x_j)^2} - \overline{\rho v_i' T'} + S, \quad (5)$$

where T is the fluid temperature ($^{\circ}\text{C}$), λ is the thermal conductivity of the fluid ($\text{W/m}\cdot\text{K}$), S is the source item, and $\overline{\rho v_i' T'}$ is the turbulent thermal diffusion term, the expression of which is shown in the following equation:

$$\overline{\rho v_i' T'} = \frac{v_T}{\text{Pr}_t}, \quad (6)$$

where v_T is the turbulent viscosity ($\text{Pa}\cdot\text{s}$), Pr_t is an empirical coefficient, the value of which is greatly affected by the material thermal properties and turbulent intensity. l is the mixing length (m).

Equations (7)–(11) give the boundary conditions of the model:

$$v_{z=0} = v_0, \quad (7)$$

$$p_{z=H} = p_0, \quad (8)$$

$$T_{air}|_{z=0} = T_0, \quad (9)$$

$$q_w = 0, \quad (10)$$

$$\lambda \frac{\partial T_{air}}{\partial x_i} \Big|_{x_i=x_1} = q = \text{const} \quad (11)$$

Combined with the governing equations and boundary conditions in this model, it can be seen that the velocity vector in the energy equation can be obtained by solving continuity equation (2) and momentum equation (3) of a certain position under the initial conditions. Furthermore, the turbulent heat diffusion value in the energy equation is obtained by the turbulent stress solved under the specific condition and the given turbulent Prandtl number, and on this basis, we can obtain the value of turbulent thermal diffusion and temperature at a certain point in this system. This process is iterated to gradually generate the velocity field and temperature field of the whole space.

A verification model was established according to the experiment of Arghode et al. [27], consistent with experimental conditions in this paper. The cold aisle temperature measured by the temperature monitoring car of racks 2–7 and racks 9–12 was compared with the simulated results, as shown in Figure 3.

Figure 3 shows experimental and simulated temperature of the cold aisle. The error of racks in the middle position is the minimum, and the mean absolute error is about 5%. It can be seen that the error is caused by uncontrollable factors between the assumed condition and the actual situation. The reason for the higher temperature of the lower servers may be that the temperature measuring car blocks the air flow in the cold aisle. The temperature shows mostly good agreement with the numerical results. It can be considered that the model is feasible.

In order to evaluate the selected scheme, RHI (Return Heat Index) and RTI (Return Temperature Index) are introduced to conduct comprehensive evaluation [15, 23], where RHI represents the utilization ratio of the air-cooling capacity of the rack, and RTI evaluates the air distribution in the DC. Details are shown in Table 1.

RHI can be used to evaluate the thermal environment and determine the existence and specific location of local hot spots, while RTI can be used to objectively evaluate the airflow distribution of the rack and the overall DC.

4. Influence of Workload Allocation on Complexity Thermal Environment

The influence of workload allocation and distribution of racks on the heat dissipation of the DC and the influence of parameters of the DC change on the optimization of heat dissipation under nonfull workload conditions are studied in this section.

4.1. Workload Allocation for Servers. According to the current common mode of busy servers allocation in DCs, 8 classic allocation modes of busy servers were designed and are shown in Table 2 and Figure 4, named by the workload allocation of the servers, and Figure 4 shows that there are

significant differences of thermal environment in the DC. There are two reasons for this phenomenon. First of all, when the cold air flows through the enclosed aisle, there is different cooling attenuation at different workload allocation of servers. In addition, under different workload distribution modes, the reexchanging heat amount of airflow with different cooling attenuation in the hot aisle is also different. The cold energy utilization in the centralized distribution models is significantly lower than that in the decentralized model. The hot zone exists in the DC with the centralized distribution model, as shown in Model 1~6, the uniformity of thermal environment of Model 7 and Model 8 is better, and the temperature difference is about 2°C. The results show that whether the thermal environment is good or not depends on the mixing degree of cold airflow in the open hot aisle, the better the heat transfer performance, the more uniform the temperature distribution and the better the overall heat dissipation. Secondly, because the trend of the vertically upward air supply in the enclosed aisle is greater than that of the side direction rack fan, less cold air flows through the lower part of the rack's servers than the upper part. This conclusion can be confirmed by the temperature comparison of Model 1, Model 2, and Model 3 in Figure 5, and heat transfer capacity is weakened successively from Model 2 and Model 3 to Model 1. In addition, the hot zone appeared in models where the workload was distributed near the lower layers, such as Model 1, Model 4, and Model 6.

According to GB50174-2017 of China, the standard range of safe operation in DCs is 18–28°C. When the busy ratio of the DC is 0.5, the temperature comparison of the overall thermal environment in 8 cases is shown in Figures 5(a)–5(h). The peak temperatures of Model 1/4/6/7 exceed the upper limit of 28°C; it will inevitably increase the consumption of refrigerating capacity and electricity cost for the stable operation. The peak temperatures of Model 2/3/5/8 are within the standard range. It indicates that an economical operation mode for DCs is to arrange the busy servers close to the middle and upper layers of the rack in the process of nonfull load operation. In addition, busy servers in Model 5, Model 2, and Model 3 are all distributed in the middle and upper layers, and they are relatively more dispersed in Model 5. Comparing the thermal environment of Model 2/3/5/8, the thermal stratification of Model 5 is more uniform, and the average temperature of the thermal environment is the lowest. On the basis of centralized distribution, proper dispersion is beneficial to improve the cooling effect, but it is not that the more dispersed the better. For example, the thermal environment of Model 8 is not as good as that of Model 5, because the servers' excessive dispersion will increase the possibility that the servers are distributed in the lower rack, and it is not conducive to cooling.

According to Table 1, RHI and RTI are obtained to evaluate the local airflow structure comprehensively. Figure 6(b) shows that RHI is relatively high in the mode that the busy servers are far away from the lower layers, for example, in Model 2, 3, and 5. It means that in nonfull load conditions, the middle and upper layout modes of the busy servers can effectively reduce the mixing of hot and cold air



FIGURE 3: Temperature comparison of experimental and simulation results in cold aisles.

TABLE 1: Description of two thermal evaluation indexes.

Thermal evaluation index	RHI	RTI
Expression	$Q/(Q + \delta Q)$	$(T_{out} - T_{in}/\Delta T) \times 100\%$
Evaluation criterion	RHI $\in (0, 1)$. The more the RHI approaches 1, the better the heat transfer, the less the mixing of cold and hot air, and the higher the utilization rate of air-cooling capacity is.	The more the RTI approaches 1, the better the air distribution is. When RTI > 1 , there is hot air backflow. While RTI < 1 , it indicates cold air bypass.

TABLE 2: Allocation modes of busy servers.

Workload allocation model	Busy servers distribution
Model 1	Concentrate in the lower layers
Model 2	Concentrate in the middle layers
Model 3	Concentrate in the upper layers
Model 4	Central free
Model 5	Upper alternating segment
Model 6	Lower alternating segment
Model 7	Alternating segment
Model 8	Single alternating

and improve the utilization of cooling capacity. Through the relative temperature index RTI, we can find that RTI of Model 7 is closest to 1, followed by Model 5. However, based on the abovementioned conclusions, in the three models with better RHI of Model 2, 3 and 5, RTI of Model 5 is closest to 1. The maximum temperature of Model 5 is about 7°C lower than Model 7, that is, Model 5 is the best model for the comprehensive evaluation of the heat and air distribution.

4.2. Influence of Busy Ratios. Based on the abovementioned conclusions, Model 2, 3, 5, and 8 are adopted to analyze the variation regularity of thermal environment performance indexes RHI and RTI, and the switch strategy on energy saving will be optimized. When the busy ratios are, respectively, 0.2, 0.35, 0.5, 0.65, and 0.8, the numbers of busy servers are, respectively, 4, 7, 10, 13, and 16. Figure 7 shows

that RTI increases with the increase of the busy ratio, and the range gradually increases from about 0.75 to 1.3. This can be attributed to that when the busy ratio is small, the subcooled zones are large, and the loss of bypass cold air occurs. As the busy ratio increases, the hot zones gradually appear instead of subcooled zones, the possibility of hot air recirculation is increased. Secondly, RHI decreases with the increase of the busy ratio. This is because the increase of the busy ratio promotes the possibility of hot air backflow, which leads to hot air mixing with cold air in the enclosed cold aisle, reducing the cooling efficiency of air supply. It can be seen that given the ideal cooling amount making the thermal environment at the same temperature gradient, RHI and RTI are closest to the ideal value at the busy ratio of 0.5, and the cooling efficiency is the highest. When the busy ratio is more than or equals to 0.5, RTI of Model 5 is closest to ideal value 1, RHI is the largest relative to other models, and the overall thermal environment is optimal. When the busy ratio is less than 0.5, Model 2 is the best choice.

5. Transient Analysis of Dynamic Switch Strategy

There are numerous transient scenarios in the actual operation of DCs. Therefore, the dynamic switch of workload is very important for the stable operation of DCs. In addition to the influence of the dynamic switch degree of the workload quantity on the cooling performance of servers,

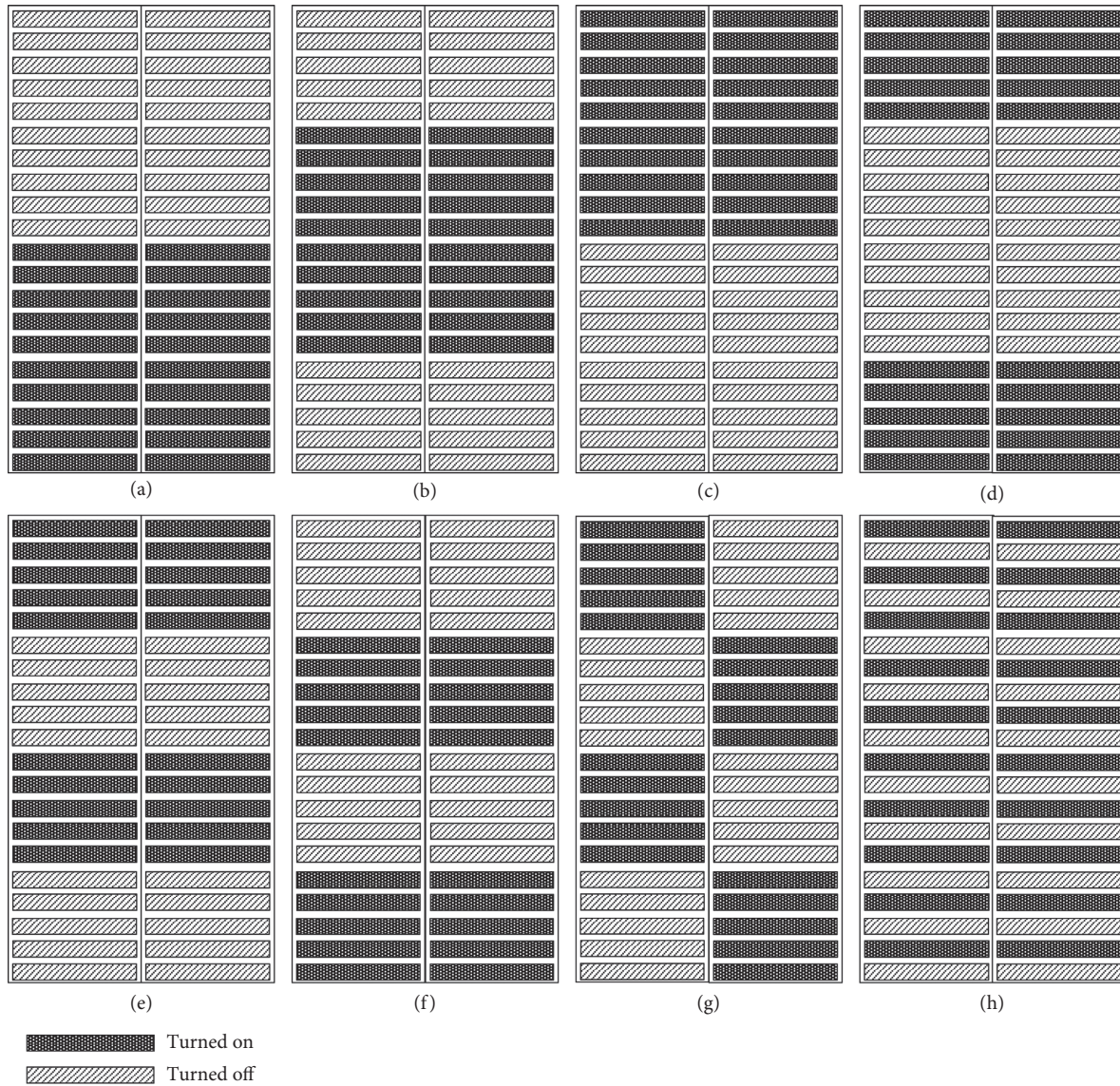


FIGURE 4: Schematic diagram of the workload allocation scheme. (a) Model 1. (b) Model 2. (c) Model 3. (d) Model 4. (e) Model 5. (f) Model 6. (g) Model 7. (h) Model 8.

the location change of busy/idle servers will also affect the transient thermal environment of DCs. In transient modeling analysis, the switch sequence of busy servers in different positions will not only affect the generation location of time-varying heat but also cause differences in cold and hot air mixing at the outlet.

Four classical cases were set up with different quantities of busy servers and different dynamic switch sequences for numerical simulation to analyze their effects on the thermal environment of DCs. In Case C_0 , the total task load is evenly distributed on each server of the rack. In other three cases, the standard 42 U rack shall be divided equally into the upper, middle, and lower layers. By adjusting the dynamic switch sequence of the servers in the upper, middle, and lower layers, the influence of busy/idle states changing of servers on the transient thermal environment will be analyzed. The busy servers in Case C_1 are started in the order of

lower-upper-middle layers as the task load increases, and each server keeps a state of full load of 200 W. Busy servers in Case C_2 are started in the order of middle-upper-lower layers, and in Case C_3 they are started in the order of upper-middle-lower layers. The total power is evenly distributed to each server in proportion, and the transient curve of power changing with time is shown in Figure 8. The total power of a single rack increases from 1.2 kW to 2.6 kW and then to the full load of 4 kW, there are two instantaneous uprush of the power at 300 s and 600 s, and the corresponding cooling capacity is increased from 30% to 65% to 100% of cooling capacity requiring at full load, and according to the simulation results, the curve of the average temperature at the 9th rack that exits in column A at the central section of the DC over time is shown in Figure 9.

From the comparison of the four groups of data, it is concluded that sudden changes in power cause temperature

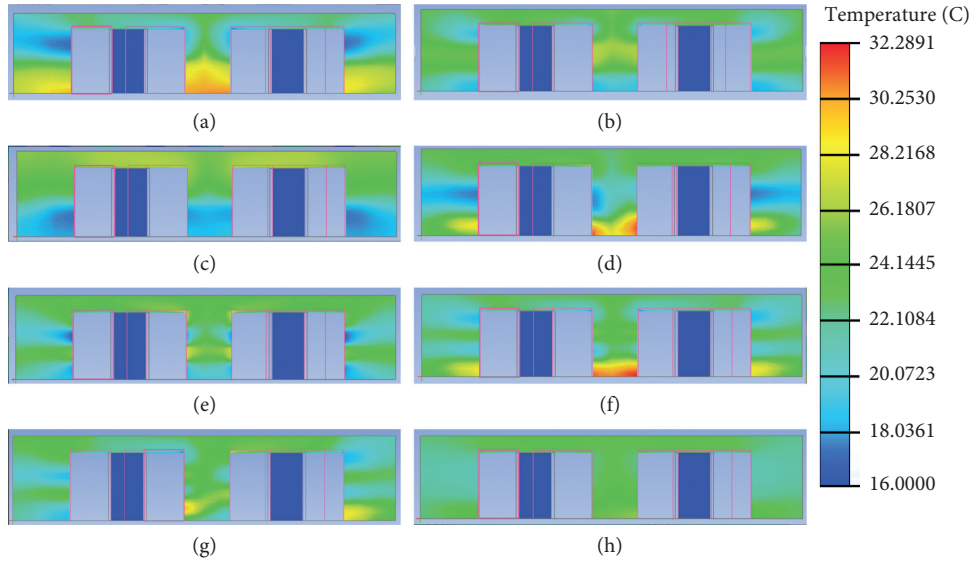


FIGURE 5: Temperature cloud diagram of different workload allocation at $X = 7$ m. (a) Model 1. (b) Model 2. (c) Model 3. (d) Model 4. (e) Model 5. (f) Model 6. (g) Model 7. (h) Model 8.

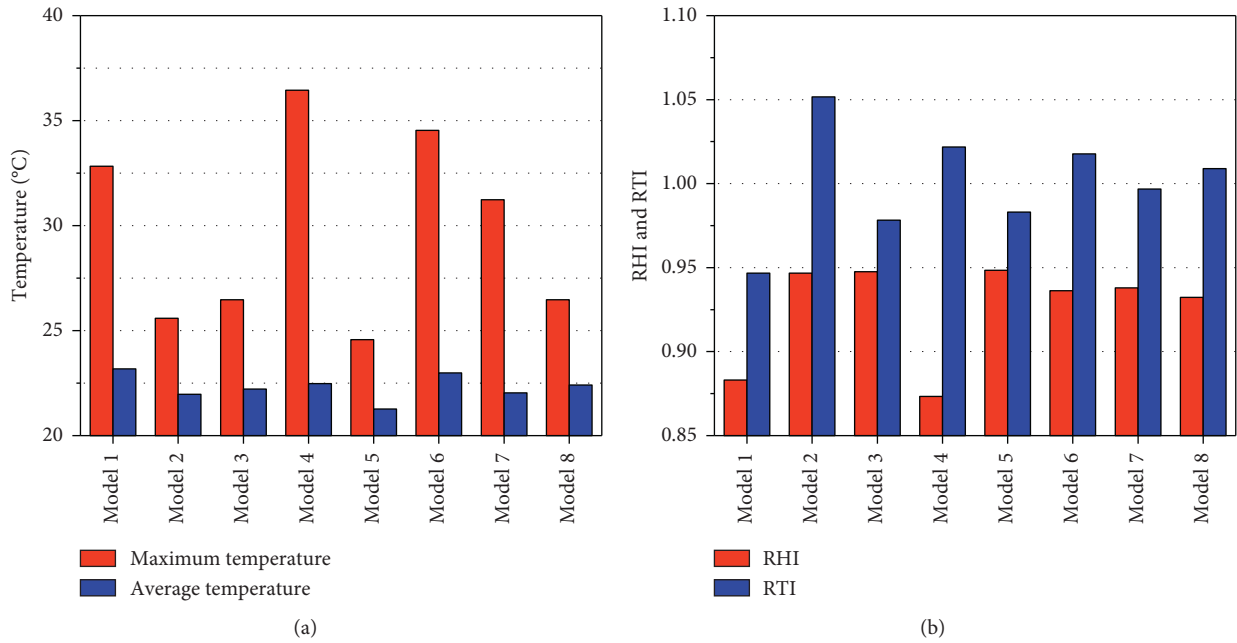


FIGURE 6: Evaluation based on temperature, RHI, and RTI of eight cases. (a) Temperature of thermal environment. (b) RHI and RTI.

fluctuations and result in the different transient effects in four cases. Considering the temperature fluctuation caused by different transient scenarios, when the load task increases, Optimal distribution of average temperature and the minimum temperature overshoot fluctuation occur in Case C_3 . While the worst temperature distribution and the strongest temperature overshoot occur in Case C_2 . The average temperature of the rack outlet with servers operating at full load finally remains the same in four cases, but the time for the average temperature to reach stability is different. This

indicates that, firstly, the dynamic change of the busy servers' location will lead to the circulation and mixing of hot and cold air around the rack outlet, and the cooling performance of different busy server locations will also be different. Secondly, as long as the parameters of the final state are consistent, changing the starting position and sequence of the servers will affect the time to reach the final stability without affecting the final thermal environment temperature. When the servers' workload increases, Case C_3 is undoubtedly a safe and feasible ideal switch strategy.

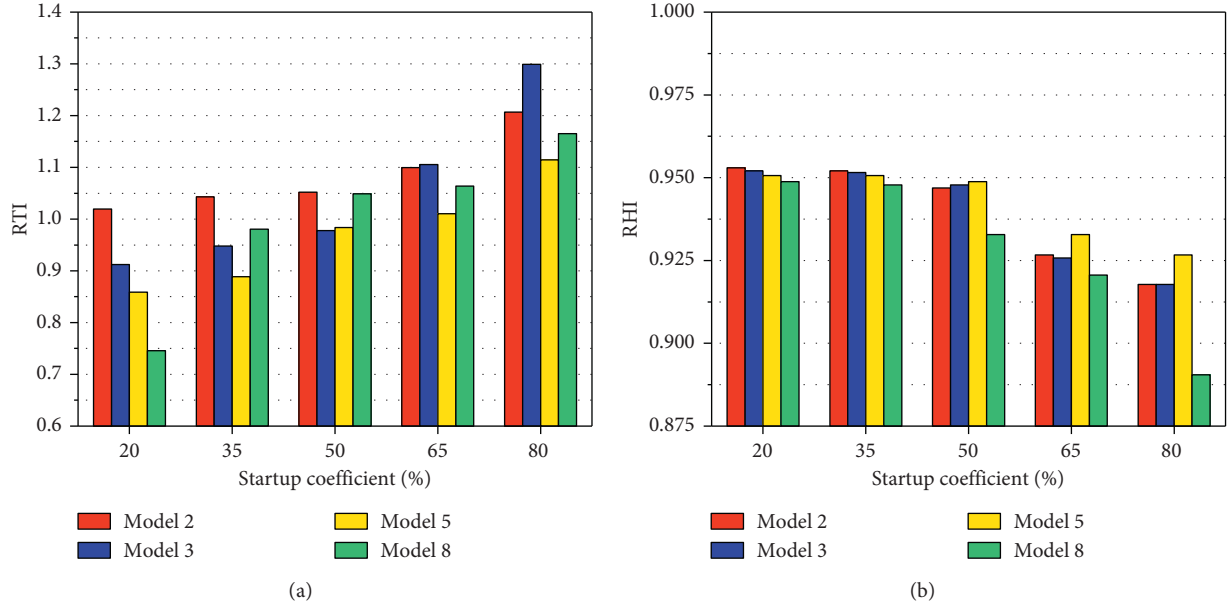


FIGURE 7: (a) RTI and (b) RHI in the DC with different busy ratios.

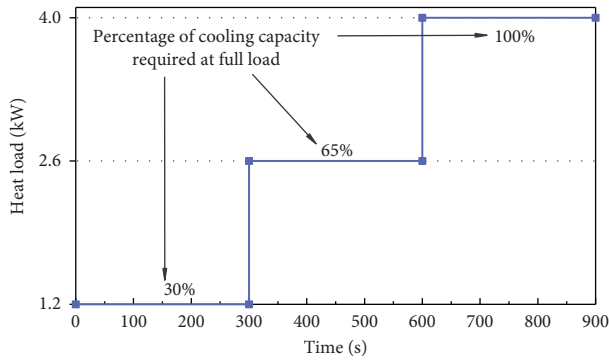


FIGURE 8: Schematic diagram of the transient attribute input file for changing the boot position.

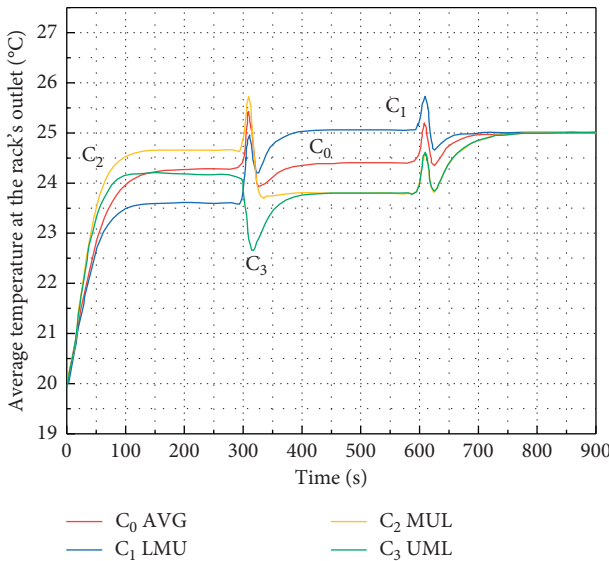


FIGURE 9: The average temperature at the outlet of the rack over time.

6. Economic Analyses

The economic benefits of a DC mainly include income and operating costs. DCs derive their revenues from the services they provide, and their costs are mainly energy bills. Energy costs include two parts: energy consumption for servers and cooling systems. Both of them are relevant to the number of servers. Meanwhile, the number of servers determines the request execution status, service quality, and server distribution mode of the DC. The former indirectly affects the benefits of the DC, while the latter indirectly affects the heat distribution and cooling costs. The relationships between the economic benefits and the relevant attributes are shown in Figure 10 including the symbols used in the section. We model and analyze the economic benefits of the DC with the following steps: firstly, the server's number of the DC is determined; secondly, the energy consumption of servers is determined, and then the energy consumption of the DC refrigeration is determined by the methods mentioned in previous sections; finally, the energy price and benefits of the DC are modeled on this basis, and the DC economic benefits are determined.

6.1. Energy Consumption for Busy Servers. Let a DC need n servers in the scheduling time t , and the time for the servers to process the request is composed of two parts: average wait time and average processing time for requests. θ is the average processing speed for the request (request/sec). γ is the arrival speed of the requests in scheduling time t (request/sec). p is the full load power of a server (watts). δ is the average waiting time for requests in t time slot (sec). R_0 is the maximum delay constraint of time of the requests (sec). q is the quality of service, i.e., the probability of task being immediately dealt with; the higher the probability, the higher quality of the service. Under the constraints, the average

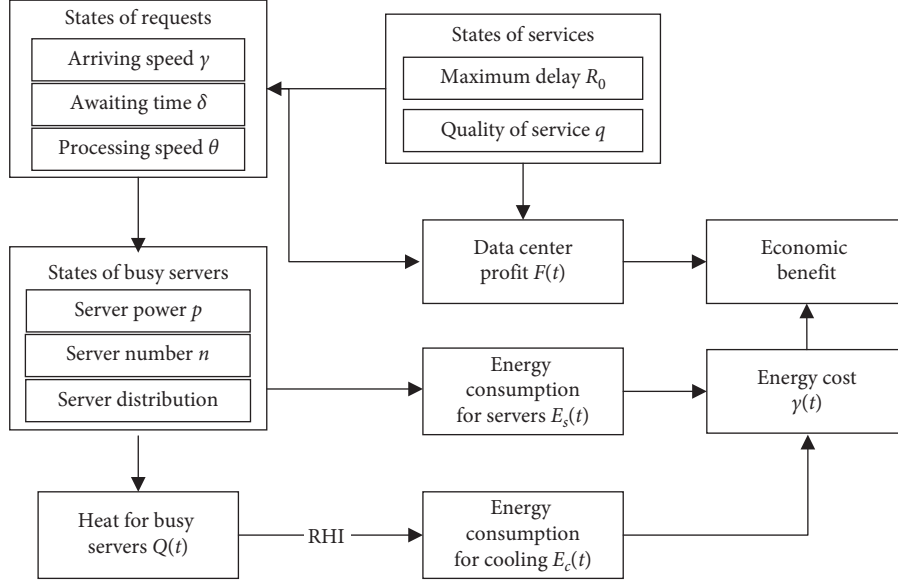


FIGURE 10: Relationships of benefits and relevant attributes.

waiting time for request is $\delta = q/(n \cdot \theta - \gamma)$, and the average response time for request R is $(1/\theta) + \delta$. Requiring $R \leq R_0$, so the following inequality is defined:

$$\frac{1}{\theta} + \frac{q}{n \cdot \theta - \gamma} \leq R_0. \quad (12)$$

Therefore, the constraint on the number of servers in the DC and the energy consumption under this constraint are as the follows:

$$E_s(t) = p \cdot n \cdot t, \quad \text{where } n \geq \frac{q}{R_0 \theta - 1} + \frac{\gamma}{\theta}. \quad (13)$$

6.2. Energy Consumption for Cooling. Based on the energy conservation law and the proposed optimization on cooling efficiency RHI, we study the energy consumption for cooling. In condition of n busy servers at time slot t , let $E_c(t)$ be the energy consumption for cooling, and $Q(t)$ be the heat produced by n servers, then $E_c(t) = Q(t) \text{RHI}^{-1}$, in which RHI is relevant to the switch strategy. When the number of running servers in the DC is n , the optimal switch strategy can be determined according to the heat distribution models in previous sections. For example, when n is half of the number of servers in the DC, the overall thermal environment of Model 5 in Table 2 is the optimal.

The mathematical expressions of $Q(t)$ can be defined using the lumped RC thermal model [28]. In the RC (resistor, capacitor circuit) model, the inside and outside of the server is considered as a heat transfer system with a certain temperature difference and thermal resistance. T_0 is the internal temperature of the servers, T_{amb} is the external temperature of servers, P is the server power, R is thermal resistance, and C is the heat capacity of the server. After t time the server temperature is shown in equation (14), and $Q(t)$ is shown in equation (15), where the parameters of equation (15) refer to the parameters in equation (12). The

refrigeration energy consumption $E_c(t)$ in the DC can be obtained.

$$T = RC(t) = PR + T_{\text{amb}} + (T_0 - PR - T_{\text{amb}}) \cdot e^{-t/RC}, \quad (14)$$

$$Q(t) = c_p G(T - T_0). \quad (15)$$

6.3. Energy Price. We utilize two different energy pricing models for energy deficient situation and energy adequate situation. Because more and more DCs apply the renewable energy, $Y(t)$ represents the time-dependent energy price for grid energy and the grid operator. We consider an exponential model [29] in energy deficient situation and flat-rate price for energy adequate situation, as shown in the following equation:

$$Y(t) = \begin{cases} y_0 e^{-\omega(t)}, & \text{if } t > t_\omega, \\ y_0, & \text{otherwise,} \end{cases} \quad (16)$$

where $\omega(t)$ is a normalized positive value of time t and t_ω represents the time slot when $\omega(t) = 0$, i.e., energy adequate situation, hence the energy price is constant y_0 .

6.4. DC Profit. The DC provides computing services for multiple users. These users share the same infrastructure, e.g., a user can share a DBMS with another in the context of databases. In return, each user pays the rent for resources to the provider according to the ‘‘pay as you go’’ model, i.e., a user only pays what it consumes [21]. Therefore, the DC’s profit in time slot t is relevant with w , R_0 , and q which are previously explained. Here, we use a logarithmic utility model, which follows the law of diminishing marginal utility and is widely used in a previous work [30]. $F(t)$ represents the time-dependent profit when the DC provides the services

with given average waiting time w , maximum delay time R_0 , and the probability of a request been processed q . $F(t)$ is calculated as the following equation:

$$F(t) = \varepsilon_0 \cdot \left(1 + k \cdot \log \frac{q}{R_0}\right) \cdot e^{-\text{ReLu}(w+\mu-R_0)}, \quad (17)$$

where ε_0 is the pricing constant, k is the adjustment coefficient, $\text{ReLu}()$ is the activation function, $\log q/R_0$ represents the contract profit which increases with expected service quality, and $e^{-\text{ReLu}(w+\mu-R_0)}$ represents the real service quality which decreases with the response delay.

6.5. Problem Definition. Aforementioned models define the problem of maximized economic benefits with the constraints. In a time slot t , the economic benefits are drawn from equations (13)–(17) as $F(t) - Y(t)[E_s(t) + E_c(t)]$, in which only n and RHI are variables, and the rest of the parameters are all constants. Besides, n and RHI are also relevant. Our heat distribution study ensures an optimal RHI for an n value. Therefore, we finally formalize the complex problem of maximizing economic benefit of the DC to the easily solved problem of the maximum value of a simple function. For long-term duration, the economic benefit is the aggregated value of each time slot t . In such conditions, each time slot in the duration is the schedule interval.

In conclusion, with the proposed model for the thermal distribution of a DC and the server distribution which could determinately change the thermal distribution, we define quantitative models for economic benefit and the relevant attributes such as energy consumption of servers and cooling system, energy price, profit, and service qualities. For maximizing the economic benefits, we remain the number of busy servers and thermal evaluation index as the schedulable attributes.

7. Conclusions

Considering the same air condition, the thermal steady-state numerical simulation is used to study the switch strategy of busy servers, and the thermal transient numerical simulation is used to study the switch strategy under transient changes in power of DCs. The conclusions are as follows:

- (1) When DC is running stably, there is a thermal stratification phenomenon in the cooling process. The thermal environment performance index is used for evaluation, and the decentralized distribution of the servers is conducive to heat dissipation. For the stable running conditions, when the busy ratio is at 0.5 or above, the upper alternating segment model has the best heat dissipation performance. For the lower busy ratio of less than 0.5, the mode that the servers concentrate in the middle layers is the best choice. Under the same temperature gradient, the cooling efficiency is the highest when the busy ratio is about 0.5.
- (2) The transient temperature characteristic under the dynamic switch of load condition is studied through

transient numerical simulation, and the effect of power change and cold quantity change on the transient characteristics of temperature is analyzed. The results show that the mode of servers in racks starting in the order of upper-middle-lower layer is an ideal strategy to meet the safety and feasible operation of DCs with enclosed cold aisles.

- (3) The influence of thermal environment on the economic benefits of DC is analyzed. We quantified the relationships between economic benefits and energy consumption for busy servers and cooling system, energy price, and profit of the DC. These models define the problem of maximized economic benefit with the constraints.

Data Availability

The experimental data used to support the findings of this study are the dataset generated according to the strategy mentioned within the article by Arghode et al. [27]. The data generation programs can be easily implemented or are available from the corresponding author upon request.

Conflicts of Interest

The authors declare that they have no conflicts of interest.

Acknowledgments

The authors would like to thank Li Jiyuan, who is a student of Thermal Engineering Department, School of Metallurgy, Northeastern University, for the calculation of the economic benefit model and improving the paper. This work was supported by the Research Grant from the National Natural Science Foundation of China (Grant no. 611662057) and the Fundamental Research Funds for the Central Universities (N182504017).

References

- [1] C. Nadjahi, H. Louahlia, and S. Lemasson, "A review of thermal management and innovative cooling strategies for data center," *Sustainable Computing: Informatics and Systems*, vol. 19, pp. 14–28, 2018.
- [2] S. Baig, W. Iqbal, J. Lluís Berral, and D. Carrera, "Adaptive sliding windows for improved estimation of data center resource utilization," *Future Generation Computer Systems*, vol. 104, pp. 212–224, 2020.
- [3] T. J. Chainer, M. D. Schultz, P. R. Parida, and M. A. Gaynes, "Improving data center energy efficiency with advanced thermal management," *IEEE Transactions on Components, Packaging and Manufacturing Technology*, vol. 7, no. 8, pp. 1228–1239, 2017.
- [4] T. L. Vasques, P. Moura, and A. De Almeida, "A review on energy efficiency and demand response with focus on small and medium data centers," *Energy Efficiency*, vol. 12, no. 5, pp. 1399–1428, 2019.
- [5] H. Rong, H. Zhang, S. Xiao, C. Li, and C. Hu, "Optimizing energy consumption for data centers," *Renewable and Sustainable Energy Reviews*, vol. 58, pp. 674–691, 2016.

- [6] P. Kumar and Y. Joshi, "Optimizing energy consumption for data centers Fundamentals of data center airflow management," *Energy Efficient Thermal Management of Data Centers*, Springer, Berlin, Germany, pp. 39–136, 2012.
- [7] W.-X. Chu, R. Wang, P.-H. Hsu, and C.-C. Wang, "Assessment on rack intake flowrate uniformity of data center with cold aisle containment configuration," *Journal of Building Engineering*, vol. 30, p. 101331, 2020.
- [8] J. Cho and J. Woo, "Development and experimental study of an independent row-based cooling system for improving thermal performance of a data center," *Applied Thermal Engineering*, vol. 169, p. 114857, 2020.
- [9] C. Jin, X. Bai, C. Yang, W. Mao, and X. Xu, "A review of power consumption models of servers in data centers," *Applied Energy*, vol. 265, p. 114806, 2020.
- [10] S. A. Nada and K. E. Elfeky, "Experimental investigations of thermal managements solutions in data centers buildings for different arrangements of cold aisles containments," *Journal of Building Engineering*, vol. 5, pp. 41–49, 2016.
- [11] M. Tatchell-Evans, N. Kapur, J. Summers, H. Thompson, and D. Oldham, "An experimental and theoretical investigation of the extent of bypass air within data centres employing aisle containment, and its impact on power consumption," *Applied Energy*, vol. 186, pp. 457–469, 2017.
- [12] V. Sundaralingam, V. K. Arghode, and Y. Joshi, "Experimental characterization of cold aisle containment for data centers," in *Proceedings of the 29th IEEE Semiconductor Thermal Measurement and Management Symposium*, March 2013.
- [13] C. Lyu, G. Chen, S. Ye, and Y. Liu, "Enclosed aisle effect on cooling efficiency in small scale data center," *Procedia Engineering*, vol. 205, pp. 3789–3796, 2017.
- [14] Y. Fulpagare, Y. Joshi, and A. Bhargav, "Rack level transient CFD modeling of data center," *International Journal of Numerical Methods for Heat & Fluid Flow*, vol. 28, no. 2, pp. 381–394, 2018.
- [15] K. Zhu, Z. Cui, Y. Wang, H. Li, X. Zhang, and C. Franke, "Estimating the maximum energy-saving potential based on IT load and IT load shifting," *Energy*, vol. 138, pp. 902–909, 2017.
- [16] S. K. Uzaman, A. u. R. Khan, J. Shuja, T. Maqsood, F. Rehman, and S. Mustafa, "A systems overview of commercial data centers," *International Journal of Information Technology and Web Engineering*, vol. 14, no. 1, pp. 42–65, 2019.
- [17] T. Y. Lawson and D. Zbigniew, "Economic framework for resource management in data centers," in *Proceedings of the 2016 IEEE International Conference on Communication Systems (ICCS)*, pp. 1–6, IEEE, Shenzhen, China, December 2016.
- [18] C. Gu, L. Fan, W. Wu, H. Huang, and X. Jia, "Greening cloud data centers in an economical way by energy trading with power grid," *Future Generation Computer Systems*, vol. 78, pp. 89–101, 2018.
- [19] W. Lu, P. Lu, Q. Sun, S. Yu, and Z. Zhu, "Profit-aware distributed online scheduling for data-oriented tasks in cloud datacenters," *IEEE Access*, vol. 6, pp. 15629–15642, 2018.
- [20] X.-D. Dong, S. Chen, L.-P. Zhao, X.-B. Zhou, H. Qi, and K.-Q. Li, "More requests, less cost: uncertain inter-datacenter traffic transmission with multi-tier pricing," *Journal of Computer Science and Technology*, vol. 33, no. 6, pp. 1152–1163, 2018.
- [21] R. Mokadem and A. Hameurlain, "A data replication strategy with tenant performance and provider economic profit guarantees in cloud data centers," *Journal of Systems and Software*, vol. 159, Article ID 110447, 2020.
- [22] S. M. MirhoseiniNejad, H. Moazamigoodarzi, G. Badawy, and G. Douglas, "Joint data center cooling and workload management: a thermal-aware approach," *Future Generation Computer Systems*, vol. 104, pp. 174–186, 2020.
- [23] K. Zhang, Y. Zhang, J. Liu, and X. Niu, "Recent advancements on thermal management and evaluation for data centers," *Applied Thermal Engineering*, vol. 142, pp. 215–231, 2018.
- [24] J. Ni, B. Jin, S. Ning, and X. Wang, "The numerical simulation of the airflow distribution and energy efficiency in data centers with three types of aisle layout," *Sustainability*, vol. 11, no. 18, 2019.
- [25] P. Dhoot, J. W. Vangilder, Z. Pardey, and C. M. Healey, "Zero-equation turbulence models for large electrical and electronics enclosure applications," US Patent 20180014427, 2018.
- [26] C. Chen and S. Jaw, *Fundamentals of Turbulence Modeling*, Taylor & Francis, Washington, DC, USA, 1998.
- [27] V. K. Arghode, V. Sundaralingam, and Y. Joshi, "Thermal characteristics of open and contained data center cold aisle," *Journal of Heat Transfer*, vol. 135, no. 6, 2013.
- [28] C. Da, P. Georges, and O. Wojciech, "Energy and thermal models for simulation of workload and resource management in computing systems," *Simulation Modeling Practice and Theory*, vol. 58, pp. 40–54, 2015.
- [29] A. M. T. Ramos, J. A. Carvalho, and G. L. Vasconcelos, "Exponential model for option prices: application to the Brazilian market," *Physica A: Statistical Mechanics and Its Applications*, vol. 445, pp. 161–168, 2016.
- [30] Z. Zhou, F. Liu, H. Jin, B. Li, B. Li, and H. Jiang, "On arbitrating the power-performance trade off in SaaS clouds," in *Proceedings of the 2013 Proceedings IEEE INFOCOM*, pp. 872–880, IEEE, Toronto, Canada, April 2013.

Research Article

The Applications and Complexity Analysis Based on Network Embedding Behaviors under Evolutionary Game Framework

Xin Su ^{1,2}, Hui Zhang,¹ and Shubing Guo ³

¹Shandong University of Finance and Economics, School of Business Administration, Jinan 250014, China

²Research Center of Government Performance Evaluation of Shandong University of Finance and Economics, Jinan 250002, China

³College of Management and Economics, Tianjin University, Tianjin, China

Correspondence should be addressed to Xin Su; sdcsx2016@126.com and Shubing Guo; sbguo20160831@126.com

Received 10 March 2020; Revised 13 April 2020; Accepted 22 April 2020; Published 15 June 2020

Academic Editor: Abdelalim Elsadany

Copyright © 2020 Xin Su et al. This is an open access article distributed under the Creative Commons Attribution License, which permits unrestricted use, distribution, and reproduction in any medium, provided the original work is properly cited.

In this paper, we use the dynamic mechanism of biological evolution to simulate the enterprises' bounded rational game. We construct game models of network embedding behaviors of horizontal and vertical enterprises in supply chain, explain the repeated games of random pairs of enterprises by replication dynamic differential equations, study the characteristics and evolution trend of this flow, conduct simulation experiments, clarify the evolution direction and law of network embedding strategy selection of supply chain enterprises, and discuss the stable state of evolutionary game and its dynamic convergence process. The results show that the probability of supply chain enterprises choosing a network embedding strategy is related to the enterprises' special assets investment cost, cooperation cost, network income, and cooperation benefits. Supply chain enterprises should reduce the special assets investment cost and cooperation cost, maximize network income and cooperation income, narrow the gap between the extra-cooperation profit and the current cooperation profit, and restrain them from violating cooperation contracts or taking opportunistic actions.

1. Introduction

With the rapid development in science and technology, the product life cycle is shortening day by day, and the uncertainty of the external market environment that enterprises are facing is getting higher and higher. It is difficult for enterprises to cope with the competitive market environment solely by their own resources endowment. In order to alleviate the adverse effects of resource constraints on the enterprises sustainable growth and strengthen their core competitive advantages, enterprises must break through their inherent boundaries or frameworks [1], establish stable cooperative relations with upstream and downstream enterprises, and form their own supply chain networks. Therefore, the competition among enterprises is no longer the independent competition among individual enterprises but the competition between supply chains and supply chains [2].

By embedding in a certain supply chain network and signing cooperative contracts with other member enterprises, enterprises can build cooperative partnerships, which is helpful to realize the resources and interests sharing among enterprises, and then improve the performance [3]. The supply chain network mainly includes suppliers, manufacturers, wholesalers, distributors, and retailers and other participants. They cooperate closely with each other in order to cultivate the overall competitive advantage and achieve a win-win situation [4, 5]. Generally speaking, the manufacturers occupy the important position as the core enterprises of the supply network. On the one hand, the manufacturers and upstream suppliers establish cooperative relations to obtain raw materials needed by the enterprises and improve the production efficiency and performance on the basis of the specialized division [6]. On the other hand, manufacturers sign cooperative contracts with downstream distributors or retailers to expand sales channels, so as to

transfer products to consumers smoothly through intermediaries, and ultimately maximize the products value and obtain network rent or excess profits [7].

Previous studies have mostly discussed the game equilibrium of supplier-manufacturer or manufacturer-distributor relationship and benefit distributions in the static supply chain [8]. They have qualitatively analyzed the supply chain relationship governance concept, connotation, and countermeasures [9, 10] or empirically studied the impacts of supply chain partnership quality, information sharing, logistics capability, joint liability governance and other factors on supply chain enterprise behaviors, supply chain integrations, operational efficiency, and performance [11–13]. However, in view of the whole supply chain, there are few literatures on the evolutionary game of enterprises' network embedding behavior in the dynamic environment, so it is difficult to effectively reflect the specific operation practice of the supply chain embedded in the dynamic environment. As a complex system composed of node enterprises, each node enterprise is an independent legal person with different resource endowments and business objectives. There are differences and conflicts in weighing the benefits and costs of cooperation, which are embodied in the rational choice and cooperation of whether each node enterprise is embedded in the supply chain network. The key to solve the above problems is to build the evolutionary game model of the network embedding behaviors of supply chain enterprises. Analyzing the influencing factors of the enterprises' network embedding behaviors and clarifying their rational choices are conducive to the sustainable development of the cooperation relationship between supply chain enterprises and the improvement of the supply chain operation ability. Therefore, in view of the fact that dynamics and complexity are the essential features of supply chain relationship network, this paper constructs evolutionary game models between supply chain participants from a systematic and dynamic perspective, discusses the characteristics and evolution trend of this flow, seeks the interests joint point of each participant in supply chain cooperation so as to maintain cooperation stability, and provides a reference basis for improving the enterprises' performance.

2. Reviews

2.1. The Definition of Supply Chain Network. A supply chain is a complex adaptive system, which refers to a logistics process around core enterprises from raw material procurement and intermediate processing to final product and product transfer to consumers, thus realizing product values [14, 15]. Supply chain is a functional network composed of suppliers, manufacturers, distributors, retailers, and consumers. And it is manifested as logistics, capital flow, and information flow, which can meet customer needs through the transfer between enterprises or functional departments, so as to maximize profits [16]. The standard logistics terminology published in China in 2011 defines the supply chain as the network structure formed by upstream and downstream enterprises that provide products and services to end-users in the production process. Some scholars also put forward that supply chain is a learning system

for knowledge sharing among enterprises in the whole chain: an important way for enterprises to acquire external knowledge and an important source for enterprises to win competitive advantage. In addition, through this learning system, enterprises can better share information, obtain more external heterogeneous knowledge, improve the supply chain operation capability, and form competitive advantages that are difficult to be replaced [17]. From the complex relationship between knowledge management and supply chain management, supply chain is not only material supply chain but also “knowledge supply chain” or “knowledge supply and demand network.”

The supply chain network is a kind of network organization between the market system and vertical integration. The suppliers, manufacturers, distributors, and retailers in the network form certain transaction links, share resources, and information and cooperate to strengthen the supply chain overall competitive advantage by signing contracts [11, 18]. In China, enterprises are more represented as economic legal persons, referring to commodity producers, operators, or economic organizations that rely on their fixed production and operation sites, funds, equipments, and employees to engage in production, processing, and service activities in order to maximize profits. The enterprises operate independently and take responsibility for their own profits and losses [19]. Based on the supply chain characteristics and enterprises concept, this paper considers that the member enterprises in supply chain network that meet the enterprises' attributes can be collectively known as supply chain enterprises, such as suppliers, manufacturers, distributors, and retailers. Each supply chain enterprise makes full use of its own superior resources and capabilities interdependently and complementarily and ultimately achieves the objectives and value increment of each link of the supply chain. Enterprise executives have long been concerned about the mechanism of complexity on enterprise operation and committed to taking measures to weaken its negative impact. Supply chain complexity is recognized as an important challenge for enterprises [20]. With the continuous enrichment of economic activities, the supply chain network complexity is getting higher and higher. The complex supply chain network is gradually replacing the simple traditional supply network structure [21, 22].

2.2. Network Embedding Theory. Polanyi first puts forward the word “embeddedness” in his book “great change” and considers that “embeddedness” belongs to the category of economic sociology [23]. The enterprises' economic behavior is embedded in certain social relations, and enterprises and external social environment interact with each other. Subsequently, the viewpoint of “embeddedness” was gradually integrated into social network research, mainly exploring the specific manifestations of enterprises' economic behaviors in social networks. Granovetter held that the path of social relations influencing enterprise behaviors and institutions is one of the classical problems of social theory. In the relevant literature, it further reveals the influence of “embeddedness” among enterprises on enterprises' economic behaviors, marketing channels, cooperative

relations, organizational adaptability, and market positioning decision-making in the context of network. The embedding viewpoint focuses on the roles of specific interpersonal relationships. And it holds that enterprises' structure plays an important role in stimulating the subject's trust perception and preventing misconduct [24]. In addition, Uzzi believed that the study of "embeddedness" is conducive to deepening the understanding of the impact mechanism of social structure on economic life. Therefore, the term "embeddedness" has become a hot research topic in the field of sociology and economics. It is of obvious characteristics such as time economy, comprehensive consistency, and complex adaptability in improving allocation efficiency [25].

The generation mechanism of "embeddedness" originates from the trust level among the member enterprises in the network. Based on the enterprises' mutual trust, each enterprise embeds its own economic behavior into the social network, which gradually forms a more stable relationship [26, 27], and realizes the resources and information sharing in the network [28, 29]. Network embedding includes the social network relationship and trust relationship formed by emotional interaction among members of the network [30]. And network embedding contains the more formal network relationship such as enterprise alliance and franchise [31]. Cluster enterprises, supply chain enterprises, or enterprises with cooperative relationships will exchange business, resources, and information with other enterprises and then build an interdependent social network relationship. The member enterprises in the network have changed from the original single or binary relationship to the interdependent multirelationship or network relationship [32, 33]. To a certain extent, this is conducive to the rapid flow and efficient transformation of resources and information in the network. Among them, the enterprises exist in the form of network "nodes," while the "edges" of the social relationship network represent the social relations formed by the transaction links among the enterprises [7, 34–37].

Therefore, network embedding behavior refers to the form of a transaction or cooperated network established by an enterprise because of its future development, transaction, or the need to cope with competitive pressures. The purpose is to achieve resource sharing and value creation in the network. As a supply-demand network organization, the relationship between the supply chain upstream and downstream nodes is mainly manifested as relational transactions. The members embedded in the network can realize feedback more quickly and clearly and obtain new solutions. For the dynamic system of the supply chain, network embedding is mainly manifested in the supply and demand network formed by the upstream and downstream enterprises based on trust or contract. Within this network, each node enterprise plays a synergistic effect and ultimately improves the supply chain operation capability on the basis of realizing resource, information exchange, and sharing.

2.3. Reviews of Supply Chain Enterprise Game. However, as a complex system, each node enterprise has differences and conflicts in balancing the cooperation benefits and costs. In

order to maximize their own interests and operate the supply chain efficiently, each node enterprise keeps playing repeated games. Based on different research perspectives, the relevant scholars discussed the game problems of supply chain operation. For example, Li thinks that the efficient operation of supply chain is the result of many factors. By constructing the game model of supply chain node enterprise strategic partner collaborative competition, the paper analyzes the important factors that affect the realization of supply chain cooperative game [38]. Nie et al. builds a supply chain model with fairness-concerns based on Stackelberg game, discusses the decision-making and coordination of the supply chain, analyzes the impact of the disagreement points on supply chain operation, and thinks that enterprises should adopt the way of price subsidy to design the joint contract to promote the coordination of the supply chain [39]. Sun uses the evolutionary game model to explore the rules and dynamic change process of B2C service enterprises' collaborative cooperation under the e-commerce platform based on the perspective of enterprise benefit distribution and puts forward countermeasures to improve the supply chain operation capability [40]. Jian et al. establishes a green supply chain game model in which manufacturers consider both profit and environmental objectives and explores the operation and cooperation strategies of different objectives at the supply chain level [41]. In addition, Jian et al. examines the contract coordination among manufacturers with peer-induced and distributional fairness concerns, constructs two game models, and analyzes the influence of a revenue sharing contract on the pricing decisions and profit distribution of a competitive supply chain considering fairness concerns [42].

It can be seen that most of the existing researches are based on different perspectives, using evolutionary game method to discuss the supply chain operation, but not involving the game of enterprise network embedding behavior, and exploring the synergistic effect of multiple factors on the enterprise network embedding behavior choice. In view of this, this paper constructs the game model of network embedding behavior of supply chain enterprises, discusses the influence of the factors such as the investment cost of special assets, cooperation cost, network income, and cooperation income on the supply chain operation, analyzes the stable state and dynamic convergence process of evolutionary game, and provides theoretical reference for the enterprises' decision-making of network embedding behavior and the maintenance of cooperation relationship.

3. Evolutionary Game Analysis of Enterprises' Embedding Behaviors

In the supply chain network, there are not only horizontal cooperative behaviors among parallel participants but also vertical cooperative behaviors between upstream and downstream enterprises [35]. It is assumed that, in the supply chain network, each participant is a bounded rational economic person with independent decision-making ability. The purpose of cooperation with upstream and downstream enterprises or horizontal enterprises is to maximize economic benefits. The cooperative behaviors among enterprises in the supply chain network are shown in Figure 1.

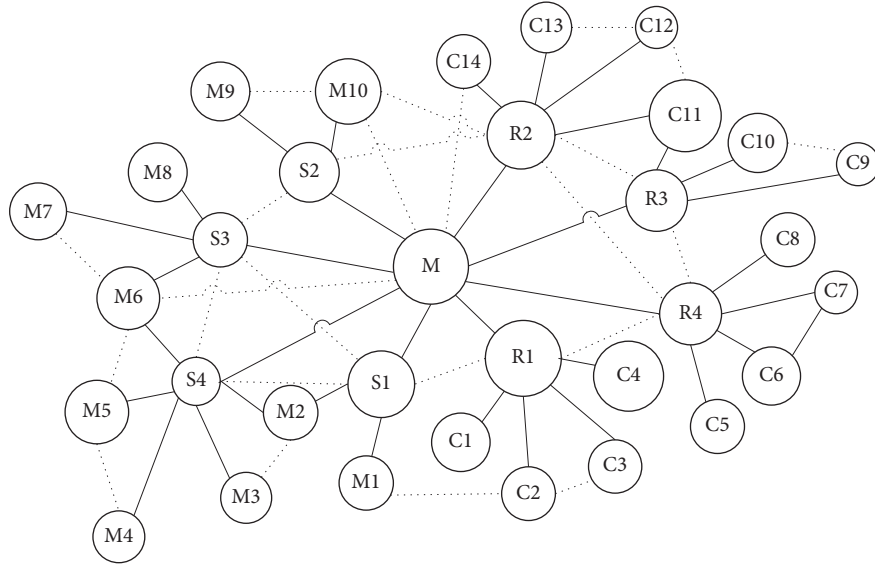


FIGURE 1: Supply chain relationship network.

The nodes represent supply chain enterprises. The supplier nodes are represented by the letter “S,” the manufacturer nodes are represented by the letter “M,” the retailer nodes are represented by the letter “R,” and the consumers are represented by the letter “C.” The solid line represents the established cooperation relationship between supply chain enterprises, while the dotted line indicates the potential cooperation relationship between the two enterprises. By embedding in a supply chain network, an enterprise will sign a cooperative contract with other member enterprises to share resources in order to improve the performance. All cooperation between S and S, M and M, and R and R are known as supply chain enterprises horizontal cooperation, while all cooperation between S and M, S and R, and M and S are called supply chain enterprises vertical cooperation. Enterprises can broaden the channels of accessing resources, so as to obtain more heterogeneous resources and information, reduce transaction costs, and ultimately enhance the production efficiency through embedding in a supply chain network.

3.1. Evolutionary Game Analysis of Horizontal Enterprises.

Horizontal enterprise cooperative behavior in a supply chain network is mainly manifested in the parallel cooperative relationship or behavior between suppliers and suppliers, manufacturers and manufacturers, or retailers and retailers. Through joint production or R&D, enterprises can enhance their innovation capability and output level.

3.1.1. Model Building. Assuming that an enterprise has the independent decision-making power to embed in supply chain relationship networks, enterprise A and enterprise B are both horizontal enterprises, and their strategy space is (embedding, nonembedding). The choice of embedding strategy means that enterprises choose to cooperate with other members of the supply chain network to form an

alliance relationship. On the one hand, enterprises can obtain heterogeneous resources and information needed for the development of enterprises by embedding in the relationship network. These resources and information can be further transformed into social capital or relational capital of enterprises. This paper calls them network gains. On the other hand, enterprises can cooperate with other member enterprises to realize the sharing of information and resources and then obtain cooperative gains. If both enterprises A and enterprise B adopt the embedding strategy, it indicates that there is a cooperative relationship between enterprise A and enterprise B, which can generate certain cooperation benefits. In addition, the probability of embedding strategy is x ($0 < x < 1$) and the probability of nonembedding strategy is $(1 - x)$. The total income of an enterprise is the sum of the income from independent production or sales and the income from cooperation.

- (1) Enterprise A adopts the embedding strategy, while enterprise B also adopts the embedding strategy, which means that there is a cooperative relationship between enterprise A and enterprise B. Enterprises A and B need to spend some energy or invest some assets when they choose to embed the supply chain relationship network; that is, the investment cost of special assets is C_{A0} ($C_{A0} > 0$) and C_{B0} ($C_{B0} > 0$), respectively, so as to obtain network income R_{A0} ($R_{A0} > 0$) and R_{B0} ($R_{B0} > 0$). In addition, when enterprise A and enterprise B form a contractual relationship and cooperation, they need to invest a certain time cost and transaction cost; that is, the cooperation cost of enterprise A is C_{AC} ($C_{AC} > 0$), and the cooperation cost of enterprise B is C_{BC} ($C_{BC} > 0$). Enterprises A and B can achieve resource integration, joint R&D of new products, or further expansion of sales channels by strengthening information exchange and interaction. Thus, enterprise A can obtain cooperative income R_{AC} ($R_{AC} > 0$)

and enterprise B can obtain cooperative income $R_{BC}(R_{BC} > 0)$.

- (2) Enterprise A adopts the embedding strategy, while enterprise B chooses the nonembedding strategy, which means that there is no cooperative relationship between enterprise A and enterprise B. When enterprise A embeds in the supply chain relationship network, the cost to be paid is C_{A0} , and the network income to be obtained is R_{A0} . When enterprise B chooses a non-embedding strategy, it can obtain profit P_B if it produces or sells independently, and enterprise A can obtain additional profit $L_A(L_A > 0)$ when it cooperates with other member enterprises in the supply chain network.
- (3) Enterprise A adopts nonembedding strategy, while enterprise B chooses embedding strategy, which indicates that there is no cooperative relationship between enterprise A and enterprise B. Enterprise B embeds in the supply chain network, which needs to pay C_{B0} for preinvestment cost, so as to obtain network revenue R_{B0} . When enterprise A adopts the nonembedding strategy, it can obtain profit P_A if it produces or sells independently. Similarly, enterprise B cooperates with other members of the supply chain network to obtain additional profit $L_B(L_B > 0)$.
- (4) Enterprise A adopts the nonembedding strategy, while enterprise B also chooses the nonembedding strategy, which means that there is no cooperative relationship between enterprise A and enterprise B. In view of this, both sides' profits from outside the supply chain network are neglected. Enterprises A and B choose nonembedding strategy in the supply chain network, so their preinvestment cost is 0, and each gains profit P_A and P_B when producing or selling products independently.

To sum up, the income matrix of embedding behavior between enterprise A and enterprise B is shown in Table 1.

3.1.2. Model Solution

- (1) According to the income matrix between enterprise A and enterprise B constructed above, when the probability of enterprise B choosing embedding strategy is x , the expected revenue of enterprise A chooses embedding strategy U_{A1} :

$$U_{A1} = x(P_A + R_{A0} + R_{AC} - C_{A0} - C_{AC}) + (1-x)(P_A + R_{A0} - C_{A0} + L_A). \quad (1)$$

Enterprise A chooses the nonembedding strategy with the expected return of U_{A2} :

$$U_{A2} = x(P_A) + (1-x)(P_A). \quad (2)$$

Therefore, the average expected return of enterprise A is U_A :

$$\begin{aligned} U_A &= x(U_{A1}) + (1-x)U_{A2} \\ &= x[x(P_A + R_{A0} + R_{AC} - C_{A0} - C_{AC}) \\ &\quad + (1-x)(P_A + R_{A0} - C_{A0} + L_A)] \\ &\quad + (1-x)[x(P_A) + (1-x)(P_A)]. \end{aligned} \quad (3)$$

When enterprise A chooses embedding strategy and nonembedding strategy with the same expected return ($U_{A1} = U_{A2}$), it achieves game equilibrium, that is,

$$x(P_A + R_{A0} + R_{AC} - C_{A0} - C_{AC}) + (1-x) \cdot (P_A + R_{A0} - C_{A0} + L_A) = xP_A + (1-x)P_A. \quad (4)$$

After sorting out, the following formula ① is obtained: $(R_{AC} - C_{AC} - L_A)x = C_{A0} - R_{A0} - L_A$; that is, $x = C_{A0} - R_{A0} - L_A / R_{AC} - C_{AC} - L_A$.

- (2) Similarly, when the probability of enterprise A choosing embedding strategy is x , the expected return of enterprise B choosing embedding strategy is U_{B1} :

$$U_{B1} = x(P_B + R_{B0} + R_{BC} - C_{B0} - C_{BC}) + (1-x)(P_B + R_{B0} - C_{B0} + L_B). \quad (5)$$

Enterprise B chooses the nonembedding strategy with the expected return of U_{B2} :

$$U_{B2} = x(P_B) + (1-x)(P_B). \quad (6)$$

Therefore, the average expected return of enterprise B is U_B :

$$\begin{aligned} U_B &= x(U_{B1}) + (1-x)U_{B2} \\ &= x[x(P_B + R_{B0} + R_{BC} - C_{B0} - C_{BC}) \\ &\quad + (1-x)(P_B + R_{B0} - C_{B0} + L_B)] \\ &\quad + (1-x)[x(P_B) + (1-x)(P_B)]. \end{aligned} \quad (7)$$

When enterprise B chooses embedding strategy and nonembedding strategy with the same expected return ($U_{B1} = U_{B2}$), it achieves game equilibrium, that is,

$$x(P_B + R_{B0} + R_{BC} - C_{B0} - C_{BC}) + (1-x) \cdot (P_B + R_{B0} - C_{B0} + L_B) = xP_B + (1-x)P_B. \quad (8)$$

After sorting out, the following formula is obtained: $(R_{BC} - C_{BC} - L_B)x = C_{B0} - R_{B0} - L_B$; that is, $x = C_{B0} - R_{B0} - L_B / R_{BC} - C_{BC} - L_B$.

It can be seen that enterprise A and enterprise B belong to the same group and have similar industrial status. There is no difference in the probability of choosing embedding strategy and nonembedding strategy. Therefore, this paper only takes enterprise A as an example to conduct a specific model analysis:

TABLE 1: Revenue matrix of horizontal enterprise.

Vertical enterprise embedding behavior		Enterprise B	
		Embedding (y)	Nonembedding ($1-y$)
Enterprise A	Embedding (x)	$P_A + R_{A0} + R_{AC} - C_{A0} - C_{AC}$, $P_B + R_{B0} + R_{BC} - C_{B0} - C_{BC}$	$P_A + R_{A0} - C_{A0} + L_A$, P_B
	Nonembedding ($1-x$)	P_A , $P_B + R_{B0} - C_{B0} + L_B$	P_A , P_B

$$\begin{aligned}
x^* &= \frac{C_{A0} - R_{A0} - L_A}{R_{AC} - C_{AC} - L_A} = \frac{L_A + (R_{A0} - C_{A0})}{L_A - (R_{AC} - C_{AC})} = 1 \\
&\quad + \frac{(R_{AC} - C_{AC}) + (R_{A0} - C_{A0})}{L_A - (R_{AC} - C_{AC})}, \\
1 - x^* &= \frac{(R_{AC} - C_{AC}) + (R_{A0} - C_{A0})}{(R_{AC} - C_{AC}) - L_A}, \\
\text{or } x^* &= \frac{C_{B0} - R_{B0} - L_B}{R_{BC} - C_{BC} - L_B} = 1 + \frac{(R_{BC} - C_{BC}) + (R_{B0} - C_{B0})}{L_B - (R_{BC} - C_{BC})}, \\
1 - x^* &= \frac{(R_{BC} - C_{BC}) + (R_{B0} - C_{B0})}{(R_{BC} - C_{BC}) - L_B}.
\end{aligned} \tag{9}$$

3.1.3. Model Analysis. In order to obtain more heterogeneous resources and information and strengthen the core competitive advantages, the enterprises should break through their inherent boundaries or frameworks and embeds in their supply chain network to seek cooperation. On this basis, they should continuously improve cooperation efficiency and maintain the stability of cooperation relations among enterprises. This paper will further analyze the interfering factors of enterprises' choice of embedding in the supply chain relationship network in order to clarify the parameters' theoretical and practical significance in the game model.

Taking enterprise A as an example, the probability of enterprise choosing embedding strategy is x^* , and we can see that the value of x^* is related to the values of R_{AC} , C_{AC} , R_{A0} , C_{A0} , and L_A from $x^* = L_A + (R_{A0} - C_{A0})/L_A - (R_{AC} - C_{AC})$. When other parameters are fixed, for the molecule of x^* value, (1) the higher the network benefit (R_{A0}) of enterprise A embedding in supply chain relationship network is, the higher the possibility of choosing embedding strategy is; (2) the more assets the enterprise A invests in the supply chain relationship network are, the greater the cost of payment (C_{A0}) is, the less the possibility of choosing embedding strategy is; (3) the greater the network profit ($R_{A0} - C_{A0}$) obtained by embedding in the chain network is, the greater the possibility of enterprise A choosing embedding strategy is. Similarly, when other parameters are fixed, for the denominator of the x^* value, (1) when enterprise B embeds in the supply chain relationship network, the greater the cooperative income (R_{AC}) obtained by cooperation between enterprise A and enterprise B is, the greater the possibility of enterprise A choosing the embedding strategy is; (2) when enterprise B embeds in the supply chain relationship network, the investment of special

assets (C_{AC}) invested by cooperation between enterprise A and enterprise B will be greater, and the less likely the enterprise A chooses the embedding strategy; (3) when enterprise B embeds in the supply chain network, the greater the cooperative profit ($R_{AC} - C_{AC}$) obtained by cooperation between enterprise A and enterprise B, the greater the possibility of enterprise A choosing the embedding strategy. In addition, it is known that $(R_{AC} - C_{AC}) + (R_{A0} - C_{A0})/(R_{AC} - C_{AC}) - L_A > 0$ from $x^* = 1 - (R_{AC} - C_{AC}) + (R_{A0} - C_{A0})/(R_{AC} - C_{AC}) - L_A$. When other parameters are fixed, the greater the difference between $R_{AC} - C_{AC}$ and L_A is, the greater the possibility of enterprise A choosing embedding strategies is and, conversely, the greater the possibility of enterprise A choosing not embedding strategies is.

In conclusion, the probability of enterprise A choosing embedding strategy or nonembedding strategy is affected by many parameters. Among them, the greater the network profit of enterprise A is, the greater the possibility of enterprise A choosing the embedding strategy is. The greater the cooperation profit is, the greater the possibility of enterprise A choosing the embedding strategy is. The cooperation profit between enterprise A and enterprise B is obviously larger than that between enterprise A and other enterprises, and enterprise A chooses the embedding strategy and forms alliance and cooperation with enterprise B is more likely with the increase of this difference.

3.1.4. Equilibrium Stability Analysis of Horizontal Enterprises. In view of the market symmetry of horizontal enterprises, this paper takes enterprise A as an example to unilaterally analyze the evolution of the embedding behavior of enterprise A.

It is assumed that both sides of the game are bounded rational. Since the decision-making of the enterprise involves collective decision-making, the player is aware of the ability to make mistakes and adjust the strategy, or the adjustment behavior of the enterprise is to slowly "evolve" rather than learn quickly. This paper discusses the generalized enterprise. We cannot assume that the enterprise can find the best strategy from the beginning but the random grouping of the large group members composed of the limited rational players with a lower rational level. If the rational level of the enterprise is low, it is impossible to find the best strategy from the beginning. It is impossible that all the game results are (embedded, nonembedded), usually embedded in the existing enterprise, and the enterprise is not embedded. This paper considers companies with different strategies as different types of players, but this type is not given, but changes with the players strategy. Therefore,

x actually represents the probability of an enterprise that is agreed to be embedded in the entire enterprise group, and $1 - x$ represents the probability of disagreeing with the embedded enterprise in the entire enterprise group. When the players in the enterprise group are randomly paired to perform the game, each enterprise may encounter either an embedded opponent or an unembedded opponent. So the enterprise benefits depend on its own type and the opponents type that are randomly matched. But with embedded or not embedded, the company's revenue is different. As long as the players have basic judgment, this difference will be discovered sooner or later, and companies with poor returns will find it more advantageous to change their own strategies and start to imitate another type of business. So x is not fixed but changes with time according to a certain speed of change. This dynamic rate of change can be represented by a replication dynamic equation. That is, the change rate of x is related to two factors. One is choosing the probability x of embedding, which implies the difficulty of imitation. The second is the degree of success, that is, the difference between the expected return of the embedded enterprise and the average income of all enterprises. The formula is as follows:

$$\frac{dx}{dt} = x(U_{A1} - U_A). \quad (10)$$

Among them, U_{A1} and U_A still represent the expected return of the members and the average expected return of the members. Therefore, the enterprise A choosing the embedded dynamic differential equation of the embedded strategy is as follows:

$$\begin{aligned} F(x) &= \frac{dx}{dt} = x(U_{A1} - U_A) = x(1-x)(U_{A1} - U_{A2}) \\ &= x(1-x)[x(R_{AC} - C_{AC} - L_A) + (R_{A0} - C_{A0} + L_A)]. \end{aligned} \quad (11)$$

Make $dx/dt = 0$, and get three critical values: $x = 0$, $x = 1$, and $x = R_{A0} - C_{A0} + L_A/L_A - R_{AC+C_{AC}} \cap [0, 1]$.

- (1) When $R_{AC} - C_{AC} - L_A > 0$ and $R_{A0} - C_{A0} + L_A < 0$, $dx/dt \geq 0$ in the interval $((C_{A0} - R_{A0} - L_A)/(R_{AC} - C_{AC} - L_A), 1]$. In this case, $x = 1$ is the evolutionary stability point, while $x = C_{A0} - R_{A0} - L_A/R_{AC} - C_{AC} - L_A$ is the unstable equilibrium point, and the embedding strategy is the evolutionary stability strategy. When $R_{AC} - C_{AC} - L_A > 0$ and $R_{A0} - C_{A0} + L_A < 0$, $dx/dt \leq 0$ in the interval $[0, C_{A0} - R_{A0} - L_A/R_{AC} - C_{AC} - L_A)$. So $x = 0$ is the evolutionary stability point, while $x = R_{A0} - C_{A0} - C_A/L_A - R_{AC} + C_{AC} - C_A$ is the unstable equilibrium point, and the nonembedding strategy is the evolutionary stability strategy. Thus, when the cooperative profit between enterprise A and enterprise B is larger than that between enterprise A and other member enterprises and the network profit of enterprise A and the cooperative profit between enterprise A and other member enterprises are not

enough to compensate for its embedding cost, the final result of the behavior evolution of enterprise A may be either embedding behavior or nonembedding behavior, and with the higher the $C_{A0} - R_{A0} - L_A/R_{AC} - C_{AC} - L_A$ value is, the greater the possibility of enterprise A evolving into embedding behavior is.

- (2) When $R_{AC} - C_{AC} - L_A \leq 0$, and $R_{A0} - C_{A0} + L_A \geq 0$, $dx/dt \geq 0$ in the interval $[0, (C_{A0} - R_{A0} - L_A)/(R_{AC} - C_{AC} - L_A))$. In this case, $x = C_{A0} - R_{A0} - L_A/R_{AC} - C_{AC} - L_A$ is the unstable equilibrium point. When $R_{AC} - C_{AC} - L_A \leq 0$ and $R_{A0} - C_{A0} + L_A \geq 0$, $dx/dt \leq 0$ in the interval $((C_{A0} - R_{A0} - L_A)/(R_{AC} - C_{AC} - L_A), 1]$. In this case, $x = C_{A0} - R_{A0} - L_A/R_{AC} - C_{AC} - L_A$ is also an unstable equilibrium point.
- (3) When $R_{AC} - C_{AC} - L_A > 0$ and $R_{A0} - C_{A0} + L_A > 0$, $dx/dt \geq 0$. At this point, $x = 1$ is the evolutionary stability point; that is, enterprise A will eventually evolve into embedding behavior and embedding strategy is the evolutionary stability strategy. The cooperative profit between enterprise A and enterprise B is larger than that between enterprise A and other member enterprises. When the network profit of enterprise A and the cooperative profit between enterprise A and other member enterprises are enough to compensate for the embedding cost, the final result of the behavior evolution of enterprise A is to adopt the embedding strategy.
- (4) When $R_{AC} - C_{AC} - L_A \leq 0$ and $R_{A0} - C_{A0} + L_A \leq 0$, $dx/dt \leq 0$. In this case, $x = 0$ is the evolutionary stability point; that is, enterprise A will eventually evolve into nonembedding behavior and nonembedding strategy is the evolutionarily stable strategy. The cooperative profit between enterprise A and enterprise B is less than that between enterprise A and other member enterprises, but when the network profit of enterprise A and the cooperative profit between enterprise A and other member enterprises are not enough to compensate for the embedded cost, the final result of the evolution of enterprise A behavior is to adopt the nonembedding behavior.

To sum up, the evolutionary results of horizontal enterprise strategic decision-making behavior may or may not be embedding strategy. On the one hand, the evolution results depend on the value of cooperative profits between enterprise A and enterprise B and between enterprise A and other supply chain members. On the other hand, the evolution results depend on whether the sum of network profits of enterprise A and the profits of cooperation between enterprise A and other member enterprises can compensate for the embedding cost of enterprise A or not. In addition, the higher the ratio of $C_{A0} - R_{A0} - L_A/R_{AC} - C_{AC} - L_A$ is, the more likely the enterprise will evolve to adopt embedding behavior.

3.1.5. Evolutionary Game Simulation of Horizontal Enterprise. According to the operation practice of supply chain enterprises, this paper assigns the parameters that affect the embedding behavior of supply chain enterprises taking enterprise A as an example. The cost of cooperation between enterprise A and other supply chain enterprises is higher than that between enterprise A and enterprise B. For the sake of simplicity and generality, this paper sets the network return rate of supplier enterprise A as r_{A0} , and then, the network return is $R_{A0} = (1 + r_{A0})C_{A0}$. The return rate of cooperation between enterprise A and other horizontal enterprises is r_A , and then, the profit of cooperation between enterprise A and other horizontal enterprises is $L_A = (1 + r_A)C_A$. And the return rate of cooperation between enterprise A and enterprise B is r_{AC} , then cooperation profit between enterprise A and enterprise B is $R_{AC} = (1 + r_{AC})C_{AC}$. On this basis, a new replicated dynamic differential equation $F(x)$ is obtained. The initial values of the parameters are set, as shown in Table 2:

$$F(x) = x(1-x)[x(R_{AC} - C_{AC} - L_A) + (R_{A0} - C_{A0} + L_A)]. \quad (12)$$

Based on the initial values of the above parameters, the network embedding behavior strategy of supply chain enterprises is simulated by using MATLAB simulation software. As shown in Figure 2, the proportion of enterprise A choosing to embed in the supply chain relationship network will eventually converge to 1, so the system will reach an ideal evolutionary stable state. In addition, with the increasing x value, that is, more and more horizontal enterprises choose the embedding strategy in the supply chain, enterprise A tends to adjust its own strategy quickly and embedding in the supply chain relationship network.

As shown in Figure 3, the initial value of r_{AC} between enterprise A and enterprise B is changed from 0.6 to 0.4 and 0.8, respectively, and different simulation results are obtained. When the cooperative rate of return between enterprise A and enterprise B decreases, that is, $r_{AC} = 0.4$, the proportion of enterprise A choosing the embedding strategy decreases, and the sensitivity to external environment change also decreases. When the cooperative rate of return between enterprise A and enterprise B increases, that is, $r_{AC} = 0.8$, the proportion of enterprise A choosing the embedding strategy increases, and the sensitivity to external environmental changes has also been improved. Thus, the higher the cooperative rate of return between supply chain enterprise A and enterprise B is, the larger the proportion of enterprise A choosing the embedding strategy is. That is, when supply chain enterprise A perceives the embedding in a supply chain relationship network, the more profitable it is to cooperate with enterprise B, the more likely it is to choose the embedding strategy.

In addition, in order to further explore the dynamic trend of horizontal enterprises' embedding behaviors in supply chain, this paper sets $a = R_{AC} - C_{AC} - L_A$ and $b = R_{A0} - C_{A0} + L_A$, and C_1 and C_2 are the initial values of replicating dynamic differential equations, respectively. The initial values of parameters are set, as shown in Table 3.

As shown in Figure 4, picture coding ②, ③, ⑤, ⑧, and ⑩ show that although the proportion of enterprise A choosing to embed in the supply chain relationship network fluctuates near the value 1, it will converge to 1 with the change of time t ; thus, the system reaches an ideal evolutionary stable state; that is, $x = 1$ is the evolutionary stable point, and the embedding strategy is the evolutionary stable strategy.

However, the picture coding ①, ④, ⑥, ⑦, and ⑨ shows that although the proportion of enterprise A choosing to embed in the supply chain relationship network oscillates near the value 0, it will eventually converge to 0 with the change in time t ; thus, the system achieves an ideal evolutionary stable state; that is, $x = 0$ is the evolutionary stable point, and the nonembedding strategy is the evolutionary stable strategy. Thus, although the initial values and parameters of the equation are different, the system will eventually stabilize at the equilibrium point of $x = 0$ or $x = 1$ with the time t changing periodically.

3.2. Evolutionary Game Analysis of Vertical Enterprises. The vertical cooperative behavior of enterprises in the supply chain network is mainly manifested in the vertical cooperative relationship or behavior between supplier and manufacturer and manufacturer and retailer. Through the specialized division of labor among enterprises, the production efficiency of enterprises and the overall operation ability of the supply chain can be improved.

3.2.1. Model Building. Assuming that an enterprise has the independent decision-making power of embedding in a supply chain relationship network, the relationship among the main bodies is a vertical cooperative relationship, and its strategy space is (embedding, nonembedding). Enterprises choose embedding strategy, which means that enterprises choose to cooperate with upstream and downstream members of the supply chain network to form an alliance relationship. On the one hand, enterprises embedding in the supply chain network can obtain heterogeneous resources and information needed for the enterprises development. These resources and information can be further transformed into social capital or relational capital. This paper names them as network gains. On the other hand, cooperation between enterprises and upstream and downstream member enterprises can reduce information asymmetry and transaction costs and then improve cooperation efficiency. Assuming that enterprise S is the supplier, enterprise M is the manufacturer, and enterprise S and enterprise M adopt the embedding strategy, indicating that there is a cooperative relationship between enterprise S and enterprise M, which can generate certain cooperation benefits. If neither enterprise S nor enterprise M decides to embeds in the supply chain network, the profits from independent production or sales are $P_S(P_S > 0)$ and $P_M(P_M > 0)$. In addition, in the vertical enterprise group, the probability of supplier group adopting embedding strategy is assumed to be $x(0 < x < 1)$, the probability of nonembedding strategy is $(1 - x)$, the probability of manufacturer group adopting embedding

TABLE 2: Initial values of parameters and implications.

Parameter name	Initial value	Parameter implication
r_{A0}	0.1	Network return rate of enterprise A
r_A	0.25	Cooperation rate of return between enterprise A and other enterprises
r_{AC}	0.6	Cooperation rate of return between enterprise A and enterprise B
C_{A0}	1	Special assets investment cost of enterprise A
C_{AC}	2	Cooperation cost between enterprise A and enterprise B
C_A	4	Cooperation cost between enterprise A and other enterprises

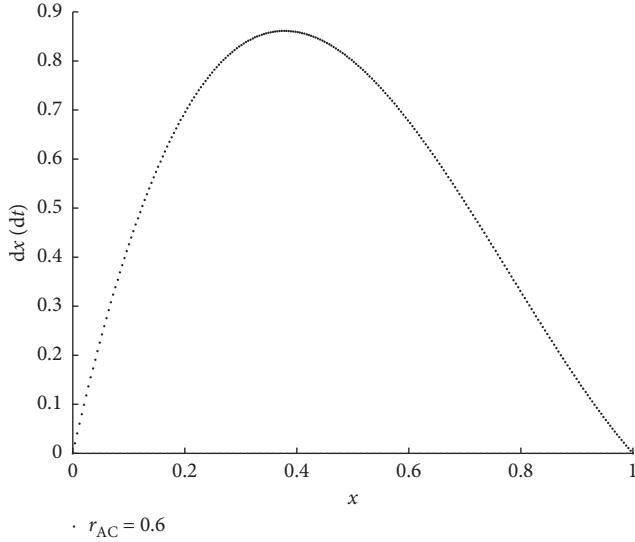


FIGURE 2: Initial simulation experiments.

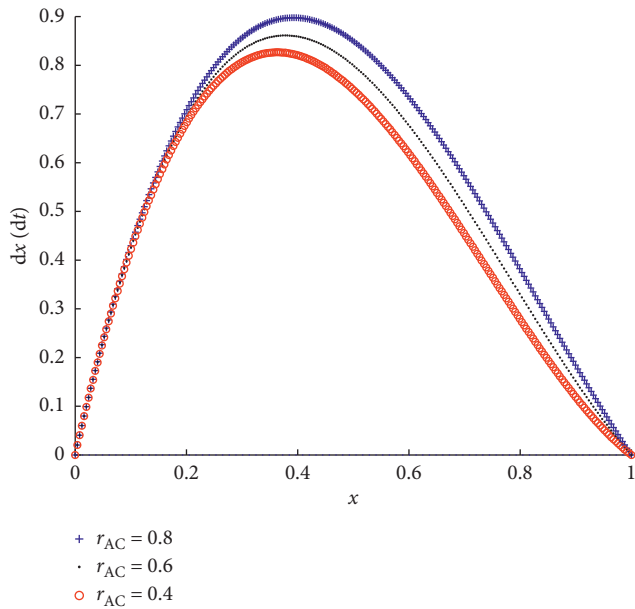


FIGURE 3: Simulation test results.

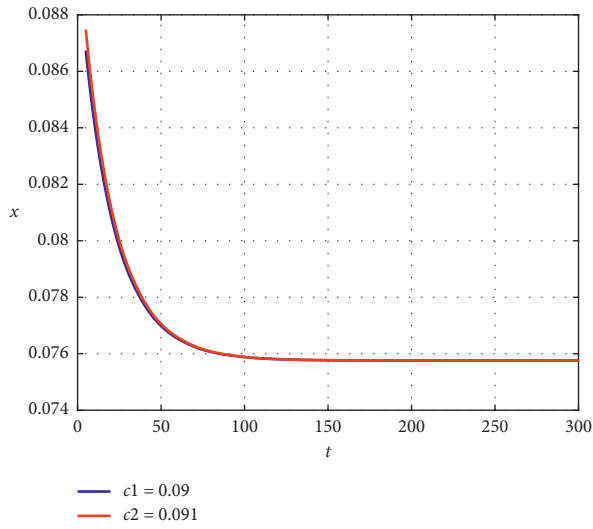
strategy is y ($0 < y < 1$), and the probability of nonembedding strategy is $(1 - y)$. The total income of an enterprise is the sum of the income from independent production or sales and the income from cooperation.

TABLE 3: Initial setting of parameters for horizontal enterprises.

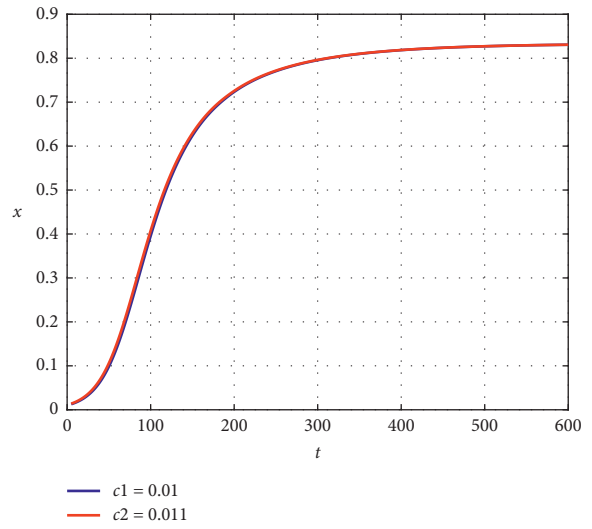
Picture coding	a	b	C_1	C_2
①	-0.660	0.050	0.090	0.091
②	-0.060	0.050	0.010	0.011
③	200	300	0.01	0.011
④	-200	-300	0.01	0.011
⑤	-6	5	0.01	0.011
⑥	6	-5	0.01	0.011
⑦	200	-3	0.01	0.011
⑧	2	1	0.01	0.011
⑨	-200	-100	0.01	0.011
⑩	-200	200	0.01	0.011

- (1) Enterprise S adopts the embedding strategy, and enterprise M also adopts the embedding strategy, which means that there is a cooperative relationship between enterprise S and enterprise M. When enterprises S and M choose to embed in supply chain network, they need to bear certain social responsibility and pay a certain cost; that is, the investment cost of special assets is C_{S0} ($C_{S0} > 0$) and C_{M0} ($C_{M0} > 0$), so as to obtain social capital; that is, network income is R_{S0} ($R_{S0} > 0$) and R_{M0} ($R_{M0} > 0$). In addition, when enterprise S and enterprise M form a contractual relationship, they need to invest a certain time cost and transaction cost; that is, the cooperation cost of enterprise S is C_{SC} ($C_{SC} > 0$), and the cooperation cost of enterprise M is C_{MC} ($C_{MC} > 0$). Enterprise S and enterprise M can effectively improve the overall specialization level and cooperation efficiency of supply chain by strengthening information interaction and cooperation. Therefore, enterprise S can further obtain cooperative revenue R_{SC} ($R_{SC} > 0$) and enterprise M can obtain cooperative revenue R_{MC} ($R_{MC} > 0$).

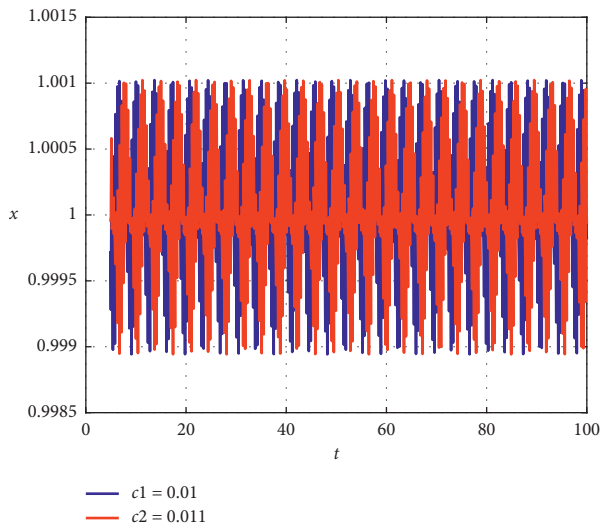
- (2) Enterprise S adopts an embedding strategy, while enterprise M chooses nonembedding strategy, which means that there is no cooperative relationship between enterprise S and enterprise M. When enterprise S embeds in the supply chain network, the cost to be paid is C_{S0} , and the social capital to be obtained is R_{S0} . When enterprise M chooses the nonembedding strategy, the additional profit obtained by cooperation between enterprise S and other manufacturers in the supply chain network is L_S ($L_S > 0$), while enterprise M can obtain profit P_M when it produces or sells independently.



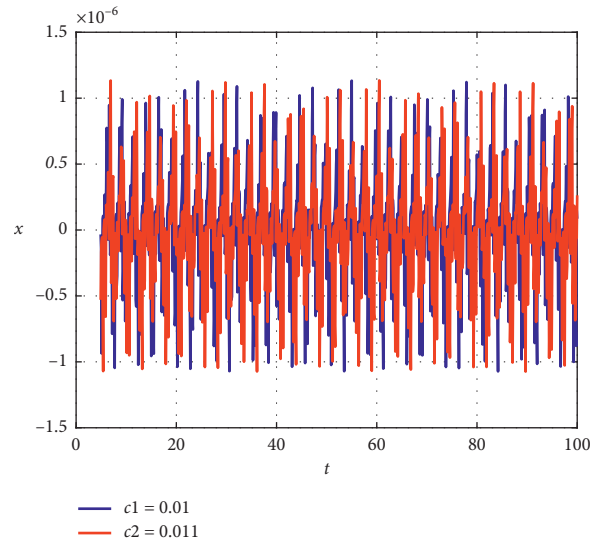
(a)



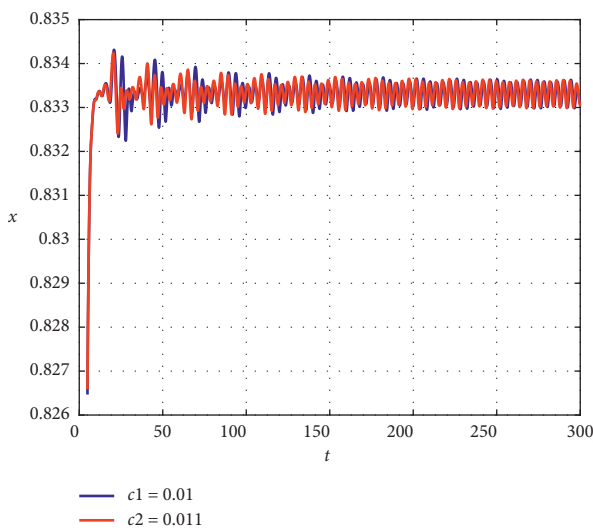
(b)



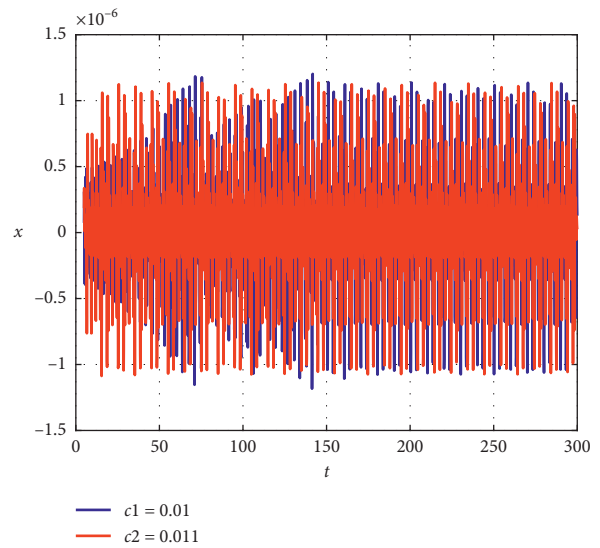
(c)



(d)



(e)



(f)

FIGURE 4: Continued.

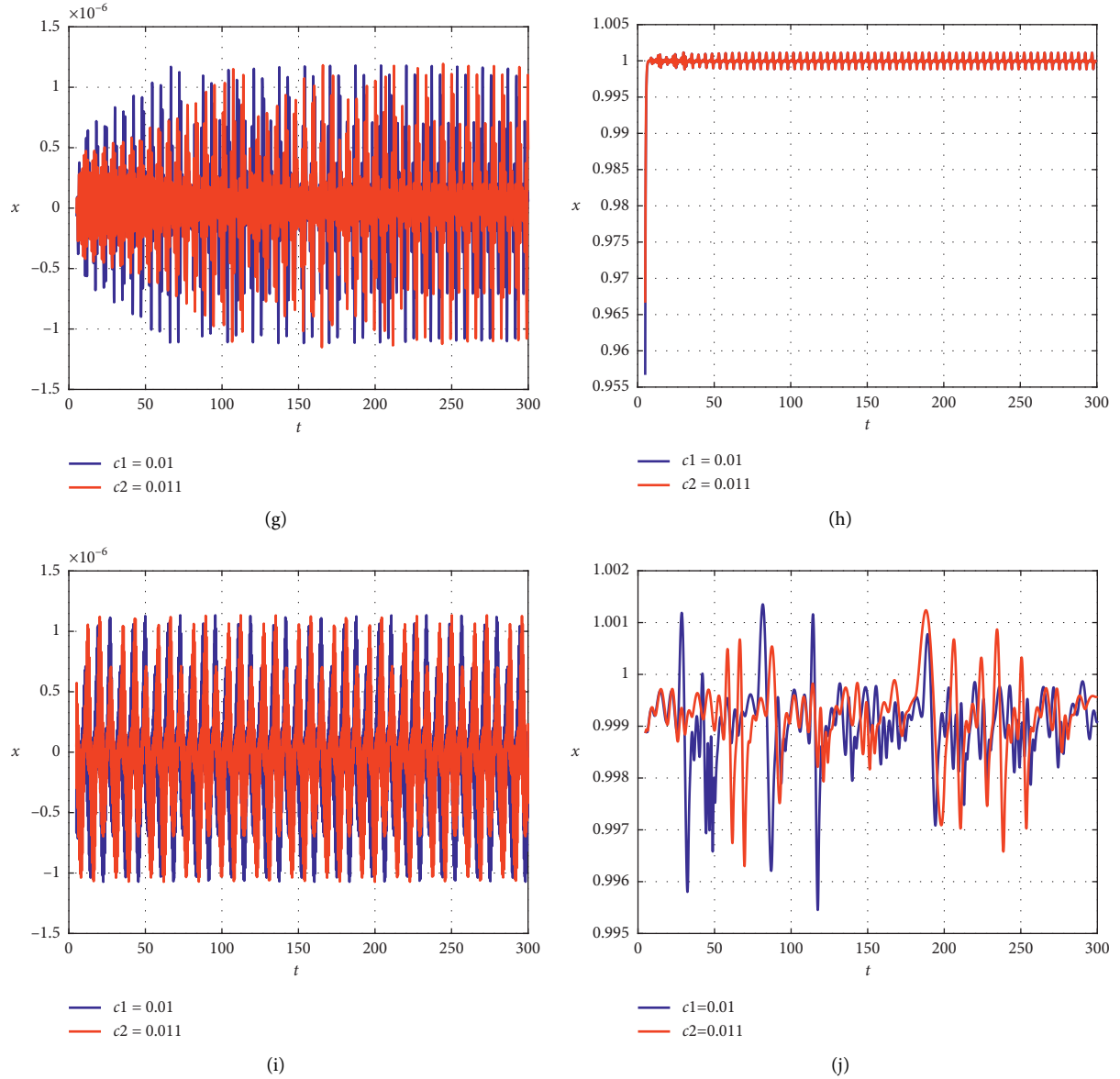


FIGURE 4: Simulated graph of horizontal enterprises: (a) ①; (b) ②; (c) ③; (d) ④; (e) ⑤; (f) ⑥; (g) ⑦; (h) ⑧; (i) ⑨; (j) ⑩.

- (3) Enterprise S adopts a nonembedding strategy, while enterprise M chooses embedding strategy, which indicates that there is no cooperative relationship between enterprise S and enterprise M. Enterprise M embeds in the supply chain network, which needs to pay C_{M0} for the preinvestment cost, so as to obtain R_{M0} network revenue. When enterprise S adopts the nonembedding strategy, the additional profit obtained by enterprise M cooperating with other suppliers in the supply chain network is $L_M (L_M > 0)$, while enterprise S can obtain the profit P_S when it produces or sells independently.
- (4) Enterprise S adopts a nonembedding strategy, and enterprise M also chooses a nonembedding strategy, which means that there is no cooperative relationship between enterprise S and enterprise M. Both

enterprise S and enterprise M choose not to embed in the supply chain relationship network, so their preinvestment cost is 0. In view of this, the profits of enterprise S and enterprise M from the outside of supply chain network are neglected, so they obtain their own profits P_S and P_M when they produce or sell independently.

To sum up, the income matrix of the embedding behavior between enterprise S and enterprise M is shown in Table 4.

3.2.2. Model Solution

- (1) According to the revenue matrix between enterprise S and enterprise M constructed above, when the probability of enterprise M choosing embedding

TABLE 4: Revenue matrix of vertical enterprises.

Vertical enterprise embedding behavior	Enterprise M	
	Embedding (y)	Nonembedding ($1 - y$)
Enterprise S	$P_S + R_{S0} + R_{SC} - C_{S0} - C_{SC}$, $P_M + R_{M0} + R_{MC} - C_{M0} - C_{MC}$ $P_S, P_M + R_{M0} - C_{M0} + L_M$	$P_S + R_{S0} - C_{S0} + L_S, P_M$ P_S, P_M

strategy is y , the expected revenue of enterprise S choosing embedding strategy is U_{S1} :

$$U_{S1} = y(P_S + R_{S0} + R_{SC} - C_{S0} - C_{SC}) + (1 - y)(P_S + R_{S0} - C_{S0} + L_S). \quad (13)$$

The expected return of enterprise S choosing non-embedding strategy is U_{S2} :

$$U_{S2} = y(P_S) + (1 - y)P_S. \quad (14)$$

Therefore, the average expected return of enterprise S is U_S :

$$\begin{aligned} U_S &= xU_{S1} + (1 - x)U_{S2} \\ &= x[y(P_S + R_{S0} + R_{SC} - C_{S0} - C_{SC}) + (1 - y) \\ &\quad \cdot (P_S + R_{S0} - C_{S0} + L_S)] + (1 - x) \\ &\quad \cdot [y(P_S) + (1 - y)P_S]. \end{aligned} \quad (15)$$

When the expected return of S choosing embedding strategy and nonembedding strategy is equal ($U_{S1} = U_{S2}$), the game equilibrium is realized, that is,

$$y(P_S + R_{S0} + R_{SC} - C_{S0} - C_{SC}) + (1 - y)(P_S + R_{S0} - C_{S0} + L_S) = y(P_S) + (1 - y)P_S. \quad (16)$$

After sorting out, the following formulas are obtained:

$$\begin{aligned} (R_{SC} - C_{SC} - L_S)y &= C_{S0} - R_{S0}, \\ y^* &= \frac{C_{S0} - R_{S0}}{R_{SC} - C_{SC} - L_S} = \frac{R_{S0} - C_{S0}}{L_S - (R_{SC} - C_{SC})} \\ &= 1 - \frac{(R_{SC} - C_{SC}) - (C_{S0} - R_{S0}) - L_S}{L_S - (R_{SC} - C_{SC})}, \\ 1 - y^* &= \frac{(R_{SC} - C_{SC}) - (C_{S0} - R_{S0}) - L_S}{L_S - (R_{SC} - C_{SC})}. \end{aligned} \quad (17)$$

- (2) Similarly, according to the revenue matrix between enterprise S and enterprise M, when the probability of enterprise S choosing embedding strategy is x , the expected revenue of enterprise M choosing embedding strategy is U_{M1} :

$$U_{M1} = x(P_M + R_{M0} + R_{MC} - C_{M0} - C_{MC}) + (1 - x)(P_M + R_{M0} - C_{M0} + L_M). \quad (18)$$

Enterprise M chooses the nonembedding strategy with the expected return of U_{M2} :

$$U_{M2} = x(P_M) + (1 - x)(P_M). \quad (19)$$

Therefore, the average expected return of enterprise M is U_M :

$$\begin{aligned} U_M &= yU_{M1} + (1 - y)U_{M2} = y[x(P_M + R_{M0} + R_{MC} - C_{M0} \\ &\quad - C_{MC}) + (1 - x)(P_M + R_{M0} - C_{M0} + L_M)] \\ &\quad + (1 - y)[x(P_M) + (1 - x)(P_M)]. \end{aligned} \quad (20)$$

When enterprise M chooses embedding strategy and nonembedding strategy with the same expected return ($U_{M1} = U_{M2}$), it achieves game equilibrium, that is,

$$x(P_M + R_{M0} + R_{MC} - C_{M0} - C_{MC}) + (1 - x)(P_M + R_{M0} - C_{M0} + L_M) = x(P_M) + (1 - x)(P_M). \quad (21)$$

After sorting out, the formula ② is obtained:

$$\begin{aligned} (R_{MC} - C_{MC} - L_M)x &= C_{M0} - R_{M0}, \\ x^* &= \frac{C_{M0} - R_{M0}}{R_{MC} - C_{MC} - L_M} = \frac{R_{M0} - C_{M0}}{L_M - (R_{MC} - C_{MC})} \\ &= 1 - \frac{(R_{MC} - C_{MC}) - (C_{M0} - R_{M0}) - L_M}{L_M - (R_{MC} - C_{MC})}, \\ 1 - x^* &= \frac{(R_{MC} - C_{MC}) - (C_{M0} - R_{M0}) - L_M}{L_M - (R_{MC} - C_{MC})}. \end{aligned} \quad (22)$$

3.2.3. Model Analysis. In order to further strengthen their core competitive advantages, enterprises should embed in their supply chain network and seek to build a cooperative relationship with upstream and downstream enterprises. On this basis, they should continuously improve the level of specialization and cooperation efficiency and maintain the stability of cooperative relationship between enterprises. This paper will further analyze the influencing factors of upstream and downstream member enterprises' choice of embedding in the supply chain network in order to clarify the theoretical and practical significance of the parameters of the game model.

- (1) The probability of enterprise S choosing embedding strategy is x^* , it is seen that x^* is related to the values of R_{MC} , C_{MC} , R_{M0} , C_{M0} , and L_M from $x^* = R_{M0} - C_{M0}/L_M - (R_{MC} - C_{MC})$. When other parameters are fixed, for the molecule of x^* value, (1)

the greater the network revenue (R_{M0}) of enterprise M embedding in the supply chain relationship network is, the greater the possibility of enterprise S choosing to embedding is; (2) the more assets the enterprise M invests in the supply chain relationship network, the greater the cost of payment (C_{M0}) is, the smaller the possibility of enterprise S choosing to embedding is; (3) the greater the network profit ($R_{M0}-C_{M0}$) of the enterprise M choosing to embedding is, the greater the possibility of enterprise S choosing embedding strategy is. Similarly, when other parameters are fixed, for the denominator of x^* value, (1) when enterprise S embeds in the supply chain network, the greater the cooperative benefit (R_{MC}) of cooperation between enterprise M and enterprise S is, the greater the possibility of enterprise S choosing the embedding strategy is; (2) when enterprise S embeds in the supply chain network, the investment of special assets invested by enterprise M and enterprise S in cooperation is greater, the greater the cost (C_{MC}) is, and the less likely the enterprise S chooses the embedding strategy; (3) when the enterprise S embeds in the supply chain network, the greater the cooperative profit ($R_{MC}-C_{MC}$) obtained by the cooperation between enterprise M and enterprise S is, the more likely the enterprise S chooses the embedding strategy; (4) when enterprise S does not embed in the supply chain network, the larger the cooperative profit (L_M) is, the smaller the possibility of S choosing embedding strategy is; (5) the smaller the difference between cooperative profit (L_M) between enterprise M and other member enterprises and cooperative profit ($R_{MC}-C_{MC}$) between enterprise M and enterprise S is, the greater the possibility of S choosing embedding strategy is, and conversely, the greater the possibility of S choosing nonembedding strategy is.

In summary, the probability of enterprise S choosing embedding strategy and nonembedding strategy is affected by many parameters of enterprise M. Among them, the greater the network profit of enterprise M embedding in the supply chain relationship network is, the greater the possibility of enterprise S choosing the embedding strategy is. The greater the cooperative profit of enterprise M and enterprise S is, the greater the possibility of enterprise S choosing the embedding strategy is. When the cooperative profit between enterprise M and other suppliers is obviously larger than that between enterprise M and enterprise S, the enterprise S chooses the embedding strategy with the increase in the gap and forms alliance and cooperating with M.

- (2) The probability of enterprise M choosing embedding strategy is y^* , and it is known that it is determined by the values of R_{SC} , C_{SC} , R_{S0} , C_{S0} , and L_S from $y^* = R_{S0} - C_{S0}/L_S - (R_{SC} - C_{SC})$. When other parameters are fixed, for the molecule of the

y^* value, (1) the greater the network revenue (R_{S0}) of enterprise S embedding in supply chain network is, the greater the possibility of enterprise M choosing to embedding is; (2) the more assets invested in supply chain relationship network invests the enterprise S, the greater the cost of payment (C_{S0}) is, and the smaller the possibility of enterprise M choosing to embedding is; and (3) the larger the network profit ($R_{S0}-C_{S0}$) is, the greater the possibility of enterprise M choosing embedding strategy is. Similarly, when other parameters are fixed, for the denominator of y^* value, (1) when enterprise M embeds in the supply chain network, the greater the cooperative benefit (R_{SC}) obtained by cooperation between enterprise S and enterprise M is, the greater the possibility of enterprise M choosing the embedding strategy is; (2) when enterprise M embeds in the supply chain network, the greater the cost (C_{SC}) of special assets invested by cooperation between enterprise S and enterprise M is, the less likely the enterprise M chooses the embedding strategy; (3) when the enterprise M embeds in the supply chain network, the greater the cooperative profit ($R_{SC}-C_{SC}$) obtained by the cooperation between enterprise S and enterprise M is, the more likely the enterprise M chooses the embedding strategy; (4) when enterprise M does not embed in the supply chain network, the larger the cooperative profit (L_S) is, the smaller the possibility of enterprise M choosing the embedding strategy is; (5) the smaller the difference ($L_S - R_{SC} + C_{SC}$) between cooperative profit (L_S) and cooperative profit ($R_{SC}-C_{SC}$) is, the greater the possibility of enterprise M choosing the embedding strategy is, and conversely, the greater the possibility of enterprise M choosing the nonembedding strategy is.

In summary, the probability of enterprise M choosing embedding strategy and nonembedding strategy is affected by many parameters of enterprise S. Among them, the greater the network profit of enterprise S embedding in the supply chain network is, the greater the possibility of enterprise M choosing the embedding strategy is. The greater the cooperative profit of enterprise S and enterprise M is, the greater the possibility of enterprise M choosing the embedding strategy is. When the cooperative profit of enterprise S and other manufacturer enterprises is obviously larger than that of enterprise S and enterprise M, the possibility of M choosing embedding strategy and forming alliance and cooperating with S with the increase in this gap becomes greater.

3.2.4. Equilibrium Stability Analysis of Enterprises. This paper analyzes the evolution of embedding behaviors of enterprise S and enterprise M, respectively.

The replication dynamic differential equation of enterprise S choosing embedding strategy is

$$\begin{aligned}
F(x) &= \frac{dx}{dt} = x(U_{S1} - U_S) = x(1-x)(U_{S1} - U_{S2}) \\
&= x(1-x)[y(R_{SC} - C_{SC} - L_S) + (R_{S0} - C_{S0} + L_S)].
\end{aligned} \tag{23}$$

Set $dx/dt = 0$, and get three critical values: $x=0$, $x=1$, and $y_0 = R_{S0} - C_{S0} + L_S/L_S - R_{SC+C_{SC}}$.

Similarly, the replication dynamic differential equation of enterprise M choosing embedding strategy is

$$\begin{aligned}
F(y) &= \frac{dy}{dt} = y(U_{M1} - U_M) = y(1-y)(U_{M1} - U_{M2}) \\
&= y(1-y)[x(R_{MC} - C_{MC} - L_M) + (R_{M0} - C_{M0} + L_M)].
\end{aligned} \tag{24}$$

Set $dy/dt = 0$, and get three critical values: $y=0$, $y=1$, and $x_0 = R_{M0} - C_{M0} + L_M/L_M - R_{MC+C_{MC}}$.

In summary, this paper gets five equilibrium points such as $A(0, 0)$, $B(1, 0)$, $C(0, 1)$, $D(1, 1)$, and $E((R_{M0} - C_{M0} + L_M)/(L_M - R_{MC+C_{MC}}), (R_{S0} - C_{S0} + L_S)/(L_S - R_{SC+C_{SC}}))$. The Jacobi matrix J is as follows: $J = \begin{pmatrix} (1-2x)[(R_{SC} - C_{SC} - L_S)y + R_{S0} - C_{S0} + L_S] & x(1-x)(R_{SC} - C_{SC} - L_S) \\ y(1-y)(R_{MC} - C_{MC} - L_M)(1-2y) & (R_{MC} - C_{MC} - L_M)x + R_{M0} - C_{M0} + L_M \end{pmatrix}$.

The above differential equations form a group dynamic system. Based on the construction of Jacobi matrix, the local stability of each equilibrium point is further discussed according to the symbolic changes in determinant and trace of Jacobi matrix under different conditions:

- (1) When $R_{SC} - C_{SC} > 0$, $R_{MC} - C_{MC} > 0$, $R_{S0} - C_{S0} > 0$, and $R_{M0} - C_{M0} > 0$, there are five equilibrium points in the system, including three unstable points, one locally asymptotical stable point, and one saddle point. When the equilibrium point of the system is $D(1, 1)$, the Jacobi matrix of the system is as follows:

$$J = \begin{pmatrix} C_{SC} - R_{SC} + C_{S0} - R_{S0} & 0 \\ 0 & C_{MC} - R_{MC} + C_{M0} - R_{M0} \end{pmatrix}. \tag{25}$$

It is found that the λ_1 and λ_2 are both negative real parts. Therefore, point $D(1, 1)$ is a locally asymptotically stable point; that is, the combination of (embedding, embedding) strategy is an evolutionarily stable strategy of the system. The practical significance of this evolutionary stabilization strategy lies in that when enterprise S and enterprise M embed in the supply chain network, and the network benefits they can obtain are greater than the network costs, and the cooperation benefits are greater than the cooperation costs; both enterprise S and enterprise M will gradually choose the embedding strategy to build the cooperative

relationship between them. With the increasing networks and cooperation profit margins of enterprise S and enterprise M, the possibility of both sides choosing the embedding strategy is greater. In addition, the symbols of determinants and traces of Jacobi matrices corresponding to each equilibrium point are shown in Table 5.

- (2) When $R_{SC} - C_{SC} + R_{S0} - C_{S0} < 0$ and $C_{M0} - R_{M0} - L_M < 0$, there are five equilibrium points in the system, including three unstable points, one locally asymptotical stable point, and one saddle point. When the equilibrium point of the system is $C(0, 1)$, the Jacobi matrix of the system is as follows:

$$J = \begin{pmatrix} R_{SC} - C_{SC} + R_{S0} - C_{S0} & 0 \\ 0 & C_{M0} - R_{M0} - L_M \end{pmatrix}. \tag{26}$$

It is found that λ_1 and λ_2 are both negative real parts. Therefore, point $C(0, 1)$ is a locally asymptotically stable point; that is, the combination of (nonembedding, embedding) strategy is an evolutionarily stable strategy of the system. The practical significance of this evolutionary stabilization strategy lies in that when enterprise S embeds in the supply chain relationship network, the network gains are insufficient to compensate for the network costs it pays for, and the cooperative gains from cooperation between enterprise S and enterprise M are difficult to compensate for the investment cost of the dedicated assets it invests, or the overall network profit and cooperative profit are less than zero; the cooperative profit obtained with other member enterprises is larger than the difference between network cost and network profit; that is to say, the cooperative profit of enterprise M is enough to compensate for the network loss or social liabilities caused by embedding in the supply chain network; the enterprise S will gradually choose the nonembedding strategy, while enterprise M will gradually choose the embedding strategy.

In addition, with the increasing sum of network loss and cooperation loss of enterprise S and the difference between network cost, network profit, and cooperation profit, the more the possibility that enterprise S will choose nonembedding strategy step by step is, and the more the probability that enterprise M chooses embedding strategy is. In addition, the symbols of determinants and traces of Jacobi matrix corresponding to each equilibrium point are shown in Table 6.

- (3) When $C_{S0} - R_{S0} - L_S < 0$, $R_{MC} - C_{MC} + R_{M0} - C_{M0} < 0$, there are five equilibrium points in the system, including three unstable points, one locally asymptotical stable point, and one saddle point. When the

TABLE 5: Local stability analysis of equilibrium points.

Equilibrium point	Symbols of Jacobi matrix determinant	Symbols of Jacobi matrix traces	Local stability
$A(0, 0)$	+	+	Instable
$B(1, 0)$	-	\pm	Instable
$C(0, 1)$	-	\pm	Instable
$D(1, 1)$	+	-	ESS
$E(x_0, y_0)$	-	0	Saddle point

TABLE 6: Local stability analysis of equilibrium points.

Equilibrium point	Symbols of Jacobi matrix determinant	Symbols of Jacobi matrix traces	Local stability
$A(0, 0)$	+	+	Instable
$B(1, 0)$	\pm	\pm	Instable
$C(0, 1)$	+	-	ESS
$D(1, 1)$	\pm	\pm	Instable
$E(x_0, y_0)$	-	0	Saddle point

equilibrium point of the system is $B(1, 0)$, the Jacobi matrix of the system is as follows:

$$J = \begin{pmatrix} C_{S0} - R_{S0} - L_S & 0 \\ 0 & R_{MC} - C_{MC} + R_{M0} - C_{M0} \end{pmatrix}. \quad (27)$$

It is found that the λ_1 and λ_2 are both negative real parts. Therefore, point $B(1, 0)$ is a locally asymptotically stable point; that is, the combination of (embedding, nonembedding) strategy is an evolutionarily stable strategy of the system. The practical significance of this evolutionary stabilization strategy lies in that when enterprise M embeds in the supply chain relationship network, the network gains are not enough to compensate for the network costs it pays for, and the cooperative gains from cooperation between enterprise M and enterprise S are difficult to compensate for the investment costs of the special assets it invests, or the overall network profits and cooperative profits are less than zero, while the cooperative profit obtained between enterprise S and other manufacturers is larger than the difference between network cost and network profit; that is to say, the cooperative profit of enterprise S is enough to compensate for the network loss or social liabilities caused by embedding in the supply chain network. Enterprise M will gradually choose the nonembedding strategy, while enterprise S will gradually choose the embedding strategy. In addition, with the increasing sum of network loss and cooperation loss of enterprise M, the network cost and network profit, and the difference between cooperation profit of enterprise S, the possibility of enterprise M choosing nonembedding strategy step by step is greater, and the probability of enterprise S choosing embedding strategy is also greater. The symbols of determinants and traces of Jacobi matrix

corresponding to each equilibrium point are shown in Table 7.

- (4) When $R_{S0} - C_{S0} + L_S < 0$ and $R_{M0} - C_{M0} + L_M < 0$, there are five equilibrium points in the system, including three unstable points, one locally asymptotically stable point, and one saddle point. When the equilibrium point of the system is $A(0, 0)$, the Jacobi matrix of the system is as follows:

$$J = \begin{pmatrix} R_{S0} - C_{S0} + L_S & 0 \\ 0 & R_{M0} - C_{M0} + L_M \end{pmatrix}. \quad (28)$$

It is found that the λ_1 and λ_2 are both negative real parts. Therefore, point $A(0, 0)$ is a locally asymptotically stable point; that is, the combination of (nonembedding, nonembedding) strategy is an evolutionarily stable strategy of the system. The practical significance of this evolutionary stabilization strategy lies in the following aspects. When the manufacturer chooses the nonembedding strategy, the total net profit obtained by the enterprise S embedding in the supply chain network and its cooperation profit with other manufacturers is not enough to compensate for the network cost. When the enterprise S chooses the nonembedding strategy, the network profit and cooperation profit obtained by cooperation with other suppliers are not enough to compensate for the network cost, that is, the social liabilities formed by the enterprise S or enterprise M embedding in the supply chain relationship network separately. At the present, both enterprise S and enterprise M will gradually choose the nonembedding strategy more likely. Moreover, with the increasing gap between the network revenue, cooperative profit, and network cost of enterprise S and enterprise M, the possibility of both sides gradually choosing the nonembedding strategy is greater. In addition, the symbols of determinants and traces of Jacobi matrix corresponding to each equilibrium point are shown in Table 8.

TABLE 7: Local stability analysis of equilibrium points.

Equilibrium point	Symbols of Jacobi matrix determinant	Symbols of Jacobi matrix traces	Local stability
$A(0, 0)$	\pm		
$B(1, 0)$	$+$	$-$	ESS
$C(0, 1)$	\pm		
$D(1, 1)$	\pm		
$E(x_0, y_0)$	$-$	0	Saddle point

TABLE 8: Local stability analysis of equilibrium points.

Equilibrium point	Symbols of Jacobi matrix determinant	Symbols of Jacobi matrix traces	Local stability
$A(0, 0)$	$+$	$-$	ESS
$B(1, 0)$	\pm	\pm	Instable
$C(0, 1)$	\pm	\pm	Instable
$D(1, 1)$	\pm	\pm	Instable
$E(x_0, y_0)$		0	Saddle point

- (5) When $0 < x_0, y_0 < 1$, the equilibrium point $E(x_0, y_0)$ is substituted into Jacobi matrix. The Jacobi matrix of the system is as follows:

$$J = \begin{pmatrix} 0 & J_{12} \\ J_{21} & 0 \end{pmatrix},$$

$$J_{12} = \frac{(R_{M0} - C_{M0} + L_M)(C_{MC} - R_{MC} + C_{M0} - R_{M0})(R_{SC} - C_{SC} - L_S)}{(L_M - R_{MC} + C_{MC})^2},$$

$$J_{21} = \frac{(R_{S0} - C_{S0} + L_S)(C_{SC} - R_{SC} + C_{S0} - R_{S0})(R_{MC} - C_{MC} - L_M)}{(L_S - R_{SC} + C_{SC})^2},$$

$$\det J = (-J_{12}) * J_{21} < 0, \quad \text{and } tr J = 0.$$

Therefore, the equilibrium point $E(x_0, y_0)$ is not the asymptotic stability point of the system but the saddle point of the system.

From the analysis of the local stability of the above evolutionary game, we can draw the following conclusions: ① when $y = y_0 (0 \leq y_0 \leq 1)$, the $F(x) = 0$; that is, no matter how x is selected within the definition range, the system will eventually reach an evolutionary stable state; when the proportion of manufacturers who adopt the embedding strategy is y_0 , no matter which strategy the supplier chooses or how likely it is to adopt a certain strategy, there is no difference in earnings. When $x = x_0 (0 \leq x_0 \leq 1)$, there will always be $F(y) = 0$; that is, no matter how y is selected within the definition range, the system will eventually reach an evolutionary stable state; when the supplier proportion of choosing embedding strategy is y_0 , no matter what strategy the manufacturer chooses or how likely it is to adopt, its benefits will be the same. ② When $y > y_0$ and $y(R_{SC} - C_{SC} - L_S) + (R_{S0} - C_{S0} + L_S) > 0$, $x = 0$ and $x = 1$ are two possible stabilization points. When $x = 0$, $\partial F(x)/\partial x = 1 > 0$; while $x = 1$ and $\partial F(x)/\partial x = -1 < 0$. Therefore, the evolutionary game will reach a stable state, and $x = 1$ is the only possible stable point; that is, the supplier strategy will

gradually shift from nonembedding to embedding, and embedding strategy will eventually become the evolutionary stable strategy of suppliers. Similarly, when $y < y_0$, $x = 0$ is the only possible stability point; that is, the supplier strategy gradually shifts from embedding to nonembedding, and the nonembedding strategy will eventually become the evolutionary stability strategy of suppliers. ③ When $x > x_0$ and $x(R_{MC} - C_{MC} - L_M) + (R_{M0} - C_{M0} + L_M) > 0$, $y = 0$ and $y = 1$ are two possible stabilization points. When $y = 0$, $\partial F(y)/\partial y = 1 > 0$; while $y = 1$, $\partial F(y)/\partial y = -1 < 0$. Therefore, the evolutionary game will reach a stable state. $y = 1$ is the only possible stable point. That is, the strategy chosen by the manufacturer will gradually shift from nonembedding to embedding. Embedding strategy will eventually become the evolutionary stable strategy of the manufacturer. Similarly, when $x < x_0$, $y = 0$ is the only possible stabilization point; that is, the strategy chosen by the manufacturer gradually shifts from embedding to nonembedding, the non-embedding strategy will eventually become the evolutionary stabilization strategy of the manufacturer. ④ Figure 5 shows that when point (x, y) falls into the CEBD area, the system will converge to the ideal state in which both enterprise S and enterprise M choose the embedding strategy, while when

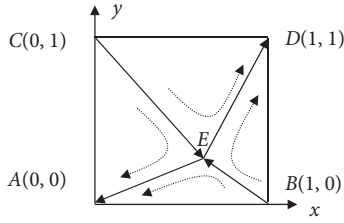


FIGURE 5: Phase diagram of evolutionary game equilibrium point.

point (x, y) falls into the CEBA area, the result of evolutionary game will tend to the bad state that both sides adopt the nonembedding strategy.

3.2.5. The Influence of Parameters Changing on Convergence Rate. The group members participating in the game have the dynamic nature of optimum reaction with myopia. The initial state will influence the behavior pattern of the participants in the game in a conventional way and ultimately determines the direction of the group equilibrium strategy movement. The more the $E(x_0, y_0)$ approaches point A, the larger the area of quadrilateral CEBA, which indicates that evolutionary game will converge to ideal state D gradually, that is, the more likely the enterprises S and M both choose the embedding strategy. The closer the $E(x_0, y_0)$ approaches point D, the larger the area of quadrilateral CEBA, which indicates that evolutionary game will gradually converge to a bad “lock-in” state, that is, the more likely both enterprises S and enterprise M will choose nonembedding strategy.

Under normal circumstances, the higher the network revenue (R_{S0}, R_{M0}) and cooperation revenue (R_{SC}, R_{MC}) can be obtained by suppliers and manufacturers embedding in the supply chain network, the closer the saddle point $E(x_0, y_0)$ moves towards point A(0, 0) on online AED, and the larger the area of quadrilateral CEBA; the system is more conducive to the ideal stable state, and the probability of both suppliers and manufacturers choosing embedding strategy increases. On the contrary, the higher the cooperation cost (C_{SC}, C_{MC}) and investment cost (C_{S0}, C_{M0}) paid by supplier and manufacturer because of embedding in supply chain relationship network, the closer the saddle point $E(x_0, y_0)$ moves towards point D(1, 1) on online AED, and relatively the larger the area of quadrilateral CEBA, so the system will gradually converge to a bad “lock-in” state; that is, the probability of supplier and manufacturer both choosing nonembedding strategy increases. Therefore, suppliers and manufacturers can effectively improve the cooperation revenue between the two sides by improving production efficiency and reducing transaction costs, thus speeding up the convergence of evolutionary game to an ideal state. In addition, when one side chooses nonembedding strategy, the higher the cooperative profits (L_S, L_M) obtained by the other side cooperating with other member enterprises, the more the saddle point $E(x_0, y_0)$ tends to move towards point D(1, 1), which is not conducive to the ideal stable state of the system; on the contrary, it promotes the system to converge gradually to the bad “lock-in” state.

3.2.6. Game Simulation Experiment of Vertical Enterprises.

In view of the fact that supplier and manufacturer enterprises occupy different network positions and have different network powers in the supply chain network, this paper assigns the parameters affecting their embedding behavior according to the operation practice of supply chain enterprises. This paper assumes that manufacturer enterprises are at the core of supply chain relationship network, so they need to pay higher C_{M0} and C_{MC} than supplier enterprises. In addition, the cost of cooperation between supplier S or manufacturer M and other supply chain enterprises is higher than that between them.

For the sake of simplicity and generality, this paper sets the network return rate of supplier enterprise S as r_{S0} , and then, the network returns $R_{S0} = (1 + r_{S0})C_{S0}$; the return rate of supplier enterprise S cooperating with other manufacturers is r_S , and then, the profit of supplier enterprise S cooperating with other manufacturers is $L_S = (1 + r_S)C_S$; the return rate of supplier enterprise S cooperating with manufacturer enterprise M is r_{SC} , and then, the profit of supplier S cooperating with manufacturer M is $R_{SC} = (1 + r_{SC})C_{SC}$. Similarly, this paper sets the network return rate of manufacturer enterprise M as r_{M0} , and then, the network return is $R_{M0} = (1 + r_{M0})C_{M0}$; the return rate of supplier enterprise S cooperating with other manufacturer enterprises is r_M , and then, the profit of supplier enterprise S cooperating with other manufacturer enterprises is $L_M = (1 + r_M)C_M$; and the return rate of supplier enterprise S cooperating with manufacturer enterprise M is r_{MC} , and then, the cooperation profit of supplier enterprise S and manufacturer enterprise M is $R_{MC} = (1 + r_{MC})C_{MC}$. On this basis, the new replicated dynamic differential equations $F(x)$ and $F(y)$ are obtained. The initial values of the parameters are set as shown in Table 9.

Based on the initial values of the above parameters, the network embedding behavior strategy of supply chain enterprises is simulated by using MATLAB simulation software. As shown in Figure 6, the proportion of supplier S and manufacturer M choosing to embed in the supply chain relationship network will eventually converge to 1, and thus, the system will reach an ideal evolutionary stable state. In addition, compared with the supplier enterprise S, the manufacturer M will achieve an ideal stable state with a faster convergence rate. With the increasing x value, more and more suppliers choose embedding strategy, and manufacturers tend to quickly adjust their own strategy and embed in the supply chain relationship network; similarly, with the increasing y value, more and more manufacturers choose embedding strategy, and supplier enterprises will also pay attention to market changes, adjust their own strategy in time, and choose to embed in supply chain networks. Generally speaking, when the other party's behavior strategy is established, the manufacturer's response time to external environmental changes is relatively short and has a strong sensitivity.

As shown in Figure 7, the initial value of r_{SC} between supplier S and manufacturer M is changed from 0.5 to 0.25 and 0.75, respectively, and different simulation results are obtained. When the cooperative return rate between supplier enterprise S and manufacturer enterprise M decreases, that is, $r_{SC} = 0.25$, the proportion of supplier enterprise

TABLE 9: Initial values of parameters and implications.

Parameter name	Initial value	Parameter implication
r_{S0}	0.1	Network return rate of S
r_S	0.25	Cooperative return rate between S and others
r_{SC}	0.5	Cooperative return rate between S and M
C_{S0}	1	Special assets investment cost of S
C_{SC}	2	Cooperation cost between S and M
C_S	4	Cooperation cost between S and others
r_{M0}	0.2	Network return rate of M
r_M	0.35	Cooperative return rate between M and others
r_{MC}	0.6	Cooperative return rate between M and M
C_{M0}	2	Special assets investment cost of M
C_{MC}	3	Cooperation cost between M and S
C_M	5	Cooperation cost between M and others

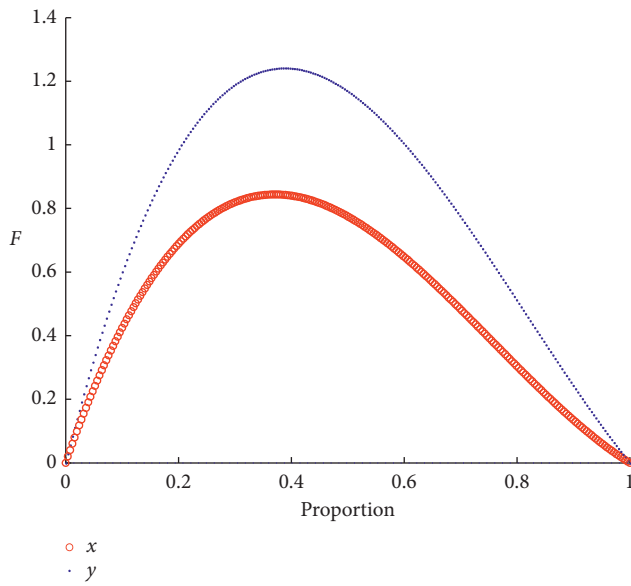


FIGURE 6: Initial simulation results.

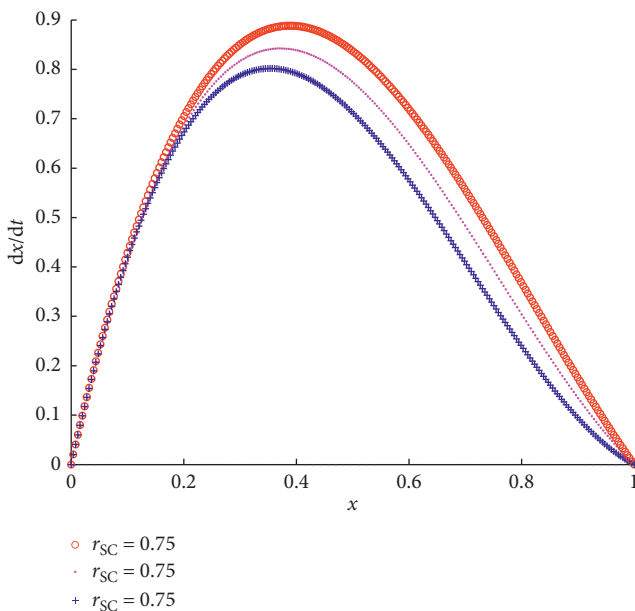


FIGURE 7: Analysis of simulation test results 1.

choosing the embedding strategy decreases, and the sensitivity to external environment changes also decreases. When the cooperative return rate between supplier enterprise S and manufacturer enterprise M increases, that is, $r_{SC} = 0.75$, the proportion of supplier enterprise choosing the embedding strategy is increased, and the sensitivity to external environmental changes is also improved. Thus, the higher the cooperative return rate between supplier enterprise S and manufacturer enterprise M is, the larger the proportion of supplier enterprise choosing the embedding strategy is. That is, when supplier enterprise perceives it is more profitable to embed in supply chain relationship network, the more likely it is to choose the embedding strategy.

Similarly, as shown in Figure 8, the initial value of r_{MC} between manufacturer M and supplier S is changed from 0.6 to 0.4 and 0.8, respectively, and different simulation results are obtained. When the cooperative return rate between manufacturer M and supplier S decreases, that is, $r_{MC} = 0.4$, the proportion of manufacturer enterprises choosing the embedding strategy decreases, and the sensitivity to external environment changes also decreases. When the cooperative return rate between manufacturer M and supplier S increases, that is, $r_{MC} = 0.8$, manufacturer enterprises choose the embedding strategy. The proportion is slightly increased, and the sensitivity to changes in the external environment is also improved. Thus, the higher the cooperative return rate between manufacturer M and supplier S is, the greater the proportion of manufacturer enterprises choosing the embedding strategy is. That is, when manufacturer enterprises perceive embedding in supply chain relationship network and cooperating with supplier enterprises more profitably, the more likely they choose the embedding strategy.

In addition, in order to further explore the dynamic trend of vertical enterprises' embedding behaviors in supply chain, this paper set $m_1 = R_{SC} - C_{SC} - L_S$, $m_2 = R_{S0} - C_{S0} + L_S$, $m_3 = R_{MC} - C_{MC} - L_M$, and $m_4 = R_{M0} - C_{M0} + L_M$, and C_{11} and C_{12} are the initial values of x and y , respectively. The initial values of parameters are set as shown in Table 10.

As shown in Figure 9, picture coding ①, ②, ⑥, ⑨, and ⑩ show that although the proportion of enterprises choosing to embed in the supply chain relationship network fluctuates near the value 1, it will converge to 1 with the change in time t . Thus,

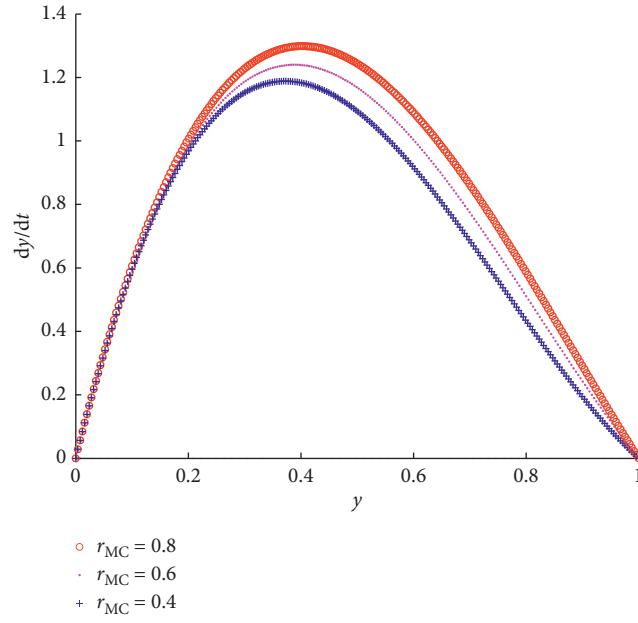


FIGURE 8: Analysis of simulation test results 2.

TABLE 10: Initial parameters of vertical enterprise.

Picture coding	m_1	m_2	m_3	m_4	C_{11}	C_{12}
①	200	200	400	200	0.99	0.50
②	1.20	1	1	2	0.50	0.50
③	1	-1	2	-1	0.01	0.01
④	-100	-100	-200	-200	0.01	0.01
⑤	-100	100	-200	200	0.05	0.01
⑥	-100	-100	2	2	0.05	0.01
⑦	0.10	-0.20	0.02	-0.02	0.05	0.01
⑧	0.10	0.20	0.20	-0.20	0.05	0.01
⑨	-0.10	-0.20	-0.20	0.20	0.05	0.01
⑩	0.10	0.20	-0.20	0.20	0.05	0.01

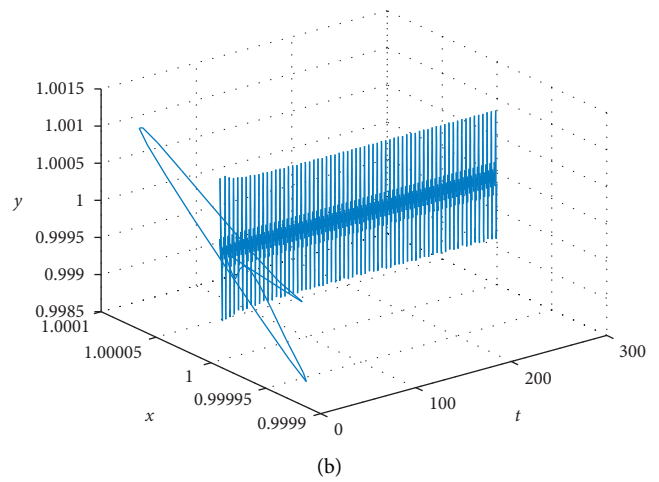
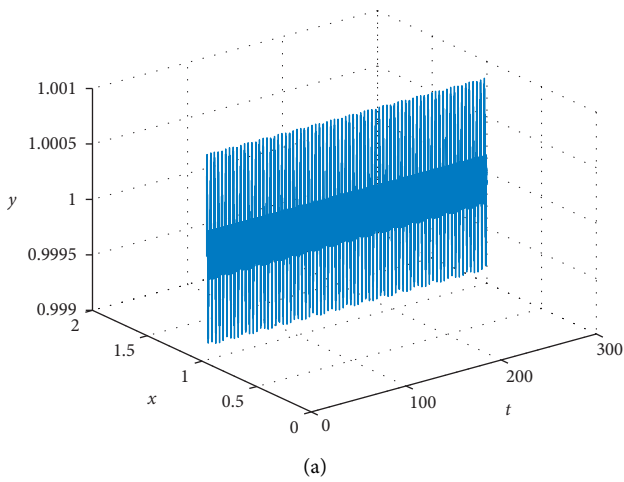


FIGURE 9: Continued.

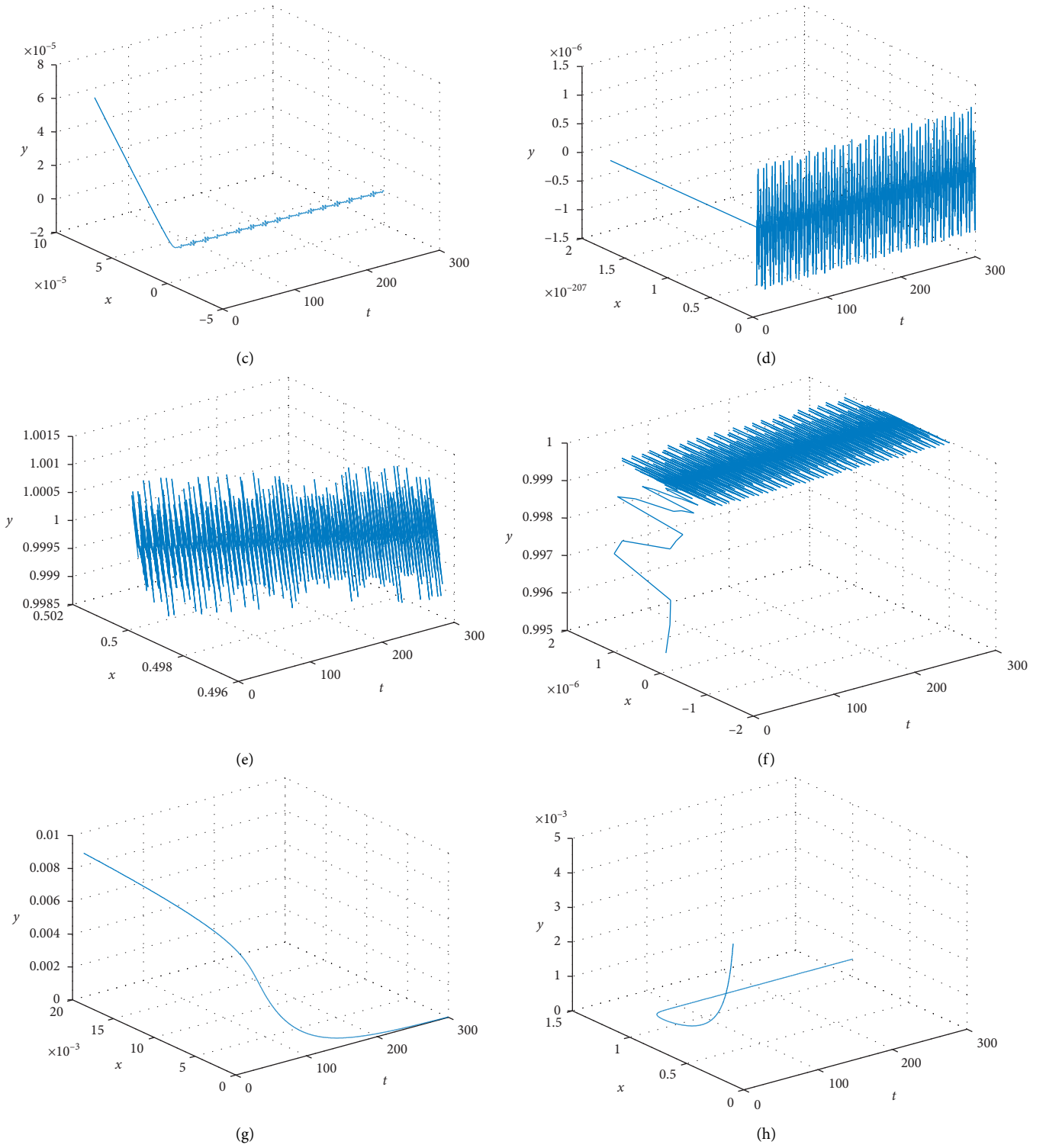


FIGURE 9: Continued.

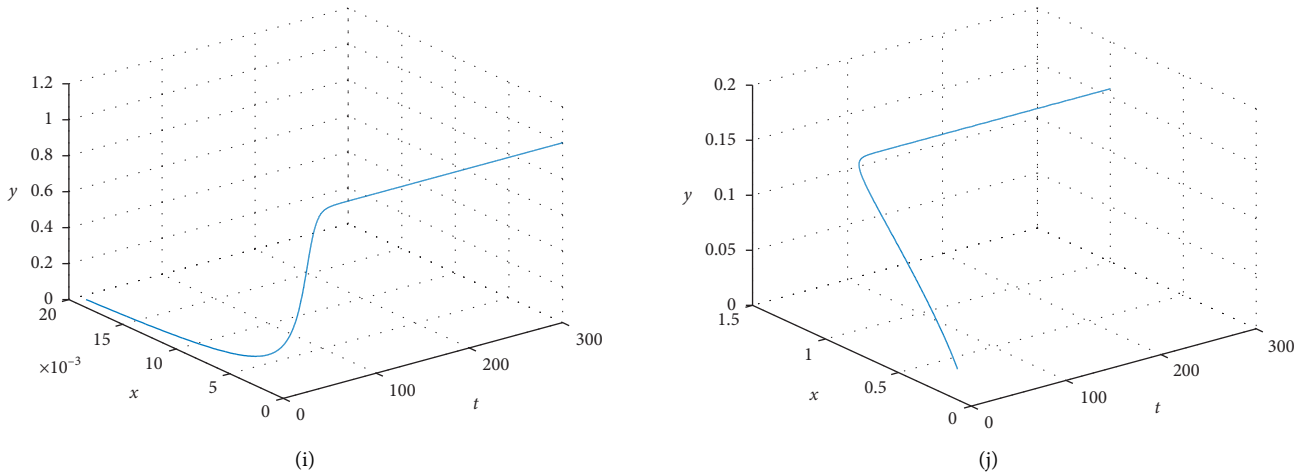


FIGURE 9: Simulated graph of vertical enterprises: (a) ①; (b) ②; (c) ③; (d) ④; (e) ⑤; (f) ⑥; (g) ⑦; (h) ⑧; (i) ⑨; (j) ⑩.

the system achieves an ideal evolutionary stable state; that is, $x=1$ is the evolutionary stable point, and the embedding strategy is the evolutionary stable strategy.

While picture coding ③, ④, ⑤, ⑦, and ⑧ show that although the proportion of enterprises choosing to embed in the supply chain relationship network oscillates near the value 0, it will eventually converge to 0 with the change in time t ; thus, the system achieves an ideal evolutionary stable state; that is, $x=0$ is the evolutionary stable point, and the nonembedding strategy is the evolutionary stable strategy. Thus, although the initial values and parameters of x and y are different, the system will eventually stabilize at the equilibrium point of $x=0$ or $x=1$ with the time-varying periodicity.

In summary, based on the external dynamic environment, enterprises often choose to embed in the supply chain relationship network, seek to sign cooperation contracts with other member enterprises and establish partnerships, so as to obtain more heterogeneous resources and information from the supply chain relationship network, and overcome the resource constraints. By speeding up the cross-border flow of capital and information in the supply chain network, supply chain enterprises can promote mutual cooperation among enterprises and develop more innovative products or services to meet the needs of the individualized and diversified market in order to realize the benefit sharing and performance improvement among enterprises.

4. Conclusion and Enlightenment

Based on the dynamic evolutionary game method, this paper clarifies the path evolution direction, law, and dynamic convergence process of supply chain enterprise's network embedding strategy selection. The conclusions of this paper mainly include the following two aspects.

On the one hand, whether supply chain enterprises adopt network embedding behavior is related to such factors as investment cost of special assets, cooperation cost, network income, cooperation income, cooperation profit with other member enterprises, and the probability of other

member enterprises choosing embedding behavior. The greater the network profit that enterprises gain when they embed in the supply chain network is, the greater the possibility of enterprises choosing the embedding strategy is. The greater the cooperative profit obtained by cooperation among enterprises is, the greater the possibility of enterprises choosing the embedding strategy is. When the cooperative profit between enterprises is obviously larger than the cooperative profit between one enterprise and other enterprises, enterprises will choose the embedding strategy with the increase in the difference more likely.

On the other hand, the evolutionary results of strategic decision-making behavior of supply chain enterprises may or may not be the embedding strategy. The result of this evolution depends on the value of interfirm cooperative profits and the net profit of enterprises and whether the sum of the profits of interfirm cooperation with other member enterprises can compensate for the embedding cost of enterprises. With the constant changes in parameters such as initial values and time t , the system will eventually converge to 1 and reach an ideal evolutionary stable state; that is, $x=1$ is the evolutionary stable point, and the embedding strategy is the evolutionary stable strategy; or if the system will eventually converge to 0, the system can reach an ideal evolutionary stable state; that is, $x=0$ is the evolutionary stable point, and the nonembedding strategy is the evolutionary stable strategy.

Therefore, under the condition that other factors remain unchanged, supply chain enterprises should reduce the investment cost and cooperation cost of special assets and realize the maximization of network revenue and cooperation income, so as to improve the possibility of adopting network embedding behavior. In addition, the enterprises should narrow the gap between the extra-cooperation profit and the current cooperation profit obtained by cooperation between supply chain enterprises and other member enterprises and restrain supply chain enterprises from violating the cooperation contract and taking opportunistic actions in order to increase the probability of choosing network embedding behavior.

In conclusion, by constructing the game model of network embedding behavior of horizontal and vertical enterprises in the supply chain, this paper clarifies the evolution direction and law of network embedding strategy selection of enterprises, discusses the stable state and dynamic convergence process of evolutionary game, and provides a reference for the enterprises' decision-making of network embedding behaviors. However, there are still a few shortcomings and deficiencies remaining. For example, this paper only discusses the factors that affect the enterprises' network embedding behaviors from two aspects of cost and benefit, ignoring the influence of external factors such as environment. In the future, we should fully consider the influence of external environmental factors on the enterprises' behaviors choosing to embed the supply chain network and the cooperation with other node enterprises and reconstruct the network embedding behavior model of supply chain enterprises. In addition, the supply chain network is more complex in reality, including multiple participants. In the future research, the supply chain network structure can be extended to the situation of one supplier (manufacturer, retailer) to multiple manufacturers (retailer) or even multiple suppliers (manufacturer, retailer) to multiple manufacturers (retailer) when constructing the supply chain enterprises' embedded behavior model in order to make it more realistic.

Data Availability

The data used to support the findings of this study are available from the corresponding author upon request.

Conflicts of Interest

The authors declare that they have no conflicts of interest.

Acknowledgments

This paper was supported by the General Projects of the National Social Science Fund (Research on industrial chain synergy mechanism of new type agricultural operators under high quality development target (19BGL150)) and Social Science Youth Project of Shandong Province (Research on the sustainable growth mechanism of farmers' professional cooperatives in Shandong Province from the perspective of network embeddedness (20DGLJ08)).

References

- [1] F. H. Zhang and T. Y. Zuo, "Network embeddedness and innovation performance of domestic firms under the circumstance of fdi clustering," *R&D Management*, vol. 25, no. 5, pp. 70–80, 2013.
- [2] H. J. Xiao, "Shared value," *Business Ecosystem and the Transformation of Competitive Paradigms for Business Reform*, vol. 17, pp. 129–141, 2015.
- [3] S. L. Vargo and R. F. Lusch, "Service-dominant logic: continuing the evolution," *Journal of the Academy of Marketing Science*, vol. 36, no. 1, pp. 1–10, 2008.
- [4] Y. Du and H. Zhang, "Research on the impact of the use of channel power on channel cooperation in the flower market—taking relationship commitment as adjustment," *Variable Review of Economy and Management*, vol. 33, no. 1, pp. 65–74, 2017.
- [5] L. Xie, J. Ma, and H. Han, "Implications of stochastic demand and manufacturers' operational mode on retailer's mixed bundling strategy and its complexity analysis," *Applied Mathematical Modelling*, vol. 55, no. 3, pp. 484–501, 2018.
- [6] J. Ma and H. Wang, "Complexity analysis of dynamic non-cooperative game models for closed-loop supply chain with product recovery," *Applied Mathematical Modelling*, vol. 38, no. 23, pp. 5562–5572, 2014.
- [7] J. Ma and X. Ma, "Measure of the bullwhip effect considering the market competition between two retailers," *International Journal of Production Research*, vol. 55, no. 2, pp. 313–326, 2017.
- [8] X. Su and H. Zhang, "Research on the governance of agricultural product channel relations from the perspective of tripartite game," *Journal of Agro-Technical Economics*, vol. 36, no. 3, pp. 42–52, 2017.
- [9] X. J. Pu and D. L. Jin, "The operational efficiency measurement of agro-food supply chains: the single farmer-supermarket direct purchase vs," *Dual Channel Chinese Journal of Management Science*, vol. 25, no. 1, pp. 98–105, 2017.
- [10] M. K. He and W. J. Wang, "International reference and China's strategies for the development of modern supply chain," *Reform*, vol. 31, no. 1, pp. 22–35, 2018.
- [11] H. M. Liu, Y. Wang, and H. J. Li, "The impact of partnership and logistics capability on," *Supply Chain Integration Chinese Journal of Management Science*, vol. 24, no. 12, pp. 148–157, 2016.
- [12] Y. Lin, "Is downstream the knowledge source for technological innovations," *Studies in Science of Science*, vol. 35, no. 3, pp. 471–479, 2017.
- [13] M. Xue, "The Influence of Supply Chain Partner Characteristics on Supply Chain Financing in Perspective of Network Capacity Variance," *Intermediary Role of Relational Capital Management Review*, vol. 30, no. 6, pp. 238–250, 2018.
- [14] G. Q. Chen, *Supply Chain Management China Soft Science*, vol. 10, pp. 101–104, 1999.
- [15] A. Surana, S. Kumara, M. Greaves, and U. N. Raghavan, "Supply-chain networks: a complex adaptive systems perspective," *International Journal of Production Research*, vol. 43, no. 20, pp. 4235–4265, 2005.
- [16] S. H. Ma, "The influence of core enterprise on the formation of strategic partnership in supply chain," *Industrial Engineering and Management*, vol. 5, no. 1, pp. 24–27, 2000.
- [17] C. L. Feng, "Research on the relationship between supply chain knowledge sharing and firm performance: the mediating and moderating effect of Supply Chain," *Agility and Environmental Dynamics Management Review*, vol. 27, no. 11, pp. 181–191, 2015.
- [18] J. Ma and L. Sun, "Complexity analysis about nonlinear mixed oligopolies game based on production cooperation," *IEEE Transactions on Control Systems Technology*, vol. 26, no. 4, pp. 1532–1539, 2018.
- [19] K. D. Zhou, *Enterprise Economics China Prospect*, Publishing House, China, 1987.
- [20] T. Neil, A. James, and B. Cecil, "A framework for understanding managerial responses to supply chain complexity," *International Journal of Operations & Production Management*, vol. 38, no. 6, pp. 1443–1466, 2018.
- [21] H. Q. Hu, "Research on the mechanism of relational capital's effect on supply chain financing from the perspective of

- complex supply chain,” *Network Management Review*, vol. 31, no. 12, pp. 306–318, 2019.
- [22] E. M. Tachizawa and C. Y. Wong, “The performance of green supply chain management governance mechanisms: a supply network and complexity perspective,” *Journal of Supply Chain Management*, vol. 51, no. 3, pp. 18–32, 2015.
- [23] K. Polanyi, *The Great Transformation: Economic and Political Origins of Our Time*, Rinehart, New York, NY, USA, 1944.
- [24] M. Granovetter, “Economic action and social structure: the problem of embeddedness,” *American Journal of Sociology*, vol. 91, no. 3, pp. 481–510, 1985.
- [25] B. Uzzi, “Social structure and competition in interfirm networks: the paradox of embeddedness,” *Administrative Science Quarterly*, vol. 42, no. 1, pp. 35–67, 1997.
- [26] H. James and K. Johan, “Multilevel embeddedness: the case of the global fisheries governance complex,” *Social Networks*, vol. 44, no. 1, pp. 281–294, 2016.
- [27] C. Y. Zhang, T. Guo, and H. D. Liu, “The impact of network embedding on the business mode innovation of technological,” *Entrepreneurship Studies in Science of Science*, vol. 36, no. 1, pp. 167–175, 2018.
- [28] M. C. Dong, F. Zeng, and C. Su, “Network embeddedness as a dependence-balancing mechanism in developing markets: differential effects for channel partners with asymmetric dependencies,” *Journal of the Academy of Marketing Science*, vol. 47, no. 6, pp. 1064–1084, 2019.
- [29] X. Xie, H. Wang, and H. Jiao, “Non-R&D innovation and firms’ new product performance: the joint moderating effect of R&D intensity and network embeddedness,” *R&D Management*, vol. 49, no. 5, pp. 748–761, 2019.
- [30] L. Tanja, C. Sylvie, and D. Pavlos, “Network embeddedness in the internationalization of biotechnology entrepreneurs,” *Entrepreneurship & Regional Development*, vol. 30, no. 3, pp. 1–23, 2018.
- [31] S. L. Zhu and Y. Z. Chen, “Reverse embedding, parenting control and overseas innovation of Chinese enterprises,” *Document Review and Future Reform of Economic System*, vol. 35, no. 2, pp. 94–99, 2017.
- [32] B. Yang and Y. Yang, “Postponement in supply chain risk management: a complexity perspective,” *International Journal of Production Research*, vol. 48, no. 7, pp. 1901–1912, 2010.
- [33] M. Erica, P. Giovanni, and S. K. Dzidziso, “Network embeddedness and new product development in the biopharmaceutical industry: the moderating role of open innovation flow,” *International Journal of Production Economics*, vol. 160, no. 2, pp. 106–119, 2015.
- [34] J. P. Xie, H. W. Kong, and W. S. Zhang, “S & T innovation platform: network characteristics, operation governance and development strategy—a case study from S & T innovation practice of zhongguancun and,” *ZhangjiangPark Business Management Journal*, vol. 39, no. 5, pp. 36–49, 2017.
- [35] G. R. Chai, “Evolutionary game analysis on the cooperative behavior in industrial cluster under supply chain,” *Networks Science Research Management*, vol. 32, no. 5, pp. 129–134, 2011.
- [36] J. Ma, W. Lou, and Y. Tian, “Bullwhip effect and complexity analysis in a multi-channel supply chain considering price game with discount sensitivity,” *International Journal of Production Research*, vol. 57, no. 17, pp. 5432–5452, 2019.
- [37] J. Ma and L. Xie, “The stability analysis of the dynamic pricing strategy for bundling goods: a comparison between simultaneous and sequential pricing mechanism,” *Nonlinear Dynamics*, vol. 95, no. 2, pp. 1147–1164, 2019.
- [38] J. Ma and L. Xie, “The stability analysis of the dynamic pricing strategy for bundling goods: a comparison between simultaneous and sequential pricing mechanism,” *Nonlinear Dynamics*, vol. 95, no. 2, pp. 1147–1164, 2019.
- [39] T. F. Nie, B. Y. He, and S. F. Du, “Supply chain operations considering fairness concerns with bargaining disagreement point,” *Journal of Management Sciences in China*, vol. 20, no. 10, pp. 92–102, 2017.
- [40] P. Sun, “Co-evolution mechanism and countermeasures of B2C,” *Logistics Service Supply Chain*, vol. 38, no. 12, pp. 93–96, 2019.
- [41] J. Jian, Y. Guo, L. Jiang, Y. An, and J. Su, “A multi-objective optimization model for green supply chain considering environmental benefits,” *Sustainability*, vol. 11, no. 21, p. 5911, 2019.
- [42] J. Jian, Y. Zhang, L. Jiang, and J. Su, “Coordination of supply chains with competing manufacturers considering fairness concerns,” *Complexity*, vol. 2020, Article ID 4372603, 15 pages, 2020.

Research Article

The Pricing Strategy of Dual Recycling Channels for Power Batteries of New Energy Vehicles under Government Subsidies

Xiaodong Zhu ^{1,2} and Wei Li³

¹School of Management Engineering, Nanjing University of Information Science and Technology, Nanjing 210044, China

²Development Institute of Jiangbei New Area, Nanjing 210044, China

³Chang Wang School of Honors, Nanjing University of Information Science and Technology, Nanjing 210044, China

Correspondence should be addressed to Xiaodong Zhu; zxd@nuist.edu.cn

Received 9 March 2020; Revised 30 April 2020; Accepted 20 May 2020; Published 13 June 2020

Guest Editor: Lei Xie

Copyright © 2020 Xiaodong Zhu and Wei Li. This is an open access article distributed under the Creative Commons Attribution License, which permits unrestricted use, distribution, and reproduction in any medium, provided the original work is properly cited.

The vigorous development of the new energy automobile industry has highlighted the issue of efficient recycling of power batteries. Using a Stackelberg game, the pricing mechanism of dual-channel power battery recycling models under different government subsidies is investigated. Consequently, sensitivity analysis and comparison analysis are conducted, providing the pricing decision and the optimal profit of closed-loop supply chain (CLSC) systems. Finally, the effects of recycling efforts, power battery greenness levels, service levels, and consumer green recycling awareness on prices of power batteries and profits are determined through numerical simulations, and the optimal prices under different strategies are compared. The results indicate that recycling prices of each party in the manufacturer subsidy model are relatively high, and consumers' green awareness and the green levels of power batteries are directly proportional to the recycling prices offered by recycling parties. Automobile 4S stores and recycling networks should pay attention to the balance between the increase in the cost and the quantity of government subsidies for their recycling efforts. For recycling enterprises, maintaining an appropriate service level can maximize their profits and positively motivate the development of them.

1. Introduction

In recent years, new-energy automobile industry in China has developed rapidly under the impetus of the government, and the sales of new energy vehicles have soared. With the vigorous development of the new energy vehicle industry, large-scale “retirement” of automotive power batteries has been observed and the subsequent recycling of new energy vehicle power batteries has become a major issue. According to the latest development plan issued by the State Council, the annual output of new energy vehicles will reach 2 million in 2020. It is expected that there will be a “scrap tidal wave,” and the quantity of scrapped power batteries will reach between 120,000 and 170,000 tons, resulting in serious environmental and resource problems. Therefore, in order to better perform environmental management and resource utilization, the recycling of used power batteries is not only

one of the key links in the new energy vehicle industry, but it can also generate huge economic and environmental benefits. Recycling and avoiding “secondary pollution” have become important concern for enterprises, society, and the country.

However, in the aspect of recycling channels of used power batteries, the system of remanufacturing in China is not complete, and that for used power batteries is rather chaotic. A considerable number of used batteries cannot be collected on a regular basis for professional recycling. Market researches show that some forward-looking remanufacturing enterprises have built their own recycling channels of waste products. Huawei, Lenovo, and other manufacturers have carried out their own recycling channels under the stimulus of production responsibility extension system. They either rely on the recovery of major networks or entrust a third party to recover e-waste and gradually

form a dual-channel supply chain consisting of recycling networks and traditional retailers. Similarly, the dual-channel supply chain has also been put into practice in the field of recycling used power batteries as well. Many regions in China have started to build and share power battery recycling networks or cooperate with 4S stores in order to form a dual-channel supply chain and explore the market-oriented pricing mechanism of used power batteries. In practice, however, recycling channels face multiple obstacles. On the one hand, there is a competitive relationship between recycling channels, and the recycling efforts of 4S stores and recycling networks affect the decision-making behavior of each party and the pricing strategy of the dual-channel supply chain. On the other hand, there is always a difference in service level between 4S stores and recycling networks, and the difference in greenness level of different power batteries poses a challenge to the pricing strategy of manufacturers. Based on the practical background, it can be seen that the research on the recycling pricing strategy of used power batteries in dual-channel supply chains is not only of theoretical significance but also of practical guiding significance.

In recent years, new-energy automobile industry has developed rapidly under government subsidies. However, the state's "transfusion-type" support for the development of the new energy industry has led to frequent occurrences of new energy vehicles "scams." According to the Public Notice on The 2017 New Energy Vehicle Promotion and Application of Subsidy Funds Liquidation Audit Final Situation issued by the Ministry of Industry and Information Technology on October 11, 2019, the subsidy audit standards of new energy vehicles are getting stricter year by year, which reflects that China is gradually tightening the supervision of the new energy vehicle industry. With the gradual decline of new energy vehicles' subsidies, China's new energy vehicle market has gradually shifted from being policy-oriented to market-oriented. Given this policy background and the high level of battery scrapping, the market space for power battery recycling is very huge. However, the government's subsidies are limited, so it is worth considering which recycling subject the government chooses to subsidize. Additionally, it is important to study how to motivate the main parties of the supply chain to maximize recycling efforts and improve consumers' green recycling awareness, as these have become urgent problems for power battery recycling. The existing recycling methods of used power batteries are mainly divided into two channels: automobile 4S stores and recycling networks.

Aligning with the abovementioned policy guidance and background and considering the impact of government subsidies, this paper builds a dual-channel power battery recycling model under a Stackelberg game. Recycling efforts, power battery greenness levels, service levels, and consumer green recycling awareness are introduced. The optimal price structures of each subject under different models and the effects of each factor on recycling prices were analyzed through numerical simulations, and the optimal prices under different strategies were compared. Finally, relevant countermeasures and suggestions for power battery

recycling are proposed based on the research results. The purpose of this article is to answer the following questions: (1) under the circumstance of different government subsidies, how do each recycling party in the supply chain carry out pricing strategies of used power batteries? (2) In a situation in which government subsidies are becoming tighter, how do government departments choose the subsidy recipient and determine the quantity of subsidy needed in order to maximize the incentive for recycling power batteries and encourage the sustainable development of new energy companies? (3) In the case that there are differences in recycling efforts and service levels between recycling channels, how do each party in the power battery recycling supply chain formulate pricing strategies to improve its own competitive advantages and benefits?

The remainder of this article is organized as follows: Section 2 reviews the literature on new energy vehicles, closed-loop supply chain (CLSC) pricing, and government subsidies; Section 3 contains the problem description and model assumptions; Section 4 introduces the construction and solution of the dual-channel CLSC model under five strategies; the Stackelberg game is used to solve the pricing and profitability problems in the models; Section 5 presents the comparison and sensitivity analyses through numerical simulations to demonstrate the application of the model; and finally, Section 6 presents the conclusions.

2. Literature Review

The literature related to this article mainly focuses on three aspects: power battery recycling of new energy vehicles, CLSC pricing, and government subsidies.

The power battery contains a large quantity of precious metal resources, which are likened to "urban minerals." Recycling nickel, cobalt, and rare metals in power batteries can generate enormous economic benefits for enterprises, effectively reducing the environmental pollution risk of power batteries and alleviating the dependence of rare precious metals on foreign resources in China. In terms of power battery recycling for new energy vehicles, Alamerew and Brissaud [1] used a system dynamics approach to study costs, revenues, strategies, and regulatory decisions. Taking electric vehicle batteries as an example, the authors discussed the main pillars of circular economy research. Zhu et al. [2] studied the optimal channel selection and battery capacity allocation strategy of electric vehicle manufacturers with regard to battery recycling. The study found that the optimal channel selection of each electric vehicle manufacturer depends on the procurement cost from external battery suppliers. Li et al. [3] studied the impact of subsidy policies and dual credit policies on the production decisions of new energy vehicles and fuel vehicles, considering battery recycling in a competitive environment. The problem of joint recycling and coordination between upstream and downstream operations of the power battery three-level CLSC was studied. Harper et al. [4] proposed that lithium-ion battery recycling by electric vehicles can provide valuable sources of secondary materials. They also summarized and evaluated the current methods of recycling and reusing

lithium-ion batteries for electric vehicles, emphasizing the future development direction. Betancourt-Torcat et al. [5] proposed an optimization decision-making method for the main energy sources and power generation, providing recommendations for the electric vehicle power battery power supply chain. Tang et al. [6] considered the application of the reward and punishment mechanism in the battery recycling of scrapped electric vehicles and established a Stackelberg game theory model to study the social, economic, and environmental impact of recycling used electric vehicle batteries.

CLSCs, which follow the theory of a circular economy with the goal of maximizing the product life cycle, is one of the effective ways to develop the remanufacturing industry. In terms of CLSC pricing, He et al. [7] explored the channel structure and pricing decisions of manufacturers through a two-channel CLSC model and studied government's subsidy policies for competing new and remanufactured products. Taleizadeh et al. [8] considered the social and environmental aspects of supply chain decision-making and proposed a tactical decision-making model that included product price and logistics decisions. Kabul and Parlaktürk [9] considered a decentralized supply chain consisting of a retailer and a supplier. The supplier provided services to forward-looking consumers in two periods and set prices from the perspective of the retailer and supplier, respectively. Chen and Ho [10] explored whether supplier sales rely on supplier participation in environmental protection practices (PEPs), and, if so, how is this relationship regulated by the customer's PEP level? Zhang and Xiong [11] considered the design of two optimal pricing contracts for retailers when the information of manufacturer's recycling cost was asymmetric. Pi et al. [12] studied pricing and service strategies under the competition and cooperation of retailers in a dual-channel supply chain system composed of one manufacturer and two retailers. Under the circumstance of revenue sharing in the forward supply chain and channel cost sharing in the reverse supply chain, Jiaping et al. [13] discussed how the product pricing and service optimization decisions can be made. Xie [14] et al. studied the contract coordination of centralized and decentralized dual-channel CLSC in the context of online/offline dual channels. Chao et al. [15] proposed a risk decentralized contract model with a loss-sharing mechanism and unilateral compensation mechanism to manage procurement inventory risk in order to stimulate retailers to expand product orders. Researches on the above two aspects mostly focus on the competition and coordination of recycling channels, manufacturers' monopoly decisions, and consumer preferences, while the literature on the impact of government subsidies on pricing strategies of recycling power batteries is relatively scarce. In this study, we mainly focus on the CLSC's reverse channel. The pricing strategy and profitability of each entity were studied through a dual-channel supply chain model.

In terms of government subsidies, Wang et al. [16] studied the allocation strategy of government subsidies under an e-waste reverse supply chain consisting of a recycler, a remanufacturer, and two retailers. The optimal pricing decision of multisubsidized government subsidies and their effects are studied. Mitra and Webster [17] studied the effect of government subsidies to promote remanufacturing activities and considered three cases in which the

government gave subsidies to manufacturers alone, remanufacturers alone, or both. Calcott and Walls [18] explored the impact of government subsidies on recycling rates in the case of manufacturer recycling. Pfeifer and Ovchinnikov [19] distinguished between customer life cycle value and consumer willingness and studied the impact of government subsidies on product demand. Guo et al. [20] considered the optimal recycling and production strategy of a CLSC in the case of supply interruption and government subsidies and provided a reference for the operation of enterprises with supply interruptions and the design of a reasonable government subsidy mechanism. Zhao and Sun [21] established two profit distribution models for CLSCs without government subsidies and with government subsidies and compared the profit distribution of members of the two models. Wan and Hong [22] established a Stackelberg game model to analyze the optimal pricing and recycling policies of a CLSC and discussed the effects of subsidy policies. Nielsen et al. [23] studied the impact of government subsidy policies on optimal pricing and investment decisions in order to improve product quality and recycling under the goal of social welfare optimization. However, among the literature on government subsidies, there are few researches related to the recycling of power batteries. This paper introduces the government subsidy and studies the pricing mechanism under different subsidy strategies. Then, we investigated and compared the pricing strategies and profits under different models, providing management suggestions for recycling enterprises in the supply chain.

Based on the above, we can conclude that there are limited researches on power battery recycling and related government regulations. From the perspective of the supply chain, the actual situation of pricing strategies and the profitability of all parties need further study. This study is different from previous research in three ways. First, this paper not only considers traditional recycling methods of power batteries, which in this paper is automobile 4S stores, but also considers the current emerging recycling method, namely, recycling networks. Consequently, a dual-channel supply chain for recycling power batteries was built based on the actual situation. Second, this study uses the Stackelberg game to study the optimal pricing strategy and its influencing factors for the main players in a supply chain led by the remanufacturer. Pricing decisions and comparative analysis under different government subsidy strategies are performed as well. Third, this paper regards the greenness level of remanufactured batteries and consumers' green recycling awareness under the government regulations; then, we introduce the recycling effort and service level for sensitivity simulation analysis and propose countermeasures and recommendations for new energy power battery recycling.

3. Problem Description and Assumptions

This study builds a two-stage CLSC consisting of a manufacturer, a new energy vehicle 4S store, and a recycling network, as shown in Figure 1. We assume that the supply

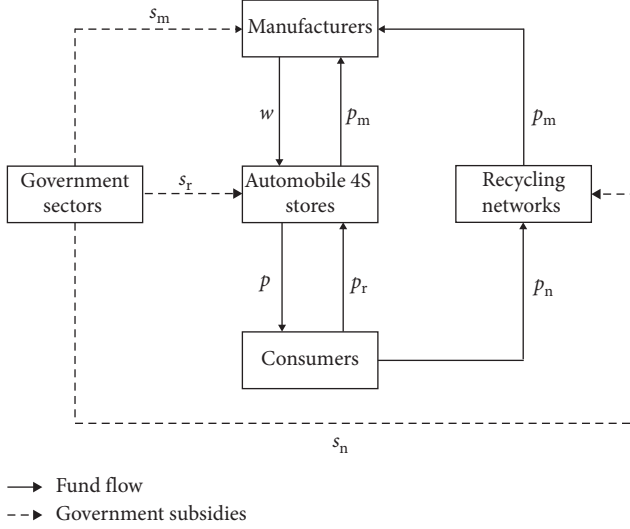


FIGURE 1: Flow chart of power battery recycling of new energy vehicles.

capacity of the market is strong enough, and new energy automobile companies can meet the purchasing demand of consumers. The market supply and demand are balanced. In the sales link, manufacturers sell power batteries to automobile 4S stores at the wholesale price w , and 4S stores sell power batteries to consumers at price p . New power batteries reach consumers through the forward supply chain. In order to characterize the relationship between the sales price of power batteries and demand, according to the analysis of Savaskan [3], it is assumed that the market demand function for remanufactured products is $q = \alpha - \beta p$, where $\alpha, \beta > 0$ and are both constant. In the recycling link, 4S stores recycle used power batteries from consumers at the price p_r , while recycling networks recycle used power batteries from consumers at the price p_n . Finally, the manufacturers recycle all used power batteries from 4S stores and recycling networks at the price p_m . The recycling power batteries are returned to the manufacturers through the reverse supply chain. To ensure the profit of each entity, $p_m > p_n$, $p_m > p_r$, and $w > p$ must be met. C_m is the unit cost of the new power battery, and C_r is the unit cost of the remanufactured power battery, so $C_r < C_m$ must exist. The difference between the two is given by $\Delta = C_m - C_r$, which represents the cost saved by remanufacturing.

According to the industry background of power battery recycling, this paper considers the influence of consumers' awareness of green recycling, greenness level of power batteries, recycling efforts, and service level of recycling outlets and 4S stores on the pricing strategy of recycling used power battery. It is assumed that consumers have the same willingness to buy new power batteries and remanufactured power batteries on the market, and the two products have the same market price. In the recycling link, the recycling quantity of used power batteries of 4S stores and recycling networks are $q_r = \theta S - b_2 p_n + b_1 p_r + \rho(v_r - v_n) + k g_m$ and $q_n = (1 - \theta)S - b_2 p_r + b_1 p_n + \rho(v_n - v_r)$, where S is the total market demand, θ is the market share of the consumer demand of 4S stores in the dual-channel supply chain, b_1 is the consumers' sensitivity coefficient to the recycling price, and b_2 is the channel competition coefficient

between 4S stores and recycling networks. In order to ensure a good competitive environment and positive profits for the recycling parties, we assume $b_1 > b_2 > 0$. k and g_m , respectively, represent consumers' awareness of green recycling and the greenness level of power batteries. When either factor improves, consumers are more willing to choose regular channels to recycle used power batteries and more willing to buy remanufactured power batteries, and the recycling quantity of power batteries of 4S stores and recycling networks will increase. Since the dual-channel recycling supply chain is considered in this paper, service level is an important factor to be considered among competitive channels. v_r and v_n represent the service levels provided by 4S stores and recycling networks to consumers, respectively. The costs spent in service levels are recorded as v_r^2 and v_n^2 [24]. ρ represents the transfer coefficient of market demand to service level differences.

In addition, this paper also considers the influence of the recycling efforts of 4S stores and recycling networks on the pricing and profit of the supply chain. In the process of recycling power batteries from consumers, the degree at which 4S stores and recycling networks respond to the national call for publicity and recycling efforts is set at e_r and e_n , respectively, and the government, according to their respective efforts, provides $e_r s_r$ and $e_n s_n$ subsidies, respectively. Since manufacturers are involved in the recycling and disassembly of power batteries, the greenness of power batteries is set to g_m . Assuming that the greenness level of batteries produced by manufacturers meets subsidy requirements, the government examines per-unit products based on the greenness of their remanufactured products. $C_r t (g_m - g)$ is the quantity of government subsidy, where t is the unit adjustment coefficient of subsidy, $t \leq 1$.

Specific notations are shown in Table 1. The superscripts "ND" and "NC" in the variables represent the decentralized and centralized decision-making models without government subsidies, respectively. In the optimal decision results, the subscripts "m," "r," and "n" represent the three main parties, the manufacturers, automobile 4S stores, and recycling networks, respectively.

4. Construction and Solution of the Dual-Channel CLSC Model under Different Strategies

Based on the operating framework of the dual-channel power battery recycling CLSC, the pricing strategies under centralized and decentralized supply chain decision-making are studied separately below. Under the decentralized decision-making model, the main parties of the supply chain aim to maximize their own profits. Under centralized decision-making, the main players of the supply chain aim to maximize the overall profit of the supply chain. The decentralized and centralized supply chain decision-makings are modelled and solved.

4.1. Decentralized Decision Model without Government Subsidy (Model ND). Under the decentralized decision-making model without government subsidies (denoted as

TABLE 1: Notations.

Notation	Definition
<i>Automobile 4S stores</i>	
p	Unit price of one new power battery
q	Consumers' demand for power batteries
q_r	Recycling quantity of used power batteries in 4S stores
p_r	The price that 4S stores pay consumers for recycling power batteries
v_r	Service level provided by 4S stores to consumers
e_r	The publicity and recycling efforts of 4S stores
μ_r	4S stores' recycling effort effect coefficient
<i>Manufacturers</i>	
C_m	Cost of new power batteries
C_r	Cost of remanufacturing power batteries
ω	Wholesale price for power batteries
p_m	The price of recycling used power batteries that manufacturers pay 4S stores and recycling networks
g_m	Greenness level of remanufactured power battery
<i>Recycling networks</i>	
p_n	The price that recycling networks pay consumers to recycle power batteries
e_n	The publicity and recycling efforts of recycling networks
μ_n	Recycling networks' recycling effort coefficient
<i>Consumer</i>	
k	Consumers' awareness of green recycling
S	Total market demand for recycling power batteries
θ	Market share of consumers' demand for recycling power batteries in the distribution channel of 4S stores
b_1	Consumers' sensitivity to recycling prices
b_2	Channel competition coefficient between 4S stores and recycling networks
ρ	The transfer coefficient of consumer demand to the difference in service level
<i>Government</i>	
s_r	The unit subsidy provided by the government to 4S stores
s_m	The unit subsidy provided by the government to manufacturers
s_n	The unit subsidy provided by the government to recycling networks
g	The minimum green level required for government subsidies
t	Government unit subsidy adjustment factor
r	Government unit subsidy coefficient

“model ND”), manufacturers, 4S stores, and recycling networks each pursue their own profit maximization. The manufacturers, 4S stores, and recycling networks play a Stackelberg game in which the manufacturers are the leader, and the 4S stores and the recycling networks are the followers. The order of decision is as follows: the manufacturers first decide the wholesale price ω and the recycling price p_m , and then, the 4S stores and the recycling networks decide the sales price p and the recycling prices p_r and p_n . At this point, the profit functions of manufacturers, 4S stores, and recycling networks are as follows:

$$\pi_m^{\text{ND}}(\omega, p_m) = (\omega - C_m)q + (C_m - C_r)(q_r + q_n) - p_m(q_r + q_n), \quad (1)$$

$$\pi_r^{\text{ND}}(p_r, p) = (p - \omega)q + (p_m - p_r)q_r - v_r^2, \quad (2)$$

$$\pi_n^{\text{ND}}(p_n) = (p_m - p_n)q_n - v_n^2. \quad (3)$$

Theorem 1. *In model ND, the optimal prices for new and remanufactured products can be calculated as follows:*

$$\begin{aligned}
\omega^{\text{ND}*} &= \frac{\alpha + \beta C_m}{2\beta}, \\
p^{\text{ND}*} &= \frac{3\alpha + \beta C_m}{4\beta}, \\
p_n^{\text{ND}*} &= \frac{B + b_1^2 b_2 (11S - 2b_2 \Delta + 10kg_m + 12A) - 2b_1^3 (-3S - b_2 \Delta - 2kg_m - 4A) + b_1 b_2^2 (-S + 2kg_m - 4A)}{4b_1 (b_1 - b_2) (4b_1^2 - b_2^2)}, \\
p_r^{\text{ND}*} &= \frac{B + b_1 b_2^2 (3S + 2kg_m + 4A) + 2b_1^3 (-S + b_2 \Delta + 2kg_m - 4A) + b_1^2 b_2 (-S - 2b_2 \Delta + 10kg_m - 12A)}{4b_1 (b_1 - b_2) (4b_1^2 - b_2^2)}, \\
p_m^{\text{ND}*} &= \frac{2b_1^3 (C_m - C_r) + b_1 b_2 (S + 2kg_m) - b_2^2 (S + 2kg_m) + b_1^2 (S - 2b_2 (C_m - C_r) + 2kg_m)}{4b_1^2 (b_1 - b_2)}.
\end{aligned} \tag{4}$$

By substituting the above optimal solution into the corresponding profit function, the optimal profits of the manufacturers, 4S stores, and recycling networks under the model ND are $\pi_m^{\text{ND}*}$, $\pi_r^{\text{ND}*}$, and $\pi_n^{\text{ND}*}$. To simplify the results, let $\rho v_n - \rho v_r - S\theta = A$ and $4b_1^4 (C_m - C_r) - b_2^3 (S + 2kg_m) = B$. Note that the proof of all theorems can be found in Appendix A, and the proof of all propositions can be found in Appendix B.

Proposition 1. *As the consumers' sensitivity coefficient of recycling prices increases, the number of used power batteries recycled by 4S stores and recycling networks both increases.*

Proposition 1 shows that the increase in the sensitivity of the recycling price has a positive feedback effect on the quantity of recycling and the profit of the supply chain. There are several reasons contributing to this conclusion. When consumers pay more attention to the recycling price level, 4S stores and recycling networks are prompted to increase recycling prices. Consequently, the recycling willingness of consumers increase and so do the recycling quantity of used power batteries.

Proposition 2. *The higher the consumers' awareness of green recycling k , the higher the recycling prices p_r and p_n paid by 4S stores and recycling networks to consumers, respectively.*

Proposition 2 shows that increased consumer awareness of green recycling will directly increase the quantity of recycled power batteries, the recycling prices, and consumers' demand for remanufactured products, stimulating manufacturers to produce power batteries. The broad market demand will also bring a higher profit space to the main players in the supply chain.

4.2. Centralized Decision Model without Government Subsidies (Model NC). Under centralized decision-making, manufacturers, 4S stores, and recycling networks are jointly pursuing the overall maximum profit of the CLSC. At this time, the total profit model is

$$\begin{aligned}
\pi^{\text{NC}}(p, p_r, p_n) &= (p - C_m)q + (C_m - C_r)(q_r + q_n) \\
&\quad - p_r q_r - p_n q_n - v_r^2 - v_n^2.
\end{aligned} \tag{5}$$

Theorem 2. *The optimal prices of model NC are as follows:*

$$\begin{aligned}
p^{\text{NC}*} &= \frac{\alpha + \beta C_m}{2\beta}, \\
p_r^{\text{NC}*} &= \frac{b_1^2 (-C_m + C_r) + b_2 (S - S\theta + b_2 (C_m - C_r) + kg_m + \rho v_n - \rho v_r) + b_1 (S\theta + kg_m - \rho v_n + \rho v_r)}{2(b_1^2 - b_2^2)}, \\
p_n^{\text{NC}*} &= \frac{b_1^2 (C_m - C_r) + b_1 (-S + S\theta - kg_m - \rho v_n + \rho v_r) - b_2 (S\theta + b_2 (C_m - C_r) + kg_m - \rho v_n + \rho v_r)}{2(b_1^2 - b_2^2)}.
\end{aligned} \tag{6}$$

The overall optimal profit $\pi^{\text{NC}*}$ of the CLSC under the model NC can be obtained by substituting the above optimal solutions in equation (5).

Proposition 3. *Whether under decentralized or centralized decision-making, when the service level difference $v_n - v_r$ increases, p_n decreases, and p_r increases.*

Proposition 3 shows that when the service level of one recycling party's increases, the party's cost of service increases; thus, the recycling price of the party decreases. Contrarily, since the service level of the other party is relatively low, it is at a competitive disadvantage; thus, the other party will increase its recycling price to improve competitive advantage and incentivize consumers to recycle power

batteries. Therefore, the increase in service level differences has opposing effects on the recycling prices of 4S stores and those of recycling networks.

4.3. Manufacturer Subsidy Strategy (Model M). This study investigates the actual background of new energy vehicle subsidies and related regulations. We found that government subsidies provided to manufacturers are closely related to the greenness levels of remanufactured power batteries produced by them. The Notice on Promoting the Application of Financial Subsidy Policies for New Energy Vehicles clearly stipulates that the fuel saving rate of plug-in hybrid electric vehicles (including extended range) must be greater than 60%. The subsidy adjustment factor for 60% to 65% fuel efficiency is 0.8, while the subsidy adjustment factor for more than 70% fuel efficiency is 1. Therefore, this study sets the government unit subsidy coefficient as $r = t(g_m - g)$, where

t is the unit subsidy adjustment coefficient factor, $t \leq 1, r \geq 0$. Therefore, the unit remanufactured power battery subsidy quantity is $C_r t(g_m - g)$. At this time, the profit functions of the manufacturers, the 4S stores, and the recycling networks are

$$\begin{aligned} \pi_m^M(\omega, p_m, t) &= (\omega - C_m)q + (C_m - C_r - p_m)(q_r + q_n) \\ &\quad + C_r t(g_m - g)(q_r + q_n), \end{aligned} \quad (7)$$

$$\pi_r^M(p_r, p) = (p - \omega)q + (p_m - p_r)q_r - v_r^2, \quad (8)$$

$$\pi_n^M(p_n) = (p_m - p_n)q_n - v_n^2. \quad (9)$$

Theorem 3. *The optimal solutions of model M are as follows:*

$$\begin{aligned} p^{M*} &= \frac{3\alpha + \beta C_m}{4\beta}, \\ \omega^{M*} &= \frac{\alpha + \beta C_m}{2\beta}, \\ p_m^{M*} &= \frac{-Sb_1^2 - Sb_1b_2 + Sb_2^2 - 2kb_1^2g_m - 2kb_1b_2g_m + 2kb_2^2g_m}{2b_1^2(b_2 - b_1)}, \\ t_m^{M*} &= \frac{Sb_1^2 + Sb_1b_2 - Sb_2^2 - 2b_1^3C_m + 2b_1^2b_2C_m + 2b_1^3C_r - 2b_1^2b_2C_r + 2kb_1^2g_m + 2kb_1b_2g_m - 2kb_2^2g_m}{2b_1^2(b_2 - b_1)C_r(g - g_m)}, \\ p_n^{M*} &= \frac{b_2^2(S + 2kg_m) + b_1b_2(3S - 2S\theta + 4kg_m + 2\rho v_n - 2\rho v_r) + b_1^2(-S + 2S\theta - 2\rho v_n + 2\rho v_r)}{2b_1(b_1 - b_2)(2b_1 + b_2)}, \\ p_r^{M*} &= \frac{b_2^2(S + 2kg_m) + b_1^2(S - 2S\theta + 2\rho v_n - 2\rho v_r) + b_1b_2(S + 2S\theta + 4kg_m - 2\rho v_n + 2\rho v_r)}{2b_1(b_1 - b_2)(2b_1 + b_2)}. \end{aligned} \quad (10)$$

By substituting the above optimal solution into the corresponding profit function, the optimal profits of the manufacturers, 4S stores, and recycling networks under model M are π_m^{M*} , π_r^{M*} , and π_n^{M*} .

Proposition 4. *When the greenness level g_m of power batteries produced by manufacturers increases, the unit subsidy adjustment coefficient factor t increases. Accordingly, the government unit subsidy coefficient r and the government unit subsidy quantity also increase.*

Proposition 4 shows that when the greenness level of power batteries increases, the government increases the unit subsidy adjustment factor for manufacturers accordingly, encouraging manufacturers to pay attention to the greenness level of power batteries in future production. Therefore, promoting the greenness level of power batteries increases consumers'

purchasing demand for power batteries, enhancing the environmental protection of the CLSC and society.

4.4. Automobile 4S Stores Subsidy Strategy (Model R). In response to the national call on the recycling of power batteries of new energy vehicles, 4S stores encourage consumers to recycle used power batteries by using publicity or feedback surveys. Therefore, the recycling quantities of 4S stores and recycling networks are $q_r^R = \theta S - b_2 p_n + b_1 p_r + \rho(v_r - v_n) + kg_m + \mu_r e_r$ and $q_n^R = (1 - \theta)S - b_2 p_r + b_1 p_n + \rho(v_n - v_r) + kg_m - \mu_r e_r$. Here, e_r stands for the recycling effort of the 4S stores, and μ_r stands for the effect of the recycling effort of the 4S stores on recycling quantities, which also is known as the recycling effort effect coefficient. Previous relevant literature [24] found that the recycling

effort cost of 4S stores was e_r^2 . Therefore, the profit function of manufacturers, 4S stores, and recycling networks is

$$\pi_m^R(\omega, p_m) = (\omega - C_m)q + (C_m - C_r)(q_n^R + q_r^R) - p_m(q_n^R + q_r^R), \quad (11)$$

$$\pi_r^R(p_r, p, s_r, e_r) = (p - \omega)q + (p_m - p_r)q_r^R + e_r s_r - e_r^2 - v_r^2, \quad (12)$$

$$p_m^{R*} = \frac{S - 2b_1(C_m - C_r) + 2b_2(C_m - C_r) - 2kg_m}{4(b_2 - b_1)},$$

$$\omega^{R*} = \frac{\alpha + \beta C_m}{2\beta},$$

$$p^{R*} = \frac{3\alpha + \beta C_m}{4\beta},$$

$$p_n^{R*} = \frac{4b_1^3\Delta + b_1b_2(7S - 2b_2\Delta - 12\mu e_r + 2kg_m + 12A) + 4b_2^2(\mu e_r + kg_m - A) + 2b_1^2(-5S - b_2\Delta + 4\mu e_r - 6kg_m - 4A)}{4(b_1 - b_2)(4b_1^2 - b_2^2)},$$

$$p_r^{R*} = \frac{4b_1^3\Delta + 4b_2^2(S - \mu e_r + kg_m + A) - 2b_1^2(S + b_2\Delta + 4\mu e_r + 6kg_m - 4A) + b_1b_2(-5S - 2b_2\Delta + 12\mu e_r + 2kg_m - 12A)}{4(b_1 - b_2)(4b_1^2 - b_2^2)},$$

$$s_r^{R*} = \frac{S\mu_r b_1 - 2S\theta\mu_r b_1 + 2\mu_r \rho b_1(v_n - v_r)}{-(2b_1 + b_2)^2},$$

$$e_r^{R*} = \frac{\mu_r b_2(S - 2S\theta + 2\rho v_n - 2\rho v_r)}{2(\mu_r^2 - 4b_1 - 2b_2)(2b_1 + b_2)}.$$

(14)

Plugging the above optimal solution into the corresponding profit function, the optimal profit of manufacturers, 4S stores, and recycling networks under the model R is π_m^{R*} , π_r^{R*} and π_n^{R*} .

Proposition 5. As k increases, p_m^{R*} increases accordingly.

Proposition 5 shows that, as consumers' awareness of green recycling increases, manufacturers' recycling prices of used power batteries increases. This indicates that increasing consumers' awareness of green recycling promotes the recycling quantity of power batteries, which influences the entire supply chain and the social environment in a positive way.

Proposition 6. As e_r^{R*} increases, p_r^{R*} decreases and p_n^{R*} increases.

Proposition 6 shows that, under the model R, due to the 4S stores' publicity and advertising, a certain cost of recycling effort is generated, and the quantity of recycling increases. Accordingly, the recycling price decreases, and recycling networks, in order to compete with 4S stores for more customers, tend to increase its own recycling price to incentivize consumers to recycle used power batteries.

4.5. Recycling Network Subsidy Strategy (Model N). On March 2, 2018, seven ministries and commissions, including

$$\pi_n^R(p_n) = (p_m - p_n)q_n^R - v_n^2. \quad (13)$$

Theorem 4. The optimal solutions of model R are as follows:

the Ministry of Industry and Information Technology of China, jointly issued the Implementation Plan for the Pilot Implementation of New Energy Vehicle Power Battery Recycling, which stipulated that the Beijing-Tianjin-Hebei, Yangtze River Delta, and Central Regions will be selected to launch new projects. The pilot work on the recycling and utilization of energy batteries for energy vehicles will currently focus on the pilot area but will expand to surrounding areas in the future. This paper combines policy requirements and realistic backgrounds, uses e_n to indicate the degree of recycling efforts of recycling networks, and uses μ_n to indicate the influence of the recovery effort on recycling quantity, which is also known as the recycling effort effect coefficient. e_n^2 is the cost of recycling effort of networks. Therefore, the recycling quantity of recycling networks and 4S stores is $q_n^N = (1 - \theta)S - b_2 p_r + b_1 p_n + \rho(v_n - v_r) + kg_m + \mu_n e_n$ and $q_r^N = \theta S - b_2 p_n + b_1 p_r + \rho(v_r - v_n) + kg_m - \mu_n e_n$. Therefore, the profit functions of manufacturers, 4S stores, and recycling networks are

$$\pi_m^N(\omega, p_m) = (\omega - C_m)q + (C_m - C_r)(q_n^N + q_r^N) - p_m(q_n^N + q_r^N), \quad (15)$$

$$\pi_r^N(p_r, p) = (p - \omega)q + (p_m - p_r)q_r^N - v_r^2, \quad (16)$$

$$\pi_n^N(p_n, s_n, e_n) = (p_m - p_n)q_n^N + e_n s_n - e_n^2 - v_n^2. \quad (17)$$

Theorem 5. *The optimal solutions of model N are as follows:*

$$\begin{aligned}
 \omega^{N*} &= \frac{\alpha + \beta C_m}{2\beta}, \\
 p^{R*} &= \frac{3\alpha + \beta C_m}{4\beta}, \\
 p_m^{N*} &= \frac{S - 2b_1(C_m - C_r) + 2b_2(C_m - C_r) - 2kg_m}{4(b_2 - b_1)}, \\
 e_n^{N*} &= \frac{(b_2 - b_1)(2b_1 + b_2)\mu_n}{2(2b_1 - b_2)(4b_1 + 2b_2 + \mu_n^2)}, \\
 s_n^{N*} &= \frac{(-4b_1^2\Delta + 2b_1(4C + S + \Delta b_2 - 2kg_m) + b_2(-4C - 3S + 2b_2\Delta - 2kg_m))\mu_n}{16b_1^2 - 4b_2^2}, \\
 p_r^{N*} &= \frac{4b_1^3\Delta + 2b_1^2(-5S - b_2\Delta - 6kg_m - 4(C + e_n\mu_n))}{4(b_1 - b_2)(4b_1^2 - b_2^2)} + \frac{4b_2^2(kg_m - A - e_n\mu_n) + b_1b_2(7S - 2b_2\Delta + 2kg_m + 12(A + e_n\mu_n))}{4(b_1 - b_2)(4b_1^2 - b_2^2)}, \\
 p_n^{N*} &= \frac{4b_1^3\Delta + b_1b_2(-5S - 2b_2\Delta + 2kg_m - 12(A + e_n\mu_n))}{4(b_1 - b_2)(4b_1^2 - b_2^2)} + \frac{2b_1^2(-S - b_2\Delta - 6kg_m + 4(A + e_n\mu_n)) + 4b_2^2(S + kg_m + A + e_n\mu_n)}{4(b_1 - b_2)(4b_1^2 - b_2^2)}.
 \end{aligned} \tag{18}$$

By substituting the above optimal solution into the corresponding main body profit function, the optimal profits of manufacturers, 4S stores, and recycling networks under the model N are π_m^{N*} , π_r^{N*} , and π_n^{N*} .

Proposition 7. *As g_m rises, p_m^{N*} increases.*

Proposition 7 shows that, as the greenness level of remanufactured power batteries increases, the greenness of the entire power battery CLSC increases. The greenness level of the recycling power batteries will thus be relatively high, so, in the reverse supply chain, manufacturers increase recycling prices.

5. Numerical Simulation

The former sections show the research and comparative analysis of the theoretical model for the dual-channel CLSC under different models, the equilibrium solutions in different situations, and several management enlightenments. Since some of the analytic solutions above are complicated, the conclusions are verified visually through numerical examples in this section. First, by comparing the five decision models in Section 4, the effectiveness analysis is performed on optimal recycling prices and profits. The sensitivity analysis is then used to study the influence of consumers' green recycling awareness k on recycling prices. The influence of the greenness of power battery g_m on the recycling prices is also analyzed and so is the impact of recycling efforts e_r and e_n and the level of service s_r and s_n on the pricing of 4S stores and recycling networks. In addition, we studied the literature related to this research [25] and combined it with the current status of the development of

new energy vehicles in China in order to better analyze and elaborate upon management implications. By combining theoretical research with the practical conditions, we assume $C_m = 10$, $C_r = 5$, $\alpha = 100$, $\beta = 2$, $\rho = 1$, $v_n = 3$, $v_r = 6$, $k = 0.5$, $S = 200$, $\theta = 0.6$, and $b_1, b_2 \in [0, 1]$.

5.1. Comparative Analysis of Optimal Prices under Different Strategies. From Table 2, the following conclusions can be obtained: (1) in the two models without government subsidies, the optimal recycling prices p_r and p_n under a decentralized model are smaller than the corresponding optimal recycling prices under a centralized model. This is because, under decentralized decision-making, each entity pursues the maximization of its own profits, which leads to the loss of profit in CLSC. (2) In all strategies, the sales price of remanufactured power batteries does not change, and in all decentralized models, the wholesale price of remanufactured power batteries also does not change, which indicates that the government's subsidies provided to the entities in the recycling link have nothing to do with the prices in the sales link. (3) In all decentralized models, p_r , p_n , and p_m are relatively high in model M, benefiting all members of the supply chain and stimulating the prosperity of the new energy vehicle industry. This is because the subsidies provided by the manufacturers have an incentive effect on the recycling of the downstream enterprises. The increase in the greenness level of power batteries is conducive to promoting the recycling of used power batteries, which increases the recycling quantity that 4S stores and recycling networks obtained. When the

TABLE 2: Comparison of optimal prices under different strategies.

Optimal price	Model ND	Model NC	Model M	Model R	Model N
p_r	184.30	260.91	195.08	194.53	228.62
p_n	197.59	249.09	205.48	217.47	218.37
p_m	291.76	\	302.01	260.61	260.61
ω	30	\	30	30	30
p	40	40	40	40	40

government increases subsidies, manufacturers can make higher profits; thus, more money is spent on the dismantling and remanufacturing of power batteries, promoting the long-term development of the new energy industry.

5.2. Sensitivity Analysis

5.2.1. Consumer Green Recycling Awareness k and Power Battery Greenness Level g_m . It can be seen from Figure 2 that, as consumers' awareness of green recycling k increases, p_r , p_n , and p_m increase. Take the optimal solutions of the model D. From the perspective of consumers, the rising recycling awareness of consumers means that they prefer to buy green batteries. Since there is more dismantling and remanufacturing value in the recycling process of green batteries, 4S stores and recycling networks will offer higher recycling prices than for batteries that are not green. Therefore, when the consumers' awareness of recycling is improving, the greater the proportion of green batteries among power batteries in the CLSC, the higher the recycling prices. In addition, from the perspective of the manufacturers, according to the increase in recycling prices p_r , p_n , and p_m due to the selected set of greenness levels $g_m \in \{3, 5, 7\}$, when consumers have the same awareness of recycling, the greater the proportion of green batteries among power batteries, the higher the corresponding recycling prices. In summary, from the manufacturers' perspective, manufacturers should proactively improve the greenness of power batteries, increase environmental consciousness, and promote the recycling of power batteries in the recycling process. From the consumers' perspective, increasing the awareness of green recycling is not only more economical and environmentally friendly for consumers who use new energy vehicles but also conducive to promoting the sales of new energy vehicles with high green levels. As a result, economic efficiency and environmental indicators will both increase in the entire CLSC.

5.2.2. Recycling Effort e_n and e_r . From Figure 3, as the 4S stores' recycling effort e_r increases, the recycling price p_r decreases, while that of its competitive channel recycling

networks increase. This is because the more the 4S stores' recycling effort, the higher the cost of its recycling effort. At the same time, the improvement of the recycling effort of 4S stores directly increases the recycling quantity; thus, the recycling prices of them decrease accordingly. On the contrary, the recycling networks compete with 4S stores for customers and will increase their recycling prices to incentivize consumers to recycle used power batteries there. Correspondingly, the impact of the recycling effort e_n of the recycling networks on the recycling prices work in the same way. Since the financial resources of recycling companies are always limited, the financial status of different recycling companies is often quite different. Although when enterprises have high levels of recycling efforts, there will be higher government subsidies. However, the cost of recycling efforts will also rise. Recycling companies are advised to balance the relationship between the level of recycling efforts and the quantity of subsidies. While ensuring a certain level of effort, they must also consider the rising costs due to the increase in the quantity of recycling.

5.2.3. Service Level v_r and v_n . As can be seen from Figures 4(a) and 4(b), when a service level rises, this party's recycling price decreases accordingly because a higher service level increases the party's service cost. However, the other party, since they have a relatively low service level and are at a competitive disadvantage, intends to increase their recycling price to improve some competitiveness in order to incentivize consumers to recycle used power batteries there. Thus, the recycling price of one party is inversely related to the service level of the other party.

From Figures 4(c) and 4(d), when the service level of one party increases, the profit of that party first increases and then decreases. For 4S stores and recycling networks in the CLSC, when the service level increases from 0 to a certain level, their profits have a positive correlation with the service level. This is because the improvement in service level attracts more consumers; thus, the recycling quantity of this party increases, and the increase in revenue due to the increase in recycling quantity is greater than the cost caused by the increase in service level. However, when the service level increases to a certain level, and the party's profit reaches its

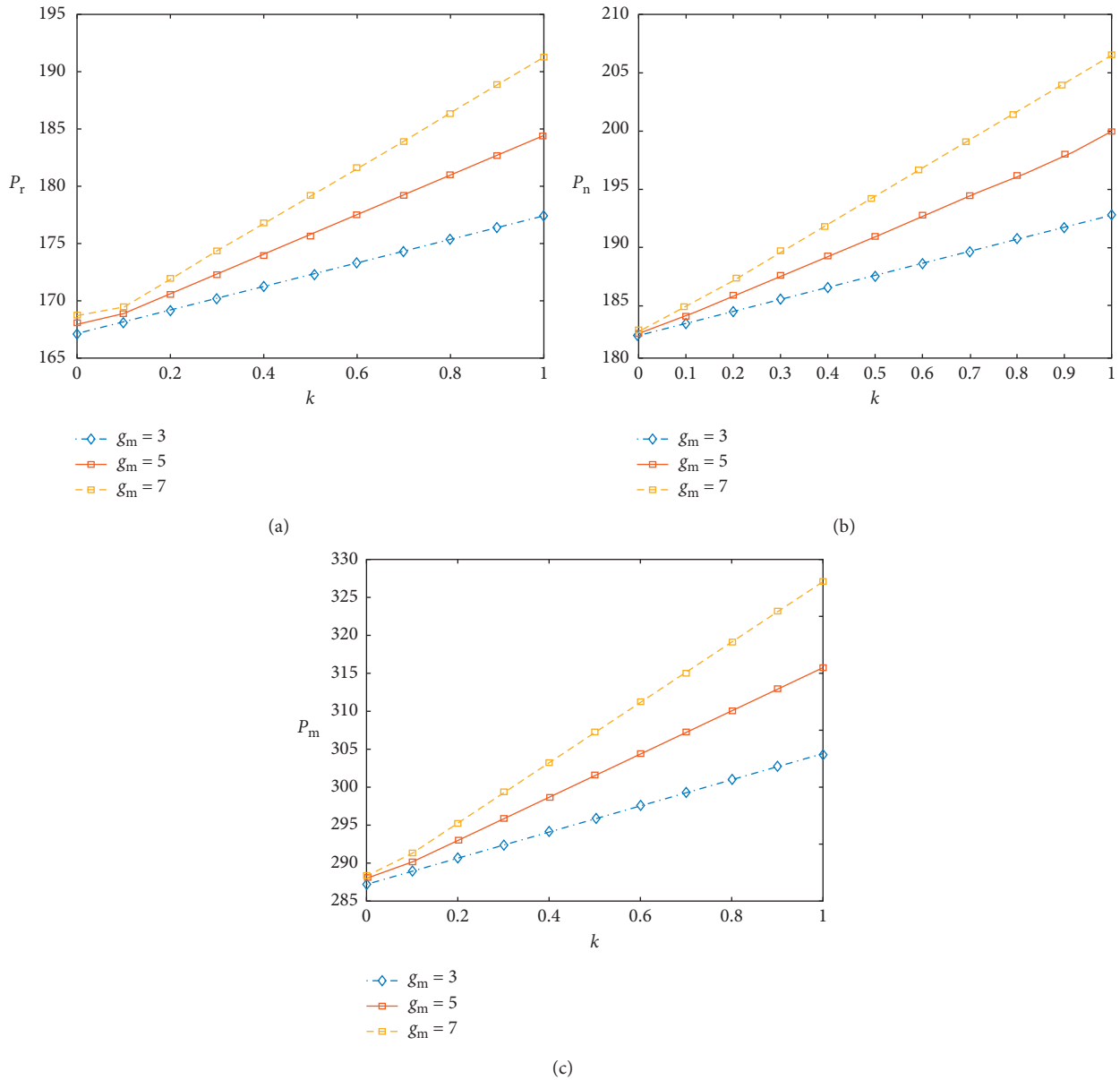


FIGURE 2: Impact of consumers' green recycling consciousness k and power battery greenness g_m on recycling prices p_r , p_n , and p_m : (a) the influence of consumers' green recycling consciousness k on recycling price p_r ; (b) the influence of consumers' green recycling consciousness k on recycling price p_n ; (c) the influence of consumers' green recycling consciousness k on recycling price p_m .

maximum, the profits of recycling parties will show a downward trend. At this time, the cost will be greater than the increase in revenue caused by a rise in demand. This brings us certain management inspiration: in the process of power battery recycling, enterprises should maintain an appropriate

service level in the light of the industry environment and their own actual conditions and take into account the cost due to the rising service level. It is inadvisable to only maintain the service level promotion blindly and neglect the balance between service level and the service level cost.

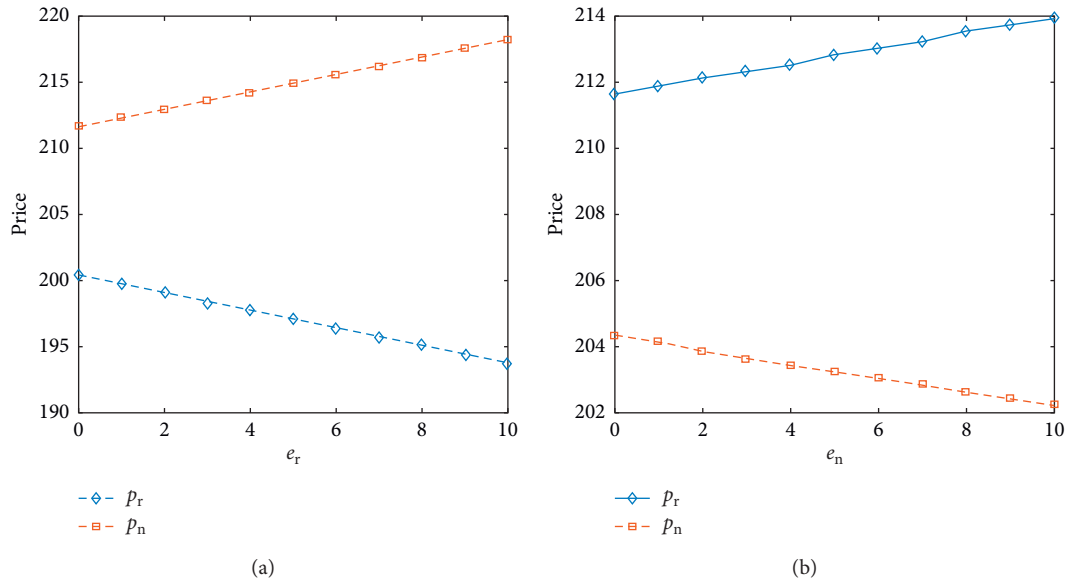


FIGURE 3: Impact of recycling effort e_n and e_r on recycling prices p_r and p_n : (a) the influence of recycling effort e_r on recycling prices p_r and p_n ; (b) the influence of recycling effort e_n on recycling prices p_r and p_n .

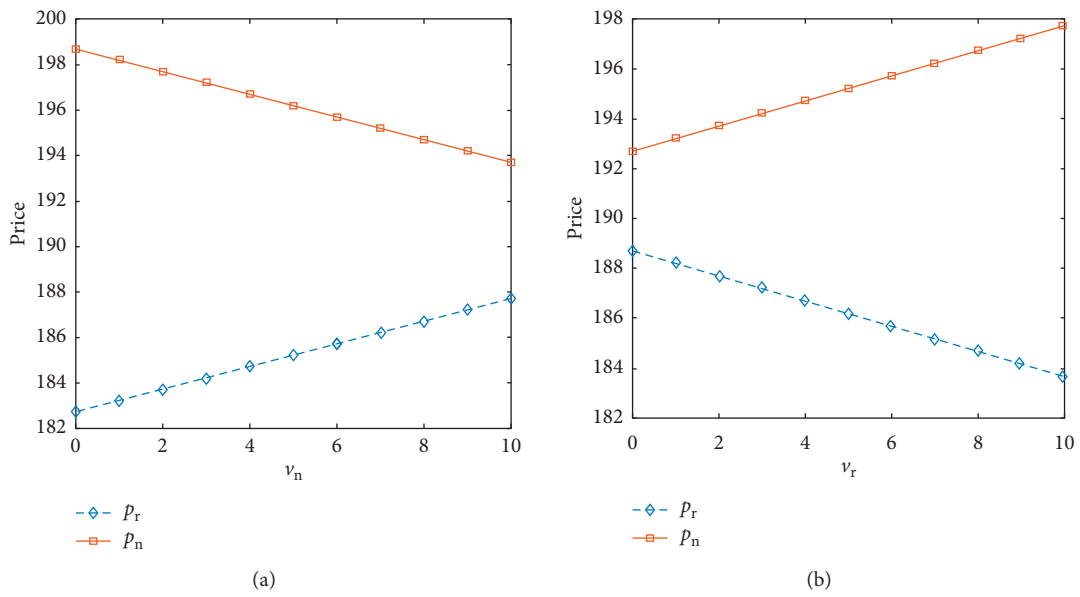


FIGURE 4: Continued.

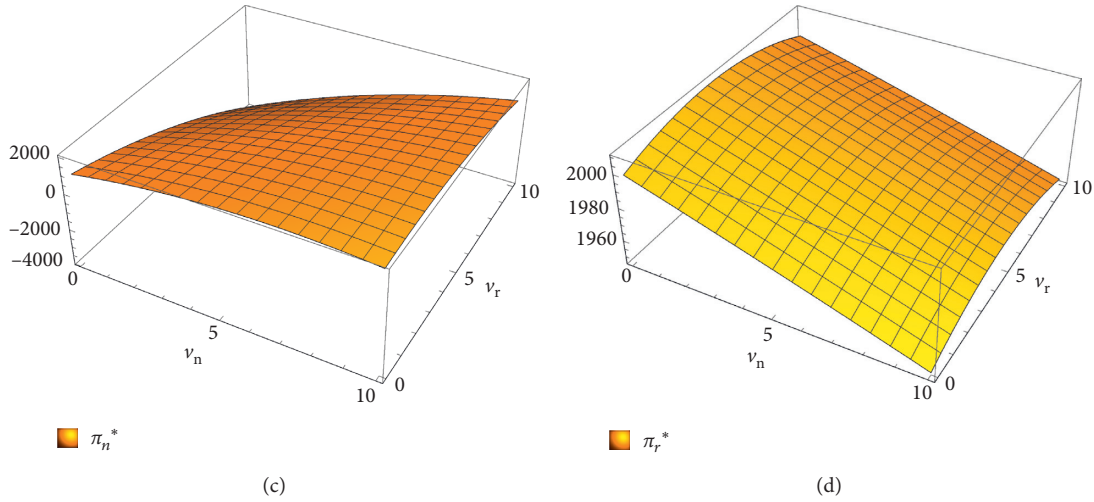


FIGURE 4: Impact of service level v_n and v_r on pricing and profit of recycling networks and automobile 4S stores: (a) the influence of recycling effort v_n on recycling prices p_r and p_n ; (b) the influence of recycling effort v_r on recycling prices p_r and p_n ; (c) the influence of recycling efforts v_n and v_r on the profit of automobile 4S stores; (d) the influence of recycling efforts v_n and v_r on the profit of recycling networks.

6. Conclusion

This paper studies the price structure and profit situation of the recycling of waste power batteries in a CLSC without government subsidies and with subsidies for each party. By introducing the recycling effort, product green levels, service levels, and consumer green awareness, the optimal price structure of each party under different models is solved, the influences of each factor on the recycling prices of power battery are analyzed, and the optimal prices under different strategies are compared. The conclusions are as follows:

- (1) In the five dual-channel models, when the government subsidizes the manufacturers, the recycling price of each main party of the supply chain is relatively high. Firstly, since the manufacturer is the first mover in the Stackelberg model game and 4S stores and recycling networks are followers, manufacturers often enjoy the first mover advantage. When there are preferential subsidy policies provided by the government, the first mover advantage is relatively obvious. Secondly, from the perspective of the recycling link of the supply chain, when subsidies are given to manufacturers, the recycling prices given by manufacturers to 4S stores and recycling networks will increase significantly compared with other subsidy policies. In this way, the recycling prices given to consumers by 4S stores and recycling networks will also increase to a certain extent. The manufacturer-subsidy strategy greatly promotes the recycling of waste power batteries by consumers. Consumers are thus willing to recycle, which increases the recycling number of waste power batteries. Thirdly, from the perspective of the sales link of the supply chain, although the government does not subsidize the sales link, due to the large number of recycled waste power batteries and the

fast turnover of the supply chain, the stock of remanufactured power batteries is sufficient, and the development of the new energy automobile industry is promoted.

- (2) The recycling price of each recycling party in the supply chain has positive correlations with the green recycling awareness of consumers and the green level of power batteries. When consumers are more aware of green recycling, they are more inclined to buy new energy vehicles with high green levels and actively recycle waste power batteries. Therefore, in the recycling process, waste power batteries with high green levels account for a relatively high proportion and are more valuable for disassembly and remanufacturing. Thus, the recycling prices given by 4S stores, recycling networks, and manufacturers can increase. This brings certain management enlightenments to recycling enterprises: we should encourage consumers to recycle power batteries, popularize the economic and environmental benefits of green products, and strive to enhance consumers' awareness of green recycling. For manufacturers, it is necessary to improve their green level in the process of power battery remanufacturing to promote the overall benefits of the CLSC.
- (3) Recycling enterprises should pay attention to balance the cost due to recycling efforts and the quantity of government subsidies and then make appropriate recycling efforts according to their economic actual situation. With improvements in recycling efforts, government subsidies given to 4S stores or recycling networks will increase, however, at the same time, so will the cost of recycling efforts. At this time, enterprises need to choose their own operation strategies according to their own financial situation and development space. It is advised to maintain

recycling efforts and government subsidies while ensuring appropriate recycling prices.

- (4) Service level is an important factor to be considered for recycling enterprises. Maintaining an appropriate service level has a positive impact on the development of enterprises. Too high or too low service levels will damage the profits of enterprises. When the service level is improved, there will be two impacts: an increase in service level cost and an increase in recycling quantity. When the increase in revenue due to the increase in recycling quantity is greater than the increase in cost due to the service level, an increase in the service level results in increased profits for the enterprise. On the contrary, when the increase in revenue due to the increase in recycling quantity is smaller than the increase in cost due to the service level, an increase in service level results in decreased profits for enterprises. Consequently, in the process of recycling power batteries, enterprises should maintain an appropriate service level in combination with the industry environment and their own actual situation and take into account the cost due to the rise of service level. It is not advised to just maintain the improvement of service level and subsequently ignore the balance between service level and service level costs.
- (5) The main management implications of this paper are as follows: first, for manufacturers who enjoy a first-mover advantage in the supply chain, government subsidies provided to them can greatly stimulate the quantity of power battery recycling and have a greater positive incentive effect on the remanufacturing industry chain. In the case of limited government subsidies, subsidies to manufacturers is a better choice. Second, it is urgent for recycling enterprises and environmental management departments to build a complete recycling network system together. In combination with the local economic development level, battery production and recycling, and other specific conditions, policies conducted to encourage consumers' recycling should be adjusted and refined. Measures such as repurchase and trade-in can be adopted to improve the enthusiasm of users to hand over waste power batteries. From the aspect of product quality, manufacturers should improve the greenness level of power batteries in order to innovate consumers to recycle. Third, in terms of the service level and recycling efforts of recycling enterprises, enterprises should maintain certain recycling efforts and service levels to improve their competitive advantages. However, excessive improvement will aggravate the competition, and vicious service competition will cause damage to the benefits of enterprises and the supply chain, which is not conducive to the long-term development of recycling enterprises. Additionally, enterprises should consider the cost caused by the increase in recycling efforts and service level and

weigh the input of both according to their own economic level, recycling, and operation capacity.

Appendix

A. Theorems

Proof of Theorem 1. The backward induction was used to solve the model. First, the first-order partial derivative of π_r^{ND} with respect to p and p_r and the first-order partial derivative of π_n^{ND} with respect to p_n are obtained; their equations can be obtained by setting their partial derivatives equal to 0 in parallel: $p^{ND} = (\alpha + \beta\omega)/2\beta$, $p_r^{ND} = (-S\theta - kg_m + b_1p_m + b_2p_n + \rho v_n - \rho v_r)/2b_1$, and $p_n^{ND} = (-S + S\theta - kg_m + b_1p_m + b_2p_r - \rho v_n + \rho v_r)/2b_1$. According to equation (2), the Hessian matrices can be easily solved as follows:

$$H(p_r, p) = \begin{pmatrix} -2\beta & & & \\ & 0 & & \\ & & 0 & \\ & & & -2b_1 \end{pmatrix}. \quad (A.1)$$

According to the assumptions, $\beta > 0$ and $b_1 > 0$. Thus, the Hessian matrix of π_r^{ND} is negative, which means that π_r^{ND} is a strictly concave function concerning p_r and p . p_n is the only variable in equation (3). Consequently, the optimal equilibrium solutions of the two equations are unique.

Plugging p^{ND} , p_r^{ND} , and p_n^{ND} into equation (1), the derivatives of π_m^{ND} with respect to ω and p_m are, respectively, obtained. According to equation (1), the Hessian matrix can be easily solved:

$$H(p_m, \omega) = \begin{pmatrix} \frac{\beta}{2} & 0 \\ 0 & b_2 - b_1 \end{pmatrix}. \quad (A.2)$$

According to the assumptions, $\beta > 0$ and $b_1 > b_2$. Thus, the Hessian matrix of π_m^{ND} is negative, which means that π_m^{ND} is a strictly concave function concerning ω and p_m , and the optimal equilibrium solutions of the equation are unique. Then, the optimal solutions p_m^{ND*} and ω^{ND*} can be solved.

By substituting p_m^{ND*} and ω^{ND*} into p_r^{ND} , p^{ND} , and p_n^{ND} , the optimal solutions p_r^{ND*} , p^{ND*} , and p_n^{ND*} can be obtained. \square

Proof of Theorem 2. First, the derivatives of π^{NC} with respect to p , p_r , and p_n were, respectively, obtained.

According to equation (5), the Hessian matrix can be easily solved as follows:

$$H(p, p_r, p_n) = \begin{pmatrix} -2\beta & 0 & 0 \\ 0 & -2b_1 & 2b_2 \\ 0 & 2b_2 & -2b_1 \end{pmatrix}. \quad (A.3)$$

According to the assumptions, $\beta > 0$ and $b_1 > b_2 > 0$. Then, $H_1 < 0$, $H_2 > 0$, and $H_3 < 0$. Thus, the Hessian matrices of π^{NC} is negative, which means that π^{NC} is a strictly concave

function concerning p , p_r , and p_n . Then, the unique optimal solutions can be solved. \square

Proof of Theorem 3. The method used is consistent with the above models. First, derive π_r^M with respect to p and p_r and derive π_n^M with respect to p_n ; then, make all equations equal to 0. The equations can be solved: $p^M = (\alpha + \beta\omega)/2\beta$, $p_r^M = (-S\theta - kg_m + b_1p_m + b_2p_n + \rho v_n - \rho v_r)/2b_1$ and $p_n^M = (-S + S\theta - kg_m + b_1p_m + b_2p_r - \rho v_n + \rho v_r)/2b_1$:

$$H(\omega, p_m, t) = \begin{pmatrix} -\beta & 0 & 0 \\ -\beta & 0 & 0 \\ 0 & \frac{4(b_2 - b_1)}{2b_1 - b_2} \frac{C_r(g_m - g)(2b_1^3 - b_1)}{b_1(2b_1 - b_2)} \end{pmatrix}. \quad (\text{A.4})$$

According to the assumptions, $\beta > 0, b_1 > b_2 > 0, C_r > 0$, and $g_m > g$. Then, $H_1 < 0, H_2 > 0$, and $H_3 < 0$. The Hessian matrices of equations (7)–(9) remain negative, and optimal solutions of model M are unique. Plugging p^M, p_r^M , and p_n^M into equation (7), the derivatives of π_m^M with respect to ω, p_m , and t are, respectively, obtained. Then, the optimal solutions p_m^{M*}, ω^{M*} , and t^{M*} can be solved. By substituting p_m^{M*} and ω^{M*} into p, p_r , and p_n , the optimal solutions p^{M*}, p_n^{M*} , and p_r^{M*} can be solved as well. \square

Proof of Theorem 4. The backward induction was used to solve the model. First, the first-order partial derivative of π_r^R with respect to p and p_r and the first-order partial derivative of π_n^R with respect to p_n are obtained, and their equations can be obtained by setting the partial derivatives equal to 0 in parallel:

$$H(p, p_r, s_r, e_r) = \begin{pmatrix} -2\beta & 0 & 0 & 0 \\ 0 & -2b_1 & -\mu_r & 0 \\ 0 & -\mu_r & -2 & 1 \\ 0 & 0 & 1 & 0 \end{pmatrix}. \quad (\text{A.5})$$

According to the assumptions, $\beta > 0$ and $b_1 > b_2 > 0$. Then, $H_1 < 0, H_2 > 0, H_3 < 0$, and $H_4 > 0$. Similar to the previous section, the optimal solutions of equations (11)–(13) are unique since the Hessian matrices are negative. Then, the following solutions can be solved: $p^R = (\alpha + \beta\omega)/2\beta$, $p_r^R = (-S\theta - \mu e_r - kg_m + b_1p_m + b_2p_n + \rho v_n - \rho v_r)/2b_1$, and $p_n^R = (-S + S\theta + \mu e_r - kg_m + b_1p_m + b_2p_r - \rho v_n + \rho v_r)/2b_1$.

Substituting p^R, p_r^R , and p_n^R into equation (11), the derivatives of π_m^R concerning ω and p_m are, respectively, obtained. Then, the optimal solutions p_m^{R*} and ω^{R*} can be solved. By substituting p_m^{R*} and ω^{R*} into p, p_r , and p_n , the optimal solutions p^{R*}, p_n^{R*} , and p_r^{R*} can be solved as well. Finally, we took the derivatives of π_r^R concerning s_r and e_r , respectively. The optimal solutions of model R can be solved. \square

Proof of Theorem 5. The first-order partial derivative of π_r^N with respect to p and p_r and the first-order partial derivative

of π_n^N with respect to p_n are obtained, and then, their equations can be obtained by setting the partial derivatives equal to 0 in parallel:

$$H(\omega, p_m, t) = \begin{pmatrix} \frac{2b_2^2 - 4b_1^2}{2b_1} & \frac{\mu_n(b_2 - 2b_1)}{2b_1} & 0 \\ \mu_n\left(\frac{b_2}{2b_1} - 1\right) & -2 & 1 \\ 0 & 1 & 0 \end{pmatrix}. \quad (\text{A.6})$$

According to the assumptions, $\beta > 0, b_1 > b_2 > 0, C_r > 0$, and $g_m > g$. Then, $H_1 < 0, H_2 > 0$, and $H_3 < 0$. The Hessian matrices of equations (15)–(17) are negative, and the optimal solutions of them are unique. Then, the optimal solutions of the simultaneous equations are $p^N = (\alpha + \beta\omega)/2\beta$, $p_n^N = (-S + S\theta - kg_m + b_1p_m + b_2p_r - \rho v_n + \rho v_r - e_n\mu_n)/2b_1$, and $p_r^N = (-S\theta - kg_m + b_1p_m + b_2p_n + \rho v_n - \rho v_r + e_n\mu_n)/2b_1$.

Plugging p^N, p_r^N , and p_n^N into equation (15), the derivatives of π_m^N with respect to ω and p_m are, respectively, obtained. Then, the optimal solutions p_m^{N*} and ω^{N*} can be solved. By substituting p_m^{N*} and ω^{N*} into p, p_r , and p_n , the optimal solutions p^{N*}, p_n^{N*} , and p_r^{N*} can be solved as well. Finally, plugging p^{N*}, p_r^{N*} , and p_n^{N*} into equation (17), we took the derivatives of π_n^N concerning s_n and e_n , respectively. The optimal solutions of model N can be solved. \square

B. Propositions

Proof of Proposition 1. $\partial q_r/\partial b_1 = p_r > 0, \partial q_n/\partial b_1 = p_n > 0$, and it can be evidently found that q_r and q_n are increasing functions concerning b_1 . \square

Proof of Proposition 2. $\partial p_r/\partial k = (4b_1^3g_m + 10b_1^2b_2g_m + 2b_1b_2^2g_m + 2b_2^3g_m)/(4b_1(b_1 - b_2)(4b_1^2 - b_2^2))$, and $\partial p_n/\partial k = (2b_1b_2^2g_m + 2b_2^3g_m + 4b_1^3g_m + 10b_1^2b_2g_m)/(4b_1(b_1 - b_2)(4b_1^2 - b_2^2))$. It can be evidently found that $\partial p_r/\partial k, \partial p_n/\partial k > 0$. Proposition 2 is proved. \square

Proof of Proposition 3. According to assumptions, $b_1 > b_2$, $\partial p_r/(\partial(v_n - v_r)) = \partial p_n/(\partial(v_n - v_r)) = (8\rho b_1^3 - 12\rho b_1^2b_2 + 4\rho b_1b_2^2)/(4b_1(b_1 - b_2)(4b_1^2 - b_2^2)) = \rho/(2b_1 + b_2) > 0$. $\partial p_n/(\partial(v_n - v_r)) = (-\rho b_1 + \rho b_2)/(2(b_1^2 - b_2^2)) < 0$. Proposition 3 is proved. \square

Proof of Proposition 4. $\partial t/\partial g_m = (-(2gk + S)b_1b_2 + (2gk + S)b_2^2 - b_1^2(-2gk + S + 2b_2(C_m - C_r)) + 2b_1^2(C_m - C_r))/(2b_1^2(b_1 - b_2)C_r(g - g_m)^2) = ((2gk + S)(b_2^2 + b_1^2 - b_1b_2) + (2b_1^3 - 2b_1^2b_2)(C_m - C_r))/(2b_1^2(b_1 - b_2)C_r(g - g_m)^2)$. Since $b_1 > b_2$ and $b_2^2 + b_1^2 - b_1b_2 > 0$, $\partial t/\partial g_m > 0$. According to the government unit subsidy coefficient $r = t(g_m - g)$, r will also increase as g_m and t both rise. \square

Proof of Proposition 5. Since $\partial p_m^{R*}/\partial k = kg_m/(2(b_1 - b_2)) > 0$, Proposition 5 is proved. \square

Proof of Proposition 6. According to assumptions, $b_1 > b_2$, then $\partial p_r^{R^*} / \partial e_r = (4\mu b_2^2 - 8\mu b_1^2 + 12\mu b_1 b_2) / (4(b_1 - b_2)(4b_1^2 - b_2^2)) < 0$ and $\partial p_n^{R^*} / \partial e_r = (4\mu b_2^2 + 8\mu b_1^2 + 12\mu b_1 b_2) / (4(b_1 - b_2)(4b_1^2 - b_2^2)) > 0$. \square

Proof of Proposition 7. $b_1 > b_2 > 0$; thus, $\partial p_m^{N^*} / \partial g_m = k / (2(b_1 - b_2)) > 0$. Proposition 7 is proved. \square

Data Availability

The data used to support the findings of this study are included within the article.

Conflicts of Interest

The authors declare that they have no conflicts of interest.

Acknowledgments

This paper received administrative and technical support from the China Institute of Manufacturing Development. This research was funded by the Ministry of China of Education of Humanities and Social Science Project (Grant no. 19YJC630240) and the Practice Innovation Training Program of College Students in Jiangsu Province (Grant no. 201910300045Z).

References

- [1] Y. A. Alamerew and D. Brissaud, "Modelling reverse supply chain through system dynamics for realizing the transition towards the circular economy: a case study on electric vehicle batteries," *Journal of Cleaner Production*, vol. 254, Article ID 120025, 2020.
- [2] M. Zhu, Z. Liu, J. Li, and S. X. Zhu, "Electric vehicle battery capacity allocation and recycling with downstream competition," *European Journal of Operational Research*, vol. 283, no. 1, pp. 365–379, 2020.
- [3] J. Li, Y. Ku, C. Liu, and Y. Zhou, "Dual credit policy: promoting new energy vehicles with battery recycling in a competitive environment?" *Journal of Cleaner Production*, vol. 243, Article ID 118456, 2020.
- [4] G. Harper, R. Sommerville, E. Kendrick et al., "Recycling lithium-ion batteries from electric vehicles," *Nature*, vol. 575, no. 7781, pp. 75–86, 2019.
- [5] A. Betancourt-Torcat, T. Poddar, and A. Almansoori, "A realistic framework to a greener supply chain for electric vehicles," *International Journal of Energy Research*, vol. 43, no. 6, pp. 2369–2390, 2019.
- [6] Y. Tang, Q. Zhang, Y. Li, H. Li, X. Pan, and B. Mcllellan, "The social-economic-environmental impacts of recycling retired EV batteries under reward-penalty mechanism," *Applied Energy*, vol. 251, p. 113313, 2019.
- [7] P. He, Y. He, and H. Xu, "Channel structure and pricing in a dual-channel closed-loop supply chain with government subsidy," *International Journal of Production Economics*, vol. 213, pp. 108–123, 2019.
- [8] A. A. Taleizadeh, F. Haghghi, and S. T. A. Niaki, "Modeling and solving a sustainable closed loop supply chain problem with pricing decisions and discounts on returned products," *Journal of Cleaner Production*, vol. 207, pp. 163–181, 2019.
- [9] M. O. Kabul and A. K. Parlaktürk, "The value of commitments when selling to strategic consumers: a supply chain perspective," *Management Science*, vol. 65, no. 10, pp. 4754–4770, 2019.
- [10] C. M. Chen and H. Ho, "Who pays you to be green? How customers' environmental practices affect the sales benefits of suppliers' environmental practices," *Journal of Operations Management*, vol. 65, no. 4, pp. 333–352, 2019.
- [11] P. Zhang and Z. Xiong, "Incentive contract design for retailers under asymmetric manufacturer recycling cost information," *Journal of Industrial Engineering and Engineering Management*, vol. 33, no. 4, pp. 144–150, 2019.
- [12] Z. Pi, W. Fang, and B. Zhang, "Service and pricing strategies with competition and cooperation in a dual-channel supply chain with demand disruption," *Computers & Industrial Engineering*, vol. 138, Article ID 106130, 2019.
- [13] J. Xie, L. Liang, G. Yang, F. Kong, and Y. Chen, "Revenue sharing and cost sharing contract coordination and optimization of complementary closed-loop supply chain," *China Journal of Management Science*, vol. 26, no. 8, pp. 94–105, 2018.
- [14] J. P. Xie, L. Liang, L. H. Liu, and P. Ieromonachou, "Coordination contracts of dual-channel with cooperation advertising in closed-loop supply chains," *International Journal of Production Economics*, vol. 183, pp. 528–538, 2017.
- [15] C. Ma, T. Zhong, J. Wang, and J. He, "Risk diversification contract with retailer effort effect under loss avoidance," *Journal of Industrial Engineering and Engineering Management*, vol. 1–9, 2019.
- [16] Z. Wang, J. Huo, and Y. Duan, "Impact of government subsidies on pricing strategies in reverse supply chains of waste electrical and electronic equipment," *Waste Management*, vol. 95, pp. 440–449, 2019.
- [17] S. Mitra and S. Webster, "Competition in remanufacturing and the effects of government subsidies," *International Journal of Production Economics*, vol. 111, no. 2, pp. 287–298, 2008.
- [18] P. Calcott and M. Walls, "Waste, recycling, and "design for environment": roles for markets and policy instruments," *Resource and Energy Economics*, vol. 27, no. 4, pp. 287–305, 2005.
- [19] P. E. Pfeifer and A. Ovchinnikov, "A note on willingness to spend and customer lifetime value for firms with limited capacity," *Journal of Interactive Marketing*, vol. 25, no. 3, pp. 178–189, 2011.
- [20] J. Guo, L. He, and M. Gen, "Optimal strategies for the closed-loop supply chain with the consideration of supply disruption and subsidy policy," *Computers & Industrial Engineering*, vol. 128, pp. 886–893, 2019.
- [21] J. Zhao and N. Sun, "Government subsidies-based profits distribution pattern analysis in closed-loop supply chain using game theory," *Neural Computing and Applications*, vol. 32, no. 6, pp. 1715–1724, 2020.
- [22] N. Wan and D. Hong, "The impacts of subsidy policies and transfer pricing policies on the closed-loop supply chain with dual collection channels," *Journal of Cleaner Production*, vol. 224, pp. 881–891, 2019.
- [23] I. E. Nielsen, S. Majumder, and S. Saha, "Game-theoretic analysis to examine how government subsidy policies affect a closed-loop supply chain decision," *Applied Sciences*, vol. 10, no. 1, p. 145, 2019.
- [24] X. Lu, J.-S. Song, and A. Regan, "Rebate, returns and price protection policies in channel coordination," *IIE Transactions*, vol. 39, no. 2, pp. 111–124, 2007.
- [25] A. Atasu, M. Sarvary, and L. N. Van Wassenhove, "Remanufacturing as a marketing strategy," *Management Science*, vol. 54, no. 10, pp. 1731–1746, 2008.

Research Article

DLI: A Deep Learning-Based Granger Causality Inference

Wei Peng 

College of Economics and Management, Shandong University of Science and Technology, Qingdao 266590, China

Correspondence should be addressed to Wei Peng; pengweisd@foxmail.com

Received 31 March 2020; Revised 1 May 2020; Accepted 9 May 2020; Published 9 June 2020

Guest Editor: Lei Xie

Copyright © 2020 Wei Peng. This is an open access article distributed under the Creative Commons Attribution License, which permits unrestricted use, distribution, and reproduction in any medium, provided the original work is properly cited.

Integrating autoencoder (AE), long short-term memory (LSTM), and convolutional neural network (CNN), we propose an interpretable deep learning architecture for Granger causality inference, named deep learning-based Granger causality inference (DLI). Two contributions of the proposed DLI are to reveal the Granger causality between the bitcoin price and S&P index and to forecast the bitcoin price and S&P index with a higher accuracy. Experimental results demonstrate that there is a bidirectional but asymmetric Granger causality between the bitcoin price and S&P index. And the DLI performs a superior prediction accuracy by integrating variables that have causalities with the target variable into the prediction process.

1. Introduction

Time series is a series of observation values of a variable arranged in a chronological order, which reflects the change of a phenomenon itself with time if there are no exogenous variables. Generally speaking, time series analysis focuses more on predicting the future based on the existing historical data [1–3] than interpreting the causalities which may exist among the variables. Exploring the causalities among financial time series can be important for portfolio management [4]. As a decentralized cryptocurrency, bitcoin has attracted more and more investors and traders owing to high-investment returns in recent years [5]. From January 1, 2014, to December 31, 2018, bitcoin price jumped from \$771 to \$3742 (USD), which made bitcoin a promising investment cryptocurrency. Interestingly, Yermack [6] asserted that bitcoin was not a currency as it performs poorly as a unit of account and as a store of value. And Corbet et al. [7] supported the conclusion of Yermack that bitcoin was a speculative asset rather than a currency. Moreover, Dyhrberg [8] proved that bitcoin can serve as a hedge against the stock market, and it is a helpful tool for both portfolio diversification and risk management. Therefore, it is of great importance for investors and traders to forecast the bitcoin price and investigate the causes of its volatility.

In most circumstances, causality inference among financial time series is based on the Granger causality [9]. As a predictive causality, the Granger causality refers to that a time series x Granger-causes y if x 's values provide statistically significant information about future values of y , i.e., predictions of y based on its prior values, and the prior values of x are better than predictions of y based only on its prior values. Some traditional approaches for Granger causality inference mainly include vector autoregression (VAR) [10], vector error correction model (VECM) [11], and their variants [12, 13]. VAR and VECM are valid mostly when the input is stationary data. However, the results of some unit root test methods, such as ADF [14], showed that most economic time series are not stationary, while they may be stationary after preprocessing. Hence, traditional Granger causality inference for nonstationary time series needs to preprocess the input to reach a stationary sequence, which may bring pretesting distortions. The Wald test [15] has attracted much attention because there is no pretesting distortion, and it is based on a standard asymptotical distribution, irrespective of the unit roots and the cointegrating properties of the data [16]. However, the Wald test method may be inefficient since it intentionally overfits the VAR. Moreover, those aforementioned approaches are not good at capturing the complex representation of the input data.

Deep learning-based architecture could learn more abstract representation from the input data without data stationarity requirement. Chong et al. [17] proposed a deep learning-based stock market forecasting model to examine the ability of three unsupervised feature extraction methods of predicting future market behaviour. Based on a deep learning model, Chen et al. [18] built a computer-aided diagnosis and decision-making system for medical data from MR images. Long et al. [19] proposed a multi-filter neural network that integrated convolutional and recurrent neurons for feature extraction on economic time series samples and price volatility prediction. And the aforementioned deep learning-based forecasting models achieved promising forecasting performances. Lahmiri and Bekiros [20] employed LSTM for cryptocurrency prediction, which proved deep learning was highly efficient in predicting the inherent chaotic dynamics of cryptocurrency markets. Those aforementioned deep learning-based models are prone to perform better than traditional econometric methods, which suggest the deep learning-based architecture is more potent in dealing with financial time series data.

In this paper, we construct a deep learning-based Granger causality inference architecture, named DLI, which consists of AE, CNN, and LSTM. The two contributions of our work are exploring the Granger causality between the bitcoin price and S&P index and predicting the bitcoin price and S&P index with a higher accuracy.

The remainder of this paper is organized as follows. Available datasets we employed are presented in Section 2. The proposed DLI is depicted in Section 3. Experiments and results are introduced in Section 4. Our contributions and future work are summarized in Section 5.

2. Data

We took the bitcoin price¹ and S &P index² as experimental datasets. Both of them can be downloaded from the Yahoo website, and their relative prices are in US dollars. Without loss of generality, we take the daily closing price as the day's price. The descriptive statistics for the bitcoin price and S&P index covering the period from January 1, 2014, to December 31, 2018, can be found in Table 1. The sample of the bitcoin price and S&P index contains 1,826 and 1,258 data points, respectively. Since stock markets are usually closed for holidays or other reasons, we employed AE to remove the data noise caused by default values.

To obtain a desirable model, we divide the experimental data into three parts: 70% training dataset, 10% validation dataset, and 20% test dataset. The training dataset is to reach a sound model, the validation dataset is to further determine the parameters of the whole network, and the test dataset is to test the generalization ability of the model.

3. Model Development

Autoencoder is a simple but powerful unsupervised deep learning model. A typical AE consists of three layers: input layer, hidden layer, and output layer, as shown in Figure 1.

TABLE 1: Descriptive statistics for the bitcoin price and S&P index.

	Bitcoin price	S&P index
Mean	2,588.19	2,255.94
Standard error	83.06	8.81
Median	638.92	2,124.25
Mode	236.15	1,920.03
Standard deviation	3,549.46	312.58
Sample variance	1.26E + 07	97,706.86
Kurtosis	6.11	2.03
Skewness	1.82	0.57
Range	19,319.3	1,188.86
Minimum	178.1	1,741.89
Maximum	19,497.4	2,930.75
Count	1,826	1,258

And its output layer is an approximate reconstruction of the input layer, which can be used for filtering and representation learning. In the proposed DLI, we adopt AE as a filter to denoise the origin input, which is helpful for improving prediction accuracy.

Long short-term memory is a widely used deep learning model, which focuses on processing sequence data, such as time series data and speech. It is an extension of the recurrent neural network by adding the gate mechanism, which shows a better performance in long-term prediction. In the proposed DLI, we hope it can achieve a long-term accurate prediction by introducing the LSTM model.

Convolutional neural network is also a widely used deep learning model [21], which focuses on processing time series data (1D CNN), image (2D CNN), and video or medical image (3D CNN). CNN includes the convolution layer and pooling layer, as shown in Figure 1. And it can greatly reduce the amount of parameters and speed up training by local receptive fields and shared weights. Moreover, LeCun and Bengio [22] showed that time series have a strong 1D structure: variables that are spatially or temporally nearby are highly correlated, and CNN can effectively extract the spatial feature of time series. Therefore, CNN is introduced into the proposed DLI to extract the spatial feature and to speed up training.

Figure 1 shows the graphic illustration of the DLI which consists AE, CNN, and LSTM. We assume that both S&P index (X) and bitcoin price (Y) are time series of length T ,

$$\text{where } X = \begin{pmatrix} x_1 \\ x_2 \\ \vdots \\ x_t \\ \vdots \\ x_T \end{pmatrix} \in \mathbb{R}^{T \times 1} \text{ and } Y = \begin{pmatrix} y_1 \\ y_2 \\ \vdots \\ y_t \\ \vdots \\ y_T \end{pmatrix} \in \mathbb{R}^{T \times 1}. \text{ Let } x_t$$

be the S&P index at time t and y_t be the bitcoin price at time t .

The DLI consists of three processing stages: denoising, feature extracting, and forecasting. As described in Section 2, since stock markets are usually closed for holidays or other reasons, the S&P index time series has many default values. Therefore, at the denoising stage, AE is firstly used for data filtering to remove the noises in the S&P index. At the feature extracting stage, the denoised S&P index and bitcoin

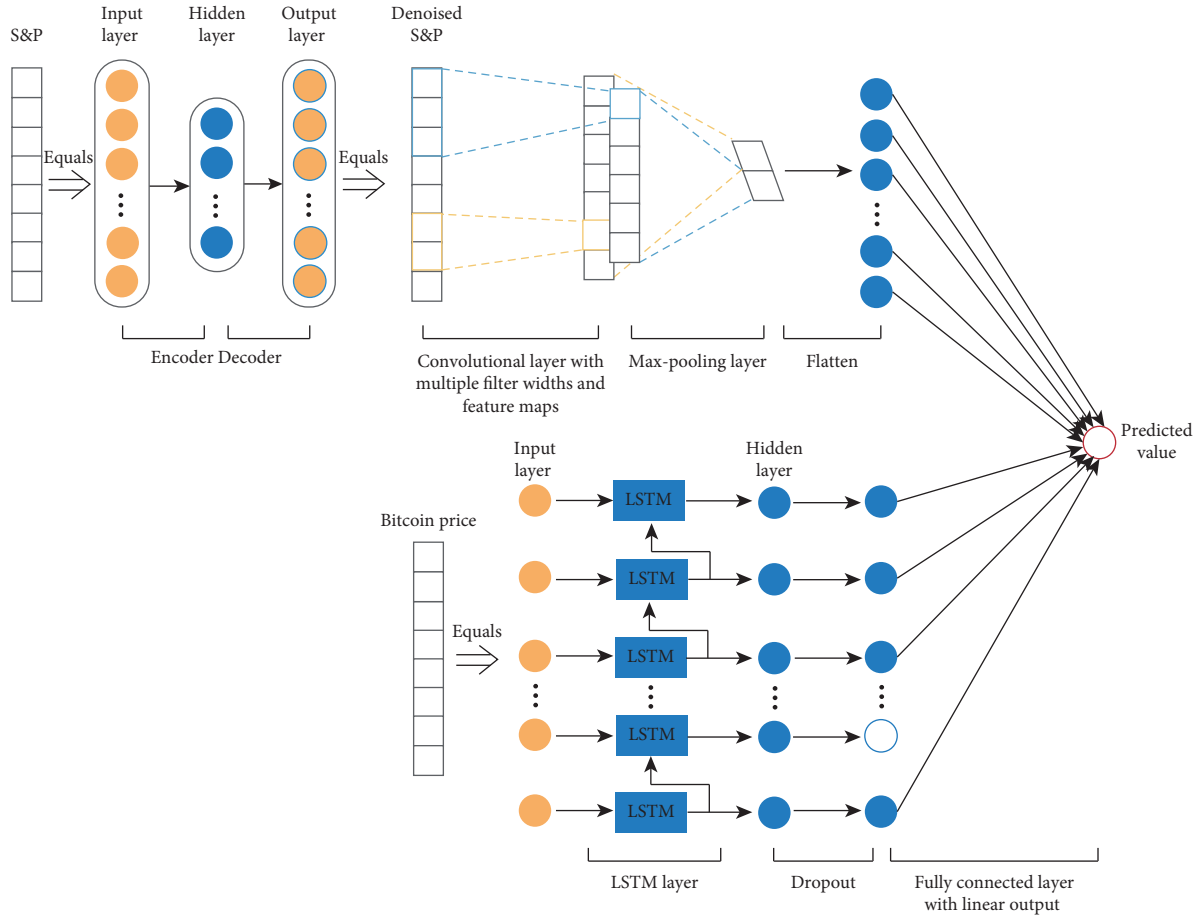


FIGURE 1: The architecture of the proposed DLI.

price would be taken as the inputs of CNN and LSTM to extract deep representations, respectively. At the forecasting stage, we would obtain the bitcoin price prediction through a fully connected layer.

The optimization of the DLI model is to minimize the reconstruction error of AE and the training error of the whole model. At the denoising stage, the output of AE is an approximate copy of the input. Therefore, we have to minimize the reconstruction error between the input and the output, which could maintain the economic significance of the S&P index. The reconstruction error of AE is defined as follows:

$$e_{AE} = \min \sum \|X - g(W' \times f(WX + b) + b')\|^2, \quad (1)$$

where $f(\cdot)$ and $g(\cdot)$ are activation functions, W and W' are weights, and b and b' are biases.

It is necessary for obtaining a sound model to minimize the training error of the whole model. The objective function of the whole model can be described as

$$e_{DLI} = \min \sum \|y_t - \hat{y}_t\|^2, \quad (2)$$

where \hat{y}_t denotes the predicted value.

4. Empirical Results

In this part, we will explore the Granger causality between the bitcoin price and S&P index. To investigate whether the S&P index Granger-causes the bitcoin price, we firstly predict the bitcoin price without considering the S&P index, as shown in Figure 2. Then, for comparison, we take the S&P index as auxiliary information to predict the bitcoin price, as shown in Figure 3. In the same way, to investigate whether the bitcoin price Granger-causes the S&P index, we firstly predict the S&P index without considering the bitcoin price, as shown in Figure 4. Then, for comparison, we take the bitcoin price as auxiliary information to predict the S&P index, as shown in Figure 5. In addition, we employ the traditional approach ARIMA to demonstrate the superiority of the proposed model. Owing to the continuous value prediction, we employ the root mean squared errors (RMSEs) as the forecasting performance indicator. The smaller the RMSE value, the better the prediction performance. And the corresponding prediction RMSEs are shown in Table 2.

From Table 2, we can see that the bitcoin price prediction RMSE of the DLI decreases by 92.10% and 23.32% compared with that of the ARIMA and LSTM, respectively. And the S&P index prediction RMSE of the DLI significantly

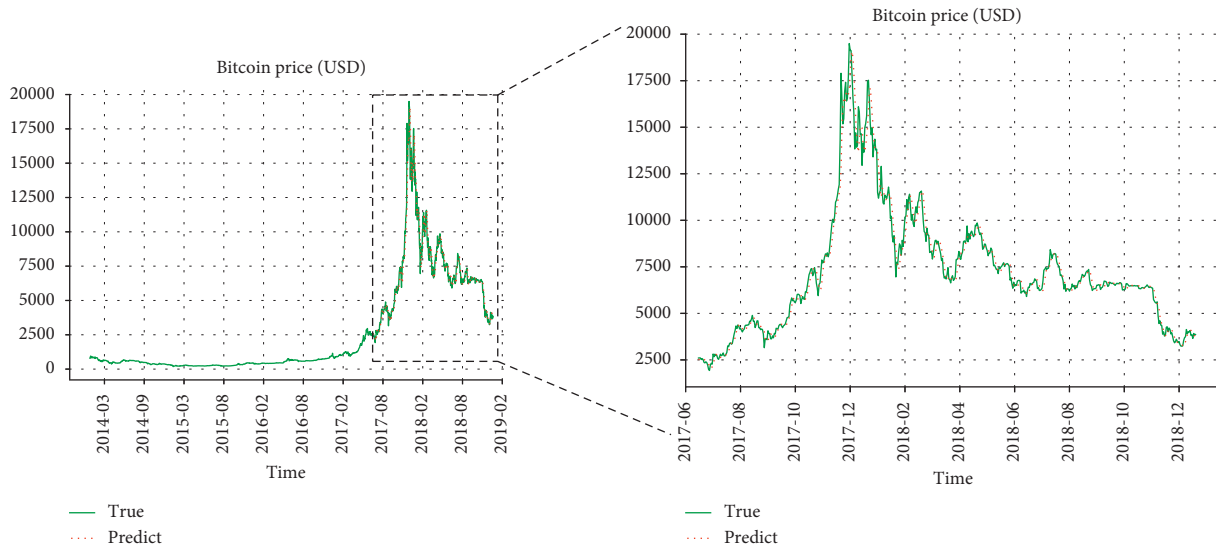


FIGURE 2: The bitcoin price prediction without consideration of the S&P index.

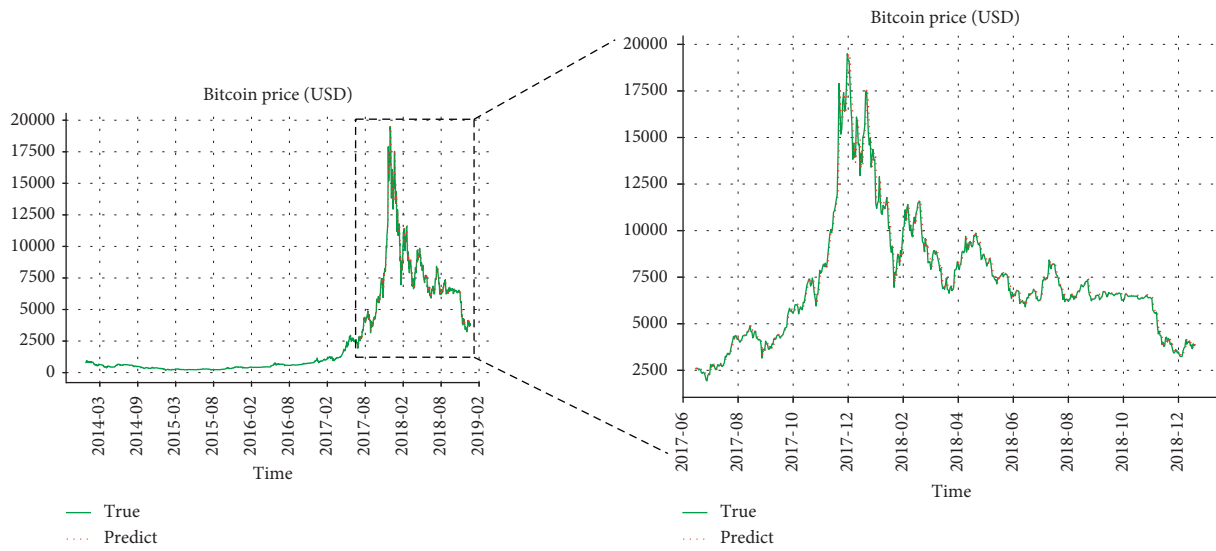


FIGURE 3: The bitcoin price prediction with consideration of the S&P index.

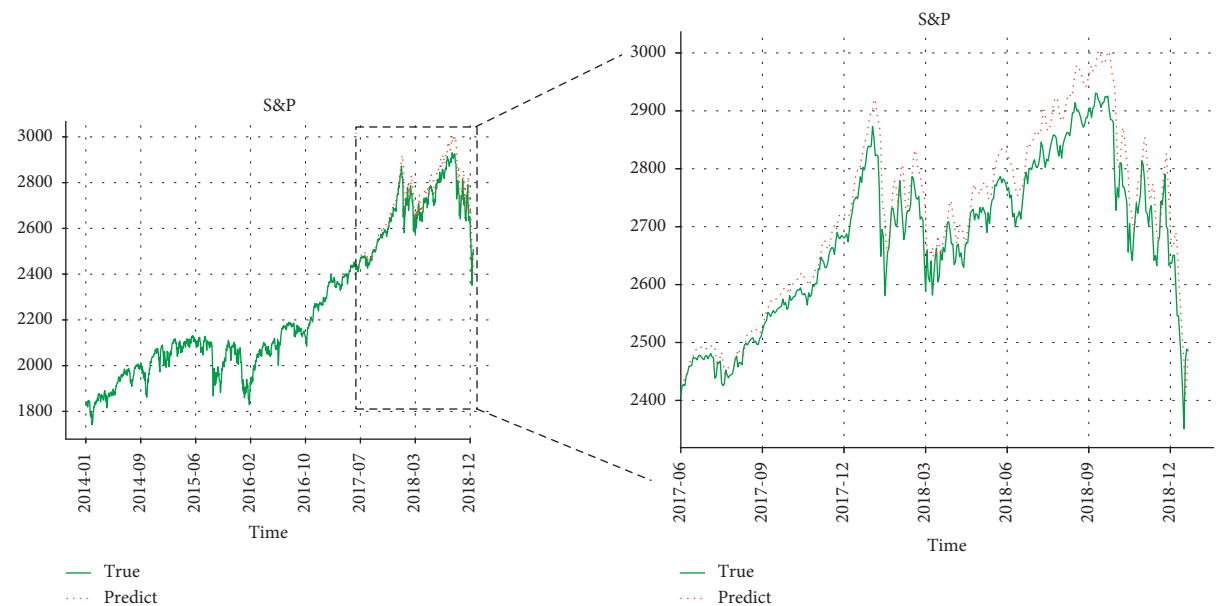


FIGURE 4: The S&P index prediction without consideration of the bitcoin price.

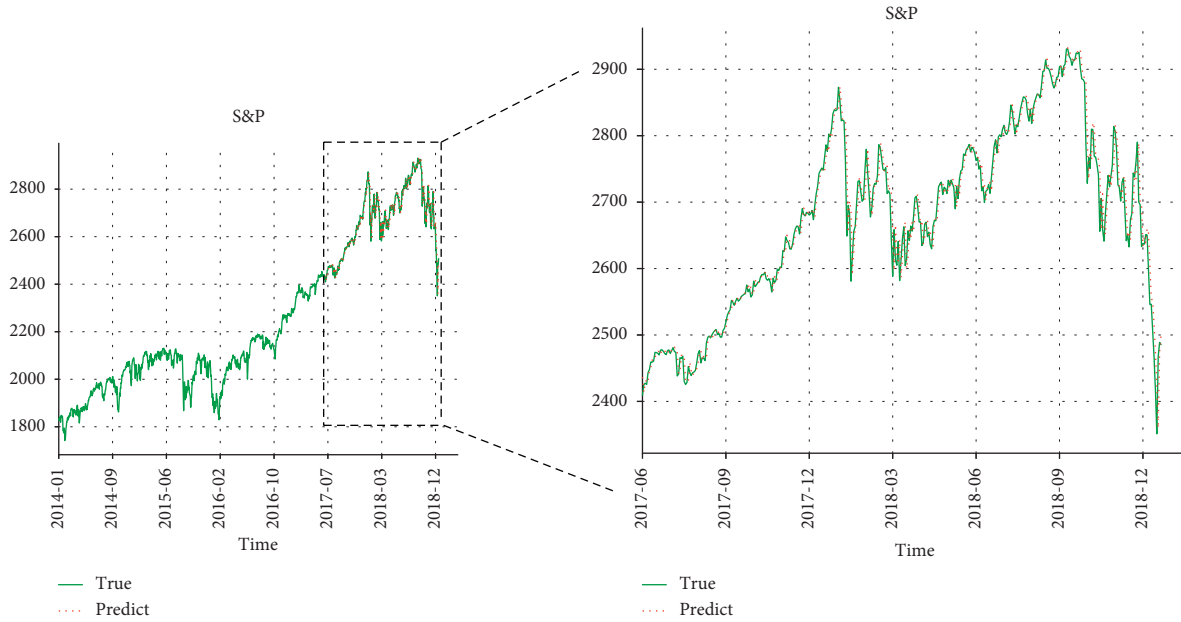


FIGURE 5: The S&P index prediction with consideration of the bitcoin price.

TABLE 2: RMSEs of the prediction.

Prediction task	Whether or not to consider auxiliary information	Approaches	RMSE
Bitcoin price prediction	Without consideration of the S&P index	ARIMA	5,932.96
		LSTM	611.47
	With consideration of the S&P index	DLI	468.87
		Without consideration of the bitcoin price	ARIMA
S&P index prediction	Without consideration of the bitcoin price	LSTM	49.63
		DLI	24.34
	With consideration of the bitcoin price	DLI	24.34

decreases by 98.06% and 50.96% compared with that of the ARIMA and LSTM, respectively. The above results demonstrate that both bitcoin price and S&P index prediction performances would be enhanced with consideration of the S&P index and bitcoin price, respectively. And the prediction performance improvement of the S&P index is more significant than that of the bitcoin price. Therefore, we can conclude that there is a bidirectional but asymmetric Granger causality between the bitcoin price and S&P index.

5. Conclusions

In this paper, we proposed an interpretable deep learning-based Granger causality inference architecture by integrating AE, CNN, and LSTM, named DLI. The proposed DLI, as a deep learning-based model, one of its advantages compared with traditional econometric models is that it can process big data efficiently and retain its original economic significance of variables after data preprocessing.

Our two contributions are exploring the Granger causality between the bitcoin price and S&P index and predicting the bitcoin price and S&P index with a higher accuracy. Our experiments reveal a bidirectional but asymmetric Granger causality between the bitcoin price and S&P index. And the DLI performs a superior prediction

accuracy by integrating variables that have causalities with the target variable into the prediction process.

In future work, the proposed DLI can be extended to some other economic variables to provide a reasonable reference for portfolio management, or it can be used for prediction in other scientific fields. Moreover, the DLI can also be extended from two variables to multivariables to determine causalities among the multitime series.

Data Availability

The raw data supporting the conclusions of this article will be made available by the authors, without undue reservation, to any qualified researcher.

Conflicts of Interest

The author declares that there are no conflicts of interest regarding the publication of this paper.

Acknowledgments

The author acknowledges the National Natural Science Foundation of China (Grant no. 11801060) and the Innovation Program of Shandong University of Science and Technology (no. SDKDYC190114).

References

- [1] Z. Zhou, T. Ren, H. Xiao, and W. Liu, "Time-consistent investment and reinsurance strategies for insurers under multi-period mean-variance formulation with generalized correlated returns," *Journal of Management Science and Engineering*, vol. 4, no. 2, pp. 142–157, 2019.
- [2] K. Wang, K. Li, L. Zhou et al., "Multiple convolutional neural networks for multivariate time series prediction," *Neurocomputing*, vol. 360, pp. 107–119, 2019.
- [3] A. Yadav, C. K. Jha, and A. Sharan, "Optimizing LSTM for time series prediction in Indian stock market," *Procedia Computer Science*, vol. 167, pp. 2091–2100, 2020.
- [4] M. Brière, K. Oosterlinck, and A. Szafarz, "Virtual currency, tangible return: portfolio diversification with bitcoin," *Journal of Asset Management*, vol. 16, no. 6, pp. 365–373, 2015.
- [5] G. Wang, Y. Tang, C. Xie, and S. Chen, "Is bitcoin a safe haven or a hedging asset? evidence from China," *Journal of Management Science and Engineering*, vol. 4, no. 3, pp. 173–188, 2019.
- [6] D. Yermack, "Chapter 2-is bitcoin a real currency? an economic appraisal," in *Handbook of Digital Currency*, D. Lee Kuo Chuen, Ed., pp. 31–43, Academic Press, Cambridge, MA, USA, 2015.
- [7] S. Corbet, B. Lucey, M. Peat, and S. Vigne, "Bitcoin futures-what use are they?" *Economics Letters*, vol. 172, pp. 23–27, 2018.
- [8] A. H. Dyhrberg, "Hedging capabilities of bitcoin. is it the virtual gold?" *Finance Research Letters*, vol. 16, pp. 139–144, 2016.
- [9] C. W. J. Granger, "Investigating causal relations by econometric models and cross-spectral methods," *Econometrica Journal of the Econometric Society*, vol. 37, no. 3, pp. 424–438, 1969.
- [10] X. Hou, S. Li, W. Li, and Q. Wang, "Bank diversification and liquidity creation: panel granger-causality evidence from China," *Economic Modelling*, vol. 71, pp. 87–98, 2018.
- [11] X. Meng and J. Han, "Roads, economy, population density, and CO₂: a city-scaled causality analysis," *Resources, Conservation and Recycling*, vol. 128, pp. 508–515, 2018.
- [12] T. Chang, F. Gatwabayege, R. Gupta, R. Inglesi-Lotz, N. C. Manjezi, and B. D. Simo-Kengne, "Causal relationship between nuclear energy consumption and economic growth in G6 countries: evidence from panel granger causality tests," *Progress in Nuclear Energy*, vol. 77, pp. 187–193, 2014.
- [13] Y. Zhao, S. A. Billings, H. Wei, F. He, and P. G. Sarrigiannis, "A new NARX-based granger linear and nonlinear causal influence detection method with applications to EEG data," *Journal of Neuroscience Methods*, vol. 212, no. 1, pp. 79–86, 2013.
- [14] D. A. Dickey and W. A. Fuller, "Distribution of the estimators for autoregressive time series with a unit root," *Journal of the American Statistical Association*, vol. 74, no. 366a, pp. 427–431, 1979.
- [15] H. Y. Toda and T. Yamamoto, "Statistical inference in vector autoregressions with possibly integrated processes," *Journal of Econometrics*, vol. 66, no. 1-2, pp. 225–250, 1995.
- [16] R. S. Hacker and A. Hatemi-J, "Tests for causality between integrated variables using asymptotic and bootstrap distributions: theory and application," *Applied Economics*, vol. 38, no. 13, pp. 1489–1500, 2006.
- [17] E. Chong, C. Han, and F. C. Park, "Deep learning networks for stock market analysis and prediction: methodology, data representations, and case studies," *Expert Systems with Applications*, vol. 83, pp. 187–205, 2017.
- [18] A. Chen, L. Zhu, H. Zang, Z. Ding, and S. Zhan, "Computer-aided diagnosis and decision-making system for medical data analysis: a case study on prostate MR images," *Journal of Management Science and Engineering*, vol. 4, no. 4, pp. 266–278, 2019.
- [19] W. Long, Z. Lu, and L. Cui, "Deep learning-based feature engineering for stock price movement prediction," *Knowledge-Based Systems*, vol. 164, pp. 163–173, 2019.
- [20] S. Lahmiri and S. Bekiros, "Cryptocurrency forecasting with deep learning chaotic neural networks," *Chaos, Solitons & Fractals*, vol. 118, pp. 35–40, 2019.
- [21] Y. Zheng, X. L. Xu, and L. Y. Qi, "Deep CNN-assisted personalized recommendation over big data for mobile wireless networks," *Wireless Communications & Mobile Computing*, vol. 2019, p. 6082047, 2019.
- [22] Y. LeCun and Y. Bengio, "Convolutional networks for images, speech, and time series," *The Handbook of Brain Theory and Neural Networks*, vol. 3361, no. 10, 1995.

Research Article

Research on the Complexity of Game Model about Recovery Pricing in Reverse Supply Chain considering Fairness Concerns

Ting Li ^{1,2}, Dongyun Yan,¹ and Shuxia Sui¹

¹School of Economics and Management, Dezhou University, Dezhou 253023, China

²School of Management, Shandong University, Jinan 250100, China

Correspondence should be addressed to Ting Li; tjlit@foxmail.com

Received 13 March 2020; Revised 25 April 2020; Accepted 29 April 2020; Published 29 May 2020

Academic Editor: Abdelalim Elsadany

Copyright © 2020 Ting Li et al. This is an open access article distributed under the Creative Commons Attribution License, which permits unrestricted use, distribution, and reproduction in any medium, provided the original work is properly cited.

A reverse recycling supply chain consisting of two recyclers is established in this paper, which takes into account the fact that the recyclers will consider the issue of fair concern in pricing. The paper discusses the local stability of the Nash equilibrium point in this price game model showing that the fair concern factors will reduce the stable area of the system. The paper also discusses the impacts of the sensitivity of the recovery price and the price cross coefficient on the stable area of the system. Through the method of system simulation and use of some indicators, such as the singular attractor, bifurcation diagram, attraction domain, power spectrum, and maximum Lyapunov exponent, the characteristics of the system at different times will be illustrated.

1. Introduction

With the information technology innovation and the deep integration of global economy in the postindustrial era, product replacement has become more frequent, resulting in more and more waste products, environmental degradation, and resource shortages. The green innovation strategy is a new idea for achieving green development and an inevitable choice for enterprise upgrading [1]. Closed-loop supply chain, a new type of logistics management mode, realizes the recycling and reuse of waste products. At present, closed-loop supply chain management has attracted widespread attention from various scholars [2].

Scholars such as Savaskan et al. [3, 4] have conducted a more comprehensive study of the recycling models. Firstly, they made analysis on three recycling models in a closed-loop supply chain; secondly, they made an analysis on the selection of the optimal recycling channels in the manufacturers' closed-loop supply chains. Hong and Yeh [5] examined the decision-making problems of the closed-loop supply chain when the retailers and the third-party recyclers make their recycling separately and pointed out that the channel recovery rate, manufacturers' profits, and total channel profits for the retailers are not always better than

those when the third parties are responsible for recycling. Choi et al. [6] studied the decision-making problem of the closed-loop supply chains under different channel forces and held that the overall performance of the closed-loop supply chains dominated by retailers was the best. On the basis of symmetric and asymmetric information, Wei et al. [7] constructed four decision models for the closed-loop supply chain under the power of two channels, namely, the manufacturer-led and retailer-led.

According to the above literature, decision makers for closed-loop supply chain are completely rational and take profit maximization as the decision objective. However, Kahnema, a behavioral economist, found that when people pay attention to their own interests, they also pay attention to the interests of others around them and show great attention to fairness [8]. A large number of experimental results show that the members in the game are generally willing to give up part of their interests for achievement to reach a fair result because of their fairness concerns. In the case of the ultimatum game, Ruffle [9] made several analysis on the decision in the case of the ultimatum game; thus, if one party thinks the other party's plan is unfair, the former will make a decision to reject the plan. In addition, many experiments, such as trust game experiment, authoritarian

game experiment, and public goods game experiment, show that people have the tendency to display fairness concern behaviors. The study conducted by Fehr and Schmidt [10] showed that the disadvantaged decision-makers pay more attention to their own benefits and compare their benefits with those of other decision-makers, in an attempt to obtain more equity through cooperation. Similarly, through other experiments, Loch and Wu [11] also showed that, in general, members in a disadvantaged position would be more inclined to focus on their own benefits and find ways to coordinate their sense of fairness by making comparison with the benefits from the other party. Tversky and Kahneman [12], on the contrary, believed that, in many cases, the existence of equity concerns has been common in organizations. In the process of operation, enterprises also constantly pay attention to the fact of whether or not their profits are “fair” compared with those of other enterprises. Therefore, the fairness concern behavior impacts on the decision-making subject of the supply chain to a certain extent. Haitao Cui et al. [13] proposed the equity concern in the newsboy model, which indicates that when the behavior of members of the supply chain display equity concern behaviors, suppliers can stimulate the coordination of the supply chain by the utilization of the wholesale price which is above the marginal cost. Li et al. [14] made study on the distribution fairness in the reverse supply chain. A simple reverse supply chain, which consisted of one recycler and one remanufacturer, was established and then extended to the situation in which one remanufacturer and two recyclers were being involved; the study made discussion on the impact which was made on the transfer prices and optimal decision-making by the fairness factors.

Without a doubt, the supply chain is a complex economic system, which entails features of human participation, being open and possessing information feedback function, but at the same time, it is not able to realize the changes in the competition process in accordance with the predesigned blueprint and preset orbit. Instead, these changes can only be realized through the interaction and game of the main players in the system. Although many studies have shown that static optimization is a stable state of dynamic evolution and can also be regarded as the fixed point of a dynamic system, the system often fails to achieve static optimization due to the disordered competition caused by different individual interests in the supply chain.

On the basis of the Cournot model, Rand [15] first found that the game results of oligarchs sometimes did not converge to the equilibrium point but presented periodic or chaotic solutions. Subsequently, a large number of scholars have conducted extensive research on the Cournot model, and the construction of the bounded rationality and incomplete information to the Cournot model is one such study, which speaks the complex behavior of decision makers. Based on Puu and Marín [16, 17], research on the production adjustment process of the Cournot model with the impacts of the elastic demand function came, and they came to the conclusion that complex phenomena such as bifurcation and chaos also occurred in the model. In respect of Bischi and Kopel [18, 19], they also introduced the

bounded rationality to the Cournot game model. Additionally, further studies were made on the impacts of the output adjustment rate on the system stability by making analysis on the critical curve and attraction domain. Agiza et al. [20] also studied mapping the symmetry of Cournot model. Xin et al. [21, 22] proposed a fractional-order energy resources demand-supply system and proposed a projective synchronization scheme.

With the improvement in the demand function, Ahmed and Hegazi [23, 24] established a duopoly game model at nonlinear cost and extended the duopoly model to a multidimensional model. In effect, Elsadany [25] studied the impacts of delay decision on Cournot model and found that the appropriate employment of delay strategy could make the system become more stable. Other scholars also introduced the chaos theory into the study of the supply chain game. Li and Ma [26, 27] studied the long-term price competition in the multichannel supply chain and found some complex phenomena like bifurcation and chaos. Li et al. [28] also conducted studies on the chaos phenomenon in the closed-loop supply chain and the control of the chaos theory effectively in the system.

This paper ultimately discussed the impacts of equity fairness concerns on the stable domain of the system and made simulation study on the system in the case of the supply chain system for reverse recovery: (1) the manufacturer does not participate in the recovery but gives subsidies to the recyclers; (2) it is assumed that one of the retailers is concerned about equity.

The structure of this paper is as follows: in the first part, the literature is being summarized; in the second part, the price game model of two recyclers would be constructed; in the third part, analysis on the local and global stability of equilibrium points should be given; in the fourth part, the relation between the equilibrium point and the parameters would be studied with the help of the simulation technique and the characteristics of system in chaos would be presented; and in the fifth part, the conclusion of the paper should be given.

2. Problem Description and Model Building

2.1. Model Description. In this article, two oligopoly recyclers in a reverse supply chain market and a competition model will be established for the study of the product recycling. Competition usually occurs through price strategies, and essentially, the competition between the two oligopolies conforms to the Bertrand game model. The structure of supply chain is as shown in Figure 1.

2.2. Symbol Description

a_1 and a_2 represent the amount of used products that consumers are willing to recycle when the price is 0; to some extent, this amount reflects the environmental awareness of consumers and the recycling influence of each recycler.

p_1 and p_2 represent the recycling prices of two recyclers, respectively.

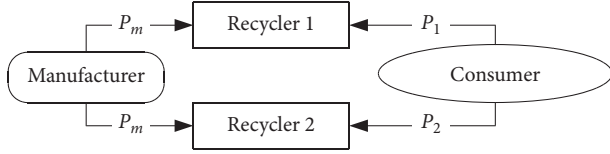


FIGURE 1: Game model for recycling supply chain.

q_1 and q_2 represent the recycling quantity of two recyclers respectively.

b represents the consumers' sensitivity to recycling prices.

d reflects the price cross coefficient between response channels.

c_1 and c_2 mean the unit cost of the two recyclers, respectively. For simplification of the analysis, we assume $c_1 = c_2 = c$.

p_m represents the subsidy given by the manufacturer to the recycler for the recycled product per unit.

For the purpose of making the model economically meaningful, we assume $a_1, a_2, b, d > 0$.

2.3. Model Construction. We assume that, in reality, two recyclers make recycling of waste products together. According to the concept of the Bertrand game model, the quantity of recycled products is related to the recycling price. When there exists more than one recycling company, the quantity is also related to the recycling prices provided by other recyclers. The model can be expressed as

$$\begin{cases} q_1 = a_1 + bp_1 - dp_2, \\ q_2 = a_2 + bp_2 - dp_1. \end{cases} \quad (1)$$

$$\begin{cases} \frac{\partial U_1}{\partial p_1} = dp_2 - bp_1 - a_1 - \lambda(a_1 + bp_1 - dp_2 + b(c + p_1 - p_m) + d(c + p_2 - p_m)) + b(p_m - c - p_1), \\ \frac{\partial U_2}{\partial p_2} = dp_1 - bp_2 - a_2 + b(p_m - c - p_2). \end{cases} \quad (4)$$

From the formula (4), we can get

$$\begin{cases} p_1^* = \frac{2a_1b(1+\lambda) + 2b^2(c - p_m - \lambda p_m + c\lambda) + a_2d + bd(c - p_m - 2\lambda p_m + 2c\lambda)}{4b^2(1+\lambda) - d^2}, \\ p_2^* = \frac{2a_2b(1+\lambda) + 2b^2(c - p_m - \lambda p_m + c\lambda)}{4b^2(1+\lambda) - d^2}. \end{cases} \quad (5)$$

In reality, corporate decisions could be limited by objective conditions like the individual ability of the decision maker, which shows that it is impossible for the decision

The model shows that when the recycler from one channel raises the price, the product recycling volume of the other channel will increase. The profit of the two recyclers can be written as

$$\begin{cases} \pi_1 = (p_m - p_1 - c_1)q_1, \\ \pi_2 = (p_m - p_2 - c_2)q_2. \end{cases} \quad (2)$$

In making price decisions, recyclers will not only consider their own profits but also the profits of their competitors. Recyclers are unwilling to determine the profit distribution of the supply chain by strength but are more willing to express concerns about fairness by directly comparing the profits with those of other recyclers. By means of dependence on the reference point, this article tries to characterize the retailer's fair concern; that is, one recycler will use the profit of another recycler as the reference point for its own profits with the purpose of showing its perception of fair concern. By introduction of λ as a fair concern coefficient, the utility function of the recycler is as follows:

$$\begin{cases} U_1 = \pi_1 - \lambda(\pi_2 - \pi_1), \\ U_2 = \pi_2. \end{cases} \quad (3)$$

The formula shows that, for recycler 1, when the profit of recycler 2 is greater than that of recycler 1, the utility of recycler 1 will decrease. λ , a fair concern coefficient, reflects the sensitivity of recycler 1 to the profit gap between competitors and themselves. Recycler 2 uses profit maximization as its decision criterion. When $\lambda = 0$, it could be stated that recycler 1 was fair and neutral.

From the formula, we can get the marginal utility of the recycler as

maker to obtain all the information in the market. Here, we make assumptions that the recycler is to be boundedly rational; price decision can be adjusted within a reasonable

range in the next cycle. Recyclers would make prediction and determination on the price of the next period based on the profit margin. In other words, if the marginal profit is

positive in the period t , the recycler will raise its price in the period $t + 1$. Conversely, recyclers will lower their prices. So, we can build a corresponding dynamic model:

$$\begin{cases} p_1(t+1) = p_1(t) + \alpha_1 p_1(t)(dp_2(t) - bp_1(t) - a_1 - \lambda(a_1 + bp_1(t) - dp_2(t) + b(c + p_1(t) - p_m) \\ + d(c + p_2(t) - p_m)) + b(p_m - c - p_1(t))), \\ p_2(t+1) = p_2(t) + \alpha_2 p_2(t)(dp_1(t) - bp_2(t) - a_2 + b(p_m - c - p_2(t))). \end{cases} \quad (6)$$

3. Stability Analysis of the Equilibrium Points

3.1. Market Equilibrium. According to the definition of fixed point, $p_i(t+1) = p_i(t)$, ($i = 1, 2$), we can get the equilibrium point of the system as

$$E_1 = (0, 0),$$

$$E_2 = \left(0, \frac{a_2 + bc - bp_m}{-2b}\right),$$

$$E_3 = \left(\frac{a_1 + bc - bp_m + \lambda(a_1 + bc - bp_m + cd - dp_m)}{-2b(\lambda + 1)}, 0\right),$$

$$E^* = \left(\frac{2a_1b(1 + \lambda) + 2b^2(c - p_m - \lambda p_m + c\lambda) + a_2d + bd(c - p_m - 2\lambda p_m + 2c\lambda)}{4b^2(1 + \lambda) - d^2}, \frac{2a_2b(1 + \lambda) + 2b^2(c - p_m - \lambda p_m + c\lambda)}{4b^2(1 + \lambda) - d^2}\right). \quad (7)$$

Since the pricing cannot be negative in reality, in order to ensure that the equilibrium point has economic meaning, the value range of the parameters should meet $E_1, E_2, E_3, E^* \geq 0$. Obviously, E_1, E_2 , and E_3 are the boundary equilibrium solution, and E^* is the only NASH equilibrium solution.

3.2. Local Stability Analysis of Equilibrium Points. For the purpose of making analysis on the local stability of the equilibrium point, we make calculation for the Jacobian matrix of the system:

$$\begin{pmatrix} 1 + \alpha_1 f_1 & dp_1 \alpha_1 \\ dp_2 \alpha_2 & 1 + \alpha_2 f_2 \end{pmatrix}. \quad (8)$$

In this matrix,

$$\begin{aligned} f_1 &= dp_2 - 2bp_1 - a_1 - \lambda(a_1 + 2bp_1 - dp_2) \\ &\quad + b(c + 2p_1 - p_m) + d(c + p_2 - p_m) + b(p_m - c - 2p_1), \\ f_2 &= dp_1 - 2bp_2 - a_2 + b(p_m - c - 2p_2). \end{aligned} \quad (9)$$

The stability of the equilibrium point is determined by the properties of the eigenvalue corresponding to the equilibrium point in the Jacobian matrix. When the equilibrium points E_1, E_2, E_3 , and E^* are substituted into the matrix, we can get the following theorem.

Theorem 1. *The equilibrium point E_1 is a stable equilibrium point.*

Proof. Substitute E_1 into the following matrix:

$$\begin{pmatrix} 1 + \alpha_1(-a_1 - \lambda(a_1 + b(c - p_m) + d(c - p_m)) + b(p_m - c)) & 0 \\ 0 & 1 + \alpha_2(-a_2 + b(p_m - c)) \end{pmatrix}. \quad (10)$$

By calculation, we get to know that the two characteristic roots of the corresponding characteristic equation for the matrix are

$$\begin{aligned} r_1 &= 1 + \alpha_1(-a_1 - \lambda(a_1 + b(c - p_m) + d(c - p_m)) + b(p_m - c)), \\ r_2 &= 1 + \alpha_2(-a_2 + b(p_m - c)). \end{aligned} \quad (11)$$

Since the value of each parameter satisfies the condition that the four equilibrium points could be positive, we can get $|r_{1,2}| > 1$, which shows that the eigenvalues of the characteristic equation are usually greater than 1 when E_1 has been in correspondence with Jacobian matrix. According to the stability judgment condition of equilibrium point, E_1 is an unstable equilibrium point. \square

Theorem 2. *The equilibrium points E_2 and E_3 are unstable saddle points.*

Proof. Substitute the equilibrium point E_2 into the matrix, the two characteristic roots of the corresponding characteristic equation could be calculated as

$$\begin{aligned} r_1 &= 1 - \alpha_1(2a_1b(1 + \lambda) + 2b^2(c - p_m - \lambda p_m + c\lambda) + a_2d \\ &\quad + bd(c - p_m - 2\lambda p_m + 2c\lambda)) > 1, \\ r_2 &= 1 + \alpha_2(a_2 + bc - bp_m) < 1. \end{aligned} \quad (12)$$

According to the judgment condition of stability for equilibrium point, equilibrium point E_2 is an unstable saddle point. In the same way, E_3 is also an unstable saddle point. \square

Theorem 3. *The local stability of the Nash equilibrium point E^* is related to the speed of price adjustment α_1 and α_2 .*

Proof. We will plug E^* in and get

$$J(E^*) = \begin{pmatrix} 1 + \alpha_1 h_1 & dp_1 \alpha_1 \\ dp_2 \alpha_2 & 1 + \alpha_2 h_2 \end{pmatrix}, \quad (13)$$

in which

$$\begin{aligned} h_1 &= dp_2^* - 2bp_1^* - a_1 - \lambda(a_1 + 2bp_1^* - dp_2^* + b(c + 2p_1^* - p_m) \\ &\quad + d(c + p_2^* - p_m)) + b(p_m - c - 2p_1^*), \\ h_2 &= dp_1^* - 2bp_2^* - a_2 + b(p_m - c - 2p_2^*). \end{aligned} \quad (14)$$

In order to determine the stable region of the Nash equilibrium point E^* regarding the speed of price adjustment α_1 and α_2 , firstly we should obtain the characteristic equation $\lambda'^2 + A\lambda + B = 0$ corresponding to its Jacobian matrix, among that

$$\begin{aligned} A &= 2 + h_1 \alpha_1 + h_2 \alpha_2, \\ B &= 1 + h_1 \alpha_1 + h_2 \alpha_2 + (h_1 h_2 - d^2 p_1^* p_2^*) \alpha_1 \alpha_2. \end{aligned} \quad (15)$$

According to Jury's argument for determining stability, which is based on the Nash equilibrium of a discrete system, the local stability E^* is determined by the formula

$$\begin{cases} 1 - A + B > 0, \\ 1 + A + B > 0, \\ 1 - B > 0. \end{cases} \quad (16)$$

Substitute the value of the parameters A and B to get

$$\begin{cases} 2 - (h_1 h_2 - d^2 p_1^* p_2^*) \alpha_1 \alpha_2 > 0, \\ 4 + 2h_1 \alpha_1 + 2h_2 \alpha_2 + (h_1 h_2 - d^2 p_1^* p_2^*) \alpha_1 \alpha_2 > 0, \\ 1 + h_1 \alpha_1 + h_2 \alpha_2 > 0, \end{cases} \quad (17)$$

In the formula, after determining the values of the other parameters α_1 and α_2 , the local stability of E^* is obtained if and only if the parameters α_1 and α_2 satisfy the formula. To satisfy all the values of this inequality formula, α_1 and α_2 means the stability domain of the Nash equilibrium point E^* related to parameters α_1 and α_2 . If the value of (α_1, α_2) is in the stable region, $(p_1(t), p_2(t))$ will keep stable at the point E^* after a long game. If the value of (α_1, α_2) is not in the stable region, after a series of games, the system will gradually lose stability and the market price will become difficult for prediction. This shows that when recyclers continue to speed up the price adjustment in order to obtain greater own profits, market competition will become disordered. \square

4. Numerical Simulation

For better understanding of the model, visual demonstration will be made for the long-term competition of the system by the means of numerical simulation. Taking the actual competition of recyclers into consideration, we make it possible as follows:

$$\begin{aligned} a_1 &= a_2 = 1, \\ b &= 1, \\ d &= 0.3, \\ c &= 1, \\ p_m &= 5, \\ \lambda &= 0.3. \end{aligned} \quad (18)$$

At this point, Nash equilibrium point is like $E^* = (1.843, 1.777)$.

4.1. Relationship between the Stability of the Equilibrium Points and the Parameters. As is shown in Figure 2, for (α_1, α_2) , the local stable area of the Nash equilibrium point is the light blue part in the figure, which indicates that if and only if the value of the price adjustment speed (α_1, α_2) is within this stable range, the price $(p_1(t), p_2(t))$ will eventually get stable at $(1.843, 1.777)$ after the long-term competition.

For the study of the impact of fairness concerns on the equilibrium point and stability of the system, we take the values of λ 0, 0.5, and 1, respectively, which represent different degrees of fair concern. As shown in Figure 3, we can

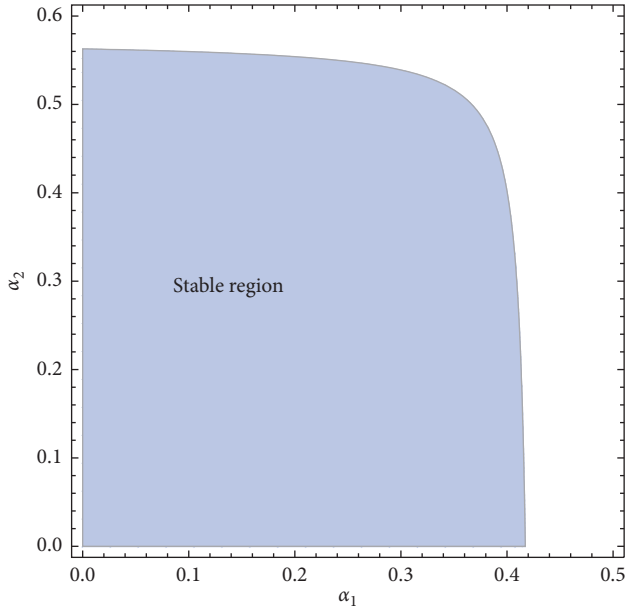


FIGURE 2: Local stability region of Nash equilibrium about (α_1, α_2) .

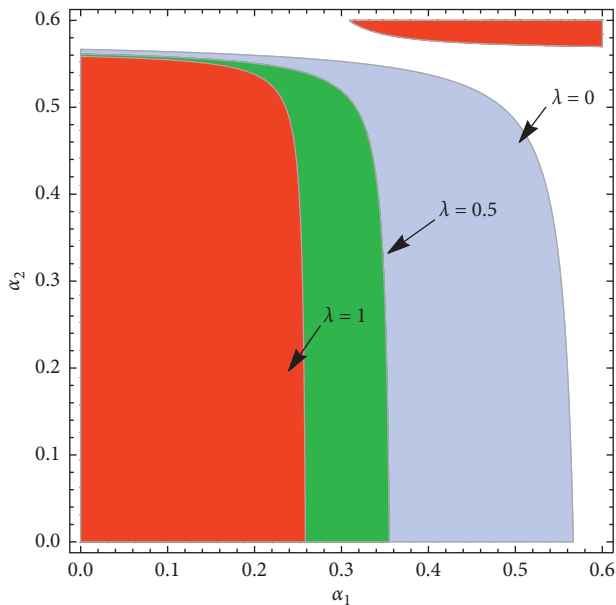


FIGURE 3: When λ is different, the local stability region of the Nash equilibrium points at (α_1, α_2) .

also obtain the stable domains of the system when λ takes different values. The corresponding Nash equilibrium points are shown in Table 1.

In Figure 3, the red, green, and light blue scopes represent the corresponding values, respectively, when $\lambda = 0, 0.5$, and 1. From Figure 3, we can know that when the value of λ increases, that is to say, recycler 1 being more concerned about the sense of fairness, the stable region of the system will get smaller. This shows that recycler 1 will adopt a fierce competition strategy for obtaining fair utility. As a result, this more intense pricing strategy will make it more difficult for the market to maintain its stability.

TABLE 1: Nash equilibrium.

λ	$\lambda = 0$	$\lambda = 0.5$	$\lambda = 1$
Nash equilibrium	(1.765, 1.765)	(1.878, 1.782)	(1.934, 1.79)

When the recyclers continue to speed up the price adjustment, the market will become unstable, and the system will become bifurcated or even chaotic. Figures 4 and 5 show the bifurcation diagrams indicating price changes of recycler 1 and recycler 2 with changes in price adjustment speed, respectively. From Figure 4, we can learn that when the price adjustment speed of recycler 1 is relatively low, with limited times of game, the price will get stable at the Nash equilibrium point (1.843, 1.777).

When the price adjustment speed gets increased and the doubling period makes bifurcation for the first time and two equilibrium solutions appeared in the system, then followed by four times period, eight times period, and so on, the system finally entered into the chaotic state. Figure 5 shows that the system will show a similar change along with the change in the price adjustment speed for the recycler 2.

By making a comparison between Figures 4 and 5, we can easily find another phenomenon: although the recyclers could gain the preferential advantage to some degrees in price competition through continuous speeding up of price adjustment, when the system enters into chaos, the party, which continues to speed up the price adjustment, would experience a huge price fluctuation, while at the same time, another party who employs the “follow strategy” will experience a smaller price fluctuation.

The type of system bifurcation, the periodic behavior of the solution, and the path to chaos are analyzed by means of the parameter 2D bifurcation diagram. First, we use the price input adjustment coefficient as the bifurcation parameter. Figure 6 shows a two-dimensional bifurcation diagram of the system, among which blue scope represents the system’s stable domain, that is, the 1-period solution; red scope represents the 2-period solution, green scope for the 3-period solution, pink scope for the 4-period solution, light blue scope for the 5-period solution, purple scope for the 6-period solution domain, yellow scope for the 7-period solution domain, brown scope for the 8-period solution domain, dark purple scope for the 9-period solution, and dark green scope for the 10-period solution; gray scope represents the chaotic region of the system, and white scope indicates that the system variables have overflowed and no meaning exists. From Figure 6, we could see that the faster the price adjustment speed becomes (that is, the more frequent the price adjustment), the more unstable the entire system will be, and the market is more prone to enter into chaos. From Figure 6, we may also see that the system can enter into chaos in two ways: firstly, the system will lead to chaos through a period-doubling bifurcation channel which is composed of those red, pink, purple, and brown scopes, called flip bifurcation; secondly, the system leads to chaos through the odd cycle which is represented by the green and light blue scopes. Finally, those intermittent odd cycle points can be found from Figure 6.

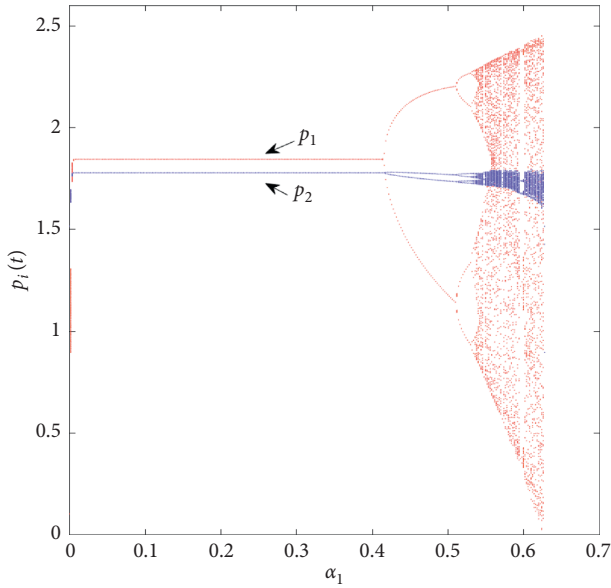


FIGURE 4: Price bifurcation diagram of the system with variations in α_1 .

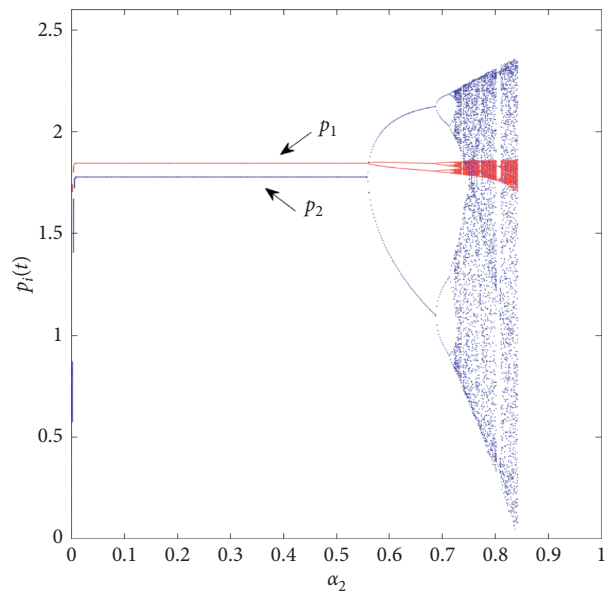


FIGURE 5: Price bifurcation diagram of the system with variations in α_2 .

Figure 7 shows a two-dimensional bifurcation diagram which reflects consumers' sensitivity to recycling prices and the speed α_1 of recycling price adjustment. It can be concluded from Figure 7 that when b becomes larger, that is, the more sensitive the consumer is to the recycling price, the narrower the blue area will become in the figure, which indicates that the stability region of the system is decreasing. The result shows that if companies can reduce the consumer's sensitivity to prices by means of advertising or improvement of consumers' environmental awareness, leading to more consumers' awareness of the importance of recycling products, they can effectively reduce consumers'

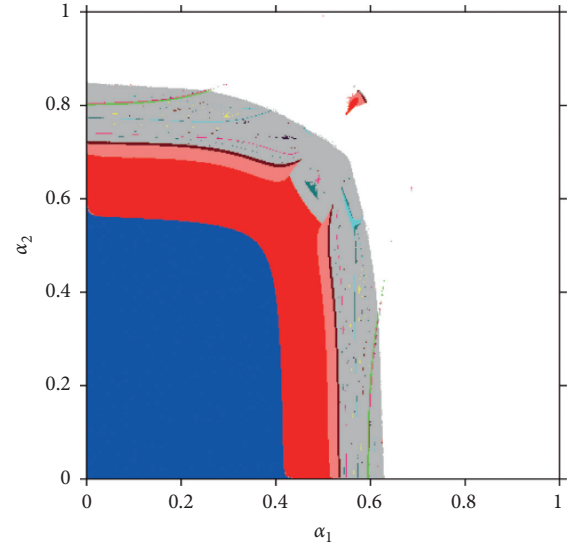


FIGURE 6: Two-dimensional bifurcation of the system with changes in (α_1, α_2) .

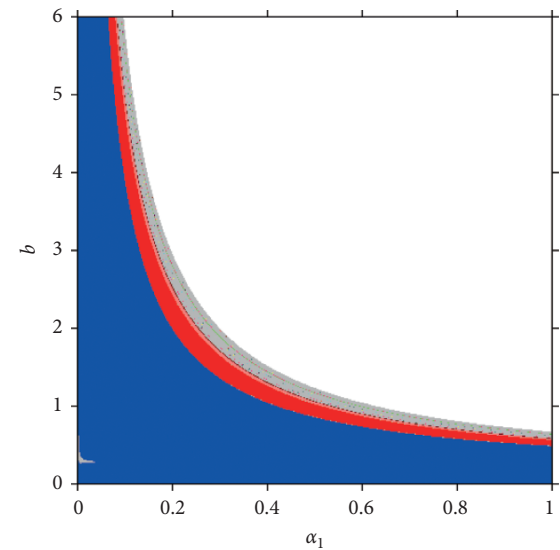


FIGURE 7: Impact of consumers' sensitivity to recycling prices on system's stability.

perception of products, increase the speed of price adjustment for themselves, gain more competitive advantages, and surely create more space.

Figure 8 shows a two-dimensional bifurcation diagram of the cross-elasticity of prices between channels and the speed of adjustment of recycling prices α_1 . It can be learned from Figure 8 that the larger the price cross-coefficient d becomes between channels, the smaller the system's stable region will get. This also shows that when consumers are more sensitive to price factors, for recyclers, the strategic space, which is employed to increase competitive advantage through price adjustment, will become smaller. At the same time, it also shows that if the manufacturer could make effective reduction of the competition between two recyclers

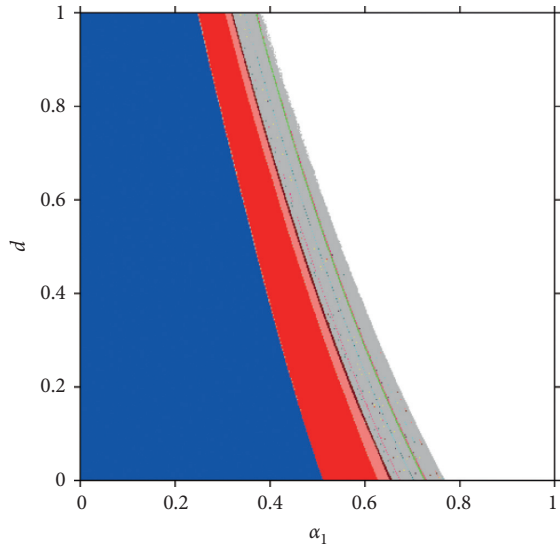


FIGURE 8: Effects of price cross coefficient on system's stability.

by means of reasonable setting of the recycling sites for two competing recyclers, he could reduce the price cross-coefficient between channels with the result that the market will become more stable. All these factors, which include consumer's sensitivity to the recycling price, the cross-elasticity of the price between channels and the retailer's recycling price adjustment speed α_2 are similar to those in Figures 7 and 8, so they will not be mentioned here again.

In fact, the initial value of the price is not necessarily close to the equilibrium point of the market. Therefore, it is necessary to make analysis on the global stability of the system (6). Figure 9 shows the attractive domain when the equilibrium points are $\alpha_1 = 0.1$ and $\alpha_2 = 0.1$. The LC curve is a trajectory of points that are mapped once and have 2 or more images. The set of these images is defined as LC_{-1} . The LC curve divides the plane into different regions Z_0, Z_2 , and Z_4 by the number of images [29], and the LC_{-1} set belongs to the set of points whose determinant Jacobian value is 0. So, we can get

$$LC_{-1} \subseteq J_0 = \{(p_m, p_r) \in R^2 | \det J(p_m, p_r) = 0\}. \quad (19)$$

System (19) defines the mapping M so that we can get $LC = M(LC_{-1})$. At the same time, since the price should be nonnegative in reality, that is, $p_m, p_r > 0$ we define a feasible region:

$$R_1 = \{((p_m, p_r) \in R^2 | p_m > 0, p_r > 0)\}. \quad (20)$$

Figure 9 shows the attractive domain of the Nash equilibrium point at that time when $\alpha_1 = 0.1$ and $\alpha_2 = 0.1$. In Figure 9, the gray area represents a feasible attractor area that satisfies the publicity (20). By making a comparison between Figures 9 and 10, we could find that the attraction domain will change from simple connection to multiple connection with the increased adjustment speed for recycler 1, and the feasible area in the direction of p_1 will also be significantly reduced which also leads to significant reduction of the entire feasible area.

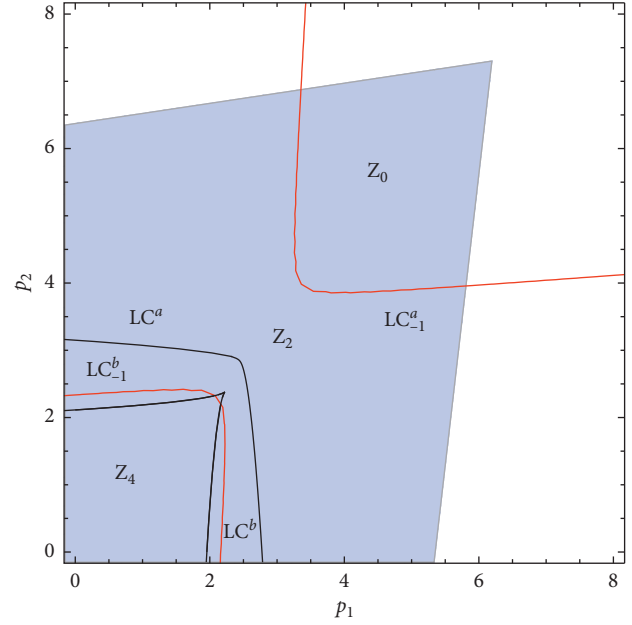


FIGURE 9: Attraction domain for equilibrium point when $\alpha_1 = 0.1$ and $\alpha_2 = 0.1$.

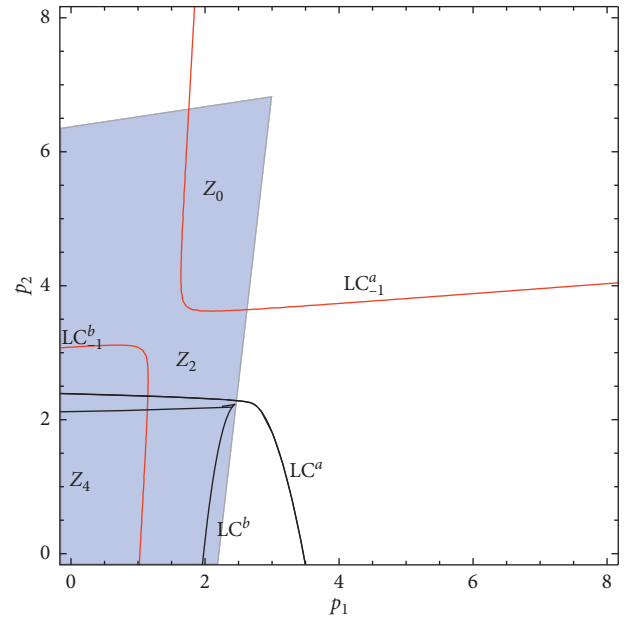


FIGURE 10: Attraction domain for equilibrium point when $\alpha_1 = 0.55$ and $\alpha_2 = 0.1$.

4.2. Characteristics of the System in Chaos. Figure 11 shows the maximum Lyapunov index in correspondence with Figure 4 as the price adjustment coefficient α_1 increases. The maximum Lyapunov index can characterize the degree of separation between two points starting at the same time and running over time. When the system is in a stable state, the maximum Lyapunov index of the system is less than zero; when the system is in the chaotic state, the maximum Lyapunov index of the system is greater than zero. From

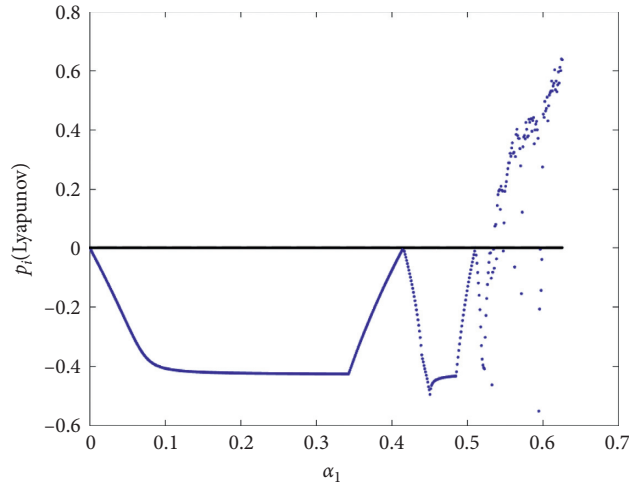


FIGURE 11: The system's largest Lyapunov index.

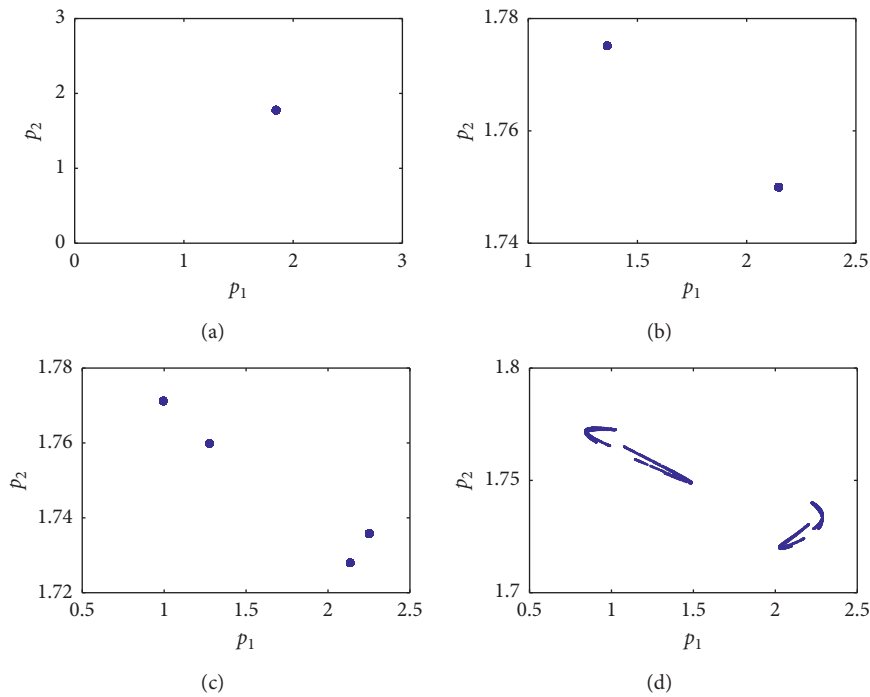


FIGURE 12: Formation process for attractor in system: (a) $\alpha_1 = 0.1, \alpha_2 = 0.1$; (b) $\alpha_1 = 0.46, \alpha_2 = 0.1$; (c) $\alpha_1 = 0.52, \alpha_2 = 0.1$; (d) $\alpha_1 = 0.54, \alpha_2 = 0.1$.

Figure 11, we can clearly see that when the maximum Lyapunov exponent is equal to 0 for the first time, the system enters into a double period bifurcation, and when the maximum Lyapunov exponent is greater than 0, it indicates that the system has entered into a chaotic state.

When the system is in chaos, another characteristic is that the system has singular attractors. The strange attractor is the result of the overall stability and local instability of the system, and it has self-similarity and fractal structure. Figure 12 shows the formation process of the singular attractor in this model at 0.1, 0.46, 0.52, and 0.54 and $\alpha_2 = 0.1$, and the system experienced a stable period, a double period, a

quadruple period, and then entered into the chaotic state. Figure 13 corresponds to the rules of price changes in different periods of the system. Figure 13(a) shows the price changes over time when the system is in a stable state. After a limited number of games, the price of the system will stabilize at the Nash equilibrium point. Figures 13(b) and 13(c) show the price changes in the system in the two-cycle and four-cycle cycles, respectively. Figure 13(d) shows the price change over time when the system is in the chaotic state. It is clearly illustrated that compared with price in the stable state, the pricing decision becomes uncertain, disordered, and unpredictable when the system is in the chaotic state.

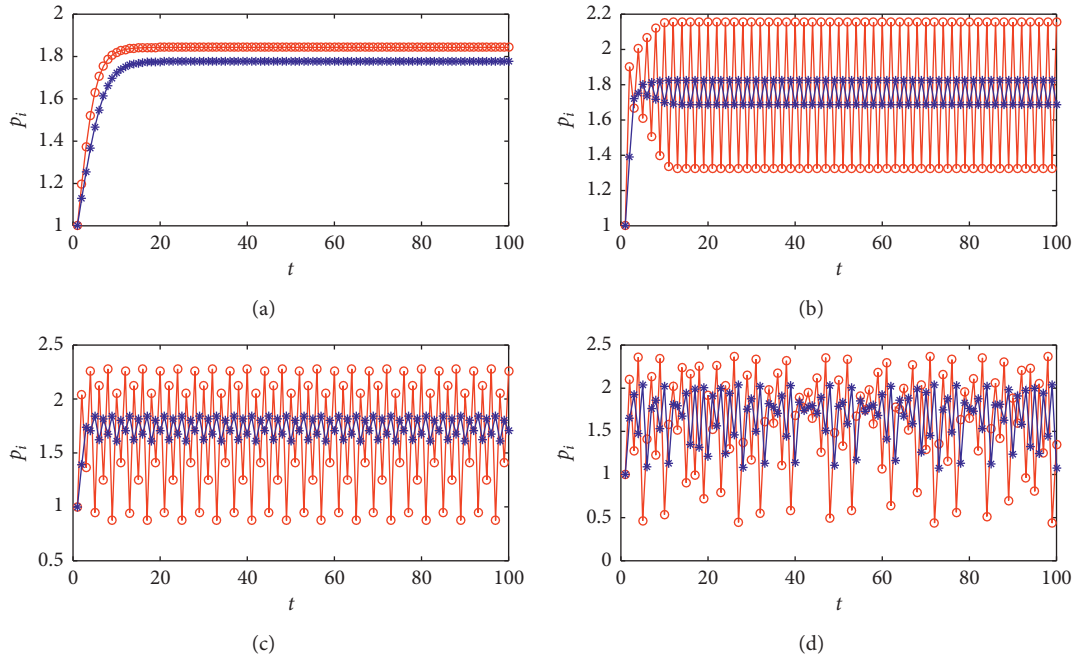


FIGURE 13: Price power spectrum of the system at different times.

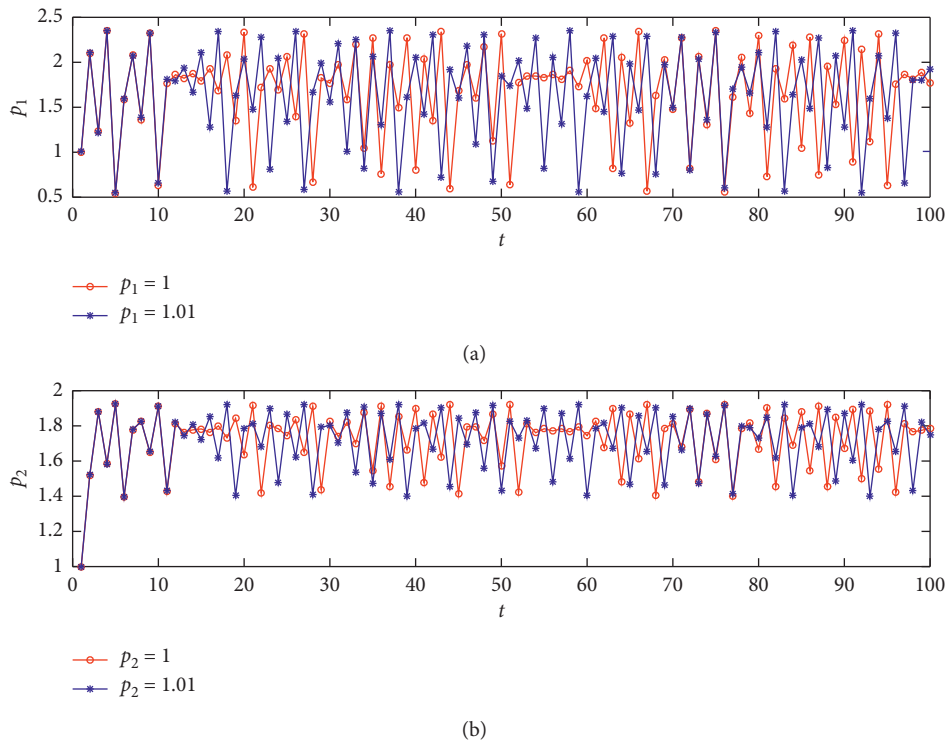


FIGURE 14: Sensitivity of the system to initial values: (a) $\alpha_1 = 0.56, \alpha_2 = 0.4$; (b) $\alpha_1 = 0.56, \alpha_2 = 0.4$.

Sensitive initial value is another important characteristic when the system is in chaos; that is, the evolution result of the system has extremely sensitive dependence on the initial value, which is what we often call the butterfly effect. Figure 14 shows the evolution of the recovery price over time when the initial pricing of recycler 1 and

recycler 2 is 1 and 1.01 and when the system is in a chaotic state ($\alpha_1 = 0.56, \alpha_2 = 0.4$). We get to know that even the initial value has only a slight difference. However, over time, the price competition has undergone a long-term evolution process, and its process has become very different.

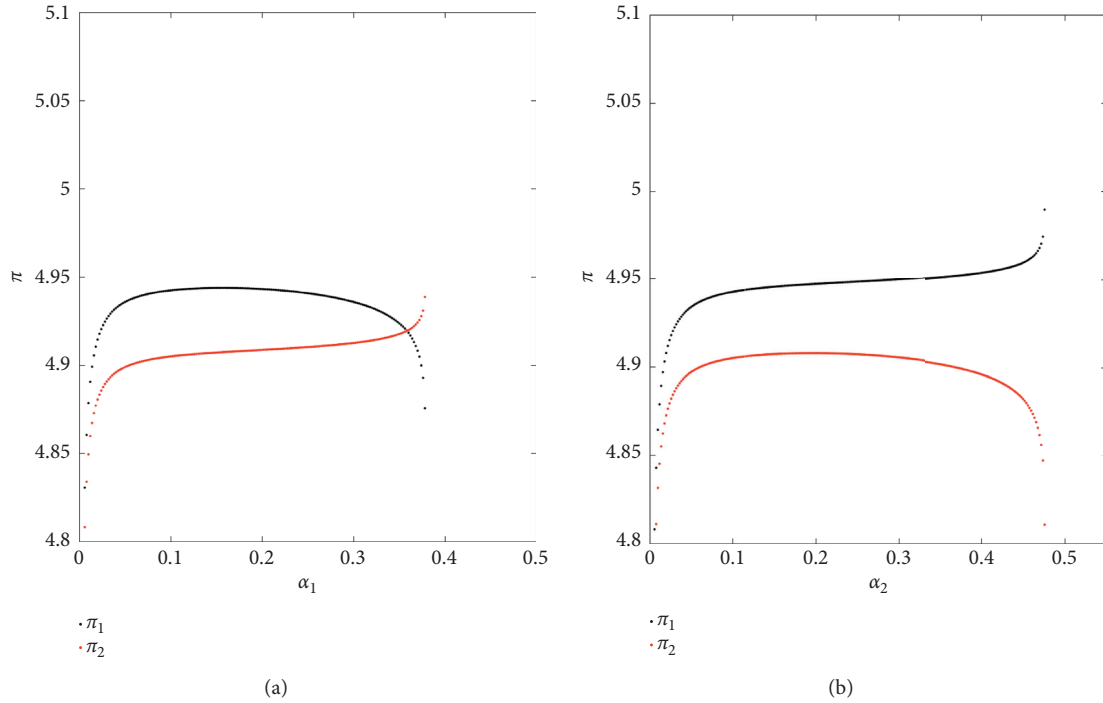


FIGURE 15: Changes in recyclers' profits with that of the price adjustment speed.

4.3. Impact of Price Adjustment Speed on Recyclers' Profits.

Figure 15 shows the changes in the profits of two recyclers with the speed of price adjustment. From Figure 15(a), we find that as the price adjustment speed of recycle 1 continues to accelerate, the profit of recycler 1 starts to decline. It is when the system is chaotic, it declines rapidly, but at the same time, the profit of recycler 2 is rising. Comparing to the enlightenment given in Figure 4, this shows that when recycler 1 speeds up the price adjustment to obtain a greater competitive advantage, exaggerated price fluctuations have also affected their own profits. Figure 15(b) and Figure 5 say that when recycler 2 speeds up the price adjustment, its profit also decreases.

5. Conclusion

This article establishes a reverse supply chain consisting of two recyclers. The two recyclers make competition through price strategies. We assume that one of the retailers is of fair concern, which makes the competition for recycling of products more intense. Through analysis on the equilibrium point stability, we find three unstable bounded equilibrium points and a Nash equilibrium point with local stability. Then, the simulation study of the system is performed. So, the following conclusions are made:

- (1) With the increase in the price adjustment speed for recyclers, some complex phenomena like bifurcation and chaos will appear in the system during the long-term process of competition. In this paper, the characteristics of the system in different periods are simulated numerically through means of the

bifurcation diagram, the maximum Lyapunov index, and the power spectrum diagram of price changes.

- (2) The fairness concerns of recyclers have a significant impact on the stability of the system. It is found that when the fair concern coefficient of the recycler becomes larger, the recyclers will care more about the sense of fairness, and the result of it is that recyclers may adopt a more aggressive price competition strategy, which may also make the system become more likely to lose its stability. By making analysis on the stability of the system, we find that amounts of the stability area for the system has decreased significantly.
- (3) Speeding up the price adjustment is a common business strategy for companies to gain competitive advantage. However, in a reverse supply chain where there is a fair concern, speeding up the price adjustment will not only cause complex phenomena such as chaos in the system but also actively accelerate the recovery of price adjustment speed. Not only does the price fluctuate greatly during chaos but profits also significantly decrease after complex behaviors such as bifurcation and chaos occurred in the system. At the same time, the relative profit of recyclers who have not actively adjusted the price adjustment rate has increased. This conclusion is different from many previous studies, which indicates that although it is easier to actively adjust prices to obtain a competitive advantage, we must also strive to maintain a competitive balance in the

market. Once the market loses its stability, continual speeding up of the price adjustment will only have negative effects on its own profits but positive effects on the profits of the opponent.

In our research, the impact of fairness factors on the complexity of the system has been taken into consideration, but many other behavioral factors that could have some influence on the retailer's decision-making still account for a large proportion. At the same time, fractional order equations, being an important form of demand function, also means an important research direction for the study which is mainly about the operators' behavior of reverse supply chain in the future.

Data Availability

The data used to support the findings of this study are available from the corresponding author upon request.

Conflicts of Interest

The authors declare that they have no conflicts of interest.

Acknowledgments

The research was supported by the China Post-doctoral Fund (no. 2016M602155), Ministry of Education Humanities and Social Sciences Project (no. 18YJCZH081), Scientific Research Projects in Shandong Universities (no. J18RA055), Talent Introduction Project of Dezhou University (no. 2015skrc05), and innovation and entrepreneurship training program for college students of the Ministry of Education (S201910448035).

References

- [1] H. Cao and Z. Chen, "The driving effect of internal and external environment on green innovation strategy-The moderating role of top management's environmental awareness," *Nankai Business Review International*, vol. 10, no. 3, pp. 342–361, 2019.
- [2] K. Govindan, H. Soleimani, and D. Kannan, "Reverse logistics and closed-loop supply chain: a comprehensive review to explore the future," *European Journal of Operational Research*, vol. 240, no. 3, pp. 603–626, 2015.
- [3] R. C. Savaskan, S. Bhattacharya, and L. N. Van Wassenhove, "Closed-loop supply chain models with product remanufacturing," *Management Science*, vol. 50, no. 2, pp. 239–252, 2004.
- [4] R. C. Savaskan and L. N. Van Wassenhove, "Reverse channel design: the case of competing retailers," *Management Science*, vol. 52, no. 1, pp. 1–14, 2006.
- [5] I.-H. Hong and J.-S. Yeh, "Modeling closed-loop supply chains in the electronics industry: a retailer collection application," *Transportation Research Part E: Logistics and Transportation Review*, vol. 48, no. 4, pp. 817–829, 2012.
- [6] T.-M. Choi, Y. Li, and L. Xu, "Channel leadership, performance and coordination in closed loop supply chains," *International Journal of Production Economics*, vol. 146, no. 1, pp. 371–380, 2013.
- [7] J. Wei, K. Govindan, Y. Li, and J. Zhao, "Pricing and collecting decisions in a closed-loop supply chain with symmetric and asymmetric information," *Computers & Operations Research*, vol. 54, pp. 257–265, 2015.
- [8] Y. Zhou, M. Bao, X. Chen, and X. Xu, "Co-op advertising and emission reduction cost sharing contracts and coordination in low-carbon supply chain based on fairness concerns," *Journal of Cleaner Production*, vol. 133, pp. 402–413, 2016.
- [9] B. J. Ruffle, "More is better, but fair is fair: tipping in dictator and ultimatum games," *Games and Economic Behavior*, vol. 23, no. 2, pp. 247–265, 1996.
- [10] E. Fehr and K. M. Schmidt, "A theory of fairness, competition, and cooperation," *The Quarterly Journal of Economics*, vol. 114, no. 3, pp. 817–868, 1999.
- [11] C. H. Loch and Y. Wu, "Social preferences and supply chain performance: an experimental study," *Management Science*, vol. 54, no. 11, pp. 1835–1849, 2008.
- [12] A. Tversky and D. Kahneman, *Rational Choice and the Framing of Decisions*, Springer, Berlin, Germany, 1989.
- [13] T. Haitao Cui, J. S. Raju, and Z. J. Zhang, "Fairness and channel coordination," *Management Science*, vol. 53, no. 8, pp. 1303–1314, 2007.
- [14] X. Li, X. Cui, Y. Li, D. Xu, and F. Xu, "Optimisation of reverse supply chain with used-product collection effort under collector's fairness concerns," *International Journal of Production Research*, pp. 1–12, 2019.
- [15] D. Rand, "Exotic phenomena in games and duopoly models," *Journal of Mathematical Economics*, vol. 5, no. 2, pp. 173–184, 1978.
- [16] T. Puu, "The chaotic monopolist," *Chaos, Solitons & Fractals*, vol. 5, no. 1, pp. 35–44, 1995.
- [17] T. Puu and M. R. Marín, "The dynamics of a triopoly Cournot game when the competitors operate under capacity constraints," *Chaos, Solitons & Fractals*, vol. 28, no. 2, pp. 403–413, 2006.
- [18] G. I. Bischi and M. Kopel, "Equilibrium selection in a nonlinear duopoly game with adaptive expectations," *Journal of Economic Behavior & Organization*, vol. 46, no. 1, pp. 73–100, 2001.
- [19] G.-I. Bischi and F. Lamantia, "Nonlinear duopoly games with positive cost externalities due to spillover effects," *Chaos, Solitons & Fractals*, vol. 13, no. 4, pp. 701–721, 2002.
- [20] H. N. Agiza, A. S. Hegazi, and A. A. Elsadany, "Complex dynamics and synchronization of a duopoly game with bounded rationality," *Mathematics and Computers in Simulation*, vol. 58, no. 2, pp. 133–146, 2002.
- [21] B. Xin, T. Chen, and Y. Liu, "Projective synchronization of chaotic fractional-order energy resources demand-supply systems via linear control," *Communications in Nonlinear Science and Numerical Simulation*, vol. 16, no. 11, pp. 4479–4486, 2011.
- [22] B. Xin and J. Zhang, "Finite-time stabilizing a fractional-order chaotic financial system with market confidence," *Nonlinear Dynamics*, vol. 79, no. 2, pp. 1399–1409, 2015.
- [23] E. Ahmed and A. S. Hegazi, "On dynamical multi-team and signaling games," *Applied Mathematics and Computation*, vol. 172, no. 1, pp. 524–530, 2006.
- [24] E. Ahmed, M. F. Elettrey, and A. S. Hegazi, "On Puu's incomplete information formulation for the standard and multi-team Bertrand game," *Chaos, Solitons & Fractals*, vol. 30, no. 5, pp. 1180–1184, 2006.
- [25] A. A. Elsadany, "Dynamics of a delayed duopoly game with bounded rationality," *Mathematical and Computer Modelling*, vol. 52, no. 9–10, pp. 1479–1489, 2010.

- [26] T. Li and J. Ma, "Complexity analysis of dual-channel game model with different managers' business objectives," *Communications in Nonlinear Science and Numerical Simulation*, vol. 20, no. 1, pp. 199–208, 2015.
- [27] T. Li and J. Ma, "Complexity analysis of the dual-channel supply chain model with delay decision," *Nonlinear Dynamics*, vol. 78, no. 4, pp. 2617–2626, 2014.
- [28] T. Li, D. Yan, and X. Ma, "Stability analysis and chaos control of recycling price game model for manufacturers and retailers," *Complexity*, vol. 2019, Article ID 3157407, 13 pages, 2019.
- [29] T. Puu, "Complex dynamics with three oligopolists," *Chaos, Solitons & Fractals*, vol. 7, no. 12, pp. 2075–2081, 1996.

Research Article

Feedback Control of a Chaotic Finance System with Two Delays

Zhichao Jiang¹ and Tongqian Zhang²

¹School of Liberal Arts and Sciences, North China Institute of Aerospace Engineering, Langfang 065000, China

²College of Mathematics and Systems Science, Shandong University of Science and Technology, Qingdao 266590, China

Correspondence should be addressed to Tongqian Zhang; zhangtongqian@sdu.edu.cn

Received 29 February 2020; Revised 26 April 2020; Accepted 4 May 2020; Published 26 May 2020

Academic Editor: Abdelalim Elsadany

Copyright © 2020 Zhichao Jiang and Tongqian Zhang. This is an open access article distributed under the Creative Commons Attribution License, which permits unrestricted use, distribution, and reproduction in any medium, provided the original work is properly cited.

In this research, we use the double-delayed feedback control (DDFC) method in order to control chaos in a finance system. Taking delays as parameters, the dynamic behavior of the system is investigated. Firstly, we study the local stability of equilibrium and the existence of local Hopf bifurcations. It can find that the delays can make chaos disappear and generate a stable equilibrium or periodic solution, which means the effectiveness of DDFC method. By using the normal form theory and center manifold argument, one derives the explicit algorithm for determining the properties of bifurcation. In addition, we also apply some mathematical methods (stability crossing curves) to show the stability changes of the financial system in two parameters' (τ_1, τ_2) plane. Finally, we give some numerical simulations by Matlab Microsoft to show the validity of theoretical analyses.

1. Introduction

In the past few decades, many scholars produced the increasing interest in nonlinear dynamic economic methods [1–11]. In the fields of finance, because of the influence of nonlinear factors, all sorts of economy problems become more and more complicated. The misalignment of certain parameters in the economic system can lead to runaway markets and possibly even a financial crisis [12–15]. Therefore, it is more and more important to study the internal structure characteristics of a complex financial system and uncover its causes, so as to predict and control the system.

A lot of work has been carried out in modeling nonlinear economic dynamics, such as Goodwin's model, van der Pol model, IS-LM model, and nonlinear finance system [14, 16–25]. However, it is well known that even a simple nonlinear system can exhibit chaotic behavior. Chaos is the inherent randomness of deterministic systems. Since the first discovery of chaos in economics from 1985, a great impact has been produced on the study of western economics because chaos in the economic system means the inherent uncertainty in macroeconomic operation. Over the past two decades, many efforts had been made to control chaos, such as stability and chaos synchronization, at unstable fixed

points. In recent years, many methods had been put forward to control and synchronize chaos, such as OGY method [26], PC method [27], fuzzy control [28], impulsive control method [29, 30], stochastic control [31–33], linear feedback control [34], delay feedback approach [35–44], and multiple delay feedback control (MDFC) [45]. Delayed feedback control (DFC) was first proposed by Pyragas [46] in order to stabilize unstable periodic orbits (UPO). Then, the DFC method was extended to the multidelay [47]. One of the main characteristics of the DFC method is that it does not need the knowledge of the internal dynamics of the system beyond the period nor does it require a preliminary understanding of the required UPO. At the same time of UPO control, using the DFC method to realize USS stability had become an area of concern and had been applied to some real systems. It is very successful in stabilizing UPO for the DFC method, but the control of USS is less efficient. In [45], authors put forward the MDFC method and conducted numerical simulations, which showed that the MDFC method preceded the DFC method in USS stability.

In [16], authors put forward a financial system describing the temporal changes using three variables: $x(t)$ denotes the interest rate, $y(t)$ expresses the investment demand, and $z(t)$ represents the price index:

$$\begin{cases} \dot{\mathbf{x}}(t) = (\mathbf{y} - a)\mathbf{x} + \mathbf{z}, \\ \dot{\mathbf{y}}(t) = 1 - b\mathbf{y} - \mathbf{x}^2, \\ \dot{\mathbf{z}}(t) = -\mathbf{x} - c\mathbf{z}, \end{cases} \quad (1)$$

where the parameters a, b , and c represent the saving amount, the investment cost, and the elasticity of market demand, respectively, and a, b , and c are positive constants. From [48], it is known that, under the parameter values $a = 0.9$, $b = 0.2$, and $c = 1.2$, system (1) exists a strange attractor, as shown in Figure 1.

In this paper, our object is to control the strange attractor by using the DDFC method and study the following system:

$$\begin{cases} \dot{\mathbf{x}}(t) = (\mathbf{y} - a)\mathbf{x} + \mathbf{z} + k_1 [\mathbf{x}(t) - \mathbf{x}(t - \tau_1)] + k_2 [\mathbf{x}(t) - \mathbf{x}(t - \tau_2)], \\ \dot{\mathbf{y}}(t) = 1 - b\mathbf{y} - \mathbf{x}^2, \\ \dot{\mathbf{z}}(t) = -\mathbf{x} - c\mathbf{z}, \end{cases} \quad (2)$$

where $k_1 \in \mathbb{R}$ and $k_2 \in \mathbb{R}$ are the feedback strengths and τ_1 and τ_2 are nonnegative delays.

The initial conditions of system (2) are given as

$$\begin{aligned} \mathbf{x}(b) &= \varphi_1(b), \\ \mathbf{y}(b) &= \varphi_2(b), \\ \mathbf{z}(b) &= \varphi_3(b), \quad b \in [-\tau, 0], \end{aligned} \quad (3)$$

where $\varphi = (\varphi_1, \varphi_2, \varphi_3)^T \in C = C([- \tau, 0], \mathbb{R}^3)$ and $\tau = \max\{\tau_1, \tau_2\}$.

The purpose of this paper is to analyze and numerically study system (2). Our results show that the stability of system varies with delays. When the delay passes a certain critical value, the chaotic oscillation disappears and can be transformed into stable equilibrium or periodic orbit, which indicates that the chaotic property changes with the changes of delays.

This article is organized as follows. In Section 2, by studying the distribution of eigenvalues of exponential polynomials and using the results in [49, 50], the local stability and existence of local Hopf bifurcation are obtained. In Section 3, the properties of Hopf bifurcation are given by using central manifold theory and normal form method. In Section 4, using the crossing curve methods, it can obtain the stable changes of equilibrium in (τ_1, τ_2) plane to overcome the problem that no information is given on the plane (τ_1, τ_2) that comes into being stable or unstable equilibrium in Section 2. To support the analysis results, some numerical simulations are carried out in Section 5. Finally, some conclusions and discussions are given.

2. Stability of Equilibrium and Hopf Bifurcation

Firstly, it gives the existence of equilibria.

Lemma 1.

(i) If $c(1 - ab) - b \leq 0$ holds, then system (2) has only a boundary equilibrium $E_0(0, 1/b, 0)$

(ii) If $c(1 - ab) - b > 0$ holds, then system (2) has two interior equilibria $E_{\pm}^*(\pm \kappa, (1 + ac/c), \mp \kappa c^{-3/2})$ besides E_0 , where $\kappa = (1 - ab - b/c)^{1/2}$.

In the following text, it always assumes that $c(1 - ab) - b > 0$ is satisfied and only considers the stability of E_{\pm}^* and the other equilibria can be analyzed similarly.

Let $u_1 = \mathbf{x} - \kappa$, $u_2 = \mathbf{y} - (1 + ac/c)$, and $u_3 = \mathbf{z} + \kappa c^{-3/2}$, then system (2) becomes

$$\begin{cases} \dot{u}_1(t) = \left(\frac{1}{c} + k_1 + k_2\right)u_1(t) + \kappa u_2(t) + u_3(t) - k_1 u_1(t - \tau_1) \\ \quad - k_2 u_1(t - \tau_2) + u_1(t)u_2(t), \\ \dot{u}_2(t) = -2\kappa u_1(t) - b u_2(t) - u_1^2(t), \\ \dot{u}_3(t) = -u_1(t) - c u_3(t), \end{cases} \quad (4)$$

whose characteristic equation is

$$\begin{aligned} \nabla(\lambda, \tau_1, \tau_2) &= \lambda^3 + a_2 \lambda^2 + a_1 \lambda + a_0 + k_1 e^{-\lambda \tau_1} (\lambda^2 + b_1 \lambda + b_0) \\ &\quad + k_2 e^{-\lambda \tau_2} (\lambda^2 + b_1 \lambda + b_0) = 0, \end{aligned} \quad (5)$$

where

$$\begin{aligned} a_0 &= c[2\kappa^2 - b(k_1 + k_2)], \\ a_1 &= 2\kappa^2 + bc - \frac{b}{c} - (b + c)(k_1 + k_2), \\ a_2 &= b + c - \left(\frac{1}{c} + k_1 + k_2\right), \\ b_0 &= bc, \\ b_1 &= b + c. \end{aligned} \quad (6)$$

Now, we use the method in [49, 50] to study the root distribution of (5). When $\tau_1 = \tau_2 = 0$, (5) becomes

$$\begin{aligned} \nabla(\lambda, 0, 0) &= \lambda^3 + (k_1 + k_2 + a_2)\lambda^2 + (k_1 b_1 + k_2 b_1 + a_1)\lambda \\ &\quad + k_1 b_0 + k_2 b_0 + a_0 = 0. \end{aligned} \quad (7)$$

By Routh–Hurwitz criterion, all roots of (7) have negative real parts if and only if

$$\begin{aligned} (H1) a_2 + k_1 + k_2 &> 0, \\ a_0 + k_1 b_0 + k_2 b_0 &> 0, \\ (a_2 + k_1 + k_2)(a_1 + k_1 b_1 + k_2 b_1) &> a_0 + k_1 b_0 + k_2 b_0, \end{aligned} \quad (8)$$

holds.

2.1. The Case $\tau_1 > 0$ and $\tau_2 = 0$. In this part, let $\tau_2 = 0$, and choose τ_1 as the parameter to study the distribution of the

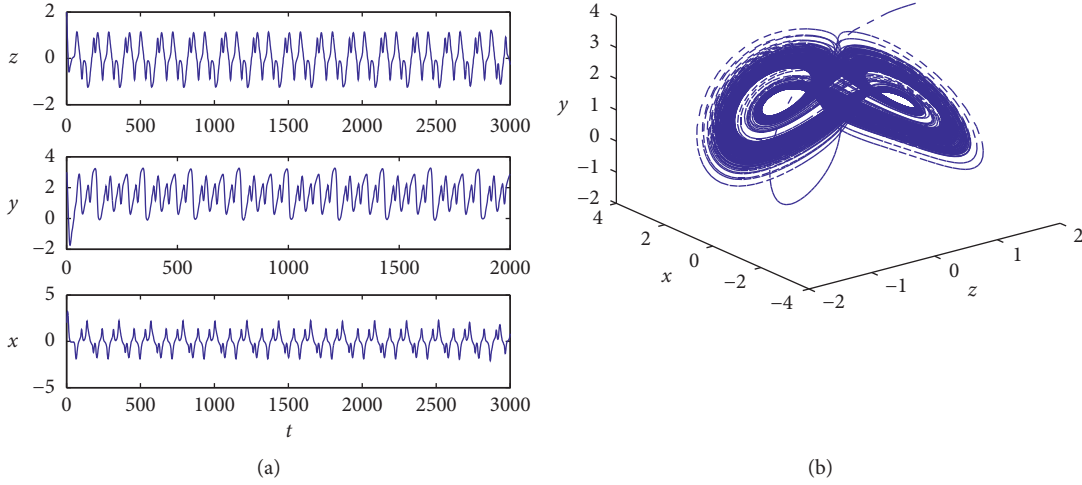


FIGURE 1: There exists chaotic attractor for system (1). (a) Time series of the solutions of system (1). (b) Three-dimensional phase diagram of system (1).

root of (5). Let $i\omega$ be the root of (5), then ω must satisfy the following equations:

$$\begin{cases} -\omega^3 + (a_1 + k_2 b_1)\omega = k_1 [(b_0 - \omega^2)\sin \omega\tau_1 - b_1 \omega \cos \omega\tau_1], \\ a_2 \omega^2 - a_0 - k_2 (b_0 - \omega^2) = k_1 [(b_0 - \omega^2)\cos \omega\tau_1 + b_1 \omega \sin \omega\tau_1]. \end{cases} \quad (9)$$

Adding the squares of both sides of (9), it yields to

$$\omega^6 + \rho \omega^4 + q \omega^2 + r = 0, \quad (10)$$

where

$$\begin{aligned} \rho &= (k_2 + a_2)^2 - 2(a_1 + k_2 b_1) - k_1^2, \\ q &= (a_1 + k_2 b_1)^2 - 2(a_2 + k_2)(a_0 + b_0 k_2) + 2b_0 k_1 - k_1^2 b_1^2, \\ r &= (a_0 + k_2 b_0)^2 - k_1^2 b_0^2. \end{aligned} \quad (11)$$

Furthermore, from (9), it can be obtained that

$$\begin{cases} \cos \omega\tau_1 = \frac{\mathcal{Q}(b_0 - \omega^2) - \rho b_1}{k_1 (b_0 - \omega^2)^2 + k_1 b_1^2 \omega^2} := \mathbb{S}_1, \\ \sin \omega\tau_1 = \frac{\rho (b_0 - \omega^2) + \mathcal{Q} b_1 \omega}{k_1 (b_0 - \omega^2)^2 + k_1 b_1^2 \omega^2} := \mathbb{S}_2, \end{cases} \quad (12)$$

where $\rho = -\omega^3 + (a_1 + k_2 b_1)\omega$ and $\mathcal{Q} = a_2 \omega^2 - a_0 - k_2 (b_0 - \omega^2)$.

Let $z = \omega^2$, then (10) becomes

$$\mathbf{h}(z) := z^3 + \rho z^2 + qz + r = 0. \quad (13)$$

Applying the results in [49], the following conclusions hold.

Lemma 2.

(i) If $r \geq 0$ and $\Delta \leq 0$ hold, then (13) has no positive root

(ii) If $r < 0$ holds, then (13) has at least a positive root
 (iii) If $r \geq 0$ and $\Delta > 0$ hold, then (13) has a positive roots iff $z_1^* > 0$ and $\mathbf{h}(z_1^*) \leq 0$, where $z_1^* = (-\rho + \sqrt{\Delta})/3$ and $\Delta = \rho^2 - 3q$

Without loss of generality, it supposes that (13) has three positive roots, denoted by z_1, z_2 , and z_3 , respectively. Then, (10) has three positive roots $\omega_k = \sqrt{z_k}$ ($k = 1, 2, 3$). Substituting ω_k into (9) gives

$$\tau_{1k}^{(j)} = \begin{cases} \frac{1}{\omega_k} \{\arccos(\mathbb{S}_1) + 2j\pi\}, & \mathbb{S}_2 \geq 0, \\ \frac{1}{\omega_k} \{-\arccos(\mathbb{S}_1) + 2(j+1)\pi\}, & \mathbb{S}_2 < 0, \end{cases} \quad (14)$$

where $k = 1, 2, 3, j = 0, 1, \dots$

Define $\tau_1^0 = \min_{k=1,2,3} \{\tau_{1k}^{(0)}\}$. Let $\lambda(\tau_1) = \gamma(\tau_1) + i\omega(\tau_1)$ be the root of (5) with $\tau_2 = 0$ satisfying $\gamma(\tau_{1k}^{(j)}) = 0$ and $\omega(\tau_{1k}^{(j)}) = \omega_k$.

Lemma 3. Suppose that $\mathbf{h}'(z_k) \neq 0$, then $(\mathbf{d}(\gamma(\tau_{1k}^{(j)})))/\mathbf{d}\tau_1 \neq 0$ and $\mathbf{Sign}\{\mathbf{d}(\gamma(\tau_{1k}^{(j)}))/\mathbf{d}\tau_1\} = \mathbf{Sign}\{\mathbf{h}'(z_k)\}$.

Proof. Let $\tau_2 = 0$, and differentiate both sides of (5) about τ_1 , and it has

$$\begin{aligned} \left[\frac{\mathbf{d}\lambda}{\mathbf{d}\tau_1} \right]^{-1} &= \frac{[3\lambda^2 + 2(b_1 + k_2)\lambda + a_1 + k_2 b_1] e^{\lambda\tau_1}}{k_1 \lambda (\lambda^2 + b_1 \lambda + b_0)} \\ &+ \frac{2\lambda + b_1}{\lambda(\lambda^2 + b_1 \lambda + b_0)} - \frac{\tau_1}{\lambda}. \end{aligned} \quad (15)$$

Hence,

$$\begin{aligned} \left[\frac{\mathbf{d}(\gamma(\tau_{1k}^{(j)}))}{\mathbf{d}\tau_1} \right]^{-1} &= \mathbf{Re} \left\{ \left[\frac{3\lambda^2 + 2(b_1 + k_2)\lambda + a_1 + k_2 b_1}{k_1 \lambda (\lambda^2 + b_1 \lambda + b_0)} e^{\lambda \tau_1} + k_1 (2\lambda + b_1) - \frac{\tau_1}{\lambda} \right] \right\} \Big|_{\tau_1 = \tau_{1k}^{(j)}} \\ &= \frac{1}{\Gamma} (3\omega_k^6 + 2\rho\omega_k^4 + \varrho\omega_k^2) = \frac{\varkappa_k}{\Gamma} \mathbf{h}'(\varkappa_k), \end{aligned} \quad (16)$$

where $\Gamma = k_1^2 [b_1^2 \omega_k^4 + (\omega_k^2 - b_0)\omega_k^2]$. Since $\Gamma > 0$ and $\varkappa_k > 0$, then we have

$$\mathbf{Sign} \left\{ \frac{\mathbf{d}(\gamma(\tau_{1k}^{(j)}))}{\mathbf{d}\tau_1} \right\} = \mathbf{Sign}\{\mathbf{h}'(\varkappa_k)\}. \quad (17)$$

By 3 and applying the Hopf bifurcation theorem in [51], for system (2) it has the following theorem. \square

Theorem 1. *It assumes that (H1) holds:*

- (i) *If $\varkappa > 0$ and $\Delta \leq 0$ hold, then, for all $\tau_1 \geq 0$, E_+^* is locally asymptotically stable (LAS)*
- (ii) *If either $\varkappa < 0$ or $\varkappa \geq 0$ and $\Delta > 0$, $\varkappa_1^* > 0$, $\mathbf{h}(\varkappa_1^*) \leq 0$ hold, then for $\tau_1 \in [0, \tau_1^0)$, E_+^* is LAS*
- (iii) *If all conditions in (ii) and $\mathbf{h}'(\varkappa_k) \neq 0$ hold, then system (2) undergoes Hopf bifurcations at E_+^* when $\tau_1 = \tau_{1k}^{(j)}$, $j = 0, 1, 2, \dots, k = 1, 2, 3$*

We know that the condition (H1) guarantees that all roots of (7) have negative real parts. If (H1) is violated, we define

$$A = a_2 + k_1 + k_2, \quad B = a_1 + (k_1 + k_2)b_1, \quad C = a_0 + (k_1 + k_2)b_0. \quad (18)$$

Let $\lambda = \Lambda - A/3$, then (7) becomes

$$\Lambda^3 + \rho_1 \Lambda + \varrho_1 = 0, \quad (19)$$

where $\rho_1 = B - A^2/3$ and $\varrho_1 = (2A^3/27) - (AB/3) + C$. Define

$$\begin{aligned} \Delta_1 &= \left(\frac{\rho_1}{3}\right)^3 + \left(\frac{\varrho_1}{2}\right)^2, \\ \alpha &= \sqrt{[3]} - \frac{\varrho_1}{2} + \sqrt{\Delta_1}, \\ \beta &= \sqrt{[3]} - \frac{\varrho_1}{2} - \sqrt{\Delta_1}. \end{aligned} \quad (20)$$

Then, from Cardano's formula, it has the following Theorem.

Theorem 2.

- (i) *If $\Delta_1 < 0$, then (19) has three real roots*
- (ii) *If $\Delta_1 > 0$, then (19) has a real root $\alpha + \beta - A/3$ and a pair of conjugate complex roots $-((\alpha + \beta)/2) + (A/3) \pm \mathbf{i}((\sqrt{3}(\alpha - \beta))/2)$*

Furthermore, we assume that

$$(H2)\Delta_1 > 0,$$

$$\frac{\alpha + \beta}{2} + \frac{A}{3} < 0, \quad (21)$$

$$\alpha + \beta - \frac{A}{3} < 0,$$

$$\alpha - \beta \neq 0.$$

Theorem 3. *It assumes that (H2) holds. For system (2), it has the following results.*

- (i) *If $\varkappa > 0$ and $\Delta \leq 0$, then, for all $\tau_1 \geq 0$, E_+^* of system (2) is unstable.*
- (ii) *If either $\varkappa < 0$ or $\varkappa \geq 0$ and $\Delta > 0$, $\varkappa_1^* > 0$, $\mathbf{h}(\varkappa_1^*) \leq 0$ hold, then for $\tau_1 \in [0, \tau_1^0)$, E_+^* of system (2) is unstable. In addition, if $\mathbf{dRe} \lambda(\tau_1^0)/\mathbf{d}\tau_1 < 0$, then E_+^* is LAS when $\tau_1 \in (\tau_1^0, \tau_1^1)$, where τ_1^1 is the second critical value.*
- (iii) *If all conditions in (ii) and $\mathbf{h}'(\varkappa_k) \neq 0$ hold, then system (2) undergoes Hopf bifurcations at E_+^* when $\tau_1 = \tau_{1k}^{(j)}$, $j = 0, 1, 2, \dots, k = 1, 2, 3$.*

From the abovementioned discussion, one can know that the stable switch may exist as τ_1 varies for system (2) with $\tau_2 = 0$. Define I as stable interval of τ_1 .

2.2. *The Case $\tau_1 \in I$ and $\tau_2 > 0$.* In this part, let $\tau_1 \in I$, $\tau_2 > 0$, and $\lambda = \mathbf{i}\omega$ ($\omega = \omega(\tau_2) > 0$) be the root of (5), and it has

$$\begin{cases} -\omega^3 + a_1 \omega - k_1 (b_0 - \omega^2) \sin \omega \tau_1 + k_1 b_1 \omega \cos \omega \tau_1 \\ = k_2 [(b_0 - \omega^2) \sin \omega \tau_2 - b_1 \omega \cos \omega \tau_2], \\ a_2 \omega^2 - a_0 - k_1 (b_0 - \omega^2) \cos \omega \tau_1 - k_1 b_1 \omega \sin \omega \tau_1 \\ = k_2 [(b_0 - \omega^2) \cos \omega \tau_2 + b_1 \omega \sin \omega \tau_2], \end{cases} \quad (22)$$

which yields to

$$\begin{cases} \cos \omega \tau_2 = \frac{\mathcal{Q}^1 (b_0 - \omega^2) - \rho^1 b_1}{k_2 (b_0 - \omega^2)^2 + k_2 b_1^2 \omega^2} := \mathbb{T}_1, \\ \sin \omega \tau_2 = \frac{\rho^1 (b_0 - \omega^2) + \mathcal{Q}^1 b_1 \omega}{k_2 (b_0 - \omega^2)^2 + k_2 b_1^2 \omega^2} := \mathbb{T}_2, \end{cases} \quad (23)$$

where

$$\rho^1 = -\omega^3 + a_1\omega - k_1(b_0 - \omega^2)\sin \omega\tau_1 + k_1b_1\omega \cos \omega\tau_1, \quad (24)$$

and

$$\mathcal{Q}^1 = a_2\omega^2 - a_0 - k_1(b_0 - \omega^2)\cos \omega\tau_1 - k_1b_1\omega \sin \omega\tau_1. \quad (25)$$

Hence, we have

$$\begin{aligned} g(\omega) := & \omega^6 + (b_1^2 - 2a_1 - k_2^2 + k_1^2)\omega^4 + [a_1^2 - 2a_0b_1 \\ & + (2b_0 - b_1^2)(k_2^2 - k_1^2)]\omega^2 \\ & + a_0^2 - b_0^2(k_2^2 - k_1^2) + 2[k_1(a_0 - b_1\omega^2)(b_0 - \omega^2) \\ & + k_1b_1\omega(a_1\omega - \omega^3)]\cos \omega\tau_1 \\ & + 2[k_1b_1\omega(a_0 - b_1\omega^2) - k_1(a_1\omega - \omega^3)(b_0 - \omega^2)] \\ & \sin \omega\tau_1 = 0, \end{aligned} \quad (26)$$

with $g(0) = a_0^2 - b_0^2(k_2^2 - k_1^2) + 2[k_1(a_0 - b_1\omega^2)(b_0 - \omega^2) + k_1b_1\omega(a_1\omega - \omega^3)]$ and $g(+\infty) = +\infty$.

It can be easily known that equation (26) has at most N positive roots, denoted by $\omega_k (k = 1, 2, \dots, N)$. From (22), we have

$$\tau_{2k}^{(i)} = \begin{cases} \frac{1}{\omega_k} \{\arccos(\mathbb{T}_1) + 2i\pi\}, & \mathbb{T}_2 \geq 0, \\ \frac{1}{\omega_k} \{-\arccos(\mathbb{T}_1) + 2(i+1)\pi\}, & \mathbb{T}_2 < 0, i = 0, 1, 2, \dots \end{cases} \quad (27)$$

Denote

$$\begin{aligned} \tau_2^0 = \tau_{2k_0}^{(0)} &= \min_{k \in \{1, 2, \dots, N\}} \{\tau_{2k}^{(0)}\}, \\ \omega_0 &= \omega_{k_0}. \end{aligned} \quad (28)$$

Let $\lambda(\tau_2) = \alpha(\tau_2) + i\omega(\tau_2)$ be the root of (5) satisfying $\alpha(\tau_{2k}^{(j)}) = 0$ and $\omega(\tau_{2k}^{(j)}) = \omega_k$. By computation, we obtain

$$\begin{aligned} \alpha(\tau_2^0) = & \mathcal{O}\{RS - TU - 2k_2^2\omega_0^2 + 2b_0k_2^2\omega_0^2 - b_1^2k_2^2\omega_0^2 + (RD\omega_0 - ET\omega_0)\sin \omega_0\tau_2^0 \\ & - (QD + PE)\omega_0 \cos \omega_0(\tau_1 + \tau_2^0) + (-EQ + PD)\omega_0 \\ & \sin \omega_0(\tau_1 + \tau_2^0) - (ER\omega_0 + DT\omega_0)\cos \omega_0\tau_2^0 + (SP + UQ)\cos \omega_0\tau_1 + (QS - PU)\sin \omega_0\tau_1\}^{-1}, \end{aligned} \quad (29)$$

where

$$\begin{aligned} \mathcal{O} &= b_1^2k_2^2\omega_0^4 + (b_0^2 - \omega_0^2)^2k_2^2\omega_0^2, \\ P &= -k_1(-b_1 + b_0\tau_1 - \tau_1\omega_0^2), \\ Q &= -k_1(-2\omega_0 + b_1\tau_1\omega_0), \\ R &= -3\omega_0^2 + a_1, \\ D &= -k_1(b_0 - \omega_0), \\ E &= -k_1b_1\omega_0, \\ S &= a_1\omega_0^2 - \omega_0^4, \\ T &= 2b_1\omega_0, \\ U &= -b_1\omega_0^3 + a_0\omega_0. \end{aligned} \quad (30)$$

To sum up, we have the following theorem.

Theorem 4. Suppose that either (H1) or (H2) is satisfied, and $\tau_1 \in I$ for system (2).

- (i) If (26) has no positive roots, then for all $\tau_2 \geq 0$, E_+^* is LAS.
- (ii) If (26) has positive roots, then E_+^* of is LAS when $\tau_2 \in [0, \tau_2^0)$. In addition, if $\alpha(\tau_2^0) \neq 0$, then system (2) undergoes Hopf bifurcation at E_+^* when $\tau_2 = \tau_2^0$.

Remark 1. Obviously, there exists a Hopf bifurcation at τ_2^0 when τ_1 is fixed in the stable interval I . However, if we

choose τ_1 in the unstable interval, then there may be no τ_2^* such that when system (2) is unstable in $\tau_2 \in [0, \tau_2^*)$, it is stable in $\tau_2 > \tau_2^*$. The result will be discussed in the latter section by using the stability crossing curve method in [52].

Remark 2. For some τ_1 and τ_2 , if (5) has two pairs of purely imaginary roots $\pm i\omega_1$ and $\pm i\omega_2$, all the other roots have negatively real parts. Let $w_1: w_2 = l_1: l_2$; then, system (2) undergoes a double Hopf bifurcation (DHB) with the ratio $l_1: l_2$. If $l_1, l_2 \in \mathbb{Z}^+$, then it is called a resonant DHB; otherwise, it is called a nonresonant DHB. Since in system (2) there are several parameters besides τ_1 and τ_2 , the co-dimension 2 bifurcation may occur. An interesting study can be found in [53].

3. Property of Hopf Bifurcation at E_+^*

In Section 3, we have obtained some sufficient conditions to guarantee that the Hopf bifurcation occurs in system (2) at E_+^* when $\tau_2 = \tau_2^0$. In this section, we assume that Theorem 4 (ii) is satisfied to establish the explicit formula for the property of Hopf bifurcation at $\tau_2 = \tau_2^0$ using the method proposed by Hassard et al. [54].

For convenience, we assume $\tau_1 > \tau_2$ and the phase space $C = C([- \tau_1, 0], \mathbb{R}^3)$. Let $\bar{\tau}_2 = \tau_2^0 + \vartheta$, $\vartheta \in \mathbb{R}$ and dropping “-”. Then, system (2) occurs Hopf bifurcation at $\vartheta = 0$. System (2) can be transformed into the following system:

$$\dot{\mathcal{U}}_t = \mathbb{L}_\vartheta(\mathcal{U}_t) + f(\vartheta, \mathcal{U}_t), \quad (31)$$

where $\mathcal{U}_t(\theta) = \mathcal{U}(t + \theta) \in C$, and $\mathbb{L}_\vartheta: C \rightarrow \mathbb{R}^3, f: \mathbb{R} \times C \rightarrow \mathbb{R}^3$ are given, respectively, by

$$\mathbb{L}_\vartheta\varphi = A_1\varphi(0) + B_1\varphi(-\tau_1) + B_2\varphi(-\tau_2^0), \quad (32)$$

where

$$A_1 = \begin{pmatrix} k_1 + k_2 + \frac{1}{c} & \kappa & 1 \\ -2\kappa & -b & 0 \\ -1 & 0 & -c \end{pmatrix},$$

$$B_1 = \begin{pmatrix} -k_1 & 0 & 0 \\ 0 & 0 & 0 \\ 0 & 0 & 0 \end{pmatrix},$$

$$B_2 = \begin{pmatrix} -k_2 & 0 & 0 \\ 0 & 0 & 0 \\ 0 & 0 & 0 \end{pmatrix},$$

$$f(\vartheta, \varphi) = \begin{pmatrix} \varphi_1(0)\varphi_2(0) \\ -\varphi_1^2(0) \\ 0 \end{pmatrix}, \quad (33)$$

where $\varphi = (\varphi_1, \varphi_2, \varphi_3)^T \in C$.

By the Riesz representation theorem, for $\Theta \in [-\tau_1, 0]$, there exists a bounded variation function $\zeta(\Theta, \vartheta)$ such that

$$\mathbb{L}_\vartheta\varphi = \int_{-\tau_1}^0 \mathbf{d}\zeta(\Theta, \vartheta)\varphi(\Theta). \quad (34)$$

In fact, one may choose

$$\zeta(\Theta, \vartheta) = \begin{cases} 0, & \Theta = -\tau_1, \\ B_1, & \Theta \in (-\tau_1, -\tau_2^0], \\ B_1 + B_2, & \Theta \in (-\tau_2^0, 0), \\ A_1 + B_1 + B_2, & \Theta = 0. \end{cases} \quad (35)$$

For $\varphi \in C^1([-\tau_1, 0], \mathbb{R}^3)$, define

$$\mathbb{A}(\vartheta)\varphi = \begin{cases} \int_{-\tau_1}^0 \mathbf{d}\zeta(s, \vartheta)\varphi(s), & \Theta = 0, \\ \dot{\varphi}(\Theta), & \Theta \in [-\tau_1, 0), \end{cases} \quad (36)$$

$$\mathbb{R}(\vartheta)\varphi = \begin{cases} f(\vartheta, \varphi), & \Theta = 0, \\ 0, & \Theta \in [-\tau_1, 0). \end{cases}$$

For $\mathcal{U}_t = \mathcal{U}(t + \theta) \in C^1$, it has $\mathbf{d}\mathcal{U}_t/\mathbf{d}\Theta = \mathbf{d}\mathcal{U}_t/\mathbf{d}t$. Then, system (31) can be rewritten as

$$\dot{\mathcal{U}}_t = \mathbb{A}(\vartheta)\mathcal{U}_t + \mathbb{R}(\vartheta)\mathcal{U}_t, \quad (37)$$

where $\mathcal{U}_t(\theta) = \mathcal{U}(t + \theta)$.

For $\alpha_1 \in C([-\tau_1, 0], \mathbb{R}^3)$ and $\psi, \alpha_2 \in C^1([0, \tau_1], \mathbb{R}^{3*})$, define

$$\mathbb{A}^*\psi(s) = \begin{cases} \int_{-\tau_1}^0 \mathbf{d}\zeta^T(t, 0)\psi(-t), & s = 0, \\ -\dot{\psi}(s), & s \in (0, \tau_1], \end{cases} \quad (38)$$

and the inner product

$$\langle \alpha_1, \alpha_2 \rangle = \bar{\alpha}_1(0)\alpha_2(0) - \int_{-\tau_1}^0 \int_{\eta=0}^{\Theta} \bar{\alpha}_1(\eta - \Theta)\mathbf{d}\zeta(\Theta)\alpha_2(\eta)\mathbf{d}\eta, \quad (39)$$

where $\zeta(\Theta) = \zeta(\Theta, 0)$. By direct computations, we obtain that $q(\Theta) = (1, \nu, \varsigma)^T e^{i\omega_0\Theta}$ is an eigenvector of \mathbb{A} corresponding to the eigenvalue $i\omega_0$, and $q^*(\eta) = \overline{\mathcal{D}}(1, \nu^*, \varsigma^*)e^{i\omega_0\eta}$ is an eigenvector of \mathbb{A}^* corresponding to the eigenvalue $-i\omega_0$. Furthermore, it has that

$$\begin{aligned} \langle q^*(\eta), q(\Theta) \rangle &= 1, \\ \langle q^*(\eta), \bar{q}(\Theta) \rangle &= 0, \end{aligned} \quad (40)$$

where

$$\nu = -\frac{2\kappa}{b + i\omega_0},$$

$$\varsigma = -\frac{1}{c + i\omega_0},$$

$$\nu^* = \frac{\kappa}{b - i\omega_0},$$

$$\varsigma^* = \frac{1}{c - i\omega_0},$$

$$\mathcal{D} = \left[1 + \nu^*\bar{\nu}^* + \varsigma^*\bar{\varsigma}^* - \tau_1 k_1 e^{-i\omega_0\tau_1} - \tau_2^0 k_2 e^{-i\omega_0\tau_2^0} \right]^{-1}. \quad (41)$$

Let \mathcal{U}_t be the solution of system (31) when $\vartheta = 0$. Define $\mathcal{X}(t) = \langle q^*, \mathcal{U}_t \rangle$; then,

$$\dot{\mathcal{X}}(t) = i\omega_0\mathcal{X}(t) + \bar{q}^*(0)\hat{f}(\mathcal{X}, \overline{\mathcal{X}}), \quad (42)$$

where

$$\hat{f} = f(0, \mathbb{W}(\mathcal{X}, \overline{\mathcal{X}}) + 2\mathbf{Re}\{\mathcal{X}q\}),$$

$$\mathbb{W}(\mathcal{X}, \overline{\mathcal{X}}) = \mathcal{U}_t - 2\mathbf{Re}\{\mathcal{X}q\}, \quad (43)$$

$$\mathbb{W}(\mathcal{X}, \overline{\mathcal{X}}) = \mathbb{W}_{20}\frac{\mathcal{X}^2}{2} + \mathbb{W}_{11}\mathcal{X}\overline{\mathcal{X}} + \mathbb{W}_{02}\frac{\overline{\mathcal{X}}^2}{2} + \dots.$$

Rewriting (42) as

$$\dot{\mathcal{U}}_t = i\omega_0\mathcal{X}(t) + \mathcal{G}(\mathcal{X}, \overline{\mathcal{X}}), \quad (44)$$

where

$$\mathcal{G}(\mathcal{X}, \overline{\mathcal{X}}) = \mathcal{G}_{20}\frac{\mathcal{X}^2}{2} + \mathcal{G}_{11}\mathcal{X}\overline{\mathcal{X}} + \mathcal{G}_{02}\frac{\overline{\mathcal{X}}^2}{2} + \mathcal{G}_{21}\frac{\mathcal{X}^2\overline{\mathcal{X}}}{2} + \dots \quad (45)$$

Furthermore,

$$\dot{W} = \begin{cases} \mathbb{A}W - 2\text{Re}\{\bar{q}^*(0)\hat{f}q(\Theta)\}, & \Theta \in [-\tau, 0), \\ \mathbb{A}W - 2\text{Re}\{\bar{q}^*(0)\hat{f}q(\Theta)\} + \hat{f}, & \Theta = 0, \end{cases} \stackrel{\text{def}}{=} \mathbb{A}W + \mathbb{H}(\mathcal{X}, \bar{\mathcal{X}}, \Theta), \quad (46)$$

where

$$\mathbb{H}(\mathcal{X}, \bar{\mathcal{X}}, \Theta) = \mathbb{H}_{20}(\Theta)\frac{\mathcal{X}^2}{2} + \mathbb{H}_{11}(\Theta)\mathcal{X}\bar{\mathcal{X}} + \mathbb{H}_{02}(\Theta)\frac{\bar{\mathcal{X}}^2}{2} + \dots \quad (47)$$

Notice that

$$\begin{aligned} \mathcal{U}_1(t) &= \mathcal{X} + \bar{\mathcal{X}} + \mathbb{W}_{20}^{(1)}(0)\frac{\mathcal{X}^2}{2} + \mathbb{W}_{11}^{(1)}(0)\mathcal{X}\bar{\mathcal{X}} + \dots, \\ \mathcal{U}_2(t) &= \nu\mathcal{X} + \bar{\nu}\bar{\mathcal{X}} + \mathbb{W}_{20}^{(2)}(0)\frac{\mathcal{X}^2}{2} + \mathbb{W}_{11}^{(2)}(0)\mathcal{X}\bar{\mathcal{X}} + \dots \end{aligned} \quad (48)$$

Hence, we can obtain the following important quantities:

$$\begin{aligned} \mathcal{G}_{20} &= 2\mathcal{D}(\nu - \bar{\nu}^*), \quad \mathcal{G}_{11} = \mathcal{D}(\nu + \bar{\nu} - 2\bar{\nu}^*), \quad \mathcal{G}_{02} = 2\mathcal{D}(\bar{\nu} - \bar{\nu}^*), \\ \mathcal{G}_{21} &= 2\mathcal{D}\left[\mathbb{W}_{11}^{(2)}(0) + \frac{1}{2}\mathbb{W}_{20}^{(2)}(0) + \mathbb{W}_{20}^{(1)}(0)\left(\frac{1}{2}\bar{\nu} - \bar{\nu}^*\right) \right. \\ &\quad \left. + \mathbb{W}_{11}^{(1)}(0)(\nu - 2\bar{\nu}^*)\right], \end{aligned} \quad (49)$$

where

$$\begin{aligned} \mathbb{W}_{20}(\Theta) &= \frac{\mathbf{i}\mathcal{G}_{20}}{\omega_0}q(0)e^{\mathbf{i}\omega_0\Theta} + \frac{\mathbf{i}\bar{\mathcal{G}}_{02}}{3\omega_0}\bar{q}(0)e^{-\mathbf{i}\omega_0\Theta} + \mathbb{E}_1e^{2\mathbf{i}\omega_0\Theta}, \\ \mathbb{W}_{11}(\Theta) &= -\frac{\mathbf{i}\mathcal{G}_{11}}{\omega_0}q(0)e^{\mathbf{i}\omega_0\Theta} + \frac{\mathbf{i}\bar{\mathcal{G}}_{11}}{\omega_0}\bar{q}(0)e^{-\mathbf{i}\omega_0\Theta} + \mathbb{E}_2, \\ \mathbb{E}_1 &= \begin{pmatrix} \mathbf{G} & -\kappa & -1 \\ 2\kappa & 2\mathbf{i}\omega_0 + b & 0 \\ 1 & 0 & 2\mathbf{i}\omega_0 + c \end{pmatrix}^{-1} \times \begin{pmatrix} \nu \\ -1 \\ 0 \end{pmatrix}, \\ \mathbb{E}_2 &= \begin{pmatrix} \frac{1}{c} & \kappa & 1 \\ -2\kappa & -b & 0 \\ -1 & 0 & -c \end{pmatrix}^{-1} \times \begin{pmatrix} -(\nu + \bar{\nu}) \\ 2 \\ 0 \end{pmatrix}, \end{aligned} \quad (50)$$

where $\mathbf{G} = 2\mathbf{i}\omega_0 - (k_1 + k_2 + 1/c) + k_1e^{-2\mathbf{i}\omega_0\tau_1} + k_2e^{-2\mathbf{i}\omega_0\tau_2}$.

Substituting \mathbb{E}_1 and \mathbb{E}_2 into $\mathbb{W}_{20}(\Theta)$ and $\mathbb{W}_{11}(\Theta)$, respectively, furthermore, \mathcal{G}_{21} can be computed. Thus, it can obtain the following quantities:

$$\begin{aligned} \mathcal{E}_1(0) &= \frac{\mathbf{i}}{2\omega_0} \left(\mathcal{G}_{20}\mathcal{G}_{11} - 2|\mathcal{G}_{11}|^2 - \frac{|\mathcal{G}_{02}|^2}{3} \right) + \frac{\mathcal{G}_{21}}{2}, \\ \mathcal{E}_2 &= -\frac{\text{Re}\{\mathcal{E}_1(0)\}}{\text{Re}\lambda'(\tau_2^0)}, \\ \mathcal{F}_2 &= -\frac{\text{Im}\{\mathcal{E}_1(0)\} + \mathcal{E}_2\text{Im}\lambda'(\tau_2^0)}{\omega_0}, \\ \mathcal{B}_2 &= 2\text{Re}\{\mathcal{E}_1(0)\}. \end{aligned} \quad (51)$$

Hence, we have the following result.

Theorem 5. *Hopf bifurcation is supercritical (subcritical) if $\mathcal{E}_2 > 0$ (< 0). The bifurcation periodic solutions are orbitally stable (unstable) if $\mathcal{B}_2 < 0$ (> 0). The period increase (decrease) if $\mathcal{F}_2 > 0$ (< 0).*

4. Crossing Curve Method

The results in Theorem 4 clearly show that the stability of system (2) changes depending on the parameters of system. However, the (τ_1, τ_2) plane analysis results for bifurcation generation are not obtained by this method in Section 2. Gu et al. [52] gave an effective approach to separate the stable and unstable regions in the (τ_1, τ_2) plane by using the stability crossing curves. In this part, we carry out the method. on the basis of equation (5), and it can define the following polynomials about λ :

$$\begin{cases} \mathcal{P}_0(\lambda) = \lambda^3 + a_2\lambda^2 + a_1\lambda + a_0, \\ \mathcal{P}_1(\lambda) = k_1(\lambda^2 + b_1\lambda + b_0), \\ \mathcal{P}_2(\lambda) = \frac{k_2}{k_1}\mathcal{P}_1(\lambda), \end{cases} \quad (52)$$

satisfying

- (i) $\deg(\mathcal{P}_0(\lambda)) \geq \max\{\deg(\mathcal{P}_1(\lambda)), \deg(\mathcal{P}_2(\lambda))\}$
- (ii) $\mathcal{P}_0(0) + \mathcal{P}_1(0) + \mathcal{P}_2(0) \neq 0$
- (iii) The polynomials $\mathcal{P}_0(\lambda)$,
- (53)
- $\mathcal{P}_1(\lambda)$ and $\mathcal{P}_2(\lambda)$ do not have any common zeros
- (iv) $\lim_{\lambda \rightarrow \infty} \left(\left| \frac{\mathcal{P}_1(\lambda)}{\mathcal{P}_0(\lambda)} \right| + \left| \frac{\mathcal{P}_2(\lambda)}{\mathcal{P}_0(\lambda)} \right| \right) < 1$

The following discussions will follow the continuity of the zeros with respect to the delay parameters as stated in the following lemma [52].

Lemma 4. *As the delays (τ_1, τ_2) continuously vary within \mathbb{R}_+^2 , the number of zeros (counting multiplicity) of $\Delta(\lambda, \tau_1, \tau_2)$ on \mathbb{C}_+ can change only if a zero appears on or across the imaginary axis.*

The characteristic equation (5) has the same zeros with the zeros of

$$\Delta(\lambda, \tau_1, \tau_2) = 1 + \delta_1(\lambda)e^{-\lambda\tau_1} + \delta_2(\lambda)e^{-\lambda\tau_2} = 0, \quad (54)$$

where $\delta_s(\lambda) = \mathcal{P}_s(\lambda)/\mathcal{P}_0(\lambda)$, $s = 1, 2$. Therefore, in general, we may obtain all the crossing points and directions of crossing from the solutions of $\Delta(\lambda, \tau_1, \tau_2) = 0$ instead of $\nabla(\lambda, \tau_1, \tau_2) = 0$. Now, based on the procedure proposed by [52], the procedure is comprised of the following steps.

The first step is to determine the crossing set Ω of ω that satisfies the feasibility condition so that the purely imaginary root exists, and geometrically, the vectors that satisfy (54) form a triangle (see Figure 2).

From Figure 2, the crossing set Ω can be represented as

$$\mathbf{L}_1(\omega) = |\delta_1(\mathbf{i}\omega)| + |\delta_2(\mathbf{i}\omega)| \geq 1, \quad (55)$$

$$\mathbf{L}_2(\omega) = |\delta_1(\mathbf{i}\omega)| - |\delta_2(\mathbf{i}\omega)| \leq 1. \quad (56)$$

The second step is to determine the inner angles $\theta_1, \theta_2 \in [0, \pi]$ of the triangle in Figure 2. From the cosine law, it has

$$\begin{cases} \cos \theta_1 = \frac{1 + |\delta_1(\mathbf{i}\omega)|^2 - |\delta_2(\mathbf{i}\omega)|^2}{2|\delta_1(\mathbf{i}\omega)|}, \\ \cos \theta_2 = \frac{1 + |\delta_2(\mathbf{i}\omega)|^2 - |\delta_1(\mathbf{i}\omega)|^2}{2|\delta_2(\mathbf{i}\omega)|}. \end{cases} \quad (57)$$

For any $\omega \in \Omega$, one can obtain (τ_1, τ_2) from (54) as follows:

$$\begin{aligned} \tau_1^{u^\pm}(\omega) &= \frac{1}{\omega} [\arg(\delta_1(\mathbf{i}\omega)) \pm \theta_1 + (2u - 1)\pi] \geq 0, \\ u &= u_0^\pm, u_0^\pm + 1, u_0^\pm + 2, \dots, \end{aligned} \quad (58)$$

and

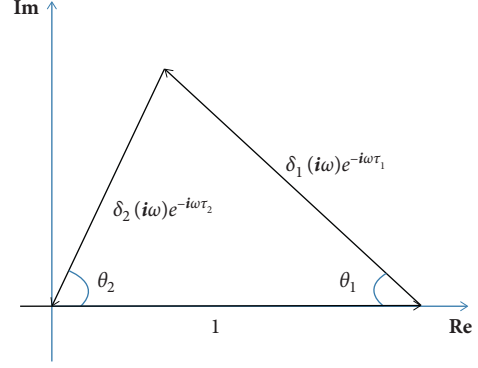


FIGURE 2: Triangle formed by 1, $|\delta_1(\mathbf{i}\omega)|$, and $|\delta_2(\mathbf{i}\omega)|$.

$$\tau_2^{\ell^\pm}(\omega) = \frac{1}{\omega} [\arg(\delta_2(\mathbf{i}\omega)) \mp \theta_2 + (2\ell - 1)\pi] \geq 0, \quad (59)$$

$$\ell = \ell_0^\pm, \ell_0^\pm + 1, \ell_0^\pm + 2, \dots,$$

where u_0^\pm and ℓ_0^\pm are the smallest integers so that the right sides of (58) and (59) are nonnegative.

Let

$$\begin{aligned} \mathcal{S}_{u,\ell}^\pm &= \left\{ \left(\tau_1^{u^\pm}(\omega), \tau_2^{\ell^\pm}(\omega) \right) \right\} \\ &= \left\{ \left(\frac{1}{\omega} [\arg(\delta_1(\mathbf{i}\omega)) + (2u - 1)\pi \pm \theta_1], \right. \right. \\ &\quad \left. \left. \frac{1}{\omega} [\arg(\delta_2(\mathbf{i}\omega)) + (2\ell - 1)\pi \mp \theta_2] \right) \right\}, \end{aligned} \quad (60)$$

then

$$\mathcal{F}_\omega = \left(\bigcup_{u \geq u_0^+, \ell \geq \ell_0^+} \mathcal{S}_{u,\ell}^+ \right) \cup \left(\bigcup_{u \geq u_0^-, \ell \geq \ell_0^-} \mathcal{S}_{u,\ell}^- \right), \quad (61)$$

which is the set of all (τ_1, τ_2) such that $\Delta(\lambda, \tau_1, \tau_2)$ has a zero at $\lambda = \mathbf{i}\omega$.

$\mathcal{F} = \{\mathcal{F}_\omega : \omega \in \Omega\}$ identifies the stability crossing curves in (τ_1, τ_2) plane, and the crossing set Ω is composed by a finite number of intervals with finite length. Let these intervals be Ω_k , $k = 1, 2, \dots, N$, arranged in such an order that the left endpoint of Ω_k increases with increasing k . Then, $\Omega = \bigcup_{k=1}^N \Omega_k$, and the left endpoints of the intervals ω_k^l and the right endpoints ω_k^r must only satisfy one of the three equations: $L_1(\omega) = 1$ and $L_2(\omega) = \pm 1$.

Let

$$\begin{aligned} \mathcal{F}_{u,\ell,k}^\pm &= \bigcup_{\omega \in \Omega_k} \mathcal{S}_{u,\ell}^\pm, \\ \mathcal{F}^k &= \bigcup_{u=-\infty}^{+\infty} \bigcup_{\ell=-\infty}^{+\infty} (\mathcal{F}_{u,\ell,k}^+ \cup \mathcal{F}_{u,\ell,k}^-) \cap \mathbf{R}_+^2. \end{aligned} \quad (62)$$

Then, $\mathcal{F} = \bigcup_{k=1}^N \mathcal{F}^k$.

Hence, we can divide these endpoints into three types according to the conditions satisfied by the equation ω_k^l or ω_k^r . If $\omega_1^l = 0$, then Ω_1 may have a special type. As stated by [52], the possible shapes of \mathcal{F}^k must belong to one of the following three types:

- (i) A series of closed curves.
- (ii) A series of spiral-like curves oriented along horizontally, vertically, or diagonally.
- (iii) A series of open-ended curves whose ends approach ∞ .

If the left endpoint of Ω_k is of Type l and its right endpoint is of Type r , we call an interval Ω_k is of Type lr . There are a total of 12 possible types, where

Type 1: $\mathbf{L}_2(\omega) = 1$ is satisfied. $\mathcal{S}_{u,\beta,k}^+$ links $\mathcal{S}_{u,\beta-1,k}^-$ at the end.

Type 2: $\mathbf{L}_2(\omega) = -1$ is satisfied. $\mathcal{S}_{u,\beta,k}^+$ links $\mathcal{S}_{u+1,\beta,k}^-$ at the end.

Type 3: $\mathbf{L}_1(\omega) = 1$ is satisfied. $\mathcal{S}_{u,\beta,k}^+$ links $\mathcal{S}_{u,\beta,k}^-$ at the end.

Type 0: $\omega_k^l = 0$. As $\omega \rightarrow 0$, $\mathcal{S}_{u,\beta,k}^+$ and $\mathcal{S}_{u,\beta,k}^-$ approach ∞ .

In 12 possible types, Type 11, Type 22, and Type 33 form a series of closed curves. Type 12 and Type 21, Type 13 and Type 31, and Type 23, and Type 32 form series spiral-like curves oriented along diagonally, vertically, and horizontally, respectively. Type 01, Type 02, and Type 03 form a series of open-ended curves.

Next, to determine the existence of Hopf bifurcation, we consider the direction of the root of (5) through the imaginary axis by the method given in [52]. By (54) and the implicit function theorem, τ_1 and τ_2 can be expressed as the function of $\lambda = i\omega$. As λ moves along the imaginary axis, $(\tau_1, \tau_2) = (\tau_1^{u^+}(\omega), \tau_2^{\beta^+}(\omega))$ moves along \mathcal{F}^k . For a fixed $\omega \in \Omega_k$, let

$$\begin{aligned} \operatorname{Re}\left(\frac{i}{\lambda} \frac{\partial \Delta(\lambda, \tau_1, \tau_2)}{\partial \lambda}\right)\Big|_{\lambda=i\omega} &= \mathfrak{R}_0, \\ \operatorname{Im}\left(\frac{i}{\lambda} \frac{\partial \Delta(\lambda, \tau_1, \tau_2)}{\partial \lambda}\right)\Big|_{\lambda=i\omega} &= \mathfrak{I}_0, \\ -\operatorname{Re}\left(\frac{1}{\lambda} \frac{\partial \Delta(\lambda, \tau_1, \tau_2)}{\partial \tau_s}\right)\Big|_{\lambda=i\omega} &= \mathfrak{R}_s, \\ -\operatorname{Im}\left(\frac{1}{\lambda} \frac{\partial \Delta(\lambda, \tau_1, \tau_2)}{\partial \tau_s}\right)\Big|_{\lambda=i\omega} &= \mathfrak{I}_s, \end{aligned} \quad (63)$$

where $s = 1, 2$.

The direction in which the ω increases is called the positive direction of the curve, which is reversed when the curve passes the point corresponding to the Ω_k endpoint. When we move in the positive direction of the curve, we also call the region on the left-hand side the region on the left. The following results come from [52].

Lemma 5. *Let $\omega \in (\omega_k^l, \omega_k^r)$ and $(\tau_1, \tau_2) \in \mathcal{F}^k$ so that $i\omega$ is a simple root of (5) and for any $\omega l \neq \omega$, $\Delta(i\omega l, \tau_1, \tau_2) \neq 0$. Then, as (τ_1, τ_2) moves from the right-side region to the left-side region of the corresponding curve in \mathcal{F}^k , a pair of roots of (54) cross the imaginary axis to the right side if $\mathfrak{R}_2\mathfrak{I}_1 - \mathfrak{R}_1\mathfrak{I}_2 > 0$. If the inequality is reversed, the crossing direction is opposite.*

Theorem 6. *Let ω, τ_1 , and τ_2 satisfy the conditions in Lemma 5. Then, when (τ_1, τ_2) crosses the curve along the direction (ℓ_1, ℓ_2) , a pair of roots of (54) cross the imaginary axis to the right side if*

$$\ell_1(\mathfrak{R}_0\mathfrak{I}_1 - \mathfrak{R}_1\mathfrak{I}_0) + \ell_2(\mathfrak{R}_0\mathfrak{I}_2 - \mathfrak{R}_2\mathfrak{I}_0) > 0. \quad (64)$$

If the inequality is reversed, the crossing direction is opposite.

5. Numerical Simulations

In this part, we will carry out some numerical simulations by using Matlab Microsoft to confirm the theoretical analyses.

Firstly, as an example, we investigate the following system:

$$\begin{cases} \dot{x}(t) = (y - 0.9)x + z - [x(t) - x(t - \tau_1)] - 2[x(t) - x(t - \tau_2)], \\ \dot{y}(t) = 1 - 0.2y - x^2, \\ \dot{z}(t) = -x - 1.2z, \end{cases} \quad (65)$$

and the initial functions are $\varphi_1(\theta) \equiv 2, \varphi_2(\theta) \equiv 3$, and $\varphi_3(\theta) \equiv 2$. With these parameters, condition (H2) holds. When $\tau_2 = 0$, (10) has two positive roots $\omega_1 \doteq 0.9752$ and $\omega_2 \doteq 1.9997$. Substituting them into (14) gives, respectively,

$$\begin{aligned} \tau_{11}^{(j)} &= 0.3795 + 6.4430j, \\ \tau_{12}^{(i)} &= 2.5811 + 3.1421i, \quad j, i = 0, 1, 2, \dots \end{aligned} \quad (66)$$

Furthermore, $\mathbf{d}(\operatorname{Re} \lambda(\tau_{11}^{(j)}))/\mathbf{d}\tau_1 < 0$ and $\mathbf{d}(\operatorname{Re} \lambda(\tau_{12}^{(i)}))/\mathbf{d}\tau_1 > 0$. By Theorem 4, E_+^* is unstable when $\tau_1 \in [0, 0.3795) \cup (2.5811, +\infty)$, and LAS when $\tau_1 \in (0.3795, 2.5811)$. The numerical simulation results are shown in Figures 3–5.

Fix $\tau_1 = 2.2 \in (0.3795, 2.5811)$, and it computes $\tau_2^0 \doteq 2.4692$. By Theorem 4, we know that E_+^* is LAS for $\tau_2 \in [0, 2.4692)$. Choosing $\tau_2 = 1$, E_+^* is stable (see Figure 6). Furthermore, by Section 3, it has $\mathcal{E}_1(0) = -10.1592 + 0.7794i, \mathcal{B}_2 < 0$ and $\mathcal{E}_2 > 0$ when $\tau_2 = 2.4692$, and the bifurcating periodic solution is stable, which is illustrated in Figure 7.

Next, one gives some examples for the crossing curve method using Matlab Microsoft. Firstly, it still chooses the parameters in system (65). It can obtain the crossing set based on the equation of $\mathbf{L}_1(\omega)$ and $\mathbf{L}_2(\omega)$. In equations (58) and (59), we regard τ_1 and τ_2 as the function of ω , by drawing the parametric equation curves in (τ_1, τ_2) plane, and it obtains the crossing curves. The crossing set has only a interval Ω_1 and $\omega_1^l = 0.9893$ and $\omega_1^r = 2.6715$, satisfying $\mathbf{L}_1(\omega) = 1$ with $\omega = \omega_1^l$ and $\omega = \omega_1^r$ (see Figure 8(a)). So, the interval Ω_1 is Type 33 and the crossing curves form a series of closed curves (see Figures 8(b) and 8(c)). Firstly, it chooses $\tau_1 = 10 > 2.5811$ and $\tau_2 = 0$, and it can obtain that E_+^* is unstable (see Figure 9). In the following, it chooses, respectively, $\tau_2 = 1, 3.35, 3.7$ for fixed $\tau_1 = 10$, and it can find that E_+^* is stable when $\tau_2 = 1$ (see Figure 10) and $\tau_2 = 3.7$ (see Figure 11), unstable when $\tau_2 = 3.35$, and there exists a stable periodic solution (see Figure 12). Furthermore, it can fix $a = 0.9, b = 0.2$, and $c = 1.2$, and let k_1 and k_2 change, and

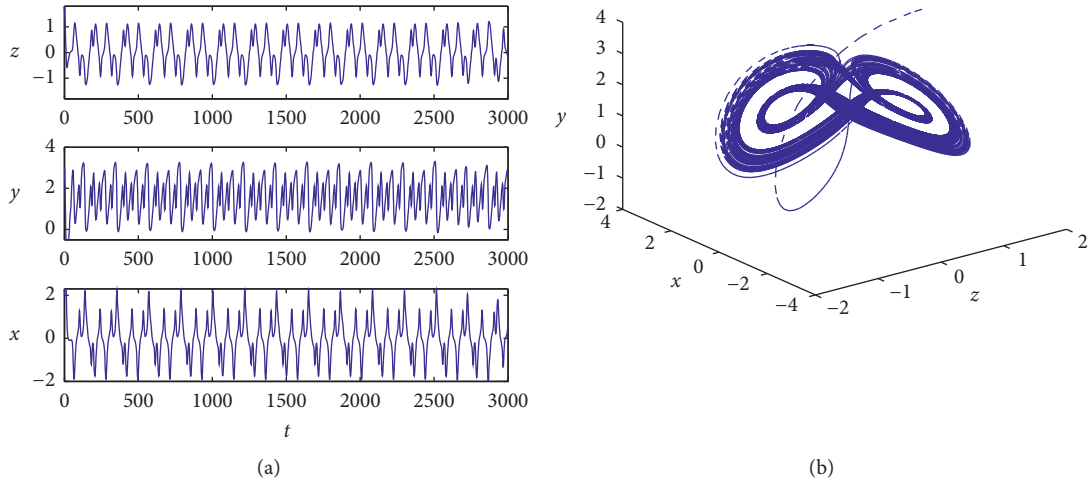


FIGURE 3: E_+^* is unstable, and chaos phenomenon still exists for system (65) when $\tau_1 = 0.1 \in [0, 0.3795]$. (a) Time series of the solutions. (b) Three-dimensional phase diagram.

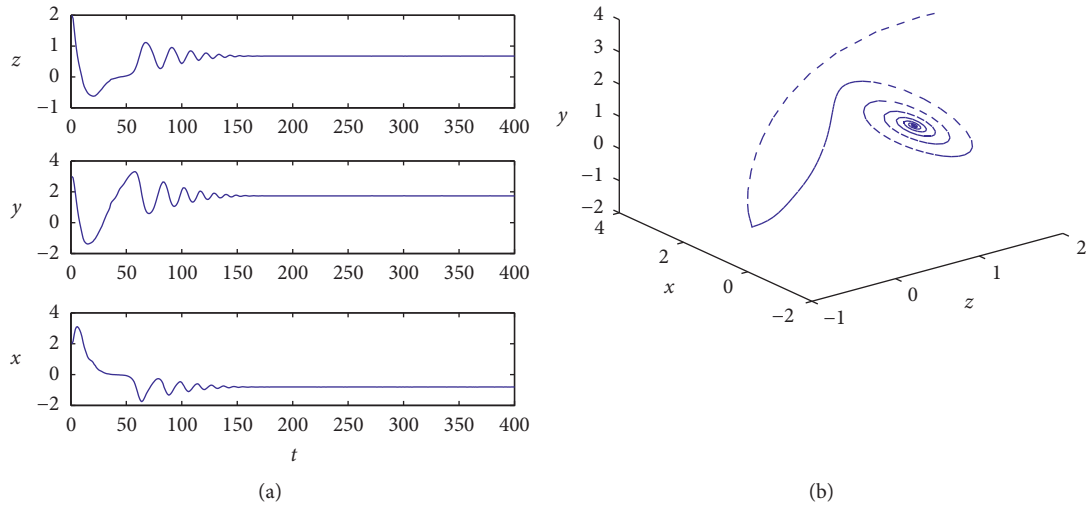


FIGURE 4: E_+^* is stable and the chaos phenomenon disappears for system (65) when $\tau_1 = 0.8 \in (0.3795, 2.5811)$. (a) Time series of the solutions. (b) Three-dimensional phase diagram.

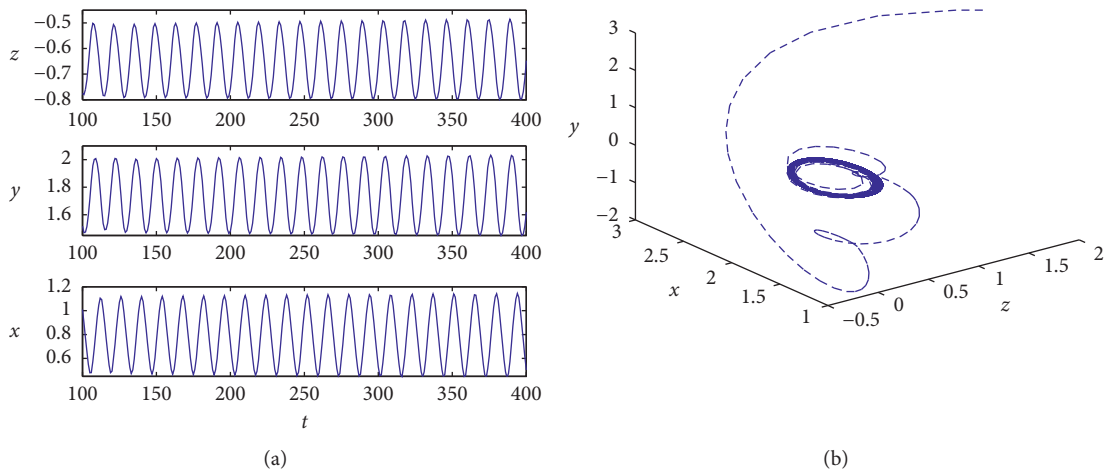


FIGURE 5: E_+^* is unstable and a stable periodic solution exists for system (65) when $\tau_1 = 2.77 > 2.5811$. (a) Time series of the solutions. (b) Three-dimensional phase diagram.

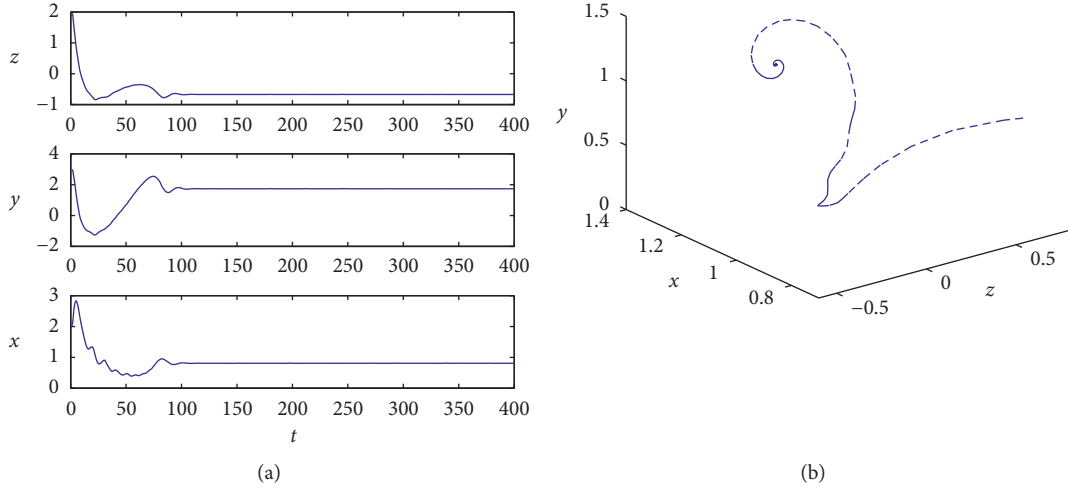


FIGURE 6: E_+^* is stable for system (65) with $\tau_1 = 2.2$ and $\tau_2 = 1$. (a) Time series of the solutions. (b) Three-dimensional phase diagram.

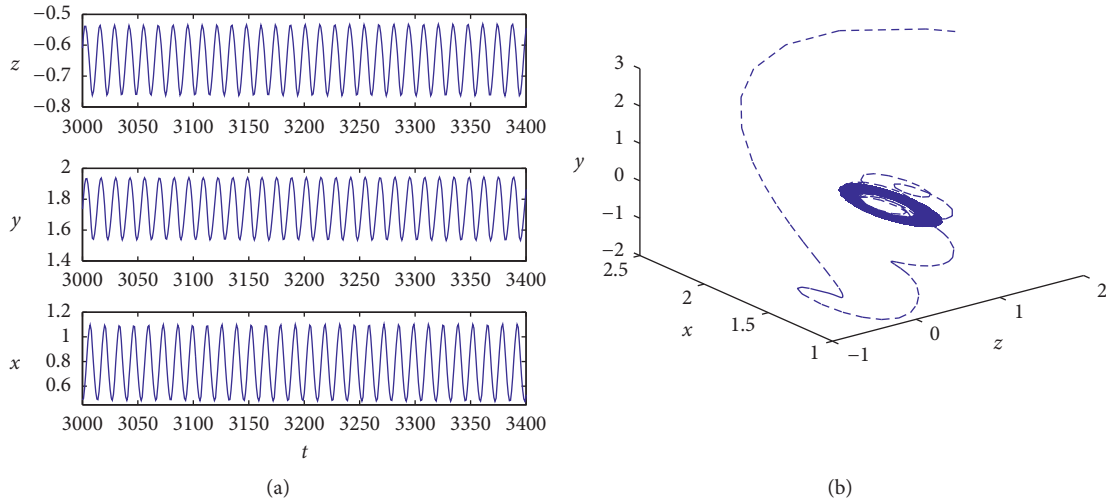


FIGURE 7: E_+^* is unstable and there exists a stable periodic solution for system (65), where $\tau_1 = 2.2$ and $\tau_2 = \tau_2^0$. (a) Time series of the solutions. (b) Three-dimensional phase diagram.

the crossing curves can produce different shapes (see Figures 13–15). When $k_1 = 1$ and $k_2 = -5$, the crossing sets have two intervals $\Omega_1 = (0.3696, 0.9733)$ and $\Omega_2 = (2.9688, 5.4793)$. Here, ω_1^l and ω_2^l satisfy $L_2(\omega) = -1$ while ω_1^l and ω_2^r satisfy $L_1(\omega) = 1$ (see Figure 13(a)). So, the interval Ω_1 belongs to Type 32 and the interval Ω_2 belongs to Type 23. The crossing curves are spatial-like curves, as shown in Figures 13(b) and 13(c). Choosing $k_1 = -4$ and $k_2 = 2$, the crossing sets include two intervals $\Omega_1 = (0.2097, 1.0151)$ and $\Omega_2 = (2.3341, 6.2418)$ (see Figure 14(a)). The crossing curves belong to Type 31 and Type 13 with the spiral-like shape (see Figure 14(b)). Here, the stability crossing curves in $\Omega_1 = (0.2097, 1.0151)$ belonging to type 31 are not drawn. If $k_1 = 3$ and $k_2 = 1$, the crossing set includes an interval $\Omega_1 = (0, 0.7486)$. Since $\omega_1^l = 0$ and $L_1(\omega_1^r) = 0$ (see Figure 15(a)), the stability crossing curves belong to Type 03 with the open-ended shapes (see Figure 15(b)). These show that the changes of the feedback strengths k_1 and k_2 can alter

the stable region of the system in (τ_1, τ_2) plane, and it has an important effect on the stability of the financial system.

In addition, for the following two systems:

$$\begin{cases} \dot{x}(t) = (y - a)x + z, \\ \dot{y}(t) = 1 - by - x^2 + k_1[y(t) - y(t - \tau_1)] \\ \quad + k_2[y(t) - y(t - \tau_2)], \\ \dot{z}(t) = -x - cz, \end{cases} \quad (67)$$

and

$$\begin{cases} \dot{x}(t) = (y - a)x + z, \\ \dot{y}(t) = 1 - by - x^2, \\ \dot{z}(t) = -x - cz + k_1[z(t) - z(t - \tau_1)] + k_2[z(t) - z(t - \tau_2)], \end{cases} \quad (68)$$

that is, delayed feedback terms appear on the investment demand or the price index, respectively. Systems (67) and

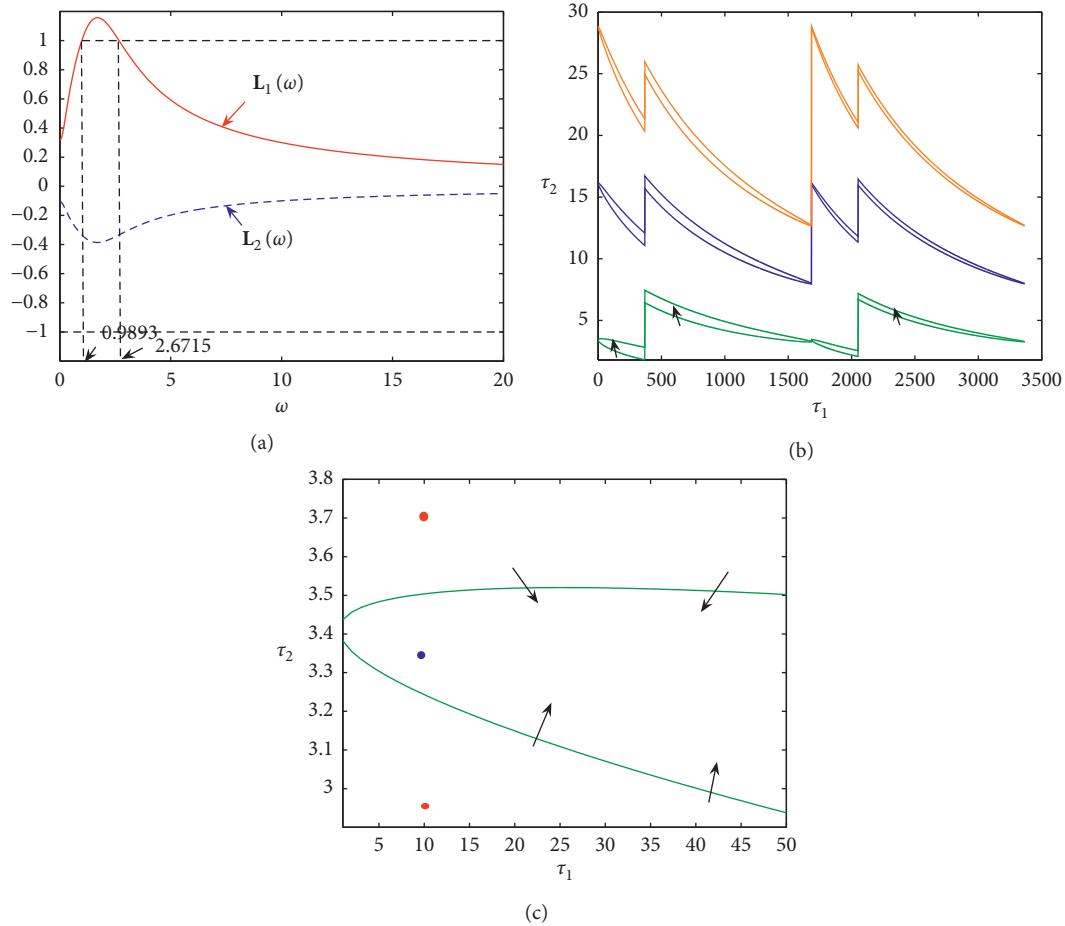


FIGURE 8: The feedback strength sets: $k_1 = -1$ and $k_2 = -2$. The arrow directions point to an unstable region. (a) The crossing set $\Omega = (0.9893, 2.6715)$. (b) Stability crossing curves τ^1 in (τ_1, τ_2) plane. (c) The zoom-in T 1 plot.

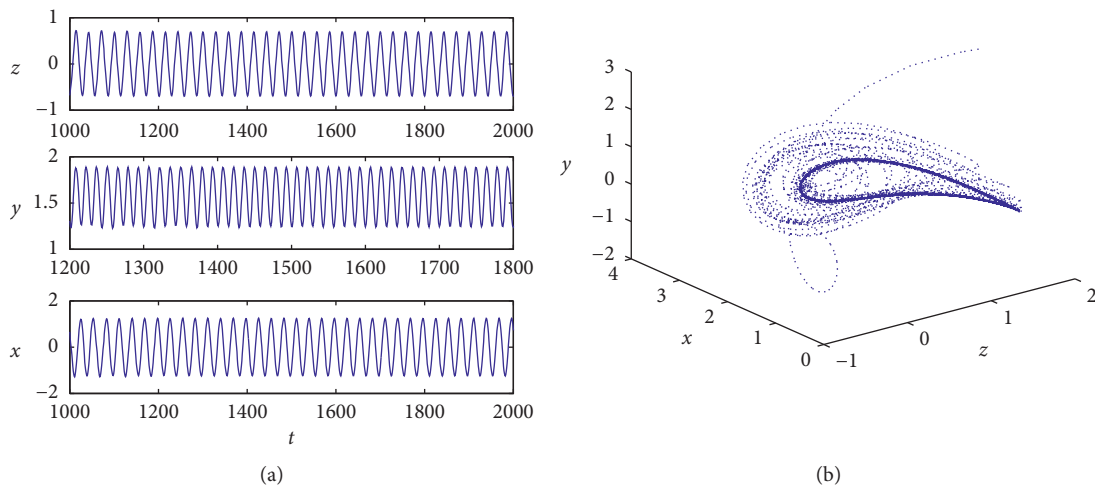


FIGURE 9: E_+^* for system (2) is unstable and there exists a stable periodic solution when $\tau_1 = 10$ and $\tau_2 = 0$ with feedback strength sets: $k_1 = -1$ and $k_2 = 0$. (a) Time series of the solutions. (b) Three-dimensional phase diagram.

(68) can be investigated as system (2) and can also obtain similar results to system (2).

The time-delay feedback controller $ke^{-d\tau}[\mathbf{u}(t) - \mathbf{u}(t - \tau)]$ with delay correlation coefficients can also be designed to

control system (1) which can modify the bifurcation characteristics of a nonlinear system to obtain some specific dynamical behaviors. Note that the strength of feedback control is in the form of $ke^{-d\tau}$, and the function decreases

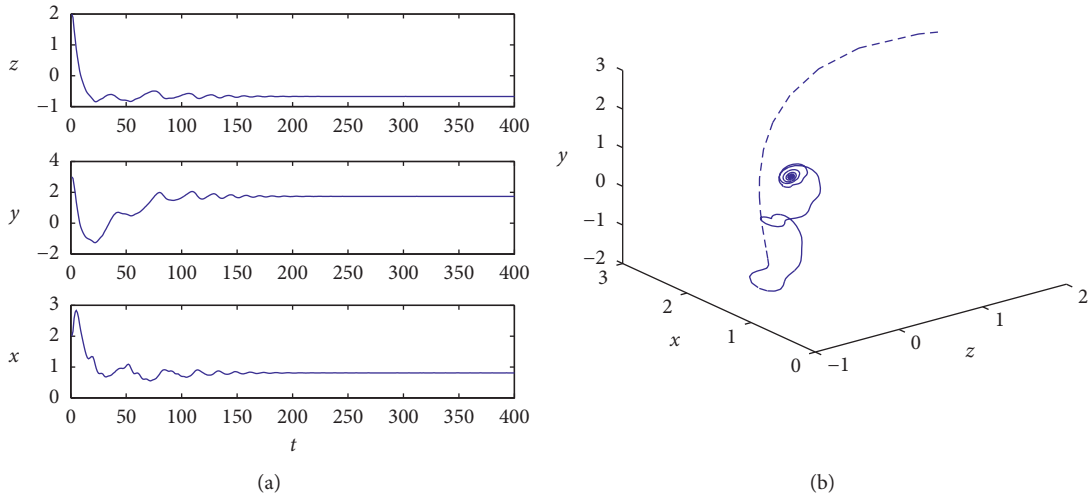


FIGURE 10: E_+^* for system (2) is stable when $\tau_1 = 10$ and $\tau_2 = 1$ with feedback strength sets: $k_1 = -1$ and $k_2 = -2$. (a) Time series of the solutions. (b) Three-dimensional phase diagram.

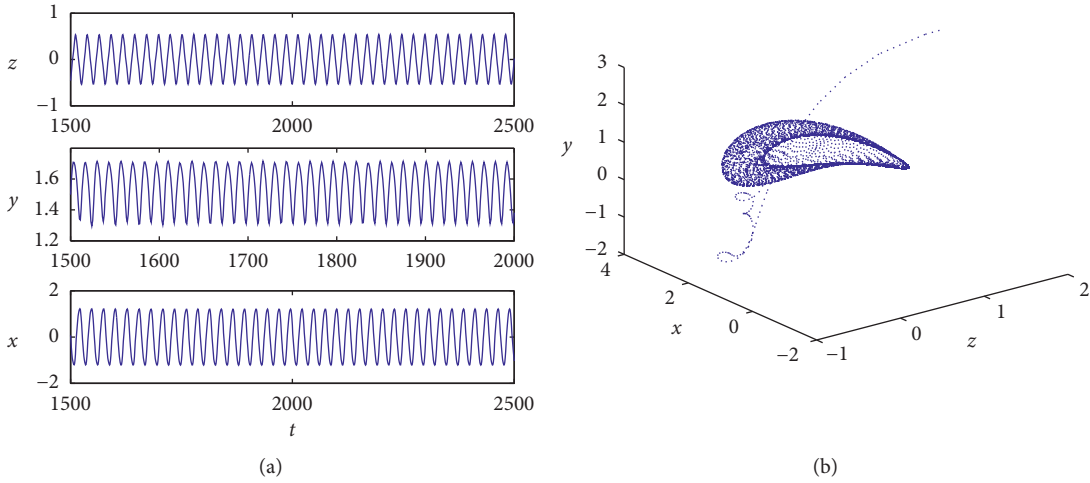


FIGURE 11: E_+^* for system (2) is stable when $\tau_1 = 10$ and $\tau_2 = 3.7$ with feedback strength sets: $k_1 = -1$ and $k_2 = -2$. (a) Time series of the solutions. (b) Three-dimensional phase diagram.

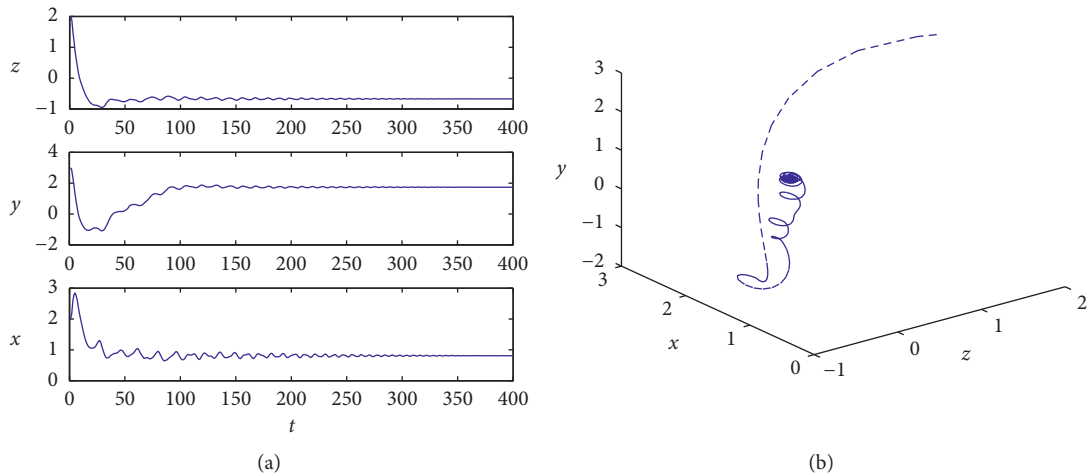


FIGURE 12: E^* for system (2) is unstable and there exists a stable periodic solution when $\tau_1 = 10$ and $\tau_2 = 3.35$ with feedback strength sets: $k_1 = -1$ and $k_2 = -2$. (a) Time series of the solutions. (b) Three-dimensional phase diagram.

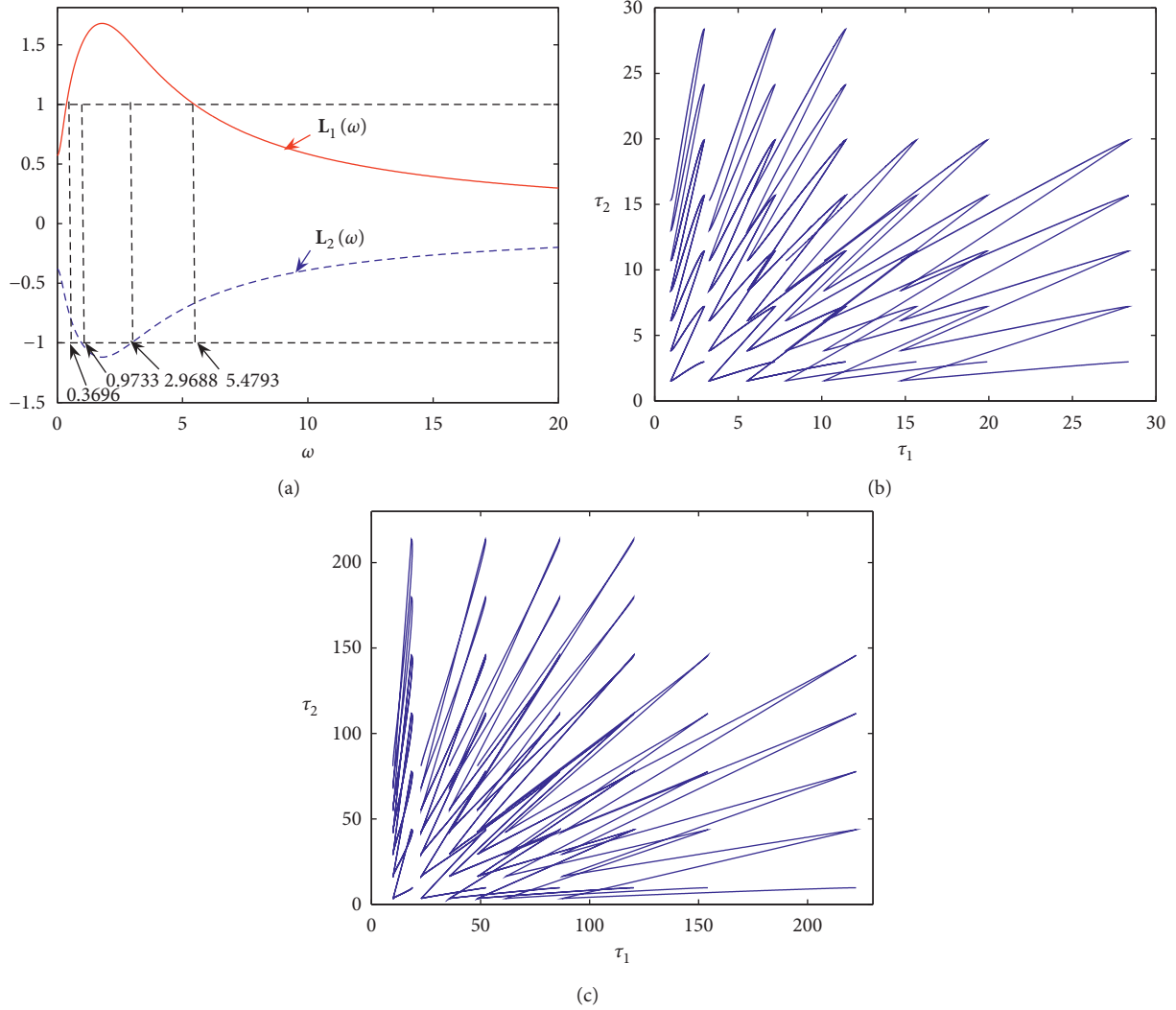


FIGURE 13: The feedback strength sets: $k_1 = 1$ and $k_2 = -5$. (a) The crossing set $\Omega = (0.3696, 0.9733) \cup (2.9688, 5.4793)$. (b) Stability crossing curves τ^1 in (τ_1, τ_2) plane. Stability crossing curves are spiral-like curves along the horizontal axis belonging to type 32 for the crossing set $\Omega_1 = (0.3696, 0.9733)$. (c) Stability crossing curves τ^2 in (τ_1, τ_2) plane. Stability crossing curves are spiral-like curves along the horizontal axis belonging to type 23 for the crossing set $\Omega_2 = (2.9688; 5.4793)$.

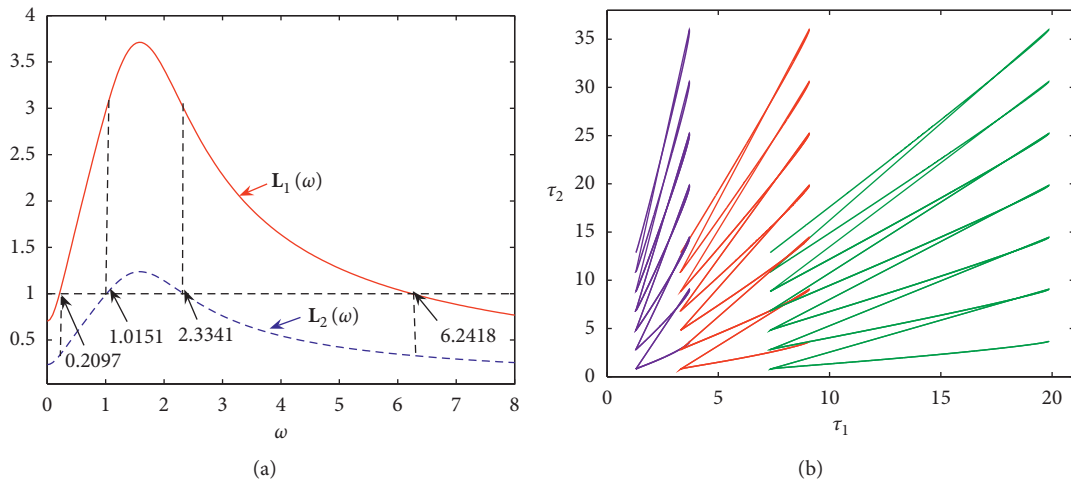


FIGURE 14: The feedback strength sets: $k_1 = -4$ and $k_2 = 2$. (a) The crossing set $\Omega = (0.2097, 1.0151) \cup (2.3341, 6.2418)$. (b) Stability crossing curves τ^2 in (τ_1, τ_2) plane. Stability crossing curves are spiral-like curves along the vertical axis belonging to type 13 for the crossing set $\Omega_2 = (2.3341, 6.2418)$.

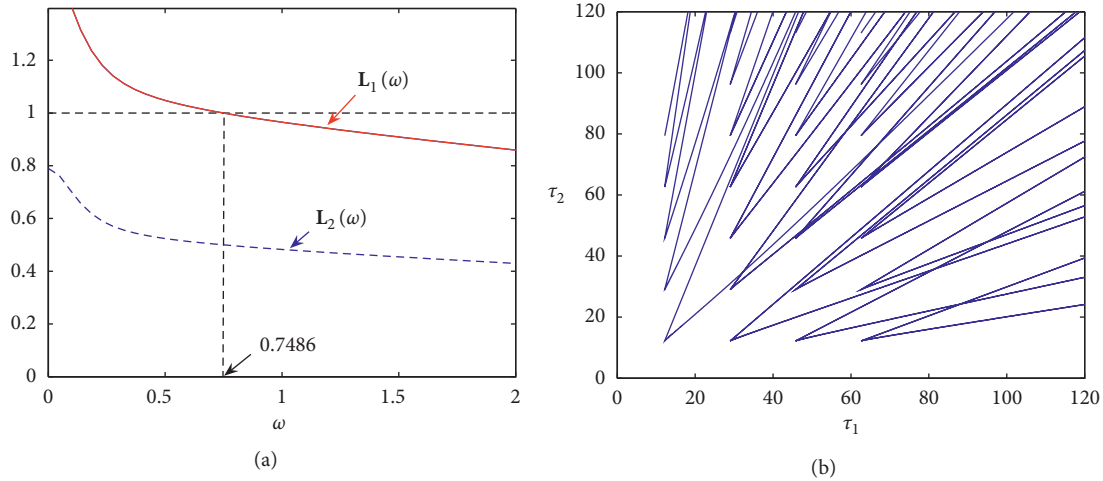


FIGURE 15: The feedback strength sets: $k_1 = 3$ and $k_2 = 1$. (a) The crossing set $\Omega = (0, 0.7486)$. (b) Stability crossing curves τ^1 in (τ_1, τ_2) plane. Stability crossing curves are open-ended curves belonging to type 03.

exponentially with delay τ . This means that the feedback effects of past states diminish over time. Hence, it can carry out the feedback with time-delay correlation coefficients in system (1). The systems with coefficient dependent delay increase the complexity of the analysis and are challenging, especially those with two time delays. The research is set aside for future consideration.

6. Conclusion

This paper analyzes a class of chaotic financial systems with two feedback delays. System (1) exists in chaos under some parameters. The purpose of this study is to control the chaos of the system. For controlling chaos, we improve the DFC method and introduce the double-delay feedback control method in system (1). We introduce the control term in the equation of the interest rate. The system may exist in three equilibria, and we choose one of these equilibria as the research target. It finds that the single delay feedback control can make the system stable and produce the stable switches, i.e., when τ_1 changes with $\tau_2 = 0$, system (2) exists stable switches and chaos may disappear. Furthermore, fixing τ_1 in a stability interval and taking the delay τ_2 as a parameter, proves the existence of the first critical value τ_2 . At this critical value, the equilibrium loses stability and Hopf bifurcation occurs. The properties of Hopf bifurcation are also studied by using central manifold theory and normal form method for determining the direction of Hopf bifurcation and the stability of bifurcating periodic solution. The abovementioned results are obtained under the condition fixed τ_1 in a stability interval; however, if we choose the τ_1 in the unstable interval, then there may exist no the critical value τ_2^0 such that τ_2^0 is the first Hopf bifurcation value. Hence, for obtaining the complete result separating the stable and unstable regions in the (τ_1, τ_2) , using the stability crossing curve methods in [52], it obtains the curve sets in which Hopf bifurcation occurs in (τ_1, τ_2) plane for fixed a, b , and c . By numerical simulations, it can find that the different shape crossing curves, and crossing sets can

produce by changing k_1 and k_2 . Theoretical analysis and numerical simulation results show that, for chaotic financial systems, chaotic oscillation can be controlled by delays. In other words, the multiple delay financial system we study has chaotic oscillations when $\tau_1 = \tau_2 = 0$. When the delay increases, the chaos disappears, the equilibrium point gains stability or the system appears periodic oscillation, and the periodic solution is generated by the Hopf bifurcation. The DDFC method can control the chaotic behavior of the system more effectively than the DFC method. When τ_1 cannot change the chaos behavior of system (2), system (2) can be stabilized by varying τ_2 value. These show that the effectiveness of the DDFC method.

Data Availability

Data sharing is not applicable to this article as all datasets are hypothetical during the current study.

Conflicts of Interest

The authors declare that there are no conflicts of interest regarding the publication of this paper.

Acknowledgments

Z. Jiang was supported by National Natural Science Foundation of China (11801014), Natural Science Foundation of Hebei Province (A2018409004), University Discipline Top Talent Selection and Training Program of Hebei Province (SLRC2019020) and Graduate Student Demonstration Course Construction of Hebei Province (KCJSX2020093), 2020 Talent Training Project Funding of Hebei Province. T. Zhang was supported by Shandong Provincial Natural Science Foundation from China (ZR2019MA003).

References

- [1] H. Lorenz, *Nonlinear Dynamical Economics and Chaotic Motion*, Springer-Verlag, Berlin, Germany, 1989.

- [2] R. Goodwin, *Chaotic Economic Dynamics*, Oxford University Press, Oxford, UK, 1990.
- [3] J. Ma and L. Xie, "The comparison and complex analysis on dual-channel supply chain under different channel power structures and uncertain demand," *Nonlinear Dynamics*, vol. 83, no. 3, pp. 1379–1393, 2016.
- [4] X. Zhan, J. Ma, and W. Re, "Research entropy complexity about the nonlinear dynamic delay game model," *Entropy*, vol. 19, pp. 1–10, 2017.
- [5] J. Ma and L. Sun, "Complexity analysis about nonlinear mixed oligopolies game based on production cooperation," *IEEE Transactions on Control Systems Technology*, vol. 26, no. 4, pp. 1532–1539, 2017.
- [6] F. Si and J. Ma, "Complex dynamics in a triopoly game with multiple delays in the competition of green product level," *International Journal of Bifurcation and Chaos*, vol. 28, no. 2, Article ID 1850027, 2018.
- [7] J. Ma and H. Ren, "Influence of government regulation on the stability of dual-channel recycling model based on customer expectation," *Nonlinear Dynamics*, vol. 94, no. 3, pp. 1775–1790, 2018.
- [8] B. Xin, W. Peng, and M. Sun, "Optimal coordination strategy for international production planning and pollution abating under cap-and-trade regulations," *International Journal of Environmental Research and Public Health*, vol. 16, pp. 1–21, 2019.
- [9] Z. Wu, G. Hou, and B. Xin, "Has the belt and road initiative brought new opportunities to countries along 205 the routes to participate in global value chains?" *SAGE Open*, vol. 10, no. 1, p. 2020.
- [10] L. Xie, J. Ma, and H. Han, "Implications of stochastic demand and manufacturers' operational mode on retailer's mixed bundling strategy and its complexity analysis," *Applied Mathematical Modelling*, vol. 55, no. 1, pp. 484–501, 2018.
- [11] J. Ma, W. Lou, and Y. Tian, "Bullwhip effect and complexity analysis in a multi-channel supply chain considering price game with discount sensitivity," *International Journal of Production Research*, vol. 57, pp. 1–21, 2018.
- [12] D. Huang and H. Li, *Theory and Method of the Nonlinear Economics*, Sichuan University Press, Chengdu, China, 1993.
- [13] J. Ma, Y. Cui, and L. Liu, "Hopf bifurcation and chaos of financial system on condition of specific combination of parameters," *Journal of Systems Science and Complexity*, vol. 21, no. 2, pp. 250–259, 2008.
- [14] Q. Gao and J. Ma, "Chaos and Hopf bifurcation of a finance system," *Nonlinear Dynamics*, vol. 58, no. 1–2, pp. 209–216, 2009.
- [15] B. Xin, W. Peng, Y. Kwon, and Y. Liu, "Modeling, discretization, and hyperchaos detection of conformable derivative approach to a financial system with market confidence and ethics risk," *Advances in Difference Equations*, vol. 2019, no. 1, pp. 1–14, 2019.
- [16] J.-h. Ma and Y.-s. Chen, "Study for the bifurcation topological structure and the global complicated character of a kind of non-linear finance system (I)," *Applied Mathematics and Mechanics*, vol. 22, no. 11, pp. 1240–1251, 2001.
- [17] X. Zhang and H. Zhu, "Hopf bifurcation and chaos of a delayed finance system," *Complexity*, vol. 2019, Article ID 6715036, 18 pages, 2019.
- [18] W.-C. Chen, "Dynamics and control of a financial system with time-delayed feedbacks," *Chaos, Solitons & Fractals*, vol. 37, no. 4, pp. 1198–1207, 2008.
- [19] F. Zhang, G. Yang, Y. Zhang, X. Liao, and G. Zhang, "Qualitative study of a 4D chaos financial system," *Complexity*, vol. 2018, Article ID 3789873, 5 pages, 2018.
- [20] Z. Jiang, Y. Guo, and T. Zhang, "Double delayed feedback control of a nonlinear finance system," *Discrete Dynamics in Nature and Society*, vol. 2019, Article ID 7254121, 17 pages, 2019.
- [21] B. Xin and Y. Qu, "Effects of smart city policies on green total factor productivity: evidence from a quasi-natural experiment in China," *International Journal of Environmental Research and Public Health*, vol. 16, pp. 1–15, 2019.
- [22] G. Kai, W. Zhang, Z. Jin, and C. Wang, "Hopf bifurcation and dynamic analysis of an improved financial system with two delays," *Complexity*, vol. 2020, Article ID 3734125, 13 pages, 2020.
- [23] Z. Wu, G. Hou, and B. Xin, "The causality between participation in GVCs, renewable energy consumption and CO₂ emissions," *Sustainability*, vol. 12, no. 3, p. 1237, 2020.
- [24] W. Lou and J. Ma, "Complexity of sales effort and carbon emission reduction effort in a two-parallel household appliance supply chain model," *Applied Mathematical Modelling*, vol. 64, pp. 398–425, 2018.
- [25] J. Ma and B. Bao, "Research on bullwhip effect in energy-efficient air conditioning supply chain," *Journal of Cleaner Production*, vol. 143, pp. 854–865, 2017.
- [26] E. Ott, C. Grebogi, and J. A. Yorke, "Controlling chaos," *Physical Review Letters*, vol. 64, no. 11, pp. 1196–1199, 1990.
- [27] L. M. Pecora and T. L. Carroll, "Synchronization in chaotic systems," *Physical Review Letters*, vol. 64, no. 8, pp. 821–824, 1990.
- [28] K. Tanaka, T. Ikeda, and H. O. Wang, "A unified approach to controlling chaos via an LMI-based fuzzy control system design," *IEEE Transactions on Circuits and Systems I: Fundamental Theory and Applications*, vol. 45, no. 10, pp. 1021–1040, 1998.
- [29] T. Zhang, T. Xu, J. Wang, Y. Song, and Z. Jiang, "Geometrical analysis of a pest management model in food-limited environments with nonlinear impulsive state feedback control," *Journal of Applied Analysis & Computation*, vol. 9, no. 6, pp. 2261–2277, 2019.
- [30] T. Zhang, N. Gao, T. Wang et al., "Global dynamics of a model for treating microorganisms in sewage by periodically adding microbial flocculants," *Mathematical Biosciences and Engineering*, vol. 17, no. 1, pp. 179–201, 2020.
- [31] H. Zhang and T. Zhang, "The stationary distribution of a microorganism flocculation model with stochastic perturbation," *Applied Mathematics Letters*, vol. 103, Article ID 106217, 2020.
- [32] N. Gao, Y. Song, X. Wang, and J. Liu, "Dynamics of a stochastic SIS epidemic model with nonlinear incidence rates," *Advances in Difference Equations*, vol. 2019, p. 41, 2019.
- [33] G. Liu, H. Qi, Z. Chang, and X. Meng, "Asymptotic stability of a stochastic May mutualism system," *Computers & Mathematics with Applications*, vol. 79, no. 3, pp. 735–745, 2020.
- [34] M. Rafikov and J. M. Balthazar, "On control and synchronization in chaotic and hyperchaotic systems via linear feedback control," *Communications in Nonlinear Science and Numerical Simulation*, vol. 13, no. 7, pp. 1246–1255, 2008.
- [35] V. Pyragas and K. Pyragas, "Delayed feedback control of the Lorenz system: an analytical treatment at a subcritical Hopf bifurcation," *Physical Review E*, vol. 73, no. 3, Article ID 036215, 2006.
- [36] S. Xu, J. Lam, and Y. Zou, "Delay-dependent approach to stabilization of time-delay chaotic systems via standard and

- delayed feedback controllers,” *International Journal of Bifurcation and Chaos*, vol. 15, no. 4, pp. 1455–1465, 2005.
- [37] D.-H. Jiang, J. Wang, X.-Q. Liang, G.-B. Xu, and H.-F. Qi, “Quantum voting scheme based on locally indistinguishable orthogonal product states,” *International Journal of Theoretical Physics*, vol. 59, no. 2, pp. 436–444, 2020.
- [38] Z. Jiang, X. Bi, T. Zhang et al., “Global Hopf bifurcation of a delayed phytoplankton-zooplankton system considering toxin producing effect and delay dependent coefficient,” *Mathematical Biosciences and Engineering*, vol. 16, no. 5, pp. 3807–3829, 2019.
- [39] Z. Jiang, J. Dai, and T. Zhang, “Bifurcation analysis and control of a delayed plankton ecosystem using delayed feedback control method,” *International Journal of Bifurcation and Chaos*, vol. 30, Article ID 2050039, 2020.
- [40] B. Xin, W. Peng, and L. Guerrini, “A continuous time Bertrand duopoly game with fractional delay and conformable derivative: modelling, discretization process, Hopf bifurcation and chaos,” *Frontiers in Physics*, vol. 7, pp. 1–9, 2019.
- [41] M. Chi and W. Zhao, “Dynamical analysis of two-microorganism and single nutrient stochastic chemostat model with Monod-Haldane response function,” *Complexity*, vol. 2019, Article ID 8719067, 13 pages, 2019.
- [42] T. Zhang, J. Wang, Z. Jiang, and X. Han, “Dynamics analysis of a delayed virus model with two different transmission methods and treatments,” *Advances in Difference Equations*, vol. 2020, p. 1, 2020.
- [43] T. Li and W. Zhao, “Periodic solution of a neutral delay Leslie predator-prey model and the effect of random perturbation on the Smith growth model,” *Complexity*, vol. 2020, Article ID 8428269, 15 pages, 2020.
- [44] W. Wang, W. Ma, and Z. Feng, “Complex dynamics of a time periodic nonlocal and time-delayed model of reaction-diffusion equations for modeling CD4⁺ T cells decline,” *Journal of Computational and Applied Mathematics*, vol. 367, p. 112430, 2020.
- [45] A. Ahlborn and U. Parlitz, “Controlling dynamical systems using multiple delay feedback control,” *Physical Review E*, vol. 72, Article ID 016206, 2005.
- [46] K. Pyragas, “Continuous control of chaos by self-controlling feedback,” *Physics Letters A*, vol. 170, no. 6, pp. 421–428, 1992.
- [47] K. Pyragas, “Control of chaos via extended delay feedback,” *Physics Letters A*, vol. 206, no. 5-6, pp. 323–330, 1995.
- [48] M. Yang and G. Cai, “Chaos control of a non-linear finance system,” *Journal of Uncertain Systems*, vol. 5, pp. 263–270, 2011.
- [49] S. Ruan and J. Wei, “On the zeros of a third degree exponential polynomial with applications to a delayed model for the control of testosterone secretion,” *Mathematical Medicine and Biology*, vol. 18, no. 1, pp. 41–52, 2001.
- [50] S. Ruan and J. Wei, “On the zeros of transcendental functions with applications to stability of delay differential equations with two delays,” *Dynamics of Continuous, Discrete and Impulsive Systems*, vol. 10, pp. 863–874, 2003.
- [51] J. Hale, *Theory of Functional Differential Equations*, Springer, New York, NY, USA, 1977.
- [52] K. Gu, S.-I. Niculescu, and J. Chen, “On stability crossing curves for general systems with two delays,” *Journal of Mathematical Analysis and Applications*, vol. 311, no. 1, pp. 231–253, 2005.
- [53] P. Bi and S. Ruan, “Bifurcations in delay differential equations and applications to tumor and immune system interaction models,” *SIAM Journal on Applied Dynamical Systems*, vol. 12, no. 4, pp. 1847–1888, 2013.
- [54] B. Hassard, N. Kazarinoff, and Y. Wan, *Theory and Application of Hopf Bifurcation*, Cambridge University Press, Cambridge, UK, 1981.

Research Article

Production Decision and Coordination Mechanism of Socially Responsible Closed-Loop Supply Chain

Xiaofeng Long ^{1,2}, Jiali Ge ³, Tong Shu ³, and Chunxia Liu ¹

¹Department of Business Administration, Hunan University of Finance and Economics, Changsha, Hunan 410205, China

²School of Economics and Trade, Hunan University, Changsha 410082, China

³School of Business Administration, Hunan University, Changsha 410082, China

Correspondence should be addressed to Xiaofeng Long; 47387681@qq.com and Jiali Ge; logjiali@163.com

Received 21 January 2020; Revised 20 April 2020; Accepted 29 April 2020; Published 23 May 2020

Guest Editor: Baogui Xin

Copyright © 2020 Xiaofeng Long et al. This is an open access article distributed under the Creative Commons Attribution License, which permits unrestricted use, distribution, and reproduction in any medium, provided the original work is properly cited.

Corporate social responsibility (CSR) has a significant impact on the operation of enterprises. This study analyzes the production and coordination decisions of closed-loop supply chain (CLSC) by establishing two assumptions of endogenous and exogenous CSR. The results reveal that, for ordinary consumers, CSR is quantified as the parameter of consumer surplus, which has an impact on the patent licensing fee, revenue-sharing ratio, and so on, and which not only increases the sales quantity in CLSC but also creates more value for the manufacturer and the retailer. Considering endogenous CSR, the study found that the manufacturer's CSR level and the manufacturer's and the retailer's profits both increase with the proportion of CSR-sensitive consumers. In the endogenous model, the manufacturer sets a higher wholesale price and lower patent licensing fee than in the exogenous model. Perfect coordination in the two models can be achieved by setting a revenue-sharing ratio related to wholesale price and patent licensing fee. In practice, improving the social responsibility consciousness of consumers and raising enterprises' CSR level can achieve a win-win situation for revenues and social welfare.

1. Introduction

In the new era, increasing attention has been paid to environmental sustainability, driven by laws, regulations, environmental pressure, and social responsibility, which has become an important indicator of supply chain management success [1]. Sustainable supply chain management focuses on environmental issues, such as closed-loop supply chain (CLSC) and corporate social responsibility (CSR).

CSR is a type of intrinsic motivation [2], which refers to an enterprise not only creating profits for shareholders but also emphasizing contributions to the environment, consumers, and society. Consumers with CSR awareness can obtain utility from the environmental attributes of products, such as remanufactured products, which is an important market driver for environmental sustainability in supply chains. According to Cotte and Trudel [3], a total of 70% of consumers are willing to pay higher prices for products with “responsible” attributes. Most consumers tend to buy

products that are socially responsible and environmentally friendly [4]. This depends in part on the CSR level of the manufacturer.

Enterprises' recycling and reuse process is also a means of strengthening their level of CSR. Enterprises can achieve the improvement and coordination of supply chains through joint CSR investments [5–7]. The manufacturer's CSR behavior is beneficial to increase channel profit and improve the recovery rate [8], and CSR investment is a feasible strategy to enhance enterprises' sales power [9].

Based on theoretical research, this study constructs CLSC production and collaboration optimization models considering CSR and examines the following questions: (1) how does endogenous and exogenous CSR affect pricing, revenue of CLSC members? (2) what are the impact and coordination functions of patent licensing fee on the decision of CLSC? (3) what is the influencing mechanism of different types of consumers on CSR and the profit of the manufacturer and the retailer?

The main contributions of this study are as follows: (1) it brings CSR behaviors into the classic framework of CLSC management, examines its impact on the operation of CLSC, and clarifies the value of CSR; (2) it considers the issue of patent licensing in CLSC and reveals the regulatory role of patent licensing; and (3) it sets a revenue-sharing ratio related to price and patent licensing fee in the two models to coordinate the profit of the manufacturer and the retailer.

The remainder of this paper is organized as follows: the related research is reviewed in Section 2, Section 3 outlines the model setting, Section 4 investigates the decision and coordination in the CLSC of exogenous CSR when there are only ordinary consumers in the market, Section 5 examines the decision and coordination in the CLSC of endogenous CSR when there are CSR-sensitive consumers and ordinary consumers in the market, and concluding remarks are presented in Section 6.

2. Literature Review

There are three streams of research related with this research: CLSC considering patent licensing, CSR activities in supply chain management, and supply chain coordination.

The first stream mainly focuses on CLSC considering patent licensing, which can be a strategy when there are multiple remanufacturing subjects in CLSC. Cruz [10] studied the impact of CSR in supply chain management using a multicriteria decision-making approach. Zhao et al. [11] investigated the best patent licensing contracts with network effects and investigated the welfare impact by setting a Stackelberg model. Huang and Wang [12] examined the CLSC model for product recycling and hybrid remanufacturing under patent licensing and discussed the impact of remanufacturing capabilities on supply chain members and environmental sustainability. Hong et al. [13] studied the quantity and collective decisions in the CLSC using two licensing models: fixed fees and unit royalty. Hao et al. [14] discussed the best game strategies for both parties under three different decision structures: two competitive models (competition with and without remanufacturing patent licensing) and cooperation models. Huang and Wang [12, 15] studied a CLSC with technology licenses. Jin et al. [16] considered the two-period game model, designed the optimal patent licensing contract and production outsourcing strategy, and analyzed the value of CSR.

The second stream is CSR activities in supply chain management. Ni and Li [17] investigated how enterprises and suppliers interact in CSR behaviors and the impact of external parameters on this interaction. Panda [18] found that revenue-sharing contracts can maximize CSR retailers' welfare. Modak et al. [19] analyzed the dual-channel supply chain of CSR and studied its impact on the successful operation of the dual channel. Panda et al. [20] discussed the issue of coordination and profit distribution in the supply chain composed of CSR manufacturer and retailer. Panda and Modak [21] examined the channel coordination and benefit distribution between CSR manufacturer and retailer through subgame perfect equilibrium and negotiations. White et al. [22] summarized the studies on CSR through

quantitative and qualitative models. Modak et al. [23] studied CSR practice in a two-echelon CLSC.

The third stream is supply chain coordination. Panda et al. [24] resolved channel conflicts and distributed surplus profits among channel members by Nash bargaining contracts. Zhang and Ren [25] studied CLSC coordination strategy for the remanufacture of patented products. Panda et al. [8] discussed the channel coordination issue of CLSC by setting a revenue-sharing contract. Seyedhosseini et al. [26] proposed a two-part tariff contract to provide a win-win situation for all supply chain members. Hosseini-Motlagh [27, 28] studied CLSC coordination of CSR considering different demand conditions. Li and Gong [29] constructed a CLSC model and designed a cost-sharing contract to achieve supply chain coordination.

The related literature mainly examines the impact of CSR on supply chain performance, decisions, and coordination. These studies reveal that environmental improvement can be obtained through supply chain management. The current study focuses on the production decision and coordination mechanism of CLSC with patent licensing from the perspective of CSR. In addition, this study considers two models of endogenous and exogenous CSR and types of customers in the market to better grasp the value of CSR. Our study differs from the existing literature in that enterprises' CSR and the social responsibility awareness of consumers are involved in the model. The related theoretical and numerical analysis reveal how the endogenous and exogenous CSR influence production decisions and coordination.

3. Model Setting

We establish a CLSC composed of a manufacturer and a retailer, in which the manufacturer sells new products through the retailer, and the retailer recycles used products from consumers, reselling them to consumers after remanufacturing. There are two types of consumers in the market: CSR-sensitive consumers (C-type consumers), which account for a ratio of ρ to market capacity, and ordinary consumers (N-type consumers), which account for a ratio of $1 - \rho$ to market capacity. The characteristic of C-type consumers is that they can obtain additional utilities by choosing products produced by a CSR manufacturer. The utility C-type consumers can obtain from buying a unit of CSR-type products is $U_C = v - p_c + Ky_m$. N-type consumers are only sensitive to product price, and the utility they can obtain from buying a unit of ordinary products is $U_N = v - p_n$. Conditions for C-type consumers purchasing CSR products is $U_C > 0$ and $U_C \geq U_N$. Conditions for N-type consumers purchasing ordinary products is $U_N > 0$ and $U_N > U_C$, in which $v \sim U[0, 1]$. Through calculation, we find the following:

- (1) When $v - p_c + Ky_m \geq v - p_n$, the market demand for CSR-type products is $q_c = a\rho(1 - p_c + Ky_m)$ and the market demand for ordinary products is $q_n = a(1 - \rho)(1 - p_n)$.
- (2) When $v - p_c + Ky_m < v - p_n$, consumers will not buy CSR products and all consumers will buy ordinary products. At this time, the market demand for CSR-type products is $q_c = 0$ and the market demand

for ordinary products is $q_n = a(1 - p_n)$. Model parameter settings are presented in Table 1.

4. Production Decision and Coordination Mechanism of CLSC Based on Exogenous CSR

This section does not distinguish between consumer groups, meaning that consumers do not know whether the enterprise has social responsibility. In addition, this section explores the impact of CSR on patent licensing, recycling rates, and profits. The CSR manufacturer will encourage the retailer to recycle, produce, or sell more remanufactured products while increasing the revenues of all parties [8]. We use $\theta \in [0, 1]$ to represent the CSR factor of the manufacturer, $\theta = 0$ is the revenue maximization of the manufacturer, and $\theta = 1$ is the welfare maximization of the manufacturer.

In the manufacturer's revenue function, the manufacturer's CSR is quantified as the proportion of consumer surplus (CS), which refers to the difference between the maximum price a consumer is willing to pay and the actual total price to pay. When the demand function is the linear function $D = a(1 - p)$, CS is $CS = \int_{(a-D)/a}^a (a - ap)dp = (D^2/2a)$ [8]. Some of the assumptions used herein are as follows:

Assumption 1: the manufacturer is the leader of the Stackelberg game.

Assumption 2: remanufactured products are used as products recycled from consumers by the retailer. To ensure the remanufacturing activities of the retailer, the saving value of remanufactured products is $\Delta > 0$.

Assumption 3: remanufactured products have no difference in quality and use function compared with new products produced by the manufacturer; consumers value both products in the same way, and they are sold at the same price in the market.

The recycling quantity of used products increases with the increase in recovery price [30]; the recycling quantity of used products G is a function of the recovery price r : $G = \alpha + \beta * r$, where α represents the quantity of used products that consumers voluntarily return and β indicates consumers' degree of sensitivity to recovery prices.

4.1. Analysis of Decentralized Decision Model. The manufacturer authorizes the retailer to remanufacture, charging a certain patent licensing fee. In addition, the manufacturer may not recycle or remanufacture products for the sake of recovery costs or branding. The retailer recycles used products from remanufacturing activities and sells new and remanufactured products together to consumers after obtaining a patent technical license.

The decision turn of the Stackelberg game is as follows: (1) as the game leader, the manufacturer first sets the wholesale price w and patent licensing fee f ; (2) after obtaining the manufacturer's patent licensing, the retailer determines the sale price of the product p and recovery price r . When CSR is not considered, the manufacturer's revenue function is

$$\max_{w, f} \pi_M = (w - c_n)(a - a * p - \alpha - \beta * r) + f * (\alpha + \beta * r), \quad (1)$$

and the retailer's revenue function is

$$\begin{aligned} \max_{p, r} \pi_R = & (p - w)(a - a * p - \alpha - \beta * r) \\ & + (p - c_n + \Delta)(\alpha + \beta * r) - (f + r)(\alpha + \beta * r). \end{aligned} \quad (2)$$

When CSR is considered, the manufacturer's revenue function is

$$\begin{aligned} \max_{w, f} v_M = & (w - c_n)(a - a * p - \alpha - \beta * r) \\ & + f * (\alpha + \beta * r) + \theta * \frac{D^2}{2a}. \end{aligned} \quad (3)$$

Proposition 1 can be obtained by the backward induction solution.

Proposition 1. *The revenue functions of the manufacturer and the retailer under decentralized decisions are nonconvex. The optimal wholesale price can be obtained as follows: $w^* = ((2 - \theta + 2c_n)/(4 - \theta))$, the optimal retail price is $p^* = ((3 - \theta + c_n)/(4 - \theta))$, the optimal recovery price is $r^* = ((\beta\Delta - 3\alpha)/4\beta)$, and the optimal patent licensing fee is $f^* = ((4\beta + 4\alpha - 2\beta\theta - \alpha\theta - 4\beta c_n + 4\beta\Delta + 2\beta c_n\theta - \beta\theta\Delta)/(2\beta(4 - \theta)))$.*

By Proposition 1, the maximum revenue of the manufacturer considering CSR is

$$v_M^* = \frac{a\alpha^2 + 2a\alpha\beta\Delta - 4\beta\alpha^2}{8} + \frac{\beta^2\Delta^2}{a\beta} - a^2\beta c_n + \frac{ac_n^2}{2(4 - \theta)}. \quad (4)$$

The maximum revenue of the retailer is

$$\pi_R^* = \frac{(\beta\Delta + \alpha)^2}{16\beta} + \frac{\alpha^2 - 2a^2c_n + a^2c_n^2}{a(4 - \theta)^2}. \quad (5)$$

The total revenue of the supply chain is

$$\begin{aligned} v^* = & \frac{(\beta\Delta + \alpha)^2}{16\beta} + \frac{\alpha^2 - 2a^2c_n + a^2c_n^2}{a(4 - \theta)^2} + \frac{a\alpha^2 + 2a\alpha\beta\Delta - 4\beta\alpha^2}{8} \\ & + \frac{\beta^2\Delta^2}{a\beta} - \beta a^2 c_n + \frac{ac_n^2}{2(4 - \theta)}. \end{aligned} \quad (6)$$

The CS is

$$CS = \frac{a(1 - c_n)^2}{2(4 - \theta)^2}. \quad (7)$$

Conclusion 1. (1) As the cost of new products increases, both wholesale and retail prices increase, the optimal patent licensing fee charged by the manufacturer decreases, the revenue of the manufacturer and the retailer decreases, and the revenue of the supply chain decreases. (2) As the

TABLE 1: Model parameter settings.

Parameter	Represents
p	Retail price per unit of product set by the retailer
w	Unit wholesale price given by the manufacturer
r	Recovery price for used products
c_n	Production cost of new products
Δ	Production cost saved by the retailer from remanufactured products
K	Impact factors of social responsibility level on consumers' willingness to pay
f	Patent licensing fee for manufacturer-licensed remanufacturing
y_m	Manufacturer's level of CSR
ρ	Ratio of CSR-sensitive consumers
a	Market capacity
π_i^j	The profit function of the enterprise i , parameter $i \in \{M, R\}$, where M represents the manufacturer and R represents the retailer

remanufacturing saving cost increases, the recovery price and recycling quantity of used products both increase, the patent licensing fee charged increases and the profits of the manufacturer, the retailer, and the supply chain all increase. (3) When the manufacturer shows stronger CSR, the wholesale and the retail prices of products are lower. The manufacturer's revenue is higher, the patent licensing fee is lower, the retailer's revenue increases, and CS increases.

4.2. Analysis of Centralized Decision Model. In the centralized decision model, the revenue function of the entire supply chain is

$$\max_{p_c, r_c} \pi_c = (p_c - c_n)(a - a * p) + (\Delta - r_c)(\alpha + \beta * r_c). \quad (8)$$

When the manufacturer's CSR is considered, the revenue function of the entire supply chain is

$$\max_{p_c, r_c} v_c = (p_c - c_n)(a - a * p) + (\Delta - r_c)(\alpha + \beta * r_c) + \theta * \frac{D^2}{2a}. \quad (9)$$

Take the partial derivatives of formula (8) with respect to p_c and r_c , $(\partial v_c / \partial p_c) = 0$, $(\partial v_c / \partial r_c) = 0$, and obtain the best solution p_c^* and r_c^* . The corresponding Hessian matrix is

$$H_c = \begin{pmatrix} \frac{\partial^2 v_c}{\partial p_c^2} & \frac{\partial^2 v_c}{\partial p_c \partial r_c} \\ \frac{\partial^2 v_c}{\partial r_c \partial p_c} & \frac{\partial^2 v_c}{\partial r_c^2} \end{pmatrix} = \begin{pmatrix} -2\beta & -2\beta \\ 0 & a\theta - 2a \end{pmatrix}. \quad (10)$$

When Hessian matrix $H_c > 0$, $2 - \theta > 0$, that is, the centralized revenue function is nonconvex, we can obtain Proposition 2.

Proposition 2. *The revenue function of the entire supply chain under centralized decisions with respect to p_c and r_c is nonconvex, and the optimal solution (p_c^*, r_c^*) is $((1 - \theta + c_n) / (2 - \theta))$, $((\beta\Delta - \alpha) / (2\beta))$. The revenue of the entire supply chain under centralized decisions is*

$$v_c^* = \frac{2a\beta + 2\alpha^2 + 2a\beta c_n^2 + 2\beta^2 \Delta^2 - \beta\alpha^2 - \theta\beta^2 \Delta^2 - 4\beta c_n + 4\alpha\beta\Delta - 2\alpha\beta\Delta\theta}{4\beta(2 - \theta)}. \quad (11)$$

4.3. Revenue-Sharing Coordination Mechanism. Traditionally, the manufacturer and the retailer act independently and maximize their own respective revenues. However, an effective supply chain network requires a cooperative relationship. Therefore, a coordination mechanism is needed to coordinate the manufacturer and the retailer. Under a revenue-sharing (RS) contract, the manufacturer offers a wholesale price and requires a small portion of the revenue from the retailer. The RS contract sets the revenue-sharing parameter as $\lambda \in (0, 1)$, and the manufacturer receives $(1 - \lambda)$ of the revenue.

Proposition 3. *Under the RS contract, the revenue function expressions of the manufacturer and the retailer are, respectively, as follows:*

$$\begin{aligned} \pi_M &= (1 - \lambda)p(a - ap) + (w - c_n)(a - ap - \alpha - \beta r) \\ &\quad + f(\alpha + \beta r), \\ \pi_R &= (\lambda p - w)(a - ap) + (w - c_n + \Delta)(\alpha + \beta r) \\ &\quad - (f + r)(\alpha + \beta r), \\ v_M &= (1 - \lambda)p(a - ap) + (w - c_n)(a - ap - \alpha - \beta r) \\ &\quad + f(\alpha + \beta r) \frac{\theta(a - ap)^2}{2a}. \end{aligned} \quad (12)$$

When the RS contract the manufacturer provided to the retailer is

$$(w^{co}, f^{co}) = \left(\frac{2c_n - \theta}{2 - \theta} \lambda, \frac{2c_n - \theta}{2 - \theta} \lambda - c_n \right), \quad (13)$$

the RS proportion λ should meet $\lambda_1 < \lambda < \lambda_2$, in which when

$$\lambda_1 = \frac{(2 - \theta)^2 (16(a - ac_n)^2 - 3a(4 - \theta)^2 (\alpha + \beta\Delta)^2)}{16\beta(4 - \theta)^2 (a - ac_n)^2},$$

$$\lambda_2 = - \left(\frac{(1 - c_n)^2}{2(\theta - 2)} + \frac{4\beta(1 - c_n)^2 + (4 - \theta)(\alpha + \beta\Delta)^2 - 3\beta^2\Delta^2\theta}{8\beta(4 - \theta)} \right) \frac{(2 - \theta)^2}{(a - ac_n)^2}, \quad (14)$$

the CLSC can be coordinated by the RS contract (see Appendix A).

Proposition 4. *Under the RS contract, it satisfies the following relationships: $p^{co} < p^*$, $w^{co} < w^*$, $f^{co} < f^*$, $r^{co} > r^*$, $\pi_R^{co} > \pi_R^*$, and $v_M^{co} > v_M^*$.*

Proposition 4 shows that when an RS contract is adopted, the manufacturer pays more attention to CSR and reduces its wholesale price and the product patent licensing fee, thus increasing the sales volume of products. Product sales are directly proportional to the CSR level of the manufacturer. In addition, the recycling intensity of the retailer increases, and in response to the manufacturer's strategies, the retailer reduces their sale prices to encourage customers to buy more products and puts more efforts into collecting used products from customers. The manufacturer's CSR therefore influences the retailer's decisions and further influences their decisions in the reverse supply chain through influencing prices. In centralized decisions, when CSR increases, the manufacturer reduces the wholesale price of products, and the sale price under the centralized decision is lower than that under the decentralized decision. As a result, there is a higher demand for products of centralized decisions. Obviously, the retailer will make more efforts to collect used products under centralization. The manufacturer, the retailer, and the entire supply chain have higher revenues under the centralized model than that under decentralized model; thus, the entire CLSC achieves coordination.

At the same time, consumers can buy new products at a lower price and sell used products at a higher price, which greatly improves consumers' utilities and achieves a win-win situation for enterprises and consumers.

4.4. Numerical Examples and Sensitivity Analysis. Numerical calculations are made based on the above conclusions. Parameter values refer to assumptions of Bakal and Akcali [30]; the market demand function of products is $D(p) = 100(1 - p)$, the supply function of old products is $G(r) = 0.8 + 10r$, and the production cost of new products is $C_n = 0.5$. The decision results of different CLSC systems are illustrated in Tables 2 and 3.

As can be seen from Table 2, under decentralized decisions, with the increasing awareness of the manufacturer's CSR, the revenues of both the manufacturer and the retailer increase, the manufacturer reduces the patent licensing fee and lowers the

wholesale prices so that the retailer sets retail prices lower and the consumer purchase quantity increases. With the increase in remanufacturing saving cost, the retailer's recycling prices rise. The manufacturer charges more patent licensing fees, and both the manufacturer's and the retailer's revenues increase. From Table 3, as the RS proportion increases, the manufacturer's wholesale price increases, the patent licensing fee decreases, the retailer's revenue increases, and the manufacturer's revenue decreases.

Sensitivity analysis is conducted on the key parameters (C_n and θ) to examine the proposed models' performance. The effects of C_n on the w , p , and f are shown in Figure 1. By increasing C_n , both wholesale prices w and retail prices p increase and the optimal patent licensing fee f decreases. When the production cost of new products C_n is higher, the manufacturer reduces the patent licensing fee to encourage the retailer to produce and recycle more used products and increase the revenue. Figure 2 illustrates the effects of θ on the w , p , and f by increasing θ and the decreases in wholesale prices w , retail prices p , and patent licensing fee f . When the manufacturer's CSR θ is stronger, the price of products is lower. The sales volume is higher, and the profits of both the manufacturer and the retailer increase. The manufacturer will reduce the patent licensing fee, encouraging the retailer to recycle and remanufacture. Therefore, patent licensing fee is an important adjustment tool for the manufacturer.

From Figure 3, the entire CLSC profit is improved under RS contracts, the profit of the manufacturer and the retailer is improved compared to the decentralized model ($\pi_R^{co} > \pi_R^*$ and $v_M^{co} > v_M^*$) and the compensation-based whole price mechanism can motivate the retailer to take part in the centralized decisions.

5. Production Decision and Coordination Mechanism of CLSC of Endogenous CSR

This section divides consumers into CSR-sensitive and ordinary types, constructs the CLSC model considering endogenous CSR, and mainly examines the impact of the proportion of CSR-sensitive consumers on CSR level, the profits of CLSC members, and RS contracts. The specific parameter settings are shown in Table 1.

5.1. Analysis of Decentralized Decision Model. When CSR is endogenous, there are CSR-sensitive consumers and

TABLE 2: Decentralized decision results of CLSC.

Parameter variation	w	p	f	π_R	v_M
$\Delta = 0.3 \quad \theta = 0.2$	0.7368	0.8684	0.4268	1.8216	3.47
$\Delta = 0.3 \quad \theta = 0.5$	0.7143	0.8571	0.4043	2.1311	3.7519
$\Delta = 0.3 \quad \theta = 0.8$	0.6875	0.8438	0.3775	2.5317	4.0868
$\Delta = 0.4 \quad \theta = 0.2$	0.7368	0.8684	0.4768	1.8753	3.5775
$\Delta = 0.4 \quad \theta = 0.5$	0.7143	0.8571	0.4543	2.1848	3.8594
$\Delta = 0.4 \quad \theta = 0.8$	0.6875	0.8438	0.4275	2.5854	4.1942

TABLE 3: Coordinated decision results under revenue-sharing contract.

Parameter variation	w^{co}	r^{co}	f^{co}	π_R^{co}	v_M^{co}
$\Delta = 0.3 \quad \lambda_1 = 0.2209$	0.0982	0.11	0.4018	1.8216	5.4839
$\theta = 0.2 \quad \lambda_2 = 0.4503$	0.2001	0.11	0.2999	3.8355	3.47
$\Delta = 0.4 \quad \lambda_1 = 0.1448$	0.0483	0.16	0.4517	2.1848	6.7245
$\theta = 0.5 \quad \lambda_2 = 0.4027$	0.1420	0.16	0.3658	5.0499	3.8594
$\Delta = 0.4 \quad \lambda_1 = 0.1157$	0.0193	0.16	0.4807	2.5854	8.4073
$\theta = 0.8 \quad \lambda_2 = 0.3584$	0.0597	0.16	0.4403	6.7984	4.1942

ordinary consumers in the market, and the revenue function of the manufacturer is

$$\begin{aligned} \max_{w_c, w_n, f, y_m} \pi_M = & (w_c - c_n)a\rho(1 - p_c + Ky_m) \\ & + (w_n - c_n)a(1 - \rho)(1 - p_n) \\ & + f(\alpha + \beta r) - y_m^2. \end{aligned} \quad (15)$$

The revenue function of the retailer is

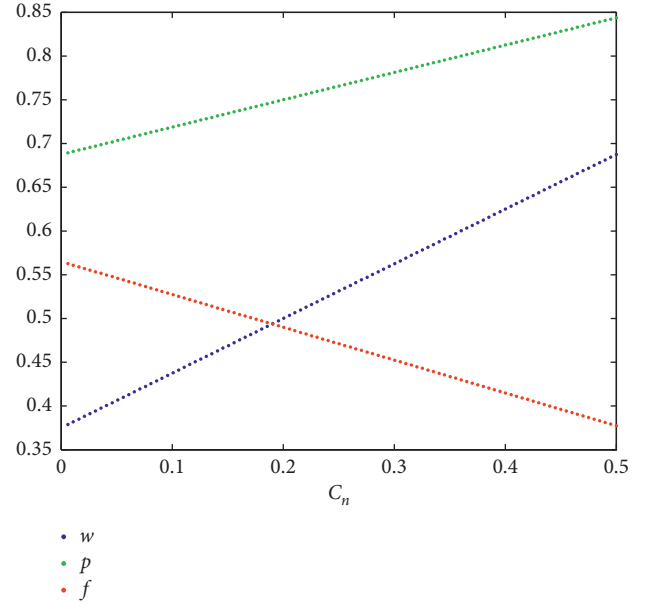
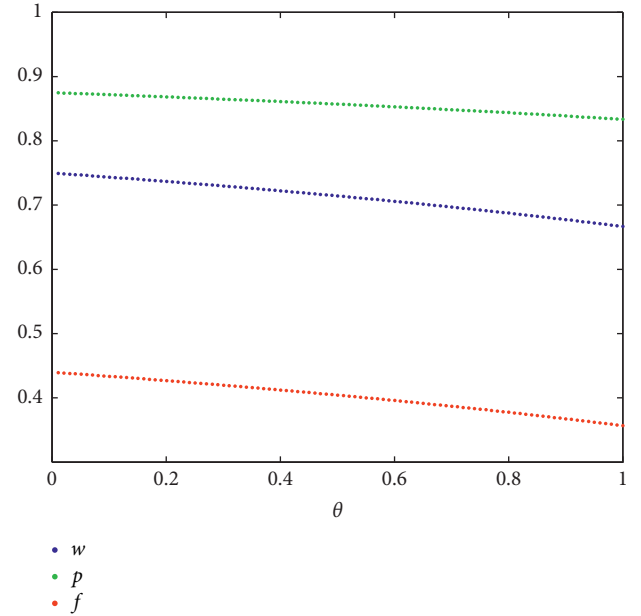
$$\begin{aligned} \max_{p_c, p_n, r} \pi_R = & (p_c - w_c)a\rho(1 - p_c + Ky_m) \\ & + (p_n - w_n)a(1 - \rho)(1 - p_n) \\ & + (\Delta - f - r)(\alpha + \beta r). \end{aligned} \quad (16)$$

Proposition 5 can be obtained through the backward induction solution.

Proposition 5. *The revenue functions of the manufacturer and the retailer are nonconvex. The optimal wholesale price of CSR-type products that can be obtained is $w_c = -(-ac_n\rho K^2 + 4c_n + 4)/(a\rho K^2 - 8)$, the optimal retail price is $p_c = -((2c_n - ac_n\rho K^2 + 6)/(a\rho K^2 - 8))$, the optimal wholesale price of ordinary products is $w_n = ((1 + c_n)/2)$, and the optimal retail price is $p_n = ((3 + c_n)/4)$. The optimal recovery price is $r = -((3\alpha - \beta\Delta)/4\beta)$, the optimal patent licensing fee is $f = ((\alpha + \beta\Delta)/2\beta)$, and the manufacturer's optimal CSR level is $y_m = -((aK\rho(1 - c_n))/(aK^2\rho - 8))$. From $p_c > 0$, $y_m > 0$, $0 < c_n < 1$, we can obtain $a\rho K^2 < 8$.*

Conclusion 2

- (1) As the cost of products increases, the retail price and the wholesale price of ordinary products increase; when $a\rho K^2 < 4$, the wholesale price of CSR-sensitive products increases. When $4 < a\rho K^2 < 8$, the wholesale price of CSR-sensitive products decreases. When

FIGURE 1: Optimal decision results when C_n changes.FIGURE 2: Optimal decision results when θ changes.

$a\rho K^2 < 2$, the retail price of CSR-sensitive products increases. When $2 < a\rho K^2 < 8$, the retail price of CSR-sensitive products decreases. Optimum patent licensing fee and recovery prices are not affected by the cost of products, and the manufacturer's CSR level decreases as the cost of products increases.

- (2) As the remanufacturing saving cost increases, the recovery price and the recycling quantity of used products both increase, the patent licensing fee increases, and the profits of the manufacturer, the retailer, and the supply chain all increase.
- (3) With the increase in the proportion of CSR-sensitive consumers, the wholesale and retail prices of CSR

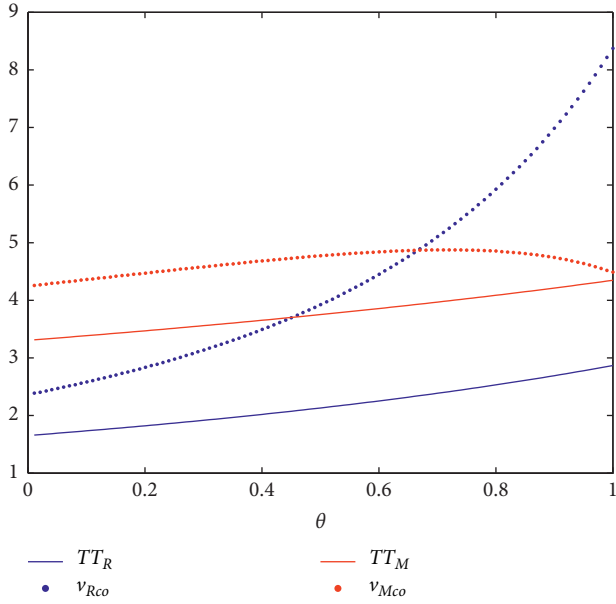


FIGURE 3: Profit comparison between decentralized and centralized decisions when θ changes.

products increase, the CSR level of the manufacturer increases, and the profits of both the manufacturer and the retailer increase.

- (4) $w_n < w_c$, $p_n < p_c$, the wholesale and selling prices of socially responsible products are higher than those of ordinary products.

5.2. Analysis of Centralized Decision Model. In the centralized decision model, the revenue function of the entire supply chain is

$$\pi = a\rho(p_c - c_n)(1 - p_c + Ky_m) + a(p_n - c_n)(1 - \rho)(1 - p_n) + (\Delta - r)(\alpha + \beta r) - y_m^2. \quad (17)$$

Proposition 6. *The revenue function of the entire supply chain under centralized decisions is nonconvex with respect to p_c , p_n , and r . The optimal solution of (p_c^*, p_n^*, r^*) is $(-\frac{((2 - a\rho K^2 + 2c_n)}{(a\rho K^2 - 4)), (1 + c_n)/2, (\beta\Delta - \alpha)/2\beta}$.*

Proposition 7. *This compares the results of decentralized and centralized decisions $p_n > p_n^*$, $r^* < r_c^*$. When $a\rho K^2 < 2$, $p_c > p_c^*$ and when $2 < a\rho K^2 < 8$, $p_c < p_c^*$.*

Conclusion 3. In the centralized decision model, (1) with the increase in remanufacturing cost savings, the maximum revenue of the entire supply chain increases and the recovery price of products increases. (2) With the increase in the proportion of CSR-sensitive consumers, the sale price of CSR products increases, and the overall revenue of the supply chain increases.

5.3. Coordination Mechanism. RS contracts are still adopted for coordination here. In RS contracts, the manufacturer

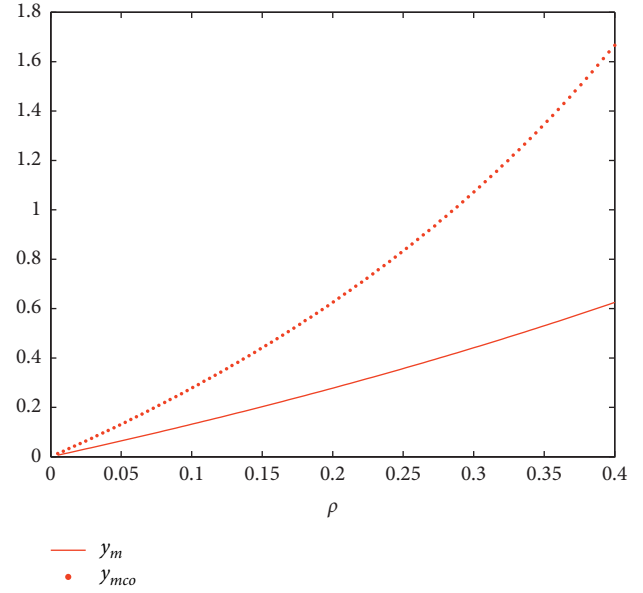


FIGURE 4: Optimal CSR results between decentralized and centralized decisions when ρ changes.

provides a wholesale price and requires a portion of the revenue from the retailer. The revenue-sharing parameter set in RS contracts is $\lambda \in (0, 1)$, and the manufacturer receives $(1 - \lambda)$ times a portion of the revenue.

The revenue function of the manufacturer is

$$\begin{aligned} \pi_M = & (1 - \lambda)(p_c a \rho (1 - p_c + Ky_m) + p_n a (1 - \rho)(1 - p_n)) \\ & + (w_c - c_n) a \rho (1 - p_c + Ky_m) \\ & + (w_n - c_n) a (1 - \rho)(1 - p_n) + f(\alpha + \beta r) - y_m^2. \end{aligned} \quad (18)$$

The retailer's revenue function is

$$\begin{aligned} \pi_R = & (\lambda p_c - w_c) a \rho (1 - p_c + Ky_m) \\ & + (\lambda p_n - w_n) a (1 - \rho)(1 - p_n) + (\Delta - f - r)(\alpha + \beta r). \end{aligned} \quad (19)$$

Proposition 8. *When the manufacturer offers the contract $w_c = -2\lambda \frac{((2 + 2c_n - a c_n \rho K^2)}{(a\rho K^2 - 4)) + ((\lambda + K\lambda y_m)/2\lambda)}$, $w_n = \lambda c_n$, and $f = ((\alpha + \beta\Delta)/2\beta)$, the CLSC can be coordinated. See Appendix B.*

5.4. Sensitivity Analysis. The data are set as in Section 4.4, $a = 100$, $G(r) = 0.8 + 10r$, $C_n = 0.5$, $\Delta = 0.3$, and $k = 0.2$. Sensitivity analysis is conducted on the key parameter ρ to examine the proposed model's performance in the following. Figure 4 illustrates the effects of ρ on y_m , and Figure 5 shows the effects of ρ on the profits of the manufacturer and the retailer under the decentralized and coordinated structures. With the increase in the proportion of CSR-sensitive consumers ρ , the CSR level of enterprises y_m increases and the profits of both the manufacturer and the retailer increase, which are more than those in the decentralized structure.

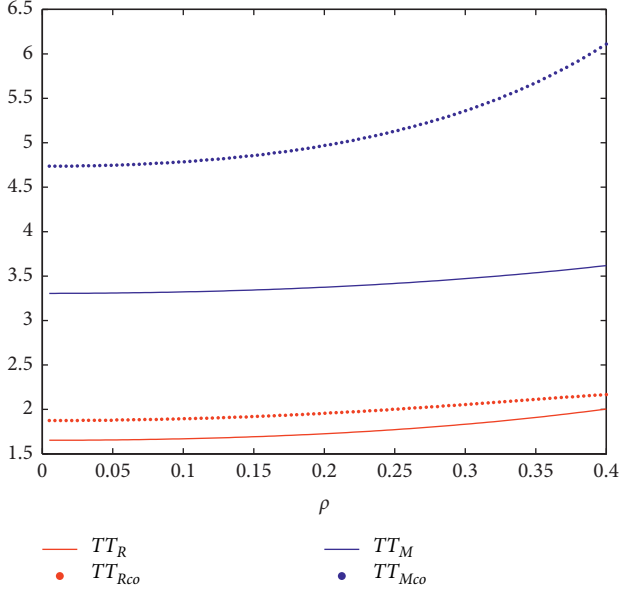


FIGURE 5: Profit comparison between decentralized and centralized decisions when ρ changes.

The result confirms those of Hosseini-Motlagh et al. [28], who used the cost-sharing contract to coordinate the CLSC.

Comparing the wholesale price, patent licensing fee, and profits in Propositions 1 and 5, we can obtain $w^* < w_n < w_c$, $p^* < p_n < p_c$, and $f^* > f$. The price of any product in the endogenous model is higher than that of the exogenous model, which means that manufacturer's CSR level has effects on CSR-sensitive consumers and further affects customers' price sensitivity. But the patent license fee in the endogenous model is lower, which is set by the manufacturer to encourage the retailer to recycle and remanufacture. However, the manufacturer and the retailer's profits in the exogenous model are not necessarily more than those in endogenous model.

6. Conclusion

This study investigates the CLSC production and coordination problem by setting endogenous and exogenous CSR assumptions. CSR level can effectively improve the revenues of the manufacturer and the retailer, and patent licensing fee has an important regulatory effect on regulating the manufacturer's revenue and encouraging the retailer to remanufacture. CLSC considering CSR is more competitive than the traditional pure profit maximization supply chain. In practice, improving consumers' social responsibility consciousness and raising enterprises' level of CSR can achieve a win-win situation for revenues and social welfare. RS contracts coordinate the CLSC of endogenous and exogenous CSR.

From the comparisons and discussions of the results among the two models, we obtained some managerial insights. The manufacturer's level of CSR affects the wholesale

price and patent licensing fee, and this result is significantly different from the profit maximization of a pure supply chain. Improving the social responsibility consciousness of consumers and raising the CSR level can achieve a win-win situation for revenues and social welfare; the manufacturer and the retailer should therefore increase the proportion of socially responsible consumers through the price mechanism. The results of sensitivity analysis reveal that the supply chain can be coordinated by using the compensation-based wholesale price mechanism. Therefore, the mechanism not only increases the profits of the CLSC and all members but also increases CSR activities for environmental, social, and economic development.

This study has several limitations and future research opportunities. This study adopts the linear demand. In terms of random demand, there remains an issue of how to solve the model. In addition, regarding the RS contract coordinating the supply chain adopted herein, we can try to adopt quantity discount contracts and bargaining models for coordination.

Appendix

A. Proof of Proposition 3

Proof of Proposition 3. The retailer's revenue function:

$$\pi_R = (\lambda p - w)(a - ap) + (w - c_n + \Delta)(\alpha + \beta r) - (f + r)(\alpha + \beta r). \quad (\text{A.1})$$

Take first derivation with respect to p and r , and get $p^{\text{co}} = ((\lambda + w)/2\lambda)$ and $r^{\text{co}} = ((-\alpha + \beta(w + \Delta - f - c_n))/2\beta)$.

Let the profits of the CLSC under the revenue-sharing contract be the same as that under centralized decisions, and it needs to satisfy $((\lambda + w)/2\lambda) = ((\alpha - \alpha\theta + ac_n)/(2a - a\theta))$, $((-\alpha + \beta(w + \Delta - f - c_n) - a\theta)/2\beta) = ((\beta\Delta - \alpha)/2\beta)$.

The manufacturer's optimum wholesale price and patent licensing fee are

$$w^{\text{co}} = \frac{2c_n - \theta}{(2 - \theta)}\lambda, \quad (\text{A.2})$$

$$f^{\text{co}} = \frac{2c_n - \theta}{(2 - \theta)}\lambda - c_n.$$

At this point, the revenues of the manufacturer and the retailer are

$$v_M^{\text{co}} = \frac{a(-c_n)^2(\theta + 2\lambda - 2)}{2(2 - \theta)^2}, \quad (\text{A.3})$$

$$\pi_R^{\text{co}} = \frac{4a\lambda\beta(1 - c_n)^2 + (2 - \theta)^2(\alpha + \beta\Delta)^2}{4\beta(2 - \theta)^2}.$$

The condition of both parties receiving the contract is $v_M^{\text{co}} > v_M^*$ and obtain $\lambda_1 < \lambda < \lambda_2$:

$$\lambda_1 = \frac{(2 - \theta)^2 (16a(1 - c_n)^2 - 3(4 - \theta)^2 (\alpha + \beta\Delta)^2)}{16a\beta(4 - \theta)^2 (-c_n)^2},$$

$$\lambda_2 = -\left(\frac{a(1 - c_n)^2}{2(\theta - 2)} + \frac{4a\beta(1 - c_n)^2 + (4 - \theta)(\alpha + \beta\Delta)^2 - 3\beta^2\Delta^2\theta}{8\beta(4 - \theta)} \right) \frac{(2 - \theta)^2}{a(1 - c_n)^2}.$$
(A.4)

B. Proof of Proposition 8

Proof of Proposition 8. The retailer's revenue function is

$$\begin{aligned} \pi_R = & (\lambda p_c - w_c) a \rho (1 - p_c + K y_m) \\ & + (\lambda p_n - w_n) a (1 - \rho) (1 - p_n) + (\Delta - f - r) (\alpha + \beta r). \end{aligned}$$
(B.1)

Take the first derivation respects to p_c , p_n , and r and obtain $p_c = ((\lambda + w_c + K\lambda y_m)/2\lambda)$, $p_n = ((\lambda + w_n)/2\lambda)$, and $r = -((\alpha - \beta\Delta)/2\beta)$.

Let the profits of the CLSC under the revenue-sharing contract be the same as that under centralized decisions, and it needs to satisfy $((\lambda + w_c + K\lambda y_m)/2\lambda) = -((2 + 2c_n - ac\rho K^2)/a\rho K^2 - 4)$ and $((\lambda + w_n)/2\lambda) = ((1 + c_n)/2)$.

The optimal wholesale price and the patent licensing fee of the manufacturer are $w_c = -2\lambda(((2 + 2c_n - ac\rho K^2)/(a\rho K^2 - 4)) + ((\lambda + K\lambda y_m)/2\lambda))$, $w_n = \lambda c_n$, and $f = ((\alpha + \beta\Delta)/2\beta)$.

The total revenue under the coordinated decision should be greater than the total revenue under the decentralized decision, $(\pi_M + \pi_R)^{co} > (\pi_M + \pi_R)^*$, and we can obtain λ_1 and λ_2 , satisfying $\lambda_1 < \lambda < \lambda_2$. \square

Data Availability

The data used to support the findings of this study are available from the corresponding author upon request.

Conflicts of Interest

The authors declare that there are no conflicts of interest regarding the publication of this paper.

Acknowledgments

This study was financially supported by Natural Science Foundation of Hunan Province (No. 2020JJ5011), Scientific Research Fund of Hunan Provincial Education Department (No. 19C0315) and National Natural Science Foundation of China (Nos. 71771080 and 71802075).

References

- [1] Z. Hong and X. Guo, "Green product supply chain contracts considering environmental responsibilities," *Omega*, vol. 83, pp. 155–166, 2019.
- [2] K. M. Amaeshi, O. K. Osuji, and P. Nnodim, "Corporate social responsibility in supply chains of global brands: a boundaryless responsibility? Clarifications, exceptions and implications," *Journal of Business Ethics*, vol. 81, no. 1, pp. 223–234, 2008.

- [3] J. Cotte and R. Trudel, "Socially conscious consumerism: a systematic review of the body of knowledge," in *Network for Business Sustainability Knowledge Project Series. Economist*, Boston University, Boston, MA, USA, 2009.
- [4] J. Gaur, M. Amini, and A. K. Rao, "Closed-loop supply chain configuration for new and reconditioned products: an integrated optimization model," *Omega*, vol. 66, pp. 212–223, 2017.
- [5] C.-F. Hsueh, "Improving corporate social responsibility in a supply chain through a new revenue sharing contract," *International Journal of Production Economics*, vol. 151, no. 3, pp. 214–222, 2014.
- [6] C.-F. Hsueh, "A bilevel programming model for corporate social responsibility collaboration in sustainable supply chain management," *Transportation Research Part E: Logistics and Transportation Review*, vol. 73, pp. 84–95, 2015.
- [7] C.-H. Wu, "Collaboration and sharing mechanisms in improving corporate social responsibility," *Central European Journal of Operations Research*, vol. 24, no. 3, pp. 681–707, 2016.
- [8] S. Panda, N. M. Modak, and L. E. Cárdenas-Barrón, "Coordinating a socially responsible closed-loop supply chain with product recycling," *International Journal of Production Economics*, vol. 188, no. 1, pp. 11–21, 2017.
- [9] S. La and B. Choi, "Perceived justice and CSR after service recovery," *Journal of Services Marketing*, vol. 33, no. 2, pp. 206–219, 2019.
- [10] J. M. Cruz, "The impact of corporate social responsibility in supply chain management: multicriteria decision-making approach," *Decision Support Systems*, vol. 48, no. 1, pp. 224–236, 2009.
- [11] D. Zhao, H. Chen, X. Hong, and J. Liu, "Technology licensing contracts with network effects," *International Journal of Production Economics*, vol. 158, pp. 136–144, 2014.
- [12] Y. Huang and Z. Wang, "Closed-loop supply chain models with product take-back and hybrid remanufacturing under technology licensing," *Journal of Cleaner Production*, vol. 142, pp. 3917–3927, 2016.
- [13] X. Hong, K. Govindan, L. Xu, and P. Du, "Quantity and collection decisions in a closed-loop supply chain with technology licensing," *European Journal of Operational Research*, vol. 256, no. 3, pp. 820–829, 2017.
- [14] S. Hao, Y. Jun, H. Jin-song, D. A. Qing-li, and W. Kai, "Research on the game strategies for the OEM and the remanufacturer under different decision structures," *Chinese Journal of Management Science*, vol. 25, no. 1, pp. 160–169, 2017.
- [15] Y. Huang and Z. Wang, "Information sharing in a closed-loop supply chain with technology licensing," *International Journal of Production Economics*, vol. 191, pp. 113–127, 2017.
- [16] L. Jin, B. Zheng, and X. Hu, "Patent licensing, production outsourcing and corporate social responsibility," *Nankai Business Review*, vol. 22, no. 3, pp. 40–53, 2019.
- [17] D. Ni and K. W. Li, "A game-theoretic analysis of social responsibility conduct in two-echelon supply chains," *International Journal of Production Economics*, vol. 138, no. 2, pp. 303–313, 2012.
- [18] S. Panda, "Coordination of a socially responsible supply chain using revenue sharing contract," *Transportation Research Part E: Logistics and Transportation Review*, vol. 67, pp. 92–104, 2014.

- [19] N. M. Modak, S. Panda, S. S. Sana, and M. Basu, "Corporate social responsibility, coordination and profit distribution in a dual-channel supply chain," *Pacific Science Review*, vol. 16, no. 4, pp. 235–249, 2015.
- [20] S. Panda, N. M. Modak, and D. Pradhan, "Corporate social responsibility, channel coordination and profit division in a two-echelon supply chain," *International Journal of Management Science and Engineering Management*, vol. 11, no. 1, pp. 22–33, 2016.
- [21] S. Panda and N. M. Modak, "Exploring the effects of social responsibility on coordination and profit division in a supply chain," *Journal of Cleaner Production*, vol. 139, pp. 25–40, 2016.
- [22] C. L. White, A. E. Nielsen, and C. Valentini, "CSR research in the apparel industry: a quantitative and qualitative review of existing literature," *Corporate Social Responsibility and Environmental Management*, vol. 24, no. 5, pp. 382–394, 2017.
- [23] N. M. Modak, N. Kazemi, and L. E. Cárdenas-Barrón, "Investigating structure of a two-echelon closed-loop supply chain using social work donation as a corporate social responsibility practice," *International Journal of Production Economics*, vol. 207, pp. 19–33, 2019.
- [24] S. Panda, N. M. Modak, M. Basu, and S. K. Goyal, "Channel coordination and profit distribution in a social responsible three-layer supply chain," *International Journal of Production Economics*, vol. 168, pp. 224–233, 2015.
- [25] C.-T. Zhang and M. Ren, "Closed-loop supply chain coordination strategy for the remanufacture of patented products under competitive demand," *Applied Mathematical Modelling*, vol. 40, no. 13–14, pp. 6243–6255, 2016.
- [26] S. M. Seyedhosseini, S.-M. Hosseini-Motlagh, M. Johari, and M. Jazinaninejad, "Social price-sensitivity of demand for competitive supply chain coordination," *Computers & Industrial Engineering*, vol. 135, pp. 1103–1126, 2019.
- [27] S.-M. Jazinaninejad, M. Nouri-Harzvili, T.-M. Choi, and S. Ebrahimi, "Reverse supply chain systems optimization with dual channel and demand disruptions: sustainability, CSR investment and pricing coordination," *Information Sciences*, vol. 503, pp. 606–634, 2019.
- [28] S.-M. Hosseini-Motlagh, S. Ebrahimi, and R. Zirakpourdehkordi, "Coordination of dual-function acquisition price and corporate social responsibility in a sustainable closed-loop supply chain," *Journal of Cleaner Production*, vol. 251, pp. 1–15, 2020.
- [29] J. Li and S. Gong, "Coordination of closed-loop supply chain with dual-source supply and low-carbon concern," *Complexity*, vol. 2020, 2020.
- [30] I. S. Bakal and E. Akcali, "Effects of random yield in remanufacturing with price-sensitive supply and demand," *Production & Operations Management*, vol. 15, no. 3, pp. 407–420, 2006.

Research Article

Dynamics of a Cournot Duopoly Game with a Generalized Bounded Rationality

A. Al-khedhairi 

Department of Statistics and Operations Researches, College of Science, King Saud University, P.O. Box: 2455, Riyadh 11451, Saudi Arabia

Correspondence should be addressed to A. Al-khedhairi; akhediri@ksu.edu.sa

Received 18 January 2020; Revised 22 March 2020; Accepted 15 April 2020; Published 23 May 2020

Guest Editor: Baogui Xin

Copyright © 2020 A. Al-khedhairi. This is an open access article distributed under the Creative Commons Attribution License, which permits unrestricted use, distribution, and reproduction in any medium, provided the original work is properly cited.

In this paper, the dynamics of Cournot duopoly game with a generalized bounded rationality is considered. The fractional bounded rationality of the Cournot duopoly game is introduced. The conditions of local stability analysis of equilibrium points of the game are derived. The effect of fractional marginal profit on the game is investigated. The complex dynamics behaviors of the game are discussed by numerical computation when parameters are varied.

1. Introduction

Many scientists have created diverse variations of Cournot oligopoly games. Cournot duopoly game was the first oligopoly game [1]. Furth [2] studied existence and equilibrium stability in oligopoly games. Oligopoly game which contains two firms is called duopoly game; these two firms are in a competition and there is no collaboration among them. In order to maximize the profit, every firm takes action on the basis of its rivals reaction to compete with its rivals. After that, the modifications of these games turned into the core interest. Dana and Montrucchio [3] investigated complex dynamics in Cournot oligopoly games. Moreover, Puu [4, 5] studied the chaotic dynamics of Cournot duopoly games. The stability analysis of naive and bounded rationality oligopoly games has been discussed in [6]. Bischi and Naimzada [7] studied dynamics duopoly game based on bounded rationality. Agiza and Elsadany [8] investigated nonlinear dynamics occurring in heterogeneous duopoly game. The duopoly game based on altering heterogeneous players has been explored in [9]. Nonlinear Chinese cold-rolled steel market game has been examined in [10]. Nonlinear oligopoly games have been reviewed in [11]. The dynamics of a discrete duopoly game with players having adaptive expectations has been studied in [12]. The stability of Cournot duopoly game with

logarithmic price function has been investigated in [13]. Hommes [14] studied heterogeneous expectations and behavioral rationality in economic models. The isoelastic duopoly game with different expectations has been introduced in [15]. Fanti and Gori [16] investigated the differentiated competition duopoly game. Sarafopoulos [17] explored the dynamics of a nonlinear duopoly game with differentiated products. Askar and Al-khedhairi [18] discussed the influences of a cubic utility function on the stability of a nonlinear differentiated Cournot duopoly game. Tramontana and Elsadany [19] and Guirao et al. [20] studied oligopoly games while increasing the number of heterogeneous competitors. Dynamical heterogeneous duopoly games and their control are investigated in many other research studies [21–24]. The modified Puu duopoly game has been analyzed [25]. Fanti [26] investigated the dynamic banking duopoly game with capital regulations. An uncertainty Cournot duopoly game based on concave demand has been introduced in [25]. The impact of delay on Cournot duopoly game has been discussed in [27]. Elsadany [28] considered the Cournot duopoly game due to relative profit. Different investigations discussed for more realistic learning of firms structures of different strategies such as choices of firms and have demonstrated that the oligopoly games may tend to complex dynamics [29–32].

In recent years, the issue of incorporating game theory with complexity theory has been discussed by many authors [33–39]. Askar and Al-khedhairi [33] examined Cournot game that is constructed based on Cobb–Douglas preferences and, especially, analyzed its nonlinear dynamics. Tian et al. [34] investigated a dynamic duopoly Stackelberg model of competition on output with stochastic perturbations. Zhao et al. [35] extend the Cournot game to the case of multimarket with bounded rationality. Peng et al. [36] analyzed complex dynamics for Cournot–remanufacturing duopoly game based on bounded rationality. Cerboni Baiardi and Naimzada [37] considered the oligopoly model with rational and imitation rules. They found that the number of firms participating in the game, called a parameter of the game, has an ambiguous effect in influencing the stationary state stability property and double stability threshold has been observed. Al-khedhairi [38] introduced a fractional-order Cournot triopoly game and discussed the effects of the memory on the dynamics of the game. Furthermore, remanufacturing Cournot duopoly game based on a nonlinear utility function has been studied by Askar and Al-khedhairi [39].

The generalized bounded rationality is more applicable than the traditional one. The later ignores the memory of the production's previous prices adopted by production buyers. The traditional bounded rationality may be used to handle total amnesia of buyers, but the generalized one is suggested to remove that issue and takes into account the effect of memory. Memory is known to be an important factor in the economy. The fractional-order derivative is based on integration. Consequently, the fractional-order derivative is a nonlocal operator. Therefore, the fractional-order derivative is appropriate for representing complex systems like biological, economic, and social systems. The case of triopoly game with differentiated products based on generalized (fractional) bounded rationality is considered by Askar and Abouhawwash [40]. They showed that, for the firms to stay stable for a long time in the market, they should play with generalized bounded rationality rather than the traditional bounded rationality. The present paper constitutes a modification of the game introduced by [40]. The aim of this work is to present the generalized-order bounded rationality method. The Cournot duopoly games are more popular models describing the competition between firms and have been intensively studied in the literature. For this reason comes our contributions in this paper. We have adopted the generalized bounded rationality introduced in [40] to show that the chaotic behavior of such games persists under fractional bounded rationality for duopoly games. In addition, our proposed model can extend some models in the literature [7]. We investigate Cournot duopoly game based on fractional marginal profit. Our proposed game is described by generalized bounded rationality decisional learning and different marginal costs.

The paper is arranged as follows: We discuss Cournot duopoly game with generalized bounded rationality in Section 2. Section 3 analyzes the equilibrium point's stability. We have also performed numerical simulation to illustrate

complex dynamics, bifurcations, and chaos of the game in Section 4, and the arrived results are discussed in Section 5.

2. Model

We assume that there are two players, named $i = 1$ and 2 , producing the same products to be purchased in the market. Creation choices of the two firms happen at discrete time periods $t = 0, 1, 2, \dots$. We consider linear demand function in the market as follows:

$$p_t = f(Q_t) = a - bQ_t, \quad (1)$$

where $q_{i,t}$ is the quantity of firm i and a and b are non-negative parameters. Also, $Q_t = q_1(t) + q_2(t)$ is the total quantity in the market. We assume that the cost function in the linear form is

$$C_i(q_{i,t}) = c_i q_{i,t}, \quad i = 1, 2, \quad (2)$$

where the marginal costs are the positive parameters c_i . Hence, the profit of the firm i has the following form:

$$\Pi_{i,t}(q_{1,t}, q_{2,t}) = q_{i,t} (a - b(q_{i,t} + q_{j,t})) - c_i q_{i,t}, \quad i = 1, 2, \quad (3)$$

Equation (3) can be given as follows:

$$\Pi_{i,t}(q_{1,t}, q_{2,t}) = (a - c_i)q_{i,t} - bq_{i,t}^2 - bq_{i,t}q_{j,t}, \quad i, j = 1, 2 \quad i \neq j, \quad (4)$$

and the marginal profit of the firm i is

$$\Phi_i = \frac{\partial \Pi_{i,t}}{\partial q_{i,t}} = a - c_i - 2bq_{i,t} - bq_{j,t}, \quad i, j = 1, 2 \quad i \neq j. \quad (5)$$

Information in the game generally is deficient, so firms may utilize more complex strategies, for example, bounded rationality method. Firms with bounded rationality do not have the total information of the game; thus, the settling yield choices depend on a local estimate of the marginal profit $\partial \Pi_{i,t} / \partial q_{i,t}$. A firm, at each time period t , plans to increase its quantity produced $q_{i,t}$ at the period $(t + 1)$ if it has a positive marginal profit or decreases its quantity produced at the period $(t + 1)$ if the marginal profit is negative. When companies make use of this type of adjustments, they are to be rational players and the two-dimensional structure that defines the dynamics of the game's economic model is formed as follows:

$$\begin{cases} q_{1,t+1} = q_{1,t} + k(q_{1,t}) \frac{\partial \Pi_{1,t}(q_{1,t}, q_{2,t})}{\partial q_{1,t}}, \\ q_{2,t+1} = q_{2,t} + k(q_{2,t}) \frac{\partial \Pi_{2,t}(q_{1,t}, q_{2,t})}{\partial q_{2,t}}, \end{cases} \quad (6)$$

where $q_{i,t+1}$ is the quantity output of i th firm at time $(t + 1)$ and k represents a speed adjustment function. In the next section, we will discuss the fractional mechanism of the marginal profit.

2.1. Fractional-Order Marginal Profit. The generalized bounded rationality introduced here is a generalization of the traditional bounded rationality [7]. As we mentioned before, our aim of this work is to analyze the effect of fractional marginal profit in a duopoly game. To do so, we can write (5) as follows:

$$\begin{aligned} \frac{\partial^\beta \Pi_{i,t}(q_{1,t}, q_{2,t})}{\partial q_{i,t}^\beta} &= (a - c_i) \frac{\partial^\beta(q_{i,t})}{\partial q_{i,t}^\beta} - b \frac{\partial^\beta(q_{i,t}^2)}{\partial q_{i,t}^\beta} \\ &\quad - bq_{j,t} \frac{\partial^\beta(q_{i,t})}{\partial q_{i,t}^\beta}, \quad i, j = 1, 2, i \neq j. \end{aligned} \quad (7)$$

To differentiate (6) where β is a fractional and $0 < \beta < 1$, we will use the following definition.

Definition 1. For $\beta \in \mathbb{R}^+$, let n be the nearest integer greater than β ; the Caputo fractional derivative of order $\beta > 0$ with $n - 1 < \beta < n$ of the power function $f(t) = t^p$ for $p \geq 0$ and $t > 0$ is given by

$$D^\beta t^p = \frac{\Gamma(p+1)}{\Gamma(p-\beta+1)} t^{p-\beta}, \quad (8)$$

where Γ is Euler's Gamma function. One can use the book Fractional Calculus such as Miller and Ross [41] for more information about fractional derivatives.

Consequently and using this definition, (6) is rewritten as follows:

$$\begin{aligned} \frac{\partial^\beta \Pi_{i,t}(q_{1,t}, q_{2,t})}{\partial q_{i,t}^\beta} &= \frac{(a - c_i)}{\Gamma(2-\beta)} q_{i,t}^{1-\beta} - \frac{bq_{j,t}}{\Gamma(2-\beta)} q_{i,t}^{1-\beta} \\ &\quad - \frac{2b}{\Gamma(3-\beta)} q_{i,t}^{2-\beta}, \quad i, j = 1, 2, i \neq j. \end{aligned} \quad (9)$$

However, to increase the profit, both firms adopt gradient mechanism in which the duopolistic changes the quantity produced based on the direction of variation of profit, the same direction in case of positive variation and opposite direction in case of negative variation.

The fractional-order marginal profit method presented here is a generalization of the classical one. It thinks about the nearness of a memory of purchasers about the past costs of the generation. The customary limited objectivity can be utilized as a part of instance of all purchasers has aggregate amnesia. Along these lines, fractional derivatives are proposed to expel amnesia and consider the impact of memory. This implies that request can rely upon changes that may happen in prices amid a limited interim of time. In addition, the parameter β representing memory decay is added to describe the degree of memory decay throughout the time interval. Now, the generalized bounded rationality (the adjustment mechanism) takes the following form:

$$q_{i,t+1} = q_{i,t} + k \frac{\partial^\beta \Pi_{i,t}(q_{1,t}, q_{2,t})}{\partial q_{i,t}^\beta}, \quad 0 < \beta \leq 1, k > 0. \quad (10)$$

For simplicity, we take a constant relation for speed of adjustment function, where k is the speed of adjustment. From (9) and (10), we get the following two-dimensional nonlinear difference equation:

$$\begin{aligned} q_{i,t+1} &= q_{i,t} + k \left[\frac{(a - c_i)}{\Gamma(2-\beta)} q_{i,t}^{1-\beta} - \frac{bq_{j,t}}{\Gamma(2-\beta)} q_{i,t}^{1-\beta} \right. \\ &\quad \left. - \frac{2b}{\Gamma(3-\beta)} q_{i,t}^{2-\beta} \right], \quad i, j = 1, 2, i \neq j. \end{aligned} \quad (11)$$

We will discuss the dynamics of the game (11) in the following sections.

3. Equilibrium and Stability

From (11), the duopoly dynamical system with generalized bounded rational firms has the following form:

$$\begin{cases} q_{1,t+1} = q_{1,t} + k \left\{ \frac{(a - c_1)}{\Gamma(2-\beta)} q_{1,t}^{1-\beta} - \frac{bq_{2,t}}{\Gamma(2-\beta)} q_{1,t}^{1-\beta} - \frac{2b}{\Gamma(3-\beta)} q_{1,t}^{2-\beta} \right\}, \\ q_{2,t+1} = q_{2,t} + k \left\{ \frac{(a - c_2)}{\Gamma(2-\beta)} q_{2,t}^{1-\beta} - \frac{bq_{1,t}}{\Gamma(2-\beta)} q_{2,t}^{1-\beta} - \frac{2b}{\Gamma(3-\beta)} q_{2,t}^{2-\beta} \right\}. \end{cases} \quad (12)$$

In order to explore the behavior of game (12), can define the fixed points of (12) as the solution of the following system:

$$\begin{cases} \frac{(a - c_1)}{\Gamma(2-\beta)} q_{1,t}^{1-\beta} - \frac{bq_{2,t}}{\Gamma(2-\beta)} q_{1,t}^{1-\beta} - \frac{2b}{\Gamma(3-\beta)} q_{1,t}^{2-\beta} = 0, \\ \frac{(a - c_2)}{\Gamma(2-\beta)} q_{2,t}^{1-\beta} - \frac{bq_{1,t}}{\Gamma(2-\beta)} q_{2,t}^{1-\beta} - \frac{2b}{\Gamma(3-\beta)} q_{2,t}^{2-\beta} = 0. \end{cases} \quad (13)$$

which is given by setting $q_{1,t+1} = q_{1,t}$ and $q_{2,t+1} = q_{2,t}$ in (12). System (13) has four fixed points:

$$\begin{aligned} E_1 &(0, 0), \\ E_2 &\left(\frac{(2-\beta)(a - c_1)}{2b}, 0 \right), \\ E_3 &\left(0, \frac{(2-\beta)(a - c_2)}{2b} \right), \end{aligned} \quad (14)$$

and $E_*(q_1^*, q_2^*)$, where

$$\begin{aligned} q_1^* &= \frac{(2-\beta)\{(2-\beta)(a - c_2) - 2(a - c_1)\}}{b[\beta^2 - 4\beta]}, \\ q_2^* &= \frac{(2-\beta)\{(2-\beta)(a - c_1) - 2(a - c_2)\}}{b[\beta^2 - 4\beta]}, \end{aligned} \quad (15)$$

which depends on the game parameters. The equilibria E_1 , E_2 , and E_3 are called the boundary equilibria [7]. E_2 and E_3 are nonnegative when

$$a > c_i, \quad i = 1, 2. \quad (16)$$

The equilibrium point E_* is the unique interior equilibrium point and has economic meaning (has nonnegative components) when

$$\begin{aligned} a &> \frac{2c_1 - (2 - \beta)c_2}{\beta}, \\ a &> \frac{2c_2 - (2 - \beta)c_1}{\beta}, \\ a &> c_i, \quad i = 1, 2, 0 < \beta < 1. \end{aligned} \quad (17)$$

In order to study the stability of the fixed points, we have to compute the Jacobian matrix of game (12) which is written as follows:

$$J(q_1, q_2) = \begin{bmatrix} \ell_{11} & \ell_{12} \\ \ell_{21} & \ell_{22} \end{bmatrix}, \quad (18)$$

where

$$\begin{aligned} \ell_{11} &= 1 + k \left[\frac{(a - c_1)}{\Gamma(1 - \beta)} q_1^{-\beta} - \frac{bq_2}{\Gamma(1 - \beta)} q_1^{-\beta} - \frac{2b}{\Gamma(2 - \beta)} q_1^{1 - \beta} \right], \\ \ell_{12} &= \frac{-kb}{\Gamma(2 - \beta)} q_1^{1 - \beta}, \\ \ell_{21} &= \frac{-kb}{\Gamma(2 - \beta)} q_2^{1 - \beta}, \text{ and} \\ \ell_{22} &= 1 + k \left[\frac{(a - c_2)}{\Gamma(1 - \beta)} q_2^{-\beta} - \frac{bq_1}{\Gamma(1 - \beta)} q_2^{-\beta} - \frac{2b}{\Gamma(2 - \beta)} q_2^{1 - \beta} \right]. \end{aligned} \quad (19)$$

The trivial equilibrium $E_1(0, 0)$ has no practical significance (no economic implications) because both the outputs of two firms are zero, so we exclude it from the analysis. The stability of equilibrium points E_2 , E_3 , and E_* will be determined by the eigenvalues of the Jacobian matrix computed at the corresponding equilibrium points.

Proposition 2. *The boundary equilibrium point $E_2(((2 - \beta)(a - c_1)/2b), 0)$ of game (12) is stable if $k < 2^{(1 - \beta)} (\Gamma(2 - \beta)/(a - c_1))((2 - \beta)(a - c_1)/b)^\beta$; otherwise, it is unstable.*

Proof. Jacobian matrix (18) at $E_2(((2 - \beta)(a - c_1)/2b), 0)$ reads

$$J(E_2) = \begin{bmatrix} \Omega_1 & \Omega_2 \\ 0 & 1 \end{bmatrix}, \quad (20)$$

where

$$\begin{aligned} \Omega_1 &= 1 - \frac{k(a - c_1)}{\Gamma(2 - \beta)} \left(\frac{(2 - \beta)(a - c_1)}{2b} \right)^{-\beta}, \\ \Omega_2 &= \frac{kb}{\Gamma(2 - \beta)} \left(\frac{(2 - \beta)(a - c_1)}{2b} \right)^{1 - \beta}. \end{aligned} \quad (21)$$

The trace of the $J(E_2)$ is given by

$$\text{Tr}J(E_2) = 2 - \frac{k(a - c_1)}{\Gamma(2 - \beta)} \left(\frac{(2 - \beta)(a - c_1)}{2b} \right)^{-\beta}. \quad (22)$$

The determinant of the $J(E_2)$ is

$$\text{Det}J(E_2) = 1 - \frac{k(a - c_1)}{\Gamma(2 - \beta)} \left(\frac{(2 - \beta)(a - c_1)}{2b} \right)^{-\beta}. \quad (23)$$

Depending on the Jury conditions (Puu [42]), the E_2 is stable if and only if

$$\begin{aligned} 1 - \text{Tr}J(E_2) + \text{Det}J(E_2) &> 0, \\ 1 + \text{Tr}J(E_2) + \text{Det}J(E_2) &> 0, \\ 1 - |\text{Det}J(E_2)| &> 0. \end{aligned} \quad (24)$$

Substituting $\text{Tr}J(E_2)$ and $\text{Det}J(E_2)$ into the above inequalities, the first and third conditions are satisfied. The second conditions becomes

$$2 - \frac{k(a - c_1)}{\Gamma(2 - \beta)} \left(\frac{(2 - \beta)(a - c_1)}{2b} \right)^{-\beta} > 0. \quad (25)$$

Therefore, the equilibrium point E_2 is stable under the following condition:

$$k < 2^{(1 - \beta)} \frac{\Gamma(2 - \beta)}{(a - c_1)} \left(\frac{(2 - \beta)(a - c_1)}{b} \right)^\beta. \quad (26)$$

This completes the proof.

By a similar argument as the proof of Proposition 2, we can prove the following proposition.

Proposition 4. *The boundary equilibrium point $E_3(0, ((2 - \beta)(a - c_2)/2b))$ of game (12) is stable if $k < 2^{(1 - \beta)} (\Gamma(2 - \beta)/(a - c_2))((2 - \beta)(a - c_2)/b)^\beta$; otherwise, it is unstable.*

Now, we discuss the local stability of the interior equilibrium point $E_*(q_1^*, q_2^*)$, linearizing game (12) at E_* . We can easily get its Jacobian matrix as follows:

$$J(E_*) = \begin{bmatrix} v_{11} & v_{12} \\ v_{21} & v_{22} \end{bmatrix}, \quad (27)$$

where

$$\begin{aligned} v_{11} &= 1 + k \left[\frac{(a - c_1)}{\Gamma(1 - \beta)} q_1^{*(-\beta)} - \frac{bq_2^*}{\Gamma(1 - \beta)} q_1^{*(-\beta)} - \frac{2b}{\Gamma(2 - \beta)} q_1^{*(1 - \beta)} \right], \\ v_{12} &= \frac{-kb}{\Gamma(2 - \beta)} q_1^{*(1 - \beta)}, \\ v_{21} &= \frac{-kb}{\Gamma(2 - \beta)} q_2^{*(1 - \beta)}, \\ v_{22} &= 1 + k \left[\frac{(a - c_2)}{\Gamma(1 - \beta)} q_2^{*(-\beta)} - \frac{bq_1^*}{\Gamma(1 - \beta)} q_2^{*(-\beta)} - \frac{2b}{\Gamma(2 - \beta)} q_2^{*(1 - \beta)} \right], \end{aligned} \quad (28)$$

where q_1^* and q_2^* are defined in (14).

The characteristics equation of $J(E_*)$ is given by

$$P(\lambda) = \lambda^2 - \text{Tra}(J(E_*))\lambda + \text{Det}(J(E_*)) = 0, \quad (29)$$

where $\text{Tra}(J(E_*))$ and $\text{Det}(J(E_*))$ are the trace and determinant of the Jacobian matrix, respectively:

$$\begin{aligned} \text{Tra}(J(E_*)) &= 2 + k \left[\frac{(a-c_1)}{\Gamma(1-\beta)} q_1^{*(-\beta)} - \frac{bq_2^*}{\Gamma(1-\beta)} q_1^{*(-\beta)} - \frac{2b}{\Gamma(2-\beta)} q_1^{*(1-\beta)} \right] + k \left[\frac{(a-c_2)}{\Gamma(1-\beta)} q_2^{*(-\beta)} - \frac{bq_1^*}{\Gamma(1-\beta)} q_2^{*(-\beta)} - \frac{2b}{\Gamma(2-\beta)} q_2^{*(1-\beta)} \right], \\ \text{Det}(J(E_*)) &= \left[1 + k \left[\frac{(a-c_1)}{\Gamma(1-\beta)} q_1^{*(-\beta)} - \frac{bq_2^*}{\Gamma(1-\beta)} q_1^{*(-\beta)} - \frac{2b}{\Gamma(2-\beta)} q_1^{*(1-\beta)} \right] \right] \times \left[1 + k \left[\frac{(a-c_2)}{\Gamma(1-\beta)} q_2^{*(-\beta)} - \frac{bq_1^*}{\Gamma(1-\beta)} q_2^{*(-\beta)} - \frac{2b}{\Gamma(2-\beta)} q_2^{*(1-\beta)} \right] \right] \\ &\quad - \frac{k^2 b^2}{(\Gamma(2-\beta))^2} q_1^{*(1-\beta)} q_2^{*(1-\beta)}. \end{aligned} \quad (30)$$

The roots of characteristic equation (19) are inside the unit disk when Jury's conditions (Puu [42]) are satisfied. Then, the interior equilibrium point E_* is asymptotically stable if and only if

$$\begin{cases} 1 + \text{Tra}(J(E_*)) + \text{Det}(J(E_*)) > 0, \\ 1 - \text{Tra}(J(E_*)) + \text{Det}(J(E_*)) > 0, \\ 1 - \text{Det}(J(E_*)) > 0. \end{cases} \quad (31)$$

By using the equations in (20), the stability conditions become

$$\begin{cases} 3 + k(u_1 - u_2 - u_3) + k(u_4 - u_5 - u_6) + [1 + k(u_1 - u_2 - u_3)][1 + k(u_4 - u_5 - u_6)] - u_7 > 0, \\ -1 - k(u_1 - u_2 - u_3) - k(u_4 - u_5 - u_6) + [1 + k(u_1 - u_2 - u_3)][1 + k(u_4 - u_5 - u_6)] - u_7 > 0, \\ 1 - [1 + k(u_1 - u_2 - u_3)][1 + k(u_4 - u_5 - u_6)] + u_7 > 0, \end{cases} \quad (32)$$

where

$$\begin{aligned} u_1 &= \frac{(a-c_1)}{\Gamma(1-\beta)} q_1^{*(-\beta)}, \\ u_2 &= \frac{bq_2^*}{\Gamma(1-\beta)} q_1^{*(-\beta)}, \\ u_3 &= \frac{2b}{\Gamma(2-\beta)} q_1^{*(1-\beta)}, \\ u_4 &= \frac{(a-c_2)}{\Gamma(1-\beta)} q_2^{*(-\beta)}, \\ u_5 &= \frac{bq_1^*}{\Gamma(1-\beta)} q_2^{*(-\beta)}, \\ u_6 &= \frac{2b}{\Gamma(2-\beta)} q_2^{*(1-\beta)}, \\ u_7 &= \frac{k^2 b^2}{(\Gamma(2-\beta))^2} q_1^{*(1-\beta)} q_2^{*(1-\beta)}. \end{aligned} \quad (33)$$

The second and third conditions of (23) are explicitly always met, while the first condition is violated. Hence, the interior equilibrium point E_* is locally stable if and only if

$$k(u_4 - u_5 - u_6) < \frac{4 + k(2u_1 - 2u_2 - 2u_3 + u_4 - u_5 - u_6) - u_7}{-1 - k(u_1 - u_2 - u_3)}. \quad (34)$$

4. Numerical Simulation

Currently, some numerical simulations are performed to have more insights into the stability of our game (12) and confirm the results obtained above. Such simulations contain bifurcation diagrams, phase portrait, and the maximal Lyapunov exponents (MLEs), to further investigate the unpredictable behavior of the game. We will study the impact of the game parameters on dynamics of game (12), the speed of adjustment parameter k , the generalized bounded rationality parameter β , and the maximum price in the market a , and these are discussed in the following.

More specifically, we illustrate the stabilizing effect of the generalized bounded rationality on the dynamics of game (12). To study this effect, we choose the fractional parameter $0 < \beta < 1$ and parameter k as bifurcation parameters (varied parameters) and other game parameters as fixed parameters, otherwise stated. Let us take the parameters by the following values $a = 6$, $b = 0.3$, $c_1 = 0.2$, $c_2 = 0.3$, and $\beta = 0.9$. The initial state of game (12) is $(0.3, 0.5)$. Figure 1(a) shows the bifurcation diagram of game (12) with respect to k ; it is clear that the equilibrium points become locally stable when the

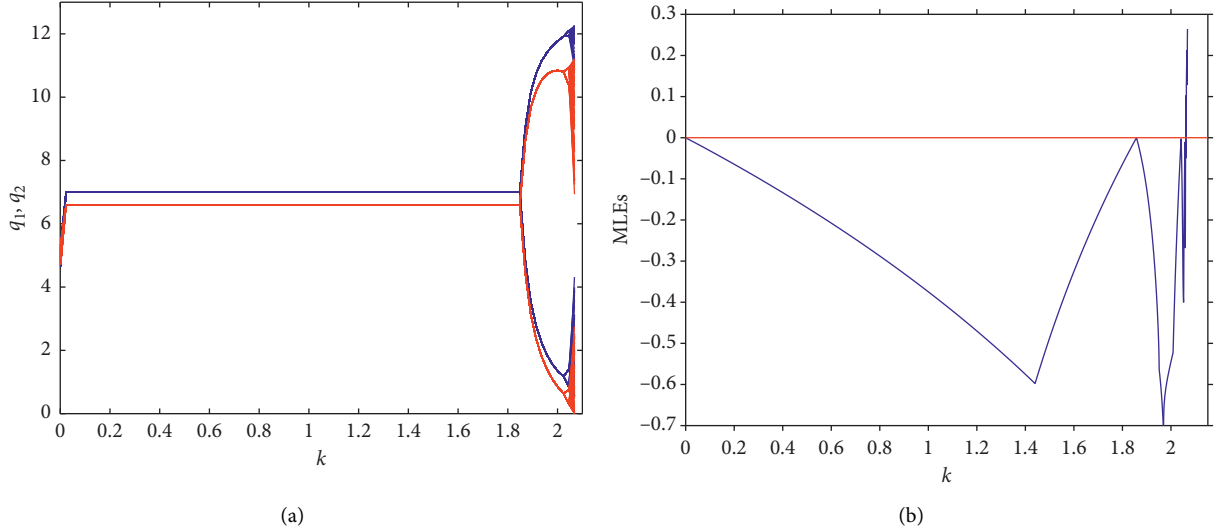


FIGURE 1: Bifurcation diagram and MLEs for game (12) with respect to control parameter k at $a = 6$, $b = 0.3$, $c_1 = 0.2$, $c_2 = 0.3$, and $\beta = 0.9$.

parameter approaches $k = 1.8$ where the appearance of period-doubling bifurcation exists. Therefore, any increase above this point makes the system enter the chaotic region. It is known that the positive Lyapunov exponent is a good indicator for chaos. The corresponding maximal Lyapunov exponents are plotted in Figure 1(b). Obviously, the period-doubling bifurcation arises as k reaches the value of $k = 1.8$. After that, the Nash equilibrium point loses its stability as k increases.

A strange attractor can be seen in Figure 2, when the dynamics of the game becomes very complicated. Bifurcation diagram of game (12) as a function of k , with $a = 6$, $b = 0.3$, $c_1 = 0.2$, $c_2 = 0.3$, and $\beta = 0.6$, is displayed in Figure 3(a). The MLEs plot corresponding to Figure 3(a) of game (12) is shown in Figure 3(b). We see that the interior equilibrium changes from stable to unstable and loses its stability via flip bifurcation. Consequently, game (12) shows irregular and unpredictable behaviors in the interval $k \in (1.3, 1.45)$. We find a rise in change speed k playing a destabilizing role. When $k = 1.45$, the phase portrait is displayed in Figure 4.

We have chosen values for the parameter β close to 1 in Figure 1(a) (which means the memory adopted by buyers is close to the current state of the market where traditional bounded rationality may be used). It is also clear that the interval of stability is better than that when we use values of memory far from the current state of the market as shown in Figure 3(a), where we take $\beta = 0.6$.

The bifurcation diagrams and associated MLEs graphs for two different values of β are given in Figures 5(a) and 5(b) and Figures 6(a) and 6(b), respectively. The bifurcation diagram of game (12) is shown in Figure 5(a) at $\beta = 0.5$, and the corresponding maximal Lyapunov exponents are plotted in Figure 5(b). Also, a bifurcation diagram of game (12) with respect to k is given in Figure 6(a) at $\beta = 0.2$, and the corresponding maximal Lyapunov exponents are plotted in Figure 6(b). The bifurcation diagrams show that increasing values of the parameter k may destabilize the

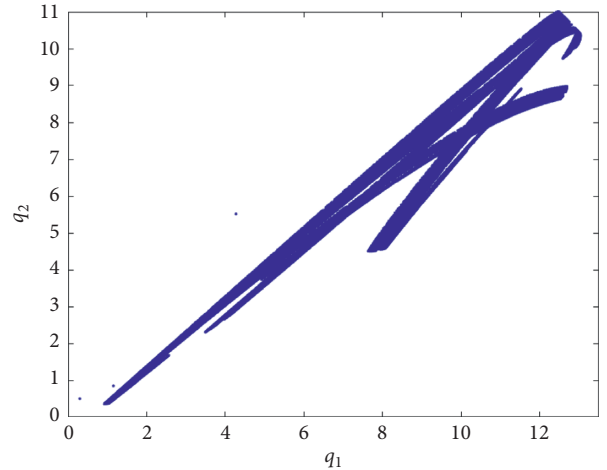


FIGURE 2: Strange attractor of the chaotic state of duopoly game (12), with the parameter values $a = 6$, $b = 0.3$, $c_1 = 0.2$, $c_2 = 0.3$, $\beta = 0.9$, and $k = 2.1$.

interior equilibrium point through flip bifurcation. This means as k goes far from the current state of the market, the equilibrium point becomes unstable, and then, we claim that the memory effect of parameter should be in a range close to 1 where traditional bounded rationality may be used. After the occurrence of the bifurcation, period doubling exists and describes the long-run behavior of the game. Chaotic attractors exist after the accumulation of a period-doubling cascade; i.e., the dynamics of the game will become more and more confused. It is observed from Figures 1–6 that increasing the parameter k and fixing the generalized-order bounded rationality parameter a destabilize game (12) and chaotic behavior occurs. It is shown that game (12) is stabilized only for a relatively small value of the parameter k . A faster adjustment speed is disadvantageous for the game to keeping the stability of game (12).

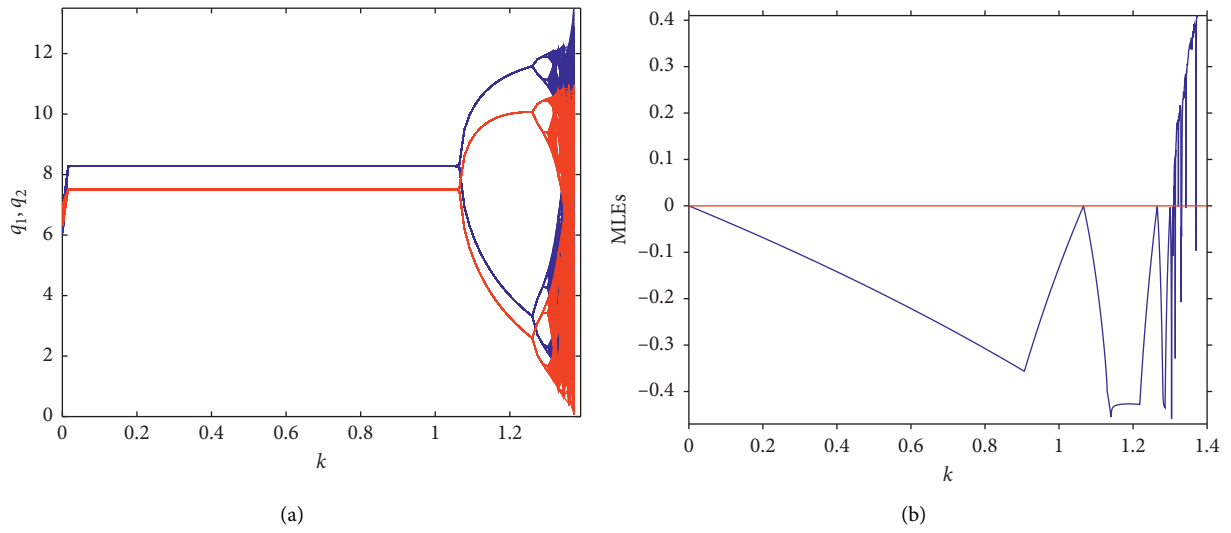


FIGURE 3: Bifurcation diagram and MLEs for game (12) with respect to control parameter k at $a = 6$, $b = 0.3$, $c_1 = 0.2$, $c_2 = 0.3$, and $\beta = 0.6$.

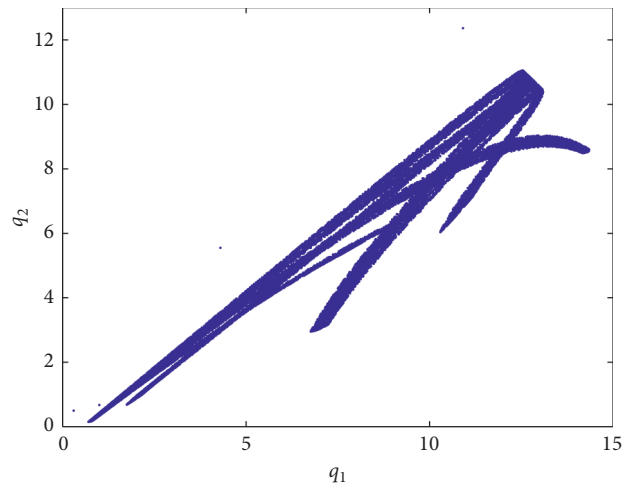


FIGURE 4: Phase portraits of the chaotic attractor of game (12) are shown using parameters values $a = 6$, $b = 0.3$, $c_1 = 0.2$, $c_2 = 0.3$, $\beta = 0.6$, and $k = 1.4$.

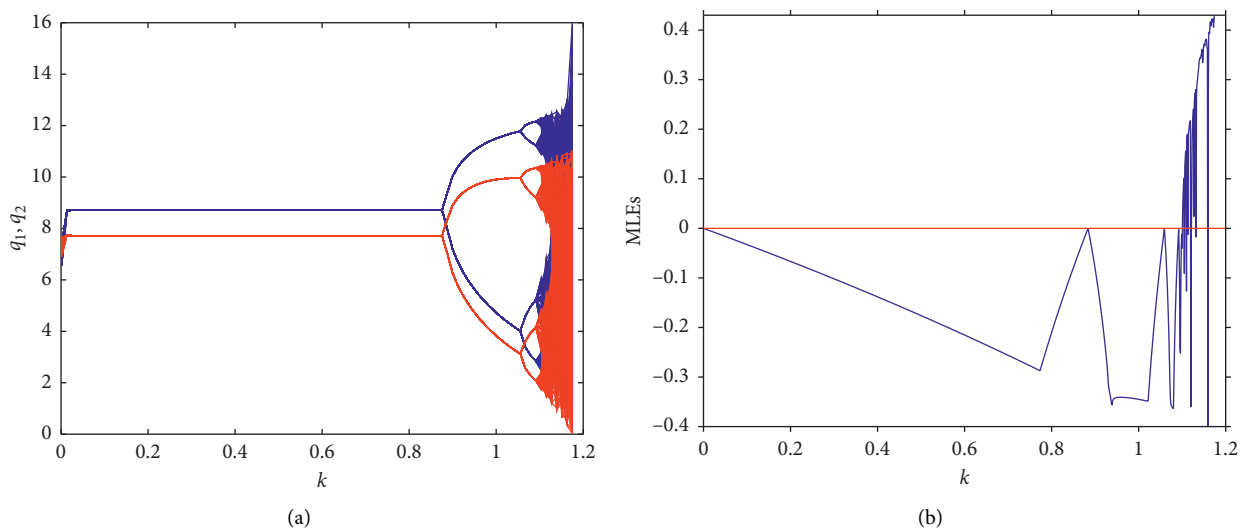


FIGURE 5: Bifurcation diagram and MLEs for game (12) as a function of k at $a = 6$, $b = 0.3$, $c_1 = 0.2$, $c_2 = 0.3$, and $\beta = 0.5$.

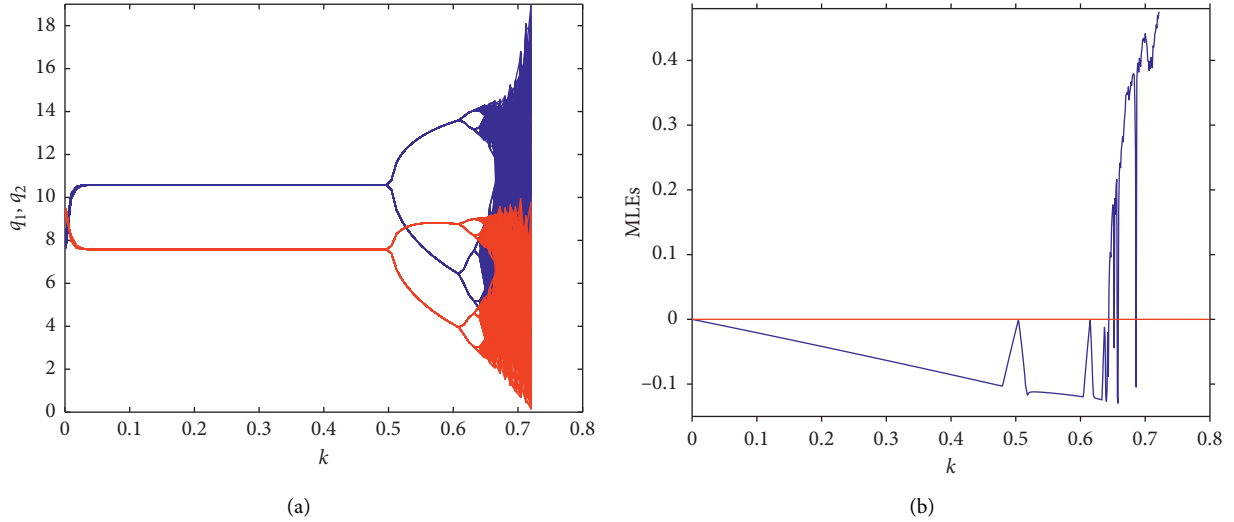


FIGURE 6: The bifurcation diagram and MLEs for game (12) with respect to control parameter k at $a = 6$, $b = 0.3$, $c_1 = 0.2$, $c_2 = 0.3$, and $\beta = 0.2$.

In Figure 7, we illustrate the impact of the parameter a on the dynamics of game (12). One can deduce that the interior equilibrium changes from stable to unstable, leading to increasingly complex attractors as a increases. From the above analysis, a high level of the speed of adjustment k and the maximum price in the market a lead to instability of the game.

4.1. Effect of the Generalized Bounded Rationality Method on the Dynamics of the Game. To study the effect of the generalized bounded rationality method on the dynamics of game (12), under variations of the parameter β , we will analyze the dynamics of game (12). We have plotted the bifurcation diagrams of game (12) with respect to the parameter β for different values of the parameter k . The bifurcation diagram as a function of β when $a = 6$, $b = 0.3$, $c_1 = 0.2$, $c_2 = 0.3$, and $k = 0.6$ is displayed in Figure 8. As can be seen in Figure 8, game (12) loses insatiability and enters the stability region with increase of β .

The bifurcation diagram of game (12) with respect to β , with $a = 6$, $b = 0.3$, $c_1 = 0.2$, $c_2 = 0.3$, and $k = 0.9$, is given in Figure 9. It is observed that the size of chaotic attractor, or in other words, the amplitude of chaotic fluctuation in quantity outputs, decreases as β increases. When the parameter has values $a = 6$, $b = 0.3$, $c_1 = 0.2$, $c_2 = 0.3$, and $k = 1.2$, the bifurcation diagram as a function of β is plotted in Figure 10. This bifurcation diagram describes that bifurcation of the backward flip occurs at $\beta = 0.65$ from the interior equilibrium point. It demonstrates that firms have a better chance of achieving the equilibrium point with an increase of β with various adjustment speed values. Therefore, it can be observed that the stability chance of interior equilibrium point when $\beta < 0.65$ is less than the one for $\beta > 0.65$ and that there is an optimal value corresponding to the most probability of stability in certain cases for $\beta \in (0.65, 1)$. Thus, it is shown that the generalized bounded rationality parameter β has an effect on the dynamics of the game. The stabilization can be

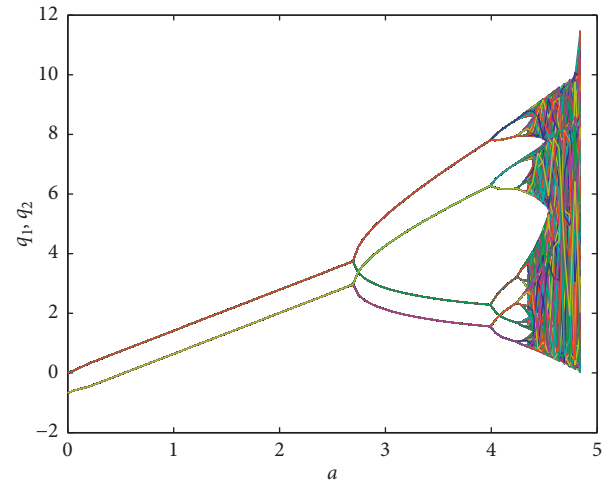


FIGURE 7: Bifurcation diagrams for game (12) as a function of a obtained at $b = 0.3$, $c_1 = 0.2$, $c_2 = 0.3$, $k = 1.5$, and $\beta = 0.5$.

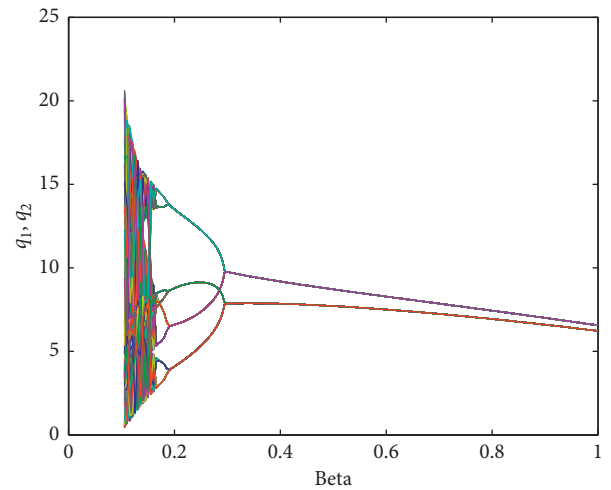


FIGURE 8: Bifurcation diagram for game (12) as a function of control parameter β when $k = 0.6$.

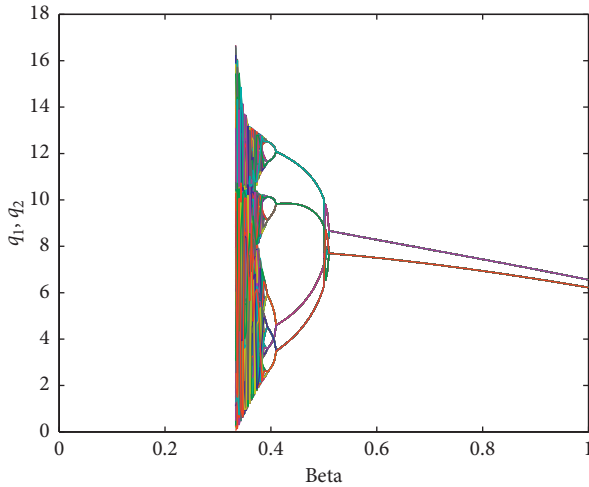


FIGURE 9: Bifurcation diagram for game (12) as a function of control parameter β when $k = 0.9$.

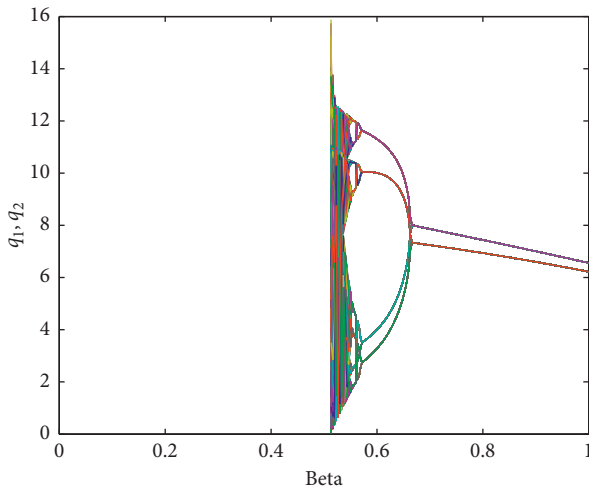


FIGURE 10: Bifurcation diagram for game (12) as a function of control parameter β when $k = 1.2$.

achieved if the generalized bounded rationality parameter takes values close to 1 where traditional bounded rationality may be used.

5. Conclusion

This paper has presented Cournot duopoly game based on generalized bounded rationality. The generalized bounded rationality method has been presented to study the dynamics of the Cournot duopoly game. The Cournot duopoly game with the fractional marginal profit approach has been analyzed on the stability of equilibria, bifurcation, and chaotic behaviors. Our motivation is to show the effect of buyer's memory when it becomes close to the current state of the market. The numerical results have investigated the dynamic behavior of duopoly game with generalized bounded rationality for different values of the memory parameter β . The basic properties of the game have been analyzed by meaning of bifurcation diagrams, the maximal Lyapunov exponents,

and phase portraits. Memory is a key economic factor. The effect of the generalized bounded rationality method has shown that it has a stabilizing effect on the dynamics of the game. This stabilization can be achieved if generalized bounded rationality parameter β takes values close to 1 where traditional bounded rationality may be used. Our obtained results have given interesting results regarding the memory effect on the game stabilization.

Data Availability

No data were used to support this study.

Conflicts of Interest

The author declares that they have no conflicts of interest.

Acknowledgments

The author would like to extend his sincere appreciation to the Deanship of Scientific Research at King Saud University for funding the research group no. RG-1438-046.


References

- [1] A. Cournot, *Researches into the Mathematical Principles of the Theory of Wealth*, Macmillan, New York, NY, USA, 1897.
- [2] D. Furth, "Stability and instability in oligopoly," *Journal of Economic Theory*, vol. 40, no. 2, pp. 197–228, 1986.
- [3] R.-A. Dana and L. Montrucchio, "Dynamic complexity in duopoly games," *Journal of Economic Theory*, vol. 40, no. 1, pp. 40–56, 1986.
- [4] T. Puu, "Complex dynamics with three oligopolists," *Chaos Solitons Fractals*, vol. 12, pp. 207–581, 1996.
- [5] T. Puu, "On the stability of Cournot equilibrium when the number of competitors increases," *Journal of Economic Behavior & Organization*, vol. 66, pp. 445–456, 2007.
- [6] L. C. Corchon and A. Mas-Colell, "On the stability of best reply and gradient systems with applications to imperfectly competitive models," *Economics Letters*, vol. 51, no. 1, pp. 59–65, 1996.
- [7] G. Bischi and A. Naimzada, "Global analysis of a duopoly game with bounded rationality," *Advance Dynamic Games and Applications*, vol. 5, pp. 361–385, 1999.
- [8] H. N. Agiza and A. A. Elsadany, "Chaotic dynamics in nonlinear duopoly game with heterogeneous players," *Applied Mathematics and Computation*, vol. 149, no. 3, pp. 843–860, 2004.
- [9] T. Dubiel-Teleszynski, "Nonlinear dynamics in a heterogeneous duopoly game with adjusting players and diseconomies of scale," *Communications in Nonlinear Science and Numerical Simulation*, vol. 16, no. 1, pp. 296–308, 2011.
- [10] Z. Sun and J. Ma, "Complexity of triopoly price game in Chinese cold rolled steel market," *Nonlinear Dynamics*, vol. 67, no. 3, pp. 2001–2008, 2012.
- [11] G. I. Bischi, C. Chiarella, M. Kopel, and F. Szidarovszky, *Nonlinear Oligopolies: Stability and Bifurcations*, Springer, Berlin, Germany, 2009.
- [12] M. Bai and Y. Gao, "Chaos control on a duopoly game with homogeneous strategy," *Discrete Dynamics in Nature and Society*, vol. 2016, Article ID 7418252, 7 pages, 2016.

- [13] S. S. Askar, A. M. Alshamrani, and K. Alnowibet, "The arising of cooperation in cournot duopoly games," *Applied Mathematics and Computation*, vol. 273, pp. 535–542, 2016.
- [14] C. Hommes, *Behavioral Rationality and Heterogeneous Expectations in Complex Economic Systems*, Cambridge University Press, Cambridge, UK, 2013.
- [15] F. Tramontana, "Heterogeneous duopoly with isoelastic demand function," *Economic Modelling*, vol. 27, no. 1, pp. 350–357, 2010.
- [16] L. Fanti and L. Gori, "The dynamics of a differentiated duopoly with quantity competition," *Economic Modelling*, vol. 29, no. 2, pp. 421–427, 2012.
- [17] G. Sarafopoulos, "On the dynamics of a duopoly game with differentiated goods," *Procedia Economics and Finance*, vol. 19, pp. 146–153, 2015.
- [18] S. S. Askar and A. Al-khedhairi, "Analysis of nonlinear duopoly games with product differentiation: stability, global dynamics, and control," *Discrete Dynamics in Nature and Society*, vol. 2017, Article ID 2585708, 13 pages, 2017.
- [19] F. Tramontana and A. E. A. Elsadany, "Heterogeneous triopoly game with isoelastic demand function," *Nonlinear Dynamics*, vol. 68, no. 1-2, pp. 187–193, 2012.
- [20] J. L. G. a. Guirao, M. Lampart, and G. H. Zhang, "On the dynamics of a 4D local Cournot model," *Applied Mathematics & Information Sciences*, vol. 7, no. 3, pp. 857–865, 2013.
- [21] J.-g. Du, Y.-q. Fan, Z.-h. Sheng, and Y.-z. Hou, "Dynamics analysis and chaos control of a duopoly game with heterogeneous players and output limiter," *Economic Modelling*, vol. 33, pp. 507–516, 2013.
- [22] J. Ma and Z. Guo, "The parameter basin and complex of dynamic game with estimation and two-stage consideration," *Applied Mathematics and Computation*, vol. 248, pp. 131–142, 2014.
- [23] L. Zhao and J. Zhang, "Analysis of a duopoly game with heterogeneous players participating in carbon emission trading," *Nonlinear Analysis: Modelling and Control*, vol. 19, no. 1, pp. 118–131, 2014.
- [24] W. Yu and Y. Yu, "The complexion of dynamic duopoly game with horizontal differentiated products," *Economic Modelling*, vol. 41, pp. 289–297, 2014.
- [25] H. N. Agiza, A. A. Elsadany, and M. M. El-Dessoky, "On a new Cournot duopoly game," *Jason Chaos*, vol. 5, p. 487803, 2013.
- [26] L. Fanti, "The dynamics of a banking duopoly with capital regulations," *Economic Modelling*, vol. 37, pp. 340–349, 2014.
- [27] A. A. Elsadany and A. E. Matouk, "Dynamic Cournot duopoly game with delay," *Journal of Complex Systems*, vol. 2014, pp. 384843–7, 2014.
- [28] A. A. Elsadany, "Dynamics of a Cournot duopoly game with bounded rationality based on relative profit maximization," *Applied Mathematics and Computation*, vol. 294, pp. 253–263, 2017.
- [29] L. Fanti, L. Gori, C. Mammana, and E. Michetti, "Local and global dynamics in a duopoly with price competition and market share delegation," *Chaos, Solitons & Fractals*, vol. 69, pp. 253–270, 2014.
- [30] L. Fanti, L. Gori, and M. Sodini, "Nonlinear dynamics in a Cournot duopoly with isoelastic demand," *Mathematics and Computers in Simulation*, vol. 108, pp. 129–143, 2015.
- [31] F. Cavalli, A. Naimzada, and F. Tramontana, "Nonlinear dynamics and global analysis of a heterogeneous Cournot duopoly with a local monopolistic approach versus a gradient rule with endogenous reactivity," *Communications in Nonlinear Science and Numerical Simulation*, vol. 23, no. 1-3, pp. 245–262, 2015.
- [32] Z. Ding, Q. Li, S. Jiang, and X. Wang, "Dynamics in a Cournot investment game with heterogeneous players," *Applied Mathematics and Computation*, vol. 256, pp. 939–950, 2015.
- [33] S. S. Askar and A. Al-khedhairi, "Cournot duopoly games: models and investigations," *Mathematics*, vol. 7, no. 11, p. 1079, 2019.
- [34] B. Tian, Y. Zhang, and J. Li, "Stochastic perturbations for a duopoly Stackelberg model," *Physica A: Statistical Mechanics and Its Applications*, vol. 545, p. 123792, 2019.
- [35] L. Zhao, J. Du, and Q. Wang, "Nonlinear analysis and chaos control of the complex dynamics of multi-market Cournot game with bounded rationality," *Mathematics and Computers in Simulation*, vol. 162, pp. 45–57, 2019.
- [36] Y. Peng, Q. Lu, Y. Xiao, and X. Wu, "Complex dynamics analysis for a remanufacturing duopoly model with nonlinear cost," *Physica A: Statistical Mechanics and Its Applications*, vol. 514, pp. 658–670, 2019.
- [37] L. Cerboni Baiardi and A. K. Naimzada, "An evolutionary Cournot oligopoly model with imitators and perfect foresight best responders," *Metroeconomica*, vol. 70, no. 3, pp. 458–475, 2019.
- [38] A. Al-khedhairi, "Dynamical analysis of fractional-order differentiated Cournot triopoly game," *Journal of Vibration and Control*, 2020.
- [39] S. S. Askar and A. Al-Khedhairi, "The dynamics of a business game: a 2D-piecewise smooth nonlinear map," *Physica A: Statistical Mechanics and Its Applications*, vol. 537, p. 122766, 2020.
- [40] S. S. Askar and M. Abouhawwash, "Quantity and price competition in a differentiated triopoly: static and dynamic investigations," *Nonlinear Dynamics*, vol. 91, no. 3, pp. 1963–1975, 2018.
- [41] R. Miller and B. Ross, *An Introduction to the Fractional Calculus and Fractional Differential Equations*, John Wiley & Sons, Hoboken, NJ, USA, 1993.
- [42] T. Puu, *Attractors, Bifurcations and Chaos: Nonlinear Phenomena in Economica*, Springer, Berlin, Germany, 2000.

Research Article

Decision-Making of Electronic Commerce Supply Chain considering EW Service

Yuyan Wang ¹, Zhaoqing Yu,¹ Liang Shen,² and Runjie Fan¹

¹School of Management Science and Engineering, Shandong University of Finance and Economics, Jinan, Shandong 250014, China

²School of Public Finance and Taxation, Shandong University of Finance and Economics, Jinan, Shandong 250014, China

Correspondence should be addressed to Yuyan Wang; wangyuyan1224@126.com

Received 25 February 2020; Revised 15 April 2020; Accepted 21 April 2020; Published 22 May 2020

Guest Editor: Baogui Xin

Copyright © 2020 Yuyan WANG et al. This is an open access article distributed under the Creative Commons Attribution License, which permits unrestricted use, distribution, and reproduction in any medium, provided the original work is properly cited.

With the rapid development of the network economy, it is a marketing strategy to provide an extended warranty (EW) service. Considering the differences in the EW service providers and dominant enterprises, this paper proposes four kinds of decision-making models and aims to study decisions of the electronic commerce supply chain, including EW price, sales price, and service level of e-platform. Through comparative analysis and numerical analysis, this research shows that, among four decision-making models, the highest system profit can be achieved when the seller provides the EW service and the e-platform dominates the system. For electronic commerce supply chain enterprises, whether to dominate the system or to provide EW service, it is conducive to the increase of profits. When the e-platform provides the EW service, the conclusion is that who dominates the system is the one who gets more profit. However, when the seller provides the EW service, the conclusion is that who dominates the system is the one who gets less profit. When the EW service is offered by the dominating enterprise, service levels of the e-platform are lower.

1. Introduction

With the development of the network economy, the electronic commerce supply chain (ECSC) has been greatly promoted and advanced. The ECSC focuses on core enterprises, integrates upstream and downstream resources, makes full use of the network technology, and ultimately achieves all-win results for supply chain participants [1, 2]. Besides, the ECSC not only improves the competitiveness of products but also solves problems in online shopping, such as excessive fakes, low transportation services, and slow after-sales processing. In the ECSC, sellers sell products with the aid of the e-commerce platform (e-platform) and consumers cannot physically contact products before receiving them. Therefore, many e-platforms and sellers have introduced an extended warranty (EW) service to alleviate consumer concerns, for example, *Home Security Service* of GOME (<http://help.gome.com.cn/question/5588.html>),

Sunshine Package for electrical appliances of SUNNING (http://issm.snisc.cn/articleDetail_A10632.htm), *Jingdong Service Steward* of JD (<http://fuwu.jd.com/service.html>), *Haier extended warranty service* of Haier (<http://www.ehaier.com/article.php?a=fixed&alias=warranty>), and *Apple Care Protection Plan* of Apple (<https://www.apple.com/legal/sales-support/applicare/countrylist.html>).

The EW service is a kind of insurance, similar to a contract that consumers can purchase to obtain opportunities for product repair after the time limit specified in the *three guarantees*. It is an optional contract that is offered by a retailer, a manufacturer, or an outsourcing service provider. The EW service provides customers with the opportunity to repair products at a low cost after the warranty period ends, which can effectively expand the product market and open up a new profit source. Many consumers would purchase EW service for home appliances, electronics, and automobiles. Statistics show that the penetration rate of EW service

in the United States has reached 35% and that of electronic products has exceeded 85% (the report is available at <http://www.315online.com/survey/331921.html>). As consumers' awareness of EW service has increased, market demand has gradually opened up, and EW service is a market with great potential.

EW service not only increases consumers' trust in products and brands but also contributes to profits for companies that provide EW service [3]. Currently, there are four main operation modes for EW service (the report is available at <https://36kr.com/coop/toutiao/5059989.html>): the retailer mode, where retail enterprises provide professional marketing for EW service; the manufacturer mode, which has technical advantages and high service quality; the third-party mode, which is professional but usually relies on retailers to sell; insurance company mode, with a high ability to bear and transfer risks, but rarely studied. With the development of the Internet economy, the ECSC has gradually developed and improved. The e-platforms have replaced the retail stores in the traditional supply chain and can independently sell EW service, especially large e-platforms, such as Tmall and Amazon. Therefore, two modes of EW service provided by the seller or the e-platform are studied in this research.

EW service is conducive to product sales [4, 5], and each node company in the supply chain is willing to provide EW service. In general, leading companies in the supply chain have greater power when making decisions. Therefore, the power structure of the supply chain has a certain impact on the EW service decision. In the network economy environment, the characteristics of online sales, especially the asymmetry of product information, lead to a deeper influence of the power structure on the EW strategy [6, 7]. Moreover, the ECSC is very different from the traditional supply chain, which causes the existing conclusions of traditional supply chains not applicable to the ECSC. The main differences between ECSCs and traditional supply chains are as follows.

Firstly, in the ECSC, e-platforms replace retail stores for product sales, but their operations are different from traditional retail stores. Manufacturers wholesale products to retail stores in traditional supply chains. Among them, the manufacturer decides the product's wholesale price and the retail store decides the retail price. However, in the ECSC, the seller directly sells products to consumers with the aid of the e-platform, which is a direct-sale model [8]. Therefore, the seller directly decides the retail price and the wholesale price to distribute profits is not involved. Also, the commission is an intermediate variable in the profit distribution between e-platforms and sellers to ensure e-platforms to provide sales services. Moreover, the commission rate is a specific percentage of the sales amount of the seller. This rate is set by the e-platform when the seller enters and is not determined based on the retail price of the product [9].

Secondly, the profit modes of sellers and e-platforms are different. The traditional retailer's unit product revenue depends on wholesale price and retail price, which depends on upstream sellers and downstream consumers. However, unit product revenue of the e-platform depends only on

upstream sellers. Therefore, in the ECSC model, the revenue of e-platform comes from the commission income and it does not involve direct unit product costs.

Finally, ECSCs and traditional supply chains are affected by different factors. In traditional supply chains, price is a major factor in sales. However, in the ECSC, the market demand for products is greatly affected by the sales service of the e-platform, including advertising promotion, return and exchange policies, and logistics services [10, 11].

At present, more and more ECSCs consisting of sellers and e-platforms are being formed and developed. In the ECSC, providing EW to alleviate consumers' concerns about product quality has become a popular sales strategy. Who is better to provide EW service? How does the power structure of ECSC affect EW? Existing research has not addressed these issues. Considering research gaps, four decision models are constructed and analyzed taking into account the differences in the power structure and EW providers in the ECSC.

This paper aims to address the following problems: what are the optimal decisions of the ECSC system when considering the EW service and the sales service of the e-platform; what is the influence of power structure and different EW service providers on the optimal decisions; what is the comparative relationship of optimal decisions in different decision models; how do enterprises provide the EW service, and whether should they provide the EW service when they dominate ECSC? With these problems in mind, the conclusions intend to provide the managerial insights for the operation of enterprises in the ECSC.

The rest of the paper is organized as follows. Section 2 discusses the related literature. Section 3 provides the model illustration and assumptions. Section 4 presents model analysis of EW being provided by the seller or the e-platform. The decisions of the four models are compared and analyzed in Section 5. Section 6 consists of the numerical analysis. Section 7 presents the conclusion.

2. Literature Review

EW service has been recognized and developed rapidly in the economic market, which has also been discussed in many kinds of literature. These studies include the following three streams.

The first stream focuses on the pricing and cost of EW in supply chains. Considering the cost of EW, Chen et al. [12] analyzed how different pricing strategies affect supply chain decisions and profits. Bouguerra et al. [13] studied the maximum payment for consumers and the minimum price for manufacturers to sell EW service. Given EW costs, Shahanaghi et al. [14] designed an EW mechanism and proposed the best operation strategy. Wu and Longhurst [15] and Jung et al. [16] analyzed the cost of EW from the perspective of consumers. Considering the dynamic change of the company's long-term EW price with the learning ability of consumers, Lei et al. [17] explored the impact of EW pricing on corporate earnings. Chen et al. [18] proposed the optimal production cycle and product pricing strategy considering the EW period. Bian et al. [19] compared

traditional EW and old-to-new EW and explored the optimal sales price for different EW modes. Based on the hypothesis of bounded rational, Zhao et al. [20] analyzed the impact of vertical competition and fair concerns on the pricing of EW.

The second stream focuses on the provider of EW in supply chains. In a two-tier duopoly supply chain system with EW provided by the retailer, Ma et al. [21] explored the decision of EW periods under supply chain competition. Also, considering that EW is provided by retailers, Zhang et al. [22] investigated the impact of EW costs on retailers' decisions. Li et al. [23] explored the impact of EW providers on decisions in the supply chain. From the perspective of the manufacturer, Su and Wang [24] and Huang et al. [25] presented a preventive maintenance strategy to reduce the cost of EW. Ashayeri et al. [26] proposed a nonconvex mixed-integer programming model and designed a closed-loop distribution network with EW provided by outsourcers.

The third stream focuses on the operation strategy of EW in the supply chain. Heese [27] constructed a supply chain for two manufacturers and one retailer who provided EW and studied the optimal EW strategy for manufacturers and the retailer. Su and Shen [28] considered three repair options for failed components and proposed the best-EW policies. Qin et al. [29] proposed a three-tier online sales supply chain model and analyzed the impact of EW periods on manufacturers' profits and EW value. Mai et al. [30] explored the impact of the way that retailers transfer revenue from manufacturers to EW prices through three methods. In a dual-channel supply chain, He et al. [31] explored the impact of customer channel preferences on EW strategies. Based on consumers' purchasing decision behavior, Zhu et al. [32] studied and coordinated the EW decision model for the closed-loop supply chain with the Stackelberg game. Zheng et al. [5] considered the carbon tax and the trade-in subsidy policy and explored the impact of the trade-in policy on the EW operation model.

Most of the abovementioned research focuses on the context of traditional supply chains and did not consider the development of the Internet economy, nor have they explored the impact of e-platforms on the operation of supply chains and the impact of system channel power structure on EW. Considering the differences in the channel power structure and EW service provider, pricing decisions and service decisions are studied in this research. The differences between this study and the existing literature are shown in Table 1.

The main contributions of this article are as follows:

- (1) Considering the differences between the ECSC and the traditional supply chain, four ECSC models are constructed. Then, EW decisions and sales strategies are analyzed. Most of the existing literature focuses on traditional supply chains and rarely considers the impact of the network economy on the supply chain.
- (2) Taking the differences of EW providers and dominant enterprises into consideration, this paper explores the impact of supply chain dominance on EW, proposes the optimal EW provider and EW mode,

and provides management insights for corporates in the ECSC.

- (3) Incorporating the service level of e-platform into the ECSC decision models, this paper explores EW decisions and pricing decisions under different EW models. The research results can guide supply chain participants to set EW price and product price to maximize ECSC profit.

3. Model Illustration and Assumptions

This paper researches an ECSC system that consists of a single seller (called her) and a single e-platform (called him), as shown in Figure 1. In this ECSC, it is assumed that the seller can release the sales information of her products with the aid of e-platform. Meanwhile, to increase sales and improve the service level, both the seller and e-platform can implement a sales strategy of providing EW.

In this ECSC, there are two types of fees paid by the seller when entering the third-party e-platform:

- (1) The fixed fee, such as technical fee and deposit, can ensure that the e-platform provides basic services; that is, e-platform allocates an online store (website) to the seller and empowers her to release sales information.
- (2) The variable fee, such as commission, changes according to the sales. Currently, many e-platforms, including Tmall (tmall.com) and JD (jd.com), charge commission based on sales revenue. Likewise, e-platform can provide various supplementary services based on the amount of commission, such as advertising (quantity, position, and slot of advertisements), the service of a quick return and exchange for goods, the propagation of online stores, and the sales preservation service (operations agent, payment and customer service, warehouse and logistics service). For instance, Tmall will provide different sales services according to the different commissions paid by the seller, especially for advertising efforts.

The notations used in the models are summarized in Table 2.

In this ECSC system, the dominant modes of the supply chain can be divided into two types: one is the decision-making process dominated by the seller; the other is dominated by the e-platform. In these two dominant modes, both the seller and e-platform individually provide EW service. Thus, the supply chain system has four different decision-making models, as shown in Figure 2.

The following four decision-making models are considered: the seller provides EW service and dominates the ECSC such as Apple that provides EW service for iPhones; the seller provides EW service but does not dominate the ECSC, such as the sellers of mobile phones on JD.com; the e-platform provides EW service and dominates the ECSC, such as GOME; it not only dominates system but also provides EW service; the platform provides EW service but

TABLE 1: Literature comparison of this study and the existing studies.

References	Pricing strategy	Sales service is involved	EW provider	Dominant enterprise	EW period is considered	Coordination contract	Managerial insights are discussed	EW cost is involved
Li et al. [23]	Y	N	Retailer/ manufacturer	Manufacturer	Y	N	Y	Y
Chiang et al. [8]	N	N	Seller	—	Y	N	N	Y
Afsahi and Shafiee [33]	Y	N	Manufacturer	—	Y	N	N	Y
Bian et al. [34]	Y	N	Two retailers	Manufacturer	Y	N	N	Y
Bian et al. [19]	Y	N	Retailer/ manufacturer	—	N	N	N	Y
Bouguerra et al. [13]	N	N	Manufacturer	—	Y	N	N	Y
Su and Shen [28]	N	N	Manufacturer	—	Y	N	N	Y
Ma et al. [21]	Y	N	Retailers	Manufacturers	Y	Y	N	Y
Huang et al. [25]	N	N	Manufacturer	—	Y	N	N	Y
He et al. [31]	Y	N	Retailer/ manufacturer	Manufacturer	N	N	N	Y
Zhao et al. [20]	Y	N	Retailer/ manufacturer	Retailer	N	N	N	N
Mai et al. [30]	Y	N	Manufacturer	Manufacturer	N	Y	N	Y
This study	Y	Y	Seller/e- platform	Seller/e- platform	N	N	Y	Y

Y = Yes; N = No; — = not consider power structure.

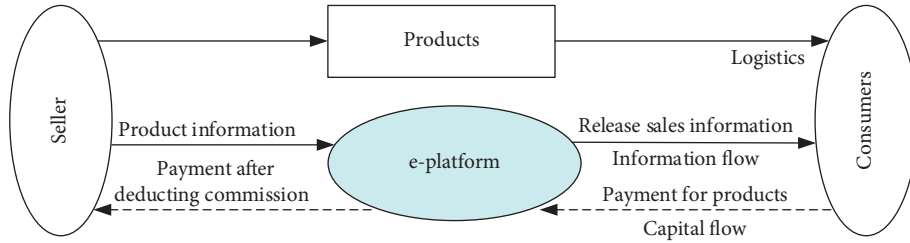


FIGURE 1: A framework of the ECSC.

does not dominate the ECSC, such as cooperation between powerful mobile phone sellers and JD.com.

4. Model Formulation and Equilibrium Solution

4.1. *EW Provided by the Seller.* In this case, the profit function of the seller who provides EW service is

$$\pi_r = (p - \rho p)q + (p_o - c_o)q_o - f. \quad (1)$$

The e-platform's profit function is

$$\pi_e = \rho p q - \frac{s^2}{2} + f. \quad (2)$$

The total profit function of the ECSC is

$$\pi = \pi_r + \pi_e. \quad (3)$$

The following sections focus on the decision-making processes of two modes: dominated by the seller or the e-platform. When the seller provides the EW service, there are the following two cases: if the ECSC is dominated by the seller, the seller first determines the sales price and the EW price and then the e-platform determines the service level, and if the ECSC is dominated by the e-platform, the e-platform first determines the service level and then the seller determines the sales price and the EW price.

4.1.1. *Decision Model with Dominant Seller.* In the ECSC, if the strength of the seller is stronger than the e-platform, the seller can dominate the ECSC and become the leader (first-mover in the game). In practice, according to the cooperation mode of Chinese retail magnate, RT-mart, and her cooperator, Feiniu (www.feiniu.com), a model with the dominant seller can be established: RT-mart sells her

TABLE 2: Description of notations.

Notations	Description
p	The sales price of the seller
f	The fixed fee paid by the seller for the technical service provided by the e-platform in the selling period
ρ	The commission rate, $0 < \rho < 1$. ρpq is the total commission charged by e-platform
s	The service level provided by the e-platform for selling products. According to Wang and Li [35] and Pokharel and Liang [36], this paper assumes that the sales service cost function satisfies $C(s) = ks^2/2$, where $k(k > 0)$ is the service cost coefficient
c_o	The unit cost of providing EW service in the warranty period
p_o	EW price
q	Market demand for products is greatly affected by sales price and service level. Based on the study of Wu [37] and Otrodi et al. [38], this paper assumes that the demand function (the form of market demand function with the sales price in existing studies includes power function [39, 40], inverse demand function [41], and linear demand function [38]. In this paper, we use the linear demand function which can reflect that demand decreases with sales price and increases with service level [22, 23]) is $q = \alpha - \beta p + \gamma s$, in which, $\alpha(\alpha > 0)$ refers to the market saturation, $\beta(\beta > 0)$ is the sales price elasticity, and $\gamma(\gamma > 0)$ represents the service level elasticity. The larger the value in β and γ , the more the demand is affected. $0 < \gamma \leq \beta < \alpha$ implies that consumers are more sensitive to price than service
q_o	Market demand for EW: this demand only emerges from consumers who purchased products. Thus, the highest demand for EW is equal to the highest demand for products without sales service. Meanwhile, the product sales price is also the main factor affecting EW demand (the price elasticity coefficient is the same in both product demand function and EW demand function). Referring to Klausner and Hendrickson [42], this paper assumes that the EW period is an exogenous constant and the EW demand function is $q_o = \alpha - \beta p - \lambda p_o$. λ is the elasticity coefficient of EW price. The larger the value in λ , the more the demand for EW service is affected. Without the loss of feasibility, $\lambda < \beta < 2\lambda$ is required, which restricts that there is no big gap between consumers' sensitivity coefficients to the product price and the EW price
Remarks	To simplify the calculations, this study assumes $\beta = 1$ and $k = 1$. The sales function can be simplified as $q = \alpha - p + \gamma s$, and the EW service demand and the cost function of the e-platform are $q_o = \alpha - p - \lambda p_o$ and $C(s) = s^2/2$, respectively. Meanwhile, it is assumed that $0 < \gamma \leq 1 < \alpha$, which indicates that consumers are more sensitive to price than service

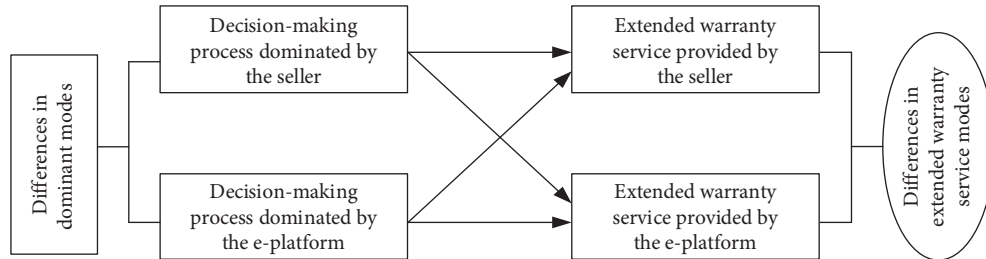


FIGURE 2: Four decision-making models in the ECSC.

products with the aid of e-platform, Feiniu, forming an ECSC system with the dominant seller and the following e-platform. In this two-echelon Stackelberg game model, the dominant seller first decides the sales price p and the EW price p_o ; then, the following e-platform decides the service level s . Both enterprises make decisions individually to maximize their profits. Optimal decisions can be derived by the backward induction method.

There is $\partial^2 \pi_e / \partial s^2 = -1 < 0$ according to equation (2); the optimal solution of π_e exists and the response function of service level can be derived as

$$s = \rho \gamma p. \quad (4)$$

Substitute equation (4) into equation (1) and take the second-order derivative of the seller's profit function with respect to the sales price and the EW price;

$$\text{Hessian matrix } H = \begin{bmatrix} \partial^2 \pi_r / \partial p^2 & \partial^2 \pi_r / \partial p \partial p_o \\ \partial^2 \pi_r / \partial p_o \partial p & \partial^2 \pi_r / \partial p_o^2 \end{bmatrix} =$$

$\begin{bmatrix} -2(1-\rho)(1-\rho\gamma^2) - 1 & -1 \\ -1 & -2\lambda \end{bmatrix}$. When $2(1-\rho)(1-\rho\gamma^2) > 0$ and $4\lambda(1-\rho)(1-\rho\gamma^2) - 1 > 0$, the optimal solution of $\pi_r(p, p_o)$ exists. The sales price and EW price can be solved by $\partial \pi_r / \partial p = 0$ and $\partial \pi_r / \partial p_o = 0$:

$$p^{rR} = \frac{[2\lambda(1-\rho) - 1]\alpha + \lambda c_o}{4\lambda(1-\rho)(1-\rho\gamma^2) - 1}, \quad (5)$$

$$p_o^{rR} = \frac{\alpha + 2c_o}{2\lambda} - \frac{[2\lambda(1-\rho) - 1]\alpha + \lambda c_o}{2\lambda[4\lambda(1-\rho)(1-\rho\gamma^2) - 1]}.$$

When equation (5) is substituted into equation (4), the optimal service level of the e-platform can be obtained. Overall, when the seller dominates the ECSC and provides the EW service, optimal pricing and service strategies are derived as follows:

The optimal product sales price is

$$p^{rR} = \frac{\alpha[2\lambda(1-\rho)-1] + \lambda c_o}{4\lambda(1-\rho)(1-\rho\gamma^2) - 1}. \quad (6)$$

The optimal EW price is

$$p_o^{rR} = \frac{\alpha + \lambda c_o}{2\lambda} - \frac{\alpha[2\lambda(1-\rho)-1] + \lambda c_o}{2\lambda[4\lambda(1-\rho)(1-\rho\gamma^2) - 1]}. \quad (7)$$

The optimal service level of e-platform is

$$s^{rR} = \frac{\rho\gamma\{\alpha[2\lambda(1-\rho)-1] + \lambda c_o\}}{4\lambda(1-\rho)(1-\rho\gamma^2) - 1}. \quad (8)$$

The optimal profit of the seller is

$$\begin{aligned} \pi_r^{rR} &= \frac{\alpha^2(1-\rho)[\lambda(1-\rho) - \rho\gamma^2]}{4\lambda(1-\rho)(1-\rho\gamma^2) - 1} + \frac{\lambda^2 c_o^2 \alpha^2(1-\rho)(1-\rho\gamma^2)}{4\lambda(1-\rho)(1-\rho\gamma^2) - 1} \\ &\quad - \frac{\alpha\lambda c_o(1-\rho)(1-2\rho\gamma^2)}{4\lambda(1-\rho)(1-\rho\gamma^2) - 1} - f. \end{aligned} \quad (9)$$

The optimal profit of e-platform is

$$\begin{aligned} \pi_e^{rR} &= \frac{\rho[\alpha - 2\alpha\lambda(1-\rho) - \lambda c_o]}{2[4\lambda(1-\rho)(1-\rho\gamma^2) - 1]^2} \\ &\quad \cdot \{\alpha[\rho\gamma^2 - 2\lambda(1-\rho)(2-3\rho\gamma^2)] + \lambda c_o(2-\rho\gamma^2)\} + f. \end{aligned} \quad (10)$$

The optimal profit of the ECSC is

$$\pi^{rR} = \pi_r^{rR} + \pi_e^{rR}. \quad (11)$$

4.1.2. Decision Model with Dominant e-Platform. In the ECSC, if the strength of e-platform is stronger than the seller, the e-platform can dominate the supply chain. This section takes Tmall as a practical case, and a model with a dominant e-platform can be established. Tmall, as a powerful platform enterprise, has the initiative to choose cooperators, including small and medium-sized sellers, thus can dominate the

whole supply chain. Therefore, in this two-echelon Stackelberg game model, the dominant e-platform first decides service level s ; then, the following seller decides sales price p and EW price p_o . The optimal decisions can be derived by the backward induction method.

Based on equation (1), $\partial^2 \pi_r / \partial p^2 = -2(1-\rho) < 0$, $\partial^2 \pi_r / \partial p_o^2 = -2\lambda$, and $\partial^2 \pi_r / \partial p \partial p_o = \partial^2 \pi_r / \partial p_o \partial p = -1$. When $4\lambda(1-\rho) - 1 > 0$, the optimal solution of $\pi_r(p, p_o)$ exists. According to $\partial \pi_r / \partial p = 0$ and $\partial \pi_r / \partial p_o = 0$, the response functions of the sales price and the EW price are as follows:

$$p = \frac{\alpha - \lambda c_o - 2\lambda[(1-\rho)(\alpha + \gamma s)]}{1 - 4\lambda(1-\rho)}, p_o = \frac{c_o + (1-\rho)(\gamma s - \alpha - 2\lambda c_o)}{1 - 4\lambda(1-\rho)}. \quad (12)$$

Substituting equation (12) into equation (2), $\partial^2 \pi_e / \partial s^2 = -4\lambda(1-\rho)(2-\rho\gamma^2)[2\lambda(1-\rho)-1] + 1/[4\lambda(1-\rho)-1]^2$; when $4\lambda(1-\rho)(2-\rho\gamma^2)[2\lambda(1-\rho)-1] + 1 > 0$, the optimal solution of $\pi_e(s)$ exists. Solving $\partial \pi_e / \partial s = 0$,

$$s^{rE} = \rho\gamma \cdot \frac{\alpha\{1 + 4\lambda[2\lambda(1-\rho)-1](1-\rho)\} - \lambda c_o}{N}. \quad (13)$$

When equation (13) is substituted into equation (12), the optimal sales price and the EW price can be obtained.

The optimal product sales price is

$$p^{rE} = \frac{2\lambda(1-\rho)}{Q} \cdot \frac{M}{N} - \frac{\alpha - \lambda c_o}{Q}. \quad (14)$$

The optimal EW price is

$$p_o^{rE} = \frac{(1-\rho)}{Q} \cdot \frac{\alpha Q^2(1-\rho\gamma^2) + \rho\gamma^2 \lambda c_o}{N} - \frac{c_o[1 - 2\lambda(1-\rho)]}{Q}. \quad (15)$$

The optimal service level of e-platform is

$$s^{rE} = \rho\gamma \cdot \frac{\alpha\{1 + 4\lambda[2\lambda(1-\rho)-1](1-\rho)\} - \lambda c_o}{N}. \quad (16)$$

The optimal profit of seller is

$$\begin{aligned} \pi_r^{rE} &= \frac{(1-\rho)}{Q} \left[2\lambda(1-\rho) \cdot \frac{M}{N} - (\alpha - \lambda c_o) \right] \left[\frac{2\lambda(1-\rho)-1}{Q} \cdot \frac{M}{N} + \frac{\alpha - \lambda c_o}{Q} \right] \\ &\quad + \frac{(1-\rho)^2}{Q^2} \left[\frac{\alpha Q^2(1-\rho\gamma^2) - \rho\gamma^2 \lambda c_o}{N} - 2\lambda c_o \right] \cdot \left[2(\alpha - \lambda c_o) - \lambda \cdot \frac{M}{N} \right] - f. \end{aligned} \quad (17)$$

The optimal profit of e-platform is

$$\pi_e^{rE} = \frac{\rho\alpha^2\{4\lambda(1-\rho)[2\lambda(1-\rho)-1] + \rho\gamma^2\} + \lambda\rho c_o\{2\alpha(1-\rho\gamma^2) - \lambda c_o(2-\rho\gamma^2)\}}{2N} + f. \quad (18)$$

The optimal profit of ECSC is $\pi = \pi_r^{rE} + \pi_e^{rE}$, in which $Q = 4\lambda(1-\rho) - 1$, $N = 4\lambda[2\lambda(1-\rho)-1](1-\rho)(2-\rho\gamma^2) + 1$, and

$$M = \alpha\{1 + \rho\gamma^2 + 8\lambda[2\lambda(1-\rho)-1](1-\rho)\} - \rho\gamma^2 \lambda c_o. \quad (19)$$

4.2. *EW Provided by e-Platform.* In order to obtain more profits, the e-platform should consider providing EW. For example, many e-platforms, such as JD (jd.com), GOME (gome.com.cn), and Suning (suning.com), would provide EW service for consumers. In this case, the profit function of the seller is

$$\pi_r = (p - \rho p)q - f. \quad (20)$$

The e-platform's profit function is

$$\pi_e = \rho p q + (p_o - c_o)q_o - \frac{s^2}{2} + f. \quad (21)$$

The total profit function of the ECSC is

$$\pi = \pi_r + \pi_e. \quad (22)$$

Similarly, there are two dominant modes: the ECSC dominated by the seller or the ECSC dominated by the e-platform. When the e-platform provides the EW service, there are the following two cases: if the ECSC is dominated by the e-platform, the e-platform first determines the service level and the EW price and then the seller determines the sales price, and if the ECSC is dominated by the seller, the seller first determines the sales price and then the e-platform determines the service level and the EW price.

4.2.1. *Decision Model with Dominant Seller.* When the seller dominates the ECSC and the e-platform provides the EW service, the seller first decides the sales price p and then the e-platform decides the service level s and the EW price p_o , forming a two-echelon Stackelberg game model.

From equation (21), $\partial^2 \pi_e / \partial s^2 = -k < 0$, $\partial^2 \pi_e / \partial p_o^2 = -2\lambda < 0$, and $\partial^2 \pi_e / \partial p_o \partial s = \partial^2 \pi_e / \partial s \partial p_o = 0$, where π_e is a strictly concave function of p_o and s . According to $\partial \pi_e / \partial p_o = 0$ and $\partial \pi_e / \partial s = 0$, we obtain

$$p_o = \frac{\alpha - p + \lambda c_o}{2\lambda}, s = \frac{\rho \gamma p}{k}. \quad (23)$$

Substituting equation (23) into equation (20), $\partial^2 \pi_r / \partial p^2 = -2(1 - \rho)(1 - \rho \gamma^2) < 0$; the optimal solution of $\pi_r(p)$ exists. Solving $\partial \pi_r / \partial p = 0$, we obtain

$$p^{eR} = \frac{\alpha}{2(1 - \rho \gamma^2)}. \quad (24)$$

Substituting equation (24) into equation (23), the optimal EW price and service level can be obtained.

The optimal product sales price is

$$p^{eR} = \frac{\alpha}{2(1 - \rho \gamma^2)}. \quad (25)$$

The optimal EW price is

$$p_o^{eR} = \frac{\alpha + \lambda c_o}{2\lambda} - \frac{\alpha}{4\lambda(1 - \rho \gamma^2)}. \quad (26)$$

The optimal service level of e-platform is

$$s^{eR} = \frac{\rho \gamma \alpha}{2(1 - \rho \gamma^2)}. \quad (27)$$

The optimal profit of the seller is

$$\pi_r^{eR} = \frac{\alpha^2(1 - \rho)}{4(1 - \rho \gamma^2)} - f. \quad (28)$$

The optimal profit of e-platform is

$$\pi_e^{eR} = \frac{\alpha^2 \rho}{4(1 - \rho \gamma^2)} + \frac{1}{16\lambda} \left[\frac{\alpha(1 - 2\rho \gamma^2)}{1 - \rho \gamma^2} - 2\lambda c_o \right]^2 - \frac{\alpha^2 \rho^2 \gamma^2}{8(1 - \rho \gamma^2)^2} + f. \quad (29)$$

The optimal profit of the ECSC is

$$\pi^{eR} = \pi_r^{eR} + \pi_e^{eR}. \quad (30)$$

4.2.2. *Decision Model with Dominant e-Platform.* When the e-platform dominates the ECSC and provides the EW service, the service level s and the EW price p_o are given first and then the seller decides the sales price p , forming a two-echelon Stackelberg game model.

According to equation (20), $\partial^2 \pi_r / \partial p^2 = -2(1 - \rho) < 0$; through $\partial \pi_r / \partial p = 0$, we obtain

$$p = \frac{(\alpha + \gamma s)}{2}. \quad (31)$$

Substituting equation (31) into equation (21), $\partial^2 \pi_e / \partial s^2 = \rho \gamma^2 / 2 - 1 < 0$, $\partial^2 \pi_e / \partial p_o^2 = -2\lambda$, and $\partial^2 \pi_e / \partial p_o \partial s = \partial^2 \pi_e / \partial s \partial p_o = -\gamma / 2$; when $8\lambda - \gamma^2(1 + 4\lambda\rho) > 0$, the optimal solution of $\pi_e(p_o, s)$ exists. According to $\partial \pi_e / \partial p_o = 0$ and $\partial \pi_e / \partial s = 0$, we obtain

$$p_o^{eE} = \frac{2\alpha(1 - \rho \gamma^2) + c_o[4\lambda - \gamma^2(1 + 2\lambda\rho)]}{8\lambda - \gamma^2(1 + 4\lambda\rho)}, s^{eE} = \frac{\gamma[2\lambda c_o - \alpha(1 - 4\lambda\rho)]}{8\lambda - \gamma^2(1 + 4\lambda\rho)}. \quad (32)$$

Substituting equation (32) into equation (31), the optimal sales price can be obtained.

The optimal product sales price is

$$p^{eE} = \frac{4\alpha\lambda - \alpha\gamma^2 + \lambda\gamma^2 c_o}{8\lambda - \gamma^2(1 + 4\lambda\rho)}. \quad (33)$$

The optimal EW price is

$$p_o^{eE} = \frac{2\alpha(1 - \rho \gamma^2) + c_o[4\lambda - \gamma^2(1 + 2\lambda\rho)]}{8\lambda - \gamma^2(1 + 4\lambda\rho)}. \quad (34)$$

The optimal service level of e-platform is

$$s^{eE} = \frac{\gamma[2\lambda c_o - \alpha(1 - 4\lambda\rho)]}{8\lambda - \gamma^2(1 + 4\lambda\rho)}. \quad (35)$$

The optimal profit of the seller is

$$\pi_r^{eE} = (1 - \rho) \left\{ \frac{\alpha(4\lambda - \gamma^2) + \lambda\gamma^2 c_o}{[8\lambda - \gamma^2(1 + 4\lambda\rho)]} \right\}^2 - f. \quad (36)$$

The optimal profit of e-platform is

$$\pi_e^{eE} = \frac{\alpha^2(1 + 4\lambda\rho - 2\rho\gamma^2) - 4\lambda c_o \alpha(1 - \rho\gamma^2)}{2[8\lambda - \gamma^2(1 + 4\lambda\rho)]} + f. \quad (37)$$

The optimal profit of the ECSC is

$$\pi^{eE} = \pi_r^{eE} + \pi_e^{eE}. \quad (38)$$

5. Analysis of Optimal Decisions

The following propositions can be obtained by comparing and analyzing the optimal decisions of the four decision-making models.

Proposition 1

- (1) Sales prices in different models: $p^{eR} > p^{eE} > p^{rE} > p^{rR}$;
EW prices in different models: $p_o^{rR} > p_o^{rE} > p_o^{eE} > p_o^{eR}$

The proof is given in Appendix A.

Because products and the EW service are the sources of profits for enterprises, there may be competition between the sales price and the EW price. Proposition 1 compares the sales price of products and the EW price under different models to find out how channel power structure and the EW service enterprise affect the sales price and the EW price. According to Proposition 1,

- (1) The comparison of product sales prices is contrary to the EW prices because the demand for EW is negatively related to the sales price. When the sales price reaches the highest, enterprises would reduce the EW price for maintaining market demand for the EW service. In these four models, when the dominant seller provides the EW service, the sales price reaches the lowest but the EW price reaches the highest; when the following e-platform provides the EW service, the sales price is the highest but the EW price is the lowest. This is because when the seller dominates the supply chain and provides the EW service simultaneously, the seller would like to stimulate product market demand through setting a lower sales price. However, the dominant seller decides a higher sales price when the following e-platform provides the EW service, and the e-platform has to set a lower EW price to maintain market demand for the EW service which is negatively related to the sales price.
- (2) Compared with the case that the seller provides the EW service, it is indicated that the sales price is higher and the EW price is lower when the e-platform becomes the provider of EW service. This is because all the profit generated from the EW service is possessed by the e-platform when it provides the EW service, the seller can only gain profit from product sales by setting a higher sales price. However, a higher sales price means that the demand for EW service may decrease, forcing the e-platform to reduce the EW price to maintain demand for the EW service. For instance, JD, a Chinese online e-platform, has been providing the EW service for electrical appliances and digital products, and the sales prices of these products are relatively higher in JD than other e-platforms, such as GOME and Suning (like the insurance for broken phone screens at <https://www.jd.com/pinpai/982-9639.html>).

Proposition 2. p^{rE} , p^{rR} , p_o^{eE} , and p_o^{eR} have a negative correlation with ρ , but p^{eR} , p^{eE} , p_o^{rR} , and p_o^{rE} have a positive correlation with ρ .

The proof is given in Appendix B.

Proposition 2 analyzes how the sales price of products and the EW price change with the commission rate of the e-platform. The commission rate is set by the platform and affects price adjustments and profit distribution between the seller and the platform, which is of significance for enterprises.

When the seller provides the EW service, the sales price decreases but the EW price increases with the commission rate. However, in the case of the e-platform providing the EW service, the results are the opposite: the sales price increases but the EW price decreases with the commission rate. This is because the seller who provides the EW service can gain profit by reducing her sales price and increasing the EW price concurrently even if the commission rate gets higher. Such behavior is more acceptable for consumers than increasing the sales price directly, thus helping the seller to implicitly occupy the consumer surplus. For example, Haier, a Chinese firm who produces and sells electric appliances, has been focusing on dynamically adjusting the sales price and the EW price to keep profitable. In 2011, in order to cope with the pressure of high operating costs, Haier increased the EW price while reducing the product sales price (<http://news.sina.com.cn/c/2011-06-28/090322718682.shtml>). However, when EW is provided by the e-platform, sellers can only gain profit from selling products and set a higher sales price with the increase in the commission rate. As for the e-platform, the provider of EW service has to reduce the EW price for the market demand for EW.

Proposition 3. The service level of the e-platform in different models: $s^{rE} > s^{eR} > s^{rR} > s^{eE}$.

The proof is given in Appendix C.

Proposition 3 compares the service level of the e-platform under four operation models to study the influence of channel power structure and EW service enterprise on the service level. According to Proposition 3,

- (1) When the following seller provides EW in an ECSC with the dominant e-platform, the service level of e-platform reaches the highest. This is because the dominant e-platform only gains profit from selling products, the higher service level is determined to attract more consumers and increase market demand for products.
- (2) When the dominant e-platform provides the EW service, the service level of e-platform reaches the lowest. The EW service is a source of the e-platform's profit, which makes e-platform pay more attention to the EW service market but neglect the product market to a certain extent. Hence, the service level for product sales would decrease. On the other hand, when the seller dominates the supply chain, the dominant seller can compel the following e-platform to increase the service level to promote product sales.

- (3) If the ECSC is dominated by the seller, the service level will be higher with the e-platform providing EW than the seller providing EW. In this case, it is extremely difficult for the e-platform to increase his profit by raising the service level, which forces the e-platform to make more efforts to improve the EW service. Therefore, in this situation, the service level will be higher with the e-platform providing the EW service than the seller providing the EW service.

In conclusion, if the ECSC is dominated by the e-platform, it is beneficial for the e-platform to increase the service level for product sales when the seller provides the EW service. Otherwise, if the seller dominates the ECSC, it is conducive for the e-platform to improve service level when the e-platform is the EW provider. In brief, the service level of product sales is always lower when the dominant enterprise in the supply chain provides the EW service compared with the following enterprise providing the EW service. This indicates that the service level can be higher as long as the dominant party and the provider of EW service are different.

6. Numerical Analysis

This section analyzes the performance of various models through numerical examples and investigates the variations in optimal decisions and profits. Suning, a Chinese online e-platform, is used to carry out the numerical analysis. Based on the laptop sales of Suning, this paper assumes that $\alpha = 1000$, $\gamma = 0.3$, $\lambda = 0.7$, $c_o = 50$, and $f = 1500$. Then, this section discusses the impact of the commission rate $\rho \in [0.03, 0.1]$ on decisions and profits. The results of the four decision-making structures are indicated in Figures 3–8.

It can be seen from Figures 3 and 4 that when the e-platform provides the EW service, the sales price increases but the EW price decreases with the commission rate and when the seller provides the EW service, the sales price decreases but the EW price increases over the commission rate. Moreover, the sales price (EW price) reaches the highest (lowest) with the e-platform providing EW than the seller providing EW. According to Figure 5, the service level of the e-platform increases with the commission rate and the service level reaches the highest with the seller providing EW and the e-platform dominating the ECSC. The service level becomes the lowest in the ECSC with the dominant e-platform which also provides the EW service. This conclusion is consistent with Proposition 3.

Proposition 4 is derived from Figures 6 and 7.

Proposition 4. Comparing the different decision-making models, there are $\pi_r^{rE} > \pi_r^{rR} > \pi_r^{eR} > \pi_r^{eE}$ and $\pi_e^{eE} > \pi_e^{eR} > \pi_e^{rR} > \pi_e^{rE}$.

As a service product, the EW service contributes to enterprise profits, so Proposition 4 compares the profits of the seller and the e-platform under the four models to analyze the influence of channel power structure and EW service enterprise on profits. According to Proposition 4,

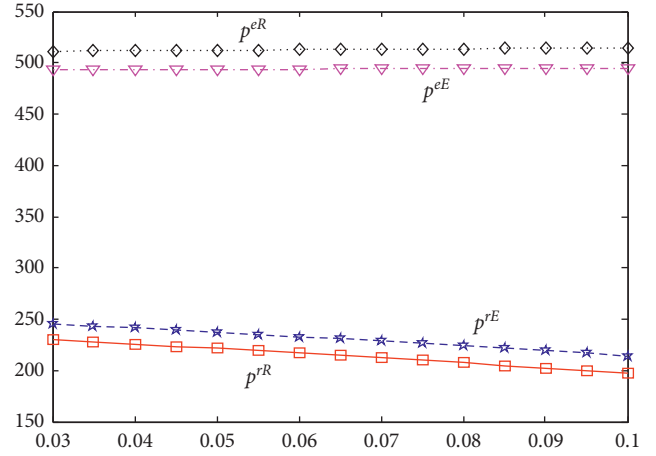


FIGURE 3: Optimal sales price over ρ .

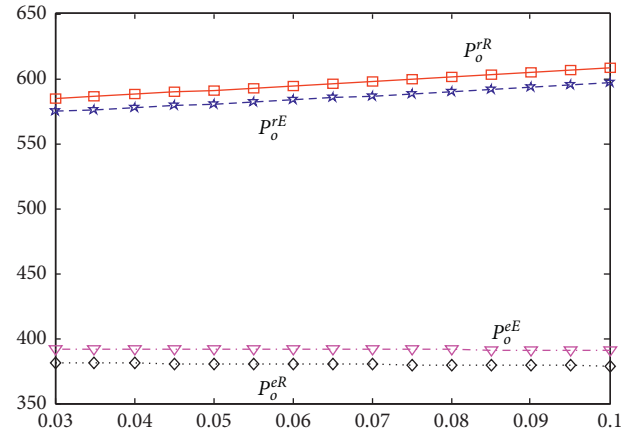


FIGURE 4: Optimal EW price over ρ .

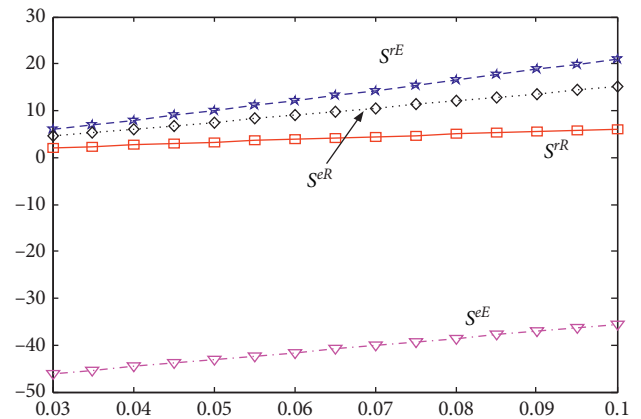
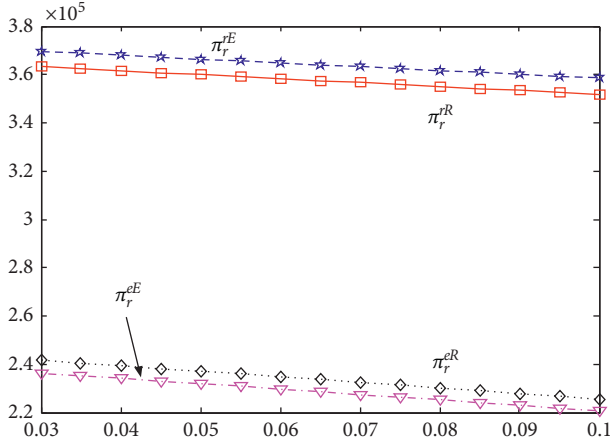
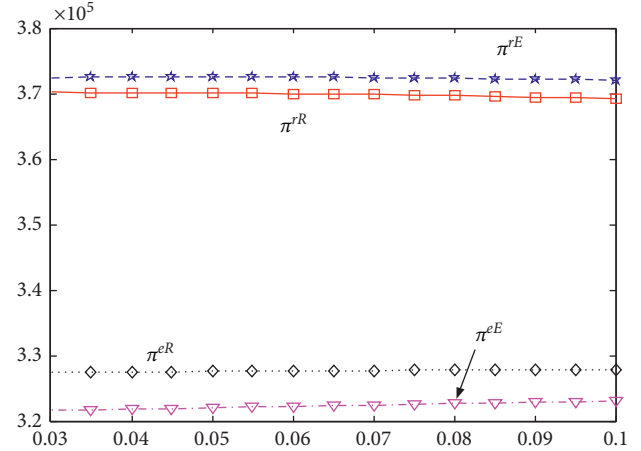
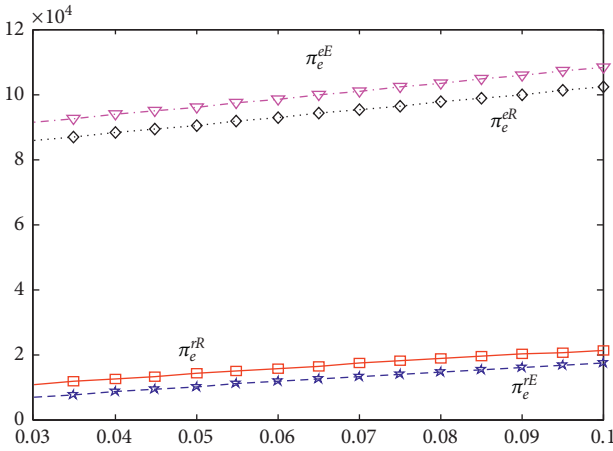


FIGURE 5: Optimal service level over ρ .

- (1) Both the seller and e-platform can obtain more profits when providing EW, which is why all supply chain members are keen on providing EW.
- (2) According to the comparison of four decision-making models, the comparison of the seller's profits has the

FIGURE 6: Optimal profit of the seller over ρ .FIGURE 8: Optimal system profit over ρ .FIGURE 7: Optimal profit of e-platform over ρ .

contrary order with the e-platform's profits. The seller's profit is the highest when the seller provides EW in a supply chain with a dominant e-platform, but the e-platform's profit is the lowest in this model. Likewise, the e-platform's profit is the highest when the e-platform provides the EW service and dominates the supply chain at the same time, but the seller's profit is the lowest. Therefore, when e-platform provides EW in an ECSC, it is profitable for supply chain members to obtain the dominant power. However, the result is the opposite when the seller provides EW, the dominant enterprise will get less profit.

Overall, for the supply chain enterprises, it is conducive to increasing profit to dominate the supply chain or provide EW.

Proposition 5 can be obtained from Figure 8.

Proposition 5. Comparing different decision-making models, there is $\pi^{rE} > \pi^{rR} > \pi^{eR} > \pi^{eE}$.

Proposition 5 compares the profits of the ECSC system under four decision-making models to show which decision-making model can achieve the highest system profit. Propositions 4 and 5 indicate that comparison results of

system profit are consistent with the results of the seller's profit. In these four decision models, the system profit reaches the highest when the seller provides the EW service and the e-platform dominates the supply chain. In this case, the sales service level also reaches the highest, and both the sales price and the EW price are relatively lower, which can improve the product demand and demand for the EW service. This is the reason why the system profit is the highest in the condition where the seller provides the EW service and the e-platform dominates the supply chain. Therefore, in practice, Suning, as a dominant e-platform enterprise in the electric appliance supply chain, leaves the EW service to sellers, such as Philips, Changhong, TCL, LG, and Samsung.

7. Discussion

7.1. Main Findings. With the rapid development of the network economy, the ECSC has been greatly promoted and advanced. In order to expand the e-commerce sales market and product diversity, a great number of enterprises in the ECSC begin to focus on EW business. Therefore, this paper builds an ECSC model with a single seller and a single e-platform and studies the pricing and EW strategies. Furthermore, this study considers the differences of providers and dominators and then constructs four decision-making models: when the seller provides EW, there are two models with the dominant seller or dominant e-platform; likewise, there are also two models when e-platform provides EW. Ultimately, this paper obtains the optimal solutions in various models and further analyzes them with numerical examples. The results show the following.

According to the comparison of four decision-making models, the total profit reaches the highest when the seller provides EW and e-platform dominates the supply chain. Meanwhile, in this case, the sales service level reaches the highest, but both the sales price and the EW price are relatively lower. For the supply chain members, dominating the supply chain or providing EW is conducive to improving profit. Therefore, when e-platform provides EW in an ECSC, it is profitable for supply chain members to obtain the dominant power. However, the result is the opposite when

the seller provides EW; it is not beneficial to obtain the dominant power.

Moreover, this paper finds that when e-platform dominates the supply chain system, it is beneficial for e-platform increasing product service level when the seller provides EW. However, when the seller dominates the whole system, it is constructive for e-platform to increase the product service level when the e-platform is the EW provider. The service level for product sales is always lower when the dominant enterprise provides EW. Besides, this study points out that the sales price is relatively higher but the EW price goes lower with the e-platform providing EW rather than the seller providing EW.

7.2. Managerial Implications. Some managerial suggestions can be derived from conclusions as follows.

By the comparative analysis of sales price and EW price, it can be known that the minimum sales price and the minimum EW price cannot be in the same decision model. The seller and the e-platform should recognize this and set a sales price and an EW price rationally.

Regardless of the seller or the e-platform providing the EW service, the provider can obtain higher profit, which indicates that the EW service can be a profit source for enterprises. Therefore, the sellers and the e-platform should actively provide the EW service to increase profits.

The findings show that when the e-platform provides the EW service, the conclusion is that who dominates the system

is the one who gets more profit; and when the seller provides the EW service, the conclusion is that who dominates the system is the one who gets less profit. Therefore, when leading the supply chain, the e-platform should provide the EW service; however, when the seller dominates the system, it is wise not to provide the EW service.

In the ECSC, if the product market demand tends to be increased through service level, the dominant enterprise and the enterprise that provides the EW service might just as well not be the same because the service level is higher in this operating model.

7.3. Limitation and Future Research. This paper only considers an ECSC system which is composed of a single seller and a single e-platform. In reality, there are also other operation modes, such as multisellers on single platform and multisellers on multiplatforms, which are the future research directions we should focus on. Besides, we also need to pay attention to the other key factor, the warranty period, which can significantly influence the decision-making process.

Appendix

A. Proof of Proposition 1

Proof

$$p^{eR} - p^{eE} = \gamma^2 \cdot \frac{\alpha(1 + 4\lambda\rho - 2\rho\gamma^2) - 2\lambda c_o(1 - \rho\gamma^2)}{2(1 - \rho\gamma^2)[8\lambda - \gamma^2(1 + 4\lambda\rho)]} > 0, \quad (\text{A.1})$$

$$p^{rE} - p^{rR} = \frac{2\alpha\lambda\rho\gamma^2(1 - \rho)\{4\lambda(1 - \rho)[2 - 2\lambda(1 - \rho) - \rho\gamma^2] - 1\} - \lambda c_o(1 - \rho)[4\lambda(1 - \rho)(2 - \rho\gamma^2) - 1]}{[4\lambda(1 - \rho)(1 - \rho\gamma^2) - 1]\{4\lambda[2\lambda(1 - \rho) - 1](1 - \rho)(2 - \rho\gamma^2) + 1\}} > 0, \quad (\text{A.2})$$

$$p_o^{eE} - p_o^{eR} = \frac{\alpha\{4\lambda(2\lambda - 1) + \gamma^2(1 - \lambda)(1 + 4\lambda\rho) - \rho\gamma^4\} - \lambda\gamma^2 c_o(1 - \rho\gamma^2)}{2\lambda(2 - \rho\gamma^2)[8\lambda - \gamma^2(1 + 4\lambda\rho)]} > 0. \quad (\text{A.3})$$

The same can be proved, $p^{eE} - p^{rE} > 0$, $p_o^{rR} - p_o^{rE} > 0$, and $p_o^{rE} - p_o^{eE} > 0$; therefore, $p^{eR} > p^{eE} > p^{rE} > p^{rR}$ and $p_o^{rR} > p_o^{rE} > p_o^{eE} > p_o^{eR}$. \square

B. Proof of Proposition 2

Proof

$$\frac{\partial p^{eR}}{\partial \rho} = \frac{\alpha\gamma^2}{2(1 - \rho\gamma^2)^2} > 0,$$

$$\frac{\partial p_o^{eR}}{\partial \rho} = \frac{\alpha\gamma^2}{2(1 - \rho\gamma^2)^2} < 0,$$

$$\frac{\partial p^{eE}}{\partial \rho} = 4\lambda\gamma^2 \cdot \frac{\alpha(4\lambda - \gamma^2) + \lambda c_o\gamma^2}{[8\lambda - \gamma^2(1 + 4\lambda\rho)]^2} > 0,$$

(B.1)

$$\frac{\partial p_o^{eE}}{\partial \rho} = \frac{-2\alpha\gamma^2(4\lambda - \gamma^2) - 2\lambda c_o\gamma^4}{[8\lambda - \gamma^2(1 + 4\lambda\rho)]^2} < 0, \quad (\text{B.2})$$

$$\frac{\partial p_o^{rR}}{\partial \rho} = 2\lambda \frac{\alpha\{-1 + \gamma^2[4\rho + 4\lambda(1 - \rho)^2 - 2]\} + 2\lambda c_o[1 + \gamma^2(1 - 2\rho)]}{[4\lambda(1 - \rho)(1 - \rho\gamma^2) - 1]^2} < 0,$$

$$\frac{\partial p_o^{rE}}{\partial \rho} = \frac{\alpha\{1 + \gamma^2[2 - 4\rho - 4\lambda(1 - \rho)^2]\} - 2\lambda c_o[1 + \gamma^2(1 - 2\rho)]}{[4\lambda(1 - \rho)(1 - \rho\gamma^2) - 1]^2} > 0. \quad (\text{B.3})$$

Similarly, $\partial p_o^{rE}/\partial \rho < 0$ and $\partial p_o^{rE}/\partial \rho > 0$. \square

C. Proof of Proposition 3

Proof

$$s^{eR} - s^{rR} = \rho\gamma \cdot \frac{\alpha(1 - 2\rho\gamma^2) - 2\lambda c_o(1 - \rho\gamma^2)}{2(1 - \rho\gamma^2)[4\lambda(1 - \rho)(1 - \rho\gamma^2) - 1]} > 0, \quad (\text{C.1})$$

$$s^{rE} - s^{eR} = \alpha\rho\gamma \cdot \frac{1 - 2\gamma^2\{1 + 2\lambda\rho(1 - \rho)[2\lambda(1 - \rho) - 1]\}}{2(1 - \rho\gamma^2)\{4\lambda[2\lambda(1 - \rho) - 1](1 - \rho)(2 - \rho\gamma^2) + 1\}} + \frac{2\lambda c_o}{2\{4\lambda[2\lambda(1 - \rho) - 1](1 - \rho)(2 - \rho\gamma^2) + 1\}} > 0. \quad (\text{C.2})$$

Similarly, $s^{rR} - s^{eE} > 0$; therefore, $s^{rE} > s^{eR} > s^{rR} > s^{eE}$. \square

Data Availability

The data used to support the findings of this study are included within the article.

Additional Points

Suning's (suning.com) sales case is referenced in this paper, but we did not use Suning's real sales data for numerical analysis. Just refer to Suning's sales and warranty extensions and make theoretical assumptions about the parameters involved in the numerical analysis so as to give simulation graphics analysis.

Conflicts of Interest

The authors declare that there are no conflicts of interest regarding the publication of this article.

Acknowledgments

This study was supported financially by the National Natural Science Foundation of China (71971129) and Science and Technology Support Program for Youth Innovation of Colleges and Universities in Shandong Province (2019RWG017).

References

- [1] A. W. Siddiqui and S. A. Raza, "Electronic supply chains: status & perspective," *Computers & Industrial Engineering*, vol. 88, pp. 536–556, 2015.
- [2] S. Y. Nof, J. Ceroni, W. Jeong, and M. Moghaddam, "Revolutionizing collaboration through e-work, e-business, and e-service," *Automation, Collaboration, & E-Services*, vol. 2, pp. 237–271, 2015.
- [3] T. Chen, A. Kalra, and B. Sun, "Why do consumers buy extended service contracts?" *Journal of Consumer Research*, vol. 36, no. 4, pp. 611–623, 2009.
- [4] T. Peng and L. Chunling, "Designing differential service strategy for two-dimensional warranty based on warranty claim data under consumer-side modularisation," *Proceedings of the Institution of Mechanical Engineers, Part O: Journal of Risk and Reliability*, vol. 17, 2019.
- [5] R. Zheng, C. Su, and Y. Zheng, "Two-stage flexible warranty decision-making considering downtime loss," *Proceedings of the Institution of Mechanical Engineers, Part O: Journal of Risk and Reliability*, vol. 17, 2019.
- [6] M. Kim and R. Narasimhan, "Designing supply networks in automobile and electronics manufacturing industries: a multiplex analysis," *Processes*, vol. 7, no. 3, p. 176, 2019.
- [7] S. Yin, B. Li, X. Zhang, and M. Zhang, "How to improve the quality and speed of green new product development?" *Processes*, vol. 7, no. 7, p. 443, 2019.
- [8] W.-y. K. Chiang, D. Chhajed, and J. D. Hess, "Direct marketing, indirect profits: a strategic analysis of dual-channel supply-chain design," *Management Science*, vol. 49, no. 1, pp. 1–20, 2003.
- [9] Y. Wang and Z. Yu, "Research on advertising and pricing in e-supply chain under different dominant modes," *Journal of Systems Science and Information*, vol. 6, no. 1, pp. 58–68, 2018.
- [10] Y. Vakulenko, P. Shams, D. Hellström, and K. Hjort, "Service innovation in e-commerce last mile delivery: mapping the e-customer journey," *Journal of Business Research*, vol. 101, pp. 461–468, 2019.
- [11] Y. Wang, Z. Yu, and X. Ji, "Coordination of e-commerce supply chain when e-commerce platform providing sales

- service and extended warranty service,” *Journal of Control and Decision*, vol. 34, pp. 1–21, 2018.
- [12] X. Chen, L. Li, and M. Zhou, “Manufacturer’s pricing strategy for supply chain with warranty period-dependent demand,” *Omega*, vol. 40, no. 6, pp. 807–816, 2012.
- [13] S. Bouguerra, A. Chelbi, and N. Rezg, “A decision model for adopting an extended warranty under different maintenance policies,” *International Journal of Production Economics*, vol. 135, no. 2, pp. 840–849, 2012.
- [14] K. Shahanaghi, R. Noorossana, S. G. Jalali-Naini, and M. Heydari, “Failure modeling and optimizing preventive maintenance strategy during two-dimensional extended warranty contracts,” *Engineering Failure Analysis*, vol. 28, pp. 90–102, 2013.
- [15] S. Wu and P. Longhurst, “Optimising age-replacement and extended non-renewing warranty policies in lifecycle costing,” *International Journal of Production Economics*, vol. 130, no. 2, pp. 262–267, 2011.
- [16] K. M. Jung, M. Park, and D. H. Park, “Cost optimization model following extended renewing two-phase warranty,” *Computers & Industrial Engineering*, vol. 79, pp. 188–194, 2015.
- [17] Y. Lei, Q. Liu, and S. Shum, “Warranty pricing with consumer learning,” *European Journal of Operational Research*, vol. 263, no. 2, pp. 596–610, 2017.
- [18] C.-K. Chen, C.-C. Lo, and T.-C. Weng, “Optimal production run length and warranty period for an imperfect production system under selling price dependent on warranty period,” *European Journal of Operational Research*, vol. 259, no. 2, pp. 401–412, 2017.
- [19] Y. Bian, J. Xie, T. W. Archibald, and Y. Sun, “Optimal extended warranty strategy: offering trade-in service or not?” *European Journal of Operational Research*, vol. 278, no. 1, pp. 240–254, 2019.
- [20] D. Zhao, X. Zhang, T. Ren, and H. Fu, “Optimal pricing strategies in a product and service supply chain with extended warranty service competition considering retailer fairness concern,” *Mathematical Problems in Engineering*, vol. 2019, pp. 1–15, 2019.
- [21] J. Ma, X. Ai, W. Yang, and Y. Pan, “Decentralization versus coordination in competing supply chains under retailers’ extended warranties,” *Annals of Operations Research*, vol. 275, no. 2, pp. 485–510, 2018.
- [22] R. Zhang, M. Li, and B. Liu, “Pricing decisions and provider choice on extended warranty service in supply chain,” *International Journal of Information Systems and Supply Chain Management*, vol. 12, no. 4, pp. 55–71, 2019.
- [23] K. Li, S. Mallik, and D. Chhajed, “Design of extended warranties in supply chains under additive demand,” *Production and Operations Management*, vol. 21, no. 4, pp. 730–746, 2012.
- [24] C. Su and X. Wang, “A two-stage preventive maintenance optimization model incorporating two-dimensional extended warranty,” *Reliability Engineering & System Safety*, vol. 155, pp. 169–178, 2016.
- [25] Y.-S. Huang, C.-D. Huang, and J.-W. Ho, “A customized two-dimensional extended warranty with preventive maintenance,” *European Journal of Operational Research*, vol. 257, no. 3, pp. 971–978, 2017.
- [26] J. Ashayeri, N. Ma, and R. Sotirov, “The redesign of a warranty distribution network with recovery processes,” *Transportation Research Part E: Logistics and Transportation Review*, vol. 77, pp. 184–197, 2015.
- [27] H. S. Heese, “Retail strategies for extended warranty sales and impact on manufacturer base warranties,” *Decision Sciences*, vol. 43, no. 2, pp. 341–367, 2012.
- [28] C. Su and J. Shen, “Analysis of extended warranty policies with different repair options,” *Engineering Failure Analysis*, vol. 25, pp. 49–62, 2012.
- [29] X. Qin, Q. Su, and S. H. Huang, “Extended warranty strategies for online shopping supply chain with competing suppliers considering component reliability,” *Journal of Systems Science and Systems Engineering*, vol. 26, no. 6, pp. 753–773, 2017.
- [30] D. T. Mai, T. Liu, M. D. S. Morris, and S. Sun, “Quality coordination with extended warranty for store-brand products,” *European Journal of Operational Research*, vol. 256, no. 2, pp. 524–532, 2017.
- [31] Z. He, D. Huang, and S. He, “Design of extended warranty service in a dual supply channel,” *Total Quality Management & Business Excellence*, vol. 29, no. 9–10, pp. 1089–1107, 2018.
- [32] X. Zhu, L. Yu, J. Zhang, C. Li, and Y. Zhao, “Warranty decision model and remanufacturing coordination mechanism in closed-loop supply chain: view from a consumer behavior perspective,” *Sustainability*, vol. 10, no. 12, p. 4738, 2018.
- [33] M. Afsahi and M. Shafiee, “A stochastic simulation-optimization model for base-warranty and extended-warranty decision-making of under- and out-of-warranty products,” *Reliability Engineering & System Safety*, vol. 197, Article ID 106772, 2020.
- [34] Y. Bian, S. Yan, W. Zhang, and H. Xu, “Warranty strategy in a supply chain when two retailer’s extended warranties bundled with the products,” *Journal of Systems Science and Systems Engineering*, vol. 24, no. 3, pp. 364–389, 2015.
- [35] Y.-Y. Wang and J. Li, “Research on pricing, service and logistic decision-making of E-supply chain with ‘Free Shipping’ strategy,” *Journal of Control and Decision*, vol. 5, no. 4, pp. 319–337, 2018.
- [36] S. Pokharel and Y. Liang, “A model to evaluate acquisition price and quantity of used products for remanufacturing,” *International Journal of Production Economics*, vol. 138, no. 1, pp. 170–176, 2012.
- [37] C.-H. Wu, “Price and service competition between new and remanufactured products in a two-echelon supply chain,” *International Journal of Production Economics*, vol. 140, no. 1, pp. 496–507, 2012.
- [38] F. Otrodi, R. G. Yaghin, and S. A. Torabi, “Joint pricing and lot-sizing for a perishable item under two-level trade credit with multiple demand classes,” *Computers & Industrial Engineering*, vol. 127, pp. 761–777, 2019.
- [39] F. Samadi, A. Mirzazadeh, and M. M. Pedram, “Fuzzy pricing, marketing and service planning in a fuzzy inventory model: a geometric programming approach,” *Applied Mathematical Modelling*, vol. 37, no. 10–11, pp. 6683–6694, 2013.
- [40] R. Y. Yaghin, “Enhancing supply chain production-marketing planning with geometric multivariate demand function (a case study of textile industry),” *Computers & Industrial Engineering*, vol. 140, 2020.
- [41] R. Y. Chenavaz, G. Feichtinger, R. F. Hartl, and P. M. Kort, “Modeling the impact of product quality on dynamic pricing and advertising policies,” *European Journal of Operational Research*, vol. 284, no. 3, pp. 990–1001, 2020.
- [42] M. Klausner and C. T. Hendrickson, “Reverse-logistics strategy for product take-back,” *Interfaces*, vol. 30, no. 3, pp. 156–165, 2000.

Research Article

Supply Chain Flexibility Evaluation Based on Matter-Element Extension

Xiaochun Luo ^{1,2}, Zilong Wang,¹ Lin Lu ² and Yan Guan²

¹College of Economics and Management, Nanjing University of Aeronautics and Astronautics, Nanjing, China

²College of Economics and Management, Guangxi Normal University, Guilin, China

Correspondence should be addressed to Lin Lu; lulin355@163.com

Received 27 March 2020; Revised 4 May 2020; Accepted 7 May 2020; Published 20 May 2020

Academic Editor: Abdelalim Elsadany

Copyright © 2020 Xiaochun Luo et al. This is an open access article distributed under the Creative Commons Attribution License, which permits unrestricted use, distribution, and reproduction in any medium, provided the original work is properly cited.

Flexibility is an important indicator to consider the uncertain information processing ability of the supply chain comprehensively. It is a powerful way to improve the efficiency and quality of supply chain operation by evaluating the level of supply chain flexibility effectively. The traditional method is used to decompose the supply chain flexibility evaluation indicators from the perspective of system structure or cost saving, but these indicators cannot truly describe the dynamics of the supply chain operation. Otherwise, supply chain flexibility evaluation is a typical multiobjective evaluation; there are some incompatibilities between these flexible evaluation indicators, and the common evaluation methods are difficult to deal with such contradictions. In this paper, the dynamic characteristics of supply chain operation are considered, and the evaluation system of supply chain flexibility is designed from the perspective of operation efficiency. The matter-element analysis theory is used to create the comprehensive appraisal model of supply chain flexibility. The matter-element matrix solves the uncertainty and incompatibility of the evaluated factors used to assess supply chain flexibility. The paper evaluates the performance of four autoservice companies and concludes that the evaluation grades of the four companies are in line with the reality, indicating that the evaluation system and the method are effective and credible.

1. Introduction

Internet information technology has promoted tremendous changes in the functions and roles of market participants. Consumers have gradually replaced producers and enterprises as the main force of economic operation, which is the core force of promoting production and market reform. Under the influence of information technology, the consumer market environment has distinct characteristics of the times: diversification, speediness, individuation, and to a greater extent, it is easy to be influenced by the herd effect. Unpredictable changes in the market environment increase the risk of business operation and investment, so the “horizontal integration” mode of thinking came into being, that is, for the flow of logistics, capital flow, information flow, and other elements among enterprises in the supply chain, to carry out efficient, integrated, seamless, real-time, and effective management, so as to promote the organic cooperation between enterprises and enhance the

competition of the whole supply chain strive to maximize the performance of the whole supply chain. The uncertainty of the market environment and the existence of risk factors make the supply chain enterprises to respond to the unexpected situation of market environment quickly. Supply chain flexibility is an important tool for dealing with uncertain information. Improving the level of supply chain flexibility plays a very positive role in improving the overall operation efficiency of the supply chain and maintaining the core competitiveness of the enterprise. It is an important way to improve the operation quality of the supply chain.

In the supply chain management environment, flexibility refers to the ability of supply chain managers to quickly and effectively reconfigure the internal supply chain in order to adapt to the changing market demand, so as to cope with the uncertainty of the internal and external environment [1, 2]. With the increasing dynamic and uncertainty of business environment and the shortening of product life cycle, the ability to respond quickly to changes becomes more and

more important for core enterprises and the whole supply chain [3]. Supply chain flexibility can not only show the ability of quick response to environmental changes but also has a certain strategic role [4], such as helping enterprises to make profits and meet customers' changing needs [5].

The research on the dimensions of the supply chain flexible system mainly includes the dimensions of supply flexibility and manufacturing flexibility [6], process flexibility and holding product inventory [7], flexible structure deployment information technology [8], supply chain contract [9], order fulfillment flexibility [10], and operation and organization absorption flexibility [11]. The evaluation indicators of supply chain flexibility are diversified. From the perspective of performance, they are divided into four primary indicators: supply chain re-engineering flexibility, supply chain collaboration flexibility, supply chain flexibility, and the establishment of supply chain risk management culture [12]. From the perspective of supply chain agility, they can be divided into 25 evaluation indicators such as organizational structure flexibility, production flexibility, market scheduling flexibility, quality control flexibility, organizational flexibility, operation flexibility, customer service flexibility, organizational structure flexibility, effective prediction flexibility, and logistics management flexibility [13], or they can be divided into 22 evaluation indicators, such as supplier flexibility, coordination flexibility among supply chain members, fast response ability, fast conversion ability, information transparency, design flexibility, production and delivery flexibility, labor flexibility, quality level, innovation degree, etc. [14]. From the perspective of organizational hierarchy, they can be divided into operational flexibility (workshop and resource level) [15], strategic flexibility (company level) [16], tactical flexibility (plant level) [17], and supply chain flexibility (network level) [18]. It is impossible to measure the flexibility of the whole supply chain by a single standard. An analysis method [19] that can evaluate the flexibility of the supply chain comprehensively and continuously is needed, such as AHP [20] and sensitivity analysis [21].

Most of the existing literature mainly focus on the supply chain model, supply chain integration, supply chain flexibility measurement, supply chain flexibility strategic level planning, and tactical level implementation and rarely involve the coexistence of incompatible indicators in the supply chain flexibility evaluation, as well as the integration of qualitative and quantitative evaluation; in addition, the traditional evaluation methods are single; only considering the results caused by a single factor cannot reflect the results caused by multiple factors, and supply chain flexibility may be accumulated through internal factors. In view of the above limitations, this paper puts forward the matter-element extension theory, which can completely and comprehensively reflect the different characteristics of the evaluation research object and overcome the disadvantages of the traditional evaluation method which can only select one-sided factors and may lead to the accidental results. At the same time, extension theory can flexibly change the evaluation indicator according to the actual characteristics of the evaluation object, and the application of the model will

not be rigid. Using this method to solve the complex problem of the incompatibility of service supply chain flexibility and to make a reasonable distinction between the level of service supply chain flexibility can effectively achieve the compatibility of multiple evaluation indicators.

2. Construction of the Supply Chain Flexibility Evaluation Indicator System

According to the connotation of supply chain flexibility, by analyzing the actual operation management of the supply chain and referring to the existing literature research results, this paper expands and extends the flexibility indicator according to the characteristics of dynamic operation of the supply chain. Supply network, operation system, internal and external organizational structure design, and information system are considered as an indispensable part of the supply chain. From the perspective of these parts, the supply chain flexibility is decomposed into ten primary indicators, such as service category and quantity flexibility, human resource flexibility, capital flexibility, logistics flexibility, and partner flexibility, each of which can be decomposed into several secondary indicators.

2.1. Service Category and Quantity Flexibility. Service category and quantity flexibility can measure the range of service category that an organization or enterprise can operate under the condition of profit, which is often related to the variety and quantity of service products that an organization can provide and the cost change brought by such change. There are four secondary indicators under such flexible indicators, including customer order missing rate (mainly involving service product inventory, demand, and shortage), average delayed order rate (mainly involving order urgency, service production capacity, service resource inventory level, and service delivery capacity), average early delivery service rate (reflecting that customers are within the acceptable time range, the ability of the enterprise to submit service first), and average customer waiting rate (mainly related to order quantity, production capacity, and service product delivery path).

2.2. Human Resource Flexibility. Human resource flexibility includes two secondary indicators: skill flexibility and behavior flexibility. Skill flexibility refers to that employees have a wealth of knowledge and skills and that enterprises can provide employees with a large number of learning and training time and opportunities so that employees can obtain the skills needed for multiple posts and different services, so as to flexibly respond to the changes of the working environment and work requirements. It mainly involves the mastery and application of skills, skill training, job rotation, job enrichment and expansion, and the adaptation of skills acquired by employees to the environment. Behavior flexibility refers to the long-term professional training of behavior or service skills, which enables employees to flexibly use a variety of preset and prepared behavior script sets to deal with emergencies in the process

of work. It mainly involves the behaviors of employees at work, as well as the adaptation of these behaviors to environmental changes and new work contents.

2.3. Capital Flexibility. Capital flexibility includes three secondary indicators: financing capacity flexibility, profitability flexibility, and price flexibility. Among them, the flexibility of financing ability is reflected by the financing cost rate, the flexibility of profitability is reflected by the operating profit rate, and the flexibility of price reflects the adjustable price space that the product can expand when the enterprise realizes the profit.

2.4. Logistics Flexibility. For the supply chain, reducing the cost of transportation, purchasing, and inventory is the key. Logistics flexibility mainly includes three secondary indicators: inventory turnover, diversity of transportation channels available, and distribution accuracy. The high indicator of inventory turnover indicates that the supply chain has a high level of flexibility. Diversity of transportation channels available reflects the ability of the supply chain to quickly select different transportation channels and modes in case of emergency. Distribution accuracy can reflect the ability of zero error distribution of raw materials, semifinished products, spare parts, and other necessary products from the upstream of the supply chain. This indicator is particularly important when the external environment changes.

2.5. Partner Flexibility. The increasingly fierce market competition makes the organic cooperation of all links in the supply chain more important. Partner flexibility is reflected in the ability of enterprises to change and adjust their partners in time when the external environment changes. Partner flexibility includes three secondary indicators: trust mechanisms' build capacity, knowledge sharing rate, and the number of partners that can be selected in time. The more willing and knowledge sharing partners are, the more partners can be adjusted in time and the higher the flexibility level of the supply chain.

2.6. Production Equipment Flexibility. Production equipment flexibility includes three secondary indicators: production equipment trouble-free continuous operation efficiency, maintenance rate of production equipment, and actual productivity of production equipment.

2.7. Technical Flexibility. Technical flexibility is the difficulty of the process of original technology updating and leaping over to new technology, including two secondary indicators of original technology and new technology.

2.8. Time Flexibility. Time flexibility reflects the time needed for the supply chain to respond to customers' needs in time, including two secondary indicators: degree of timely response and delivery flexibility. The higher the degree of

timely response, the shorter the response time and the higher the level of supply chain flexibility. Delivery flexibility reflects the ability of the supply chain to respond to changes when delivery time changes.

2.9. Service Supply Flexibility. Service supply flexibility includes two dimensions: hybrid flexibility and new service supply flexibility.

Hybrid flexibility can not only measure the maximum range of different kinds of services that enterprises can produce or provide in a specific time but also measure the response time that service providers need to change the service product mix, including two secondary indicators: hybrid flexibility range and hybrid flexibility time.

New service supply flexibility reflects the degree of difficulty for enterprises to produce or introduce new service products. On the one hand, it considers the time needed for new service products to be introduced into the existing supply system, and on the other hand, it considers the cost needed for the existing service supply system to introduce new service products, including two secondary indicators: new service flexibility time and new service flexibility cost.

2.10. Information Response Flexibility. Information response flexibility of the supply chain is embodied in the ability of members of the supply chain to accept and take action in time to process business information, including three secondary indicators: information response time, information response range, and information distribution accuracy. Information response time is the time taken by each entity in the supply chain to receive and respond to business information. Information response range is the range that the information system can accept and respond to information at the same time. Information distribution accuracy can reflect the ability of the supply chain information system to deal with uncertainty.

According to the above content, the supply chain flexible evaluation indicator system is constructed, which is divided into primary indicators, secondary indicators, secondary indicator description, and indicator nature. The quantitative indicators in secondary indicators are expressed by the calculation formula according to the indicator meaning and data availability. The evaluation standard division of qualitative indicators can be referred to previous studies or yearbook data related to indicators, as shown in Table 1.

3. Construct the Matter-Element Model of Supply Chain Flexibility Evaluation

Extension theory was founded by Chinese scholar Cai [22] in the 1980s. It combines matter-element theory with extension set theory, studies matter-element and its changing trend, and studies and solves the changing law of complex problems in a qualitative and quantitative way. The important feature of this theory is that it provides an effective tool to solve the problem of incompatibility. Based on the matter-element model, extension set, and correlation function theory of extension science, the method of multi-indicator

TABLE 1: Supply chain flexibility evaluation indicator system.

Primary indicators	Secondary indicators	Secondary indicator description	Indicator nature	
Service category and quantity flexibility, p_1	Customer order missing rate, c_1	Number of service delivery failures/total number of service products available	Quantitative	Negative
	Average delayed order rate, c_2	Number of delayed services/total number of service products available	Quantitative	Negative
	Average early delivery service rate, c_3	Number of services provided in advance/total number of service products available	Quantitative	Positive
	Average customer waiting rate, c_4	Number of customers waiting for service/total number of times to receive service products	Quantitative	Negative
Human resource flexibility, p_2	Skill flexibility, c_5	The classification of evaluation criteria can be referred to the previous studies, for example, it can be divided according to the following dimensions: (1) The number of effective skills currently possessed by human resources (2) The speed of human resources learning new and effective skills (3) The ability to quickly reintegrate and reconfigure multiple skill value chains	Qualitative	Positive
		The classification of evaluation criteria can be referred to the previous studies, for example, it can be divided according to the following dimensions: (1) The ability of human resources to “script” beneficial behaviors (2) The ability to coordinate and integrate multiple behavioral “scripts”		
Capital flexibility, p_3	Behavioral flexibility, c_6	(1) The ability of human resources to “script” beneficial behaviors (2) The ability to coordinate and integrate multiple behavioral “scripts”	Qualitative	Positive
	Financing capacity flexibility, c_7	Fund use fee/(total amount of financing – financing expenses)	Quantitative	Negative
	Profitability flexibility, c_8	Operating profit/sales revenue	Quantitative	Positive
	Price flexibility, c_9	Average market price of products – product actual cost	Quantitative	Positive
Logistics flexibility, p_4	Inventory turnover, c_{10}	Cost of sales/average inventory balance	Quantitative	Positive
		The division of the evaluation criteria can be referred to the China statistical yearbook on transportation, for example, it can be divided into the following sections: (1) Be able to select five modes of transportation to cope with the change of service demand, scoring range (2) Be able to select more than three modes of transportation to cope with the change of service demand, scoring range (3) Only two or more modes of transportation can be selected to cope with the change of service demand, scoring range (4) Single transportation channel, only able to meet the most basic needs of customers, scoring range	Qualitative	Positive
	Diversity of transportation channels available, c_{11}	Number of orders delivered correctly/number of delivered orders		
	Distribution accuracy, c_{12}	Number of orders delivered correctly/number of delivered orders	Quantitative	Positive

TABLE 1: Continued.

Primary indicators	Secondary indicators	Secondary indicator description	Indicator nature				
Partner flexibility, p_5	Trust mechanisms' build capacity, c_{13}	The evaluation criteria can be divided according to the previous studies, for example, they can be divided into the following intervals: (1) Have a common strategic goal and can share risks in a complex environment (2) In the event of divergence of interest, it is necessary to resolve the conflict through consultation and discussion (3) It has a normal cooperative relationship on the premise of not violating the signed contract or contract (4) There are often disagreements and contradictions in the decision-making of key issues	Qualitative	Positive			
		Knowledge sharing rate, c_{14}			The amount of knowledge shared by enterprises in time and accurately/the amount of knowledge enterprises should share	Quantitative	Positive
		Number of partners that can be selected in time, c_{15}			Number of partners with fast access + number of partners that can exit quickly	Quantitative	Positive
Production equipment flexibility, p_6	Production equipment trouble-free continuous operation efficiency, c_{16}	Production equipment trouble-free operation time/total operation time of production equipment	Quantitative	Positive			
	Maintenance rate of production equipment, c_{17}	Number of production equipment actually maintained/total production equipment	Quantitative	Negative			
	Actual productivity of production equipment, c_{18}	Actual capacity of production equipment/maximum capacity of production equipment	Quantitative	Positive			
Technical flexibility, p_7	Original technology, c_{19}	The classification of evaluation criteria can refer to previous studies, for example, it can be divided according to the following dimensions: (1) The degree to which a product and/or service can be added (2) Scope of application to a variety of products and technologies (3) It helps to improve customers' sense of identity with products and technologies	Qualitative	Positive			
		New technique, c_{20}			The classification of evaluation criteria can refer to the previous studies, for example, it can be divided according to the following dimensions: (1) Ability to develop new technologies (2) The ability to introduce new technology into enterprise activities (3) Innovation and transformation ability of new technology	Qualitative	Positive
					Degree of timely response, c_{21}		
Time flexibility, p_8	Delivery capability, c_{22}	Delivery time that can be shortened/total time required to complete delivery	Quantitative	Positive			
	Hybrid flexible range, c_{23}	Types and quantities of products that can be provided by enterprises in each link of the supply chain in a certain period of time	Quantitative	Positive			
Service supply flexibility, p_9	Hybrid flexibility time, c_{24}	The transition time required to change from one product mix type to another	Quantitative	Negative			
	New service flexibility time, c_{25}	Time required to introduce a new service portfolio	Quantitative	Negative			
	New service flexibility cost, c_{26}	Cost of introducing new service products	Quantitative	Negative			
	Information response time, c_{27}	Information acquisition time + processing time + feedback time	Quantitative	Negative			
Information response flexibility, p_{10}	Information response range, c_{28}	The total number of information that an enterprise can respond effectively/number of members that an enterprise can connect to	Quantitative	Positive			
	Information distribution accuracy, c_{29}	Number of accurate information/number of all information	Quantitative	Positive			

extension comprehensive analysis is a new method of multivariate data quantitative decision-making. In this study, matter-element is used to describe the level and object of supply chain flexibility, extension set, and correlation function which are used to establish the evaluation criteria and the degree of supply chain flexibility, and a multi-attribute evaluation model is established to represent the level of supply chain flexibility.

3.1. Matter-Element Model of Supply Chain Flexibility. Suppose the supply chain flexibility is N , and its quantitative value about feature C is V ; then, this ternary ordered group is called the fundamental element of things, referred to as matter-element, denoted as $R = (N, C, V)$. N , C , and V are called the three elements of matter-element R . If the supply chain flexibility has n characteristics, it is denoted as $c_1, c_2, c_3, \dots, c_n$, and the corresponding characteristic value is denoted as $v_1, v_2, v_3, \dots, v_n$; then, R is denoted as n -dimensional matter-element, which can be expressed as the following formula [22, 23]:

$$R = (N, C, V) = \begin{bmatrix} N & c_1 & v_1 \\ & c_2 & v_2 \\ & \vdots & \vdots \\ & c_n & v_n \end{bmatrix}. \quad (1)$$

3.2. Evaluation Model of Supply Chain Flexibility

3.2.1. Classical Domain, Node Domain, and Object to Be Evaluated of Supply Chain Flexibility. Classical domain refers to the value range of each supply chain flexibility evaluation indicator under different levels of supply chain flexibility. There are m supply chain flexibility levels N_1, N_2, \dots, N_m , and the corresponding matter-elements are established as shown in the following formula [22, 23]:

$$R_j = (N_j, c_i, v_{ij}) = \begin{bmatrix} N_j & c_1 & v_{1j} \\ & c_2 & v_{2j} \\ & \vdots & \vdots \\ & c_n & v_{nj} \end{bmatrix} = \begin{bmatrix} N_j & c_1 & \langle a_{1j}, b_{1j} \rangle \\ & c_2 & \langle a_{2j}, b_{2j} \rangle \\ & \vdots & \vdots \\ & c_n & \langle a_{nj}, b_{nj} \rangle \end{bmatrix}, \quad (2)$$

where N_j represent the divided j ($j = 1, 2, \dots, m$) supply chain flexible grades, c_i ($i = 1, 2, \dots, n$) represent the N_j characteristics of the supply chain flexible grades, v_{ij} represents the quantitative value range of c_i specified by N_j , that is, the numerical range of each supply chain flexible grade with respect to the corresponding characteristics represented by $v_{ij} = \langle a_{ij}, b_{ij} \rangle$, a_{ij} and b_{ij} are the upper and lower limits of the classical domain, respectively, and R_j is the classical domain of supply chain flexibility.

Its nodal domain R_p is constructed by the classical domain, and $R_p = R_j$, as shown in the following formula [22, 23]:

$$R_p = (N_p, c_i, v_{ip}) = \begin{bmatrix} N_p & c_1 & v_{1p} \\ & c_2 & v_{2p} \\ & \vdots & \vdots \\ & c_n & v_{np} \end{bmatrix} = \begin{bmatrix} N_p & c_1 & \langle a_{1p}, b_{1p} \rangle \\ & c_2 & \langle a_{2p}, b_{2p} \rangle \\ & \vdots & \vdots \\ & c_n & \langle a_{np}, b_{np} \rangle \end{bmatrix}, \quad (3)$$

where N_p represents the total supply chain flexibility level and v_{ip} is the range of values taken by N_p with respect to c_i represented by $v_{ip} = \langle a_{ip}, b_{ip} \rangle$, a_{ip} and b_{ip} are the upper and lower limits of the node domain, respectively.

For the object to be evaluated, the evaluation indicator information is represented by matter-element, which is called the flexible object of the supply chain to be evaluated, as shown in the following formula [22, 23]:

$$R_o = (P_o, c_i, t_i) = \begin{bmatrix} P_o & c_1 & t_1 \\ & c_2 & t_2 \\ & \vdots & \vdots \\ & c_n & t_n \end{bmatrix}, \quad (4)$$

where P_o is the matter-element to be evaluated and t_i is the measurement value of P_o with respect to c_i , that is, the actual measurement value of the indicator of the object to be evaluated.

3.2.2. Calculate the Correlation Degree of Supply Chain Flexibility. The correlation degree of each supply chain flexibility level of the object to be evaluated is calculated by the correlation function. The value of the i ($i = 1, 2, \dots, n$)-th indicator belongs to the correlation function of the j ($j = 1, 2, \dots, m$)-th supply chain flexibility level, as shown in the following formula [22, 23]:

$$K_j(t_i) = \begin{cases} \frac{\rho(t_i, v_{ij})}{\rho(t_i, v_{ip}) - \rho(t_i, v_{ij})}, & t_i \notin v_{ij}, \\ \frac{-\rho(t_i, v_{ij})}{|v_{ij}|}, & t_i \in v_{ij}, \end{cases} \quad (5)$$

where $K_j(t_i)$ is the correlation degree of each supply chain flexibility indicator with respect to each evaluation level, $\rho(t_i, v_{ij})$ is the distance between t_i and $v_{ij} = \langle a_{ij}, b_{ij} \rangle$ in a finite interval, and $\rho(t_i, v_{ip})$ is the distance between t_i and $v_{ip} = \langle a_{ip}, b_{ip} \rangle$ in a finite interval, and the distance calculation formulae are shown in formulae (6) and (7) [22, 23]:

$$\rho(t_i, v_{ij}) = \left| t_i - \frac{1}{2}(a_{ij} + b_{ij}) \right| - \frac{1}{2}(b_{ij} - a_{ij}), \quad (6)$$

$$\rho(t_i, v_{ip}) = \left| t_i - \frac{1}{2}(a_{ip} + b_{ip}) \right| - \frac{1}{2}(b_{ip} - a_{ip}). \quad (7)$$

3.2.3. Calculate the Weight of the Evaluation Indicator. The supply chain flexibility is regarded as a system, and each evaluation indicator is a subsystem. The value of each

evaluation object under the indicator can be regarded as the possible result of the subsystem, and the entropy weight of the indicator can be calculated according to its probability. According to the definition of entropy, the entropy of m evaluation objects and n indicators is calculated as shown in the following formula [24]:

$$E_i = -\frac{\sum_{j=1}^m T_{ij} \ln T_{ij}}{\ln m}, \quad i = 1, 2, \dots, n; j = 1, 2, \dots, m, \quad (8)$$

where $T_{ij} = (t_{ij} / \sum_{j=1}^m t_{ij}) (T_{ij} \neq 0)$ and $T_{ij} = ((1 + t_{ij}) / \sum_{j=1}^m (1 + t_{ij})) (T_{ij} = 0)$, t_{ij} is the value of the i -th indicator of the j -th evaluation object. The calculation formulae of entropy weight λ_i and weight W of evaluation indicators are shown in formulae (9) and (10) [24]:

$$\lambda_i = \frac{1 - E_i}{\sum_{i=1}^n (1 - E_i)}, \quad (9)$$

$$W = (\lambda_i)_{1 \times n}. \quad (10)$$

3.2.4. Calculation of Comprehensive Correlation Degree and Evaluation of Grade. The correlation degree between each evaluation indicator and the grade standard is weighted and summed to get the comprehensive correlation degree, as shown in the following formula [22, 23]:

$$K_j(R_o) = \sum_{i=1}^n \lambda_i K_j(t_i). \quad (11)$$

If $K_j(R_o) = \max\{K_j(R_o)\} (j = 1, 2, \dots, m)$, then the supply chain flexibility grade is j .

4. Example Analysis

In recent years, the automobile service industry has been developing rapidly in China, and its supply chain flexibility is representative. In this paper, four automobile service companies (A, B, C, and D) in N city of China are selected as research objects to evaluate and analyze their supply chain flexibility.

4.1. Supply Chain Flexibility Classification. In order to better reflect the level of supply chain flexibility, it is necessary to classify the level of supply chain flexibility of the automobile service industry. The supply chain flexibility level is divided into four levels according to industry reports over the years such as China's automobile service industry market status survey and development prospect analysis report (2019–2025) and China's automobile service industry development status survey and development trend analysis report (2018–2024). The level of supply chain flexibility from superior to inferior corresponds to I (excellent), II (good), III (medium), and IV (poor), and the meaning of each level of supply chain flexibility is shown in Table 2. By using the concept of the extension set, the gradual classification relationship of {excellent \rightarrow good \rightarrow medium \rightarrow poor} is extended from qualitative description to quantitative

description, so as to identify the hierarchical relationship of this concept. The evaluation of supply chain flexibility is expressed as $P = \{\text{excellent} \rightarrow \text{good} \rightarrow \text{medium} \rightarrow \text{poor}\}$, $I = \{\text{excellent}\}$, $II = \{\text{good}\}$, $III = \{\text{medium}\}$, and $IV = \{\text{poor}\}$, $I, II, III, IV \in P$. For any $p \in P$, it is judged that it belongs to I, II, III, or IV.

4.2. Determination of Classical Domain, Nodal Domain, and Weight. To autoservice industry based on the above cognizance of flexible supply chain hierarchies, combined with years of China's autoservice industry market research report, in reference to the China N city area actual situation on the basis of the background value and expert advice, determine range of supply chain flexible evaluation of each indicator hierarchy standard, the resulting classical domain and joint domain value interval values, and by formulae (8)~(10) to determine evaluation indicator weights, and the results are shown in Table 3.

4.3. Determination of Matter-Element to Be Evaluated. To evaluate the supply chain flexibility level of four automobile service companies (company A, company B, company C, and company D) in N city, China, it is necessary to determine the actual value of each company's supply chain flexibility to be evaluated, that is, t_i in formula (4). The evaluation indicator system constructed in this paper has 29 secondary indicators, including 23 quantitative indicators and 6 qualitative indicators. The acquisition of quantitative indicator data is mainly through the collection of the original data of each company, including the company's operation report, financial report, annual report, and field research data. The qualitative indicator data were obtained mainly by means of self-filled questionnaire and structured interview, and a seven-level Likert scale was designed for experts and staff to evaluate and score the indicator and quantify the qualitative indicator. After the positive indicator is quantified, the higher the score is, the higher the flexibility level of the indicator is. According to this, the supply chain flexible matter-element models of four automobile service companies are constructed.

4.4. Calculation of Correlation Degree and Determination of Evaluation Grade. According to the volume value t_i of each evaluation indicator c_i of the automobile service company and formulae (5)~(7), the correlation degree $K_j(t_i)$ of each company's supply chain flexibility evaluation secondary indicator with respect to the evaluation grade can be obtained, respectively. By judging the degree that the actual volume value t_i in the object to be evaluated R_o tends to the adjacent grade N_j , it can reflect a trend of the level change of the object to be evaluated. If $K_j(t_i) < -1$, it means that the supply chain flexibility does not belong to grade j and does not have the conditions to meet the grade standard; the smaller the value is, the larger the gap is; if $-1 \leq K_j(t_i) \leq 0$, it means that the supply chain flexibility does not belong to grade j but has the conditions to convert to the grade; the larger the value is, the easier to convert; and if $K_j(t_i) > 0$, it means that the supply chain flexibility meets the

TABLE 2: Classification of supply chain flexibility in the automobile service industry.

Grade	Characterization of supply chain flexibility grade
I (excellent)	(1) The specialty of the supply chain, the adaptability, and flexibility of service are strong
	(2) On the basis of specialization, it tends to be more personalized
	(3) It has a strong ability to effectively respond to changes in demand, a strong ability to respond to service supply chain, and a high level of flexibility
II (good)	(1) The specialty of the supply chain, the adaptability, and flexibility of service are stronger
	(2) On the basis of specialization, it can be more personalized
	(3) The ability to effectively respond to the change of demand is stronger, the response ability of service supply chain is stronger, and the level of flexibility is higher
III (medium)	(1) The specialty of the supply chain, the adaptability, and flexibility of service are general
	(2) The flow efficiency of information exchange among the main parts of the supply chain is general.
	(3) The ability to effectively respond to changes in demand is general, the response ability of the supply chain is general, and the level of flexibility is general
IV (poor)	(1) The specialty of the supply chain, the adaptability, and flexibility of service are weak
	(2) The flow efficiency of information exchange among the main parts of the supply chain is low
	(3) The ability to deal with the change of demand effectively is weak, the response ability of the supply chain is weak, and the level of flexibility is low

TABLE 3: Classic domain, node domain, and weight of supply chain flexibility evaluation indicators of the automobile service industry.

Indicators	Classical domain value interval				Node domain value interval	Weight
	I (excellent)	II (good)	III (medium)	IV (poor)		
c_1	[0, 0.056]	[0.056, 0.166]	[0.166, 0.222]	[0.222, 0.333]	[0, 0.333]	0.0886
c_2	[0.053, 0.156]	[0.156, 0.215]	[0.215, 0.315]	[0.315, 0.421]	[0.053, 0.421]	0.0151
c_3	[0.85, 0.94]	[0.75, 0.85]	[0.65, 0.75]	[0.55, 0.65]	[0.55, 0.94]	0.0079
c_4	[0, 0.166]	[0.166, 0.253]	[0.253, 0.368]	[0.368, 0.588]	[0, 0.588]	0.0065
c_5	[6, 7]	[4, 6]	[2, 4]	[1, 2]	[6, 7]	0.0014
c_6	[6, 7]	[5, 6]	[3, 5]	[1, 3]	[6, 7]	0.0003
c_7	[0.1, 0.3]	[0.3, 0.4]	[0.4, 0.5]	[0.5, 0.7]	[0.1, 0.7]	0.0882
c_8	[0.17, 0.25]	[0.15, 0.17]	[0.04, 0.15]	[0.01, 0.04]	[0.01, 0.25]	0.0383
c_9	[279, 360]	[200, 279]	[119, 200]	[87, 119]	[87, 360]	0.0805
c_{10}	[5.54, 7.29]	[3.13, 5.54]	[0.95, 3.13]	[0.65, 0.95]	[0.65, 7.29]	0.1416
c_{11}	[6, 7]	[4, 6]	[2, 4]	[1, 2]	[1, 7]	0.1280
c_{12}	[0.94, 1]	[0.79, 0.94]	[0.62, 0.79]	[0.38, 0.62]	[0.38, 1]	0.0124
c_{13}	[6, 7]	[4, 6]	[2, 4]	[1, 2]	[1, 7]	0.1282
c_{14}	[0.82, 0.94]	[0.64, 0.82]	[0.49, 0.64]	[0.23, 0.49]	[0.23, 0.94]	0.0476
c_{15}	[17, 20]	[14, 17]	[9, 14]	[5, 9]	[5, 20]	0.0656
c_{16}	[0.71, 0.98]	[0.63, 0.71]	[0.51, 0.63]	[0.32, 0.51]	[0.32, 0.98]	0.0033
c_{17}	[0.11, 0.23]	[0.23, 0.41]	[0.41, 0.57]	[0.57, 0.72]	[0.11, 0.72]	0.0107
c_{18}	[0.9, 1]	[0.8, 0.9]	[0.7, 0.8]	[0.6, 0.7]	[0.6, 1]	0.0013
c_{19}	[6, 7]	[5, 6]	[4, 5]	[3, 4]	[3, 7]	0.0142
c_{20}	[6, 7]	[5, 6]	[4, 5]	[3, 4]	[3, 7]	0.0019
c_{21}	[0.37, 0.48]	[0.48, 0.51]	[0.51, 0.65]	[0.65, 0.98]	[0.37, 0.98]	0.0077
c_{22}	[0.76, 0.85]	[0.59, 0.76]	[0.29, 0.59]	[0.09, 0.29]	[0.09, 0.85]	0.0429
c_{23}	[20, 30]	[15, 20]	[11, 15]	[5, 11]	[5, 30]	0.0078
c_{24}	[1, 2]	[2, 3]	[3, 6]	[6, 7]	[1, 7]	0.0025
c_{25}	[1, 2]	[2, 3]	[3, 4]	[4, 5]	[1, 5]	0.0197
c_{26}	[7, 9]	[9, 13]	[13, 17]	[17, 24]	[7, 24]	0.0181
c_{27}	[3, 5]	[5, 7]	[7, 9]	[9, 14]	[3, 14]	0.0073
c_{28}	[0.8, 0.9]	[0.7, 0.8]	[0.5, 0.7]	[0.3, 0.5]	[0.3, 0.9]	0.0071
c_{29}	[0.84, 0.92]	[0.77, 0.84]	[0.6, 0.77]	[0.42, 0.6]	[0.42, 0.92]	0.0052

requirements of grade j , the higher the value is. Tables 4 and 5 show the secondary indicator correlation and evaluation grade of supply chain flexibility evaluation of four automobile service companies.

By substituting the weight of each indicator in Table 3 and the correlation degree $K_j(t_i)$ of each secondary indicator in Table 4 into formula (11), the correlation degree and

comprehensive correlation degree of the primary indicators of supply chain flexibility evaluation from company A to company D can be obtained, respectively, so as to evaluate the correlation degree of each company's primary indicators of supply chain flexibility and the level of each company's supply chain flexibility. The calculation results are shown in Tables 6–8.

TABLE 4: Secondary indicator correlation degree and grade of supply chain flexibility evaluation of companies A and B.

Indicators	Company A				Grade	Company B				Grade
	I	II	III	IV		I	II	III	IV	
c_1	0.0607	-0.0607	-0.6831	-0.7631	Excellent	-0.3187	0.4473	-0.3663	-0.5261	Good
c_2	-0.2571	0.0763	-0.0278	-0.3989	Good	-0.0169	0.0305	-0.3531	-0.6000	Good
c_3	-0.7283	-0.5925	-0.1850	0.1850	Poor	-0.2869	0.3940	-0.2074	-0.4807	Good
c_4	-0.3964	-0.2397	0.3017	-0.1199	Medium	-0.5822	-0.4737	-0.1986	0.1986	Poor
c_5	-0.3503	0.4150	-0.2767	-0.5660	Good	-0.3848	0.1650	-0.1100	-0.4660	Good
c_6	-0.3322	0.0100	-0.0050	-0.5025	Good	-0.3408	-0.0327	0.0350	-0.4825	Medium
c_7	0.0105	-0.0105	-0.3403	-0.5053	Excellent	0.3290	-0.3290	-0.5527	-0.6645	Excellent
c_8	-0.4825	-0.4086	0.4800	-0.3894	Medium	-0.2475	-0.1387	0.1745	-0.4324	Medium
c_9	-0.8177	-0.6903	0.0370	-0.0789	Medium	-0.1955	0.3291	-0.3313	-0.5560	Good
c_{10}	-0.9425	-0.8867	-0.0630	0.0630	Poor	-0.3044	0.4350	-0.2520	-0.5092	Good
c_{11}	-0.8600	-0.7667	-0.3000	0.3000	Poor	-0.3077	0.4000	-0.4000	-0.6400	Good
c_{12}	-0.6802	-0.5632	-0.2538	0.2538	Poor	-0.4005	0.1953	-0.1395	-0.5245	Good
c_{13}	-0.8235	-0.7059	-0.1176	0.1176	Poor	-0.2730	0.3006	-0.4663	-0.6798	Good
c_{14}	-0.7429	-0.6300	-0.4165	0.4165	Poor	-0.1618	0.1594	-0.5043	-0.6696	Good
c_{15}	-0.9167	-0.8889	-0.7500	0.2500	Poor	-0.2857	0.3333	-0.1667	-0.5455	Good
c_{16}	0.2267	-0.2267	-0.4034	-0.5557	Excellent	0.3411	-0.3411	-0.4917	-0.6215	Excellent
c_{17}	-0.4286	-0.0968	0.1875	-0.3171	Medium	-0.5714	-0.3226	0.3750	-0.2222	Medium
c_{18}	-0.1984	0.3290	-0.3355	-0.5570	Good	0.0890	-0.0890	-0.5445	-0.6963	Excellent
c_{19}	-0.3214	0.1000	-0.0500	-0.3667	Good	-0.5667	-0.3500	0.3000	-0.1875	Medium
c_{20}	-0.2500	0.5000	-0.2500	-0.5000	Good	0.0400	-0.0400	-0.5200	-0.6800	Excellent
c_{21}	-0.8732	-0.8651	-0.8079	0.1921	Poor	-0.5534	-0.5249	-0.3233	0.3233	Poor
c_{22}	-0.9651	-0.9532	-0.8830	0.1170	Poor	-0.8245	-0.7648	-0.4120	0.4120	Poor
c_{23}	-0.0833	0.2000	-0.2667	-0.4211	Good	-0.2000	0.4000	-0.1429	-0.3333	Good
c_{24}	-0.8400	-0.8000	-0.2000	0.2000	Poor	-0.8800	-0.8500	-0.4000	0.4000	Poor
c_{25}	-0.4333	-0.1500	0.3000	-0.2917	Medium	-0.5000	-0.2500	0.5000	-0.2500	Medium
c_{26}	-0.4167	-0.1250	0.2500	-0.3000	Medium	-0.3333	0.5000	-0.3333	-0.6000	Good
c_{27}	-0.3750	-0.1667	0.5000	-0.1667	Medium	-0.5556	-0.4286	-0.2000	0.2000	Poor
c_{28}	-0.5118	-0.3898	0.2205	-0.1530	Medium	-0.3514	-0.0770	0.0910	-0.4545	Medium
c_{29}	-0.7381	-0.6857	-0.3889	0.3889	Poor	-0.6667	-0.6000	-0.2222	0.2222	Poor

4.5. *Data Analysis.* It can be seen from Table 8 that the comprehensive evaluation grade of company A is transformation to poor, company B is good, company C is medium, and company D is transformation to poor. It can be seen that company B has the highest rating among the four companies, which reflects its professional supply chain, strong ability to effectively respond to demand changes, and high flexibility. Company A and company D have weak adaptability, weak response ability, and low flexibility in the supply chain. The supply chain of company C is generally flexible.

The data in Tables 6 and 7 are used to analyze the results in Table 8, that is, the supply chain flexibility level of each company is analyzed one by one. Among the primary indicators of company B, there are one excellent, five good, two medium, one poor, one transformation to poor, 80% of which are above medium, and 60% of which are above good. Therefore, the indicators to be concerned are p_6 production equipment flexibility and p_7 technology flexibility, and the key indicators are p_8 time flexibility and p_{10} information response flexibility. In the same way, company C accounts for 70% of the indicators above the medium level (including transformation to medium), while company C accounts for only 20% of the indicators above the good level. This shows that the supply chain flexibility of the company is in general in most aspects, and there is a huge room for improvement.

Company A and company D account for 60% of the indicators above the medium level (including transformation to medium). The difference is that company D accounts for 40% of the indicators above the good level (including transformation to good). It also shows that the performance of p_3 capital flexibility, p_5 partner flexibility, p_6 production equipment flexibility, and p_8 time flexibility, which is currently poor, is the focus of future work improvement of the company. Through the overall analysis of the primary indicators, we can see that the four companies' indicator p_2 human resource flexibility has reached a good level, and the performance of indicator p_9 service supply flexibility is also good, reaching above the medium level, but p_8 time flexibility of the four companies is in a poor grade.

By analyzing the data in Table 4, we can get the secondary indicators that affect the supply chain flexibility level of each company. Taking company D as an example, because p_3 capital flexibility, p_5 partner flexibility, p_6 production equipment flexibility, and p_8 time flexibility are the four primary indicators that need to be focused on, combined with the secondary indicator correlation in Table 4, it is found that the secondary indicators c_7 under p_3 , c_{13} , c_{15} and c_{15} under p_5 , c_{17} , under p_6 , c_{21} , and c_{22} under p_8 are all in poor grades. Based on the further analysis of the investigation of company D, c_7 financing capacity flexibility is poor mainly because the development of the

TABLE 5: Secondary indicator correlation degree and grade of supply chain flexibility evaluation of companies C and D.

Indicators	Company C				Grade	Company D				Grade
	I	II	III	IV		I	II	III	IV	
c_1	-0.3993	-0.0036	0.0107	-0.2498	Medium	-0.3852	0.1455	-0.0964	-0.3243	Good
c_2	-0.2812	-0.0408	0.0720	-0.3542	Medium	-0.3547	-0.1699	0.3500	-0.2754	Medium
c_3	0.3078	-0.3078	-0.6721	-0.7852	Excellent	-0.2632	0.5000	-0.2632	-0.5172	Good
c_4	-0.4953	-0.3642	-0.0318	0.0318	Poor	-0.6597	-0.5713	-0.3473	0.3473	Poor
c_5	-0.3634	0.3350	-0.2233	-0.5340	Good	-0.3387	0.4750	-0.3167	-0.5900	Good
c_6	-0.3512	-0.0763	0.0900	-0.4550	Medium	-0.3175	0.1300	-0.0650	-0.5325	Good
c_7	-0.2953	-0.0603	0.1810	-0.2251	Medium	-0.8855	-0.8473	-0.7710	0.2290	Poor
c_8	0.2950	-0.2950	-0.4360	-0.7314	Excellent	-0.1633	0.0300	-0.0060	-0.5267	Good
c_9	-0.4375	-0.0442	0.0617	-0.4130	Medium	-0.9583	-0.9292	-0.7500	0.2500	Poor
c_{10}	-0.6596	-0.3289	0.3741	-0.4505	Medium	-0.3203	0.3528	-0.2044	-0.4780	Good
c_{11}	-0.6500	-0.4167	0.3750	-0.3000	Medium	0.2400	-0.2400	-0.7467	-0.8480	Excellent
c_{12}	-0.4460	-0.2410	0.4253	-0.1903	Medium	-0.4112	0.0740	-0.0529	-0.4766	Good
c_{13}	-0.3799	0.2095	-0.1396	-0.4838	Good	-0.8414	-0.7356	-0.2069	0.2069	Poor
c_{14}	-0.4725	-0.2410	0.3413	-0.1413	Medium	-0.6585	-0.5085	-0.2250	0.2250	Poor
c_{15}	-0.5833	-0.4444	0.2000	-0.1667	Medium	-0.7500	-0.6667	-0.2500	0.2500	Poor
c_{16}	-0.1425	0.3275	-0.0749	-0.3111	Good	0.2456	-0.2456	-0.4180	-0.5666	Excellent
c_{17}	-0.7347	-0.5806	-0.1333	0.1333	Poor	-0.8163	-0.7097	-0.4000	2.0000	Poor
c_{18}	-0.3286	0.0410	-0.0205	-0.3470	Good	-0.2961	0.2740	-0.1370	-0.4247	Good
c_{19}	-0.9000	-0.8500	-0.7000	0.3000	Poor	-0.4333	-0.1500	0.3000	-0.2917	Medium
c_{20}	0.4000	-0.4000	-0.7000	-0.8000	Excellent	-0.1875	0.3000	-0.3500	-0.5667	Good
c_{21}	-0.5066	-0.4751	-0.2524	0.2524	Poor	-0.3892	-0.3500	-0.0713	0.0706	Poor
c_{22}	-0.7546	-0.6712	-0.1780	0.1780	Poor	-0.8361	-0.7804	-0.4510	0.4510	Poor
c_{23}	-0.1429	0.4000	-0.2000	-0.3684	Good	0.3000	-0.3000	-0.5333	-0.6316	Excellent
c_{24}	-0.6800	-0.6000	0.2000	-0.2727	Medium	-0.8600	-0.8250	-0.3000	0.3000	Poor
c_{25}	-0.2222	0.4000	-0.3000	-0.5333	Good	-0.1875	0.3000	-0.3500	-0.5667	Good
c_{26}	-0.4667	-0.2727	0.2500	-0.1111	Medium	-0.6000	-0.4545	-0.1429	0.1429	Poor
c_{27}	-0.5222	-0.3857	-0.1400	0.1400	Poor	-0.6667	-0.5714	-0.4000	0.4000	Poor
c_{28}	-0.3236	0.0830	-0.0415	-0.5208	Good	-0.2922	0.2970	-0.1485	-0.5743	Good
c_{29}	-0.5476	-0.4571	0.0588	-0.0500	Medium	-0.4000	-0.2727	0.4706	-0.2500	Medium

TABLE 6: Primary indicators' correlation degree and grade of supply chain flexibility evaluation of companies A and B.

Indicators	Company A				Grade	Company B				Grade
	I	II	III	IV		I	II	III	IV	
p_1	-0.0580	-0.0886	-0.5115	-0.6175	Transformation to poor	-0.2924	0.3395	-0.3447	-0.4926	Good
p_2	-0.4052	0.2566	-0.7414	-1.1726	Good	-0.6696	0.4704	-0.4297	-0.9614	Good
p_3	-0.4027	-0.3484	-0.0419	-0.3181	Transformation to medium	0.0185	-0.0379	-0.3321	-0.5794	Excellent
p_4	-0.8935	-0.8179	-0.1790	0.1790	Poor	-0.3101	0.4085	-0.3142	-0.5692	Good
p_5	-0.8329	-0.7406	-0.3484	0.2125	Poor	-0.2545	0.2817	-0.3924	-0.6413	Good
p_6	-0.2670	-0.0898	0.0158	-0.3888	Medium	-0.3184	-0.3073	0.1105	-0.3482	Medium
p_7	-0.3129	0.1480	-0.0740	-0.3827	Good	-0.4939	-0.3128	0.2017	-0.2465	Medium
p_8	-0.9511	-0.9398	-0.8716	0.1284	Poor	-0.7833	-0.7284	-0.3985	0.3985	Poor
p_9	-0.3913	-0.1175	0.1630	-0.2902	Medium	-0.4083	0.1066	0.0351	-0.3614	Good
p_{10}	-0.5205	-0.3847	0.1637	-0.0146	Medium	-0.5113	-0.3471	-0.1009	-0.0303	Transformation to poor

company is in the transition stage from introducing innovation to independent innovation, the innovation work in all aspects is not mature enough, and the cost of capital invested at the current stage is high, resulting in high capital use fee, thus improving the financing cost rate. c_{13} trust mechanism build ability, c_{14} knowledge sharing rate, and c_{15} number of partners that can be selected in time are rated as poor grades mainly due to the limited efficiency of information transfer between suppliers and all parties, the

weak ability to enhance their own competitive strength with the help of partners, the poor communication and cooperation between the main parts of the supply chain, and the low efficiency of information transfer, resulting in low supply flexibility level of the chain. The main reason for the poor c_{17} maintenance rate of production equipment is that the training of professional skills of the company's employees is not in place, and the employees are not proficient in the use of equipment. The poor grade of c_{21}

TABLE 7: Primary indicators' correlation degree and grade of supply chain flexibility evaluation of companies C and D.

Indicators	Company C				Grade	Company D				Grade
	I	II	III	IV		I	II	III	IV	
p_1	-0.3422	-0.0486	-0.0294	-0.2834	Transformation to medium	-0.3883	0.0892	-0.0642	-0.2939	Good
p_2	-0.7034	0.2155	-0.1988	-0.8038	Good	-0.7234	0.5048	-0.3375	-0.8740	Good
p_3	-0.2414	-0.0975	0.0206	-0.3918	Medium	-0.7803	-0.7170	-0.6214	0.0975	Poor
p_4	-0.6458	-0.3648	0.3768	-0.3707	Medium	-0.0701	0.0715	-0.4438	-0.6458	Good
p_5	-0.4534	-0.0570	0.0475	-0.3301	Medium	-0.7805	-0.6721	-0.2222	0.2222	Poor
p_6	-0.5723	-0.3318	-0.1113	-0.0030	Transformation to poor	-0.5424	-0.5274	-0.3822	1.2414	Poor
p_7	-0.7441	-0.7960	-0.7000	0.1681	Poor	-0.4039	-0.0960	0.2221	-0.3246	Medium
p_8	-0.7170	-0.6414	-0.1893	0.1893	Poor	-0.7683	-0.7151	-0.3934	0.3932	Poor
p_9	-0.3251	0.0949	-0.0508	-0.3341	Good	-0.2984	-0.1400	-0.2993	-0.2652	Transformation to good
p_{10}	-0.4572	-0.2355	-0.0518	-0.1488	Transformation to medium	-0.4609	-0.1789	-0.0787	-0.1238	Transformation to medium

TABLE 8: Comprehensive correlation degree and grade of supply chain flexibility evaluation of each company.

Company	I	II	III	IV	Grade
A	-0.6301	-0.5511	-0.2380	-0.0579	Transformation to poor
B	-0.2624	0.1675	-0.3085	-0.5014	Good
C	-0.4642	-0.1924	0.0922	-0.3065	Medium
D	-0.4932	-0.3352	-0.3536	-0.1257	Transformation to poor

degree of timely response and c_{22} delivery flexibility is due to the company's relatively lagging response to market changes or changes in customer demand, the long time taken to respond to changes and uncertainties, the low sensitivity of delivery time, and the difficulty of shortening and changing the delivery service time at any time.

5. Conclusion

The development of each industry is faced with the uncertainty and risk brought by the external market environment. The flexibility level of the supply chain affects the market competitiveness and market position of enterprises. The results show that the improvement of supply chain flexibility depends on the efficient operation of the information system. Enterprises should find the information system suitable for their own business development needs, scientifically combine the business and data processing in actual work, realize the seamless connection between online and offline, and improve the ability of employees to use the information system and information platform. In addition, enterprises should balance the input of innovation resources. In addition to strengthening the innovation of product manufacturing technology, they should also pay attention to the sharing of information resources in the supply chain and strengthen the ability of obtaining internal and external information and identifying value information in the supply chain. In addition to the information system, the intelligent and high-tech service auxiliary equipment should also include the storage management and the provision of additional services in the customer waiting area. It is also very

important to strengthen the cooperation with the internal and external enterprises of the supply chain. The enterprises in each link of the supply chain need to correctly handle the relationship between competition and cooperation, rationalize the division of labor, strengthen flexible cooperation, so as to jointly improve the ability to deal with market risks.

This paper designs a comprehensive and feasible evaluation system for supply chain flexibility research from the perspective of enterprise dynamic management and uses the matter-element evaluation method to effectively solve the problems of possible incompatibility of flexible indicators and multi-objective evaluation so that the evaluation results are more scientific and comprehensive, the key indicators affecting the evaluation results are more easily identified, and different evaluations of different research samples are made. The contrast and gap between the results are clearer. In the matter-element evaluation method, the construction of the matter-element extension evaluation model is the key to the research. The setting of classical domain and nodal domain and the design of correlation function have great room for improvement, which will be the future research direction.

Data Availability

The data used to support the findings of this study are available from the corresponding author upon request.

Conflicts of Interest

The authors declare that they have no conflicts of interest.

Acknowledgments

This work was supported by the Key Projects of the National Social Science Fund of China (no. 18AGL028).

References

- [1] R. Srinivasan and M. Swink, "An investigation of visibility and flexibility as complements to supply chain analytics: an organizational information processing theory perspective,"

- Production and Operations Management*, vol. 27, no. 10, pp. 1849–1867, 2018.
- [2] S. Fayezi, A. Zutshi, and A. O’Loughlin, “Understanding and development of supply chain agility and flexibility: a structured literature review,” *International Journal of Management Reviews*, vol. 19, no. 4, pp. 379–407, 2017.
 - [3] Y. Jin, M. Vonderembse, T. S. Ragu-Nathan, and J. T. Smith, “Exploring relationships among IT-enabled sharing capability, supply chain flexibility, and competitive performance,” *International Journal of Production Economics*, vol. 153, pp. 24–34, 2014.
 - [4] A. Rojo, J. Llorens-Montes, and M. N. Perez-Arostegui, “The impact of ambidexterity on supply chain flexibility fit,” *Supply Chain Management: An International Journal*, vol. 21, no. 4, pp. 433–452, 2016.
 - [5] D. Eckstein, M. Goellner, C. Blome, and M. Henke, “The performance impact of supply chain agility and supply chain adaptability: the moderating effect of product complexity,” *International Journal of Production Research*, vol. 53, no. 10, pp. 3028–3046, 2015.
 - [6] R. Sreedevi and H. Saranga, “Uncertainty and supply chain risk: the moderating role of supply chain flexibility in risk mitigation,” *International Journal of Production Economics*, vol. 193, pp. 332–342, 2017.
 - [7] D. Simchi-Levi, H. Wang, and Y. Wei, “Increasing supply chain robustness through process flexibility and inventory,” *Production and Operations Management*, vol. 27, no. 8, pp. 1476–1491, 2018.
 - [8] J. H. M. Manders, M. C. J. Caniels, and P. W. T. Ghijsen, “Supply chain flexibility,” *The International Journal of Logistics Management*, vol. 28, no. 4, pp. 964–1026, 2017.
 - [9] J. S. Kim, S. I. Park, and K. Y. Shin, “A quantity flexibility contract model for a system with heterogeneous suppliers,” *Computers & Operations Research*, vol. 41, pp. 98–108, 2014.
 - [10] R. Ishfaq and A. Narayanan, “Incorporating order-fulfillment flexibility in automotive supply chain through vehicle trades,” *Decision Sciences*, vol. 50, no. 1, pp. 84–117, 2018.
 - [11] A. Rojo, M. Stevenson, F. J. Lloréns Montes, and M. N. Perez-Arostegui, “Supply chain flexibility in dynamic environments,” *International Journal of Operations & Production Management*, vol. 38, no. 3, pp. 636–666, 2018.
 - [12] A. K. Sahu, S. Datta, and S. S. Mahapatra, “Evaluation of performance index in resilient supply chain: a fuzzy-based approach,” *Benchmarking: An International Journal*, vol. 24, no. 1, pp. 118–142, 2017.
 - [13] B. Singh Patel, C. Samuel, and S. K. Sharma, “Evaluation of agility in supply chains: a case study of an indian manufacturing organization,” *Journal of Manufacturing Technology Management*, vol. 28, no. 2, pp. 212–231, 2017.
 - [14] S. Routroy, A. Bhardwaj, S. K. Sharma, and B. K. Rout, “Analysis of manufacturing supply chain agility performance using Taguchi loss functions and design of experiment,” *Benchmarking: An International Journal*, vol. 25, no. 8, pp. 3296–3319, 2018.
 - [15] I. Kazemian and S. Aref, “Multi-echelon supply chain flexibility enhancement through detecting bottlenecks,” *Global Journal of Flexible Systems Management*, vol. 17, no. 4, pp. 357–372, 2016.
 - [16] K. T. Shubin, A. Gunasekaran, T. Papadopoulos, R. Dubey, M. Singh, and S. F. Wamba, “Enablers and barriers of flexible green supply chain management: a total interpretive structural modeling approach,” *Global Journal of Flexible Systems Management*, vol. 17, no. 2, pp. 171–188, 2016.
 - [17] R. Dubey, A. Gunasekaran, and S. J. Childe, “Big data analytics capability in supply chain agility: the moderating effect of organizational flexibility,” *Management Decision*, vol. 57, no. 8, pp. 2092–2112, 2019.
 - [18] D. Ivanov, A. Das, and T.-M. Choi, “New flexibility drivers for manufacturing, supply chain and service operations,” *International Journal of Production Research*, vol. 56, no. 10, pp. 3359–3368, 2018.
 - [19] G. Seebacher and H. Winkler, “A capability approach to evaluate supply chain flexibility,” *International Journal of Production Economics: manufacturing System Strategy Design*, vol. 167, pp. 177–186, 2015.
 - [20] A. Chaudhuri, H. Boer, and Y. Taran, “Supply chain integration, risk management and manufacturing flexibility,” *International Journal of Operations & Production Management*, vol. 38, no. 3, pp. 690–712, 2018.
 - [21] A. R. Somarin, S. Asian, F. Jolai, and S. Chen, “Flexibility in service parts supply chain: a study on emergency resupply in aviation MRO,” *International Journal of Production Research*, vol. 56, no. 10, pp. 3547–3562, 2018.
 - [22] W. Cai, *Matter-element Analysis*, Guangdong Higher Education Press, Guangdong, China, 1987.
 - [23] W. Cai, *Matter-Element Model and Its Application*, Science Press, Beijing, China, 1994.
 - [24] P. Y. Li, J. H. Wu, and H. Qian, “Groundwater quality assessment based on entropy weighted osculating value method,” *International Journal of Environmental Sciences*, vol. 4, pp. 621–630, 2010.

Research Article

The Effect of Shadow Banking on the Systemic Risk in a Dynamic Complex Interbank Network System

Hong Fan  and **Hongjie Pan**

Glorious Sun School of Business and Management, Donghua University, Shanghai 200051, China

Correspondence should be addressed to Hong Fan; hongfan@dhu.edu.cn

Received 4 February 2020; Revised 4 April 2020; Accepted 15 April 2020; Published 18 May 2020

Guest Editor: Baogui Xin

Copyright © 2020 Hong Fan and Hongjie Pan. This is an open access article distributed under the Creative Commons Attribution License, which permits unrestricted use, distribution, and reproduction in any medium, provided the original work is properly cited.

After the financial crisis triggered by the subprime mortgage crisis in the United States in 2008, many scholars believed that the unstable transmission of shadow banking business in the banking system is the main factor causing financial turmoil. This paper proposes a dynamic complex interbank network system model with shadow banking in which the dynamic complex interbank network system differs from the traditional banking network and is formed by the interrelated business between shadow banks and commercial banks to explore the effect of shadow banking on the systemic risk. The results show that the existence of shadow banking will increase the systemic risk, accelerate the speed of bankruptcy of banks, reduce the survival ratio of banks, and increase the strength of central bank assistance. The smaller the number of shadow banks in the system, the higher the degree of credit connection among commercial banks and the smaller the systemic risk.

1. Introduction

The outbreak of the global financial crisis has shown that the occurrence of systemic risk would lead to a tremendous destructive effect on the financial system [1, 2]. Therefore, the research of the systemic risk has drawn more and more attention [3, 4]. In the existing studies of systemic risk, most of them focus on the analysis of the systemic risk that is conducted from the perspective of interbank lending and it is believed that interbank lending relationship has an important impact on the systemic risk [5–7]. The network structure formed by interbank lending as a carrier of risk contagion [8, 9] plays an important role in the systemic risk [6, 7]. Kaufman and Scott [10] argued that the systemic risk will be triggered by risks or possible systemic collapses in the interbank lending market. Allen and Gale [11] studied the effects of a complete market structure and an incomplete market structure on the systemic risk and found that the complete market structure is more stable than the incomplete market structure. Iori and Jafarey [12] found that the homogeneous banking system is more stable than the heterogeneous banking system. Nier et al. [13] pointed out that

the impact of banking network concentration on the systemic risk is nonmonotonous. Lenzu and Tedeschi [14] analyzed the impact of different network topologies on the systemic risk and found that the random network structure is more stable than the scale-free network structure. Caccioli et al. [15] showed that the scale-free network has better flexibility, but its systemic risk is significantly higher than other networks. Godlewski et al. [16] argued that the small-world network structure is conducive to enhancing assets connectivity between banks, reducing loan spreads and the systemic risk. Georg et al. [17, 18] stressed that the central bank stabilizes interbank markets in the short run alone and the money-centric network is more stable than the random network. Lux [19] presented that the interbank network shows a “core periphery” structure. The core banks could provide financial support for peripheral banks to prevent systemic risk. Berardi and Tedeschi [20] showed that the banking network presents a centralized structure and the increase in the number of attractive banks will reduce the systemic risk.

The existing studies mainly analyzed the systemic risk caused by the crisis from the perspective of the interbank

market and different interbank lending networks. The effect of shadow banking on systemic risk is almost lacking. As defined in Page and Wooder [21], shadow banks are non-bank financial institutions that operate outside the traditional banking regulation system. Shadow banks are not directly regulated by central banks, and they are not included in the safety net. According to Financial Stability Board (FSB) [22], the shadow banking system is a credit intermediary system which is free from the formal banking system and may cause systemic financial risks and regulatory arbitrage risks. The FSB also sets out several classes of shadow banking sectors: (i) sectors susceptible to runs, such as certain mutual funds, credit hedge funds, and real-estate funds; (ii) nonbank lenders dependent on short-term funding, such as finance companies, leasing companies, factoring companies, and consumer-credit companies; (iii) market intermediaries dependent on short-term funding or on the secured funding of client assets, such as broker dealers; (iv) companies facilitating credit creation, such as credit insurance companies, financial guarantors, and monoline insurers; and (v) securitization-based intermediaries. Shadow banking brings prosperity to the financial market, but at the same time, it also brings great vulnerability to the financial system. Therefore, the interest in the impact of shadow banking on financial markets is becoming a growing area within systemic risk literature. Pozsar et al. [23] and Tucker [24] discussed that the size of shadow banking showed a pattern of sudden increase before the outbreak of the global financial crisis and shadow banking was considered as one of the main reasons that could trigger financial systemic risk. Bernanke et al. [25] believed that shadow banking utilizes the balance sheets to provide credit loans similar to commercial banks and uses term conversion to avoid bankruptcy risk, which induces systemic risk. Diamond [26] found that the diversification of shadow banking's portfolio by buying and selling risky loans would result in the accumulation of the systemic risk. Gennaioli et al. [27] used an improved shadow banking model to study the relationship between shadow banking and the systemic risk and discovered if reasonably expected, shadow banking could help withstand the systemic risk and maintain the system stable. Elgin and Oztunali [28] found through a two-sector dynamic general equilibrium model that the relative size of shadow banking sector will affect systemic risk. Colombo et al. [29] constructed a shadow banking model to emphasize that the form of propagation after a crisis shock will reduce the ability of the financial system to resist future shocks, and the level of the systemic risk will increase.

Although the above research concerning the impact of shadow banking on the systemic risk examines the relationship between shadow banking and the systemic risk, it does not reveal the mechanism of systemic risk well, as they neglected the complicated interactions among banks. It is widely believed that the systemic risk mainly originated from the cascading failures of banks due to the complicated interactions among banks. Therefore, the study of the impact of shadow banking on the systemic risk should be integrated with the interbank network system. In view of the above considerations, a dynamic complex interbank network

system model with shadow banking is proposed. The dynamic evolution of the systematic risk in the existence and absence of shadow banking is studied in this study; furthermore, the impact of shadow banking on the number of default banks, bank survival rate, ratio of default rate to commercial bank survival rate, and central bank assistance are compared. Moreover, the time course of the systemic risk (dynamic evolutionary systemic risk) other than a fixed systemic risk is obtained in this paper, as the calculation of the systemic risk is based on a dynamic interbank network model. This enables us to observe the trend of the systemic risk, making the results of shadow banking effect on the systemic risk more valuable.

2. Model of a Dynamic Complex Interbank Network System with Shadow Banking

2.1. The Structure of Interbank Network with Shadow Banking.

A dynamic complex interbank network system with shadow banking is constructed, in which commercial banks and shadow banks form a network including connections to the real economy; here, the real economy represents the rest of economy, namely, the economy outside of banking. The number of agents of commercial banks is denoted by M , and N is the number of agents of shadow banks. Thus, $U = M + N$ is the sum of all the banks in the system. When $N = 0$, the interbank network system can be regarded as the traditional interbank network system. t ($t = 1, 2, \dots$) is the dynamic evolution time step of the system. At any time t , there are a finite number of banks U . Figure 1 shows the structure of interbank network with shadow banking. Commercial banks are overseen by the central bank. They are operating within the protection net provided by the central bank and receive the central bank's aid like CB_t^j when bank j defaults. According to the definition proposed by Pozsar et al. [23], shadow banks are financial institutions that operate outside of the central bank's regulatory. Thus, there is no need for shadow banks to obey the central bank's regulations (such as legal reserves and investment restrictions). Meanwhile, they cannot receive aid from the central bank.

In the banking system, bank failure is often caused by a lack of liquidity. The liquidity of a bank is mainly related to deposit, financing, investment, and interbank lending. When banks are short of liquidity, they will borrow from each other in the interbank network, which is shown in Figure 1. The directed line segments between banks represent the amounts of borrowing or lending from one bank to another. For example, the arrow from commercial bank M_j points to commercial bank M_k , indicating that commercial bank M_j is the debt bank of commercial bank M_k , and its debt is $b_t^{j,k}$; the arrow from commercial bank M_k points to commercial bank M_i , indicating that commercial bank M_i is commercial bank M_k 's creditor bank with a claim of $b_t^{k,i}$. Since shadow banks have the characteristics of independence and information opacity [30], there is a business relationship between shadow banks and commercial banks, while no interbank lending between shadow banks is considered in this paper. For example, $b_t^{j|M,q|N}$ indicates that

commercial bank M_j borrows from shadow bank N_q and $b_t^{w|N,j|M}$ indicates that shadow bank N_w borrows from commercial bank M_j . $b_t^{q|N,k|M}$ and $b_t^{k|M,i|N}$ represent the interbank claims and debts between commercial bank M_k and shadow bank N_q and shadow bank N_j , respectively. Similarly, $b_t^{l|N,i|M}$ and $b_t^{i|M,w|N}$ represent the interbank claims and debts between commercial bank M_i and shadow bank N_i and shadow bank N_w , respectively. Moreover, according to the policy restrictions on the relationship between commercial banks and shadow banks, in our model, the interbank lending relationship between a shadow bank and commercial banks will be limited by the number (the number is represented by d , that is, the maximum number of commercial banks that a shadow bank can borrow).

In addition to interbank interactions, in order to be more in line with the real financial state, according to the research of Gong and Page [31], the model proposed in this paper includes connections to the real economy S^n . To simplify the system, this paper divides the state of the real economy into three, that is, $S^n (n=1,2,3)$. The banking system and real economy feature a two-sided interaction. The state of the real economy influences the banking system by determining the allocation of investment. For each state of the real economy, there is an investment project $K^n (n=1, 2, 3)$. As shown in Figure 1, a bank selects project K^n to invest in the real economy S^n . The return of the projects K^n is subject to the state of the real economy (detailed in the below section). With reference to Pareto's principle [32], using Pareto's economic model [33] and taking the bank default rate (the ratio of the number of default banks to the total number of banks) as a measure, the three critical values for dividing the real economy are calculated. When the bank default rate is less than 10%, it is in a good economic case S^1 , corresponding to the investment project K^1 with low risk and high return; when the bank default rate is between 10% and 20%, it is in a stable economic case S^2 , corresponding to the investment project K^2 with medium risk and return; when the bank default rate exceeds 20%, it is in a depressed economic case S^3 , corresponding to the investment project K^3 with high risk and low return. The real economy S^n will change with the dynamic evolution of the bank default rate in the system. Banks in the system will default but the number of banks will not increase.

2.2. Traditional Interbank Network System. The traditional interbank network refers to the network formed by the interbank lending of commercial banks. This paper refers to the studies of Iori et al. [12] and Georg et al. [17, 18], and the interbank network is set up as a random network. In a random network, banks are randomly connected and the connectivity relationship is represented by binary matrix J . $J_{i,j}$ is either one or zero. $J_{i,j}=1$ indicates that there is a credit linkage between bank i and bank j , and $J_{i,j}=0$ means that there is no relationship. c indicates the probability of a credit linkage between any two banks, i.e., $c \in [0,1]$. At one extreme, $c=0$ means there is no interbank lending, while $c=1$ means interbank network's structure is a fully connected structure.

The bank dynamic evolution is based on the banks' balance sheet. Every bank's assets and liabilities in the banking system are dynamically changing at each time step. The balance sheet of each bank in the system evolves dynamically as follows:

$$L_{t-1}^i = A_{t-1}^i + B_{t-1}^i + V_{t-1}^i - \sum_{j=1}^{\tau} I_{t-j}^i, \quad (1)$$

where L_{t-1}^i is the liquidity asset of bank i at time $t-1$; A_{t-1}^i is the deposit of bank i at time $t-1$; V_{t-1}^i is the owner's equity of bank i at time $t-1$; $\sum_{j=1}^{\tau} I_{t-j}^i$ is the total investment of bank i in τ investment periods; and $B_{t-1}^i = \sum_{k=1}^U b_{t-1}^{i,k}$ is the total borrowing amount of bank i at time $t-1$; $b_{t-1}^{i,k} > 0$ if bank i borrows from bank k and $b_{t-1}^{k,i} < 0$ if bank k loans to bank i , where $b_{t-1}^{i,k} = -b_{t-1}^{k,i}$. $b_{t-1}^{i,k} = -b_{t-1}^{k,i} = 0$ if there is no lending relationship between banks.

2.3. Interbank Network System with Shadow Banking. Besides the dynamically changing assets and liabilities of every bank, the interbank lending network also changes dynamically at each time step. It should be noted that there is no interbank lending between shadow banks in this paper. Therefore, the binary matrix J among shadow banks is always set to zero. The balance sheet of banks in the interbank network system with shadow banking is evolved same as equation (1); however, if bank i is a shadow bank, then $B_{t-1}^i = \sum_{k=1}^d b_{t-1}^{i|N,k|M}$, indicating the total borrowing amount of shadow bank i at time $t-1$. $b_{t-1}^{i|N,k|M} > 0$ if shadow bank i borrows from commercial bank k and $b_{t-1}^{k|M,i|N} < 0$ if commercial bank k borrows from to shadow bank i , where $b_{t-1}^{i|N,k|M} = -b_{t-1}^{k|M,i|N}$. $b_{t-1}^{i|N,k|M} = -b_{t-1}^{k|M,i|N} = 0$ if there is no lending relationship between shadow bank i and commercial bank k . The sequence of activities in each time is as follows. At the start of each time, each bank inherits the initial liquidity asset. Then, the liquidity asset of banks will change dynamically with the inflow and outflow of funds. The liquidity asset of bank i is updated to

$$L_t^i = L_{t-1}^i + (A_t^i - A_{t-1}^i) - r_a A_{t-1}^i + \rho \sum_{j=1}^{\tau} I_{t-j}^i + I_{t-\tau}^i, \quad (2)$$

where $r_a A_{t-1}^i$ is the interest paid by the commercial bank to depositors or the interest paid by the shadow bank to financiers and r_a is the deposit interest rate or the financing interest rate; $\rho \sum_{j=1}^{\tau} I_{t-j}^i$ and $I_{t-\tau}^i$ are investment income and the investment recovered at maturity; and ρ is the rate of return on investment of each time. Since the deposit and financing patterns of customers are fluctuating and unpredictable, each bank receives stochastic shocks to its liquidity reserves. Therefore, it is assumed that the deposits or financing A_t^i for the bank i obeys the normal distribution: $A_t^i = |\bar{A} + \bar{A}\delta_A \varepsilon_t|$, $\varepsilon_t \sim N(0,1)$, where \bar{A} is the mean of random deposits of commercial banks or random financing of shadow banks and δ_A is the standard deviation of commercial banks' random deposits or shadow banks' random financing.

If $L_t^i > 0$, it denotes that bank i has sufficient liquidity. Such bank can undertake dividend payments to

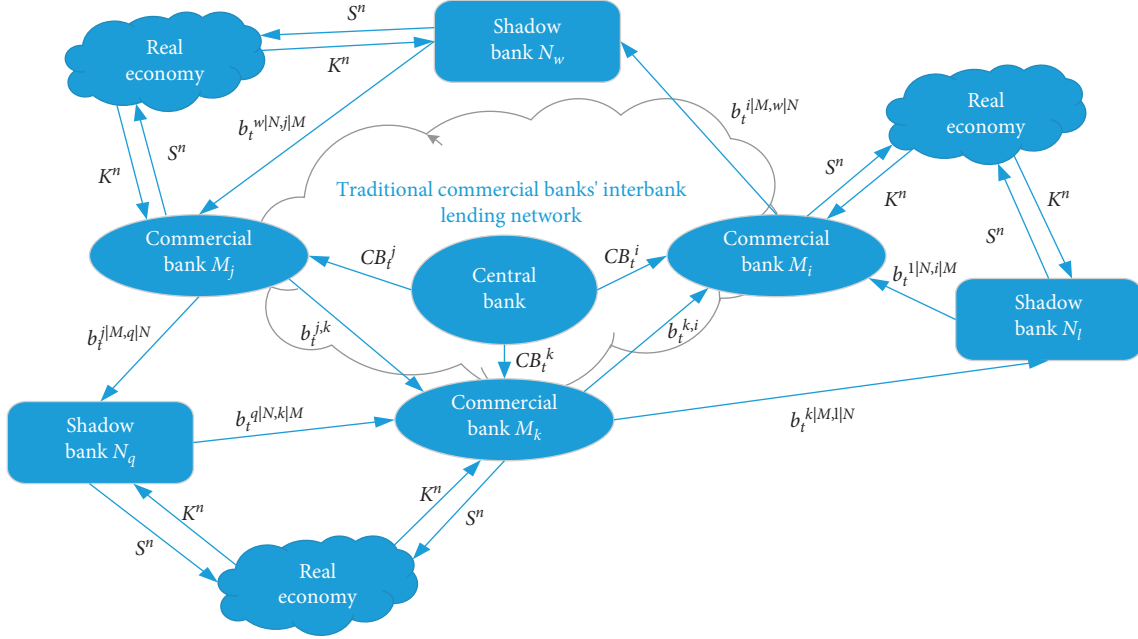


FIGURE 1: The structure of interbank network with shadow banking.

shareholders. Dividend distribution is different in commercial banks and shadow banks. When bank i is a commercial bank, dividend distribution D_t^{iM} can be described as follows:

$$D_t^{iM} = \max \left[0, \min \left[\rho \sum_{j=1}^{\tau} I_{t-j}^i - r_a A_{t-1}^i, L_t^i - R_t^i, L_t^i + \sum_{j=1}^{\tau-1} I_{t-j}^i - (1 + \chi) A_t^i \right] \right], \quad (3)$$

where $R_t^i = \beta A_t^i$ is the legal deposit reserve kept by commercial bank i , β is the deposit reserve ratio, and χ is the deposit ratio. When bank i is a shadow bank, dividend distribution D_t^{iN} is as follows:

$$D_t^{iN} = \max \left[0, \min \left[\chi \left(\rho \sum_{j=1}^{\tau} I_{t-j}^i - r_a A_{t-1}^i \right), L_t^i \right] \right], \quad (4)$$

where χ is the financing ratio; for simplicity, the financing ratio is equal to the deposit ratio in this paper.

After the dividends have been paid, the bank undertakes reinvestment. Corresponding to the real economy S^n , bank i chooses project K^n to reinvest under its available liquidity and investment opportunity. Different projects have different returns on investment. As the value of n increases, the economic condition declines and the return on investment decreases. The return on investment of the project can be expressed as

$$R_o | S^n = \begin{cases} 0, & 1 - p_n \\ R_o^{S^n}, & p_n \end{cases} (n = 1, 2, 3), \quad (5)$$

where $R_o^{S^n}$ is the investment return corresponding to project K^n under the state of the real economy S^n . The value of $R_o^{S^n}$ is

set according to the existing investment return rate of banks and the loan income rate of financial companies. p_n is the investment recovery probability corresponding to project K^n , indicating the risk of the project; with the increase of the risk of the project, the investment recovery probability decreases. And the initial value is set by referring to the real bank's nonperforming loan interest ratio. The better the real economy, the lower the risk and the higher the return of investment and the investment recovery probability.

The reinvestment of commercial bank i is $I_t^{iM} | K^n$, and the reinvestment of shadow bank i is $I_t^{iN} | K^n$:

$$I_t^{iM} | K^n = \min \left[\max \left[0, L_t^i - D_t^{iM} - R_t^i \right], \omega_t^i \right], \quad (6)$$

$$I_t^{iN} | K^n = \min \left[\max \left[0, L_t^i - D_t^{iN} \right], \omega_t^i \right], \quad (7)$$

where ω_t^i is the investment opportunity of bank i . The investment opportunity of bank i at time t is subject to a normal distribution: $\omega_t^i = |\bar{\omega} + \bar{\omega} \delta_\omega \eta_t|$, $\eta_t \sim N(0, 1)$. $\bar{\omega}$ is the average investment opportunity of banks, and δ_ω is the standard deviation of banks' investment opportunity. The difference between the two types of reinvestment is that there is no need for shadow banks to pay the legal deposit reserve to the central bank.

After completing the above dividend distribution and reinvestment, if bank i 's liquidity asset $L_t^i \geq 0$, it can continue interbank lending. Conversely, if $L_t^i < 0$, bank i becomes a member of defaulted set F at time step t . When defaulted bank i is a commercial bank, even if it is unable to borrow enough money to restore its liquidity, it can go back to the banking system because it will be bailed out by the central bank. The form of the assistance of the central bank will be described as follows:

$$CB_t^i = \begin{cases} R_t^i - L_t^i, & R_t^i > L_t^i, \\ 0, & \text{otherwise.} \end{cases} \quad (8)$$

When $R_t^i > L_t^i$, the central bank's assistance amount to commercial bank i is $R_t^i - L_t^i$. After getting the assistance of the central bank, commercial bank i 's debts update to 0 ($B_t^i = 0$) and go into the next time step. Otherwise, the commercial bank i pays legal deposit reserve by itself and evolves to the next time step. Protected by the central bank, commercial banks only default and do not go bankrupt.

Alternatively, if a bank experiencing negative liquidity is a shadow bank i (i.e., $L_t^i < 0$), it will be cleared by the central bank. Following Eisenberg and Noe [34], this paper assumes that shadow banks with insufficient liquidity to cover their debts pay their debts proportionally. The debt repayment is calculated as follows:

$$PB_t^{iN,k|M} = \begin{cases} V_t^{iN} * \frac{b_t^{iN,k|M}}{\sum_{k=1}^d b_t^{iN,k|M}}, & \text{if } b_t^{iN,k|M} > 0 \\ & \text{and } V_t^{iN} > 0, \\ 0, & \text{otherwise,} \end{cases} \quad (9)$$

where V_t^{iN} represents the owner's equity of shadow bank i , $b_t^{iN,k|M}$ is the loan amount of commercial bank k to shadow bank i , and $\sum_{k=1}^d b_t^{iN,k|M}$ is the total amount of shadow bank i borrowed from no more than d commercial banks. d is the number of commercial banks that is borrowed by shadow bank i . Then, the shadow bank i 's debts update to 0, and it becomes a member of bankruptcy set D .

2.4. Dynamic Process Algorithm of Interbank Network System with Shadow Banking. In the interbank network system with shadow banking, banks conduct interbank lending when their liquidity is insufficient, including interbank lending among commercial banks and business relationship between commercial banks and shadow banks. The dynamic process algorithm of the interbank network with shadow banking is shown in Figure 2, which is divided into the following 4 steps:

Step 1: at time $t = 1$, the initial real economy S^0 is set to S^1 , and the initial calculation of the initial deposit of the commercial banks, the initial financing of the shadow bank, and each parameter and variable is, respectively, performed.

Step 2: the real economy S^0 is determined and the asset liquidity L_t of each bank at time t is calculated. According to the number of default banks at time $t-1$, the bank default rate is calculated to determine the real economy S^0 in time t , and the value of relevant parameters is determined by S^0 . Then, the liquidity of the survival bank at time t is calculated, the banks with sufficient liquidity ($L_t > 0$) carry out dividend distribution D_t and reinvestment I_t , and the banks that lack

liquidity ($L_t \leq 0$) enter into Step 3 and start interbank lending.

Step 3: according to the liquidity of each bank in Step 2, the bank with liquidity $L_t > 0$ is the creditor bank and the bank with liquidity $L_t \leq 0$ is the debt bank. The debt bank and the creditor bank establish a connection through a random network and conduct interbank lending according to the liquidity of the banks. If the debt bank j can borrow sufficient funds from the creditor banks to repay the previous loan and interest, i.e., $L_t^j - (1 + r_b)B_{t-1}^j \geq 0$ (r_b is the interbank lending rate), bank j enters the next time step; if the debt bank j cannot borrow sufficient funds to repay the previous loan and interest, i.e., $L_t^j - (1 + r_b)B_{t-1}^j < 0$, the debt bank j becomes a member of defaulted set F and gets into Step 4.

Step 4: the insolvent default debt bank is bailed out or cleared. If the default bank j is a shadow bank, it will partially repay the debt according to its owner's equity and then get into the bankruptcy set D ; if the default bank j is a commercial bank, the central bank will aid it to make its liquidity meet the legal deposit reserve. The debts of banks, which are bailed out or cleared, update to 0 ($B_t^j = 0$).

3. Simulation and Analysis

The interbank network system with shadow banking constructed in this paper can simulate the real dynamic evolutionary process of the interbank network system. The bank's balance sheet is dynamically evolved, such as liquidity L , owner's equity V , deposit A , and investment I . Related indicators will change dynamically over time t . By observing the dynamic evolution process of the interbank network system, the impact of shadow banking on the systemic risk is studied. Due to the heterogeneity of banks, banks in the interbank network will be exposed to risks owing to different operating conditions and business strategies, resulting in a series of, and even large-scale, chain failure. The systemic risk of the interbank network is not only affected by the banks' own factors (internal factors) but also by shadow banking (external factors). To objectively reflect the effect of shadow banking on the banking system and measure the systemic risk of the banking network, the average number of default banks in the $[t+1, t+T]$ time zone was normalized, and the calculated value was recorded as $Risk(t)$. It is calculated as follows:

$$Risk(t) = \frac{1}{TR_e} \sum_{i=1}^{R_e} \sum_{j=t+1}^{t+T} \frac{C_j^i}{S_j^i} \quad (10)$$

where the T is the time interval, and the average proportion of default banks in the future T time (that is, the average probability of default banks) can indicate the systemic risk of the system at a certain moment. This paper sets $T = 10$. R_e is the time number of the simulation, C_j^i is the number of banks that default at time j in the i th simulation, and S_j^i is the number of banks that survived at time j in the i th simulation.

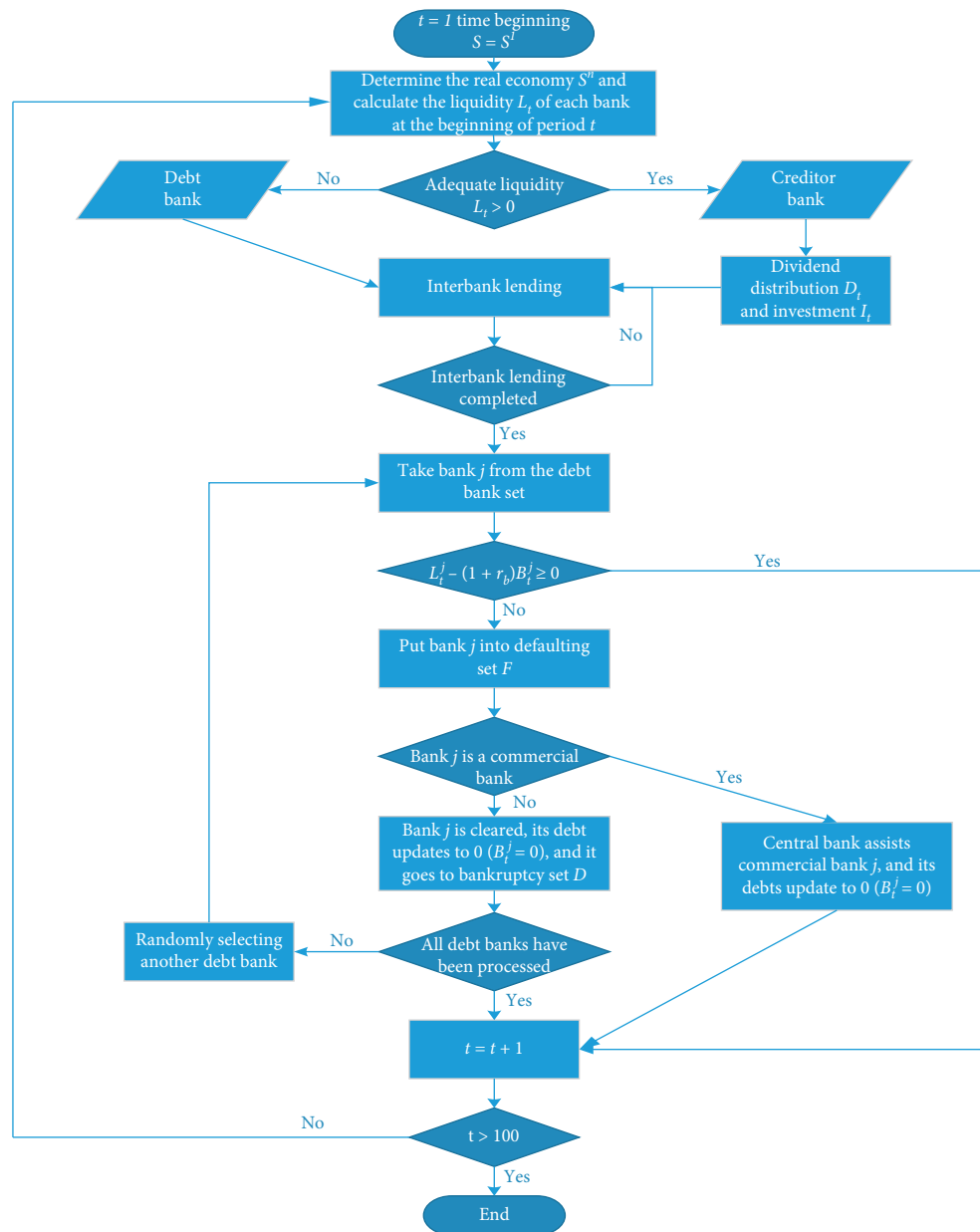


FIGURE 2: Dynamic process algorithm of the interbank system with shadow banking.

400 banks were selected as research objects (sufficient to reflect the characteristics of the banking network system), including 100 commercial banks ($M=100$) and 300 shadow banks ($N=300$), and the maximum simulation time step was set to $t = 100$ (the simulated 100-step system has approached stability).

3.1. The Impact of Shadow Banking on the Systemic Risk. Figure 3 plots the systemic risk of the interbank network with the existence of shadow banking and no shadow banking over time. It can be seen from Figure 3 that in any case, the systemic risk exists from the beginning of the simulation, which is related to the heterogeneity of the banks. Different banks have different operating activities,

which lead to the initial risk of the banking system. It is further found that although there is a systemic risk in the banking system with no shadow banking, its value fluctuates only within a small range close to 0 and is relatively stable. However, the systemic risk of the system with shadow banking has been relatively high and fluctuating, which indicates that shadow banking is affected by the high-risk characteristics of its own business activities, which will bring significant systemic risk impact to the banking system. With the extension of time steps, the systemic risk has shown a downward trend. This may be due to the bankruptcy of the shadow bank, which caused the termination of the interbank lending between the shadow bank and the commercial bank. At the same time, the banking system can self-regulate digestive risks, which is also an important reason to resist

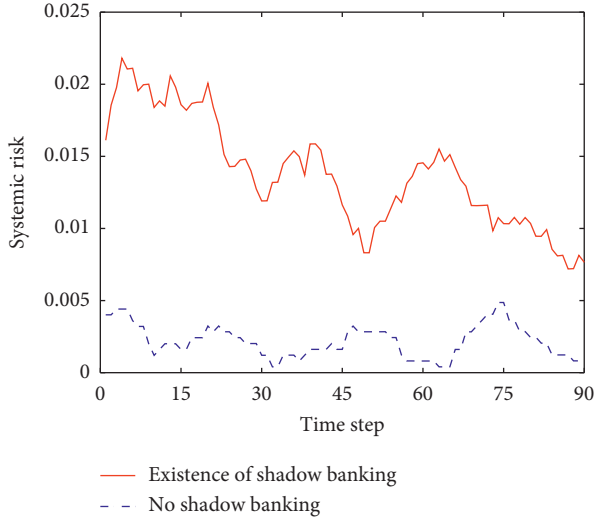


FIGURE 3: The impact of the existence of shadow banking on the systemic risk (the parameters are set as follows: $r_a = 0.0035$, $r_b = 0.023$, $\beta = 0.15$, $\chi = 0.3$, $\sigma_A = 0.3$, $\sigma_\omega = 0.03$, $c = 0.03$, $\bar{A} = 1000$, $\bar{\omega} = \bar{I} = 500$, $\rho = 0.045$, $\tau = 3$, $d = 3$, $R_o^{s1} = 0.07$, $R_o^{s2} = 0.03$, $R_o^{s3} = 0.01$, $p_1 = 0.95$, $p_2 = 0.5$, $p_3 = 0.3$, $U = 400$, $M = 400$, and $N = 0$ for the case of no shadow banking and $M = 100$ and $N = 300$ for the case of existence of shadow banking).

external shock and maintain the stability of the banking system.

3.2. The Impact of Shadow Banking on the Cumulative Number of Default Banks, Bank Survival Rate, Ratio of Bank Default Rate to Commercial Bank Survival Rate, and the Amount of Central Bank Assistance in the Banking System. To effectively describe the specific performance of the impact of the existence of shadow banking on the systemic risk of banks, we calculated the cumulative number of default banks, bank survival rate, ratio of bank default rate to commercial bank survival rate, and the amount of central bank assistance in the banking system through simulation. Figure 4(a) shows the impact of the existence of shadow banking on the cumulative number of default banks in the system. It can be found that the cumulative number of default banks in the banking system with shadow banking is significantly higher than that of the banking system with no shadow banking, and the difference between the two is multiplied as the time step is extended. When the time step reaches 100, the cumulative number of default banks in the banking system with no shadow banking is stable at 6, while that in the banking system with shadow banking is as high as 20. The existence of shadow banking can significantly increase the number of default banks within the system. The emergence of default banks under the existence of shadow banking is mainly due to the decline in liquidity of the system caused by the interbank lending between shadow banks and commercial banks. Table 1 shows the liquidity of the system under the existence of shadow banking and no shadow banking at evolutionary time. Under the influence of business activities such as

investment, the existence of shadow banking aggravates the interbank lending between shadow banks and commercial banks, resulting in a significant decline in the liquidity of the system. Debt banks cannot repay their debts on time, resulting in an increase in the number of default banks.

Figure 4(b) shows the impact of the existence of shadow banking on changes in bank survival ratio in the system. It can be seen that the bank survival ratio in the banking system with no shadow banking decreased with the extension of the time step, but the decline was relatively small, and the fluctuation was stable and finally stayed at around 0.92. This shows that the banking system with no shadow banking is generally stable. However, the bank survival ratio in the banking system with shadow banking has shown a notable decline from the beginning. As the time step is extended, the rate of decline has not slowed down, and there is still a significant downward trend until 100 steps. It shows that the existence of shadow banking significantly reduces the number of surviving banks in the system, undermines the stability of the banking system, has a big shock on the banking system, and increases the possibility of inducing systemic risk in the banking system. The condition of commercial banks in the banking system can directly reflect the stability of the banking system, and it is meaningful to calculate the ratio of the bank default rate to the survival rate of commercial banks. Figure 4(c) depicts the impact of the existence of shadow banking on the ratio of bank default rate to commercial bank survival rate. With the introduction of shadow banking, the contagion risk induced by shadow banking results in the decline of commercial bank survival ratio and the increase of bank default rate; the ratio of default rate to commercial bank survival rate is significantly higher than that in the case with no shadow banking, and ultimately, the stability of the banking system is damaged. Figure 4(d) shows the impact of the existence of shadow banking on the change in the amount of central bank assistance. The central bank assistance to commercial banks can be clearly observed from about 60 steps as shown in the figure. The existence of shadow banking has significantly aggravated the central bank assistance to commercial banks. This once again emphasizes the interbank lending between shadow banks and commercial banks will greatly reduce the liquidity of the system (as shown in Table 1). The bankruptcy of the shadow banks will cause commercial banks to fall into a liquidity dilemma because they cannot recover the loan funds on time. Eventually, commercial banks closed down. The ability of the system to withstand risks is reduced, causing systemic risk.

3.3. The Impact of Changes in Correlation Indicators between Shadow Banks and Commercial Banks on Systemic Risk of Banks. In the case of a finite number of banks in the system, that is, $U = 400$, the combination of the number of shadow banks and commercial banks will affect the scope of the lending between them, and the liquidity of the system will change and thus affect the systemic risk. Figure 5 shows the systemic risk curve under the number combination of three

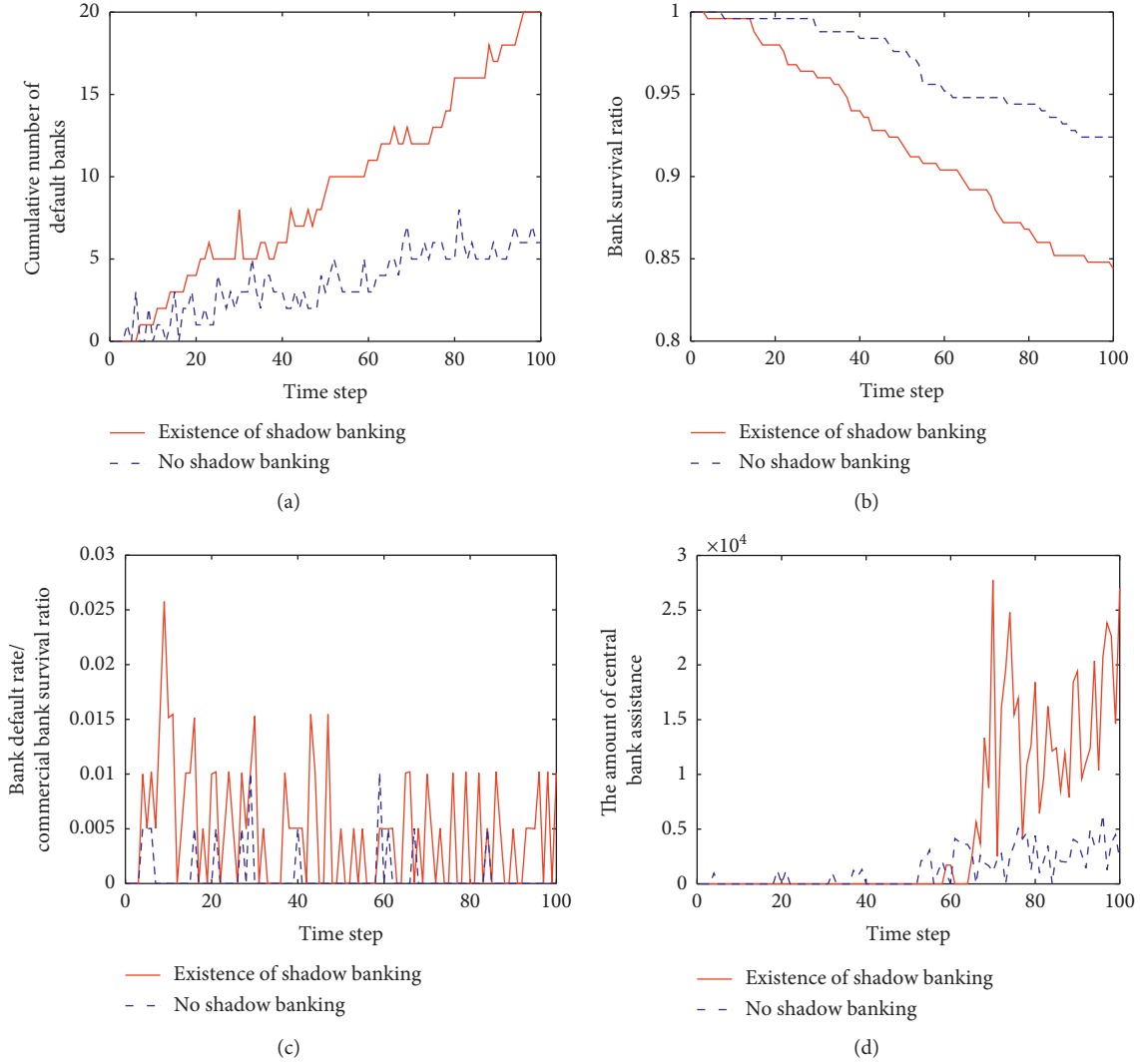


FIGURE 4: (a) The impact of the existence of shadow banking on the cumulative number of default banks in the banking system. (b) The impact of the existence of shadow banking on changes in bank survival ratio in the banking system. (c) The impact of the existence of shadow banking on the ratio of bank default rate to commercial bank survival rate. (d) The impact of the existence of shadow banking on the changes in the amount of central bank assistance (the parameter settings are the same as in Figure 3).

TABLE 1: The liquidity of the system under the existence of shadow banking and no shadow banking at evolutionary time.

	Time step			
	20	40	60	80
Existence of shadow banking	70319.3	74651.0	73180.7	72943.4
No shadow banking	73994.4	72397.3	75185.8	81082.3

types of shadow banks and commercial banks ($M: N=100:300$, $M: N=200:200$, and $M: N=300:100$). It can be seen that as the number of shadow banks in the system decreases from 300 to 100 and the number of commercial banks increases from 100 to 300, the systemic risk gradually decreases and tends to be stable, and the possibility of bank default in the system is also reduced. It shows that the more the number of shadow banks in the banking system compared to

the number of commercial banks, the greater the risk impact of the system. The high number of shadow banks will reduce the maintenance role of the regulatory authorities and the central bank on the stability of the banking system, bring a large and uncertain risk impact to the banking system, weaken the ability of the banking system to deal with risks, and accelerate bank failure.

Iori et al. [12] and Georg [18] studied traditional banking network systems and pointed out that the higher the credit connection between banks, the lower the systemic risk. To further examine the impact of shadow banking on the systemic risk, Figure 6 plots the systemic risk changes under different credit connections ($c=0.01$, $c=0.03$, and $c=0.05$) between shadow banks and commercial banks. The result is similar to the traditional view. Under the structure of the interbank network with shadow banking, the higher the credit connection between shadow banks and commercial banks, the lower and more stable the systemic risk. This

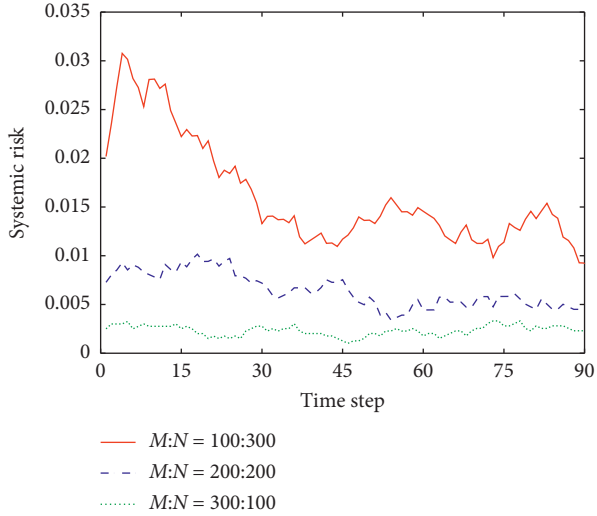


FIGURE 5: The impact of the change in the number combination between the shadow banks and the commercial banks on the systemic risk curve (the parameter setting is the same as in Figure 3 except for M and N).

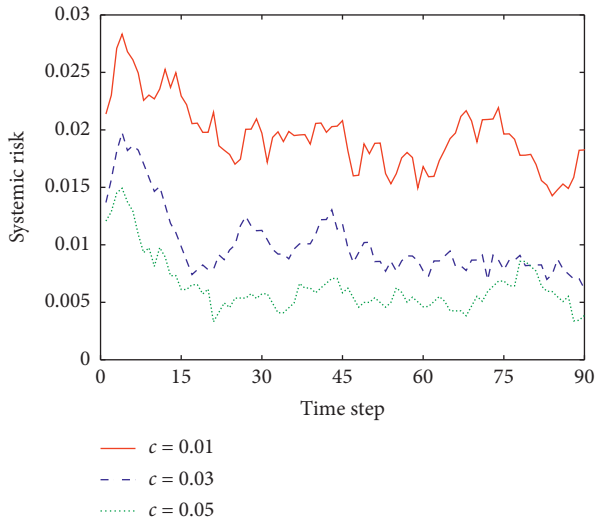


FIGURE 6: The impact of changes in credit connection between shadow banks and commercial banks on systemic risk curves (the parameter setting is the same as in Figure 3 except $M = 100$, $N = 300$, and c).

illustrates that with the increase of the credit connection between shadow banks and commercial banks, the possibility of interbank lending between shadow banking and commercial banks is increased. The existence of shadow banking shares part of the systemic risk, improves the stability of the banking system, and reduces the possibility of bankruptcy.

4. Conclusions

The growth of shadow banking has led to fundamental changes in the global financial architecture. As an important

part of the contemporary complex financial system, shadow banking is considered to be one of the important reasons for causing systemic risk. In order to better explain the effect of shadow banking on systemic risk, a dynamic complex interbank network model with shadow banking is constructed in this paper. Based on the traditional banking network model, the model used the relationship between shadow banks and commercial banks to form a banking system network and analyzed the impact of shadow banking on the systemic risk. In addition, the banks' balance sheet and the interbank lending network are dynamically evolved in this model, which is closer to real bank operations and depicts the specific impact of shadow banking on systemic risk from a microlevel. Through numerical simulation, we have obtained a series of conclusions as follows:

- (i) Compared with the traditional banking network system, the existence of shadow banking does affect the systemic risk.
- (ii) The existence of shadow banking will have an impact on the stability of the banking system, resulting in an increase in the number of default banks in the system, a decline in bank survival rates, and an increase in the number of central bank assistance. The liquidity of funds within the system is reduced, which increases the occurrence of systemic risk.
- (iii) When the number of shadow banks is greater than the number of commercial banks, the systemic risk will be enormous. However, higher credit connection between shadow banks and commercial banks will reduce the systemic risk.

The aforementioned conclusions not only have practical significance for quantitative research on the systemic risk but also have important reference value for preventing financial risks. In addition, the definition of shadow banking is different and the banking system is relatively complex. Therefore, there are still many problems that can be discussed in future work, for example, government policy interference factors under macroeconomic conditions should be considered [35], a more in-depth network structure of interbank lending [36] (not only random network) should be constructed, and the real-world interbank lending network should be estimated by using real data.

Data Availability

The data used to support the findings of this study are available from the corresponding author upon request.

Conflicts of Interest

The authors declare that they have no conflicts of interest.

Acknowledgments

This study was supported by the National Natural Science Foundation of China (71971054), the Shanghai Natural Science Foundation (19ZR1402100), and the Fundamental Research Funds for the Central Universities (19D110803).

References

- [1] Y. Jin and Z. Zeng, "Banking risk and macroeconomic fluctuations," *Journal of Banking & Finance*, vol. 48, pp. 350–360, 2014.
- [2] S. Poledna, J. L. Molina-Borboa, S. Martínez-Jaramillo, M. van der Leij, and S. Thurner, "The multi-layer network nature of systemic risk and its implications for the costs of financial crises," *Journal of Financial Stability*, vol. 20, pp. 70–81, 2015.
- [3] A. R. Neveu, "A survey of network-based analysis and systemic risk measurement," *Journal of Economic Interaction and Coordination*, vol. 1, pp. 1–41, 2016.
- [4] M. Pollak and Y. Guan, "Partially overlapping ownership and contagion in financial networks," *Complexity*, vol. 2017, Article ID 9895632, 16 pages, 2017.
- [5] W. Silva, H. Kimura, and V. A. Sobreiro, "An analysis of the literature on systemic financial risk: a survey," *Journal of Financial Stability*, vol. 28, pp. 91–114, 2016.
- [6] M. Kanno, "Assessing systemic risk using interbank exposures in the global banking system," *Journal of Financial Stability*, vol. 20, pp. 105–130, 2015.
- [7] T. Schuler and L. Corrado, "Interbank market failure and macro-prudential policies," *Journal of Financial Stability*, vol. 33, pp. 133–149, 2016.
- [8] F. Castiglionesi, "Financial contagion and the role of the central bank," *Journal of Banking & Finance*, vol. 31, no. 1, pp. 81–101, 2007.
- [9] A. Hasman and M. Samartín, "Information acquisition and financial contagion," *Journal of Banking & Finance*, vol. 32, no. 10, pp. 2136–2147, 2008.
- [10] G. G. Kaufman and K. E. Scott, "What is systemic risk, and do bank regulators retard or contribute to it?" *Independent Review*, vol. 7, no. 3, pp. 371–391, 2003.
- [11] F. Allen and D. Gale, "Financial contagion," *Journal of Political Economy*, vol. 108, no. 1, pp. 1–33, 2000.
- [12] G. Iori, S. Jafarey, and F. G. Padilla, "Systemic risk on the interbank market," *Journal of Economic Behavior & Organization*, vol. 61, no. 4, pp. 525–542, 2006.
- [13] E. Nier, J. Yang, T. Yorulmazer, and A. Alentorn, "Network models and financial stability," *Journal of Economic Dynamics and Control*, vol. 31, no. 6, pp. 2033–2060, 2007.
- [14] S. Lenzu and G. Tedeschi, "Systemic risk on different interbank network topologies," *Physica A: Statistical Mechanics and Its Applications*, vol. 391, no. 18, pp. 4331–4341, 2012.
- [15] F. Caccioli, T. A. Catanach, and J. D. Farmer, "Heterogeneity, correlations and financial contagion," *Advances in Complex Systems*, vol. 15, Article ID 1250058, 2012.
- [16] C. J. Godlewski, B. Sanditov, and T. Burger-Helmchen, "Bank lending networks, experience, reputation, and borrowing costs: empirical evidence from the French syndicated lending market," *Journal of Business Finance and Accounting*, vol. 39, no. 1–2, pp. 113–140, 2012.
- [17] C. P. Georg and J. Poschmann, *Systemic Risk in a Network Model of Interbank Markets with Central Bank Activity*, Jena Economic Research Papers, 2010.
- [18] C.-P. Georg, "The effect of the interbank network structure on contagion and common shocks," *Journal of Banking & Finance*, vol. 37, no. 7, pp. 2216–2228, 2013.
- [19] T. Lux, "Emergence of a core-periphery structure in a simple dynamic model of the interbank market," *Journal of Economic Dynamics and Control*, vol. 52, pp. A11–A23, 2015.
- [20] S. Berardi and G. Tedeschi, "From banks' strategies to financial (in)stability," *International Review of Economics & Finance*, vol. 47, pp. 255–272, 2017.
- [21] J. H. F. Page and M. Wooders, "Networks and Stability," in *Computational Complexity*, R. Meyers, Ed., pp. 6024–6048, Springer, New York, NY, USA, 2012.
- [22] Financial Stability Board, *Global Shadow Banking Monitoring Report 2015*, Financial Stability Board, Basel, Switzerland, 2015.
- [23] Z. Pozsar, T. Adrian, A. Ashcraft et al., *Shadow Banking Federal Reserve Bank of New York*, Staff Reports, vol. 105, no. 458, pp. 447–457, New York, NY, USA, 2010.
- [24] P. Tucker, "Shadow banking, financing markets and financial stability," in *Proceedings of the Remarks at a Bernie Gerald Cantor Partners Seminar*, vol. 21, Oxford University Press, London, UK, January 2010.
- [25] B. S. Bernanke, C. C. Bertaut, L. Demarco et al., "International capital flows and the returns to safe assets in the United States, 2003–2007," *FRB International Finance Discussion Paper*, vol. 1014, 2011.
- [26] D. W. Diamond, "Financial intermediation and delegated monitoring," *The Review of Economic Studies*, vol. 51, no. 3, pp. 393–414, 1984.
- [27] N. Gennaioli, A. Shleifer, and R. W. Vishny, "A model of shadow banking," *The Journal of Finance*, vol. 68, no. 4, pp. 1331–1363, 2013.
- [28] C. Elgin and O. Oztunali, "Shadow economies around the world: model based estimates," *Bogazici University Department of Economics working Papers*, vol. 5, no. 2012, pp. 1–48, 2012.
- [29] E. Colombo, L. Onnis, and P. Tirelli, "Shadow economies at times of banking crises: empirics and theory," *Journal of Banking & Finance*, vol. 62, no. 9, pp. 180–190, 2016.
- [30] T. V. Dang, G. Gorton, and B. Holmstrom, *Opacity and the Optimality of Debt for Liquidity Provision*, Manuscript Yale University, New Haven, CT, USA, 2009.
- [31] R. Gong and F. H. Page, "Shadow banks and systemic risks," *SSRN Electronic Journal*, 2015.
- [32] J. M. Juran, "Pareto, lorenz, Bernoulli, juran and others," *Industrial Quality Control*, vol. 25, no. 10, 1960.
- [33] F. Basile, "Great management ideas can work for you," *Indianapolis Business Journal*, vol. 16, no. 1, pp. 53–54, 1996.
- [34] L. Eisenberg and T. H. Noe, "Systemic risk in financial systems," *Management Science*, vol. 47, no. 2, pp. 236–249, 2001.
- [35] A. R. Admati, P. M. DeMarzo, M. F. Hellwig, and P. Pfleiderer, "The leverage ratchet effect," *The Journal of Finance*, vol. 73, no. 1, pp. 145–198, 2018.
- [36] S. Gabrieli, "The microstructure of the money market before and after the financial crisis: a network perspective," *SSRN Electronic Journal*, vol. 9, no. 181, 2011.

Research Article

Analyzing Interactions between Japanese Ports and the Maritime Silk Road Based on Complex Networks

Zhi-Hua Hu ¹, Chan-Juan Liu,¹ and Paul Tae-Woo Lee²

¹Logistics Research Center, Shanghai Maritime University, Shanghai 20135, China

²Ocean College, Zhejiang University, Zhoushan 316021, China

Correspondence should be addressed to Zhi-Hua Hu; zhhu@shmtu.edu.cn

Received 12 March 2020; Accepted 21 April 2020; Published 15 May 2020

Guest Editor: Lei Xie

Copyright © 2020 Zhi-Hua Hu et al. This is an open access article distributed under the Creative Commons Attribution License, which permits unrestricted use, distribution, and reproduction in any medium, provided the original work is properly cited.

This article considers how the Japanese ports interact with the ports of China and along the 21st century Maritime Silk Road (MSR) while they are embedded in the global port network, especially in the context of China's Belt and Road Initiative. At a port level, it primarily uses connectivity analysis to analyze the port relations and significances in the maritime network. In contrast, at the network level, it applies the methods from network sciences to analyze the significances of these maritime networks and the interactions among the maritime networks of Japan, China, and MSR. This article extracts a large-scale maritime network from ports and vessels' profiles and data of vessels' Automatic Identification System (AIS). It then examines the relations among the networks (including Japan, China, MSR, and global ports) after defining the maritime networks, network generation schemes, and port network analysis tools. Based on the analysis results and findings, this study draws some implications for regional ports and shipping development and the global supply network.

1. Introduction

A maritime system consists of ports and shipping lines [1]. A global maritime network undertakes 80–90% cargo trade in the world, and its traffic is even estimated to increase by 240–1,209% by 2050 [2]. This article considers a maritime country as a network of ports. China initiated the Belt and Road Initiative (BRI) comprising of the 21st century Maritime Silk Road (MSR) and the Silk Road Economic Belt (SREB) in 2013 [3]. They also can be taken as maritime networks consisting of the ports and vessel flows along the BRI or MSR. The ports, countries with ports, and regional port systems are interweaved in the complicated global port and shipping networks. Thus, this study attempts to raise and answer a research question: how do the maritime networks represent the country- and region-level interactions embedded in the global maritime network?

China publicly released a document entitled “Vision and Actions on Jointly Building Silk Road Economic Belt and 21st-Century Maritime Silk Road” [3, 4]. The document proposed the principles and framework which form the

foundation of the BRI, including two parts, MSR and SREB. This article investigates the relation between Japan and MSR. The 21st century Maritime Silk Road goes from China's coast to Europe through the South China Sea and the Indian Ocean in one route and from China's coast through the South China Sea to the South Pacific in the other [5]. Since the inception of the BRI in 2013, it has motivated researchers, businessmen, and policy-makers to address its impact in a multidimensional way. The official document of MSR does not include Japan. However, Japan is an ancient maritime country with numerous maritime ports and advanced maritime transport [6]. It locates near one end of the MSR. Most importantly, Japan is an important trade partner of China.

Japan has begun to pay more and more attention to the BRI with increasing anticipations [7]. From 2013 to 2015, the Japanese government and the Diets Committee have discussed the Asian Infrastructure Investment Bank (AIIB) membership issue intensively. Only after 2015, the discussion covered the BRI with a wider range of topics. By looking at responses by the Japanese government, the initial response

until 2016 was “nonparticipation”; however, after 2017, the government has shifted attitude to “conditional engagement” through business cooperation in the third countries, especially plus-sum dimension [8].

Hu et al. [1, 9] have established a port and shipping data system using the data from the Internet and commercial providers. Their studies preprocessed the data of maritime ports (6945 ports), terminals (more than 14322 terminals), and berths based on various port data categories and verified by web crawlers and long-time manual processing. They obtained the vessel profiles mainly by web crawlers and so they may not be complete when comparing the real set of active vessels in the world. The ports and vessels’ profiles may be changed, and seemingly no official or commercial organization manages such data centrally. Therefore, the acquisition and verification of these data are time-consuming. We generated the shipping connections among maritime ports from the vessels’ Automatic Identification System (AIS) (3,000,000 vessels) data of 2016. There is an AIS data-sharing network in the world to ensure vessel traveling safety [10]. The AIS data may be recorded in units of second or minute for each vessel when the AIS devices have been installed. Therefore, the AIS data volume is massive. By the present technologies used by us, it will take at least two months to process the data of 2016. From the vessel tracks recorded in AIS, we identified the vessels’ calling sequences of ports. The data system does not collect the cargo volumes or containers carried by vessels or handled by maritime ports. Therefore, we used the vessels’ weight capacities as estimates of the flows of vessels. As described above, the vessels’ calling sequences of ports can be utilized and so we can establish a maritime network (maritime ports and vessel flows) as the base of this study.

This study formulates Japan by a network of its ports and vessel flows among the ports, while the country is not isolated but is connected to other ports, countries, and the global maritime network, as well as China. Simultaneously, China, different countries, and even the global maritime system are all such maritime networks in the global maritime network. The MSR consists of a group of countries, especially with maritime ports and transport connections, which also contribute to a maritime network.

In the era of big data, the bridge of data and qualitative methods emerge in industries [11]. Data storytelling case studies become a vital stream of qualitative researches [12, 13]. In this study, we take the Japanese maritime network in the global maritime network and interact with various other maritime networks as a case that consists of a series of analysis driven by the data system and network analysis methods (see Section 3).

In the following, we first review the relevant studies that provide general insights into the research question. Then, we develop maritime network analysis methods with eight definitions and computing procedures by extending general network analysis methods. This article used a data system as described in our previous studies [1, 4], and we present the details related to data and visualization in Section 4. Then, a series of scenarios are analyzed using the data system and proposed network analysis methods. Finally, we discuss the

study’s empirical findings and conclusions with implications for theory and future research.

2. Background and Literature Review

2.1. Network Analysis. The study of networks has a long history in graph theory and sociology. The modern chapter of network science emerged in the background of complexity, complex network, and complex system. The most explosive works in network sciences are helpful to the study of random networks in graph theory [14] and the social network [15]. Various complex networks exist in telecommunication networks, computer networks, biological networks, cognitive and semantic networks, and social networks. The emergence of network science presents the following natures: interdisciplinary, empirical, and data-driven, quantitative and mathematical, and computational nature. Thus, many scholars developed various models and algorithms by using principles and technologies in mathematics and computer sciences for analyzing the network natures and characteristics by considering distinct nodes (elements, actors, nodes, or vertices) and the connections (links or edges). Network science provides various methods to assess the node, edge, and network complexities (e.g., centrality analysis [15] and link prediction [16]), detect the network structures (e.g., clustering and community analysis [17, 18]), and examine the network behaviors (e.g., synchronization and diffusion [19, 20]).

In this study, upon network science, the maritime networks and their relations are examined. We formulate the countries and regions as maritime networks and their interactions. Thus, the methods in network science can be used and tuned to analyze the shipping, cargo, and trade relations in the port, country, region, and global levels with different granularities of stakeholders.

2.2. Maritime Networks. In a maritime network, a maritime port itself is a hierarchical organization generally with some terminals that contain berths as primary vessel handling facilities; additionally, a port is also a part of a port city that borders with its hinterlands [1]. Due to these hierarchies, the maritime network is geographically a multilayer multiscale system. Meanwhile, it is also associated with logistics, supply chain, industrial chain, trade, and even societies and environments. In this article, we restrict the maritime network to a network of ports and shipping connections; then, we investigate the relations between ports and countries (or independent economies and regions) based on this network.

The maritime network studies can be categorized into three by the method used. First, the maritime networks are studied by network programming to optimize the network structures or deploy the resources operating the networks [21, 22]. Second, many studies investigate the characteristics of finely modeled networks by using the complex network and social network analysis methods [23–25]. Third, the maritime networks are studied broadly by using comprehensive methods [3, 4]. This article belongs to the second category. In Table 1, we reviewed ten studies and identified a set of

TABLE 1: Maritime network studies using network analysis methods.

No.	Articles	Networks	Analysis methods
1	[26]	(1) Containerized maritime network (1164–1342 vessels and 330–390 ports); (2) general cargo maritime network (1515–1654 vessels and 938–1232 ports); (3) the data were queried from the Lloyd’s Register database (generated using AIS data).	Centrality analysis.
2	[27]	(1) Containerized maritime network for the East-West corridor from 1995 to 2011; (2) the network was constructed by the Containerization International Yearbooks (2012).	Degree centrality and distribution, concentration, and regional network analysis.
3	[23]	The Greek Maritime Transportation Network (GMN) is a maritime transportation system that connects 229 ports among regions of Greece.	Centrality, clustering, modularity, average path length, and degree distribution analysis.
4	[25]	A network (2001–2012) among 17 regions comes from the International Containerization (CI-Online) database that provides container deployment data (in TEU) among world regions of the top 100 container lines in terms of the total TEU capacity, and it updates monthly.	Centrality and vulnerability analysis.
5	[28]	The baseline container shipping network (2012) has 1113 nodes and 15916 links obtained from Lloyd’s List Intelligence.	Centrality, community, degree distribution, and vulnerability analysis.
6	[24]	(1) The maritime container transportation network consisted of 39 major container ports, including the 18 major container ports in East Asia, with a throughput of a minimum of 1.5 million TEUs. in 2013; (2) edges between ports are weighted by the weekly transportation capacity (in TEUs) deployed by the top 20 liner shipping companies; (3) the typical transit time between pairs of ports is estimated based on http://www.searates.com .	Centrality analysis.
7	[29]	(1) A multiplex shipping network used the data on liner shipping services in the Americas for the 32 countries and the 139 container ports located in them; (2) the primary data source is the Containerization International Yearbook (2011).	Centrality, clustering, attack simulation, and vulnerability analysis.
8	[30]	(1) Created a container shipping network by using the data from Alphaliner in 2014; (2) the network comprises 439 nodes and 2331 edges.	Centrality, core-periphery, and community analysis.
9	[31]	Based on the AIS data, from January 2014 to March 2015, three maritime networks were built: the container shipping network has 577 nodes and 5794 edges; the tanker shipping network has 708 nodes and 13,935 edges; the bulk carrier shipping network has 700 nodes and 15,337 edges in the MSR shipping network.	Degree distribution, centrality, and flow spatial distribution analysis.
10	[32]	(1) Used AIS data to build three cargo ship transportation networks (oil tanker, container ship, and bulk carrier); (2) the container, oil tanker, and bulk carrier ship networks contain 1488, 2042, and 1969 ports individually.	Centrality, degree distribution, attack analysis, and network robustness assessment.
11	[33]	The Greek Maritime Network connects 229 ports via 231 bidirectional shipping routes.	Graph density, centrality, clustering, modularity, and average path length.

Source: compiled by the authors.

networks and analysis methods: the original data of constructing the networks mainly come from yearbooks, Internet data queries, and AIS data; analysis methods mainly include centrality, attack test, clustering, and community detection.

2.3. Japanese Maritime Network. Japan is a typical maritime country. In our data system, Japan has 994 ports in total, of which 125 ports are considered essential both in international and domestic maritime networks [34]. Maritime ports are critically crucial to the national and local economies. Because Japan is mountainous, major metropolitan areas are all developed on the coastal planes of the country. The three most significant metropolitan areas of Kanto, Chukyo, and Kinki are all developed along with the large terminals, namely, the Bays of Tokyo, Ise, and Osaka, respectively [34].

Historically, large maritime ports have played a critically important role in the economy as well as the urban development of these bay areas.

Developing a maritime system is critically important to Japan. First, Japan heavily depends on the import of raw materials for domestic production and the daily life of people. For instance, Japan imported more than 90% of energy and more than 60% of foods from overseas. Japan is a leading hi-tech country, and many industrial products are exported to the world market by seaborne trade. Second, Japan consists of about 6,800 islands, including four main islands. Most cities develop along the coastal lines of the country, and each of them has developed its port. Ports are critical to the local economy and development. Third, the cost of developing Japanese ports is high and increasing due to severe ocean conditions. Port investment is infeasible

when the government cannot recognize the ports as essential parts of the development strategies of the nation and local governments. Fourth, limited land availability of port cities restricts the Japanese port developments. The marine terminals, logistics activities, and the port cities demand a large volume of lands. Therefore, the governments must optimize the lands' efficiency and develop multiuse modes to cope with these conditions. Due to severe trade and economic dependence on maritime transport and shortage of land resources, Japanese ports and the shipping industry faces fierce competition in domestic markets and the Asian maritime system. South Korea and China both present competitive power in ports and shipping. The interaction between Japan and neighborhoods and the embeddedness in the global maritime network may indicate potential opportunities for the Japanese port system.

2.4. Summary. The network and maritime studies suggest that network formulation of the maritime network of ports and shipping is beneficial to investigate the structures and behaviors of maritime networks. However, existing studies [26, 32] mainly focused on a single network for a country of a region, the network analysis methods coupling two or more maritime networks is still in development. Considering Japan and its interactions with other countries or regions, it is challenging to construct large-scale networks for analysis.

3. Maritime Network Analysis Methods

3.1. A Systematic Framework. Figure 1 presents a systematic framework for this study. Considering the knowledge of interactions among the global maritime network, Japan, China, and MSR, we develop four modules in this study as a too-level framework. First, the previous study on the Shipping Earth data system [1, 4] is the base of this study. Second, we construct the maritime networks as the base of analysis. Third, in the analysis module, eight scenarios are investigated by constructing assessment methods for maritime network analysis. We demonstrate all these data systems, developed concepts, and methods by using the data system.

The global maritime network is defined, followed by general maritime networks. Then, we elucidate two network generation procedures and schemes: we generate a network from a vessel's port calling sequence; we construct a new network from these two interconnected maritime networks. Finally, the network analyzing methods mainly used in this study (Section 5) are given based on the abovementioned network notations. Based on the degree and PageRank centralities, we conceptualize a metric using the flows among nodes as primary (or top- n) flows and significances of flow interactions among the maritime networks.

3.2. Maritime Networks

3.2.1. Structures of Maritime Networks. We denote a global maritime network as $G = (N, E, P, W)$, where N, E, P, W are the port set, connection set, port properties, and connection properties. $E = \{(i, j) \mid i, j \in N\}$; $P = \{P^k\}$, $P^k = [P_i^k]$, $i \in N$;

$W = \{W^k\}$, $W^k = [P_e^k]$, $e \in E$. Here, k is the name or index of properties, and each property is a vector corresponding to the set of nodes or connections. The notations $start(e)$ and $end(e)$ are used to access the two end nodes of a connection $e \in E$. Define the operators $innode(i)$, $outnode(i)$ as the sets of nodes targeting or originating from the node i , as denoted by the following:

$$innode(i) = \{start(e) \mid e \in E, end(e) = i\}, \quad i \in N, \quad (1)$$

$$outnode(i) = \{end(e) \mid e \in E, start(e) = i\}, \quad i \in N. \quad (2)$$

In (1), the set of nodes entering a node i contains the starting nodes of the edges whose ending nodes are the node i . Similarly, the set of nodes leaving a node i contains the ending nodes of the edges whose starting nodes are the node i .

Any maritime network is a part of the global maritime network. Given a node subset, $N^s \subseteq N$, a maritime network is denoted as $G(N^s) = (N^s, E(N^s), P(N^s), W(N^s))$ in the following:

$$E(N^s) = \{(i, j) \mid i \in N^s, j \in N^s\} \subseteq E, \quad (3)$$

$$P(N^s) = \{P^k(N^s)\} = \left\{ \left\{ P_i^k \mid i \in N^s \right\} \right\}, \quad (4)$$

$$W(N^s) = \{W^k(N^s)\} = \left\{ \left\{ P_e^k \mid e \in E(N^s) \right\} \right\}. \quad (5)$$

The maritime network of a given set of ports N^s can be reformulated in the form of $G = (N, E, P, W)$ as defined above. Here, the new port set is N^s . The new edge set contains the edges whose starting and ending nodes that are in N^s , as denoted by (3). The port property set is a set of properties, where a property is a data vector corresponding to N^s , as denoted by (4). Similarly, the edge property set is a set of properties, where a property is a data vector corresponding to the edge set computed by (3).

The centrality measures include degree, closeness, and betweenness measures of centrality [15]. These basic centralities assess the importance (in various aspects) of a node in a network.

A vessels' shipping traffic network is different from general connectivity-based networks because a vessel's movement may depend on several previous calling ports [35]. Based on this observation, we develop the network of calling sequences by considering the vessels' movements. Besides, because the final network is a composition of all edges generated by the calling sequences, the final network utilized the local information (the calls to neighbor ports) to reduce the random errors in AIS data [36].

3.2.2. Generating Maritime Networks. In the context of maritime studies, we define a calling sequence (denoting a sequence by v in a sequence set V) as a sequence of network nodes and a weight attached to the sequence, namely, (\vec{N}^v, W^v) , where $\vec{N}^v = i_1, i_2, \dots, i_{\lfloor \vec{N}^v \rfloor}$, $i_* \in N$, and a constant weighted is W^v . The sequence \vec{N}^v travels from the port i_k to the port i_{k+j} . We say that the sequence travels for j jumps.

The network of calling sequence is defined by a $\{(\vec{N}^v, W^v)\}$. By $\{(\vec{N}^v, W^v)\}$, a maritime network

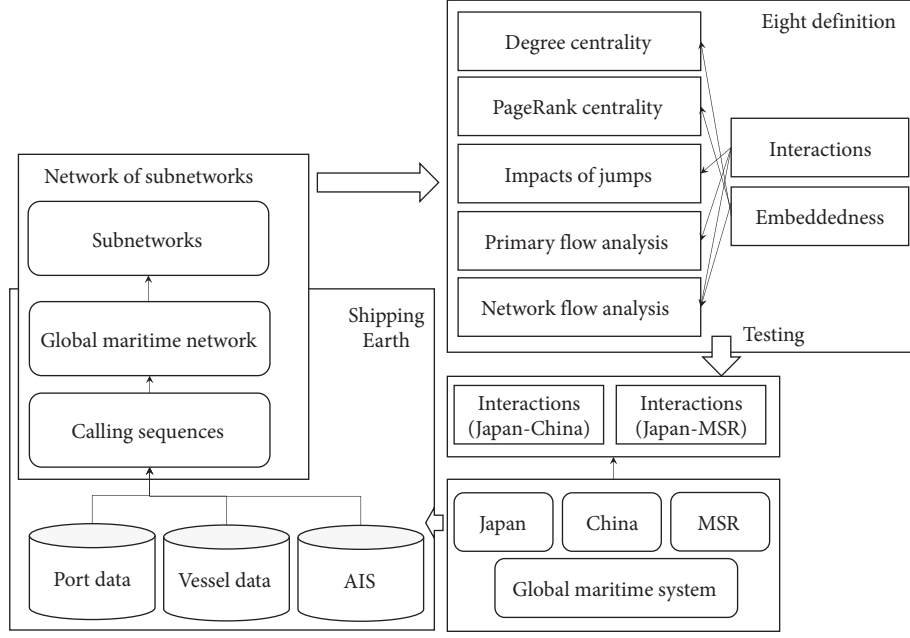


FIGURE 1: A systematic framework.

$G = (N, E, P, W)$ can be generated as (6)–(8). In (8), W^{*v} is used to represent the original weight of the calling sequence, while W^v is generated for the network.

$$N = \text{set}\left(\cup_v \text{set}\left(\vec{N}^v\right)\right), \quad (6)$$

$$E = \left\{ (i, j) \mid \exists v, i, j \in \vec{N}^v \right\}, \quad (7)$$

$$W_{(i,j)}^v = \sum_{\langle i,j \rangle \in \vec{N}^v} W^{*v}. \quad (8)$$

In (6)–(8), we generate N, E, W from a set of calling sequences. Notably, a calling sequence visits a series of ports one by one. Therefore, the direct connections from a visited port to an adjacent port just after visiting the port can be extracted from the sequence gradually. That is, a set of $N - 1$ connections (edges) can be extracted from a sequence of N ports, as denoted by (7). For a given sequence, we can calculate and determine some properties, e.g., the weight and size of the vessel of this sequence. Therefore, each edge can inherit the property of the sequence, as denoted by (8).

In the abovementioned formulations, only direct transition (one jump) from a port to its adjacent port in \vec{N}^v is used to the network G . Indeed, the transitions from a port to its successors all can present indirect transitions with a multiplier of possible smaller coefficients. In (9), all transitions from a port to its successor in the calling sequence indicate connections among ports; in (10), the weight of a connection is reduced by a multiplier, $1/(t_2 - t_1)$, which indicates that long-distance transition (more jumps) impacts less on the weight. Notably, in (9) and (10), by using $i \notin \vec{N}^v [(t_1 + 1) \sim t_2]$, the jump from node i will “stop” when it meets i .

$$E = \left\{ (i, j) \mid \exists v \in V, t_1 < t_2, t_2 - t_1 > \text{jumps}, \right. \\ \left. i \notin \vec{N}^v [(t_1 + 1) \sim t_2]: i = \vec{N}^v [t_1], j = \vec{N}^v [t_2] \right\}, \quad (9)$$

$$W_{(i,j)}^v = \sum_{\substack{i = \vec{N}^v [t_1], j = \vec{N}^v [t_2], t_1 < t_2, \\ i \notin \vec{N}^v [(t_1 + 1) \sim t_2], t_2 - t_1 > \text{jumps}}} \frac{W_{(i,j)}^{*v}}{t_2 - t_1}, \quad \forall v \in V. \quad (10)$$

As the difference between (9) and (7), they use one jump or multijumps to construct the sets of edges from a sequence. The number of jumps can amend the impacts on the edge properties, as denoted by (10).

Hence, we can set an arbitrary upper boundary number of jumps ($\text{jumps} \leq n$) to generate E and $W_{(i,j)}^v$, and so the resulting E and $W_{(i,j)}^v$ are denoted by $E|_{\text{jumps} \leq n}$ and $W_{(i,j)}^v|_{\text{jumps} \leq n}$. The resulting network will also affect the centrality and network analysis results. Therefore, this notation indicates the settings of the upper boundary jump number for generating networks. In this study, we generate the networks used in the following sections with $\text{jumps} \leq 15$. “Jumps” is a new concept introduced to represent the behaviors of the sequence.

\vec{N}^v is a time series and other two accompanied series can be defined, \vec{T}^v and \vec{D}^v , which are the visiting times and durations. By using these two series, \vec{N}^v can be segmented into short series for periodical pattern analysis.

We can generate a maritime network from a set of maritime networks whose ports come from the original networks, whose port properties aggregate the properties of the ports, and whose edge connections aggregate the weights of connections between the ports of connections.

Given two maritime networks (N^a, N^b) , new E^c, P^c, W^c are generated as (11)–(16), where \otimes and \oplus are aggregate operators upon the properties and weights; $E(N^a, N^b)$ is a set of connections between N^a and N^b . Notably, we insert two possible new connections into the connection set E^c when connections exist between the given networks, as denoted by (13) and (14).

$$N^c = N^a \cup N^b, \quad (11)$$

$$E(N^a, N^b) = \{(i, j) \mid i \in N^a, j \in N^b\}, \quad (12)$$

$$E^c \leftarrow (a, b), \quad \text{if } |E(N^a, N^b)| > 0, \quad (13)$$

$$E^c \leftarrow (b, a), \quad \text{if } |E(N^b, N^a)| > 0, \quad (14)$$

$$P = \left\{ \otimes_{i \in N^a} (P_i^k), \otimes_{i \in N^b} (P_i^k) \mid k \right\}, \quad (15)$$

$$W = \left\{ \oplus_{e \in E(N^a, N^b)} (W_e^k) \mid (a, b) \in E^c \right\}. \quad (16)$$

In (11)–(16), we deduce two maritime networks, N^a and N^b . In (11), the nodes of a top network come from these subnetworks. In (12), an operator computes the edge set between the nodes of two networks. In (13) and (14), if there are edges between two networks, an edge is added to the edge set of the top network. The node and edge property sets are different. Hence, we introduce aggregation operators in (15) and (16). For example, the throughput property of a network is the sum ($\otimes = +$) of the throughputs of the port nodes of the network. Similarly, the transportation volume between two networks is the sum ($\oplus = +$) of the volumes of all edges between these two networks.

3.3. Analysis Tools for Maritime Networks. Two categories of network analysis are studied here: node-based and edge-based analysis tools.

3.3.1. Node-Based Analysis. The node-based tools are defined based on centralities in complex networks, namely, the degree centrality and PageRank centrality [37]. The degree centrality can represent the significance of nodes with inflows and outflows (delegating the port throughputs in maritime studies). In contrast, the PageRank centrality can reflect the network significance of a node (delegating some important hub ports in a maritime network).

We derive the definitions of the weighted degree centrality as (17)–(19) [15], where $C^{\text{indegree}}(i)$ and $C^{\text{outdegree}}(i)$ are in- and out-degrees when the network is considered as a directional one, and $C^{\text{degree}}(i)$ is the centrality degree when we consider the network as a bidirectional one. When analyzing connection networks, the degree is simplified to account the connection times, as defined by (20)–(22). $N^{\text{io}}(i)$ is a set of connected nodes, while the number of connected nodes is $|N^{\text{io}}(i)|$.

$$C^{\text{indegree}}(i) = \sum_{\text{end}(e)=i} W_e^k, \quad \forall i \in N, \quad (17)$$

$$C^{\text{outdegree}}(i) = \sum_{\text{start}(e)=i} W_e^k, \quad \forall i \in N, \quad (18)$$

$$C^{\text{degree}}(i) = C^{\text{indegree}}(i) + C^{\text{outdegree}}(i), \quad \forall i \in N, \quad (19)$$

$$N^{\text{in}}(i) = \{j \mid (j, i) \in E\}, \quad \forall i \in N, \quad (20)$$

$$N^{\text{out}}(i) = \{j \mid (i, j) \in E\}, \quad \forall i \in N, \quad (21)$$

$$N^{\text{io}}(i) = N^{\text{in}}(i) \cup N^{\text{out}}(i), \quad \forall i \in N. \quad (22)$$

In the PageRank centrality, the importance of the nodes pointing to i represents the importance of a node i , denoted by *innode* (i), while the nodes pointed by connections from i is denoted by *outnode* (i). The PageRank centrality is conceptually defined by

$$C^{\text{pagerank}}(i) = c \sum_{j \in \text{innode}(i)} \frac{C^{\text{pagerank}}(j)}{|\text{outnode}(j)|}, \quad i \in N. \quad (23)$$

The ‘‘PageRank’’ [38, 39] centrality is rooted in a random walk of the network. Given a node in a graph, we decide the next node with the ‘‘Follow Probability’’ from the set of alternatives (successors) of the current node (neighbors for the undirected case). Otherwise, when a node has no alternatives (successors), the next node is selected from all nodes. We use the PageRank algorithm implemented in MATLAB 2016.

3.3.2. Edge-Based Analysis. Two edge-based tools are defined: the primary flows among a maritime network, and the flows among two maritime networks in the context of the global maritime network.

The primary flows are top- N flows between two maritime networks. Given two maritime networks with node sets N^a and N^b , the connections from N^a to N^b are $E(N^a, N^b)$. The flow is denoted by W_e^{flow} for each $e \in E(N^a, N^b)$. Hence, the connections can be ranked by the flows decreasingly. The set of the top- N connections is $\Delta^n(N^a, N^b)$. Here, n is a number indicating n connections in the set.

The mutual maritime flows occur between two maritime networks in the context of a global network. The network flows are assessed in three criteria: number calling sequences, number of calls, and weighted flow volume.

Given two node sets N^a and N^b as two maritime networks, the three assessment criteria for mutual network flows are $F^{\text{seq}}(N^a, N^b)$, $F^{\text{visit}}(N^a, N^b)$, and $F^{\text{weight}}(N^a, N^b)$ ((24)–(26)).

$$F^{\text{seq}}(N^a, N^b) = \sum_{v \in V} \left(\left| N^a \cap \vec{N}^v \right| > 0 \wedge \left| N^b \cap \vec{N}^v \right| > 0 \right), \quad (24)$$

$$F^{\text{visit}}(N^a, N^b) = \sum_{v \in V, i \in \vec{N}^v} (i \in N^a \wedge i + 1 \in N^b), \quad (25)$$

$$F^{weight}(N^a, N^b) = \sum_{e \in E(N^a, N^b)} W_e^{flow} + \sum_{e \in E(N^b, N^a)} W_e^{flow}. \quad (26)$$

We further explain the abovementioned three criteria. In (24), we compute the number of vessels' calling sequences visiting the two maritime networks (visiting a port in a maritime network and visiting another port in another maritime network), which is approximately equal to the number of vessels calling the two maritime networks. It can answer the general question: how many vessels visit the two maritime networks simultaneously? The number should represent the connection strength of two maritime networks. In (25), if a sequence visits a port in a maritime network and then a port in another maritime network, F^{visit} will be increased by one. That is to answer the question: how many visits to the two maritime networks? Similarly, by (26), we try to answer: how much volume on the visits between the two networks when the edge property is volume? By these three computing formulas, the relations between the two networks are determined.

3.4. An Example. Considering two calling sequences or maritime ports, $\langle 1, 2, 3, 4, 5, 6, 5, 3 \rangle$ with a flow of 500 tons and $\langle 2, 3, 4, 5, 7, 3, 1 \rangle$ with 700 tons. The berths of the ports 1–7 are 4, 4, 3, 3, 5, 5, and 5 individually. Therefore, a network $G = (N, E, P, W)$ can be established:

- (1) $N = \{1, 2, \dots, 7\}$
- (2) Consider a set of eight edges: $E = \{(1, 2), (2, 3), (3, 4), (5, 6), (5, 3), (5, 7), (7, 3), (3, 1)\}$
- (3) $P = \{P^{berths}\}$ and $P^{berths} = \{4, 4, 3, 3, 5, 5, 5\}$
- (4) $W = \{W^{flow}\}$ and $W^{flow} = \{500, 1200, 1200, 1200, 500, 700, 700, 700\}$

We can identify two maritime networks from the seven maritime ports, namely, $N^a = \{1, 2, 3\}$ and $N^b = \{4, 5, 6, 7\}$. Set two aggregate operators \otimes and \oplus to \sum . A new network of the submaritime networks $G^c = (N^c, E^c, P^c, W^c)$ can be extracted:

- (1) $N^c = \{a, b\}$
- (2) $E^c = \{(a, b), (b, a)\}$
- (3) $P^c = \{P^{berths}\}$, and $P^{berths} = \{11 = 4 + 4 + 3, 18 = 3 + 5 + 5 + 5\}$
- (4) $W^c = \{W^{flow}\}$, and $W^{flow} = \{1200, 1900 = 1200 + 700\}$

4. Data

In this study, we use the data of more than 300,000 vessels' AIS tracks and 6000 maritime ports of 2016 to construct a maritime network $G = (N, E, P, W)$ by using the methods developed in Section 3. A vessel's track of its positions recorded in AIS can be processed to be a calling sequence of maritime ports. By this process, we can obtain the port calling sequences of all vessels. Within these vessels, only about two of the third can have port calling sequences. Here,

N is a set of maritime ports in the global maritime network; E is a set of connections among ports. We can generate E by the method described in Section 3. P denotes a property, namely, economic entity (ee), $P = \{P^{ee}\}$. The original weight (W^{*s} in (8) and (10)) of a vessel calling sequence is the weight of the vessel.

Use $ee \in \{world, Japan, China, MSR\}$ to represent the complete port set (*world*), the Japanese port set (*Japan*) and Chinese port set (*China*), and a set of ports along the Maritime Silk Road (*MSR*), $N^{world} (= N)$, N^{Japan} , N^{China} , and N^{MSR} . Their supplementary sets are denoted by \emptyset (empty set), \bar{N}^{Japan} , \bar{N}^{China} , and \bar{N}^{MSR} . Additionally, the Japanese ports include two sets, domestic port set N^{Jd} and international port set N^{Ji} . A Japanese maritime port is called if and only if at least a vessel visits at least one port, not in N^{Japan} . We introduce $Visits(n)$ representing the number of vessels visiting Japanese ports for at least n times, as denoted in (27). Besides, in (28), $Countries(v)$ computes the number of countries whose ports are visited by the vessel v .

$$Visits(n) = \sum_{v \in S} (F^{seq}(N^{Japan}, \bar{N}^{Japan}) > n), \quad (27)$$

$$Countries(v) = \left| \left\{ P^{country}[i] \mid i \in \bar{N}^v \right\} \right|, \quad \forall v \in V. \quad (28)$$

Table 2 summarizes the vessels visiting the Japanese ports N^{Japan} . First, we classify the trading vessels into domestic and international trading vessels. More vessels are international trading vessels visiting the Japanese ports. Only a very few vessels visited Japan once in 2016, while most vessels visited the country for more than ten times. Considering the time of vessel callings, the distributions of vessels to the visiting times ($Visits(i) - Visits(i+1)$) and countries ($Countries(v)$) are depicted (see Figure 2).

Further, the distributions of F^{visit} and F^{weight} computed from $\{\bar{N}^v\}$ can be depicted for dates and months using $\{\bar{T}^v\}$ and $\{\bar{D}^v\}$ (see Figure 3). The seasonality of the distribution is slight at least for the distributions of F^{visit} and F^{weight} .

The jumps have impacts on F^{weight} , F^{seq} , N^{io} , and F^{visit} (see Figure 4). Therefore, the choice of the parameter "jumps" is essential. When the number is too small, the impacts of indirect connections among ports on the results are not observable. The "jumps" represent the visiting behavior of vessels to the ports. If a vessel visits port A just before port C, the number of jumps is one from C to A; if a vessel visits port A before visiting B and C, the number of jumps is two from C to A (Section 3). In this study, we set the number of jumps to 15 in (9) and (10).

5. Results and Analysis

In the following, we construct the maritime networks and analyze the interactions among the maritime networks (N^{Japan} , N^{China} , N^{MSR} , \bar{N}^{Japan} , \bar{N}^{China} , \bar{N}^{MSR} , N^{Jd} , and N^{Ji}) in the context of the global network (N^{world}) by using the node- and edge-based analysis tools.

TABLE 2: Summary of vessel visits to Japanese ports.

Total vessels	N^{Japan}	13925
Trading vessels	$N^{J domestic}$	6419
	$N^{J international}$	7506
Vessel visits	$Visits(200)$	3562
	$Visits(100)$	5118
	$Visits(50)$	6772
	$Visits(20)$	8769
	$Visits(10)$	10270
	$Visits(1)$	13287
	$Visits(0) - Visits(1)$	638

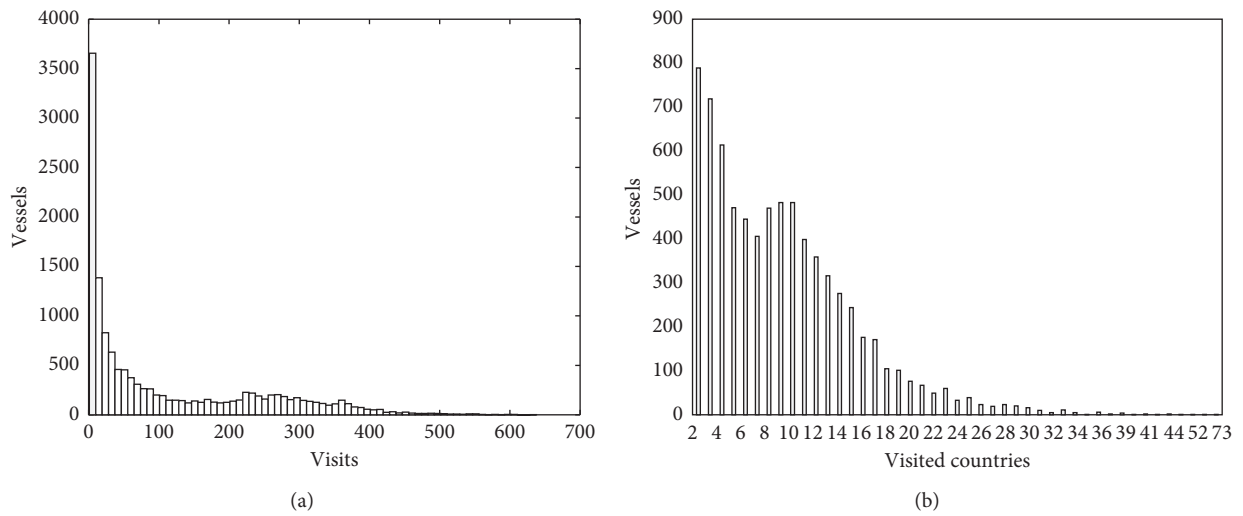


FIGURE 2: Vessel visiting times and countries. (a) $Visits(i) - Visits(i + 1)$. (b) $Countries(v)$.

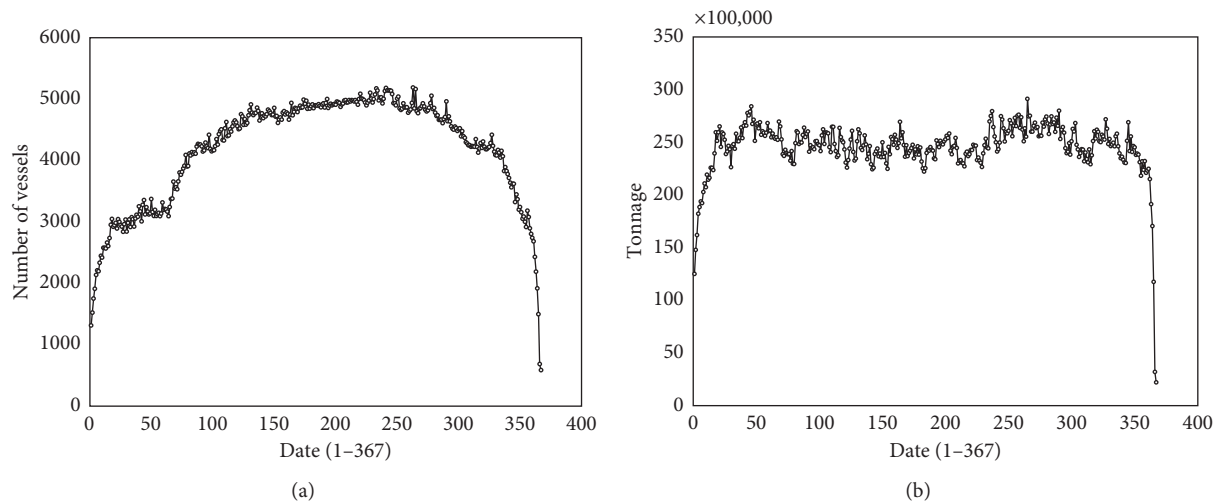


FIGURE 3: Continued.

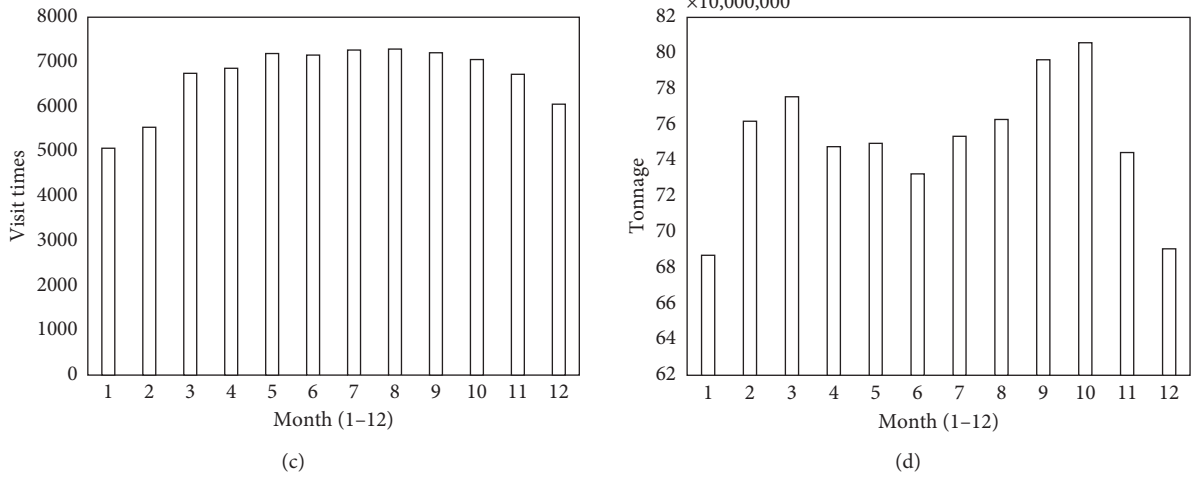


FIGURE 3: Periodical vessel visits and flows. (a) F^{visit} by date. (b) F^{weight} by date. (c) F^{visit} by month. (d) F^{weight} by month.

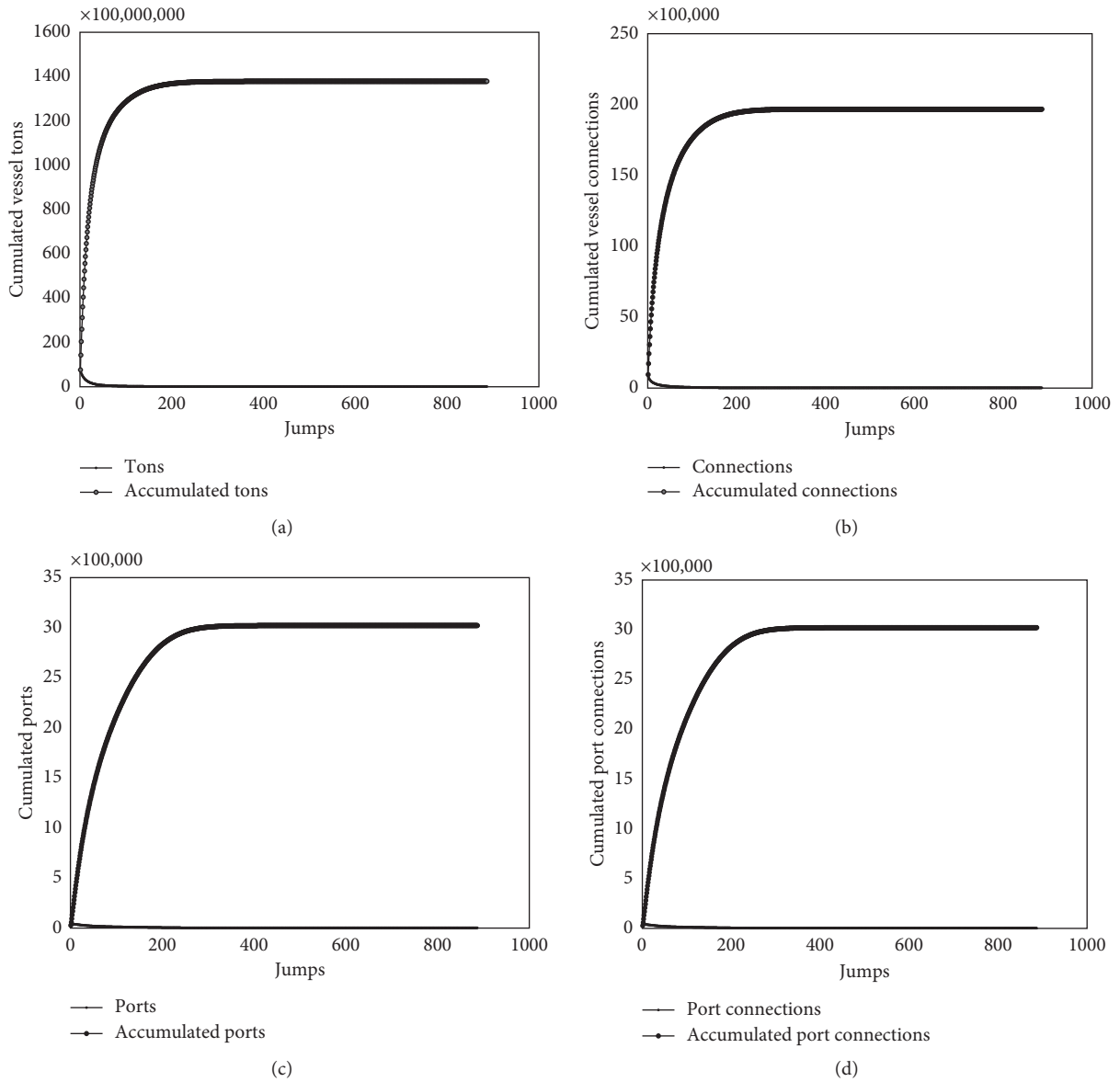


FIGURE 4: Japanese port distributions impacted by jumps. (a) $F^{weight}|_{jumps \leq n}$. (b) $F^{seq}|_{jumps \leq n}$. (c) $N^{io}|_{jumps \leq n}$. (d) $F^{visit}|_{jumps \leq n}$.

5.1. One-Jump Connections with the World. As defined in (12), The direct connections ($jumps = 1, E(N^{Japan}, \overline{N}^{Japan})$) between Japanese ports (N^{Japan}) and the world (\overline{N}^{Japan}) mean the ones directly connecting the Japanese ports and the ports of all countries/regions (see Figure 5). Here, 26097 connections and 922 ports are involved. In other words, the number of jumps (as defined in Figure 3) is one. The vessel connections (see Figures 5(a) and 5(b)) and the top primary flows (see Figures 5(c) and 5(d) for $\Delta^{2000}(N^{Japan}, \overline{N}^{Japan})$) help to identify most maritime trading regions.

5.2. Multijump Connections with the World. All connections between Japanese ports (N^{Japan}) and the world (\overline{N}^{Japan}) are the ones connecting the Japanese ports and the ports of all countries/regions by various numbers of jumps ($jumps > 1$) (see Figures 6 and 7). Here, 114673 connections and 2520 ports are involved. The maritime trading regions can be identified (see Figures 6(a) and 6(b)), as well as the top primary flows (see Figures 6(c) and 6(d) for $\Delta^{2000}(N^{Japan}, \overline{N}^{Japan})$). The settings' multijump connections reveal possible indirect maritime trading partners for Japan.

5.3. The Maritime Network of Domestic Trading Flows. The domestic connections (see E^{Jd} computed by (29)) can be summarized in terms of port connections, vessel visits (N^{Japan}), and flow, as well as the connecting domestic ports (see Table 3). The 149 active ports almost entirely interconnect with each other (see N^{Jd} computed by (30)) in the connection graph (see Figure 8). The flow throughput of port i is computed by (31)–(34).

$$E^{Jd} = \{(i, j) \mid (i, j) \in E; i, j \in N^{Japan}\}, \quad (29)$$

$$N^{Jd} = \{j \mid (i, j) \in E; i, j \in N^{Japan}\} \cup \{j \mid (j, i) \in E; j, i \in \overline{N}^{Japan}\}, \quad (30)$$

$$Vessels(i) = \sum_{v \in V} (\exists j: \overline{N}^v[j] = i), \quad (31)$$

$$C^{windegreed}(i) = \sum_{\substack{e \in E^{Jd}, \\ end(e)=i}} W_e^{flow}, \quad \forall i \in N^{Japan}, \quad (32)$$

$$C^{woutdegreed}(i) = \sum_{\substack{e \in E^{Jd}, \\ start(e)=i}} W_e^{flow}, \quad \forall i \in N^{Japan}, \quad (33)$$

$$C^{wd}(i) = C^{woutdegreed}(i) + C^{windegreed}(i). \quad (34)$$

From the top 20 primary flows (Table 4), we can identify the primary port connections, by using $\Delta^{20}(N^{Japan}, N^{Japan})$. The last three columns are defined by similar formulas, as presented in (24)–(26).

The abovementioned analysis provides tools to identify important or potentially critical domestic ports and maritime transport channels for Japan.

5.4. The Maritime Network of International Trading Flows. From the resulting international trading connections of 149 Japanese ports (Table 5), most Japanese ports (N^{Japan}) connect to more than 1000 ports (in \overline{N}^{Japan}), as defined in (36) where E^{Ji} is given by (35), and only one port is purely a domestic trading port. From the top 20 ports with the most significant flows (Table 6), only one port (Yanai, that is the purely domestic port) is listed. Therefore, Japan is a typical maritime country because its ports are almost international active ports.

$$E^{Ji} = \{(i, j) \mid (i, j) \in E; i \in N^{Japan}, j \in \overline{N}^{Japan}\}, \quad (35)$$

$$N^{Ji} = \{j \mid (i, j) \in E^{Ji}; i \in N^{Japan}, j \in \overline{N}^{Japan}\} \cup \{j \mid (j, i) \in E; j \in N^{Japan}, i \in \overline{N}^{Japan}\}. \quad (36)$$

5.5. Primary Maritime Flows between Japan and the World. From the primary flows (Figure 8, $\Delta^{20}(N^{Japan}, \overline{N}^{Japan})$) between Japan (N^{Japan}) and the world (\overline{N}^{Japan}), all prominent flows are to or from China (N^{China}), Chinese Hong Kong, and Singapore. From the top 20 connections between Japan and the world (Table 6, $\Delta^{20}(N^{Japan}, \overline{N}^{Japan})$), the most prominent flows are active between Japan and the MSR (mainly Hong Kong, Singapore, and Malaysia in N^{MSR}). Hongkong and Singapore are essential hubs for Japanese products' trade; China is an essential market of Japanese industries.

The network flows between Japan (N^{Japan}) and the world (\overline{N}^{Japan}) can be computed (see Table 7). By assessing the ratios of the flows between Japanese and the world as presented in the last two rows in Table 8, the flows of Japanese ports contribute less to the global maritime network (0.56~2.31%), while contributing to its domestic trade dominantly (11.04~28.89%).

5.6. Ranking Ports by Trading, Connection, and Centralities. Using the global connection data of the Japanese ports, we rank the ports, as shown in Table 7. Kobe is the first grade.

The Japanese ports are not different in terms of ranking of their throughput (using $C^{degree}(i)$ in Section 3) and network impact (using $C^{pagerank}(i)$ in Section 3) (see Table 9).

5.7. Primary Maritime Flows with the Maritime Silk Road. As seen from the primary maritime flows between Japan (N^{Japan}) and the MSR (N^{MSR}) (Figure 9), China, Singapore, and Malaysia are the central import countries connected to Japan.

From the top 20 connections between Japan and MSR ($\Delta^{20}(N^{Japan}, N^{MSR})$, Table 10), we can identify three essential stakeholders: Hong Kong, Singapore, and Malaysia along the MSR.

Table 11 indicates the ratios of flows between Japan (N^{Japan}) and the MSR (N^{MSR}); about 20% of vessel flows of Japanese international trade are directed to the MSR, while Japan contributes to the MSR by a tiny ratio (from 0.52% to 4.49%) of flows. It implies that although the BRI document

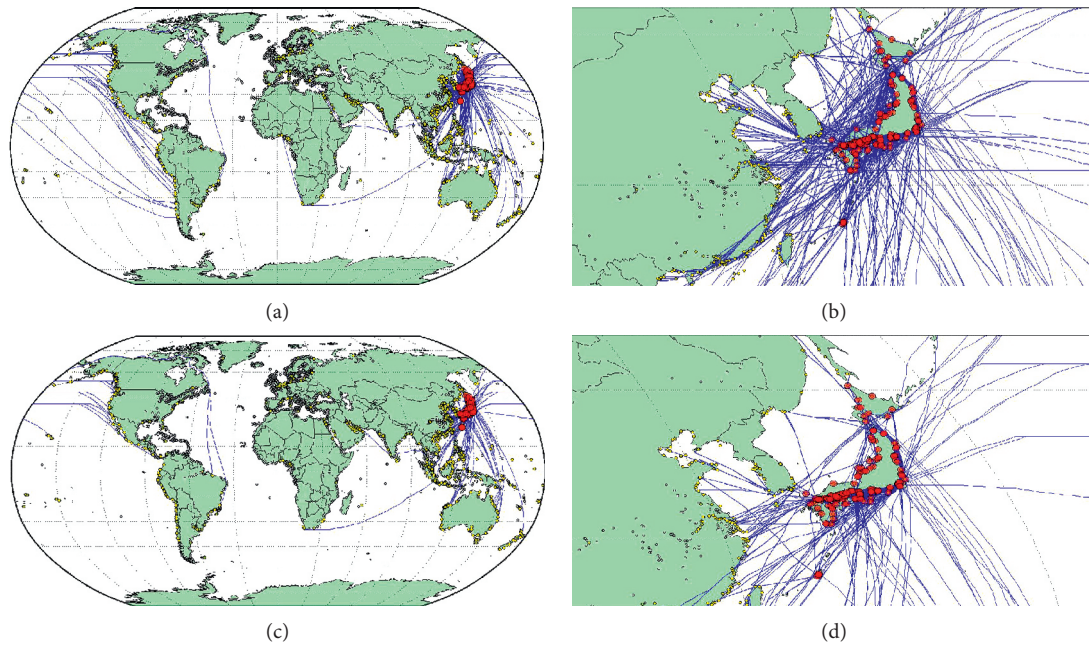


FIGURE 5: One-jump connections from Japanese ports to the world. (a) Global view (all). (b) Regional view (all). (c) Global view (top 2000). (d) Regional view (top 2000).

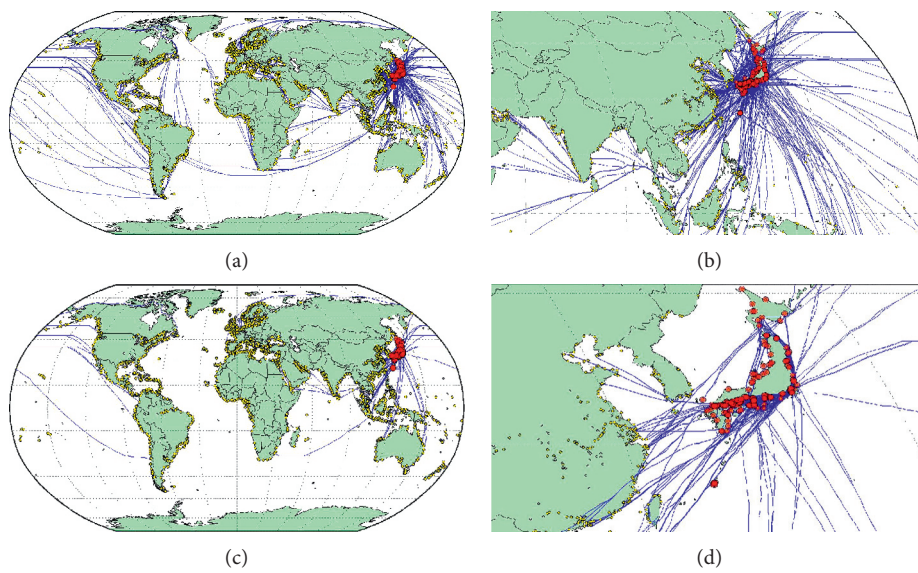


FIGURE 6: Multijump connections from Japanese ports. (a) Global view (all). (b) Regional view (all). (c) Global view (Top 2000). (d) Regional view (Top 2000).

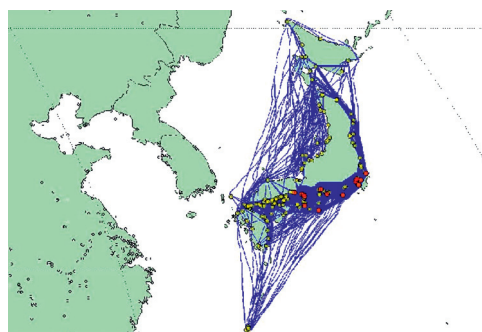


FIGURE 7: The network of the domestic connections among Japanese ports.

TABLE 3: Domestic trading connections among Japanese ports.

No	Port i	$ N^{Jd} $	$ E^{Jd} $	$Vessels(i)$	$C^{wd}(i)$
1	Kobe	148	30803	641079	3889659765
2	Chiba	148	31709	741774	3366894217
3	Higashi-Harima	148	31411	661387	3326670783
4	Yokohama	148	28089	526251	3238421359
5	Kawasaki	148	29732	615061	3102537203
6	Tokyo	148	24638	378676	2719177017
7	Osaka	148	27932	499966	2680658048
8	Yura	148	26314	397915	2612079462
9	Nagoya	148	26425	392824	2480934235
10	Shingu	148	26196	463112	2061133397
11	Atsumi	148	25148	373972	2047806866
12	Omaezaki	148	26578	425549	2009067062
13	Kurihama	148	26087	360035	1704348133
14	Kashima	148	25772	362319	1641696605
15	Wakayama	148	25682	348348	1624227948
16	Kinuura	148	23559	292885	1601320693
17	Sakai	148	25455	369813	1580207446
18	Shimotsu	148	25646	314510	1553780512
19	Kisarazu	148	22072	252279	1452599256
20	Yokkaichi	148	24174	250812	1323937715
	Mean	145	14416	117407	588070354
	Std	7	7372	148324	785733186
	Median	147	14140	56969	263031014
	Min	95	1087	1488	9762340
	Max	148	31709	741774	3889659765

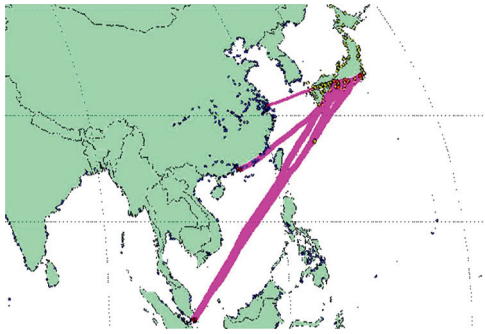


FIGURE 8: Primary flows between the Japanese ports and the world.

has not mentioned Japan, Japan has high connectivity with the BRI at least by the MSR.

5.8. Primary Maritime Flows with China. In the connections between Japan (N^{Japan}) and China (N^{China}) (see Figure 10 and Table 12), Hong Kong, Shanghai, Ningbo, and Guangzhou play essential roles. Although the flows between Japan and China account for 4.59~9.21% of Japan, while just 0.61~3.44% of China (see Table 13).

6. Discussion

Maritime networks are complex because they are agents of various stakeholders (port operators, ship operators, carriers, local port authorities and hinterlands, and multilevel governments). A port's structure and behaviors are results of games among these stakeholders, while the maritime

TABLE 4: Primary connections among the Japanese ports.

No	Port 1 (i)	Port 2 (j)	$F^{seq}(i, j)$	$F^{visit}(i, j)$	$F^{weight}(i, j)$
1	Kobe	Higashi-Harima	250	34949	220124245
2	Yokohama	Kawasaki	285	42931	203249921
3	Kobe	Osaka	262	31040	201807171
4	Kobe	Yura	350	17253	188052477
5	Chiba	Kawasaki	301	37817	183681995
6	Tokyo	Yokohama	236	19043	178290254
7	Kobe	Tokyo	230	13540	176406397
8	Kobe	Yokohama	268	18386	169435330
9	Chiba	Yokohama	260	31115	147186482
10	Kobe	Kawasaki	255	18863	139285118
11	Nagoya	Tokyo	232	11033	137489434
12	Chiba	Kobe	307	21150	125182377
13	Nagoya	Yokohama	268	13718	124939805
14	Higashi-H	Yura	351	16247	12642033
15	Kobe	Nagoya	265	12969	121850569
16	Tokyo	Yura	232	10251	120032488
17	Osaka	Higashi-H	237	24613	118952735
18	Osaka	Yura	240	13184	116414044
19	Yokohama	Yura	283	12341	115379092
20	Chiba	Higashi-Harima	247	21324	114699162

TABLE 5: International trading connections of Japanese ports.

No	Port (i)	N^{Ji}	$F^{seq}(i, N^{Ji})$	$F^{visit}(i, N^{Ji})$	$F^{weight}(i, N^{Ji})$
1	Yokohama	1700	32775	135776	3918894154
2	Kobe	1877	36019	148559	3858658354
3	Yura	1709	28592	97336	2936131922
4	Kawasaki	1654	30115	119850	2664481393
5	Tokyo	1272	20868	81832	2484460931
6	Chiba	1525	22223	79823	2381060732
7	Nagoya	1362	24272	82599	2044676910
8	Higashi-Harima	1548	23966	84684	1908593486
9	Osaka	1227	19578	72866	1743441359
10	Atsumi	1342	22509	64844	1627764831
11	Yokkaichi	1284	15458	36013	1265426014
12	Kurihama	1402	20064	55552	1251518174
13	Kashima	1413	14892	38522	1244728048
14	Shimotsu	1374	17638	46588	1137514011
15	Hakodate	1363	11926	25809	1123361951
16	Kinuura	1270	17715	44918	1117380582
17	Shirashima	1517	21622	69880	1099396186
18	Kisarazu	1263	12905	27995	936574231
19	Omaezaki	1088	16299	43395	765324362
20	Yokohama	1700	32775	135776	3918894154
149	Yanai	1	3	3	13692
	Mean	625	5856	14577	336818333
	Std	427	7214	26068	688285152
	Median	542	2994	3755	70536055
	Min	1	3	3	13692
	Max	1877	36019	148559	3918894154

network in a country or region is a holistic emergency upon them. The real-world global maritime network consists of more than 6000 ports belonging to more than 200 economic entities. In the background of the maritime network, a lot of companies, organizations, and governments are involved.

TABLE 6: Top 20 connections between Japan and the world.

No	Japanese port i	Maritime network	Top 20 port j	$F^{seq}(i, j)$	$F^{visit}(i, j)$	$F^{weight}(i, j)$
1	Kobe	Singapore	Singapore	134	5767	199498420
2	Yokohama	Singapore	Singapore	129	5289	182321787
3	Yura	Singapore	Singapore	133	4378	165408050
4	Yokohama	Hong Kong	Hong Kong	167	5263	154132255
5	Tokyo	Hong Kong	Hong Kong	164	5038	148066398
6	Chiba	Singapore	Singapore	84	3091	144850261
7	Kawasaki	Singapore	Singapore	91	5072	143696392
8	Kobe	Hong Kong	Hong Kong	157	5107	140651890
9	Tokyo	Singapore	Singapore	133	2825	115904354
10	Kobe	Malaysia	Pengerang Terminal	121	2795	112761468
11	Nagoya	Singapore	Singapore	123	3642	109875485
12	Chiba	Malaysia	Pengerang Terminal	78	1642	103776273
13	Yura	Malaysia	Pengerang Terminal	108	2164	100662393
14	Higashi-Harima	Singapore	Singapore	83	2498	95781992
15	Yokohama	China	Chiwan	152	2850	93425199
16	Kawasaki	Malaysia	Pengerang Terminal	78	2526	92901159
17	Yura	Hong Kong	Hong Kong	138	3173	91028161
18	Atsumi	Singapore	Singapore	128	2685	90333871
19	Yokohama	Malaysia	Pengerang Terminal	118	2459	87395691
20	Yokohama	China	Shanghai	162	4702	84396110

TABLE 7: Ranking Japanese ports by trading-related values.

No	Japanese port i	Ranked by			
		$ N^{io}(i) $	$F^{seq}(i, N^{world})$	$F^{visit}(i, N^{world})$	$F^{weight}(i, N^{world})$
1	Kobe	Kobe	Kobe	Chiba	Kobe
2	Yura	Yura	Yokohama	Kobe	Yokohama
3	Yokohama	Yokohama	Kawasaki	Higashi-Harima	Kawasaki
4	Kawasaki	Kawasaki	Higashi-Harima	Kawasaki	Chiba
5	Shirashima	Higashi-Harima	Yura	Yokohama	Yura
6	Higashi-Harima	Chiba	Chiba	Osaka	Higashi-Harima
7	Nagoya	Shirashima	Nagoya	Shingu	Tokyo
8	Chiba	Kashima	Atsumi	Yura	Nagoya
9	Kisarazu	Kurihama	Osaka	Nagoya	Osaka
10	Kurihama	Wakayama	Kurihama	Omaezaki	Atsumi
11	Wakayama	Shimotsu	Tokyo	Tokyo	Kurihama
12	Kinuura	Hakodate	Shimotsu	Atsumi	Kashima
13	Atsumi	Nagoya	Omaezaki	Kurihama	Omaezaki
14	Saganoseki	Atsumi	Kinuura	Kashima	Kinuura
15	Tokyo	Yokkaichi	Kashima	Sakai	Shimotsu
16	Amagasaki-NA	Tokyo	Wakayama	Wakayama	Yokkaichi
17	Kashima	Kinuura	Shingu	Shimotsu	Shingu
18	Omaezaki	Kisarazu	Yokkaichi	Komatsushima	Kisarazu
19	Shimotsu	Saganoseki	Shirashima	Kinuura	Wakayama
20	Yokkaichi	Osaka	Sakai	Takamatsu	Shirashima

TABLE 8: Ratios of flows between Japan and the world.

	Maritime network	F^{seq}	F^{visit}	F^{weight}
Flow	$F^J = F^*(N^{Japan}, N^{world})$	3020537	19665614	1.37808 E + 11
	$F^X = F^*(N^{Japan}, \overline{N}^{Japan})$	872595	2172000	50185931561
	$F^W = F^*(N^{world}, N^{world})$	37786321	390829144	3.89796 E + 12
Ratio (%)	F^X/F^J	28.89	11.04	36.42
	F^X/F^W	2.31	0.56	1.29

Their demands and benefits make the network alive and complicated in its structure and behaviors. The maritime networks are typically adaptive and complex, which

indicates that no entity controls the network, or such control is finally impossible. The maritime network is a representative of related stakeholders. For example, a maritime

TABLE 9: Ranking the Japanese ports by degree and PageRank centralities.

Throughput $C^{degree}(i)$		Network impact $C^{pagerank}(i)$	
Rank	Port i	Rank	Port i
1	Chiba	1	Chiba
2	Higashi-Harima	2	Higashi-Harima
3	Kobe	3	Kobe
4	Kawasaki	4	Kawasaki
5	Yokohama	5	Yokohama
6	Osaka	6	Osaka
7	Shingu	7	Shingu
8	Omaezaki	8	Omaezaki
9	Yura	9	Yura
10	Nagoya	10	Nagoya
11	Tokyo	11	Tokyo
12	Atsumi	12	Sakai
13	Sakai	13	Atsumi
14	Kashima	14	Kashima
15	Kurihama	15	Kurihama
16	Wakayama	16	Wakayama
17	Komatsushima	17	Komatsushima
18	Shimotsu	18	Shimotsu
19	Kinuura	19	Kinuura
20	Takamatsu	20	Takamatsu

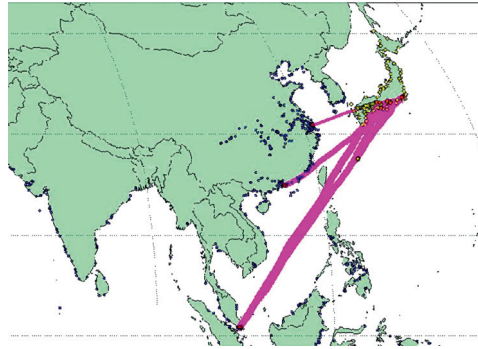


FIGURE 9: Primary flows between the Japanese ports and the MSR.

TABLE 10: Top 20 connections between Japan and the MSR.

No	Japan port (i)	Region	MSR port (j)	$F^{seq}(i, j)$	$F^{visit}(i, j)$	$F^{weight}(i, j)$
1	Kobe	Singapore	Singapore	134	5767	199498420
2	Yokohama	Singapore	Singapore	129	5289	182321787
3	Yura	Singapore	Singapore	133	4378	165408050
4	Yokohama	Hong Kong	Hong Kong	167	5263	154132255
5	Tokyo	Hong Kong	Hong Kong	164	5038	148066398
6	Chiba	Singapore	Singapore	84	3091	144850261
7	Kawasaki	Singapore	Singapore	91	5072	143696392
8	Kobe	Hong Kong	Hong Kong	157	5107	140651890
9	Tokyo	Singapore	Singapore	133	2825	115904354
10	Kobe	Malaysia	Pengerang Terminal	121	2795	112761468
11	Nagoya	Singapore	Singapore	123	3642	109875485
12	Chiba	Malaysia	Pengerang Terminal	78	1642	103776273
13	Yura	Malaysia	Pengerang Terminal	108	2164	100662393
14	Higashi-Harima	Singapore	Singapore	83	2498	95781992
15	Yokohama	China	Chiwan	152	2850	93425199
16	Kawasaki	Malaysia	Pengerang Terminal	78	2526	92901159
17	Yura	Hong Kong	Hong Kong	138	3173	91028161
18	Atsumi	Singapore	Singapore	128	2685	90333871
19	Yokohama	Malaysia	Pengerang Terminal	118	2459	87395691
20	Shanghai	Japan	Yokohama	162	4702	84396110

TABLE 11: Ratios of flows between Japan and the Maritime Silk Road.

	Maritime network	F^{seq}	F^{visit}	F^{weight}
Flow	$F^J = F^*(N^{Japan}, N^{world})$	3020537	19665614	$1.37808 E + 11$
	$F^X = F^*(N^{Japan}, N^{MSR})$	566579	1565250	31290144747
	$F^{MSR} = F^*(N^{MSR}, N^{world})$	12627333	301703689	$2.64665 E + 12$
Ratio (%)	F^X/F^J	18.76	7.96	22.71
	F^X/F^{MSR}	4.49	0.52	1.18



FIGURE 10: Primary flows between Japan and China.

TABLE 12: Top 20 connections between Japan and China.

No	Chinese port (i)	Japanese port (j)	$F^{seq}(i, j)$	$F^{visit}(i, j)$	$F^{weight}(i, j)$
1	Hong Kong	Yokohama	167	5263	154132255
2	Hong Kong	Tokyo	164	5038	148066398
3	Hong Kong	Kobe	157	5107	140651890
4	Chiwan	Yokohama	152	2850	93425199
5	Hong Kong	Yura	138	3173	91028161
6	Shanghai	Yokohama	162	4702	84396110
7	Hong Kong	Nagoya	135	3242	83980715
8	Yangshan	Yokohama	62	1000	75735976
9	Hong Kong	Osaka	147	3459	72617308
10	Shanghai	Kobe	182	5458	71786723
11	Shanghai	Tokyo	168	3809	71102550
12	Chiwan	Tokyo	155	2694	66382585
13	Ningbo	Yokohama	95	1616	65644572
14	Chiwan	Kobe	140	2608	64020112
15	Qingdao	Yokohama	128	2124	63518997
16	Guangzhou	Yokohama	175	1843	55636718
17	Hong Kong	Atsumi	149	2280	55437416
18	Shanghai	Osaka	187	3804	53315366
19	Yantian	Yokohama	93	837	50783540
20	Shanghai	Kawasaki	152	3447	50111425
269 Chinese ports		149 Japanese ports			

TABLE 13: Ratios of flows between China and Japan.

	Maritime network	F^{seq}	F^{visit}	F^{weight}
Flow	$F^J = F^*(N^{Japan}, N^{world})$	3020537	19665614	$1.37808 E + 11$
	$F^X = F^*(N^{Japan}, N^{China})$	278311	902653	12468012503
	$F^{China} = F^*(N^{China}, N^{world})$	8083920	284973537	$2.05516 E + 12$
Ratio (%)	F^X/F^J	9.21	4.59	9.05
	F^X/F^{China}	3.44	0.32	0.61

network of the ports of a country delegates the benefits and powers of the country. Therefore, we use the maritime network to analyze the relations and behaviors of the stakeholders.

Some studies formulated the maritime ports a maritime network by methods in network sciences (see Table 1). The ports interconnect with each other by shipping liners or vessel movements. Mainly, centrality-based methods are used to reveal the port significances in the network and impacts on the network. Network-based statistics help reveal network-level structures and behaviors [1]. The pioneering studies seldom investigate the countries or regional port systems in the global maritime network by data-driven methods due to that constructing large-scale or global maritime networks is challenging. This article results in the linkage between the maritime network and the country-level stakeholders in the context of the global maritime network.

Geographically, Japan is isolated from the land covered by the BRI and MSR while it has many connections with China, Asia, and Eurasia by seaborne trades. In the results presented in Section 5, although Japanese ports account for less vessel flows in the global maritime system, the interaction flow between Japan and China (also the MSR) is prominent when comparing the overall flows of Japan while it is just a small portion of the flows of China and MSR. The study provides enough reasons for Japan considering the essential connections with the MSR and Eurasia. In Section 3, the network definitions and analysis tools are formulated corresponding to a series of quantitative computing methods by extending the concepts and algorithms in network sciences. We take Japan, China, MSR, and the world maritime system as typical maritime networks here, and so we can analyze the interactions among the maritime networks of various countries or independent economies embedded in a global network in similar ways.

7. Conclusion

In this article, we addressed the research question: how do the maritime networks represent the country- and region-level interactions in the context of the global maritime network? We examined the interactions between Japan marine ports and the MSR by a data system and analysis tools. Japan connects with the MSR closely by seaborne transportation; a network of maritime networks contributes to the implications of interacted economical entities represented by the maritime networks, especially in the context of the global maritime network; prominent interactions among the maritime networks emerge by using the node- and edge-based network analysis tools. We construct a sample of a global maritime network with more than 6000 maritime ports to test and confirm the study. Although there are pioneering studies using methods in network sciences to investigate maritime networks (see Table 1), this article is the first large-scale study to link country-level and regional level analysis and maritime networks upon a global maritime network.

This study makes several scholarly contributions. It examines maritime network interactions embedded in a global maritime network, where the maritime networks are agents for country-level and regional level entities, e.g., Japan, China, MSR, and the world maritime system. Besides, it is a first ever study to examine the interactions through maritime ports and shipping between Japan and China (and MSR and the world) using a reliable method in association with AIS data. In particular, although most studies of maritime networks use data of container liner shipping as a base, this article uses a novel secondary dataset that captures the port and vessel profile data and the vessels' global movement tracks (AIS). This comprehensive dataset reflects the diversification in empirical methods in the big data and artificial intelligence era [40]. While the ports and shipping data and the AIS data have been used extensively in transport and resource management areas, we developed definitions and tools for the data-driven maritime networks.

There are limitations in the data and methods applied to this study. We construct the networks using the data of 2016, while the maritime system evolves in the economic and trade systems in recent years. To obtain a concise large-scale maritime network, we must process, repair, and synthesize by many steps. The data and its processing are expensive and time-consuming at the present stage of this study. The data system will finally provide benchmark datasets for maritime networks that will be assessable by academic communities. Therefore, the data chain is so long to guarantee and test the data quality. We focused on the application methods based on network sciences to constructed networks. However, the present developed analysis methods cannot handle the uncertainty, dynamics, and even random errors of the real-world maritime networks completely [41]. The stakeholders at the national and regional levels are complicated, and their observations and decisions must be affected by various sources of information. The maritime networks should integrate with various sources in holistic decision-making environments.

Several future studies would be desirable. First, we can extend the proposed models to examine other economy-, policy-, and sustainability-related impacts of maritime network interactions on regional and global maritime networks. At the port, national, and regional levels, the impacts are different and mutually affected. It is beneficial to construct a multilayer network for studying the evolutionary behaviors of the networks of subnetworks [35, 42]. Second, we mainly extend the network presentation, generation, and necessary analyzing concepts and methods, which can be further verified and promoted in generalized networks, especially by coupling with methods in complex systems. Third, we use the maritime networks that are generated by a set of ports in the global maritime network. In the view of network structure, we may use community detection and clustering algorithms to develop self-adaptive and evolutionary maritime networks by using the developed data system. It may contribute to new algorithms in network analysis. In summary, this study is the start of studying the network of networks.

Data Availability

The data used to support the findings of this study are available from the corresponding author upon reasonable request.

Conflicts of Interest

The authors declare that they have no conflicts of interest.

Acknowledgments

The National Natural Science Foundation of China (71871136) and the Science and Technology Commission of Shanghai Municipality (17DZ2280200) partially supported this study.

References

- [1] Z.-H. Hu, "Vietnam's connectivity and embeddedness in the maritime silk road and global maritime network," *IEEE Access*, vol. 7, no. 1, pp. 79592–79601, 2019.
- [2] A. Sardain, E. Sardain, and B. Leung, "Global forecasts of shipping traffic and biological invasions to 2050," *Nature Sustainability*, vol. 2, no. 4, pp. 274–282, 2019.
- [3] P. T.-W. Lee, Z.-H. Hu, S.-J. Lee, K.-S. Choi, and S.-H. Shin, "Research trends and agenda on the Belt and Road (B&R) initiative with a focus on maritime transport," *Maritime Policy & Management*, vol. 45, no. 3, pp. 282–300, 2018.
- [4] P. T.-W. Lee, S.-W. Lee, Z.-H. Hu, K.-S. Choi, N. Y. H. Choi, and S.-H. Shin, "Promoting Korean international trade in the east Sea economic rim in the context of the Belt and road initiative," *Journal of Korea Trade*, vol. 22, no. 3, pp. 212–227, 2018.
- [5] National Development and Reform Commission (NRDC) of China, *Vision and Actions on Jointly Building Silk Road Economic Belt and 21st-Century*, 2015, http://en.ndrc.gov.cn/newsrelease/201503/t20150330_669367.html.
- [6] Y. Wangping and L. Xiaolu, "Study on the interaction between China and Japan's economy based on FDI, import and export trade," *Studies in Business and Economics*, vol. 13, no. 1, pp. 194–208, 2018.
- [7] S. Nanwani, "Belt and road initiative: responses from Japan and India - bilateralism, multilateralism and collaborations," *Global Policy*, vol. 10, no. 2, pp. 284–289, 2019.
- [8] A. Ito, "China's belt and road initiative and Japan's response: from non-participation to conditional engagement," *East Asia*, vol. 36, no. 2, pp. 115–128, 2019.
- [9] Z. H. Hu, C. J. Liu, W. Chen, Y. G. Wang, and C. Wei, "Maritime convection and fluctuation between Vietnam and China: a data-driven study," *Research in Transportation Business and Management*, 2019.
- [10] D. A. Kroodsma, J. Mayorga, T. Hochberg et al., "Tracking the global footprint of fisheries," *Science*, vol. 359, no. 6378, pp. 904–908, 2018.
- [11] D. Karamshuk, F. Shaw, J. Brownlie, and N. Sastry, "Bridging big data and qualitative methods in the social sciences: a case study of Twitter responses to high profile deaths by suicide," *Online Social Networks and Media*, vol. 1, no. 1, pp. 33–43, 2017.
- [12] V. Boldosova, "Deliberate storytelling in big data analytics adoption," *Information Systems Journal*, vol. 29, no. 6, pp. 1126–1152, 2019.
- [13] A. Ojo and B. Heravi, "Patterns in award winning data storytelling," *Digital Journalism*, vol. 6, no. 6, pp. 693–718, 2018.
- [14] R. Albert and A.-L. Barabási, "Statistical mechanics of complex networks," *Reviews of Modern Physics*, vol. 74, no. 1, pp. 47–97, 2002.
- [15] L. C. Freeman, "Centrality in social networks conceptual clarification," *Social Networks*, vol. 1, no. 3, pp. 215–239, 1978.
- [16] Z. Bu, Y. Wang, H.-J. Li, J. Jiang, Z. Wu, and J. Cao, "Link prediction in temporal networks: integrating survival analysis and game theory," *Information Sciences*, vol. 498, no. 1, pp. 41–61, 2019.
- [17] J. Cao, Z. Bu, Y. Wang, H. Yang, J. Jiang, and H.-J. Li, "Detecting prosumer-community groups in smart grids from the multiagent perspective," *IEEE Transactions on Systems, Man, and Cybernetics: Systems*, vol. 49, no. 8, pp. 1652–1664, 2019.
- [18] M. E. J. Newman and M. Girvan, "Finding and evaluating community structure in networks," *Physical Review E-Statistical, Nonlinear, and Soft Matter Physics*, vol. 69, no. 2, 2004.
- [19] A. Arenas, A. Díaz-Guilera, J. Kurths, Y. Moreno, and C. Zhou, "Synchronization in complex networks," *Physics Reports*, vol. 469, no. 3, pp. 93–153, 2008.
- [20] Z. Wang, Q. Guo, S. Sun, and C. Xia, "The impact of awareness diffusion on SIR-like epidemics in multiplex networks," *Applied Mathematics and Computation*, vol. 349, no. 1, pp. 134–147, 2019.
- [21] R. Agarwal and O. Ergun, "Ship scheduling and network design for cargo routing in liner shipping," *Transportation Science*, vol. 42, no. 2, pp. 175–196, 2008.
- [22] Q. Meng, S. Wang, H. Andersson, and K. Thun, "Containership routing and scheduling in liner shipping: overview and future research directions," *Transportation Science*, vol. 48, no. 2, pp. 265–280, 2014.
- [23] D. Tsiotas and S. Polyzos, "Analyzing the maritime transportation system in Greece: a complex network approach," *Networks and Spatial Economics*, vol. 15, no. 4, pp. 981–1010, 2015.
- [24] Y. Wang and K. Cullinane, "Determinants of port centrality in maritime container transportation," *Transportation Research Part E: Logistics and Transportation Review*, vol. 95, no. 1, pp. 326–340, 2016.
- [25] M. Xu, Z. Li, Y. Shi, X. Zhang, and S. Jiang, "Evolution of regional inequality in the global shipping network," *Journal of Transport Geography*, vol. 44, no. 1, pp. 1–12, 2015.
- [26] C. P. Montesn, M. J. F. Seoane, and F. G. Laxe, "General cargo and containership emergent routes: a complex networks description," *Transport Policy*, vol. 24, no. 1, pp. 126–140, 2012.
- [27] N. K. Tran and H.-D. Haasis, "Empirical analysis of the container liner shipping network on the East-West corridor (1995–2011)," *NETNOMICS: Economic Research and Electronic Networking*, vol. 15, no. 3, pp. 121–153, 2014.
- [28] N. M. Viljoen and J. W. Joubert, "The vulnerability of the global container shipping network to targeted link disruption," *Physica A: Statistical Mechanics and Its Applications*, vol. 462, no. 1, pp. 396–409, 2016.
- [29] A. Calatayud, J. Mangan, and R. Palacin, "Vulnerability of international freight flows to shipping network disruptions: a multiplex network perspective," *Transportation Research Part E: Logistics and Transportation Review*, vol. 108, no. 1, pp. 195–208, 2017.
- [30] C. Liu, J. Wang, and H. Zhang, "Spatial heterogeneity of ports in the global maritime network detected by weighted ego

- network analysis,” *Maritime Policy & Management*, vol. 45, no. 1, pp. 89–104, 2018.
- [31] N. Mou, C. Liu, L. Zhang et al., “Spatial pattern and regional relevance analysis of the maritime silk road shipping network,” *Sustainability*, vol. 10, no. 4, p. 977, 2018.
- [32] P. Peng, S. Cheng, J. Chen et al., “A fine-grained perspective on the robustness of global cargo ship transportation networks,” *Journal of Geographical Sciences*, vol. 28, no. 7, pp. 881–889, 2018.
- [33] D. Tsiotas and S. Polyzos, “Effects in the network topology due to node aggregation: empirical evidence from the domestic maritime transportation in Greece,” *Physica A: Statistical Mechanics and Its Applications*, vol. 491, no. 1, pp. 71–88, 2018.
- [34] S. Inoue, “Realities and challenges of port alliance in Japan-ports of Kobe and Osaka,” *Research in Transportation Business & Management*, vol. 26, no. 1, pp. 45–55, 2018.
- [35] J. Xu, T. L. Wickramaratne, and N. V. Chawla, “Representing higher-order dependencies in networks,” *Science Advances*, vol. 2, no. 5, Article ID e1600028, 2016.
- [36] Y. Luo, L. Wang, S. Sun, and C. Xia, “Community detection based on local information and dynamic expansion,” *IEEE Access*, vol. 7, no. 8515203, pp. 8142773–8142786, 2018.
- [37] J. Wang, C. Li, and C. Xia, “Improved centrality indicators to characterize the nodal spreading capability in complex networks,” *Applied Mathematics and Computation*, vol. 334, no. 1, pp. 388–400, 2018.
- [38] S. Brin and L. Page, “The anatomy of a large-scale hypertextual web search engine,” *Computer Networks and ISDN Systems*, vol. 30, no. 1-7, pp. 107–117, 1998.
- [39] M. Scholz, J. Pfeiffer, and F. Rothlauf, “Using PageRank for non-personalized default rankings in dynamic markets,” *European Journal of Operational Research*, vol. 260, no. 1, pp. 388–401, 2017.
- [40] V. Singhal, B. B. Flynn, P. T. Ward, A. V. Roth, and V. Gaur, “Editorial: empirical elephants-Why multiple methods are essential to quality research in operations and supply chain management,” *Journal of Operations Management*, vol. 26, no. 3, pp. 345–348, 2008.
- [41] H.-J. Li, H. Wang, and L. Chen, “Measuring robustness of community structure in complex networks,” *EPL (Europhysics Letters)*, vol. 108, no. 6, p. 68009, 2014.
- [42] C. Xia, Z. Wang, C. Zheng et al., “A new coupled disease-awareness spreading model with mass media on multiplex networks,” *Information Sciences*, vol. 471, no. 1, pp. 185–200, 2019.

Research Article

Reliability Modeling for Multistate System with Preventive Maintenance under Customer Demand

Jinlei Qin ^{1,2} and Zheng Li ^{1,2}

¹Department of Computer, North China Electric Power University, Baoding, China

²Engineering Research Center of Intelligent Computing for Complex Energy Systems, Ministry of Education, North China Electric Power University, Baoding, China

Correspondence should be addressed to Jinlei Qin; jlqin717@163.com

Received 19 February 2020; Revised 20 April 2020; Accepted 21 April 2020; Published 12 May 2020

Academic Editor: Abdelalim Elsadany

Copyright © 2020 Jinlei Qin and Zheng Li. This is an open access article distributed under the Creative Commons Attribution License, which permits unrestricted use, distribution, and reproduction in any medium, provided the original work is properly cited.

The performance level of a multistate system (MSS) can vary among different values rather than only two states (perfect functioning and complete failure). To improve the reliability of MSSs, a maintenance strategy has been adopted to satisfy customer demand, and reliability modeling of MSS with preventive maintenance and customer demand is proposed. According to the regular degradation and random failure at each state, based on the Markov random process, the proposed MSS with preventive maintenance can be modeled to satisfy the customer demand in a specific state. This model can also be adapted to compute other reliability indices. Based on this model, the effect of different preventive maintenance actions on the reliability indices can be analyzed and further compared. Two numerical examples have been illustrated to show the validity of the proposed model. The reliability model presented in this study can be used to assess the type of MSS and help reliability engineers to compare different maintenance actions quantitatively and make optimal decisions.

1. Introduction

Generally, all systems and/or components will undergo an aging process before complete failure. This aging process is often modeled as a continuous and deterministic function of time. For example, the failure rate is usually depicted as a bath tub curve as a function of time. However, in most real-life situations, the failure rate depends not only on time but also on the states of the systems and/or components. Moreover, the traditional binary reliability theory assumes that there are only two states: perfect functioning and complete failure. The binary-state assumption may oversimplify the practical circumstances. A multistate degradation system may operate in an intermediate state between perfect functioning and complete failure. These intermediate states can be caused by system deterioration or peripheral factors, such as fatigue, burn-in, vibration, efficiency, failure of nonessential components, and the number of random shocks. Furthermore, the sojourn times in every state are

typically uncertain, which can result in the uncertainty of the state-dependent failure rate. Therefore, reliability modeling and evaluation of such multistate degraded systems have been impelled, some of which are discussed in the following.

The basic concepts, such as models, definitions of the structure function, and the properties of a stochastic multistate degradation system, were developed [1–3]. The notions of minimal path set, minimal cut set, coherence, and component relevancy have also been introduced. Based on these concepts, some corresponding performance measures, such as reliability, availability, mean time-to-failure, and redundancy can be deduced as the reliability description of the system under study [4–13].

To retain the reliability of a degraded system at a desired level, maintenance plays an important role. There are two types of maintenance that are based on time: corrective maintenance (CM) and preventive maintenance (PM). An optimal PM scheduling for a system consisting of deteriorating components was developed, and the simulated

annealing method was employed to obtain the optimum solution [14]. A reliability model based on Markov was presented to evaluate a three-state system, and a novel approach based on the Markov process to solve the differential equations reduced the computational time significantly [15]. The system reliability of a multistate network with multiple sinks was modeled as one of the probabilities, and an efficient algorithm was developed [16]. To improve the availability of nuclear power systems, the PM optimization for the series-parallel structure was modeled and a metaheuristic method was applied to solve the formulated problem [17]. Aiming at the degradation modeling and failure probability quantification of nuclear power plant piping systems, a multistate physics modeling approach had been proposed and applied to the piping system of a pressured water reactor undergoing thermal fatigue [18]. Some researchers have focused on the multistate k -out-of- n system with identical and nonidentical components, and a novel recursive algorithm to assess the reliability and the optimal design to improve the reliability were developed by them [19–24]. For a mission-based system, where missions are executed successfully with random durations, periodic and random inspection policy with postponed replacement is introduced [25]. An age-based preventive replacement policy is performed for components and a recursive method is developed to obtain its availability measure [26]. Although most of the models for reliability analysis have assumed that degradation will induce a decrease in system reliability, they have not considered the sudden abrupt failure from a normal working state.

Furthermore, maintenance actions are not always able to restore a system back to its “as-good-as-new” condition. If that were the case, the system might be used for an infinite period of time or for an unlimited number of missions. It is well known that this is something almost impossible to achieve in actual situations. Once a system fails stochastically, either in a perfect or degraded working state, a proper maintenance action will bring the system back to the state that existed just before the failure. As mentioned above, CM can be adopted when systems fall into the failure state, and PM can improve the performance when systems are in degraded states. Perfect PM will bring the system to as-good-as-new conditions; however, most PMs are imperfect due to limited maintenance resources such as time, budget, maintenance tools, technical level of maintenance engineers, and working environment [27]. An imperfect PM model is depicted as one in which, upon failure, the system will be replaced with probability p and be minimally repaired with probability $q = 1 - p$ [28]. Such a model was given and the extended great deluge optimization method was illustrated to give the best solution [29]. Similarly, under imperfect PM, an optimal selective maintenance strategy was resolved by a genetic algorithm [30, 31]. A systematic replacement model with minimal repair based on the cumulative repair-cost limit and an optimal PM policy based on a cumulative damage model for the used system were proposed and analyzed, respectively [32, 33]. For the system with two competing failure modes, degradation-based and shock-based failure, a condition-based maintenance model is

proposed [34]. When shocks arrive according to a nonhomogeneous Poisson process, it can significantly weaken the safety of system operating in an uncertain dynamic environment [35].

After the concept of imperfect maintenance had been introduced in the literature, the application of imperfect PM for multistate degraded systems has drawn the attention of many researchers. Because the scheduled PMs can be either imperfect or perfect, the optimal PM policies and repair decisions have been studied in order to significantly improve the maintenance efficiency of MSS modeled by the nonhomogeneous continuous time Markov process [36]. The difference from the MSS model previously mentioned is that the model proposed in this study is not only based on the homogeneous Markov chain but also on features such as Poisson failure and customer demand, which are all incorporated into this model. Here, a multistate degraded system with stochastic failure and imperfect PM has been modeled. Under the satisfaction of customer demand, this kind of system can fail stochastically in any state between perfect functioning and complete failure. When a system degrades to an unacceptable state, PM can be chosen to restore the system to one state. Based on the Markov chain theory and imperfect maintenance theory, the corresponding differential equations have been built up. Some reliability measures have also been developed and can be obtained by solving the model.

The rest of this article is composed of five sections. Section 2 formulates the MSS and stochastic model based on Markov chain theory. In Section 3, some reliability indices based on this model are deduced. The detailed method of modeling MSS is given in Section 4. Several illustrative examples are shown in Section 5. Section 6 discusses and concludes that the proposed model for reliability analysis is valid for practical application.

2. System Description and Modeling

2.1. System Description. The degraded system considered herein can be of $k + 1$ performance levels including $k - 1$ degraded states. Initially, the system will be in perfect functioning denoted by state 1. As time progresses, it can fall into one of the two states: failure state $k + 1$ (because of an abrupt failure), and the first deterioration state 2 (which is at a lower performance level or production rate). This type of failure, which occurs randomly and suddenly, is often named as Poisson failure, which is ubiquitous in many working environments [28, 32, 33, 37–39]. Upon a Poisson failure occurring at the failure rate λ_1 from state 1, the minimal repair will be implemented immediately at the repair rate μ_1 , which will restore the system back to state 1. If the system falls into the degraded state 2 from initial state 1 at the failure rate α_1 , it will proceed in the same manner. In other words, the system will transit from state 2 to the second degraded state 3 at the failure rate α_2 or to the repairable Poisson failure state $k + 2$ at the failure rate λ_2 . The other states are mimics of the transition state as can be seen in Figure 1. When it reaches the last degraded state k , it will

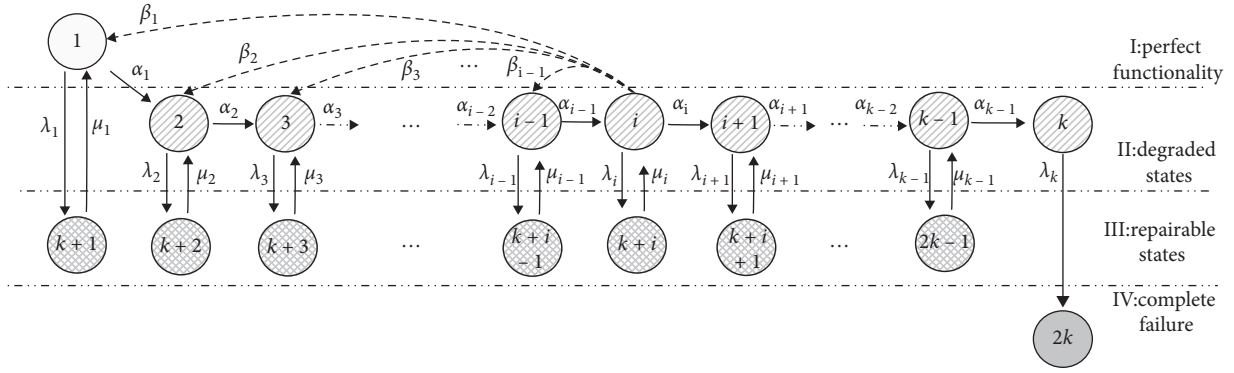


FIGURE 1: State transition diagram of the system.

only fall into the complete failure state $2k$ at the failure rate λ_k .

The deterioration states can be observed through some system parameters provided by some online supervised systems, and the time for inspection is also neglected. All the states of the system can be categorized into four types. State 1 is the perfect state with the perfect performance G_1 . State 2 to state k are the degraded states with corresponding performance or production rate ranging from G_2 to G_k ($G_2 > G_3 > \dots > G_i > \dots > G_k$). State $k+1$ to state $2k-1$ are repairable states of corresponding maintenance rate that can restore back to the corresponding state, which increase the Poisson failure. At the same time, the repairable states are of zero production rate $G_{k+1} = G_{k+2} = \dots = G_{2k-1} = 0$. The last state $2k$ is of complete failure with no repair and zero performance level $G_{2k} = 0$. For the purpose of clarity, the backgrounds of different states are shown in distinctive shades and patterns.

To satisfy customer demand w , the system performance will be restored to a better state, resorting the PM before the last state k . There are several PM actions that can be chosen, from minor to major maintenance. The system will be restored to the previous deteriorated state by minor maintenance, while the major maintenance will take the system back to the initial as-good-as-new condition. We can suppose that the state i is the state that satisfies customer demand at the lowest performance level. It can be expressed by

$$\begin{cases} G_i \geq w, \\ G_{i+1} < w, \\ 1 < i < k. \end{cases} \quad (1)$$

When an inspection finds that a system falls into the last acceptable state, a PM should be implemented to restore the system to one of the previous higher performance level at the maintenance rate. The maintenance rates are different corresponding to different states, as shown in Figure 1. Furthermore, we can assume that only one transition from state i to state j , $1 \leq j \leq i-1$, will occur. For example, the transition rate β_3 denotes the state transition from i to 3 after a minor maintenance is chosen.

2.2. Stochastic Modeling. As mentioned previously, the order of the performance level of system states can be expressed as follows:

$$\begin{cases} G_1 > G_2 > \dots > G_k > 0, \\ G_{k+1} = G_{k+2} = \dots = G_{2k} = 0. \end{cases} \quad (2)$$

These performance levels are represented by the set $\mathbf{G} = \{G_1, G_2, \dots, G_k, G_{k+1}, \dots, G_{2k}\}$. At any time $t \geq 0$, the system performance level is a random variable $G(t)$ which takes its value from the set \mathbf{G} . When the system operates after a time interval $[0, T]$, the performance level can be treated as a stochastic process. At an instant time t , the probabilities associated with the respective state are expressed as the set $\mathbf{P}(t) = \{P_1(t), P_2(t), \dots, P_i(t), \dots, P_{2k}(t)\}$, where

$$\begin{cases} P_i(t) = \Pr\{G(t) = G_i\}, \\ \sum_i P_i(t) = 1, \\ i = 1, 2, \dots, 2k. \end{cases} \quad (3)$$

Usually, the customer demand $W(t)$ can also be seen as a discrete stochastic variable taking a value from the set $\mathbf{W} = \{w_1, w_2, \dots, w_n\}$. For a specific system, we can assume that the customer demand takes a constant value w . The acceptability of the system performance level is usually dependent on the relation between the system performance level G_i and customer demand w . If we assume that the state i is the last acceptable state, the deterioration states after it will mean nothing. According to equation (5), those states between state $i+1$ and state k will be out of consideration and can be aggregated into one single failed state $i+1$ with performance level $G_{i+1} = 0$. Consequently, these repairable states after state $k+i$ can also be omitted. Thus, Figure 1 can be simplified further, as shown in Figure 2.

To assess the effect caused by a PM, a binary variable can be defined as

$$\delta_{i,j} = \begin{cases} 1, & \text{if a PM is implemented from state } i \text{ to state } j, \\ 0, & \text{otherwise,} \end{cases} \quad (4)$$

where $1 \leq j \leq i-1$. Because only one PM can be performed such that

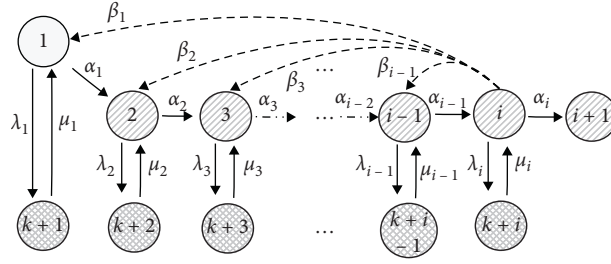


FIGURE 2: Simplified state transition diagram.

$$\sum_1^{i-1} \delta_{i,j} = 1. \quad (5)$$

If we assume that all the transition rates (including the Poisson failure rate, repairable rate, degraded rate, and PM

rate) are all constant values and exponentially distributed, then the transition process can be depicted by the Markov process. According to Figure 2 and the assumptions mentioned above, the Chapman-Kolmogorov equations corresponding to the Markov model are written as

$$\left\{ \begin{array}{l} \frac{dP_1(t)}{dt} = -(\alpha_1 + \lambda_1)P_1(t) + \mu_1 P_{k+1}(t) + \beta_1 \delta_{i,1} P_i(t), \\ \frac{dP_j(t)}{dt} = -(\alpha_j + \lambda_j)P_j(t) + \mu_j P_{k+j}(t) + \beta_j \delta_{i,j} P_i(t), \quad \text{for } j = 2, 3, \dots, i-1, \\ \frac{dP_i(t)}{dt} = -(\alpha_i + \lambda_i + \beta_j \delta_{i,j})P_i(t) + \mu_i P_{k+i}(t) + \alpha_{i-1} P_{i-1}(t), \quad \text{for } j \text{ corresponding to } \delta_{i,j} = 1, \\ \frac{dP_{k+j}(t)}{dt} = \lambda_j P_j(t) - \mu_j P_{k+j}(t), \quad \text{for } j = 1, 2, \dots, i, \\ \frac{dP_{i+1}(t)}{dt} = \alpha_i P_i(t), \end{array} \right. \quad (6)$$

with the following initial conditions:

$$\left\{ \begin{array}{l} P_1(0) = 1, \\ P_j(0) = 0, \quad j = 2, 3, \dots, i+1, \\ P_{k+j}(0) = 0, \quad j = 1, 2, \dots, i. \end{array} \right. \quad (7)$$

These state probabilities can be obtained by solving the differential equations given by equations (6) and (7). According to these state probabilities, reliability indices can be calculated further.

3. Reliability Indices

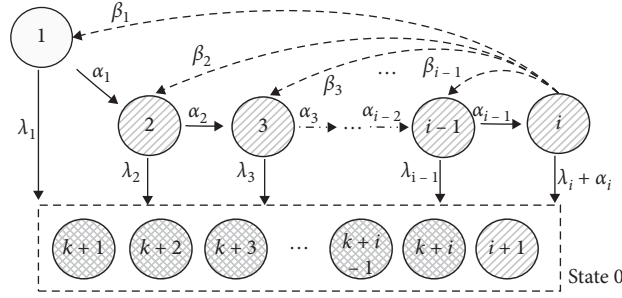
3.1. Reliability, Availability, and Production Rate. The reliability function $R(t)$ is the probability of the event that there will be successful operation of the repairable degraded system without any interruption until the time t . The time t is usually the time to the first failure, which is a random

variable T defined as the time from the beginning of the system life up to the instant that the degraded system reaches the first degraded or unacceptable state. Under this condition, the initial performance level of the degraded system can satisfy the customer demand w , and the reliability function will be given by

$$R(t) = \Pr\{T \geq t \mid G(t) \geq w\}. \quad (8)$$

To determine $R(t)$ in Figure 2, the repairable states and the unacceptable state should be grouped into one absorbing state denoted by state 0. In addition, all the repairs that make the degraded system transit from state 0 to any degraded state are removed. The failure rate from the last acceptable state i to state 0 is equal to the sum of α_i and λ_i . Based on the analysis mentioned above, the Markov model can be built, as shown in Figure 3.

According to Figure 3, the differential equations will take the form

FIGURE 3: State transition diagram for determination of $R(t)$.

$$\begin{cases} \frac{dP_j(t)}{dt} = -\lambda_j P_j(t) + \beta_j \delta_{i,j} P_i(t), & \text{for } j = 1, 2, \dots, i-1, \\ \frac{dP_i(t)}{dt} = -(\alpha_i + \lambda_i + \beta_j \delta_{i,j}) P_i(t) + \alpha_{i-1} P_{i-1}(t), & \text{for } j \text{ corresponding to } \delta_{i,j} = 1, \\ \frac{dP_0(t)}{dt} = \sum_{j=1}^{i-1} \lambda_j P_j(t) + (\lambda_i + \alpha_i) P_i(t), \end{cases} \quad (9)$$

where the initial probability is

$$\begin{cases} P_1(0) = 1, \\ P_0(0) = 0, \\ P_j(0) = 0, \quad \text{for } j = 2, 3, \dots, i-1, i. \end{cases} \quad (10)$$

These state probabilities can be solved and used to calculate the reliability function. Whenever the degraded system enters into the absorbing state 0, it will never leave it. The state probability $P_0(t)$ can be easily used to calculate the reliability function because it characterizes the $R(t)$, which will be written as

$$R(t) = 1 - P_0(t) = \sum_{j=1}^i P_j(t). \quad (11)$$

It is to be noted that as time progresses to infinity, the final state probabilities of the degraded system are $P_0(t) = 0$ and others are all equal to zero, because the degraded system always enters the final absorbing state 0.

The instantaneous availability function $A(t)$ is the probability that the degraded system will be found in the operational state at time t . For the system described in Figure 2, these states of working efficiency are the perfect and the degraded states. That is to say, $A(t)$ is the sum of the probability that the degraded system is in state 1 and one of the other acceptable degraded states at time t . Combining the results of foregoing equations (6) and (7),

$$A(t) = \Pr\{G(t) \geq w\} = \sum_{j=1}^i P_j(t). \quad (12)$$

At the same time, the production rate can also be obtained by the probability distribution of each state. The instantaneous production rate function $\rho(t)$ at time t is a de

facto output performance expectation, viz., $E(G(t))$. The value can be given by

$$\rho(t) = E(G(t)) = \sum_{j=1}^i G_j P_j(t). \quad (13)$$

3.2. Other Indices. Assuming that the life time of a degraded system is the time to reach the designated state i due to degradation, the unavailability of the system due to Poisson failure can be calculated as

$$D(t) = \sum_{j=1}^i P_{k+j}(t). \quad (14)$$

Hence, the probability that the degraded system fails completely at the state i can be defined as

$$F(t) = 1 - A(t) - D(t). \quad (15)$$

During time t , the expected operational time spent in each state is as follows:

$$E_j(t) = \int_0^t P_j(x) dx, \quad (16)$$

where $j = 1, 2, \dots, i, k+1, k+2, \dots, k+i$.

Further, the expected operational time (EOT) and the expected down time (EDT) during time t are given by

$$\begin{cases} \text{EOT}(t) = \int_0^t \sum_{j=1}^i P_j(x) dx, \\ \text{EDT}(t) = t - \text{EOT}(t). \end{cases} \quad (17)$$

Furthermore, the mean life time (MLT) is the expected life time of the system:

$$MLT = \int_0^{\infty} (1 - F(t))dt = \int_0^{\infty} (A(t) + D(t))dt. \quad (18)$$

The mean operational life time (MOLT) is the expected operational life time of the system, which is given by

$$MOLT = \int_0^{\infty} A(t)dt. \quad (19)$$

The mean time to first failure (MTTFF) of the degraded system is the expected time to the first failure which can be obtained by

$$MTTFF = \int_0^{\infty} R(t)dt. \quad (20)$$

4. Method for Modeling

Based on the abovementioned analysis, the method for modeling an MSS with Poison failure under customer demand can be summarized as follows:

- S1. According to the practical production system, its Markov model can be sketched by drawing the state transition diagram, as shown in Figure 1
- S2. Considering the customer demand on the performance level of this system, the Markov model shown in Figure 1 will be simplified to Figure 2
- S3. State probability of the system can be obtained by solving equations (6) and (7)
- S4. Relevant indices can be calculated according to equations (12) to (19)
- S5. In order to obtain the reliability function of the system, the model shown in Figure 2 needs to be altered to Figure 3
- S6. Solving equations (9) and (10), the probability at each state can be obtained
- S7. The reliability function and MTTFF can be calculated easily by using equations (11) and (20)

After the abovementioned steps are fulfilled, the reliability evaluation based on the MSS model will be performed according to the relevant equations.

5. Application Examples

5.1. Example without PM. Given a degraded system shown in Figure 4 where the parameters are signed, reliability indices can be obtained according to the model equations (6) and (7) to illustrate an example without PM using this model.

The differential equations are built up according to Figure 4, and the results of some indices can be found. The expected times spent in each state are $E_1 = 1000$, $E_2 = E_4 = 500$, and $E_5 = 2500$. The relations of $A(t)$, $D(t)$, and $F(t)$ are depicted as follows.

From the abovementioned curves during the time interval $[0, 200]$, it can be observed that the system availability $A(t)$ decreases with time. However, the unavailability $D(t)$ increases with time. The probability curve of $F(t)$ is near to

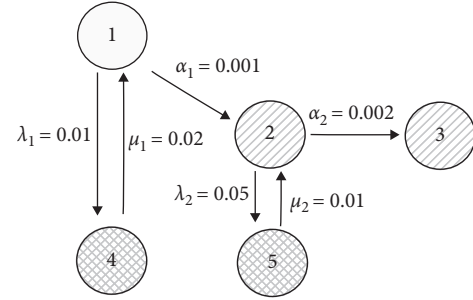


FIGURE 4: State transition diagram of the example without PM.

zero, indicating that complete failure at state i is nearly impossible. At the time $t = 100$, the values of the three indices are shown in Figure 5.

The results of the EOT and EDT listed in Table 1 are based on 5 chosen time intervals.

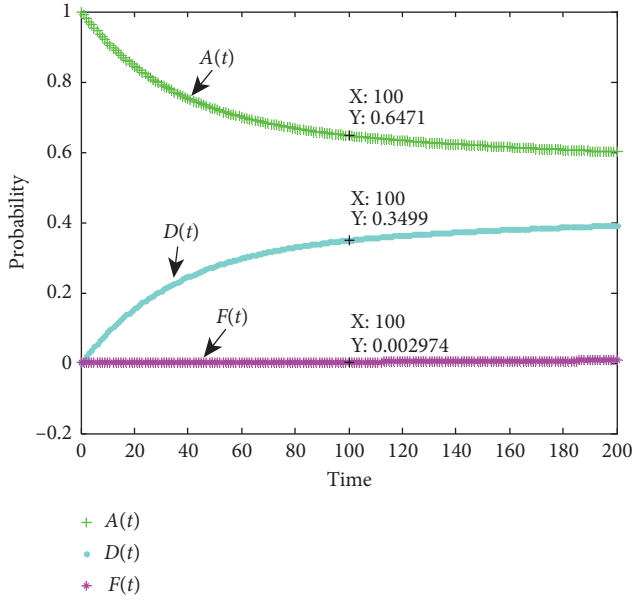
According to equations (18) and (19), $MLT = 4500$ and $MOLT = 1500$. Obviously, MLT is greater than $MOLT$. However, $MOLT$ is higher than $EOT(t)$ which increases with time t .

In order to obtain the reliability function for this example, equations (9) and (10) of the model will be adopted. After solving the equations, the reliability function can be found using equation (11). The curve of $R(t)$ is shown in Figure 6.

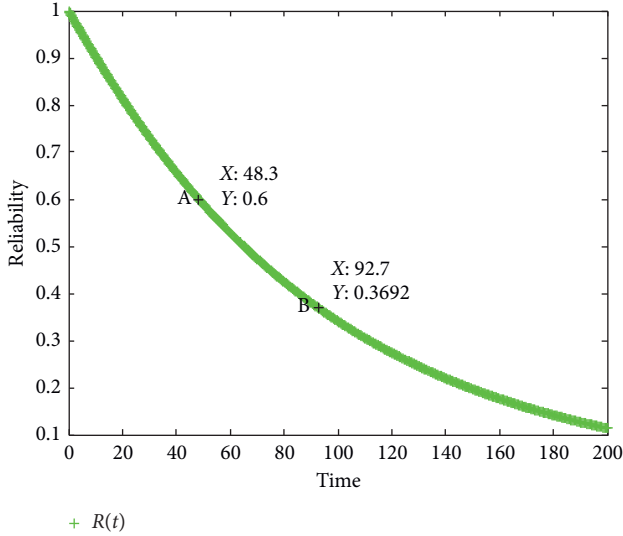
Combining equation (20), we obtain $MTTFF = 92.7$ and $R(MTTFF) = 0.3692$, and the point B shown in Figure 6. If the probability value needs to be greater than or equal to 0.6, $t \leq 48.3$ would be adequate as the point A implies.

5.2. Example with PM. A more practical example with PM actions can also be illustrated using the model. For the feeding water system in the power plant, its performance level can be measured usually by the weight of water pumped to the boiler. According to the different needs of generating power in one district, the production rate of feeding water system can be ranged from 2000, 1500, or 700 to 0 tons/hour. In other words, there are some different states corresponding to those production rates. State 1 is the perfect functioning of the 2000 performance level. State 2 and 3 are the degraded states whose performance levels are 1500 and 700, respectively. State 4 is the unacceptable state whose performance level is below the requirement. The other states are the Poison failures. With regard to this degraded feeding water system which has 7 states, some PM actions may be required to be adopted. The state transition diagram of this system is given in Figure 7.

Two PM actions can be chosen at state 3: one is the imperfect PM with the transition rate β_2 and the other is the perfect PM with the transition rate β_1 . The values of all transition rates are listed in Table 2 where their meanings correspond to Figure 7. The production rate at each state are 1000, 750, and 600 for states 1, 2, and 3, respectively. The other states can be seen as the failure state whose production rate is zero. Furthermore, the customer demand for this system can be assumed by $w \geq 600$. Therefore, when the

FIGURE 5: The curves of $A(t)$, $D(t)$, and $F(t)$.TABLE 1: Results of EOT(t) and EDT(t).

t	40	80	120	160	200
EOT(t)	34.2058	62.3437	88.2709	113.1894	137.4682
EDT(t)	5.7942	17.6563	31.7291	46.8106	62.5318

FIGURE 6: The curve of $R(t)$ for the example without PM.

system degrades to state 3, one PM action should be taken to meet the customer demand.

Using equations (6) and (7) from the model, the probabilities of each state can be obtained. Then, the availability function $A(t)$ will be evaluated by equation (12). To compare the effectiveness of the PM actions, three types of actions are adopted. The first is to do nothing, that is, without PM. The second is imperfect PM with the transition rate β_2 , and the last is perfect PM with the transition rate β_1 .

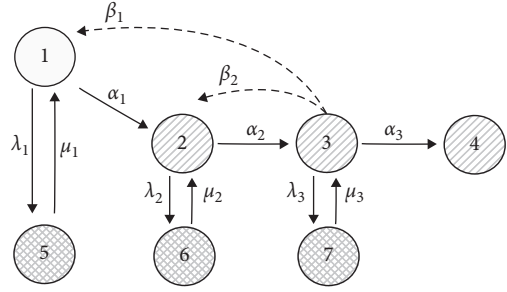


FIGURE 7: State transition diagram of the example with PM.

TABLE 2: Performance distribution of components.

Transition rate	State						
	1	2	3	5	6	7	
α	0.03	0.05	0.07	—	—	—	
λ	0.005	0.228	0.01	—	—	—	
μ	—	—	—	0.01	0.02	0.04	
β	0.02	0.08	—	—	—	—	

The results of the three PM actions on $A(t)$ are depicted in Figure 8 within the interval $t \in [0, 200]$.

From Figure 8, it can be observed that the availability rate decreases with time. When PM actions are implemented, availability rate is improved. Perfect PM has higher characteristics of improving than imperfect PM. The availability rates of three types of PM actions at time $t = 100$ are shown by points A, B, and C, respectively.

Similarly, the production rate will be calculated according to equation (13). The results of production rate $\rho(t)$ are shown in Figure 9. At time $t = 100$, the production rates are shown as points A, B, and C for the three types of PM actions, respectively. Although the production rate decreases with time, the findings show that the PM will improve the production rate of this system.

In order to calculate the reliability function, equations (9) and (10) from the model are used. Combining the three types of PM actions, the changing trends of $R(t)$ are depicted in Figure 10.

In this figure, the changing trends of $R(t)$ decrease with time. PM actions have the property of making the reliability higher. For example, the reliability of three PM actions at time $t = 100$ are the points A, B, and C for the three types of actions, respectively, as shown in Figure 10.

Furthermore, the MTTF of the system will be calculated. According to equation (20), this index under three types of PM actions can be obtained as $MTTFF_{DoNothing} = 52.5862$, $MTTFF_{ImperfectPM} = 55.3733$, and $MTTFF_{PerfectPM} = 76.1119$. Obviously, the PM actions prolong the mean time to first failure significantly.

6. Discussion and Conclusion

In this study, reliability modeling for a degraded MSS was considered. Its practical implication includes two aspects. First, it takes into account a sudden and random failure called Poison failure, which may occur with certain failure rate at

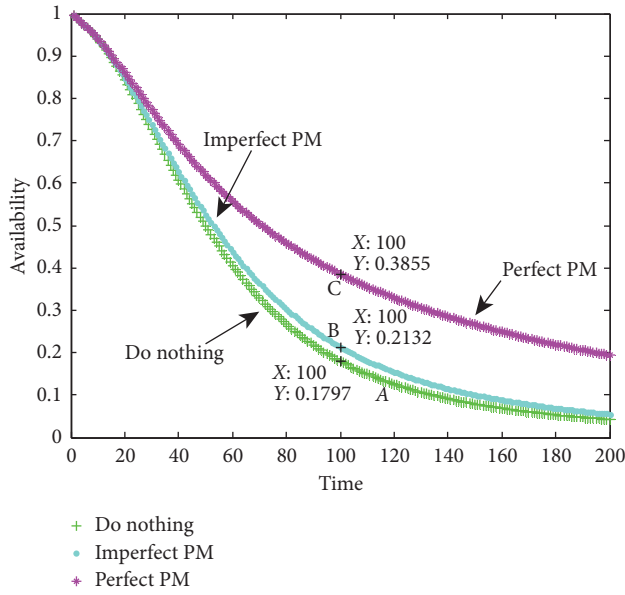


FIGURE 8: The comparison of three actions on $A(t)$.

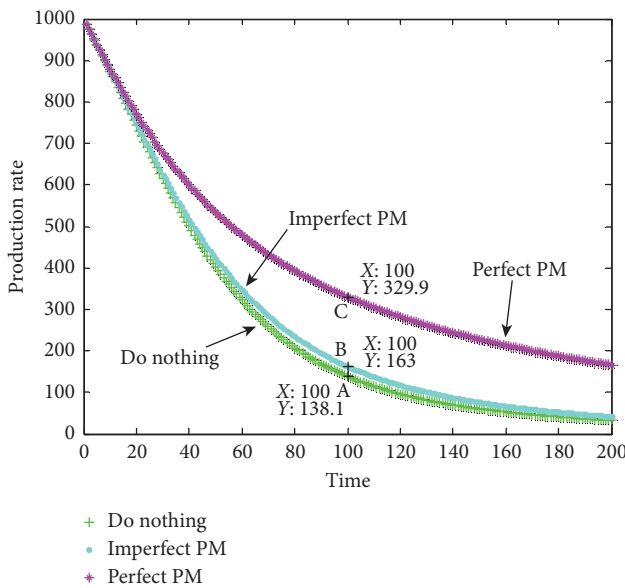


FIGURE 9: The curves of $\rho(t)$ on three actions.

each degraded state, and maintenance action can restore the system back to the state just before the Poisson failure at certain maintenance rate. Second, it includes the customer demand on the performance level. When the performance level of the MSS degrades to a level below the customer's specified demand, the model will be simplified to meet the customer's performance limit. Moreover, some PM actions can be adopted to restore the system back to a better state at certain transition rate in order to improve the reliability of the degraded MSS. The proposed method is not only convenient to model the degraded MSS under a customer's specific reliability demand but also suitable to calculate those reliability indices for the qualification of PM actions.

The proposed model can be applied in many practical situations because it can respond to a situation based on the

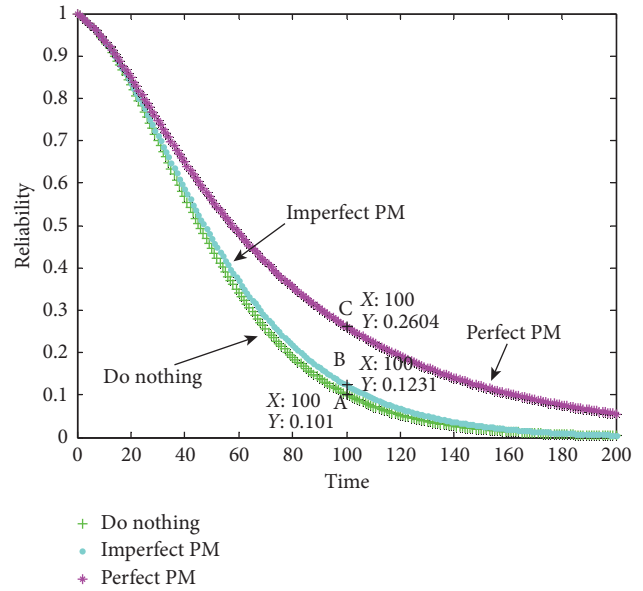


FIGURE 10: The changing trends of $R(t)$ on three types of PM actions.

needs to assure a customer's reliability demands. Furthermore, some PM actions can be qualified and expressions of reliability indices can be easily derived and compared by maintenance engineers for making decision. A limitation of this study is that the transition rates among states are considered constant. A model that treats the transition rates as a type of distribution rather than as constants will be part of our future work to strengthen the proposed model.

Data Availability

The data used to support the findings of this study are included within the article.

Conflicts of Interest

The authors declare that they have no conflicts of interest.

Acknowledgments

This work was supported financially in part by a grant from the Fundamental Research Funds for the Central Universities (nos. 2018MS076 and 2020MS120) and China Scholarship Council (no. 201906735027).



References

- [1] R. E. Barlow and A. S. Wu, "Coherent systems with multi-state components," *Mathematics of Operations Research*, vol. 3, no. 4, pp. 275–281, 1978.
- [2] E. El-Newehi, F. Proschan, and J. Sethuraman, "Multistate coherent systems," *Journal of Applied Probability*, vol. 15, no. 4, pp. 675–688, 1978.
- [3] S. M. Ross, "Multivalued state component systems," *The Annals of Probability*, vol. 7, no. 2, pp. 379–383, 1979.
- [4] H. Pham, A. Suprasad, and R. B. Misra, "Availability and mean life time prediction of multistage degraded system with partial repairs," *Reliability Engineering & System Safety*, vol. 56, no. 2, pp. 169–173, 1997.

- [5] S. Wu, "Joint importance of multistate systems," *Computers & Industrial Engineering*, vol. 49, no. 1, pp. 63–75, 2005.
- [6] M. J. Zuo and Z. Tian, "Performance evaluation of generalized multi-state," *IEEE Transactions on Reliability*, vol. 55, no. 2, pp. 319–327, 2006.
- [7] T. Zhigang, M. J. Zuo, and H. Hongzhong, "Reliability-redundancy Allocation for multi-state series-parallel systems," *IEEE Transactions on Reliability*, vol. 57, no. 2, pp. 303–310, 2008.
- [8] A. H. Tai and L.-Y. Chan, "Maintenance models for a continuously degrading system," *Computers & Industrial Engineering*, vol. 58, no. 4, pp. 578–583, 2010.
- [9] J. Qin, Y. Niu, and Z. Li, "A combined method for reliability analysis OF multi-state system OF minor-repairable components," *Eksplotacja I Niezawodnosc-Maintenance and Reliability*, vol. 18, no. 1, pp. 80–88, 2016.
- [10] J. L. Qin, Z. Li, Y.-G. Niu, and G.-Q. Meng, "Simulated method for reliability evaluation of multi-state coherent system," *Iranian Journal of Science and Technology Transaction A-Science*, vol. 42, no. 3, pp. 1363–1371, 2018.
- [11] X. Huang, Y. Li, Y. Zhang, and X. Zhang, "A new direct second-order reliability analysis method," *Applied Mathematical Modelling*, vol. 55, pp. 68–80, 2018.
- [12] Z. Li and J. Qin, "A modified particle swarm optimization with elite archive for typical multi-objective problems," *Iranian Journal of Science and Technology, Transactions A: Science*, vol. 43, no. 5, pp. 2351–2361, 2019.
- [13] J. L. Qin and Z. Li, "Reliability and sensitivity analysis method for a multistate system with common cause failure," *Complexity*, vol. 2019, Article ID 6535726, 8 pages, 2019.
- [14] M. Doostparast, F. Kolahan, and M. Doostparast, "A reliability-based approach to optimize preventive maintenance scheduling for coherent systems," *Reliability Engineering & System Safety*, vol. 126, pp. 98–106, 2014.
- [15] P. P. Guilani, M. Sharifi, S. T. A. Niaki, and A. Zaretalab, "Reliability evaluation of non-reparable three-state systems using Markov model and its comparison with the UGF and the recursive methods," *Reliability Engineering & System Safety*, vol. 129, pp. 29–35, 2014.
- [16] Y.-K. Lin and C.-F. Huang, "Reliability evaluation of a multi-state network with multiple sinks under individual accuracy rate constraint," *Communications in Statistics-Theory and Methods*, vol. 43, no. 21, pp. 4519–4533, 2014.
- [17] A. Rami, H. Hamdaoui, H. Sayah, and A. Zebblah, "Efficient harmony search optimization for preventive-maintenance-planning for nuclear power systems," *International Journal for Simulation and Multidisciplinary Design Optimization*, vol. 5, p. A17, 2014.
- [18] F. Di Maio, D. Colli, E. Zio, L. Tao, and J. Tong, "A multi-state physics modeling approach for the reliability assessment of nuclear power plants piping systems," *Annals of Nuclear Energy*, vol. 80, pp. 151–165, 2015.
- [19] E. M. Scheuer, "Reliability of an m-out-of-n system when component failure induces higher failure rates in survivors," *Reliability, IEEE Transactions on*, vol. 37, no. 1, pp. 73–74, 1988.
- [20] B. N. Sur, "Reliability evaluation of k-out-of-n redundant system with partially energized stand-by units," *Microelectronics Reliability*, vol. 36, no. 3, pp. 379–383, 1996.
- [21] W. Li and M. J. Zuo, "Reliability evaluation of multi-state weighted k-out-of-n systems," *Reliability Engineering & System Safety*, vol. 93, no. 1, pp. 160–167, 2008.
- [22] W. Li and M. J. Zuo, "Optimal design of multi-state weighted k-out-of-n systems based on component design," *Reliability Engineering & System Safety*, vol. 93, no. 11, pp. 1673–1681, 2008.
- [23] T. Zhigang, R. C. M. Yam, M. J. Zuo, and H.-Z. Huang, "Reliability Bounds for multi-State k-out-of-n systems," *IEEE Transactions on Reliability*, vol. 57, no. 1, pp. 53–58, 2008.
- [24] Y. C. Mo, L. Xing, S. V. Amari, and J. B. Dugan, "Efficient analysis of multi-state k-out-of-n systems," *Reliability Engineering & System Safety*, vol. 133, pp. 95–105, 2015.
- [25] L. Yang, X. Ma, Q. Zhai, and Y. Zhao, "A delay time model for a mission-based system subject to periodic and random inspection and postponed replacement," *Reliability Engineering & System Safety*, vol. 150, pp. 96–104, 2016.
- [26] Q. Qiu, L. Cui, and D. Kong, "Availability and maintenance modeling for a two-component system with dependent failures over a finite time horizon," *Proceedings of the Institution of Mechanical Engineers, Part O: Journal of Risk and Reliability*, vol. 233, no. 2, pp. 200–210, 2019.
- [27] M. Pandey, M. J. Zuo, and R. Moghaddass, "Selective maintenance modeling for a multistate system with multistate components under imperfect maintenance," *IIE Transactions*, vol. 45, no. 11, pp. 1221–1234, 2013.
- [28] M. Brown and F. Proschan, "Imperfect repair," *Journal of Applied Probability*, vol. 20, no. 4, pp. 851–859, 1983.
- [29] N. Nahas, A. Khatab, A.-K. Daoud, and M. Nourelfath, "Extended great deluge algorithm for the imperfect preventive maintenance optimization of multi-state systems," *Reliability Engineering & System Safety*, vol. 93, no. 11, pp. 1658–1672, 2008.
- [30] Y. Liu, H.-Z. Huang, and M. J. Zuo, "Optimal selective maintenance for multi-state systems under imperfect maintenance," in *Proceedings of the Reliability and Maintainability Symposium*, IEEE, Fort Worth, TX, USA, January 2009.
- [31] L. Yu and H. Hong-Zhong, "Optimal selective maintenance Strategy for multi-state systems under imperfect maintenance," *IEEE Transactions on Reliability*, vol. 59, no. 2, pp. 356–367, 2010.
- [32] C.-C. Chang, S.-H. Sheu, and Y.-L. Chen, "Optimal number of minimal repairs before replacement based on a cumulative repair-cost limit policy," *Computers & Industrial Engineering*, vol. 59, no. 4, pp. 603–610, 2010.
- [33] Y.-L. Chen, "A bivariate optimal imperfect preventive maintenance policy for a used system with two-type shocks," *Computers & Industrial Engineering*, vol. 63, no. 4, pp. 1227–1234, 2012.
- [34] L. Yang, X. Ma, and Y. Zhao, "A condition-based maintenance model for a three-state system subject to degradation and environmental shocks," *Computers & Industrial Engineering*, vol. 105, pp. 210–222, 2017.
- [35] Q. Qiu and L. Cui, "Reliability evaluation based on a dependent two-stage failure process with competing failures," *Applied Mathematical Modelling*, vol. 64, pp. 699–712, 2018.
- [36] S.-H. Sheu, C.-C. Chang, Y.-L. Chen, and Z. G. Zhang, "Optimal preventive maintenance and repair policies for multi-state systems," *Reliability Engineering & System Safety*, vol. 140, pp. 78–87, 2015.
- [37] R. Barlow and L. Hunter, "Optimum preventive maintenance policies," *Operations Research*, vol. 8, no. 1, pp. 90–100, 1960.
- [38] H. Chin-Yu, M. R. Lyu, and K. Sy-Yen, "A unified scheme of some Nonhomogenous Poisson process models for software reliability estimation," *IEEE Transactions on Software Engineering*, vol. 29, no. 3, pp. 261–269, 2003.
- [39] P. Roy, G. S. Mahapatra, and K. N. Dey, "Neuro-genetic approach on logistic model based software reliability prediction," *Expert Systems with Applications*, vol. 42, no. 10, pp. 4709–4718, 2015.

Research Article

The Formation Mechanism of Green Dairy Industry Chain from the Perspective of Green Sustainable Development

Hongli Chen ^{1,2} and Xiuli Liu ^{1,3}

¹University of Chinese Academy of Sciences, Beijing 100049, China

²Xinjiang Tianshan Army Reclamation Co., Ltd, Xinjiang 832000, China

³Academy of Mathematics and Systems Sciences Chinese Academy of Sciences, Beijing 100190, China

Correspondence should be addressed to Hongli Chen; chenhongli2050@sina.com

Received 15 March 2020; Accepted 16 April 2020; Published 11 May 2020

Guest Editor: Baogui Xin

Copyright © 2020 Hongli Chen and Xiuli Liu. This is an open access article distributed under the Creative Commons Attribution License, which permits unrestricted use, distribution, and reproduction in any medium, provided the original work is properly cited.

By constructing an evolutionary game model of green dairy industry chain from the perspective of green sustainable development, this paper analyzed the evolution process of strategy selection of dairy farmers and dairy enterprises under the supervision of the government. The study found the following. (1) In the absence of supervision, even if the initial cooperation willingness of dairy farmers and dairy enterprises is strong, once the additional cost of their input of “green production” is less than the additional benefit, they will eventually choose noncooperative strategy. (2) In the case of government supervision, when the government punishment or subsidy is not strong enough, the strategic choice of dairy farmers and dairy enterprises will fluctuate repeatedly, and the game equilibrium cannot be reached. However, when the government punishments and subsidies are strong enough, dairy farmers and dairy enterprises will choose to cooperate in their own interests. At this time, government subsidies have a greater impact on the evolution of bilateral cooperation than government punishments. (3) The reduction of green production cost can promote the formation of the green dairy industry chain, which is conducive to the green dairy industry chain system to achieve an ideal equilibrium state.

1. The Introduction

The concept of “green development” which was put forward at the fifth Plenary Session of the 18th CPC Central Committee has been deeply rooted in people’s hearts. Green development has become the theme of The Times. From the perspective of industrial transformation and upgrading, the green transformation of the entire industrial chain should also be an inevitable theme. The green industrial chain refers to promoting the green development of all links in the whole industrial value chain, realizing the benign interaction with nature and relevant groups in society, achieving the unity of short-term interests and long-term development, and realizing the sustainable development of the industry. With the support of the state for green industry, green supply chain will have a great development in the future. Dairy industry is a basic industry related to national economy and people’s livelihood. The formation of the green dairy industry chain is

conducive to the change of industrial model and the improvement of dairy product quality and safety. At present, China Mengniu dairy and Yili Milk, as the first camp member of global dairy industry and the leader of China’s dairy industry, have been committed to the development goal of “environmental protection” and “win-win” and have promoted the green and sustainable development of all links of the industrial chain with the mode of sustainable development.

Scholars have also conducted a multiangle and multilevel research on dairy industry, dairy industry chain, and green industry chain.

1.1. Dairy Products Quality and Safety Research. Economic research on food safety began in the 1960s [1], and people began to pay more attention to food safety after the 1980s. Lankveld [2] found that the quality of dairy products

in Poland and other countries improved significantly after they joined the EU, which verified the effectiveness of the EU dairy supply chain. Dornon [3] put forward that the dairy processing industry was a vertically integrated industry, which should pay attention not only to food safety in the processing link of the supply chain but also to pasture. Cardoso et al. [4] pointed out that dairy enterprises and da-related professionals should educate dairy farmers on animal welfare because dairy farmers believed that production was more important than the welfare of calves. Noordhuizen, Koca et al. believed that the use of hazard analysis and the application of critical control points could effectively guarantee the quality and safety of dairy enterprises [5]. Sorge et al. [6] investigated the execution procedures of bovine *tuberculosis* control in 238 dairy farmers in Canada and found that communication and communication with dairy farmers could effectively improve disease control behaviors. Liu et al. [7] used the principle of quality control diagram to test standard samples of milk powder and found through experiments that it could improve the quality of monitored products. Wu et al. [8] determined the influencing factors of the intention to implement the comprehensive quality control behavior of dairy farmers by using the multiorder Logit model. The research shows that behavioral attitude, cooperative and coordinating attitude, and government encouragement and support are the surface direct factors. Zhang and Gong [9], based on the industrial chain perspective and discussion on dairy safety issues, put forward suggestions on strengthening the degree of integration, supervising the quality and safety of the supply chain, improving the benefit connection mechanism between enterprises and dairy farmers, and playing the supporting role of the government.

1.2. Dairy Industry Chain Research. The research on the dairy industry chain mainly focuses on how to improve the competitiveness of the industry chain and increase the value of the industry chain and the relationship between the main bodies of the industry chain. Bryndis and Martin [10], on the basis of the research on the dairy industry chain, considered to reduce the energy consumption in production by replacing milk powder with concentrated milk powder. Dries et al. [11] found through investigation of several countries in central and Eastern Europe that small dairy farms benefited from more cost and higher value market channels. Ding et al [12] studied whether the participation of federal, state, and local governments would affect the performance of the dairy industry chain. Based on the farmer survey, the determinants of market channel selection for small milk producers were analyzed and the effects of these market channel choices on farmers' income and technology adoption were studied. Nyokabi et al. [13], Kilelu et al. [14], and Gorton et al. [15] studied the multistakeholder relationship in the process of value chain appreciation of dairy products and its impact on value appreciation and industrial chain development.

1.3. Study on the Green Development of Dairy Products. The research on the green development of dairy products mainly focuses on the environmental management of dairy

products production, supply chain management, and green infrastructure construction. Yawar and Kauppi [16] and Goesch et al. [17] pointed out the role of the government in the green development of dairy products through research on the environmental management practice of dairy production. Kirilova and Vaklieva-Bancheva [18], Powell et al. [19], Yazdani et al. and McWilliam and Balzarova [20, 21], Rajabian Tabesh et al. [22], and Shibin et al. [23, 24] put forward that the guiding and supervising role of the government is of great significance to promote the green and sustainable development of the whole dairy industry chain.

Relevant studies by domestic and foreign experts and scholars show that optimizing the behavior of subjects in the dairy industry chain, improving the cooperative relationship between subjects and giving full play to the "self-organizing" role of the dairy industry chain, and seeking green, healthy, and sustainable development are effective ways to solve the quality and safety problems of dairy products [25, 26]. At present, although China and dairy companies attach great importance to the formation and development of green dairy industry chain, the effect of green dairy supply chain is not obvious. Due to the large number of subjects involved in the dairy industry chain, in addition to the uncertainty and complexity of the external factors affecting the formation of the green dairy industry chain, the balance of interests among the subjects is also the main factor affecting the formation of the green dairy industry chain. For example, for dairy farmers, green production requires higher production cost and production technology, which makes them pay more human, material, and financial resources. For dairy enterprises, it is not only necessary to supervise the raw milk materials provided by dairy farmers but also to innovate in technology. The high cost of green production for dairy farmers and dairy enterprises is the obstacle and resistance to the formation of green dairy industry chain. In order to effectively promote the formation of the green dairy industry chain, it is necessary for the government to guide, support, and supervise, so as to reduce the contrast between internalized costs and externalized benefits of green production for dairy farmers and dairy enterprises. Therefore, what are the influencing factors of cooperation between dairy farmers and dairy enterprises under government supervision? What is the mechanism of government guidance for the formation of the green dairy industry chain? How can faster and more efficient design promote the formation of the green industrial chain? These problems are of great significance for vigorously promoting the cooperation among the main players of the green dairy industry chain and enhancing the value of the green industry chain. Based on this, this paper established an evolutionary game model for the sustainable development of the green dairy industry chain from the perspective of government supervision, which considered the influences of the government's penalty and reward policies on the behavior strategy choices of main bodies involved in the dairy industry. A sustainable green dairy industry chain formation mechanism was proposed and further discussed by means of simulation study.

2. Model Construction

Game refers to the process in which each player chooses his or her own strategy (action) based on the information he or she has mastered, so as to realize the maximization of benefits and the minimization of risks and costs [27, 28]. Evolutionary game theory was first applied to analyze the stability of a trait against variation in the evolution of biological population [29, 30]. Later, economists introduced evolutionary game into economics and management [31–33]. Evolutionary game theory is a method that combines game and dynamic evolution, which can study the stable structure of the game system and the strategy selection process of the players by means of introducing dynamic mechanism. The basic idea is that, in a group of a certain size, game players are not super rational players, and it is impossible to find the optimal equilibrium point in every game, but repeated game can achieve equilibrium through trial and correction. Thus, the best strategy for game players is to imitate and improve the strategies in the past. Through long-term imitation and improvement, all game players will tend to choose a certain stable strategy.

“Green” products are based on the ecological environment, with strict product quality requirements and core competitiveness. The green dairy industry is based on green food, and more emphasis is placed on the production and consumption of nonpolluting dairy products with high nutrition, high quality, and environmental ecology on the basis of safety. The green dairy industry chain is based on the entire dairy industry chain, starting from the source of the industry chain, until the sale of green dairy products to the end consumer. Therefore, it is necessary to supervise each production process of green dairy products to ensure green milk. The whole process of product control is the basic guarantee for realizing the food safety of dairy products.

At the early stage of green dairy industry chain formation, there are contradiction between dairy farmers and dairy enterprises, enterprises’ profits and social responsibility, and short-term economic profit and long-term sustainable development. Besides, resources endowment and the understanding of the green dairy industry chain make it difficult for the parties to achieve their optimal strategies. Continuous trial and error correction, learning, and improvement are needed to form evolutionary stable strategy of a game. Due to the complex game relationship involved in the green dairy industry chain and various factors affecting strategy selection, this paper first conducted a literature retrieval on the green dairy industry chain formation, which shows that the basic benefits of dairy farmers and milk enterprises, green input costs, double income from the green production, and punishment for nongreen production are the core factors affecting the formation of the green dairy industry chain [34–37]. Therefore, based on the existing research results, this paper, taking these main factors as the main parameters, constructed an evolutionary game model of the formation mechanism of the green dairy industry chain from the perspective of sustainable development.

2.1. Model Assumptions

Hypothesis 1. In the process of the green dairy industry chain formation, there are many stakeholders involved. In this paper, dairy farmers and dairy enterprises are studied as main game players.

Hypothesis 2. It is assumed that, in the process of the green dairy industry chain formation, dairy farmers and dairy enterprises are bounded rational, the strategy selection is characterized with inertia, the players make decisions based on existing strategies, and their ultimate purpose is to maximize their own interests.

Hypothesis 3. In the early stage of the game, the proportion of dairy farmers choosing “green production” and “nongreen production” are x and $1 - x$, respectively. The proportion of dairy enterprises choosing “green production” and “nongreen production” are y and $1 - y$, respectively.

2.2. Model Symbol Description. In this paper, the hypothesis of profit and loss variables and related parameters of the interest game players are set as follows.

The basic income of the dairy farmers in the dairy industry chain is R_1 . Owing to the fact that the production needs to input a certain amount of human, material, and financial resources, the resulting cost is C_1 . When dairy farmers choose green production, they need to invest additional costs in technology, equipment, and other aspects ΔC_1 . If enterprises also choose green production at the same time, dairy farmers will get additional benefits ΔR_1 . If the enterprise chooses green production, the enterprise can examine the behavioral decisions of the dairy farmers through the milk source tracing system. If the dairy farmers do not adopt green production, they will be compensated for violating the cooperation agreement between the two parties, which is set as Π .

The basic income of dairy enterprises in the industrial chain is R_2 , and the input cost in the production process of dairy products is C_2 . When dairy enterprises choose green production and dairy farmers do not choose green production, the enterprises need to invest additional costs ΔC_2 in technology and equipment, etc. If the dairy farmers choose green production, the additional costs that the enterprises need to invest are ΔC_2 . Obviously, there is $\Delta C_2 > \Delta' C_2$. When dairy enterprises choose green production, they will gain additional benefits ΔR_2 due to the recognition of green food by consumers.

The game profit and loss matrix of the two under different strategies is shown in Table 1.

3. Evolutionary Game Model Construction

3.1. Construction of Replicated Dynamic Equations. Based on the abovementioned assumptions and payment matrix, dairy farmers and dairy products companies will obtain corresponding benefits by adopting different strategies and can establish a replication dynamic system.

TABLE 1: Game income matrix of dairy farmers and dairy production enterprises.

		Dairy production enterprises	
		Green production (y)	Nongreen production ($1 - y$)
Dairy farmers	Green production (x)	$R_1 - C_1 + \Delta R_1 - \Delta C_1$, $R_2 - C_2 + \Delta R_2 - \Delta C_2$	$R_1 - C_1 - \Delta C_1$, $R_2 - C_2$
	Nongreen production ($1 - x$)	$R_1 - C_1 - \Pi$, $R_2 - C_2 + \Delta R_2 - \Delta C_2 + \Pi$	$R_1 - C_1$, $R_2 - C_2$

According to Malthusian equation in evolutionary game theory, in the process of green development of the dairy industry chain, the expected benefits of dairy farmers choosing “green production” strategy and “nongreen production” are E_1^1 and E_1^2 , respectively:

$$\begin{aligned} E_1^1 &= y(R_1 - C_1 + \Delta R_1 - \Delta C_1) + (1 - y)(R_1 - C_1 - \Delta C_1), \\ E_1^2 &= y(R_1 - C_1 - \Pi) + (1 - y)(R_1 - C_1), \end{aligned} \quad (1)$$

where E_1^1 and E_1^2 are actually the gains obtained by dairy farmers when they adopt different strategies, so the average benefits of the mixed strategy of “green production” and “nongreen production” selected by dairy farmers are as \bar{E}_1 :

$$\bar{E}_1 = xE_1^1 + (1 - x)E_1^2. \quad (2)$$

Therefore, the replication dynamic equation that dairy farmers choose “green production” strategy is as follows:

$$F(x) = \frac{dx}{dt} = x(E_1^1 - \bar{E}_1) = x(1 - x)[y(\Delta R_1 + \Pi) - \Delta C_1]. \quad (3)$$

Similarly, the expected benefits of dairy enterprises choosing “green production” and “nongreen production” are E_2^1 and E_2^2 :

$$\begin{aligned} E_2^1 &= x(R_2 - C_2 + \Delta R_2 - \Delta C_2) + (1 - x) \\ &\quad (R_2 - C_2 + \Delta R_2 - \Delta C_2 + \Pi), \\ E_2^2 &= x(R_2 - C_2) + (1 - x)(R_2 - C_2). \end{aligned} \quad (4)$$

The average benefits of dairy enterprises’ mixed strategies of “green production” and “nongreen production” are \bar{E}_2 :

$$\bar{E}_2 = yE_2^1 + (1 - y)E_2^2. \quad (5)$$

Therefore, the replication dynamic equation that dairy enterprises choose “green production” are as follows:

$$\begin{aligned} D(y) &= \frac{dy}{dt} = y(E_2^1 - \bar{E}_2) = y(1 - y) \\ &\quad \cdot [x(\Delta C_2 - \Delta C_2 - \Pi) + \Delta R_2 - \Delta C_2 + \Pi]. \end{aligned} \quad (6)$$

The two-dimensional dynamic system (I) of the replication dynamic equation involved dairy farmers and milk enterprise can be gotten in accordance with equations (3) and (6).

From the abovementioned analysis, it can be seen that only when the income and payment cost of dairy farmers

and dairy product enterprises adopting “noncooperation” are less than the revenue and payment cost of cooperation between the two parties, both parties of the rational person will adopt the “cooperation” strategy. At this time, $x = 1$ and $y = 1$, respectively, indicate that the dairy farmers and dairy products companies choose the “green production” behavior strategy.

3.2. Stability Analysis of Equilibrium Point

Proposition 1. *If the dairy farmers and dairy enterprises constitute a two-dimensional dynamic system (I), there are $2^2 = 4$ group strategy equilibrium points, namely, (1, 1), (1, 0), (0, 1), and (0, 0). At the same time, there should be an equilibrium point of a mixed strategy, which satisfies $(x^*, y^*), x^* \in [0, 1]$, and $y^* \in [0, 1]$:*

$$\begin{aligned} x^* &= \frac{\Delta R_2 - \Delta C_2 + \Pi}{\Delta C_2 - \Delta C_2 + \Pi} = M, \\ y^* &= \frac{\Delta C_1}{\Delta R_1 + \Pi} = N. \end{aligned} \quad (7)$$

Proof. For two-dimensional dynamic system (I), when $x = 0$ or $x = 1$ and $y = 0$ or $y = 1$, there is $F(x) = 0$ and $D(y) = 0$. Therefore, (1, 1), (1, 0), (0, 1), and (0, 0) are the equilibrium points of the system. When $0 < x < 1$ and $0 < y < 1$, if $y(\Delta R_1 + \Pi) - \Delta C_1 = 0$ and $x(\Delta C_2 - \Delta C_2 - \Pi) + \Delta R_2 - \Delta C_2 + \Pi = 0$, then there is $F(x) = 0$, $D(y) = 0$. Solve the system of equation (8) and obtain that (x^*, y^*) is the possible equilibrium point of two-dimensional dynamic system (I):

$$\begin{cases} y(\Delta R_1 + \Pi) - \Delta C_1 = 0, \\ x(\Delta C_2 - \Delta C_2 - \Pi) + \Delta R_2 - \Delta C_2 + \Pi = 0. \end{cases} \quad (8)$$

According to [27], the equilibrium of a two-dimensional dynamic system (I) can be defined as an evolutionarily stable strategy (ESS for short) only through the stability test, which means the local stability of Jacobian matrix can be used to judge the stability of the equilibrium.

The Jacobian Matrix of the system is as below:

$$J = \begin{bmatrix} \frac{\partial G(x)}{\partial x} & \frac{\partial G(x)}{\partial y} \\ \frac{\partial F(y)}{\partial x} & \frac{\partial F(y)}{\partial y} \end{bmatrix} = \begin{bmatrix} a_{11} & a_{12} \\ a_{21} & a_{22} \end{bmatrix}, \quad (9)$$

where

$$\begin{aligned}
a_{11} &= (1 - 2x)[y(\Delta R_1 + \Pi) - \Delta C_1], \\
a_{12} &= x(1 - x)(\Delta R_1 + \Pi), \\
a_{21} &= y(1 - y)(\Delta' C_2 - \Delta C_2 - \Pi), \\
a_{22} &= (1 - 2y)[x(\Delta' C_2 - \Delta C_2 - \Pi) + \Delta R_2 - \Delta' C_2 + \Pi].
\end{aligned} \tag{10}$$

If the following two conditions are satisfied, the equilibrium point of the replication dynamic equation is the evolutionary stable strategy (ESS):

- (1) $tr J = a_{11} + a_{22} < 0$ (trace condition)
- (2) $\det J = \begin{vmatrix} a_{11} & a_{12} \\ a_{21} & a_{22} \end{vmatrix} = a_{11}a_{22} - a_{12}a_{21} > 0$ (Jacobian condition)

From the abovementioned calculation results, it can be seen that there is $a_{11} + a_{22} = 0$ at the local equilibrium point (M, N) , which does not conform to the equilibrium point. Therefore, (M, N) is definitely not the system's evolutionary stable strategy (ESS). As for the remaining four equilibrium points, according to the determinant and trace values of the Jacobian matrix J , the local stability of the equilibrium points can be judged. The results are shown in Table 2.

4. Result Analysis

According to ESS analysis of Table 2 and the replicated dynamic equation, it can be known as follows.

Proposition 2. *When $\Delta R_2 - \Delta' C_2 + \Pi < 0$, since $-\Delta C_1 < 0$, the evolutionary stable strategy (ESS) of two-dimensional dynamical system (I) is $(0, 0)$.*

Proof. It can be judged according to the determinant and trace of Jacobian.

This shows that, in the process of the formation of the green dairy industry chain, the sum of the extra income ΔR_2 obtained by the dairy enterprises when they choose green production and the cost Π fined by the dairy farmers when they do not choose green production is less than the extra cost $\Delta' C_2$ required by the enterprises when they choose green production, and the enterprises will choose noncooperative strategy. At the same time, if dairy farmers choose green production, they will need to invest additional costs ΔC_1 . At this time, dairy enterprises choose noncooperative strategy, and dairy farmers have no additional benefits, so they will choose noncooperative strategy. In summary, both the dairy enterprises and the dairy farmers choose nongreen production. Therefore, $(0, 0)$ is the stable point of the system evolution.

Proposition 3. *If $\Delta R_1 + \Pi - \Delta C_1 < 0$ and $\Delta R_2 - \Delta' C_2 + \Pi > 0$, the evolutionary stable strategy (ESS) of two-dimensional dynamical system (I) is $(0, 1)$.*

Proof. It can be judged according to the determinant and trace of Jacobian.

TABLE 2: Determinant values and traces of local equilibrium points.

	a_{11}	a_{12}	a_{21}	a_{22}
$(0, 0)$	$-\Delta C_1$	0	0	$\Delta R_2 - \Delta' C_2 + \Pi$
$(0, 1)$	$\Delta R_1 + \Pi - \Delta C_1$	0	0	$-\Delta R_2 - \Delta' C_2 + \Pi$
$(1, 0)$	ΔC_1	0	0	$\Delta R_2 - \Delta C_2$
$(1, 1)$	$-\Delta R_1 + \Pi - \Delta C_1$	0	0	$-\Delta R_2 - \Delta C_2$
(x^*, y^*)	0	M	N	0

This means that, in the process of formation of the green dairy industry chain, when the sum of extra income ΔR_1 gained by the green production and opportunity cost Π that enterprises choose nongreen enterprises is less than the extra cost of investment ΔC_1 that dairy farmers choose green production, farmers will choose noncooperative strategy for their own benefit maximization. At the same time, dairy enterprises will choose cooperation because the overall benefit is greater than the cost. In other words, when dairy farmers choose green production, their own interests will be damaged, while dairy enterprises choose green production, and their own profits will increase. Therefore, both sides of the game ultimately choose nongreen production strategy and green production strategy. Therefore, $(0, 1)$ is the stable point of the system evolution.

Proposition 4. *Two-dimensional dynamical system (I) does not have an evolutionary stable strategy (ESS) of $(1, 0)$.*

Proof. It can be judged according to the determinant and trace of Jacobian.

This shows that when dairy enterprises do not choose green production, dairy farmers will choose green production because there is no supervision of dairy enterprises. In other words, if there is no external force imposed, dairy farmers have no motivation to carry out green production because it requires extra investment but does not get additional benefits. As a rational person, it will definitely choose nongreen production, so there is no ESS of $(1, 0)$ for the two-dimensional dynamical system.

Proposition 5. *If $\Delta R_1 + \Pi - \Delta C_1 > 0$ and $\Delta R_2 - \Delta C_2 > 0$, the evolutionary stable strategy (ESS) of two-dimensional dynamical system (I) is $(1, 1)$.*

It can be judged according to the determinant and trace of Jacobian.

This shows that, in the process of green dairy industry chain formation, when both dairy farmers and dairy enterprises choose green production, their overall benefits are greater than their costs, and they will eventually choose cooperation strategy. In other words, at this time, both rational parties have maximized interests and they tend to adopt cooperative strategies. Therefore, $(1, 1)$ is the stable point of the evolution of the system.

It can be seen from the abovementioned analysis that if the extra input cost of dairy farmers and dairy enterprises does not get a large profit in the process of forming the green dairy industry chain, or the input cost is far greater than the profit, the rational people will not choose green production. Due to the frequent occurrence of agricultural products and

food safety incidents in recent years, the state has continuously strengthened the supervision of agricultural products and food, and the formation of the green dairy industry chain is also imminent. Therefore, in the process of forming the green dairy industry chain, the government's reward and punishment mechanism will play a huge role. It is assumed that the government can ensure its ability to inspect green production in the process of forming the green dairy industry chain, and it will not cover up the noncooperative strategy of the other party due to corruption and bribery.

It is assumed that, in the process of the formation of the green dairy industry chain, the government will punish dairy farmers or dairy enterprises once they are found to be uncooperative and provide policy subsidies to dairy farmers or dairy enterprises that have actively cooperated with them. In this case, the probability that government agencies supervise are z and $1 - z$, and the government, dairy farmers, and dairy enterprises are rational people.

In this paper, the government is regarded as a game player and its main income is tax and fines for noncooperative game players. Moreover, when both dairy farmers and dairy enterprises choose green production, the green

development benefits of the government will be promoted, but the cooperative game players need to be rewarded. Therefore, the profit and loss analysis of the government is as follows: the government rewards to dairy farmers and dairy enterprises for choosing green production are G_1 and G_2 , respectively, and the fines for dairy farmers and dairy enterprises for choosing green production are g_1 and g_2 , respectively. The investment the government pays for supervising the formation of the green dairy industry chain is C_3 , basic revenue from government taxation is R_3 , and the benefits obtained from dairy farmers and dairy enterprises to choose green production are ΔR_3 and $\Delta' R_3$, respectively. Therefore, the revenue matrix of the government being a game player in the process of forming the green dairy industry chain is shown in Table 3 below.

The income matrix of the government in the formation process of the green dairy industry chain can be calculated according to Table 3. In the process of the green development of the dairy industry chain, the expected benefits of the government choosing supervision strategy and non-supervision strategy are E_3^1 and E_3^2 , respectively:

$$\begin{aligned} E_3^1 &= [xy(R_3 + \Delta R_3 + \Delta' R_3 - G_1 - G_2 - C_3) + x(1 - y)(R_3 + \Delta R_3 + g_2 - C_3 - G_1)] \\ &\quad + [(1 - x)y(R_3 + \Delta' R_3 + g_1 - C_3 - G_2) + (1 - x)(1 - y)(R_3 - C_3 + g_1 + g_2)], \\ E_3^2 &= [xy(R_3 + \Delta R_3 + \Delta' R_3) + x(1 - y)(R_3 + \Delta R_3)] + [(1 - x)y(R_3 + \Delta' R_3) + (1 - x)(1 - y)R_3]. \end{aligned} \quad (11)$$

The average benefits of the mixed strategy of supervision strategy and nonsupervision strategy chosen by the government are as follows:

$$\bar{E}_3 = zE_3^1 + (1 - z)E_3^2. \quad (12)$$

Therefore, the replication dynamic equation that the government chooses supervision strategy is as follows:

$$\begin{aligned} G(x) = \frac{dz}{dt} &= z(E_3^1 - \bar{E}_3) = z(1 - z)[-x(G_1 - g_1) \\ &\quad - y(G_2 - g_2) + g_1 + g_2]. \end{aligned} \quad (13)$$

Under the government's reward and punishment mechanism, the replication dynamic equation of dairy farmers and dairy enterprises will also change during the formation of the green dairy industry chain, which is shown as follows:

$$\begin{aligned} F_1(x) = \frac{dx}{dt} &= x(1 - x)[y(\Delta R_1 + \Pi) + zG_1 + yz g_2 \\ &\quad + (1 - y)z g_1 - \Delta C_1], \end{aligned} \quad (14)$$

$$\begin{aligned} D_1(y) = \frac{dy}{dt} &= y(1 - y)[x(\Delta' C_2 - \Delta C_2 - \Pi) \\ &\quad + zG_2 + xz g_1 + (1 - x)z g_2 + \Delta R_2 - \Delta' C_2 + \Pi]. \end{aligned} \quad (15)$$

In the process of forming the green dairy industry chain, the government rewards and penalizes dairy farmers and dairy enterprises, which can reduce the volatility of the game and accelerate the speed of all parties to reach the equilibrium state. According to the basic nature of the evolutionary game, (x^*, y^*, z^*) is substituted into equations (13)–(15). When $F_1'(x) < 0$, $D_1'(y) < 0$, $G(z) < 0$, (x^*, y^*, z^*) is the stable strategy of dairy farmers, dairy enterprises, and the government under the multiplayer game formed by the green dairy industry chain. Since the government plays the role of supervision and support, this paper only analyzes the gradual stability of dairy farmers and dairy enterprises in the industrial chain, and the results are as follows.

4.1. Progressive Stability Analysis of Dairy Farmers

- ① If $y(\Delta R_1 + \Pi) + zG_1 + yz g_2 + (1 - y)z g_1 - \Delta C_1 = 0$, then there is $F_1(x) \equiv 0$, which means the strategy selection of dairy farmers is in a stable state in the process of forming the green dairy industry chain, that is, the proportion of dairy farmers' strategy selection will not change with the passing of time.
- ② If $y(\Delta R_1 + \Pi) + zG_1 + yz g_2 + (1 - y)z g_1 - \Delta C_1 > 0$, let $F_1(x) = 0$, then $x = 0$ and $x = 1$ are two stable points of x . $F_1'(x) = (1 - 2x)[y(\Delta R_1 + \Pi) + zG_1 +$

TABLE 3: The income matrix of the government in the forming process of the green dairy industry chain.

		Governments	
		Supervising (z)	Nonsupervising ($1 - z$)
Strategy choices of dairy enterprises and dairy farmers	Both parties have chosen cooperative strategies (x, y)	$R_3 + \Delta R_3 + \Delta' R_3 - G_1 - G_2 - C_3$	$R_3 + \Delta R_3 + \Delta' R_3$
	Dairy farmers and dairy enterprises choose cooperative strategy and noncooperative strategy ($x, 1 - y$)	$R_3 + \Delta R_3 + g_2 - C_3 - G_1$	$R_3 + \Delta R_3$
	Dairy farmers and dairy enterprises choose noncooperative strategy and cooperative strategy ($1 - x, y$)	$R_3 + \Delta' R_3 + g_1 - C_3 - G_2$	$R_3 + \Delta' R_3$
	Both parties have chosen noncooperative strategies ($1 - x, 1 - y$)	$R_3 - C_3 + g_1 + g_2$	R_3

$yzg_2 + (1 - y)zg_1 - \Delta C_1$], and then there is $F'_1(0) > 0$ and $F'_1(1) < 0$, so $x = 1$ is the balance point of dairy farmers' strategy. It shows that extra profits ΔR_1 and government subsidies G_1 obtained by the dairy farmers when they choose green production, the opportunity cost g_1 and g_2 and Π of being fined when they choose green production, and the extra cost ΔC_1 of investment required by the dairy farmers when they choose green production are all key factors that affect the strategy selection of dairy farmers. At this time, subsidies for the green dairy industry chain under government supervision and penalties for noncooperation of dairy farmers and dairy enterprises accelerate the emergence of cooperative behaviors of dairy farmers. Therefore, government supervision is of great significance to the formation of cooperative behaviors of dairy farmers in the green dairy industry chain.

- ③ Similarly, if $y(\Delta R_1 + \Pi) + zG_1 + yzg_2 + (1 - y)zg_1 - \Delta C_1 < 0$, then $F'_1(0) < 0$ and $F'_1(1) > 0$, so $x = 0$ is the balance point of dairy farmers' selection strategy. This shows that once the sum of the benefits of green production (including additional benefits and government incentives) and the opportunity cost of noncooperation is smaller than the additional cost of green production, the dairy farmers will choose noncooperative strategy because the input cost of green production is too high. Therefore, in the process of forming the green dairy industry chain, the government and dairy enterprises need not only supervise the dairy farmers but also provide support for green production technology and equipment.

4.2. Progressive Stability Analysis of Dairy Enterprises

- ① If $x(\Delta' C_2 - \Delta C_2 - \Pi) + zG_2 + xzg_1 + (1 - x)zg_2 + \Delta R_2 - \Delta' C_2 + \Pi = 0$, then there is $D'_1(y) \equiv 0$, which means the strategic choice of dairy enterprises is a stable state, that is, the proportion of dairy industry strategic choice will not change with the passage of time.

- ② If $x(\Delta' C_2 - \Delta C_2 - \Pi) + zG_2 + xzg_1 + (1 - x)zg_2 + \Delta R_2 - \Delta' C_2 + \Pi > 0$, let $D_1(y) = 0$, then $y = 0$ and $y = 1$ are two stable points of y . There is $D'_1(y) = (1 - 2y)[x(\Delta' C_2 - \Delta C_2 - \Pi) + zG_2 + xzg_1 + (1 - x)zg_2 + \Delta R_2 - \Delta' C_2 + \Pi]$, $F'_2(0) > 0$, and $F'_2(1) < 0$, so $y = 1$ is the stable points of dairy enterprises' strategies. This shows that the extra income ΔR_2 when the dairy enterprises choose the green production, the government's penalty Π and subsidy G_2 , the opportunity cost when the dairy enterprises choose green production and nongreen production g_1 and g_2 , and the additional cost of dairy companies when the dairy farmers choose cooperative strategy and noncooperative strategy $\Delta' C_2$ and ΔC_2 are the key factors influencing the dairy products enterprise strategy choice. Similarly, subsidies for the green dairy industry chain under government supervision and penalties for noncooperation of dairy farmers and dairy enterprises accelerate the generation of cooperative behaviors of dairy enterprises. Therefore, government supervision is of great significance to the formation of cooperative behaviors of dairy enterprises in the green dairy industry chain.

- ③ Similarly, if $x(\Delta' C_2 - \Delta C_2 - \Pi) + zG_2 + xzg_1 + (1 - x)zg_2 + \Delta R_2 - \Delta' C_2 + \Pi < 0$, then there is $F'_1(0) < 0$ and $F'_1(1) > 0$, so $x = 0$ is the balance point of dairy enterprises' selection strategy. This shows that the sum of the benefits the dairy enterprises choose green production (including the additional income and penalties and rewards from the governments) and the opportunity cost when the dairy enterprises choose noncooperative strategy is less than the additional expected cost $x\Delta C_2 + (1 - x)\Delta' C_2$, and dairy companies will choose noncooperative strategies due to too high production cost. Therefore, in addition to government supervision, the behavior of dairy farmers at the initial stage of the industrial chain also has a huge impact on the behavior of dairy enterprises in the process of the formation of the green dairy industry chain.

All in all, the government can increase the cooperation income of dairy farmers and enterprises through subsidies

and can also increase the noncooperative opportunity cost through penalties, so as to supervise and guide the formation of the green supply chain, and eventually realize the sustainable development of the dairy industry chain.

5. Numerical Simulation

Based on the analysis of the formation of green dairy industry chain under the supervision of the government, this paper compared the behavioral strategies of dairy farmers and dairy enterprises with or without government rewards and punishments to choose the evolutionary path and discussed the impact of the change of green production cost on the formation of the green dairy industry chain. Firstly, it is assumed that, in the early stage of the green dairy industry chain, dairy farmers, and dairy enterprises finally failed to reach cooperation intention, that is, ESS is $(0, 0)$, at which time the parameters meet $\Delta R_2 - \Delta C_2 + \Pi < 0$. It is assumed that the value of relevant parameters in the game matrix is $\Delta R_1 = \Delta R_2 = 1$, $\Delta C_2 = 3$, $\Pi = 0.5$, $\Delta C_1 = 1.5$, and $\Delta C_2 = 2$. Based on the abovementioned parameters, it is assumed that at the beginning of the green dairy industry chain, dairy farmers and dairy enterprises have a strong desire to cooperate, that is, at the beginning $x = y = 0.9$. Government rewards and punishments, as well as the influence of changes in green production costs on the behavioral strategies of dairy farmers and dairy enterprises are simulated below.

5.1. The Impact of Government Subsidies on the Formation of Green Dairy Industry Chain. As shown in Figure 1, when there is no government subsidies, even if the initial willingness of dairy farmers and dairy enterprises to cooperate is strong, after a certain period of game learning, they will choose noncooperative because the income is less than the input. When the government intends to promote the formation of the green dairy industry chain, it can be obtained from the evolutionary game dynamics system that the critical point of dairy farmers for government's rewards is $G_1 = 0.15$ and the critical point of dairy enterprises is $G_2 = 1.05$. That is to say, when the government reward is higher than the critical point, dairy farmers and dairy enterprises will choose cooperative strategies. If one critical point is reached, assuming government subsidies $G_1 = G_2 = 0.7$, dairy farmers and dairy enterprises will maximize their own interests and choose strategies that fluctuate between $(0, 1)$ in the learning process of evolutionary game, eventually leading to the failure of both parties to reach a stable equilibrium state (as shown in Figure 2).

Only when the government subsidy is greater than the critical point, if $G_1 = 1.5$ and $G_2 = 2$, then dairy farmers and dairy enterprises will choose green production strategy. At this time, the dairy farmers and dairy enterprises can take the initiative to gain high net benefits from green production, which are also the results of continuous learning of dairy farmers and dairy companies. Therefore, it can be concluded that government subsidies can effectively promote green production of dairy farmers and dairy enterprises, promote

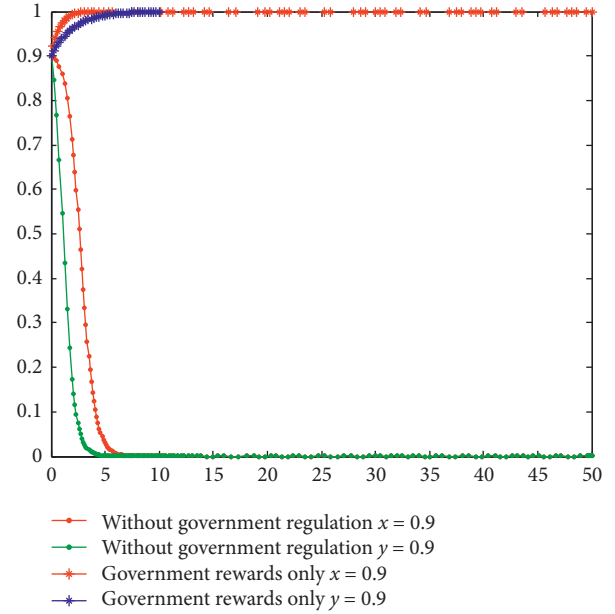


FIGURE 1: Influence of government subsidies on the formation of the green dairy industry chain.

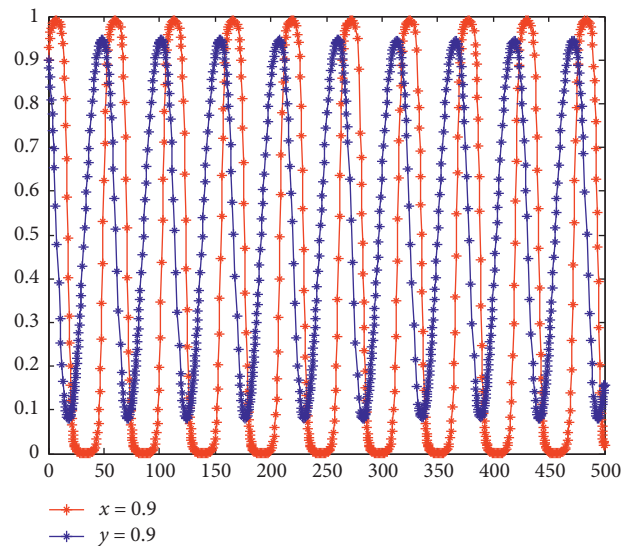


FIGURE 2: Influence of critical points of government subsidies on the formation of the green dairy industry chain.

the formation of green dairy industry chain, and help the green dairy industry chain system to reach an ideal equilibrium state.

5.2. The Impact of Government Punishment on the Formation of Green Dairy Industry Chain. When the government intends to promote the formation of green industry chain by means of punishment, it can be obtained from the evolutionary game power system that if the initial cooperation intention between the dairy farmers and dairy enterprises is strong as $x = y = 0.9$, the critical point for dairy farmers on government punishment is $g_1 = (93/80)$ and the critical

point on dairy enterprises is $g_2 = (3/80)$, which means when the government punishment is higher than the critical point, the dairy farmers and dairy companies will choose cooperative strategy for fear of excessive punishment on non-cooperation. Likewise, if the government only implements punishment policy for the formation of the green industry chain, there is only one critical point. Assuming that punishment from the government is $g_1 = 1$ and $g_2 = 1.8$, farmers and dairy companies will maximize their own interests, and their selection strategy in the learning process of evolutionary game fluctuates between (0, 1), resulting in the fact that both sides cannot reach a stable equilibrium state (as shown in Figure 3). In the process of the game during 500 unit of time, the influence of contrast Figures 2 and 3 shows that the situation exists that the learning speed of the players below the critical points of the government rewards is far from higher than that with government punishment. This shows that the sensitivity of the influence of learning speed over government rewards is much higher than that over government punishment. Of course, it also related to dairy farmers and milk enterprise initial cooperation will.

Only when the government for dairy farmers and dairy enterprises punishment is greater than the critical point, $g_1 = g_2 = 2.5$, dairy farmer and dairy companies will choose green production strategy. At this time, the dairy farmers and dairy enterprises would rather take the initiative to conduct green production than get heavy punishment. It is also the results of the final selection through continuous learning process, as shown in Figure 4. Therefore, it can be concluded that, in the absence of government subsidies, increasing government punishment can also effectively promote the green production of dairy farmers and dairy enterprises, promote the formation of the green dairy industry chain, and help the green dairy industry chain system to reach an ideal equilibrium state. It should be noted that the government's punishment is a mandatory measure, which may reduce the enthusiasm of dairy farmers and dairy enterprises to participate in the formation of the dairy industry chain and force them out of the industry.

5.3. The Impact of Government Subsidies and Penalties on the Formation of Green Dairy Industry Chain. Based on the analysis on (1) and (2), government subsidies and government punishment promote the evolutionary game equilibrium function (as shown in Figure 5). Obviously, the combination of government subsidies and government punishment will accelerate the game when the formation of ESS. When dairy farmers and dairy enterprises choose green production strategy, the government will give subsidies, and the opportunity cost will be exempted from government punishment. When the opportunity cost of subsidies and punishment is greater than the net gain without cooperation, both sides will avoid their own losses and choose cooperation.

Of course, the convergence speed of evolution game equilibrium solution for dairy farmers and dairy enterprises is different. That is to say, increasing the government subsidy by one unit or increasing the government punishment by one unit or both will speed up the cooperation between the

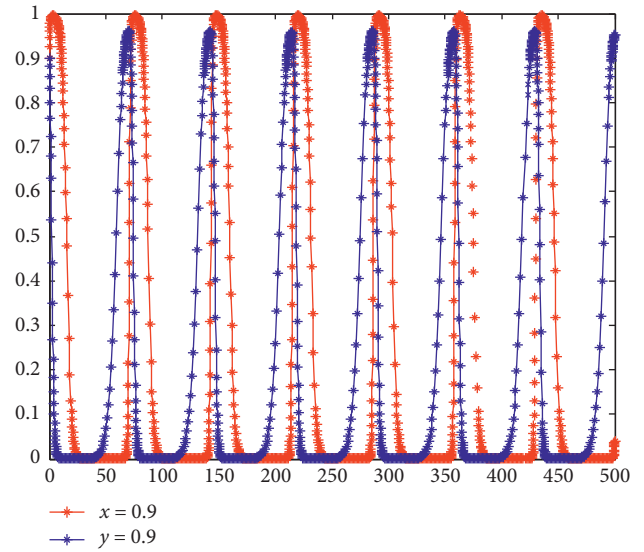


FIGURE 3: Influence of critical point of government punishment on the formation of green dairy industry chain.

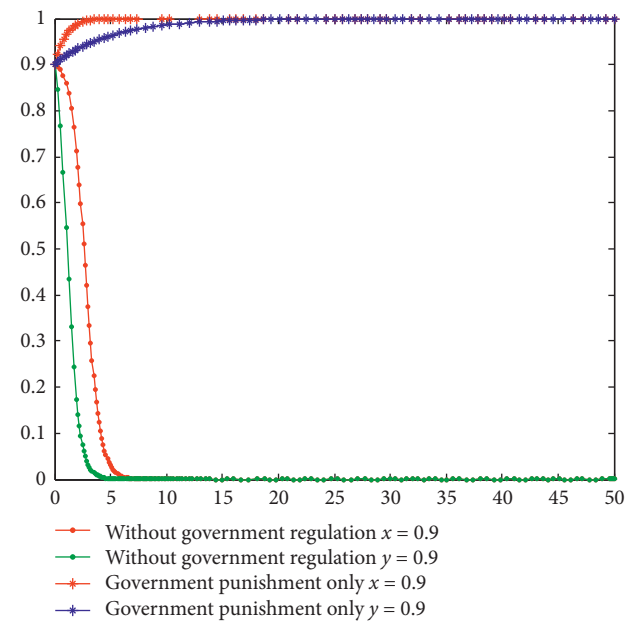


FIGURE 4: Influence of government punishment on the formation of the green dairy industry chain.

two parties. As shown in Figure 6, coexisting of government subsidy and government punishment has bigger promoting effect than only with government subsidy or with punishment, and the subsidy has more significant influence than the punishment. It is most effective when there are both government subsidies and government punishments. Cooperation can also be promoted when there are only government subsidies and government punishments, but subsidies and punishments must be strengthened.

5.4. The Influence of Green Production Cost on the Formation of Green Dairy Industry Chain. Green production cost is also

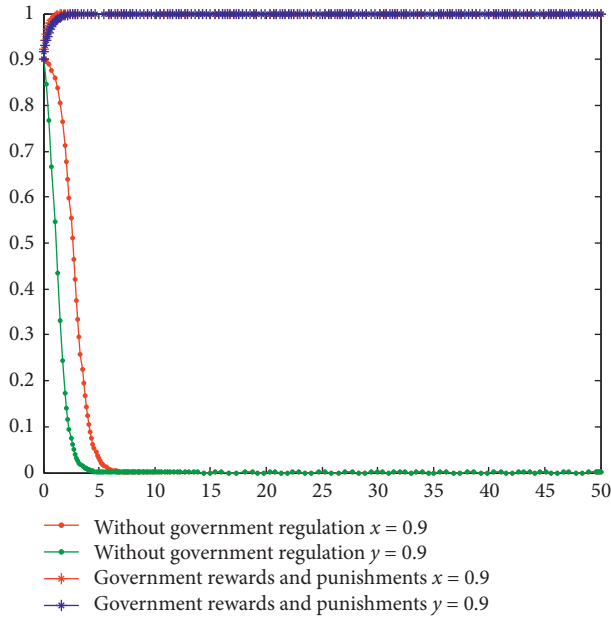


FIGURE 5: Influence of government subsidy and punishment on the formation of green dairy industry chain.

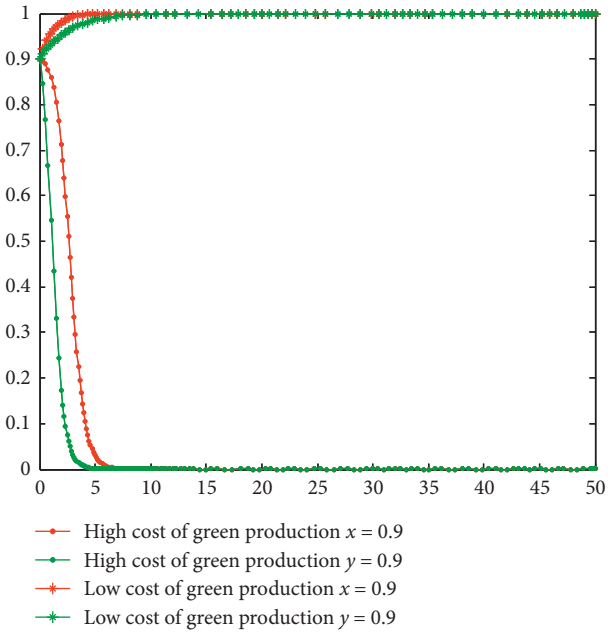


FIGURE 7: Influence of green production cost on the formation of green dairy industry chain.

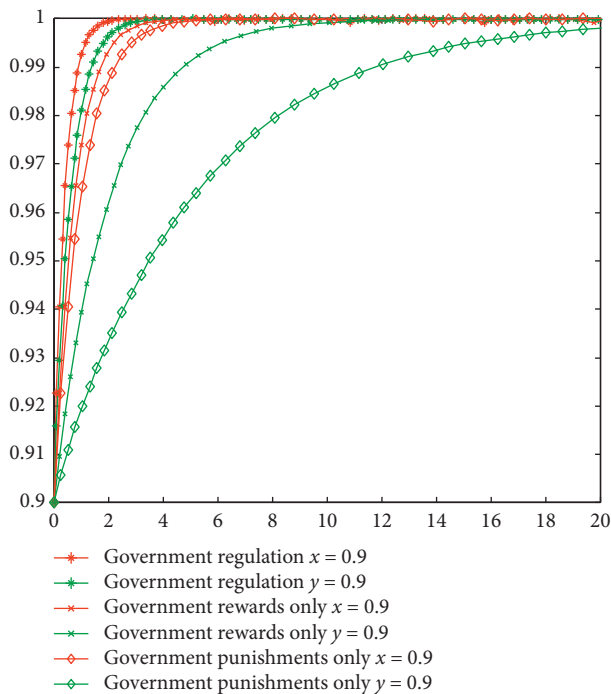


FIGURE 6: Comparison of convergence speed of government subsidies and punishments on the game between dairy farmers and dairy enterprises.

extremely important for the formation of the green dairy industry chain. In fact, the reduction of green production cost will eventually improve the net income of dairy farmers and dairy enterprises. In accordance with the evolutionary game power system, if the cooperation intention of both sides is as strong as $x = y = 0.9$, the crucial point of green

production costs on dairy farmers is $\Delta C_1 = 1.35$, and on dairy enterprises is $\Delta C_2 = 1$ and $\Delta C_2' = 1.5$. In other words, when the production cost is higher than the critical point, dairy farmers and dairy enterprises will choose noncooperative strategy for the high cost and deficit of net income. The cooperation between dairy farmers and dairy enterprises can only be promoted by scientific and technological innovation through government training and green production cost reduction. When the green production cost is reduced through technical means and scientific and technological innovation, it is assumed that $\Delta C_1 = 0.5$, $\Delta C_2 = 0.3$, and $\Delta C_2' = 1$, and the initial intention of cooperation between dairy farmers and dairy enterprises is $x = y = 0.9$, both sides of the game will obtain higher net benefits through green production and finally choose cooperation (as shown in Figure 7). Therefore, the reduction of green production cost is also an important factor to promote the formation of the green dairy industry chain, which can promote the green dairy industry chain system to reach an ideal equilibrium state.

6. Conclusion

Based on the basic theory of evolutionary game, this paper analyzed the forming mechanism of the green dairy industry chain under government supervision. The results showed that when dairy farmers and dairy enterprises have a strong desire to build a green dairy industry chain, if the cost of green production invested by dairy farmers and dairy enterprises does not get a large profit, both sides of the game will give up cooperation. When there is no government supervision, or the government supervision is not enough, the evolutionary game between dairy farmers and dairy enterprises is either uncooperative or changes periodically, which cannot achieve the effect of cooperation. Therefore, in

the process of forming the green dairy industry chain, the government's supervision is extremely urgent. Under the condition of strict government supervision, government subsidies and punishments can greatly promote the formation of green dairy industry chain. The more government subsidies are, the more serious the government punishments will be and the less likely dairy farmers and dairy enterprises will choose the behavior strategy of nongreen production. Of course, promoting technological innovation and reducing green production costs through government training are also important means to promote bilateral cooperation. Therefore, establishing a government-led supervision mechanism, appropriately increasing subsidies, strengthening penalties, and reducing green production costs can effectively improve the cooperation between dairy farmers and dairy enterprises, so as to ensure the formation of a green dairy industry chain and protect the interests of the public.

Based on the abovementioned conclusions and analysis, the following suggestions are proposed for the formation of the green dairy industry chain.

Firstly, the government should reasonably formulate the reward and punishment system for the green dairy industry chain. In the process of promoting the formation of the green dairy industry chain, the government should consider various constraints, weigh the interests of all parties on the industrial chain, and formulate a reward and punishment system conducive to the formation of green dairy industry chain. Of course, this means that the government not only needs to pay more administrative costs in supervision but also needs to invest more incentive costs. Therefore, the government can develop a scientific and reasonable third-party supervision system to effectively supervise dairy farmers and dairy enterprises.

Secondly, reduce the cost of green production for dairy farmers and dairy companies. The government can provide basic training for dairy farmers and dairy enterprises so that they can acquire necessary green production skills and improve their overall production quality. At the same time, it is also possible to make use of the technological advantages of universities and research institutes to carry out technical research on green production through industry-university-research, so as to solve the technical problems existing in the process of green production. At the same time, the government can also equip dairy farmers and dairy companies with advanced green production testing equipment to reduce their production costs.

Thirdly, dairy products enterprises should establish a green development strategic plan. In addition to constantly innovating the design and development of dairy products, it is also necessary to use the green dairy product standard as a guideline to meet consumer demand for safe and high-quality dairy products. In terms of operation, we need to improve the control of dairy products processing and sales and improve the level of green and sustainable development of the company.

Data Availability

The data used to support the findings of this study are available from the corresponding author upon request.

Conflicts of Interest

The authors declare no conflicts of interest.

Acknowledgments

This work was supported by the National Natural Science Foundation of China (Project no. 71874184) and Xinjiang Tianshan army reclamation co., Ltd. (Project no. 2019ZH04). The funders had no role in the design of the study; in the collection, analyses, or interpretation of data; in the writing of the manuscript; or in the decision to publish the results.

References

- [1] G. Tognon, L. M. Nilsson, D. Shungin, L. Lissner, J. H. Jansson et al., "Nonfermented milk and other dairy products: associations with all-cause mortality," *The American Journal of Clinical Nutrition*, vol. 105, 2017.
- [2] J. M. G. Lankveld, "Quality, safety and value optimization of the milk supply chain in rapidly evolving central and Eastern European markets," *Leerstoelgroep Productontwerpen en Kwaliteskunde*, vol. 9, p. 14, 2004.
- [3] H. Dornon, *Guide to Good Dairy Farming Practices 2004*, Introduction FAO/IDF, Paris, France, 2006.
- [4] C. S. Cardoso, M. A. Keyserlingk, M. J. Hotzel et al., "Trading of animal welfare and production goals: Brazilian dairy farmers' perspectives on calf dehorning," *Livestock Science*, vol. 187, no. 2, pp. 102–108, 2016.
- [5] T. Koca, M. Akcam, F. Serdaroglu et al., "Breakfast habits, dairy product consumption, physical activity, and their associations with body mass index in children aged 6–18," *European Journal of Pediatrics*, vol. 176, no. 9, pp. 1251–1257, 2017.
- [6] U. Sorge, D. Kelton, K. Lissemore et al., "Attitudes of Canadian dairy farmers toward a voluntary Johne's disease control program," *Journal of Dairy Science*, vol. 93, no. 4, pp. 0–1499, 2010.
- [7] Q. Liu, C. Yi, and Z. Y. Dai, "Application of control chart in quality control of dairy enterprises," *Journal of Food Safety and Quality Inspection*, vol. 9, no. 21, pp. 240–248, 2018.
- [8] Q. Wu, Y. Y. Zhang, and S. M. Sun, "Analysis on the behavior of total quality control of dairy farmers based on Logit-ISM model," *Journal of Agrotechnical Economics*, vol. 2017, no. 3, pp. 55–65, 2017.
- [9] X. X. Zhang and X. J. Gong, "Research progress of dairy product safety based on industrial chain optimization," *Journal of Dairy Science and Technology*, vol. 40, no. 3, pp. 24–28, 2017.
- [10] B. Stefansdottir and M. Grunow, "Selecting new product designs and processing technologies under uncertainty: two-stage stochastic model and application to a food supply chain," *International Journal of Production Economics*, vol. 201, pp. 89–101, 2018.
- [11] L. Dries, E. Gemenji, N. Noev, and J. F. Swinnen, "Farmers, vertical coordination, and the restructuring of dairy supply chains in Central and Eastern Europe," *World Development*, vol. 37, no. 11, pp. 1742–1758, 2009.
- [12] H. Ding, Y. Fu, L. Zheng, and Z. Yan, "Determinants of the competitive advantage of dairy supply chains: evidence from the Chinese dairy industry," *International Journal of Production Economics*, vol. 209, pp. 360–373, 2019.

- [13] S. Nyokabi, S. J. Oosting, B. O. Bebe et al., "The Kenyan dairy sector: stakeholder roles and relationships, and their impact on milk quality," in *Farming Systems: Facing Uncertainties and Enhancing Opportunities*, Wageningen University & Research, Wageningen, Netherlands, 2018.
- [14] C. Kilelu, L. Klerkx, A. Omore, I. Baltenweck, C. Leeuwis, and J. Githinji, "Value chain upgrading and the inclusion of smallholders in markets: reflections on contributions of multi-stakeholder processes in dairy development in Tanzania," *The European Journal of Development Research*, vol. 29, no. 5, pp. 1102–1121, 2017.
- [15] M. Gorton, R. Angell, L. Dries, V. Urutyanyan, E. Jackson, and J. White, "Power, buyer trustworthiness and supplier performance: evidence from the Armenian dairy sector," *Industrial Marketing Management*, vol. 50, pp. 69–77, 2015.
- [16] S. A. Yawar and K. Kauppi, "Understanding the adoption of socially responsible supplier development practices using institutional theory: dairy supply chains in India," *Journal of Purchasing and Supply Management*, vol. 24, no. 2, pp. 164–176, 2018.
- [17] T. Goesch, K. Lawson, R. Green, and K. Morey, *Australia's Beef Supply Chains Infrastructure Issues and Implications*, ABARES Research Report 15.7, ABARES, Canberra, Australia, 2015.
- [18] E. G. Kirilova and N. G. Vakiieva-Bancheva, "Environmentally friendly management of dairy supply chain for designing a green products' portfolio," *Journal of Cleaner Production*, vol. 167, pp. 493–504, 2017.
- [19] D. Powell, S. Lundebj, L. Chabada, and H. Dreyer, "Lean Six Sigma and environmental sustainability: the case of a Norwegian dairy producer," *International Journal of Lean Six Sigma*, vol. 8, no. 1, pp. 53–64, 2017.
- [20] W. McWilliam and M. Balzarova, "The role of dairy company policies in support of farm green infrastructure in the absence of government stewardship payments," *Land Use Policy*, vol. 68, pp. 671–680, 2017.
- [21] M. Yazdani, P. Chatterjee, E. K. Zavadskas, and S. H. Zolfani, "Integrated QFD-MCDM framework for green supplier selection," *Journal of Cleaner Production*, vol. 142, pp. 3728–3740, 2017.
- [22] A. Rajabian Tabesh, P. J. Batt, and B. Butler, "Modelling the impact of environmental and organizational determinants on green supply chain innovation and performance," *Journal of Food Products Marketing*, vol. 22, no. 4, pp. 436–454, 2016.
- [23] J. C. V. Martínez and J. C. Fransoo, "Green facility location," in *Sustainable Supply Chains*, pp. 219–234, Springer, Berlin, Germany, 2017.
- [24] K. T. Shubin, A. Gunasekaran, T. Papadopoulos, R. Dubey, M. Singh, and S. F. Wamba, "Enablers and barriers of flexible green supply chain management: a total interpretive structural modeling approach," *Global Journal of Flexible Systems Management*, vol. 17, no. 2, pp. 171–188, 2016.
- [25] M. P. Squicciarini, A. Vandeplas, E. Janssen, and J. Swinnen, "Supply chains and economic development: insights from the Indian dairy sector," *Food Policy*, vol. 68, pp. 128–142, 2017.
- [26] S. Yildiz Çankaya and B. Sezen, "Effects of green supply chain management practices on sustainability performance," *Journal of Manufacturing Technology Management*, vol. 30, no. 1, pp. 98–121, 2019.
- [27] J. W. Friedman, *Game theory with applications to economics*, Oxford University Press, Oxford, UK, 1986.
- [28] R. B. Myerson, *Game Theory*, Harvard University Press, Cambridge, MA, USA, 2013.
- [29] C. F. Camerer, *Behavioral Game Theory: Experiments in Strategic Interaction*, Princeton University Press, Princeton, NJ, USA, 2011.
- [30] J. W. Weibull, *Evolutionary Game Theory*, MIT press, Cambridge, MA, USA, 1997.
- [31] K. E. Boulding, *Evolutionary Economics*, Sage Publications, New York, NY, USA, 1981.
- [32] D. Friedman, "On economic applications of evolutionary game theory," *Journal of Evolutionary Economics*, vol. 8, no. 1, pp. 15–43, 1998.
- [33] P. Ji, X. Ma, and G. Li, "Developing green purchasing relationships for the manufacturing industry: an evolutionary game theory perspective," *International Journal of Production Economics*, vol. 166, pp. 155–162, 2015.
- [34] A. Abedullah, N. Mtimet, N. Teufel, M. N. Ibrahim, Z. Mustafa, and A. Ahmad, *Dairy value chains in Pakistan Stakeholders' Involvement and Constraints Analysis*, vol. 9, p. 14, 2015.
- [35] A. Criscuolo and F. Cuomo, *Market Opportunities for Green Upgrading and Innovation: Sustainability Demand Analysis for the Beef, Soy, Dairy and Tourism Industries*, Chandigarh, India, 2018.
- [36] C. W. Kilelu, L. Klerkx, and C. Leeuwis, "Supporting smallholder commercialisation by enhancing integrated coordination in agrifood value chains: experiences with dairy hubs in Kenya," *Experimental Agriculture*, vol. 53, no. 2, pp. 269–287, 2017.
- [37] S. B. Tsai, B. Liu, and Y. Li, Eds., *Green Production Strategies For Sustainability*, IGI Global, PA, USA, 2017.

Research Article

An Eco-Inefficiency Dominance Probability Approach for Chinese Banking Operations Based on Data Envelopment Analysis

Feng Li ¹, Lunwen Wu,¹ Qingyuan Zhu ,^{2,3} Yanling Yu,¹ Gang Kou ¹ and Yi Liao ¹

¹School of Business Administration, Southwestern University of Finance and Economics, Chengdu 611130, China

²College of Economics and Management, Nanjing University of Aeronautics and Astronautics, Nanjing 211106, China

³Research Centre for Soft Energy Science, Nanjing University of Aeronautics and Astronautics, Nanjing 211106, China

Correspondence should be addressed to Qingyuan Zhu; zqynuaa@nuaa.edu.cn

Received 23 February 2020; Revised 30 March 2020; Accepted 10 April 2020; Published 4 May 2020

Guest Editor: Baogui Xin

Copyright © 2020 Feng Li et al. This is an open access article distributed under the Creative Commons Attribution License, which permits unrestricted use, distribution, and reproduction in any medium, provided the original work is properly cited.

Data envelopment analysis (DEA) has proven to be a powerful technique for assessing the relative performance of a set of homogeneous decision-making units (DMUs). A critical feature of conventional DEA approaches is that only one or several sets of optimal virtual weights (or multipliers) are used to aggregate the ratio performance efficiencies, and thus, the efficiency scores might be too extreme or even unrealistic. Alternatively, this paper aims at developing a new performance dominance probability approach and applying it to analyze the banking operations in China. Towards that purpose, we first propose an extended eco-inefficiency model based on the DEA methodology to address banking activities and their possible relative performances. Since the eco-inefficiency will be obtained using a set of optimal weights, we further build a performance dominance structure by considering all sets of feasible weights from a data-driven perspective. Then, we develop two pairwise eco-inefficiency dominance concepts and propose the inefficiency dominance probability model. Finally, we illustrate the eco-inefficiency dominance probability approach with 32 Chinese listed banks from 2014 to 2018 to demonstrate the usefulness and efficacy of the proposed method.

1. Introduction

Forty years have gone by since the great reform and opening policy of 1978, and China has made substantial progress in economic development with an annual increase of almost nine percent in gross domestic product from 149.541 billion dollars in 1978 to 13.608 trillion dollars in 2018. It is rather remarkable that the banking industry of China, especially state-owned and listed banks, has played a great role in Chinese economic growth [1, 2]. Throughout the ever-increasing national economic development, the banking industry in China has also been promoted and developed considerably. For example, the total assets of the Chinese banking industry reached almost 41 trillion dollars in 2018, which is more than three times the gross domestic product in current US dollars in the same year. Meanwhile, the unprecedented competition within Chinese banks and between Chinese domestic banks and foreign banks has become increasingly fierce since the opening of financial markets. To participate in the ongoing competitive

challenges all over the world, it is of vital importance for Chinese banks to pay special attention to their operation performances [1, 3, 4]. In addition, it is also an inherent requirement of guaranteeing and promoting the healthy and sustainable economic development of China to address the banking performance.

Among the family of existing performance evaluation methods, data envelopment analysis (DEA) is one of the major approaches because of its general applicability [5–10]. DEA, first introduced by Charnes et al. [11] and further extended by Banker et al. [12], is a data analytics approach that can be used for evaluating the relative performances of a group of homogeneous decision-making units (DMUs), which in practice consume multiple inputs to gain multiple outputs. The basic logic behind the DEA methodology is that it compares DMUs' real activity levels relative to the ideal status by projecting their actual input-output bundle onto the production frontier. To obtain the production frontier, all DMUs' observed inputs and outputs are used to construct a production possibility set (PPS) with a set of certain

axiomatic hypothesis, while the production frontier is an envelopment of the production possibility set. The DEA methodology has many apparent characteristics/advantages, and since its inception work in Charnes et al. [11], DEA has been applied to many kinds of activities in various different contexts [13–16]. In addition, the DEA methodology has also proven to be a powerful and preferable method for performance evaluation in the banking industry and has been frequently applied to this industry [2–4, 17].

The conventional DEA methods allow each DMU to generate a set of relative weights to maximize its ratio efficiency of aggregated weighted outputs to aggregated weighted inputs while ensuring that the same ratio is no more than one for all DMUs, and the maximum ratio is considered the performance index for the evaluated DMU [18, 19]. The weight determination is critical to performance evaluation results, but there are some significant concerns that reduce the applicability of DEA-based performance analytics and applications [20, 21]. On the one hand, each DMU selects its most favorable set of weights to maximize its efficiency ratio, and thus, the efficiency score of each DMU might be too optimistic or even impossible due to the unrealistic set of weights. On the other hand, each DMU selects its set of weights separately, and as a result, their performance scores are obtained under different standards and thus are not comparable.

Many studies have been proposed for more reasonable performance analytics by focusing on the selection of feasible weights. Cook et al. [22] and Roll et al. [23] suggest a common set of weights method that attempts to find a common set of weights, and the performance assessment is implemented using that common set of weights. Cook and Kress [24] also address the common set of weights by minimizing the gap of upper and lower bounds of weights. Kao and Hung [25] suggest generating a common set of weights by minimizing the sum of squared difference between the possible efficiency scores for the common set of weights and the CCR efficiency score across all DMUs. Similar studies can also be found in Liu & Peng [26], Kao [27], Zohrehbandian et al. [28], Ramazani-Tarkhorani et al. [29], Shabani et al. [30], Li et al. [31], and Li et al. [32]. Although the common set of weights method can provide a common evaluation standard for all DMUs, its major problem is that it still considers only one possibility for weights upon which the performance is estimated. Moreover, the determination of the common set of weights is still a big problem that will affect the performance analytics results relative to different common sets of weights, and a consensus regarding this has not been reached thus far.

Another research stream focuses on the cross-efficiency method, in which each DMU selects a set of common weights and then the set of common weights is used to evaluate each DMU [33]. It is notable that the classic DEA approach evaluates each DMU's relative efficiency using its favorable set of weights [18, 34], while the cross-efficiency method requires that each DMU's favorable set of weights be used to evaluate itself as well as the other DMUs' relative efficiency. As a result, several sets of weights are used to measure the relative performance, which is a great

improvement relative to classic DEA approaches considering only one set of weights. Furthermore, each DMU will have a maximal efficiency score based on self-appraisal and several smaller efficiency scores based on peer appraisal. The ultimate cross-efficiency score can be aggregated with these self-appraisal and peer appraisal scores for each individual DMU [35–41]. The DEA cross-efficiency method has some preferable characteristics, such as satisfied discrimination power between good and poor performances [42], a full ranking of all DMUs [43], and more realistic weights attached to various inputs and outputs [44]. The literature has witnessed numerous studies on various cross-efficiency evaluation approaches for many kinds of real applications [45–47]. Although the cross-efficiency method considers several sets of weights to measure the performance, it is insufficient to involve all performance possibilities. Moreover, the determination of nonunique weights from each DMU's perspective will also reduce the applicability of cross-efficiency methods, as does the aggregation of individual cross-efficiencies [41, 48–50].

The recent research by Salo and Punkka [21] suggests developing ratio-based efficiency analysis over all sets of feasible weights. Salo and Punkka [21] build ranking intervals, dominance relations, and efficiency bounds to show how the DMUs' efficiency ratios relate to each other for all sets of feasible weights rather than for some sets of weights that are typically used in classic DEA studies. More specifically, Tang et al. [51] propose a novel efficiency probability dominance model and develop the dominance efficiency probability over all sets of feasible weights, but their approach is based on a radial model under the constant returns to scale (CRS) assumption, and only traditional desirable outputs are considered by ignoring undesirable outputs. Shi [52] extends the Salo and Punkka [21] model over sets of all feasible weights to a more common and practical case considering the internal two-stage production structure. The proposed approach calculates each DMU's efficiency bounds for the overall system as well as the efficiency bounds for each subsystem. Li et al. [53] build the efficiency ranking interval for two-stage production systems and calculate each DMU's ranking interval for the overall system, as well as for each substage. Li et al. [54] propose a fixed cost allocation approach based on the efficiency ranking concept, which addresses the performance and efficiency ranking interval by considering all relative weights. It is of vital significance to consider all sets of feasible weights because doing so can address all possibilities from a data analytics perspective and provide evaluation results that are more logical and fairer.

In this paper, we will develop a dominance probability approach with undesirable outputs to assess the ratio performance based on DEA models, and the proposed approach is illustrated with Chinese listed banks. From a data-driven analytics perspective, we will consider all sets of feasible weights that are used for estimating the ratio performance. Towards that purpose, we first build a performance evaluation model to address the banking activities in the classic DEA framework by considering only a set of optimal weights. Since banking operations inevitably yield some

undesirable by-products, such as bad debts that are jointly produced with incomes, an extended eco-inefficiency model is developed. Furthermore, the eco-inefficiency model is used to develop the pair dominance structure taking all sets of weights into account based on Tang et al. [51]. The performance dominance probability is proposed to calculate the average probability of a certain DMU's performance dominating all DMUs. A larger performance dominance probability indicates that it is easier for that DMU to dominate all other DMUs, implying that its inefficiency score is more likely to be smaller than that of other DMUs in the sense of data-driven analytics. Finally, the proposed approach is applied to a four-year dataset of 32 Chinese listed banks, and the empirical results show that (1) the inefficiency dominance probability is largely different from inefficiency scores; (2) these state-owned commercial banks are more likely to have a better dominance performance, while local rural commercial banks might have very promising inefficiency performances in some extreme situations but are likely to have poor performance in the sense of inefficiency dominance probability; and (3) China Construction Bank, Industrial and Commercial Bank of China, and Industrial Bank are the top three listed banks based on operations analytics, and on the contrary, Suzhou Rural Commercial Bank, Rural Commercial Bank of Zhangjiagang, and Jiangyin Rural Commercial Bank are the lowest three banks with inefficiency dominance probability. This paper contributes to the literature in at least the following aspects. First, this paper extends a new approach in the DEA framework by taking all sets of feasible weights into account, whereas previous studies have considered only one or several sets of weights. Second, this paper establishes a pairwise performance dominance concept, which can help decision-makers analyze the performance relation in any context with price information (i.e., weights or multipliers). Third, this paper analyzes the performance of Chinese listed banks and provides some empirical findings, which can facilitate the banking industries in China.

The remainder of this paper is organized as follows. Section 2 develops the mathematical methodology of an extended eco-inefficiency model with undesirable outputs and performance dominance structure using inefficiency scores. Afterwards, the proposed approach is used to study the empirical performance analytics of 32 listed banks in Section 3. Finally, Section 4 concludes and summarizes this paper.

2. Mathematical Modeling

We first propose an extended eco-inefficiency model to address banking activities and possible relative performances in Section 2.1. Furthermore, we build a performance dominance structure considering all sets of feasible weights in Section 2.2.

2.1. An Extended Eco-Inefficiency Model. Suppose a set of n peer banks, with each bank using m inputs for the sake of

producing s traditional desirable outputs as well as q undesirable outputs, such as bad debt in the illustrative application. A bad debt or nonperforming loan is a jointly produced and unavoidable by-product in the banking industry. Without loss of generality, we consider each bank as a homogeneous decision-making unit (DMU) in the DEA framework. Furthermore, $DMU_j (j = 1, \dots, n)$ consume inputs $X_j = (x_{1j}, \dots, x_{mj})$ to produce desirable outputs $Y_j = (y_{1j}, \dots, y_{sj})$ and undesirable outputs $B_j = (b_{1j}, \dots, b_{qj})$, respectively. Before constructing the modeling, a core task is to identify appropriate methods to handle undesirable outputs. It is clear that the strong and weak disposability assumption of undesirable outputs and desirable outputs are the two most common and natural methods in the literature [55–57]. A significant feature between the strong and weak disposability assumption is whether undesirable outputs can be produced without damage or subsequent cost to desirable outputs [58]. If undesirable outputs can be freely generated without damage or subsequent cost, implying that both inputs and outputs can change unilaterally without compromising each other, then undesirable outputs are assumed to be strongly disposable. In contrast, if the production of undesirable outputs indeed has some damage or subsequent cost to inputs or desirable outputs, implying that a reduction in undesirable outputs would result in a reduction of desirable outputs simultaneously [59, 60], then undesirable outputs are assumed to be weakly disposable. Here, we consider the weak disposability assumption because it is more suitable for the real world and, more specifically, for the empirical application of banking operations, where it is very difficult to freely reduce bad debts without affecting incomes and changing banking operations. To this end, the production possibility set (PPS) under the variable returns to scale (VRS) assumption can be formulated as follows:

$$PPS = \left\{ (x_i, y_r, b_p) \left| \begin{array}{l} \sum_{j=1}^n \lambda_j x_{ij} \leq x_i, \quad i = 1, \dots, m \\ \rho_j \sum_{j=1}^n \lambda_j y_{rj} \geq y_r, \quad r = 1, \dots, s \\ \rho_j \sum_{j=1}^n \lambda_j b_{pj} = b_p, \quad p = 1, \dots, q \\ \sum_{j=1}^n \lambda_j = 1 \\ 0 \leq \rho_j \leq 1, \lambda_j \geq 0, \quad j = 1, \dots, n \end{array} \right. \right\}. \quad (1)$$

The above formula is nonlinear since both the reduction factor ρ_j and intensity variable λ_j are unknown. Furthermore, we can equivalently change formula (1) into a linear version, which is presented in the following formula:

$$PPS = \left\{ (x_i, y_r, b_p) \left| \begin{array}{l} \sum_{j=1}^n (\lambda_j + \eta_j) x_{ij} \leq x_i, \quad i = 1, \dots, m \\ \sum_{j=1}^n \lambda_j y_{rj} \geq y_r, \quad r = 1, \dots, s \\ \sum_{j=1}^n \lambda_j b_{pj} = b_p, \quad p = 1, \dots, q \\ \sum_{j=1}^n (\lambda_j + \eta_j) = 1, \quad \lambda_j, \eta_j \geq 0, \quad j = 1, \dots, n \end{array} \right. \right\}. \quad (2)$$

Based on formula (2), both desirable and undesirable outputs are weighted by nondisposed intensity variables λ_j , whereas the inputs are weighted by the sum of nondisposed intensity variables λ_j and disposed intensity variables η_j . In addition, the VRS assumption is ensured by summing the total nondisposed intensity variables λ_j and disposed intensity variables η_j to 1, i.e., $\sum_{j=1}^n (\lambda_j + \eta_j) = 1$.

Based on the above PPS in formula (2), we can build mathematical models to compute the relative performance of DMUs. In this paper, we follow the practice of Chen and Delmas [58] to develop an extended eco-inefficiency model for performance evaluation since the eco-inefficiency model has some advantages in modeling activities with undesirable outputs compared with four well-established models in the literature (undesirable outputs as inputs, transformation of undesirable outputs, directional distance function, and hyperbolic efficiency model. Readers can refer Chen and Delmas [58] for details on the comparison). The extended eco-inefficiency model is formulated as follows:

$$\begin{aligned}
 inE_d^* = \text{Max} \quad & \frac{\sum_{i=1}^m g_i^x / x_{id} + \sum_{r=1}^s g_r^y / y_{rd} + \sum_{p=1}^q g_p^b / b_{pd}}{m + s + q} \\
 \text{s.t.} \quad & \sum_{j=1}^n (\lambda_j + \eta_j) x_{ij} \leq x_{id} - g_i^m, \quad i = 1, \dots, m \\
 & \sum_{j=1}^n \lambda_j y_{rj} \geq y_{rd} + g_r^y, \quad r = 1, \dots, s \\
 & \sum_{j=1}^n \lambda_j b_{pj} = b_{pd} - g_p^b, \quad p = 1, \dots, q \\
 & \sum_{j=1}^n (\lambda_j + \eta_j) = 1 \\
 & \lambda_j, \eta_j, g_i^m, g_r^y, g_p^b \geq 0, \quad j = 1, \dots, n; \\
 & r = 1, \dots, s; p = 1, \dots, q.
 \end{aligned} \tag{3}$$

In model (3), the variables g_i^x , g_r^y , and g_p^b represent the amount of potential improvements in inputs, desirable outputs, and undesirable outputs, respectively, that the evaluated DMU can make relative to its current input usage and output production to reach its ideal benchmark target on the efficiency frontier. The potential improvements reflect input reduction potentials and desirable output expansion potentials (or undesirable output reduction potentials) instead of actual input usage and output production [61, 62]. Model (3) uses a slack-based formula that is similar to the directional distance function (DDF) model to maximize the average additive inefficiency index across all input and output measures, where the inefficiency index represents potential improvements divided by observed inputs or outputs. More specifically, the optimal direction vector of model (3) can be endogenously obtained in a similar way as that of Arabi et al. [63]. For that purpose, suppose

$g_i^x = \beta \cdot \bar{g}_i$, $g_r^y = \beta \cdot \bar{g}_r$, and $g_p^b = \beta \cdot \bar{g}_p$, where the direction vector is $\mathbf{g} = (\bar{g}_i, \bar{g}_r, \bar{g}_p)$. Solving model (3) determines an optimal solution $(g_i^{x*}, g_r^{y*}, g_p^{b*})$, then we have $\beta = (g_i^{x*} / \bar{g}_i) = (g_r^{y*} / \bar{g}_r) = (g_p^{b*} / \bar{g}_p)$ ($i = 1, \dots, m; r = 1, \dots, s; p = 1, \dots, q$). Hence, we have a system of $(m + s + q + 1)$ unknown variables $(\beta, \bar{g}_i, \bar{g}_r, \bar{g}_p)$ and $(m + s + q)$ linearly independent equations $g_1^{x*} \bar{g}_2 = g_2^{x*} \bar{g}_1, \dots, g_m^{x*} \bar{g}_1 = g_1^{x*} \bar{g}_m$, $g_1^{y*} \bar{g}_2 = g_2^{y*} \bar{g}_1, \dots, g_s^{y*} \bar{g}_1 = g_1^{y*} \bar{g}_s$, $g_1^{b*} \bar{g}_2 = g_2^{b*} \bar{g}_1, \dots, g_{q-1}^{b*} \bar{g}_q = g_q^{b*} \bar{g}_{q-1}$, and $g_q^{b*} = \beta \cdot \bar{g}_q$. Together with another equation such as $\sum_{i=1}^m \bar{g}_i + \sum_{r=1}^s \bar{g}_r + \sum_{p=1}^q \bar{g}_p = 1$ that is used to ensure a bounded and closed space, we then have a system of $(m + s + q + 1)$ unknown variables and $(m + s + q + 1)$ linearly independent equations. Therefore, this system has a unique solution and we can obtain a unique optimal direction.

Model (3) is slightly different from that of Chen and Delmas [58] in several aspects: first, we also take the input improvement into account, while Chen and Delmas [58] studied only the output improvement; secondly, we assume the weak disposability assumption of desirable outputs and undesirable outputs, while the strong disposability assumption was modeled in Chen and Delmas [58]. In addition, the VRS assumption is considered in model (3) such that it is more suitable for real applications. Since the individual inefficiency index theoretically has a value ranging from zero to unity for inputs and undesirable outputs and a value from zero to infinity for desirable outputs, the overall average inefficiency of DMU_d also takes a value from zero to infinity. The larger the average inefficiency index is, the more inefficient the evaluated DMU is. An average inefficiency index of zero value means that the considered DMU is on the efficiency frontier and has no slack for improvement, and hence, the DMU is efficient.

Furthermore, model (4) is a dual formulation of the above model (3) in its multiplier formulation:

$$\begin{aligned}
 inE_d^* = \text{Min} \quad & \sum_{i=1}^m v_i x_{id} - \sum_{r=1}^s u_r y_{rd} + \sum_{p=1}^q w_p b_{pd} + u_0 \\
 \text{s.t.} \quad & \sum_{i=1}^m v_i x_{ij} - \sum_{r=1}^s u_r y_{rj} + \sum_{p=1}^q w_p b_{pj} + u_0 \geq 0, \\
 & j = 1, \dots, n \\
 & \sum_{i=1}^m v_i x_{ij} + u_0 \geq 0, \quad j = 1, \dots, n \\
 & v_i \geq 1 / (m + s + q) x_{id}, \quad i = 1, \dots, m \\
 & u_r \geq 1 / (m + s + q) y_{rd}, \quad r = 1, \dots, s \\
 & w_p \geq 1 / (m + s + q) b_{pd}, \quad p = 1, \dots, q \\
 & v_i, u_r \geq 0, i = 1, \dots, m; r = 1, \dots, s; \\
 & w_p, u_0 \text{ are free}, p = 1, \dots, q.
 \end{aligned} \tag{4}$$

Model (4) computes the inefficient component (i.e., the difference between aggregated inputs and aggregated outputs) for the evaluated DMU, yet the inefficient component is nonnegative for all DMUs, and some constraints on

multipliers are held. Solving model (4) for each DMU_{*d*} (*d* = 1, . . . , *n*) determines a series of inefficiency scores inE_d^* using a series of optimal solutions $(u_r^{d*}, v_i^{d*}, w_p^{d*}, u_0^{d*})$. The inefficiency score can be used for a performance indicator among all DMUs, and the smaller the inefficiency score is, the better the performance of DMU_{*d*} is.

2.2. Dominance Probability Based on Inefficiency Scores.

It is notable that the inefficiency score inE_d^* obtained previously can be used to analyze the performance of Chinese listed banks, but there are two main concerns. On the one hand, it is calculated by only considering the optimal weight plan $(u_r^{d*}, v_i^{d*}, w_p^{d*}, u_0^{d*})$ while ignoring any other feasible weights, and thus, the obtained inefficiency score inE_d^* might be too extreme or even unrealistic. On the other hand, the inefficiency score inE_d^* is calculated separately for each DMU_{*d*} (*d* = 1, . . . , *n*), and different weights will be preferred by different DMUs; thus, the results are not completely comparable.

Since the resulting inefficiency indexes can change relative to different sets of weights, it is important to explore the performance associated with all sets of feasible input/output weights. To this end, we focus on the efficiency dominance concept of Salo and Punkka [21]. As well defined and discussed in Salo and Punkka [21] and Tang et al. [51], the dominance relation is determined through a pairwise efficiency comparison among DMUs. Furthermore, a certain DMU dominates another DMU if and only if its efficiency score is as large as that of the other for all sets of feasible input/output weights and is larger for at least some sets of feasible input/output weights. Here, we follow the same idea of Salo and Punkka [21] and Tang et al. [51] to determine the dominance relation of Chinese listed banks. For comparison, we take inevitable undesirable outputs in banking operations, such as bad debts, into account. Furthermore, we follow Chen and Delmas [58] in focusing on eco-inefficiency scores rather than efficiency scores through a nonradial directional distance function model. To this end, we first build the inefficiency dominance concept as follows.

Definition 1. DMU_{*d*} dominates DMU_{*k*} (denoted as $DMU_d \succ DMU_k$) if and only if DMU_{*d*} always has a smaller inefficiency score relative to DMU_{*k*} for all sets of feasible input and output weights.

The dominance relation based on inefficiency scores is determined if the inefficiency score for a certain DMU_{*d*} is as small as that of DMU_{*k*} for all sets of feasible input/output weights and is smaller for at least some sets of feasible input/output weights. The dominance relation between DMU_{*d*} and DMU_{*k*} is determined through their inefficiency comparison. By rethinking the idea of model (3) and model (4), which calculate the maximal inefficiency score, we can formulate model (5) to calculate the inefficiency range of DMU_{*d*} when DMU_{*k*} is fixed with a prespecified inefficiency level of zero by requiring the constraint that $inE_k = \sum_{i=1}^m v_i x_{ik} - \sum_{r=1}^s u_r y_{rk} + \sum_{p=1}^q w_p b_{pk} + u_0 = 0$. In fact, the inefficiency level of DMU_{*k*} can be set to any nonnegative value *M*, and by substituting u_0 with $u_0 - M$, we can get the same dominance

probability as given in Definition 2 and Definition 3; hence, we immediately set the inefficiency level of DMU_{*k*} to zero for simplification in the following model:

$$\begin{aligned} \frac{inE_{dk}^{\max}}{inE_{dk}^{\min}} &= \frac{\text{Min} \sum_{i=1}^m v_i x_{id} - \sum_{r=1}^s u_r y_{rd} + \sum_{p=1}^q w_p b_{pd} + u_0}{\text{Max} \sum_{i=1}^m v_i x_{id} - \sum_{r=1}^s u_r y_{rd} + \sum_{p=1}^q w_p b_{pd} + u_0} \\ \text{s.t.} \quad &\sum_{i=1}^m v_i + \sum_{r=1}^s u_r + \sum_{p=1}^q w_p = 1 \\ &\sum_{i=1}^m v_i x_{ik} - \sum_{r=1}^s u_r y_{rk} + \sum_{p=1}^q w_p b_{pk} + u_0 = 0 \\ &\sum_{i=1}^m v_i x_{ij} + u_0 \geq 0, \quad j = d, k \\ &v_i \geq \frac{1}{(m+s+q)x_{id}}, \quad i = 1, \dots, m \\ &u_r \geq \frac{1}{(m+s+q)y_{rd}}, \quad r = 1, \dots, s \\ &w_p \geq \frac{1}{(m+s+q)b_{pd}}, \quad p = 1, \dots, q \\ &v_i, u_r \geq 0, i = 1, \dots, m; r = 1, \dots, s; \\ &w_p, u_0 \text{ are free, } p = 1, \dots, q. \end{aligned} \tag{5}$$

An additional constraint that $\sum_{i=1}^m v_i + \sum_{r=1}^s u_r + \sum_{p=1}^q w_p = 1$ is inserted into model (5) to make the feasible weight space closed and bounded. The optimal objective function for model (5) shows the lower and upper bounds on how much different DMU_{*d*}'s inefficiency score can be relative to DMU_{*k*} across all sets of feasible input/output weights. Using model (5), the dominance structure can be determined for any pairwise DMUs. More specifically, if the inefficiency level of DMU_{*k*} is fixed to zero and if $inE_{dk}^{\max} < 0$, which means that DMU_{*d*} will always have a smaller inefficiency score compared with DMU_{*k*}, then DMU_{*d*} dominates DMU_{*k*}. In contrast, if $inE_{dk}^{\min} > 0$, which means that DMU_{*d*} will always have a larger inefficiency score than DMU_{*k*} (which has an inefficiency level of zero), then DMU_{*d*} is dominated by DMU_{*k*}. For more general cases, however, we cannot obtain the complete dominance relation, which is usually true in practice. Therefore, we propose determining the performance dominance probability. To this end, we follow the work of Tang et al. [51] in building the inefficiency dominance probability concept, as given in Definition 2.

Definition 2. When DMU_{*k*} has an inefficiency score of inE_k , the probability that DMU_{*d*} dominates DMU_{*k*} over all sets of feasible input and output weights is calculated by $P_{d \succ k} = (inE_k - inE_{dk}^{\min}) / (inE_{dk}^{\max} - inE_{dk}^{\min})$.

It is clear that, if $inE_k \leq inE_{dk}^{\min}$, which means that DMU_{*d*} will always have a larger inefficiency by remaining the inefficiency inE_k for DMU_{*k*}, the inefficiency dominance

probability of DMU_d relative to DMU_k would take a nonpositive value. That is, it is impossible for DMU_d to dominate DMU_k . For the sake of a bounded range, we assume that $P_{\bar{d}>k} = 0$ if $inE_k \leq inE_{\bar{d}k}^{\min}$. For a more general case in which $inE_{\bar{d}k}^{\min} \leq inE_k \leq inE_{\bar{d}k}^{\max}$, the probability that DMU_d dominates DMU_k takes a value from zero to unity. A larger value of $P_{\bar{d}>k}$ means that it is more likely for DMU_d to have a smaller inefficiency score compared with DMU_k over all sets of feasible input/output weights.

Note in addition that Definition 2 fixes the inefficiency level of DMU_k to calculate the inefficiency range of DMU_d and further computes the inefficiency dominance probability of DMU_d relative to DMU_k . In contrast, we can also compute the inefficiency dominance probability of DMU_d relative to DMU_k by fixing the inefficiency level of DMU_d and calculating the inefficiency range of DMU_k . The above idea is formulated in model (6), which is very similar to model (5) but substitutes DMU_k for DMU_d :

$$\begin{aligned} \frac{inE_{\bar{d}k}^{\max}}{inE_{\bar{d}k}^{\min}} &= \frac{\text{Min} \sum_{i=1}^m v_i x_{ik} - \sum_{r=1}^s u_r y_{rk} + \sum_{p=1}^q w_p b_{pk} + u_0}{\text{Max} \sum_{i=1}^m v_i x_{ik} - \sum_{r=1}^s u_r y_{rk} + \sum_{p=1}^q w_p b_{pk} + u_0} \\ \text{s.t.} \quad &\sum_{i=1}^m v_i + \sum_{r=1}^s u_r + \sum_{p=1}^q w_p = 1 \\ &\sum_{i=1}^m v_i x_{id} - \sum_{r=1}^s u_r y_{rd} + \sum_{p=1}^q w_p b_{pd} + u_0 = 0 \\ &\sum_{i=1}^m v_i x_{ij} + u_0 \geq 0, \quad j = d, k \\ &v_i \geq \frac{1}{(m+s+q)x_{ik}}, \quad i = 1, \dots, m \\ &u_r \geq \frac{1}{(m+s+q)y_{rk}}, \quad r = 1, \dots, s \\ &w_p \geq \frac{1}{(m+s+q)b_{pk}}, \quad p = 1, \dots, q \\ &v_i, u_r \geq 0, i = 1, \dots, m; r = 1, \dots, s; \\ &w_p, u_0 \text{ are free, } p = 1, \dots, q. \end{aligned} \quad (6)$$

An alternative inefficiency dominance probability of DMU_d relative to DMU_k by fixing the inefficiency level of DMU_d is given in Definition 3.

Definition 3. When DMU_d has an inefficiency score of inE_d , the probability that DMU_d dominates DMU_k over all sets of feasible input and output weights is calculated by $P_{d>k} = (inE_{\bar{d}k}^{\max} - inE_d / inE_{\bar{d}k}^{\max} - inE_{\bar{d}k}^{\min})$.

Furthermore, the overall probability that the inefficiency score of DMU_d dominates that of DMU_k is the average of the two probabilities by fixing the inefficiency level of DMU_d and DMU_k . More specifically, Definition 4 gives the pairwise

performance dominance probability with regard to inefficiency scores.

Definition 4. The pairwise performance dominance probability of DMU_d relative to DMU_k over all sets of feasible input and output weights is $P_{d>k} = ((P_{\bar{d}>k} + P_{d>\bar{k}})/2)$.

The classic DEA methods allow each DMU to generate a set of relative weights to maximize its ratio of aggregated weighted outputs to aggregated weighted inputs while ensuring that the same ratio is no more than one for all DMUs, and the maximum ratio is considered the efficiency score for the evaluated DMU. By taking all sets of feasible weights and the inefficiency dominance structure into account, the overall inefficiency dominance probability for a certain DMU_d among all DMUs can be calculated by the average of pair inefficiency dominance probabilities across all DMUs. The above idea is given in Definition 5.

Definition 5. The performance dominance probability of DMU_d across all DMUs over all sets of feasible input and output weights is $P_d = \sum_{k=1}^n P_{d>k} / n$.

The classic DEA approaches use deterministic (in)efficiency scores to measure the relative performance, while the performance dominance probability is an alternative performance indicator from a data analytics perspective that considers all sets of feasible weights that are stochastic to determine the relative performance. It is rather remarkable that different sets of weights will cause different performance measures, and the performance dominance probability involves all possibilities over all sets of feasible input and output weights. The performance dominance probability of DMU_d calculates the probability of its performance dominating the set of all DMUs. A larger performance dominance probability indicates that it is much easier for that DMU to dominate other DMUs, implying that its inefficiency score is more likely to be smaller than that of other DMUs.

3. Illustrative Application of Chinese Listed Banks

In this section, we illustrate the proposed approach using empirical performance analytics for 32 Chinese listed banks. Since the proposed approach considers all sets of feasible weights, the performance relations and ratio index results are more comprehensive and reasonable.

3.1. Data Description. This section addresses the performance of listed banks in China. For simplification and research purposes, we consider only those banks that have been registered in China and that are listed in the mainland of China. More specifically, only banks that are owned by Chinese organizations and are listed on the Shenzhen Stock Exchange and Shanghai Stock Exchange are collected. In contrast, neither Chinese banks listed on other stock exchanges nor foreign banks listed on the Shenzhen Stock Exchange and Shanghai Stock Exchange are involved in this study. As a result, we have 32 listed banks. For the research

purpose, we give these 32 banks and their corresponding codes in Table 1.

In practice, each bank will consume multiple inputs to generate multiple outputs and more specifically mainly for profits. In this study, we follow similar studies such as Wang et al. [4], Zha et al. [1], Fukuyama and Matousek [64], Li et al. [65], and Zhu et al. [2] in taking employment referring to human resource investment and manpower, fixed asset referring to the asset value of physical capital that can be used for business activities, and operation cost as three inputs. Note in addition that the operation cost in this study excludes the expense of labor input that occurs in banking operations because the employment has already taken the labor input into account. Furthermore, we consider three different outputs generated in banking operations, with interest income and noninterest income being two desirable outputs and nonperforming bad loan percentage in the current year as an undesirable output. The interest income is derived directly from the gap between the interest paid on deposits and the interest earned from loans, while the noninterest income is primarily derived from commissions, securities investments, fees, and other business activity incomes. However, a bad loan is a jointly produced and unavoidable by-product that will greatly harm the bank. The inputs and outputs to be used in this study are summarized in Table 2.

Our empirical study contains operation data for 32 Chinese listed banks over the 2014–2018 period, accounting for 160 observations. All data for these listed banks were collected from official sources of bank annual reports and the financial reports of banks in China Stock Market Accounting Research (CSMAR) during 2014–2018. Table 3 shows the descriptive statistics of the inputs, desirable outputs, and undesirable outputs of these 160 observations. It can be found that both the average fixed asset and operation cost among the 32 listed banks are increasing year by year, but the average employment and bad debt percentage increased to a peak in 2016 and then decreased continuously. Furthermore, both interest income and noninterest income show an increasing trend but decreased in a year.

3.2. Result Analysis. To provide data analytics of bank performance, we first calculate the inefficiency scores using model (3) or model (4) in the nonradial DDF-based formulation under the VRS property. The inefficiencies of these 32 banks from 2014 to 2018 are given in Table 4. Since the inefficiency score represents potential improvements divided by the observed inputs or outputs, an inefficiency score of zero indicates that there will be no improvement potential. Table 4 shows that, by selecting the optimal set of weights to aggregate inputs and outputs, many listed banks will be extremely efficient without improvement potentials. There are always ten banks that have an inefficiency score larger than zero, but the average inefficiency score across these 32 listed banks fluctuates according to the year. Since the VRS analysis is adopted in this study, we may not draw any significant conclusion as to inefficiency changes year by year. Furthermore, some banks (DMU₆, Bank of Guiyang;

TABLE 1: Codes for 32 Chinese listed banks.

DMUs	Banks	Abbreviation
DMU ₁	Bank of Beijing	BOB
DMU ₂	Changshu Rural Commercial Bank	CRCB
DMU ₃	Bank of Chengdu	BCD
DMU ₄	Industrial and Commercial Bank of China	ICBC
DMU ₅	China Everbright Bank	CEB
DMU ₆	Bank of Guiyang	BOG
DMU ₇	Bank of Hangzhou	BOH
DMU ₈	Huaxia Bank	HB
DMU ₉	China Construction Bank	CCB
DMU ₁₀	Bank of Jiangsu	BOJ
DMU ₁₁	Jiangyin Rural Commercial Bank	JRCB
DMU ₁₂	Bank of Communications	BC
DMU ₁₃	China Minsheng Bank	CMSB
DMU ₁₄	Bank of Nanjing	BON
DMU ₁₅	Bank of Ningbo	BN
DMU ₁₆	Agricultural Bank of China	ABC
DMU ₁₇	Ping An Bank	PB
DMU ₁₈	Shanghai Pudong Development Bank	SPDB
DMU ₁₉	Bank of Qingdao	BOQ
DMU ₂₀	Qingdao Rural Commercial Bank	QRCB
DMU ₂₁	Bank of Shanghai	BOS
DMU ₂₂	Suzhou Rural Commercial Bank	SRCB
DMU ₂₃	Wuxi Rural Commercial Bank	WRCB
DMU ₂₄	Bank of Xian	BOX
DMU ₂₅	Industrial Bank	IB
DMU ₂₆	Rural Commercial Bank of Zhangjiagang	RCBZ
DMU ₂₇	Bank of Changsha	BCS
DMU ₂₈	China Merchants Bank	CMB
DMU ₂₉	Bank of Zhengzhou	BOZ
DMU ₃₀	Bank of China	BOC
DMU ₃₁	China CITIC Bank	CCB
DMU ₃₂	Zijin Rural Commercial Bank	ZRCB

TABLE 2: Input and output variables.

Input/output	Variable	Notation	Unit
Inputs	Employment	x_1	Person count
	Fixed assets	x_2	Million yuan
	Operation costs	x_3	Million yuan
Desirable outputs	Interest income	y_1	Million yuan
	Noninterest income	y_2	Million yuan
Undesirable outputs	Bad debt percentage	z_1	Percentage

DMU₈, Huaxia Bank; DMU₁₅, Bank of Ningbo; and DMU₃₂, Zijin Rural Commercial Bank) will always have a nonzero inefficiency, meaning that these banks always show very terrible performance compared with banks that have a zero-value inefficiency index.

Since the previous inefficiency scores are separately derived by considering only one optimal set of weights, the resulting performance information might be unrealistic and unreasonable. Therefore, we can use the proposed eco-inefficiency dominance probability approach in this paper to analyze the banking performance considering all sets of feasible weights. To this end, we first use model (5) to

TABLE 3: Descriptive statistics for input-output measures.

Year	Statistics	x_1	x_2	x_3	y_1	y_2	z_1
2014	Max	493583	196238	271132	849879	165370	2.7100
	Min	1089	412.01	1151.41	3533.90	109.48	0.7500
	Mean	67582	28499.15	48231.62	154112.69	25685.99	1.2531
	SD	135316	55898.04	78151.35	235785.69	44163.22	0.4237
2015	Max	503082	221502	306395	871779	189780	2.3900
	Min	1180	418.04	1245.26	3486.11	130.69	0.8300
	Mean	69772	31335.97	57387.23	162109.41	30344.05	1.5308
	SD	136444	60262.26	87459.17	243294.78	49419.92	0.4226
2016	Max	496698	243619	282712	791480	204045	2.4100
	Min	1352	413.99	1235.88	3268.89	162.62	0.8700
	Mean	70266	34778.86	58285.96	151790.21	35560.52	1.6013
	SD	134489	65118.10	85168.72	220693.57	57189.80	0.3678
2017	Max	487307	245687	331518	861594	204424	2.3900
	Min	1426	462.93	1260.89	3789.14	166.05	0.8200
	Mean	69782	36383.26	60079.96	166927.92	35168.24	1.5431
	SD	132071	66621.76	91681.04	239463.71	53045.31	0.3240
2018	Max	473691	253525	368966	948094	201271	2.4700
	Min	1454	418.08	1733.55	4567.00	203.17	0.7800
	Mean	69354	38380.34	67444.02	183050.26	39183.08	1.5034
	SD	129697	70061.74	100964.72	261751.20	55000.40	0.3382

TABLE 4: Inefficiency scores of 32 listed banks from 2014 to 2018.

Banks	2014	2015	2016	2017	2018
DMU ₁	0.0000	0.0000	0.0000	0.0000	0.0000
DMU ₂	0.0000	0.3483	0.6442	0.5430	0.3483
DMU ₃	0.0000	0.0979	0.2730	0.0000	0.0979
DMU ₄	0.0000	0.0000	0.0000	0.0000	0.0000
DMU ₅	0.0000	0.0590	0.0000	0.1087	0.0590
DMU ₆	0.2345	0.3469	0.3273	0.5898	0.3469
DMU ₇	0.1798	0.0000	0.0000	0.0000	0.0000
DMU ₈	0.2880	0.3059	0.2288	0.2768	0.3059
DMU ₉	0.0000	0.0000	0.0000	0.0000	0.0000
DMU ₁₀	0.0000	0.0000	0.0000	0.0000	0.0000
DMU ₁₁	0.0000	0.0000	0.0000	0.0000	0.0000
DMU ₁₂	0.1449	0.0000	0.0000	0.0000	0.0000
DMU ₁₃	0.0000	0.0000	0.0000	0.0000	0.0000
DMU ₁₄	0.2088	0.1072	0.1415	0.0000	0.1072
DMU ₁₅	0.2793	0.2415	0.2018	0.2225	0.2415
DMU ₁₆	0.1926	0.0000	0.0000	0.0000	0.0000
DMU ₁₇	0.0000	0.0000	0.0000	0.0000	0.0000
DMU ₁₈	0.0567	0.0000	0.0000	0.0000	0.0000
DMU ₁₉	0.0000	0.0000	0.0827	0.0000	0.0000
DMU ₂₀	0.0000	0.0000	0.0000	0.0000	0.0000
DMU ₂₁	0.0000	0.0000	0.0000	0.0000	0.0000
DMU ₂₂	0.0000	0.0000	0.0000	0.2032	0.0000
DMU ₂₃	0.0000	0.0000	0.0000	0.0000	0.0000
DMU ₂₄	0.0000	0.0000	0.0000	0.0000	0.0000
DMU ₂₅	0.0000	0.0000	0.0000	0.0000	0.0000
DMU ₂₆	0.0000	0.0000	0.0000	0.0000	0.0000
DMU ₂₇	0.0000	0.2287	0.2670	0.6379	0.2287
DMU ₂₈	0.0000	0.0000	0.0000	0.0000	0.0000
DMU ₂₉	0.0000	0.0000	0.1373	0.0967	0.0000
DMU ₃₀	0.0000	0.0000	0.0000	0.0000	0.0000
DMU ₃₁	0.0634	0.0799	0.0000	0.0000	0.0799
DMU ₃₂	0.5982	0.2792	0.3526	0.5700	0.2792
Mean	0.0702	0.0655	0.0830	0.1015	0.0655

calculate the inefficiency score intervals and then use Definition 2 to calculate the first-level pairwise dominating probability in 2018. Since the pairwise dominating probability involves an $n \times n$ matrix that is hard to present in this paper, we arbitrarily take the Bank of Jiangsu (BOJ), Agricultural Bank of China (ABC), and Rural Commercial Bank of Zhangjiagang (RCBZ) for instance, and the first-level inefficiency dominating probability for these three banks across all 32 banks is listed in the second, third, and fourth columns of Table 5, namely, $P_{BOJ>k}^{\sim}$, $P_{ABC>k}^{\sim}$, and $P_{RCBZ>k}^{\sim}$ (it is also possible to consider any other banks as examples to show the calculation results). The results represent the probability of the considered bank having a smaller inefficiency index across any other bank, with different sets of weights being attached to inputs and outputs to ensure an efficient status for other banks. For example, the value of 0.2699 implies that, by fixing the inefficiency score of the Bank of Beijing (DMU_1) to zero, the inefficiency score of the Bank of Jiangsu will be smaller with a probability of 0.2699 and larger with a probability of 0.7301 ($1-0.2699$). At the same time, we can use model (6) and Definition 3 to calculate another dominating probability, and the second-level results of Bank of Jiangsu (BOJ), Agricultural Bank of China (ABC), and Rural Commercial Bank of Zhangjiagang (RCBZ) in 2018 are given in the last three columns of Table 5.

Without loss of generality, each DMU will always dominate itself, as these three banks will have a dominating probability of 1 to itself regardless of whether the first-level dominance probability or the second-level dominance probability is considered. From Table 5, we can find that all three banks have a larger second-level dominance probability than the first-level dominance probability to other banks, and it is indeed also held for all banks. This difference is due to the definition style of pairwise dominances, and we cannot arbitrarily use one dominating probability to represent the performance assessment with the other being ignored. By averaging the two pairwise dominating probabilities, we can calculate the pairwise dominance probability as well as the dominated probability. Reconsidering the three banks in Table 5, we show the pairwise dominance probability as well as dominated probability for Bank of Jiangsu, Agricultural Bank of China, and Rural Commercial Bank of Zhangjiagang in Table 6. Taking the inefficiency dominance probability of Bank of Jiangsu to Bank of Beijing (DMU_1), for example, the arithmetic mean of 0.2699 and 0.3515 by Definition 4 is exactly the pairwise inefficiency dominance probability of Bank of Jiangsu to Bank of Beijing, 0.3107. Since the pairwise dominance probability shows the probability of the inefficiency score of Bank of Jiangsu relative to any other banks, by considering all sets of feasible input and output weights, it means that the inefficiency score of Bank of Jiangsu is smaller than that of Bank of Beijing with a probability of 0.3107. In contrast, the inefficiency of Bank of Jiangsu will be dominated by Bank of Beijing with a probability of 0.6893.

Furthermore, by aggregating the pairwise inefficiency dominance probability across all banks, we can obtain the average performance dominance probability in terms of inefficiency scores for these three banks, as given in the last

TABLE 5: Two kinds of dominating probabilities for BOJ, ABC, and RCBZ in 2018.

Banks	Definition 2			Definition 3		
	BOJ	ABC	RCBZ	BOJ	ABC	RCBZ
DMU_1	0.2699	0.5964	0.0093	0.3515	0.9452	0.2111
DMU_2	0.8578	0.6238	0.2563	0.9850	0.9959	0.4689
DMU_3	0.8520	0.6207	0.0496	0.9662	0.9910	0.1966
DMU_4	0.0288	0.3164	0.0016	0.3339	0.3822	0.3216
DMU_5	0.1671	0.5897	0.0074	0.3446	0.9119	0.2663
DMU_6	0.8592	0.6197	0.0386	0.9599	0.9887	0.1905
DMU_7	0.8518	0.6159	0.0253	0.9337	0.9821	0.1961
DMU_8	0.3056	0.6073	0.0106	0.4337	0.9419	0.2603
DMU_9	0.0315	0.1127	0.0017	0.3121	0.1311	0.2989
DMU_{10}	1.0000	0.6052	0.0088	1.0000	0.9589	0.1523
DMU_{11}	0.8514	0.6230	0.3883	0.9915	0.9977	0.4059
DMU_{12}	0.0835	0.5315	0.0042	0.3563	0.7917	0.3073
DMU_{13}	0.1096	0.5695	0.0054	0.3154	0.8709	0.2684
DMU_{14}	0.8678	0.6123	0.0146	0.9135	0.9736	0.1657
DMU_{15}	0.9666	0.6173	0.0286	0.9704	0.9791	0.2599
DMU_{16}	0.0411	1.0000	0.0023	0.3948	1.0000	0.3768
DMU_{17}	0.2062	0.5856	0.0089	0.4109	0.9140	0.3081
DMU_{18}	0.0921	0.5531	0.0046	0.3014	0.8476	0.2634
DMU_{19}	0.8593	0.6219	0.0995	0.9780	0.9943	0.2510
DMU_{20}	0.8454	0.6226	0.1170	0.9772	0.9942	0.2986
DMU_{21}	0.5626	0.6048	0.0133	0.5695	0.9618	0.2139
DMU_{22}	0.8492	0.6230	0.2009	0.9916	0.9978	0.2256
DMU_{23}	0.8463	0.6225	0.1454	0.9886	0.9971	0.1876
DMU_{24}	0.8473	0.6222	0.0825	0.9808	0.9951	0.1796
DMU_{25}	0.0724	0.5560	0.0038	0.2395	0.8469	0.2161
DMU_{26}	0.8477	0.6232	1.0000	0.9912	0.9977	1.0000
DMU_{27}	0.8790	0.6204	0.0512	0.9669	0.9892	0.2431
DMU_{28}	0.1159	0.5628	0.0058	0.3840	0.8491	0.3310
DMU_{29}	0.8588	0.6202	0.0662	0.9644	0.9908	0.2669
DMU_{30}	0.0389	0.3718	0.0021	0.3274	0.4493	0.3107
DMU_{31}	0.1246	0.5690	0.0060	0.3564	0.8716	0.2997
DMU_{32}	0.8494	0.6222	0.1199	0.9848	0.9960	0.2093

column of Table 6. Furthermore, proceeding in the same manner as above, we can determine the inefficiency dominance probability for all 32 Chinese listed banks from 2014 to 2018, as shown in Table 7.

As Table 7 shows, these banks have very different inefficiency dominance probabilities over all sets of feasible weights relative to the inefficiency scores derived from only an optimal set of weights. For example, Huaxia Bank (DMU_8) always has a positive inefficiency in each year, and that bank will be ranked after most banks. However, Huaxia Bank will have an inefficiency dominance probability of 0.6105, 0.5885, 0.5749, 0.5640, and 0.5857 in the 2014–2018 period, respectively. This phenomenon implies that Huaxia Bank is more likely to have an inefficiency index smaller than that of half of all banks. In contrast, by considering only the optimal set of weights, the Rural Commercial Bank of Zhangjiagang (DMU_{26}) is extremely efficient with an inefficiency score of zero for all years, but it has a relatively small inefficiency dominance probability in each year (0.2405, 0.2264, 0.2289, 0.2039, and 0.1864, respectively), implying that the performance of Rural Commercial Bank of Zhangjiagang in the sense of inefficiency scores is at a disadvantage to other banks by addressing all weight possibilities.

TABLE 6: Pairwise dominance probability for BOJ, ABC, and RCBZ in 2018.

Banks	Dominating			Dominated		
	BOJ	ABC	RCBZ	BOJ	ABC	RCBZ
DMU ₁	0.3107	0.7708	0.1102	0.6893	0.2292	0.8898
DMU ₂	0.9214	0.8098	0.3626	0.0786	0.1902	0.6374
DMU ₃	0.9091	0.8058	0.1231	0.0909	0.1942	0.8769
DMU ₄	0.1813	0.3493	0.1616	0.8187	0.6507	0.8384
DMU ₅	0.2559	0.7508	0.1369	0.7441	0.2492	0.8631
DMU ₆	0.9096	0.8042	0.1145	0.0904	0.1958	0.8855
DMU ₇	0.8928	0.7990	0.1107	0.1072	0.2010	0.8893
DMU ₈	0.3696	0.7746	0.1354	0.6304	0.2254	0.8646
DMU ₉	0.1718	0.1219	0.1503	0.8282	0.8781	0.8497
DMU₁₀	1.0000	0.7820	0.0805	1.0000	0.2180	0.9195
DMU ₁₁	0.9214	0.8104	0.3971	0.0786	0.1896	0.6029
DMU ₁₂	0.2199	0.6616	0.1557	0.7801	0.3384	0.8443
DMU ₁₃	0.2125	0.7202	0.1369	0.7875	0.2798	0.8631
DMU ₁₄	0.8906	0.7929	0.0902	0.1094	0.2071	0.9098
DMU ₁₅	0.9685	0.7982	0.1442	0.0315	0.2018	0.8558
DMU₁₆	0.2180	1.0000	0.1895	0.7820	1.0000	0.8105
DMU ₁₇	0.3086	0.7498	0.1585	0.6914	0.2502	0.8415
DMU ₁₈	0.1968	0.7004	0.1340	0.8032	0.2996	0.8660
DMU ₁₉	0.9187	0.8081	0.1752	0.0813	0.1919	0.8248
DMU ₂₀	0.9113	0.8084	0.2078	0.0887	0.1916	0.7922
DMU ₂₁	0.5661	0.7833	0.1136	0.4339	0.2167	0.8864
DMU ₂₂	0.9204	0.8104	0.2132	0.0796	0.1896	0.7868
DMU ₂₃	0.9174	0.8098	0.1665	0.0826	0.1902	0.8335
DMU ₂₄	0.9141	0.8086	0.1311	0.0859	0.1914	0.8689
DMU ₂₅	0.1559	0.7014	0.1099	0.8441	0.2986	0.8901
DMU₂₆	0.9195	0.8105	1.0000	0.0805	0.1895	1.0000
DMU ₂₇	0.9229	0.8048	0.1472	0.0771	0.1952	0.8528
DMU ₂₈	0.2499	0.7060	0.1684	0.7501	0.2940	0.8316
DMU ₂₉	0.9116	0.8055	0.1666	0.0884	0.1945	0.8334
DMU ₃₀	0.1832	0.4106	0.1564	0.8168	0.5894	0.8436
DMU ₃₁	0.2405	0.7203	0.1529	0.7595	0.2797	0.8471
DMU ₃₂	0.9171	0.8091	0.1646	0.0829	0.1909	0.8354
Mean	0.6096	0.7375	0.1864	0.4217	0.2938	0.8448

Furthermore, it can be found that all banks have a relatively stable inefficiency dominance probability in the period of 2014–2018, with the largest variation being 0.1343 (0.2956–0.1613) for Zijin Rural Commercial Bank (DMU₃₂) and the smallest variation being 0.0087 (0.7331–0.7244) for Shanghai Pudong Development Bank (DMU₁₈). All banks always have an eco-inefficiency dominance probability that is either larger than 0.50 or less than 0.50 in the five-year sample (0.5 is a threshold where the dominating probability is equal to the dominated probability), implying that all banks can be divided into two groups, one for superior banks and another for inferior banks. The categories are shown in Table 8. From the average sense, we find that China Construction Bank (DMU₉), Industrial and Commercial Bank of China (DMU₄), Industrial Bank (DMU₂₅), Bank of China (DMU₃₂), and Shanghai Pudong Development Bank (DMU₁₈) are the top five listed banks for operation performance. In contrast, the lowest five banks are Suzhou Rural Commercial Bank (DMU₂₂), Rural Commercial Bank of Zhangjiagang (DMU₂₆), Jiangyin Rural Commercial Bank (DMU₁₁), Zijin Rural Commercial Bank (DMU₃₂), and Changshu Rural Commercial Bank (DMU₂), all of which

TABLE 7: Inefficiency dominance probability of 32 listed banks from 2014 to 2018.

Banks	2014	2015	2016	2017	2018	Mean
DMU ₁	0.6175	0.6149	0.6142	0.6173	0.6235	0.6175
DMU ₂	0.2872	0.2633	0.2243	0.2184	0.2293	0.2445
DMU ₃	0.4257	0.4131	0.3831	0.3685	0.3971	0.3975
DMU ₄	0.7964	0.7936	0.7786	0.7920	0.8056	0.7932
DMU ₅	0.6770	0.6678	0.6790	0.6815	0.6411	0.6693
DMU ₆	0.3007	0.3382	0.3529	0.3928	0.4268	0.3623
DMU ₇	0.4582	0.4853	0.4794	0.4922	0.4908	0.4812
DMU ₈	0.6105	0.5885	0.5749	0.5640	0.5857	0.5847
DMU ₉	0.8039	0.8091	0.7945	0.8038	0.8132	0.8049
DMU₁₀	0.5439	0.5812	0.5893	0.6105	0.6096	0.5869
DMU ₁₁	0.2742	0.2571	0.2469	0.2246	0.2099	0.2425
DMU ₁₂	0.7623	0.7480	0.7216	0.7106	0.7032	0.7291
DMU ₁₃	0.7042	0.6892	0.6916	0.7231	0.6982	0.7013
DMU ₁₄	0.5130	0.5143	0.5269	0.5392	0.5413	0.5269
DMU ₁₅	0.4937	0.4849	0.4806	0.4678	0.4710	0.4796
DMU₁₆	0.7135	0.7209	0.7130	0.7232	0.7375	0.7216
DMU ₁₇	0.6272	0.6105	0.5922	0.6169	0.6155	0.6125
DMU ₁₈	0.7315	0.7255	0.7244	0.7324	0.7331	0.7294
DMU ₁₉	0.3614	0.3654	0.3772	0.3510	0.3212	0.3552
DMU ₂₀	0.2796	0.2947	0.3033	0.2929	0.3048	0.2951
DMU ₂₁	0.5859	0.5885	0.6007	0.5769	0.5712	0.5846
DMU ₂₂	0.1967	0.1937	0.1941	0.1786	0.2062	0.1939
DMU ₂₃	0.2875	0.3021	0.2897	0.2705	0.2559	0.2812
DMU ₂₄	0.2823	0.2992	0.3333	0.3240	0.3304	0.3138
DMU ₂₅	0.7851	0.7710	0.7642	0.7895	0.7747	0.7769
DMU₂₆	0.2405	0.2264	0.2289	0.2039	0.1864	0.2172
DMU ₂₇	0.3743	0.3810	0.4116	0.3980	0.4038	0.3938
DMU ₂₈	0.7060	0.6765	0.6573	0.6634	0.6801	0.6766
DMU ₂₉	0.4041	0.4260	0.4448	0.4405	0.3855	0.4202
DMU ₃₀	0.7721	0.7665	0.7577	0.7673	0.7795	0.7686
DMU ₃₁	0.7224	0.6996	0.7011	0.6738	0.6721	0.6938
DMU ₃₂	0.1613	0.2040	0.2686	0.2909	0.2956	0.2441

have an average inefficiency dominance probability of less than 0.2500.

The eco-inefficiency and eco-inefficiency dominance probabilities of these 32 listed banks are given in Tables 4 and 7, respectively. It is clear that the proposed approach will give performance indexes that are different from those of previous approaches. Furthermore, we give the ranking comparison of eco-inefficiency and eco-inefficiency dominance probabilities in Table 9. It can be found from Table 9 that, on the one hand, the proposed approach will give performance rankings that are largely different from those of previous approaches. On the other hand, the traditional DEA model cannot discriminate all banks, and more seriously, more than twenty banks are ranked as the first based on inefficiency scores, while the eco-inefficiency dominance probability approach can indeed give a full ranking of all banks. From this perspective, the proposed approach can give a more reasonable and discriminating performance assessment.

All 32 listed banks can be mainly categorized into four groups according to the ownership, namely, state-owned banks, joint-stock banks, city commercial banks, and rural commercial banks. Table 10 shows the divisions, and Table 11 gives the average inefficiency dominance probabilities for different kinds of banks.

TABLE 8: Superior and inferior listed banks.

Category	Banks
Superior (>0.5000)	Bank of Beijing, Industrial and Commercial Bank of China, China Everbright Bank, Huaxia Bank, China Construction Bank, Bank of Jiangsu, Bank of Communications, China Minsheng Bank, Bank of Nanjing, Agricultural Bank of China, Ping An Bank, Shanghai Pudong Development Bank, Bank of Shanghai, Industrial Bank, China Merchants Bank, Bank of China, China CITIC Bank
Inferior (<0.5000)	Changshu Rural Commercial Bank, Bank of Chengdu, Bank of Guiyang, Bank of Hangzhou, Jiangyin Rural Commercial Bank, Bank of Ningbo, Bank of Qingdao, Qingdao Rural Commercial Bank, Suzhou Rural Commercial Bank, Wuxi Rural Commercial Bank, Bank of Xian, Rural Commercial Bank of Zhangjiagang, Bank of Changsha, Bank of Zhengzhou, Zijin Rural Commercial Bank

TABLE 9: Ranking of inefficiency and inefficiency dominance probabilities.

Banks	2014		2015		2016		2017		2018	
DMU ₁	1	13	1	12	1	12	1	12	1	12
DMU ₂	1	26	32	28	32	31	29	30	32	29
DMU ₃	1	20	25	21	29	22	1	23	25	22
DMU ₄	1	2	1	2	1	2	1	2	1	2
DMU ₅	1	11	23	11	1	10	25	9	23	11
DMU ₆	29	24	31	24	30	24	31	22	31	20
DMU ₇	26	19	1	18	1	19	1	18	1	18
DMU ₈	31	14	30	15	27	16	28	16	30	15
DMU ₉	1	1	1	1	1	1	1	1	1	1
DMU ₁₀	1	16	1	16	1	15	1	14	1	14
DMU ₁₁	1	29	1	29	1	29	1	29	1	30
DMU ₁₂	25	5	1	5	1	6	1	8	1	7
DMU ₁₃	1	10	1	9	1	9	1	7	1	8
DMU ₁₄	28	17	26	17	25	17	1	17	26	17
DMU ₁₅	30	18	28	19	26	18	27	19	28	19
DMU ₁₆	27	8	1	7	1	7	1	6	1	5
DMU ₁₇	1	12	1	13	1	14	1	13	1	13
DMU ₁₈	23	6	1	6	1	5	1	5	1	6
DMU ₁₉	1	23	1	23	23	23	1	24	1	25
DMU ₂₀	1	28	1	27	1	26	1	26	1	26
DMU ₂₁	1	15	1	14	1	13	1	15	1	16
DMU ₂₂	1	31	1	32	1	32	26	32	1	31
DMU ₂₃	1	25	1	25	1	27	1	28	1	28
DMU ₂₄	1	27	1	26	1	25	1	25	1	24
DMU ₂₅	1	3	1	3	1	3	1	3	1	4
DMU ₂₆	1	30	1	30	1	30	1	31	1	32
DMU ₂₇	1	22	27	22	28	21	32	21	27	21
DMU ₂₈	1	9	1	10	1	11	1	11	1	9
DMU ₂₉	1	21	1	20	24	20	24	20	1	23
DMU ₃₀	1	4	1	4	1	4	1	4	1	3
DMU ₃₁	24	7	24	8	1	8	1	10	24	10
DMU ₃₂	32	32	29	31	31	28	30	27	29	27

It can be learned from Table 11 that the four kinds of listed banks exhibit considerably different performance dominance probabilities. More specifically, those five state-owned banks have the highest average inefficiency dominance probability, which is almost three times that of the lowest rural commercial banks. This result shows that these state-owned banks are more likely to have better performance compared with other banks over all sets of weights. In contrast, those rural commercial banks are more likely to have worse performance relative to other banks. Furthermore, joint-stock banks are inferior to state-owned banks and superior to city commercial banks, which are further superior to rural commercial banks.

By using the proposed inefficiency dominance probability approach, we can provide a performance analysis of 32 Chinese listed banks that is derived from the real world. Since the proposed approach considers all sets of feasible weights, which is different from classic DEA approaches that focus on only one or several optimal sets of weights, the resulting performance analytics are more reasonable due to taking full weights and all possibilities into account. Furthermore, by considering all sets of feasible weights, the performance dominance probability is largely different from traditional performance indexes that are obtained with some extreme weights, and the corresponding ranking orders are also changed considerably. Therefore, it makes sense for the

TABLE 10: Categories of different listed banks.

Category	Banks
State-owned banks (5)	Industrial and Commercial Bank of China
	China Construction Bank
	Bank of Communications
	Agricultural Bank of China
	Bank of China
Joint-stock banks (8)	China Everbright Bank, Huaxia Bank
	China Minsheng Bank, Ping An Bank
	Shanghai Pudong Development Bank
	Industrial Bank, China Merchants Bank
	China CITIC Bank
City commercial banks (12)	Bank of Beijing, Bank of Chengdu
	Bank of Guiyang, Bank of Hangzhou
	Bank of Jiangsu, Bank of Nanjing
	Bank of Ningbo, Bank of Qingdao
	Bank of Shanghai, Bank of Xian
	Bank of Changsha, Bank of Zhengzhou
Rural commercial banks (7)	Changshu Rural Commercial Bank
	Jiangyin Rural Commercial Bank
	Qingdao Rural Commercial Bank
	Suzhou Rural Commercial Bank
	Wuxi Rural Commercial Bank
	Rural Commercial Bank of Zhangjiagang
Zijin Rural Commercial Bank	

TABLE 11: Average inefficiency dominance probabilities for four kinds of listed banks.

Banks	2014	2015	2016	2017	2018	Mean
State-owned banks	0.7696	0.7676	0.7531	0.7594	0.7678	0.7635
Joint-stock banks	0.6955	0.6786	0.6731	0.6806	0.6751	0.6806
City commercial banks	0.4467	0.4577	0.4662	0.4649	0.4644	0.4600
Rural commercial banks	0.2467	0.2488	0.2508	0.2400	0.2412	0.2455

proposed approach because it can provide a comprehensive performance assessment instead of only some extreme performances from a data analytics perspective.

4. Conclusion

This paper proposes a new DEA-based approach for assessing the operation performance of Chinese listed banks. Since the conventional DEA approaches consider only a set of optimal and extreme weights to measure the relative performance, the resulting performance indexes might be unreasonable and even unrealistic in practice. From a data-driven decision-making perspective, this paper proceeds to take all sets of feasible input/output weights into account rather than only some special weights. For that purpose, we

first propose an extended eco-inefficiency model to address banking activities and build a pairwise performance dominance structure in terms of inefficiency scores. Furthermore, we calculate the overall inefficiency dominance probability based on all sets of feasible weights, and the inefficiency dominance probability can be used for data-driven performance analytics of those Chinese listed banks. The proposed approach can provide data analytics on relative performances instead of only some extreme possibilities, and it is further used for the empirical analytics of operation performances for 32 listed banks in China.

This paper can be extended with regard to several aspects. First, this paper considers the possible inefficiency score range but ignores its associated possibility. That is, we consider each possible performance score coequally, but it is common that some performance scores are more likely than others. Therefore, future research can be developed to take the possibilities of various performances based on different sets of weights into account. Second, an important research avenue in the DEA field is how to address the internal production structure of DMUs, and thus, similar studies can be designed for situations with complex internal structures and linking connections. Third, similar approaches based on all sets of weights can also be developed for other purposes, such as fixed cost and resource allocation and target setting in real applications.

Data Availability

The illustration data used to support the findings of this study are collected from annual financial reports that are publicly produced by these listed banks in Shenzhen Stock Exchange and Shanghai Stock Exchange in China. In addition, the data are available from the corresponding author upon request.

Conflicts of Interest

The authors declare that there are no conflicts of interest regarding the publication of this article.

Acknowledgments

This work was financially supported by the National Natural Science Foundation of China (nos. 71901178, 71904084, 71910107002, and 71725001), the Natural Science Foundation of Jiangsu Province (no. BK20190427), the Social Science Foundation of Jiangsu Province (no. 19GLC017), the Fundamental Research Funds for the Central Universities at Southwestern University of Finance and Economics (nos. JBK2003021, JBK2001020, and JBK190504) and at Nanjing University of Aeronautics and Astronautics (no. NR2019003), and the Innovation and Entrepreneurship Foundation for Doctor of Jiangsu Province, China.

References

- [1] Y. Zha, N. Liang, M. Wu, and Y. Bian, "Efficiency evaluation of banks in China: a dynamic two-stage slacks-based measure approach," *Omega*, vol. 60, pp. 60–72, 2016.

- [2] N. Zhu, J. L. Hougarrd, Z. Yu, and B. Wang, "Ranking Chinese commercial banks based on their expected impact on structural efficiency," *Omega*, vol. 94, Article ID 102049, 2019.
- [3] N. K. Avkiran, "Opening the black box of efficiency analysis: an illustration with UAE banks," *Omega*, vol. 37, no. 4, pp. 930–941, 2009.
- [4] K. Wang, W. Huang, J. Wu, and Y.-N. Liu, "Efficiency measures of the Chinese commercial banking system using an additive two-stage DEA," *Omega*, vol. 44, pp. 5–20, 2014.
- [5] Q. An, X. Tao, B. Dai, and J. Li, "Modified distance friction minimization model with undesirable output: an application to the environmental efficiency of China's regional industry," *Computational Economics*, 2019.
- [6] Q. An, X. Tao, and B. Xiong, "Benchmarking with data envelopment analysis: an agency perspective," *Omega*, Article ID 102235, 2020.
- [7] J. Chu, J. Wu, C. Chu, and T. Zhang, "DEA-based fixed cost allocation in two-stage systems: leader-follower and satisfaction degree bargaining game approaches," *Omega*, vol. 94, Article ID 102054, 2019.
- [8] Y. Li, L. Wang, and F. Li, "A data-driven prediction approach for sports team performance and its application to National Basketball Association," *Omega*, Article ID 102123, 2019.
- [9] P. Yin, J. Chu, J. Wu, J. Ding, M. Yang, and Y. Wang, "A DEA-based two-stage network approach for hotel performance analysis: an internal cooperation perspective," *Omega*, vol. 93, Article ID 102035, 2020.
- [10] Q. Zhu, M. Song, and J. Wu, "Extended secondary goal approach for common equilibrium efficient frontier selection in DEA with fixed-sum outputs," *Computers & Industrial Engineering*, vol. 144, Article ID 106483, 2020.
- [11] A. Charnes, W. W. Cooper, and E. Rhodes, "Measuring the efficiency of decision making units," *European Journal of Operational Research*, vol. 2, no. 6, pp. 429–444, 1978.
- [12] R. D. Banker, A. Charnes, and W. W. Cooper, "Some models for estimating technical and scale inefficiencies in data envelopment analysis," *Management Science*, vol. 30, no. 9, pp. 1078–1092, 1984.
- [13] W. Chen, R. He, and Q. Wu, "A novel efficiency measure model for industrial land use based on subvector data envelope analysis and spatial analysis method," *Complexity*, vol. 2017, Article ID 9516267, 11 pages, 2017.
- [14] F. Li, Q. Zhu, and L. Liang, "A new data envelopment analysis based approach for fixed cost allocation," *Annals of Operations Research*, vol. 274, no. 1-2, pp. 347–372, 2019.
- [15] Q. Zhu, X. Li, F. Li, and A. Amirteimoori, "Data-driven approach to find the best partner for merger and acquisitions in banking industry," *Industrial Management & Data Systems*, 2020.
- [16] Q. Zhu, X. Li, F. Li, and D. Zhou, "The potential for energy saving and carbon emission reduction in China's regional industrial sectors," *Science of the Total Environment*, vol. 716, Article ID 135009, 2020.
- [17] J. C. Paradi and H. Zhu, "A survey on bank branch efficiency and performance research with data envelopment analysis," *Omega*, vol. 41, no. 1, pp. 61–79, 2013.
- [18] H.-H. Liu, Y.-Y. Song, and G.-L. Yang, "Cross-efficiency evaluation in data envelopment analysis based on prospect theory," *European Journal of Operational Research*, vol. 273, no. 1, pp. 364–375, 2019.
- [19] J. Wu, J. Chu, J. Sun, and Q. Zhu, "DEA cross-efficiency evaluation based on Pareto improvement," *European Journal of Operational Research*, vol. 248, no. 2, pp. 571–579, 2016.
- [20] R. G. Dyson, R. Allen, A. S. Camanho, V. V. Podinovski, C. S. Sarrico, and E. A. Shale, "Pitfalls and protocols in DEA," *European Journal of Operational Research*, vol. 132, no. 2, pp. 245–259, 2011.
- [21] A. Salo and A. Punkka, "Ranking intervals and dominance relations for ratio-based efficiency analysis," *Management Science*, vol. 57, no. 1, pp. 200–214, 2011.
- [22] W. D. Cook, Y. Roll, and A. Kazakov, "A dea model for measuring the relative efficiency of highway maintenance patrols," *INFOR: Information Systems and Operational Research*, vol. 28, no. 2, pp. 113–124, 1990.
- [23] Y. Roll, W. D. Cook, and B. Golany, "Controlling factor weights in data envelopment analysis," *IIE Transactions*, vol. 23, no. 1, pp. 2–9, 1991.
- [24] W. D. Cook and M. Kress, "A data envelopment model for aggregating preference rankings," *Management Science*, vol. 36, no. 11, pp. 1302–1310, 1990.
- [25] C. Kao and H.-T. Hung, "Data envelopment analysis with common weights: the compromise solution approach," *Journal of the Operational Research Society*, vol. 56, no. 10, pp. 1196–1203, 2005.
- [26] F.-H. F. Liu and H. Hsuan Peng, "Ranking of units on the DEA frontier with common weights," *Computers & Operations Research*, vol. 35, no. 5, pp. 1624–1637, 2008.
- [27] C. Kao, "Malmquist productivity index based on common-weights DEA: the case of Taiwan forests after reorganization," *Omega*, vol. 38, no. 6, pp. 484–491, 2010.
- [28] M. Zohrehbandian, A. Makui, and A. Alinezhad, "A compromise solution approach for finding common weights in DEA: an improvement to Kao and Hung's approach," *Journal of the Operational Research Society*, vol. 61, no. 4, pp. 604–610, 2010.
- [29] S. Ramezani-Tarkhorani, M. Khodabakhshi, S. Mehrabian, and F. Nuri-Bahmani, "Ranking decision-making units using common weights in DEA," *Applied Mathematical Modelling*, vol. 38, no. 15-16, pp. 3890–3896, 2014.
- [30] A. Shabani, F. Visani, P. Barbieri, W. Dullaert, and D. Vigo, "Reliable estimation of suppliers' total cost of ownership: an imprecise data envelopment analysis model with common weights," *Omega*, vol. 87, pp. 57–70, 2019.
- [31] Y. Li, F. Li, A. Emrouznejad, L. Liang, and Q. Xie, "Allocating the fixed cost: an approach based on data envelopment analysis and cooperative game," *Annals of Operations Research*, vol. 274, no. 1-2, pp. 373–394, 2019.
- [32] F. Li, Q. Zhu, and Z. Chen, "Allocating a fixed cost across the decision making units with two-stage network structures," *Omega*, vol. 83, pp. 139–154, 2019.
- [33] T. R. Sexton, R. H. Silkman, and A. J. Hogan, "Data envelopment analysis: critique and extensions," *New Directions for Program Evaluation*, vol. 1986, no. 32, pp. 73–105, 1986.
- [34] F. Li, Q. Zhu, and L. Liang, "Allocating a fixed cost based on a DEA-game cross efficiency approach," *Expert Systems with Applications*, vol. 96, pp. 196–207, 2018.
- [35] M. Davtalab-Olyaie, "A secondary goal in DEA cross-efficiency evaluation: a "one home run is much better than two doubles" criterion," *Journal of the Operational Research Society*, vol. 70, no. 5, pp. 807–816, 2019.
- [36] F. Li, Q. Zhu, Z. Chen, and H. Xue, "A balanced data envelopment analysis cross-efficiency evaluation approach," *Expert Systems with Applications*, vol. 106, pp. 154–168, 2018.
- [37] L. Liang, J. Wu, W. D. Cook, and J. Zhu, "Alternative secondary goals in DEA cross-efficiency evaluation," *International Journal of Production Economics*, vol. 113, no. 2, pp. 1025–1030, 2008.
- [38] J. L. Ruiz and I. Sirvent, "On the DEA total weight flexibility and the aggregation in cross-efficiency evaluations," *European*

- Journal of Operational Research*, vol. 223, no. 3, pp. 732–738, 2012.
- [39] Y.-M. Wang and K.-S. Chin, “The use of OWA operator weights for cross-efficiency aggregation,” *Omega*, vol. 39, no. 5, pp. 493–503, 2011.
- [40] Y. M. Wang and S. Wang, “Approaches to determining the relative importance weights for cross-efficiency aggregation in data envelopment analysis,” *Journal of the Operational Research Society*, vol. 64, no. 1, pp. 60–69, 2013.
- [41] G.-L. Yang, J.-B. Yang, W.-B. Liu, and X.-X. Li, “Cross-efficiency aggregation in DEA models using the evidential-reasoning approach,” *European Journal of Operational Research*, vol. 231, no. 2, pp. 393–404, 2013.
- [42] A. Boussofiane, R. G. Dyson, and E. Thanassoulis, “Applied data envelopment analysis,” *European Journal of Operational Research*, vol. 52, no. 1, pp. 1–15, 1991.
- [43] J. R. Doyle and R. H. Green, “Cross-evaluation in DEA: improving discrimination among DMUs,” *INFOR: Information Systems and Operational Research*, vol. 33, no. 3, pp. 205–222, 1995.
- [44] T. R. Anderson, K. Hollingsworth, and L. Inman, “The fixed weighting nature of a cross-evaluation model,” *Journal of Productivity Analysis*, vol. 17, no. 3, pp. 249–255, 2002.
- [45] M. Falagario, F. Sciancalepore, N. Costantino, and R. Pietroforte, “Using a DEA-cross efficiency approach in public procurement tenders,” *European Journal of Operational Research*, vol. 218, no. 2, pp. 523–529, 2012.
- [46] S. Lim, K. W. Oh, and J. Zhu, “Use of DEA cross-efficiency evaluation in portfolio selection: an application to Korean stock market,” *European Journal of Operational Research*, vol. 236, no. 1, pp. 361–368, 2014.
- [47] S. Lim and J. Zhu, “DEA cross-efficiency evaluation under variable returns to scale,” *Journal of the Operational Research Society*, vol. 66, no. 3, pp. 476–487, 2015.
- [48] M. Carrillo and J. M. Jorge, “An alternative neutral approach for cross-efficiency evaluation,” *Computers & Industrial Engineering*, vol. 120, pp. 137–145, 2018.
- [49] L. Liang, J. Wu, W. D. Cook, and J. Zhu, “The DEA game cross-efficiency model and its Nash equilibrium,” *Operations Research*, vol. 56, no. 5, pp. 1278–1288, 2008.
- [50] Y.-M. Wang and K.-S. Chin, “Some alternative models for DEA cross-efficiency evaluation,” *International Journal of Production Economics*, vol. 128, no. 1, pp. 332–338, 2010.
- [51] X. Tang, Y. Li, M. Wang, and L. Liang, “A DEA efficiency probability dominance method,” *Systems Engineering-Theory & Practice*, vol. 36, no. 10, pp. 2641–2647, 2016.
- [52] X. Shi, “Efficiency bounds for two-stage production systems,” *Mathematical Problems in Engineering*, vol. 2018, Article ID 2917537, 9 pages, 2018.
- [53] Y. Li, X. Shi, A. Emrouznejad, and L. Liang, “Ranking intervals for two-stage production systems,” *Journal of the Operational Research Society*, vol. 71, no. 2, pp. 209–224, 2020.
- [54] F. Li, Z. Yan, Q. Zhu, M. Yin, and G. Kou, “Allocating a fixed cost across decision making units with explicitly considering efficiency rankings,” *Journal of the Operational Research Society*, pp. 1–15, 2020.
- [55] F. Li, A. Emrouznejad, G.-I. Yang, and Y. Li, “Carbon emission abatement quota allocation in Chinese manufacturing industries: an integrated cooperative game data envelopment analysis approach,” *Journal of the Operational Research Society*, pp. 1–30, 2019.
- [56] X. Li, F. Li, N. Zhao, and Q. Zhu, “Measuring environmental sustainability performance of freight transportation seaports in China: a data envelopment analysis approach based on the closest targets,” *Expert Systems*, Article ID e12334, 2018.
- [57] M. Song, Q. An, W. Zhang, Z. Wang, and J. Wu, “Environmental efficiency evaluation based on data envelopment analysis: a review,” *Renewable and Sustainable Energy Reviews*, vol. 16, no. 7, pp. 4465–4469, 2012.
- [58] C.-M. Chen and M. A. Delmas, “Measuring eco-inefficiency: a new frontier approach,” *Operations Research*, vol. 60, no. 5, pp. 1064–1079, 2012.
- [59] T. Kuosmanen, “Weak disposability in nonparametric production analysis with undesirable outputs,” *American Journal of Agricultural Economics*, vol. 87, no. 4, pp. 1077–1082, 2005.
- [60] F. Li, Q. Zhu, and J. Zhuang, “Analysis of fire protection efficiency in the United States: a two-stage DEA-based approach,” *OR Spectrum*, vol. 40, no. 1, pp. 23–68, 2018.
- [61] M. Asmild, J. L. Hougaard, D. Kronborg, and H. K. Kvist, “Measuring inefficiency via potential improvements,” *Journal of Productivity Analysis*, vol. 19, no. 1, pp. 59–76, 2003.
- [62] P. Bogetoft and J. L. Hougaard, “Efficiency evaluations based on potential (non-proportional) improvements,” *Journal of Productivity Analysis*, vol. 12, no. 3, pp. 233–247, 1999.
- [63] B. Arabi, S. Munisamy, and A. Emrouznejad, “A new slacks-based measure of Malmquist-Luenberger index in the presence of undesirable outputs,” *Omega*, vol. 51, pp. 29–37, 2015.
- [64] H. Fukuyama and R. Matousek, “Modelling bank performance: a network DEA approach,” *European Journal of Operational Research*, vol. 259, no. 2, pp. 721–732, 2017.
- [65] F. Li, L. Liang, Y. Li, and A. Emrouznejad, “An alternative approach to decompose the potential gains from mergers,” *Journal of the Operational Research Society*, vol. 69, no. 11, pp. 1793–1802, 2018.

Research Article

The Dominance Degree-Based Heterogeneous Linguistic Decision-Making Technique for Sustainable 3PRLP Selection

Xiaolu Zhang ¹ and Ting Su²

¹The Collaborative Innovation Center, Jiangxi University of Finance and Economics, Nanchang 330013, China

²School of Business, Shanghai University of Finance and Economics, Shanghai 200433, China

Correspondence should be addressed to Xiaolu Zhang; xiaolu_jy@163.com

Received 18 March 2020; Revised 6 April 2020; Accepted 7 April 2020; Published 28 April 2020

Guest Editor: Baogui Xin

Copyright © 2020 Xiaolu Zhang and Ting Su. This is an open access article distributed under the Creative Commons Attribution License, which permits unrestricted use, distribution, and reproduction in any medium, provided the original work is properly cited.

This study develops a novel dominance degree-based heterogeneous linguistic decision-making technique for identifying the most sustainable third-party reverse logistics providers (3PRLPs) under complex input environments. First, qualitative and uncertain inputs that arise from real-world 3PRLP evaluation process are successfully managed by using linguistic terms, hesitant fuzzy linguistic terms, and probabilistic linguistic term sets with different granularities. Then, the dominance degrees of each 3PRLP related to the other 3PRLPs are calculated based on a new ratio index-based probabilistic linguistic ranking method and the dominance matrix is constructed. Furthermore, to represent the closeness of each 3PRLP to the ideal solution, we propose a sort of measures including the dominance-based group utility measure, the dominance-based individual regret measure, and the dominance-based compromise measure. Accordingly, the selection results of 3PRLPs are obtained according to these measures. Finally, the developed method is applied to a case study from car manufacture industry, and the comparison analysis shows that the proposed method is reliable and stable for dealing with the problem of the 3PRLP selection. The main advantage of the developed method is that it cannot only well avoid the potential loss risks but also balance group utility scores and individual regret scores.

1. Introduction

Growing environmental concerns and potential economic profitability have driven more and more corporations to outsource their logistics activities to third-party reverse logistics providers (3PRLPs) [1]. To achieve the goals of cost reduction and environmental protection, it is crucial for manufacturers to select the best available 3PRLP. Considering the qualitative nature of assessed criteria in the selection process of 3PRLPs, linguistic expression forms [2] are quite comfortable and straightforward for evaluators to capture their uncertain preferences. For example, Mavi et al. [3] and Zarbakhshnia et al. [4] employed single linguistic terms (LTs) to express performances of 3PRLPs. With the need of modeling more complexity uncertain information, two new extensions of linguistic variables, hesitant fuzzy linguistic term set (HFLTSS) [5–7] and probabilistic linguistic

term set (PLTS) [8–11], are recently developed. These new linguistic forms provided more freedom for evaluators to express their uncertain preferences [12–14], especially for the 3PRLP evaluation contexts.

In the practical 3PRLP evaluating process, for example, one evaluator may employ single LT like “good” or “poor” to express performances of 3PRLPs under the quality criterion and utilize comparative linguistic expression (CLE) like “at least good” to model performances of 3PRLPs from the aspect of green technology capability, and use one PLTS {fair(0.6), good(0.4)} to represent performances of 3PRLPs from the aspect of the employment stability. This PLTS means that the preference for the evaluator is “good” with a degree of 40% and “fair” with a degree of 60%. It is evident that diverse linguistic expression forms of decision information, such as LTs, HFLTSSs, and PLTSs, are simultaneously involving with the real-world 3PRLP selection problems

under complex assessed contexts. This situation is called a kind of heterogeneous linguistic information-based 3PRLP selection problems. However, the majority of the existing techniques developed for 3PRLP selection problems only consider the situations where the performance scores of 3PRLPs are described in a uniform mathematical format. Therefore, the one challenge need to be addressed imperatively is how to deal with the qualitative and heterogeneous uncertain inputs.

On the other hand, in the real-world 3PRLP selection process, the decision maker (DM) is usually bounded rational and the behavior factor of DM greatly affects the final decision results [15, 16]. A recent study by Li et al. [1] has also been proved that the psychological behavior of DM in 3PRLP selection under environmental pressure weighed heavily with decision solution. But the majority of the current 3PRLP selection techniques that are constructed under a strict hypothesis that DM is completely rational in decision making fail to investigate 3PRLP selection problems with consideration of the psychological behavior of DM. Therefore, one other challenge urgently needed to deal with is how to identify the most preferred 3PRLP with full consideration of DM's psychological behavior.

In order to deal with these two challenges, this study attempts to develop a new dominance degree-based heterogeneous linguistic decision-making method to identify the optimal 3PRLP in case of considering the DM's psychological behavior. The remainder of this paper is organized as follows: Section 2 provides literature review and Section 3 introduces briefly the basic concepts of different linguistic forms and formulates the 3PRLP selection problems. Section 4 develops a dominance degree-based heterogeneous linguistic decision-making method. Section 5 provides an empirical study to demonstrate the usefulness of our proposed method, and Section 6 presents our conclusions.

2. Literature Review

Reverse logistics management has been one of the most heated topics discussed in the supply chain management research domain, which mainly focuses on the backward flow of materials and raw equipment from customers to suppliers [3]. Its biggest advantage is able to provide customers with a chance to return end-of-life products to the manufacturer and to allow this manufacturer to reevaluate them and utilize them again in the production cycle [17]. In other words, reverse logistics can not only bring economic benefits but also protect the resources of raw materials as the environment [18]. The pressure from environmental protection and sustainable development has driven the majority of manufacturers to outsource logistics activities to 3PRLPs. To identify the most sustainable 3PRLP, the manufacturers have to address two key issues in the 3PRLP selection. The first one is to determine the optimal selection criteria. In the early research, the majority of the identified 3PRLP evaluation criteria are from economic, environmental, and social dimensions [19–25], such as the quality or cost factor from the economic aspect and the recycle or disposal factor from

the perspective of environment. Recent studies [3, 26] have demonstrated that the risk factors including operational and financial risks play an important role in selecting the most preferred 3PRLPs. The study [4] had further discussed the relationships between the operational risk and the financial risk and provided the sixteen criteria-based evaluation index system. Following the pioneering works of Zarebakhshnia [4, 27], the sixteen evaluation criteria from economic, environmental, social, and risk dimensions are taking into account in this study when evaluating 3PRLPs, and the key criteria for the selection of sustainable 3PRLPs are summarized in Table 1.

The second one is to propose an evaluation and selection method. Multicriteria decision-making (MCDM) methods, which conduct the selection and ranking process by evaluating lots of criteria in different dimensions simultaneously, have been widely used in the 3PRLP selection, such as the TOPSIS method [33], the VIKOR method [34–36], the ELECTRE method [28], and the DEA method [37, 38]. Table 2 summarizes the prevailing approaches to evaluation and selection of 3PRLPs in the existing literature. It is easy to see that the majority of the current 3PRLP selection techniques are constructed under a strict hypothesis that the DM is completely rational in decision making. In other words, few aforementioned techniques have investigated 3PRLP selection problems with consideration of the psychological behavior of DM.

3. Preliminaries

3.1. Basic Concepts. LTs, HFLTSSs, and PLTSs are three frequently used linguistic expression forms and are adopted in this study to capture uncertain performances of 3PRLPs. Their basic concepts are introduced as follows.

Definition 1 (see [43]). The label set $L = \{l_i \mid i = 0, 1, \dots, \tau\}$ is called the ordinal scale-based linguistic variable when $l_i \geq l_j$ if $i \geq j$ ($i, j = 0, 1, \dots, \tau$) and $N(l_i) = l_j$ if $j = \tau - i$ ($N(\bullet)$ is the negation operator and τ is a positive integer).

Definition 2 (see [7]). HFLTSS is defined as one ordered finite subset of consecutive LTs based on the predefined LT set, which is denoted by $H_L = \{l_i, l_{i+1}, \dots, l_j\}$ and $l_k \in L$ ($k = i, i + 1, \dots, j$).

Definition 3 (see [44]). The PLTS is defined as $L(p) = \{l_\sigma(p_\sigma) \mid l_\sigma \in L, p_\sigma \geq 0, \sigma \in \Lambda, \sum_{\sigma \in \Lambda} p_\sigma \leq 1\}$, where $\Gamma = \{1, 2, \dots, \tau\}$ be a set of the subscripts of LTs in L and Λ be a subset of Γ .

In the practical operation process, the LT $l_i \in L$ is equivalent to the special PLTS $L(p) = \{l_i(1.0)\}$, and the HFLTSS $H_L = \{l_i, l_{i+1}, \dots, l_j \mid l_k \in L, k = i, i + 1, \dots, j\}$ can be mathematically rewritten the PLTS as follows:

$$L(p) = \left\{ l_i \left((q - g + 1)^{-1} \right) \mid i = g, g + 1, \dots, q \right\}. \quad (1)$$

Definition 4 (see [44]). Given a set of PLTSs $\wp = \{L_1(p), L_2(p), \dots, L_m(p)\}$, the element $L_i(p) \in \wp$ is

TABLE 1: Criteria used for the selection of sustainable 3PRLPs.

Dimensions	Criteria	Optimal references											
		[17]	[28]	[19]	[20]	[29]	[30]	[31]	[32]	[26]	[3]	[4]	[27]
Economic	Quality		✓	✓	✓	✓			✓	✓	✓	✓	✓
	Cost	✓	✓	✓	✓	✓		✓	✓	✓	✓	✓	✓
	Lead time	✓								✓	✓	✓	✓
	Delivery and services	✓		✓	✓	✓			✓	✓	✓	✓	✓
	Transportation					✓			✓	✓	✓	✓	✓
Environment	Recycle			✓		✓	✓	✓	✓	✓	✓	✓	✓
	Disposal			✓		✓			✓	✓	✓	✓	✓
	Remanufacture and reuse			✓		✓			✓	✓	✓	✓	✓
	Green technology capability		✓	✓				✓	✓		✓	✓	✓
	Environment protection certification									✓		✓	✓
	Eco-design production							✓				✓	✓
Social	Health and safety		✓					✓				✓	✓
	Voice of customer	✓					✓					✓	✓
	Employment stability				✓	✓			✓			✓	✓
Risk	Operational risk		✓							✓		✓	✓
	Financial risk		✓							✓		✓	✓

TABLE 2: Summary of the prevailing methods to select the optimal 3PRLPs.

Selection methods	Optimal references															
	[3]	[4]	[27]	[36]	[34]	[35]	[39]	[40]	[41]	[33]	[28]	[20]	[42]	[1]	[37]	[38]
AHP			✓			✓	✓			✓						
ANP								✓	✓							
TOPSIS				✓						✓			✓			
VIKOR				✓	✓	✓										
ELECTRE											✓					
SWARA	✓	✓														
MOORA	✓		✓													
COPRAS		✓														
DEA															✓	✓
Other methods													✓	✓		

denoted by $L_i(p) = \{l_\sigma(p_\sigma^i) \mid \sigma \in \Lambda_i\}$. $L_i(p)$ is called a partial PLTS when $\sum_{\sigma \in \Lambda_i} p_\sigma^i < 1$, and $L_i(p)$ is called a complete PLTS when $\sum_{\sigma \in \Lambda_i} p_\sigma^i = 1$. Then, the normalization process of the set of PLTSs \wp is shown as follows:

- (1) If $L_i(p)$ is a partial PLTS, then it should be normalized into the complete PLTS $\hat{L}_i(p) = \{l_\sigma(p_\sigma^i + \tau^{-1}(1 - \sum_{\sigma \in \Lambda_i} p_\sigma^i)), l_\rho(\tau^{-1}(1 - \sum_{\sigma \in \Lambda_i} p_\sigma^i)) \mid \sigma \in \Lambda_i, \rho \in (\Gamma \setminus \Lambda_i)\}$
- (2) Let $\Lambda_\wp = \Lambda_1 \cup \Lambda_2 \cup \dots \cup \Lambda_m$ and $\Lambda^+ = \Lambda_i \cap \Lambda_\wp$, if $\Lambda_i \subset \Lambda_\wp$ ($i = 1, 2, \dots, m$), the set of LTs $L^+ = \{l_\rho \mid \rho \in \Lambda^+\}$ is added in $\hat{L}_i(p)$ until $\Lambda_i = \Lambda_\wp$, and probabilities of all added LTs are zero

Definition 5. Considering two complete PLTSs denoted by $L_1(p) = \{l_\sigma(p_\sigma^1) \mid \sigma \in \Lambda_1\}$ and $L_2(p) = \{l_\sigma(p_\sigma^2) \mid \sigma \in \Lambda_2\}$, probabilistic linguistic distance between $L_1(p)$ and $L_2(p)$ is provided as follows:

$$d(L_1(p), L_2(p)) = \frac{1}{\tau} \left| \sum_{\sigma \in \Lambda_1 \cap \Lambda_2} \sigma \times (p_\sigma^1 - p_\sigma^2) + \sum_{(\sigma \in \Lambda \setminus \Lambda_2)} p_\sigma^1 - \sum_{(\sigma \in \Lambda \setminus \Lambda_1)} p_\sigma^2 \right|, \quad (2)$$

where $\Lambda = \Lambda_1 \cup \Lambda_2$.

The above probabilistic linguistic distance measure is motivated by the idea of linguistic distribution distance measure reported in [45], and it is easy to prove that this measure possesses the following desirable properties.

Proposition 1. Let $L_1(p) = \{l_\sigma(p_\sigma^1) \mid \sigma \in \Lambda_1\}$, $L_2(p) = \{l_\nu(p_\nu^2) \mid \nu \in \Lambda_2\}$, and $L_3(p) = \{l_\nu(p_\nu^3) \mid \nu \in \Lambda_3\}$ be three complete PLTSs, and $L_1(p) > L_2(p)$ when $\min_{\sigma \in \Lambda_1} \sigma > \max_{\nu \in \Lambda_2} \nu$, then we have

- (P1.1) $0 \leq d(L_1(p), L_2(p)) \leq 1$
(P1.2) $d(L_1(p), L_2(p)) = 0$ if and only if $L_1(p) = L_2(p)$
(P1.3) $d(L_1(p), L_2(p)) = d(L_2(p), L_1(p))$
(P1.4) If $L_1(p) > L_2(p) > L_3(p)$, then $d(L_1(p), L_2(p)) < d(L_1(p), L_3(p))$ and $d(L_2(p), L_3(p)) < d(L_1(p), L_3(p))$

3.2. Formulation of the 3PRLP Selection Problems. The practical 3PRLP selection usually needs to take into account lots of factors from the following four aspects (also called main criteria): economic criterion (mc_1), social criterion (mc_2), environment criterion (mc_3), and risk criterion (mc_4). Every main criterion mc_j ($j \in \{1, 2, 3, 4\}$) is assumed to include $o_j - o_{j-1}$ subcriteria $\{c_{o_{j-1}+1}, c_{o_{j-1}+2}, \dots, c_{o_j}\}$ ($o_0 = 0$), where o_4 denotes the total number of subcriteria. Let $A = \{a_1, a_2, \dots, a_m\}$ be a set of feasible 3PRLPs, $C = \{c_1, c_2, \dots, c_{o_4}\}$ be the set of subcriteria, and r_{if} denote the performance score of a_i ($i \in \{1, 2, \dots, m\}$) under the subcriterion c_f ($f \in \{1, 2, \dots, o_4\}$). Owing to the fact that the expression form of 3PRLPs performances generally depends on the nature of the criteria in the real-life complex assessed contexts [46, 47], the performance scores under different criteria may be represented by different expression forms of information. In this study, the criterion c_f in the subcriteria set C is assumed to be evaluated using one of three distinct information forms (i.e., LTs, HFLTSS, and PLTSS). The criteria set is divided into three different criteria subsets, i.e., $C = C_1 \cup C_2 \cup C_3$ and $C_1 \cap C_2 \cap C_3 = \emptyset$. Without loss of generality, it is stipulated that

- (i) If $c_f \in C_1$, then $r_{if} = l_{if}^{g(f_1)}$ is represented by single LT based on $L^{g(f_1)} = \{l_1, l_2, \dots, l_{g(f_1)}\}$
- (ii) If $c_f \in C_2$, then $r_{if} = (H_L)_{if}^{g(f_2)}$ is represented by a HFLTSS based on $L^{g(f_2)} = \{l_1, l_2, \dots, l_{g(f_2)}\}$
- (iii) If $c_f \in C_3$, then $r_{if} = L_{if}^{g(f_3)}(p)$ is represented by a PLTSS based on $L^{g(f_3)} = \{l_1, l_2, \dots, l_{g(f_3)}\}$

where $g(f_k)$ ($k = 1, 2, 3$) is the granularity of the LT set.

Then, the 3PRLP selection problem is concisely expressed in the form of heterogeneous linguistic decision matrix $R = (r_{if})_{m \times o_4}$ which is shown in Table 3.

4. The Developed Dominance Degree-Based Heterogeneous Linguistic Decision-Making Technique

To well evaluate and identify the sustainable 3PRLP, this section will develop a new dominance degree-based heterogeneous linguistic decision-making method. There are two influencing factors: the first one is to determine the dominance matrix (which is solved in Section 4.1), and the second one is to identify the group utility and the individual regret (which is dealt with in Section 4.2).

4.1. Determining the Dominance Matrix. Usually, the dominance degree of each 3PRLP under each criterion over the other 3PRLPs is determined by comparing the magnitudes of their performance values. Owing to the fact that all the performance values r_{if} take the form of PLTSSs, the first task is to develop a useful ranking method for comparing the magnitudes of performance values. Thus, a new probabilistic linguistic distance-based ratio index is introduced in Definition 6.

Definition 6. Given two complete PLTSSs $L_1(p)$ and $L_2(p)$, let $\mathcal{O}^+ = \{l_\tau(1.0)\}$ and $\mathcal{O}^- = \{l_1(1.0)\}$ be the positive ideal PLTS and the negative ideal PLTS, respectively, the ratio index of $L_j(p)$ ($j = 1, 2$) is defined as follows:

$$\mathcal{F}(L_j(p)) = \frac{d(L_j(p), \mathcal{O}^-)}{1 + \max\{d(L_1(p), \mathcal{O}^-), d(L_2(p), \mathcal{O}^-)\}} - \frac{d(L_j(p), \mathcal{O}^+)}{1 + \min\{d(L_1(p), \mathcal{O}^+), d(L_2(p), \mathcal{O}^+)\}} \quad (3)$$

where $d(\bullet, \bullet)$ is probabilistic linguistic distance measure defined in equation (2).

In the practical 3PRLP selecting process under PLTSS context, if the evaluation value of one 3PRLP under a criterion provided by the DM is the PLTS $\{l_\tau(1.0)\}$ based on $L^{(\tau)} = \{l_1, l_2, \dots, l_\tau\}$, then the 3PRLP is regarded as the best one for the evaluator from the perspective of this criterion and the evaluation value can be regarded as the positive ideal PLTS $\mathcal{O}^+ = \{l_\tau(1.0)\}$. On the contrary, if the assessment value is $\{l_1(1.0)\}$, which means that this preference for the evaluator is the worst and the evaluation value can be regarded as the negative ideal PLTS $\mathcal{O}^- = \{l_1(1.0)\}$. Apparently, if $L_1(p)$ has much shorter distance from \mathcal{O}^+ than $L_2(p)$ and has much farther distance from \mathcal{O}^- than $L_2(p)$, then $L_1(p)$ is superior to $L_2(p)$. That is to say, the bigger the $\mathcal{F}(L_j(p))$ ($j = 1, 2$) is, the larger the PLTS $L_j(p)$ is, and thus, the comparison law between $L_1(p)$ and $L_2(p)$ is provided as follows:

- (i) If $\mathcal{F}(L_1(p)) < \mathcal{F}(L_2(p))$, then $L_1(p) <_{\mathcal{F}} L_2(p)$
- (ii) If $\mathcal{F}(L_1(p)) = \mathcal{F}(L_2(p))$, then $L_1(p) \sim_{\mathcal{F}} L_2(p)$
- (iii) If $\mathcal{F}(L_1(p)) > \mathcal{F}(L_2(p))$, then $L_1(p) >_{\mathcal{F}} L_2(p)$

where the symbol $>$ means “is superior to,” the symbol \sim means “is equivalent to,” and the symbol $<$ means “is inferior to,” respectively.

Proposition 2. Given two PLTSSs $L_1(p)$ and $L_2(p)$, the ratio index of $L_j(p)$ ($j = 1, 2$) which is denoted by $\mathcal{F}(L_j(p))$ possesses the following properties:

- (P2.1) $-1 \leq \mathcal{F}(L_j(p)) \leq 0.5$
- (P2.2) $\mathcal{F}(L_j(p)) = 0.5$ if and only if $L_j(p) = \mathcal{O}^+$
- (P2.3) $\mathcal{F}(L_j(p)) = -1$ if and only if $L_j(p) = \mathcal{O}^-$

TABLE 3: Heterogeneous linguistic decision matrix R for performances of 3PRLPs.

3PRLPs	Main criteria/subcriteria											
	Economic mc ₁			Social mc ₂			Environment mc ₃			Risk mc ₄		
	c ₁	...	c _{o₁}	c _{o₁+1}	...	c _{o₂}	c _{o₂+1}	...	c _{o₃}	c _{o₃+1}	...	c _{o₄}
a ₁	r ₁₁	...	r _{1o₁}	r _{1(o₁+1)}	...	r _{1o₂}	r _{1(o₂+1)}	...	r _{1o₃}	r _{1(o₃+1)}	...	r _{1o₄}
a ₂	r ₂₁	...	r _{2o₁}	r _{2(o₁+1)}	...	r _{2o₂}	r _{2(o₂+1)}	...	r _{2o₃}	r _{2(o₃+1)}	...	r _{2o₄}
...
a _m	r _{m1}	...	r _{mo₁}	r _{m(o₁+1)}	...	r _{mo₂}	r _{m(o₂+1)}	...	r _{mo₃}	r _{m(o₃+1)}	...	r _{mo₄}

(P2.4) If $d(L_1(p), \mathcal{O}^-) > d(L_2(p), \mathcal{O}^-)$ and $d(L_1(p), \mathcal{O}^+) < d(L_2(p), \mathcal{O}^+)$, namely, $L_1(p)$ is superior to $L_2(p)$, then $\mathcal{F}(L_2(p)) < \mathcal{F}(L_1(p))$

$$\mathcal{F}(L_1(p)) = \frac{d(L_1(p), \mathcal{O}^-)}{1 + d(L_1(p), \mathcal{O}^-)} - \frac{d(L_1(p), \mathcal{O}^+)}{1 + d(L_1(p), \mathcal{O}^+)}, \quad (8)$$

$$\mathcal{F}(L_2(p)) = \frac{d(L_2(p), \mathcal{O}^-)}{1 + d(L_2(p), \mathcal{O}^-)} - \frac{d(L_2(p), \mathcal{O}^+)}{1 + d(L_2(p), \mathcal{O}^+)}$$

Proof. (P2.1) Owing to $0 \leq d(L_j(p), \mathcal{O}^-), d(L_j(p), \mathcal{O}^+) \leq 1$, we have

$$0 \leq \max_{j=1}^n \{d(L_j(p), \mathcal{O}^-)\}, \quad (4)$$

$$\min_{j=1}^n \{d(L_j(p), \mathcal{O}^+)\} \leq 1.$$

It is easy to obtain

$$0 \leq \frac{d(L_j(p), \mathcal{O}^-)}{1 + \max_{j=1}^n \{d(L_j(p), \mathcal{O}^-)\}} \leq 0.5, \quad (5)$$

$$-1 \leq -\frac{d(L_j(p), \mathcal{O}^+)}{1 + \min_{j=1}^n \{d(L_j(p), \mathcal{O}^+)\}} \leq 0.$$

According to the definition of $\mathcal{F}(L_j(p))$, we can conclude $-1 \leq \mathcal{F}(L_j(p)) \leq 0.5$.

(P2.2) If $\mathcal{F}(L_j(p)) = 0.5$, according to the proof of (1) in Proposition 2, we have

$$\frac{d(L_j(p), \mathcal{O}^-)}{1 + \max_{j=1}^n \{d(L_j(p), \mathcal{O}^-)\}} = 0.5, \quad (6)$$

$$\frac{d(L_j(p), \mathcal{O}^+)}{1 + \min_{j=1}^n \{d(L_j(p), \mathcal{O}^+)\}} = 0.$$

Further, we conclude $d(L_j(p), \mathcal{O}^-) = \max_{j=1}^n \{(L_j(p), \mathcal{O}^-)\} = 1$ and $d(L_j(p), \mathcal{O}^+) = 0$. By the definition of probabilistic linguistic distance measure, we have $L_j(p) = \mathcal{O}^-$. On the contrary, if $L_j(p) = \mathcal{O}^+$, then $d(L_j(p), \mathcal{O}^+) = 0$ and $d(L_j(p), \mathcal{O}^-) = 1$, namely, $\mathcal{F}(L_j(p)) = 0.5$.

(P2.3) This proof is similar to the proof of (P2.2) in Proposition 2.

(P2.4) If $d(L_1(p), \mathcal{O}^-) > d(L_2(p), \mathcal{O}^-)$ and $d(L_1(p), \mathcal{O}^+) < d(L_2(p), \mathcal{O}^+)$, then we have

$$\begin{aligned} \max\{d(L_1(p), \mathcal{O}^-), d(L_2(p), \mathcal{O}^-)\} &= d(L_1(p), \mathcal{O}^-), \\ \min\{d(L_1(p), \mathcal{O}^+), d(L_2(p), \mathcal{O}^+)\} &= d(L_1(p), \mathcal{O}^+), \end{aligned} \quad (7)$$

and then we conclude

Obviously, $\mathcal{F}(L_1(p)) > \mathcal{F}(L_2(p))$.

The proof of Proposition 2 is completed.

Analogously, the ranking law for a set of PLTSs $\Theta = \{L_1(p), L_2(p), \dots, L_n(p)\}$ ($n > 2$) is provided as follows:

(i) If $\mathcal{F}(L_1(p)) < \mathcal{F}(L_2(p)) < \dots < \mathcal{F}(L_n(p))$, then $L_1(p) <_{\mathcal{F}} L_2(p) <_{\mathcal{F}} \dots <_{\mathcal{F}} L_n(p)$

(ii) If $\mathcal{F}(L_1(p)) = \mathcal{F}(L_2(p)) = \dots = \mathcal{F}(L_n(p))$, then $L_1(p) \sim_{\mathcal{F}} L_2(p) \sim_{\mathcal{F}} \dots \sim_{\mathcal{F}} L_n(p)$

(iii) If $\mathcal{F}(L_1(p)) > \mathcal{F}(L_2(p)) > \dots > \mathcal{F}(L_n(p))$, then $L_1(p) >_{\mathcal{F}} L_2(p) >_{\mathcal{F}} \dots >_{\mathcal{F}} L_n(p)$

where $\mathcal{F}(L_j(p))$ is the ratio index of $L_j(p) \in \Theta$ and is defined as follows:

$$\begin{aligned} \mathcal{F}(L_j(p)) &= \frac{d(L_j(p), \mathcal{O}^-)}{1 + \max_{j=1}^n \{d(L_j(p), \mathcal{O}^-)\}} \\ &\quad - \frac{d(L_j(p), \mathcal{O}^+)}{1 + \min_{j=1}^n \{d(L_j(p), \mathcal{O}^+)\}}. \end{aligned} \quad (9)$$

Based on the developed ratio index of PLTSs, we next present a new defuzzification function of PLTSs to manage probabilistic linguistic assessment-based criteria weights. \square

Definition 7. Given a set of PLTSs $\Theta = \{L_1(p), L_2(p), \dots, L_n(p)\}$, the ratio index-based defuzzification function of $L_j(p)$ ($j = 1, 2, \dots, n$) is defined as follows:

$$\mathcal{E}(L_j(p)) = \frac{1 + \mathcal{F}(L_j(p))}{\sum_{j=1}^n (1 + \mathcal{F}(L_j(p)))}. \quad (10)$$

Proposition 3. Given a set of PLTSs $\Theta = \{L_1(p), L_2(p), \dots, L_n(p)\}$, the ratio index-based defuzzification function of $L_j(p)$ which is denoted by $\mathcal{E}(L_j(p))$ ($j = 1, 2, \dots, n$) possesses the following properties:

$$(P3.1) \quad 0 \leq \mathcal{E}(L_j(p)) \leq 1$$

$$(P3.2) \quad \sum_{j=1}^n \mathcal{E}(L_j(p)) = 1$$

(P3.3) If $L_1(p) < L_2(p)$, then $\mathcal{E}(L_1(p)) < \mathcal{E}(L_2(p))$

The proof of Proposition 3 is straightforward and is omitted here.

By equation (10), the defuzzification score of the main criterion weight $w(mc_i)$ can be calculated by the following expression:

$$\mathcal{E}(w(mc_i)) = (1 + \mathcal{F}(w(mc_i)))^{-1} \sum_{i=1}^4 (1 + \mathcal{F}(w(mc_i))),$$

$$i = 1, 2, 3, 4,$$
(11)

where $\mathcal{F}(w(mc_i)) = d(w(mc_i), \mathcal{O}^-) / (1 + \max_{i=1}^4 \{d(w(mc_i), \mathcal{O}^-)\}) - d(w(mc_i), \mathcal{O}^+) / (1 + \min_{i=1}^4 \{d(w(mc_i), \mathcal{O}^+)\})$.

Analogously, the defuzzification score of the subcriterion weight $w(c_f)$ is determined by the following expression:

$$\mathcal{E}(w(c_f)) = (1 + \mathcal{F}(w(c_f)))^{-1} \sum_{f=1}^{o_4} (1 + \mathcal{F}(w(c_f))),$$

$$f = 1, 2, \dots, o_4,$$
(12)

where $\mathcal{F}(w(c_f)) = d(w(c_f), \mathcal{O}^-) / (1 + \max_{f=1}^{o_4} \{d(w(c_f), \mathcal{O}^-)\}) - d(w(c_f), \mathcal{O}^+) / (1 + \min_{f=1}^{o_4} \{d(w(c_f), \mathcal{O}^+)\})$.

Then, the final weight score for each subcriterion $w_f (f = 1, 2, \dots, o_4)$ is determined as follows:

$$\begin{pmatrix} w_1 \\ w_2 \\ \vdots \\ w_{o_1} \end{pmatrix} = \mathcal{E}(w(mc_1)) \otimes \begin{pmatrix} \mathcal{E}(w(c_1)) \\ \mathcal{E}(w(c_2)) \\ \vdots \\ \mathcal{E}(w(c_{o_1})) \end{pmatrix},$$

$$\begin{pmatrix} w_{o_1+1} \\ w_{o_1+2} \\ \vdots \\ w_{o_2} \end{pmatrix} = \mathcal{E}(w(mc_2)) \otimes \begin{pmatrix} \mathcal{E}(w(c_{o_1+1})) \\ \mathcal{E}(w(c_{o_1+2})) \\ \vdots \\ \mathcal{E}(w(c_{o_2})) \end{pmatrix},$$

$$\begin{pmatrix} w_{o_2+1} \\ w_{o_2+2} \\ \vdots \\ w_{o_3} \end{pmatrix} = \mathcal{E}(w(mc_3)) \otimes \begin{pmatrix} \mathcal{E}(w(c_{o_2+1})) \\ \mathcal{E}(w(c_{o_2+2})) \\ \vdots \\ \mathcal{E}(w(c_{o_3})) \end{pmatrix},$$

$$\begin{pmatrix} w_{o_3+1} \\ w_{o_3+2} \\ \vdots \\ w_{o_4} \end{pmatrix} = \mathcal{E}(w(mc_4)) \otimes \begin{pmatrix} \mathcal{E}(w(c_{o_3+1})) \\ \mathcal{E}(w(c_{o_3+2})) \\ \vdots \\ \mathcal{E}(w(c_{o_4})) \end{pmatrix},$$
(13)

which is the product of the main criterion weight score and the subcriterion weight score with respect to the corresponding main criterion.

Furthermore, we can calculate the dominance degree of the 3PRLP a_i over the 3PRLP a_k concerning the criterion $c_f (f = 1, 2, \dots, o_4)$ using the following expression:

$$\phi_f(a_i, a_k) = \begin{cases} \tau^{-1} \left| \sum_{\sigma \in \Lambda_{r_{if}} \cap \Lambda_{r_{kf}}} \sigma \times (p_{\sigma}^{r_{if}} - p_{\sigma}^{r_{kf}}) + \sum_{(\sigma \in \Lambda \setminus \Lambda_{r_{kf}})} p_{\sigma}^{r_{if}} - \sum_{(\sigma \in \Lambda \setminus \Lambda_{r_{if}})} p_{\sigma}^{r_{kf}} \right|, & \text{if } \mathcal{F}(r_{if}) - \mathcal{F}(r_{kf}) > 0, \\ 0, & \text{if } \mathcal{F}(r_{if}) - \mathcal{F}(r_{kf}) = 0, \\ -(\theta\tau)^{-1} \left| \sum_{\sigma \in \Lambda_{r_{kf}} \cap \Lambda_{r_{if}}} \sigma \times (p_{\sigma}^{r_{kf}} - p_{\sigma}^{r_{if}}) + \sum_{(\sigma \in \Lambda \setminus \Lambda_{r_{if}})} p_{\sigma}^{r_{kf}} - \sum_{(\sigma \in \Lambda \setminus \Lambda_{r_{kf}})} p_{\sigma}^{r_{if}} \right|, & \text{if } \mathcal{F}(r_{if}) - \mathcal{F}(r_{kf}) < 0. \end{cases}$$
(14)

In equation (14), the parameter θ represents the attenuation factor of the losses.

In the practical decision analysis processes, $\phi_f(a_i, a_k)$ is usually regarded as a gain when $\mathcal{F}(r_{if}) - \mathcal{F}(r_{kf}) > 0$,

$\phi_f(a_i, a_k)$ is deemed to be a nil when $\mathcal{F}(r_{if}) - \mathcal{F}(r_{kf}) = 0$, and $\phi_f(a_i, a_k)$ is counted to be a loss when $\mathcal{F}(r_{if}) - \mathcal{F}(r_{kf}) < 0$.

Then, the dominance matrix for the criterion $c_f (f = 1, 2, \dots, o_4)$ is obtained as follows:

$$D_f = [\phi_f(a_i, a_k)]_{m \times m} = \begin{bmatrix} & a_1 & a_2 & \cdots & a_m \\ a_1 & 0 & \phi_f(a_1, a_2) & \cdots & \phi_f(a_1, a_m) \\ a_2 & \phi_f(a_2, a_1) & 0 & \cdots & \phi_f(a_2, a_m) \\ \vdots & \vdots & \vdots & \vdots & \vdots \\ a_m & \phi_f(a_m, a_1) & \phi_f(a_m, a_2) & \cdots & 0 \end{bmatrix}. \quad (15)$$

Next, the total dominance degree of the 3PRLP $a_i (i = 1, 2, \dots, m)$ under $c_f (f = 1, 2, \dots, o_4)$ can be calculated by the following form:

$$\vartheta_f(a_i) = \sum_{k=1}^m \phi_f(a_i, a_k). \quad (16)$$

Accordingly, the total dominance matrix is determined as below:

$$D = [\vartheta_f(a_i)]_{m \times o_4} = \begin{bmatrix} & c_1 & c_2 & \cdots & c_{o_4} \\ a_1 & \sum_{k=1}^m \phi_1(a_1, a_k) & \sum_{k=1}^m \phi_2(a_1, a_k) & \cdots & \sum_{k=1}^m \phi_{o_4}(a_1, a_k) \\ a_2 & \sum_{k=1}^m \phi_1(a_2, a_k) & \sum_{k=1}^m \phi_2(a_2, a_k) & \cdots & \sum_{k=1}^m \phi_{o_4}(a_2, a_k) \\ \vdots & \vdots & \vdots & \vdots & \vdots \\ a_m & \sum_{k=1}^m \phi_1(a_m, a_k) & \sum_{k=1}^m \phi_2(a_m, a_k) & \cdots & \sum_{k=1}^m \phi_{o_4}(a_m, a_k) \end{bmatrix}. \quad (17)$$

4.2. Identifying the Group Utility and the Individual Regret. On the basis of the obtained dominance matrix $D = (\vartheta_f(a_i))_{m \times o_4}$, the dominance degree-based positive

ideal solutions (PISs) $\vartheta^+ = (\vartheta_1^+, \vartheta_2^+, \dots, \vartheta_{o_4}^+)$ is determined by the following equation:

$$\begin{aligned} \vartheta^+ &= (\vartheta_1^+, \vartheta_2^+, \dots, \vartheta_{o_4}^+) \\ &= \left(\max_{i=1}^m \sum_{k=1}^m \phi_1(a_i, a_k), \max_{i=1}^m \sum_{k=1}^m \phi_2(a_i, a_k), \dots, \max_{i=1}^m \sum_{k=1}^m \phi_{o_4}(a_i, a_k) \right), \end{aligned} \quad (18)$$

and the dominance degree-based negative ideal solutions (NISs) $\vartheta^- = (\vartheta_1^-, \vartheta_2^-, \dots, \vartheta_{o_4}^-)$ is calculated according to the following form:

$$\begin{aligned} \vartheta^- &= (\vartheta_1^-, \vartheta_2^-, \dots, \vartheta_{o_4}^-) \\ &= \left(\min_{i=1}^m \sum_{k=1}^m \phi_1(a_i, a_k), \min_{i=1}^m \sum_{k=1}^m \phi_2(a_i, a_k), \dots, \min_{i=1}^m \sum_{k=1}^m \phi_{o_4}(a_i, a_k) \right). \end{aligned} \quad (19)$$

Thus, the dominance degree-based maximum group utility $\text{Dom } S_i$ for the 3PRLP $a_i (i = 1, 2, \dots, m)$ is obtained by the following equation:

$$\text{Dom } S_i = \sum_{f=1}^{o_i} \mathcal{E}(w(c_f)) \bullet \frac{d(\vartheta_f^+, \vartheta_{if})}{d(\vartheta_f^+, \vartheta_f^-)}, \quad (20)$$

and the dominance degree-based minimum individual regret $\text{Dom } R_i$ for $a_i (i = 1, 2, \dots, m)$ is determined as follows:

$$\text{Dom } R_i = \max_{j=1}^{o_i} \mathcal{E}(w(c_f)) \bullet \frac{d(\vartheta_f^+, \vartheta_{if})}{d(\vartheta_f^+, \vartheta_f^-)}, \quad (21)$$

where $d(\vartheta_f^+, \vartheta_{if})$ is defined as follows:

$$d(\vartheta_f^+, \vartheta_{if}) = \max_{i=1}^m \sum_{k=1}^m \phi_f(a_i, a_k) - \sum_{k=1}^m \phi_f(a_i, a_k), \quad (22)$$

and $d(\vartheta_f^+, \vartheta_f^-)$ is defined as follows:

$$d(\vartheta_f^+, \vartheta_f^-) = \max_{i=1}^m \sum_{k=1}^m \phi_f(a_i, a_k) - \min_{i=1}^m \sum_{k=1}^m \phi_f(a_i, a_k). \quad (23)$$

Accordingly, the compromise solution of the 3PRLP $a_i (i = 1, 2, \dots, m)$ is obtained as follows:

$$\begin{aligned} \text{Dom } Q_i = t & \frac{\text{Dom } S_i - \min_i \{\text{Dom } S_i\}}{\max_i \{\text{Dom } S_i\} - \min_i \{\text{Dom } S_i\}} \\ & + (1-t) \frac{\text{Dom } R_i - \min_i \{\text{Dom } R_i\}}{\max_i \{\text{Dom } R_i\} - \min_i \{\text{Dom } R_i\}}, \end{aligned} \quad (24)$$

where the parameter $t (t \in [0, 1])$ is used to construct a convex combination of $\text{Dom } S_i$ and $\text{Dom } R_i$.

At length, we rank the 3PRLPs by sorting the scores of $\text{Dom } S_i$, $\text{Dom } R_i$, $\text{Dom } Q_i (i = 1, 2, \dots, m)$ in a decreasing order, and three ranking lists of 3PRLPs are obtained. Let $a_{\sigma(1)}$ be the 3PRLP with the first position in the ranking list derived by $\text{Dom } Q_i (i = 1, 2, \dots, m)$, and it is the compromise solution if the following two conditions (Cd1 and Cd2) are satisfied simultaneously [48, 49]:

- (i) Cd1: $\text{Dom } Q(a_{\sigma(2)}) - \text{Dom } Q(a_{\sigma(1)}) \geq (m-1)^{-1}$
- (ii) Cd2: the 3PRLP $a_{\sigma(1)}$ is also the 3PRLP with the first position in the ranking lists derived by $\text{Dom } S_i (i = 1, 2, \dots, m)$ and/or $\text{Dom } R_i (i = 1, 2, \dots, m)$

If Cd1 is not satisfied, we should identify the maximum value of M according to the following formula: $\text{Dom } Q(a_{\sigma(M)}) - \text{Dom } Q(a_{\sigma(1)}) < (1/(m-1))$, and the set of 3PRLPs $\{a_{\sigma(1)}, a_{\sigma(2)}, \dots, a_{\sigma(M)}\}$ is the compromise solution for the DM; if Cd2 is not satisfied, the set of 3PRLPs $\{a_{\sigma(1)}, a_{\sigma(2)}\}$ is the set of the compromise solutions.

Based on the above analysis, a brief algorithm of the proposed method is presented in Figure 1.

5. Case Study and Comparison Analysis

With the increasing cost of raw materials and pressure to minimize the environmental impacts of business activities, more and more car manufacturers plan to outsource their logistics activities to a sustainable 3PRLP. We here introduce a car manufacture case study to illustrate the usefulness and application of the developed method to the 3PRLP selection.

5.1. Description of the Selection Problems of 3PRLPs. The car manufacturer X considered for this research mainly produces business cars, home cars, and batteries in China. Its production capacity is more than hundred thousand cars annually. This manufacture follows the development route of independent R&D, production and brand and is determined to create a truly affordable national vehicle. Owing to lack of the available infrastructure and expertise, the management team of the manufacturer X recently plans to outsource the logistics activities to a sustainable 3PRLP. In order to select a most preferred 3PRLP from five potential 3PRLPs {3PRLP1, 3PRLP2, 3PRLP3, 3PRLP4, 3PRLP5} to cooperate with, 16 qualified assessed criteria from economic, environmental, social, and risk aspects are identified and are listed in Table 4 [4]. Considering the complexity and uncertainty of the realistic evaluation contexts, the weights of all evaluating criteria are represented by PLTSs and are provided in Table 4. LTs, HFLTSSs, and PLTSs with different granularities are simultaneously provided for assessors to capture the qualitative and uncertain performances of 3PRLPs. The performances of five 3PRLPs in terms of 16 criteria are provided in Table 5.

It is worthy mentioned in Table 5 that (1) the performances of 3PRLPs under *quality criterion*, *disposal criterion*, *eco-design production criterion*, and *operational risk criterion* are represented by single LTs based on LT set with the granularity $g(1) = 7$; (2) the performances of 3PRLPs under *cost criterion*, *recycle criterion*, *remanufacture and reuse criterion*, *environment protection certification criterion*, *green technology capability criterion*, and *voice of customer criterion* are represented by PLTSs based on LT set with the granularity $g(2) = 5$; (3) the performances of 3PRLPs under *lead time criterion* and *transportation criterion* are represented by single LTs based on LT set with the granularity $g(3) = 5$; (4) the performances of 3PRLPs under *delivery and services criterion* and *health and safety criterion* are represented by HFLTSSs based on LT set with the granularity $g(4) = 7$; (5) the performances of 3PRLPs under *lead time criterion* and *transportation criterion* are represented by single LTs based on LT set with the granularity $g(3) = 5$; and (6) the performances of 3PRLPs under *employment stability criterion* and *financial risk criterion* are represented by PLTSs based on LT set with the granularity $g(5) = 7$.

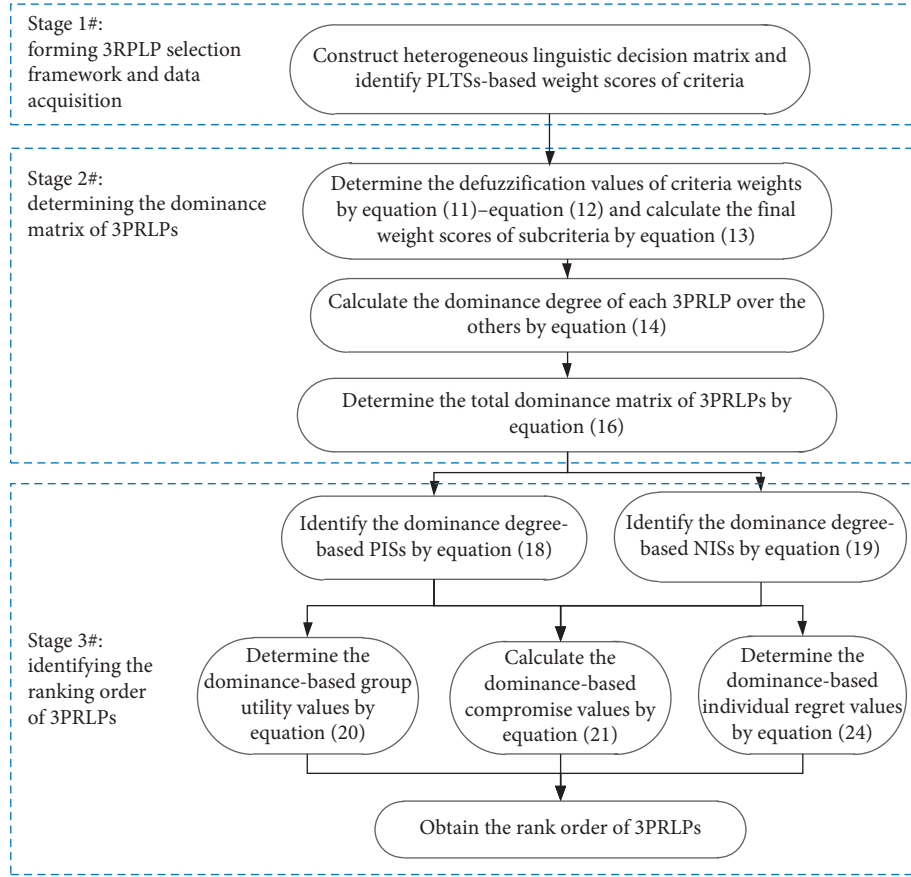


FIGURE 1: Flowchart of the algorithm of the developed method.

TABLE 4: The main criteria and subcriteria for 3PRLP selection and criteria weights.

Main criteria	Weights of main criteria	Subcriteria	Weights of subcriteria
C_1	$\{I_4^{(5)}(0.4), I_5^{(5)}(0.6)\}$	c_1	$\{I_3^{(5)}(0.2), I_4^{(5)}(0.4), I_5^{(5)}(0.4)\}$
		c_2	$\{I_4^{(5)}(0.7), I_5^{(5)}(0.3)\}$
		c_3	$\{I_4^{(5)}(1.0)\}$
		c_4	$\{I_2^{(5)}(0.3), I_3^{(5)}(0.7)\}$
		c_5	$\{I_3^{(5)}(0.3), I_4^{(5)}(0.4), I_5^{(5)}(0.3)\}$
C_2	$\{I_3^{(5)}(0.3), I_4^{(5)}(0.4), I_5^{(5)}(0.3)\}$	c_6	$\{I_3^{(5)}(1.0)\}$
		c_7	$\{I_3^{(5)}(0.3), I_4^{(5)}(0.4), I_5^{(5)}(0.3)\}$
		c_8	$\{I_2^{(5)}(0.3), I_3^{(5)}(0.7)\}$
		c_9	$\{I_4^{(5)}(1.0)\}$
		c_{10}	$\{I_3^{(5)}(0.7), I_4^{(5)}(0.3)\}$
		c_{11}	$\{I_3^{(5)}(1.0)\}$
C_3	$\{I_3^{(5)}(1.0)\}$	c_{12}	$\{I_3^{(5)}(0.6), I_4^{(5)}(0.4)\}$
		c_{13}	$\{I_4^{(5)}(1.0)\}$
		c_{14}	$\{I_4^{(5)}(0.7), I_5^{(5)}(0.3)\}$
C_4	$\{I_3^{(5)}(0.6), I_4^{(5)}(0.4)\}$	c_{15}	$\{I_3^{(5)}(0.3), I_4^{(5)}(0.4), I_5^{(5)}(0.3)\}$
		c_{16}	$\{I_3^{(5)}(0.6), I_4^{(5)}(0.4)\}$

5.2. Selection Results Derived by the Developed Method. With the aid of the dominance degree-based heterogeneous linguistic decision-making technique, the most preferred

3PRLP will be determined for the case company. The detailed calculation and selection processes are introduced as follows. First, all the nonhomogeneous linguistic assessed

TABLE 5: The performances of five 3PRLPs under 16 criteria.

	Quality	Cost	Lead time	Delivery and services
3PRLP1	$I_5^{(7)}$	$\{I_3^{(5)}(0.3), I_4^{(5)}(0.4), I_5^{(5)}(0.3)\}$	$I_3^{(5)}$	$\{I_4^{(7)}, I_5^{(7)}\}$
3PRLP2	$I_3^{(7)}$	$\{I_4^{(5)}(1.0)\}$	$I_4^{(5)}$	$\{I_3^{(7)}\}$
3PRLP3	$I_6^{(7)}$	$\{I_3^{(5)}(0.6), I_4^{(5)}(0.4)\}$	$I_3^{(5)}$	$\{I_4^{(7)}\}$
3PRLP4	$I_3^{(7)}$	$\{I_3^{(5)}(1.0)\}$	$I_5^{(5)}$	$\{I_2^{(7)}, I_3^{(7)}\}$
3PRLP5	$I_4^{(7)}$	$\{I_4^{(5)}(0.7), I_5^{(5)}(0.3)\}$	$I_2^{(5)}$	$\{I_3^{(7)}, I_4^{(7)}, I_5^{(7)}\}$
	Transportation	Recycle	Disposal	Remanufacture and reuse
3PRLP1	$I_4^{(5)}$	$\{I_2^{(5)}(0.3), I_3^{(5)}(0.7)\}$	$I_5^{(7)}$	$\{I_4^{(5)}(0.7), I_5^{(5)}(0.3)\}$
3PRLP2	$I_2^{(5)}$	$\{I_3^{(5)}(1.0)\}$	$I_3^{(7)}$	$\{I_4^{(5)}(1.0)\}$
3PRLP3	$I_3^{(5)}$	$\{I_4^{(5)}(0.7), I_5^{(5)}(0.3)\}$	$I_6^{(7)}$	$\{I_3^{(5)}(0.6), I_4^{(5)}(0.4)\}$
3PRLP4	$I_5^{(5)}$	$\{I_3^{(5)}(0.4), I_4^{(5)}(0.4), I_5^{(5)}(0.2)\}$	$I_4^{(7)}$	$\{I_4^{(7)}(0.5), I_5^{(7)}(0.3), I_6^{(7)}(0.2)\}$
3PRLP5	$I_3^{(5)}$	$\{I_5^{(5)}(1.0)\}$	$I_6^{(7)}$	$\{I_4^{(5)}(0.7), I_5^{(5)}(0.3)\}$
	Health and safety	Environment protection certification	Eco-design production	Green technology capability
3PRLP1	$\{I_3^{(7)}, I_4^{(7)}, I_5^{(7)}\}$	$\{I_2^{(5)}(0.6), I_3^{(5)}(0.4)\}$	$I_4^{(7)}$	$\{I_2^{(5)}(1.0)\}$
3PRLP2	$\{I_4^{(7)}, I_5^{(7)}\}$	$\{I_3^{(5)}(0.5), I_4^{(5)}(0.2), I_5^{(5)}(0.3)\}$	$I_3^{(7)}$	$\{I_4^{(5)}(0.7), I_5^{(5)}(0.3)\}$
3PRLP3	$\{I_6^{(7)}\}$	$\{I_4^{(5)}(0.7), I_5^{(5)}(0.3)\}$	$I_4^{(7)}$	$\{I_3^{(5)}(0.6), I_4^{(5)}(0.4)\}$
3PRLP4	$\{I_5^{(7)}\}$	$\{I_3^{(5)}(1.0)\}$	$I_6^{(7)}$	$\{I_4^{(5)}(1.0)\}$
3PRLP5	$\{I_6^{(7)}, I_7^{(7)}\}$	$\{I_3^{(5)}(0.2), I_4^{(5)}(0.8)\}$	$I_4^{(7)}$	$\{I_3^{(5)}(0.4), I_4^{(5)}(0.4), I_5^{(5)}(0.2)\}$
	Voice of customer	Employment stability	Operational risk	Financial risk
3PRLP1	$\{I_5^{(5)}(1.0)\}$	$\{I_4^{(7)}(0.5), I_5^{(7)}(0.3), I_6^{(7)}(0.2)\}$	$\{I_6^{(7)}, I_7^{(7)}\}$	$\{I_4^{(7)}(1.0)\}$
3PRLP2	$\{I_3^{(5)}(0.6), I_4^{(5)}(0.4)\}$	$\{I_5^{(7)}(0.6), I_6^{(7)}(0.4)\}$	$\{I_5^{(7)}\}$	$\{I_2^{(7)}(0.2), I_3^{(7)}(0.8)\}$
3PRLP3	$\{I_4^{(5)}(1.0)\}$	$\{I_4^{(7)}(1.0)\}$	$\{I_4^{(7)}, I_5^{(7)}\}$	$\{I_4^{(7)}(0.4), I_5^{(7)}(0.3), I_6^{(7)}(0.3)\}$
3PRLP4	$\{I_4^{(5)}(0.8), I_5^{(5)}(0.2)\}$	$\{I_6^{(7)}(1.0)\}$	$\{I_5^{(7)}\}$	$\{I_5^{(7)}(1.0)\}$
3PRLP5	$\{I_2^{(5)}(0.3), I_3^{(5)}(0.7)\}$	$\{I_3^{(7)}(0.3), I_4^{(7)}(0.7)\}$	$\{I_3^{(7)}, I_4^{(7)}, I_5^{(7)}\}$	$\{I_4^{(7)}(0.7), I_5^{(7)}(0.3)\}$

values in Table 5 are unified into the form of PLTSs and are shown in Table 6.

In light of the assessment data in Table 4, the defuzzification scores of the main criteria weights are determined according to equation (11) as follows:

$$\begin{aligned}
 \mathcal{E}(w(\text{mc}_1)) &= 0.3089, \\
 \mathcal{E}(w(\text{mc}_2)) &= 0.2673, \\
 \mathcal{E}(w(\text{mc}_3)) &= 0.1981, \\
 \mathcal{E}(w(\text{mc}_4)) &= 0.2258.
 \end{aligned} \tag{25}$$

According to equations (12) and (13), the final weight scores of the subcriteria are obtained in Table 7.

Afterwards, take *voice of customer criterion* for example, we can calculate the dominance degrees of one 3PRLP over another one under this criterion according to equation (14), and the dominance matrix under *voice of customer criterion* is obtained as follows:

$$D_{(\text{voice of customer})} = \begin{bmatrix} & 3\text{PRLP}_1 & 3\text{PRLP}_2 & 3\text{PRLP}_3 & 3\text{PRLP}_4 & 3\text{PRLP}_5 \\ 3\text{PRLP}_1 & 0 & 0.32 & 0.20 & 0.16 & 0.46 \\ 3\text{PRLP}_2 & -0.32 & 0 & -0.12 & -0.16 & -0.14 \\ 3\text{PRLP}_3 & -0.20 & 0.12 & 0 & -0.04 & 0.26 \\ 3\text{PRLP}_4 & -0.16 & 0.16 & 0.04 & 0 & 0.30 \\ 3\text{PRLP}_5 & -0.46 & 0.14 & 0.26 & 0.30 & 0 \end{bmatrix}. \tag{26}$$

TABLE 6: Probabilistic linguistic-based performances of five 3PRLPs under 16 criteria.

	Quality	Cost	Lead time	Delivery and services
3PRLP1	$\{I_5^{(7)}(1.0)\}$	$\{I_3^{(5)}(0.3), I_4^{(5)}(0.4), I_5^{(5)}(0.3)\}$	$\{I_3^{(5)}(1.0)\}$	$\{I_4^{(7)}(0.5), I_5^{(7)}(0.5)\}$
3PRLP2	$\{I_3^{(7)}(1.0)\}$	$\{I_4^{(5)}(1.0)\}$	$\{I_4^{(5)}(1.0)\}$	$\{I_5^{(7)}(1.0)\}$
3PRLP3	$\{I_6^{(7)}(1.0)\}$	$\{I_3^{(5)}(0.6), I_4^{(5)}(0.4)\}$	$\{I_3^{(5)}(1.0)\}$	$\{I_4^{(7)}(1.0)\}$
3PRLP4	$\{I_3^{(7)}(1.0)\}$	$\{I_5^{(5)}(1.0)\}$	$\{I_5^{(5)}(1.0)\}$	$\{I_2^{(7)}(0.5), I_3^{(7)}(0.5)\}$
3PRLP5	$\{I_4^{(7)}(1.0)\}$	$\{I_4^{(5)}(0.7), I_5^{(5)}(0.3)\}$	$\{I_2^{(5)}(1.0)\}$	$\{I_3^{(7)}(\frac{1}{3}), I_4^{(7)}(\frac{1}{3}), I_5^{(7)}(\frac{1}{3})\}$
	Transportation	Recycle	Disposal	Remanufacture and reuse
3PRLP1	$\{I_4^{(5)}(1.0)\}$	$\{I_2^{(5)}(0.3), I_3^{(5)}(0.7)\}$	$\{I_5^{(7)}(1.0)\}$	$\{I_4^{(5)}(0.7), I_5^{(5)}(0.3)\}$
3PRLP2	$\{I_2^{(5)}(1.0)\}$	$\{I_3^{(5)}(1.0)\}$	$\{I_3^{(7)}(1.0)\}$	$\{I_4^{(5)}(1.0)\}$
3PRLP3	$\{I_3^{(5)}(1.0)\}$	$\{I_4^{(5)}(0.7), I_5^{(5)}(0.3)\}$	$\{I_6^{(7)}(1.0)\}$	$\{I_3^{(5)}(0.6), I_4^{(5)}(0.4)\}$
3PRLP4	$\{I_5^{(5)}(1.0)\}$	$\{I_3^{(5)}(0.4), I_4^{(5)}(0.4), I_5^{(5)}(0.2)\}$	$\{I_4^{(7)}(1.0)\}$	$\{I_4^{(7)}(0.5), I_5^{(7)}(0.3), I_6^{(7)}(0.2)\}$
3PRLP5	$\{I_3^{(5)}(1.0)\}$	$\{I_5^{(5)}(1.0)\}$	$\{I_6^{(7)}(1.0)\}$	$\{I_4^{(5)}(0.7), I_5^{(5)}(0.3)\}$
	Health and safety	Environment protection certification	Eco-design production	Green technology capability
3PRLP1	$\{I_3^{(7)}(\frac{1}{3}), I_4^{(7)}(\frac{1}{3}), I_5^{(7)}(\frac{1}{3})\}$	$\{I_2^{(5)}(0.6), I_3^{(5)}(0.4)\}$	$\{I_4^{(7)}(1.0)\}$	$\{I_2^{(5)}(1.0)\}$
3PRLP2	$\{I_4^{(7)}(0.5), I_5^{(7)}(0.5)\}$	$\{I_3^{(5)}(0.5), I_4^{(5)}(0.2), I_5^{(5)}(0.3)\}$	$\{I_3^{(7)}(1.0)\}$	$\{I_4^{(5)}(0.7), I_5^{(5)}(0.3)\}$
3PRLP3	$\{I_6^{(7)}(1.0)\}$	$\{I_4^{(5)}(0.7), I_5^{(5)}(0.3)\}$	$\{I_4^{(7)}(1.0)\}$	$\{I_3^{(5)}(0.6), I_4^{(5)}(0.4)\}$
3PRLP4	$\{I_5^{(7)}(1.0)\}$	$\{I_3^{(5)}(1.0)\}$	$\{I_6^{(7)}(1.0)\}$	$\{I_4^{(5)}(1.0)\}$
3PRLP5	$\{I_6^{(7)}(0.5), I_7^{(7)}(0.5)\}$	$\{I_3^{(5)}(0.2), I_4^{(5)}(0.8)\}$	$\{I_4^{(7)}(1.0)\}$	$\{I_3^{(5)}(0.4), I_4^{(5)}(0.4), I_5^{(5)}(0.2)\}$
	Voice of customer	Employment stability	Operational risk	Financial risk
3PRLP1	$\{I_5^{(5)}(1.0)\}$	$\{I_4^{(7)}(0.5), I_5^{(7)}(0.3), I_6^{(7)}(0.2)\}$	$\{I_6^{(7)}(0.5), I_7^{(7)}(0.5)\}$	$\{I_4^{(7)}(1.0)\}$
3PRLP2	$\{I_3^{(5)}(0.6), I_4^{(5)}(0.4)\}$	$\{I_5^{(7)}(0.6), I_6^{(7)}(0.4)\}$	$\{I_5^{(7)}(1.0)\}$	$\{I_2^{(7)}(0.2), I_3^{(7)}(0.8)\}$
3PRLP3	$\{I_4^{(5)}(1.0)\}$	$\{I_4^{(7)}(1.0)\}$	$\{I_4^{(7)}(0.5), I_5^{(7)}(0.5)\}$	$\{I_4^{(7)}(0.4), I_5^{(7)}(0.3), I_6^{(7)}(0.3)\}$
3PRLP4	$\{I_4^{(5)}(0.8), I_5^{(5)}(0.2)\}$	$\{I_6^{(7)}(1.0)\}$	$\{I_5^{(7)}(1.0)\}$	$\{I_5^{(7)}(1.0)\}$
3PRLP5	$\{I_2^{(5)}(0.3), I_3^{(5)}(0.7)\}$	$\{I_3^{(7)}(0.3), I_4^{(7)}(0.7)\}$	$\{I_3^{(7)}(\frac{1}{3}), I_4^{(7)}(\frac{1}{3}), I_5^{(7)}(\frac{1}{3})\}$	$\{I_4^{(7)}(0.7), I_5^{(7)}(0.3)\}$

TABLE 7: The final weight scores of sixteen subcriteria.

Subcriteria	Weight scores	Subcriteria	Weight scores
Quality	0.0851	Transportation	0.0810
Cost	0.0871	Recycle	0.0526
Lead time	0.0810	Disposal	0.0701
Delivery and services	0.0539	Remanufacture and reuse	0.0467
Health and safety	0.0701	Voice of customer	0.0520
Environment protection certification	0.0579	Employment stability	0.0559
Eco-design production	0.0526	Operational risk	0.0592
Green technology capability	0.0442	Financial risk	0.0504

Similarly, the dominance matrix under the other criteria can be calculated. Further, the total dominance degrees of 3PRLPs under different criteria are determined according to equation (16) and are shown in Table 8.

By using equations (18) and (19), the dominance degree-based PISs $\vartheta^+ = (\vartheta_1^+, \vartheta_2^+, \dots, \vartheta_{16}^+)$ and the dominance degree-

based NISs $\vartheta^- = (\vartheta_1^-, \vartheta_2^-, \dots, \vartheta_{16}^-)$ are determined, respectively, and these calculation results are shown in Table 9.

In light of the obtained data in Tables 7–9, the dominance degree-based maximum group utility scores and the dominance degree-based minimum individual regret scores are calculated according to equations (20) and (21),

TABLE 8: The total dominance degrees of 3PRLPs over different criteria.

	Quality	Cost	Lead time	Delivery and services
3PRLP1	0.5714	0.42	-0.4	0.6714
3PRLP2	-0.8571	0.22	0.6	-0.4
3PRLP3	1.2857	-0.38	-0.4	0.3143
3PRLP4	-0.8571	-0.78	1.6	-0.9
3PRLP5	-0.1429	0.52	-1.4	0.3143
	Transportation	Recycle	Disposal	Remanufacture and reuse
3PRLP1	0.6	-1.06	0.1429	0.16
3PRLP2	-1.4	-0.76	-1.2857	-0.14
3PRLP3	-0.4	0.54	0.8571	-0.74
3PRLP4	1.6	0.04	-0.5714	0.56
3PRLP5	-0.4	1.24	0.8571	0.16
	Health and safety	Environment protection certification	Eco-design production	Green technology capability
3PRLP1	-0.8571	-1.06	-0.1429	-1.5
3PRLP2	-0.5	0.34	-0.8571	0.8
3PRLP3	0.5714	0.84	-0.1429	-0.1
3PRLP4	-0.1429	-0.46	1.2857	0.5
3PRLP5	0.9286	0.34	-0.1429	0.3
	Voice of customer	Employment stability	Operational risk	Financial risk
3PRLP1	1.14	-0.0429	1.0714	-0.1429
3PRLP2	-0.74	0.4571	0	-1
3PRLP3	0.14	0.5429	-0.3571	0.5
3PRLP4	0.34	0.8857	0	0.5714
3PRLP5	-0.88	-0.7571	-0.7143	0.0714

respectively. These calculation results are shown in Table 10. Let the value of t be 0.5 from an equilibrium point of view, the dominance degree-based compromise scores of $3PRLP_i$ ($i = 1, 2, 3, 4, 5$) are calculated according to equation (24) and are also shown in Table 10.

From the calculation results in Table 10, we can see that 3PRLP3 is the best in the ranking lists according to the values of $Dom S_i$, $Dom R_i$, and $Dom Q_i$, respectively. Obviously, 3PRLP3 is the best choice for the car manufacturer X and this selection result simultaneously satisfies the conditions of $Cd1$ and $Cd2$. Clearly, the proposed approach provides informative insights to managers/DMs of car manufacturers for selecting an appropriate 3PRLP to cooperate with. First, this developed method offers DMs an insight of cognitive contribution of 3PRLP criteria and provides a good way for DMs to evaluate 3PRLPs under heterogeneous linguistic environments. Second, the developed method gives a better understanding of the influence of DM's psychology in the 3PRLP selection. The results indicate that the developed method not only well avoids the potential loss risks but also balances group utility scores and individual regret scores. The authenticity of 3PRLP selection results can be greatly enhanced.

5.3. Sensitivity Analysis. In our developed method, a parameter t is introduced to coordinate the group utility and the individual regret. One of the advantages of the developed method is that it allows DM to modify the value of t according to his/her individual preferences. For example, when one DM highlights the maximization of group utility, the value of t will become larger, and $0.5 \leq t \leq 1$, conversely, the value of t will become smaller when DM has emphasized

on the minimization of individual regret, and $0 \leq t \leq 0.5$ [50]. We next analyze the effects of the parameter t on ranking orders of 3PRLPs. We calculate the ranking results of 3PRLPs by modifying the value of t from 1.0 to 0. The corresponding ranking results of 3PRLPs with the different values of t ($t = 1.0, 0.8, 0.6, 0.4, 0.2, 0.0$) are obtained. These calculation results are shown in Table 11 and are depicted in Figure 2.

It is easily observed from Table 11 and Figure 2 that the compromise scores of 3PRLP2 are increasing as the value of the parameter t changes from 0.0 to 1.0, the compromise scores of 3PRLP3 are constant, while the compromise scores of 3PRLP1, 3PRLP4 and 3PRLP5 are decreasing. In particular, when the value of the parameter t is provided as 1.0, then the ranking order of 3PRLPs is $3PRLP3 > 3PRLP4 > 3PRLP5 > 3PRLP1 > 3PRLP2$ which means that the developed method only takes the maximization of group utility into account, and while the value of the parameter t is assigned as 0.0, then the ranking order of 3PRLPs is $3PRLP3 > 3PRLP1 > 3PRLP5 > 3PRLP2 > 3PRLP4$, and in this situation, the developed method only takes the minimization of individual regret into account. When $t = 0.8, 0.6, 0.4, 0.2$, the ranking orders of 3PRLPs are consistent ($3PRLP3 > 3PRLP1 > 3PRLP5 > 3PRLP4 > 3PRLP2$) although the ranking scores of 3PRLPs are different, which trade-offs the group utility and the individual regret. Clearly, all of these ranking orders of 3PRLPs show that 3PRLP3 is the best choice for this manufacture although the DM has different preferences between group utility and individual regret. In other words, the ranking result of 3PRLPs is insensitive to the values of t when using our developed method in the above case study.

TABLE 9: The dominance-based PISs and dominance-based NISs under various criteria.

	Quality	Cost	Lead time	Delivery and services
PIS	1.2857	0.52	1.6	0.6714
NIS	-0.8571	-0.78	-1.4	-0.9
	Transportation	Recycle	Disposal	Remanufacture and reuse
PIS	1.6	1.24	0.8571	0.56
NIS	-1.4	-1.06	-1.2857	-0.74
	Health and safety	Environment protection certification	Eco-design production	Green technology capability
PIS	0.9286	0.84	1.2857	0.8
NIS	-0.8571	-1.06	-0.8571	-1.5
	Voice of customer	Employment stability	Operational risk	Financial risk
PIS	1.14	0.8857	1.0714	0.5714
NIS	-0.88	-0.7571	-0.7143	-1

TABLE 10: The scores of $\text{Dom } S_i$, $\text{Dom } R_i$, and $\text{Dom } Q_i$ of each 3PRLP and the corresponding rank.

	$\text{Dom } S_i$	Ranking order	$\text{Dom } R_i$	Ranking order	$\text{Dom } Q_i$	Ranking order
3PRLP1	0.4683	4	0.0701	2	0.3172	2
3PRLP2	0.6639	5	0.0851	4	0.9623	5
3PRLP3	0.3968	1	0.0603	1	0.0000	1
3PRLP4	0.4439	2	0.0871	5	0.5882	4
3PRLP5	0.4615	3	0.0810	3	0.5078	3

TABLE 11: The compromise scores of 3PRLPs with different values of t .

	3PRLP1	3PRLP2	3PRLP3	3PRLP4	3PRLP5
$t = 1.0$	0.2676	1.0000	0.0000	0.1765	0.2420
$t = 0.8$	0.3172	0.9623	0.0000	0.5882	0.5078
$t = 0.6$	0.3073	0.9698	0.0000	0.5059	0.4547
$t = 0.4$	0.3272	0.9547	0.0000	0.6706	0.5610
$t = 0.2$	0.3470	0.9396	0.0000	0.8353	0.6673
$t = 0.0$	0.3669	0.9246	0.0000	1.0000	0.7737

5.4. Comparison Analysis. The aforementioned 3PRLP selection methods including TOPSIS selection method [33], VIKOR selection method [34], and VIKOR-TOPSIS selection method [36], which ranked and selected 3PRLPs based on the relative closeness to the ideal solution without considering the psychological factors of DM, are closest to our developed method. It is worth mentioning that these three methods are only suitable to deal with the data represented by real numbers, single LTs, and/or neighborhood rough set but are not able to manage the assessed data represented by HFLTSS and/or PLTSS as the above-mentioned case study. To deal with this issue, these three methods are next modified. Firstly, probabilistic linguistic PISs and NISs are determined by the following equations:

$$\begin{aligned}
3\text{PRLP}^+ &= \left\{ \langle c_f, \max_i \mathcal{F}(L_{if}(p)) \rangle \mid f \in \{1, 2, \dots, o_4\} \right\} \\
&= \{ \langle c_1, L_1^+(p) \rangle, \langle c_2, L_2^+(p) \rangle, \dots, \langle c_{o_4}, L_{o_4}^+(p) \rangle \}, \\
3\text{PRLP}^- &= \left\{ \langle c_f, \min_i \mathcal{F}(L_{if}(p)) \rangle \mid f \in \{1, 2, \dots, o_4\} \right\} \\
&= \{ \langle c_1, L_1^-(p) \rangle, \langle c_2, L_2^-(p) \rangle, \dots, \langle c_{o_4}, L_{o_4}^-(p) \rangle \},
\end{aligned} \tag{27}$$

where $\mathcal{F}(\bullet)$ is the probabilistic linguistic ranking function proposed in Definition 6.

In terms of the modified TOPSIS method [33], the relative closeness index Id_i of the 3PRLP a_i ($i = 1, 2, \dots, m$) to the ideal solution can be calculated by using the following formula:

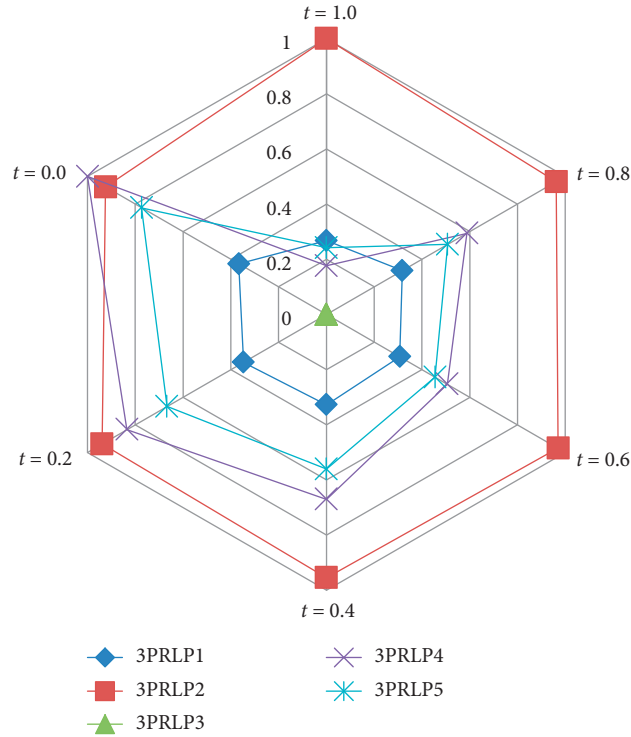


FIGURE 2: The diagrammatic presentation of the 3PRLP compromise scores.

$$Id_i = \frac{\sum_{f=1}^{o_4} \mathcal{E}(w(c_f))d(L_{if}(p), L_f^-(p))}{\sum_{f=1}^{o_4} \mathcal{E}(w(c_f))d(L_{if}(p), L_f^+(p)) + \sum_{f=1}^{o_4} \mathcal{E}(w(c_f))d(L_{if}(p), L_f^-(p))}, \quad (28)$$

where $\mathcal{E}(\bullet)$ is the ratio index-based probabilistic linguistic defuzzification function proposed in Definition 7 and $d(\bullet, \bullet)$ is probabilistic linguistic distance measure introduced in Definition 5.

By equation (28), the ranking order of 3PRLPs in the abovementioned case study is obtained based on the modified TOPSIS method and is shown in Table 12.

In terms of the modified VIKOR method [34], the maximum group utility S_i of the 3PRLP a_i ($i = 1, 2, \dots, m$) is obtained as follows:

$$S_i = \sum_{f=1}^{o_4} \mathcal{E}(w(c_f)) \bullet d(L_{if}(p), L_f^+(p)) d(L_f^+(p), L_f^-(p))^{-1}. \quad (29)$$

And the minimum individual regret R_i of a_i ($i = 1, 2, \dots, m$) is calculated by the following equation:

$$R_i = \max_{j=1}^{o_4} \mathcal{E}(w(c_j)) d(L_{if}(p), L_f^+(p)) d(L_f^+(p), L_f^-(p))^{-1}. \quad (30)$$

Then, the compromise solution Q_i of a_i ($i = 1, 2, \dots, m$) is obtained as follows:

$$Q_i = \chi \frac{S_i - \min_i\{S_i\}}{\max_i\{S_i\} - \min_i\{S_i\}} + (1 - \chi) \frac{R_i - \min_i\{R_i\}}{\max_i\{R_i\} - \min_i\{R_i\}}, \quad 0 \leq \chi \leq 1. \quad (31)$$

By equation (31) with $\chi = 0.5$, the ranking order of these five 3PRLPs is obtained based on the modified VIKOR method and is shown in Table 12.

TABLE 12: Ranking orders of 3PRLPs obtained by different 3PRLP selection methods.

3PRLP selection methods	Ranking orders of 3PRLPs
The modified TOPSIS method [33]	3PRLP4 > 3PRLP5 > 3PRLP1 > 3PRLP3 > 3PRLP2
The modified VIKOR method [34]	3PRLP4 > 3PRLP5 > 3PRLP3 > 3PRLP1 > 3PRLP2
The modified TOPSIS-VIKOR method [36]	3PRLP4 > 3PRLP3 > 3PRLP5 > 3PRLP2 > 3PRLP1
Our proposed method	3PRLP3 > 3PRLP1 > 3PRLP5 > 3PRLP4 > 3PRLP2

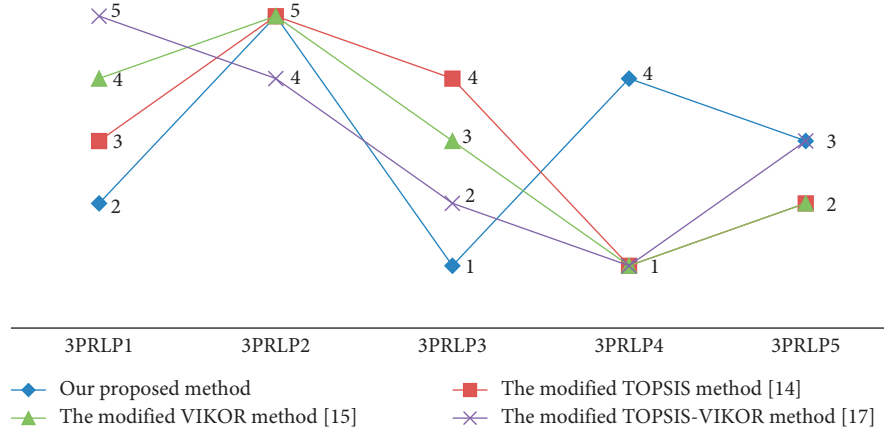


FIGURE 3: The pictorial representation of ranking orders of 3PRLPs.

In terms of the modified TOPSIS-VIKOR method [36], the relative closeness index Rd_i of each 3PRLP to the ideal solution is determined as follows:

$$Rd_i = \eta \times \frac{\sum_{f=1}^{o_4} E(w(c_f))d(L_{if}(p), L_f^-(p))}{\sum_{f=1}^{o_4} E(w(c_f))d(L_{if}(p), L_f^+(p)) + \sum_{f=1}^{o_4} E(w(c_f))d(L_{if}(p), L_f^-(p))} + (1 - \eta) \times \frac{\min_i(E(w(c_f))d(L_{if}(p), L_f^-(p)))}{\max_i(E(w(c_f))d(L_{if}(p), L_f^+(p))) + \min_i(E(w(c_f))d(L_{if}(p), L_f^-(p)))}. \quad (32)$$

Accordingly, by equation (32) with $\eta = 0.5$, the ranking order of these five 3PRLPs is obtained based on the modified TOPSIS-VIKOR method and is shown in Table 12. All the above comparison results in Table 12 are depicted in Figure 3.

The comparison results in Table 12 and in Figure 3 indicate that the ranking order of 3PRLPs obtained by the developed method is completely different from that obtained by the modified 3PRLP selection methods [33, 34, 36]. Specifically, 3PRLP3 was regarded as the most preferred alternative by the proposed dominance-based heterogeneous linguistic decision-making method, while the modified TOPSIS [33], the modified VIKOR [34], and the modified TOPSIS-VIKOR [36] all preferred 3PRLP4. The main reason for these differences lies in that the assumptions of DM's rationality between our developed method and the modified methods were distinct. The modified methods

[33, 34, 36] ranked the 3PRLPs under the strict assumption that the DM is complete rationality. In contrast, the proposed dominance-based heterogeneous linguistic MCDM method is under the assumption that the DM is bounded rationality and taking fully into account psychology behavior of DM. Therefore, it is not hard to see that the biggest advantage of our proposed method, compared with the modified 3PRLP selection methods [33, 34, 36], is that it took fully into consideration the bounded rationality of DM and the selection result with the most preferred 3PRLP was more consistent with the reality.

6. Conclusions

Selecting an appropriate 3PRLP to cooperate with is a key step for manufacturers to achieve the goals of sustainable development and environmental protection. In this paper,

we have developed a dominance degree-based heterogeneous linguistic decision-making method for aiding manufacturers to identify a sustainable 3PRLP. The first advantage of the developed method is that it successfully manages qualitative and heterogeneous uncertain inputs that usually arise from real-world 3PRLP evaluation process. Heterogeneous linguistic expression forms with different granularities give great freedom for evaluators to provide their preferences on 3PRLPs and can well improve the accuracy of evaluation data. The second advantage is that the dominance degrees of each 3PRLP under various criteria related to the others are taken fully into account. It can consider the psychological factor of DM in the 3PRLP selection process and well avoid the potential loss risks. The third advantage is that it carefully balances the maximum group utility and the minimum individual regret. The sensitivity analysis and the comparison analysis with similar 3PRLP selection methods [33, 34, 36] indicated that the developed dominance-based heterogeneous linguistic MCDM method can obtain more precise and reliable selection results. On the other hand, we have developed a new ratio index-based probabilistic linguistic ranking method for comparing the magnitude of PLTSs and have proved its desirable properties. We have also proposed a useful ratio-based defuzzification function of PLTSs, which can well model probabilistic linguistic-based weights of criteria. Despite its advantage, this study has several limitations which may sever as suggestions for further research. First of all, the relationships among the assessed criteria of 3PRLPs are assumed in the developed method to be independent. How to deal with various types of relationships which exist among criteria is an interesting research issue with challenges, especially for the selection of 3PRLPs. Moreover, in order to deal automatically with complex 3PRLP selection problems, how to construct an appropriate decision support system on the basis of the developed technique is also an interesting research idea.

Data Availability

All data used in our study are provided in this manuscript. The reviewers and readers can access the data by Tables 4–11 in the manuscript.

Conflicts of Interest

The authors declare that they have no conflicts of interest.

Acknowledgments

The work was supported by the National Natural Science Foundation of China (nos. 71661010 and 71901112), the Major Program of the National Social Science Foundation of China (no. 19ZDA111), the Natural Science Foundation of Jiangxi Province of China (no. 20161BAB211020), and the Technology Project of Education Department of Jiangxi Province of China (no. GJJ170340).

References

- [1] Y.-L. Li, C.-S. Ying, K.-S. Chin, H.-T. Yang, and J. Xu, "Third-party reverse logistics provider selection approach based on hybrid-information MCDM and cumulative prospect theory," *Journal of Cleaner Production*, vol. 195, pp. 573–584, 2018.
- [2] Z. Xu, "Deviation measures of linguistic preference relations in group decision making," *Omega*, vol. 33, no. 3, pp. 249–254, 2005.
- [3] R. K. Mavi, M. Goh, and N. Zarebakhshnia, "Sustainable third-party reverse logistic provider selection with fuzzy SWARA and fuzzy MOORA in plastic industry," *The International Journal of Advanced Manufacturing Technology*, vol. 91, no. 5–8, pp. 2401–2418, 2017.
- [4] N. Zarebakhshnia, H. Soleimani, and H. Ghaderi, "Sustainable third-party reverse logistics provider evaluation and selection using fuzzy SWARA and developed fuzzy COPRAS in the presence of risk criteria," *Applied Soft Computing*, vol. 65, pp. 307–319, 2018.
- [5] H. Liao, R. Qin, C. Gao, X. Wu, A. Hafezalkotob, and F. Herrera, "Score-HeDLiSF: a score function of hesitant fuzzy linguistic term set based on hesitant degrees and linguistic scale functions: an application to unbalanced hesitant fuzzy linguistic MULTIMOORA," *Information Fusion*, vol. 48, pp. 39–54, 2019.
- [6] Y. Liu, R. M. Rodriguez, H. Hagrass, H. Lu, K. Qin, and L. Martinez, "Type-2 fuzzy envelope of hesitant fuzzy linguistic term set: a new representation model of comparative linguistic expression," *IEEE Transactions on Fuzzy Systems*, vol. 27, no. 12, pp. 2312–2326, 2019.
- [7] R. M. Li, L. Martinez, and F. Herrera, "Hesitant fuzzy linguistic term sets for decision making," *IEEE Transactions on Fuzzy Systems*, vol. 20, no. 1, pp. 109–119, 2012.
- [8] Q. Pang, H. Wang, and Z. Xu, "Probabilistic linguistic term sets in multi-attribute group decision making," *Information Sciences*, vol. 369, pp. 128–143, 2016.
- [9] H. Liao, X. Mi, and Z. Xu, "A survey of decision-making methods with probabilistic linguistic information: bibliometrics, preliminaries, methodologies, applications and future directions," *Fuzzy Optimization and Decision Making*, vol. 19, no. 1, pp. 81–134, 2020.
- [10] X. Mi, H. Liao, X. Wu, and Z. Xu, "Probabilistic linguistic information fusion: a survey on aggregation operators in terms of principles, definitions, classifications, applications, and challenges," *International Journal of Intelligent Systems*, vol. 35, no. 3, pp. 529–556, 2020.
- [11] M. Tang and H. C. Liao, "From conventional group decision making to large-scale group decision making: what are the challenges and how to meet them in big data era? A state-of-the-art survey," *Omega*, 2019, In press.
- [12] X. Wu and H. Liao, "A consensus-based probabilistic linguistic gained and lost dominance score method," *European Journal of Operational Research*, vol. 272, no. 3, pp. 1017–1027, 2019.
- [13] P. Liu and F. Teng, "Probabilistic linguistic TODIM method for selecting products through online product reviews," *Information Sciences*, vol. 485, pp. 441–455, 2019.
- [14] S.-z. Luo, H.-y. Zhang, J.-q. Wang, and L. Lin, "Group decision-making approach for evaluating the sustainability of constructed wetlands with probabilistic linguistic preference relations," *Journal of the Operational Research Society*, vol. 70, no. 12, pp. 2039–2055, 2019.
- [15] C. Camerer, "Bounded rationality in individual decision making," *Experimental Economics*, vol. 1, no. 2, pp. 163–183, 1998.

- [16] G. Charness and M. Rabin, "Expressed preferences and behavior in experimental games," *Games and Economic Behavior*, vol. 53, no. 2, pp. 151–169, 2005.
- [17] T. Efendigil, S. Ö en, and E. Kongar, "A holistic approach for selecting a third-party reverse logistics provider in the presence of vagueness," *Computers & Industrial Engineering*, vol. 54, no. 2, pp. 269–287, 2008.
- [18] K. Govindan and H. Soleimani, "A review of reverse logistics and closed-loop supply chains: a Journal of Cleaner Production focus," *Journal of Cleaner Production*, vol. 142, pp. 371–384, 2017.
- [19] P. Sasikumar and A. N. Haq, "Integration of closed loop distribution supply chain network and 3PRLP selection for the case of battery recycling," *International Journal of Production Research*, vol. 49, no. 11, pp. 3363–3385, 2011.
- [20] G. Soleimani, S. Pokharel, and P. S. Kumar, "A hybrid approach using ISM and fuzzy TOPSIS for the selection of reverse logistics provider," *Resources, Conservation and Recycling*, vol. 54, no. 1, pp. 28–36, 2009.
- [21] A. Aguezzoul, "Third-party logistics selection problem: a literature review on criteria and methods," *Omega*, vol. 49, pp. 69–78, 2014.
- [22] S. Agrawal, R. K. Singh, and Q. Murtaza, "A literature review and perspectives in reverse logistics," *Resources, Conservation and Recycling*, vol. 97, pp. 76–92, 2015.
- [23] S. Pokharel and A. Mutha, "Perspectives in reverse logistics: a review," *Resources, Conservation and Recycling*, vol. 53, no. 4, pp. 175–182, 2009.
- [24] K. Govindan, H. Soleimani, and D. Kannan, "Reverse logistics and closed-loop supply chain: a comprehensive review to explore the future," *European Journal of Operational Research*, vol. 240, no. 3, pp. 603–626, 2015.
- [25] H. Prajapati, R. Kant, and R. Shankar, "Bequeath life to death: state-of-art review on reverse logistics," *Journal of Cleaner Production*, vol. 211, pp. 503–520, 2019.
- [26] M. Tavana, M. Zareinejad, F. J. Santos-Arteaga et al., "A conceptual analytic network model for evaluating and selecting third-party reverse logistics providers," *The International Journal of Advanced Manufacturing Technology*, vol. 86, no. 5–8, pp. 1705–1721, 2016.
- [27] N. Zarbakhshnia, Y. Wu, K. Govindan, and H. Soleimani, "A novel hybrid multiple attribute decision-making approach for outsourcing sustainable reverse logistics," *Journal of Cleaner Production*, vol. 242, p. 118461, 2020.
- [28] K. Govindan, M. Kadziński, R. Ehling, and G. Miebs, "Selection of a sustainable third-party reverse logistics provider based on the robustness analysis of an outranking graph kernel conducted with ELECTRE I and SMAA," *Omega*, vol. 85, pp. 1–15, 2019.
- [29] K. Govindan, M. Palaniappan, Q. Zhu, and D. Kannan, "Analysis of third party reverse logistics provider using interpretive structural modeling," *International Journal of Production Economics*, vol. 140, no. 1, pp. 204–211, 2012.
- [30] K. Kannan, J. Sarkis, and M. Palaniappan, "An analytic network process-based multicriteria decision making model for a reverse supply chain," *The International Journal of Advanced Manufacturing Technology*, vol. 68, no. 1–4, pp. 863–880, 2013.
- [31] J. L. d. S. Guimarães and V. A. P. Salomon, "ANP applied to the evaluation of performance indicators of reverse logistics in footwear industry," *Procedia Computer Science*, vol. 55, pp. 139–148, 2015.
- [32] C. Prakash and M. K. Barua, "An analysis of integrated robust hybrid model for third-party reverse logistics partner selection under fuzzy environment," *Resources, Conservation and Recycling*, vol. 108, pp. 63–81, 2016.
- [33] A. Jayant, P. Gupta, S. K. Garg, and M. Khan, "TOPSIS-AHP based approach for selection of reverse logistics service provider: a case study of mobile phone industry," *Procedia Engineering*, vol. 97, pp. 2147–2156, 2014.
- [34] A. H. Khan, A. Asiaei, and S. Zailani, "Green decision-making model in reverse logistics using FUZZY-VIKOR method," *Resources, Conservation and Recycling*, vol. 103, pp. 125–138, 2015.
- [35] C. Prakash and M. K. Barua, "A combined MCDM approach for evaluation and selection of third-party reverse logistics partner for Indian electronics industry," *Sustainable Production and Consumption*, vol. 7, pp. 66–78, 2016.
- [36] C. Bai and J. Sarkis, "Integrating and extending data and decision tools for sustainable third-party reverse logistics provider selection," *Computers & Operations Research*, vol. 110, pp. 188–207, 2019.
- [37] M. Miebs and R. F. Saen, "A new chance-constrained data envelopment analysis for selecting third-party reverse logistics providers in the existence of dual-role factors," *Expert Systems with Applications*, vol. 38, no. 10, pp. 12231–12236, 2011.
- [38] E. Momeni, M. Azadi, and R. F. Saen, "Measuring the efficiency of third party reverse logistics provider in supply chain by multi objective additive network DEA model," *International Journal of Shipping and Transport Logistics*, vol. 7, no. 1, pp. 21–41, 2015.
- [39] V. Jain and S. A. Khan, "Application of AHP in reverse logistics service provider selection: a case study," *International Journal of Business Innovation and Research*, vol. 12, no. 1, pp. 94–119, 2017.
- [40] S. Jharkharia and R. Shankar, "Selection of logistics service provider: an analytic network process (ANP) approach," *Omega*, vol. 35, no. 3, pp. 274–289, 2007.
- [41] V. Ravi, R. Shankar, and M. K. Tiwari, "Analyzing alternatives in reverse logistics for end-of-life computers: ANP and balanced scorecard approach," *Computers & Industrial Engineering*, vol. 48, no. 2, pp. 327–356, 2005.
- [42] A. Liu, X. Ji, H. Lu, and H. Liu, "The selection of 3PRLs on self-service mobile recycling machine: interval-valued Pythagorean hesitant fuzzy best-worst multi-criteria group decision-making," *Journal of Cleaner Production*, vol. 230, pp. 734–750, 2019.
- [43] R. R. Yager, "An approach to ordinal decision making," *International Journal of Approximate Reasoning*, vol. 12, no. 3–4, pp. 237–261, 1995.
- [44] X. Zhang, "A novel probabilistic linguistic approach for large-scale group decision making with incomplete weight information," *International Journal of Fuzzy Systems*, vol. 20, no. 7, pp. 2245–2256, 2018.
- [45] Z. Zhang, C. Guo, and L. Martínez, "Managing multigranular linguistic distribution assessments in large-scale multi-attribute group decision making," *IEEE Transactions on Systems, Man, and Cybernetics: Systems*, vol. 47, no. 11, pp. 3063–3076, 2016.
- [46] X. Zhang, Z. Xu, and H. Wang, "Heterogeneous multiple criteria group decision making with incomplete weight information: a deviation modeling approach," *Information Fusion*, vol. 25, pp. 49–62, 2015.
- [47] X. Zhang, "Multicriteria pythagorean fuzzy decision analysis: a hierarchical QUALIFLEX approach with the closeness index-based ranking methods," *Information Sciences*, vol. 330, pp. 104–124, 2016.

- [48] H. Liao, Z. Xu, and X.-J. Zeng, "Hesitant fuzzy linguistic VIKOR method and its application in qualitative multiple criteria decision making," *IEEE Transactions on Fuzzy Systems*, vol. 23, no. 5, pp. 1343–1355, 2015.
- [49] S. Opricovic and G.-H. Tzeng, "Compromise solution by MCDM methods: a comparative analysis of VIKOR and TOPSIS," *European Journal of Operational Research*, vol. 156, no. 2, pp. 445–455, 2004.
- [50] W.-z. Liang, G.-y. Zhao, and C.-s. Hong, "Performance assessment of circular economy for phosphorus chemical firms based on VIKOR-QUALIFLEX method," *Journal of Cleaner Production*, vol. 196, pp. 1365–1378, 2018.

Research Article

Research on Coordination Complexity of E-Commerce Logistics Service Supply Chain

Yaoguang Zhong,¹ Fangfang Guo,¹ Huajun Tang ,² and Xumei Chen ³

¹School of Economics and Management, Dongguan University of Technology, Guangdong 523808, China

²School of Business, Macau University of Science and Technology, Macau 999078, China

³School of Traffic and Transportation, Beijing Jiaotong University, Beijing 100044, China

Correspondence should be addressed to Huajun Tang; hjtang@must.edu.mo

Received 16 February 2020; Revised 26 March 2020; Accepted 31 March 2020; Published 28 April 2020

Guest Editor: Baogui Xin

Copyright © 2020 Yaoguang Zhong et al. This is an open access article distributed under the Creative Commons Attribution License, which permits unrestricted use, distribution, and reproduction in any medium, provided the original work is properly cited.

With the rapid growth of E-commerce business, logistics service, especially the last-mile distribution, has become one bottleneck, which leads to the rise of coordination complexity of logistics service supply chain (LSSC). This research, based on Stackelberg's game theory, studies the coordination of a new three-echelon LSSC consisting of an E-commerce mall, an express company, and a terminal distribution service provider and investigates the optimal solutions and profits for each party within the semicentralized and centralized LSSC alliances, respectively. To accomplish this, it firstly shows that the three-echelon LSSC can lead to global optimum under the centralized decision-making scenario and then deploys the contract coordination schemes, including revenue sharing, cost sharing, and unit delivery price contracts, in three semicentralized alliances, so as to achieve the same performance of the centralized decision-making scenario, in which each party in the LSSC can achieve the win-win situation. Finally, numerical examples are provided to illustrate the feasibility and the effectiveness of the proposed coordination strategies. This study enriches the coordination theory in the field of LSSC and provides managerial insights for decision makers in LSSC.

1. Introduction

In recent years, the booming development of E-commerce in China is promoting the rapid growth of the logistics express industry. According to the data of the State Post Office in 2019, the national express business revenue reached RMB745 billion with an annual increase of 23%, and the total express business volume exceeded 63 billion pieces with an increase of 24%. However, the lag of logistics and distribution services has been seriously mismatched with the development of E-commerce, which has become one of the main complaints of online shopping consumers. Logistics and distribution, especially the terminal last-mile distribution, has become the bottleneck of the development of E-commerce business [1]. Hence, it is urgent to coordinate logistics service supply chain (LSSC) so as to improve the service level and keep E-commerce industry sustainable.

Spengler [2] was the first to introduce the idea of supply chain coordination and proved that a double marginalization effect naturally led to a suboptimal supply chain. Supply chain coordination aims to provide a win-win mechanism to stimulate all the partners in the supply chain to cooperate together. Recently, supply chain coordination has been one popular topic in the field of supply chain management. The main research streams for this topic focus on all kinds of supply chain coordination strategies, including buyback contract, revenue sharing contract, cost sharing contract, sales rebate policy, quantity flexibility scheme, and quantity discount contract [3]. For instance, Luo and Chen [4] studied the retailer's optimal order policy and the supplier's optimal production policy under revenue sharing contract. Xie et al. [3] integrated the revenue sharing contract in the forward channel with the cost sharing contract and deployed the Stackelberg game to investigate the contract coordination mechanism. Most recently, Zhao et al. [5] focused on

the combination of a buy-back contract and a revenue sharing contract so as to improve the efficiency of a supply chain. However, most existing literatures mainly focus on the coordination of upstream partners (e.g., supplier or manufacturer) and downstream partners (e.g., retailer). There is a lack of literature in studying about this topic in the field of terminal distribution. Hence, there is a need to study the coordination of LSSC, including E-commerce mall, express company, and terminal distribution provider.

The aim of this study is to propose several coordination strategies, including revenue sharing scheme, cost sharing contract, and coordination of unit delivery price, in order to make three semicentralized alliances achieve the global optimal performance under centralized decision-making scenario. The results of this research suggest that all the three schemes, based on Stackelberg's game theory, can help the whole LSSC realize the win-win status. The contribution of this work enriches the supply chain coordination in the field of downstream three-echelon LSSC including the terminal distribution, takes the price and effort level of logistics service dependent demand into account, develops effective coordination strategies, such as revenue sharing and cost sharing contracts, and unit delivery price coordination, and provides managerial insights for decision makers to choose appropriate alliance in real business.

The structure of this study is as follows. In Section 2, the main literatures related to the research topic are reviewed. In Section 3, the research problem and decision models are proposed. In Section 4, semicentralized and centralized LSSC decision models are put forward. In Section 5, the coordination schemes in different alliances are derived: revenue sharing, cost sharing, and coordination of the unit delivery price. Section 6 provides numerical analysis to test the feasibility of the coordination strategies. Section 7 summarizes the research, provides management suggestions, and puts forward the limitations of this study for future research.

2. Literature Review

There exist various literatures on supply chain coordination. The research object ranges from the two-echelon supply chain composed of manufacturers and retailers, to the purchasing and retailing supply chain composed of manufacturers, online retailers, and the third-party logistics (3PL), and then to the LSSC system including E-commerce malls, express companies, and terminal distribution service providers. For the sake of clarity, two main stream of literatures on analytical methods and supply chain coordination are reviewed, respectively.

There always exist one leader and his followers in a supply chain, in which the leader can obtain the followers' optimal decision and then make his own optimal decision. Hence, game theory is widely applied in existing literatures. For instance, Luo and Chen [4] studied the role of revenue sharing contracts in the coordination of supply chains with random yield and stochastic market demand. With game theory, they derived the retailer's optimal order decision and the supplier's optimal production policy under revenue

sharing contracts. Wu et al. [6] deployed game theory to study the coordination of supply chain pricing and advertising decision taking into account the impact of platform users on demand. The results showed that the coordination of supply chain based on the revenue sharing contract can improve the total supply chain performance. Song and Gao [7] constructed game models under centralized and decentralized scenarios, based on revenue sharing contracts. The results showed that revenue sharing contract can effectively improve the greening level of products and the overall profitability of supply chain. Xie et al. [3] combined the revenue sharing contract in the forward channel with the channel investment cost sharing contract and introduced the Stackelberg game to investigate the contract coordination mechanism. Yan et al. [8] used game theory to study the pricing strategy in a dual channel supply chain consisting of a supplier with limited capital and an e-retailer providing capital. Hua et al. [9, 10] proposed four games to investigate the optimal pricing strategy in a two-echelon reverse supply chain.

As for supply chain coordination, there are various existing studies with the following perspectives:

- (1) Quantity discount perspective. For instance, Pang et al. [11] studied the coordination role of revenue sharing contract in a three-echelon supply chain including manufacturers, distributors, and retailers and proposed an improved revenue sharing contract based on quantity discount policy. Pang et al. [12] proposed an improved revenue sharing contract based on quantity discount strategy. Taleizadeh et al. [13] deployed quantity discount policies in the coordination of a two-echelon supply chain in presence of market segmentation and credit payment.
- (2) Demand perspective. Sang [14] studied the revenue sharing contract of multilevel supply chain with customer demand and retail price as fuzzy variables and proposed a revenue sharing contract with fuzzy demand and information asymmetry. Zhao et al. [5] studied the effect of joint buyback and revenue sharing contracts on supply chain coordination between risk neutral suppliers and risk averse retailers under stochastic demand. Cai et al. [15] designed a flexible contract for VMI supply chain with service-sensitive demand. Zhao et al. [16] investigated the coordination of fuzzy closed-loop supply chain, in which demand was price-dependent and information was asymmetric.
- (3) Resource-constrained perspective. Zhao et al. [17] established a model consisting of manufacturer and capital constrained retailer and studied the pricing and the coordination of green supply chain with capital constraint. Yan et al. [18] analyzed the coordination feasibility with supply chain financing and concluded that the financing solution with a suitable combination of decision preferences can realize the coordination. Furthermore, Yan et al. [8] investigated the pricing coordination strategy in a dual-channel supply chain including one capital-

constrained supplier and one e-retailer providing finance.

- (4) Supply chain partner perspective. Many scholars focused on two-echelon supply chain in the research of supply chain coordination. For example, Zhang et al. [19] constructed a supply chain model with one manufacturer and one retailer for deteriorating items, in which they designed a revenue sharing and cooperative investment contract. Bai et al. [20] studied a two-phase sustainable supply chain system composed of producers and retailers and the revenue coordination under carbon emission cap and trade control. Giri et al. [21] proposed a two-stage closed-loop supply chain game model consisting of a manufacturer and a retailer to coordinate the performance of the supply chain through revenue sharing contracts. Heydari and Ghasemi [22] investigated a two-echelon reverse supply chain (RSC) consisting of a single remanufacturer and a single collector. Peng et al. [23] used Stackelberg model to explore a supply chain composed of suppliers and manufacturers and studied the production, price, and carbon emission reduction decisions of decentralized and centralized supply chain. Zou et al. [24] constructed a sustainable closed-loop supply chain coordination mechanism consisting of one manufacturer and two retailers competing in price to coordinate the profits of supply chain members through revenue sharing contracts. Mohammadi et al. [25] studied the supply chain composed of a single supplier and a single vendor and proposed new revenue and preservation technology investment sharing coordination contract based on the fresh supply chain coordination mechanism. Ghazanfari et al. [26] used two different methods to model the supply chain composed of supplier and buyer based on the Stackelberg game model: (1) the traditional selling cycle in the open market without considering the government's incentives and (2) the modern selling cycle in the organized market considering the government's incentives. There also exist some studies on the multi-echelon supply chain. For instance, Zhong et al. [27] expanded from a two-level supply chain composed of an E-commerce platform and a logistics service provider to a three-level supply chain composed of an E-commerce platform, an express company, and a terminal distributor and studied the profit distribution scheme based on revenue sharing contract in the e-commerce environment. Pang et al. [28] studied the revenue coordination of a three-stage supply chain consisting of a manufacturer, a distributor, and a retailer. Hou et al. [29] focused on a three-echelon supply chain composed of a manufacturer, a distributor, and a retailer for a single selling period. Based on a revenue sharing contract, the coordination of the decentralized supply chain with the simultaneous move game or the leader-follower game was analyzed. Yuan et al. [30] constructed a three-tier seafood online retail logistics service supply chain LSSC including online retailers,

logistics service integrators, and functional logistics service providers. Liu and Yi [31] constructed a three-stage supply chain coordination strategy consisting of a manufacturer, a retailer, and a data company and analyzed four benefit models of BDI investment in the decentralized and centralized supply chain. Giri and Sarker [32] studied the contract coordination of a three-level supply chain system, which is composed of a raw material supplier, a manufacturer, and a retailer.

- (5) Policy perspective. In addition, some researchers took the related policy into account. For example, Liu et al. [33] analyzed the coordination between supply chains and retailers through revenue sharing contracts under the government price control policy after the demand disruption of oil, natural gas, and agricultural products which were subject to government price restrictions. Meng et al. [34] established an agent-based revenue sharing negotiation model to study the complexity of stakeholders' revenue sharing in time compression of construction projects.

In summary, the above literatures mainly focus on the traditional production or retailing supply chain or logistics supply chain, but it involves less coordination between the E-commerce mall and logistics service providers. The existing coordination mechanisms mainly included revenue sharing and cost sharing, but seldom involves the coordination of unit delivery price. In the supply chain coordination, most of the literatures focused on the coordination between centralized decision-making and decentralized decision-making. However, as online shopping has become a popular trend, the relationship between E-commerce malls and logistics service providers tends to be closer. Hence, the purpose of this research is to establish three semicentralized alliances in the three-echelon down-stream supply chain consisting of E-commerce mall, express company, and terminal distribution service company and design some reasonable coordination strategies so as to make all the supply chain partners achieve the win-win situation. Table 1 lists some key-related literatures.

3. Problem Description and Research Models

3.1. Problem Description. The logistics service supply chain (LSSC) in this study includes an E-commerce mall, an express company, and a terminal distribution service provider. The E-commerce mall purchases products and sells them online to customers. The express company is responsible for carrying products to terminal distribution service provider network, and the terminal distribution service provider is responsible for delivering them to final customers. Each partner in the LSSC has to make some decision. The E-commerce mall should determine the selling price, the express company should determine the unit price of transportation service and the effort level of logistics service, and the terminal distribution service provider should determine the unit delivery price so as to make their own profit optimal. The problem of this work is how to develop appropriate coordination strategies to stimulate all the partners to cooperate together and achieve the all-win situation.

TABLE 1: List of key-related literatures.

Author(s) and Ref. no.	Journal Title and Year	Factors considered in the research problems			
		Supply chain partners	Coordination strategy	Supply chain system	Demand
Pang et al. [11]	Discrete Dynamics in Nature and Society, 2014	A supplier, and a manufacturer	Revenue sharing	Decentralized and centralized	Sales effort dependent
Heydari and Ghasemi [22]	Journal of Cleaner Production, 2018	A remanufacturer and a collector	Revenue sharing	Decentralized and centralized	Stochastic
Liu and Yi [31]	Annals of Operation Research, 2018	A manufacturer, a retailer, and a data company	Revenue sharing	Decentralized and centralized	Stochastic
Mohammadi et al. [25]	Journal of Cleaner Production, 2019	A supplier and a buyer	Revenue-and-preservation-technology-investment-sharing	Decentralized and centralized	Retail price and freshness degree of products dependent
Ghazanfari et al. [26]	IEEE Transactions on Engineering Management, 2019	A supplier and a buyer	Short-term tax breaks and a single-window system	Traditional selling cycle and modern selling cycle	Stochastic multifactor-dependent
Zeng and Hou, [35]	International Journal of Production Economics, 2019	A supplier and a distributor	Quantity discount	Decentralized and centralized	Price-dependent
Ye et al. [36]	Operational Research, 2020	An agribusiness firm and multiple risk-averse farmers	Revenue sharing, production cost sharing, guaranteed money	Decentralized and centralized	Stochastic
Zhao et al. [37]	European Journal of Operational Research, 2020	Two manufacturers and a major retailer	Revenue sharing consignment	Decentralized and centralized	Shelf space and sales price dependent
This study		E-commerce mall, express company, terminal distribution service provider	Revenue sharing, cost sharing, unit delivery price	Semicentralized and centralized	Sales price-dependent, effort level of logistics service dependent

3.2. *Symbol Description.* The basic symbols and descriptions are defined in Table 2.

3.3. Assumption and Models

- (1) All the members in LSSC are risk neutral
- (2) All the members are rational who make their own decisions to maximize their own profit
- (3) The product demand is affected by the price and the effort level of logistics service [27]
- (4) The cost function of logistics service effort is defined as $g(s) = ks^2$ [38], which is the cost paid by logistics service providers to improve the efficiency of logistics service in order to satisfy customers and increase product sales, where $k > 0$ represents the effort cost coefficient of logistics services

This study includes an E-commerce mall M , an express company E , and a terminal distribution service provider T . Based on Chiang et al. and Huang's linear demand functions [39, 40], it is assumed that the E-commerce mall sells only one product and the terminal distribution service provider cost is borne by the E-commerce mall, which is in line with the reality that Tmall subsidizes the Cainiao station. The E-commerce mall plays a dominant role in the supply chain, and the market demand Q is affected by the price p and the effort level of logistics service s , which decreases with the

TABLE 2: Symbols and descriptions of research models.

Symbols	Descriptions
q	Market demand for product
Q_0	Market base demand for product
α	The elasticity coefficient of market demand to price
β	The elasticity coefficient of market demand to logistics service
p	Selling price of E-commerce product
s	Effort level of logistics service
k	The sensitivity coefficient of logistics service
Δp	Marginal profit of E-commerce mall or alliances
η	Cost sharing ratio
C_M	Unit cost of procurement and operation for E-commerce product
C_E	Unit cost of express company
C_T	Unit delivery cost of terminal distribution service provider
$g(s)$	Service cost of logistics service provider
W_E	Unit price of express company
W_T	Unit price of terminal distribution service provider
W_{ET}	Service quotation of express company and terminal distribution service provider alliance
θ	Revenue sharing ratio
φ	Increase ratio of unit delivery price

increasing price and increases with the effort level of logistics service. Suppose the relationship among the three is $Q = Q_0 - \alpha p + \beta s$ and $Q_0 > 0$, $\alpha > 0$, and $\beta > 0$. According to the

market demand, the suppliers decide the order quantity and assuming that there is no shortage.

The express company determines its own effort level of logistics service s , whose unit operating cost is C_E and unit service price is W_E . Assuming there are no capacity restrictions, it can meet any service requirements, but it must pay the corresponding incremental operating costs. The unit operating cost of the terminal distribution service provider is C_T , and the unit price of service is W_T . In order to ensure the decision variables p , s , W_E , and W_T are positive, the relationship between variables is satisfied that $2\alpha k - \beta^2 > 0$ and $Q_0 - \alpha(C_M + C_E + C_T) > 0$.

The market demand of the product is

$$Q = Q_0 - \alpha p + \beta s. \quad (1)$$

The profit of the E-commerce mall is

$$\prod_M = (p - C_M - W_E - W_T)q. \quad (2)$$

The profit of the express company is

$$\prod_E = (W_E - C_E)q - g(s) = (W_E - C_E)q - ks^2. \quad (3)$$

The profit of the terminal distribution service provider is

$$\prod_T = (W_T - C_T)q. \quad (4)$$

The profit of the E-commerce mall and the terminal distribution service provider alliance is

$$\prod_{MT} = (p - W_E - C_M - C_T)q. \quad (5)$$

The profit of the E-commerce mall and the express company is

$$\prod_{ME} = (p - W_T - C_M - C_E)q - ks^2. \quad (6)$$

The profit of the express company and the terminal distribution service provider alliance is

$$\prod_{ET} = (W_{ET} - C_E - C_T)q - ks^2. \quad (7)$$

The system profit is

$$\begin{aligned} \prod &= \prod_M + \prod_E + \prod_T = (p - C_M - C_E - C_T)q - g(s) \\ &= (p - C_M - C_E - C_T)q - ks^2. \end{aligned} \quad (8)$$

4. Semicentralized and Centralized Decision Models

In this study, the E-commerce mall is the main leader, and the express company and the terminal distribution service provider are the followers. Based on Stackelberg's game theory, the E-commerce mall determines the unit price of the product p and then the express company decides the unit price of transportation service W_B and the effort level of logistics service s , and the terminal distribution service provider determines the unit delivery price W_C [28].

4.1. Semicentralized Decision Models. In the case of semicentralized decision-making, the LSSC consists of one alliance and another partner, in which the alliance includes the other two partners. There are three situations below:

Semicentralized Model 1. The E-commerce mall and the terminal distribution service provider form an alliance, which is equivalent to the self-operated terminal network of the E-commerce mall

Semicentralized Model 2. The E-commerce mall and the express company form an alliance, which is equivalent to the self-operated distribution of the E-commerce mall

Semicentralized Model 3. The express company and the terminal distribution service provider form an alliance, which is equivalent to the whole process of the express company from the E-commerce warehouse to the customer

4.1.1. Decision Analysis of Semicentralized Model 1. The E-commerce mall and the terminal distribution service provider form an alliance, which is equivalent to the self-operated terminal network of the E-commerce mall. In this case, the alliance is the leader and the express company is the follower. In the first stage, the alliance determines the selling price of its product p according to the market information so as to maximize its own profit. In the second stage, the express company decides the best express service price W_B and the effort level of logistics service s according to the market information and the information provided by the alliance.

In order to ensure that the E-commerce alliance is profitable, there is

$$p = C_M + W_E + W_T + \Delta p. \quad (9)$$

Then, the objective functions of the alliance and the express company are

$$\begin{cases} \max \Pi_E = (W_E - C_E)[Q_0 - \alpha(C_M + C_E + W_E + \Delta p) + \beta s] - ks^2, \\ \max \Pi_{MT} = (p - C_M - W_E - C_T)[Q_0 - \alpha(C_M + C_T + W_E + \Delta p) + \beta s]. \end{cases} \quad (10)$$

Use the reverse induction method to solve the problem. First, solving the first partial derivatives of W_E and s about Π_E in formula (10) is

$$\frac{\partial \Pi_E}{\partial W_E} = Q_0 - \alpha(C_M - C_E + C_T + \Delta p) + \beta s - 2\alpha W_E, \quad (11)$$

$$\frac{\partial \Pi_E}{\partial s} = \beta(W_E - C_E) - 2ks.$$

The second-order partial derivative of W_E and s about Π_E in formula (10) is

$$\frac{\partial^2 \Pi_E}{\partial W_E^2} = -2\alpha < 0, \quad (12)$$

$$\frac{\partial^2 \Pi_E}{\partial s^2} = -2k < 0.$$

The Hessian matrix is $H = \begin{pmatrix} -2\alpha & \beta \\ \beta & -2k \end{pmatrix}$, whose first-order determinant $|H_1| = -2\alpha < 0$ and $|H_2| = 4\alpha k - \beta^2 > 0$. It is shown that the Hessian matrix is negative definite, and there is a unique optimal (W_E, s) , leading the Π_E to be maximum.

Let $(\partial \Pi_E / \partial W_E) = 0$ and $(\partial \Pi_E / \partial s) = 0$, then

$$W_E = \frac{Q_0 - \alpha(C_M - C_E + C_T + \Delta p) + \beta s}{2\alpha}, \quad (13)$$

$$s = \frac{\beta(W_E - C_E)}{2k}. \quad (14)$$

Integrate equations (13) and (14), we get the expressions of W_E and s for Δp as follows:

$$\begin{cases} W_E = \frac{2k[Q_0 - \alpha(C_M - C_T + \Delta p)] + (2\alpha k - \beta^2)C_B}{4\alpha k - \beta^2}, \\ s = \frac{\beta[Q_0 - \alpha(C_M + C_E + C_T + \Delta p)]}{4\alpha k - \beta^2}. \end{cases} \quad (15)$$

Bring equation (15) into equation (14), then

$$\prod_{MT} = \Delta p \frac{2\alpha k[Q_0 - \alpha(C_M + C_E + C_T + \Delta p)]}{4\alpha k - \beta^2}. \quad (16)$$

Then, the first partial derivative of Δp about R_{AC} in formula (16) is $(\partial \prod_{MT} / \partial \Delta p) = ((2\alpha k[Q_0 - \alpha(C_M + C_E + C_T + 2\Delta p)]) / (4\alpha k - \beta^2))$. The second-order partial derivative is $(\partial^2 \prod_{MT} / \partial \Delta p^2) = (-4\alpha^2 k / (4\alpha k - \beta^2)) < 0$. This implies that \prod_{MT} is the concave function about Δp , so there

is only one Δp that makes the \prod_{MT} optimal. Let $(\partial \prod_{MT} / \partial \Delta p) = 0$, then

$$\Delta p = \frac{Q_0 - \alpha(C_M + C_E + C_T)}{2\alpha}. \quad (17)$$

Bring equation (17) into equation (15), then

$$W_{E1}^* = \frac{k[Q_0 - \alpha(C_M + C_T)] + (3\alpha k - \beta^2)C_E}{4\alpha k - \beta^2}, \quad (18)$$

$$s_1^* = \frac{\beta[Q_0 - \alpha(C_M + C_E + C_T)]}{2(4\alpha k - \beta^2)}. \quad (19)$$

Bring equations (18)-(19) into equations (1) and (9), then

$$q_1^* = \frac{\alpha k[Q_0 - \alpha(C_M + C_E + C_T)]}{4\alpha k - \beta^2}, \quad (20)$$

$$p_1^* = \frac{(6\alpha k - \beta^2)Q_0 + \alpha(2\alpha k - \beta^2)(C_M + C_E + C_T)}{2\alpha(4\alpha k - \beta^2)}.$$

Then, we can get the optimal profit of the alliance, the express company, and the whole system:

$$\begin{aligned} \prod_{MT}^* &= \frac{k[Q_0 - \alpha(C_M + C_E + C_T)]^2}{2(4\alpha k - \beta^2)}, \\ \prod_{E1}^* &= \frac{k[Q_0 - \alpha(C_M + C_E + C_T)]^2}{4(4\alpha k - \beta^2)}, \\ \prod_{I1}^* &= \frac{3k[Q_0 - \alpha(C_M + C_E + C_T)]^2}{4(4\alpha k - \beta^2)}. \end{aligned} \quad (21)$$

4.1.2. Decision Analysis of Semicentralized Model 2. The E-commerce mall and the express company form an alliance, which is equivalent to the self-operated distribution of the E-commerce mall. In this case, the alliance is the leader and the terminal distribution service provider is the follower. In the first stage, the alliance decides the selling price p and the effort level of logistics service s according to the market information so as to maximize its own profit. In the second stage, the terminal distribution service provider decides the optimal service price W_C according to the market information and the information provided by the alliance.

In order to ensure that the E-commerce alliance is profitable, there is

$$p = C_M + W_E + C_M + \Delta p. \quad (22)$$

Then, the objective functions of the alliance and the terminal distribution service provider are

$$\begin{cases} \max \Pi_T = (W_T - C_T)[Q_0 - \alpha(C_M + C_E + W_T + \Delta p) + \beta s], \\ \max \Pi_{ME} = (p - C_M - C_E - W_T)[Q_0 - \alpha(C_M + C_E + W_T + \Delta p) + \beta s] - ks^2. \end{cases} \quad (23)$$

Similarly, the corresponding optimal solutions are obtained as follows:

$$\begin{aligned} W_{T2}^* &= \frac{2k[Q_0 - \alpha(C_M + C_E)] + (6\alpha k - \beta^2)C_T}{8\alpha k - \beta^2}, \\ s_2^* &= \frac{\beta[Q_0 - \alpha(C_M + C_E + C_T)]}{8\alpha k - \beta^2}, \\ q_2^* &= \frac{2\alpha k[Q_0 - \alpha(C_M + C_E + C_T)]}{8\alpha k - \beta^2}, \\ p_2^* &= \frac{6kQ_0 + (2\alpha k - \beta^2)(C_M + C_E + C_T)}{8\alpha k - \beta^2}, \end{aligned} \quad (24)$$

$$\begin{aligned} \Pi_{ME}^* &= \frac{k[Q_0 - \alpha(C_M + C_E + C_T)]^2}{8\alpha k - \beta^2}, \\ \Pi_{T2}^* &= \frac{4\alpha k^2[Q_0 - \alpha(C_M + C_E + C_T)]^2}{(8\alpha k - \beta^2)^2}, \\ \Pi_2^* &= \frac{k(12\alpha k - \beta^2)[Q_0 - \alpha(C_M + C_E + C_T)]^2}{(8\alpha k - \beta^2)^2}. \end{aligned}$$

4.1.3. Decision Analysis of Semicentralized Model 3. The express company and the terminal distribution service provider form an alliance, which is equivalent to the whole process of the express company from the E-commerce warehouse to the consumer. In this case, the E-commerce mall is the leader and the alliance is the follower. In the first stage, the E-commerce mall decides the selling price p according to the market information so as to maximize its own profit. In the second stage, the terminal distribution service provider decides the optimal service price W_{BC} and the effort level of logistics service s according to the market information and the information provided by the E-commerce mall.

In order to ensure that the E-commerce alliance is profitable, there is

$$p = C_M + W_{ET} + \Delta p. \quad (25)$$

Then, the objective functions of the E-commerce mall and the alliance are

$$\begin{cases} \max \Pi_{ET} = (W_{ET} - C_E - C_T)[Q_0 - \alpha(C_M + W_{ET} + \Delta p) + \beta s] - ks^2, \\ \max \Pi_M = (p - C_M - W_{ET})[Q_0 - \alpha(C_M + W_{ET} + \Delta p) + \beta s]. \end{cases} \quad (26)$$

Similarly, the corresponding optimal solutions are obtained in the following:

$$\begin{aligned} W_{ET}^* &= \frac{k(Q_0 - \alpha C_M) + (3\alpha k - \beta^2)(C_E + C_T)}{4\alpha k - \beta^2}, \\ s_3^* &= \frac{\beta[Q_0 - \alpha(C_M + C_E + C_T)]}{2(4\alpha k - \beta^2)}, \\ q_3^* &= \frac{\alpha k[Q_0 - \alpha(C_M + C_E + C_T)]}{4\alpha k - \beta^2}, \\ p_3^* &= \frac{(6\alpha k - \beta^2)Q_0 + \alpha(2\alpha k - \beta^2)(C_M + C_E + C_T)}{2\alpha(4\alpha k - \beta^2)}, \\ \Pi_{M3}^* &= \frac{k[Q_0 - \alpha(C_M + C_E + C_T)]^2}{2(4\alpha k - \beta^2)}, \\ \Pi_{ET}^* &= \frac{k[Q_0 - \alpha(C_M + C_E + C_T)]^2}{4(4\alpha k - \beta^2)}, \\ \Pi_3^* &= \frac{3k[Q_0 - \alpha(C_M + C_E + C_T)]^2}{4(4\alpha k - \beta^2)}. \end{aligned} \quad (27)$$

4.2. Centralized Decision Model. Centralized decision-making is similar to the whole process of E-commerce from self-operated products to customers; that is, the E-commerce mall, the express company, and the terminal distribution service provider are regarded as a joint alliance, and their profit maximization is investigated from the perspective of the whole LSSC.

Bring equation (1) into (8), then

$$\begin{aligned} \Pi &= [p - (C_M + C_E + C_T)](Q_0 - \alpha p + \beta s) - ks^2, \\ p_4^* &= \frac{2kQ_0 + (2\alpha k - \beta^2)(C_M + C_E + C_T)}{4\alpha k - \beta^2}, \\ s_4^* &= \frac{\beta[Q_0 - \alpha(C_M + C_E + C_T)]}{4\alpha k - \beta^2}, \\ q_4^* &= \frac{2\alpha k[Q_0 - \alpha(C_M + C_E + C_T)]}{4\alpha k - \beta^2}, \end{aligned} \quad (28)$$

$$\Pi_4^* = \frac{k[Q_0 - \alpha(C_M + C_E + C_T)]^2}{4\alpha k - \beta^2}.$$

4.3. Comparative Analysis of Semicentralized and Centralized Decision Models. In this subsection, three propositions are derived so as to compare the corresponding profit and the effort level of logistics service, order quantity, and selling price between the semicentralized models and the centralized model.

Proposition 1. *The overall profit of centralized decision is better than that of semicentralized decision-making. That is, $\Pi_4^* > \Pi_1^* = \Pi_3^* > \Pi_2^*$ and $\Pi_4^* = (4/3)\Pi_1^*$.*

It is proved as follows:

$$\frac{\Pi_4^*}{\Pi_1^*} = \frac{(k[Q_0 - \alpha(C_M + C_E + C_T)]^2/4\alpha k - \beta^2)}{(3k[Q_0 - \alpha(C_M + C_E + C_T)]^2/4(4\alpha k - \beta^2))} = \frac{4}{3} > 1, \text{ so } \Pi_4^* > \Pi_1^* \text{ and } \Pi_4^* = (4/3)\Pi_1^*,$$

$$\Pi_1^* - \Pi_2^* = \frac{\beta^2(16\alpha k - \beta^2)[Q_0 - \alpha(C_M + C_E + C_T)]^2}{4(4\alpha k - \beta^2)^2(8\alpha k - \beta^2)^2} > 0, \text{ so } \Pi_1^* = \Pi_3^* > \Pi_2^*.$$

Proposition 2. *Under centralized decision-making, the effort of the express company is higher than that of semicentralized decision-making. That is, $s_4^* > s_3^* = s_1^* > s_2^*$ and $s_4^* = 2s_3^* = 2s_1^*$. The sales volume of the product under the centralized decision is higher than that in the individual*

decision. That is, $q_4^ > q_3^* = q_1^* > q_2^*$ and $q_4^* = 2q_3^* = 2q_1^*$. The selling price of the product under the individual decision is higher than that in the semicentralized decision. That is, $p_2^* > p_1^* = p_3^* > p_4^*$.*

$$\left(\frac{s_4^*}{s_3^*}\right) = \frac{(\beta[Q_0 - \alpha(C_M + C_E + C_T)]/4\alpha k - \beta^2)}{(\beta[Q_0 - \alpha(C_M + C_E + C_T)]/2(4\alpha k - \beta^2))} = 2, \text{ so } s_4^* > s_3^* \text{ and } s_4^* = 2s_3^*,$$

$$\frac{s_1^*}{s_2^*} = \frac{(\beta[Q_0 - \alpha(C_M + C_E + C_T)]/2(4\alpha k - \beta^2))}{(\beta[Q_0 - \alpha(C_M + C_E + C_T)]/8\alpha k - \beta^2)} = \frac{8\alpha k - \beta^2}{2(4\alpha k - \beta^2)} > 1, \text{ so } s_1^* > s_2^*,$$

$$\frac{q_4^*}{q_3^*} = \frac{(2\alpha k[Q_0 - \alpha(C_M + C_E + C_T)]/4\alpha k - \beta^2)}{(\alpha k[Q_0 - \alpha(C_M + C_E + C_T)]/4\alpha k - \beta^2)} = 2, \text{ so } q_4^* > q_3^*, \text{ and } q_4^* = 2q_3^*,$$

$$\frac{q_1^*}{q_2^*} = \frac{(\alpha k[Q_0 - \alpha(C_M + C_E + C_T)]/4\alpha k - \beta^2)}{(2\alpha k[Q_0 - \alpha(C_M + C_E + C_T)]/8\alpha k - \beta^2)} = \frac{8\alpha k - \beta^2}{2(4\alpha k - \beta^2)} > 1, \text{ so } q_2^* > q_3^*,$$

$$\frac{q_3^*}{q_1^*} = \frac{(2\alpha k[Q_0 - \alpha(C_M + C_E + C_T)]/8\alpha k - \beta^2)}{(\alpha k[Q_0 - \alpha(C_M + C_E + C_T)]/8\alpha k - \beta^2)} = 2, \text{ so } q_3^* > q_1^*, \text{ and } q_1^* > q_2^*,$$

$$p_2^* - p_1^* = \frac{\beta^2(2\alpha k - \beta^2)[Q_0 - \alpha(C_M + C_E + C_T)]}{2\alpha(4\alpha k - \beta^2)(8\alpha k - \beta^2)} > 0, \text{ so } p_1^* = p_3^* < p_2^*,$$

$$p_3^* - p_4^* = \frac{(2\alpha k - \beta^2)[Q_0 - \alpha(C_M + C_E + C_T)]}{2\alpha(4\alpha k - \beta^2)} > 0, \text{ so } p_4^* < p_3^* = p_1^*.$$

Proposition 3. *Among the three models of semicentralized decision-making, the total profits of semicentralized models 1 and 3 are both superior to that of semicentralized model 2. Furthermore, E-commerce mall can achieve the highest profit in semicentralized model 3.*

It is proved below.

From Propositions 1 and 2, it is obvious that $\Pi_1^* = \Pi_3^* > \Pi_2^*$, $s_3^* = s_1^* > s_2^*$, $q_3^* = q_1^* > q_2^*$, and $p_2^* > p_1^* = p_3^*$, so when E-commerce mall and end-distributor alliance and express company and end-distributor alliance, the overall effect of logistics service supply

chain is better than E-commerce mall and express company alliance:

$$\Pi_{M3}^* = \Pi_{ET}^* = \frac{k[Q_0 - \alpha(C_M + C_E + C_T)]^2}{2(4\alpha k - \beta^2)}$$

$$> \Pi_{M3}^* \frac{k[Q_0 - \alpha(C_M + C_E + C_T)]^2}{8\alpha k - \beta^2}.$$

That is, when the express company forms an alliance with the terminal distribution service provider, the profit of

the E-commerce mall \prod_{M3}^* is equal to the overall profit of the E-commerce mall and the terminal distribution service provider alliance \prod_{ET}^* and is higher than the overall profit of the E-commerce mall and the express company alliance \prod_{ME}^* . Therefore, the E-commerce mall can achieve the highest profit in semicentralized model 3.

5. Contract Coordination Mechanism

Based on Table 2, the overall profit of LSSC under centralized decision-making is significantly higher than that under semicentralized decision-making models. Therefore, to achieve the performance of centralized decision-making under semicentralized scenarios, supply chain coordination strategies are introduced to improve the overall profit and achieve the win-win situation.

This section firstly discusses the profit range of each partner for the three semicentralized alliances. Secondly, it introduces the specific coordination schemes. Since the alliance of semicentralized model 3 is equivalent to a two-echelon LSSC composed of the E-commerce mall and the logistics service provider, this study mainly focuses on the coordination of semicentralized models 1 and 2. Then, the contract coordination scheme for semicentralized model 1 are discussed in the two cases: (1) $3\beta^2 - 4\alpha k > 0$ and (2) $3\beta^2 - 4\alpha k < 0$. Finally, this work investigates the contract coordination scheme semicentralized model 2.

5.1. Profit Range of Three Semicentralized Models

5.1.1. Profit Range of Semicentralized Model 1

Proposition 4. *Under the supply chain coordination, the profit ranges of the alliance formed by the E-commerce mall and the terminal distribution service provider and the express company are obtained below, respectively:*

$$\frac{k[Q_0 - \alpha(C_M + C_E + C_T)]^2}{2(4\alpha k - \beta^2)} \leq \prod_{MT} \leq \frac{3k[Q_0 - \alpha(C_M + C_E + C_T)]^2}{4(4\alpha k - \beta^2)},$$

$$\frac{k[Q_0 - \alpha(C_M + C_E + C_T)]^2}{4(4\alpha k - \beta^2)} \leq \prod_E \leq \frac{k[Q_0 - \alpha(C_M + C_E + C_T)]^2}{2(4\alpha k - \beta^2)}. \quad (32)$$

It is proved as follows.

§e purpose of the contract coordination between the alliance including the E-commerce mall, the terminal distribution service provider, and the express company is to achieve the performance of centralized decision-making and all-win status. §at is, the profits of all parties are not lower than the profit before the coordination since

$$\prod_{MT} + \prod_E = \frac{k[Q_0 - \alpha(C_M + C_E + C_T)]^2}{4\alpha k - \beta^2},$$

$$\prod_{MT} \geq \frac{k[Q_0 - \alpha(C_M + C_E + C_T)]^2}{2(4\alpha k - \beta^2)}, \quad (33)$$

$$\prod_E \geq \frac{k[Q_0 - \alpha(C_M + C_E + C_T)]^2}{4(4\alpha k - \beta^2)}.$$

Therefore,

$$\frac{k[Q_0 - \alpha(C_M + C_E + C_T)]^2}{2(4\alpha k - \beta^2)} \leq \prod_{MT} \leq \frac{3k[Q_0 - \alpha(C_M + C_E + C_T)]^2}{4(4\alpha k - \beta^2)},$$

$$\frac{k[Q_0 - \alpha(C_M + C_E + C_T)]^2}{4(4\alpha k - \beta^2)} \leq \prod_E \leq \frac{k[Q_0 - \alpha(C_M + C_E + C_T)]^2}{2(4\alpha k - \beta^2)}. \quad (34)$$

5.1.2. Profit Range of Semicentralized Model 2

Proposition 5. *Under the supply chain coordination, the profit ranges of the alliance including the E-commerce mall and the express company and the terminal distribution service provider are below:*

$$\frac{k[Q_0 - \alpha(C_M + C_E + C_T)]^2}{8\alpha k - \beta^2} \leq \prod_{ME} \leq \frac{k(48\alpha^2 k^2 - 12\alpha k \beta^2 + \beta^4)[Q_0 - \alpha(C_M + C_E + C_T)]^2}{(8\alpha k - \beta^2)^2(4\alpha k - \beta^2)}, \quad (35)$$

$$\frac{4\alpha k^2[Q_0 - \alpha(C_M + C_E + C_T)]^2}{(8\alpha k - \beta^2)^2} \leq \prod_T \leq \frac{4\alpha k^2[Q_0 - \alpha(C_M + C_E + C_T)]^2}{(8\alpha k - \beta^2)(4\alpha k - \beta^2)}.$$

It is proved as follows.

§e purpose of the contract coordination between the alliance composed of the E-commerce mall and the express company and the terminal distribution service provider is to

make the profits of the two parties after the coordination reach the effect of centralized decision-making, and the profits of the parties are not lower than the profits before the coordination. Hence,

$$\begin{aligned}\prod_{ME} + \prod_T &= \frac{k[Q_0 - \alpha(C_M + C_E + C_T)]^2}{4\alpha k - \beta^2}, \\ \prod_{ME} &\geq \frac{k[Q_0 - \alpha(C_M + C_E + C_T)]^2}{8\alpha k - \beta^2}, \\ \prod_T &\geq \frac{4\alpha k^2 [Q_0 - \alpha(C_M + C_E + C_T)]^2}{(8\alpha k - \beta^2)^2}.\end{aligned}\quad (36)$$

Therefore,

$$\begin{aligned}\frac{k[Q_0 - \alpha(C_M + C_E + C_T)]^2}{8\alpha k - \beta^2} &\leq \prod_{ME} \leq \frac{k(48\alpha^2 k^2 - 12\alpha k\beta^2 + \beta^4)[Q_0 - \alpha(C_M + C_E + C_T)]^2}{(8\alpha k - \beta^2)^2(4\alpha k - \beta^2)}, \\ \frac{4\alpha k^2 [Q_0 - \alpha(C_M + C_E + C_T)]^2}{(8\alpha k - \beta^2)^2} &\leq \prod_T \leq \frac{4\alpha k^2 [Q_0 - \alpha(C_M + C_E + C_T)]^2}{(8\alpha k - \beta^2)(4\alpha k - \beta^2)}.\end{aligned}\quad (37)$$

5.1.3. Profit Range of Semicentralized Model 3

Proposition 6. Under the contract coordination mechanism, the profit range of the express company and the terminal distribution service provider alliance and the E-commerce mall are derived as follows, respectively:

$$\begin{aligned}\frac{k[Q_0 - \alpha(C_M + C_E + C_T)]^2}{2(4\alpha k - \beta^2)} &\leq \prod_M \leq \frac{3k[Q_0 - \alpha(C_M + C_E + C_T)]^2}{4(4\alpha k - \beta^2)}, \\ \frac{k[Q_0 - \alpha(C_M + C_E + C_T)]^2}{4(4\alpha k - \beta^2)} &\leq \prod_{ET} \leq \frac{k[Q_0 - \alpha(C_M + C_E + C_T)]^2}{2(4\alpha k - \beta^2)}.\end{aligned}\quad (38)$$

It is proved below.

The purpose of the contract coordination between the alliance composed of the express company and the terminal distribution service provider and the E-commerce mall is to make the profits of the two parties after the coordination reach the effect of centralized decision-making, and the profits of the parties are not lower than the profits before the coordination. Hence,

$$\begin{aligned}\prod_M + \prod_{ET} &= \frac{k[Q_0 - \alpha(C_M + C_E + C_T)]^2}{4\alpha k - \beta^2}, \\ \prod_M &\geq \frac{k[Q_0 - \alpha(C_M + C_E + C_T)]^2}{2(4\alpha k - \beta^2)}, \\ \prod_{ET} &\geq \frac{k[Q_0 - \alpha(C_M + C_E + C_T)]^2}{4(4\alpha k - \beta^2)}.\end{aligned}\quad (39)$$

Therefore,

$$\begin{aligned}\frac{k[Q_0 - \alpha(C_M + C_E + C_T)]^2}{2(4\alpha k - \beta^2)} &\leq \prod_M \leq \frac{3k[Q_0 - \alpha(C_M + C_E + C_T)]^2}{4(4\alpha k - \beta^2)}, \\ \frac{k[Q_0 - \alpha(C_M + C_E + C_T)]^2}{4(4\alpha k - \beta^2)} &\leq \prod_{ET} \leq \frac{k[Q_0 - \alpha(C_M + C_E + C_T)]^2}{2(4\alpha k - \beta^2)}.\end{aligned}\quad (40)$$

5.2. Coordination Strategy of Semicentralized Model 1

Proposition 7. When $3\beta^2 - 4\alpha k > 0$, the alliance needs to transfer some profit to the express company, and when $3\beta^2 - 4\alpha k < 0$, it suggests that one partner should share some profit with the other.

It is proved as follows.

When

$$\begin{aligned}s_4^* &= \frac{\beta[Q_0 - \alpha(C_M + C_E + C_T)]}{4\alpha k - \beta^2}, \\ p_4^* &= \frac{2kQ_0 + (2\alpha k - \beta^2)(C_M + C_E + C_T)}{4\alpha k - \beta^2},\end{aligned}\quad (41)$$

$$W_E = \frac{k[Q_0 - \alpha(C_M + C_T)] + (3\alpha k - \beta^2)C_E}{4\alpha k - \beta^2},$$

then

$$\begin{aligned}\prod_{MT} &= \frac{2\alpha k^2 [Q_0 - \alpha(C_M + C_E + C_T)]^2}{(4\alpha k - \beta^2)^2}, \\ \prod_E &= \frac{k(2\alpha k - \beta^2)[Q_0 - \alpha(C_M + C_E + C_T)]^2}{(4\alpha k - \beta^2)^2}.\end{aligned}\quad (42)$$

Because

$$\frac{k[Q_0 - \alpha(C_M + C_E + C_T)]^2}{2(4\alpha k - \beta^2)} \leq \prod_{MT} \leq \frac{3k[Q_0 - \alpha(C_M + C_E + C_T)]^2}{4(4\alpha k - \beta^2)},$$

$$\frac{k[Q_0 - \alpha(C_M + C_E + C_T)]^2}{4(4\alpha k - \beta^2)} \leq \prod_E \leq \frac{k[Q_0 - \alpha(C_M + C_E + C_T)]^2}{2(4\alpha k - \beta^2)}. \quad (43)$$

When $3\beta^2 - 4\alpha k > 0$, $\prod_{MT} > \prod_{MT \max} = (3k [Q_0 - \alpha(C_M + C_E + C_T)]^2 / 4(4\alpha k - \beta^2))$, and the alliance needs to transfer some profit to the express company. When $3\beta^2 - 4\alpha k < 0$, $\prod_{MT} < \prod_{MT \max} = (3k [Q_0 - \alpha(C_M + C_E + C_T)]^2 / 4(4\alpha k - \beta^2))$, and one partner should share some profit with the other.

Based on this, there are two situations in the contract coordination scheme. When $3\beta^2 - 4\alpha k > 0$, the contract coordination scheme is (1) the strategy of transferring part of the profit to the express company by the alliance including E-commerce mall and the terminal distribution service provider, (2) the strategy of the alliance bearing part of the logistics service cost for the express companies, and (3) the strategy of increasing unit delivery price of the express company. When $3\beta^2 - 4\alpha k < 0$, the contract coordination scheme is (1) the strategy of transferring some revenue to the express company from the alliance of E-commerce mall and the terminal distribution service provider, (2) the strategy of the alliance undertaking part of the logistics service cost, (3) the strategy of raising the unit delivery price of express company logistics services, and (4) the strategy of transferring some revenue to the express company from the alliance of E-commerce mall and the terminal distribution service provider.

5.2.1. Case 1: $3\beta^2 - 4\alpha k > 0$. As mentioned above, there are three kinds of contract coordination schemes when $3\beta^2 - 4\alpha k > 0$, (1) the alliance transfers part of the profit to the express company, (2) the alliance bears some logistics service cost of the express company, and (3) the alliance increases the unit delivery price of the express company.

A1: Revenue Sharing Coordination in Semicentralized Model 1.

Proposition 8. *In order to achieve the centralized decision-making selling price p and the effort level of logistics service s and the unit delivery price, W_B remains unchanged, assuming that the revenue sharing ratio of the alliance composed of the E-commerce mall and the terminal distribution service provider to the express company is θ_1 ; when $((3\beta^2 - 4\alpha k) [Q_0 - \alpha(C_M + C_E + C_T)] / 8\alpha [2kQ_0 + (2\alpha k - \beta^2)(C_M + C_E + C_T)]) \leq \theta_1 \leq (\beta^2 [Q_0 - \alpha(C_M + C_E + C_T)] / 4\alpha [2kQ_0 + (2\alpha k - \beta^2)(C_M + C_E + C_T)])$, the profit coordination between the alliance and express company can be realized.*

It is proved as follows.

Assuming the revenue sharing ratio of the alliance to the express company is θ_1 and $0 < \theta_1 < 1$, then the profit of the alliance is $\prod_{MT} = [(1 - \theta_1)p - C_M - C_T - W_E]q$ and the

profit of the express company is $\prod_E = (W_E + \theta_1 p - C_E)q - ks^2$.

When

$$p = \frac{2kQ_0 + (2\alpha k - \beta^2)(C_M + C_E + C_T)}{4\alpha k - \beta^2},$$

$$s = \frac{\beta [Q_0 - \alpha(C_M + C_E + C_T)]}{4\alpha k - \beta^2}, \quad (44)$$

$$W_E = \frac{k[Q_0 - \alpha(C_M + C_T)] + (3\alpha k - \beta^2)C_E}{4\alpha k - \beta^2},$$

then

$$\prod_{MT} = \frac{2\alpha k [Q_0 - \alpha(C_M + C_E + C_T)]}{(4\alpha k - \beta^2)^2} \{ (1 - 2\theta_1)kQ_0 - [(1 + 2\theta_1)\alpha k - \theta_1\beta^2](C_M + C_E + C_T) \},$$

$$\prod_E = \frac{k[Q_0 - \alpha(C_M + C_E + C_T)]}{(4\alpha k - \beta^2)^2} \{ [(1 + 2\theta_1)2\alpha k - \beta^2]Q_0 - \alpha(1 - 2\theta_1)(2\alpha k - \beta^2)(C_M + C_E + C_T) \}. \quad (45)$$

Since

$$\frac{k[Q_0 - \alpha(C_M + C_E + C_T)]^2}{2(4\alpha k - \beta^2)} \leq \prod_{MT} \leq \frac{3k[Q_0 - \alpha(C_M + C_E + C_T)]^2}{4(4\alpha k - \beta^2)},$$

$$\frac{k[Q_0 - \alpha(C_M + C_E + C_T)]^2}{4(4\alpha k - \beta^2)} \leq \prod_E \leq \frac{k[Q_0 - \alpha(C_M + C_E + C_T)]^2}{2(4\alpha k - \beta^2)}, \quad (46)$$

then

$$\frac{(3\beta^2 - 4\alpha k)[Q_0 - \alpha(C_M + C_E + C_T)]}{8\alpha [2kQ_0 + (2\alpha k - \beta^2)(C_M + C_E + C_T)]} \leq \theta_1$$

$$\leq \frac{\beta^2 [Q_0 - \alpha(C_M + C_E + C_T)]}{4\alpha [2kQ_0 + (2\alpha k - \beta^2)(C_M + C_E + C_T)]}. \quad (47)$$

B1: Cost Sharing Coordination in Semicentralized Model 1.

Proposition 9. *In order to achieve the centralized decision-making of sales price p and the logistics service s and keep the unit delivery price W_E unchanged, assuming that the cost sharing proportion of s by the alliance is η_1 , $0 < \eta_1 < 1$, then when $(3\beta^2 - 4\alpha k / 4\beta^2) \leq \eta_1 \leq (1/2)$, the alliance and the express company can achieve the profit coordination.*

It is proved in the following.

Assuming that the cost sharing ratio of logistics service cost is η_1 and $0 < \eta_1 < 1$, the profit of the alliance is $\prod_{MT} = (p - C_M - C_T - W_E)q - \eta_1 ks^2$ and the profit of the express company is $\prod_E = (W_E + \theta_1 p - C_E)q - ks^2$.

When

$$p = \frac{2kQ_0 + (2\alpha k - \beta^2)(C_M + C_E + C_T)}{4\alpha k - \beta^2},$$

$$s = \frac{\beta[Q_0 - \alpha(C_M + C_E + C_T)]}{4\alpha k - \beta^2}, \quad (48)$$

$$W_E = \frac{k[Q_0 - \alpha(C_M + C_T)] + (3\alpha k - \beta^2)C_E}{4\alpha k - \beta^2},$$

then

$$\prod_{MT} = \frac{k(2\alpha k - \eta_1 \beta^2)[Q_0 - \alpha(C_M + C_E + C_T)]^2}{(4\alpha k - \beta^2)^2},$$

$$\prod_E = \frac{k[2\alpha k - (1 - \eta_1)\beta^2][Q_0 - \alpha(C_M + C_E + C_T)]^2}{(4\alpha k - \beta^2)^2}. \quad (49)$$

Since

$$\frac{k[Q_0 - \alpha(C_M + C_E + C_T)]^2}{2(4\alpha k - \beta^2)} \leq \prod_{MT} \leq \frac{3k[Q_0 - \alpha(C_M + C_E + C_T)]^2}{4(4\alpha k - \beta^2)},$$

$$\frac{k[Q_0 - \alpha(C_M + C_E + C_T)]^2}{4(4\alpha k - \beta^2)} \leq \prod_E \leq \frac{k[Q_0 - \alpha(C_M + C_E + C_T)]^2}{2(4\alpha k - \beta^2)}, \quad (50)$$

then

$$\frac{3\beta^2 - 4\alpha k}{4\beta^2} \leq \eta_1 \leq \frac{1}{2}. \quad (51)$$

CI: Coordination of Unit Delivery Price in Semi-centralized Model 1.

Proposition 10. *In order to achieve the centralized decision-making selling price p and the effort level of express service s , the unit price of express service W_B remains unchanged; if the alliance increases the unit delivery price by φ_1 , $0 < \varphi_1 < 1$, when $((3\beta^2 - 4\alpha k)[Q_0 - \alpha(C_M + C_E + C_T)] / 8\alpha\{k[Q_0 - \alpha(C_M + C_T)] + (3\alpha k - \beta^2)C_E\}) \leq \varphi_1 \leq (\beta^2[Q_0 - \alpha(C_M + C_E + C_T)] / 4\alpha\{k[Q_0 - \alpha(C_M + C_T)] + (3\alpha k - \beta^2)C_E\})$ ($3\beta^2 - 4\alpha k > 0$), then the alliance and the express company can achieve profit coordination.*

It is proved as follows.

Assume that the rate of increase in express unit price is φ and $0 < \varphi < 1$, then the profit of the alliance is $\prod_{MT} = [p - C_M - C_T - (1 + \varphi_1)W_E]q$, and the profit of the express company is $\prod_E = [(1 + \varphi_1)W_E - C_E]q - ks^2$.

When

$$p = \frac{2kQ_0 + (2\alpha k - \beta^2)(C_M + C_E + C_T)}{4\alpha k - \beta^2},$$

$$s = \frac{\beta[Q_0 - \alpha(C_M + C_E + C_T)]}{4\alpha k - \beta^2}, \quad (52)$$

$$W_E = \frac{k[Q_0 - \alpha(C_M + C_T)] + (3\alpha k - \beta^2)C_E}{4\alpha k - \beta^2},$$

then

$$\prod_{MT} = \frac{2\alpha k[Q_0 - \alpha(C_M + C_E + C_T)]}{(4\alpha k - \beta^2)^2} \{(1 - \varphi_1)k$$

$$\cdot [Q_0 - \alpha(C_M + C_T)] - [(1 + 3\varphi_1)\alpha k - \varphi_1\beta^2]C_E\},$$

$$\prod_E = \frac{k[Q_0 - \alpha(C_M + C_E + C_T)]}{(4\alpha k - \beta^2)^2} \{[(1 + \varphi_1)2\alpha k - \beta^2]$$

$$\cdot [Q_0 - \alpha(C_M + C_T)] + \alpha[(3\varphi_1 - 1)2\alpha k + (1 - 2\varphi_1)\beta^2]C_E\}. \quad (53)$$

Since

$$\frac{k[Q_0 - \alpha(C_M + C_E + C_T)]^2}{2(4\alpha k - \beta^2)} \leq \prod_{MT} \leq \frac{3k[Q_0 - \alpha(C_M + C_E + C_T)]^2}{4(4\alpha k - \beta^2)},$$

$$\frac{k[Q_0 - \alpha(C_M + C_E + C_T)]^2}{4(4\alpha k - \beta^2)} \leq \prod_E \leq \frac{k[Q_0 - \alpha(C_M + C_E + C_T)]^2}{2(4\alpha k - \beta^2)}, \quad (54)$$

then

$$\frac{(3\beta^2 - 4\alpha k)[Q_0 - \alpha(C_M + C_E + C_T)]}{8\alpha\{k[Q_0 - \alpha(C_M + C_T)] + (3\alpha k - \beta^2)C_E\}} \leq \varphi_1$$

$$\leq \frac{\beta^2[Q_0 - \alpha(C_M + C_E + C_T)]}{4\alpha\{k[Q_0 - \alpha(C_M + C_T)] + (3\alpha k - \beta^2)C_E\}}. \quad (55)$$

5.2.2. Case 2: $3\beta^2 - 4\alpha k < 0$. As mentioned above, when $3\beta^2 - 4\alpha k < 0$, there are four coordination schemes: (1) the alliance transfers part of the revenue to the express company; (2) the alliance bears some of the logistics service effort cost for the express companies; (3) the alliance increases the unit delivery price of the express company; and (4) the express company transfers some of the revenue to the alliance.

A2: Revenue Sharing Coordination in Semicentralized Model 1

Proposition 11. *In order to achieve the centralized decision-making sales price p and the effort level of logistics service s , the service unit price of the express deliver W_B remains unchanged, assuming that the revenue sharing ratio of the alliance composed of the E-commerce mall and the terminal distribution service provider to the express company is θ_2 , $0 < \theta_2 < 1$; when $0 < \theta_2 \leq (\beta^2[Q_0 - \alpha(C_M + C_E + C_T)] / 4\alpha[2kQ_0 + (2\alpha k - \beta^2)(C_M + C_E + C_T)])$, the profit coordination between the alliance and express company can be realized.*

With the similar proof in Proposition 7, we can obtain that

$$0 < \theta_2 \leq \frac{\beta^2[Q_0 - \alpha(C_M + C_E + C_T)]}{4\alpha[2kQ_0 + (2\alpha k - \beta^2)(C_M + C_E + C_T)]}. \quad (56)$$

B2: Cost Sharing Coordination in Semicentralized Model 1

Proposition 12. *In order to achieve the centralized decision-making of sales price p and effort level of express service s , keep the unit price of the express service W_E unchanged, assuming that the sharing proportion of the logistics service effort cost is η_2 , $0 < \eta_2 < 1$, then when $0 < \eta_2 \leq (1/2)$, the alliance and the express company can achieve profit coordination.*

With the similar proof in Proposition 8, we have

$$0 < \eta_2 \leq \frac{1}{2}. \quad (57)$$

C2: Coordination of Unit Delivery Price of Logistics Service in Semicentralized Model 1

Proposition 13. *In order to achieve the centralized decision-making sales price p and the effort level of express service s , the unit price of express service W_B remains unchanged; if the alliance increases the unit delivery price by φ_2 , $0 < \varphi_2 < 1$, when $0 < \varphi_2 \leq (\beta^2 [Q_0 - \alpha(C_M + C_E + C_T)] / 4\alpha \{k[Q_0 - \alpha(C_M + C_T)] + (3\alpha k - \beta^2)C_E\})$, then the alliance and the express company can achieve profit coordination.*

With the similar proof in Proposition 8, we have

$$0 < \varphi_2 \leq \frac{\beta^2 [Q_0 - \alpha(C_M + C_E + C_T)]}{4\alpha \{k[Q_0 - \alpha(C_M + C_T)] + (3\alpha k - \beta^2)C_E\}}. \quad (58)$$

D2: Coordination Strategy of Transferring Part of the Express Company's Profit to the Alliance

Proposition 14. *In order to achieve the centralized decision-making of sales price p and the effort level of logistics service s , the service unit price of the express service provider W_E remains unchanged, assuming that the revenue sharing ratio of the express company is δ , $0 < \delta < 1$, then when $0 < \delta \leq ((4\alpha k - 3\beta^2)[Q_0 - \alpha(C_M + C_E + C_T)] / 8\alpha \{k[Q_0 - \alpha(C_M + C_T)] + (3\alpha k - \beta^2)C_E\})$, the alliance and the express company can achieve profit coordination.*

It is proved as follows.

Assume that the revenue sharing ratio of the express company is δ , and $0 < \delta < 1$, then the profit of the alliance is $\prod_{MT} = [p - C_M - C_T - (1 - \delta)W_E]q - ks^2$, and the profit of the express company is $\prod_E = [(1 - \delta)W_E - C_E]q$.

When

$$\begin{aligned} p &= \frac{2kQ_0 + (2\alpha k - \beta^2)(C_M + C_E + C_T)}{4\alpha k - \beta^2}, \\ s &= \frac{\beta [Q_0 - \alpha(C_M + C_E + C_T)]}{4\alpha k - \beta^2}, \\ W_E &= \frac{k [Q_0 - \alpha(C_M + C_T)] + (3\alpha k - \beta^2)C_E}{4\alpha k - \beta^2}, \end{aligned} \quad (59)$$

then

$$\begin{aligned} \prod_{MT} &= \frac{2\alpha k [Q_0 - \alpha(C_M + C_E + C_T)]}{(4\alpha k - \beta^2)^2} \{(1 + \delta)k \\ &\quad \cdot [Q_0 - \alpha(C_M + C_T)] + [(3\delta - 1)\alpha k - \delta\beta^2]C_E\}, \\ \prod_E &= \frac{k [Q_0 - \alpha(C_M + C_E + C_T)]}{(4\alpha k - \beta^2)^2} \{[(1 - \delta)2\alpha k - \beta^2] \\ &\quad \cdot [Q_0 - \alpha(C_M + C_T)] - \alpha [(1 + 3\delta)2\alpha k - (1 + 2\delta)\beta^2]C_E\}. \end{aligned} \quad (60)$$

Since

$$\begin{aligned} \frac{k [Q_0 - \alpha(C_M + C_E + C_T)]^2}{2(4\alpha k - \beta^2)} &\leq \prod_{MT} \leq \frac{3k [Q_0 - \alpha(C_M + C_E + C_T)]^2}{4(4\alpha k - \beta^2)}, \\ \frac{k [Q_0 - \alpha(C_M + C_E + C_T)]^2}{4(4\alpha k - \beta^2)} &\leq \prod_E \leq \frac{k [Q_0 - \alpha(C_M + C_E + C_T)]^2}{2(4\alpha k - \beta^2)}, \end{aligned} \quad (61)$$

hence

$$0 < \delta \leq \frac{(4\alpha k - 3\beta^2)[Q_0 - \alpha(C_M + C_E + C_T)]}{8\alpha \{k[Q_0 - \alpha(C_M + C_T)] + (3\alpha k - \beta^2)C_E\}}. \quad (62)$$

5.2.3. *Summary.* It can be seen from the above analysis that there are two situations in the contract coordination scheme. When $3\beta^2 - 4\alpha k > 0$, this study proposes three supply chain coordination schemes: (1) the strategy of sharing revenue by the alliance with the express company, (2) the strategy of bearing some of the express company's logistics cost by the alliance, and (3) the strategy of raising the unit delivery price of the express company. When $3\beta^2 - 4\alpha k < 0$, it develops the four coordination schemes: (1) the strategy of transferring some revenue of the alliance to the express company, (2) the strategy of bearing part of the logistics service effort cost by the alliance, (3) the strategy of increasing the unit delivery price of the express company, and (4) the strategy of transferring part of the express company's profit to the alliance.

5.3. Coordination Strategy of Semicentralized Model 2

Proposition 15. *Assuming that the E-commerce mall and the express company alliance and the terminal distribution service provider realize the centralized decision-making sales volume through revenue sharing contract, when the unit price of the terminal distribution service provider remains unchanged, the profits of the terminal distribution service provider will increase.*

It is proved as follows.

When

$$q = \frac{2\alpha k [Q_0 - \alpha(C_M + C_E + C_T)]}{4\alpha k - \beta^2},$$

$$W_T = \frac{2k [Q_0 - \alpha(C_M + C_E)] + (6\alpha k - \beta^2)C_T}{8\alpha k - \beta^2}, \quad (63)$$

then

$$\begin{aligned} \prod_T &= (W_T - C_T)q = \frac{4\alpha k^2 [Q_0 - \alpha(C_M + C_E + C_T)]^2}{(4\alpha k - \beta^2)(8\alpha k - \beta^2)} \\ &= \prod_{T \max} > \prod_{E2}^* = \frac{4\alpha k^2 [Q_0 - \alpha(C_M + C_E + C_T)]^2}{(8\alpha k - \beta^2)^2}, \\ &\frac{4\alpha k^2 [Q_0 - \alpha(C_M + C_E + C_T)]^2}{(8\alpha k - \beta^2)^2} \leq \prod_T \\ &\leq \frac{4\alpha k^2 [Q_0 - \alpha(C_M + C_E + C_T)]^2}{(8\alpha k - \beta^2)(4\alpha k - \beta^2)}. \end{aligned} \quad (64)$$

It can be seen that, in the coordination scheme between the alliance and the terminal distribution service provider, only the terminal distribution service provider can share revenue or undertake some cost with the alliance. Hence, there are two coordination schemes: (1) the strategy of sharing revenue of the terminal distribution service provider with the alliance and (2) the strategy of bearing some logistics service effort cost of the alliance by the terminal distribution service provider.

5.3.1. Revenue Sharing Coordination of Semicentralized Model 2

Proposition 16. In order to achieve the centralized decision-making of sales price p and the effort level of logistics service s , the service unit price of the terminal distribution service provider W_C remains unchanged, assuming that the proportion of sharing the revenue of the terminal distribution service provider is θ_3 , $0 < \theta_3 < 1$, then when $0 < \theta_3 \leq (8\alpha k^2 [Q_0 - \alpha(C_M + C_E + C_T)] / (8\alpha k - \beta^2)) \{2k [Q_0 - \alpha(C_M + C_E)] + (6\alpha k - \beta^2)C_T\}$, the alliance and the terminal distribution service provider can achieve profit coordination.

It is proved as follows.

Assume that the revenue sharing ratio of the terminal distribution service provider is θ_3 and $0 < \theta_3 < 1$, then the profit of the alliance is $\prod_{ME} = [p - C_M - C_E - (1 - \theta_3)W_T]q - ks^2$, and the profit of the terminal distribution service provider is $\prod_T = [(1 - \theta_3)W_T - C_T]q$.

When

$$\begin{aligned} p &= \frac{2kQ_0 + (2\alpha k - \beta^2)(C_M + C_E + C_T)}{4\alpha k - \beta^2}, \\ s &= \frac{\beta [Q_0 - \alpha(C_M + C_E + C_T)]}{4\alpha k - \beta^2}, \\ W_T &= \frac{2k [Q_0 - \alpha(C_M + C_E)] + (6\alpha k - \beta^2)C_T}{8\alpha k - \beta^2}, \end{aligned} \quad (65)$$

then

$$\begin{aligned} \prod_{ME} &= \frac{k [Q_0 - \alpha(C_M + C_E + C_T)]}{(4\alpha k - \beta^2)(8\alpha k - \beta^2)} \{ [4\alpha k (1 + \theta_3) - \beta^2] \\ &\quad \cdot [Q_0 - \alpha(C_M + C_E)] + \alpha [4\alpha k (3\theta_3 - 1) + (1 - 2\theta_3)C_T] \}, \\ \prod_T &= \frac{2k (1 - \theta_3) [Q_0 - \alpha(C_M + C_E)] + [2\alpha k (1 - 3\theta_3) - \theta_3 \beta^2] C_T}{(4\alpha k - \beta^2)(8\alpha k - \beta^2)} \\ &\quad \cdot [Q_0 - \alpha(C_M + C_E + C_T)]. \end{aligned} \quad (66)$$

Since

$$\frac{k [Q_0 - \alpha(C_M + C_E + C_T)]^2}{8\alpha k - \beta^2} \leq \prod_{ME} \leq \frac{k (48\alpha^2 k^2 - 12\alpha k \beta^2 + \beta^4) [Q_0 - \alpha(C_M + C_E + C_T)]^2}{(8\alpha k - \beta^2)^2 (4\alpha k - \beta^2)}, \quad (67)$$

$$\frac{4\alpha k^2 [Q_0 - \alpha(C_M + C_E + C_T)]^2}{(8\alpha k - \beta^2)^2} \leq \prod_T \leq \frac{4\alpha k^2 [Q_0 - \alpha(C_M + C_E + C_T)]^2}{(8\alpha k - \beta^2)(4\alpha k - \beta^2)},$$

hence

$$0 < \theta_3 \leq \frac{8\alpha k^2 [Q_0 - \alpha(C_M + C_E + C_T)]}{(8\alpha k - \beta^2) \{2k [Q_0 - \alpha(C_M + C_E)] + (6\alpha k - \beta^2)C_T\}}. \quad (68)$$

5.3.2. Cost Sharing Coordination of Semicentralized Model 2

Proposition 17. In order to determine the centralized decision-making sales price p and the express service effort level s , the service unit price of the terminal distribution service provider W_T remains unchanged; it is assumed that the

bearing ratio of the logistics service effort cost by the terminal distribution service provider is η_3 , $0 < \eta_3 < 1$, then when $0 < \eta_3 \leq (16\alpha^2 k^2 (4\alpha k - \beta^2) / (8\alpha k - \beta^2)^2 \beta^2)$, the alliance and the terminal distribution service provider can achieve the profit coordination.

It is proved in the following.

Assume that the cost sharing ratio of logistics service effort by the terminal distribution service provider is η_3 and $0 < \eta_3 < 1$, then the profit of the alliance is $\Pi_{ME} = (p - C_M - C_E - W_T)q - (1 - \eta_3)ks^2$, and the profit of the terminal distribution service provider is $\Pi_T = (W_T - C_T)q - \eta_3 ks^2$.

When

$$\begin{aligned} p &= \frac{2kQ_0 + (2\alpha k - \beta^2)(C_M + C_E + C_T)}{4\alpha k - \beta^2}, \\ s &= \frac{\beta[Q_0 - \alpha(C_M + C_E + C_T)]}{4\alpha k - \beta^2}, \\ W_T &= \frac{2k[Q_0 - \alpha(C_M + C_E)] + (6\alpha k - \beta^2)C_T}{8\alpha k - \beta^2}, \end{aligned} \quad (69)$$

then

$$\begin{aligned} \Pi_{ME} &= \frac{k[Q_0 - \alpha(C_M + C_E + C_T)]^2}{(4\alpha k - \beta^2)^2 (8\alpha k - \beta^2)} \left[(4\alpha k - \beta^2)^2 \right. \\ &\quad \left. + \eta_3 \beta^2 (8\alpha k - \beta^2) \right], \\ \Pi_T &= \frac{k[Q_0 - \alpha(C_M + C_E + C_T)]^2}{(4\alpha k - \beta^2)(8\alpha k - \beta^2)} \left[4\alpha k (4\alpha k - \beta^2) \right. \\ &\quad \left. - \eta_3 \beta^2 (8\alpha k - \beta^2) \right]. \end{aligned} \quad (70)$$

Since

$$\begin{aligned} \frac{k[Q_0 - \alpha(C_M + C_E + C_T)]^2}{8\alpha k - \beta^2} &\leq \Pi_{ME} \leq \frac{k(48\alpha^2 k^2 - 12\alpha k \beta^2 + \beta^4)[Q_0 - \alpha(C_M + C_E + C_T)]^2}{(8\alpha k - \beta^2)^2 (4\alpha k - \beta^2)}, \\ \frac{4\alpha k^2 [Q_0 - \alpha(C_M + C_E + C_T)]^2}{(8\alpha k - \beta^2)^2} &\leq \Pi_T \leq \frac{4\alpha k^2 [Q_0 - \alpha(C_M + C_E + C_T)]^2}{(8\alpha k - \beta^2)(4\alpha k - \beta^2)}, \end{aligned} \quad (71)$$

then

$$0 < \eta_3 \leq \frac{16\alpha^2 k^2 (4\alpha k - \beta^2)}{(8\alpha k - \beta^2)^2 \beta^2}. \quad (72)$$

5.4. Summary of Coordination Schemes. According to the above analysis in this section, this study develops the corresponding coordination schemes for semicentralized models 1 and 2. For semicentralized model 1, there are three coordination strategies if $3\beta^2 - 4\alpha k > 0$. Otherwise, there are four coordination strategies. For semicentralized model 2, there are two coordination strategies, which can lead to the win-win status.

6. Numerical Analysis

It is assumed that an E-commerce logistics market includes an E-commerce mall M , an express company E , and a terminal distribution service provider T . The E-commerce mall only sells one product, and the market demand function of the product is $q = 450 - 8p + 15s$. The logistics service cost of express company is $g(s) = 16s^2$. It is assumed that the unit product cost of E-commerce mall C_M is 30, the unit service cost of express company C_E is 12, and the unit

distribution cost of terminal distribution service provider C_T is 3.

6.1. Numerical Analysis of Centralized and Semicentralized Decision Models. Take the above data into Table 3 and get the optimal solution and profit of each partner in semicentralized decision-making and centralized decision-making models, respectively (see Table 4).

Compared with the three semicentralized decision-making models, the logistics service quality of the express companies is higher, the price of products is lower, and the sales volume is higher, so the overall profit of the system is higher under the centralized decision-making model. Furthermore, semicentralized models 1 and 3 have the same effort level of logistics service, product price, and sales volume, thus bringing the same overall profit of the system. In the case of semicentralized model 2, the effort level of logistics service is low, the product price is high, and the sales volume is low, so the overall profit of the system is low. However, due to the fact that the E-commerce mall cannot control the effort level of logistics service when the express company and the terminal distribution service provider are in an alliance, and it is difficult to solve the practical problem that the end distribution cannot meet the customer demand.

TABLE 3: Variables and profit levels in semicentralized decision models.

	The E-commerce mall and the terminal distribution service provider form an alliance (semicentralized 1)	The E-commerce mall and the express company form an alliance (semicentralized 2)	The express company and the terminal distribution service provider form an alliance (semicentralized 3)
s	$(\beta[Q_0 - \alpha(C_M + C_E + C_T)]/2(4\alpha k - \beta^2))$	$(\beta[Q_0 - \alpha(C_M + C_E + C_T)]/8\alpha k - \beta^2)$	$(\beta[Q_0 - \alpha(C_M + C_E + C_T)]/2(4\alpha k - \beta^2))$
p	$((6\alpha k - \beta^2)Q_0 + \alpha(2\alpha k - \beta^2)(C_M + C_E + C_T)/2\alpha(4\alpha k - \beta^2))$	$(6kQ_0 + (2\alpha k - \beta^2)(C_M + C_E + C_T)/8\alpha k - \beta^2)$	$((6\alpha k - \beta^2)Q_0 + \alpha(2\alpha k - \beta^2)(C_M + C_E + C_T)/2\alpha(4\alpha k - \beta^2))$
q	$(\alpha k[Q_0 - \alpha(C_M + C_E + C_T)]/4\alpha k - \beta^2)$	$(2\alpha k[Q_0 - \alpha(C_M + C_E + C_T)]/8\alpha k - \beta^2)$	$(\alpha k[Q_0 - \alpha(C_M + C_E + C_T)]/4\alpha k - \beta^2)$
W_E	$(k[Q_0 - \alpha(C_M + C_T)] + (3\alpha k - \beta^2)C_E/4\alpha k - \beta^2)$	—	—
W_T	—	$(2k[Q_0 - \alpha(C_M + C_E)] + (6\alpha k - \beta^2)C_T/8\alpha k - \beta^2)$	—
W_{ET}	—	—	$(k(Q_0 - \alpha C_M) + (3\alpha k - \beta^2)(C_E + C_T)/4\alpha k - \beta^2)$
Π_{MT}	$(k[Q_0 - \alpha(C_M + C_E + C_T)]^2/2(4\alpha k - \beta^2))$	—	—
Π_{ME}	—	$(k[Q_0 - \alpha(C_M + C_E + C_T)]^2/8\alpha k - \beta^2)$	—
Π_{ET}	—	—	$(k[Q_0 - \alpha(C_M + C_E + C_T)]^2/4(4\alpha k - \beta^2))$
Π_M	$(k[Q_0 - \alpha(C_M + C_E + C_T)]^2/4(4\alpha k - \beta^2))$	—	—
Π_E	—	$(4\alpha k^2[Q_0 - \alpha(C_M + C_E + C_T)]^2/(8\alpha k - \beta^2)^2)$	—
Π_T	$(3k[Q_0 - \alpha(C_M + C_E + C_T)]^2/4(4\alpha k - \beta^2))$	$(k(12\alpha k - \beta^2)[Q_0 - \alpha(C_M + C_E + C_T)]^2/(8\alpha k - \beta^2)^2)$	$(3k[Q_0 - \alpha(C_M + C_E + C_T)]^2/4(4\alpha k - \beta^2))$
Π	—	—	—

TABLE 4: Optimal solution and profit with different decision models.

Parameter	Semicentralized 1	Semicentralized 2	Semicentralized 3	Centralized decision-making
s	2.35	1.69	2.35	4.70
p	55.64	55.81	55.64	55.03
q	40.14	28.84	40.14	80.28
W_E	17.02			
W_T		6.60		
W_{ET}			20.17	
\prod_M			225.78	
\prod_E	112.89			
\prod_T		103.94		
\prod_{MT}	225.78			
\prod_{ME}		162.20		
\prod_{ET}			112.89	
\prod	338.67	266.14	338.67	451.77

Therefore, the alliance between the E-commerce mall and the express company or the terminal distribution service provider is the key to solve the logistics service quality and improve the logistics service. Compared with the alliance of E-commerce mall and the express company, the alliance of E-commerce mall and terminal distribution service provider has a higher effort level of logistics service, lower product price, and higher overall profit of the system.

To maximize the overall profit of the LSSC including the E-commerce mall, the express company, and the terminal distribution service provider, the express company should work harder so as to help the E-commerce mall obtain more orders, but its cost would increase. Therefore, it is necessary for all partners involved to cooperate on the basis of contract coordination so as to achieve all-win situation.

6.2. Numerical Analysis Based on Coordination Schemes

6.2.1. Numerical Analysis of Semicentralized Model 1.

According to the analysis of Section 5, if $3\beta^2 - 4ak > 0$, then there are three coordination schemes: (1) the alliance transfers part of the profit to the express company, (2) the alliance bears some logistics service cost of the express company, and (3) the alliance increases the unit delivery price of the express company.

A1: Coordination of Revenue Sharing. Taking the above data into formula (47), then $0.0145 \leq \theta_1 \leq 0.040$

That is, when the transferring ratio is within the interval $[0.0145, 0.040]$, the profit of both parties can be coordinated and the profit of centralized decision-making can be achieved. The higher the transferring ratio, the less the profit it will earn. Otherwise, the alliance will get a higher profit. The specific transferring ratio depends on the negotiations between the two partners. The profit that can be realized by the two parties under different transfer ratios is shown in Table 5.

From Table 5 and Figure 1, it can be seen that the lower the proportion of revenue sharing by the alliance is, and the higher the profit of the alliance is. However, in any case, the total profits of the alliance and the express company are higher than the profits before the agreement of the contract

TABLE 5: Coordination results of revenue sharing in semi-centralized model 1.

Parameter	Alliance	Profit coordination		
s	2.35			
p	55.64			
q	40.14			
W_E	17.02			
θ_1	—	0.02	0.025	0.035
\prod_{MT}	225.78	313.85	291.76	247.58
\prod_E	112.89	137.92	160.01	204.19
\prod	338.67	451.77	451.77	451.77

coordination scheme, which implies that the contract coordination scheme of revenue sharing can play an effective role.

B1: Coordination of Cost Sharing. Bringing the above data into formula (51), then $0.18 \leq \eta_1 \leq 0.5$.

That is, the alliance, including the E-commerce mall and the terminal distribution service provider, bears the range of the effort cost of the express company within the interval $[0.18, 0.5]$, and the coordination of the profit of both parties can be realized within the range. The specific cost range depends on the negotiations between the two parties. The profit that can be realized by both parties under different sharing ranges is shown in Table 6.

It can be seen from Table 6 and Figure 2 that the lower the proportion of cost sharing by the alliance is, the higher the profit of the alliance is. However, in any case, the total profits of the alliance and express companies are higher than the profits before the contract coordination scheme is reached, which shows that the contract coordination scheme can help the whole system achieve the all-win situation.

C1: Coordination of the Unit Price of Express Service. Bringing the above values into formula (55), then $0.047 \leq \varphi_1 \leq 0.13$.

That is, the range of the unit price increase ratio of the express service is located in $[0.047, 0.13]$, and the coordination of the profit of both parties can be realized within the range. The proportion of specific upward adjustment depends on the

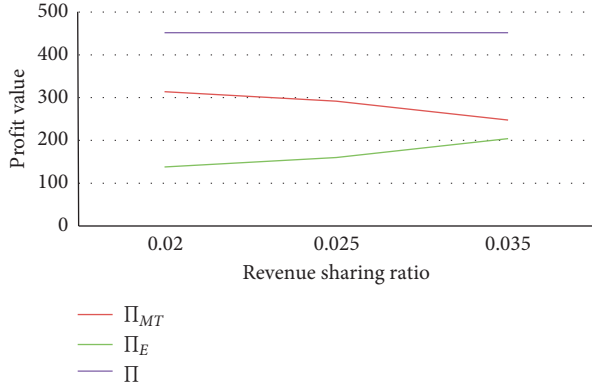


FIGURE 1: Sensitivity of revenue sharing in semicentralized model 1.

TABLE 6: Coordination results of cost sharing in semicentralized model 1.

Parameter	Alliance	Profit coordination		
s	2.35	4.70		
p	55.64	55.03		
q	40.14	80.28		
W_E	17.02	18.04	18.38	18.72
η_1	—	0.2	0.3	0.4
\prod_{MT}	225.78	331.51	296.17	260.83
\prod_E	112.89	120.26	155.60	190.94
\prod	338.67	451.77	451.77	451.77

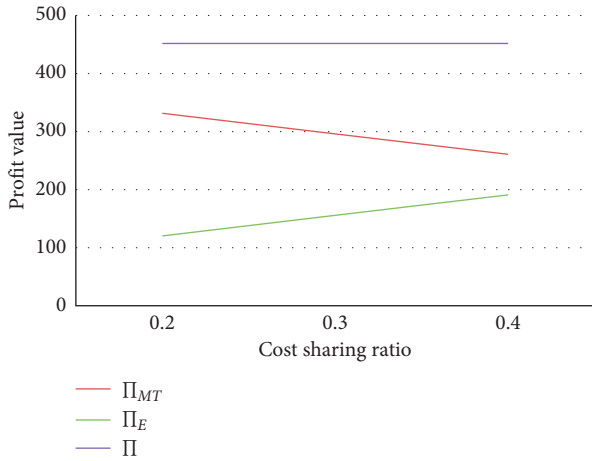


FIGURE 2: Sensitivity of cost sharing in semicentralized model 1.

results of negotiations between the two parties. The profits that can be realized by the two parties under different upward adjustment ratios are shown in Table 7.

From Table 7 and Figure 3, it can be seen that the lower the proportion of increasing the unit delivery price of the express company is, the higher the profit of the alliance is. However, in any case, the total profits of the alliance and the express company are higher than the profits before the contract coordination plan is reached, which shows that the contract coordination can make all the partners in the LSSC achieve the win-win status.

TABLE 7: Coordination result of the unit price of express service in semicentralized model 1.

Parameter	Alliance	Profit coordination		
s	2.35	4.70		
p	55.64	55.03		
q	40.14	80.28		
W_E	17.02	18.04	18.38	18.72
φ_1	—	0.06	0.08	0.10
\prod_{MT}	225.78	320.22	292.89	265.57
\prod_E	112.89	131.55	158.88	186.20
\prod	338.67	451.77	451.77	451.77



FIGURE 3: Sensitivity of the unit delivery price in semicentralized model 1.

6.2.2. Numerical Analysis of Semicentralized Model 2

A3: Coordination of Revenue Sharing by the Terminal Distribution Service Provider. Take the above data into Formula (68), then $0 < \theta_3 \leq 0.35$.

That is, if the revenue sharing ratio of the terminal distribution service provider with the alliance is within the range of $(0, 0.35]$, then all the partners can achieve the all-win situation. The specific ratio depends on the outcome of the negotiations between the two parties. The profit between the two parties with different ratios is shown in Table 8.

From Table 8 and Figure 4, it can be seen that the overall profit of the supply chain can be greatly improved, with an increase rate of 69.75% after the revenue sharing by the terminal distribution service provider. Furthermore, the smaller the proportion of revenue shared by the terminal distribution service provider is, the higher the profit of the terminal distribution service provider is. However, in any case, the total profits of the alliance and the terminal distribution service provider are higher than the profits before the contract coordination scheme is reached, which shows that the contract coordination scheme can lead to the all-win status.

B3: Coordination of Cost Sharing by the Terminal Distribution Service Provider. Bringing the above data into formula (72), then $0 < \eta_3 \leq 0.52$.

TABLE 8: Coordination results of revenue sharing in semicentralized model 2.

Parameter	Alliance	Profit coordination		
s	1.69		4.70	
p	55.81		55.03	
q	28.84		80.28	
W_T	6.60	5.94	5.28	4.62
θ_3	—	0.1	0.2	0.3
Π_{ME}	162.20	215.75	268.73	321.71
Π_T	103.94	236.02	183.04	130.06
Π	266.14	451.77	451.77	451.77

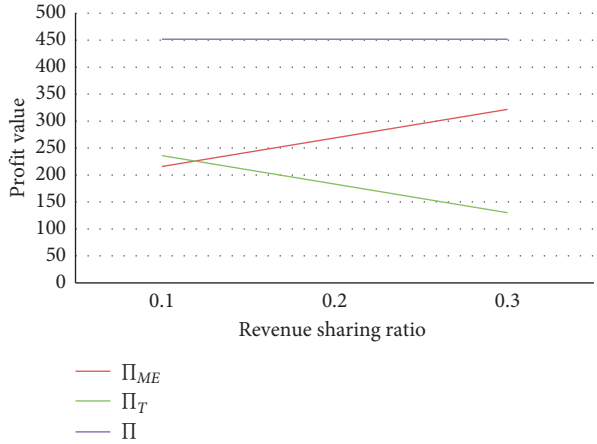


FIGURE 4: Sensitivity of revenue sharing in semicentralized model 2.

TABLE 9: Coordination results of cost sharing in semicentralized model 2.

Parameter	Alliance	Profit coordination		
s	1.69		4.70	
p	55.81		55.03	
q	28.84		80.28	
W_T	6.60		6.60	
η_3	—	0.1	0.3	0.45
Π_{ME}	162.20	198.10	268.79	321.81
Π_T	103.94	253.67	182.98	129.96
Π	266.14	451.77	451.77	451.77

That is, the terminal distribution service provider undertakes some percentage of the service effort cost. If the ratio ranges within the interval of $(0, 0.52]$, then the coordination can be realized. The specific cost-bearing ratio depends on the results of negotiation between the two sides. The profits realized by the two sides under different share ratios are shown in Table 9.

From Table 9 and Figure 5, it can be seen that the overall profit of the supply chain can also be greatly improved, with an increase of 69.75% after the cost sharing by the terminal distribution service provider. Specifically, the smaller the bearing proportion of effort cost by the terminal distribution service provider is, the higher the profit of the terminal distribution service provider is. However, in any case, the total profits of the alliance and the terminal distribution

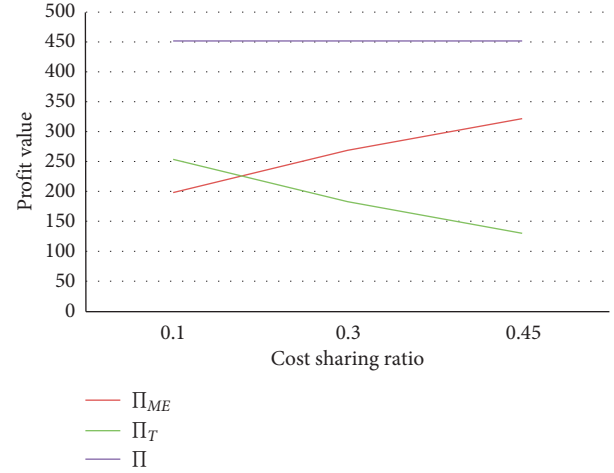


FIGURE 5: Sensitivity of cost sharing in semicentralized model 2.

service provider are higher than the profits before the contract coordination scheme is reached, which suggests that the contract coordination scheme can stimulate all the partners to cooperate together and get the win-win situation.

7. Conclusion and Future Research

This study focuses on the E-commerce LSSC system consisting of an E-commerce mall, an express company, and a terminal distribution service provider and studies the coordination strategy of semicentralized and centralized decision models. With comparative analysis, it is found that the performance of the centralized model is better than that of semicentralized models.

To achieve the global profit level of centralized decision-making and promote the cooperation to establish alliances, it is necessary to apply coordination strategies to achieve long-term win-win cooperation. Based on this, it discusses the profit coordination schemes of the two semicentralized alliances. In the profit coordination scheme of the semicentralized model 1, coordination strategies are discussed according to the two situations. When $3\beta^2 - 4\alpha k > 0$, three coordination strategies are discussed: revenue sharing, cost sharing, and coordination of the unit delivery price. When $4\alpha k - 3\beta^2 > 0$, four coordination strategies are proposed: the alliance's revenue sharing, cost sharing, coordination of the unit delivery price, and the express company's revenue sharing. In the coordination scheme of semicentralized model 2, two coordination schemes are developed, which are the strategy of revenue sharing and cost sharing by the terminal distribution service provider.

Furthermore, through the numerical analysis, the revenue transferring ratio, the proportion of cost sharing, and the unit delivery price of logistics service under the semicentralized decision models are analyzed, respectively. Under the coordination strategy, the ratios of revenue sharing and cost sharing are different in the above semicentralized decision models. The choice of specific contract scheme depends on the comparative advantage of each partner in the negotiation. The research results also provide

some practical support for decision makers to choose appropriate cooperation models based on their real business environment.

Finally, it concludes that the E-commerce mall can get the highest profit when the express company and the terminal distribution service provider join the alliance. However, the E-commerce business may not be sustainable because the E-commerce mall cannot control the logistics service quality and cannot solve the bottleneck problem of the last-mile delivery in reality, which is a key issue for customers. The alliance of E-commerce mall and terminal distribution service providers can improve the quality of logistics service, solve the bottleneck problem of terminal distribution, and improve the overall profit of LSSC. E-commerce mall and terminal distribution service providers can join the alliance with express companies through supply chain coordination, such as revenue sharing, cost sharing, and adjusting the unit delivery price. When the E-commerce mall and express company join the alliance, we need to coordinate the terminal distribution service provider to share some revenue or undertake some cost of logistics service so as to make all the partners achieve the all-win status. Therefore, for E-commerce LSSC, the alliance including E-commerce mall and terminal distribution service providers can be a better choice. The rookie alliance in real life is a typical embodiment.

This research, with respect to existing studies, extends the supply chain coordination in the field of downstream three-echelon LSSC including the terminal distribution, takes the price and effort level of logistics service dependent demand into account, develops effective coordination strategies, such as revenue sharing and cost sharing contracts, and unit delivery price coordination, and provides managerial implication for decision makers to choose appropriate alliance in real business and develop effective coordination strategy.

However, there also exist the following limitations. (1) In real business, the price and demand functions are affected by many factors and are not simply linear or quadratic functions. In the subsequent research, the influences of various factors on price and demand will be considered to establish more practical decision models. (2) In the supply chains with both online and offline business, the sales volume of online platform will be fluctuated by the influence of offline sales. The future research will explore the problem with stochastic demand and information asymmetry and consider the decision-making with a dual-channel online and offline business.

Data Availability

The data used to support the findings of this study are included within the article.

Conflicts of Interest

The authors declare that there are no conflicts of interest regarding the publication of this paper.

Acknowledgments

This study was supported by Humanities and Social Sciences foundation of Ministry of Education in China (Grant 17YJC630230), Social Sciences Federation of Guangdong in China (Grant GD17XGL11), and Macau University of Science and Technology Foundation (Grant FRG-19-033-MSB).

References

- [1] D. A. Hensher, Z. Y. Zhang, and J. Rose, "Transport and logistics challenges for China: drivers of growth, and bottlenecks constraining development," *Road & Transport Research*, vol. 24, no. 2, pp. 32–41, 2015.
- [2] J. J. Spengler, "Vertical integration and antitrust policy," *Journal of Political Economy*, vol. 58, no. 4, Article ID 347e352, 1950.
- [3] J. Xie, W. Zhang, L. Liang, Y. Xia, J. Yin, and G. Yang, "The revenue and cost sharing contract of pricing and servicing policies in a dual-channel closed-loop supply chain," *Journal of Cleaner Production*, vol. 191, pp. 361–383, 2018.
- [4] J. Luo and X. Chen, "Coordination of random yield supply chains with improved revenue sharing contracts," *European Journal of Industrial Engineering*, vol. 10, no. 1, pp. 81–102, 2016.
- [5] H. Zhao, S. Song, Y. Zhang, J. N. D. Gupta, A. G. Devlin, and R. Chiong, "Supply chain coordination with a risk-averse retailer and a combined buy-back and revenue sharing contract," *Asia-Pacific Journal of Operational Research*, vol. 36, no. 5, Article ID 1950028, 2019.
- [6] Z. H. Wu, L. C. Feng, and D. Y. Chen, "Coordinating pricing and advertising decisions for supply chain under consignment contract in the dynamic setting," *Complexity*, vol. 2018, Article ID 7697180, 11 pages, 2018.
- [7] H. Song and X. Gao, "Green supply chain game model and analysis under revenue-sharing contract," *Journal of Cleaner Production*, vol. 170, pp. 183–192, 2018.
- [8] N. Yan, Y. Liu, X. Xu, and X. He, "Strategic dual-channel pricing games with e-retailer finance," *European Journal of Operational Research*, vol. 283, no. 1, pp. 138–151, 2020.
- [9] M. Hua, I. K. W. Lai, and H. Tang, "Analysis of advertising and a points-exchange incentive in a reverse supply chain for unwanted medications in households based on Game Theory," *International Journal of Production Economics*, vol. 217, pp. 259–268, 2019.
- [10] M. N. Hua, H. J. Tang, and I. K. W. Lai, "Game theoretic analysis of pricing and cooperative advertising in a reverse supply chain for unwanted medications in households," *Sustainability*, vol. 9, no. 10, 2017.
- [11] Q. H. Pang, Y. E. Chen, and Y. L. Hu, "Coordinating three-level supply chain by revenue-sharing contract with sales effort dependent demand," *Discrete Dynamics in Nature and Society*, vol. 2014, Article ID 561081, 10 pages, 2014.
- [12] Q. H. Pang, X. Y. Wu, and M. L. Tan, "Supply chain coordination using revenue-sharing contract with DISTRIBUTOR'S effort dependent demand," *International Journal of Simulation Modelling*, vol. 14, no. 2, pp. 335–348, 2015.
- [13] A. A. Taleizadeh, N. Rabiei, and M. Noori-Daryan, "Coordination of a two-echelon supply chain in presence of market segmentation, credit payment, and quantity discount policies," *International Transactions in Operational Research*, vol. 26, no. 4, pp. 1576–1605, 2019.

- [14] S. Sang, "Revenue sharing contract in a multi-echelon supply chain with fuzzy demand and asymmetric information," *International Journal of Computational Intelligence Systems*, vol. 9, no. 6, pp. 1028–1040, 2016.
- [15] J. Cai, X. Hu, P. R. Tadikamalla, and J. Shang, "Flexible contract design for VMI supply chain with service-sensitive demand: revenue-sharing and supplier subsidy," *European Journal of Operational Research*, vol. 261, no. 1, pp. 143–153, 2017.
- [16] J. Zhao, J. Wei, and X. C. Sun, "Coordination of fuzzy closed-loop supply chain with price dependent demand under symmetric and asymmetric information conditions," *Annals of Operations Research*, vol. 257, no. 1-2, pp. 469–489, 2017.
- [17] L. M. Zhao, L. Li, Y. Song, C. Li, and Y. Wu, "Research on pricing and coordination strategy of a sustainable green supply chain with a capital-constrained retailer," *Complexity*, vol. 2018, Article ID 6845970, 12 pages, 2018.
- [18] N. Yan, T. Tong, and H. Dai, "CAPITAL-CONSTRAINED supply chain with multiple decision attributes: decision optimization and coordination analysis," *Journal of Industrial & Management Optimization*, vol. 15, no. 4, pp. 1831–1856, 2019.
- [19] J. Zhang, G. Liu, Q. Zhang, and Z. Bai, "Coordinating a supply chain for deteriorating items with a revenue sharing and cooperative investment contract," *Omega*, vol. 56, pp. 37–49, 2015.
- [20] Q. Bai, M. Chen, and L. Xu, "Revenue and promotional cost-sharing contract versus two-part tariff contract in coordinating sustainable supply chain systems with deteriorating items," *International Journal of Production Economics*, vol. 187, pp. 85–101, 2017.
- [21] B. C. Giri, C. Mondal, and T. Maiti, "Analysing a closed-loop supply chain with selling price, warranty period and green sensitive consumer demand under revenue sharing contract," *Journal of Cleaner Production*, vol. 190, pp. 822–837, 2018.
- [22] J. Heydari and M. Ghasemi, "A revenue sharing contract for reverse supply chain coordination under stochastic quality of returned products and uncertain remanufacturing capacity," *Journal of Cleaner Production*, vol. 197, pp. 607–615, 2018.
- [23] H. Peng, T. Pang, and J. Cong, "Coordination contracts for a supply chain with yield uncertainty and low-carbon preference," *Journal of Cleaner Production*, vol. 205, pp. 291–302, 2018.
- [24] H. Zou, J. Qin, P. Yang, and B. Dai, "A coordinated revenue-sharing model for a sustainable closed-loop supply chain," *Sustainability*, vol. 10, no. 9, 2018.
- [25] H. Mohammadi, M. Ghazanfari, M. S. Pishvae, and E. Teimoury, "Fresh-product supply chain coordination and waste reduction using a revenue-and-preservation-technology-investment-sharing contract: a real-life case study," *Journal of Cleaner Production*, vol. 213, pp. 262–282, 2019.
- [26] M. Ghazanfari, H. Mohammadi, M. S. Pishvae, and E. Teimoury, "Fresh-product trade management under government-backed incentives: a case study of fresh flower market," *Ieee Transactions on Engineering Management*, vol. 66, no. 4, pp. 774–787, 2019.
- [27] Y. G. Zhong, F. Guo, Z. Wang, and H. Tang, "Coordination analysis of revenue sharing in E-commerce logistics service supply chain with cooperative distribution," *SAGE Open*, vol. 9, no. 3, Article ID 215824401987053, 2019.
- [28] Q. H. Pang, Y. L. Hou, and Y. F. Lv, "Coordinating three-level supply chain under disruptions using revenue-sharing contract with effort dependent demand," *Mathematical Problems in Engineering*, vol. 2016, Article ID 9167864, 10 pages, 2016.
- [29] Y. Hou, F. Wei, S. X. Li, Z. Huang, and A. Ashley, "Coordination and performance analysis for a three-echelon supply chain with a revenue sharing contract," *International Journal of Production Research*, vol. 55, no. 1, pp. 202–227, 2017.
- [30] Y. Yuan, S. Ju, Y. Fan, and W. Bian, "The revenue-sharing model of logistics service supply chain for online seafood retailing," *Journal of Coastal Research*, vol. 94, no. sp1, pp. 659–665, 2019.
- [31] P. Liu and S. P. Yi, "Investment decision-making and coordination of a three-stage supply chain considering Data Company in the Big Data era," *Annals of Operations Research*, vol. 270, no. 1-2, pp. 255–271, 2018.
- [32] B. C. Giri and B. R. Sarker, "Coordinating a multi-echelon supply chain under production disruption and price-sensitive stochastic demand," *Journal of Industrial and Management Optimization*, vol. 15, no. 4, pp. 1631–1651, 2019.
- [33] X. F. Liu, J. Li, J. Wu, and G. Zhang, "Coordination of supply chain with a dominant retailer under government price regulation by revenue sharing contracts," *Annals of Operations Research*, vol. 257, no. 1-2, pp. 587–612, 2017.
- [34] Q. F. Meng, J. X. Chen, and K. Qian, "The complexity and simulation of revenue sharing negotiation based on construction stakeholders," *Complexity*, vol. 2018, Article ID 5698170, 11 pages, 2018.
- [35] A. Z. Zeng and J. Hou, "Procurement and coordination under imperfect quality and uncertain demand in reverse mobile phone supply chain," *International Journal of Production Economics*, vol. 209, pp. 346–359, 2019.
- [36] F. Ye, Q. Lin, and Y. Li, "Coordination for contract farming supply chain with stochastic yield and demand under CVaR criterion," *Operational Research*, vol. 20, no. 1, pp. 369–397, 2020.
- [37] J. Zhao, Y.-W. Zhou, Z.-H. Cao, and J. Min, "The shelf space and pricing strategies for a retailer-dominated supply chain with consignment based revenue sharing contracts," *European Journal of Operational Research*, vol. 280, no. 3, pp. 926–939, 2020.
- [38] R. Yan and Z. Pei, "Retail services and firm profit in a dual-channel market," *Journal of Retailing and Consumer Services*, vol. 16, no. 4, pp. 306–314, 2009.
- [39] W.-y. K. Chiang, D. Chhajed, and J. D. Hess, "Direct marketing, indirect profits: a strategic analysis of dual-channel supply-chain design," *Management Science*, vol. 49, no. 1, pp. 1–20, 2003.
- [40] W. Huang and J. M. Swaminathan, "Introduction of a second channel: implications for pricing and profits," *European Journal of Operational Research*, vol. 194, no. 1, pp. 258–279, 2009.

Research Article

Supply Chain Decisions and Coordination under the Combined Effect of Overconfidence and Fairness Concern

Zhang Zhijian,¹ Peng Wang ,¹ Miyu Wan,² Junhua Guo,¹ and Jian Liu ²

¹School of Transportation and Logistics, East China Jiaotong University, Nanchang 330013, China

²School of Information Technology, Jiangxi University of Finance and Economics, Nanchang 330013, China

Correspondence should be addressed to Peng Wang; wangpeng_wl@126.com

Received 9 January 2020; Revised 8 March 2020; Accepted 10 April 2020; Published 25 April 2020

Guest Editor: Baogui Xin

Copyright © 2020 Zhang Zhijian et al. This is an open access article distributed under the Creative Commons Attribution License, which permits unrestricted use, distribution, and reproduction in any medium, provided the original work is properly cited.

The purpose of this study was to examine the joint effect of overconfidence and fairness concern on supply chain decisions and design contracts to achieve a win-win situation within the supply chain. For this study, a centralized supply chain model was established without considering the retailers' overconfidence and fairness concern. Furthermore, the retailers' overconfidence and fairness concerns were introduced into the decentralized supply chain, while the Stackelberg game model between the manufacturer and the retailer was built. Furthermore, an innovative supply chain contract, i.e., buyback contract, with promotional cost sharing was designed to achieve supply chain coordination along with overconfidence and fairness concern. Finally, a numerical analysis was also conducted to analyze the effect of overconfidence, fairness concern, and the validity of the contract. The principal findings of the study include the positive correlation between retailers' overconfidence and optimal order quantity, sales effort, expected utility, and profit. Although the order quantity and sales efforts were not affected by the fairness concern of the retailer, the contract achieved coordination with a win-win outcome when the level of overconfidence and fairness concern was moderate.

1. Introduction

In a global supply chain, the manufacturer sells their product to the retailer at a wholesale price set by the manufacturer, and in response, the retailer chooses the order quantity. Retailers sell goods to consumers through various promotional methods. Besides the interaction between manufacturer and retailer, a reasonable wholesale price, appropriate order quantity, and valid promotion are crucial factors for supply chain members. However, players in the supply chain often tend to show characteristics of bounded rationality in complex and uncertain environments, such as overconfidence [1] and fairness concern [2]. These two behavior preferences were observed anecdotally in practice. For example, Eastman Kodak Company overestimated its technical ability and ignored the planning for the future, which led to declined sales and eventually bankruptcy [3]; Gome in March 2016 was concerned about distributional fairness and wanted to capitalize on its dominating power in the retailing

industry to extract more profit from the manufacturer [4]. Overconfidence is the most widespread cognitive bias in the decision-making process. Fairness concern is the reflection of sociological emotions, which are related to social preferences in the supply chain. Therefore, overconfidence and fairness concern could affect decision-making profoundly in a wide range of areas, such as ordering, pricing, and sales effort.

In general, the above two behavioral preferences, i.e., overconfidence and fairness concern, coexist in the decision-making process. A typical case can be used to illustrate the phenomenon. During the Chinese shopping festival "Double 11" of 2014, Alibabas' transaction value exceeded RMB 57.1 billion. Before the onset of Double 11, the CEO of Taobao predicted that the refund rate would be in single-digit percentage points. However, the real refund rate was 69%, and the real complaint rate was higher than usual, for example, Haier complaint rate was 54.2% [5]. The significant discount on the activity motivated a large number of end

customers with irrational shopping behavior, which resulted in return orders and complaint rate. This case indicated that overconfidence and fairness concern coexisted in the decision-making process. On the one hand, the prediction by the CEO and the high refund rate indicated that a large number of people were overconfident. Consequently, wrong decisions caused losses, which included seller and consumer concern fairness issues that resulted in a high complaint rate. Hence, the coexistence of overconfidence and fairness concern was not occasional but inevitable. In the context of the supply chain, numerous interactions existed between overconfidence and fairness concern. Overconfidence on-demand prediction triggered retailer overordering, while fairness concern had an opposite effect on the retailer's decisions. For instance, in the "Double 11" shopping festival, a retailer of China believed that he possessed better marketing capabilities than others and thus ordered more products from a large manufacturer, e.g., Procter & Gamble (P&G). However, the retailer made lower-than-expected profit due to excessive inventory and marketing expenses. Meanwhile, the retailer reduced order quantity and increased retail price because he felt that P&G was unfairly seizing a disproportionate share of the profit [6]. Therefore, this paper introduces overconfidence and fairness concern into the context of the supply chain. Based on random market demands, we analyzed the retailer's behavioral preferences in decision-making, which affects the decision-making ability, profits, and utility in the supply chain.

The decision makers of the decentralized supply chain are sufficiently rational. However, they suffer when manufacturers charge a wholesale price higher than the production cost so that the amount of order quantity in the decentralized channel is lower in the centralized channel analog [7]. Therefore, coordination is a critical issue in supply chain management. At the same time, the members of the supply chain aim to maximize their profits, which results in the well-known problem of "double marginalization." In order to solve this problem, various coordinating contracts were proposed in different supply chain structures. However, coordinating conditions and the degrees of difficulty during coordination changes depend on behavioral factors [8]. Among many different types of contracts, combined contract, i.e., the combination of two or more contracts, has received widespread attention and proved to be effective in resolving these conflicts [9]. As compared to the centralized supply chain, optimal decisions or profits in a decentralized supply chain are always suboptimal when the retailer has behavioral preferences in the decentralized supply chain.

Based on these challenges, two critical scenarios are considered: (a) the centralized supply chain, wherein the manufacturer and retailer make decisions as a whole to maximize the total expected profit, and (b) the decentralized supply chain consisting of a rational manufacturer and a retailer with overconfidence and fairness concern, wherein members are independent decision makers and aim to maximize their profits. We then assessed the effect of behavioral preferences on the equilibrium outcome for this decentralized supply chain and compared these effects to

their centralized channel analogs. We observed that the two cognitive biases could trigger the decision makers of decentralized supply chain members to deviate from their optimal decisions in the centralized supply chain, which reduces the profitability of the decentralized supply chain. Thus, a valid buyback contract with promotional cost sharing was proposed to coordinate the decentralized supply chain with overconfidence and fairness concern. Such a contract is based on two types of conventional contracts: buyback contract and promotional cost-sharing contract. In the buyback contract, the upstream manufacturer commits to buying back unsold goods from the downstream retailer at the end of the selling season in order to encourage the retailer to order more. The latter contract is designed to share the cost of retailers' sales efforts on increasing sales. The buyback contract with promotional cost sharing has been widely applied in various industries, such as procurement of industrial materials [10], medical devices [11], and retailing [12].

The remainder of the paper is organized as follows: the relevant papers are described in Section 2, whereas Section 3 formalizes the problem. The two important models are presented and solved, i.e., (a) the centralized supply chain model wherein the members are both rational and (b) the decentralized supply chain model wherein the retailer has overconfidence and fairness concern. The combined effect of overconfidence and fairness concern on supply chain decisions has also been discussed. In Section 4, the buyback contract with promotional cost sharing is proposed to coordinate supply chain decisions in the presence of cognitive biases. A numerical analysis is conducted to examine the theoretical models and propositions in Section 5. Lastly, the conclusions and directions for future studies are discussed in Section 6.

2. Literature Review

There are three streams of literature related to our paper: overconfidence, fairness concern, and supply chain coordination. In this section, the recent literature on these three topics has been reviewed and summarized.

2.1. Overconfidence. Some studies have investigated overconfidence in supply chain management (SCM). Croson et al. [13] first introduced overconfidence into the supply chain and analyzed the decisions of overconfident newsvendors. Li et al. [14] examined the implications and influences of overconfidence in a competitive newsvendor setting. Similarly, Liu et al. [15] presented a two-period service capacity procurement model and found that a dynamic wholesale price mechanism could eliminate the negative effect of overconfidence. Xu et al. [16] explored the effects of overconfidence on retailers in different games. Li [17] identified that overconfidence could reduce the double marginalization effect in a decentralized supply chain. The papers mentioned above defined the decision makers' overconfidence based on a biased belief that the variance of demand was underestimated. Hence, in this paper, the

retailers' overconfidence had the same definition. Besides, we also considered that the overconfident retailer overestimated the mean of market demand and the effects of their own sales effort on demand. Moreover, the most existing papers only focused on the effect of overconfidence on the ordering or pricing; we extended previous research and analyzed the effect of overconfidence on pricing, ordering, and sales effort.

2.2. Fairness Concern. Fairness concern has been studied extensively in SCM. Cui et al. [18] analytically and experimentally evaluated how fairness significantly affected the pricing decisions of the manufacturer and the retailer. Similar issues were considered by Wu et al. [19], who examined the influence of fairness concern on the retailers' profit allocation in the newsvendors' model. A recent paper by Chen et al. [20] also analyzed the interactions between fairness concern and decisions, including pricing and service level in a dual-channel supply chain consisting of a manufacturer and two retailers. Also, Liu et al. [21] investigated the impact of different fairness concerns on order allocation in the logistics service supply chain. Zhang et al. [22] revealed the characteristics of price changes when fairness concern was categorized into unfavorable and favorable disutility, respectively. The above papers mainly studied how fairness concerns affected decision variables in various supply chain structures. Motivated by those papers, we also analyzed the decision-making problems of members in a two-echelon supply chain wherein the retailer had fairness concerns. However, we extended previous studies and analyzed the impact of fairness concern on pricing, ordering, and the sales effort, while other papers ignored sales effort.

2.3. Supply Chain Coordination. It can be seen from Sections 2.1 and 2.2 that both overconfidence and fairness concern had a systematic effect on the decision-making and performance in supply chains; they also cause decision-making bias. Therefore, in order to pursue a win-win situation and reduce decision biases, appropriate coordination mechanisms are especially necessary. To date, various contracts have been developed in behavioral supply chain management. For fairness concern, Cui et al. [18] incorporated fairness concern into a conventional supply chain and considered its influence on channel coordination between a manufacturer and a retailer. Cui's model was then extended by Liu et al. [21] to include a nonlinear demand. They further devised a revenue-sharing contract to coordinate a two-echelon CLSC with both members' fairness concerns. Nevertheless, Zheng et al. [4] proposed a cooperative game approach to coordinate a three-echelon closed-loop supply chain with fairness concern. For overconfidence, based on the principal-agent theory, Wang et al. [23] designed an optional contract to achieve a two-echelon supply chain with overconfidence coordination and Pareto improvement. Jiang et al. [24] studied the effect of supplier overconfidence on buyback contracts in a financing supply chain. These studies revealed that fairness concerns and overconfidence could complicate coordination in a supply chain, and

existing research along this line is generally confined to a supply chain within a non-cooperative game setting.

Based on these critical features of our model, we tabulated our research in the context of a proper literature review (Table 1). The table revealed that the majority of the literature concentrates on the coordination of different structure supply chains with single-behavioral preference, i.e., overconfidence or fairness concern. However, overconfidence and fairness concern coexist in practice, and this paper extends the depth and breadth of related literature about behavioral preferences. Besides, the two cognitive biases (overconfidence and fairness concern) were simultaneously taken into consideration, and the buyback contract with promotional cost sharing was proposed in this paper. Nevertheless, the focus of our paper was to investigate the impact of retailers' fairness concern and overconfidence on the coordination results of a two-echelon supply chain by employing a Stackelberg game approach. We examined the validity of the contract under conditions that the retailer had cognitive biases, which were aligned with previous research.

3. Assumptions and Models

3.1. Assumptions. A two-echelon supply chain was considered, which included the rational manufacturer as the leader of the supply chain, while the retailer had overconfidence and fairness concern. The manufacturer produced products at unit production cost c and then sold them at unit wholesale price w to the retailer. The retailer then sold those to customers at unit retail price p . The manufacturer and the retailer showed risk neutrality. Let s be the unit salvage value, v be the unit stockout cost, and q be the order quantity of the retailer. According to Ma et al. [25], we assumed that the sales effort cost of the retailer was monotonically increasing as convex function, i.e., $C(e)$ denoted the sales effort cost, where $C(e) = (1/2)\gamma e^2$ ($\gamma > 0$) is the sales cost coefficient and e ($e > 0$) is the retailers' sales effort denoted by the promotional effort level. Without loss of generality, we assumed that $0 < s < c < v < p$, $w > c$, and $q > 0$.

In the two-echelon supply chain, the manufacturer determined the wholesale price w , and the retailer determined the order quantity q and sales effort e , i.e., w , q , and e were decision variables of supply chain members. s , v , and γ were assumed to be exogenous variables. Note that the retail price p was also assumed to be exogenous.

3.2. Centralized Supply Chain Model. In this section, we considered the scenario wherein the manufacturer and the retailer made decisions as individuals. The model with no behavioral preferences was analyzed as a benchmark. Besides, the goal of the coordination contract in Section 4 was to allow supply chain performance to achieve the optimal situation under complete rationality. Hence, the benchmark was kept under complete rationality [8, 26]. However, the only goal was to maximize the overall profitability of the supply chain by determining the optimal order quantity q and sales effort e . Previous studies proved that when decision makers were entirely rational, the equilibrium solutions of

TABLE 1: Differences between this paper and relevant studies.

Papers	Overconfidence	Fairness concern	Demand function	Coordination
Crosron et al. [13]	✓		Stochastic demand	
Li et al. [14]	✓		Deterministic demand	
Liu et al. [15]	✓		Deterministic demand	
Xu et al. [16]	✓		Stochastic demand	
Li [17]	✓		Stochastic demand	
Cui et al. [18]		✓	Deterministic demand	Wholesale price contract
Wu et al. [19]		✓	Stochastic demand	
Chen et al. [20]		✓	Deterministic demand	Revenue sharing contract
Liu et al. [21]		✓	Deterministic demand	Membership-profit share contract
Zhang et al. [22]		✓	Deterministic demand	
Zheng et al. [4]	✓		Deterministic demand	Cooperative game mechanism
Wang et al. [23]	✓		Stochastic demand	Option contract
Jiang et al. [24]	✓		Stochastic demand	Wholesale price contract with buyback
This study	✓	✓	Stochastic demand	Buyback contract with promotion cost sharing

the centralized supply chain were always better than the decentralized behavioral supply chain [27, 28]. In order to explore research problems and compare optimal decision variables to the decentralized supply chain with behavioral preference analogs, we assumed that the decision maker was rational in the centralized supply chain. According to Xu et al. [16], the stochastic demand function is as follows:

$$D = a - bp + e + \theta, \quad (1)$$

where a signifies the market scale, while b is the price sensitivity coefficient of random demand. The above function indicated that sales effort e has a positive influence on demand D ($D > 0$). The sales price p is exogenous; therefore, we assumed that θ denotes the uncertainty of the demand, which was a random variable following a uniform distribution on the interval $[-A, A]$, wherein $A > 0$ denotes the variation range of the random variable. For variable θ , the cumulative distribution function is $F(\theta)$, and the probability density function is $f(\theta)$. According to the assumption, $f(\theta) = (1/2A)$ and $F(\theta) = (\theta - A/2A)$. Also, to avoid trivial cases, we assumed $A < a$ and $a - bp > 0$, which guaranteed that the demand is nonnegative.

Under settings that did not guarantee market demand, we took q to be more than the demand D , i.e., the decision maker faced the situation of overstock. Under such a situation, we assumed $-A < \theta < q - (a - bp + e)$. In contrast, when q was less than D , $q - (a - bp + e) < \theta < A$ was obtained, which indicated that the decision maker faced a situation of stockout. We assumed that $\theta_0 = q - (a - bp + e)$ indicated that order quantity was equal to the actual market demand D . Hence, $f(\theta_0) = (1/2A)$ and $F(\theta_0) = ((c - v)/(s - v))$.

The profit for the centralized supply chain can be expressed as

$$\max_{q, e} \int_0^c \Pi = pE[\min\{q, D\}] + E[s(q - D)]^+ - E[v(D - q)]^+ - cq - C(e). \quad (2)$$

The first term in equation (2) is the expected revenue of the supply chain, while the second term signifies the expected surplus value if the situation of overstock happened. The third is the expected loss provided the decision makers' order quantity was out of stock. The term cq is the total production cost, and the last term indicated promotion effort, i.e., the cost of sales.

The first-order derivatives of equation (2) with respect to q and e are

$$\begin{cases} \frac{\partial E(\Pi^c)}{\partial q} = (s - v)F(\theta_0) + v - c = 0, \\ \frac{\partial E(\Pi^c)}{\partial e} = (p - v) + (v - s)F(\theta_0) - \gamma e = 0. \end{cases} \quad (3)$$

Therefore, the Hessian matrix is

$$H(q, e) = \begin{pmatrix} (s - v)f(\theta_0) & 0 \\ 0 & (s - v)f(\theta_0) - \gamma \end{pmatrix}. \quad (4)$$

Note that $s - v < 0$ and $f(\theta_0) > 0$; thus, the Hessian matrix Π^c is a negative definite for q and e . We can obtain optimal order quantity and sales effort as follows:

$$\begin{cases} q^{c*} = \frac{(v - s)[(a - bp)\gamma + (p - c)] + A\gamma(v + s - 2c)}{(v - s)\gamma}, \\ e^{c*} = \frac{(p - c)}{\gamma}. \end{cases} \quad (5)$$

3.3. Decentralized Supply Chain Model. In this section, the overconfidence and fairness concerns were incorporated into the two-echelon supply chain, wherein the

manufacturer was reported to be rational, while the retailer had a cognitive bias. We assumed an overconfident retailer who not only underestimated the variance of demand but also overestimated the mean of demand and the effect of sales effort on demand. According to Chen et al. [3], we adopted mean-increasing and variance-reducing transformation of the actual market demand D . Thus, the market demand can be explained as follows:

$$D_O = a - bp + (1 + \beta)e + (1 - \beta)\theta = a - bp + (1 + \beta)e + \theta_1, \quad (6)$$

wherein β indicates the overconfident level ($0 < \beta < 1$). Moreover, the continuous random variable θ_1 is equal to $(1 - \beta)\theta$, which is a random noisy signal and assumed to be uniformly distributed, i.e., $\theta_1 \sim U(-A, A)$. When $\beta = 0$, the retailer had no overconfidence, whereas for $0 < \beta < 1$, the mean of D_O increased and the variance of D_O decreased as compared to the mean and variance of D , i.e., $E(D_O) > E(D)$ and $\text{var}(D_O) < \text{var}(D)$. Meanwhile, the impact of the promotion effort ($(1 + \beta)e > e$) on market demand was overestimated, i.e., the influence of e on market demand increased as β increased.

Similarly, when market demand was uncertain, we considered an order quantity q for the retailer with overconfidence and fairness concern provided q was more than the random demand D_O . Such an arrangement indicated that the retailer faced an overstock situation. In this situation, we have $-A < \theta_1 < q - [a - bp + (1 + \beta)e]$. In contrast, if q was less than D_O , $q - [a - bp + (1 + \beta)e] < \theta_1 < A$ was obtained, which indicated that the retailer faced a stockout situation, i.e., we assumed that $\theta_2 = q - [a - bp + (1 + \beta)e]$. Hence, $F(\theta_2) = (\mu(w - c) + (1 + \mu)(w - v)/(s - v)(1 + \mu))$. The utility of the overconfident retailer is as follows:

$$\begin{aligned} \max_{q, e} U_r^o &= pE[\min\{q, D_O\}] + E[s(q - D_O)^+] \\ &\quad - E[v(D_O - q)]^+ - wq - C(e). \end{aligned} \quad (7)$$

The reference framework for a retailer with fairness concern is the F-S model [29]:

$$U_r^f = \prod_r -\mu \left(\prod_m - \prod_r, 0 \right) - \lambda \left(\prod_r - \prod_m, 0 \right), \quad (8)$$

where μ is the degree of fairness concern and λ is the coefficient of sympathy, $\mu, \lambda \geq 0$, and $0 < \lambda < 1$. The first part of equation (12) reflected the retailer's profit, whereas the second part evaluated the utility loss from disadvantageous inequality for the retailer when $\pi_m > \pi_r$, and the third part measured the loss from advantageous inequality for the retailer when $\pi_m < \pi_r$. Note that if the retailer's profit was worse than the manufacturers' profit (i.e.,

$\pi_m > \pi_r$), the retailer will have negative utility under the condition of unfair aversion. In contrast, if his profit was more significant than the manufacturers', the retailer will also suffer positive utility because of the sympathy. However, Qin et al. [30] demonstrated that the profit of the leader in a supply chain often accounted for more than half of the overall profit when the Stackelberg game was carried out. In this paper, the retailer is a weak follower as compared to the manufacturer who served as the leader. Alongside this, we found out that the profit of the manufacturer was twice that of the retailer when the manufacturer and the retailer were both unboundedly rational. Figures 4 and 5 validate the result in Section 5 when $\mu = 0, \beta = 0$; hence, the retailer had the negative utility of unfair aversion. Therefore, according to equation (8), when the retailer had fairness concern only, his utility function was corrected to

$$U_r^f = \prod_r -\mu \left(\prod_m - \prod_r \right) = (1 + \mu) \prod_r - \mu \prod_m, \quad (9)$$

where \prod_r and \prod_m denotes the profit of the rational retailer and the rational manufacturer, respectively. $\mu > 0$ is the degree of fairness concern.

According to the theories of overconfidence and fairness concern, the utility of the retailer with the two behavioral preferences which was replaced by \prod_r in equation (9) with U_r^o in equation (7) is as follows:

$$\max_{q, e} U \left(\prod_r^d \right) = (1 + \mu) U_r^o - \mu \prod_m^d. \quad (10)$$

The retailer with behavioral preference orders q from the manufacturer, the rational manufacturer profit function is

$$\max_w \prod_m^d = (w - c)q. \quad (11)$$

The Stackelberg game model, where the manufacturer was serving as the leader and the retailer served as the follower, was established in the decentralized supply chain. The events of the model are described as follows. Firstly, the manufacturer decided the wholesale price w . Then, the retailer made decisions about the order quantity q and the sales effort e based on the decision of the manufacturer and market demand. To solve the subgame perfect equilibrium, the backward induction method was applied. The equilibrium solutions under the Stackelberg game model were considered when the retailer had a cognitive bias. The solutions are as follows. The proof is given in Appendix A.

$$w^{d*} = \frac{(a - bp)(1 + \mu)(v - s)\gamma + (v - s)(1 + \beta)^2[(1 + \mu)p + (1 + 3\mu)c] + A\gamma[(s + v)(1 + \mu) + 2(1 + 3\mu)c]}{2(1 + 2\mu)[2A\gamma + (v - s)(1 + \beta)^2]}, \quad (12)$$

$$q^{d*} = \frac{(a - bp)(v - s)\gamma + (1 + \beta)^2(v - s)(p - c) + A\gamma(s + v - 2c)}{2(v - s)\gamma}, \quad (13)$$

$$e^{d*} = \frac{(1 + \beta)[(a - bp)(s - v)\gamma + (p - c)(v - s)(1 + \beta)^2 + 2A\gamma(2p - c - s - v)]}{2\gamma[2A\gamma + (1 + \beta)^2(v - s)]}. \quad (14)$$

Based on the above equilibrium solutions in the decentralized supply chain, the propositions about the effect of overconfidence and fairness concern (β and μ) on decision variables (q^{d*} , e^{d*} , and w^{d*}) are shown as in the following. Note that the proof of all propositions can be found in Appendix B.

Proposition 1. *When the retailer had both overconfidence and fairness concern, the optimal order quantity q^{d*} and sales effort e^{d*} were both positively correlated with the overconfident level β but had nothing to do with the degree of fairness concern μ . Furthermore, q^{d*} is a strictly convex function with respect to β .*

Proposition 1 indicated that the overconfident drives the retailer to increase order volume and improve sales efforts. The reason is that overconfidence had two main effects. On the one hand, the retailer overestimated the average market demand and exaggerated the effectiveness of sales effort, which directly motivated the retailer to make a more considerable sales effort (for example, increasing promotions). On the other hand, the retailer overestimated that the variance of the “random impact factor θ_1 ” is smaller than the actual level. In other words, from his point of view, a smaller market demand fluctuation influenced prediction. Thus, the two effects made the retailer order more product quantities and pay more sales effort for more revenue. Meanwhile, it was easy to find that q^{d*} and e^{d*} were only related to β as per equations (13) and (14), which revealed that the retailers’ decisions on ordering and sales efforts were not affected by fairness concern.

Proposition 2. *When the retailer has both overconfidence and fairness concern, the optimal wholesale price w^{d*} is positively proportional to the overconfident level β but inversely proportional to the degree of fairness concern μ .*

Proposition 2 illustrated that the cognitive bias of the retailer had an opposite effect on the manufacturers’ decision. Firstly, the moment the rational manufacturer realized that the overconfident retailer could increase the order quantity, he raised the wholesale price of the product to maximize the profit, which was consistent with the anecdotes that merchants in real world could take advantage of others’ overconfidence to maximize their profit. Besides, when the manufacturer understood the features of the retailers’ fairness concern, he lowered the

wholesale price to alleviate the retailers’ unfair aversion, which implied that the retailer could boost his bargaining power in the supply chain while he was concerned with the fairness. Therefore, the rational manufacturer was required to set a reasonable wholesale price to balance the influence of the two cognitive biases. Next, we compared the equilibrium outcomes in the centralized supply chain model with those in the decentralized supply chain model. There is a proposition as follows.

Proposition 3. *q^{c*} may be more than or less than q^{d*} ; e^{c*} may be more than or less than e^{d*} . Interestingly, $\Delta q = q^{d*} - q^{c*}$, and $\Delta e = e^{d*} - e^{c*}$ increases as the overconfidence level β increases, respectively.*

According to Proposition 3, the effect of overconfidence, the optimal order quantity, and sales effort on the decentralized supply chain could deviate from the optimal equilibrium solution in the centralized supply chain, which resulted in a loss of the expected profits, thereby increasing the revenue gap between manufacturer and retailer.

4. Buyback Contract with Promotion Cost Sharing

It can be seen from Section 3.3 that due to the cognitive bias of the retailer, his decisions deviated from the optimal decisions in the centralized supply chain, which affected the profit or utility of supply chain members. Thereby, in order to coordinate the profit or utility between the supply chain members and ensure the maximized performance of the two-echelon supply chain, according to Bai et al. [31], the buyback contract with promotional cost sharing was proposed in this section. Here, the manufacturer served as the leader, who buys back the unsold products from the retailer at the buyback price and shared the promotional cost. We denoted this contract factor as (w^{sc} , r , and $1 - \phi$), where w^{sc} is the wholesale price, r is the buyback price, and $1 - \phi$ is the fraction of promotional costs that the rational manufacturer paid, while the retailer undertook ϕ portion of the cost ($0 < \phi < 1$). In order to avoid retailers’ over-ordering and encourage the retailer to accept the contract, we assumed $0 < s \leq r < w^{sc}$. Based on these descriptions and assumptions above, the manufacturers’ profit and retailers’ utility are given by the following expression:

$$\prod_m^{sc} = (w - c)q + E[(s - r)(q - D_O)]^+ - (1 - \phi)C(e), \quad (15)$$

$$U\left(\prod_r^{sc}\right) = (1 + \mu)\{p[(a - bp + (1 + \beta)e)] + E[r(q - D_O)^+]\} - E[v(D_O - q)^+] - wq - \phi C(e) - \mu \prod_m^{sc}, \quad (16)$$

wherein equation (15) is the profit when the manufacturer buys back the unsold products at buyback price r from the retailer and thus obtained the surplus value of these products. $(1 - \phi)C(e)$ is the promotional costs which the manufacturer undertook. $r(q - D_O)^+$ in equation (16) is the revenue when the retailer sells the unsold inventory of

$$w^{sc*} = \frac{[\beta(1 + \mu) + 1 - \phi(1 + 2\mu)]p + [\beta\mu + (1 + 2\mu)\phi]c}{(1 + 2\mu)(1 + \beta)}, \quad (18)$$

$$r^* = \frac{(v - s)(p - c)(1 + \beta)(1 + \mu)v\beta + 2A[\gamma\phi(p - c)(1 + 2\mu) + \beta cv(1 + \mu)] - 2A\gamma\{p(v - s)[1 + \beta + (2 + \beta)\beta\mu] - sv(1 + \beta)(1 + \mu)\}}{(1 + 2\mu)(1 + \beta)[\beta(p - c)(v - s) + 2A\gamma(c - v)]} \quad (19)$$

The purpose of the buyback contract with promotion cost sharing was to design a reasonable profit allocation scheme between the rational manufacturer and the retailer with cognitive bias. It should be noted that if the profit of supply chain members became lower, the contract was unacceptable. The contract was acceptable if and only if $\prod_m^{sc} \geq \prod_m^{d*}$ and $U(\prod_r^{sc}) \geq U(\prod_r^{d*})$.

Based on the above equilibrium solutions in the contract, the following propositions were obtained. Due to the sophisticated formula of the buyback price, this section discussed the effect of overconfidence and fairness concern on wholesale price.

Proposition 4. *The optimal wholesale price in the buyback contract with promotion cost sharing was negatively correlated with μ and ϕ . Nevertheless, if $\phi < (\mu/(1 + 2\mu))$, the wholesale price w^{sc*} is positively correlated with β . In contrast, if $\phi < (\mu/(1 + 2\mu))$, it is negatively correlated with β .*

Proposition 4 implied that the contract was adopted, and the negative effect of fairness concern μ on wholesale price w^{sc*} remained consistent with Proposition 2. Besides, as w^{sc} increased, ϕ decreased and $1 - \phi$ increased accordingly, which meant that the manufacturer bore more promotional cost when the wholesale price rose, which is in line with the practice. Meanwhile, the values of μ and ϕ determined the impact of β (positive or negative influence) on the wholesale price w^{sc} , which indicated that fairness concern μ and promotional cost portion $1 - \phi$ were critical to manufacturer's decisions on the wholesale price w^{sc} . Thus, when the

products to the manufacturer at the end of the selling season. $\phi C(e)$ is the promotional costs which he pay.

According to the first derivations of equation (16) based on q and e , the following expression is obtained:

$$\begin{cases} q^{sc} = \frac{2A(1 + \mu)(v - w) - \mu(w - c)}{(1 + \mu)(v - r) + \mu(s - r)} + a - bp + (1 + k)e^{sc} - A, \\ e^{sc} = \frac{(1 + \beta)[\mu(p + c - 2w) + p - w]}{(2\mu\phi - \mu + \phi)\gamma}. \end{cases} \quad (17)$$

In the buyback contract with promotion cost sharing to achieve supply chain coordination, the optimal decisions of the retailer were the same as those under the centralized supply chain model, that is, $q^{sc} = q^{c*}$ and $e^{sc} = e^{c*}$ [25, 26]. Therefore, equation (17) needs to be equal to equation (5) as the contract factors (w^{sc}, r) were obtained:

two types of behavioral preferences coexisted in the contract, the effect of overconfidence on the optimal wholesale price depended on the relationship between fairness degree and fraction of promotion cost. Since the utility and profit functions in the supply chain included a large number of unknown parameters under three scenarios (i.e., Sections 3.2, 3.3, and 4), it was difficult to compare and analyze the effects of the cognitive biases. Thus, numerical methods were utilized to conduct further analysis in the next section.

5. Numerical Analysis

In this section, a numerical study approach was adopted to allow a more in-depth insight into the two behavioral preferences. First, a numerical experiment was conducted to show how equilibrium solutions and profit (utility) in the two-echelon supply chain changed along with the levels of overconfidence and fairness concern (i.e., β and μ) and to examine the robustness of propositions. Then, we also determined the effect of overconfidence and fairness concern on the buyback contract with promotional cost sharing.

In our experiments, some parameters were gathered from the existing papers. For the parameters related to overconfidence, Ren et al. [1] set $\beta \in [0, 1]$ and $c = \{0.5, 0.6, 0.8, 0.9\}$ to perform their numerical experiments, and Li et al. [7] set $\beta \in (0, 1)$ and $c = 5$ to conduct their study. For the parameters related to fairness concern, Zheng et al. [4] set $\mu \geq 0$, $c = 20$, and $a = 100$ to implement their numerical analysis, and Guo et al. [9] set $\mu \geq 0$ to perform their studies. According to the parameters above,

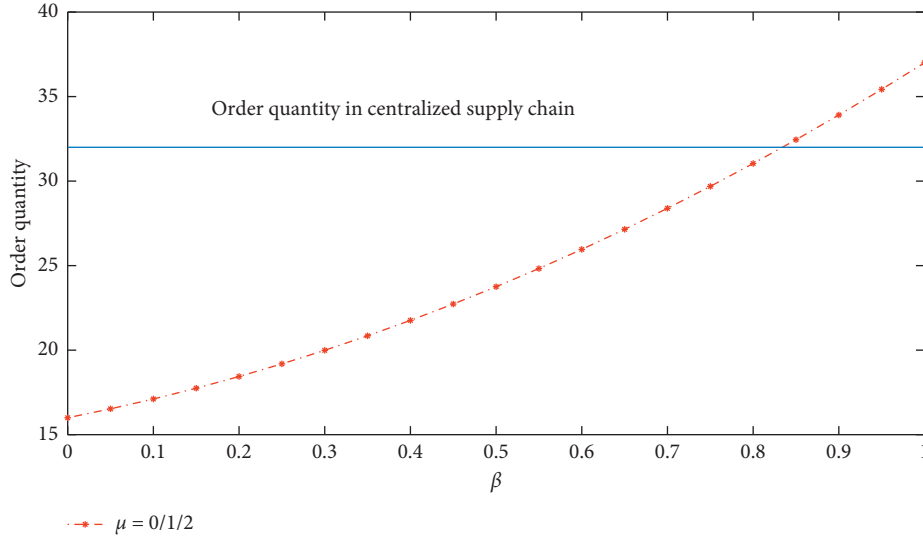


FIGURE 1: The effect of the cognitive biases on optimal order quantity.

we assumed $\beta \in [0, 1)$ and $\mu = \{0, 1, 2\}$ to reflect the level of overconfidence and fairness concern in this paper. When $\beta = 0$ and $\mu = 0$, the retailer was considered to be rational. Similarly, other fundamental parameter values were set in experiments as follows: $a = 50$, $\theta \sim U(-30, 30)$, $c = 4$, $p = 20$, $v = 7$, $s = 2$, $b = 2$, and $\gamma = 1$. All the parameters satisfied the constraint conditions and assumptions of the three models in Sections 3.2, 3.3, and 4. The parameter values were also in line with the real situation of the market. We could easily obtain $q^{c*} = 32$, $e^{c*} = 16$, and $\prod^c = 252$ in the centralized supply chain.

5.1. Effect of Overconfidence and Fairness Concern on the Supply Chain. The changes in the decision variables (w , q , and e), manufacturer profit, and retailer expected utility when the level of overconfidence and fairness concern (β and μ) changed are shown in Figures 1–5.

As shown in Figures 1 and 2, when the retailer was rational (e.g., $\beta = 0$ and $\mu = 0$) in the decentralized supply chain, both optimal order quantity and sales effort were lower than those under the centralized supply chain. Next, when the retailer had overconfidence and fairness concern simultaneously, overconfidence could only affect the retailer's optimal order quantity and sales effort of the retailer because the optimal order quantity and sales effort were a function of overconfidence in equations (13) and (14). Moreover, the order quantity was monotonically increasing as concave function with respect to β . In comparison, sales effort was monotonically increasing as convex function with respect to it. Furthermore, there existed a threshold ($\beta = 0.83$), when β was less than 0.83, and the two decision variables were both less than the optimal values ($q^{c*} = 32$, $e^{c*} = 16$) under the centralized decision scenario. Nevertheless, once β was larger than 0.83, the two decision variables were both more than them. The above discussion verified the correctness of Proposition 1. In short, overconfidence was the main factor that affected the retailer's optimal strategies of order quantity

and sales effort in the decentralized supply chain. However, the above findings contradicted with the conclusions from a study conducted by Xu et al. [16], which examined the effect of retailer's overconfidence on the supply chain, and the result suggested that a higher level of overconfident resulted in the lower ordering quantity.

In Figure 3, we observed that the higher overconfident level resulted in the high wholesale price; in contrast, a high degree of fairness concern resulted in low price, which demonstrated that Proposition 2 was robust. This figure implied that when the information for both parties was symmetric, the rational manufacturer knew that the retailer was overconfident, that is, the retailer was optimistic about the market demand and increased the order quantity. As a result, the manufacturer also raised the wholesale price to maximize its revenue. Also, if the overconfident retailer paid attention to the unfairness of profit allocation in the decision-making process, the retailer's bargaining power was enhanced [32]. Hence, for better performance in the supply chain, the leading manufacturer was required to lower wholesale prices to ease the feeling of unfairness by the retailer, which is consistent with the actual economic phenomenon. Furthermore, these findings are consistent with the result concluded by Cui et al. [2], which indicated that a high degree of the retailer's fairness concern could lower the wholesale price. Interestingly, as the levels of the cognitive bias increased, its effect on wholesale price gradually decreased, which highlighted its effect on decreased wholesale prices.

Figure 4 displays the impact of the cognitive bias on the retailer's utility. The graph showed that the retailer expected utility increased gradually with the overconfident level and the degree of fairness concern, which suggested that two cognitive biases were beneficial to the retailer. The reasons for such a phenomenon were that both cognitive biases could increase the optimal order quantity and sales effort, thus enhancing the utility of the retailer.

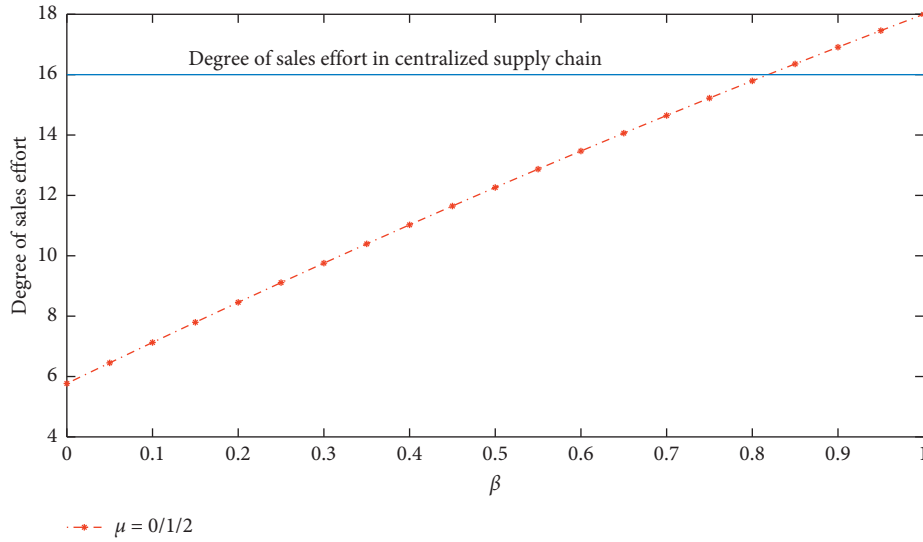


FIGURE 2: The effect of the cognitive biases on optimal sales effort.

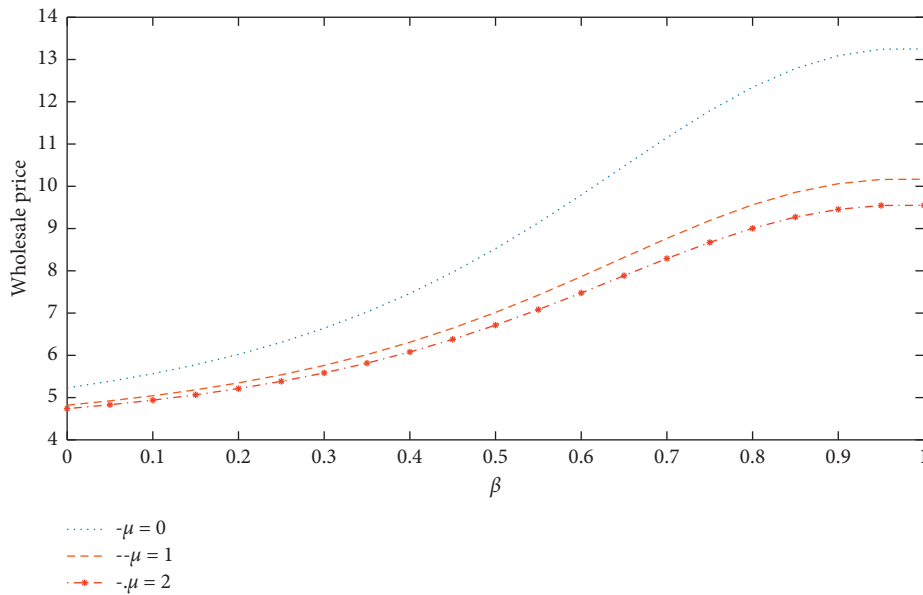


FIGURE 3: The effect of the cognitive biases on the optimal wholesale price.

Figure 5 illustrates the impact of overconfidence and fairness concern on the manufacturer's profit. That is, the optimal manufacturer's profit is an increasing function of β but a decreasing function of μ . According to Figure 3, the graph of the manufacturer's profit was similar to the graph of the wholesale price, which indicated that the manufacturer's profit was firmly related to wholesale price. Figure 5 also illustrates the effect of the cognitive bias β on the manufacturer's decreasing profit.

5.2. Effect of Overconfidence and Fairness Concern on Supply Chain Coordination. As can be seen from Section 5.1, there exist deviations between the optimal decisions under the

benchmark and the decisions in the presence of the retailer's cognitive biases. Therefore, the buyback contract with promotion cost sharing was necessary to coordinate the revenue of supply chain members and optimize the performance of the supply chain.

Here, we discussed the validity of the contract. When the optimal order quantity and sales effort of the retailer under the contract were the same as the optimal decision variables in the centralized supply chain, i.e., $q^{sc} = q^{c*} = 32$ and $e^{sc} = e^{c*} = 16$, the buyback contract with promotion cost sharing achieved supply chain coordination. First, the effect of overconfidence and fairness concern (β and μ) on contract factors w^{sr*} , r^* , and ϕ is shown in Figures 6 and 7 and Table 1. For clearly analyzing the effect of β and μ on w^{sr*}

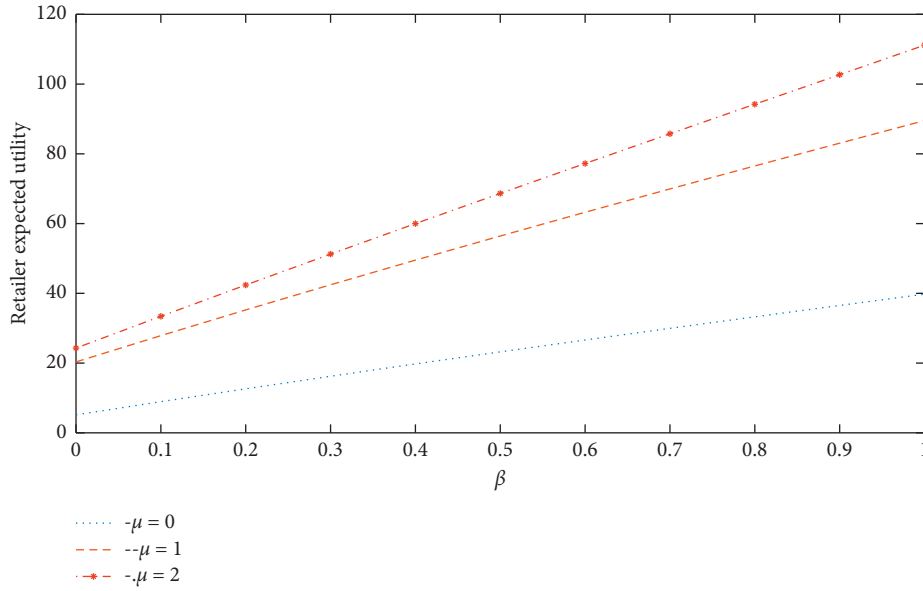


FIGURE 4: The effect of the cognitive biases on retailer utility.

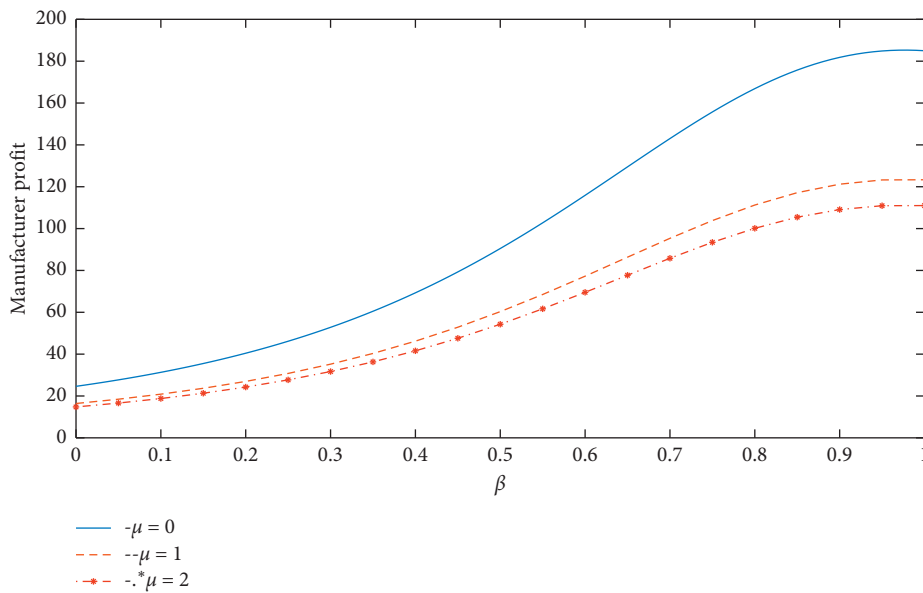


FIGURE 5: The effect of the cognitive biases on manufacturer profit.

and r^* , we let $\phi = 1$ in equations (18) and (19), which meant that the manufacturer proposed the buyback contract only, and the retailer bore all sales effort costs.

According to Figure 6, it was revealed that the optimal wholesales price is a strictly increasing function of the overconfidence level β but a strictly decreasing function of the degree of fairness concern μ , which confirmed the result of Proposition 4. Similarly, Figure 7 highlights that the optimal buyback price sharply increased with β but decreased with μ . Moreover, in the buyback contract, w^{sr*} was always greater than or equal to 4, and r^* was always greater than or equal to 2 in different cognitive bias levels. Hence,

the optimal buyback price r^* satisfied the assumption $s = 2 \leq r$. Note that the above characteristics influenced cognitive biases; hence, contract factors w^{sr*} and r^* were also correct when ϕ is equal to other values (such as $\phi = 0.3, 0.5, 0.8$) under conditions in which the buyback contract had promotion cost sharing.

However, data from Figure 7 can be compared with the data in Figure 6, which showed r^{sr*} is more significant than w^{sr*} when β was within a specific range (for example, $0.4 \leq \beta < 1$), which did not match the assumption $r < w^{sr}$. Therefore, the buyback contract did not achieve the coordination of the behavioral supply chain.

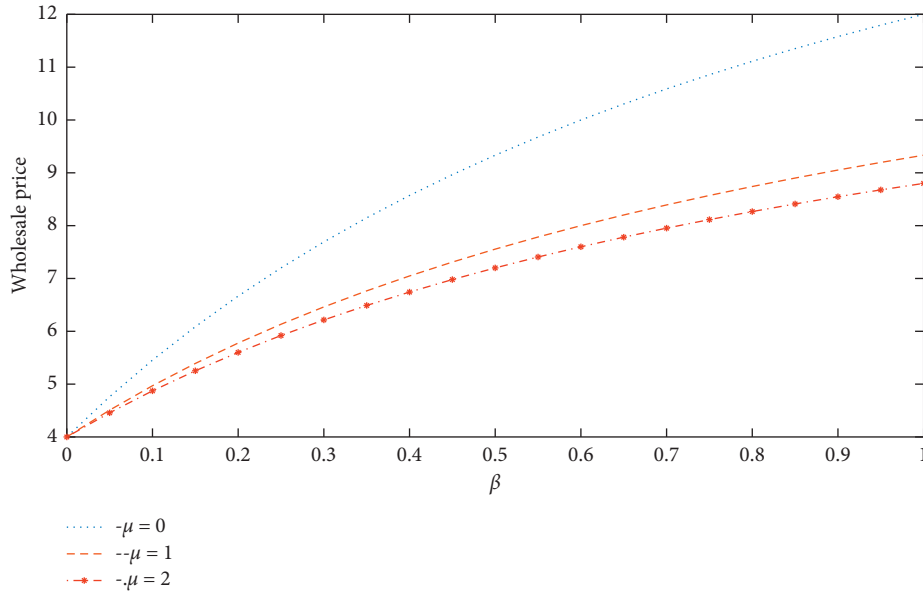


FIGURE 6: The effect of the cognitive biases on wholesale price w^{sr*} .

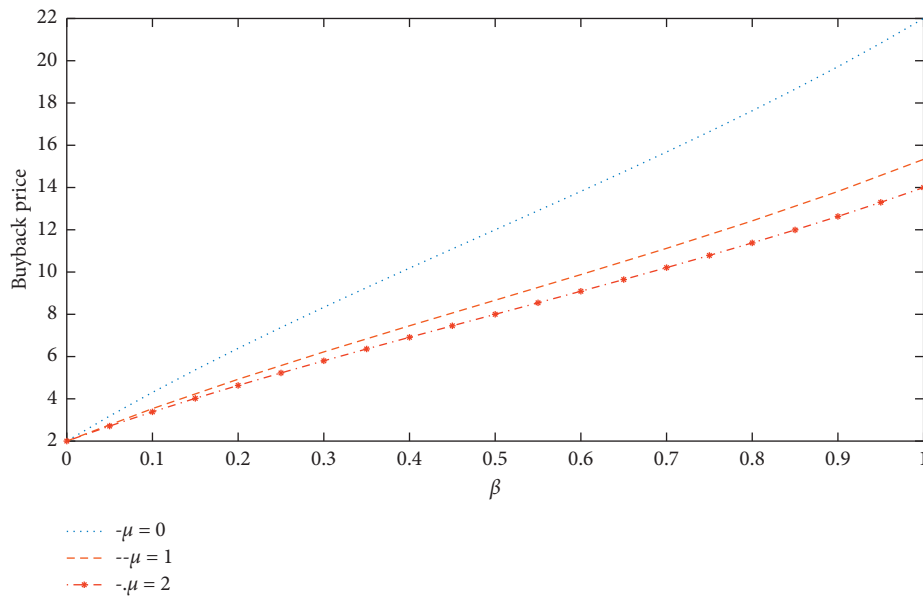


FIGURE 7: The effect of the cognitive biases on buyback price r^* .

As described in Section 4, if the supply chain members accepted the buyback contract with promotion cost sharing, the assumptions $\prod_m^{sc} \geq \max \prod_m^d$ and $U(\prod_r^{sc}) \geq \max U(\prod_r^d)$ had to be satisfied. Also, according to the assumptions, the value ϕ must satisfy $\prod_m^{sc} \geq \max \prod_m^d$ and $U(\prod_r^{sc}) \geq \max U(\prod_r^d)$. Thus, we kept the values of parameters to be the same (i.e., $a = 50$, $\theta \sim U(-30, 30)$, $c = 4$, $p = 20$, $v = 7$, $s = 2$, $b = 2$, and $\gamma = 1$) to capture a likely domain of ϕ .

As can be seen from Table 2, the overconfident level β increased the upper and lower limits of ϕ , which had a clear upward trend. In contrast, the upper and lower limits of ϕ

showed a definite declining trend as the degree of fairness concern μ increased. These trends illustrated that in order to coordinate the revenue of both parties and optimize the performance of the supply chain, the manufacturer needs to bear less promotional costs as β increased but bear more promotional costs as μ value increased. Besides, when β and μ increased, the interval of sharing cost portion ϕ shrunk, which indicated that the buyback contract with promotional cost sharing had certain flexibility to coordinate the revenue between supply chain members. However, the flexibility could be weakened with the rise of the cognitive bias level. For supply chain members, the possibility of negotiation or

TABLE 2: The effect of the cognitive biases on the feasible domain of promotion cost-sharing portion ϕ .

μ	β					
	0	0.2	0.4	0.6	0.8	0.81
0	[0.2884, 0.4976]	[0.3683, 0.5587]	[0.4528, 0.6199]	[0.6343, 0.7754]	[0.7835, 0.8669]	—
1	[0.2545, 0.4741]	[0.3310, 0.5331]	[0.4167, 0.5908]	[0.6207, 0.7516]	[0.7800, 0.8560]	—
2	[0.2352, 0.4600]	[0.3101, 0.5156]	[0.4034, 0.5719]	[0.6094, 0.7321]	[0.7736, 0.8478]	—

TABLE 3: The effect of the cognitive biases on the coordination of the supply chain.

$\mu = 1$	β				
	0	0.2	0.4	0.6	0.8
q^{sc}	32	32	32	32	32
e^{sc}	16	16	16	16	16
ϕ	[0.2545, 0.4741]	[0.3310, 0.5331]	[0.4167, 0.5908]	[0.6207, 0.7516]	[0.7800, 0.8560]
r	[2.100, 3.5363]	[2.8268, 3.9188]	[3.0555, 4.2637]	[3.6209, 4.4215]	[4.0485, 4.9164]
w^{sc}	[4.9205, 5.3687]	[4.9016, 5.3522]	[5.4092, 6.9568]	[6.2513, 7.2626]	[8.0407, 8.7453]
\prod_m^d	16.4103	26.9591	46.1996	77.2619	111.2545
$U(\prod_m^{sc})$	[16.8722, 21.7850]	[26.9600, 33.6882]	[46.3175, 50.0938]	[77.2619, 81.4300]	[111.2545, 112.0376]
\prod_r^d	20.333	35.2396	49.5161	63.2422	76.5317
$U(\prod_r^{sc})$	[20.333, 24.3043]	[35.2396, 40.0595]	[49.5161, 52.5161]	[63.2422, 65.7581]	[76.5317, 78.4632]

cooperation between manufacturers and retailers also decreased with an increase in retailers' cognitive bias level. When the overconfident level was more than 0.81, the retailer's utility from decentralized decisions was greater than the utility in the contract environment, wherein the two parties could not reach a cooperation agreement. Thus, the supply chain could not achieve coordination as different levels of cognitive bias under the contract had the same influence on decision variables, profit, and utility. Table 2 shows a clear picture wherein μ is equal to 1 and β falls within the range of (0, 0.8) which were used to analyze the effect of the cognitive biases on the coordination of the supply chain.

The results of the numerical simulation in Table 3 indicate that the contract factors, i.e., ϕ , r , wholesale price, the profit, and utility of members existed as flexible intervals when $\beta \in (0, 0.8)$ and $\mu = 1$. Besides, the order quantity q^{sc} and the degree of sales effort e^{sc} under the contract are equal to q^{c*} and e^{c*} in a centralized supply chain, respectively. Meanwhile, the buyback price r was less than the wholesale price w^{sc} and higher than the unit salvage value s , which satisfied the constrains $s \leq r < w^{sc*}$. Thus, the buyback contract with promotion cost could achieve the coordination of the two-echelon supply chain. Also, the buyback price r was positively correlated with the portion ϕ of promotion cost sharing. Notably, the wholesale price w^{sc} dropped as ϕ increased when β was in the range of (0, 0.2) in Table 3. However, the situation reversed when it was in the range of (0.2, 0.8), which was inconsistent since the manufacturer lowered the wholesale price when the retailer paid more promotional costs in the contract. The reason for such an observation was that the wholesale price was not related to ϕ but positively related to the overconfident level β when the degree of fairness concern was moderate. Furthermore, the retailer accepted the contract designed by manufacturers since the term $U(\prod_r^{sc}) \geq \max U(\prod_r^d)$ was guaranteed in Table 3.

6. Conclusions

6.1. Main Conclusions. In this paper, we analyzed the effect of cognitive bias on equilibrium solutions, including the wholesale price, sales price, sales effort, and expected profits under demand uncertainty by introducing both overconfidence and fairness concern into the two-echelon supply chain. The most important conclusion from the study was that, for retailers with the two cognitive biases, overconfidence was positive and the main bias that affected supply chain decisions, and the retailers' utility benefits were not only due to overconfidence but also fairness concern. For manufacturers, overconfidence could increase the wholesale price and profit. However, the fairness concern had a negative effect on them. Furthermore, the decisions of the retailer in the decentralized supply chain deviated from the optimal decisions in the centralized supply chain model. Especially, when the threshold of overconfidence was more than a fixed value, the decision variables under decentralized decision-making were actually higher than the optimal variables under centralized decision-making. Also, the buyback contract with promotional cost sharing achieved behavioral supply chain coordination. In contrast, the promotional cost-sharing portion and buyback price both benefited from overconfidence, but fairness concern had a detrimental effect on them. However, as the retailers' overconfidence level increased and fairness concern was equal to 1, the flexibility of contract coordination was weakened. When the overconfidence level was more than 0.8, the contract became invalid, and members were not able to cooperate.

6.2. Management Insights. This paper provided some interesting managerial insights for decision makers in the decentralized supply chain wherein retailers had two preferences. First, overconfidence was beneficial to them in terms of decision variables, and yet, the fairness concern

only damaged the wholesale price. Second, the two behavioral preferences were both conducive to utilities for the retailer but not necessarily beneficial for the manufacturer to receive profit, and overconfidence helped to increase manufacturers' profit, which led to nonoptimal decisions that dragged down the performance of the two-echelon supply chain. Finally, for the two behavioral preferences of the retailer, the manufacturer assessed the degree of overconfidence and fairness concern (especially, the overconfidence) via historical data and the current order quantity or other indicators. In contrast, factual data indicated that two behavioral preferences were in the right range (such as $\beta \in (0, 0.8)$ and $\mu \in (0, 2)$). The manufacturers introduced the buyback contract with promotional cost sharing into the practice of pricing and ordered decentralized supply chains. Furthermore, they designed a reasonable promotional cost-sharing portion and buyback price, thereby achieving an optimized decision and utility. In practice, the manufacturers could analyze whether the sellers had two behavioral preferences based on the historical data by cooperating with downstream enterprises, i.e., if two behavioral preferences existed, they referred to the papers' conclusions to redesign a reasonable contract mechanism.

6.3. *Future Research.* Since cognitive biases could exist among all members of supply chains, it is necessary to explore the manufacturers' cognitive biases and analyze the supply chain coordination problem in the presence of the two behavior preferences. Besides, the overconfidence and fairness concern considered in our centralized decision are a future research direction.

Appendix

A. Decentralized Supply Chain Model

In a decentralized supply chain consisting of a rational manufacturer and a retailer with cognitive biases, maximum profit or utility is the only goal. The backward inductive method can be applied to solve a Stackelberg game wherein the manufacturer is the leader, and the retailer is a follower. The proof of the equilibrium solutions in equations (12)–(14) is as follows.

The profit of the manufacturer and expected utility of retailers are as follows, respectively:

$$\max_w \prod_m^d = (w - c)q, \quad (\text{A.1})$$

$$\begin{aligned} \max_{q,e} U \left(\prod_r^d \right) &= (1 + \mu) \left\{ p[a - bp + (1 + \beta)e] + s \int_{-A}^{\theta_2} (q - (a - bp + (1 + \beta)e + \theta_1))f(\theta_1) d\theta_1 \right. \\ &\quad \left. - v \int_{\theta_2}^A ((a - bp + (1 + \beta)e + \theta_1 - q))f(\theta_1) d\theta_1 - wq - \frac{1}{2}\gamma e^2 \right\} - \mu(w - c)q. \end{aligned} \quad (\text{A.2})$$

Solving the first-order partial derivatives of the retailer's expected utility concerning q^d and e^d which equal to 0, we obtained the following equations:

$$\frac{\partial U^e(\prod_r^d)}{\partial q} = (1 + \mu)[v - w + F(\theta_2)(s - v)] - \mu(w - c) = 0, \quad (\text{A.3})$$

$$\frac{\partial U^e(\prod_r^d)}{\partial e} = (1 + \beta)[p - v + (v - s)F(\theta_2)] - \gamma e = 0. \quad (\text{A.4})$$

Hessian matrix:

$$H(q, e) = \begin{pmatrix} (s - v)f(\theta_2) & (v - s)(1 + \beta)f(\theta_2) \\ (v - s)f(\theta_2) & (s - v)(1 + \beta)f(\theta_2) - \gamma \end{pmatrix}. \quad (\text{A.5})$$

According to the assumptions, $v > s > 0$, $f(\theta_2) > 0$, and $\beta \in [0, 1)$. Thus, the Hessian matrix of $U(\prod_r^d)$ is a negative definite for q and e , which meant that the optimal order quantity and sales effort of retailers existed in the decentralized supply chain. Therefore, we obtained the following formula of the retailers' order quantity and sales effort by jointly solving equations (A.3) and (A.4):

$$q^d = \frac{(a - bp)(v - s)(1 + \mu)\gamma + (1 + \beta)^2(v - s)[(1 + \mu)(p - w) + \mu c] + A\gamma[(s + v)(1 + \mu) + 2\mu c - w]}{(v - s)(1 + \mu)\gamma}, \quad (\text{A.6})$$

$$e^d = \frac{(1 + \beta)[(1 + \mu)p + \mu c - (1 + 2\mu)w]}{(1 + \mu)\gamma}. \quad (\text{A.7})$$

Substituting equations (A.6) into (A.1), we attained

$$\max_w \prod_m^d = \frac{(w-c)\{(a-bp)(v-s)(1+\mu)\gamma + (1+\beta)^2(v-s)[(1+\mu)p + \mu c] + A\gamma[(s+v)(1+\mu) + 2\mu c] - (1+2\mu)w[2A\gamma + (1+\beta)^2(v-s)]\}}{(v-s)(1+\mu)\gamma}. \quad (\text{A.8})$$

Taking into account the first-order condition of equation (A.7) with respect to w rounded off to 0, we obtained

$$\frac{\partial \prod_m^d}{\partial e} = \frac{(a-bp)(v-s)(1+\mu)\gamma + (1+\beta)^2(v-s)[(1+\mu)p + \mu c] + A\gamma[(s+v)(1+\mu) + 2\mu c] - (2w-c)(1+2\mu)[2A\gamma + (1+\beta)^2(v-s)]}{(v-s)(1+\mu)\gamma}. \quad (\text{A.9})$$

Solving equation (A.8), we found that the optimal wholesale price of the manufacturer is as follows:

$$w^{d*} = \frac{(a-bp)(1+\mu)(v-s)\gamma + (v-s)(1+\beta)^2[(1+\mu)p + (1+3\mu)c] + A\gamma[(s+v)(1+\mu) + 2(1+3\mu)c]}{2(1+2\mu)[2A\gamma + (v-s)(1+\beta)^2]}. \quad (\text{A.10})$$

By substituting equation (A.9) into equations (A.6) and (A.7), we attained the optimal order quantity and sales effort, which are displayed in equations (13) and (14).

to β in equations (13) and (14), respectively. Meanwhile, taking the second-order derivative of q^{d*} with respect to β , we obtained

B. Propositions

Proof of Proposition 1. We solved the first derivatives of optimal order quantity q^{d*} and sales effort e^{d*} with respect

$$\frac{\partial q^{d*}}{\partial \beta} = \frac{(1+\beta)(p-c)}{\gamma}, \quad \frac{\partial^2 q^{d*}}{\partial \beta^2} = \frac{p-c}{\gamma}, \quad (\text{B.1})$$

$$\frac{\partial e^{d*}}{\partial \beta} = \frac{4(p-c)(v-s)^2\beta(\beta^3 + 4\beta^2 + 6\beta + 4) + (a-bp)\gamma(1+\beta)^2(v-s)^2 + A\gamma(v-s)(1+\beta)^2[(2(p-c) + v+s) + 2(A\gamma)^2(4p-c-s-v)]}{2\gamma[(1+\beta)^2(v-s) + 2A\gamma]^2}. \quad (\text{B.2})$$

Since the second derivative of e^{d*} with respect to β was very complicated, there was no need to solve it. According to the assumptions $p > v > c > s > 0$, $\beta \in (0, 1)$, $a - bp > 0$, and $\gamma > 0$, so $(\partial q^{d*} / \partial \beta) > 0$, $(\partial^2 q^{d*} / \partial \beta^2) > 0$, and $(\partial e^{d*} / \partial \beta) > 0$.

Proof of Proposition 2. Based on the process above, we took the first-order and second-order partial derivatives of optimal wholesale price w^{d*} with respect to β and μ in equation (12), respectively:

$$\frac{\partial w^{d*}}{\partial \beta} = \frac{\gamma(v-s)(1+\mu)(1+\beta)[(a-bp)(v-s) + A(2p-s-v)]}{(1+2\mu)[(1+\beta)^2(v-s) + 2A\gamma]^2}, \quad (\text{B.3})$$

$$\frac{\partial w^{d*}}{\partial \mu} = -\frac{[(a-bp)(v-s)\gamma + (p-c)(v-s)(1+\beta)^2 + A\gamma(s+v-2c)]}{2(1+2\mu)^2[(v-s)(1+\beta)^2 + 2A\gamma]}. \quad (\text{B.4})$$

According to the optimal result of order quantity in equation (13) and the assumption $q > 0$, the condition $s + v - 2c > 0$ is found. According to the assumptions we had, $(\partial w^{d*}/\partial \beta) > 0$ and $(\partial w^{d*}/\partial \mu) < 0$.

Proof of Proposition 3. The gap between q^{d*} and q^{c*} , denoted by Δq , is as follows:

$$\Delta q = q^{d*} - q^{c*} = \frac{(p-c)(v-s)[(1+\beta)^2 - 2] - A\gamma(s+v-2c) - (a-bp)(v-s)\gamma}{2\gamma(v-s)}. \quad (\text{B.5})$$

If $(p-c)(v-s)[(1+\beta)^2 - 2]$ is more than $A\gamma(s+v-2c) + (a-bp)(v-s)\gamma$, we have $\Delta q > 0$, i.e., $q^{d*} > q^{c*}$. In contrast, if $(p-c)(v-s)[(1+\beta)^2 - 2]$ is less

than $A\gamma(s+v-2c) + (a-bp)(v-s)\gamma$, $\Delta q < 0$, i.e., $q^{d*} < q^{c*}$.

The gap between e^{d*} and e^{c*} , denoted by Δe , is as follows:

$$\Delta e = e^{d*} - e^{c*} = \frac{A\beta\gamma(4p-2c-s-v) - A\gamma(s+v-2c) - (v-s)(1+\beta)[(a-bp)\gamma + (1-\beta^2)(p-c)]}{2\gamma[2A\gamma + (1+\beta)^2(v-s)]}. \quad (\text{B.6})$$

Similarly, if $A\beta\gamma(4p-2c-s-v) > A\gamma(s+v-2c) + (v-s)(1+\beta)[(a-bp)\gamma + (1-\beta^2)(p-c)]$, we have $\Delta e = e^{d*} - e^{c*} > 0$. In contrast, if $A\beta\gamma(4p-2c-s-v) < A\gamma(s+v-2c) +$

$(v-s)(1+\beta)[(a-bp)\gamma + (1-\beta^2)(p-c)]$, we have $\Delta e = e^{d*} - e^{c*} < 0$.

Upon solving the first-order derivative of Δq and Δe with respect to β , respectively, we obtained

$$\frac{\partial \Delta q}{\partial \beta} = \frac{(1+\beta)(p-c)}{\gamma}, \quad (\text{B.7})$$

$$\frac{\partial \Delta e}{\partial \beta} = \frac{4(p-c)(v-s)^2(\beta^3 + 4\beta^2 + 6\beta + 4)\beta + (a-bp)\gamma(1+\beta)^2(v-s)^2 + A\gamma(v-s)(1+\beta)^2[2(p-c) + v + s] + 2(A\gamma)^2(4p-c-s-v)}{2\gamma[(1+\beta)^2(v-s) + 2A\gamma]^2}. \quad (\text{B.8})$$

According to the assumptions $p > v > c > s > 0$, $\beta \in (0, 1)$, $\gamma > 0$, and $a - bp > 0$, $(\partial \Delta q / \partial \beta) > 0$ and $(\partial \Delta e / \partial \beta) > 0$ can be proved. Hence, the gaps increased as a function with respect to β .

$(\partial w^{sc*} / \partial \beta)$, if $\phi > (\mu / (1 + 2\mu))$ is more than 0; otherwise, $\phi > (\mu / (1 + 2\mu))$ is less than 0. Thus, w^{sc} could be increasing with respect to β , nevertheless, decreasing with respect to β . Besides, according to the assumptions, $p > v > c > s > 0$, $\beta \in (0, 1)$, $\gamma > 0$, and $a - bp > 0$, it can be evidently found that $(\partial w^{sc*} / \partial \mu) > 0$ and $(\partial w^{sc*} / \partial \phi) > 0$.

Proof of Proposition 4. The proof for Proposition 4 is similar to Proposition 2. Herein, we took first-order and second-order partial derivatives of optimal wholesale price w^{sc*} with respect to β , μ , and ϕ in equation (18), respectively. The solving results are as follows:

$$\begin{aligned} \frac{\partial w^{sc*}}{\partial \beta} &= \frac{[(1+2\mu)\phi - \mu](p-c)}{(1+2\mu)(1+\beta)^2}, \\ \frac{\partial w^{sc*}}{\partial \mu} &= -\frac{(p-c)\beta}{(1+\beta)(1+2\mu)^2}, \\ \frac{\partial w^{sc*}}{\partial \phi} &= \frac{p-c}{1+\beta}, \end{aligned} \quad (\text{B.9})$$

Data Availability

The data used to support the findings of this study are included within the article.

Conflicts of Interest

The authors declare no conflicts of interest.

Acknowledgments

This work was supported by a major project financed by the National Social Science Fund of China (Approval nos. 71461009, 71662011, and 71761015).

References

- [1] Y. Ren, D. C. Croson, and R. T. A. Croson, "The overconfident newsvendor," *Journal of the Operational Research Society*, vol. 68, no. 5, pp. 496–506, 2017.
- [2] T. H. Cui and P. Mallucci, "Fairness ideals in distribution channels," *Journal of Marketing Research*, vol. 53, no. 6, pp. 969–987, 2016.
- [3] K. Chen, X. Wang, M. Huang, and W.-K. Ching, "Salesforce contract design, joint pricing and production planning with asymmetric overconfidence sales agent," *Journal of Industrial & Management Optimization*, vol. 13, no. 2, pp. 873–899, 2017.
- [4] X. X. Zheng, Z. Liu, K. W. Li et al., "Cooperative game approaches to coordinating a three-echelon closed-loop supply chain with fairness concerns," *International Journal of Production Economic*, vol. 212, pp. 92–110, 2018.
- [5] China Internet Watch, *False Prosperity behind Double 11: Refund Rate Increased to 69%*, 2014, <https://www.chinainternetwatch.com/11643/false-prosperity-behind-double-11-refund-rate-increased-to-69/>.
- [6] C. L. Lu, "P&G's collaborative supply chain transformation," *Enterprise Management*, vol. 10, pp. 79–80, 2016.
- [7] M. Li, N. C. Petruzzi, and J. Zhang, "Overconfident competing newsvendors," *Management Science*, vol. 63, no. 8, pp. 2637–2646, 2016.
- [8] T. Nie, "Dual-fairness supply chain with quantity discount contracts," *European Journal of Operational Research*, vol. 258, no. 2, pp. 491–500, 2017.
- [9] X. Du and B. Jiang, "Signaling through price and quality to consumers with fairness concerns," *Journal of Marketing Research*, vol. 53, no. 6, pp. 988–1000, 2016.
- [10] V. Kurz, A. Orland, and K. Posadzy, "Fairness versus efficiency: how procedural fairness concerns affect coordination," *Experimental Economics*, vol. 21, no. 3, pp. 601–626, 2018.
- [11] S. Villa and J. A. Castañeda, "Transshipments in supply chains: a behavioral investigation," *European Journal of Operational Research*, vol. 269, no. 2, pp. 715–729, 2018.
- [12] B. Gu, Y. Fu, and Y. Li, "Fresh-keeping effort and channel performance in a fresh product supply chain with loss-averse consumers' returns," *Mathematical Problems in Engineering*, vol. 2018, Article ID 4717094, 20 pages, 2018.
- [13] D. Croson, R. Croson, and Y. Ren, *How to Manage an Overconfident Newsvendor*, 2008, <http://cbees.utdallas.edu/papers/CrosonRenCmsonMS2008>.
- [14] M. Li, "Overconfident distribution channels," *Production and Operations Management*, vol. 28, no. 6, pp. 1347–1365, 2019.
- [15] W. Liu, D. Wang, O. Tang, and D. Zhu, "The impacts of logistics service integrator's overconfidence behaviour on supply chain decision under demand surge," *European Journal of Industrial Engineering*, vol. 12, no. 4, pp. 558–597, 2018.
- [16] L. Xu, X. Shi, P. Du, K. Govindan, and Z. Zhang, "Optimization on pricing and overconfidence problem in a duopolistic supply chain," *Computers & Operations Research*, vol. 101, pp. 162–172, 2019.
- [17] Y. Li and M. Shan, "Advance selling decisions with overconfident consumers," *Journal of Industrial and Management Optimization*, vol. 2, no. 3, pp. 891–905, 2016.
- [18] T. H. Cui, J. S. Raju, and Z. J. Zhang, "Fairness and channel coordination," *Management Science*, vol. 53, no. 8, pp. 1303–1314, 2007.
- [19] X. Wu and J. A. Niederhoff, "Fairness in selling to the newsvendor," *Production and Operations Management*, vol. 23, no. 11, pp. 2002–2022, 2014.
- [20] Z. Chen and S.-I. Ivan Su, "Social welfare maximization with the least subsidy: photovoltaic supply chain equilibrium and coordination with fairness concern," *Renewable Energy*, vol. 132, pp. 1332–1347, 2019.
- [21] W. Liu, D. Wang, X. Shen, X. Yan, and W. Wei, "The impacts of distributional and peer-induced fairness concerns on the decision-making of order allocation in logistics service supply chain," *Transportation Research Part E: Logistics and Transportation Review*, vol. 116, pp. 102–122, 2018.
- [22] L. Zhang, H. Zhou, Y. Liu, and R. Lu, "Optimal environmental quality and price with consumer environmental awareness and retailer's fairness concerns in supply chain," *Journal of Cleaner Production*, vol. 213, pp. 1063–1079, 2019.
- [23] X. L. Wang, S. Q. Hu, and X. B. Liu, "Supply coordination with option contract considering overconfidence under random demand and yields," *Computer Integrated Manufacturing System*, vol. 24, no. 11, pp. 2898–2908, 2018.
- [24] W. Jiang and J. Liu, "Inventory financing with overconfident supplier based on supply chain contract," *Mathematical Problems in Engineering*, vol. 2018, Article ID 5054387, 12 pages, 2018.
- [25] P. Ma, H. Wang, and J. Shang, "Contract design for two-stage supply chain coordination: integrating manufacturer-quality and retailer-marketing efforts," *International Journal of Production Economics*, vol. 146, no. 2, pp. 745–755, 2013.
- [26] J. Liu, W. F. Jiang, and Y. P. Tang, "The supply chain coordination based on carbon reduction of overconfident manufacturer," *Journal of Jiangxi Normal University (Natural Science)*, vol. 42, no. 2, pp. 203–207, 2018.
- [27] R. Dubey, N. Altay, and C. Blome, "Swift trust and commitment: the missing links for humanitarian supply chain coordination?" *Annals of Operations Research*, vol. 283, no. 1–2, pp. 159–177, 2019.
- [28] C. Cui, Z. Feng, and C. Tan, "Credibilistic loss aversion nash equilibrium for bimatrix games with triangular fuzzy payoffs," *Complexity*, vol. 2018, Article ID 7143586, 16 pages, 2018.
- [29] E. Fehr and K. M. Schmidt, "A theory of fairness, competition, and cooperation," *The Quarterly Journal of Economics*, vol. 114, no. 3, pp. 817–868, 1999.
- [30] Z. Qin and J. Yang, "Analysis of a revenue-sharing contract in supply chain management," *International Journal of Logistics Research and Applications*, vol. 11, no. 1, pp. 17–29, 2008.
- [31] S.-Z. Bai and J. Ni, "Research on buy-back contract with sales effort cost sharing," in *Proceedings of the 2009 Chinese Control and Decision Conference*, IEEE, Guilin, China, pp. 1917–1921, June 2009.
- [32] E. Karagözoğlu and K. Keskin, "Time-varying fairness concerns, delay, and disagreement in bargaining," *Journal of Economic Behavior and Organization*, vol. 147, pp. 115–128, 2018.

Research Article

Cooperative Innovation in the Medical Supply Chain Based on User Feedback

Ran Chen, Gui-sheng Hou, and Yu Wang 

School of Economics and Management, Shandong University of Science and Technology, Qindao 266590, China

Correspondence should be addressed to Yu Wang; yuwang17@sdust.edu.cn

Received 17 February 2020; Revised 17 March 2020; Accepted 30 March 2020; Published 21 April 2020

Guest Editor: Lei Xie

Copyright © 2020 Ran Chen et al. This is an open access article distributed under the Creative Commons Attribution License, which permits unrestricted use, distribution, and reproduction in any medium, provided the original work is properly cited.

Given the importance of users in medical innovation, positive user participation can boost the cooperative innovation process within the medical supply chain. A stochastic differential model based on user feedback is proposed to study the relationship between user feedback and the medical supply chain. The stability and sensitivity of the medical supply chain is analysed through different parameters. The results show that the effect of patient feedback and suggestions from hospitals on the innovation level of medical services and medical products is positive, such that the impact of the innovation level of medical services on users and the effect of patient feedback are positively related to marginal profits and that cooperative innovation is beneficial for medical product and service innovation and the improvement of demand and profits.

1. Introduction

With economic growth and increasing health awareness, demand for and spending on advanced medical products and services have increased due to the pursuit of longer lifespans and better living conditions [1, 2]. Consumers are increasingly willing to pay more for advanced medical products and services [3].

Medical manufacturers develop and produce innovative medical products to meet this diverse and complex demand. Medical products include medicines, medical devices, and other supplementary medical products. Medical devices are necessary for patient recovery and physical rehabilitation. In most countries, the majority of medical device companies is small and medium-sized enterprises (SMEs); in the Netherlands, for example, the ratio of SMEs in this sector is approximately 80% [4]. The main market for their products is domestic. These companies have few opportunities to attract large investments, and it is difficult to launch new medical products owing to regulatory restrictions and licensing systems [5, 6]. High technological capacity and innovative capacity are two main drivers of competition in the medical industry. Cooperating with other firms in this industry has been suggested due to the uncertainty involved

in the technological innovation process, hysteresis, and revenue leakages [5]. Cooperation enables firms to earn more profits [7]. Cooperation in medical technological innovation is vital for companies that have a heavy dependence on the import of technology and advanced products. Alliances among enterprises, universities, and research institutes play an important role in decreasing research risk and speeding up the identification of medical innovation breakthroughs. Thus, appropriate medical products and services can be developed in a shorter time [8]. Cooperation among industry, academia, hospitals, and patients is beneficial for the effective integration of various resources, the construction of an expansive knowledge network for medical innovation [9], and the development of open innovation platforms [10]. Patients not only are those who need a cure but also are consumers of medical products and services [11]. As a key knowledge source and the main consumers of such products and services, patients help lead long-term medical innovation and drive the primary trend of the market [12]. Users provide new ideas to companies and enable them to understand real demands and expectations, reduce costs, develop product design and safety, and identify potential problems with medical products in the development stage [13, 14]. Users also offer real-time

feedback after the introduction of new products in the market [12]. However, companies must involve users in product development at the right time using the right methods to make the cooperation work [15].

Users include both patients and hospitals. For hospitals, the aim of medical services is the promotion of the public good instead of profit maximum [16]. Hospital managers need to consider effectiveness, patient safety, budget, treatment requirements, reputation, and cost in developing a hospital's medical technology strategy [17]. The hospital cooperates with medical suppliers, provides medical services, and collects patient information and feedback. An adequate understanding of patient needs and effective interaction and communication with patients during the process of supplying medical services are indispensable for increasing the quality of medical services. Feedback from patients on their own diseases and relevant treatments has high heterogeneity and direction [18]. Physician participation is beneficial for building medical information systems to gather more accurate information [19]. Surgeons are receptive to the marketing of medical products and to patient feedback [20]. While some elements of patient feedback are characterized by low credibility, communication between medical companies and patients has some impact on the value of feedback [21]. To improve feedback credibility, most medical companies prefer to offer commissions to hospitals. The authors in [3] point out that the commission rate is dependent upon hospitals' effort level.

The identification of unmet and unrecognized needs [22], interaction with patients and their families, and an emphasis on patient feedback are critical to the construction of a patient-oriented healthcare system [23]. The incentives to further these objectives should be relevant, practical, and sustainable [24]. Governments often make some efforts: the British government, for example, has established healthcare technology cooperatives to boost cooperation among hospitals, patients, industry, and academia to develop new products and update existing ones [25]. In addition, in many countries, excellent licensing, technology evaluation, and payment systems have been established [26]. Brazil's government has passed incentives to enhance cooperation between universities and public medical institutes [27]. In other countries, green approval channels have been setup for some medical devices and medicine.

Currently, only a few medical companies prefer to collect suggestions extensively at the concept design stage, and a small number of users are invited to participate in the development and testing stages [28]. Most companies do not invite users to join in the product design and development phases [20] and ignore the significant impacts of user participation. Companies that do want to bring users into their development system need to take into account how user participation will affect product innovation, how to promote the positive role of users and hospitals in cooperative medical innovation, and how to deal with the impacts of the inherent randomness of the market and consumer choice using optimal strategies. In this paper, a strategic model is constructed based on stochastic differential game theory to solve the problems mentioned above. The model is

chosen due to the following benefits: compared with other strands of game theory, stochastic differential theory allows the randomness in the process and uncertainty during the decision-making process to be approached effectively and fits the real world better. The theory has been widely applied in the fields of economics and operations research. In [29], the authors find strategies with reduced risks by using stochastic differential game theory. The authors in [30] study cooperation in green building technology by using stochastic differential game theory to model the uncertainty of the external environment. The current research aims to promote cooperation among users, hospitals, and companies based on users' feedback and hospitals' suggestions, while considering uncertainty.

The contribution of this study is to group feedback into two types—patient feedback and hospital suggestions—and analyse the impacts of both types on the optimal strategies for cooperative innovation and for the innovation partners. Uncertainty of choice and the environment is considered to reflect the real world.

This study is organized into six parts as follows. Section 1 introduces the background. The stochastic differential model is constructed in Section 2. Sections 3 and 4 present the process of model solving. Finally, the discussion, numerical simulations, and conclusion can be found in Sections 5 and 6.

2. Proposed Stochastic Differential Model

A two-echelon supply chain has been widely applied in related research [31–33]. Here, the supply chain includes a medical manufacturer and a hospital. The medical manufacturer is the leader and responsible for the supply of medical products. The hospital is the follower and provides the corresponding medical services and treatment for patients; both players are risk neutral. The medical manufacturer is dominant in the market and sets monopoly prices to attain profits [1, 34, 35]. The manufacturer makes development decisions based on feedback from the hospital. Innovation in the medical supply chain can include the development of new medical products and medical services and treatments simultaneously. The medical manufacturer decides the wholesale price of new products and the innovation level, and the hospital decides the retail price. The conceptual model is shown in Figure 1.

Considering the existing research [3, 36, 37], the cost functions of the medical manufacturer and the hospital are set as

$$\begin{aligned} C_s(L) &= \frac{\alpha}{2(1+\chi_2)} L^2(t), \\ C_h(G) &= \frac{\beta}{2(1+\chi_1)} G^2(t), \end{aligned} \quad (1)$$

where $\alpha > 0$ and $\beta > 0$ are the cost-effectiveness of the medical products and services, respectively; $L(t)$ and $G(t)$ are the innovation levels of the medical products and services at time t , respectively; and $\chi_1 > 0$ $\chi_2 > 0$ are the

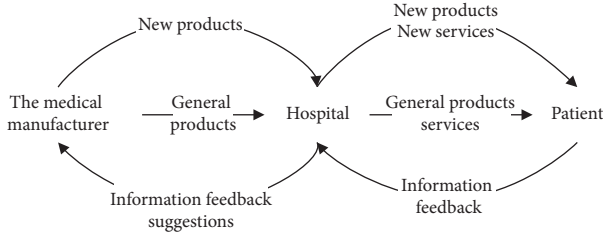


FIGURE 1: The concept of feedback in the medical supply chain innovation process.

effectiveness of the feedback from patients and the hospital, respectively.

When demand is unknown, there are some methods to describe the demand function, such as the exponential smoothing algorithm [38]. In this work, users purchase medical products and services based on the innovation level. That is, demand is a stochastic process that depends on the innovation level of medical products and services:

$$\begin{cases} dX(t) = [\delta L(t) + \gamma G(t) - \varepsilon X(t)]dt + \sigma(X(t))dW(t), \\ X(0) = X_0 \geq 0, \end{cases} \quad (2)$$

where $X(t)$ is the demand at time t , δ , and γ are the impacts of medical products and services on demand, respectively, $\varepsilon > 0$ is the demand error term, $W(t)$ is the standard Wiener process at time t , and $\sigma(X(t))$ is the random interference coefficient.

The medical manufacturer and the hospital share the profits based on a previous contract, whereby the medical manufacturer earns $n \in (0, 1)$ and the hospital receives $1 - n$. The medical manufacturer shares costs with the hospital in the ratio $j(t) \in (0, 1)$, where $j(t)$ denotes the commission rate. Subsidy I is paid by the government. The discount rate for the medical manufacturer and hospital is ρ ($\rho > 0$), and t is omitted in the following functions. The profit functions of the whole medical supply chain [39, 40], the medical manufacturer, and the hospital are as follows:

$$\begin{aligned} \pi(t) &= pX(t), \\ \max_{L,j} J_s(X_0) &= E \int_0^\infty e^{-\rho t} \left\{ n\pi(t) - \frac{\alpha}{2(1+\chi_2)} L^2(t) \right. \\ &\quad \left. - j(t) \frac{\beta}{2(1+\chi_1)} G^2(t) + I \right\} dt, \\ \max_G J_h(X_0) &= E \int_0^\infty e^{-\rho t} \left\{ (1-n)\pi(t) \right. \\ &\quad \left. - [1-j(t)] \frac{\beta}{2(1+\chi_1)} G^2(t) \right\} dt, \end{aligned} \quad (3)$$

where p is the retail price.

TABLE 1: Nomenclature.

Symbol	means
I	Government subsidy
X	Demand
G	Innovation level of medical services
p	Retail price
σ	Random interference coefficient
ε	Demand error
W	Standard Wiener process
j	Commission rate
ρ	Discount rate
α	Cost-effectiveness of the medical products
L	Innovation level of new products
β	Cost-effectiveness of medical services
χ_1	Effectiveness of feedback from patients
χ_2	Effectiveness of feedback from the hospital
δ	Impact of medical products on demand
γ	Impact of medical services on demand
n	Profit ratio for the medical manufacturer

All the variables used in the following model are listed in Table 1.

3. Solving of the Model

3.1. Decentralized Model. The medical manufacturer and the hospital maximize their profits, and the optimal strategy is

$$\begin{cases} G^* = \frac{2\gamma(1+\chi_1)(1-n)^2 p}{\beta(\rho+\varepsilon)(1+n)}, \\ L^* = \frac{\delta(1+\chi_2)np}{\alpha(\rho+\varepsilon)}, \\ j^* = \frac{3n-1}{n+1}, n \in \left(\frac{1}{3}, 1\right). \end{cases} \quad (4)$$

Proof. Feedback control with better capacity is widely applied in the economy [41]. The optimal value functions are $V_h(X)$ and $V_s(X)$, which should satisfy the Hamilton–Jacobi–Bellman (HJB) function:

$$\begin{aligned} \rho V_h(X) &= \max_G \left\{ (1-n)pX - (1-j) \frac{\beta}{2(1+\chi_1)} G^2 \right. \\ &\quad \left. + V'_h(X)(\delta L + \gamma G - \varepsilon X) + \frac{\sigma^2(X)}{2} V''_h(X) \right\}, \end{aligned} \quad (5)$$

$$\begin{aligned} \rho V_s(X) &= \max_{L,j} \left\{ npX - \frac{\alpha}{2(1+\chi_2)} L^2 - j \frac{\beta}{2(1+\chi_1)} G^2 + I \right. \\ &\quad \left. + V'_s(X)(\delta L + \gamma G - \varepsilon X) + \frac{\sigma^2(X)}{2} V''_s(X) \right\}, \end{aligned} \quad (6)$$

where $V'_h(X)$ and $V''_h(X)$ are the first and second partial derivatives of $V_h(X)$ and $V'_s(X)$ and $V''_s(X)$ are the first and second partial derivatives of $V_s(X)$.

Then, solve equation (7) and insert it into equation (6) to achieve equation (8). Maximize equation (8) to obtain equations (9) and (10). Insert (5) and (6) to obtain equations (11) and (12).

$$G = \frac{\gamma V'_h(X)(1 + \chi_1)}{(1 - j)\beta}, \quad (7)$$

$$\rho V_s(X) = \max_{L,j} \left\{ npX - \frac{\alpha}{2(1 + \chi_2)} L^2 - \frac{j(1 + \chi_1)\gamma^2 V_h'^2(X)}{2(1 - j)^2\beta} + I + V'_s(X) \left(\delta L + \frac{\gamma^2(1 + \chi_1)V'_h(X)}{(1 - j)\beta} - \varepsilon X \right) + \frac{\sigma^2(X)}{2} V_s''(X) \right\}, \quad (8)$$

$$L = \frac{\delta V'_s(X)(1 + \chi_2)}{\alpha}, \quad (9)$$

$$j = \frac{2V'_s(X) - V'_h(X)}{2V'_s(X) + V'_h(X)}, \quad (10)$$

$$\rho V_h(X) = \max_G \left\{ [(1 - n)p - \varepsilon V'_h(X)]X + \frac{\delta^2 V_h'^2(X)(1 + \chi_2)}{\alpha} + \frac{\gamma^2(1 + \chi_1)V'_h(X)[2V'_s(X) + V'_h(X)]}{4\beta} + \frac{\sigma^2(X)}{2} V_h''(X) \right\}, \quad (11)$$

$$\rho V_s(X) = \max_{L,j} \left\{ [np - \varepsilon V'_s(X)]X + \frac{\gamma^2(1 + \chi_1)[2V'_s(X) + V'_h(X)]^2}{8\beta} + I + \frac{\delta^2 V_h'^2(X)(1 + \chi_2)}{2\alpha} + \frac{\sigma^2(X)}{2} V_s''(X) \right\}. \quad (12)$$

Set $V_h(X) = f_1 X + f_2$ and $V_s(X) = k_1 X + k_2$, which are denoted by the optimal linear functions, where f_1 , f_2 , k_1 , and k_2 are constants. Insert them into (11) and (12) to obtain

$$\begin{cases} f_1 = \frac{(1 - n)p}{\rho + \varepsilon}, \\ f_2 = \frac{\delta^2(1 + \chi_2)(1 - n)^2 p^2}{\alpha\rho(\rho + \varepsilon)^2} + \frac{\gamma^2(1 + \chi_1)(1 - n)^2 p^2}{4\beta\rho(\rho + \varepsilon)^2}, \\ k_1 = \frac{np}{\rho + \varepsilon}, \\ k_2 = \frac{\gamma^2(1 + \chi_1)(p + np)^2}{8\beta\rho(\rho + \varepsilon)^2} + \frac{\delta^2(1 + \chi_2)(1 - n)^2 p^2}{2\alpha\rho(\rho + \varepsilon)^2} + I. \end{cases} \quad (13)$$

The optimal value functions of the medical manufacturer and the hospital are

$$\begin{aligned} V_h(X) &= \frac{(1 - n)p}{\rho + \varepsilon} X + \frac{\delta^2(1 + \chi_2)(1 - n)^2 p^2}{\alpha\rho(\rho + \varepsilon)^2} \\ &\quad + \frac{\gamma^2(1 + \chi_1)(1 - n)^2 p^2}{4\beta\rho(\rho + \varepsilon)^2}, \\ V_s(X) &= \frac{np}{\rho + \varepsilon} X + \frac{\gamma^2(1 + \chi_1)(p + np)^2}{8\beta\rho(\rho + \varepsilon)^2} \\ &\quad + \frac{\delta^2(1 + \chi_2)(1 - n)^2 p^2}{2\alpha\rho(\rho + \varepsilon)^2} + I. \end{aligned} \quad (14)$$

□

Corollary 1. *The innovation level of medical services is positively related to demand, the effectiveness of feedback from patients, the retail price, and the commission rate ($(\partial G/\partial\gamma) > 0$, $(\partial G/\partial\chi_1) > 0$, $(\partial G/\partial p) > 0$, $(\partial G/\partial j) > 0$). The more real and effective the feedback from patients, the better are the medical services. The cost and demand error are negatively related to the innovation level of medical services ($(\partial G/\partial\beta) < 0$, $(\partial G/\partial\varepsilon) < 0$).*

Corollary 2. *The innovation level of medical products is positively related to demand, the effectiveness of feedback from the hospital, and the retail price ($(\partial L/\partial\delta) > 0$, $(\partial L/\partial\chi_2) > 0$, $(\partial L/\partial p) > 0$). The positive effects of the innovation level of medical products on demand are significant for the development of products. The cost and demand error are negatively related to the innovation level of medical products ($(\partial L/\partial\alpha) < 0$, $(\partial L/\partial\varepsilon) < 0$).*

Considering the method proposed in [42], the optimal strategy is inserted into (2) to obtain

$$\begin{cases} dX(t) = [\Omega - \varepsilon X(t)]dt + \sigma(X(t))dW(t), \\ X(0) = X_0 \geq 0, \end{cases} \quad (15)$$

where $\Omega = (\delta^2(1 + \chi_2)(1 - n)p/\alpha(\rho + \varepsilon) + (2\gamma^2(1 + \chi_1)(1 - n)^2 p/(1 + n)\beta(\rho + \varepsilon))$ is constant. The higher the innovation level of medical products, the larger the Ω . Set $\sigma(X(t))dW(t) = \sigma\sqrt{X}dW(t)$ to obtain

$$X(t) = X(0) + \int_0^t [\Omega - \varepsilon X(s)]ds + \int_0^t \sigma(X(s))dW(s). \quad (16)$$

The expectation of equation (16) is $E(X(t)) = X(0) + \int_0^t [\Omega - \varepsilon X(s)]ds$. The initial condition is $E(X(0)) = X_0$.

$$\begin{aligned} E(X(t)) &= \frac{\Omega}{\varepsilon} (1 - e^{-\varepsilon t}) + e^{-\varepsilon t} X_0 \\ &= \left[\frac{\delta^2(1 + \chi_2)(1 - n)p}{\alpha(\rho + \varepsilon)\varepsilon} + \frac{\gamma^2(1 + \chi_1)(1 - n)p}{(1 - j)\beta(\rho + \varepsilon)\varepsilon} \right] \\ &\quad \cdot (1 - e^{-\varepsilon t}) + e^{-\varepsilon t} X_0, \\ \lim_{t \rightarrow \infty} E(X(t)) &= \frac{\Omega}{\varepsilon}. \end{aligned} \quad (17)$$

Substitute the Itô function into equation (15) to obtain

$$\begin{cases} dX^2(t) = [2X(\Omega - \varepsilon X) + \sigma^2 X]dt + 2X\sigma\sqrt{X}dW(t), \\ X^2(0) = X_0^2 \geq 0. \end{cases} \quad (18)$$

Then, integrate equations (15) and (18) to obtain the following equation:

$$D[X(t)] = \frac{\sigma^2 e^{-2\varepsilon t} (e^{-\varepsilon t} - 1)[(e^{-\varepsilon t} - 1)\Omega + 2\varepsilon X_0]}{2\varepsilon^2},$$

$$\lim_{t \rightarrow \infty} D[X(t)] = \frac{\sigma^2 \Omega}{2\varepsilon^2}. \quad (19)$$

3.2. Centralized Model. When the players plan to cooperate, the objective becomes the profit maximization of the overall medical supply chain. The profit function is

$$\begin{aligned} \max_{L,G} J_{\text{HS}}(X_0) = E \int_0^\infty e^{-\rho t} \left\{ pX(t) - \frac{\alpha}{2(1+\chi_2)} L^2(t) \right. \\ \left. - \frac{\beta}{2(1+\chi_1)} G^2(t) + I \right\} dt(t). \end{aligned} \quad (20)$$

The optimal strategy in cooperation is

$$\begin{cases} L_{\text{HS}}^* = \frac{\delta(1+\chi_2)p}{\alpha(\rho+\varepsilon)}, \\ G_{\text{HS}}^* = \frac{\gamma(1+\chi_1)p}{\beta(\rho+\varepsilon)}. \end{cases} \quad (21)$$

The optimal value function is

$$V_{\text{HS}}(X) = \frac{p}{\rho+\varepsilon} X + \frac{\delta^2(1+\chi_2)p^2}{2\alpha\rho(\rho+\varepsilon)^2} + \frac{\gamma^2(1+\chi_1)p^2}{2\beta\rho(\rho+\varepsilon)^2} + I. \quad (22)$$

Corollary 3. *The innovation level of medical products and services is positively related to demand, the effectiveness of feedback from the hospital and patients, and the retail price ($(\partial G_{\text{HS}}^*/\partial \gamma) > 0$, $(\partial G_{\text{HS}}^*/\partial \chi_1) > 0$, $(\partial G_{\text{HS}}^*/\partial p) > 0$, $(\partial L_{\text{HS}}^*/\partial \delta) > 0$, $(\partial L_{\text{HS}}^*/\partial \chi_2) > 0$, $(\partial L_{\text{HS}}^*/\partial p) > 0$).*

The same method proposed before is used to obtain the expectation, variance, and stable value in the centralized strategy:

$$\begin{aligned} E_{\text{HS}}(X(t)) &= \frac{\mathcal{U}}{\varepsilon} (1 - e^{-\varepsilon t}) + e^{-\varepsilon t} X_0, \\ \lim_{t \rightarrow \infty} E_{\text{HS}}(X(t)) &= \frac{\mathcal{U}}{\varepsilon}, \\ D_{\text{HS}}[X(t)] &= \frac{\sigma^2 e^{-2\varepsilon t} (e^{-\varepsilon t} - 1)[(e^{-\varepsilon t} - 1)\mathcal{U} + 2\varepsilon X_0]}{2\varepsilon^2}, \\ \lim_{t \rightarrow \infty} D_{\text{HS}}[X(t)] &= \frac{\sigma^2 \mathcal{U}}{2\varepsilon^2}. \end{aligned} \quad (23)$$

4. Discussion

Insight 1. The innovation level of medical products in a centralized strategy is higher than that in a decentralized strategy. The difference between the medical product innovation level in the centralized and decentralized strategies depends on the impacts of innovation on demand and the effectiveness of the feedback from the hospital:

$$\begin{aligned} \Delta L = L_{\text{HS}}^* - L^* &= \frac{\delta(1+\chi_2)(1-n)p}{\alpha(\rho+\varepsilon)} > 0, \\ \frac{\partial \Delta L}{\partial \delta} > 0, \frac{\partial \Delta L}{\partial \chi_2} > 0. \end{aligned} \quad (24)$$

Insight 2. The innovation level of medical services in a centralized strategy is higher than that in a decentralized strategy. The difference between medical service innovation level in the centralized and decentralized strategies depends on the impacts of innovation on demand and the effectiveness of the feedback from patients:

$$\begin{aligned} \Delta G = G_{\text{HS}}^* - G^* &= \frac{\gamma(1+\chi_1)p[(1+n) - 2(1-n)^2]}{\beta(\rho+\varepsilon)(1+n)}, \\ n \in \left(\frac{1}{3}, 1\right), \Delta G > 0, \frac{\partial \Delta G}{\partial \gamma} > 0, \frac{\partial \Delta G}{\partial \chi_1} > 0. \end{aligned} \quad (25)$$

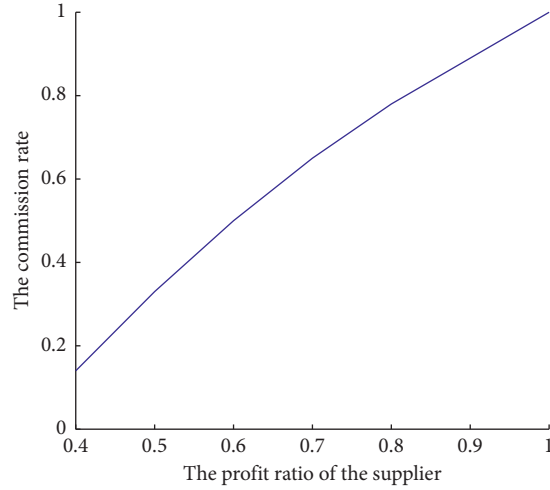


FIGURE 2: The commission rate in the decentralized strategy.

Insight 3. When $n \in ((4\sqrt{5}/5) - 1, 1)$, profits are higher in the centralized strategy than in the decentralized strategy:

$$\begin{aligned} \Delta V &= V_{\text{HS}}(X) - [V_h(X) + V_s(X)] \\ &= \frac{\delta^2(1 + \chi_2)p^2(1 - 3(1 - n)^2)}{2\alpha\rho(\rho + \varepsilon)^2} \\ &\quad + \frac{\gamma^2(1 + \chi_1)p^2(5n^2 - 11 - 10n)}{8\beta\rho(\rho + \varepsilon)^2}, \end{aligned} \quad (26)$$

$$n \in \left(\frac{4\sqrt{5}}{5} - 1, 1 \right), \quad \Delta V > 0.$$

Insight 4. The expectation and variance of the innovation level of medical products and services and their stable values are higher in the centralized strategy than in the decentralized strategy:

$$\because \mathcal{U} - \Omega = \frac{n\delta^2(1 + \chi_2)p}{\alpha(\rho + \varepsilon)} + \frac{\gamma^2(1 + \chi_1)p(1 - n)^3}{\beta(\rho + \varepsilon)(n + 1)^2} > 0,$$

$$\therefore E_{\text{HS}}(X(t)) - E(X(t)) = \frac{\mathcal{U} - \Omega}{\varepsilon}(1 - e^{-\varepsilon t}) > 0,$$

$$\lim_{t \rightarrow \infty} E_{\text{HS}}(X(t)) - \lim_{t \rightarrow \infty} E(X(t)) = \frac{\mathcal{U} - \Omega}{\varepsilon} > 0, \quad (27)$$

$$D_{\text{HS}}(X(t)) - D(X(t)) = D_{\text{HS}}[X(t)] = \frac{\sigma^2 e^{-2\varepsilon t} (e^{-\varepsilon t} - 1)^2 (\mathcal{U} - \Omega)}{2\varepsilon^2} > 0,$$

$$\lim_{t \rightarrow \infty} D_{\text{HS}}(X(t)) - \lim_{t \rightarrow \infty} D(X(t)) = \frac{\sigma^2 (\mathcal{U} - \Omega)}{2\varepsilon^2} > 0.$$

5. Numerical Simulation

5.1. Optimal Strategy of the Medical Manufacturer and the Hospital. Set $\gamma = 0.7$, $\delta = 0.8$, $\alpha = 5$, $\beta = 4$, $\rho = 0.8$, $\varepsilon = 0.1$, and $p = 10$ to study the impacts of user feedback and the share of profits on the optimal strategy.

Figures 2–4 give some information about the decentralized model. From Figure 2, the profits of the medical manufacturer are positively related to the commission rate. The more profits the medical manufacturer receives, the higher the commission rate the medical manufacturer offers. The positive impacts of feedback and suggestions from the

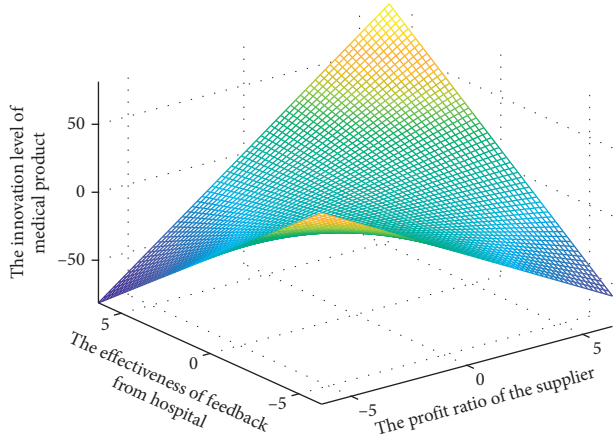


FIGURE 3: The innovation level of medical products in the decentralized strategy.

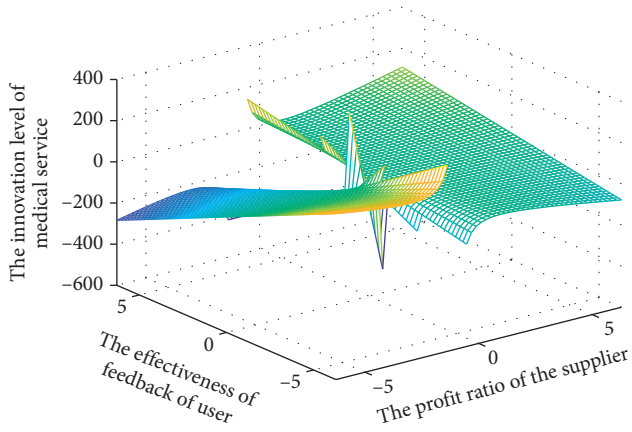


FIGURE 4: The innovation level of medical service in the decentralized strategy.

hospital and the profit ratio for the medical manufacturer on the innovation level of medical products can be found in Figure 3. That is, the real and effective information gathered and valuable suggestions supported by the hospital are beneficial for the improvement of medical products and meet the increasingly sophisticated demand. Figure 4 shows that there are positive impacts of feedback from patients and the profit ratio for the medical manufacturer on the innovation level of medical services. Though the hospital may receive lower profits, the commission makes up the gap. Figure 5 shows information about the positive impacts of the effectiveness of user feedback on the innovation level of medical products and services in the centralized strategy.

5.2. Effects of Demand and Demand Expectations. Set $\sigma = 5$, $X_0 = 0$, $\chi_1 = \chi_2 = 0.7$, $n = 0.7$, and time step $\Delta t = 1$. Based on the method presented in [42], (15) is discretized:

$$X(t + \Delta t) = X(t) + (0.97 - \varepsilon X(t))\Delta t + \sigma\sqrt{X(t)}\sqrt{\Delta t}\zeta(t), \quad (28)$$

where $\zeta(t)$ is the standard normal random variable.

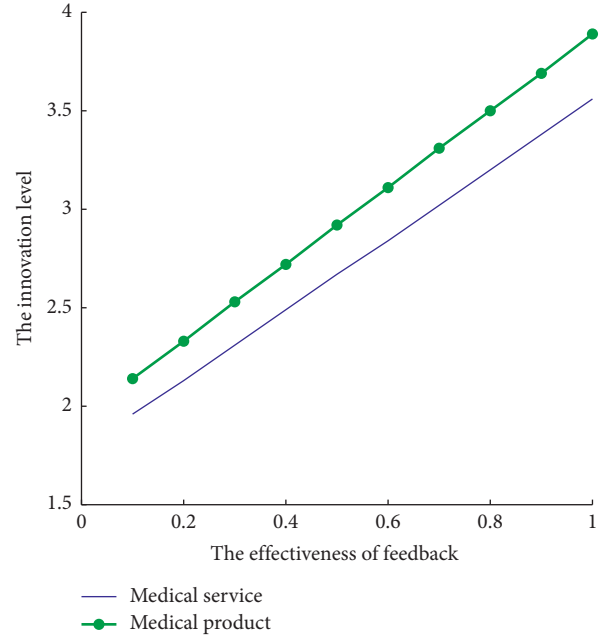


FIGURE 5: The impacts of feedback on the innovation level of medical products in the centralized strategy.

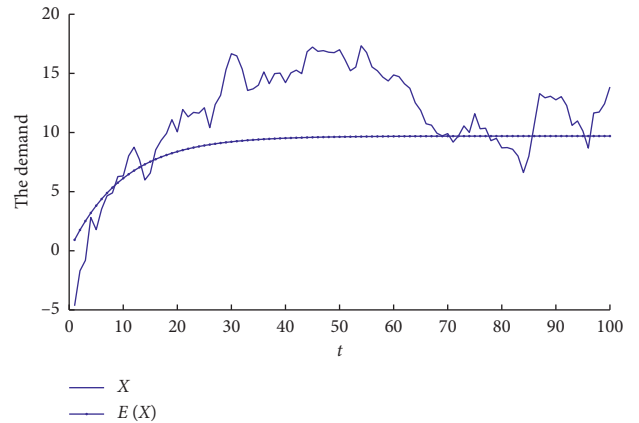


FIGURE 6: The changing effects of demand and demand expectations over time.

In Figure 6, demand fluctuates above and below its expected level. In real economies, demand is affected by various factors. It is difficult to obtain the actual data. The approximation of demand enables managers to make better decisions. Confidence intervals can describe real demand. The 95% confidence interval is

$$(E[X(t)] - 1.96\sqrt{D[X(t)]}, E[X(t)] + 1.96\sqrt{D[X(t)]}). \quad (29)$$

6. Conclusion

Cooperation among medical manufacturers, medical service providers, and patients is fundamental to the construction of healthcare systems. In this paper, an innovation system

involving patients, the medical manufacturer, and the hospital is established to allow for the consideration of user feedback. The medical manufacturer in this work is willing to collect suggestions from users and hospitals to achieve valuable feedback in the development and testing stage, highlighting the significant impacts of user participation. Stochastic differential game theory is used to find the optimal strategies in a decentralized and a centralized context. The results show that there are positive impacts of demand, the effectiveness of user feedback, and the retail price on the innovation level of medical products and services. User participation in the form of feedback has positive impacts on medical innovation. The cost and demand error term are negatively related to the innovation level of medical products and services. The innovation level of medical products and services is higher in the centralized strategy than in the decentralized strategy. It is possible to promote cooperation among users and hospitals in medical innovation by sharing the hospital's costs. The impacts of the inherent randomness of the market and consumer choice on the optimal strategies are described by the stochastic differential game model. The expectation and variance of the innovation level of medical products and services and their stable values are higher in the centralized strategy than in the decentralized strategy.

This study is beneficial in helping medical manufacturers adjust their commission rates to increase the effectiveness of user feedback, realize the importance of user feedback for cooperative innovation, and reduce costs. It is vital to build a positive cooperation cycle to boost medical products and service upgrades and updates.

Some limitations need to be addressed in the future. In real economies, there are more than two members in the medical supply chain, and the number of agents in the medical supply chain will be increased in the following study. Some other key factors, such as user feedback, need to be elaborated upon to further this study. Finally, enriching the cooperation design to reflect cooperation among industry, universities, research institutes, hospitals, and patients is another direction for future study.

Data Availability

All data, the models used during the study that appear in the submitted article, and the codes used to support the findings of this study are available from the corresponding author upon request.

Conflicts of Interest

The authors declare that there are no conflicts of interest regarding the publication of this paper.

Acknowledgments

Thanks are extended for the help from lecturer Lu Liu. This study was supported by the Shandong University of Science and Technology innovation programme (no. SDKDYC180110).

References

- [1] A. M. Garber, C. I. Jones, and P. Romer, "Insurance and incentives for medical innovation," *Forum for Health Economics & Policy*, vol. 9, no. 2, 2011.
- [2] V. Peiffer, C. A. Yock, P. G. Yock, and J. B. Pietzsch, "Value-based care: a review of key challenges and opportunities relevant to medical technology innovators," *Journal of Medical Devices, Transactions of the ASME*, vol. 13, no. 2, 2019.
- [3] Y. J. Lu, Y. Q. Deng, and X. F. Xu, "Research on incentive mechanism of medical service supply chain under information asymmetry," *Journal of UESTC (Social Sciences Edition)*, vol. 21, no. 5, pp. 88–95, 2019.
- [4] A. J. J. Pullen, P. C. De Weerd-Nederhof, A. J. Groen, and O. A. M. Fisscher, "Open innovation in practice: goal complementarity and closed NPD networks to explain differences in innovation performance for SMEs in the medical devices sector," *Journal of Product Innovation Management*, vol. 29, no. 6, pp. 917–934, 2012.
- [5] Y. Su, "Research on the cooperative innovation model of medical device industry in the processes of production-study-research-application based on information theory," *Technology Intelligence Engineering*, vol. 2, no. 2, pp. 34–44, 2016.
- [6] M. Lee, S. Park, and K. S. Lee, "What are the features of successful medical device start-ups? Evidence from Korea," *Sustainability*, vol. 11, no. 7, pp. 1–17, 2019.
- [7] Z. Li and Z. Q. Ma, "Research on benefit distribution of essential drugs supply chain in purchase pattern of medical insurance bidding," *Industrial Engineering and Management*, vol. 24, no. 5, pp. 64–71, 2019.
- [8] L. Puslecki and M. Staszko, "New cooperation modes: an opportunity for polish biotechnological clusters," *Managing Global Transitions: International Research Journal*, vol. 13, no. 2, pp. 171–188, 2015.
- [9] K. de Jager, C. Chimhundu, T. Saidi, and T. S. Douglas, "Medical device innovation in South Africa: evolution of collaboration networks (2001–2013)," *South African Journal of Industrial Engineering*, vol. 30, no. 2, pp. 26–44, 2019.
- [10] C. F. Daiberl, S. J. Oks, A. Roth, K. M. Möslein, and S. Alter, "Design principles for establishing a multi-sided open innovation platform: lessons learned from an action research study in the medical technology industry," *Electronic Markets*, vol. 29, no. 4, pp. 711–728, 2019.
- [11] F. Djellal and F. Gallouj, "Mapping innovation dynamics in hospitals," *Research Policy*, vol. 34, no. 6, pp. 817–835, 2005.
- [12] C. Lettl, C. Hienert, and H. G. Gemuenden, "Exploring how lead users develop radical innovation: opportunity recognition and exploitation in the field of medical equipment technology," *IEEE Transactions on Engineering Management*, vol. 55, no. 2, pp. 219–233, 2008.
- [13] S. Ghulam, S. Shah, and I. Robinson, "Benefits of and barriers to involving users in medical device technology development and evaluation," *International Journal of Technology Assessment in Health Care*, vol. 23, no. 1, pp. 131–137, 2007.
- [14] S. G. S. Shah, I. Robinson, and S. Alshawi, "Developing medical device technologies from users' perspectives: a theoretical framework for involving users in the development process," *International Journal of Technology Assessment in Health Care*, vol. 25, no. 4, pp. 514–521, 2009.
- [15] C. Lettl, "User involvement competence for radical innovation," *Journal of Engineering and Technology Management*, vol. 24, no. 1–2, pp. 53–75, 2007.

- [16] L. Y. Gao and X. L. Wang, "Study on coordination in medical service supply chains with social benefit under revenue sharing contract," *Soft Science*, vol. 32, no. 8, pp. 91–97, 2018.
- [17] S. Gurtner, "Making the right decisions about new technologies," *Health Care Management Review*, vol. 39, no. 3, pp. 245–254, 2014.
- [18] D. Lee, "A model for designing healthcare service based on the patient experience," *International Journal of Healthcare Management*, vol. 12, no. 3, pp. 180–188, 2017.
- [19] S. Martikainen, J. Viitanen, M. Korpela, and T. Lääveri, "Physicians' experiences of participation in healthcare IT development in Finland: willing but not able," *International Journal of Medical Informatics*, vol. 81, no. 2, pp. 98–113, 2012.
- [20] A. G. Money, J. Barnett, J. Kuljis, M. P. Craven, J. L. Martin, and T. Young, "The role of the user within the medical device design and development process: medical device manufacturers' perspectives," *BMC Medical Informatics and Decision Making*, vol. 11, no. 1, 2011.
- [21] M. P. Manary, W. Boulding, R. Staelin, and S. W. Glickman, "The patient experience and health outcomes," *New England Journal of Medicine*, vol. 368, no. 3, pp. 201–203, 2013.
- [22] A. D. McCarthy, L. Sproson, O. Wells, and W. Tindale, "Unmet needs: relevance to medical technology innovation?" *Journal of Medical Engineering & Technology*, vol. 39, no. 7, pp. 382–387, 2015.
- [23] K. Luxford, D. G. Safran, and T. Delbanco, "Promoting patient-centered care: a qualitative study of facilitators and barriers in healthcare organizations with a reputation for improving the patient experience," *International Journal for Quality in Health Care*, vol. 23, no. 5, pp. 510–515, 2011.
- [24] P. Lehoux, B. Williams-Jones, F. Miller, D. Urbach, and S. Tailliez, "What leads to better health care innovation? Arguments for an integrated policy-oriented research agenda," *Journal of Health Services Research & Policy*, vol. 13, no. 4, pp. 251–254, 2008.
- [25] D. N. M. Heron and P. W. B. Tindale Obe, "Healthcare technology co-operatives: innovative about innovation," *Journal of Medical Engineering & Technology*, vol. 39, no. 7, pp. 378–381, 2015.
- [26] Z. P. Ye, M. Tang, H. Y. Wang, and C. L. Jin, "The management system and payment framework of innovative medical technology in the United Kingdom," *Chinese Health Resources*, vol. 22, no. 4, pp. 321–325, 2019.
- [27] M. P. Ryan, "Patent incentives, technology markets, and public-private bio-medical innovation networks in Brazil," *World Development*, vol. 38, no. 8, pp. 1082–1093, 2010.
- [28] W. G. Biemans, "User and third-party involvement in developing medical equipment innovations," *Technovation*, vol. 11, no. 3, pp. 163–182, 1991.
- [29] S. Mataramvura and B. Øksendal, "Risk minimizing portfolios and HJBI equations for stochastic differential games," *Stochastics*, vol. 80, no. 4, pp. 317–337, 2008.
- [30] S. Yin and B. Li, "Transferring green building technologies from academic research institutes to building enterprises in the development of urban green building: a stochastic differential game approach," *Sustainable Cities and Society*, vol. 39, pp. 631–638, 2018.
- [31] Y. Tian, J. H. Ma, and W. D. Lou, "Research on supply chain stability driven by consumer's channel preference based on complexity theory," *Complexity*, vol. 2018, Article ID 7812784, 13 pages, 2018.
- [32] Q. Li, Y. Zhang, and Y. Huang, "The complexity analysis in dual-channel supply chain based on fairness concern and different business objectives," *Complexity*, vol. 2018, no. 2, pp. 1–13, 2018.
- [33] Q. Li, X. Chen, Y. Huang, H. Gui, and S. Liu, "The impacts of green innovation input and channel service in a dual-channel value chain," *International Journal of Environmental Research and Public Health*, vol. 16, no. 22, p. 4566, 2019.
- [34] J. Ma and Z. Guo, "The influence of information on the stability of a dynamic Bertrand game," *Communications in Nonlinear Science and Numerical Simulation*, vol. 30, no. 1–3, pp. 32–44, 2016.
- [35] J. H. Ma and Z. B. Guo, "Implications for firms with limited information to take advantage of reference price effect in competitive settings," *Complexity*, vol. 2017, Article ID 9712626, 16 pages, 2017.
- [36] J. G. Du, P. P. Dou, and L. W. Zhao, "The impact of retailer's risk aversion and fairness preference on green supply chain operation," *Journal of Industrial Technological Economics*, vol. 7, pp. 3–9, 2017.
- [37] G. Hou, Y. Wang, and B. Xin, "A coordinated strategy for sustainable supply chain management with product sustainability, environmental effect and social reputation," *Journal of Cleaner Production*, vol. 228, no. 10, pp. 1143–1156, 2019.
- [38] Q. Li, "The dynamic behaviors of a supply chain with stock-dependent demand considering competition and deteriorating items," *Kybernetes*, vol. 45, no. 7, pp. 1109–1128, 2016.
- [39] Y. M. Huang, Q. X. Li, and Y. H. Zhang, "The complexity analysis for price game model of risk-averse supply chain considering fairness concern," *Complexity*, vol. 2018, Article ID 9216193, 15 pages, 2018.
- [40] Q. Li, X. Chen, and Y. Huang, "The stability and complexity analysis of a low-carbon supply chain considering fairness concern behavior and sales service," *International Journal of Environmental Research and Public Health*, vol. 16, no. 15, p. 2711, 2019.
- [41] Y. Feng, "Fuzzy stochastic differential systems," *Fuzzy Sets and Systems*, vol. 115, no. 3, pp. 351–363, 2000.
- [42] A. Prasad and S. P. Sethi, "Competitive advertising under uncertainty: a stochastic differential game approach," *Journal of Optimization Theory and Applications*, vol. 123, no. 1, pp. 163–185, 2004.